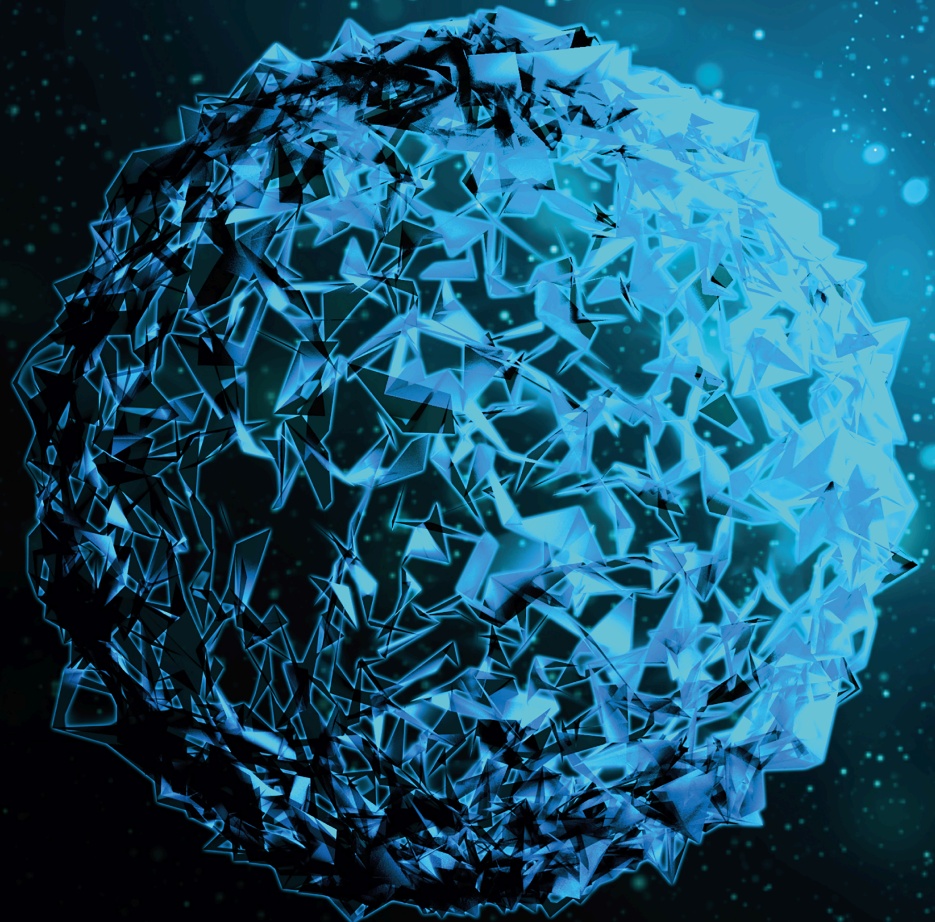


# Minimally Invasive Treatment Protocols in Clinical Dentistry

Lead Guest Editor: Dinesh Rokaya

Guest Editors: Pokpong Amornvit, Sasiwimol Sanohkan, and Zohaib  
Khurshid Sultan





---

# **Minimally Invasive Treatment Protocols in Clinical Dentistry**



BioMed Research International

---

## **Minimally Invasive Treatment Protocols in Clinical Dentistry**

Lead Guest Editor: Dinesh Rokaya

Guest Editors: Pokpong Amornvit, Sasiwimol  
Sanohkan, and Zohaib Khurshid Sultan



---

Copyright © 2023 Hindawi Limited. All rights reserved.


This is a special issue published in "BioMed Research International." All articles are open access articles distributed under the Creative Commons Attribution License, which permits unrestricted use, distribution, and reproduction in any medium, provided the original work is properly cited.

## Section Editors


Penny A. Asbell, USA  
David Bernardo , Spain  
Gerald Brandacher, USA  
Kim Bridle , Australia  
Laura Chronopoulou , Italy  
Gerald A. Colvin , USA  
Aaron S. Dumont, USA  
Pierfrancesco Franco , Italy  
Raj P. Kandpal , USA  
Fabrizio Montecucco , Italy  
Mangesh S. Pednekar , India  
Letterio S. Politi , USA  
Jinsong Ren , China  
William B. Rodgers, USA  
Harry W. Schroeder , USA  
Andrea Scribante , Italy  
Germán Vicente-Rodriguez , Spain  
Momiao Xiong , USA  
Hui Zhang , China

## Academic Editors

### Dentistry

Ali I. Abdalla, Egypt  
Carlos M. Ardila , Colombia  
Nicola Cirillo , Australia  
Fernanda Faot , Brazil  
Luca Fiorillo , Italy  
Flavia Gonçalves , Brazil  
Vincenzo Grassia , Italy  
Yeliz Guven , Turkey  
Heng Bo Jiang , China  
Saber Khazaei , Iran  
H. Y. Kim, USA  
Carlo Medina-Solis, Mexico  
Nenad Mitrović , Serbia  
Pablo G. Moreno, Spain  
Piero Papi , Italy  
Romeo Patini, Italy  
Giorgio Pompa, Italy

Joao Paulo Mendes Tribst, The Netherlands

Giuseppe Varvara , Italy

Li Wu Zheng , Hong Kong

# Contents

**Retracted: Exploring Purification Methods of Exosomes from Different Biological Samples**

BioMed Research International

Retraction (1 page), Article ID 9826329, Volume 2023 (2023)

**Retracted: Intra- and Interrater Agreement of Face Esthetic Analysis in 3D Face Images**

BioMed Research International

Retraction (1 page), Article ID 9824574, Volume 2023 (2023)

**Retracted: Strategies of Bioceramics, Bioactive Glasses in Endodontics: Future Perspectives of Restorative Dentistry**

BioMed Research International

Retraction (1 page), Article ID 9814703, Volume 2023 (2023)

**Retracted: Silencing lncRNA 93358 Inhibits the Apoptosis of Myocardial Cells in Myocardial Infarction Rats by Inducing the Expression of SLC8A1**

BioMed Research International

Retraction (1 page), Article ID 9812061, Volume 2023 (2023)

**Retracted: Kukoamine A Improves *Mycoplasma pneumoniae* Pneumonia by Regulating miR-222-3p/Superoxide Dismutase 2**

BioMed Research International

Retraction (1 page), Article ID 9786745, Volume 2023 (2023)

**Retracted: The Effect of Hyperlipidemia on Peri-Implant Health: A Clinical and Radiographical Prospective Study**

BioMed Research International

Retraction (1 page), Article ID 9783253, Volume 2023 (2023)

**Retracted: Automatic Segmentation of Calcification Areas in Digital Breast Images**

BioMed Research International

Retraction (1 page), Article ID 9832038, Volume 2023 (2023)

**Retracted: The Current Antimicrobial and Antibiofilm Activities of Synthetic/Herbal/Biomaterials in Dental Application**

BioMed Research International

Retraction (1 page), Article ID 9830262, Volume 2023 (2023)

**Retracted: Investigation of the Role of *Leuconostoc mesenteroides* subsp. *cremoris* in Periodontitis around Abutments of Fixed Prosthesis**

BioMed Research International

Retraction (1 page), Article ID 9764690, Volume 2023 (2023)

**Retracted: Study on the Mechanism of Xiaotan Sanjie Recipe in the Treatment of Colon Cancer Based on Network Pharmacology**

BioMed Research International

Retraction (1 page), Article ID 9897128, Volume 2023 (2023)



**Retracted: Innovate a Standard for the Future Model of Nursing Care at Medical-Surgical Units in Najran University**

BioMed Research International

Retraction (1 page), Article ID 9854765, Volume 2023 (2023)

**Retracted: Mutation Detection and Functional Analysis of MSX1, PAX9, AXIN2, and BMP in Nonsyndromic Congenital Missing Teeth Based on Intelligent Image Detection**

BioMed Research International

Retraction (1 page), Article ID 9832761, Volume 2023 (2023)

**Retracted: Treatment Protocols in the Efficacy and Safety of Anti-EGFR Medicines in Combination with Standard Therapy for Patients with Nasopharyngeal Cancer: A Meta-Analysis**

BioMed Research International

Retraction (1 page), Article ID 9830710, Volume 2023 (2023)

**Retracted: Effect of Supplementation of Vitamin D in Patients with Periodontitis Evaluated before and after Nonsurgical Therapy**

BioMed Research International

Retraction (1 page), Article ID 9850874, Volume 2023 (2023)

**Retracted: Detection of WBC, RBC, and Platelets in Blood Samples Using Deep Learning**

BioMed Research International

Retraction (1 page), Article ID 9864640, Volume 2023 (2023)

**Retracted: Hui Medicine Moxibustion Promotes the Absorption of Lumbar Disc Herniation and the Recovery of Motor Function in Rats through Fas/FasL Signaling Pathway**

BioMed Research International

Retraction (1 page), Article ID 9837346, Volume 2023 (2023)

**Retracted: *In Vivo* Growth Inhibition of Human Caucasian Prostate Adenocarcinoma in Nude Mice Induced by Amygdalin with Metabolic Enzyme Combinations**

BioMed Research International

Retraction (1 page), Article ID 9829041, Volume 2023 (2023)

**Retracted: Segmentation of Oral Leukoplakia (OL) and Proliferative Verrucous Leukoplakia (PVL) Using Artificial Intelligence Techniques**

BioMed Research International

Retraction (1 page), Article ID 9826519, Volume 2023 (2023)

**Retracted: Visual Analysis of Nutrient Deficiency and Treatment Protocols in Bariatric Surgery Based on VOSviewer**

BioMed Research International

Retraction (1 page), Article ID 9793724, Volume 2023 (2023)

## Contents

---

**Retracted: Prevalence and Correlation of Metabolic Syndrome in Patients with Bipolar Disorder in NGH, Riyadh**

BioMed Research International

Retraction (1 page), Article ID 9756976, Volume 2023 (2023)

**Retracted: Early Detection of Autism Spectrum Disorders (ASD) with the Help of Data Mining Tools**

BioMed Research International

Retraction (1 page), Article ID 9819043, Volume 2023 (2023)

**Retracted: Efficacy of Various Types of Berries Extract for the Synthesis of ZnO Nanocomposites and Exploring Their Antimicrobial Potential for Use in Herbal Medicines**

BioMed Research International

Retraction (1 page), Article ID 9815767, Volume 2023 (2023)

**Retracted: A Comparison of Decision Tree Algorithms in the Assessment of Biomedical Data**

BioMed Research International

Retraction (1 page), Article ID 9810245, Volume 2023 (2023)

**Retracted: Use of Composite Acellular Dermal Matrix-Ultrathin Split-Thickness Skin in Hand Hot-Crush Injuries: A One-Step Grafting Procedure**

BioMed Research International

Retraction (1 page), Article ID 9802521, Volume 2023 (2023)

**Retracted: Deep Learning-Based Networks for Detecting Anomalies in Chest X-Rays**

BioMed Research International

Retraction (1 page), Article ID 9801414, Volume 2023 (2023)

**Retracted: Biogenic Analysis of the Effect of TERC on Cell Proliferation and Migration of Oral Squamous Cell Carcinoma under Digital Minimally Invasive Treatment**

BioMed Research International

Retraction (1 page), Article ID 9798465, Volume 2023 (2023)

**Retracted: The Predictive Value of Neutrophil-Lymphocyte Ratio in Patients with Polycythemia Vera at the Time of Initial Diagnosis for Thrombotic Events**

BioMed Research International

Retraction (1 page), Article ID 9792783, Volume 2023 (2023)

**Retracted: The Use of Chest Radiographs and Machine Learning Model for the Rapid Detection of Pneumonitis in Pediatric**

BioMed Research International

Retraction (1 page), Article ID 9792648, Volume 2023 (2023)

**Retracted: Red Raspberry Extract Decreases Depression-Like Behavior in Rats by Modulating Neuroinflammation and Oxidative Stress**

BioMed Research International

Retraction (1 page), Article ID 9792454, Volume 2023 (2023)

**Retracted: Dapagliflozin Improves Diabetic Cardiomyopathy by Modulating the Akt/mTOR Signaling Pathway**

BioMed Research International

Retraction (1 page), Article ID 9765065, Volume 2023 (2023)

**Retracted: A Novel Method for Parkinson's Disease Diagnosis Utilizing Treatment Protocols**

BioMed Research International

Retraction (1 page), Article ID 9763896, Volume 2023 (2023)

**Retracted: Processing Decision Tree Data Using Internet of Things (IoT) and Artificial Intelligence Technologies with Special Reference to Medical Application**

BioMed Research International

Retraction (1 page), Article ID 9762317, Volume 2023 (2023)

**Retracted: Big Data Analysis of Manufacturing and Preclinical Studies of Nanodrug-Targeted Delivery Systems: A Literature Review**

BioMed Research International

Retraction (1 page), Article ID 9759424, Volume 2023 (2023)

**Retracted: Awareness of Medical Students toward Circadian Rhythm and Sleep Disorder Based on Biomedical Diagnosis**

BioMed Research International

Retraction (1 page), Article ID 9758681, Volume 2023 (2023)

**Retracted: Knowledge and Behavior toward Venous Thromboembolism Event Prophylaxis and Treatment Protocols among Medical Interns in Riyadh**

BioMed Research International

Retraction (1 page), Article ID 9758250, Volume 2023 (2023)

**Retracted: Hysterectomy by Transvaginal Natural Orifice Transluminal Endoscopic Surgery versus Transumbilical Laparoscopic Single-Site Surgery: A Single-Center Experience from East China**

BioMed Research International

Retraction (1 page), Article ID 9753569, Volume 2023 (2023)

**Retracted: Gait Improvement in Patients with Knee Osteoarthritis after Proximal Fibular Osteotomy**

BioMed Research International

Retraction (1 page), Article ID 9878636, Volume 2023 (2023)

**Retracted: DNMT3A Regulates miR-149 DNA Methylation to Activate NOTCH1/Hedgehog Pathway to Promote the Development of Junctional Osteosarcoma**

BioMed Research International

Retraction (1 page), Article ID 9869065, Volume 2023 (2023)



## Contents

**Retracted: The Expression of the Long Noncoding RNA AFAP1-AS1 in Laryngeal Carcinoma Affects the Proliferation, Invasion, Migration, and Apoptosis of TU212 Cell Line**

BioMed Research International

Retraction (1 page), Article ID 9846419, Volume 2023 (2023)

**[Retracted] The Effect of Hyperlipidemia on Peri-implant Health: A Clinical and Radiographical Prospective Study**

Paolo De Angelis , Edoardo Rella, Paolo Francesco Manicone, Giulio Gasparini , Valerio Giovannini, Margherita Giorgia Liguori, Francesca Camodeca, Giuseppe De Rosa, Camilla Cavalcanti, and Antonio D'Addona




Research Article (8 pages), Article ID 7570587, Volume 2023 (2023)

**[Retracted] Exploring Purification Methods of Exosomes from Different Biological Samples**

Xiaoqing Qian, Feng Xie , and Daxiang Cui 

Research Article (9 pages), Article ID 2336536, Volume 2023 (2023)

**[Retracted] Intra- and Interrater Agreement of Face Esthetic Analysis in 3D Face Images**

Minsoo Park , Hang-Nga Mai , Mai Yen Mai, Thaw Thaw Win, Du-Hyeong Lee , and Cheong-Hee Lee


Research Article (7 pages), Article ID 3717442, Volume 2023 (2023)

**Retracted: Effect of Early Low-Calorie Enteral Nutrition Support in Critically Ill Patients: A Systematic Review and Meta-analysis**

BioMed Research International

Retraction (1 page), Article ID 9783495, Volume 2023 (2023)

**[Retracted] Treatment Protocols in the Efficacy and Safety of Anti-EGFR Medicines in Combination with Standard Therapy for Patients with Nasopharyngeal Cancer: A Meta-Analysis**

Yakun Fang, Jinlei Fan, and Chao Yan 

Research Article (7 pages), Article ID 9477442, Volume 2023 (2023)

**Retracted: Hot Air Treatment Elicits Disease Resistance against *Colletotrichum gloeosporioides* and Improves the Quality of Papaya by Metabolomic Profiling**

BioMed Research International

Retraction (1 page), Article ID 9862038, Volume 2023 (2023)

**Retracted: The Effect of Social Cognitive Interaction Training on Schizophrenia: A Systematic Review and Meta-Analysis of Comparison with Conventional Treatment**

BioMed Research International

Retraction (1 page), Article ID 9837847, Volume 2023 (2023)

**Retracted: miR-211-5p Alleviates the Myocardial Ischemia Injury Induced by Ischemic Reperfusion Treatment via Targeting FBXW7**

BioMed Research International

Retraction (1 page), Article ID 9824729, Volume 2023 (2023)



**Retracted: Ferroptosis-Related lncRNA for the Establishment of Novel Prognostic Signature and Therapeutic Response Prediction to Endometrial Carcinoma**

BioMed Research International

Retraction (1 page), Article ID 9829634, Volume 2022 (2022)

**Retracted: Clinical Efficacy and Safety Analysis of PD-1/PD-L1 Inhibitor vs. Chemotherapy in the Treatment of Advanced Non-Small-Cell Lung Cancer: A Systematic Review and Meta-Analysis**

BioMed Research International

Retraction (1 page), Article ID 9808495, Volume 2022 (2022)

**Retracted: Peroxisome Proliferator-Activated Receptor Gene Knockout Promotes Podocyte Injury in Diabetic Mice**

BioMed Research International

Retraction (1 page), Article ID 9764610, Volume 2022 (2022)

**Retracted: Systematic Review and Meta-Analysis of Complications after Laparoscopic Surgery and Open Surgery in the Treatment of Pelvic Abscess**

BioMed Research International


Retraction (1 page), Article ID 9847375, Volume 2022 (2022)

**Retracted: Factors Influencing Cerebrospinal Fluid Leaking following Pituitary Adenoma Transsphenoidal Surgery: A Meta-Analysis and Comprehensive Review**

BioMed Research International


Retraction (1 page), Article ID 9762805, Volume 2022 (2022)

**[Retracted] Biogenic Analysis of the Effect of TERC on Cell Proliferation and Migration of Oral Squamous Cell Carcinoma under Digital Minimally Invasive Treatment**

Wenao Chen, Zilong Zhang, Yiyao Jin, Ruijie Zeng, Xi Sun, Zihan Zhou , Kabna Kasim, Joshua Grant, Vumika Kuraki, Felix Schmid, and Gabin Lucas





Review Article (6 pages), Article ID 2102795, Volume 2022 (2022)

**[Retracted] Awareness of Medical Students toward Circadian Rhythm and Sleep Disorder Based on Biomedical Diagnosis**

Asma Alanazi , Haifa Alhawas, Munirah Aldossari, Dana Almutairi, Dana Almatroudi, Afnan Alenazi, Leen Almadhi, and Maram Albalawi

Research Article (6 pages), Article ID 8645183, Volume 2022 (2022)


**[Retracted] Visual Analysis of Nutrient Deficiency and Treatment Protocols in Bariatric Surgery Based on VOSviewer**

Jihong Tang , Mei He , Guirong Li , Juan He , Xianhua Wang , Zhuoxin Yang , and Hongjin Wu 





Research Article (10 pages), Article ID 8228831, Volume 2022 (2022)

## Contents

**[Retracted] The Effect of Social Cognitive Interaction Training on Schizophrenia: A Systematic Review and Meta-Analysis of Comparison with Conventional Treatment**

Yan Tang, Linhua Yu, Dongyang Zhang, Fang Fang, and Zhaoxia Yuan   
Review Article (11 pages), Article ID 3394978, Volume 2022 (2022)



**[Retracted] Efficacy of Various Types of Berries Extract for the Synthesis of ZnO Nanocomposites and Exploring Their Antimicrobial Potential for Use in Herbal Medicines**

Amara Dar , Rabia Rehman , Ayesha Mohyuddin, Maria Aziz, Jamil Anwar, Gashew Tadele , Noor Mohammed Kadhim, Ali H. Alamri, and Rami M. Alzhrani   
Research Article (9 pages), Article ID 9914173, Volume 2022 (2022)






**[Retracted] Factors Influencing Cerebrospinal Fluid Leaking following Pituitary Adenoma Transsphenoidal Surgery: A Meta-Analysis and Comprehensive Review**

Jiao Zhang, Jingyun Liu, and Liyan Huang   
Review Article (9 pages), Article ID 5213744, Volume 2022 (2022)



**[Retracted] Effect of Supplementation of Vitamin D in Patients with Periodontitis Evaluated before and after Nonsurgical Therapy**

Shree Mohan Mishra, P. L. Ravishankar, V. Pramod, Prem Blaisie Rajula, K. Gayathri, Mohammad Khursheed Alam, A. Thirumal Raj, Shilpa Bhandi , and Shankargouda Patil   
Research Article (5 pages), Article ID 5869676, Volume 2022 (2022)



**[Retracted] The Predictive Value of Neutrophil-Lymphocyte Ratio in Patients with Polycythemia Vera at the Time of Initial Diagnosis for Thrombotic Events**

Xuekun Wang , Yansong Tu, Mei Cao, Xiaoyan Jiang, Yazhi Yang, Xiaoyan Zhang , Hurong Lai , Huaijun Tu , and Jian Li   
Research Article (8 pages), Article ID 9343951, Volume 2022 (2022)



**[Retracted] Hysterectomy by Transvaginal Natural Orifice Transluminal Endoscopic Surgery versus Transumbilical Laparoscopic Single-Site Surgery: A Single-Center Experience from East China**

Bin Yan, Hui-Xian Miao, You Wang, Jia-Mu Xu, Xiu-Qing Lu, Wan-Hong He, Wen Di , and Wei-Hua Lou   
Research Article (7 pages), Article ID 8246761, Volume 2022 (2022)


**[Retracted] Study on the Mechanism of Xiaotan Sanjie Recipe in the Treatment of Colon Cancer Based on Network Pharmacology**

Xiao-wei Wang , Ci-an Zhang, and Min Ye   
Research Article (9 pages), Article ID 9498109, Volume 2022 (2022)

**[Retracted] Hot Air Treatment Elicits Disease Resistance against *Colletotrichum gloeosporioides* and Improves the Quality of Papaya by Metabolomic Profiling**





Bo Liu, Meiling Xue, Jiao Zhou, Hongxia Zhang, Lili Ren , and Jianting Fan   
Research Article (13 pages), Article ID 5162845, Volume 2022 (2022)

**[Retracted] The Expression of the Long Noncoding RNA AFAP1-AS1 in Laryngeal Carcinoma Affects the Proliferation, Invasion, Migration, and Apoptosis of TU212 Cell Line**

Xin Chen, Ziwei Hu, Liao Bing, Xinhua Zhu, Ke Liu, Yuehui Liu, and Jianguo Liu 





Research Article (8 pages), Article ID 2337447, Volume 2022 (2022)

**[Retracted] A Novel Method for Parkinson's Disease Diagnosis Utilizing Treatment Protocols**

Shaha Al-Otaibi , Sarra Ayouni , Md Maruf Haque Khan , and Malek Badr 





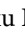
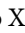



Research Article (6 pages), Article ID 6871623, Volume 2022 (2022)

**[Retracted] The Current Antimicrobial and Antibiofilm Activities of Synthetic/Herbal/Biomaterials in Dental Application**

Ali Moghaddam, Reza Ranjbar , Mohsen Yazdanian , Elahe Tahmasebi , Mostafa Alam, Kamyar Abbasi, Zahra Sadat Hosseini, and Hamid Tebyaniyan 



Review Article (26 pages), Article ID 8856025, Volume 2022 (2022)

**[Retracted] Big Data Analysis of Manufacturing and Preclinical Studies of Nanodrug-Targeted Delivery Systems: A Literature Review**

Qiang Cao , Xiaochen Li , Qi Zhang , Kexuan Zhou , Ying Yu , Zixu He , Zhibiao Xiang , Yi Qiang , and Wei Qi 





Review Article (10 pages), Article ID 1231446, Volume 2022 (2022)

**[Retracted] Strategies of Bioceramics, Bioactive Glasses in Endodontics: Future Perspectives of Restorative Dentistry**

S. Chitra , Nibin K. Mathew, S. Jayalakshmi, S. Balakumar, S. Rajeshkumar , and R. Ramya

Review Article (12 pages), Article ID 2530156, Volume 2022 (2022)

**[Retracted] Ferroptosis-Related lncRNA for the Establishment of Novel Prognostic Signature and Therapeutic Response Prediction to Endometrial Carcinoma**

Xin-Ying Zhou , Hai-Yan Dai , Hu Zhang , Jian-Long Zhu, and Hua Hu 

Research Article (16 pages), Article ID 2056913, Volume 2022 (2022)

**[Retracted] Dapagliflozin Improves Diabetic Cardiomyopathy by Modulating the Akt/mTOR Signaling Pathway**

Mengxiang Ren, Dabin Pan , Dayong Zha, and Zeyang Shan





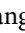





Research Article (10 pages), Article ID 9687345, Volume 2022 (2022)

**[Retracted] Deep Learning-Based Networks for Detecting Anomalies in Chest X-Rays**

Malek Badr , Shaha Al-Otaibi , Nazik Alturki, and Tanvir Abir 

Research Article (10 pages), Article ID 7833516, Volume 2022 (2022)

**[Retracted] Hui Medicine Moxibustion Promotes the Absorption of Lumbar Disc Herniation and the Recovery of Motor Function in Rats through Fas/FasL Signaling Pathway**

Jianfeng Xu , Qiang Luo , Junyao Song , Yanming Zhang , Yingxu Wang , Lei Yang , Yinyin Sha, Bowen Sun , Na You, Xinbao Tian , Ruizhu Lin , and Yongli Wu 

Research Article (9 pages), Article ID 9172405, Volume 2022 (2022)




## Contents

**[Retracted] The Use of Chest Radiographs and Machine Learning Model for the Rapid Detection of Pneumonitis in Pediatric**

Khalaf Alshamrani , Hassan A. Alshamrani , Abdullah A. Asiri, F. F. Alqahtani , Walid Theib Mohammad , and Ali H. Alshehri


Research Article (11 pages), Article ID 5260231, Volume 2022 (2022)

**[Retracted] Segmentation of Oral Leukoplakia (OL) and Proliferative Verrucous Leukoplakia (PVL) Using Artificial Intelligence Techniques**

Samar Zuhair Alshawwa , Asmaa Saleh, Malek Hasan , and Mohd Asif Shah 

Research Article (11 pages), Article ID 2363410, Volume 2022 (2022)

**[Retracted] DNMT3A Regulates miR-149 DNA Methylation to Activate NOTCH1/Hedgehog Pathway to Promote the Development of Junctional Osteosarcoma**

Shigao Cheng and Wanchun Wang 



Research Article (9 pages), Article ID 3261213, Volume 2022 (2022)

**[Retracted] Use of Composite Acellular Dermal Matrix-Ultrathin Split-Thickness Skin in Hand Hot-Crush Injuries: A One-Step Grafting Procedure**

Youfen Fan, Yanyan Pan , Cui Chen, Shengyong Cui, Jiliang Li, Guoying Jin, Neng Huang, and Sida Xu

Research Article (12 pages), Article ID 1569084, Volume 2022 (2022)

**[Retracted] Innovate a Standard for the Future Model of Nursing Care at Medical-Surgical Units in Najran University**

Abeer Y. Mahdy Shalby  and DaifAllah D. AlThubaity 


Research Article (7 pages), Article ID 2959583, Volume 2022 (2022)

**[Retracted] Knowledge and Behavior toward Venous Thromboembolism Event Prophylaxis and Treatment Protocols among Medical Interns in Riyadh**

Zohair Al Aseri , Jumanah Meshari Muammar , Najd Fahad Aldakkan, Afnan A. Alhazmi, Hadeel Hamad Albraik, Aeshah Abdullah Alasmari, Lyla Mohammed Ashry, Shaik S. Ahmed, and Aamer Aleem

Research Article (7 pages), Article ID 7191178, Volume 2022 (2022)

**[Retracted] Prevalence and Correlation of Metabolic Syndrome in Patients with Bipolar Disorder in NGHHA, Riyadh**

Asma Alanazi , Saud Alsadhan, Sultan Aldosari, Abdullah Alharbi, Mohammed Albawardi, Saud Arabah, Haifa Alhawas, and Maram Albalawi




Research Article (5 pages), Article ID 5847175, Volume 2022 (2022)

**[Retracted] Detection of WBC, RBC, and Platelets in Blood Samples Using Deep Learning**

Lamia Alhazmi 

Research Article (10 pages), Article ID 1499546, Volume 2022 (2022)


**[Retracted] A Comparison of Decision Tree Algorithms in the Assessment of Biomedical Data**

Fahima Hajjei , Manal Abdullah Alohal, Malek Badr , and Md Adnan Rahman 

Research Article (9 pages), Article ID 9449497, Volume 2022 (2022)




**[Retracted] Silencing lncRNA 93358 Inhibits the Apoptosis of Myocardial Cells in Myocardial Infarction Rats by Inducing the Expression of SLC8A1**

Jiumei Cai, Xiaoping Wang, Wei Liao, Yiming Zhong, Lingling Chen, and Zhiwei Zhang 


Research Article (11 pages), Article ID 1138709, Volume 2022 (2022)

**[Retracted] Effect of Early Low-Calorie Enteral Nutrition Support in Critically Ill Patients: A Systematic Review and Meta-analysis**

Qidong Jiang and Tao Xu 


Review Article (8 pages), Article ID 7478373, Volume 2022 (2022)

**[Retracted] Systematic Review and Meta-Analysis of Complications after Laparoscopic Surgery and Open Surgery in the Treatment of Pelvic Abscess**

Xiaolu Chen, Jun Su, Lina Xu, and Huiping Zhang 



Review Article (8 pages), Article ID 3650213, Volume 2022 (2022)

**[Retracted] Red Raspberry Extract Decreases Depression-Like Behavior in Rats by Modulating Neuroinflammation and Oxidative Stress**

Yanhua Chen, Xia Yang, Hui Li, and Jianqun Fang 

Research Article (11 pages), Article ID 9943598, Volume 2022 (2022)

**[Retracted] Peroxisome Proliferator-Activated Receptor Gene Knockout Promotes Podocyte Injury in Diabetic Mice**

Rui Yan, Ye Zhang, Yuxing Yang, Lingling Liu, Lirong Liu, Ziwei Guo, Haiyan Yu, Yuanyuan Wang , and Bing Guo 


Research Article (8 pages), Article ID 9018379, Volume 2022 (2022)

**[Retracted] Processing Decision Tree Data Using Internet of Things (IoT) and Artificial Intelligence Technologies with Special Reference to Medical Application**

Latefa Hamad Al Fryan , Mahasin Ibrahim Shomo , Malik Bader Alazzam , and Md Adnan Rahman 









Research Article (9 pages), Article ID 8626234, Volume 2022 (2022)

**[Retracted] Clinical Efficacy and Safety Analysis of PD-1/PD-L1 Inhibitor vs. Chemotherapy in the Treatment of Advanced Non-Small-Cell Lung Cancer: A Systematic Review and Meta-Analysis**

Wei-wei Guo, Tian-wei Zhang, Bin-liang Wang, Li-qun Mao, and Xiao-bo Li 

Review Article (9 pages), Article ID 9500319, Volume 2022 (2022)


**[Retracted] Gait Improvement in Patients with Knee Osteoarthritis after Proximal Fibular Osteotomy**

Xiaotong Li , Yuqing Cao , Zhenguo Cao , Pengfei Zheng , Andrew Merryweather , Hui Wang , Ding Chen , and Hang Xu 

Research Article (8 pages), Article ID 1869922, Volume 2022 (2022)


# Contents

**[Retracted] Kukoamine A Improves *Mycoplasma pneumoniae* Pneumonia by Regulating miR-222-3p/Superoxide Dismutase 2**

Xiu-Xiu Liu, Ming-Jing Wang, Qian-Na Kan, Cui Li, Zhen Xiao, Yong-Hong Jiang, Wen Li, Xiao Li, and Zhi-Yan Jiang 

Research Article (12 pages), Article ID 2064013, Volume 2022 (2022)

**[Retracted] Automatic Segmentation of Calcification Areas in Digital Breast Images**

Ammar Akram Abdulrazzaq, Yasser Muhammed, Asaad T. Al-Douri, A. A. Hamad Mohamad, and Abdelrahman Mohamed Ibrahim 


Research Article (7 pages), Article ID 2525433, Volume 2022 (2022)

**[Retracted] miR-211-5p Alleviates the Myocardial Ischemia Injury Induced by Ischemic Reperfusion Treatment via Targeting FBXW7**

Yonghui Liu, Jiatian Meng, Hongqin Di, Liheng Zheng, and Zili Meng 

Research Article (7 pages), Article ID 5423929, Volume 2022 (2022)

**[Retracted] Early Detection of Autism Spectrum Disorders (ASD) with the Help of Data Mining Tools**

Ammar Akram Abdulrazzaq, Sana Sulaiman Hamid, Asaad T. Al-Douri, A. A. Hamad Mohamad, and Abdelrahman Mohamed Ibrahim 


Research Article (10 pages), Article ID 1201129, Volume 2022 (2022)

**[Retracted] *In Vivo* Growth Inhibition of Human Caucasian Prostate Adenocarcinoma in Nude Mice Induced by Amygdalin with Metabolic Enzyme Combinations**

Ahmed Mohammed Alwan  and Jalil Tavakol Afshari 

Research Article (7 pages), Article ID 4767621, Volume 2022 (2022)

**[Retracted] Investigation of the Role of *Leuconostoc mesenteroides* subsp. *cremoris* in Periodontitis around Abutments of Fixed Prostheses**

Saif Ali Mohammed Hussein, Rehab Aamer Kareem, Ali Maki Hamed Al-Dahbi, and Mequanint Birhan 

Research Article (6 pages), Article ID 8790096, Volume 2022 (2022)

**[Retracted] Mutation Detection and Functional Analysis of MSX1, PAX9, AXIN2, and BMP in Nonsyndromic Congenital Missing Teeth Based on Intelligent Image Detection**

Xueqin Yao , Cheng Zhang, Peipei Gao, Zixuan Meng, Yonghong Hao, Jingjing Yan, and Wenbo Yao

Research Article (7 pages), Article ID 6217399, Volume 2022 (2022)

## *Retraction*

# **Retracted: Exploring Purification Methods of Exosomes from Different Biological Samples**

### **BioMed Research International**

Received 5 December 2023; Accepted 5 December 2023; Published 6 December 2023

Copyright © 2023 BioMed Research International. This is an open access article distributed under the Creative Commons Attribution License, which permits unrestricted use, distribution, and reproduction in any medium, provided the original work is properly cited.

This article has been retracted by Hindawi, as publisher, following an investigation undertaken by the publisher [1]. This investigation has uncovered evidence of systematic manipulation of the publication and peer-review process. We cannot, therefore, vouch for the reliability or integrity of this article.

Please note that this notice is intended solely to alert readers that the peer-review process of this article has been compromised.

Wiley and Hindawi regret that the usual quality checks did not identify these issues before publication and have since put additional measures in place to safeguard research integrity.

We wish to credit our Research Integrity and Research Publishing teams and anonymous and named external researchers and research integrity experts for contributing to this investigation.

The corresponding author, as the representative of all authors, has been given the opportunity to register their agreement or disagreement to this retraction. We have kept a record of any response received.

### **References**

- [1] X. Qian, F. Xie, and D. Cui, "Exploring Purification Methods of Exosomes from Different Biological Samples," *BioMed Research International*, vol. 2023, Article ID 2336536, 9 pages, 2023.

## *Retraction*

# **Retracted: Intra- and Interrater Agreement of Face Esthetic Analysis in 3D Face Images**

### **BioMed Research International**

Received 5 December 2023; Accepted 5 December 2023; Published 6 December 2023

Copyright © 2023 BioMed Research International. This is an open access article distributed under the Creative Commons Attribution License, which permits unrestricted use, distribution, and reproduction in any medium, provided the original work is properly cited.

This article has been retracted by Hindawi, as publisher, following an investigation undertaken by the publisher [1]. This investigation has uncovered evidence of systematic manipulation of the publication and peer-review process. We cannot, therefore, vouch for the reliability or integrity of this article.

Please note that this notice is intended solely to alert readers that the peer-review process of this article has been compromised.

Wiley and Hindawi regret that the usual quality checks did not identify these issues before publication and have since put additional measures in place to safeguard research integrity.

We wish to credit our Research Integrity and Research Publishing teams and anonymous and named external researchers and research integrity experts for contributing to this investigation.

The corresponding author, as the representative of all authors, has been given the opportunity to register their agreement or disagreement to this retraction. We have kept a record of any response received.

### **References**

- [1] M. Park, H.-N. Mai, M. Y. Mai, T. T. Win, D.-H. Lee, and C.-H. Lee, "Intra- and Interrater Agreement of Face Esthetic Analysis in 3D Face Images," *BioMed Research International*, vol. 2023, Article ID 3717442, 7 pages, 2023.



## *Retraction*

# **Retracted: Strategies of Bioceramics, Bioactive Glasses in Endodontics: Future Perspectives of Restorative Dentistry**

### **BioMed Research International**

Received 5 December 2023; Accepted 5 December 2023; Published 6 December 2023

Copyright © 2023 BioMed Research International. This is an open access article distributed under the Creative Commons Attribution License, which permits unrestricted use, distribution, and reproduction in any medium, provided the original work is properly cited.

This article has been retracted by Hindawi, as publisher, following an investigation undertaken by the publisher [1]. This investigation has uncovered evidence of systematic manipulation of the publication and peer-review process. We cannot, therefore, vouch for the reliability or integrity of this article.

Please note that this notice is intended solely to alert readers that the peer-review process of this article has been compromised.

Wiley and Hindawi regret that the usual quality checks did not identify these issues before publication and have since put additional measures in place to safeguard research integrity.

We wish to credit our Research Integrity and Research Publishing teams and anonymous and named external researchers and research integrity experts for contributing to this investigation.

The corresponding author, as the representative of all authors, has been given the opportunity to register their agreement or disagreement to this retraction. We have kept a record of any response received.

### **References**

- [1] S. Chitra, N. K. Mathew, S. Jayalakshmi, S. Balakumar, S. Rajeshkumar, and R. Ramya, "Strategies of Bioceramics, Bioactive Glasses in Endodontics: Future Perspectives of Restorative Dentistry," *BioMed Research International*, vol. 2022, Article ID 2530156, 12 pages, 2022.

## *Retraction*

# **Retracted: Silencing lncRNA 93358 Inhibits the Apoptosis of Myocardial Cells in Myocardial Infarction Rats by Inducing the Expression of SLC8A1**

### **BioMed Research International**

Received 5 December 2023; Accepted 5 December 2023; Published 6 December 2023

Copyright © 2023 BioMed Research International. This is an open access article distributed under the Creative Commons Attribution License, which permits unrestricted use, distribution, and reproduction in any medium, provided the original work is properly cited.

This article has been retracted by Hindawi, as publisher, following an investigation undertaken by the publisher [1]. This investigation has uncovered evidence of systematic manipulation of the publication and peer-review process. We cannot, therefore, vouch for the reliability or integrity of this article.

Please note that this notice is intended solely to alert readers that the peer-review process of this article has been compromised.

Wiley and Hindawi regret that the usual quality checks did not identify these issues before publication and have since put additional measures in place to safeguard research integrity.

We wish to credit our Research Integrity and Research Publishing teams and anonymous and named external researchers and research integrity experts for contributing to this investigation.

The corresponding author, as the representative of all authors, has been given the opportunity to register their agreement or disagreement to this retraction. We have kept a record of any response received.

## **References**

- [1] J. Cai, X. Wang, W. Liao, Y. Zhong, L. Chen, and Z. Zhang, "Silencing lncRNA 93358 Inhibits the Apoptosis of Myocardial Cells in Myocardial Infarction Rats by Inducing the Expression of SLC8A1," *BioMed Research International*, vol. 2022, Article ID 1138709, 11 pages, 2022.

## *Retraction*

# **Retracted: Kukoamine A Improves *Mycoplasma pneumoniae* Pneumonia by Regulating miR-222-3p/Superoxide Dismutase 2**

### **BioMed Research International**

Received 5 December 2023; Accepted 5 December 2023; Published 6 December 2023

Copyright © 2023 BioMed Research International. This is an open access article distributed under the Creative Commons Attribution License, which permits unrestricted use, distribution, and reproduction in any medium, provided the original work is properly cited.

This article has been retracted by Hindawi, as publisher, following an investigation undertaken by the publisher [1]. This investigation has uncovered evidence of systematic manipulation of the publication and peer-review process. We cannot, therefore, vouch for the reliability or integrity of this article.

Please note that this notice is intended solely to alert readers that the peer-review process of this article has been compromised.

Wiley and Hindawi regret that the usual quality checks did not identify these issues before publication and have since put additional measures in place to safeguard research integrity.

We wish to credit our Research Integrity and Research Publishing teams and anonymous and named external researchers and research integrity experts for contributing to this investigation.

The corresponding author, as the representative of all authors, has been given the opportunity to register their agreement or disagreement to this retraction. We have kept a record of any response received.

### **References**

- [1] X.-X. Liu, M.-J. Wang, Q.-N. Kan et al., “Kukoamine A Improves *Mycoplasma pneumoniae* Pneumonia by Regulating miR-222-3p/Superoxide Dismutase 2,” *BioMed Research International*, vol. 2022, Article ID 2064013, 12 pages, 2022.

## *Retraction*

# **Retracted: The Effect of Hyperlipidemia on Peri-Implant Health: A Clinical and Radiographical Prospective Study**

### **BioMed Research International**

Received 5 December 2023; Accepted 5 December 2023; Published 6 December 2023

Copyright © 2023 BioMed Research International. This is an open access article distributed under the Creative Commons Attribution License, which permits unrestricted use, distribution, and reproduction in any medium, provided the original work is properly cited.

This article has been retracted by Hindawi, as publisher, following an investigation undertaken by the publisher [1]. This investigation has uncovered evidence of systematic manipulation of the publication and peer-review process. We cannot, therefore, vouch for the reliability or integrity of this article.

Please note that this notice is intended solely to alert readers that the peer-review process of this article has been compromised.

Wiley and Hindawi regret that the usual quality checks did not identify these issues before publication and have since put additional measures in place to safeguard research integrity.

We wish to credit our Research Integrity and Research Publishing teams and anonymous and named external researchers and research integrity experts for contributing to this investigation.

The corresponding author, as the representative of all authors, has been given the opportunity to register their agreement or disagreement to this retraction. We have kept a record of any response received.

### **References**

- [1] P. De Angelis, E. Rella, P. F. Manicone et al., “The Effect of Hyperlipidemia on Peri-Implant Health: A Clinical and Radiographical Prospective Study,” *BioMed Research International*, vol. 2023, Article ID 7570587, 8 pages, 2023.

## Retraction

# Retracted: Automatic Segmentation of Calcification Areas in Digital Breast Images

### BioMed Research International

Received 10 October 2023; Accepted 10 October 2023; Published 11 October 2023

Copyright © 2023 BioMed Research International. This is an open access article distributed under the Creative Commons Attribution License, which permits unrestricted use, distribution, and reproduction in any medium, provided the original work is properly cited.

This article has been retracted by Hindawi following an investigation undertaken by the publisher [1]. This investigation has uncovered evidence of one or more of the following indicators of systematic manipulation of the publication process:

- (1) Discrepancies in scope
- (2) Discrepancies in the description of the research reported
- (3) Discrepancies between the availability of data and the research described
- (4) Inappropriate citations
- (5) Incoherent, meaningless and/or irrelevant content included in the article
- (6) Peer-review manipulation

The presence of these indicators undermines our confidence in the integrity of the article's content and we cannot, therefore, vouch for its reliability. Please note that this notice is intended solely to alert readers that the content of this article is unreliable. We have not investigated whether authors were aware of or involved in the systematic manipulation of the publication process.

In addition, our investigation has also shown that one or more of the following human-subject reporting requirements has not been met in this article: ethical approval by an Institutional Review Board (IRB) committee or equivalent, patient/participant consent to participate, and/or agreement to publish patient/participant details (where relevant).

Wiley and Hindawi regrets that the usual quality checks did not identify these issues before publication and have since put additional measures in place to safeguard research integrity.

We wish to credit our own Research Integrity and Research Publishing teams and anonymous and named external researchers and research integrity experts for contributing to this investigation.

The corresponding author, as the representative of all authors, has been given the opportunity to register their agreement or disagreement to this retraction. We have kept a record of any response received.

### References

- [1] A. A. Abdulrazzaq, Y. Muhammed, A. T. Al-Douri, A. A. H. Mohamad, and A. M. Ibrahim, "Automatic Segmentation of Calcification Areas in Digital Breast Images," *BioMed Research International*, vol. 2022, Article ID 2525433, 7 pages, 2022.

## Retraction

# Retracted: The Current Antimicrobial and Antibiofilm Activities of Synthetic/Herbal/Biomaterials in Dental Application

### BioMed Research International

Received 10 October 2023; Accepted 10 October 2023; Published 11 October 2023

Copyright © 2023 BioMed Research International. This is an open access article distributed under the Creative Commons Attribution License, which permits unrestricted use, distribution, and reproduction in any medium, provided the original work is properly cited.

This article has been retracted by Hindawi following an investigation undertaken by the publisher [1]. This investigation has uncovered evidence of one or more of the following indicators of systematic manipulation of the publication process:

- (1) Discrepancies in scope
- (2) Discrepancies in the description of the research reported
- (3) Discrepancies between the availability of data and the research described
- (4) Inappropriate citations
- (5) Incoherent, meaningless and/or irrelevant content included in the article
- (6) Peer-review manipulation

The presence of these indicators undermines our confidence in the integrity of the article's content and we cannot, therefore, vouch for its reliability. Please note that this notice is intended solely to alert readers that the content of this article is unreliable. We have not investigated whether authors were aware of or involved in the systematic manipulation of the publication process.

In addition, our investigation has also shown that one or more of the following human-subject reporting requirements has not been met in this article: ethical approval by an Institutional Review Board (IRB) committee or equivalent, patient/participant consent to participate, and/or agreement to publish patient/participant details (where relevant).

Wiley and Hindawi regrets that the usual quality checks did not identify these issues before publication and have since put additional measures in place to safeguard research integrity.

We wish to credit our own Research Integrity and Research Publishing teams and anonymous and named external researchers and research integrity experts for contributing to this investigation.

The corresponding author, as the representative of all authors, has been given the opportunity to register their agreement or disagreement to this retraction. We have kept a record of any response received.

### References

- [1] A. Moghaddam, R. Ranjbar, M. Yazdani et al., "The Current Antimicrobial and Antibiofilm Activities of Synthetic/Herbal/Biomaterials in Dental Application," *BioMed Research International*, vol. 2022, Article ID 8856025, 26 pages, 2022.

## Retraction

# Retracted: Investigation of the Role of *Leuconostoc mesenteroides* subsp. *cremoris* in Periodontitis around Abutments of Fixed Prostheses

### BioMed Research International

Received 10 October 2023; Accepted 10 October 2023; Published 11 October 2023

Copyright © 2023 BioMed Research International. This is an open access article distributed under the Creative Commons Attribution License, which permits unrestricted use, distribution, and reproduction in any medium, provided the original work is properly cited.

This article has been retracted by Hindawi following an investigation undertaken by the publisher [1]. This investigation has uncovered evidence of one or more of the following indicators of systematic manipulation of the publication process:

- (1) Discrepancies in scope
- (2) Discrepancies in the description of the research reported
- (3) Discrepancies between the availability of data and the research described
- (4) Inappropriate citations
- (5) Incoherent, meaningless and/or irrelevant content included in the article
- (6) Peer-review manipulation

The presence of these indicators undermines our confidence in the integrity of the article's content and we cannot, therefore, vouch for its reliability. Please note that this notice is intended solely to alert readers that the content of this article is unreliable. We have not investigated whether authors were aware of or involved in the systematic manipulation of the publication process.

In addition, our investigation has also shown that one or more of the following human-subject reporting requirements has not been met in this article: ethical approval by an Institutional Review Board (IRB) committee or equivalent, patient/participant consent to participate, and/or agreement to publish patient/participant details (where relevant).

Wiley and Hindawi regrets that the usual quality checks did not identify these issues before publication and have since put additional measures in place to safeguard research integrity.

We wish to credit our own Research Integrity and Research Publishing teams and anonymous and named external researchers and research integrity experts for contributing to this investigation.

The corresponding author, as the representative of all authors, has been given the opportunity to register their agreement or disagreement to this retraction. We have kept a record of any response received.

### References

- [1] S. A. M. Hussein, R. A. Kareem, A. M. H. Al-Dahbi, and M. Birhan, "Investigation of the Role of *Leuconostoc mesenteroides* subsp. *cremoris* in Periodontitis around Abutments of Fixed Prostheses," *BioMed Research International*, vol. 2022, Article ID 8790096, 6 pages, 2022.

## Retraction

# Retracted: Study on the Mechanism of Xiaotan Sanjie Recipe in the Treatment of Colon Cancer Based on Network Pharmacology

### BioMed Research International

Received 3 October 2023; Accepted 3 October 2023; Published 4 October 2023

Copyright © 2023 BioMed Research International. This is an open access article distributed under the Creative Commons Attribution License, which permits unrestricted use, distribution, and reproduction in any medium, provided the original work is properly cited.

This article has been retracted by Hindawi following an investigation undertaken by the publisher [1]. This investigation has uncovered evidence of one or more of the following indicators of systematic manipulation of the publication process:

- (1) Discrepancies in scope
- (2) Discrepancies in the description of the research reported
- (3) Discrepancies between the availability of data and the research described
- (4) Inappropriate citations
- (5) Incoherent, meaningless and/or irrelevant content included in the article
- (6) Peer-review manipulation

The presence of these indicators undermines our confidence in the integrity of the article's content and we cannot, therefore, vouch for its reliability. Please note that this notice is intended solely to alert readers that the content of this article is unreliable. We have not investigated whether authors were aware of or involved in the systematic manipulation of the publication process.

Wiley and Hindawi regrets that the usual quality checks did not identify these issues before publication and have since put additional measures in place to safeguard research integrity.

We wish to credit our own Research Integrity and Research Publishing teams and anonymous and named external researchers and research integrity experts for contributing to this investigation.

The corresponding author, as the representative of all authors, has been given the opportunity to register their agreement or disagreement to this retraction. We have kept a record of any response received.

### References

- [1] X. Wang, C. Zhang, and M. Ye, "Study on the Mechanism of Xiaotan Sanjie Recipe in the Treatment of Colon Cancer Based on Network Pharmacology," *BioMed Research International*, vol. 2022, Article ID 9498109, 9 pages, 2022.



## Retraction

# Retracted: Innovate a Standard for the Future Model of Nursing Care at Medical-Surgical Units in Najran University

### BioMed Research International

Received 3 October 2023; Accepted 3 October 2023; Published 4 October 2023

Copyright © 2023 BioMed Research International. This is an open access article distributed under the Creative Commons Attribution License, which permits unrestricted use, distribution, and reproduction in any medium, provided the original work is properly cited.

This article has been retracted by Hindawi following an investigation undertaken by the publisher [1]. This investigation has uncovered evidence of one or more of the following indicators of systematic manipulation of the publication process:

- (1) Discrepancies in scope
- (2) Discrepancies in the description of the research reported
- (3) Discrepancies between the availability of data and the research described
- (4) Inappropriate citations
- (5) Incoherent, meaningless and/or irrelevant content included in the article
- (6) Peer-review manipulation

The presence of these indicators undermines our confidence in the integrity of the article's content and we cannot, therefore, vouch for its reliability. Please note that this notice is intended solely to alert readers that the content of this article is unreliable. We have not investigated whether authors were aware of or involved in the systematic manipulation of the publication process.

Wiley and Hindawi regrets that the usual quality checks did not identify these issues before publication and have since put additional measures in place to safeguard research integrity.

We wish to credit our own Research Integrity and Research Publishing teams and anonymous and named external researchers and research integrity experts for contributing to this investigation.

The corresponding author, as the representative of all authors, has been given the opportunity to register their agreement or disagreement to this retraction. We have kept a record of any response received.

### References

- [1] A. Y. Mahdy Shalby and D. D. AlThubaity, "Innovate a Standard for the Future Model of Nursing Care at Medical-Surgical Units in Najran University," *BioMed Research International*, vol. 2022, Article ID 2959583, 7 pages, 2022.

## Retraction

# Retracted: Mutation Detection and Functional Analysis of MSX1, PAX9, AXIN2, and BMP in Nonsyndromic Congenital Missing Teeth Based on Intelligent Image Detection

### BioMed Research International

Received 3 October 2023; Accepted 3 October 2023; Published 4 October 2023

Copyright © 2023 BioMed Research International. This is an open access article distributed under the Creative Commons Attribution License, which permits unrestricted use, distribution, and reproduction in any medium, provided the original work is properly cited.

This article has been retracted by Hindawi following an investigation undertaken by the publisher [1]. This investigation has uncovered evidence of one or more of the following indicators of systematic manipulation of the publication process:

- (1) Discrepancies in scope
- (2) Discrepancies in the description of the research reported
- (3) Discrepancies between the availability of data and the research described
- (4) Inappropriate citations
- (5) Incoherent, meaningless and/or irrelevant content included in the article
- (6) Peer-review manipulation

The presence of these indicators undermines our confidence in the integrity of the article's content and we cannot, therefore, vouch for its reliability. Please note that this notice is intended solely to alert readers that the content of this article is unreliable. We have not investigated whether authors were aware of or involved in the systematic manipulation of the publication process.

Wiley and Hindawi regrets that the usual quality checks did not identify these issues before publication and have since put additional measures in place to safeguard research integrity.

We wish to credit our own Research Integrity and Research Publishing teams and anonymous and named external researchers and research integrity experts for contributing to this investigation.

The corresponding author, as the representative of all authors, has been given the opportunity to register their agreement or disagreement to this retraction. We have kept a record of any response received.

### References

- [1] X. Yao, C. Zhang, P. Gao et al., "Mutation Detection and Functional Analysis of MSX1, PAX9, AXIN2, and BMP in Nonsyndromic Congenital Missing Teeth Based on Intelligent Image Detection," *BioMed Research International*, vol. 2022, Article ID 6217399, 7 pages, 2022.

## Retraction

# Retracted: Treatment Protocols in the Efficacy and Safety of Anti-EGFR Medicines in Combination with Standard Therapy for Patients with Nasopharyngeal Cancer: A Meta-Analysis

### BioMed Research International

Received 3 October 2023; Accepted 3 October 2023; Published 4 October 2023

Copyright © 2023 BioMed Research International. This is an open access article distributed under the Creative Commons Attribution License, which permits unrestricted use, distribution, and reproduction in any medium, provided the original work is properly cited.

This article has been retracted by Hindawi following an investigation undertaken by the publisher [1]. This investigation has uncovered evidence of one or more of the following indicators of systematic manipulation of the publication process:

- (1) Discrepancies in scope
- (2) Discrepancies in the description of the research reported
- (3) Discrepancies between the availability of data and the research described
- (4) Inappropriate citations
- (5) Incoherent, meaningless and/or irrelevant content included in the article
- (6) Peer-review manipulation

The presence of these indicators undermines our confidence in the integrity of the article's content and we cannot, therefore, vouch for its reliability. Please note that this notice is intended solely to alert readers that the content of this article is unreliable. We have not investigated whether authors were aware of or involved in the systematic manipulation of the publication process.

Wiley and Hindawi regrets that the usual quality checks did not identify these issues before publication and have since put additional measures in place to safeguard research integrity.

We wish to credit our own Research Integrity and Research Publishing teams and anonymous and named external researchers and research integrity experts for contributing to this investigation.

The corresponding author, as the representative of all authors, has been given the opportunity to register their agreement or disagreement to this retraction. We have kept a record of any response received.

### References

- [1] Y. Fang, J. Fan, and C. Yan, "Treatment Protocols in the Efficacy and Safety of Anti-EGFR Medicines in Combination with Standard Therapy for Patients with Nasopharyngeal Cancer: A Meta-Analysis," *BioMed Research International*, vol. 2023, Article ID 9477442, 7 pages, 2023.

## *Retraction*

# **Retracted: Effect of Supplementation of Vitamin D in Patients with Periodontitis Evaluated before and after Nonsurgical Therapy**

### **BioMed Research International**

Received 18 July 2023; Accepted 18 July 2023; Published 27 September 2023

Copyright © 2023 BioMed Research International. This is an open access article distributed under the Creative Commons Attribution License, which permits unrestricted use, distribution, and reproduction in any medium, provided the original work is properly cited.

This article has been retracted by Hindawi following an investigation undertaken by the publisher. This investigation has uncovered evidence that the peer review process was compromised. We cannot, therefore, vouch for its reliability. Please note that this notice is intended solely to alert readers that the peer review of this article is compromised.

We have subsequently provided the authors with the opportunity to re-submit their article and undergo a new and independent peer-review process.

Wiley and Hindawi regret that the usual quality checks did not identify these issues before publication and have since put additional measures in place to safeguard research integrity.

We wish to credit our Research Integrity and Research Publishing teams and anonymous and named external researchers and research integrity experts for contributing to this investigation.

The corresponding author, as the representative of all authors, has been given the opportunity to register their agreement or disagreement to this retraction. We have kept a record of any response received.

## **References**

- [1] S. M. Mishra, P. L. Ravishankar, V. Pramod et al., "Effect of Supplementation of Vitamin D in Patients with Periodontitis Evaluated before and after Nonsurgical Therapy," *BioMed Research International*, vol. 2022, Article ID 5869676, 5 pages, 2022.

## Retraction

# Retracted: Detection of WBC, RBC, and Platelets in Blood Samples Using Deep Learning

### BioMed Research International

Received 18 July 2023; Accepted 18 July 2023; Published 19 July 2023

Copyright © 2023 BioMed Research International. This is an open access article distributed under the Creative Commons Attribution License, which permits unrestricted use, distribution, and reproduction in any medium, provided the original work is properly cited.

This article has been retracted by Hindawi following an investigation undertaken by the publisher [1]. This investigation has uncovered evidence of one or more of the following indicators of systematic manipulation of the publication process:

- (1) Discrepancies in scope
- (2) Discrepancies in the description of the research reported
- (3) Discrepancies between the availability of data and the research described
- (4) Inappropriate citations
- (5) Incoherent, meaningless and/or irrelevant content included in the article
- (6) Peer-review manipulation

The presence of these indicators undermines our confidence in the integrity of the article's content and we cannot, therefore, vouch for its reliability. Please note that this notice is intended solely to alert readers that the content of this article is unreliable. We have not investigated whether authors were aware of or involved in the systematic manipulation of the publication process.

Wiley and Hindawi regrets that the usual quality checks did not identify these issues before publication and have since put additional measures in place to safeguard research integrity.

We wish to credit our own Research Integrity and Research Publishing teams and anonymous and named external researchers and research integrity experts for contributing to this investigation.

The corresponding author, as the representative of all authors, has been given the opportunity to register their agreement or disagreement to this retraction. We have kept a record of any response received.

### References

- [1] L. Alhazmi, "Detection of WBC, RBC, and Platelets in Blood Samples Using Deep Learning," *BioMed Research International*, vol. 2022, Article ID 1499546, 10 pages, 2022.

## Retraction

# Retracted: Hui Medicine Moxibustion Promotes the Absorption of Lumbar Disc Herniation and the Recovery of Motor Function in Rats through Fas/FasL Signaling Pathway

### BioMed Research International

Received 18 July 2023; Accepted 18 July 2023; Published 19 July 2023

Copyright © 2023 BioMed Research International. This is an open access article distributed under the Creative Commons Attribution License, which permits unrestricted use, distribution, and reproduction in any medium, provided the original work is properly cited.

This article has been retracted by Hindawi following an investigation undertaken by the publisher [1]. This investigation has uncovered evidence of one or more of the following indicators of systematic manipulation of the publication process:

- (1) Discrepancies in scope
- (2) Discrepancies in the description of the research reported
- (3) Discrepancies between the availability of data and the research described
- (4) Inappropriate citations
- (5) Incoherent, meaningless and/or irrelevant content included in the article
- (6) Peer-review manipulation

The presence of these indicators undermines our confidence in the integrity of the article's content and we cannot, therefore, vouch for its reliability. Please note that this notice is intended solely to alert readers that the content of this article is unreliable. We have not investigated whether authors were aware of or involved in the systematic manipulation of the publication process.

Wiley and Hindawi regrets that the usual quality checks did not identify these issues before publication and have since put additional measures in place to safeguard research integrity.

We wish to credit our own Research Integrity and Research Publishing teams and anonymous and named external researchers and research integrity experts for contributing to this investigation.

The corresponding author, as the representative of all authors, has been given the opportunity to register their agreement or disagreement to this retraction. We have kept a record of any response received.

### References

- [1] J. Xu, Q. Luo, J. Song et al., "Hui Medicine Moxibustion Promotes the Absorption of Lumbar Disc Herniation and the Recovery of Motor Function in Rats through Fas/FasL Signaling Pathway," *BioMed Research International*, vol. 2022, Article ID 9172405, 9 pages, 2022.

## Retraction

# Retracted: *In Vivo* Growth Inhibition of Human Caucasian Prostate Adenocarcinoma in Nude Mice Induced by Amygdalin with Metabolic Enzyme Combinations

### BioMed Research International

Received 18 July 2023; Accepted 18 July 2023; Published 19 July 2023

Copyright © 2023 BioMed Research International. This is an open access article distributed under the Creative Commons Attribution License, which permits unrestricted use, distribution, and reproduction in any medium, provided the original work is properly cited.

This article has been retracted by Hindawi following an investigation undertaken by the publisher [1]. This investigation has uncovered evidence of one or more of the following indicators of systematic manipulation of the publication process:

- (1) Discrepancies in scope
- (2) Discrepancies in the description of the research reported
- (3) Discrepancies between the availability of data and the research described
- (4) Inappropriate citations
- (5) Incoherent, meaningless and/or irrelevant content included in the article
- (6) Peer-review manipulation

The presence of these indicators undermines our confidence in the integrity of the article's content and we cannot, therefore, vouch for its reliability. Please note that this notice is intended solely to alert readers that the content of this article is unreliable. We have not investigated whether authors were aware of or involved in the systematic manipulation of the publication process.

In addition, our investigation has also shown that one or more of the following human-subject reporting requirements has not been met in this article: ethical approval by an Institutional Review Board (IRB) committee or equivalent, patient/participant consent to participate, and/or agreement to publish patient/participant details (where relevant).

Wiley and Hindawi regrets that the usual quality checks did not identify these issues before publication and have since put additional measures in place to safeguard research integrity.

We wish to credit our own Research Integrity and Research Publishing teams and anonymous and named external researchers and research integrity experts for contributing to this investigation.

The corresponding author, as the representative of all authors, has been given the opportunity to register their agreement or disagreement to this retraction. We have kept a record of any response received.

### References

- [1] A. M. Alwan and J. T. Afshari, "*In Vivo* Growth Inhibition of Human Caucasian Prostate Adenocarcinoma in Nude Mice Induced by Amygdalin with Metabolic Enzyme Combinations," *BioMed Research International*, vol. 2022, Article ID 4767621, 7 pages, 2022.

## Retraction

# Retracted: Segmentation of Oral Leukoplakia (OL) and Proliferative Verrucous Leukoplakia (PVL) Using Artificial Intelligence Techniques

### BioMed Research International

Received 18 July 2023; Accepted 18 July 2023; Published 19 July 2023

Copyright © 2023 BioMed Research International. This is an open access article distributed under the Creative Commons Attribution License, which permits unrestricted use, distribution, and reproduction in any medium, provided the original work is properly cited.

This article has been retracted by Hindawi following an investigation undertaken by the publisher [1]. This investigation has uncovered evidence of one or more of the following indicators of systematic manipulation of the publication process:

- (1) Discrepancies in scope
- (2) Discrepancies in the description of the research reported
- (3) Discrepancies between the availability of data and the research described
- (4) Inappropriate citations
- (5) Incoherent, meaningless and/or irrelevant content included in the article
- (6) Peer-review manipulation

The presence of these indicators undermines our confidence in the integrity of the article's content and we cannot, therefore, vouch for its reliability. Please note that this notice is intended solely to alert readers that the content of this article is unreliable. We have not investigated whether authors were aware of or involved in the systematic manipulation of the publication process.

In addition, our investigation has also shown that one or more of the following human-subject reporting requirements has not been met in this article: ethical approval by an Institutional Review Board (IRB) committee or equivalent, patient/participant consent to participate, and/or agreement to publish patient/participant details (where relevant).

Wiley and Hindawi regrets that the usual quality checks did not identify these issues before publication and have since put additional measures in place to safeguard research integrity.

We wish to credit our own Research Integrity and Research Publishing teams and anonymous and named external researchers and research integrity experts for contributing to this investigation.

The corresponding author, as the representative of all authors, has been given the opportunity to register their agreement or disagreement to this retraction. We have kept a record of any response received.

### References

- [1] S. Z. Alshawwa, A. Saleh, M. Hasan, and M. A. Shah, "Segmentation of Oral Leukoplakia (OL) and Proliferative Verrucous Leukoplakia (PVL) Using Artificial Intelligence Techniques," *BioMed Research International*, vol. 2022, Article ID 2363410, 11 pages, 2022.



## *Retraction*

# **Retracted: Visual Analysis of Nutrient Deficiency and Treatment Protocols in Bariatric Surgery Based on VOSviewer**

### **BioMed Research International**

Received 18 July 2023; Accepted 18 July 2023; Published 19 July 2023

Copyright © 2023 BioMed Research International. This is an open access article distributed under the Creative Commons Attribution License, which permits unrestricted use, distribution, and reproduction in any medium, provided the original work is properly cited.

This article has been retracted by Hindawi following an investigation undertaken by the publisher [1]. This investigation has uncovered evidence of one or more of the following indicators of systematic manipulation of the publication process:

- (1) Discrepancies in scope
- (2) Discrepancies in the description of the research reported
- (3) Discrepancies between the availability of data and the research described
- (4) Inappropriate citations
- (5) Incoherent, meaningless and/or irrelevant content included in the article
- (6) Peer-review manipulation

The presence of these indicators undermines our confidence in the integrity of the article's content and we cannot, therefore, vouch for its reliability. Please note that this notice is intended solely to alert readers that the content of this article is unreliable. We have not investigated whether authors were aware of or involved in the systematic manipulation of the publication process.

In addition, our investigation has also shown that one or more of the following human-subject reporting requirements has not been met in this article: ethical approval by an Institutional Review Board (IRB) committee or equivalent, patient/participant consent to participate, and/or agreement to publish patient/participant details (where relevant).

Wiley and Hindawi regrets that the usual quality checks did not identify these issues before publication and have since put additional measures in place to safeguard research integrity.

We wish to credit our own Research Integrity and Research Publishing teams and anonymous and named external researchers and research integrity experts for contributing to this investigation.

The corresponding author, as the representative of all authors, has been given the opportunity to register their agreement or disagreement to this retraction. We have kept a record of any response received.

### **References**

- [1] J. Tang, M. He, G. Li et al., "Visual Analysis of Nutrient Deficiency and Treatment Protocols in Bariatric Surgery Based on VOSviewer," *BioMed Research International*, vol. 2022, Article ID 8228831, 10 pages, 2022.

## Retraction

# Retracted: Prevalence and Correlation of Metabolic Syndrome in Patients with Bipolar Disorder in NGHA, Riyadh

### BioMed Research International

Received 18 July 2023; Accepted 18 July 2023; Published 19 July 2023

Copyright © 2023 BioMed Research International. This is an open access article distributed under the Creative Commons Attribution License, which permits unrestricted use, distribution, and reproduction in any medium, provided the original work is properly cited.

This article has been retracted by Hindawi following an investigation undertaken by the publisher [1]. This investigation has uncovered evidence of one or more of the following indicators of systematic manipulation of the publication process:

- (1) Discrepancies in scope
- (2) Discrepancies in the description of the research reported
- (3) Discrepancies between the availability of data and the research described
- (4) Inappropriate citations
- (5) Incoherent, meaningless and/or irrelevant content included in the article
- (6) Peer-review manipulation

The presence of these indicators undermines our confidence in the integrity of the article's content and we cannot, therefore, vouch for its reliability. Please note that this notice is intended solely to alert readers that the content of this article is unreliable. We have not investigated whether authors were aware of or involved in the systematic manipulation of the publication process.

In addition, our investigation has also shown that one or more of the following human-subject reporting requirements has not been met in this article: ethical approval by an Institutional Review Board (IRB) committee or equivalent, patient/participant consent to participate, and/or agreement to publish patient/participant details (where relevant).

Wiley and Hindawi regrets that the usual quality checks did not identify these issues before publication and have since put additional measures in place to safeguard research integrity.

We wish to credit our own Research Integrity and Research Publishing teams and anonymous and named external researchers and research integrity experts for contributing to this investigation.

The corresponding author, as the representative of all authors, has been given the opportunity to register their agreement or disagreement to this retraction. We have kept a record of any response received.

### References

- [1] A. Alanazi, S. Alsadhan, S. Aldosari et al., "Prevalence and Correlation of Metabolic Syndrome in Patients with Bipolar Disorder in NGHA, Riyadh," *BioMed Research International*, vol. 2022, Article ID 5847175, 5 pages, 2022.

## Retraction

# Retracted: Early Detection of Autism Spectrum Disorders (ASD) with the Help of Data Mining Tools

### BioMed Research International

Received 20 June 2023; Accepted 20 June 2023; Published 21 June 2023

Copyright © 2023 BioMed Research International. This is an open access article distributed under the Creative Commons Attribution License, which permits unrestricted use, distribution, and reproduction in any medium, provided the original work is properly cited.

This article has been retracted by Hindawi following an investigation undertaken by the publisher [1]. This investigation has uncovered evidence of one or more of the following indicators of systematic manipulation of the publication process:

- (1) Discrepancies in scope
- (2) Discrepancies in the description of the research reported
- (3) Discrepancies between the availability of data and the research described
- (4) Inappropriate citations
- (5) Incoherent, meaningless and/or irrelevant content included in the article
- (6) Peer-review manipulation

The presence of these indicators undermines our confidence in the integrity of the article's content and we cannot, therefore, vouch for its reliability. Please note that this notice is intended solely to alert readers that the content of this article is unreliable. We have not investigated whether authors were aware of or involved in the systematic manipulation of the publication process.

Wiley and Hindawi regrets that the usual quality checks did not identify these issues before publication and have since put additional measures in place to safeguard research integrity.

We wish to credit our own Research Integrity and Research Publishing teams and anonymous and named external researchers and research integrity experts for contributing to this investigation.

The corresponding author, as the representative of all authors, has been given the opportunity to register their agreement or disagreement to this retraction. We have kept a record of any response received.

### References

- [1] A. A. Abdulrazzaq, S. S. Hamid, A. T. Al-Douri, A. A. H. Mohamad, and A. M. Ibrahim, "Early Detection of Autism Spectrum Disorders (ASD) with the Help of Data Mining Tools," *BioMed Research International*, vol. 2022, Article ID 1201129, 10 pages, 2022.

## *Retraction*

# **Retracted: Efficacy of Various Types of Berries Extract for the Synthesis of ZnO Nanocomposites and Exploring Their Antimicrobial Potential for Use in Herbal Medicines**

### **BioMed Research International**

Received 20 June 2023; Accepted 20 June 2023; Published 21 June 2023

Copyright © 2023 BioMed Research International. This is an open access article distributed under the Creative Commons Attribution License, which permits unrestricted use, distribution, and reproduction in any medium, provided the original work is properly cited.

This article has been retracted by Hindawi following an investigation undertaken by the publisher [1]. This investigation has uncovered evidence of one or more of the following indicators of systematic manipulation of the publication process:

- (1) Discrepancies in scope
- (2) Discrepancies in the description of the research reported
- (3) Discrepancies between the availability of data and the research described
- (4) Inappropriate citations
- (5) Incoherent, meaningless and/or irrelevant content included in the article
- (6) Peer-review manipulation

The presence of these indicators undermines our confidence in the integrity of the article's content and we cannot, therefore, vouch for its reliability. Please note that this notice is intended solely to alert readers that the content of this article is unreliable. We have not investigated whether authors were aware of or involved in the systematic manipulation of the publication process.

Wiley and Hindawi regrets that the usual quality checks did not identify these issues before publication and have since put additional measures in place to safeguard research integrity.

We wish to credit our own Research Integrity and Research Publishing teams and anonymous and named external researchers and research integrity experts for contributing to this investigation.

The corresponding author, as the representative of all authors, has been given the opportunity to register their agreement or disagreement to this retraction. We have kept a record of any response received.

### **References**

- [1] A. Dar, R. Rehman, A. Mohyuddin et al., "Efficacy of Various Types of Berries Extract for the Synthesis of ZnO Nanocomposites and Exploring Their Antimicrobial Potential for Use in Herbal Medicines," *BioMed Research International*, vol. 2022, Article ID 9914173, 9 pages, 2022.

## Retraction

# Retracted: A Comparison of Decision Tree Algorithms in the Assessment of Biomedical Data

### BioMed Research International

Received 20 June 2023; Accepted 20 June 2023; Published 21 June 2023

Copyright © 2023 BioMed Research International. This is an open access article distributed under the Creative Commons Attribution License, which permits unrestricted use, distribution, and reproduction in any medium, provided the original work is properly cited.

This article has been retracted by Hindawi following an investigation undertaken by the publisher [1]. This investigation has uncovered evidence of one or more of the following indicators of systematic manipulation of the publication process:

- (1) Discrepancies in scope
- (2) Discrepancies in the description of the research reported
- (3) Discrepancies between the availability of data and the research described
- (4) Inappropriate citations
- (5) Incoherent, meaningless and/or irrelevant content included in the article
- (6) Peer-review manipulation

The presence of these indicators undermines our confidence in the integrity of the article's content and we cannot, therefore, vouch for its reliability. Please note that this notice is intended solely to alert readers that the content of this article is unreliable. We have not investigated whether authors were aware of or involved in the systematic manipulation of the publication process.

Wiley and Hindawi regrets that the usual quality checks did not identify these issues before publication and have since put additional measures in place to safeguard research integrity.

We wish to credit our own Research Integrity and Research Publishing teams and anonymous and named external researchers and research integrity experts for contributing to this investigation.

The corresponding author, as the representative of all authors, has been given the opportunity to register their agreement or disagreement to this retraction. We have kept a record of any response received.

### References

- [1] F. Hajje, M. A. Alohal, M. Badr, and M. A. Rahman, "A Comparison of Decision Tree Algorithms in the Assessment of Biomedical Data," *BioMed Research International*, vol. 2022, Article ID 9449497, 9 pages, 2022.

## *Retraction*

# **Retracted: Use of Composite Acellular Dermal Matrix-Ultrathin Split-Thickness Skin in Hand Hot-Crush Injuries: A One-Step Grafting Procedure**

### **BioMed Research International**

Received 20 June 2023; Accepted 20 June 2023; Published 21 June 2023

Copyright © 2023 BioMed Research International. This is an open access article distributed under the Creative Commons Attribution License, which permits unrestricted use, distribution, and reproduction in any medium, provided the original work is properly cited.

This article has been retracted by Hindawi following an investigation undertaken by the publisher [1]. This investigation has uncovered evidence of one or more of the following indicators of systematic manipulation of the publication process:

- (1) Discrepancies in scope
- (2) Discrepancies in the description of the research reported
- (3) Discrepancies between the availability of data and the research described
- (4) Inappropriate citations
- (5) Incoherent, meaningless and/or irrelevant content included in the article
- (6) Peer-review manipulation

The presence of these indicators undermines our confidence in the integrity of the article's content and we cannot, therefore, vouch for its reliability. Please note that this notice is intended solely to alert readers that the content of this article is unreliable. We have not investigated whether authors were aware of or involved in the systematic manipulation of the publication process.

Wiley and Hindawi regrets that the usual quality checks did not identify these issues before publication and have since put additional measures in place to safeguard research integrity.

We wish to credit our own Research Integrity and Research Publishing teams and anonymous and named external researchers and research integrity experts for contributing to this investigation.

The corresponding author, as the representative of all authors, has been given the opportunity to register their agreement or disagreement to this retraction. We have kept a record of any response received.

### **References**

- [1] Y. Fan, Y. Pan, C. Chen et al., "Use of Composite Acellular Dermal Matrix-Ultrathin Split-Thickness Skin in Hand Hot-Crush Injuries: A One-Step Grafting Procedure," *BioMed Research International*, vol. 2022, Article ID 1569084, 12 pages, 2022.

## Retraction

# Retracted: Deep Learning-Based Networks for Detecting Anomalies in Chest X-Rays

### BioMed Research International

Received 20 June 2023; Accepted 20 June 2023; Published 21 June 2023

Copyright © 2023 BioMed Research International. This is an open access article distributed under the Creative Commons Attribution License, which permits unrestricted use, distribution, and reproduction in any medium, provided the original work is properly cited.

This article has been retracted by Hindawi following an investigation undertaken by the publisher [1]. This investigation has uncovered evidence of one or more of the following indicators of systematic manipulation of the publication process:

- (1) Discrepancies in scope
- (2) Discrepancies in the description of the research reported
- (3) Discrepancies between the availability of data and the research described
- (4) Inappropriate citations
- (5) Incoherent, meaningless and/or irrelevant content included in the article
- (6) Peer-review manipulation

The presence of these indicators undermines our confidence in the integrity of the article's content and we cannot, therefore, vouch for its reliability. Please note that this notice is intended solely to alert readers that the content of this article is unreliable. We have not investigated whether authors were aware of or involved in the systematic manipulation of the publication process.

In addition, our investigation has also shown that one or more of the following human-subject reporting requirements has not been met in this article: ethical approval by an Institutional Review Board (IRB) committee or equivalent, patient/participant consent to participate, and/or agreement to publish patient/participant details (where relevant).

Wiley and Hindawi regrets that the usual quality checks did not identify these issues before publication and have since put additional measures in place to safeguard research integrity.

We wish to credit our own Research Integrity and Research Publishing teams and anonymous and named external researchers and research integrity experts for contributing to this investigation.

The corresponding author, as the representative of all authors, has been given the opportunity to register their agreement or disagreement to this retraction. We have kept a record of any response received.

### References

- [1] M. Badr, S. Al-Otaibi, N. Alturki, and T. Abir, "Deep Learning-Based Networks for Detecting Anomalies in Chest X-Rays," *BioMed Research International*, vol. 2022, Article ID 7833516, 10 pages, 2022.

## Retraction

# Retracted: Biogenic Analysis of the Effect of TERC on Cell Proliferation and Migration of Oral Squamous Cell Carcinoma under Digital Minimally Invasive Treatment

### BioMed Research International

Received 20 June 2023; Accepted 20 June 2023; Published 21 June 2023

Copyright © 2023 BioMed Research International. This is an open access article distributed under the Creative Commons Attribution License, which permits unrestricted use, distribution, and reproduction in any medium, provided the original work is properly cited.

This article has been retracted by Hindawi following an investigation undertaken by the publisher [1]. This investigation has uncovered evidence of one or more of the following indicators of systematic manipulation of the publication process:

- (1) Discrepancies in scope
- (2) Discrepancies in the description of the research reported
- (3) Discrepancies between the availability of data and the research described
- (4) Inappropriate citations
- (5) Incoherent, meaningless and/or irrelevant content included in the article
- (6) Peer-review manipulation

The presence of these indicators undermines our confidence in the integrity of the article's content and we cannot, therefore, vouch for its reliability. Please note that this notice is intended solely to alert readers that the content of this article is unreliable. We have not investigated whether authors were aware of or involved in the systematic manipulation of the publication process.

In addition, our investigation has also shown that one or more of the following human-subject reporting requirements has not been met in this article: ethical approval by an Institutional Review Board (IRB) committee or equivalent, patient/participant consent to participate, and/or agreement to publish patient/participant details (where relevant).

Wiley and Hindawi regrets that the usual quality checks did not identify these issues before publication and have since put additional measures in place to safeguard research integrity.

We wish to credit our own Research Integrity and Research Publishing teams and anonymous and named external researchers and research integrity experts for contributing to this investigation.

The corresponding author, as the representative of all authors, has been given the opportunity to register their agreement or disagreement to this retraction. We have kept a record of any response received.

### References

- [1] W. Chen, Z. Zhang, Y. Jin et al., "Biogenic Analysis of the Effect of TERC on Cell Proliferation and Migration of Oral Squamous Cell Carcinoma under Digital Minimally Invasive Treatment," *BioMed Research International*, vol. 2022, Article ID 2102795, 6 pages, 2022.



## Retraction

# Retracted: The Predictive Value of Neutrophil-Lymphocyte Ratio in Patients with Polycythemia Vera at the Time of Initial Diagnosis for Thrombotic Events

### BioMed Research International

Received 20 June 2023; Accepted 20 June 2023; Published 21 June 2023

Copyright © 2023 BioMed Research International. This is an open access article distributed under the Creative Commons Attribution License, which permits unrestricted use, distribution, and reproduction in any medium, provided the original work is properly cited.

This article has been retracted by Hindawi following an investigation undertaken by the publisher [1]. This investigation has uncovered evidence of one or more of the following indicators of systematic manipulation of the publication process:

- (1) Discrepancies in scope
- (2) Discrepancies in the description of the research reported
- (3) Discrepancies between the availability of data and the research described
- (4) Inappropriate citations
- (5) Incoherent, meaningless and/or irrelevant content included in the article
- (6) Peer-review manipulation

The presence of these indicators undermines our confidence in the integrity of the article's content and we cannot, therefore, vouch for its reliability. Please note that this notice is intended solely to alert readers that the content of this article is unreliable. We have not investigated whether authors were aware of or involved in the systematic manipulation of the publication process.

In addition, our investigation has also shown that one or more of the following human-subject reporting requirements has not been met in this article: ethical approval by an Institutional Review Board (IRB) committee or equivalent, patient/participant consent to participate, and/or agreement to publish patient/participant details (where relevant).

Wiley and Hindawi regrets that the usual quality checks did not identify these issues before publication and have since put additional measures in place to safeguard research integrity.

We wish to credit our own Research Integrity and Research Publishing teams and anonymous and named external researchers and research integrity experts for contributing to this investigation.

The corresponding author, as the representative of all authors, has been given the opportunity to register their agreement or disagreement to this retraction. We have kept a record of any response received.

### References

- [1] X. Wang, Y. Tu, M. Cao et al., "The Predictive Value of Neutrophil-Lymphocyte Ratio in Patients with Polycythemia Vera at the Time of Initial Diagnosis for Thrombotic Events," *BioMed Research International*, vol. 2022, Article ID 9343951, 8 pages, 2022.

## Retraction

# Retracted: The Use of Chest Radiographs and Machine Learning Model for the Rapid Detection of Pneumonitis in Pediatric

### BioMed Research International

Received 20 June 2023; Accepted 20 June 2023; Published 21 June 2023

Copyright © 2023 BioMed Research International. This is an open access article distributed under the Creative Commons Attribution License, which permits unrestricted use, distribution, and reproduction in any medium, provided the original work is properly cited.

This article has been retracted by Hindawi following an investigation undertaken by the publisher [1]. This investigation has uncovered evidence of one or more of the following indicators of systematic manipulation of the publication process:

- (1) Discrepancies in scope
- (2) Discrepancies in the description of the research reported
- (3) Discrepancies between the availability of data and the research described
- (4) Inappropriate citations
- (5) Incoherent, meaningless and/or irrelevant content included in the article
- (6) Peer-review manipulation

The presence of these indicators undermines our confidence in the integrity of the article's content and we cannot, therefore, vouch for its reliability. Please note that this notice is intended solely to alert readers that the content of this article is unreliable. We have not investigated whether authors were aware of or involved in the systematic manipulation of the publication process.

Wiley and Hindawi regrets that the usual quality checks did not identify these issues before publication and have since put additional measures in place to safeguard research integrity.

We wish to credit our own Research Integrity and Research Publishing teams and anonymous and named external researchers and research integrity experts for contributing to this investigation.

The corresponding author, as the representative of all authors, has been given the opportunity to register their agreement or disagreement to this retraction. We have kept a record of any response received.

### References

- [1] K. Alshamrani, H. A. Alshamrani, A. A. Asiri, F. F. Alqahtani, W. T. Mohammad, and A. H. Alshehri, "The Use of Chest Radiographs and Machine Learning Model for the Rapid Detection of Pneumonitis in Pediatric," *BioMed Research International*, vol. 2022, Article ID 5260231, 11 pages, 2022.

## *Retraction*

# **Retracted: Red Raspberry Extract Decreases Depression-Like Behavior in Rats by Modulating Neuroinflammation and Oxidative Stress**

### **BioMed Research International**

Received 20 June 2023; Accepted 20 June 2023; Published 21 June 2023

Copyright © 2023 BioMed Research International. This is an open access article distributed under the Creative Commons Attribution License, which permits unrestricted use, distribution, and reproduction in any medium, provided the original work is properly cited.

This article has been retracted by Hindawi following an investigation undertaken by the publisher [1]. This investigation has uncovered evidence of one or more of the following indicators of systematic manipulation of the publication process:

- (1) Discrepancies in scope
- (2) Discrepancies in the description of the research reported
- (3) Discrepancies between the availability of data and the research described
- (4) Inappropriate citations
- (5) Incoherent, meaningless and/or irrelevant content included in the article
- (6) Peer-review manipulation

The presence of these indicators undermines our confidence in the integrity of the article's content and we cannot, therefore, vouch for its reliability. Please note that this notice is intended solely to alert readers that the content of this article is unreliable. We have not investigated whether authors were aware of or involved in the systematic manipulation of the publication process.

Wiley and Hindawi regrets that the usual quality checks did not identify these issues before publication and have since put additional measures in place to safeguard research integrity.

We wish to credit our own Research Integrity and Research Publishing teams and anonymous and named external researchers and research integrity experts for contributing to this investigation.

The corresponding author, as the representative of all authors, has been given the opportunity to register their agreement or disagreement to this retraction. We have kept a record of any response received.

### **References**

- [1] Y. Chen, X. Yang, H. Li, and J. Fang, "Red Raspberry Extract Decreases Depression-Like Behavior in Rats by Modulating Neuroinflammation and Oxidative Stress," *BioMed Research International*, vol. 2022, Article ID 9943598, 11 pages, 2022.

## Retraction

# Retracted: Dapagliflozin Improves Diabetic Cardiomyopathy by Modulating the Akt/mTOR Signaling Pathway

### BioMed Research International

Received 20 June 2023; Accepted 20 June 2023; Published 21 June 2023

Copyright © 2023 BioMed Research International. This is an open access article distributed under the Creative Commons Attribution License, which permits unrestricted use, distribution, and reproduction in any medium, provided the original work is properly cited.

This article has been retracted by Hindawi following an investigation undertaken by the publisher [1]. This investigation has uncovered evidence of one or more of the following indicators of systematic manipulation of the publication process:

- (1) Discrepancies in scope
- (2) Discrepancies in the description of the research reported
- (3) Discrepancies between the availability of data and the research described
- (4) Inappropriate citations
- (5) Incoherent, meaningless and/or irrelevant content included in the article
- (6) Peer-review manipulation

The presence of these indicators undermines our confidence in the integrity of the article's content and we cannot, therefore, vouch for its reliability. Please note that this notice is intended solely to alert readers that the content of this article is unreliable. We have not investigated whether authors were aware of or involved in the systematic manipulation of the publication process.

Wiley and Hindawi regrets that the usual quality checks did not identify these issues before publication and have since put additional measures in place to safeguard research integrity.

We wish to credit our own Research Integrity and Research Publishing teams and anonymous and named external researchers and research integrity experts for contributing to this investigation.

The corresponding author, as the representative of all authors, has been given the opportunity to register their agreement or disagreement to this retraction. We have kept a record of any response received.

### References

- [1] M. Ren, D. Pan, D. Zha, and Z. Shan, "Dapagliflozin Improves Diabetic Cardiomyopathy by Modulating the Akt/mTOR Signaling Pathway," *BioMed Research International*, vol. 2022, Article ID 9687345, 10 pages, 2022.

## Retraction

# Retracted: A Novel Method for Parkinson's Disease Diagnosis Utilizing Treatment Protocols

### BioMed Research International

Received 20 June 2023; Accepted 20 June 2023; Published 21 June 2023

Copyright © 2023 BioMed Research International. This is an open access article distributed under the Creative Commons Attribution License, which permits unrestricted use, distribution, and reproduction in any medium, provided the original work is properly cited.

This article has been retracted by Hindawi following an investigation undertaken by the publisher [1]. This investigation has uncovered evidence of one or more of the following indicators of systematic manipulation of the publication process:

- (1) Discrepancies in scope
- (2) Discrepancies in the description of the research reported
- (3) Discrepancies between the availability of data and the research described
- (4) Inappropriate citations
- (5) Incoherent, meaningless and/or irrelevant content included in the article
- (6) Peer-review manipulation

The presence of these indicators undermines our confidence in the integrity of the article's content and we cannot, therefore, vouch for its reliability. Please note that this notice is intended solely to alert readers that the content of this article is unreliable. We have not investigated whether authors were aware of or involved in the systematic manipulation of the publication process.

In addition, our investigation has also shown that one or more of the following human-subject reporting requirements has not been met in this article: ethical approval by an Institutional Review Board (IRB) committee or equivalent, patient/participant consent to participate, and/or agreement to publish patient/participant details (where relevant).

Wiley and Hindawi regrets that the usual quality checks did not identify these issues before publication and have since put additional measures in place to safeguard research integrity.

We wish to credit our own Research Integrity and Research Publishing teams and anonymous and named external researchers and research integrity experts for contributing to this investigation.

The corresponding author, as the representative of all authors, has been given the opportunity to register their agreement or disagreement to this retraction. We have kept a record of any response received.

### References

- [1] S. Al-Otaibi, S. Ayouni, M. M. H. Khan, and M. Badr, "A Novel Method for Parkinson's Disease Diagnosis Utilizing Treatment Protocols," *BioMed Research International*, vol. 2022, Article ID 6871623, 6 pages, 2022.

## *Retraction*

# **Retracted: Processing Decision Tree Data Using Internet of Things (IoT) and Artificial Intelligence Technologies with Special Reference to Medical Application**

### **BioMed Research International**

Received 20 June 2023; Accepted 20 June 2023; Published 21 June 2023

Copyright © 2023 BioMed Research International. This is an open access article distributed under the Creative Commons Attribution License, which permits unrestricted use, distribution, and reproduction in any medium, provided the original work is properly cited.

This article has been retracted by Hindawi following an investigation undertaken by the publisher [1]. This investigation has uncovered evidence of one or more of the following indicators of systematic manipulation of the publication process:

- (1) Discrepancies in scope
- (2) Discrepancies in the description of the research reported
- (3) Discrepancies between the availability of data and the research described
- (4) Inappropriate citations
- (5) Incoherent, meaningless and/or irrelevant content included in the article
- (6) Peer-review manipulation

The presence of these indicators undermines our confidence in the integrity of the article's content and we cannot, therefore, vouch for its reliability. Please note that this notice is intended solely to alert readers that the content of this article is unreliable. We have not investigated whether authors were aware of or involved in the systematic manipulation of the publication process.

Wiley and Hindawi regrets that the usual quality checks did not identify these issues before publication and have since put additional measures in place to safeguard research integrity.

We wish to credit our own Research Integrity and Research Publishing teams and anonymous and named external researchers and research integrity experts for contributing to this investigation.

The corresponding author, as the representative of all authors, has been given the opportunity to register their agreement or disagreement to this retraction. We have kept a record of any response received.

### **References**

- [1] L. H. Al Fryan, M. I. Shomo, M. B. Alazzam, and M. A. Rahman, "Processing Decision Tree Data Using Internet of Things (IoT) and Artificial Intelligence Technologies with Special Reference to Medical Application," *BioMed Research International*, vol. 2022, Article ID 8626234, 9 pages, 2022.

## *Retraction*

# **Retracted: Big Data Analysis of Manufacturing and Preclinical Studies of Nanodrug-Targeted Delivery Systems: A Literature Review**

### **BioMed Research International**

Received 20 June 2023; Accepted 20 June 2023; Published 21 June 2023

Copyright © 2023 BioMed Research International. This is an open access article distributed under the Creative Commons Attribution License, which permits unrestricted use, distribution, and reproduction in any medium, provided the original work is properly cited.

This article has been retracted by Hindawi following an investigation undertaken by the publisher [1].

This investigation has uncovered evidence of one or more of the following indicators of systematic manipulation of the publication process:

- (1) Discrepancies in scope
- (2) Discrepancies in the description of the research reported
- (3) Discrepancies between the availability of data and the research described
- (4) Inappropriate citations
- (5) Incoherent, meaningless and/or irrelevant content included in the article
- (6) Peer-review manipulation

The presence of these indicators undermines our confidence in the integrity of the article's content and we cannot, therefore, vouch for its reliability. Please note that this notice is intended solely to alert readers that the content of this article is unreliable. We have not investigated whether authors were aware of or involved in the systematic manipulation of the publication process.

Wiley and Hindawi regrets that the usual quality checks did not identify these issues before publication and have since put additional measures in place to safeguard research integrity.

We wish to credit our own Research Integrity and Research Publishing teams and anonymous and named

external researchers and research integrity experts for contributing to this investigation.

The corresponding author, as the representative of all authors, has been given the opportunity to register their agreement or disagreement to this retraction. We have kept a record of any response received.

### **References**

- [1] Q. Cao, X. Li, Q. Zhang et al., "Big Data Analysis of Manufacturing and Preclinical Studies of Nanodrug-Targeted Delivery Systems: A Literature Review," *BioMed Research International*, vol. 2022, Article ID 1231446, 10 pages, 2022.

## Retraction

# Retracted: Awareness of Medical Students toward Circadian Rhythm and Sleep Disorder Based on Biomedical Diagnosis

### BioMed Research International

Received 20 June 2023; Accepted 20 June 2023; Published 21 June 2023

Copyright © 2023 BioMed Research International. This is an open access article distributed under the Creative Commons Attribution License, which permits unrestricted use, distribution, and reproduction in any medium, provided the original work is properly cited.

This article has been retracted by Hindawi following an investigation undertaken by the publisher [1]. This investigation has uncovered evidence of one or more of the following indicators of systematic manipulation of the publication process:

- (1) Discrepancies in scope
- (2) Discrepancies in the description of the research reported
- (3) Discrepancies between the availability of data and the research described
- (4) Inappropriate citations
- (5) Incoherent, meaningless and/or irrelevant content included in the article
- (6) Peer-review manipulation

The presence of these indicators undermines our confidence in the integrity of the article's content and we cannot, therefore, vouch for its reliability. Please note that this notice is intended solely to alert readers that the content of this article is unreliable. We have not investigated whether authors were aware of or involved in the systematic manipulation of the publication process.

In addition, our investigation has also shown that one or more of the following human-subject reporting requirements has not been met in this article: ethical approval by an Institutional Review Board (IRB) committee or equivalent, patient/participant consent to participate, and/or agreement to publish patient/participant details (where relevant).

Wiley and Hindawi regrets that the usual quality checks did not identify these issues before publication and have

since put additional measures in place to safeguard research integrity.

We wish to credit our own Research Integrity and Research Publishing teams and anonymous and named external researchers and research integrity experts for contributing to this investigation.

The corresponding author, as the representative of all authors, has been given the opportunity to register their agreement or disagreement to this retraction. We have kept a record of any response received.

### References

- [1] A. Alanazi, H. Alhawas, M. Aldossari et al., "Awareness of Medical Students toward Circadian Rhythm and Sleep Disorder Based on Biomedical Diagnosis," *BioMed Research International*, vol. 2022, Article ID 8645183, 6 pages, 2022.



## Retraction

# Retracted: Knowledge and Behavior toward Venous Thromboembolism Event Prophylaxis and Treatment Protocols among Medical Interns in Riyadh

### BioMed Research International

Received 20 June 2023; Accepted 20 June 2023; Published 21 June 2023

Copyright © 2023 BioMed Research International. This is an open access article distributed under the Creative Commons Attribution License, which permits unrestricted use, distribution, and reproduction in any medium, provided the original work is properly cited.

This article has been retracted by Hindawi following an investigation undertaken by the publisher [1]. This investigation has uncovered evidence of one or more of the following indicators of systematic manipulation of the publication process:

- (1) Discrepancies in scope
- (2) Discrepancies in the description of the research reported
- (3) Discrepancies between the availability of data and the research described
- (4) Inappropriate citations
- (5) Incoherent, meaningless and/or irrelevant content included in the article
- (6) Peer-review manipulation

The presence of these indicators undermines our confidence in the integrity of the article's content and we cannot, therefore, vouch for its reliability. Please note that this notice is intended solely to alert readers that the content of this article is unreliable. We have not investigated whether authors were aware of or involved in the systematic manipulation of the publication process.

Wiley and Hindawi regrets that the usual quality checks did not identify these issues before publication and have since put additional measures in place to safeguard research integrity.

We wish to credit our own Research Integrity and Research Publishing teams and anonymous and named external researchers and research integrity experts for contributing to this investigation.

The corresponding author, as the representative of all authors, has been given the opportunity to register their agreement or disagreement to this retraction. We have kept a record of any response received.

### References

- [1] Z. Al Aseri, J. M. Muammar, N. F. Aldakkan et al., "Knowledge and Behavior toward Venous Thromboembolism Event Prophylaxis and Treatment Protocols among Medical Interns in Riyadh," *BioMed Research International*, vol. 2022, Article ID 7191178, 7 pages, 2022.

## Retraction

# Retracted: Hysterectomy by Transvaginal Natural Orifice Transluminal Endoscopic Surgery versus Transumbilical Laparoscopic Single-Site Surgery: A Single-Center Experience from East China

### BioMed Research International

Received 20 June 2023; Accepted 20 June 2023; Published 21 June 2023

Copyright © 2023 BioMed Research International. This is an open access article distributed under the Creative Commons Attribution License, which permits unrestricted use, distribution, and reproduction in any medium, provided the original work is properly cited.

This article has been retracted by Hindawi following an investigation undertaken by the publisher [1]. This investigation has uncovered evidence of one or more of the following indicators of systematic manipulation of the publication process:

- (1) Discrepancies in scope
- (2) Discrepancies in the description of the research reported
- (3) Discrepancies between the availability of data and the research described
- (4) Inappropriate citations
- (5) Incoherent, meaningless and/or irrelevant content included in the article
- (6) Peer-review manipulation

The presence of these indicators undermines our confidence in the integrity of the article's content and we cannot, therefore, vouch for its reliability. Please note that this notice is intended solely to alert readers that the content of this article is unreliable. We have not investigated whether authors were aware of or involved in the systematic manipulation of the publication process.

In addition, our investigation has also shown that one or more of the following human-subject reporting requirements has not been met in this article: ethical approval by

an Institutional Review Board (IRB) committee or equivalent, patient/participant consent to participate, and/or agreement to publish patient/participant details (where relevant).

Wiley and Hindawi regrets that the usual quality checks did not identify these issues before publication and have since put additional measures in place to safeguard research integrity.

We wish to credit our own Research Integrity and Research Publishing teams and anonymous and named external researchers and research integrity experts for contributing to this investigation.

The corresponding author, as the representative of all authors, has been given the opportunity to register their agreement or disagreement to this retraction. We have kept a record of any response received.

### References

- [1] B. Yan, H. Miao, Y. Wang et al., "Hysterectomy by Transvaginal Natural Orifice Transluminal Endoscopic Surgery versus Transumbilical Laparoscopic Single-Site Surgery: A Single-Center Experience from East China," *BioMed Research International*, vol. 2022, Article ID 8246761, 7 pages, 2022.

## Retraction

# Retracted: Gait Improvement in Patients with Knee Osteoarthritis after Proximal Fibular Osteotomy

### BioMed Research International

Received 20 June 2023; Accepted 20 June 2023; Published 21 June 2023

Copyright © 2023 BioMed Research International. This is an open access article distributed under the Creative Commons Attribution License, which permits unrestricted use, distribution, and reproduction in any medium, provided the original work is properly cited.

This article has been retracted by Hindawi following an investigation undertaken by the publisher [1]. This investigation has uncovered evidence of one or more of the following indicators of systematic manipulation of the publication process:

- (1) Discrepancies in scope
- (2) Discrepancies in the description of the research reported
- (3) Discrepancies between the availability of data and the research described
- (4) Inappropriate citations
- (5) Incoherent, meaningless and/or irrelevant content included in the article
- (6) Peer-review manipulation

The presence of these indicators undermines our confidence in the integrity of the article's content and we cannot, therefore, vouch for its reliability. Please note that this notice is intended solely to alert readers that the content of this article is unreliable. We have not investigated whether authors were aware of or involved in the systematic manipulation of the publication process.

Wiley and Hindawi regrets that the usual quality checks did not identify these issues before publication and have since put additional measures in place to safeguard research integrity.

We wish to credit our own Research Integrity and Research Publishing teams and anonymous and named external researchers and research integrity experts for contributing to this investigation.

The corresponding author, as the representative of all authors, has been given the opportunity to register their agreement or disagreement to this retraction. We have kept a record of any response received.

### References

- [1] X. Li, Y. Cao, Z. Cao et al., "Gait Improvement in Patients with Knee Osteoarthritis after Proximal Fibular Osteotomy," *BioMed Research International*, vol. 2022, Article ID 1869922, 8 pages, 2022.

## Retraction

# Retracted: DNMT3A Regulates miR-149 DNA Methylation to Activate NOTCH1/Hedgehog Pathway to Promote the Development of Junctional Osteosarcoma

### BioMed Research International

Received 20 June 2023; Accepted 20 June 2023; Published 21 June 2023

Copyright © 2023 BioMed Research International. This is an open access article distributed under the Creative Commons Attribution License, which permits unrestricted use, distribution, and reproduction in any medium, provided the original work is properly cited.

This article has been retracted by Hindawi following an investigation undertaken by the publisher [1]. This investigation has uncovered evidence of one or more of the following indicators of systematic manipulation of the publication process:

- (1) Discrepancies in scope
- (2) Discrepancies in the description of the research reported
- (3) Discrepancies between the availability of data and the research described
- (4) Inappropriate citations
- (5) Incoherent, meaningless and/or irrelevant content included in the article
- (6) Peer-review manipulation

The presence of these indicators undermines our confidence in the integrity of the article's content and we cannot, therefore, vouch for its reliability. Please note that this notice is intended solely to alert readers that the content of this article is unreliable. We have not investigated whether authors were aware of or involved in the systematic manipulation of the publication process.

In addition, our investigation has also shown that one or more of the following human-subject reporting requirements has not been met in this article: ethical approval by an Institutional Review Board (IRB) committee or equivalent, patient/participant consent to participate, and/or agreement to publish patient/participant details (where relevant).

Wiley and Hindawi regrets that the usual quality checks did not identify these issues before publication and have since put additional measures in place to safeguard research integrity.

We wish to credit our own Research Integrity and Research Publishing teams and anonymous and named external researchers and research integrity experts for contributing to this investigation.

The corresponding author, as the representative of all authors, has been given the opportunity to register their agreement or disagreement to this retraction. We have kept a record of any response received.

### References

- [1] S. Cheng and W. Wang, "DNMT3A Regulates miR-149 DNA Methylation to Activate NOTCH1/Hedgehog Pathway to Promote the Development of Junctional Osteosarcoma," *BioMed Research International*, vol. 2022, Article ID 3261213, 9 pages, 2022.

## Retraction

# Retracted: The Expression of the Long Noncoding RNA AFAP1-AS1 in Laryngeal Carcinoma Affects the Proliferation, Invasion, Migration, and Apoptosis of TU212 Cell Line

### BioMed Research International

Received 20 June 2023; Accepted 20 June 2023; Published 21 June 2023

Copyright © 2023 BioMed Research International. This is an open access article distributed under the Creative Commons Attribution License, which permits unrestricted use, distribution, and reproduction in any medium, provided the original work is properly cited.

This article has been retracted by Hindawi following an investigation undertaken by the publisher [1]. This investigation has uncovered evidence of one or more of the following indicators of systematic manipulation of the publication process:

- (1) Discrepancies in scope
- (2) Discrepancies in the description of the research reported
- (3) Discrepancies between the availability of data and the research described
- (4) Inappropriate citations
- (5) Incoherent, meaningless and/or irrelevant content included in the article
- (6) Peer-review manipulation

The presence of these indicators undermines our confidence in the integrity of the article's content and we cannot, therefore, vouch for its reliability. Please note that this notice is intended solely to alert readers that the content of this article is unreliable. We have not investigated whether authors were aware of or involved in the systematic manipulation of the publication process.

In addition, our investigation has also shown that one or more of the following human-subject reporting requirements has not been met in this article: ethical approval by an Institutional Review Board (IRB) committee or equivalent, patient/participant consent to participate, and/or agreement to publish patient/participant details (where relevant).

Wiley and Hindawi regrets that the usual quality checks did not identify these issues before publication and have since put additional measures in place to safeguard research integrity.

We wish to credit our own Research Integrity and Research Publishing teams and anonymous and named external researchers and research integrity experts for contributing to this investigation.

The corresponding author, as the representative of all authors, has been given the opportunity to register their agreement or disagreement to this retraction. We have kept a record of any response received.

### References

- [1] X. Chen, Z. Hu, L. Bing et al., "The Expression of the Long Non-coding RNA AFAP1-AS1 in Laryngeal Carcinoma Affects the Proliferation, Invasion, Migration, and Apoptosis of TU212 Cell Line," *BioMed Research International*, vol. 2022, Article ID 2337447, 8 pages, 2022.

## *Retraction*

# **Retracted: The Effect of Hyperlipidemia on Peri-Implant Health: A Clinical and Radiographical Prospective Study**

### **BioMed Research International**

Received 5 December 2023; Accepted 5 December 2023; Published 6 December 2023

Copyright © 2023 BioMed Research International. This is an open access article distributed under the Creative Commons Attribution License, which permits unrestricted use, distribution, and reproduction in any medium, provided the original work is properly cited.

This article has been retracted by Hindawi, as publisher, following an investigation undertaken by the publisher [1]. This investigation has uncovered evidence of systematic manipulation of the publication and peer-review process. We cannot, therefore, vouch for the reliability or integrity of this article.

Please note that this notice is intended solely to alert readers that the peer-review process of this article has been compromised.

Wiley and Hindawi regret that the usual quality checks did not identify these issues before publication and have since put additional measures in place to safeguard research integrity.

We wish to credit our Research Integrity and Research Publishing teams and anonymous and named external researchers and research integrity experts for contributing to this investigation.



The corresponding author, as the representative of all authors, has been given the opportunity to register their agreement or disagreement to this retraction. We have kept a record of any response received.

### **References**

- [1] P. De Angelis, E. Rella, P. F. Manicone et al., “The Effect of Hyperlipidemia on Peri-Implant Health: A Clinical and Radiographical Prospective Study,” *BioMed Research International*, vol. 2023, Article ID 7570587, 8 pages, 2023.

## Research Article

# The Effect of Hyperlipidemia on Peri-implant Health: A Clinical and Radiographical Prospective Study

**Paolo De Angelis** <sup>1</sup>, **Edoardo Rella**,<sup>1</sup> **Paolo Francesco Manicone**,<sup>1</sup> **Giulio Gasparini** <sup>1</sup>,  
**Valerio Giovannini**,<sup>1</sup> **Margherita Giorgia Liguori**,<sup>1</sup> **Francesca Camodeca**,<sup>1</sup>  
**Giuseppe De Rosa**,<sup>1</sup> **Camilla Cavalcanti**,<sup>1</sup> and **Antonio D'Addona**<sup>2</sup>

<sup>1</sup>Department of Head and Neck and Sensory Organs, Division of Oral Surgery and Implantology, Fondazione Policlinico Universitario A. Gemelli IRCCS–Università Cattolica del Sacro Cuore, Rome, Italy

<sup>2</sup>Department of Head and Neck and Sensory Organs, Division of Oral and Maxillofacial Surgery, Fondazione Policlinico Universitario A. Gemelli IRCCS–Università Cattolica del Sacro Cuore, Rome, Italy

Correspondence should be addressed to Paolo De Angelis; [dr.paolodeangelis@gmail.com](mailto:dr.paolodeangelis@gmail.com)

Received 26 June 2022; Accepted 13 July 2022; Published 26 April 2023

Academic Editor: Dinesh Rokaya

Copyright © 2023 Paolo De Angelis et al. This is an open access article distributed under the Creative Commons Attribution License, which permits unrestricted use, distribution, and reproduction in any medium, provided the original work is properly cited.

High levels of cholesterol and triglycerides may have a negative effect on the immune system and bone health, leading to lower bone mineral density, an increased risk of osteoporosis, and bone fractures, and could therefore also be related to a significant worsening of peri-implant health. The purpose of the following study was to evaluate whether the altered lipid profile in patients who undergo implant insertion surgery represents a prognostic factor capable of influencing clinical outcomes. This prospective observational study was conducted on 93 subjects; patients were required to have taken blood tests to obtain triglycerides (TG), total cholesterol, low-density lipoprotein (LDL), and high-density lipoprotein (HDL) levels prior to the surgical procedure to classify them according to current American Heart Association guidelines. The outcomes considered were marginal bone loss (MBL) 3 years after implant placement, full-mouth plaque score (FMPS), and full-mouth bleeding score (FMBS) 3 years after surgery. A statistically significant correlation was found between hypertriglyceridemia and MBL as well as between total cholesterol and MBL. There is no statistically significant correlation between the variables analyzed and the secondary outcomes 3 years after implant placement. Peri-implant marginal bone loss may be influenced by hyperlipidemia. However, further studies are needed, with larger samples and more extensive follow-ups, to confirm these results.

## 1. Introduction

The atherogenic, or high-fat (HF), diet induces hyperlipidemia, a state with an abnormal lipid profile characterized by elevated blood concentrations of triglycerides, high levels of total and low density lipoprotein (LDL) cholesterol, and reduced levels of high density lipoprotein (HDL) cholesterol [1].

An HF diet is associated with the pathophysiology of several diseases, including atherosclerosis, vascular calcifications, and osteoporosis, which are major causes of morbidity and mortality in the aging population [2–5].

The current American Heart Association guidelines define hyperlipidemia by levels of total cholesterol (>240 mg/dL), LDL cholesterol (>160 mg/dL), or triglycerides (>200 mg/dL). Because low HDL levels (<40 mg/dL in men and <50 mg/dL in women) are also considered atherogenic, the terms “dyslipidemia” and “atherogenic lipid profile” are also used [6].

Under conditions of hyperlipidemia, protein-bound lipid particles pass through the endothelial wall to the subendothelial level, where they are captured and oxidatively modified by reactive oxygen species produced by metabolically active nearby smooth muscle cells and macrophages.



A similar phenomenon occurs in human osteoporotic bone, with lipid particles bound to oxidized proteins collecting at the perivascular and subendothelial levels. Osteoblasts can also oxidatively modify protein-bound lipid particles, and oxidized lipid products have been detected in the bone marrow of hyperlipidemic mice [7, 8].

Krieger et al. [9] showed an increase in the number of osteoclasts, inhibition of osteoblastic activity, and a reduction in bone remodeling in hyperlipidemic rats. According to Luegmarly et al. [10], high-cholesterol levels can lead to an imbalance in the bone remodeling processes, reducing bone mass by increasing osteoclast activity and differentiation.

Because of the deleterious effects of hyperlipidemia on bone, it has been hypothesized that hyperlipidemia may interfere with bone grafting and dental implant therapy, as the quantity, quality, and healing potential of the host play an important role in the osseointegration and bone regeneration process [11–14].

Only one study investigated the effects of hyperlipidemia on implant osseointegration in mice by implant push-in test and microcomputed tomography (micro-CT) analysis. In this study, Keuroghlian et al. [15] found that mice fed a high-fat diet had a significantly increased chance of implant failure as well as reduced bone-implant interface formation and strength.

Three studies by the same author investigated the relationship between hypercholesterolemia and dental implant failure in humans, but none of the three reported any causal relationship between hypercholesterolemia and implant failure rates [16–18].

To the best of our knowledge, peri-implant tissue healing and bone graft maturation in the presence of hyperlipidemia have not yet been extensively studied.

The increasing number of patients with hyperlipidemia represents a challenge due to the high number of procedures and the risks of directly compromising clinical outcomes and increasing therapeutic failures.

The present prospective study is aimed at testing the null hypothesis that hyperlipidemia does not influence peri-implant marginal bone level (MBL) 3 years after implant placement.

## 2. Materials and Methods

This prospective study enrolled 93 patients treated at the Department of Oral Surgery and Implantology of the Catholic University of the Sacred Heart of Rome. All investigations have been performed in accordance with the 1975 Declaration of Helsinki, revised in 2013 for ethical approval. All participants have provided written informed consent after receiving all relevant information regarding the objectives and procedures of the study.

Ethical approval was obtained from the Catholic University of the Sacred Heart, Rome, Italy (ID: 4130).

All surgeries were performed by the same trained and experienced surgeon.

Patients were selected on the basis of the following inclusion criteria:

- (1) Patients who needed a single implant to treat a partial edentulism
- (2) Healthy patient or stable periodontitis patient
- (3) Total cholesterol, LDL-cholesterol (LDL-c), HDL-cholesterol (HDL-c), and triglyceride values recorded no more than 3 months before enrollment

- (4) Age > 20 years

The exclusion criteria were as follows:

- (1) Periodontal disease
- (2) Taking any medication known to affect oral status and bone turnover or that contraindicate surgical treatments (therapy with immunosuppressants, corticosteroids, or bisphosphonates)
- (3) Previous radiotherapy or chemotherapy
- (4) Smokers
- (5) Excessive alcohol consumption
- (6) Conditions associated with an altered relationship between glycated hemoglobin and blood glucose such as sickle cell anemia, pregnancy, glucose-6-phosphate dehydrogenase deficiency, HIV, hemodialysis, recent transfusion, or erythropoietin therapy

The following factors were evaluated and collected prior to implant placement:

- (1) Age
- (2) Gender
- (3) BMI (Body Mass Index)
- (4) Ethnicity
- (5) Regenerative bone graft therapy prior to implant placement (yes/no)

Patients were classified according to the current American Heart Association guidelines [19].

Patients were divided into four groups based on triglyceride levels (1: <150 mg/dL, 2: 150–199 mg/dL, 3: 200–499 mg/dL, and 4: ≥500 mg/dL); into two groups based on total cholesterol levels (1: <200 mg/dL, 2: ≥200 mg/dL); into two groups based on LDL levels (1: <100 mg/dL, 2: ≥100 mg/dL); and into two groups based on HDL levels (women—1: ≥50 mg/dL, 2: <50 mg/dL; men—1: ≥40 mg/dL, 2: <40 mg/dL).

The following clinical outcome variables were assessed before surgery by the same operator, using a University of North Carolina periodontal probe (UNC15, Hu-Friedy, USA).

- (i) Probing pocket depth (PPD)
- (ii) Full-mouth bleeding score (FMBS)
- (iii) Full-mouth plaque score (FMPS)

PPD was measured for each site and then averaged.



Each patient underwent a preoperative cone-beam computed tomography (CBCT) scan to complete the preoperative planning and evaluate the bone volume. Before the surgical phase, all subjects were enrolled in a rigorous oral hygiene regimen.

Surgery was performed under local anesthesia (articaine 4% with epinephrine 1:100000). A crestal incision was performed, and it was continued intrasulcularly involving the mesial and distal tooth. A mucoperiosteal flap was raised, and the bone was exposed and carefully curetted. An osteotomic site was created following company protocol, and a bone-level implant was placed, with the implant neck positioned crestally. During the implant placement, primary stability was assessed via the insertion torque and hand testing; single sutures were placed to obtain a primary intention closure.

Patients were instructed to rinse twice daily with a 0.2% chlorhexidine mouth rinse. In addition, analgesics (Ketoprofen) were prescribed for the next 3 days according to individual needs. Patients were also instructed to refrain from mechanical plaque removal in the surgical site. The sutures were removed 7–10 days after surgery.

Four months after implant positioning, a digital or a conventional impression was taken. After prosthesis delivery, all the patients were enrolled in a periodontal maintenance program.

A CBCT scan was then taken at the 3-year follow-up.

The primary outcome of the study was the change in peri-implant MBL 3 years after implant placement, measured using the CBCT scan (Orthophos XG 3D, Sirona Dental Systems GmbH). The CBCT scan was transferred into a dedicated software system (Implant Studio, 3Shape, Copenhagen K Denmark) used to perform the measurements, carried out by one designated examiner. For the most accurate details, the study used a field of view of  $5 \times 5$  cm with a voxel size of  $100 \mu\text{m}$ . All radiographic and tomographic images were taken by the same trained operator. On the CBCT coronal and sagittal section, the distances between the implant neck and the buccal/palatal bone and from the implant neck to the mesial and distal bone were measured in millimeters, and the higher value was considered for each implant.

Adverse events (e.g., wound infection, graft exposure, and soft tissue dehiscence or necrosis) were recorded during follow-up.

A sample size of 82 subjects was required to achieve a power of 80%, at a significance level of 0.05, expecting to build a final model with eight predictors with an effect size of 0.2.

**2.1. Statistical Analysis.** Categorical data were analyzed as absolute and relative frequency, whereas numerical data were reported as means and standard deviations.

A multiple regression analysis was performed to evaluate the effects of the variables on MBL and FMBS; only the variables that had a statistically significant outcome in univariable models were inserted in the multivariable analysis. Statistical analysis was conducted using STATA (StataCorp. 2021. Stata Statistical Software: Release 17. College Station, TX: StataCorp LLC).

TABLE 1: The demographic characteristics of the sample.

Variable	Absolute frequency
<i>Gender</i>	
Male	54
Female	39
<i>Race</i>	
Caucasian	87
Asian	3
Latino-American	2
Afro-American	1
<i>Previous regenerative therapy</i>	
Underwent a regenerative surgery	17
Did not undergo a regenerative surgery	76
<i>Adherence to the maintenance program</i>	
Followed the maintenance program	70
Did not follow the maintenance program	23
<i>Occurrence of complication</i>	
Suffered a complication	5
Did not suffer a complication	88

TABLE 2: The “nutritional” values of the sample.

Variable	Absolute frequency
<i>BMI</i>	
1	38
2	35
3	17
4	3
<i>Triglyceride levels</i>	
1	42
2	29
3	22
<i>Cholesterol levels</i>	
1	38
2	55
<i>LDL levels</i>	
1	42
2	51
<i>HDL levels</i>	
1	35
2	58

### 3. Results

The analyzed sample is composed of 93 patients, with a mean age of  $56.97 \pm 13.76$ . Tables 1–3 show the demographic, distribution, and periodontal data. All patients underwent the described implant surgery procedures; five patients were affected by postoperative complications.

The results of the univariable analysis are reported in Tables 4 and 5. A previous regenerative therapy, the occurrence of complications, higher BMI level, higher levels of

TABLE 3: The periodontal values of the sample.

Variable	Mean	Standard deviation
FMBS	15.48	4.40
FMPS	16.84	4.56
PPD	2.92	0.57
MBL	0.53	0.42

TABLE 4: The results of the univariable analyses for the outcome MBL.

Variable (MBL)	Coefficient	P value
Gender	-0.11	0.27
Age	0.005	0.16
Ethnicity	-0.37	0.70
Previous regenerative therapy	0.27	0.03*
Adherence to the maintenance program	-0.39	0.7
Occurrence of complication	0.62	0.004*
BMI	0.25	0.0001*
Triglyceride levels	0.25	0.0001*
Cholesterol levels	0.36	0.0001*
HDL levels	0.31	0.002*
LDL levels	0.29	0.003*
FMPS	0.05	0.0001*
PPD	0.13	0.13

TABLE 5: The results of the univariable analyses for the outcome FMBS.

Variable (FMBS)	Coefficient	P value
Gender	-0.87	0.34
Age	-0.01	0.75
Ethnicity	-0.3	0.70
Previous regenerative therapy	-0.8	0.94
Adherence to the maintenance program	-1	0.3
Development of complication	4.13	0.04*
BMI	1.3	0.01*
Triglyceride levels	0.6	0.27
Cholesterol levels	1.5	0.09
HDL levels	1.82	0.05
LDL levels	1.53	0.09
FMPS	0.57	0.0001*
PPD	1.42	0.07

triglycerides, higher levels of LDL cholesterol and total cholesterol, lower levels of HDL cholesterol, and a higher FMPS had an impact on the amount of MBL, according to the univariable model.

Only the variables that had a significant effect were inserted in the multivariable analysis, and the results are reported in Tables 6 and 7.

TABLE 6: The results of the multivariable analysis for the outcome MBL.

Variable (MBL)	Coefficient	Confidence interval	P value
Previous regenerative therapy	0.23	0.03–0.44	0.02*
Development of complication	0.15	-0.22–0.52	0.42
<i>BMI</i>			
2	0.05	-0.11–0.22	0.52
3	0.19	-0.05–0.44	0.12
4	0.66	0.24–1.09	0.003
<i>Triglyceride levels</i>			
2	0.17	-0.26–0.36	0.09
3	0.26	0.01–0.51	0.04*
<i>Cholesterol levels</i>			
2	0.16	-0.21–0.54	0.4*
<i>HDL levels</i>			
2	-0.10	-0.44–0.23	0.54
<i>LDL levels</i>			
2	-0.05	-0.27–0.17	0.66
FMPS	0.045	0.03–0.06	0.001*

TABLE 7: The results of the multivariable analysis for the outcome FMBS.

Variable (FMBS)	Coefficient	Confidence interval	P value
Development of complication	2.49	-1.26–6	0.16
<i>BMI</i>			
2	1.05	-.61–2.7	0.52
3	0.64	-1.6–2.89	0.57
4	1.77	-2.47–6	0.4
FMPS	5	0.37–0.7	0.001

Only a previous regenerative therapy, a higher FMPS and higher levels of triglycerides and total cholesterol had an impact on the amount of MBL, according to the multivariable model. HDL and LDL had no effect in this model, even if patients who had a higher level of LDL and lower level of HDL revealed a notable increase in the MBL (Figures 1 and 2); this was probably caused by the high collinearity found in the present data sample because patients who had higher levels of cholesterol and triglycerides also had high levels of LDL and lower levels of HDL.

Regarding the FMBS, a significant effect was found only for the FMPS, according to the multivariable model.

#### 4. Discussion

Implant therapy has become a widely used procedure for dental rehabilitation; it is considered safe and has a high survival and success rate, although certain conditions can affect

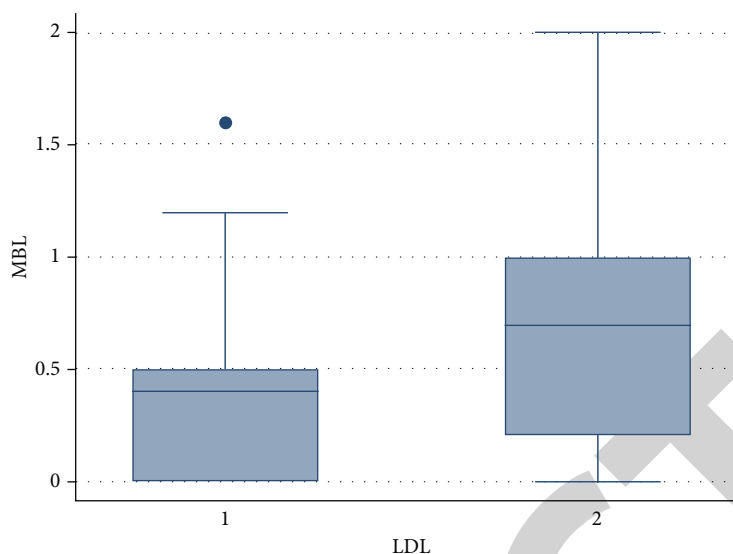


FIGURE 1: Box plot outlining marginal bone loss distribution considering the LDL levels.

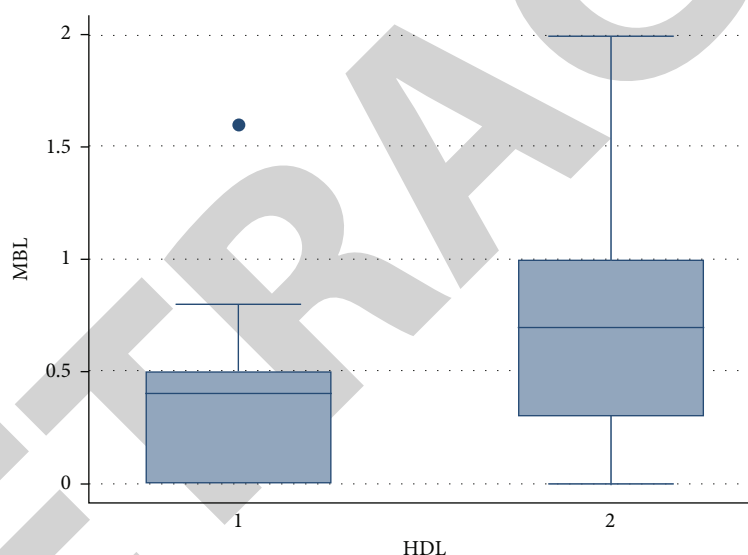


FIGURE 2: Box plot outlining marginal bone loss distribution considering the HDL levels.

the predictability of outcomes. One of these conditions may be an abnormal lipid profile due to its influence on the peri-implant hard and soft tissues [20].

The primary purpose of this study was to examine the hyperlipidemia influence on peri-implant marginal bone level (MBL) at 3 years after implant placement. Marginal bone loss surrounding dental implants is one parameter that has been commonly used to determine implant success and health and is associated with the long-term success of implant treatment [21]. Although bone regeneration is an efficient process in physiological conditions, many variables such as phlogosis, hormonal changes, and elevated serum lipid levels may be associated with the impaired or delayed healing process [22]. Recently, a correlation between atherosclerotic vascular disease and bone loss has been demonstrated [23], and it is accepted that a high-fat diet (HFD)

reduces bone density and increases bone resorption activity [24]. The role of lipid and lipid-bound protein oxidation in the pathophysiology of osteoporosis has been reported by a variety of studies [25, 26].

In their experimental study, Lu et al. [27] reported that the bone mineral content and the area of trabecular bone were significantly decreased in the HFD group compared to the controls. Moreover, they reported that in a cell culture study on aspirated bone marrow derived from mice, the colony-forming unit osteoblasts were significantly decreased in the HFD sample compared to the control [27].

The deleterious effects of HFD on osseointegration and stability of peri-implant hard tissues can be explained by more than one mechanism. At a cellular level, hyperlipidemic conditions lead to inhibition of osteogenic signaling, reductions in the number of mature osteoblasts, a higher

expression of molecular markers of bone remodeling, enhancement of osteoclast differentiation and activity, and increased bone resorption [28, 29].

In clinical practice, the influence that the lipid profile can have on the peri-implant bone remains a subject of controversy. Some studies report a correlation between lipid levels and peri-implant bone; other studies conflict with these conclusions. The latter category includes a study by Dundar et al. [8] who reported no differences in bone-to-implant contact (BIC) 12 weeks after implant placement between rabbits following a 3-month high-fat diet versus normal diet.

Other authors have investigated the influence of the lipid profile on periodontal disease and alveolar bone resorption. Hyperlipidemia seems to have a dysregulatory effect on immune system and wound healing, increasing the susceptibility to periodontal disease and other infections [26, 30, 31].

Macri et al. [32] focused on the effect of an atherogenic cholesterol-rich diet on the alveolar bone loss in rats with ligature-induced experimental periodontitis, and they concluded that an atherogenic cholesterol-rich diet induced hyperlipidemia and appeared to be a risk factor for the onset and progression of experimentally induced periodontitis. However, Valera-Lopez's study on rabbits showed that HFD could exacerbate some aspects of periodontitis, but the presence of some oral microorganisms in the subgingival plaque is essential for this exacerbation [33]. Another study by Kirzioğlu et al. [34] showed that no additive effect of cholesterol-enriched diet to alveolar bone loss (ABL) was found in rats with ligature-induced experimental periodontitis. The relationship between hyperlipidemia and periodontal disease may involve also the bacterial interaction. Choi et al., in a human study, performed a multivariable analysis and after adjusting for periodontitis and other potential risk factors found that a higher burden of periodontal bacteria was independently associated with lower HDL and higher TG in serum. This result may suggest also a possible link between exposure to periodontal bacteria and increased risk of dyslipidemia [19].

It must be considered that most of the studies in the literature on this topic have been conducted using experimental animal models; therefore, one of the notable features of the present study consists in having taken a human experimental model as a reference.

The results of the present study demonstrate that the variables that appear to have the greatest effect on MBL are having received previous regenerative therapy, a higher FMPS, and higher levels of triglycerides and total cholesterol. At the same time, it seems that the levels of LDL and HDL do not have a statistically significant effect on the primary outcome. This was probably caused by the high collinearity found in the data sample.

The absence of correlation with LDL and HDL levels is in line with the results obtained from three studies by Alsaadi et al. conducted between [16–18]. In those three studies conducted on a human experimental model, the authors did not report any causal relationship between hypercholesterolemia and implant failure, but hypercholesterolemia was analyzed in association with many other local and systemic factors; consequently, the results may not be

accurate. Furthermore, the method of measuring hypercholesterolemia had not been adequately clarified. Another retrospective cohort study did not find a significant association between an elevated triglyceride level and implant failure [23]. However, in the present study, MBL was analyzed as a primary outcome. Interestingly, in studies showing an inverse association between cholesterol levels and bone mineral density, this association is the same for both TG and LDL-cholesterol levels, whereas in our study, it was not the same [35, 36]. Therefore, further studies are required to better investigate the association between hypercholesterolemia and hypertriglyceridemia and their effect on bone metabolism.

Several *in vivo* animal studies demonstrate that a hyperlipidemic diet significantly increases implant loss as well as reduced bone-implant interface formation and strength. Obviously, human clinical correlation is required.

The limitations of the present study are related to the lack of previous clinical studies analyzing the effect of hyperlipidemia on MBL, the small study sample, the relatively short follow-up, and the lack of a bacterial analysis. Furthermore, patients' lipid profile was measured only once, at the beginning of the study, and it could have suffered variations during the follow-up.

## 5. Conclusions

Despite the limitations of the present study, the results support the hypothesis that peri-implant marginal bone loss may be influenced by a condition of hyperlipidemia. However, further studies are needed, with a larger sample and more extensive follow-up, to confirm these results.

## Data Availability

The datasets used and/or analyzed during the current study are available from the corresponding author on reasonable request.

## Ethical Approval

The present study received ethic approval from the ethical committee of Università Cattolica Del Sacro Cuore, with approval number N 4130.

## Consent

All patients were informed of their role in the present study and provided written informed consent.

## Disclosure

The abstract of the paper has been presented as a poster in "Rimini 23-25 Settembre 2021 Palazzo dei Congressi-per Odontoiatri Igienisti Dentali e Studenti-SIDP."

## Conflicts of Interest

The authors declare that they have no competing interests.

## References

- [1] T. Saxlin, L. Suominen-Taipale, A. Kattainen, J. Marniemi, M. Knuutila, and P. Ylöstalo, "Association between serum lipid levels and periodontal infection," *Journal of Clinical Periodontology*, vol. 35, no. 12, pp. 1040–1047, 2008.
- [2] R. L. Corwin, T. J. Hartman, S. A. Maczuga, and B. I. Graubard, "Dietary saturated fat intake is inversely associated with bone density in humans: analysis of NHANES III," *The Journal of Nutrition*, vol. 136, no. 1, pp. 159–165, 2006.
- [3] M. S. Huang, S. Morony, J. Lu et al., "Atherogenic phospholipids attenuate osteogenic signaling by BMP-2 and parathyroid hormone in osteoblasts," *The Journal of Biological Chemistry*, vol. 282, no. 29, pp. 21237–21243, 2007.
- [4] F. Pirih, J. Lu, F. Ye et al., "Adverse effects of hyperlipidemia on bone regeneration and strength," *Journal of Bone and Mineral Research*, vol. 27, no. 2, pp. 309–318, 2012.
- [5] Y. Tintut, S. Morony, and L. L. Demer, "Hyperlipidemia promotes osteoclastic potential of bone marrow cells ex vivo," *Arteriosclerosis, Thrombosis, and Vascular Biology*, vol. 24, no. 2, pp. e6–10, 2004.
- [6] Y. Tintut and L. L. Demer, "Effects of bioactive lipids and lipoproteins on bone," *Trends in Endocrinology and Metabolism*, vol. 25, no. 2, pp. 53–59, 2014.
- [7] M. R. Brodeur, L. Brissette, L. Falstrault, P. Ouellet, and R. Moreau, "Influence of oxidized low-density lipoproteins (LDL) on the viability of osteoblastic cells," *Free Radical Biology & Medicine*, vol. 44, no. 4, pp. 506–517, 2008.
- [8] S. Dündar, F. Yaman, M. F. Ozupek et al., "The effects of high-fat diet on implant osseointegration: an experimental study," *Journal of the Korean Association of Oral and Maxillofacial Surgeons*, vol. 42, no. 4, pp. 187–192, 2016.
- [9] M. Krieger, "The "best" of cholesterol, the "worst" of cholesterol: a tale of two receptors," *Proceedings of the National Academy of Sciences of the United States of America*, vol. 95, no. 8, pp. 4077–4080, 1998.
- [10] E. Luegmayer, H. Glantschnig, G. A. Wesolowski et al., "Osteoclast formation, survival and morphology are highly dependent on exogenous cholesterol/lipoproteins," *Cell Death and Differentiation*, vol. 11, Suppl 1, pp. S108–S118, 2004.
- [11] J. Choukroun, G. Khoury, F. Khoury et al., "Two neglected biological risk factors in bone grafting and implantology: high low-density lipoprotein cholesterol and low serum vitamin D," *The Journal of Oral Implantology*, vol. 40, no. 1, pp. 110–114, 2014.
- [12] S. Fedele, W. Sabbah, N. Donos, S. Porter, and F. D' Aiuto, "Common oral mucosal diseases, systemic inflammation, and cardiovascular diseases in a large cross-sectional US survey," *American Heart Journal*, vol. 161, no. 2, pp. 344–350, 2011.
- [13] E. C. Gaetti-Jardim, J. F. Santiago-Junior, M. C. Goiato, E. P. Pellizer, O. Magro-Filho, and E. G. Jardim Junior, "Dental implants in patients with osteoporosis," *The Journal of Craniofacial Surgery*, vol. 22, no. 3, pp. 1111–1113, 2011.
- [14] R. Olivares-Navarrete, A. L. Raines, S. L. Hyzy et al., "Osteoblast maturation and new bone formation in response to titanium implant surface features are reduced with age," *Journal of Bone and Mineral Research*, vol. 27, no. 8, pp. 1773–1783, 2012.
- [15] A. Keuroghlian, A. D. Barroso, G. Kirikian et al., "The effects of hyperlipidemia on implant osseointegration in the mouse femur," *The Journal of Oral Implantology*, vol. 41, no. 2, pp. e7–e11, 2015.
- [16] G. Alsaadi, M. Quirynen, A. Komárek, and D. van Steenberghe, "Impact of local and systemic factors on the incidence of oral implant failures, up to abutment connection," *Journal of Clinical Periodontology*, vol. 34, no. 7, pp. 610–617, 2007.
- [17] G. Alsaadi, M. Quirynen, A. Komarek, and D. van Steenberghe, "Impact of local and systemic factors on the incidence of late oral implant loss," *Clinical Oral Implants Research*, vol. 19, no. 7, pp. 670–676, 2008.
- [18] G. Alsaadi, M. Quirynen, K. Michiles, W. Teughels, A. Komárek, and D. van Steenberghe, "Impact of local and systemic factors on the incidence of failures up to abutment connection with modified surface oral implants," *Journal of Clinical Periodontology*, vol. 35, no. 1, pp. 51–57, 2008.
- [19] Y. H. Choi, T. Kosaka, M. Ojima et al., "Relationship between the burden of major periodontal bacteria and serum lipid profile in a cross-sectional Japanese study," *BMC Oral Health*, vol. 18, no. 1, p. 77, 2018.
- [20] G. Gómez-Moreno, A. Aguilar-Salvatierra, J. Rubio Roldán, J. Guardia, J. Gargallo, and J. L. Calvo-Guirado, "Peri-implant evaluation in type 2 diabetes mellitus patients: a 3-year study," *Clinical Oral Implants Research*, vol. 26, no. 9, pp. 1031–1035, 2015.
- [21] P. Galindo-Moreno, A. Leon-Cano, I. Ortega-Oller, A. Monje, F. O'Valle, and A. Catena, "Marginal bone loss as success criterion in implant dentistry: beyond 2 mm," *Clinical Oral Implants Research*, vol. 26, no. 4, pp. e28–e34, 2015.
- [22] M. B. Tekin and H. Toker, "The effect of hyperlipidemia on bone graft regeneration of peri-implant created defects in rabbits," *Int J Implant Dent*, vol. 5, no. 1, p. 18, 2019.
- [23] F. Tirone, S. Salzano, L. D'Orsi, P. Paola, and D. Rodi, "Is a high level of total cholesterol a risk factor for dental implants or bone grafting failure? A retrospective cohort study on 227 patients," *European Journal of Oral Implantology*, vol. 9, no. 1, pp. 77–84, 2016.
- [24] A. Insua, A. Monje, H. L. Wang, and R. J. Miron, "Basis of bone metabolism around dental implants during osseointegration and peri-implant bone loss," *Journal of Biomedical Materials Research. Part A*, vol. 105, no. 7, pp. 2075–2089, 2017.
- [25] F. Parhami, "Possible role of oxidized lipids in osteoporosis: could hyperlipidemia be a risk factor?," *Prostaglandins, Leukotrienes, and Essential Fatty Acids*, vol. 68, no. 6, pp. 373–378, 2003.
- [26] N. M. Rajamannan, "Low-density lipoprotein and aortic stenosis," *Heart*, vol. 94, no. 9, pp. 1111–1112, 2008.
- [27] X. M. Lu, H. Zhao, and E. H. Wang, "A high-fat diet induces obesity and impairs bone acquisition in young male mice," *Molecular Medicine Reports*, vol. 7, no. 4, pp. 1203–1208, 2013.
- [28] J. Lange, T. Barz, A. Ekkernkamp, I. Klötting, and N. Follak, "Gene expression profile in bone of diabetes-prone BB/OK rats fed a high-fat diet," *Genes & Nutrition*, vol. 8, no. 1, pp. 99–104, 2013.
- [29] A. P. Sage, J. Lu, E. Atti et al., "Hyperlipidemia induces resistance to PTH bone anabolism in mice via oxidized lipids," *Journal of Bone and Mineral Research*, vol. 26, no. 6, pp. 1197–1206, 2011.
- [30] D. Rokaya, V. Srimaneepong, W. Wisitrasameewon, M. Humagain, and P. Thunyakitpisal, "Peri-implantitis update: risk indicators, diagnosis, and treatment," *Eur J Dent*, vol. 14, no. 4, pp. 672–682, 2020.



## *Retraction*

# **Retracted: Exploring Purification Methods of Exosomes from Different Biological Samples**

### **BioMed Research International**

Received 5 December 2023; Accepted 5 December 2023; Published 6 December 2023

Copyright © 2023 BioMed Research International. This is an open access article distributed under the Creative Commons Attribution License, which permits unrestricted use, distribution, and reproduction in any medium, provided the original work is properly cited.

This article has been retracted by Hindawi, as publisher, following an investigation undertaken by the publisher [1]. This investigation has uncovered evidence of systematic manipulation of the publication and peer-review process. We cannot, therefore, vouch for the reliability or integrity of this article.

Please note that this notice is intended solely to alert readers that the peer-review process of this article has been compromised.

Wiley and Hindawi regret that the usual quality checks did not identify these issues before publication and have since put additional measures in place to safeguard research integrity.

We wish to credit our Research Integrity and Research Publishing teams and anonymous and named external researchers and research integrity experts for contributing to this investigation.

The corresponding author, as the representative of all authors, has been given the opportunity to register their agreement or disagreement to this retraction. We have kept a record of any response received.

### **References**

- [1] X. Qian, F. Xie, and D. Cui, "Exploring Purification Methods of Exosomes from Different Biological Samples," *BioMed Research International*, vol. 2023, Article ID 2336536, 9 pages, 2023.

## Research Article

# Exploring Purification Methods of Exosomes from Different Biological Samples

Xiaoqing Qian,<sup>1,2</sup> Feng Xie<sup>ID</sup>,<sup>3</sup> and Daxiang Cui<sup>ID</sup><sup>2</sup>

<sup>1</sup>School of Biomedical Engineering, Shanghai Jiao Tong University, Shanghai, China

<sup>2</sup>School of Sensing Science and Engineering, Shanghai Jiao Tong University, Shanghai, China

<sup>3</sup>Department of Thoracic Surgery, Renji Hospital, School of Medicine, Shanghai Jiao Tong University, 160 Pujian Road, Shanghai 200127, China

Correspondence should be addressed to Daxiang Cui; [dx cui@sjtu.edu.cn](mailto:dx cui@sjtu.edu.cn)

Received 8 June 2022; Revised 14 August 2022; Accepted 18 August 2022; Published 19 April 2023

Academic Editor: Dinesh Rokaya

Copyright © 2023 Xiaoqing Qian et al. This is an open access article distributed under the Creative Commons Attribution License, which permits unrestricted use, distribution, and reproduction in any medium, provided the original work is properly cited.

**Objective.** Exosomes were extracted from a variety of biological samples using several different purification processes, and our goal was to determine which method and sample were the most effective for exosome extraction. **Methods.** We used ExoQuick-TC combined with ultrafiltration to separate and purify exosomes from the supernatant of gastric cancer cells, while we used the ExoQuick kit and ultracentrifugation to purify exosomes from human serum samples. Furthermore, exosomes were isolated and purified from human urine samples by diafiltration and from postparturition human breast milk samples by the filtration-polyethylene glycol precipitation method. The isolated exosomes were morphologically analyzed using a transmission electron microscope, the particle size was measured by NanoSight, and the protein content was analyzed by western blotting. **Results.** The isolated exosomes showed an obvious cup holder shape, with a clear outline and typical exosome morphological characteristics. The sizes of exosomes derived from gastric cancer cell supernatant, serum, urine, and milk were  $65.8 \pm 26.9$  nm,  $87.6 \pm 50.9$  nm,  $197.5 \pm 55.2$  nm, and  $184.1 \pm 68.7$  nm, respectively. Western blot results showed that CD9 and TSG101 on the exosomes were expressed to varying degrees based on the exosome source. Exosome abundance was higher in the serum, urine, and breast milk than in the supernatant. It is suggested that its exosomes can be extracted to obtain an excellent potential biological source of exosomes. **Conclusion.** In this study, the extraction and separation methods of foreign bodies from different biological samples were obtained, and it was found that human breast milk was a potential excellent material for administration because of its high abundance.

## 1. Introduction

To study the internal components of exosomes, it is important to extract them with high quality. Due to their small size, NanoSight detects exosomes along with other biomolecules. Furthermore, the separation and purification of exosomes are difficult, which hinders further research on them. In recent years, researchers have developed various separation and purification methods based on the physicochemical properties of exosomes. These techniques consist of ultracentrifugation [1], density gradient ultracentrifugation [2], ultrafiltration [3], polymer

precipitation utilizing polyethylene glycol (PEG) [4], immunomagnetic beads [5], and kit separation [6–8]. To successfully isolate exosomes, it is necessary to first evaluate the quality of the extraction, which involves checking the purity, vesicle state, yield, and repeatability of the process. Next, the appropriate technical approaches should be chosen.

Exosomes may be found in a variety of biological materials, such as cell supernatant, serum, urine, and milk. The purpose of this research was to identify procedures that are practicable, trustworthy, effective, and cost-effective for separating and purifying exosomes.

## 2. Materials and Methods

**2.1. Different Candidate Biological Samples.** The exosomes were isolated from various biological samples from four candidates, including gastric cancer cell supernatant, serum, urine, and breast milk. The purity and relative yield of exosomes from the different samples were compared. The research was authorized by the Medical Ethics Committee of Renji Hospital with informed patient consent (Number 2018160).

**2.2. Exosome Purification from Gastric Cancer Cell Supernatant.** SGC7901 is a gastric cancer cell line that was developed in our laboratory. To prepare a complete cell culture medium, 10 mL of inactivated fetal bovine serum (FBS) and 1 mL of penicillin-streptomycin were added to 90 mL of Dulbecco's modified Eagle medium (DMEM) minimal medium or 90 mL of RPMI 1640 basal medium. The mixture was then placed in the refrigerator at a temperature of 4 degrees Celsius until it was ready for use. The cells were cultivated in medium containing 1% FBS, and they were allowed to grow until they reached approximately 80% confluency. Before collecting the cell supernatants, the medium described above was switched out for one that was devoid of exosomes and serum and waited 24 hours. We isolated exosomes from the cell culture supernatant using the ExoQuick-TC kit (System Biosciences, CA, USA) according to the manufacturer's protocol. Briefly, the cell culture supernatant was collected and centrifuged ( $3000 \times g$ , 15 min) to remove cells or cell debris. After centrifugation, we transferred the supernatant to a sterile tube and added 2 mL of ExoQuick-TC extract per 10 mL of cell culture supernatant with an overnight incubation at 4°C. After incubation, the solution was centrifuged at 4°C at  $1500 \times g$  for 30 min. A whitish precipitate was observed at the bottom of the centrifuge tube, and the supernatant was removed and centrifuged again with phosphate-buffered saline (PBS) at  $1500 \times g$  for 5 min. Subsequently, after carefully removing the liquid components from the upper layer, the precipitate was resuspended in PBS.

Because the ExoQuick-TC method directly extracts the cell culture supernatant to obtain more precipitates and few effective exosomes, the exosomes in the cell culture supernatant were concentrated and then precipitated for extraction. Alternatively, we could combine the ExoQuick-TC method with ultrafiltration. In this method, the cell culture supernatant was taken, and the cells or cell debris was removed by centrifugation ( $3000 \times g$ , 15 min). The supernatant was then transferred to a 30 kDa Millipore-Ultra 15 ultrafiltration tube and centrifuged (4°C,  $4000 \times g$ , 30 min), and the ultrafiltrate from the inner network was aspirated. The ExoQuick-TC extract was added to the supernatant at a 1:5 ratio, and the tubes were centrifuged upside down, mixed evenly, and left at 4°C overnight. After overnight incubation followed by centrifugation (4°C,  $1500 \times g$ , 30 min), an off-white precipitate appeared at the bottom of the centrifuge tube. The supernatant was removed and centrifuged again after adding buffer ( $1500 \times g$ , 5 min), the

liquid portion was carefully removed from the upper layer, and the precipitate was resuspended in PBS.

We found that both the ExoQuick-TC precipitation method for direct exosome extraction and the extraction of exosomes by ExoQuick-TC combined with ultrafiltration have few effective exosomes and more pseudoproteins. To further extract the effective exosomes, the shape and size of the exosomes were examined. Extraction was carried out using a modified version of the gold standard ultracentrifugation method for extracting exosomes. The collected cell supernatant (200 mL) was placed in four 50 mL centrifuge tubes. The dead cells were removed by centrifugation, followed by the removal of the cell debris (4°C,  $2000 \times g$ , 10 min and 4°C,  $1000 \times g$ , 30 min). The supernatant was transferred to 40 mL ultra-high-speed centrifuge tubes and subjected to ultra-high-speed centrifugation at  $110000 \times g$  for 70 min. After centrifugation, we discarded the supernatant while retaining 5 mL of liquid at the bottom of the centrifuge tube. The resuspended liquid was gently blown through a sterile straw to make the exosome adhere to the centrifuge tube. The second centrifugation at  $110000 \times g$  for 70 min revealed a pale yellow precipitate at the bottom of the centrifuge tube, leaving 1 mL of liquid after removal of the supernatant. The precipitate was resuspended in PBS to the required volume of 5 mL. After the third centrifugation ( $110000 \times g$  for 70 min), the supernatant was carefully removed to leave 200  $\mu$ L of liquid, which was resuspended in PBS for precipitation to the required volume of 5 mL. After the fourth centrifugation at  $110000 \times g$  for 70 min, we discarded the supernatant, transferred the collected exosomes to 1.5 mL Eppendorf tubes, and stored them at -80°C for subsequent use.

Finally, exosomes were isolated from the cell supernatants. Ten milliliters of the supernatants was centrifuged at three thousand revolutions per minute for ten minutes to remove dead cells and cell debris. The remaining supernatants were centrifuged at ten thousand revolutions per minute for sixty minutes and filtered through a sterile filter with a 0.22-micron opening. After aspirating the supernatant, an equivalent volume of a self-prepared PEG solution that contained 16 grams of PEG6000 and 5.844 grams of NaCl in 100 milliliters of double-distilled water was added. The exosome solution was brought to its final concentration of 8% PEG6000 by the precipitation process. After incubating the combination at 4 degrees Celsius for 12 hours, centrifuging it at 12,000 revolutions per minute for thirty minutes, and then resuspending the pellet in sterile PBS, it was placed in storage at either 4 degrees Celsius or -80 degrees Celsius for later use.

**2.3. Serum Exosome Purification.** Two alternative approaches were used for exosome purification from serum samples. For the ExoQuick (System Biosciences) separation method, serum was collected and centrifuged ( $3000 \times g$ , 15 min) to remove cells or cell debris. The supernatants were transferred to a clean sterile tube, 50  $\mu$ L of ExoQuick extract per 250  $\mu$ L of serum was added, and the centrifuge tube was incubated at 4°C for 30 min, followed by centrifugation (4°C,  $1500 \times g$ , 30 min). We observed an off-white precipitate at the bottom



of the centrifuge tube, and the supernatant was removed and centrifuged again after adding buffer ( $1500 \times g$ , 5 min). Subsequently, the liquid components on the upper layer were carefully removed, and the precipitate was resuspended in one-tenth of the original volume of sterile water.

We further used an alternative method to purify serum exosomes by ultracentrifugation. After ultracentrifugation and lysing,  $250 \mu\text{L}$  of cell-free serum samples were thawed on ice, diluted with 3 mL of PBS, filtered through a  $0.22 \mu\text{m}$  filter, and centrifuged ( $15,000 \times g$ ,  $4^\circ\text{C}$ , overnight). The supernatant was discarded and centrifuged ( $15,000 \times g$ ,  $4^\circ\text{C}$ , 2 h) with 1 mL of PBS-resuspended precipitate. Subsequently, the supernatant was removed and stored at  $-80^\circ\text{C}$  for subsequent use.

**2.4. Urine Exosome Purification.** We centrifuged 20 mL of freshly obtained urine at 3000 rpm for 5 min. The resulting supernatant was filtered through a sterile  $0.22 \mu\text{m}$  filter to remove larger impurity particles. Subsequently, 10–20 mL of the filtrate obtained in the above procedure was added to a 300 kDa dialysis bag (Spectrum). The dialysis was carried out in PBS for 6–10 h, with approximately 800 mL of PBS replaced every 3 h. The miscellaneous proteins and other molecules were dialyzed out, leaving the exosomes. The exosome concentration was diluted due to more PBS addition. The diluted exosome was added into a 100 kDa ultrafiltration tube and ultrafiltered at 3000 rpm for 5–8 min to concentrate the exosome volume.

**2.5. Purification of Breast Milk Exosomes.** Three tubes (approximately 10 mL per tube) of breast milk samples were collected at 7 h, 1 d, 7 d, 14 d, and 28 d after delivery and stored in liquid nitrogen for subsequent experiments. We centrifuged 5 mL of breast milk at 3000 rpm for 10 min to remove the fat globules and cells from the milk. Furthermore, the supernatant was centrifuged at 10000 rpm for 60 min and filtered through a  $0.22 \mu\text{m}$  sterile filter to remove the debris. The supernatant was aspirated, and an equal volume of the self-prepared PEG solution was added. Subsequently, a final concentration of 8% PEG6000 in the exosome solution was precipitated and incubated at  $4^\circ\text{C}$  for 12 h. The mixtures were centrifuged at 12,000 rpm for 30 min, and the precipitate was resuspended in sterile PBS and stored at  $4^\circ\text{C}$  or  $-80^\circ\text{C}$ .

**2.6. Morphological Analysis of Exosomes.** The extracted exosomes were resuspended in PBS to obtain a 50-fold dilution, and  $20 \mu\text{L}$  drops were sucked onto the sample-carrying copper mesh with an aperture of 2 nm by a pipette gun. After standing for 2 min, the excess liquid was removed with filter paper. The exosomes were negatively stained with  $30 \mu\text{L}$  of 2% uranium acetate solution for 5 min at room temperature. Following the removal of the surplus liquid using filter paper, the sample was allowed to dry at room temperature before being imaged using a transmission electron microscope.

**2.7. Detection of Exosome Particle Size by NanoSight.** Dynamic light scattering was used for the detection and study of the particle size distribution of exosomes. The collected exosomes were diluted to a particle concentration of

106–109/mL by PBS and injected into the NanoSight NS300 nanoparticle tracking analyzer (Malvern Panalytical, UK) with a 1 mL syringe for nanoparticle tracking analysis (NTA).

**2.8. Quantitative Analysis of Protein.** We used the bicinchoninic acid (BCA) assay kit for quantitative protein estimation. First, to cleave the exosome proteins, the exosome sample that had been frozen at  $-80^\circ\text{C}$  was removed and thawed on ice for 10 min at room temperature. Then,  $200 \mu\text{L}$  of RIPA lysis buffer containing an inhibitory enzyme was added. After lysis was performed on ice for 15 min, the lysate was centrifuged at  $12,000 \times g$  for 5 min, and the supernatant was collected for analysis.

Next, a 25 mg/mL protein standard solution was prepared, and  $20 \mu\text{L}$  was removed and diluted to  $0.5 \text{ mg}/\mu\text{L}$  by adding  $980 \mu\text{L}$  of diluent. Based on the number of samples, the BCA working solution was prepared in a 50:1 ratio of BCA reagent solution A and solution B. Eight gradients of standard protein concentrations were prepared, and  $20 \mu\text{L}$  of the standards was added to a 96-well plate. After the samples were diluted,  $20 \mu\text{L}$  of the samples was also added to a 96-well plate, and two wells were set for each sample. Next,  $200 \mu\text{L}$  of the working solution was added to each well. The 96-well plate was shaken gently and placed in a  $37^\circ\text{C}$  incubator for 30 min, and the optical density (OD) value was quantified at a wavelength of 562 nm.

For western blotting, we employed the Wes automated system. This device uses Simple Western technology to subvert the classic western blot approach used for more than 30 years. It separates, captures, fixes, immunodetects, and analyzes samples in the same tube. It is employed in protein property identification, quantitative analysis, function study, modification, differential expression, and antibody research.

We performed western blotting according to the manufacturer's instructions. Briefly, we switched on the instrument and computer and opened the Compass software. Next, the reagents and protein samples were added to the microplate and centrifuged at 2500 rpm for 5 min at room temperature. Then, the aluminum foil on the prepared microplate was carefully torn off, and the microplate was placed in the position of the plate holder. A capillary was placed in the cartridge holder position, and the hatch was closed. Then, we set the assay conditions on the Compass software. It is recommended to start the experiment with the default program, namely, protein separation, voltage 375 V, separation time of 25 min, antibody blocking time of 15 min, primary and secondary antibody incubation for 30 min each, a sample loading time of 9 s, a concentration time of 15 s, and an exposure time of 15–480 s. We monitored the running status of the instrument and the expected end time of the experiment by selecting the Run Summary key on the software.

### 3. Results

**3.1. Analysis of Nanoparticle Size and Morphology of the Exosomes.** The TEM images of exosomes isolated from the different biological samples are shown in Figure 1. The

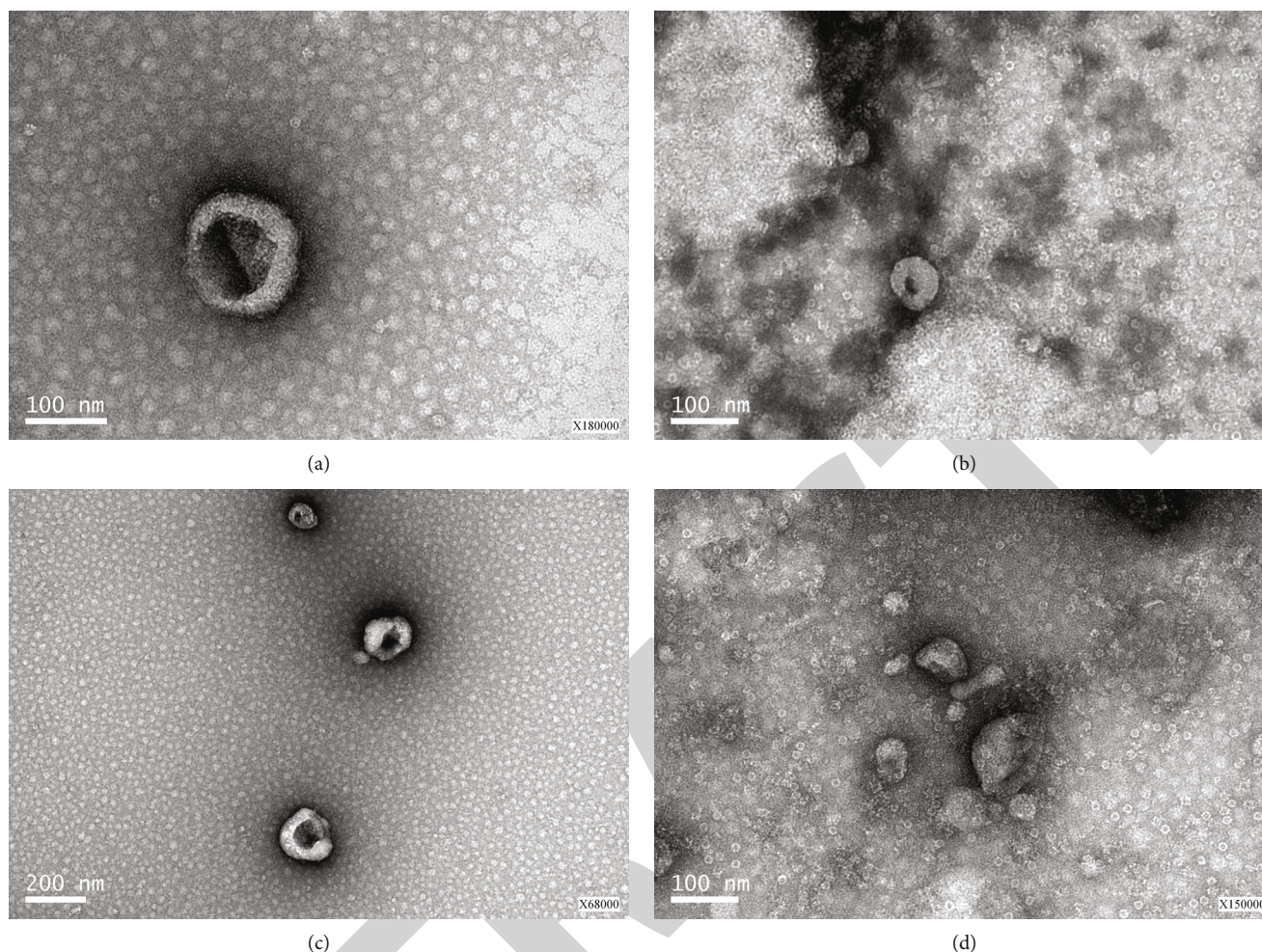


FIGURE 1: TEM images of exosomes from each biological sample. (a) Cell supernatant exosomes. (b) Serum exosomes. (c) Urine exosomes. (d) Milk exosomes.

particle size and distribution of exosomes from different samples were analyzed, and the results are shown in Figure 2.

As shown in Table 1, the parameters of the particle size of D10, D50, and D90 represent the size values measured by 10%, 50%, and 90% of the particle size. D10 refers to the particle size corresponding to when the particle distribution number reaches 10% after adding the fraction of all particle sizes smaller or larger than it. D50 (median diameter or median particle size) refers to the size of the particles in a sample when 50% of the particles are of a size lower than it and 50% of the particles are of a size greater than it. The value D50 is utilized as a representation of the powder's typical particle size. D90 refers to the particle size at which 90% of all particles have a size that is either lower than or greater than D90.

**3.2. Analysis of the Expression Level of Exosome Markers.** The purified exosomes isolated from normal human serum, normal human urine, gastric cancer serum, gastric cancer urine, and breast milk samples were examined by western blot for the expression levels of exosome markers TSG101 and CD9, and  $\beta$ -actin was used as an internal reference.

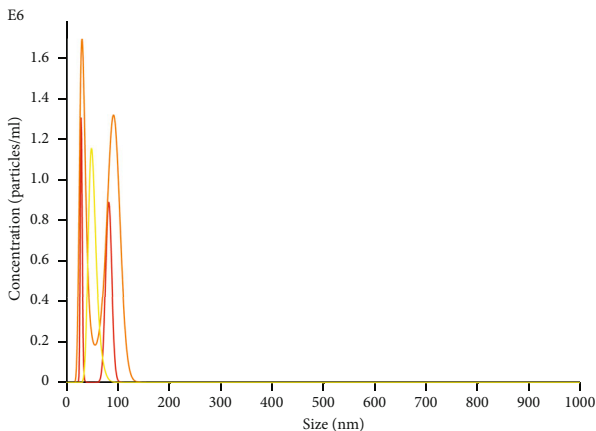
We found that the abundance of exosomes in serum, urine, and breast milk was high. This indicated that serum, urine, and breast milk could potentially be used as biological sources for extracting exosomes (Figure 3).

#### 4. Discussion

In this study, we explored the extraction and separation methods of exosomes derived from gastric cancer cell supernatant, serum, urine, and milk and analyzed the obtained exosomes with a biological transmission electron microscope, NTA particle size, and protein CD9 and TSG101 expressions. We found that breast milk samples had abundant exosome content. This finding corroborates some previous studies that have analyzed the structure, properties, and components, especially the nutritional components, of animal milk-derived exosomes or extracellular vesicles in cattle and sheep [9]. Milk-derived extracellular vesicles have unique biological characteristics and physiological functions. The outer vesicles of milk-derived cells contain various miRNAs (including miR-148a-3p, miR-182-5p, miR-30b-5p, let-7b, let-7a and let-7f, miR-148a, miR-200a-3p, Let-7a, let-7b, let-7f, miR-148a-3p, miRNA-320, and miRNA-

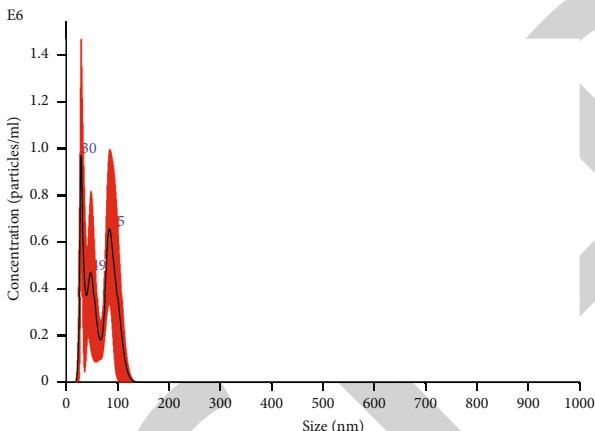
# NANOSIGHT

1-1 1 2019-01-22 16-05-38



FTLA Concentration/Size graph for Experiment:  
1-1 1 2019-01-22 16-05-38

- 1-1 1 2019-01-22 16-05-52~16-05-52
- 1-1 1 2019-01-22 16-06-14~16-06-14
- 1-1 1 2019-01-22 16-06-35~16-06-35

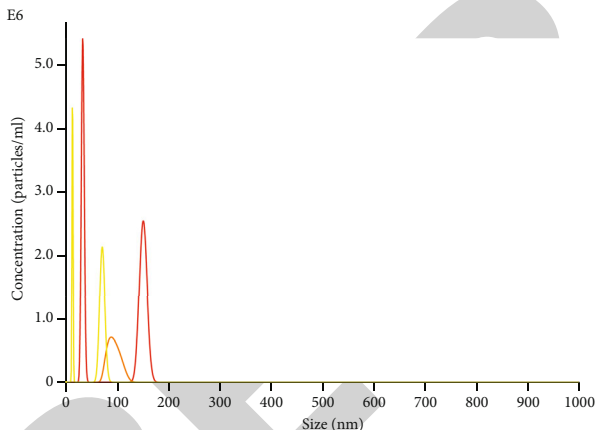


Averaged FTLA Concentration/Size for Experiment:  
1-1 1 2019-01-22 16-05-38

Error bars indicate +/- 1 standard error of the mean

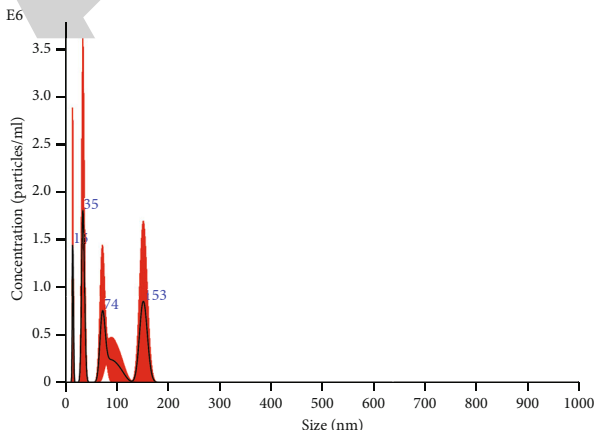
# NANOSIGHT

3-1 2019-01-22 16-32-49



FTLA Concentration/Size graph for Experiment:  
3-1 2019-01-22 16-32-49

- 3-1 2019-01-22 16-33-02~16-33-02
- 3-1 2019-01-22 16-33-24~16-33-24
- 3-1 2019-01-22 16-33-45~16-33-45



Averaged FTLA Concentration/Size for Experiment:  
3-1 2019-01-22 16-32-49

Error bars indicate +/- 1 standard error of the mean

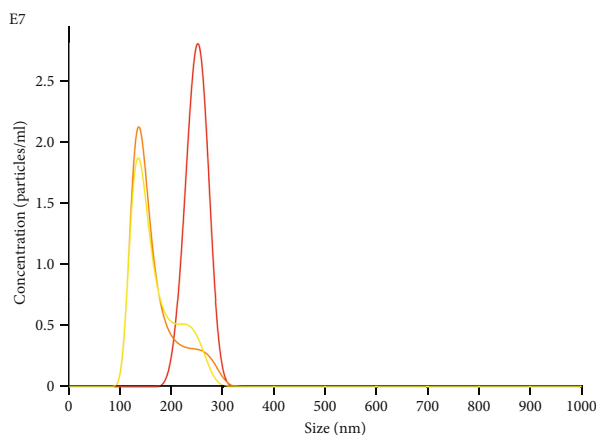
(b)

FIGURE 2: Continued.



# NANOSIGHT

5 2019-01-22 12-30-20



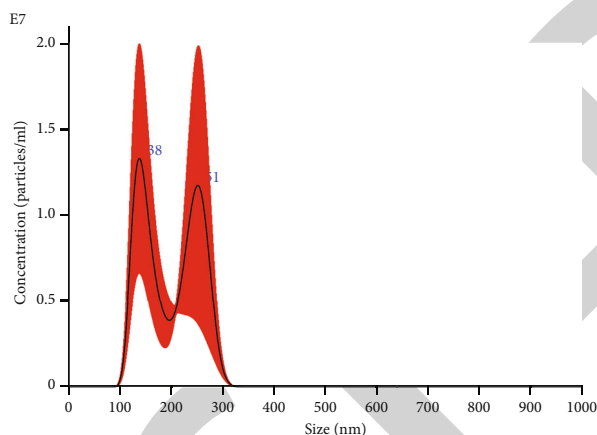
FTLA Concentration/Size graph for Experiment:

5 2019-01-22 12-30-20

— 5-12-30-31

— 5-12-30-55

— 5-12-31-25



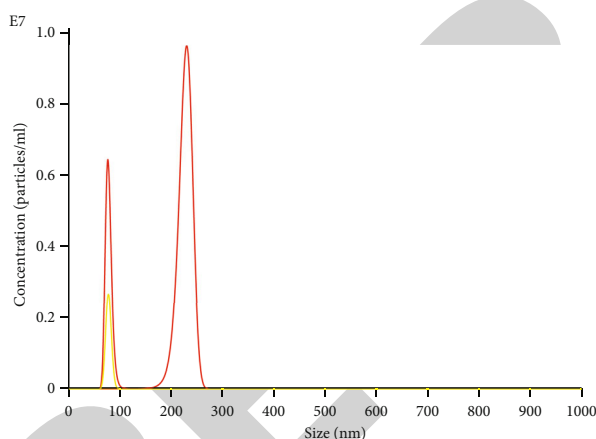
Averaged FTLA Concentration/Size for Experiment:

5 2019-01-22 12-30-20

Error bars indicate +/-1 standard error of the mean

# NANOSIGHT

2 2019-01-23 14-16-16



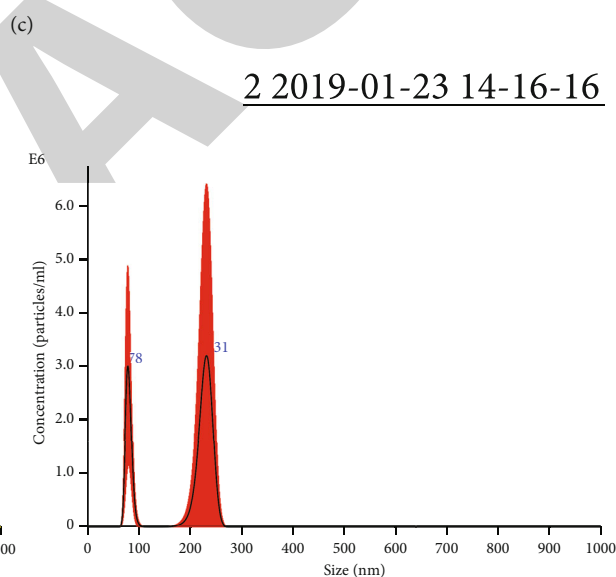
FTLA Concentration/Size graph for Experiment:

2 2019-01-23 14-16-16

— 2-14-16-46

— 2-14-17-07

— 2-14-17-28



Averaged FTLA Concentration/Size for Experiment:

2 2019-01-23 14-16-16

Error bars indicate +/-1 standard error of the mean

(d)

FIGURE 2: Graph of NTA test results for each biological sample. (a) Cell supernatant. (b) Serum exosome. (c) Urine exosome. (d) Milk exosome.

TABLE 1: Particle size distribution of exosomes from different biological samples.

Sample source	Mean (nm)	SD (nm)	D10 (nm)	D50 (nm)	D90 (nm)
Gastric cancer cell supernatant	65.8	26.9	29.1	66.4	99.2
Serum	87.6	50.9	30.0	76.9	155.0
Urine	197.5	55.2	126.5	198.0	267.2
Breast milk	184.1	68.7	75.4	220.2	241.4

SD: standard deviation.

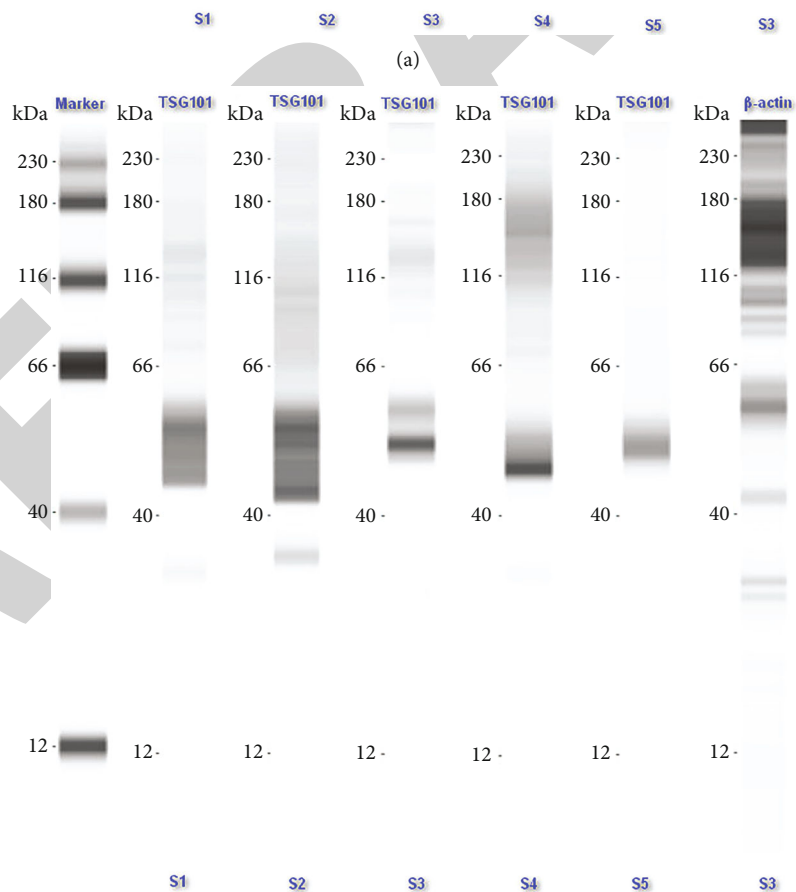
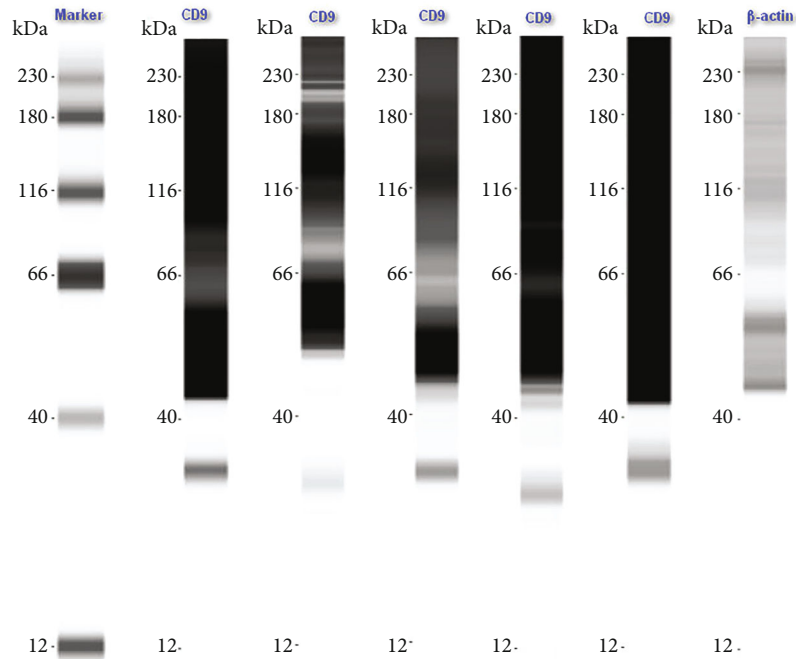


FIGURE 3: CD9 (a) and TSG101 (b) expressions on exosomes from each sample. S1: normal human serum; S2: normal urine; S3: serum of gastric cancer patients; S4, urine of a gastric cancer patient; S5: breast milk.

375) [10–14], which can be absorbed by the intestinal tract of the baby. The miRNAs of milk-derived extracellular vesicles can resist an acidic environment and enzymatic hydrolysis of the digestive tract [15]. Due to the contents of milk-derived exosomes, animals suffering from conditions such as osteoporosis and colitis are more likely to benefit from treatment with these exosomes [16, 17]. In a similar manner, tiny extracellular vesicles generated from swine milk have the ability to boost quantities of immunoglobulins secreted by the intestines as well as raise the expression of polymeric immunoglobulin receptors [18]. Yak milk-derived exosomes reduce lipopolysaccharide-induced intestinal inflammation by inhibiting the activation of the PI3K/AKT/C3 pathway [19].

In this study, TSG101 and CD9 were used as exosome markers. The vesicle-related molecules used for exosome identification other than TSG101 and CD9 include CD63 and CD81 [20]. In addition, CD14, Flot-1, and VDAC1 are also known exosomal markers [21]. TSG101 is one of the most commonly known exosomes [22]. The TSG101 protein belongs to a group of apparently inactive homologs of ubiquitin-binding enzymes. It is a component of the ESCRT-I complex and a regulator of vesicle transport. TSG101 mediates exosome biogenesis and promotes exosome release and has been widely used as a marker to identify the composition and abundance of exosomes [23–25]. The release of exosomes requires the joint coordination of TSG101 and SDCBP, CD63, and syndecan [26]. CD9, another critical exosome marker after CD63 and TSG101, is a member of the four-transmembrane protein family. Four-transmembrane protein is a cell surface glycoprotein with four transmembrane domains that can form multimeric complexes with other cell surface proteins. CD9 is more abundant than CD63 in terms of stability and release [27]. Several studies have monitored the changes in CD9 to understand the modulation of the secretion ability and stability of exosomes [28–31]. The expression of TSG101 was shown to have a positive correlation with that of CD9 in this investigation, indicating that there was consistency in the indication of exosome concentration.

## 5. Conclusion

In this work, techniques for extracting and separating exosomes originating from various biological resources were investigated. Based on our findings, we concluded that human breast milk is a potentially ideal material for exosome administration owing to the high exosome abundance it contains.

## Data Availability

The datasets used and analyzed during this study are available from the corresponding author on reasonable request.

## Conflicts of Interest

The authors declare that they have no competing interests.

## Authors' Contributions

Xiaoqing Qian and Daxiang Cui designed and directed the study. Xiaoqing Qian and Feng Xie collected the data and wrote the paper. All authors read and approved the final manuscript. Xiaoqing Qian and Feng Xie have contributed equally to this work.

## Acknowledgments

This work was supported by grants from the National Key Research and Development Program of China (No. 2017YFA0205301 and No. 2017YFA0205304) and the National Natural Science Foundation of China (No. 81903169, No. 82072767, No. 81770145, and No. 81602192).

## References

- [1] D. Yang, W. Zhang, H. Zhang et al., "Progress, opportunity, and perspective on exosome isolation - efforts for efficient exosome-based theranostics," *Theranostics*, vol. 10, no. 8, pp. 3684–3707, 2020.
- [2] Z. Zhang, C. Wang, T. Li, Z. Liu, and L. Li, "Comparison of ultracentrifugation and density gradient separation methods for isolating Tca8113 human tongue cancer cell line-derived exosomes," *Oncology Letters*, vol. 8, no. 4, pp. 1701–1706, 2014.
- [3] M. Hayashi, K. Kuroda, K. Ihara, T. Iwaya, and E. Isogai, "Suppressive effect of an analog of the antimicrobial peptide of LL-37 on colon cancer cells via exosome-encapsulated miRNAs," *International Journal of Molecular Medicine*, vol. 42, no. 6, pp. 3009–3016, 2018.
- [4] K. Otani, Y. Fujioka, M. Okada, and H. Yamawaki, "Optimal isolation method of small extracellular vesicles from rat plasma," *International Journal of Molecular Sciences*, vol. 20, no. 19, p. 4780, 2019.
- [5] Q. Tan, D. Xia, and X. Ying, "miR-29a in exosomes from bone marrow mesenchymal stem cells inhibit fibrosis during endometrial repair of intrauterine adhesion," *International Journal of Stem Cells*, vol. 13, no. 3, pp. 414–423, 2020.
- [6] Y. Chen, Y. Song, J. Huang et al., "Increased circulating exosomal miRNA-223 is associated with acute ischemic stroke," *Frontiers in Neurology*, vol. 8, p. 57, 2017.
- [7] H. Wei, X. Qian, F. Xie, and D. Cui, "Isolation of exosomes from serum of patients with lung cancer: a comparison of the ultra-high speed centrifugation and precipitation methods," *Annals of translational medicine*, vol. 9, no. 10, p. 882, 2021.
- [8] A. Weber, S. S. Liu, L. Cardone et al., "The course of circulating small extracellular vesicles in patients undergoing surgical aortic valve replacement," *BioMed Research International*, vol. 2020, Article ID 6381396, 12 pages, 2020.
- [9] S. L. Ong, C. Blenkiron, S. Haines et al., "Ruminant milk-derived extracellular vesicles: a nutritional and therapeutic opportunity?," *Nutrients*, vol. 13, no. 8, p. 2505, 2021.
- [10] N. Kosaka, H. Izumi, K. Sekine, and T. Ochiya, "microRNA as a new immune-regulatory agent in breast milk," *Silence*, vol. 1, no. 1, p. 7, 2010.
- [11] M. J. C. van Herwijnen, T. A. P. Driedonks, B. L. Snoek et al., "Abundantly present miRNAs in milk-derived extracellular vesicles are conserved between mammals," *Frontiers in Nutrition*, vol. 5, p. 81, 2018.

## *Retraction*

# **Retracted: Intra- and Interrater Agreement of Face Esthetic Analysis in 3D Face Images**

### **BioMed Research International**

Received 5 December 2023; Accepted 5 December 2023; Published 6 December 2023

Copyright © 2023 BioMed Research International. This is an open access article distributed under the Creative Commons Attribution License, which permits unrestricted use, distribution, and reproduction in any medium, provided the original work is properly cited.

This article has been retracted by Hindawi, as publisher, following an investigation undertaken by the publisher [1]. This investigation has uncovered evidence of systematic manipulation of the publication and peer-review process. We cannot, therefore, vouch for the reliability or integrity of this article.

Please note that this notice is intended solely to alert readers that the peer-review process of this article has been compromised.

Wiley and Hindawi regret that the usual quality checks did not identify these issues before publication and have since put additional measures in place to safeguard research integrity.

We wish to credit our Research Integrity and Research Publishing teams and anonymous and named external researchers and research integrity experts for contributing to this investigation.

The corresponding author, as the representative of all authors, has been given the opportunity to register their agreement or disagreement to this retraction. We have kept a record of any response received.

### **References**

- [1] M. Park, H.-N. Mai, M. Y. Mai, T. T. Win, D.-H. Lee, and C.-H. Lee, "Intra- and Interrater Agreement of Face Esthetic Analysis in 3D Face Images," *BioMed Research International*, vol. 2023, Article ID 3717442, 7 pages, 2023.

## Research Article

# Intra- and Interrater Agreement of Face Esthetic Analysis in 3D Face Images

Minsoo Park <sup>1</sup>, Hang-Nga Mai <sup>2,3</sup>, Mai Yen Mai<sup>1</sup>, Thaw Thaw Win<sup>1</sup>, Du-Hyeong Lee <sup>1,3</sup>, and Cheong-Hee Lee<sup>1</sup>

<sup>1</sup>Department of Prosthodontics, School of Dentistry, Kyungpook National University, 2177 Dalgubeoldae-ro, Jung-Gu, Daegu 41940, Republic of Korea

<sup>2</sup>Dental School of Hanoi University of Business and Technology, 10000 Hanoi, Vietnam

<sup>3</sup>Institute for Translational Research in Dentistry, Kyungpook National University, 2177 Dalgubeoldae-ro, Jung-Gu, Daegu 41940, Republic of Korea

Correspondence should be addressed to Du-Hyeong Lee; deweylee@knu.ac.kr

Received 12 August 2022; Revised 21 September 2022; Accepted 25 January 2023; Published 10 April 2023

Academic Editor: Dinesh Rokaya

Copyright © 2023 Minsoo Park et al. This is an open access article distributed under the Creative Commons Attribution License, which permits unrestricted use, distribution, and reproduction in any medium, provided the original work is properly cited.

The use of three-dimensional (3D) facial scans for facial analysis is increasing in maxillofacial treatment. The aim of this study was to investigate the consistency of two-dimensional (2D) and 3D facial analyses performed by multiple raters. Six men and four women (25–36-year-old) participated in this study. The 2D images of the smiling and resting faces in the frontal and sagittal planes were obtained. The 3D facial and intraoral scans were merged to generate virtual 3D faces. Ten clinicians performed facial analyses by investigating 14 indices of 2D and 3D faces. Intra- and interrater agreements of the results of 2D and 3D facial analyses within and among the participants were evaluated. The intrarater agreement between the 2D and 3D facial analyses varied according to the indices. The highest and lowest agreements were found for the dental crowding index (0.94) and smile line curvature index (0.56) in the frontal plane, and Angle's classification (canine) index (0.98) and occlusal plane angle index (0.55) in the profile plane. In the frontal plane, the interrater agreements were generally higher for the 3D images than for the 2D images, while in the profile plane, the interrater agreements were high in the Angle's classification (canine) index however low in the other indices. Several occlusion-related indices were missing in the 2D images because the posterior teeth were not observed. Esthetic analysis results between 2D and 3D face images can differ according to the evaluation indices. The use of 3D faces is recommended over 2D images to increase the reliability of facial analyses, as it can fully assess both esthetic and occlusion-related indices.

## 1. Introduction

A symmetrical face, along with an attractive smile, is essential for maintaining and improving a person's esthetic appearance, self-esteem, and quality of life [1]. Therefore, to enhance treatment quality, facial esthetic analysis has been performed as a routine diagnostic method in various dental fields such as orthodontics, prosthetics, and maxillofacial surgery [2]. Face analysis is performed to evaluate the structure of a face using various esthetic indicators [3]. This analysis provides valuable data to effectively plan the treatment, enable direct consultations with the patient, and help predict the prognosis of treatment [4]. Therefore, a visualized treatment plan can be

established through the results of the analysis and consultations for clinicians to effectively communicate with the patient and finalize the goal of treatment.

In the past, esthetic analysis primarily consisted of two-dimensional (2D) radiographs and camera photographs [5]. Panoramic radiographs and lateral cephalometry were used to perform skeletal analysis [6], and soft tissues were analyzed in a static state using camera photographs [7]. With these static images, various methods were suggested to analyze the face for ideal beauty. For the simple and intuitive comparison, evaluation of the facial symmetry, and the proportion of each facial part using the golden ratio has been considered the most fundamental method [8, 9]. Moreover, growth analysis, such



as the Ricketts, Downs, and Steiner methods, and computational analysis by Pascal are conducted [2, 10]. However, in this 2D analysis, image distortion and related errors can occur. For instance, 2D radiographic techniques, such as panoramic and lateral cephalometry, lack transverse information and the precise location of anatomical structures [11]. In addition, 2D profile photographs may not completely reflect actual facial perceptions because facial depth and shape are not considered [3]. As traditional 2D images cannot exactly reflect real three-dimensional (3D) results, communication between dentists and patients becomes challenging.

With the advancement of digital dentistry, devices, and computer software for facial esthetic analysis have been developed [12, 13]. Currently, 3D reconstruction of the jaws using cone-beam computed tomography is widely used for radiographic diagnosis in dental treatments [14]. The 3D soft tissue data on the face can also be obtained using 3D face scanning [15]. To obtain the structure of the oral cavity, intraoral optical scanning is currently replacing conventional physical impressions and stone-cast fabrication [16]. When extraoral and intraoral data are acquired digitally, it becomes possible to produce a virtual face in 3D. Although 3D facial analysis has attracted significant interest, there have been only a few studies on the reproducibility of 3D analysis. Therefore, we aimed to compare the consistency of the 3D-face-based facial esthetic analysis conducted by multiple evaluators with that of conventional 2D-photographic-based facial analysis.

## 2. Materials and Methods

To collect images for facial analysis, 10 adults (six men, four women; 25–36 years of age) with no history of facial injury, pathology, or cosmetic/maxillofacial surgery were recruited. The participants provided consent and were aware of the purpose of the study. The study procedure is shown in Figure 1 and was approved by the ethical research board of Kyungpook National University Dental Hospital (approval number: KNUDH-2021-11-05-00).

For data collection, 2D facial images of all participants were obtained using a digital camera (D5600, Nikon, Tokyo, Japan) with a macro lens (AF-S Dx Micro Nikkor 85 mm 1:3.5G ED VR, Nikon, Tokyo, Japan) (Figures 2(a) and 2(b)). Frontal and sagittal-plane photographs of the smiling and resting faces were taken. The distance between the camera and the participant was set at 2 m, and the head position was maintained with the Frankfort plane parallel to the floor. Smile photographs were obtained pronouncing “cheese” sounds to make participants smile consistently. To eliminate the impact caused by the change of light source, all photographs were taken in the same place indoors with led lights. All photos were taken with the setting of aperture of  $f/11$ , shutter speed of  $1/60$ s, and standard ISO speeds 200. Photographs were saved in the joint photographic expert’s group (JPEG) format with a resolution of 3000 dots per inch (DPI). The 3D facial images were collected using a 3D facial scanner (RAYFace; Ray, Seoul, Korea) (Figure 2(c) and 2(d)). The 3D images were acquired of smiling and resting faces with and without an extraoral marker tray [17]. The dental arch was scanned using an intraoral scanner (i700, MEDIT, Seoul, Korea) to acquire

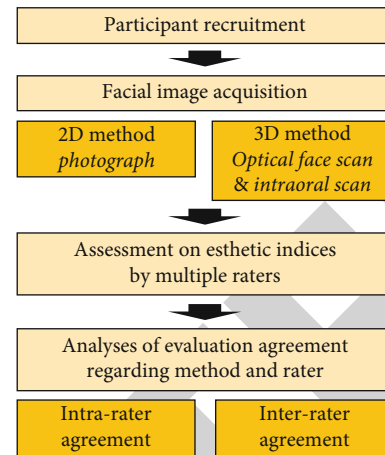


FIGURE 1: Workflow of this study.

images of the dentition, which were saved in the polygon file format. In image management software (RAYFace), the 3D facial and intraoral scan images were merged using the extraoral marker tray images (Figure 3). All 2D and 3D image collections were performed by a trained clinician

Facial esthetic analysis was performed by investigating 14 indices (Table 1). Among these, eight indices were evaluated in the frontal images, and six indices were evaluated in the profile image (Figure 4). Ten clinicians participated in the esthetic analysis. Before initiating the analysis, the evaluators were educated regarding the definition and evaluation methods of each esthetic index. All evaluations were performed in images without a built-in measurement tool. The degrees of intrarater agreement between the results of 2D and 3D esthetic facial analyses in the same participant and interrater agreement among the evaluators on the results of 2D and 3D esthetic facial analyses were evaluated.

## 3. Results

In the facial esthetic evaluation at the frontal plane, the degree of intrarater agreement between 2D and 3D face image analyses was the highest for the dental crowding index (0.94) and the lowest for the smile line curvature index (0.56) (Table 2). Overall, the interpupillary line, midline deviation, and dental crowding indices showed high interrater agreement, while the smile line curvature, lip line level, and facial type indices demonstrated low interrater agreement values (Table 3). The interrater agreement in the commissural line and facial symmetry indices was higher in the 3D images than in the 2D images; meanwhile, the degree of agreement in midline deviation and lip line level indices was lower in 3D images than in 2D images.

Regarding facial esthetic evaluation at the profile plane, the intrarater agreement of results between 2D and 3D face image analyses was the highest in the Angle’s classification (canine) index (0.98) and the lowest in the occlusal plane angle index (0.55) (Table 4). The interrater agreement was high for Angle’s classification index; however, for the other indices, the agreement values were generally low (Table 5). There were missing values in the evaluation of the 2D images for occlusal plane

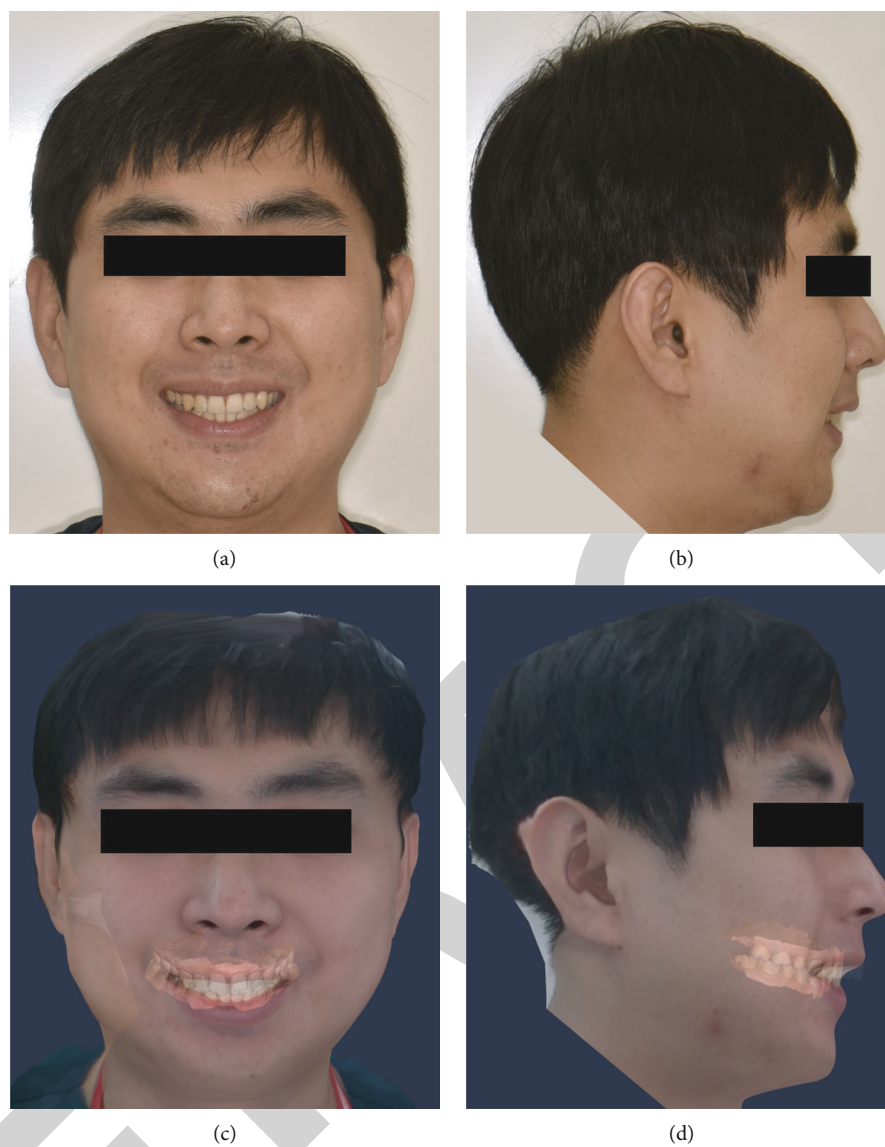


FIGURE 2: Face image collection. (a) Two-dimensional (2D) photograph at the frontal plane. (b) 2D photograph at the sagittal plane. (c) Three-dimensional (3D) scan image at the frontal plane. (d) 3D scan image at the sagittal plane.

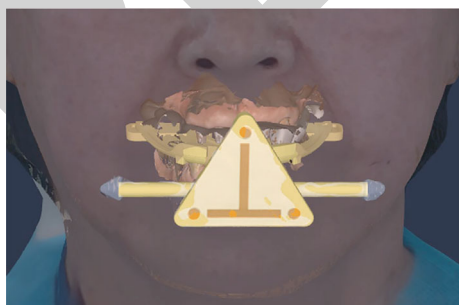


FIGURE 3: Facial scan with an extraoral marker tray.

angle and Angle's classification indices. In particular, Angle's classification index, which is based on the relationship with the first molar, could not be examined by a single evaluator in the 2D images. For all indices of the profile images, the

interrater agreements in the 3D images were similar to those in the 2D images.

#### 4. Discussion

This study was designed to investigate the consistency between 2D and 3D facial analyses and to examine the degree of agreement among ratters. The results of this study showed that the intrarater agreement of the results between 2D and 3D face image analyses differed according to the evaluation indices. For example, an intrarater agreement between 2D and 3D face images was high for Angle's classification (canine) index, whereas it was low for the occlusal plane angle index. Therefore, it is thought that different face analyses can be made in the same evaluator according to the image the decision was made.

In the frontal plane evaluations, the indices with a high interrater agreement in both 2D and 3D images were the

TABLE 1: Evaluation index for facial esthetic analysis.

View	Facial expression	Evaluation index	Level		
Frontal	Smile	Interpupillary line	Parallel Rt. slanted Lt. Slanted		
		Commissural line	Parallel Rt. slanted Lt. Slanted		
		Smile line curvature	Upward Straight Downward		
		Midline deviation	Accompany Rt. Lt.		
		High lip line	High Intermediate Low		
	Resting		Dental crowding	Crowding Normal Spacing	
			Facial type	Dolichocephalic Mesocephalic Brachycephalic	
			Facial symmetry	Symmetrical Asymmetrical	
			Smile	Occlusal plane angle	Parallel Clockwise Counter clockwise
					Angle's classification (canine)
Angle's classification (first molar)	I II III				
Profile	Resting	Profile shape	Normal Convex Concave		
		Frankfort-mandibular plane angle (FMA)	High Average Low		
		Lip protrusion	Protruded Intermediate Retruded		

interpupillary line, midline deviation, dental crowding, and Angle's classification indices, because these esthetic indices are easy to observe and less affected by the angle of viewing the image and have objective judgement criteria. As for the profile plane evaluations, Angle's classification index demonstrated high intra- and interrater agreement because it was evaluated according to a fixed reference point: the buccal groove of the mandibular first molar and mesiobuccal cusp of the maxillary first molar. Meanwhile, the smile line curvature, lip line level, facial type, profile shape, Frankfort-mandibular plane angle, and lip protrusion indices showed a low interrater agreement. The inconsistency of judgements may arise from the subjective characteristics of the criteria because the observers' perspectives

could be different, depending on the viewing angle [18]. In this study, the interrater agreement was low for most indices that used reference planes such as the occlusal, Camper's, mandibular, and Frankfort planes evaluated in the profile plane. As these planes are imagined, intuitive evaluation of these planes without directly observing them on an image may be less objective [19]. In esthetic evaluations, subjective judgments may occur, which may cause differences in judgments between ratters [20]. Therefore, rather than the type of image, the precise definition of the index for facial analysis and the evaluation method that can be performed objectively are considered important.

In 2D facial images, Angle's classification of molars was not evaluated. This was because the molars could not be

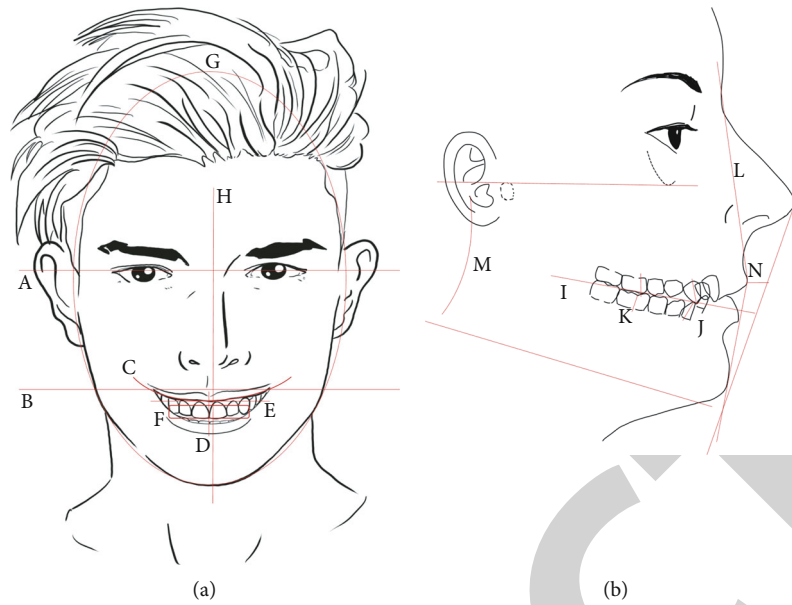


FIGURE 4: Evaluation index for facial esthetic analysis. (a) Frontal image. (b) Profile image. (A) Interpupillary line. (B) Commissural line. (C) Smile line curvature. (D) Midline deviation. (E) High lip line. (F) Dental crowding. (G) Facial type. (H) Facial symmetry. (I) Occlusal plane angle. (J) Angle’s classification (canine). (K) Angle’s classification (first molar). (L) Profile shape. (M) Frankfort-mandibular plane angle (FMA). (N) Lip protrusion.

TABLE 2: Intrarater agreement of evaluation results between the two-dimensional (2D) and three-dimensional (3D) frontal face images.

Evaluation index	Image	N	AR (%)
Interpupillary line	2D-3D	100	88
Commissural line	2D-3D	100	74
Smile line curvature	2D-3D	100	56
Midline deviation	2D-3D	100	82
Lip line level	2D-3D	100	74
Dental crowding	2D-3D	100	94
Facial type	2D-3D	100	78
Facial symmetry	2D-3D	100	82

AR: agreement ratio; 2D-3D: between 2D and 3D images.

observed in the 2D facial profile photographs. The 3D imaging technologies have been used in dentistry [21]. Currently, the facial and intraoral scan images can be merged to generate a complete virtual 3D face with a full dental arch. Furthermore, polygonal resources such as tooth and jaw models can be managed using 3D computer image software; thus, the state of the dentition can be evaluated by adjusting the transparency of the facial scan image and clinicians can also obtain an in-depth perception of both the teeth and face by freely changing the angle of view [22]. Accordingly, the 3D method enabled occlusion-related evaluations, which were impossible using the 2D method. Furthermore, 3D image presentation can aid in measuring the actual sizes and shapes of anatomical structures [23]. Thus, 3D environmental settings may facilitate treatment planning and virtual treatment practices [24, 25].

The accuracy of the image integration of the digital dental model and the 3D facial image is affected by the capability of the 3D face scans to provide a clear appearance of the anterior teeth [26]. In the photogrammetry face scanning method,

TABLE 3: Interrater agreement of evaluation results in the two-dimensional (2D) and three-dimensional (3D) frontal face images.

Evaluation index	Image	N	AR (%)
Interpupillary line	2D	100	94
	3D	100	86
Commissural line	2D	100	70
	3D	100	82
Smile line curvature	2D	100	59
	3D	100	54
Midline deviation	2D	100	91
	3D	100	81
Lip line level	2D	100	71
	3D	100	59
Dental crowding	2D	100	96
	3D	100	94
Facial type	2D	100	62
	3D	100	62
Facial symmetry	2D	100	79
	3D	100	87

AR: Agreement ratio.

multiple single-lens reflex cameras are positioned at a fixed distance and angle from the object to ensure overlapping fields of view; thus, the oral area image in the face scan is often deformed because of limitations in the depth recognition of device and light accessibility. The faulty image reconstruction of the tooth structure on the face scan could be problematic for the tooth-based matching method to correctly conduct the dentofacial image integrations [17]. In this study, to enhance the accuracy of image matching, an extraoral marker tray was used. The artificial markers supply distinct reference



TABLE 4: Intrarater agreement of evaluation results between the two-dimensional (2D) and three-dimensional (3D) profile face images.

Evaluation index	Image	N	AR (%)
Occlusal plane angle	2D-3D	93	0.55
Angle's classification (canine)	2D-3D	49	0.98
Angle's classification (1st molar)	2D-3D	0	—
Profile shape	2D-3D	100	0.73
Frankfort-mandibular plane angle	2D-3D	100	0.63
Lip protrusion	2D-3D	100	0.64

AR: Agreement ratio, 2D-3D: Between 2D and 3D images.

TABLE 5: Interrater agreement of evaluation results in the two-dimensional (2D) and three-dimensional (3D) profile face images.

Evaluation index	Image	N	AR (%)
Occlusal plane angle	2D	93	59
	3D	100	64
Angle's classification (canine)	2D	49	98
	3D	100	88
Angle's classification (1st molar)	2D	0	—
	3D	100	81
Profile shape	2D	100	57
	3D	100	58
Frankfort-mandibular plane angle	2D	100	60
	3D	100	63
Lip protrusion	2D	100	53
	3D	100	51

AR: agreement ratio.

landmarks that appeared in both the oral and facial images; thereby facilitating the image-matching process and enhancing the accuracy of the matching results.

This study attempted to include the effects of human-related factors by involving multiple participants and raters; however, the sample size was limited. Considering the diversity of ethnicity and clinical experience, large-scale clinical studies are required to generalize the findings of this study [27]. Additionally, the use of only a single 3D face scanner could be another limitation of this study. Previous studies reported that ambient spectral light could influence the quality of images in the scanners with stereophotogrammetry, but had little impact in the scanners with laser and structured-light technologies [28, 29]. During 3D image taking, direct and strong ambient light may cause a glare effect that obscures the surface details [28]. Thus, further studies should include various types of 3D face scanners and computer software for 3D visualization with various light sources.

## 5. Conclusions

Within the limitations of this study, the following conclusions were drawn:

- (1) Based on the agreement ratio of the 2D and 3D facial analyses, the facial analysis results within and among

the evaluators could be different according to the evaluation indices and type of facial images

- (2) Esthetic indices that are less affected by the angle of viewing the image and have objective judgment criteria exhibited higher interrater agreement in both 2D and 3D images. Thus, to increase the reliability of the facial analysis, objective assessment criteria, and evaluation methods are needed
- (3) The use of 3D faces combined with tooth images is recommended over 2D images, as it enables both esthetic and occlusion-related evaluations, which were not allowed in the 2D method

## Data Availability

The data used to support the findings of this study have been included in this manuscript.

## Conflicts of Interest

The authors declare that there is no conflict of interest regarding the publication of this paper.

## Authors' Contributions

All authors have seen the manuscript and approved to submit to this journal. Du-Hyeong Lee and Cheong-Hee Lee contributed equally to this work.

## Acknowledgments

This research was supported by the Korea Medical Device Development Fund grant funded by the Korean Government (the Ministry of Science and ICT, the Ministry of Trade, Industry and Energy, the Ministry of Health & Welfare, Republic of Korea, and the Ministry of Food and Drug Safety) (202011A02) and the Bio & Medical Technology Development Program of the National Research Foundation of Korea grant funded by the Korean Government (2020R1I1A1A01062967).

## References

- [1] M. E. Moskowitz and A. Nayyar, "Determinants of dental esthetics: a rationale for smile analysis and treatment," *Compendium of Continuing Education in Dentistry*, vol. 16, no. 12, pp. 1164–1166, 1995.
- [2] P. Margossian, G. Laborde, S. Koubi, D. Tardivo, and P. Magne, "Determination of facial references for esthetic restorative treatment," *The International Journal of Periodontics & Restorative Dentistry*, vol. 41, no. 1, pp. 113–119, 2021.
- [3] D. M. Sarver and M. B. Ackerman, "Dynamic smile visualization and quantification: part 2. Smile analysis and treatment strategies," *American Journal of Orthodontics and Dentofacial Orthopedics*, vol. 124, no. 2, pp. 116–127, 2003.
- [4] M. Benecke, J. Kasper, C. Heesen, N. Schäffler, and D. R. Reissmann, "Patient autonomy in dentistry: demonstrating the role for shared decision making," *BMC Medical Informatics and Decision Making*, vol. 20, no. 1, p. 318, 2020.

## *Retraction*

# **Retracted: Effect of Early Low-Calorie Enteral Nutrition Support in Critically Ill Patients: A Systematic Review and Meta-analysis**

### **BioMed Research International**

Received 9 February 2023; Accepted 9 February 2023; Published 14 February 2023

Copyright © 2023 BioMed Research International. This is an open access article distributed under the Creative Commons Attribution License, which permits unrestricted use, distribution, and reproduction in any medium, provided the original work is properly cited.

*BioMed Research International* has retracted the article titled “Effect of Early Low-Calorie Enteral Nutrition Support in Critically Ill Patients: A Systematic Review and Meta-analysis” [1] due to concerns that the peer review process has been compromised.

Following an investigation conducted by the Hindawi Research Integrity team [2], significant concerns were identified with the peer reviewers assigned to this article; the investigation has concluded that the peer review process was compromised. We therefore can no longer trust the peer review process and the article is being retracted with the agreement of the editorial board.

### **References**

- [1] Q. Jiang and T. Xu, “Effect of Early Low-Calorie Enteral Nutrition Support in Critically Ill Patients: A Systematic Review and Meta-analysis,” *BioMed Research International*, vol. 2022, Article ID 7478373, 8 pages, 2022.
- [2] L. Ferguson, “Advancing Research Integrity Collaboratively and with Vigour,” 2022, <https://www.hindawi.com/post/advancing-research-integrity-collaboratively-and-vigour/>.

## Retraction

# Retracted: Treatment Protocols in the Efficacy and Safety of Anti-EGFR Medicines in Combination with Standard Therapy for Patients with Nasopharyngeal Cancer: A Meta-Analysis

### BioMed Research International

Received 3 October 2023; Accepted 3 October 2023; Published 4 October 2023

Copyright © 2023 BioMed Research International. This is an open access article distributed under the Creative Commons Attribution License, which permits unrestricted use, distribution, and reproduction in any medium, provided the original work is properly cited.

This article has been retracted by Hindawi following an investigation undertaken by the publisher [1]. This investigation has uncovered evidence of one or more of the following indicators of systematic manipulation of the publication process:

- (1) Discrepancies in scope
- (2) Discrepancies in the description of the research reported
- (3) Discrepancies between the availability of data and the research described
- (4) Inappropriate citations
- (5) Incoherent, meaningless and/or irrelevant content included in the article
- (6) Peer-review manipulation

The presence of these indicators undermines our confidence in the integrity of the article's content and we cannot, therefore, vouch for its reliability. Please note that this notice is intended solely to alert readers that the content of this article is unreliable. We have not investigated whether authors were aware of or involved in the systematic manipulation of the publication process.

Wiley and Hindawi regrets that the usual quality checks did not identify these issues before publication and have since put additional measures in place to safeguard research integrity.

We wish to credit our own Research Integrity and Research Publishing teams and anonymous and named external researchers and research integrity experts for contributing to this investigation.

The corresponding author, as the representative of all authors, has been given the opportunity to register their agreement or disagreement to this retraction. We have kept a record of any response received.

### References

- [1] Y. Fang, J. Fan, and C. Yan, "Treatment Protocols in the Efficacy and Safety of Anti-EGFR Medicines in Combination with Standard Therapy for Patients with Nasopharyngeal Cancer: A Meta-Analysis," *BioMed Research International*, vol. 2023, Article ID 9477442, 7 pages, 2023.

## Research Article

# Treatment Protocols in the Efficacy and Safety of Anti-EGFR Medicines in Combination with Standard Therapy for Patients with Nasopharyngeal Cancer: A Meta-Analysis

Yakun Fang,<sup>1</sup> Jinlei Fan,<sup>1</sup> and Chao Yan <sup>2</sup>

<sup>1</sup>Obstetrics Department, Qingdao Municipal Hospital, Qingdao 266071, China

<sup>2</sup>Department of Radiation Oncology, Qilu Hospital (Qingdao), Cheeloo College of Medicine, Shandong University, 266035, China

Correspondence should be addressed to Chao Yan; [yanchaodoctor@hotmail.com](mailto:yanchaodoctor@hotmail.com)

Received 21 July 2022; Revised 4 August 2022; Accepted 11 August 2022; Published 6 February 2023

Academic Editor: Dinesh Rokaya

Copyright © 2023 Yakun Fang et al. This is an open access article distributed under the Creative Commons Attribution License, which permits unrestricted use, distribution, and reproduction in any medium, provided the original work is properly cited.

**Objective.** This study was conducted to compare the efficacy of standard therapy (radiotherapy/RT/CT) with that of antiepidermal growth factor receptor (anti-EGFR) monoclonal antibody (NPC) therapy in patients with advanced nasopharyngeal cancer. **Methods.** A meta-analysis was performed to meet the objective of this study. The English databases PubMed, Cochrane Library, and Web of Science were searched. The literature review compared anti-EGFR-targeted therapy with conventional therapy practices. The main outcome measure was overall survival (OS). Secondary goals were progression-free survival (PFS), locoregional recurrence-free survival (LRRFS), distant metastasis-free survival (DMFS), and adverse events (grade 3). **Results.** The database search resulted in 11 studies, with a total of 4219 participants. It was found that combining an anti-EGFR regimen with conventional therapy did not enhance OS (hazard ratio [HR] = 1.18; 95% confidence interval [CI] = 0.51 – 2.40;  $p = 0.70$ ) or PFS appreciably (HR = 0.95; 95%CI = 0.51 – 1.48;  $p = 0.88$ ) in patients with nasopharyngeal carcinoma. While LRRFS increased considerably (HR = 0.70; 95%CI = 0.67 – 1.00;  $p = 0.01$ ), the combined regimen did not improve DMFS (HR = 0.86; 95%CI = 0.61 – 1.12;  $p = 0.36$ ). Treatment-related adverse events included haematological toxicity (RR = 0.2; 95%CI = 0.08 – 0.45;  $p = 0.01$ ), cutaneous reactions (RR = 7.05; 95%CI = 2.15 – 23.09;  $p = 0.01$ ), and mucositis (RR = 1.96; 95%CI = 1.58 – 2.09;  $p = 0.01$ ). **Conclusions.** Individuals who have nasopharyngeal cancer do not have an increased chance of surviving until a local recurrence of their disease if they get normal therapy in addition to an anti-EGFR regimen. However, this combination does not enhance overall survival. On the other hand, this factor adds to an increase in the number of adverse effects.

## 1. Introduction

In 2018, more than 129,000 new cases of nasopharyngeal carcinoma (NPC) were recorded worldwide, with over 70% occurring in southern China and southeast Asia [1, 2], and they were commonly detected at an advanced stage [3]. Radiotherapy and chemotherapy are the main treatment options for NPC, and they considerably improve patient outcomes. However, recurrence and metastasis occur in 25% of cases, making them the most common reasons for treatment failure in advanced NPC cases [4]. Immune checkpoint therapy is now used to treat recurrent or metastatic nasopharyngeal carcinoma [5–7].

The epidermal growth factor receptor (EGFR) is a transmembrane glycoprotein belonging to the epidermal growth factor (EGF) family [8], and increased EGFR expression has been linked to a poor prognosis and outcome for a variety of cancers [9]. Systemic anti-EGFR medicines, such as cetuximab (CXT) and nimotuzumab (NTZ), have shown modest efficacy in clinical trials for nasopharyngeal cancer [10], but the results have been inconsistent [11–13]. It is also unknown whether combining anti-EGFR medicines with standard therapy increases the risk of bad outcomes. Therefore, to explore the efficacy and safety of anti-EGFR in combination with standard therapy for nasopharyngeal cancer patients, a comprehensive search and meta-analysis of



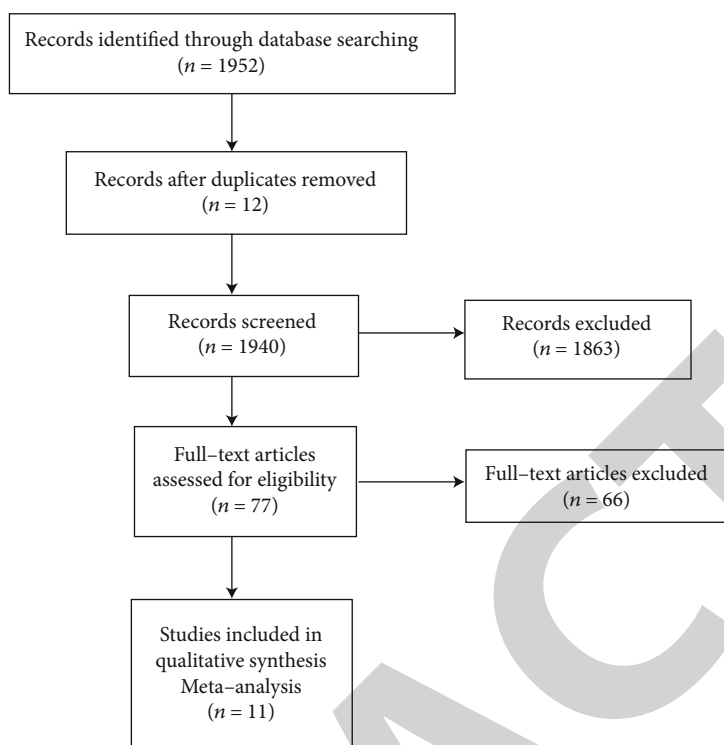


FIGURE 1: Selection procedure flowchart illustration.

randomised controlled trials were conducted in this study with the aim of rereporting relevant data for future therapy recommendations and clinical trials.

## 2. Data and Methods

**2.1. Literature Review.** Two independent reviewers combed through PubMed, Cochrane Library, Web of Science, and Embase for relevant articles from the time the databases were conceived to May 2022. They followed references given in the literature to reduce the likelihood of omissions and searched for grey literature. Nasopharyngeal neoplasms, EGFR inhibitor, cetuximab, panitumumab, and nimotuzumab were popular keywords [14, 15].

**2.2. Admission and Exclusion Criteria.** The eligibility criteria included the following: (i) articles examining the English language's linguistics, (ii) studies on reported case size, (iii) comparing EGFR-targeted therapy with standard treatment for individuals with nasopharyngeal cancer, and (iv) researches that clearly provide overall survival (OS) [16–18].

The exclusion criteria included the following: (i) publications that were not unique, (ii) publications we were unable to get the full text of, (iii) inadequate outcome indicators and evaluation standards, and (iv) indicators of result variability.

**2.3. Information Gathering.** The titles and abstracts of articles were examined, and duplicate articles and plainly unrelated or noncompliant literature were excluded. When the abstract and title were insufficient to determine whether the inclusion criteria were met, the entire content was scru-

tinised: the first author, year of publication, research stage, number of patients (per group), and outcomes (overall survival [OS], progression-free survival [PFS], locoregional recurrence-free survival [LRRFS], and distant metastasis-free survival [DMFS] as well as serious adverse events [SAEs]). The main result is OS, with PFS, LRRFS, and DMFS as supplementary endpoints [19–24]. Furthermore, various common SAEs between anti-EGFR drugs plus standard treatment and standard treatment alone were analysed. The data collection and analysis for this project were collaboratively performed by two researchers, with conflicts resolved through a consensus discussion or with the participation of a third researcher.

**2.4. Statistical Methods.** Data were collected and analysed using RevMan 5.3 software. The clinical heterogeneity of each included study was analysed first, followed by a chi-square examination of statistical heterogeneity. If  $I^2$  was less than 50%, a fixed-effects model was used for the data analysis. Furthermore, if there was no statistical heterogeneity between studies when the  $p$  value was greater than 0.05, a random-effects model was used and the sources of heterogeneity addressed [25–27]. RevMan 5.3 was used to check for possible publication bias, and the results were visually depicted. Meta-analysis of the included 11 research literatures should exclude the following three research results: those of poor quality, those with high weighting, and those with results that differed from other investigations. If two outcomes were identical, the conclusions were deemed stable; otherwise, they were unstable.

TABLE 1: Characteristics of included studies.

Author (yr)	Age (years), median (range)		Median follow-up	
	Anti-EGFR	Control	Anti-EGFR	Control
Wu (2014)	36 (26-57)	47 (32-63)	RT+h-R3	RT
Mei (2018)	45 (25-68)	44 (15-67)	CTX/NTX+CCRT	IC+CCRT
You (2017)	45 (12-69)	46 (15-74)	CTX/NTX+CCRT	CCRT
Mao (2019)	44 (17-72)	43 (13-73)	NTX/CTX+CRT	CRT
Hao (2018)	42 (36-51)	44 (36-51)	CTX/NTX+IC	IC
Wu (2007)	36 (26-57)	47 (32 + 63)	RT+h-R3	RT
Wang (2019)	44 (34-55)	44 (32-55)	NTZ+IMRT	IMRT
Li (2016)	60 (25-68)	60 (25-67)	RT+h-R3	RT+CDDP
Xia (2017)	44 (32-52)	44 (32-52)	CTX+CCRT	CCRT
Yang (2017)	46 (25-64)	46 (28-66)	CTX+CCRT	CCRT
You (2017)	46 (18-75)	47 (15-74)	CTX/NTX+IMRT	IMRT+CDDP

Note: anti-EGFR: anti-epidermal growth factor receptor. CTX; NTX; h-R3; IMRT; CDDP.

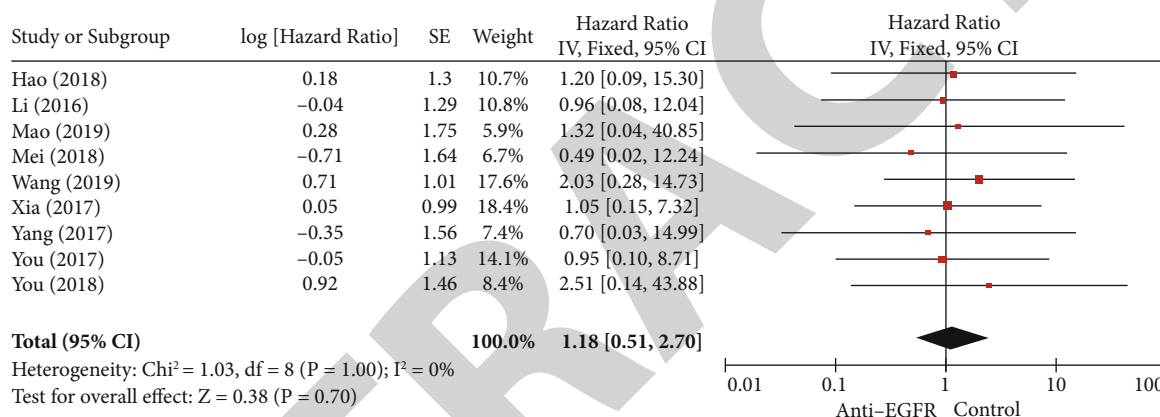


FIGURE 2: Forest diagram: anti-EGFR regimen plus standard therapy and standard therapy alone. Results: overall survival (OS).

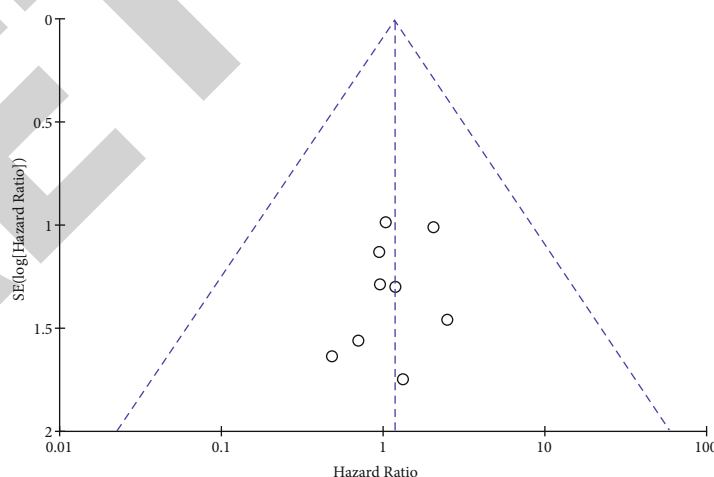


FIGURE 3: Comparison funnel chart: anti-EGFR regimen plus standard therapy and standard therapy alone; results: overall survival (OS).

### 3. Results

3.1. Literature Retrieval. Initially, 1952 related literatures were separately evaluated by title and abstract. After consolidation, 12 duplicate articles, 1650 animal-related studies,

189 meta-analyses, 12 inaccessible full-text articles, and 11 articles were eliminated from the full-text browsing synthesis (see Figure 1).

The inclusion criteria were met by 4129 observations (study subjects reported between 2007 and 2019, see Table 1).

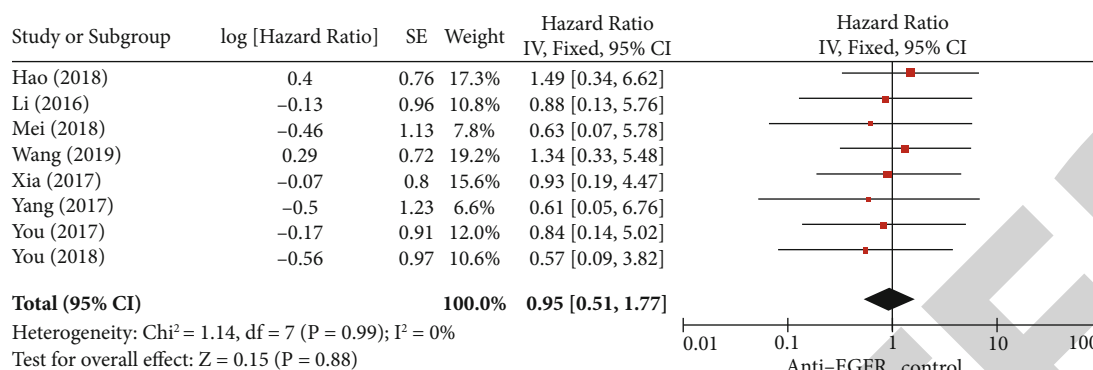


FIGURE 4: Forest diagram: anti-EGFR regimen plus standard treatment and standard treatment alone. Results: progression-free survival (PFS).

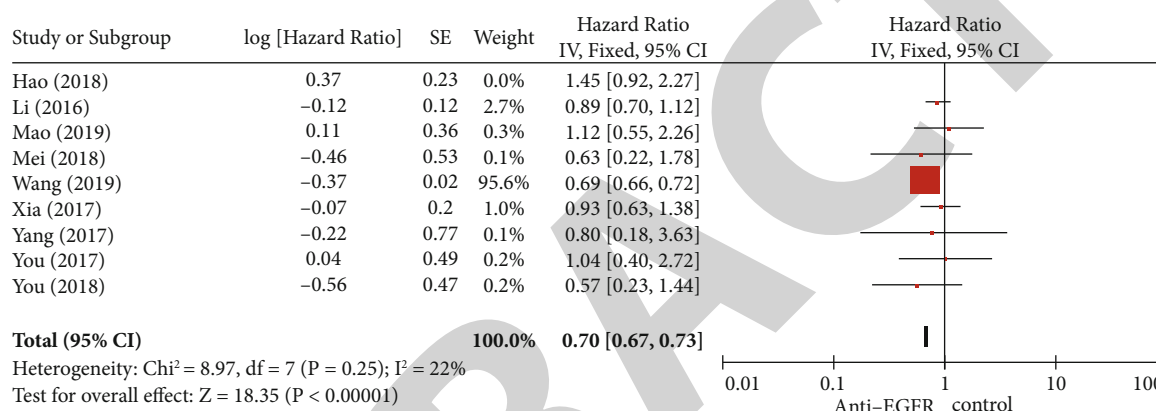


FIGURE 5: Forest diagram: anti-EGFR regimen plus standard treatment and standard treatment alone. Results: locoregional recurrence-free survival (LRRFS) rate.

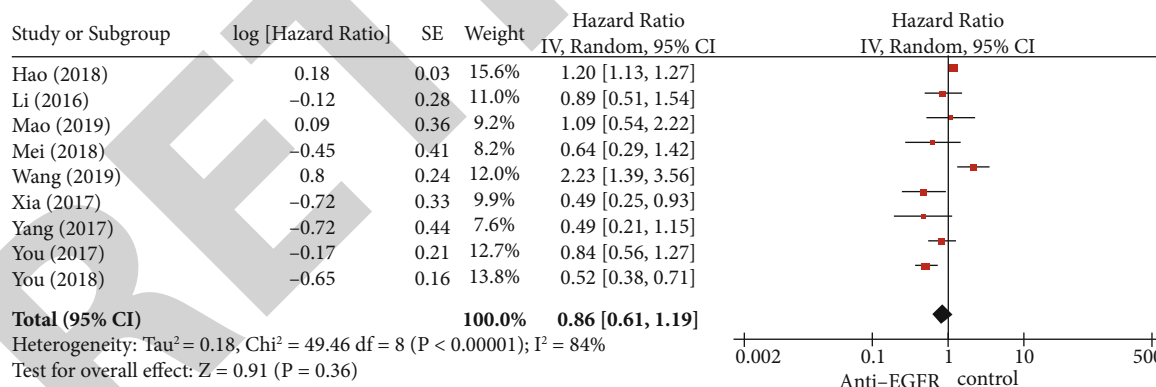


FIGURE 6: Forest plots of survival without distant metastases. Forest diagram: anti-EGFR regimen plus standard treatment and standard treatment alone. Results: survival without distant metastasis (DMFS).

Nine publications were tested for heterogeneity;  $I^2 = 0 < 50\%$ , and Q-test  $p = 1 > 0.05$  revealed that there was no substantial heterogeneity, due to which the meta-analysis was conducted using a fixed-effects model.

**3.2. Overall Survival.** Individuals with nasopharyngeal cancer who underwent anti-EGFR in addition to conventional therapy were found to have better survival rates, but the difference was not statistically significant ( $\text{HR} = 1.18$ ;  $95\% \text{CI} = 0.52 -$

$2.40$ ;  $p = 0.7$ ). Figure 2 presents a comparison between the OS rates of anti-EGFR therapy combined with standard therapy and standard therapy alone. The funnel plot comparing the two treatment approaches has the goal of assessing overall survival (OS). The symmetric funnel plot in this research demonstrates that there is no publishing bias (see Figure 3).

**3.3. Progression-Free Survival and Local Control.** In the heterogeneity tests, eight studies were included in this study,

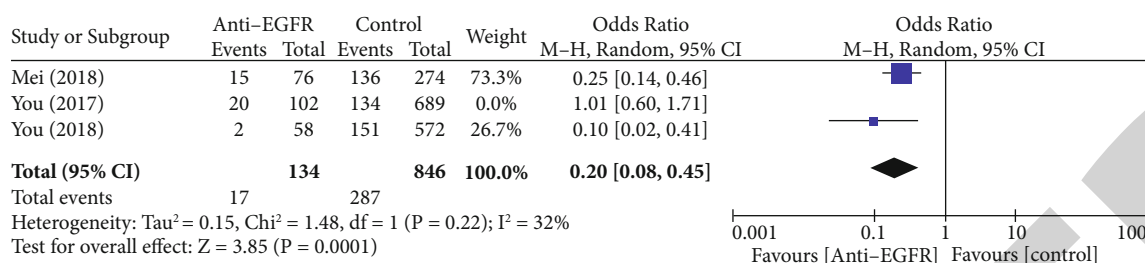


FIGURE 7: Forest diagram: results of anti-EGFR regimen plus standard treatment and standard treatment alone: blood toxicity.

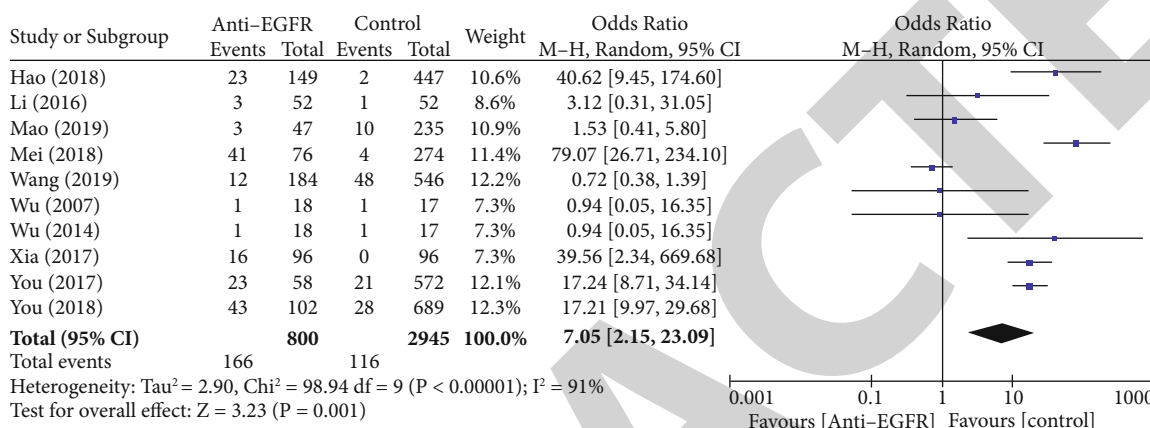


FIGURE 8: Forest diagram: anti-EGFR regimen plus standard treatment and standard treatment alone. Results: skin toxicity.

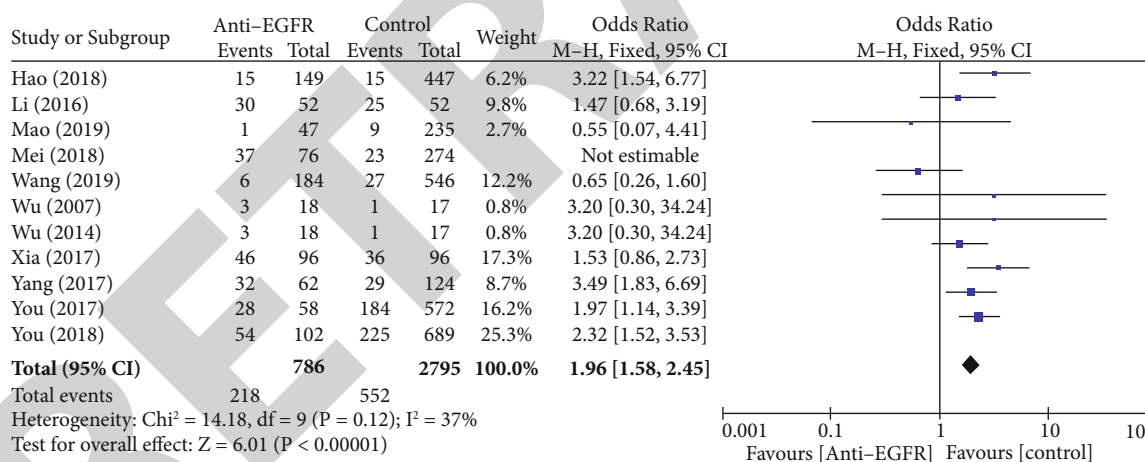


FIGURE 9: Forest diagram: anti-EGFR regimen plus standard treatment and standard treatment alone. Results: mucosal reaction.

and after heterogeneity test,  $I^2 = 0 < 50\%$ , and Q-test  $p = 0.99 > 0.05$ , which indicated that there was no obvious heterogeneity among the literatures included in this study, so the fixed-effects model was selected for meta-analysis. PFS did not improve significantly among patients receiving anti-EGFR in addition to conventional therapy (HR = 0.95; 95%CI = 0.51 – 1.88;  $p = 0.88$ ) (Figure 4).

This meta-analysis included eight LRRFS trials. A heterogeneity test revealed that the included literature was heterogeneous ( $I^2 = 53\% > 50\%$  and Q-test  $p = 0.1 > 0.05$ ); accordingly, a random-effects model was employed for the meta-analysis (see Figure 5). It means that compared with the control group, the survival time of local recurrence

increased by 70% when anti-EGFR drugs were added to the standard treatment. The random-effects model revealed that adding anti-EGFR agents to standard therapy increased patients' local area recurrence survival (HR = 0.70; 95%CI = 0.67 – 1.02;  $p = 0.01$ ) (Figure 5) as well as local survival by local survival area (HR = 0.70; 95%CI = 0.67 – 1.02;  $p = 0.01$ ). After omitting Hao et al. [20] publication from the sensitivity analysis, heterogeneity test  $I^2 = 0 < 50\%$ ; thus, a random-effects model was chosen.

3.4. *Survival Is Achievable in the Absence of Distant Metastases.* The DMFS meta-analysis involved nine investigations. Based on the results of a heterogeneity test

( $I^2 = 84\% > 50\%$  and Q-test  $p = 0.01 > 0.05$ ), which demonstrated heterogeneity across the included studies, a random-effects model was chosen for the meta-analysis. No statistically significant improvement was seen in disease-free survival among patients who took anti-EGFR medicine in addition to undergoing standard therapy (HR = 0.86; 95%CI = 0.61 – 1.16;  $p = 0.36$ ) (Figure 6). Sensitivity analysis, arbitrarily rejecting the literature in this study, will not affect the results of this study. It means that the calculation results of the above random effects are stable and reliable.

**3.5. Serious Adverse Events.** Anti-EGFR plus conventional therapy was compared to conventional therapy alone (DMFS). The addition of anti-EGFR to conventional patient care resulted in haematological toxicity, skin responses, and mucositis, among others. Since the combined haematological toxicity data indicated heterogeneity, a random-effects model was constructed. Excluding the data from You's [17] sensitivity analysis caused  $I^2$  to reduce from 89% to 32%. Anti-EGFR medication was linked with an increased incidence of haematotoxicity (RR = 0.22; 95%CI = 0.08 – 0.45;  $p = 0.01$ ) (Figure 7). Variations in the data were determined ( $I^2 = 91\%$ ,  $p = 0.01$ ), confirming the suitability of the random-effects model. Anti-EGFR therapy was linked with a greater frequency of skin toxicity (relative risk [RR] = 7.05; 95%CI = 2.15 – 23.0;  $p = 0.01$ ) (Figure 8) and an increase in the incidence of severe mucositis (RR = 1.96; 95%CI = 1.58 – 2.00;  $p = 0.01$ ) (Figure 9). Figure 7 depicts the forest plots for the hepatotoxic consequences among patients who underwent an anti-EGFR regimen in addition to conventional treatment compared to those treated with conventional treatment alone. A forest plot comparison of the two treatment approaches in terms of skin poisoning as a consequence is given in Figure 8. Figure 9 shows a comparison of forest plots for induced mucosal reactivity.

#### 4. Discussion

This study assessed the efficacy and safety of combining anti-EGFR medication with standard NPC treatment. It was found that anti-EGFR therapy improves LRRFS but has no effect on OS, PFS, or DMFS and that treatment-related adverse effects increase. Consistent anticancer efficacy has been seen when anti-EGFR medication is paired with conventional therapy for EGFR-expressing cancers, such as non-small cell lung cancer (NSCLC), squamous cell carcinoma of the head and neck (SCCHN), and colorectal cancer [10]. However, conflicting results were found in this meta-analysis, indicating that additional factors are at play. For tumour cells to be susceptible to drugs that target the DNA repair mechanism, this targeting process must be active. Anti-EGFR medications and conventional combination therapy drugs (e.g., platinum) may induce radiosensitivity by inhibiting the repair of radiation-induced DNA damage. Sensitivity to radiation and chemotherapy is generally affected by cancer cells and tumour microenvironments. Anti-EGFR or chemotherapy might have a greater impact on tumour cells than on tumour microenvironments. Thus,

with an increase in radiotherapy/chemotherapy resistance, the use of chemotherapy, anti-EGFR, or both in combination with radiotherapy can eradicate the vast majority of cancer cell molecules in a more efficient manner. Using medications that target the vascular endothelial growth factor and thus change tumour microenvironments is the only way to make the remaining cells more receptive to treatment following CRT. It is important to note that pairing anti-EGFR therapy with conventional treatment results in increased haematotoxicity, mucositis, and radiation dermatitis.

Our research still has some limitations. When exploring alternate treatments, it is critical to boost prediction findings and the quality of long-term survival. More research, especially prospective research, is required.

#### 5. Conclusions

Individuals who have nasopharyngeal cancer do not have an increased chance of surviving until a local recurrence of their disease if they get normal therapy in addition to an anti-EGFR regimen. However, this combination does not enhance overall survival. On the other hand, this factor adds to an increase in the number of adverse effects.

#### Data Availability

The datasets used and analyzed during the current study are available from the corresponding author upon reasonable request.

#### Conflicts of Interest

The authors declare that they have no conflicts of interest.

#### References

- [1] R. Liang, L. Yang, and X. Zhu, "Nimotuzumab, an anti-EGFR monoclonal antibody, in the treatment of nasopharyngeal carcinoma," *Cancer Control*, vol. 28, 2021.
- [2] E. T. Chang, W. Ye, Y. X. Zeng, and H. O. Adami, "The evolving epidemiology of nasopharyngeal carcinoma," *Cancer Epidemiology, Biomarkers & Prevention*, vol. 30, no. 6, pp. 1035–1047, 2021.
- [3] L. P. Tan, G. W. Tan, V. M. Sivanesan et al., "Systematic comparison of plasma EBV DNA, anti-EBV antibodies and miRNA levels for early detection and prognosis of nasopharyngeal carcinoma," *International Journal of Cancer*, vol. 146, no. 8, pp. 2336–2347, 2020.
- [4] R. Guo, Y. P. Mao, L. L. Tang, L. Chen, Y. Sun, and J. Ma, "The evolution of nasopharyngeal carcinoma staging," *The British Journal of Radiology*, vol. 92, no. 1102, article 20190244, 2019.
- [5] Y. P. Chen, A. T. C. Chan, Q. T. Le, P. Blanchard, Y. Sun, and J. Ma, "Nasopharyngeal carcinoma," *The Lancet*, vol. 394, no. 10192, pp. 64–80, 2019.
- [6] M. B. Alazzam, N. Tayyib, S. Z. Alshawwa, and M. Ahmed, "Nursing care systematization with case-based reasoning and artificial intelligence," *Journal of Healthcare Engineering*, vol. 2022, Article ID 1959371, 9 pages, 2022.
- [7] H. M. Lee, K. S. Okuda, F. E. González, and V. Patel, "Current perspectives on nasopharyngeal carcinoma," *Advances in Experimental Medicine and Biology*, vol. 1164, pp. 11–34, 2019.



## *Retraction*

# **Retracted: Hot Air Treatment Elicits Disease Resistance against *Colletotrichum gloeosporioides* and Improves the Quality of Papaya by Metabolomic Profiling**

### **BioMed Research International**

Received 12 November 2022; Accepted 12 November 2022; Published 19 January 2023

Copyright © 2023 BioMed Research International. This is an open access article distributed under the Creative Commons Attribution License, which permits unrestricted use, distribution, and reproduction in any medium, provided the original work is properly cited.

*BioMed Research International* has retracted the article titled “Hot Air Treatment Elicits Disease Resistance against *Colletotrichum gloeosporioides* and Improves the Quality of Papaya by Metabolomic Profiling” [1] due to concerns that the peer review process has been compromised.

Following an investigation conducted by the Hindawi Research Integrity team [2], significant concerns were identified with the peer reviewers assigned to this article; the investigation has concluded that the peer review process was compromised. We therefore can no longer trust the peer review process and the article is being retracted with the agreement of the editorial board.

### **References**

- [1] B. Liu, M. Xue, J. Zhou, H. Zhang, L. Ren, and J. Fan, “Hot Air Treatment Elicits Disease Resistance against *Colletotrichum gloeosporioides* and Improves the Quality of Papaya by Metabolomic Profiling,” *BioMed Research International*, vol. 2022, Article ID 5162845, 13 pages, 2022.
- [2] L. Ferguson, “Advancing Research Integrity Collaboratively and with Vigour,” 2022, <https://www.hindawi.com/post/advancing-research-integrity-collaboratively-and-vigour/>.

## *Retraction*

# **Retracted: The Effect of Social Cognitive Interaction Training on Schizophrenia: A Systematic Review and Meta-Analysis of Comparison with Conventional Treatment**

### **BioMed Research International**

Received 12 November 2022; Accepted 12 November 2022; Published 18 January 2023

Copyright © 2023 BioMed Research International. This is an open access article distributed under the Creative Commons Attribution License, which permits unrestricted use, distribution, and reproduction in any medium, provided the original work is properly cited.

*BioMed Research International* has retracted the article titled “The Effect of Social Cognitive Interaction Training on Schizophrenia: A Systematic Review and Meta-Analysis of Comparison with Conventional Treatment” [1] due to concerns that the peer review process has been compromised.

Following an investigation conducted by the Hindawi Research Integrity team [2], significant concerns were identified with the peer reviewers assigned to this article; the investigation has concluded that the peer review process was compromised. We therefore can no longer trust the peer review process and the article is being retracted with the agreement of the editorial board.

### **References**

- [1] Y. Tang, L. Yu, D. Zhang, F. Fang, and Z. Yuan, “The Effect of Social Cognitive Interaction Training on Schizophrenia: A Systematic Review and Meta-Analysis of Comparison with Conventional Treatment,” *BioMed Research International*, vol. 2022, Article ID 3394978, 11 pages, 2022.
- [2] L. Ferguson, “Advancing Research Integrity Collaboratively and with Vigour,” 2022, <https://www.hindawi.com/post/advancing-research-integrity-collaboratively-and-vigour/>.



## *Retraction*

# **Retracted: miR-211-5p Alleviates the Myocardial Ischemia Injury Induced by Ischemic Reperfusion Treatment via Targeting FBXW7**

### **BioMed Research International**

Received 12 November 2022; Accepted 12 November 2022; Published 18 January 2023

Copyright © 2023 BioMed Research International. This is an open access article distributed under the Creative Commons Attribution License, which permits unrestricted use, distribution, and reproduction in any medium, provided the original work is properly cited.

*BioMed Research International* has retracted the article titled “miR-211-5p Alleviates the Myocardial Ischemia Injury Induced by Ischemic Reperfusion Treatment via Targeting FBXW7” [1] due to concerns that the peer review process has been compromised.

Following an investigation conducted by the Hindawi Research Integrity team [2], significant concerns were identified with the peer reviewers assigned to this article; the investigation has concluded that the peer review process was compromised. We therefore can no longer trust the peer review process and the article is being retracted with the agreement of the editorial board.

### **References**

- [1] Y. Liu, J. Meng, H. Di, L. Zheng, and Z. Meng, “miR-211-5p Alleviates the Myocardial Ischemia Injury Induced by Ischemic Reperfusion Treatment via Targeting FBXW7,” *BioMed Research International*, vol. 2022, Article ID 5423929, 7 pages, 2022.
- [2] L. Ferguson, “Advancing Research Integrity Collaboratively and with Vigour,” 2022, <https://www.hindawi.com/post/advancing-research-integrity-collaboratively-and-vigour/>.

## *Retraction*

# **Retracted: Ferroptosis-Related lncRNA for the Establishment of Novel Prognostic Signature and Therapeutic Response Prediction to Endometrial Carcinoma**

### **BioMed Research International**

Received 24 November 2022; Accepted 24 November 2022; Published 27 December 2022

Copyright © 2022 BioMed Research International. This is an open access article distributed under the Creative Commons Attribution License, which permits unrestricted use, distribution, and reproduction in any medium, provided the original work is properly cited.

*BioMed Research International* has retracted the article titled “Ferroptosis-Related lncRNA for the Establishment of Novel Prognostic Signature and Therapeutic Response Prediction to Endometrial Carcinoma” [1] due to concerns that the peer review process has been compromised.

Following an investigation conducted by the Hindawi Research Integrity team [2], significant concerns were identified with the peer reviewers assigned to this article; the investigation has concluded that the peer review process was compromised. We therefore can no longer trust the peer review process and the article is being retracted with the agreement of the editorial board.

The authors agree to the retraction.

## **References**

- [1] X.-Y. Zhou, H.-Y. Dai, H. Zhang, J.-L. Zhu, and H. Hu, “Ferroptosis-Related lncRNA for the Establishment of Novel Prognostic Signature and Therapeutic Response Prediction to Endometrial Carcinoma,” *BioMed Research International*, vol. 2022, Article ID 2056913, 16 pages, 2022.
- [2] L. Ferguson, “Advancing Research Integrity Collaboratively and with Vigour,” 2022, <https://www.hindawi.com/post/advancing-research-integrity-collaboratively-and-vigour/>.

## *Retraction*

# **Retracted: Clinical Efficacy and Safety Analysis of PD-1/PD-L1 Inhibitor vs. Chemotherapy in the Treatment of Advanced Non-Small-Cell Lung Cancer: A Systematic Review and Meta-Analysis**

### **BioMed Research International**

Received 24 November 2022; Accepted 24 November 2022; Published 25 December 2022

Copyright © 2022 BioMed Research International. This is an open access article distributed under the Creative Commons Attribution License, which permits unrestricted use, distribution, and reproduction in any medium, provided the original work is properly cited.

*BioMed Research International* has retracted the article titled “Clinical Efficacy and Safety Analysis of PD-1/PD-L1 Inhibitor vs. Chemotherapy in the Treatment of Advanced Non-Small-Cell Lung Cancer: A Systematic Review and Meta-Analysis” [1] due to concerns that the peer review process has been compromised.

Following an investigation conducted by the Hindawi Research Integrity team [2], significant concerns were identified with the peer reviewers assigned to this article; the investigation has concluded that the peer review process was compromised. We therefore can no longer trust the peer review process and the article is being retracted with the agreement of the editorial board.

The authors do not agree to the retraction.

### **References**

- [1] W.-w. Guo, T.-w. Zhang, B.-l. Wang, L.-q. Mao, and X.-b. Li, “Clinical Efficacy and Safety Analysis of PD-1/PD-L1 Inhibitor vs. Chemotherapy in the Treatment of Advanced Non-Small-Cell Lung Cancer: A Systematic Review and Meta-Analysis,” *BioMed Research International*, vol. 2022, Article ID 9500319, 9 pages, 2022.
- [2] L. Ferguson, “Advancing Research Integrity Collaboratively and with Vigour,” 2022, <https://www.hindawi.com/post/advancing-research-integrity-collaboratively-and-vigour/>.

## *Retraction*

# **Retracted: Peroxisome Proliferator-Activated Receptor Gene Knockout Promotes Podocyte Injury in Diabetic Mice**

### **BioMed Research International**

Received 12 November 2022; Accepted 12 November 2022; Published 23 November 2022

Copyright © 2022 BioMed Research International. This is an open access article distributed under the Creative Commons Attribution License, which permits unrestricted use, distribution, and reproduction in any medium, provided the original work is properly cited.

*BioMed Research International* has retracted the article titled “Peroxisome Proliferator-Activated Receptor Gene Knockout Promotes Podocyte Injury in Diabetic Mice” [1] due to concerns that the peer review process has been compromised.

Following an investigation conducted by the Hindawi Research Integrity team [2], significant concerns were identified with the peer reviewers assigned to this article; the investigation has concluded that the peer review process was compromised. We therefore can no longer trust the peer review process and the article is being retracted with the agreement of the editorial board.

### **References**

- [1] R. Yan, Y. Zhang, Y. Yang et al., “Peroxisome Proliferator-Activated Receptor Gene Knockout Promotes Podocyte Injury in Diabetic Mice,” *BioMed Research International*, vol. 2022, Article ID 9018379, 8 pages, 2022.
- [2] L. Ferguson, “Advancing Research Integrity Collaboratively and with Vigour,” 2022, <https://www.hindawi.com/post/advancing-research-integrity-collaboratively-and-vigour/>.

## *Retraction*

# **Retracted: Systematic Review and Meta-Analysis of Complications after Laparoscopic Surgery and Open Surgery in the Treatment of Pelvic Abscess**

### **BioMed Research International**

Received 12 November 2022; Accepted 12 November 2022; Published 22 November 2022

Copyright © 2022 BioMed Research International. This is an open access article distributed under the Creative Commons Attribution License, which permits unrestricted use, distribution, and reproduction in any medium, provided the original work is properly cited.

*BioMed Research International* has retracted the article titled “Systematic Review and Meta-Analysis of Complications after Laparoscopic Surgery and Open Surgery in the Treatment of Pelvic Abscess” [1] due to concerns that the peer review process has been compromised.

Following an investigation conducted by the Hindawi Research Integrity team [2], significant concerns were identified with the peer reviewers assigned to this article; the investigation has concluded that the peer review process was compromised. We therefore can no longer trust the peer review process and the article is being retracted with the agreement of the editorial board.

### **References**

- [1] X. Chen, S. Jun, L. Xu, and H. Zhang, “Systematic Review and Meta-Analysis of Complications after Laparoscopic Surgery and Open Surgery in the Treatment of Pelvic Abscess,” *BioMed Research International*, vol. 2022, Article ID 3650213, 8 pages, 2022.
- [2] L. Ferguson, “Advancing Research Integrity Collaboratively and with Vigour,” 2022, <https://www.hindawi.com/post/advancing-research-integrity-collaboratively-and-vigour/>.

## *Retraction*

# **Retracted: Factors Influencing Cerebrospinal Fluid Leaking following Pituitary Adenoma Transsphenoidal Surgery: A Meta-Analysis and Comprehensive Review**

### **BioMed Research International**

Received 12 November 2022; Accepted 12 November 2022; Published 22 November 2022

Copyright © 2022 BioMed Research International. This is an open access article distributed under the Creative Commons Attribution License, which permits unrestricted use, distribution, and reproduction in any medium, provided the original work is properly cited.

*BioMed Research International* has retracted the article titled “Factors Influencing Cerebrospinal Fluid Leaking following Pituitary Adenoma Transsphenoidal Surgery: A Meta-Analysis and Comprehensive Review” [1] due to concerns that the peer review process has been compromised.

Following an investigation conducted by the Hindawi Research Integrity team [2], significant concerns were identified with the peer reviewers assigned to this article; the investigation has concluded that the peer review process was compromised. We therefore can no longer trust the peer review process and the article is being retracted with the agreement of the editorial board.

### **References**

- [1] J. Zhang, J. Liu, and L. Huang, “Factors Influencing Cerebrospinal Fluid Leaking following Pituitary Adenoma Transsphenoidal Surgery: A Meta-Analysis and Comprehensive Review,” *BioMed Research International*, vol. 2022, Article ID 5213744, 9 pages, 2022.
- [2] L. Ferguson, “Advancing Research Integrity Collaboratively and with Vigour,” 2022, <https://www.hindawi.com/post/advancing-research-integrity-collaboratively-and-vigour/>.

## Retraction

# Retracted: Biogenic Analysis of the Effect of TERC on Cell Proliferation and Migration of Oral Squamous Cell Carcinoma under Digital Minimally Invasive Treatment

### BioMed Research International

Received 20 June 2023; Accepted 20 June 2023; Published 21 June 2023

Copyright © 2023 BioMed Research International. This is an open access article distributed under the Creative Commons Attribution License, which permits unrestricted use, distribution, and reproduction in any medium, provided the original work is properly cited.

This article has been retracted by Hindawi following an investigation undertaken by the publisher [1]. This investigation has uncovered evidence of one or more of the following indicators of systematic manipulation of the publication process:

- (1) Discrepancies in scope
- (2) Discrepancies in the description of the research reported
- (3) Discrepancies between the availability of data and the research described
- (4) Inappropriate citations
- (5) Incoherent, meaningless and/or irrelevant content included in the article
- (6) Peer-review manipulation

The presence of these indicators undermines our confidence in the integrity of the article's content and we cannot, therefore, vouch for its reliability. Please note that this notice is intended solely to alert readers that the content of this article is unreliable. We have not investigated whether authors were aware of or involved in the systematic manipulation of the publication process.

In addition, our investigation has also shown that one or more of the following human-subject reporting requirements has not been met in this article: ethical approval by an Institutional Review Board (IRB) committee or equivalent, patient/participant consent to participate, and/or agreement to publish patient/participant details (where relevant).

Wiley and Hindawi regrets that the usual quality checks did not identify these issues before publication and have since put additional measures in place to safeguard research integrity.

We wish to credit our own Research Integrity and Research Publishing teams and anonymous and named external researchers and research integrity experts for contributing to this investigation.

The corresponding author, as the representative of all authors, has been given the opportunity to register their agreement or disagreement to this retraction. We have kept a record of any response received.

### References

- [1] W. Chen, Z. Zhang, Y. Jin et al., "Biogenic Analysis of the Effect of TERC on Cell Proliferation and Migration of Oral Squamous Cell Carcinoma under Digital Minimally Invasive Treatment," *BioMed Research International*, vol. 2022, Article ID 2102795, 6 pages, 2022.



## Review Article

# Biogenic Analysis of the Effect of TERC on Cell Proliferation and Migration of Oral Squamous Cell Carcinoma under Digital Minimally Invasive Treatment

Wenao Chen,<sup>1</sup> Zilong Zhang,<sup>1</sup> Yiyao Jin,<sup>1</sup> Ruijie Zeng,<sup>1</sup> Xi Sun,<sup>1</sup> Zihan Zhou ,<sup>2</sup> Kabna Kasim,<sup>3</sup> Joshua Grant,<sup>4</sup> Vumika Kuraki,<sup>5</sup> Felix Schmid,<sup>6</sup> and Gabin Lucas<sup>7</sup>

<sup>1</sup>I.M. Borovsky Institute of Dentistry, I.M. Sechenov First Moscow State Medical University, Moscow 119991, Russia

<sup>2</sup>Stomatological Hospital of Anhui Province, Anhui Medical University, Hefei, Anhui 230031, China

<sup>3</sup>University of Kragujevac, Kragujevac, Serbia

<sup>4</sup>University of Melbourne, Melbourne, Australia

<sup>5</sup>Kobe University, Kobe, Japan

<sup>6</sup>Carleton University, Ottawa, Canada

<sup>7</sup>University of British Columbia, Vancouver, Canada

Correspondence should be addressed to Zihan Zhou; [b20160801614@stu.ccsu.edu.cn](mailto:b20160801614@stu.ccsu.edu.cn)

Received 12 July 2022; Revised 25 July 2022; Accepted 3 August 2022; Published 18 August 2022

Academic Editor: Dinesh Rokaya

Copyright © 2022 Wenao Chen et al. This is an open access article distributed under the Creative Commons Attribution License, which permits unrestricted use, distribution, and reproduction in any medium, provided the original work is properly cited.

**Objective.** To investigate the correlation between TERC gene and cell proliferation and migration of oral squamous cell carcinoma. **Methods.** By comparing the traditional surgical treatment with the minimally invasive treatment of digital technology, the influence of Shengxin analysis method on the proliferation and migration of oral squamous cell carcinoma cells was analyzed. **Results.** Digital technology minimally invasive treatment has a great impact on the operation and survival rate of patients. TERC has a significant impact on the proliferation and migration of oral squamous cell carcinoma cells. Digital technology minimally invasive treatment can prevent TERC from great changes. **Conclusion.** TERC under the minimally invasive treatment of digital technology has little effect on the proliferation and migration of oral squamous cell carcinoma cells. It can promote the proliferation of oral squamous cell carcinoma cells. The inhibitors of migration and invasion can play an effective role in antiproliferation.

## 1. Introduction

With the improvement of living standards, people's quality of life has also changed. People are also increasingly concerned about health. They will have regular physical examination every year to pay attention to any problems that may occur in their physical functions. However, there are many diseases that cannot be found in the early stage. It is possible that the occurrence of a disease will cause problems in other organs. Today, many cancers cannot be cured. People are suffering from cancer, both physically and at home. With the change of living conditions, people are also pursuing some so-called "game," in which many bacteria and viruses are eaten into the stomach. What cannot be absorbed by itself will lead to

physical problems, such as oral squamous cell carcinoma, which refers to the malignant tumor occurring in the mouth and mainly composed of squamous cells. It is the most malignant and harmful tumor in the head and neck, accounting for 50% of the cases of head and neck squamous cell carcinoma. How does the mode of medical care integration affect oral squamous cell carcinoma? Jia (2022) and others analyzed the impact of integrated management intervention on oral squamous cell carcinoma patients and discussed their oral health, quality of life, and psychological status. The results showed that it could effectively improve their quality of life and psychological enthusiasm and more effectively alleviate patients' anxiety [1]. We can more accurately understand how to treat the proliferation and migration of cancer cells. Feng (2022)

and others analyzed and mechanism it and studied the inhibitory effect of interleukin on the proliferation of cancer cells [2]. In order to better control and inhibit the dispersion of cancer cells, Yingying (2022) and others used long-chain noncoding RNA *col11a1-208* to analyze the effect of its cell proliferation and invasion. *Col11a1-208* can promote its cell proliferation and invasion ability and play an important role in the occurrence and progress [3]. The progress of medicine and the development of scientific research, compared with the previous incurable diseases, are many. First, now, we are also studying how to treat them to alleviate the pain of patients faster, but there are also many diseases that deteriorate, which are closely related to psychological effects. The strength of psychological quality is crucial to physical function. Li (2022) and others analyzed and discussed the impact of their postoperative psychological state and used dialectical behavior therapy to effectively promote the positive growth of their postoperative patients' traumatic psychology, improve their psychological state, and improve their survival level [4].

There are about 100000 new oral cancer patients in the world every year. A large number of patients with oral cancer are mainly of high malignancy. The treatment is mainly a combination of surgery, radiotherapy, and chemotherapy. However, the survival rate of patients within 5 years fell to 50%. In this regard, Lin (2022) and others analyzed the value-added of their disease, and the results showed that this research and analysis could inhibit the value-added of cancer cells and promote cell apoptosis [5]. For the change of postoperative nutritional status of patients and the analysis of its influencing factors, Mair Haba (2022) and others analyzed the status and influencing factors during the treatment process, so as to better understand the situation of postoperative patients [6]. In the process of clinical treatment, the clinical characteristics of oral squamous cell carcinoma cells are variable. For this, Zhao (2022) and others discussed the correlation between their characteristics and prognosis, which can make the difference between the treatment of their disease and prognosis clearer [7]. In order to understand the important role of early epithelial stromal transformation in regulating the dryness and metastasis of cancer cells, Zhu (2022) and others analyzed the role and mechanism of its transformation, which can play a key role in the treatment of patients [8]. In this study, in order to better treat and control the proliferation and migration of oral squamous cell carcinoma cells, TERC under the minimally invasive treatment of digital technology was used to conduct genetic analysis and research.

## 2. Patient Information

**2.1. General Information.** 80 patients with oral squamous cell carcinoma treated in our hospital from 2018 to 2022 were selected, including 58 males and 22 females. The age of male patients is 32~68 years old, and the age of female patients is 37~66 years old. Among them, 18 cases were tongue lesions, 22 cases were palate lesions, 11 cases were buccal lesions, 7 cases were floor of mouth lesions, and 22 cases were lesions in other parts.

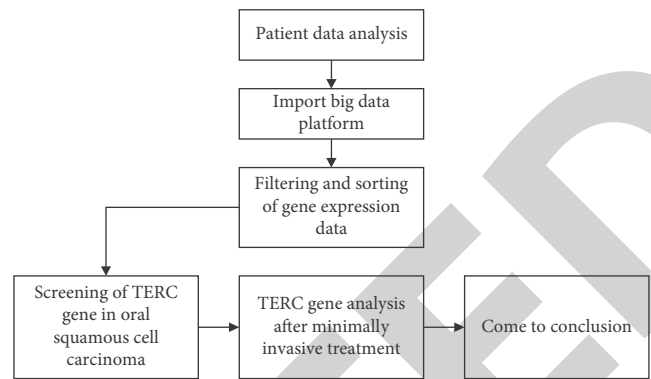


FIGURE 1: Flowchart of bioinformatics analysis of the effect of TERC gene on oral squamous cell carcinoma cells.

### 2.2. Inclusion and Exclusion Criteria

- (1) All patients were patients with simple oral squamous cell carcinoma, including oral squamous cell carcinoma caused by different reasons such as heredity, environment, and living habits
- (2) All other organs of all patients have complete structures and are normal after medical examination
- (3) All physical indicators of all patients were normal
- (4) Those who did not return to the hospital on time were excluded in the observation stage
- (5) Patients who did not comply with medication were excluded in the observation stage
- (6) All patients have no infectious diseases or are allergic to drugs for the treatment of the disease

## 3. Method

**3.1. Routine Surgical Treatment.** Oral squamous cell carcinoma is mainly treated by surgery for a wide range of excised lesions. Because of oral squamous cell carcinoma, the main purpose of surgery is functional repair. For example, if squamous lesions occur in tongue or buccal mucosa, they can be directly closed and sutured if they are removed early. For extensive invasion, there must be good repair methods, such as taking the forearm flap or taking the lateral oral flap. When the squamous cell carcinoma develops seriously, it may be necessary to cut off part of the jaw, including the maxilla, mandible, and oropharynx, which will cause the loss of oral function. In this case, more complex repair methods will be used to restore the patient's oral function while removing the lesion.

**3.2. Digital Technology Minimally Invasive Treatment.** Use digital technology to analyze the precise focus before operation, scan and image the maxillofacial bone, and make a personalized operation plan according to the results. Using minimally invasive surgery, according to the preoperative plan, the squamous cell carcinoma cells in the oral cavity were accurately removed and neck lymph node dissection,

TABLE 1: Comparison of surgical impact of patients under different methods.

Grouping	<i>n</i>	Focus localization	Focal debridement	Recurrence rate
Routine surgical treatment	40	78%	73%	14%
Digital technology minimally invasive treatment	40	92%	95%	5%
<i>t</i>		8.523	7.675	7.936
<i>p</i>		0.015	0.012	0.023

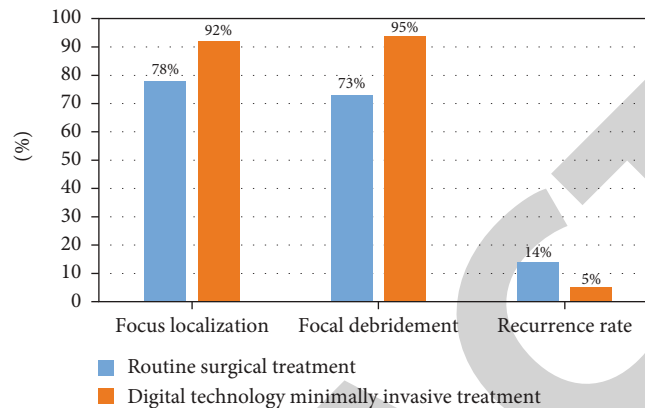


FIGURE 2: Comparison of surgical impact of patients under different methods.

and then microsurgical vascular anastomosis and defect repair were performed. In the early stage, there can be no symptoms. With the progression of the tumor, local masses can appear, accompanied by ulceration and easy bleeding. Surgical treatment should be the first choice after the diagnosis of oral cancer. The specific surgical method also needs to be determined according to the size of the tumor, the scope of invasion, and whether there is metastasis in other parts. If there is no metastasis and the focus is small, it can be minimally invasive without sweeping other tissues.

**3.3. Shengxin Analysis.** Bioinformatics analysis refers to the analysis of biological information, which reflects the state and mode of biological movement. Biological information is mainly biological genetic genes. All kinds of tumors and cancers are diseases that cause cells to stimulate the formation of new organisms due to DNA mutations. With the development of gene sequencing technology, the impact of TERC gene on the proliferation and migration of oral squamous cell carcinoma cells was identified through biological information analysis. The bioscience analysis process is shown in Figure 1.

Analyze the data of its cancer patients, input the data into the big data platform, filter and sort out the gene expression data through the big data platform to obtain the available data, screen the TERC gene of its cell cancer, analyze and discuss the impact of TERC on the proliferation and migration of cancer cells after minimally invasive treatment with digital technology, and finally draw a conclusion. This method is not only the fastest but also the most effective treatment method. It can more intuitively carry out a more specific biochemical analysis of oral squamous cell carcinoma cells and have a deeper understanding of the patient's

condition, so that the treatment is more conducive to the patient's treatment plan.

**3.4. Statistical Methods.** The study set up the conventional surgical treatment group and the digital technology minimally invasive treatment group, the statistical data are different according to the different treatment of patients. According to the statistical information obtained in the above treatment methods, group analysis was carried out to analyze the statistical correlation and corresponding relationship between the data. The statistical software platform is IBM SPSS 24.0 data analysis platform, and the bivariate *t*-test method is used to compare the differences of data. When  $t < 10.000$ , it is considered that there is statistical difference in the data and the significance *p* value of the statistical data. When  $p < 0.05$ , it is considered that the statistical results are credible, and when  $p < 0.01$ , it is considered that the statistical results have significant statistical significance.

## 4. Results

**4.1. Comparison of Patients' Surgical Impact under Different Methods.** Oral mucosal epithelium belongs to squamous epithelium. The cancer that occurs in oral mucosal epithelium is called oral squamous cell carcinoma, namely, oral squamous cell carcinoma. Oral squamous cell carcinoma is a common and harmful malignant tumor in the mouth. Now, patients with oral squamous cell carcinoma are treated in groups, and the effects of the two methods on surgical focus location, intraoperative focus clearance, and postoperative recurrence rate are compared. The data are made into Table 1 as follows.

TABLE 2: Analysis of the effect of TERC on cell proliferation and migration of oral squamous cell carcinoma under the two methods.

Grouping	<i>n</i>	Gene amplification rate	Gene migration rate
Routine surgical treatment	40	20%	17.5%
Digital technology minimally invasive treatment	40	7.5%	5%

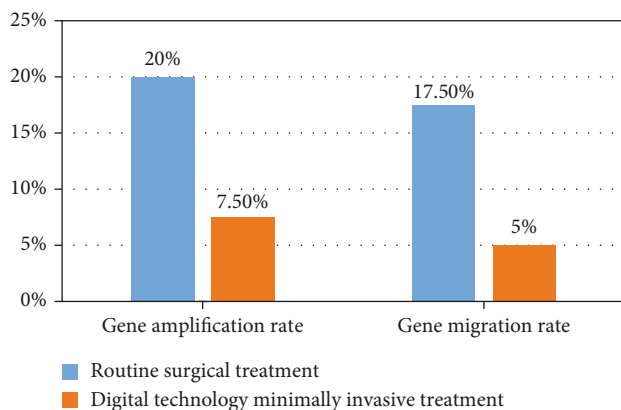


FIGURE 3: Effect of TERC on cell proliferation and migration of oral squamous cell carcinoma under two methods.

As shown in Table 1, the location of the focus of patients using digital technology minimally invasive treatment is more accurate than that of conventional surgery, and both the clearance rate and recurrence rate of the focus are better than those of patients undergoing conventional surgery. Make the data in Table 1 into a visual diagram, as shown in Figure 2.

In Figure 2, the digital technology minimally invasive treatment method performs well in all aspects of treatment. Compared with traditional treatment methods, digital technology minimally invasive treatment method is more effective, which is more conducive to patients to alleviate pain, improve treatment rate, and lay the foundation for survival rate. It can be considered that different treatment methods have a certain impact on the focus location, focus clearance, and recurrence rate of oral squamous cell carcinoma. The treatment method under the minimally invasive digital technology has a better effect on the treatment and prognosis of oral squamous cell carcinoma.

**4.2. Correlation Analysis of the Effects of TERC on Cell Proliferation and Migration of Oral Squamous Cell Carcinoma under the Two Methods.** In normal human cells, telomerase activity is closely regulated. Only in cells that constantly divide and clone can telomerase activity be detected. In this tumor cell, TERC gene expression increased, which indicates that TERC gene plays an important role in this cancer cell. The effects of TERC on cell proliferation and migration under the two methods are analyzed, and Table 2 and Figure 3 are obtained.

It can be seen in Table 2 and Figure 3 that the value-added rate of oral squamous cell carcinoma cells using conventional surgical methods is 20% and the cell migration rate is 17.5%, while the value-added rate and migration rate of oral squamous cell carcinoma cells under the minimally

invasive treatment method of digital technology are 7.5% and 5%, respectively, which is significantly lower than that of conventional surgical methods. Oral squamous cell carcinoma has many high-risk factors and complex pathogenic factors, which is conducive to the diagnosis, treatment, and prevention of oral squamous cell carcinoma, and has important clinical value.

**4.3. Comparison of Patient Survival Rate under Different Methods.** At present, the prevalence of cancer is increasing year by year, but there are also many cancers that cannot be cured. Once found, some cancers may be in the late stage of cancer, or even in the middle stage, and the survival rate is low. In this regard, the survival rate of oral cancer must be found earlier and treated in time. It also has a certain relationship with the standardization of treatment. For example, if standardized surgery is carried out and other treatments are followed up, its cure rate can be greatly improved. If it is found late or does not get standardized treatment, and the best treatment time and treatment period are delayed, its survival rate will be reduced by half. In this regard, two different treatment methods were used to compare the survival rates of the same number of patients. The survival rates of 1, 3, and 5 years were compared. Table 3 was drawn according to the data values obtained from the analysis.

In Table 3, the number of patients with the two treatment methods is the same. According to the survival rate in different time periods, the survival rate in routine surgical treatment is also increasing year by year, and the five-year survival rate data value is about 60%. Compared with the minimally invasive treatment of digital technology, the 5-year survival rate is increased to more than 70%, which can effectively improve the survival rate and reduce mortality. According to the statistical method, there was  $t < 10.000$  and  $p < 0.05$  between the two comparisons of the data, which was statistically significant. In order to observe the data values in the two different treatment methods more intuitively, Figure 4 is drawn according to the data in Table 3.

As shown in Figure 4, taking one year as an example, the survival rate of traditional treatment is 80%, while the data of digital technology treatment is 93%, which has a more significant effect. In this regard, in the new information age, the application of scientific research technology in medicine is the gospel of the majority of patients, which not only improves the survival rate but also reduces the treatment time for doctors in the treatment process, provides the basis for patients in the later treatment, and reduces patients' pain. What is more, it reduces the doctor-patient disputes in the hospital, provides the basis for building a harmonious hospital environment, and greatly alleviates the contradictions between medical staff and patients.



TABLE 3: Comparison of survival rate of patients with different treatment methods.

Grouping	<i>n</i>	1-year survival rate	3-year survival rate	5-year survival rate
Routine surgical treatment	40	80%	73%	61%
Digital technology minimally invasive treatment	40	93%	81%	74%
<i>t</i>		8.125	9.012	8.756
<i>p</i>		0.048	0.041	0.032

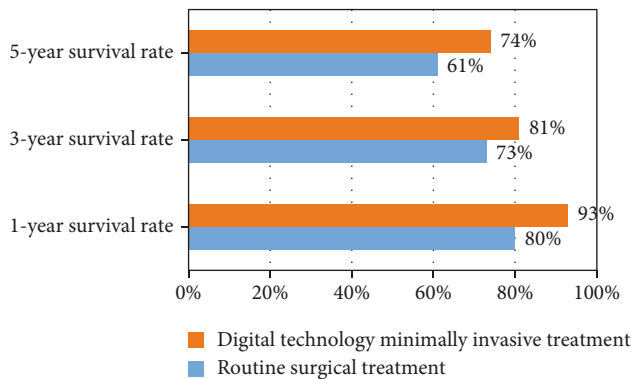


FIGURE 4: Visualization of survival rate of patients with different treatment methods.

## 5. Discussion

With the acceleration of the pace of life and the increase of social pressure, more and more people suffer from cancer, and the symptoms are becoming more and more complex. In this regard, Cong (2022) and others talked about the possible mechanism of aspirin inhibiting the proliferation of its cells by inducing apoptosis [9]. At present, some drugs can inhibit the proliferation of cancer cells. All trans-retinoic acid combined with apatinib has a qualitative inhibitory effect on the proliferation of oral squamous cell carcinoma cells. Therefore, Pan et al. (2022) studied it and showed that all trans-retinoic acid combined with apatinib can inhibit the proliferation of oral squamous cell carcinoma cells by promoting cell aging and affecting cell dryness [10]. This can alleviate the suffering caused by the pain, but this relief is also to a certain extent, and cannot completely control the disease. All diseases must be treated with drugs or drugs, but the overdose of some drugs will lead to the reduction of drug resistance, which cannot achieve the desired effect. For this, Sun (2022) and others studied and analyzed the drug resistance of oral squamous cell carcinoma, activated and inhibited the proliferation of cisplatin resistant cells in oral squamous cell carcinoma, promoted apoptosis, and reduced the resistance of oral squamous cell carcinoma cells to cisplatin [11]. Yun et al. (2022) also analyzed the influence on the invasion and migration ability of its cancer cells, and vines can significantly inhibit the invasion, migration, and tumor growth ability of oral squamous cell carcinoma cells [12]. Honor et al. (2022) studied the cell cycle arrest and apoptosis of oral squamous cell carcinoma. Transfection of si-neat1 can inhibit the proliferation of oral squamous cell carcinoma cells, induce apoptosis, and cause cycle arrest [13]. Although drug treatment can alleviate this disease, it

cannot be better treated in routine treatment. In the continuous updating and reform of scientific research technology, digital technology minimally invasive treatment has a certain impact on its disease, which can better treat the value-added and migration of this disease. It can better control the incidence of oral squamous cell carcinoma, slightly alleviate the pain caused by the disease, help to get a specific understanding of the development of oral squamous cell carcinoma disease, and better formulate a treatment plan in the treatment process.

## 6. Summary

Based on TERC under digital technology minimally invasive treatment, this study studied the influence of cell proliferation and migration of oral squamous cell carcinoma. Through the comparison of surgical effects and survival rates of patients under different treatment methods, the influence of TERC gene changes on cell proliferation and migration was studied and analyzed. Under the new technology research, the application of digital technology minimally invasive treatment can effectively control and treat its disease. With the rapid development of precision medicine and information technology, digital technology is gradually applied to various fields of medicine, which can promote the development of medicine towards precision and minimally invasive. Improve the accuracy of diagnosis, treatment, and nursing in the treatment process, improve the effect of treatment, and reduce labor intensity. In the digital information age, medicine needs to follow rules and regulations, but also needs innovation and development to obtain more extensive applications. No matter in any field or industry, the impact of digitalization has an inseparable relationship with the development of all walks of life, which is more conducive to the progress of social economy and the rapid development of society.

## Data Availability

The data underlying the results presented in the study are available within the manuscript.

## Disclosure

We confirm that the content of the manuscript has not been published or submitted for publication elsewhere.

## Conflicts of Interest

There is no potential conflicts of interest in our paper.

## Retraction

# Retracted: Awareness of Medical Students toward Circadian Rhythm and Sleep Disorder Based on Biomedical Diagnosis

### BioMed Research International

Received 20 June 2023; Accepted 20 June 2023; Published 21 June 2023

Copyright © 2023 BioMed Research International. This is an open access article distributed under the Creative Commons Attribution License, which permits unrestricted use, distribution, and reproduction in any medium, provided the original work is properly cited.

This article has been retracted by Hindawi following an investigation undertaken by the publisher [1]. This investigation has uncovered evidence of one or more of the following indicators of systematic manipulation of the publication process:

- (1) Discrepancies in scope
- (2) Discrepancies in the description of the research reported
- (3) Discrepancies between the availability of data and the research described
- (4) Inappropriate citations
- (5) Incoherent, meaningless and/or irrelevant content included in the article
- (6) Peer-review manipulation

The presence of these indicators undermines our confidence in the integrity of the article's content and we cannot, therefore, vouch for its reliability. Please note that this notice is intended solely to alert readers that the content of this article is unreliable. We have not investigated whether authors were aware of or involved in the systematic manipulation of the publication process.

In addition, our investigation has also shown that one or more of the following human-subject reporting requirements has not been met in this article: ethical approval by an Institutional Review Board (IRB) committee or equivalent, patient/participant consent to participate, and/or agreement to publish patient/participant details (where relevant).

Wiley and Hindawi regrets that the usual quality checks did not identify these issues before publication and have

since put additional measures in place to safeguard research integrity.

We wish to credit our own Research Integrity and Research Publishing teams and anonymous and named external researchers and research integrity experts for contributing to this investigation.


The corresponding author, as the representative of all authors, has been given the opportunity to register their agreement or disagreement to this retraction. We have kept a record of any response received.

### References

- [1] A. Alanazi, H. Alhawas, M. Aldossari et al., "Awareness of Medical Students toward Circadian Rhythm and Sleep Disorder Based on Biomedical Diagnosis," *BioMed Research International*, vol. 2022, Article ID 8645183, 6 pages, 2022.

## Research Article

# Awareness of Medical Students toward Circadian Rhythm and Sleep Disorder Based on Biomedical Diagnosis

Asma Alanazi <sup>1,2</sup>, Haifa Alhawas,<sup>1,2</sup> Munirah Aldossari,<sup>1</sup> Dana Almutairi,<sup>1</sup> Dana Almatroudi,<sup>1</sup> Afnan Alenazi,<sup>1</sup> Leen Almadhi,<sup>1</sup> and Maram Albalawi<sup>3</sup>

<sup>1</sup>Department of Basic Medical Sciences, College of Medicine, King Saud bin Abdulaziz University for Health Sciences (KSAU-HS), Riyadh, Saudi Arabia

<sup>2</sup>King Abdullah International Medical Research Center, Riyadh, Saudi Arabia

<sup>3</sup>Department of Biostatistics and Bioinformatics, King Abdullah International Medical Research Center, Riyadh, Saudi Arabia

Correspondence should be addressed to Asma Alanazi; [anazia@ksau-hs.edu.sa](mailto:anazia@ksau-hs.edu.sa)

Received 20 July 2022; Revised 1 August 2022; Accepted 4 August 2022; Published 18 August 2022

Academic Editor: Dinesh Rokaya

Copyright © 2022 Asma Alanazi et al. This is an open access article distributed under the Creative Commons Attribution License, which permits unrestricted use, distribution, and reproduction in any medium, provided the original work is properly cited.

**Background.** Sleep disorders affect an individual's mental and physical health and vice versa. Sleep medicine is underrecognized as a specialty; therefore, many sleep disorders go undiagnosed. This study is aimed at assessing the knowledge of medical students toward circadian neuroscience and sleep disorder based on biomedical diagnosis. **Methods.** This cross-sectional study was conducted in both male and female medical colleges from the third to the sixth year. A self-administered structured questionnaire consisting of sociodemographic data and the Assessment of Sleep Knowledge in Medical Education (ASKME) survey assessed the students' general knowledge and attitude towards sleep disorder and sleep medicine. Chi-square/Fisher exact tests were used to analyse the participants' knowledge level toward specific sociodemographic data. Also, for two-level continuous variables, the Wilcoxon two-sample test was used. **Results.** The total number of participants was 296, with 154 female and 142 male participants. The prevalence of inadequate knowledge was considerable with 96.62% of students, compared to adequate knowledge with only 3.38%. The students' attitude to sleep medicine was negative 14.53% and positive among 85.47%. We found that gender was significantly associated with attitude with a  $p$  value = 0.0057. The specific interest in sleep medicine had a significant association with knowledge and attitude,  $p$  value of 0.0522 and 0.0059, respectively. **Conclusion.** This study concluded that medical students possess inadequate knowledge regarding sleep medicine, yet they have a positive attitude towards it.

## 1. Introduction

Sleep affects an individual's mental health and psychological state due to its close connection to mental health [1]. As sleep can affect one's mental health, having mental health problems could lead to sleep disorders [1]. Sleep disorders are defined as a disturbance in an individual's sleep pattern [2]. It can be caused by various environmental conditions and factors [2]. Delayed sleep phase disorder, shift work sleep disorder, restless leg syndrome, insomnia, and sleep apnea are common sleep disorders [2].

Moreover, sleep disorders are prevalent among Saudi medical students, especially female students, according to a study done by Abdulghani et al. [3]. The need for sleep medicine, a medical specialty that focuses on sleep-related prob-

lems, is anticipated to increase significantly due to the increased prevalence of sleep disorders in the Saudi population [4]. Both sleep disorders and sleep medicine are underrecognized by healthcare workers and public workers [5]. Sleep medicine specialties' underrecognition could be because it is a relatively new specialty in the medical profession [5]. The latest International Classification of Sleep Disorders (ICSD) approved that more than seventy disorders were divided into seven major categories [6]. Although there are accurate diagnostic instruments and efficient therapies for many sleep disorders, sleep testing and treatments are still unavailable [7]. There are many sleep disorders and inadequate numbers of sleep health professionals in parts of the world [7]. According to a study conducted in Saudi Arabia in 2007, there are limited studies investigating the prevalence of sleep disorders,



although there are widespread sleep disorders among the Saudi population [8]. A survey revealed that sleep medicine in Saudi Arabia is underdeveloped compared to developed countries, and there are two main problems facing the progress of this specialty [8]. One of these obstacles includes an insufficient number of sleep-medicine experts and a lack of insurance coverage and funding [8]. Both health workers and general health practitioners do not consider sleep medicine an independent specialty [5].

Moreover, most people in Saudi Arabia do not have adequate knowledge about sleep medicine and sleep disorders. Since sleep medicine is a relatively new specialty, many people do not acknowledge its existence—people in the healthcare profession, especially medical students, lack awareness of sleep medicine as a specialty. According to a study conducted at Qassim University, medical students appeared to have limited knowledge about sleep medicine, but they showed a positive attitude towards it [9]. A study was done to assess the knowledge of sleep medicine among medical students in Riyadh and found that over 80% of the students rated their knowledge of sleep medicine to be below average [10]. In addition, it claimed that it is an obstacle that sleep medicine is considered a low priority in the medical school curriculum [10]. Early detection of specific sleeping disorders depends on the knowledge of the Primary Healthcare (PHC) physician in KSA. However, insufficient education on sleep medicine during medical school and residency training leads to inadequate knowledge in physicians, which would compromise the quality of patient care [5].

Moreover, since the physicians are uninformed about sleep medicine, patients with sleeping disorders go undiagnosed, which may lead to further complications [11]. Furthermore, Saudi PHC physicians do not fully understand sleep medicine as a specialty. According to Saleem et al.'s study, 25.7% of participant physicians admit that they would not take sleep medicine history from their patients as an essential part of their history-taking practice [12]. Moreover, 39.2% deem sleep disturbances a lifestyle problem rather than a medical condition [12]. Also, only 63% of physicians realize that obstructive sleep apnea (OSA) increases the risk of motor vehicle accidents, as mentioned in the BaHammams study [13].

According to several studies, OSA is prevalent among PHC physicians' clinic patients [13–16]. However, OSA and other sleep disorders commonly go undiagnosed because sleep medicine is underdeveloped as a specialty; hence, there is a lack of specialists, especially in KSA [5, 8]. It is impractical to expect a limited amount of sleep medicine specialists to diagnose all the sleep disorders. Alternatively, educational interventions have proven to help raise the awareness and diagnosis of sleep disorders among PHC physicians [17]. Consequently, the primary purpose of this study was to assess the knowledge and attitude regarding sleep medicine among medical students at King Saud bin Abdulaziz University for Health Sciences (KSAU-HS), Riyadh branch, using a cross-sectional study.

## 2. Methods

Based on an online survey, a cross-sectional study was conducted in KSAU-HS, Riyadh branch, regarding the knowledge

TABLE 1: Sociodemographic characteristics of participants ( $n = 296$ ).

Study variables	N (%)
Gender	
(i) Female	154 (52)
(ii) Male	142 (47.97)
Age	
(i) Less than 25	280 (94.5)
(ii) More than 25	16 (5.41)
Year of study	
(i) 3 <sup>rd</sup> year	70 (23.65)
(ii) 4 <sup>th</sup> year	93 (31.42)
(iii) 5 <sup>th</sup> year	65 (21.96)
(iv) 6 <sup>th</sup> year	68 (22.97)
GPA	
(i) 2.4-4.0	24 (8.11)
(ii) 4.1-5.0	272 (91.89)
Preferred specialty	
(i) Medicine	169 (57.09)
(ii) Surgery	88 (29.73)
(iii) Others	39 (13.18)
Specific interest in sleep medicine	
(i) Yes	56 (18.92)
(ii) No	240 (81.08)
Importance of sleep medicine	
(i) Absolutely not important	7 (2.36)
(ii) Not important	10 (3.38)
(iii) Average	76 (25.68)
(iv) Important	104 (35.14)
(v) Very important	99 (33.45)

and attitude of medical students towards sleep medicine as a specialty. The study population included medical students. The inclusion criteria were male and female medical students from the third year to the sixth year. The exclusion criteria were graduated students as well as those whose data were incomplete. The Raosoft sample size calculator was used to calculate the sample size with a population size of 1200 students, a 95% confidence interval, a margin of error of 5%, and the response distribution was 50% of medical students with adequate knowledge. Therefore, the sample size became 292.

The data collection was through a self-administered questionnaire consisting of three parts: each part consists of closed-end questions. The three parts were, namely, socio-demographic data, knowledge about sleep and sleep disorder, and attitude toward sleep medicine. The first part of the questionnaire is about the student's sociodemographic characteristics (age, year of study, gender, GPA, preferred specialty, specific interest in sleep medicine, and students' perspective on the importance of sleep medicine). The second part assesses the students' knowledge about sleep medicine using the Assessment of Sleep Knowledge in Medical Education

TABLE 2: General knowledge toward circadian and sleep disorder based on biomedical diagnosis ( $n = 296$ ).

Knowledge questions	Correct answers N (%)
(Q1) When does the need for sleep decrease in a person?	144 (48.65)
(Q2) When does the body increase its secretion of melatonin?	229 (77.36)
(Q3) When does dream sleep or rapid eye movement sleep (REM) occur?	168 (56.76)
(Q4) How does a person make up for his loss of sleep during the work week?	179 (60.47)
(Q5) How much time do newborn infants spend sleeping per 24 hours?	227 (76.69)
(Q6) What is the prevalence of insomnia between older men and women?	35 (11.82)
(Q7) What should we do to a young (preadolescent) child who regularly has trouble getting to sleep at night?	59 (19.93)
(Q8) What is the typical age of symptom onset for narcolepsy?	43 (14.53)
(Q9) When does the ability to sleep increase?	86 (29.05)
(Q10) When is the slow-wave sleep more prominent?	52 (17.57)
(Q11) When does the amount of slow-wave sleep increase?	35 (11.82)
(Q12) Episodes of sleepwalking tend to occur which third of the night?	77 (26.01)
(Q13) When do episodes of REM sleep tend to lengthen?	124 (41.89)
(Q14) During REM sleep, what happens to periodic limb movements?	74 (25)
(Q15) In children, inadequate sleep can exacerbate which of the following?	48 (16.22)
(Q16) With alcoholics in recovery, how long of alcohol abstention does it take to normalize their sleep?	24 (8.11)
(Q17) What is recommended in patients with difficulty in initiating sleep?	17 (5.74)
(Q18) What is often an indicator in the treatment of primary snoring or mild obstructive sleep apnea?	116 (39.19)
(Q19) What enhanced slow-wave sleep?	63 (21.28)
(Q20) What drug could cause chronic bedwetting in children?	120 (40.54)
(Q21) Nightmare are more common within?	49 (16.55)
(Q22) Heart rate, respiration, and blood pressure are more variable during?	100 (33.78)
(Q23) Do antihypertensive drugs cause sleep difficulties as side effects?	50 (16.89)
(Q24) What is true regarding early morning awakening in the elderly?	99 (33.45)
(Q25) What is correct regarding the benefit from alcohol?	159 (53.72)
(Q26) What statement is correct?	158 (53.38)
(Q27) Episode of sleepwalking commonly occurs at which stage?	49 (16.55)
(Q28) Who is at higher risk of developing symptoms of sleep apnea?	146 (49.32)
(Q29) What can increase the incidence of sleepwalking in children?	182 (61.49)
(Q30) What is the most symptom that correlates with narcolepsy?	75 (25.34)

(ASKME) survey [18]. Experts developed and validated the questionnaire using a pilot study to find reliability. The questionnaire contains a 30-question survey in which the outcome variables were (a) questions on students' knowledge of basic sleep principles, (b) circadian sleep/wake control, (c) normal sleep architecture, (d) common sleep disorders, and (e) the effect of drugs and alcohol on sleep. Each question had four choices: one correct answer, two wrong answers, and an "I do not know" choice. The correct answer was coded as one, while all the other answers were coded as zero.

The minimum score was 0, and the maximum score was 30 after summing up the score of thirty questions. Participants were classified into two categories by applying the cut-off points of 18/30 (60% of the total score). If the score range was from 0 to 17 points, we classified them as having inadequate knowledge; on the other hand, if the score range was from 18 to 30 points, the student's knowledge was categorized as adequate knowledge. The third part assesses the participants' attitudes toward sleep and sleep disorder using a questionnaire containing ten questions adapted from the

ASKME survey [18]. The response to the attitude questions was a 5-point Likert scale (from strongly agree = 5 to strongly disagree = 1). The total score ranged from 10 to 50. Participants who scored 30 (60% of the total score) or more were categorized as having a positive attitude. In contrast, the participants whose scores were less than 30 were categorized as having a negative attitude.

### 3. Data Analysis

All data analyses were performed using the Statistical Analysis System (SAS) Version 9.4 software. Descriptive statistics for all qualitative variables will be presented as numbers and percentages, while the mean  $\pm$  standard deviation for all quantitative variables will be presented. Chi-square/Fisher exact tests were used to analyse the participants' knowledge level with the sociodemographic profile (gender, GPA, year of study, and specific interest). Additionally, the Wilcoxon two-sample test was used for two-level continuous variables.

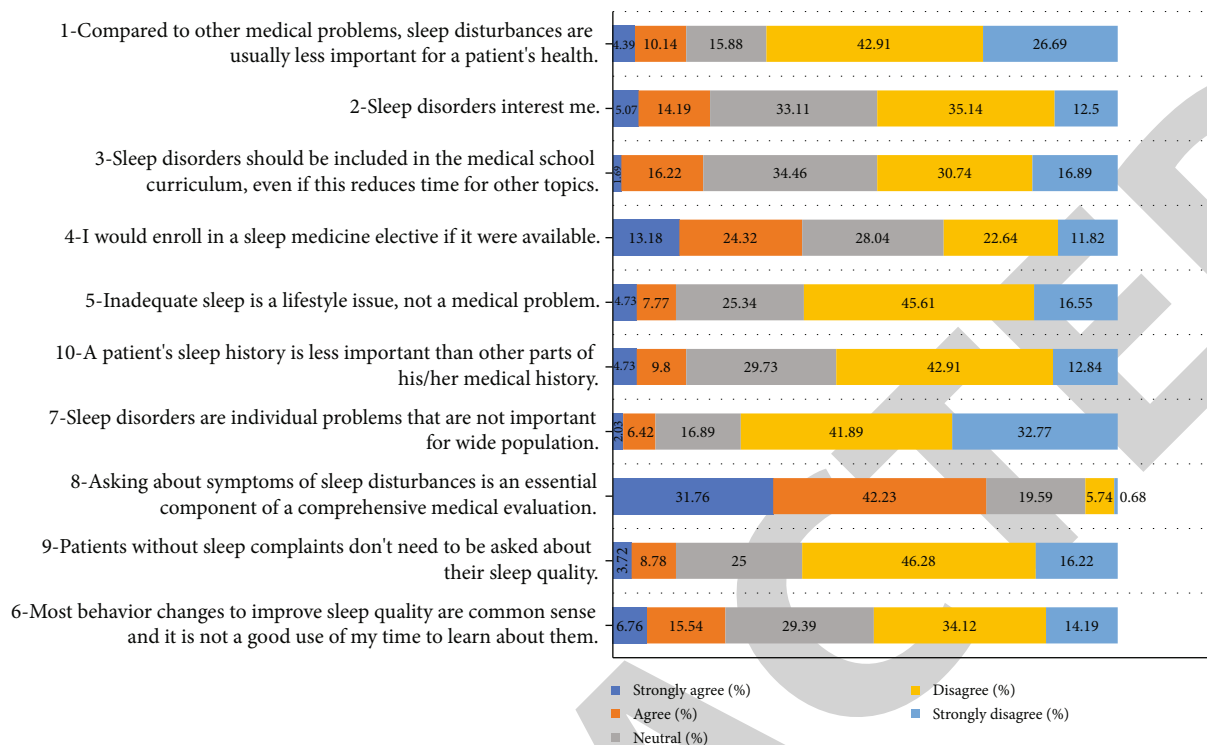


FIGURE 1: General attitude of the students toward sleep medicine.

TABLE 3: Knowledge and attitude.

Predictor variable	N (%)
Level of knowledge	
(i) Adequate	10 (3.38)
(ii) Inadequate	286 (96.62)
Attitude	
(i) Positive	253 (85.47)
(ii) Negative	43 (14.53)
Knowledge score (mean ± SD)	10.09 ± 4.15
Attitude total score (mean ± SD)	35.56 ± 5.61

The *p* value < 0.05 will be considered statistically significant for all tests applied with a 95% confidence interval.

The study proposal was approved by the King Abdullah International Medical Research Center (KAIMRC), registered at the National Committee of Bio & Med. Ethics (NCBE) (Registration No. SP21R\168\04). Consent was taken through the questionnaire, and no personal information was taken from the participants. In addition, the participants were given no compensation or benefit in any form. Only the research team had access to all the data, as all the data was kept classified throughout the entire study.

#### 4. Results

The questionnaire was distributed randomly among the third-, fourth-, fifth-, and sixth-year medical students, and there were 296 responses. The sociodemographic characteristics of the students who participated in this study are listed in Table 1. The students' ages were classified from less than 25 to more than 25; most of the participants, 280 (94.5%), were under 25 years old, with a slight inclination towards the female respondents being 154 (52%). The fourth-year medical student had the highest responses compared to the other students. Moreover, most of the participants, 272 (91.89%), had a 4.1 or higher (GPA). According to their preferred area of specialization, many students preferred medicine as a specialty 169 (57.09%). Most of the participants are not interested in sleep medicine, 240 (81.08%); despite that, many students believe sleep medicine is important.

Table 2 represents the result of the ASKME questionnaire, which indicates the number of correct responses. The ques-

tions that had the highest correct response rate were “when does the body increase the secretion of melatonin,” “how much time do newborn infants spend sleeping per 24 hours,” and “what can increase the incidence of sleepwalking in children” with 77.36%, 76.69%, and 61.49% of students answering it correctly, respectively. The question that had the least correct responses was “what is recommended in patients with difficulty in initiating sleep” with 17 (5.74%) students.

The general attitude of the medical students in this study is presented in Figure 1. Most of the students disagreed with every statement, especially statements 1 and 7. However, most of the students agreed with statement 8, with 94 (31.76%) strongly agreeing and 125 (42.23%) agreeing. In addition, statement 4 had mixed responses in which 28.04% responses were neutral, and the choices “agree” and “disagree” had approximate percentages 24.32% and 22.64%, respectively.

TABLE 4: Comparison between the sociodemographic data.

N = 296	Knowledge		Attitude	
	Adequate N (%)	Inadequate N (%)	Positive N (%)	Negative N (%)
Gender				
Female	6 (3.9)	148 (96.1)	140 (90.91)	14 (9.09)
Male	4 (2.82)	138 (97.18)	113 (79.58)	98 (20.48)
<i>p</i> value		0.7518		0.0057*
GPA				
4.1-5	9 (3.31)	263 (96.69)	234 (86.03)	38 (13.97)
2.4-4	1 (4.17)	23 (95.83)	19 (79.17)	5 (20.83)
<i>p</i> value		0.5765		0.3651
Year of study				
3 <sup>rd</sup> year	1 (1.43)	69 (98.57)	58 (82.86)	12 (17.14)
4 <sup>th</sup> year	2 (2.15)	91 (97.85)	77 (82.8)	16 (17.2)
5 <sup>th</sup> year	4 (6.15)	61 (93.85)	59 (90.77)	6 (9.23)
6 <sup>th</sup> year	3 (4.41)	65 (95.59)	59 (86.76)	9 (13.24)
<i>p</i> value		0.4059		0.4785
Specific interest				
Yes	3 (5.36)	53 (94.64)	49 (87.5)	7 (12.5)
No	7 (2.92)	233 (97.08)	204 (85)	36 (15)
<i>p</i> value		0.0522*		0.0059*

\*Significant at  $p \leq 0.05$ .

The characteristics of the students' knowledge and attitude toward sleep medicine in Table 3 show that the mean knowledge score was 10.09 ( $\pm 4.15$ ) out of 30. In this study, the prevalence of inadequate knowledge was considerable with 286 (96.62%) students, compared to adequate knowledge with 10 (3.38%) students. The mean attitude score was 35.56 ( $\pm 5.61$ ) out of 50. Moreover, only 43 (14.53%) participants had a negative attitude towards sleep medicine, whereas 253 (85.47%) participants had a positive attitude toward it.

Table 4 shows the comparison between socio-demographic data of participants and their knowledge and attitude scores. There is statistical significance in the positive attitude of females compared to males with a  $p$  value = 0.0057, although their knowledge scores are not statistically significant. Using the Wilcoxon test, the mean score of students' knowledge and attitude with a specific interest is higher and statistically significant with a  $p$  value = 0.0522 for the knowledge and a  $p$  value of 0.0059 for the attitude than those who do not have a specific interest.

## 5. Discussion

The main goal of this study was to assess the knowledge and attitude of medical students at King Saud bin Abdulaziz University for Health Sciences toward circadian neuroscience and sleep disorder based on biomedical diagnosis. The final analysis found that the students' knowledge was poor 286 (96.62%). In another study conducted in 2020 at King Abdulaziz University in Jeddah by Alghamdi et al., the ASKME questionnaire was used [19]. They classified the results into two categories: low scores (<60%) and high

scores (>60%) [19]. A total of 568 medical students participated, out of which the mean score was 9.89 ( $\pm 4.89$ ) and 97.7% had low scores [19]. Additionally, they found no statistically significant difference between both genders' knowledge scores as the findings in this study [19]. Another local study done at Qassim University by Alrebdi et al. had 116 medical students [9]. While using the ASKME questionnaire, they found that 94.8% of the participants had poor knowledge with positive attitude among the students, which was consistent with the results of this study [9]. In a study from Egypt, they had 726 participants complete the survey, of which there were 573 sixth-year medical students [20, 21]. Their results indicated poor knowledge among medical students [22]. Furthermore, there was a statistically significant difference in the knowledge scores of participants' gender and the knowledge scores, which conflicts with our findings [23, 24].

## 6. Conclusion

The medical students in the KSAU-HS Riyadh branch have poor knowledge toward sleep disorder and sleep medicine, indicating a need for sleep medicine to be added to the medical curriculum of KSAU-HS. Also, the students' positive attitude towards sleep medicine demonstrates that they are willing to learn about it. To acquire proper knowledge among medical students, we recommend that the professors be educated about sleep medicine and its importance in the medical field. In our study, there is a significant association between attitude and gender. Also, there is a significant association between knowledge and attitude with a specific interest in sleep medicine. However, our study did not find any

## Retraction

# Retracted: Visual Analysis of Nutrient Deficiency and Treatment Protocols in Bariatric Surgery Based on VOSviewer

### BioMed Research International

Received 18 July 2023; Accepted 18 July 2023; Published 19 July 2023

Copyright © 2023 BioMed Research International. This is an open access article distributed under the Creative Commons Attribution License, which permits unrestricted use, distribution, and reproduction in any medium, provided the original work is properly cited.

This article has been retracted by Hindawi following an investigation undertaken by the publisher [1]. This investigation has uncovered evidence of one or more of the following indicators of systematic manipulation of the publication process:

- (1) Discrepancies in scope
- (2) Discrepancies in the description of the research reported
- (3) Discrepancies between the availability of data and the research described
- (4) Inappropriate citations
- (5) Incoherent, meaningless and/or irrelevant content included in the article
- (6) Peer-review manipulation

The presence of these indicators undermines our confidence in the integrity of the article's content and we cannot, therefore, vouch for its reliability. Please note that this notice is intended solely to alert readers that the content of this article is unreliable. We have not investigated whether authors were aware of or involved in the systematic manipulation of the publication process.

In addition, our investigation has also shown that one or more of the following human-subject reporting requirements has not been met in this article: ethical approval by an Institutional Review Board (IRB) committee or equivalent, patient/participant consent to participate, and/or agreement to publish patient/participant details (where relevant).

Wiley and Hindawi regrets that the usual quality checks did not identify these issues before publication and have since put additional measures in place to safeguard research integrity.

We wish to credit our own Research Integrity and Research Publishing teams and anonymous and named external researchers and research integrity experts for contributing to this investigation.

The corresponding author, as the representative of all authors, has been given the opportunity to register their agreement or disagreement to this retraction. We have kept a record of any response received.

### References

- [1] J. Tang, M. He, G. Li et al., "Visual Analysis of Nutrient Deficiency and Treatment Protocols in Bariatric Surgery Based on VOSviewer," *BioMed Research International*, vol. 2022, Article ID 8228831, 10 pages, 2022.



## Research Article

# Visual Analysis of Nutrient Deficiency and Treatment Protocols in Bariatric Surgery Based on VOSviewer

Jihong Tang <sup>1,2</sup>, Mei He <sup>3</sup>, Guirong Li <sup>2</sup>, Juan He <sup>1,2</sup>, Xianhua Wang <sup>1,2</sup>,  
Zhuoxin Yang <sup>1,2</sup> and HongJin Wu <sup>1,2</sup>

<sup>1</sup>School of Nursing, Chengdu Medical College, 610500, China

<sup>2</sup>Nursing Department, Mianyang Central Hospital, 621000, China

<sup>3</sup>President's Office, Mianyang Central Hospital, 621000, China

Correspondence should be addressed to Mei He; hemeimy@163.com

Received 4 July 2022; Revised 22 July 2022; Accepted 1 August 2022; Published 16 August 2022

Academic Editor: Dinesh Rokaya

Copyright © 2022 Jihong Tang et al. This is an open access article distributed under the Creative Commons Attribution License, which permits unrestricted use, distribution, and reproduction in any medium, provided the original work is properly cited.

**Objective.** To analyze the global literature on nutritional deficiencies in bariatric surgery (BS) since January 1, 1985, and to discuss the current status of research, research hotspots, and new development trend and treatment of nutritional deficiency in bariatric surgery. It provides ideas and basis for promoting the development of bariatric surgery and new alternative therapy or treatment protocols. **Methods.** The Web of Science (WOS) database core collection was used as the data source, and VOSviewer 1.6.17 software was used to search the literature on the topic of “nutritional deficiencies in bariatric surgery.” The number of published literature, the distribution of authors, institutions, and countries, keyword cooccurrences, and journal cocitations were visualized and analyzed. **Results.** A total of 1015 relevant publications was obtained after searching and screening, and the overall trend of literature published was on the rise. The most published countries, institutions, and authors were USA, University of Sao Paulo, Ramalho, Andrea; Obesity Surgery has been the most frequently cited journal (7943 citations), and the top 10 journals had high impact factors. Keyword cooccurrence analysis showed that “bariatric surgery” and “nutritional deficiencies” are the hot topics of research in this field. **Conclusion.** There is an urgent need for bariatric surgery issuing institutions and authors to strengthen cross-institutional, cross-team, and multicenter and multidisciplinary cooperation, to promote and facilitate the exchange and cooperation in the field of bariatric surgery between developed countries in Europe and America and developing countries in Asia, Africa, and Latin America, to draw the attention of developing countries to the health problems caused by obesity, and to encourage and support the development of developing countries in this field. Bariatric surgery, obesity, weight loss, Y-type gastric bypass, gastric bypass, and nutritional deficiency are the hot research topics in the field of nutritional deficiency in bariatric surgery, and metabolic surgery, single anastomosis gastric bypass, micronutrient supplementation, micronutrient deficiency, intestinal microbiology, and guidelines are the new trends in this field.

## 1. Introduction

Obesity is officially recognized as a global disease and a persistent risk factor for chronic diseases [1]. Obese patients are frequently accompanied by other comorbidities, such as type 2 diabetes, dyslipidemia, insulin resistance, and cardiovascular disease [2]. In 2016, more than 1.9 billion adults aged 18 years and older were overweight globally, of whom more than 650 million were obese, and 39% of adults aged 18 years and older were overweight and 13% were obese [3]. According to the World Health Organization, it is estimated that by

2025, about one-fifth of the world's adults will be obese [4]. And the Report on the Status of Nutrition and Chronic Diseases in China (2020) shows that the problem of overweight and obesity in urban and rural residents of all age groups continues to be highlighted, with more than half of the adult population being overweight and obese [5]. Options for treating obesity include three main categories: lifestyle interventions, drug therapy, and bariatric surgery. Lifestyle interventions and pharmacotherapy alone have been shown to be ineffective in sustaining weight loss [6]. The results of the study demonstrate that bariatric surgery is an effective

treatment for obesity [7] and gets more attention. According to the China Bariatric Metabolic Surgery Database Annual Report 2020, the actual total number of bariatric surgery cases nationwide is projected to be about 14,037 [8], and the acceptance of bariatric surgery by the general public is gradually increasing. However, weight loss surgery has strict criteria, international recommendations for body mass index (BMI) > 40 or BMI in the range of 35-39.9 and suffer from one of the metabolic complications associated with obesity, surgery is recommended, BMI in about 30 to consider surgery [9]. According to the ethnic characteristics and differences of the East Asian population, surgery is actively recommended in China for BMI  $\geq 37.5$  kg/m<sup>2</sup>; to 32.5 kg/m<sup>2</sup>  $\leq$  BMI < 37.5 kg/m<sup>2</sup>, surgery is recommended; for 27.5 kg/m<sup>2</sup>  $\leq$  BMI < 32.5 kg/m<sup>2</sup>, which is difficult to control with lifestyle changes and medical treatment and at least 2 components of metabolic syndrome are met or comorbidities exist [10]. The two most commonly used procedures internationally are SG (sleeve gastrectomy) and Roux-en-Y-gastric bypass (RYGB) [11]; SG is done by removing approximately 80% of the size of the stomach; RYGB is a Y-shaped division of the stomach into upper and lower parts, with the small upper part anastomose with the distal small intestine and the severed proximal small intestine anastomose with the distal end laterally to form a Y shape. Both procedures achieve sustained weight loss and are also effective in the improvement of comorbidities. However, postoperative complications remain deserving of our attention. Nutritional deficiency is the most frequent postoperative complication of bariatric surgery and is associated with anemia [12], secondary hyperparathyroidism, and metabolic bone disease [13]. Nutritional deficiencies in bariatric surgery can be related to partial gastrectomy or foods, bypassing key nutrient absorption sites (e.g., duodenum/jejunum proximal), which limits dietary intake and decreases nutrient uptake [9, 14]. The results of related studies [15, 16] suggest that nutritional deficiencies in bariatric surgery can be improved through perioperative lifestyle interventions, long-term nutritional monitoring and postoperative follow-up, and increased patient awareness through a guided collaborative/participatory nurse-patient model to reduce postoperative nutritional deficiency complications and significantly improve patient compliance. VOSviewer software enables quantitative and visual analysis of knowledge structures, research hotspots, and frontiers [17]. Based on the Web of Science core collection database, this paper analyzes the current status, hotspots, and development trends of domestic and international research on nutrient deficiencies in bariatric surgery since January 1, 1985, using VOSviewer software, hoping to bring some new references and data for future research work.

## 2. Materials and Methods

**2.1. Sources and Literature Search.** The search was conducted using the core collection on the Web of Science, an English-language literature repository with a wide academic impact, as the data source, and a search strategy was constructed in the advanced search interface, including English

search terms related to bariatric surgery, nutrients, and deficiencies. ((TS=(Bariatric surgery or Metabolic Surgery or Bariatric Surgical Procedures or obesity surgery or gastric bypass or sleeve gastrectomy or laparoscopic Roux-en-Y gastric bypass or laparoscopic sleeve gastrectomy or laparoscopic gastric bypass or Endoscopic weight loss surgery or adjustable gastric banding or laparoscopic adjustable gastric banding or one-anastomosis gastric bypass or mini gastric bypass or Biliopancreatic diversion with duodenal switch or duodenal-jejunal bypass or transit bipartition or jejunal-jejunal bypass or jejunoileal bypass or duodenal switch/single-anastomosis duodenoileal bypass with sleeve gastrectomy or Fundoplication or Balloon or Stomach Stapling)) AND TS=(defici\*)) AND TS=(Nutri\*)) AND DT=(Review OR Article). The search was conducted from January 1, 1985, to March 13, 2022, in any language, and 1017 articles were retrieved, and 1015 valid articles were obtained by further eliminating duplicates using the EndNote Document Manager.

**2.2. Methods and Tools.** All the retrieved literature was exported; tab-delimited files were selected; information was entered as “full record with cited references” and saved as a “plain text” file in savedrecs.txt format to the specified path. By using VOSviewer 1.6.17 software, the search results were analyzed in terms of author, institution, country, keywords, and journal citations to explore the current status, trends, and hotspots in the field.

## 3. Results

**3.1. Analysis of the Amount of Literature Published.** A total of 1015 papers was collected from 1985 to March 13, 2022. As shown in Figure 1, there is an overall upward trend in the number of publications related to nutritional deficiency research on BS. From 41 articles in 2009 to 115 articles in 2021, the number of articles increased approximately 2.8 times during this twelve-year period. The number of publications showed an increasing trend from 2009 to 2020, with a small decline in 2013, 2015, and 2018, followed by a significant increase in 2020 and 2021. As of the search date of March 13, 2022, 24 articles have been published.

**3.2. Analysis of the Distribution of Coauthors and Institutions.** Visual analysis of authors and institutions was done, publication of research in the field of nutrition deficiencies in bariatric surgery. The analysis type was coauthorship, and the minimum number of publications in the default software for authors and institutions was 5. Out of 4797 authors, a total of 71 authors met this threshold, and out of 1674 institutions, a total of 97 institutions met this threshold. In the field of nutritional deficiencies in bariatric surgery, the top three authors with the most scientific publications were Ramalho, Andrea (17), Saboya, Carlos (14), and Ben-Porat, Tair (14), and the other authors with the most publications are detailed in Table 1. A total of 15 research or medical institutions had 10 or more publications, with the top three most published institutions being the University of São Paulo (29), Mayo Clinic (25), and the Assuta



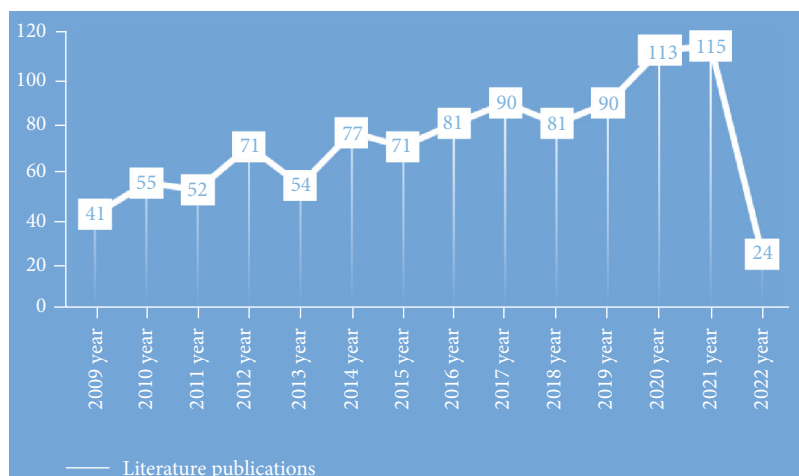


FIGURE 1: Literature publications.

TABLE 1: Ranking of authors with 10 or more publications.

Institution	Documents	Citations	Total link strength
Ramalho, Andrea	17	185	40
Saboya, Carlos	14	151	39
Ben-Porat, Tair	14	260	37
Pereira, Silvia	11	119	35
Aarts, Edo, O.	11	340	21
Sherf-dagan, Shiri	10	34	34
Coupaye, Muriel	10	385	25
Kaifarentzos, Fotis	10	489	4

Medical Center (17). Refer to Table 2 for more details on the volume of articles issued by other institutions. In Figures 2 and 3, one color represents one group, and each group represents one team of authors or one institutional consortium. A collaboration between authors is primarily restricted to internal team members, and team-to-team collaboration is extremely poor, as shown in the visual analysis table of the authors' collaboration in Figure 2. There is some cooperation between the institutions, but it is still relatively limited and most of them do not cooperate with one another. The visual analysis chart of institutional cooperation is detailed in Figure 3.

**3.3. Analysis of Country Distribution.** Visualization of countries with research in the field of nutritional deficiencies in bariatric surgery was done. The analysis type is coauthorship, and the default country minimum number of publications is 5. Out of 68 countries, a total of 39 meet this threshold and the publication of scientific results is mainly concentrated in European and North American countries. The largest number was from the United States, with 348 articles or 34.28%. Although Brazil, China, and Israel also appear in the ranking, they account for a very small percentage, and the specific ranking of country issuance is detailed in Table 3. In Figure 4, there are as many as 253 connecting lines between countries, with a total linkage intensity of 546, with particularly strong links between European and Amer-

ican countries. The visual analysis chart of country cooperation and distribution is detailed in Figure 4.

**3.4. Keyword Analysis.** The visual analysis of keywords by VOSviewer software can reflect the hotspots and development trends in the field of malnutrition in bariatric surgery and explore potential new development directions and research hotspots in the field. Figure 5 shows that the larger the size of the sphere, the higher the frequency of keywords and the more focused the research focus. Figure 6 shows that the more the color of the sphere tends to be yellow, the newer the direction of research in this area is represented. Figure 7 shows that the color brightness is positively correlated with the study hotspots. The minimum frequency of keywords was set to 5, and 351 out of 3309 keywords met the threshold requirements, and the specific results are shown in Table 4. The top 6 keywords in terms of frequency were "bariatric surgery (642)", "obesity (371)", "weight loss (221)", "Y-shaped gastric fraction (221)", and "Y-shaped gastric fraction (221)". "Weight loss (221)", "Y-shaped gastric bypass (220)", "gastric bypass (193)", and "nutrient deficiency (183)" suggest a strong relationship between nutrient deficiency and bariatric surgery, which is one of the important complications of bariatric surgery [15]. Other keywords such as "outcome", "complications", "anemia", "vitamins", and "malnutrition" indicate that postoperative complications are related to deficiencies of nutritional elements and micronutrients [12, 16]. Notably, "female" and "pregnancy" also appear in the keywords, and Mead et al. [18] showed that weight loss surgery not only affects women's nutritional deficiencies during pregnancy but also the risk of low mean birth weight of the newborn. Starting in 2019, "celiac disease", "vitamin D supplementation", "single anastomosis gastric bypass", and "healthy nutrition guidelines" have become new research directions and concerns, suggesting that healthcare professionals need to pay more attention to perioperative nutritional deficiencies in bariatric surgery and take active countermeasures to correct and improve them. A visualization of the coverage of keywords evolving over time is shown in Figure 6.

TABLE 2: Ranking of institutions with 10 or more publications.

Institution	Documents	Citations	Total link strength
Univ Sao Paulo	29	612	5
Mayo Clin	25	2404	27
Assuta Med Ctr	17	242	64
Katholieke Univ Leuven	15	1038	13
Univ Fed Rio de Janeiro	15	187	3
Hebrew Univ Jerusalem	13	273	41
Univ Minnesota	13	824	12
Rijnstate Hosp	13	444	9
Hadassah Hebrew Univ	12	269	34
Brigham & Women's Hosp	12	613	9
Harvard Med Sch	11	151	11
Harvard Univ	10	1306	33
Hadassah Hebrew Univ Med Ctr	10	124	22
Univ Hosp Leuven	10	297	8
Med Univ Vienna	10	1924	6

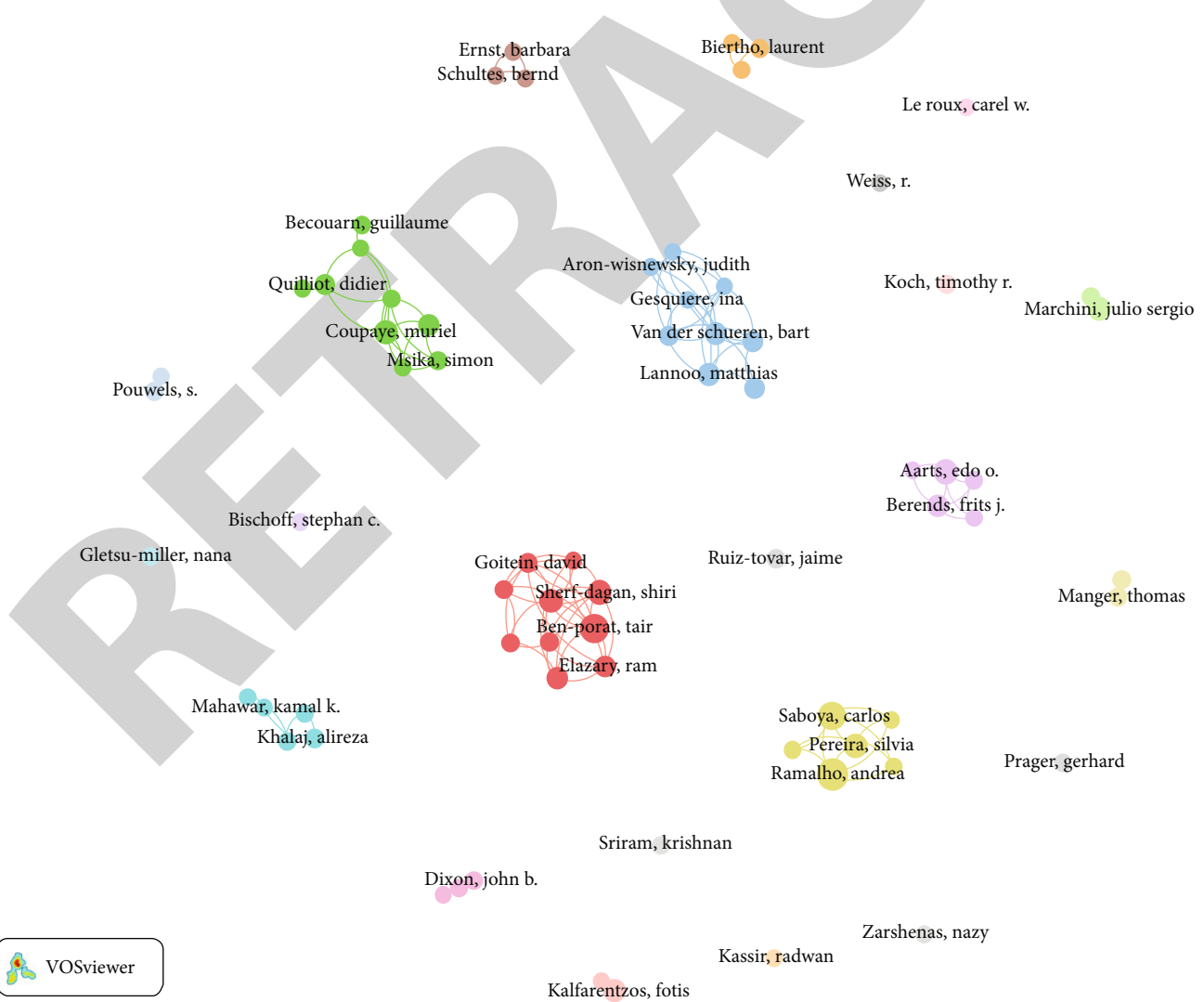


FIGURE 2: Analysis of coauthor distribution.

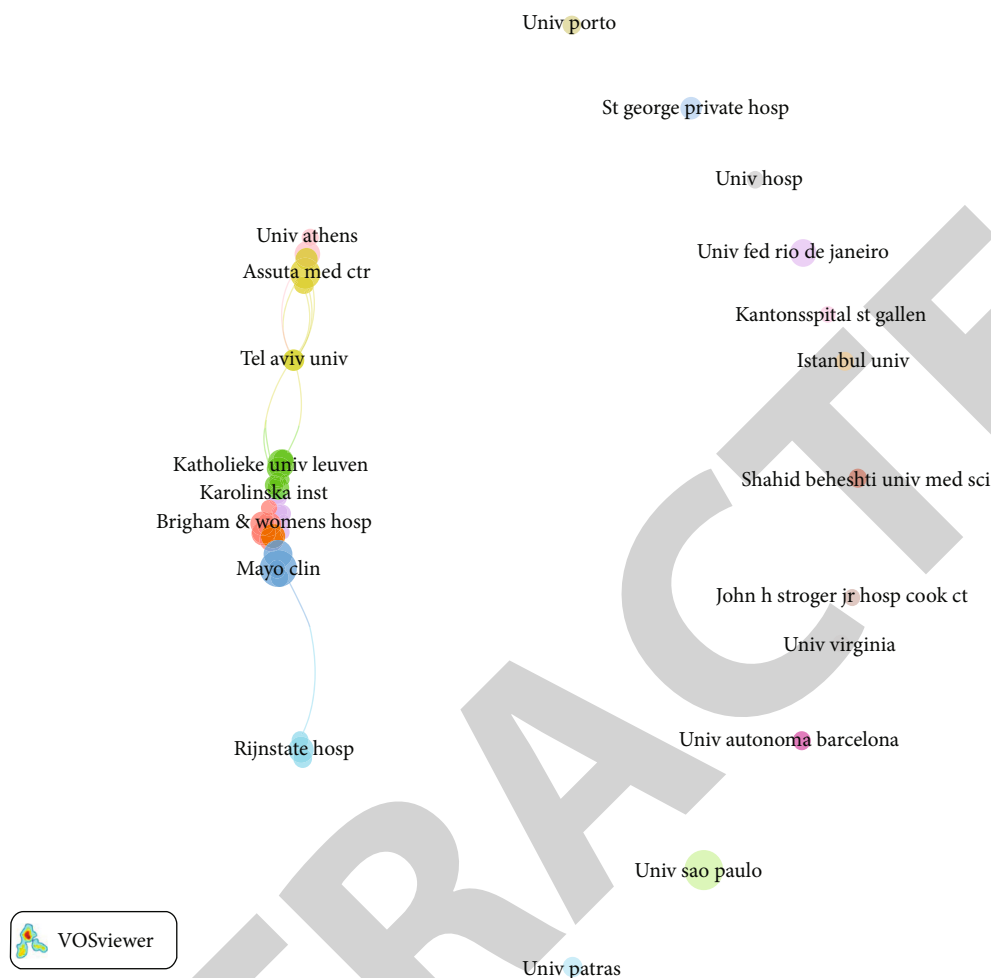


FIGURE 3: Analysis of the institutional distribution of coauthors.

TABLE 3: Top 15 ranking of coauthors' countries in terms of number of publications.

Country	Number of articles published	Percentage
USA	348	34.28%
France	91	8.97%
Brazil	83	8.2%
UK	68	6.7%
Italy	64	6.3%
Spain	60	5.9%
Germany	49	4.8%
Netherlands	43	4.2%
Canada	41	4.0%
Australia	39	3.8%
Belgium	35	3.4%
Israel	35	3.4%
China	30	3.0%
Switzerland	28	2.8%
Greek	25	2.4%

3.5. *Journal Cocitation Analysis.* A cocitation analysis of the source journals for literature related to nutritional deficiencies in bariatric surgery showed that the top three journals cited were Obesity Surgery, Surgery for Obesity and Related Diseases, and American Journal of Clinical Nutrition. The quality of the journals is relatively high in terms of citation counts and impact factors, and research on nutritional deficiencies in bariatric surgery has entered a phase of high-quality research and is receiving increasing attention. The journal citation rankings are detailed in Table 5. The connectivity between different journals is dense, and the journals are more closely linked to each other. Visual analysis of journal cocitations is shown in Figure 8.

#### 4. Conclusion

An analysis of the literature on nutritional deficiencies in bariatric surgery included in the Web of Science database since January 1, 1985, showed an overall upward trend in the number of articles published. During this period, research on nutritional deficiencies in bariatric surgery developed rapidly and achieved remarkable results. Ramalho, Andrea was the most published author whose research focuses on the complications associated with

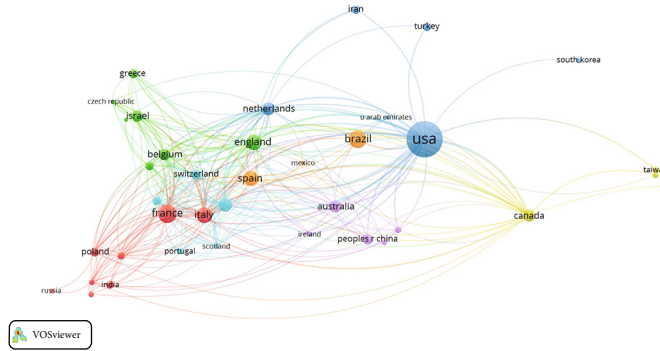


FIGURE 4: Analysis of the country distribution of coauthors.

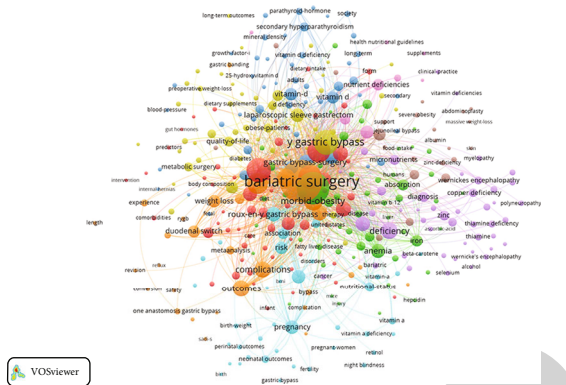


FIGURE 5: Frequency analysis of keyword occurrence.

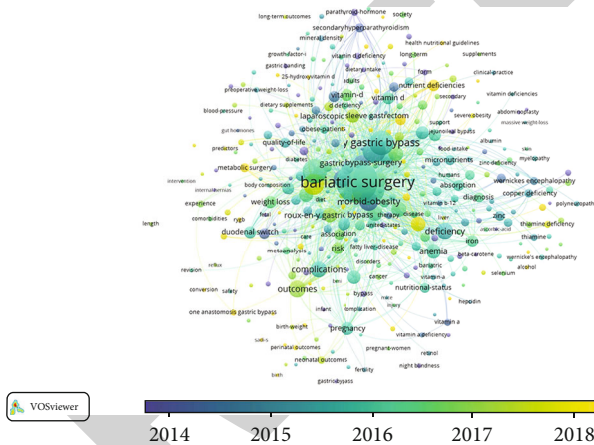


FIGURE 6: Analysis of changes in keywords by year.

micronutrient deficiencies in women, pregnancy, and bariatric surgery. While the United States, France, Brazil, the United Kingdom, and Italy are the five countries with the highest number of publications, the University of São Paulo, Mayo Clinic, and Assuta Medical Center are the main research institutions that are leaders in the field with their comprehensive and in-depth research in the area of nutritional deficiencies in bariatric surgery.

Analysis of the degree of cooperation between author groups and publishing institutions provides an overall picture of the depth and breadth of research activities in related

fields [19]. The analysis of the distribution of authors, institutions, and countries shows that the authors of studies on nutritional deficiencies in bariatric surgery come from different countries, indicating that the problem of nutritional deficiencies in bariatric surgery has gradually started to receive continuous attention in various countries around the world and is being studied in depth with “globalization” and scientific and technological advances. There is also a degree of exchange and cooperation between research or medical institutions in different countries and regions. This indicates that the problem of nutritional deficiencies in obesity and bariatric surgery is no longer a regional or local problem, but a global one that is difficult to solve on its own and requires the search for cooperation and win-win solutions. The visual analysis of authors and institutions in maps shows that the authors have many teams that work closely together and have developed a large influence, but the collaboration between authors is mostly limited to within teams, and there is almost no collaboration between teams. At the same time, cooperation among agencies is fragmented and less continuous, with a few agencies working closely with each other, but mostly as different units under the same agency. It may be related to geographic restrictions, especially after COVID-19, when countries have intensified the difficulty of cross-regional and cross-country communication and cooperation due to epidemic prevention and control requirements. From the visual analysis of the country distribution, it is known that the research results on nutritional deficiencies in bariatric surgery are mainly concentrated in Europe and North America, with a significantly higher number of Western European countries than Southern Europe, which may be related to the culture and eating habits of the Southern European diet (Mediterranean diet [20]). There are very few developing countries conducting research and producing scientific results in the field of weight loss, mainly in Asia and South America, probably influenced by the level of economic development and traditional culture, with less research on metabolic surgery nutritional deficiencies and less exchange and cooperation in this field with developed countries in Europe and America. However, it is interesting to note that Brazil and China are the 3rd and 13th countries, respectively, in terms of scientific publications in the field of nutritional deficiencies in bariatric surgery. This may be related to two things. (1) With the

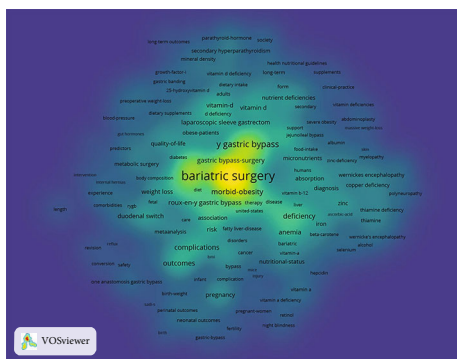


FIGURE 7: Analysis of keyword hotspot.

TABLE 4: Frequency of keywords.

Keywords	Frequency of occurrence	Total linkage strength
Bariatric surgery	642	5149
Obesity	371	3071
Weight loss	221	1949
Y gastric bypass	220	1964
Gastric bypass	193	1601
Nutritional deficiencies	183	1590
Sleeve gastrectomy	160	1440
Morbid-obesity	130	1203
Biliopancreatic diversion	117	1081
Outcomes	106	882
Deficiency	100	767
Complications	93	781
Surgery	85	626
Nutrition	79	643
Gastric-bypass surgery	78	672
Deficiencies	78	632
Guidelines	76	698
Roux-en-Y gastric bypass	76	685
Anemia	73	679
Follow-up	71	663
Malnutrition	70	592
Laparoscopic sleeve gastrectomy	66	636
Women	66	591
Prevalence	66	573
Pregnancy	65	582
Vitamin	64	600

rapid economic development, the fast pace of life and work, and the advancement of mobile payment technology, the takeout industry relying on major technology platforms is gradually becoming popular and blooming among young people, especially in the postepidemic era [21]. While technology has brought about the ability to enjoy food without leaving home, dietary patterns and habits are quietly changing, with a preference for diets or beverages high in fat, oil,

salt, and sugar and a decreasing willingness to exercise, leading to a rapid increase in the number of obese people [22]. In addition, young people work and study under pressure [23] and often stay up late [24, 25]; these unhealthy lifestyles also caused the growth of the number of obesity. (2) In the field of bariatric surgery, although Brazil and China started late, they had a high starting point. With the popularization of laparoscopic technology and minimally invasive surgery concept, BS is gradually becoming familiar to the public, and more and more people are undergoing BS. Therefore, when facing the health problems caused by obesity and the problem of nutritional deficiency after bariatric surgery, the whole world should unite to actively deal with it, start an ice-breaking action, remove barriers, adopt the methods of online network meetings and offline experience exchange and sharing, and strengthen the communication and cooperation among transnational, cross-regional, cross-center, and cross-institution, to allow more obese patients to gain health.

Analysis of the keyword network shared knowledge graph revealed that the hotspots of research on nutritional deficiencies in bariatric surgery can be broadly classified into 4 categories: (1) keywords that reflect the type of obesity are obese and morbid-obesity; (2) the keywords that reflect the type of treatment are bariatric surgery, weight loss, Y gastric bypass, gastric bypass, sleeve gastrectomy, biliopancreatic diversion, surgery, gastric-bypass surgery, Roux-en-Y gastric bypass, and laparoscopic sleeve gastrectomy; (3) the keywords that reflect the type of postoperative outcome are nutritional deficiencies, outcomes, deficiency, complications, deficiencies, anemia, and malnutrition; (4) keywords that reflect the type of postoperative nutritional management. Among them, “bariatric surgery”, “obesity”, “weight loss”, “Y-shaped gastric bypass”, “gastric bypass”, and “nutritional deficiency” are the keywords that appear most frequently and become the hotspots of research, indicating that surgical treatment of obesity is gradually becoming mainstream. Still, the problem of postoperative nutritional deficiency is also becoming more and more prominent, which requires bariatric surgeons and researchers to jointly explore the mechanisms and causes behind its occurrence and find treatment methods from the root. Other keywords such as “outcome”, “complications”, “anemia”, “vitamins”, and “malnutrition” suggest a link between nutritional deficiency as an adverse outcome after bariatric surgery and other related complications. It is recommended [26] that a multidisciplinary collaborative and integrated treatment and treatment model of perioperative nutritional management throughout the process of preoperative assessment, intraoperative monitoring, postoperative rehabilitation, and postoperative follow-up can effectively alleviate and prevent perioperative nutrient deficiencies in bariatric surgery.

In addition, Smelt et al. [27] showed that specific bariatric multivitamins targeted for individualization can improve micronutrient deficiencies. It is noteworthy that more and more authors are becoming concerned about the impact of BS of nutrient deficiencies in women during pregnancy, early/recurrent miscarriage, and low birth weight in newborns [18, 26]. Guidelines recommend that the provision







has a relatively high level of national economy, but with a large population and low per capita income level, coupled with the fact that obesity is not currently considered a disease in China and is not covered by medical insurance, the vast majority of patients who want to reduce their weight through surgery are turned away. The late start of bariatric surgery in China, the lack of data, and the relative lag in research have resulted in significantly fewer research results being published in international high-quality journals than in developed countries in Europe and the United States. As a non-English speaking country, most authors also prefer to publish their research in Chinese domestic journals, which to some extent diminishes the international influence of China in the field of bariatric surgery. In order to eliminate the large number of obese people in China as soon as possible, it is recommended that China adopt a strategic approach of “bringing in” and “going out.” “Bringing in” is based on China’s established bariatric surgery database, introducing advanced international technology and equipment and concepts, employing full-time bariatric surgeons and bariatric case managers, and combining MDT teams to improve surgical quality and safety while reducing post-operative complications. “Going out” is to strengthen exchanges and cooperation with developing countries in the field of bariatric surgery, such as visiting schools, attending conferences, and exchanging experiences, so as to produce more high-quality clinical research results and improve medical quality and clinical efficacy for the benefit of patients.

## 5. Summary

This study visualized and analyzed the collected literature on nutritional deficiencies in bariatric surgery from multiple perspectives by using VOSviewer software to derive the current status of research, research hotspots, and new research trends in this field and to actively explore possible new treatment options for future new treatment protocols. Nutritional deficiencies in bariatric surgery have received widespread attention from scholars around the world, with closer collaboration between institutions than between authors, but there is an urgent need for cross-institutional, cross-team, and cross-national academic exchange and collaboration between authors, institutions, and countries. The WOS Core Collection database is an authoritative database of academic information worldwide, which includes important academic journals and international conferences worldwide with a strict screening mechanism, and the literature included in WOS belongs to the type supported by the operation of VOSviewer software, so the literature from the WOS Core Collection database was selected for analysis. Multidatabase analysis was not conducted in this study, which has the defect of incomplete data, and multidatabase analysis will be conducted in other studies in the future.

## Data Availability

The data used to support the findings of this study are included within the article.

## Conflicts of Interest

The authors declare that there is no conflict of interest regarding the publication of this paper.

## Authors’ Contributions

The authors’ responsibilities were as follows: JT, MH, and GL designed the research; JT performed the research; XW, ZY, and HJW contributed to the acquisition of data; JT and JH analyzed the data; JT wrote the first version of the manuscript; MH revised the manuscript for essential intellectual content. All authors read and approved the final manuscript.

## References

- [1] J. I. Mechanick, C. Apovian, S. Brethauer et al., “Clinical practice guidelines for the perioperative nutrition, metabolic, and nonsurgical support of patients undergoing bariatric procedures -2019 update:cosponsored by American Association of Clinical Endocrinologists/American College of Endocrinology, The Obesity Society, American Society for Metabolic and Bariatric Surgery, Obesity Medicine Association, and American Society of Anesthesiologists,” *Obesity*, vol. 28, no. 4, pp. O1–O58, 2020.
- [2] M. Blüher, “Obesity: global epidemiology and pathogenesis,” *Nature Reviews. Endocrinology*, vol. 15, no. 5, pp. 288–298, 2019.
- [3] World Health Organization, “Obesity and overweight,” <https://www.who.int/zh/news-room/fact-sheets/detail/obesity-and-overweight>.
- [4] World Health Organization, “WHO Discussion Paper:Draft recommendations for the prevention and management of obesity over the life course, including potential targets,” <https://www.who.int/publications/m/item/who-discussion-paper-draft-recommendations-for-the-prevention-and-management-of-obesity-over-the-life-course-including-potential-targets>.
- [5] State Council Information Office of the People’s Republic of China, “Report on nutrition and chronic diseases status of Chinese residents,” *Chinese Journal of Nutrition*, vol. 42, no. 6, p. 521, 2020.
- [6] E. Faccio, A. Nardin, and S. Cipolletta, “Becoming ex-obese: narrations about identity changes before and after the experience of the bariatric surgery,” *Journal of Clinical Nursing*, vol. 25, no. 11-12, pp. 1713–1720, 2016.
- [7] S.-H. Chang, C. R. T. Stoll, J. Song, J. E. Varela, C. J. Eagon, and G. A. Colditz, “The effectiveness and risks of bariatric surgery:an updated systematic review and meta-analysis, 2003-2012,” *JAMA Surgery*, vol. 149, no. 3, pp. 275–287, 2014.
- [8] H. Yang, Y. Chen, Z. Y. Dong et al., “The Chinese obesity metabolic surgery database:annual report 2020,” *Chinese Journal of Obesity and Metabolic Diseases*, vol. 7, no. 1, pp. 1–7, 2021.
- [9] A. Gasmi, G. Björklund, P. K. Mujawdiya et al., “Micronutrients deficiencies in patients after bariatric surgery,” *European journal of nutrition*, vol. 61, no. 1, pp. 55–67, 2022.
- [10] Y. Wang, C. C. Wang, S. H. Zhu, P. Zhang, and H. Liang, “China’s obesity and type 2 diabetes surgery guide (2019 edition),” *Chinese Journal of Practical Surgery*, vol. 39, no. 4, pp. 301–306, 2019.

## *Retraction*

# **Retracted: The Effect of Social Cognitive Interaction Training on Schizophrenia: A Systematic Review and Meta-Analysis of Comparison with Conventional Treatment**

### **BioMed Research International**

Received 12 November 2022; Accepted 12 November 2022; Published 18 January 2023

Copyright © 2023 BioMed Research International. This is an open access article distributed under the Creative Commons Attribution License, which permits unrestricted use, distribution, and reproduction in any medium, provided the original work is properly cited.

*BioMed Research International* has retracted the article titled “The Effect of Social Cognitive Interaction Training on Schizophrenia: A Systematic Review and Meta-Analysis of Comparison with Conventional Treatment” [1] due to concerns that the peer review process has been compromised.

Following an investigation conducted by the Hindawi Research Integrity team [2], significant concerns were identified with the peer reviewers assigned to this article; the investigation has concluded that the peer review process was compromised. We therefore can no longer trust the peer review process and the article is being retracted with the agreement of the editorial board.

### **References**

- [1] Y. Tang, L. Yu, D. Zhang, F. Fang, and Z. Yuan, “The Effect of Social Cognitive Interaction Training on Schizophrenia: A Systematic Review and Meta-Analysis of Comparison with Conventional Treatment,” *BioMed Research International*, vol. 2022, Article ID 3394978, 11 pages, 2022.
- [2] L. Ferguson, “Advancing Research Integrity Collaboratively and with Vigour,” 2022, <https://www.hindawi.com/post/advancing-research-integrity-collaboratively-and-vigour/>.

## Review Article

# The Effect of Social Cognitive Interaction Training on Schizophrenia: A Systematic Review and Meta-Analysis of Comparison with Conventional Treatment

Yan Tang,<sup>1</sup> Linhua Yu,<sup>1</sup> Dongyang Zhang,<sup>1</sup> Fang Fang,<sup>2</sup> and Zhaoxia Yuan<sup>1</sup> 

<sup>1</sup>Department of Psychiatry, Affiliated Mental Health Center & Hangzhou Seventh People's Hospital, Zhejiang University School of Medicine, Hangzhou, Zhejiang 310013, China

<sup>2</sup>Department of Emergency, Affiliated Mental Health Center & Hangzhou Seventh People's Hospital, Zhejiang University School of Medicine, Hangzhou, Zhejiang 310013, China

Correspondence should be addressed to Zhaoxia Yuan; [yuanzx82@163.com](mailto:yuanzx82@163.com)

Received 12 July 2022; Revised 27 July 2022; Accepted 3 August 2022; Published 16 August 2022

Academic Editor: Dinesh Rokaya

Copyright © 2022 Yan Tang et al. This is an open access article distributed under the Creative Commons Attribution License, which permits unrestricted use, distribution, and reproduction in any medium, provided the original work is properly cited.

**Background.** Existing antipsychotic medications may alleviate the majority of patients' symptoms, but they have no discernible impact on improving social function and quality of life. Psychotherapy is required for the treatment of schizophrenia. However, contemporary psychotherapy technology intervention techniques are limited to a single intervention, and there is a lack of holistic and complete intervention approaches. Social cognition and interaction training is a comprehensive therapy strategy that has been employed in clinical practice; however, the therapeutic efficacy has been inconsistently reported. As a result, we included controlled clinical trials for meta-analysis in order to carefully assess the efficacy of this therapy. **Methods.** This meta-analysis searched all RCT literatures related to social cognitive interaction training (SCIT) published before April 2022 and assessed the effect of this method in the treatment of schizophrenia. The data in the literatures were combined, and the standardized mean difference (SMD) and mean difference (MD) with 95% confidence interval (95% CI) were calculated to predict the negative symptom score, positive symptom score, PANSS score, and social function score of the patients after treatment. **Results.** 14 RCT studies including 1167 inpatients with schizophrenia were included in this study using a retrospective observational study method, including 590 patients treated with SCIT and 577 patients treated with treatment as usual (TAU). The pooled analysis showed that patients after SCIT had lower negative symptom scores (SMD = -1.66, 95% CI (-2.32, -1.00),  $P < 0.0001$ ), lower positive symptom scores (MD = -4.03, 95% CI (-7.69, -0.36),  $P = 0.03$ ), lower PANSS total scores (MD = -6.33, 95% CI (-12.43, -0.23),  $P = 0.02$ ), and higher social functioning scores (SMD = 0.77, 95% CI (0.34, 1.20),  $P < 0.001$ ) than those after TAU. **Conclusion.** Our findings support that SCIT is helpful to improve the relief of symptoms and the improvement of social function in patients with schizophrenia, providing a basis for the application of SCIT in hospitalized patients and community patients, and can guide the treatment and intervention of patients with schizophrenia.

## 1. Introduction

Schizophrenia is a common chronic persistent disease in psychiatry, which is characterized by high disability rate and high recurrence rate [1]. The condition is characterized by severe cognitive impairment, which may affect patients' social functions such as self-care, daily living, communication, and family life and significantly diminish their quality of life [2]. Existing antipsychotic drugs can relieve most of

the symptoms of patients but have no significant effect on the improvement of social function and quality of life of patients, and the side effects of drugs can aggravate the mental burden of patients and affect their prognosis [3]. At present, many psychotherapy techniques have been applied in the treatment of schizophrenia, which is of great significance for controlling symptoms, improving treatment compliance, and improving the social function of patients [4, 5]. However, existing psychotherapeutic techniques have a single

intervention and lack holistic and comprehensive intervention methods [6]. Social cognitive interaction training (SCIT) is a therapy hypothesis developed by Roberts in 2007, which holds that the cognitive impairment caused by schizophrenia is separated into three parts: emotional perception, theory of mind, and attribution mode. As a result, the intervention for patients should provide holistic therapy from all three perspectives in order to significantly enhance patients' social cognitive performance [7]. At present, this treatment has been applied in a number of studies, but there are inconsistent reports on its therapeutic effect. The results of the study by Rocha et al. [8] showed that SCIT was effective in improving attribution bias and social function in patients. But another study by Dark et al. [9] showed that SCIT did not show any additional benefit in social cognition improvement compared with conventional treatment methods. In order to address the inconsistencies between different studies and to understand the important role of SCIT for the improvement of the prognosis of patients with schizophrenia, we performed this meta-analysis on the basis of the existing published literature.

The implementation of this quantitative meta-analysis is guided by the PRISMA recommended guidelines (the Preferred Reporting Items for Systematic Reviews and Meta-Analyses).

## 2. Method

**2.1. Inclusion and Exclusion Criteria for Studies.** The inclusion and exclusion criteria related to this meta-analysis were as follows: (i) subjects: all subjects were hospitalized patients with confirmed schizophrenia, without limiting that patients were in the first attack, relapse, and remission stages. To avoid heterogeneity, we excluded studies whose subjects were discharged patients in the rehabilitation stage. (ii) Grouping and control: all patients were divided into the intervention group and control group. Randomization sequence and allocation concealment study were preferred. Baseline data were compared between the two groups. (iii) The intervention group: on the basis of conventional drug therapy, social cognitive interaction training (SCIT) was given. (iv) Control group: routine medication and routine care were given, and studies with other specific methods, such as training in affect recognition (TAR) [10], were excluded from the control group. (v) Outcome indicators: PANSS score, negative symptom score, positive symptom score, and social function score after treatment were the main outcome indicators. (vi) Study type: included studies are quasirandomized controlled studies or cohort studies.

**2.2. Literature Search Strategy.** We focused on the databases PubMed (<https://pubmed.ncbi.nlm.nih.gov/>), WOS (<https://www.webofscience.com/>), Scopus (<https://www.scopus.com/>), China National Knowledge Infrastructure (CNKI, <https://www.cnki.net>), and Weipu (<https://www.cqvip.com/>), a comprehensive and systematic search was performed, and all articles were published before April 2022. The search was performed by two researchers using a keyword free search mode with keywords including (“social cognitive

interaction training” OR “SCIT” OR “cognitive behavioral social skills training” OR “CBSST”) AND (“schizophrenia”).

**2.3. Selection of Literatures.** Two researchers exported the retrieved articles from each database in a format that EndNote could identify, such as PubMed export suffix “.Nbib” and other databases’ file storage with “.ris” suffix. All the retrieved literatures were imported into EndNote management, and the repeated literatures were removed by using the “repeated literature identification” function of the software. According to the established inclusion and exclusion criteria, two researchers read the title and abstract of the literature one by one to complete the screening of most of the articles. After screening the remaining articles on the Internet (or directly contacting the original author), receive the full text of the articles, read the full text of the articles, further screen, and obtain the final collection of included articles. If there was a disagreement regarding whether or not to include a particular piece, a third person was requested to make a decision.

**2.4. Data Extraction.** The researchers obtained the data required for meta-analysis from the included literatures and recorded it in a tabular form. Data included gender ratio, mean age, initial PANSS score (mean  $\pm$  variance), education level (%), residence, family psychiatric history, name of the published journal, first author, study region, study type, random sequence generation method, and outcome data of included patients. If the data of the study is not provided, it was marked as NR (not reported).

**2.5. Literature Quality Assessment and Risk of Bias.** Cochrane risk of bias 2.0 [11] was used to evaluate the risk of bias of the included studies, including 6 levels, and each level was given “low,” “some concern of risk,” and “high” for risk evaluation.

**2.6. Statistical Methods.** (i) Effect sizes: since different literatures may adopt different scales for the evaluation of the same indicator, we use standard mean difference (SMD) and 95% CI as effect size for the analysis of outcome indicators (except PANSS total score) and mean difference (MD) and 95% CI as effect size for PANSS total score. (ii) Heterogeneity test: for the heterogeneity of literatures displayed during analysis, we expressed it as  $\tau^2$ , and standard error (SE),  $I^2$ , and Q tests were used for the test of heterogeneity;  $I^2 > 50\%$  or  $P < 0.1$  indicated that the heterogeneity was not statistically significant, and there was heterogeneity between literatures. (iii) Effect model selection: random effects mode was used for analysis. (iv) Analytical tools: the analysis was completed using the R language toolkit metafor released by Cran-Project to present the analysis results in a forest plot. (v) Heterogeneity survey: metaregression analysis, the radial plot or Galbraith plot, and normal quantile-quantile (QQ) plot were used to analyze publication bias. (vi) Publication bias analysis: publication bias was analyzed by funnel plot and Egger’s test, and  $Pr > |z| < 0.05$  was considered statistically significant.



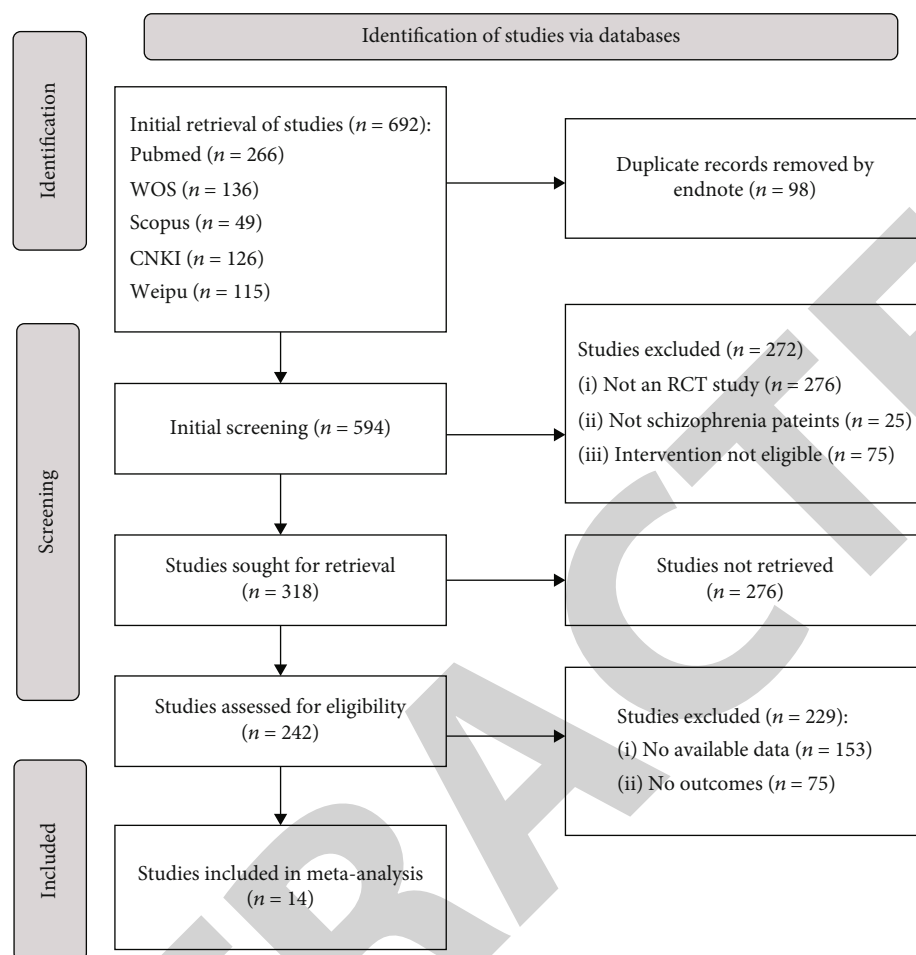


FIGURE 1: The selection flow chart following PRISMA.

### 3. Results

**3.1. Literature Screening Process and Results.** The identification, screening, and inclusion process according to PRISMA regulations is shown in Figure 1. In this study, 692 literatures were initially searched, 266 were searched by PubMed, 136 were searched by WOS, 49 were searched by Scopus, 126 were searched by CNKI (Chinese), and 115 were searched by Weipu. After all literatures were imported into EndNote, a total of 98 repeated literatures were repeatedly judged. After removing the repeated literatures, the remaining 594 literatures were initially screened, non-RCT studies (176 literatures) and nonschizophrenia patients (25 literatures) were excluded. After inappropriate intervention methods (75 literatures), the remaining 318 literatures were included in the usability analysis; the full text could not be obtained in 76 literatures. The literatures without outcome indicators and with unusable data were further excluded. Finally, 14 literatures [8, 9, 12–23] were included.

**3.2. Basic Characteristics of Literatures.** A total of 1167 patients with schizophrenia were included in this study, and all studies were RCT studies, including 590 patients treated with SCIT and 577 patients treated with TAU. There

was 1 literature [12] on children (aged <18 years), and the remaining study subjects were all adult patients; the intervention duration ranged from 4 to 36 weeks, as shown in Table 1.

**3.3. Quality Assessment of Literature.** Figure 2 summarizes the details of methodological assessment of eligible studies assessed according to the Cochrane ROB 2.0. The overall quality of the 14 studies included in this study was good, with 0 articles (0.00%) for “high risk of bias,” 8 articles (57.14%) for “low risk of bias,” and 6 articles (42.86%) for “some concern of risk.” The results of the Cochrane ROB 2.0 confirmed that there was no significant bias in this meta-analysis.

#### 3.4. Meta-Analysis Results

**3.4.1. Comparison of Negative Symptom Scores after Intervention.** Among all 14 included studies, a total of 8 literatures [8, 12, 14, 15, 20–23] tried to compare SCIT with TSU for the comparison of negative symptom scores of patients with schizophrenia after treatment, the literatures [8, 14, 21, 22] were assessed by the SANS scale, and the literatures [12, 15, 20, 23] were assessed by the negative

TABLE 1: Basic characteristics of the included studies.

First author, year	Observation group (SCIT)		Control group (TAU)		Population (O/C)	Duration of intervention	Outcome indicators
	M/F	Age	M/F	Age			
Rocha et al., 2021 [8]	5/1	29.5 ± 13.38	5/0	27 ± 6.12	6/5	20 weeks	(a)(b)(c)(d)
Dark et al., 2020 [9]	46/15	36.1 ± 10.7	40/19	37.5 ± 10.1	61/59	12 weeks	(d)(e)
Li et al., 2020 [12]	54/52	16.11 ± 1.44	55/47	16.13 ± 1.43	106/102	24 weeks	(a)(b)(c)(d)
Gordon et al., 2018 [13]	7/14	19-55	5/10	19-54	21/15	10 weeks	(e)(g)
Wang et al., 2019 [14]	20/10	26.4 ± 9.7	20/10	27.1 ± 8.5	30/30	4 weeks	(a)(f)
Zhang et al., 2019 [15]	32/26	42.5 ± 9.2	31/29	42.6 ± 8.1	58/60	9 weeks	(a)(b)(c)(d)
Tao et al., 2011 [16]	20/18	37.1 ± 11.5	18/20	39.0 ± 11.8	38/38	6 weeks	(d)(g)
Roberts et al., 2014 [17]	22/11	40.0 ± 12.2	22/11	39.4 ± 12.8	33/33	20 weeks	(d)(e)(g)
Wang et al., 2013 [18]	12/10	43.86 ± 11.65	8/9	40.88 ± 10.15	22/17	20 weeks	(d)
Lian et al., 2017 [19]	38/16	31.7 ± 8.2	36/15	33.0 ± 7.5	54/51	4 weeks	(g)
Shen et al., 2018 [20]	25/20	27.96 ± 7.66	21/24	31.06 ± 9.76	45/45	10 weeks	(a)(b)(c)(d)(g)
Mahmood et al., 2021 [21]	9/17	47.73 ± 11.36	50/50	53.24 ± 7.35	13/16	12.5 weeks	(a)(e)
Granhölm et al., 2014 [22]	46/27	41.1 ± 10.4	53/23	41.6 ± 9.2	73/76	36 weeks	(a)(b)(e)
Xu et al., 2011 [23]	17/13	37.1 ± 14.9	17/13	35.6 ± 13.0	30/30	6 weeks	(a)(c)(d)

(a) Negative symptoms, (b) positive symptoms, (c) PANSS total score, (d) social function assessment, (e) social skills and performance, (f) rehabilitation efficacy, and (g) quality of life. M/F: male/female; O/C: observation/control; PANSS: positive and negative syndrome scale; TAU: treatment as usual.

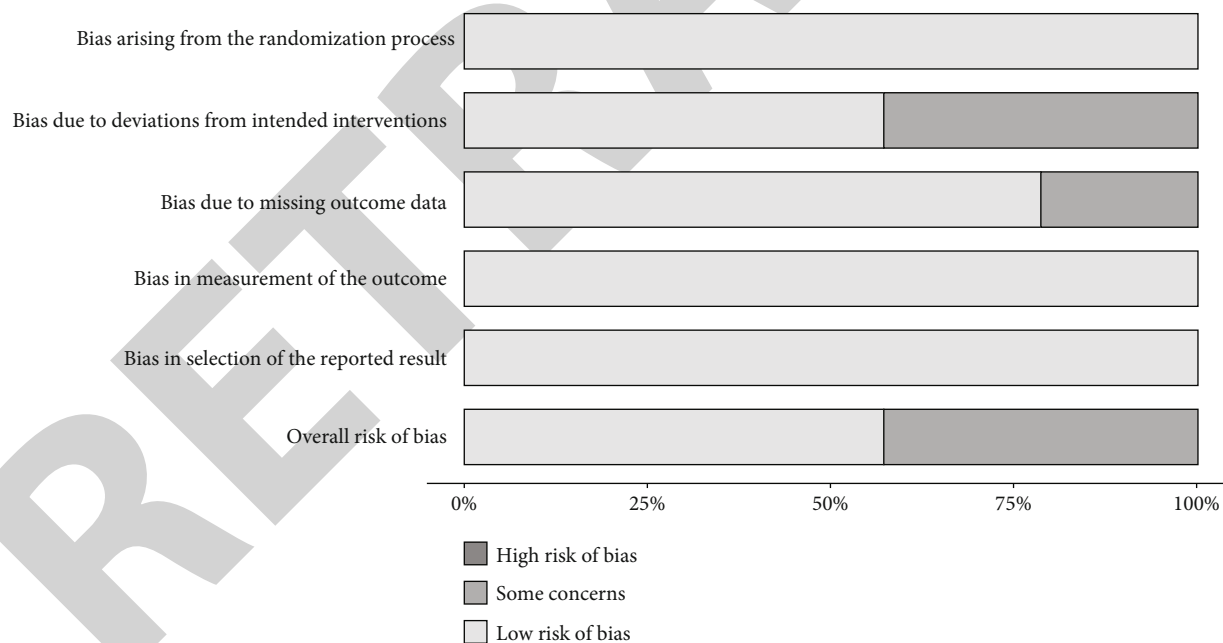


FIGURE 2: Summary plot of literature bias analysis.

symptom subscale of PANSS scale. In the analysis, it was found that there was significant heterogeneity between the literatures ( $\tau^2 = 0.7979$  ( $SE = 0.4864$ ),  $I^2 = 92.62\%$ , Cochran Q test,  $P < 0.0001$ ). The pooled ES obtained using the random effects model was  $SMD = -1.66$  (95% CI (-2.32, -1.00),  $P < 0.0001$ ), suggesting that patients had lower negative symptom scores after SCIT than after TSU treatment. A forest plot of pooled effects is shown in Figure 3.

**3.4.2. Positive Symptom Score after Intervention.** Among all 14 included studies, a total of 4 literatures [8, 15, 20, 22] tried to compare the positive symptom scores of SCIT and TSU for patients with schizophrenia after treatment. All literatures were assessed by the positive symptom subscale of PANSS scale. The analysis found that there was significant heterogeneity between the literatures ( $\tau^2 = 12.878$  ( $SE = 11.395$ ),  $I^2 = 96.91\%$ , Cochran Q test,  $P < 0.0001$ ).



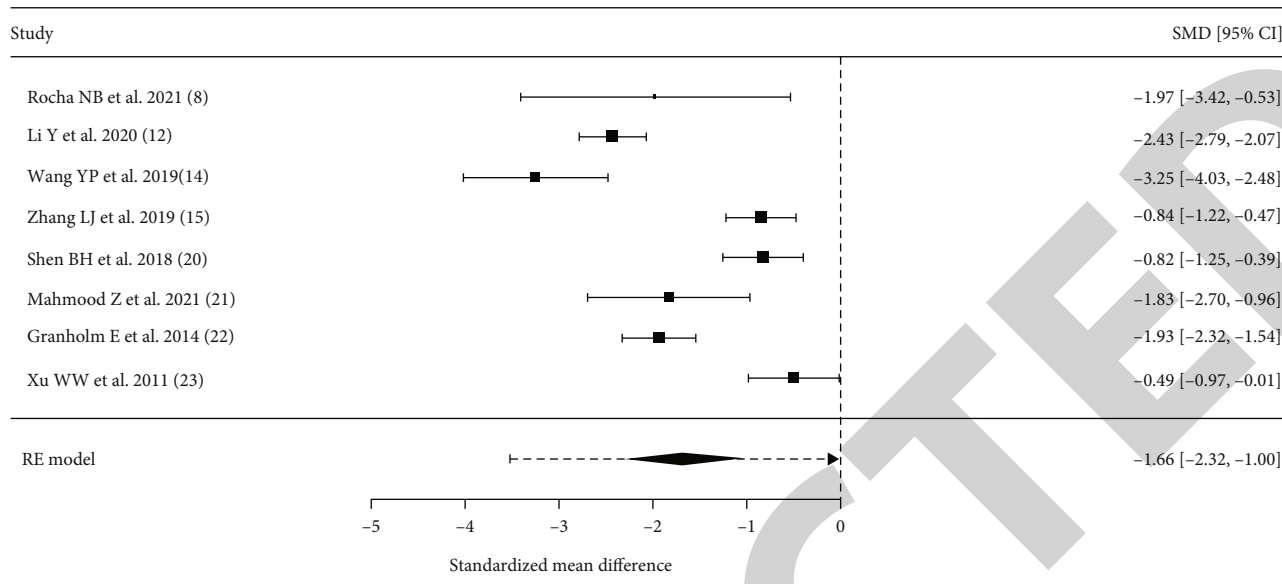


FIGURE 3: Comparison of negative symptom scores after treatment between the two groups.

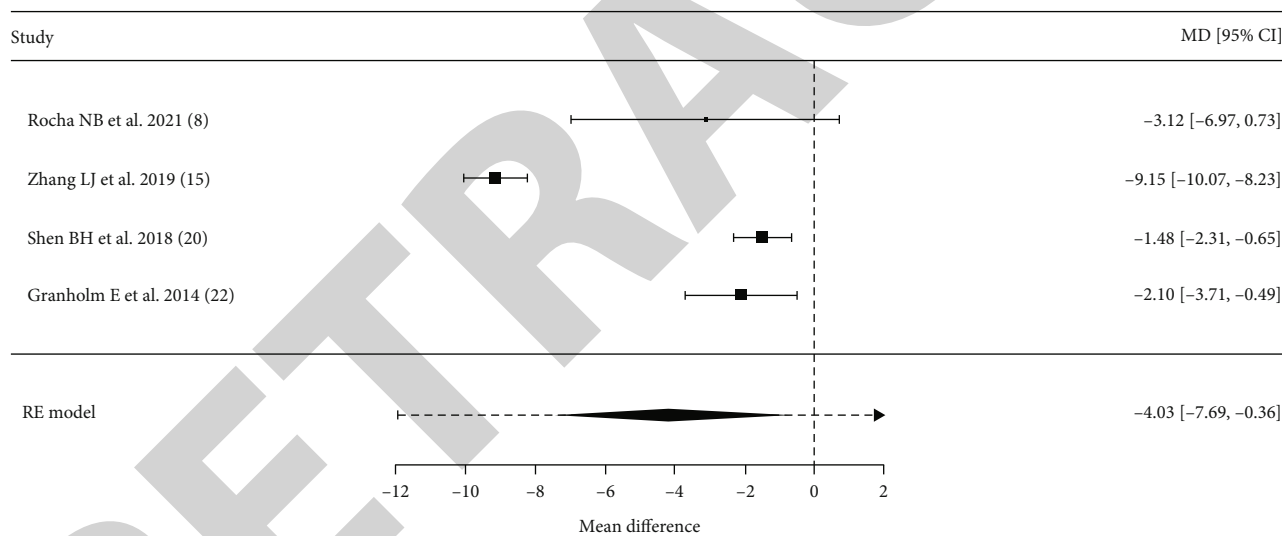


FIGURE 4: Comparison of PANSS positive symptom scores after treatment between the two groups.

The pooled ES obtained using the random effects model was MD = -4.03 (95% CI (-7.69, -0.36),  $P = 0.03$ ), suggesting that patients had lower positive symptom scores after SCIT than after TSU treatment. Forest plots of pooled effects are shown in Figure 4.

3.4.3. *PANSS Total Score after Intervention.* Among all 14 included studies, a total of 5 literatures [8, 12, 15, 20, 23] tried to compare SCIT with TSU for the PANSS total score after treatment in patients with schizophrenia, and significant heterogeneity was found between the literatures in the analysis ( $\tau^2 = 41.63$  (SE = 34.21),  $I^2 = 91.30\%$ , Cochran Q test,  $P < 0.0001$ ). The pooled ES obtained using the random effects model was MD = -6.33 (95% CI (-12.43, -0.23),  $P = 0.02$ ), suggesting that the PANSS total score was lower in

patients after SCIT than after TSU treatment. A forest plot of pooled effects is shown in Figure 5.

3.4.4. *Social Function after Intervention.* Only 8 articles [8, 12, 15, 17, 18, 20, 23] attempted to compare the effects of SCIT with TSU on posttreatment social functioning in patients with schizophrenia, and significant heterogeneity was found between the articles in the analysis ( $\tau^2 = 0.257$  (SE = 0.193),  $I^2 = 82.15\%$ , Cochran Q test,  $P < 0.0001$ ). The pooled ES obtained using the random effects model was SMD = 0.77 (95% CI (0.34, 1.20),  $P < 0.001$ ), suggesting that the social function of patients was improved after SCIT compared with TSU treatment. A forest plot of pooled effects is shown in Figure 6.

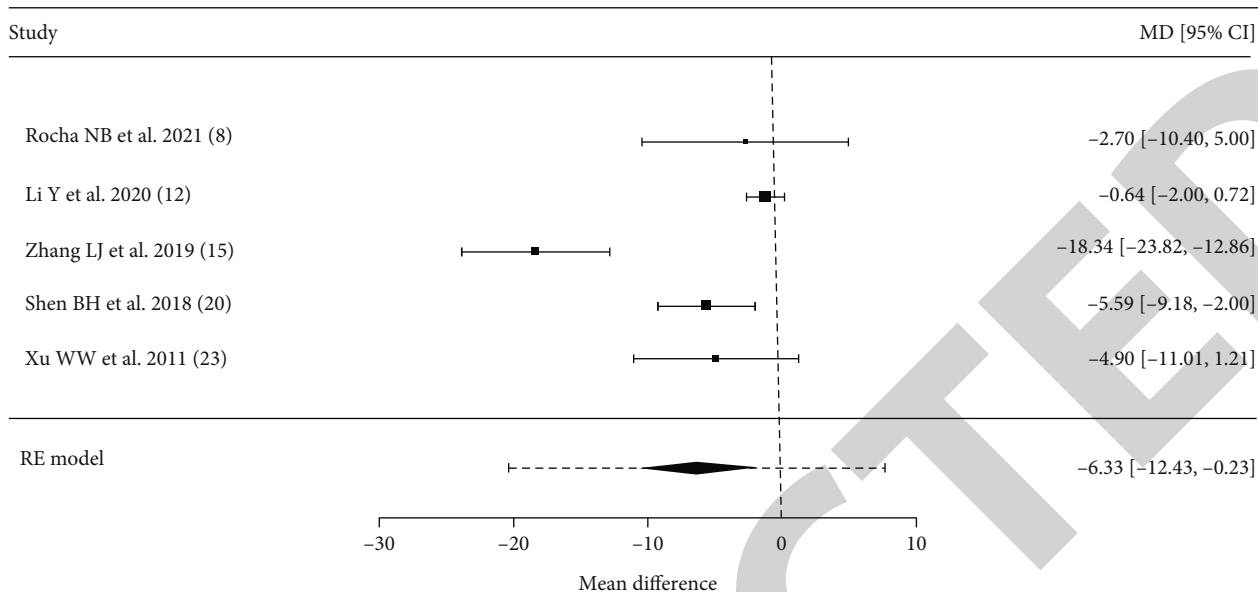


FIGURE 5: Comparison of the PANSS total score after treatment between the two groups.

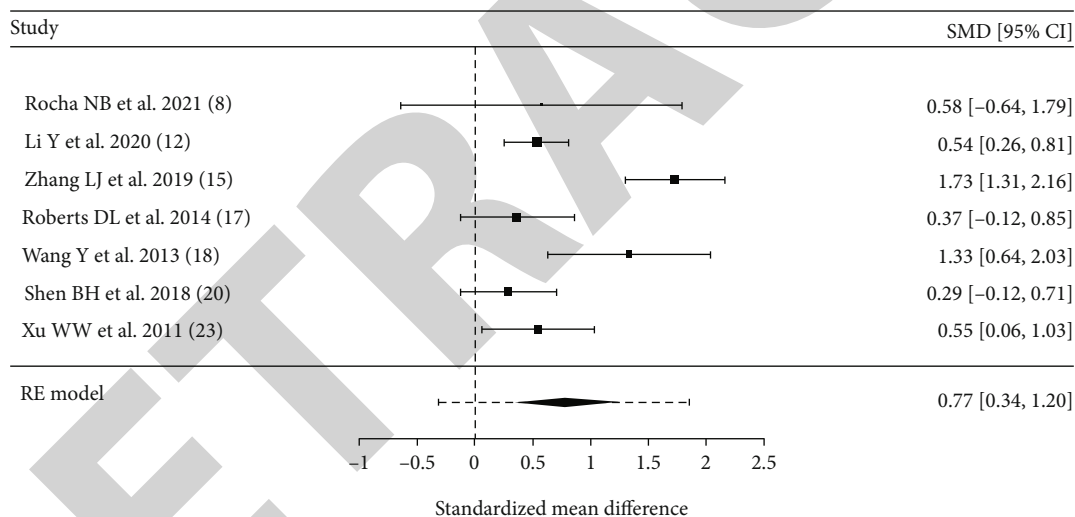


FIGURE 6: Comparison of social function scores after treatment between the two groups.

### 3.4.5. Heterogeneity Survey

(1) *Regression Analysis.* This meta-analysis tried to find whether “age” was the result affecting the negative symptom score after treatment, and the results showed that  $P > |t| = 0.553$ ; age was not the source of heterogeneity, as shown in Figure 7.

(2) *Radial Plot.* The comparison of negative symptom scores after treatment was shown by radial plot, and it can be seen from the presentation that all 8 articles were within the range without significant deviation, as shown in Figure 8.

(3) *Normal Quantile-Quantile (QQ) Plot.* The comparison of negative symptom scores after treatment was shown by the QQ plot, and it showed that 8 articles were within the range and without significant deviation, as shown in Figure 9.

3.4.6. *Analysis of Publication Bias.* In the publication bias for the comparison of negative symptom scores after treatment, the funnel plot showed that the 8 literatures showed uneven distribution on both sides of the funnel, possibly with bias; however, in the quantitative analysis using Egger’s test,  $P > |t| = 0.660$ , suggesting that there was no statistically significant publication bias, as shown in Figures 10 and 11.

## 4. Discussion

SCIT is a comprehensive psychotherapeutic approach based on improving emotional perception, attribution style, and theory of mind ability in patients with schizophrenia [24]. Unlike existing cognitive theories, this approach focuses treatment on three categories of social cognition [25]. The results of existing clinical studies have shown that SCIT can significantly

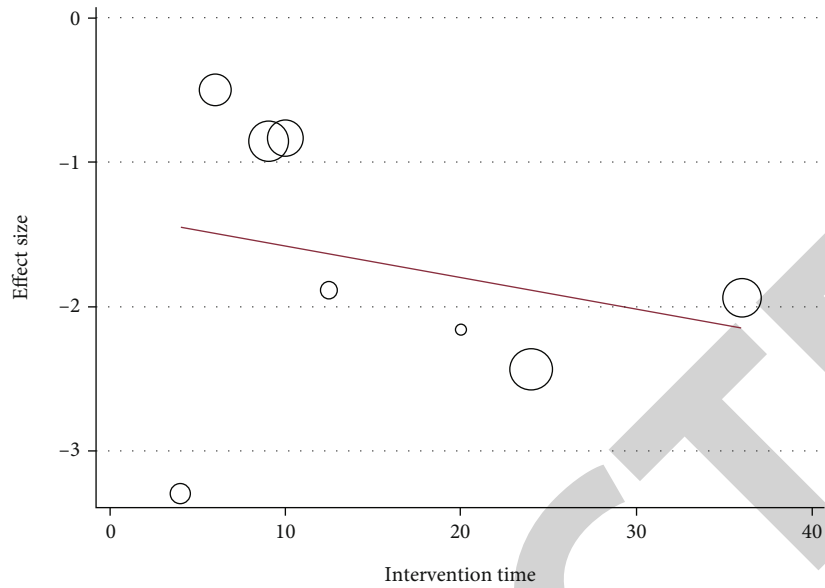


FIGURE 7: Regression analysis by age factor.

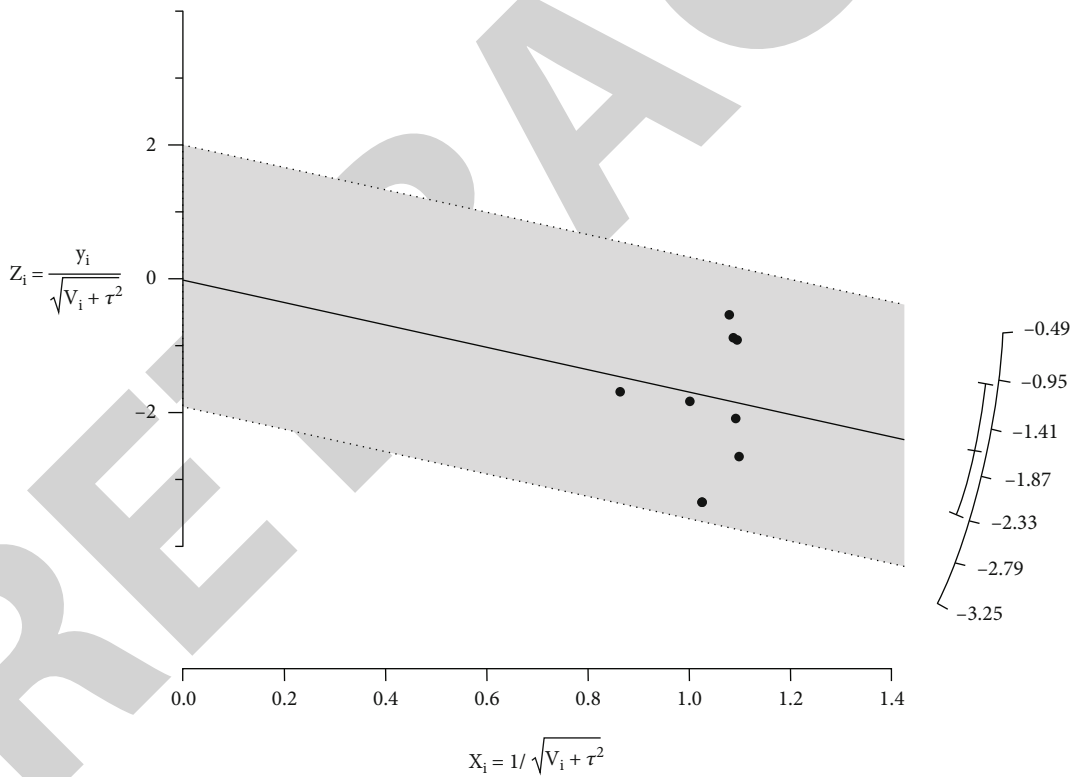


FIGURE 8: Radial plot.

improve the emotional cognition, suggestion, and attribution methods of patients, thereby reducing the aggressive behavior of patients, improving the cognitive flexibility of patients, enhancing the needs of intimate relationships, and improving the social relationships of patients [26, 27]. In the study by Rocha et al. [8], SCIT improved these indicators compared with conventional treatment, as patients' cognitive bias, emo-

tion recognition, theory of mind, and social perception were measured before and after treatment.

As the core symptom cluster of schizophrenia, negative symptoms are the main cause of protracted course and mental disability, and their occurrence is closely related to the abnormal cognitive pattern of patients to negative life events [28]. Patients generally tend to attribute multiple symptoms

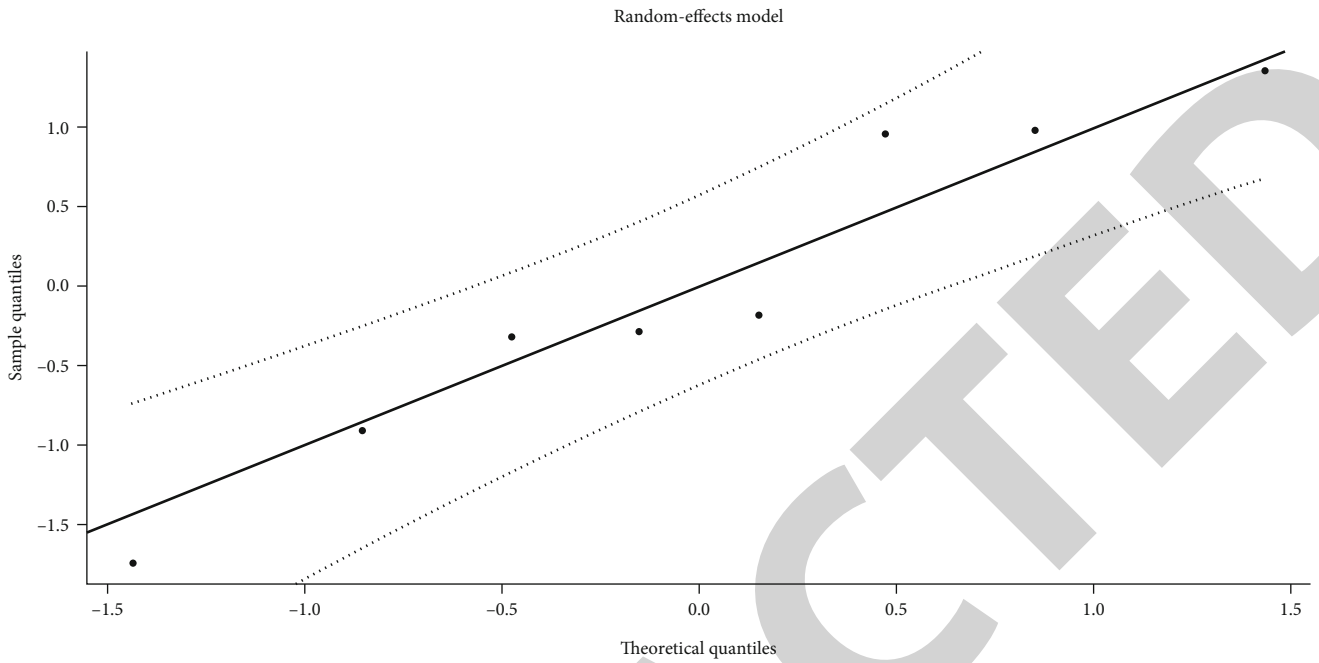


FIGURE 9: Normal quantile-quantile (QQ) plot.

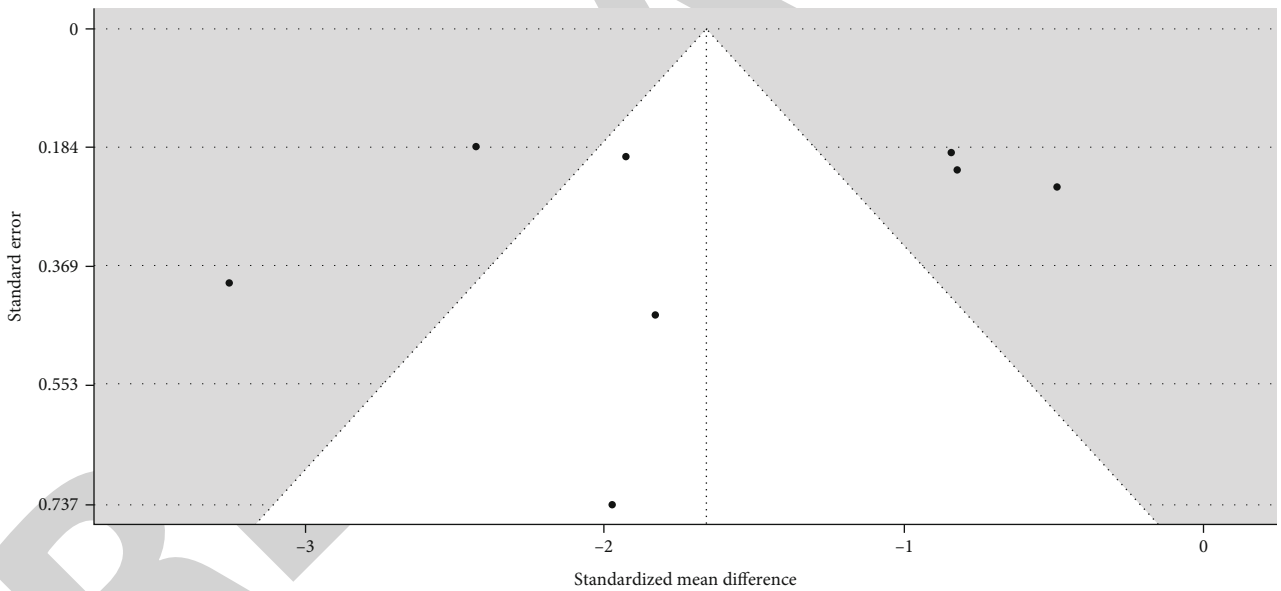


FIGURE 10: Publication bias: funnel plot.

to the outside world, especially others in the outside world [29]. SCIT focuses on the correction of patient’s unreasonable cognition, encourages patients to self-expose their emotions, ideas, and behaviors, guides patients to develop in an objective and correct direction when thinking about problems, improves patients’ ability to solve realistic problems by changing patients’ views and attitudes about people or things, and reduces patients’ negative symptoms from the perspective of improving social cognition [30]. Although some studies [23] suggested that SCIT did not improve the negative symptoms of patients, the results of this pooled analysis showed that SCIT had a lower negative symptom

score than TSU treatment (SMD = -1.66, 95% CI (-2.32, -1.00),  $P < 0.0001$ ). The severity of negative symptoms is positively correlated with the degree of emotional cognitive deficits shown statically, and apathy, diminished volition, interest, or social impairment among negative symptoms may reduce the patient’s theory of mind ability and make the patient’s social experience accumulate less [31]. In SCIT training, patients are guided to share their own life examples, to bring patients to real social events, to continuously enrich their inner experience in sufficient discussion and practice role exchange, to cultivate the ability of patients to stand at each other’s perspective in social communication to think

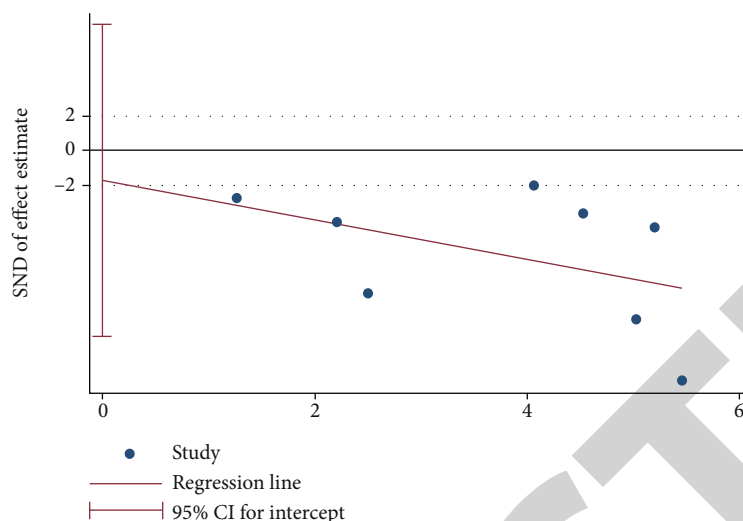


FIGURE 11: Publication bias: Egger's quantification.

about problems, to improve the patient's theory of mind level, to activate subjective initiative, and to continuously improve the patient's emotion [22].

Furthermore, the combined findings of this research revealed that the positive symptom score and PANSS total score of patients after SCIT were lower than those following TSU therapy, indicating that SCIT treatment was helpful to the patient's illness recovery. Presumably, it is successful in alleviating positive symptoms in individuals with schizophrenia spectrum disorders, particularly delusions, by explaining what delusions are, describing the numerous possibilities of event occurrence, and differentiating facts from hypothesis through images and videos [14].

In the 8 literatures included in this study, we tried to compare the effect of SCIT and TSU on the social function of patients with schizophrenia after treatment. The pooled ES was  $SMD = 0.77$  (95% CI (0.34, 1.20),  $P < 0.001$ ), suggesting that the social function of patients after SCIT is improved compared with TSU. As a systematic social skills training, SCIT integrates behavioral therapy with behavior modification techniques, contains a large number of basic social skills such as eye contact, facial expression, sound size, and fluency of language, provides patients with sufficient practice opportunities, guides patients to adopt new social skills for emotional communication with others, reminds patients to make appropriate behaviors on different occasions to reduce frustration, and continuously obtains positive feedback from peers, which qualitatively corrects and improves patients' behaviors and improves patients' social skills [16]. SCIT's intervention process also employs the concept of team therapy, allowing patients to experience the strength of being accepted and supported, activating patients' ability to be interested in the surrounding things and thus reducing negative coping styles, improving patients' enthusiasm to participate in occupational therapy, and significantly improving patients' psychological and social functions [19]. The results of Hooker et al. [32] showed that the positive effect

of SCIT on social cognitive skills may arise from its altered patient neural activity mechanisms.

The patients included in this study were all inpatients and did not include any community schizophrenic patients with stable disease. Roberts et al.'s study [33] attempted to apply this treatment to discharged patients and found that SCIT may be a promising intervention for community institutions that can serve psychiatric patients seeking to improve social functioning. In a Japanese study [34], it was shown that the application of SCIT in the community was feasible and tolerated by patients. Based on the improvement of social function in patients with mental illness, SCIT can be applied not only to patients with schizophrenia but also to patients with other mental illnesses such as autism and bipolar disorder [35, 36]. It has recently been shown that the human microbiome also has some influence on mood. Therefore, drugs capable of modulating the human microbiota, for example, amoxicillin [37] and ornidazole [38], also deserve attention.

Although the general quality of the included literatures in this research was excellent, there was no substantial publication bias, and the radial plot and normal quantile-quantile plot indicated stable findings; it should be noted that this meta-analysis had limitations. For starters, there was clear variability among the literatures. We tried to explore the source of heterogeneity and found that the length of intervention did not affect the results. The heterogeneity of literatures may be related to that the patients included in different studies had different disease types and age levels and may also be related to different intervention methods implemented in each study (different therapeutic drugs, differences in the methods implemented by SCIT) or related to different scales used for outcome measurement. Because of numerous factors, we could not analyze them one by one. Second, there were too few included articles and only eight reports on negative symptom indicators, which may cause insufficient study data. Finally, we did not have group discussions on different countries and regions. Therefore,

studies on this topic require more homogeneous, good-quality RCT literature to continue to be explored in depth.

Despite some limitations, the results of this meta-analysis support that SCIT helps to improve the relief of symptoms and the improvement of social function in patients with schizophrenia. However, more research is still needed to be deeply explored.

## Data Availability

The datasets used during the current study are available from the corresponding author on request.

## Conflicts of Interest

The author declares no conflicts of interest.

## References

- [1] R. Tandon, W. Gaebel, D. M. Barch et al., "Definition and description of schizophrenia in the DSM-5," *Schizophrenia Research*, vol. 150, no. 1, pp. 3–10, 2013.
- [2] J. Tomasik, H. Rahmoune, P. C. Guest, and S. Bahn, "Neuroimmune biomarkers in schizophrenia," *Schizophrenia Research*, vol. 176, no. 1, pp. 3–13, 2016.
- [3] P. Stępnicki, M. Kondej, and A. A. Kaczor, "Current concepts and treatments of schizophrenia," *Molecules*, vol. 23, no. 8, p. 2087, 2018.
- [4] G. P. Strauss, E. Granholm, J. L. Holden et al., "The effects of combined oxytocin and cognitive behavioral social skills training on social cognition in schizophrenia," *Psychological Medicine*, vol. 49, no. 10, pp. 1731–1739, 2019.
- [5] W. K. Lee, "Effectiveness of computerized cognitive rehabilitation training on symptomatological, neuropsychological and work function in patients with schizophrenia," *Asia-Pacific Psychiatry*, vol. 5, no. 2, pp. 90–100, 2013.
- [6] R. Lawrence, T. Bradshaw, and H. Mairs, "Group cognitive behavioural therapy for schizophrenia: a systematic review of the literature," *Journal of Psychiatric and Mental Health Nursing*, vol. 13, no. 6, pp. 673–681, 2006.
- [7] D. R. Combs, S. D. Adams, D. L. Penn, D. Roberts, J. Tiegreen, and P. Stem, "Social cognition and interaction training (SCIT) for inpatients with schizophrenia spectrum disorders: preliminary findings," *Schizophrenia Research*, vol. 91, no. 1-3, pp. 112–116, 2007.
- [8] N. B. Rocha, C. Campos, J. M. Figueiredo et al., "Social cognition and interaction training for recent-onset schizophrenia: a preliminary randomized trial," *Early Intervention in Psychiatry*, vol. 15, no. 1, pp. 206–212, 2021.
- [9] F. Dark, J. G. Scott, A. Baker et al., "Randomized controlled trial of social cognition and interaction training compared to befriending group," *The British Journal of Clinical Psychology*, vol. 59, no. 3, pp. 384–402, 2020.
- [10] G. Lahera, A. Rebores, A. Vallespi et al., "Social cognition and interaction training (SCIT) versus training in affect recognition (TAR) in patients with schizophrenia: a randomized controlled trial," *Journal of Psychiatric Research*, vol. 142, pp. 101–109, 2021.
- [11] T. Lu, C. Lu, H. Li et al., "The reporting quality and risk of bias of randomized controlled trials of acupuncture for migraine: methodological study based on STRICTA and RoB 2.0," *Complementary Therapies in Medicine*, vol. 52, article 102433, 2020.
- [12] Y. Li, K. Sun, D. Liu et al., "The effects of combined social cognition and interaction training and paliperidone on early-onset schizophrenia," *Frontiers in Psychiatry*, vol. 11, article 525492, 2020.
- [13] A. Gordon, P. J. Davis, S. Patterson et al., "A randomized waitlist control community study of social cognition and interaction training for people with schizophrenia," *The British Journal of Clinical Psychology*, vol. 57, no. 1, pp. 116–130, 2018.
- [14] N. B. F. Rocha and C. Queirós, "Metacognitive and social cognition training (MSCT) in schizophrenia: A preliminary efficacy study," *Schizophrenia Research*, vol. 150, no. 1, pp. 64–68, 2013.
- [15] J. Addington, T. A. Girard, B. K. Christensen, and D. Addington, "Social cognition mediates illness-related and cognitive influences on social function in patients with schizophrenia-spectrum disorders," *Journal of Psychiatry and Neuroscience*, vol. 35, no. 1, pp. 49–54, 2010.
- [16] D. Turkington, R. Dudley, D. M. Warman, and A. T. Beck, "Cognitive-behavioral therapy for schizophrenia: a review," *Focus*, vol. 10, no. 2, pp. 5–233, 2006.
- [17] D. L. Roberts, D. R. Combs, M. Willoughby et al., "A randomized, controlled trial of social cognition and interaction training (SCIT) for outpatients with schizophrenia spectrum disorders," *The British Journal of Clinical Psychology*, vol. 53, no. 3, pp. 281–298, 2014.
- [18] Y. Wang, D. L. Roberts, B. Xu, R. Cao, M. Yan, and Q. Jiang, "Social cognition and interaction training for patients with stable schizophrenia in Chinese community settings," *Psychiatry Research*, vol. 210, no. 3, pp. 751–755, 2013.
- [19] M. M. Kurtz, K. T. Mueser, W. R. Thime, S. Corbera, and B. E. Wexler, "Social skills training and computer-assisted cognitive remediation in schizophrenia," *Schizophrenia Research*, vol. 162, no. 1-3, pp. 35–41, 2015.
- [20] I. Hasson-Ohayon, M. Avidan-Msika, M. Mashiach-Eizenberg et al., "Metacognitive and social cognition approaches to understanding the impact of schizophrenia on social quality of life," *Schizophrenia Research*, vol. 161, no. 2-3, pp. 386–391, 2015.
- [21] Z. Mahmood, R. Van Patten, A. V. Keller et al., "Reducing negative symptoms in schizophrenia: feasibility and acceptability of a combined cognitive-behavioral social skills training and compensatory cognitive training intervention," *Psychiatry Research*, vol. 295, article 113620, 2021.
- [22] E. Granholm, J. Holden, P. C. Link, and J. R. McQuaid, "Randomized clinical trial of cognitive behavioral social skills training for schizophrenia: improvement in functioning and experiential negative symptoms," *Journal of Consulting and Clinical Psychology*, vol. 82, no. 6, pp. 1173–1185, 2014.
- [23] P. D. Harvey and M. Strassnig, "Predicting the severity of everyday functional disability in people with schizophrenia: cognitive deficits, functional capacity, symptoms, and health status," *World Psychiatry*, vol. 11, no. 2, pp. 73–79, 2012.
- [24] G. Voutilainen, T. Kouhia, D. L. Roberts, and J. Oksanen, "Social cognition and interaction training (SCIT) for adults with psychotic disorders: a feasibility study in Finland," *Behavioural and Cognitive Psychotherapy*, vol. 44, no. 6, pp. 711–716, 2016.
- [25] G. Lahera, A. Benito, J. M. Montes, A. Fernández-Liria, C. M. Olbert, and D. L. Penn, "Social cognition and interaction



## *Retraction*

# **Retracted: Efficacy of Various Types of Berries Extract for the Synthesis of ZnO Nanocomposites and Exploring Their Antimicrobial Potential for Use in Herbal Medicines**

### **BioMed Research International**

Received 20 June 2023; Accepted 20 June 2023; Published 21 June 2023

Copyright © 2023 BioMed Research International. This is an open access article distributed under the Creative Commons Attribution License, which permits unrestricted use, distribution, and reproduction in any medium, provided the original work is properly cited.

This article has been retracted by Hindawi following an investigation undertaken by the publisher [1]. This investigation has uncovered evidence of one or more of the following indicators of systematic manipulation of the publication process:

- (1) Discrepancies in scope
- (2) Discrepancies in the description of the research reported
- (3) Discrepancies between the availability of data and the research described
- (4) Inappropriate citations
- (5) Incoherent, meaningless and/or irrelevant content included in the article
- (6) Peer-review manipulation

The presence of these indicators undermines our confidence in the integrity of the article's content and we cannot, therefore, vouch for its reliability. Please note that this notice is intended solely to alert readers that the content of this article is unreliable. We have not investigated whether authors were aware of or involved in the systematic manipulation of the publication process.

Wiley and Hindawi regrets that the usual quality checks did not identify these issues before publication and have since put additional measures in place to safeguard research integrity.

We wish to credit our own Research Integrity and Research Publishing teams and anonymous and named external researchers and research integrity experts for contributing to this investigation.

The corresponding author, as the representative of all authors, has been given the opportunity to register their agreement or disagreement to this retraction. We have kept a record of any response received.

### **References**

- [1] A. Dar, R. Rehman, A. Mohyuddin et al., "Efficacy of Various Types of Berries Extract for the Synthesis of ZnO Nanocomposites and Exploring Their Antimicrobial Potential for Use in Herbal Medicines," *BioMed Research International*, vol. 2022, Article ID 9914173, 9 pages, 2022.

## Research Article

# Efficacy of Various Types of Berries Extract for the Synthesis of ZnO Nanocomposites and Exploring Their Antimicrobial Potential for Use in Herbal Medicines

Amara Dar <sup>1</sup>, Rabia Rehman <sup>2</sup>, Ayesha Mohyuddin,<sup>3</sup> Maria Aziz,<sup>3</sup> Jamil Anwar,<sup>1,3</sup> Gashew Tadele <sup>4</sup>, Noor Mohammed Kadhim,<sup>5</sup> Ali H. Alamri,<sup>6</sup> and Rami M. Alzhrani <sup>7</sup>

<sup>1</sup>Centre for Analytical Chemistry, School of Chemistry, University of the Punjab, Quaid-e-Azam Campus, Lahore 54590, Pakistan

<sup>2</sup>Centre for Inorganic Chemistry, School of Chemistry, University of the Punjab, Quaid-e-Azam Campus, Lahore 54590, Pakistan

<sup>3</sup>Chemistry Department, University of Management & Technology, Lahore, Punjab, Pakistan

<sup>4</sup>Mizan Tepi University, College of Natural and Computational Sciences, Department of Chemistry, Ethiopia

<sup>5</sup>Department of Medical Instruments engineering Techniques, Al-Farahidi University, Baghdad 10021, Iraq

<sup>6</sup>Department of Pharmaceutics, College of Pharmacy, King Khalid University, Abha 62529, Saudi Arabia

<sup>7</sup>Department of Pharmaceutics and Industrial Pharmacy, College of Pharmacy, Taif University, P.O. Box 11099, Taif 21944, Saudi Arabia

Correspondence should be addressed to Rabia Rehman; [grinorganic@yahoo.com](mailto:grinorganic@yahoo.com) and Gashew Tadele; [gashaw@mtu.edu.et](mailto:gashaw@mtu.edu.et)

Received 19 July 2022; Accepted 3 August 2022; Published 16 August 2022

Academic Editor: Dinesh Rokaya

Copyright © 2022 Amara Dar et al. This is an open access article distributed under the Creative Commons Attribution License, which permits unrestricted use, distribution, and reproduction in any medium, provided the original work is properly cited.

Nanoscience has developed various greener approaches as an alternate method for the synthesis of nanoparticles and nanocomposites. The present study discusses the efficacy of berries extract for the synthesis of ZnO nanocomposites. Characterization of synthesized nanocomposite were done by SEM, UV/VIS spectrophotometry, Fourier transform infrared (FTIR) spectroscopy, and XRD techniques. The crystalline nature of the synthesized nanoparticles was verified by XRD pattern in the range of 10-80 nm. The UV absorption peak of *Elaeagnus umbellata* (ZnO-EU) nanocomposite at 340 nm, *Rubus idaeus* (ZnO-Ri) nanocomposite at 360 nm, and *Rubus fruticosus* (ZnO-Rf) nanocomposite at 360 nm was observed. The nanocomposites were analyzed for their antimicrobial activity and found to be effective against three phytopathogens. The antimicrobial activity of ZnO nanocomposites showed good results against *Escherichia coli* (341), *Staphylococcus aureus* (345B), and *Pseudomonas aeruginosa* (5994 NLF). This study presents a simple and inexpensive approach for synthesizing zinc oxide nanocomposites with effective antibacterial activity.

## 1. Introduction

Nanoscience is an advanced field of science that has brought a revolution in different areas of science like photocatalysis, medicine, chemical synthesis, and agriculture. This is mainly due to the size and morphology of synthesized materials that increase the potential applications in the said areas. Nanomaterials are called “a wonder of modern medicine” [1]. Researchers are using ecofriendly methods to synthesize different metal nanoparticles for pharmaceutical applications because of the increasing demand [2]. Nanoparticles are tiny objects which behave as

a single unit in terms of properties. Nanoparticles can be classified as metal nanoparticles, nonmetal nanoparticles, semiconductor nanoparticles, nonmetal ceramic nanoparticles, and also carbon nanoparticles, based upon the type of the material used for synthesis of this single moiety [3].

Metal oxide NPs were used in different fields like soil stabilization, solar cells, biomedicine, gas sensors, wastewater treatment, and light-emitting devices [4]. Different metals have been successfully incorporated so far for the synthesis of nanoparticles and the applications of these particles has been studied in different fields. Metals like Cu, Au, Ag, Se,

Ni, and Zn have been used for the synthesis of nanoparticles, and their applications in agriculture and industry have been studied. Ag has got natural tendency as an antibacterial agent, that is why it has been used in various skin ointments. Zinc oxide nanoparticles appear to be the best choice for antimicrobial activity and antibacterial activity [5]. Various plant materials are recently used for the synthesis of nanoparticles, and this approach proved an easy and low-cost method for the preparation of nanomaterials; synthesized material in turn possesses a large surface-to-volume ratio due to having small particle size, surface morphology, and size distribution [1].

Nanocomposites are composites that have at least one phase with nanometer-scale dimensions. Composite materials are synthesized to create new materials with superior qualities. In the case of metal nanocomposites, any material organic, inorganic, or polymeric can be incorporated into metals/nonmetals to synthesize the nanocomposite with tailored qualities [6]. Zinc oxide biosynthesis can be achieved with different biological materials, including fungi, plant extract, and bacteria [7].

*Elaeagnus umbellata* belongs to the family of *Elaeagnaceae* and is a large shrub. It is known locally as 'Kankoli.' It is a widespread medicinal shrub that grows wild in Azad Kashmir between 1372 and 1829 meters above sea level [8]. The purpose is to enhance the knowledge about *Elaeagnus umbellata* and to evaluate their fruits as a potential source of bioactive and antioxidant compounds [9]. *Elaeagnus umbellata* is an ornamental plant. The fruit has carotenoid lycopene, which is used against myocardial infarction and various types of cancer [10]. The fruits were included in the traditional diet because of their long-lasting application in the treatment of diarrhea, fracture, antihepatitis, and injury. The fruit is used for the preparation of foodstuffs, jams, preserves, and juices.

*Rubus idaeus* belong to the *Rosaceae* family and its common name is "Raspberry." *Rubus idaeus* is high in vitamins, minerals, and bioactive compounds such as phenolics, anthocyanins, and organic acids. This wild fruit have a high content of vitamin C and mineral elements. *Rubus idaeus* fruit is visually appealing, delicious, juicy, and with a distinct aroma [11]. *Rubus idaeus* is well-known for its antioxidant properties. It is used to treat cardiovascular disease, diabetes, Alzheimer, cancer, and obesity [12].

*Rubus fruticosus* is a medicinal shrub that belongs to the *Rosaceae* family. *Rubus* is the largest genus in the *Rosaceae* family, with over 700 species. *Rubus fruticosus* is known by several names in different parts of the world. Its common name is "Blackberry." *Rubus fruticosus* is a great source of phenolic compounds exhibiting antioxidant activities. *Rubus fruticosus* has a good quantity of minerals such as calcium, selenium, fluoride, iron, phosphorus, potassium, zinc, copper, and manganese. They are a good source of vitamins and minerals. These berries are consumed both fresh and processed, as they are used to make jams, syrups, and jellies [13].

In the present study, the synthesis of ZnO nanocomposites by using extracts of berries like *Elaeagnus umbellata*, *Rubus fruticosus*, and *Rubus idaeus* is a novel approach.

Using plant extract in nanocomposite synthesis is a green approach that does not need sophisticated instrumentation and toxic chemicals. The use of eco-friendly harmless materials in the synthesis of ZnO nanomaterials can add many potential benefits for applications in different fields. For environmental risk management, such approach for developing material by environmentally safer route and possessing numerous benefits is highly appreciated and used in herbal and homeopathic medicines. These are usually have long-term effects and less side effects because their components are made up of natural products derived from plants. They do not have lethal effects like allopathic medicines [14–22].

## 2. Materials and Methods

Zinc acetate dihydrate ( $\text{Zn}(\text{CH}_3\text{COO})_2 \cdot 2\text{H}_2\text{O}$ ) was purchased from United laboratory chemicals and Sodium hydroxide from Merck.

**2.1. Collection of Plant Material.** *Elaeagnus umbellata* berries were collected in spring, and *Rubus fruticosus* and *Rubus idaeus* berries were collected in summer from Rawalakot (Azad Kashmir). The collected plant material was washed with tap water to remove dust and other impurities and finally rinsed with distilled water before the preparation of fruit extract.

**2.2. Preparation of Fruit Extract.** For the preparation of fruit extract of *Elaeagnus umbellata*, *Rubus fruticosus*, and *Rubus idaeus*, 5 g each of washed and crushed fruit was taken separately in a 250 mL borosil beaker and added 100 mL distilled water. The mixture was boiled for 10 min until the color turns reddish. The mixture was cooled at room temperature. The fruit extract was filtered by using filter paper and saved in an airtight jar for further procedure.

### 2.3. Preparation of Reagents

- (i) Zinc acetate dihydrate solution was prepared by weighing 0.219 g of zinc acetate dihydrate and adding to it little water to dissolve, then making the volume up to mark in 50 mL measuring flask

**2.4. Synthesis of Zinc Oxide Nanocomposites.** Zinc oxide nanocomposites were synthesized by using zinc acetate dihydrate. Zinc acetate solution was added into the round bottom flask and stirred for 1 hour using a magnetic stirrer hot plate at 70°C. After this, 25 mL fruit extract was added into the solution of zinc acetate solution. The salt solution was then homogeneously combined with fruit extract of *Elaeagnus umbellata*, *Rubus fruticosus*, and *Rubus idaeus*, and gradual change in color from red to reddish-brown was observed. The mixture was covered and placed for 1 hour at room temperature. After 1 hour, the mixture was centrifuged for 12 minutes at 6000 rpm. Precipitates were dried at room temperature. Figure 1 shows a study layout of ZnO-NCs can be obtained from fruit extracts of *Rubus fruticosus*, *Elaeagnus umbellata*, and *Rubus idaeus*.

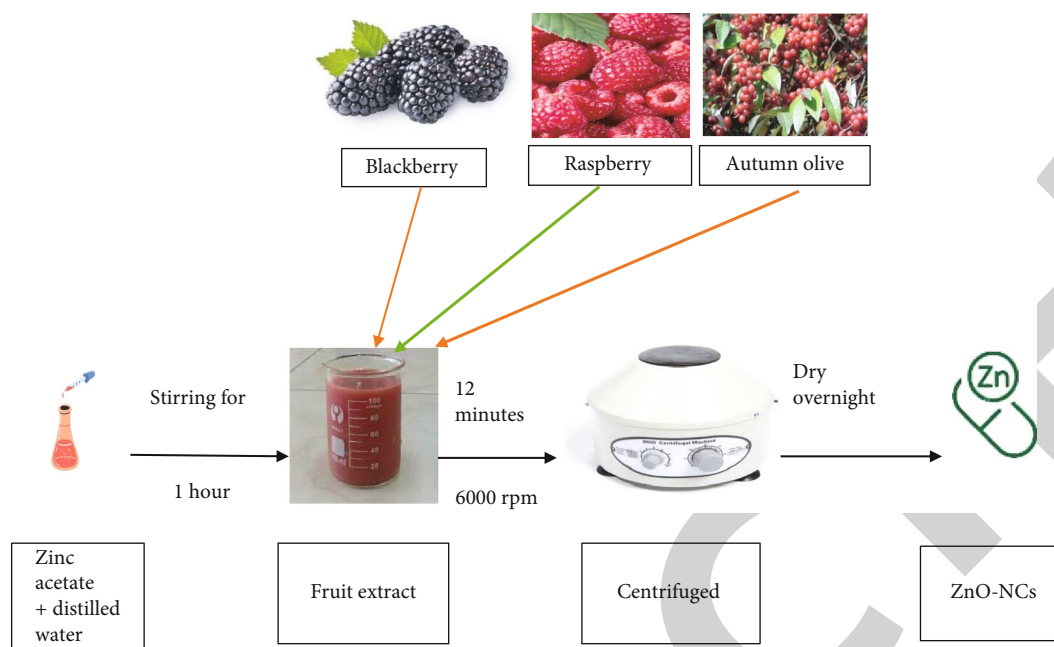


FIGURE 1: Synthesis of zinc oxide nanocomposites using fruit extracts.

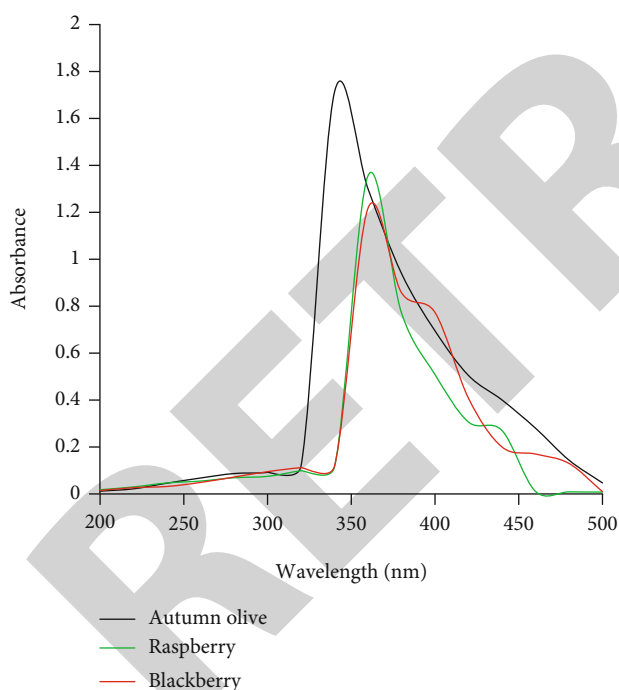


FIGURE 2: UV/VIS spectra of *Elaeagnus umbellata* (autumn olive), *Rubus idaeus* (raspberry), and *Rubus fruticosus* (blackberry).

### 2.5. Characterization of Zinc Oxide Nanocomposites

(i) UV/Vis analysis for synthesized nanocomposites was performed in the range of 250 to 550 nm using a double beam OPTIZEN POP UV/Vis spectrophotometer. All the three nanocomposites were ana-

lyzed in the UV/Vis region using methanol as a reference solvent, to find out the characteristic absorption value

(ii) FTIR analysis of ZnO nanocomposites was performed in the range of 4000 to 400  $\text{cm}^{-1}$  using Agilent Technologies Cary 630 FTIR spectrophotometer, to compare the shifts and appearance of bands in extracts and after the formation of nanocomposites

(iii) XRD was used for the determination of the crystalline structure. Rigaku D/Max 2500 VBZ+/PC diffractometer was used for structural analysis of the nanocomposites in the range of  $10^\circ$  to  $80^\circ$ . The mean size of the crystals of zinc oxide nanocomposites synthesized from *Rubus fruticosus*, *Elaeagnus umbellata*, and *Rubus idaeus* was measured with the help of the Debye-Scherrer equation

(iv) Surface morphology, shape, and particle size of the nanocomposites were studied by performing SEM. FEI Nova 450 Nano SEM machine was used to analyze morphology, shape, and particle size of the synthesized nanocomposites

**2.6. Antimicrobial Activity.** Clinically isolated three bacterial strains like *Escherichia coli* (341), *Pseudomonas aeruginosa* (5994 NLF), and *Staphylococcus aureus* (345B) were obtained from Sheikh Zayed Hospital, Lahore. These bacterial strains were selected as they are water and food-borne pathogens and degrade the quality of food and cause different diseases [23]. A small quantity of ZnO-NCs of *Elaeagnus umbellata*, *Rubus idaeus*, and *Rubus*

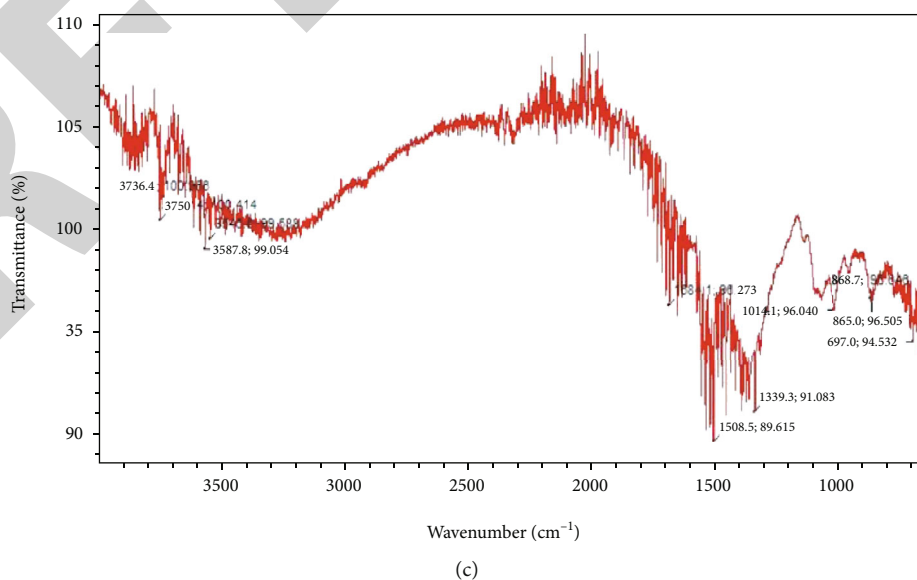
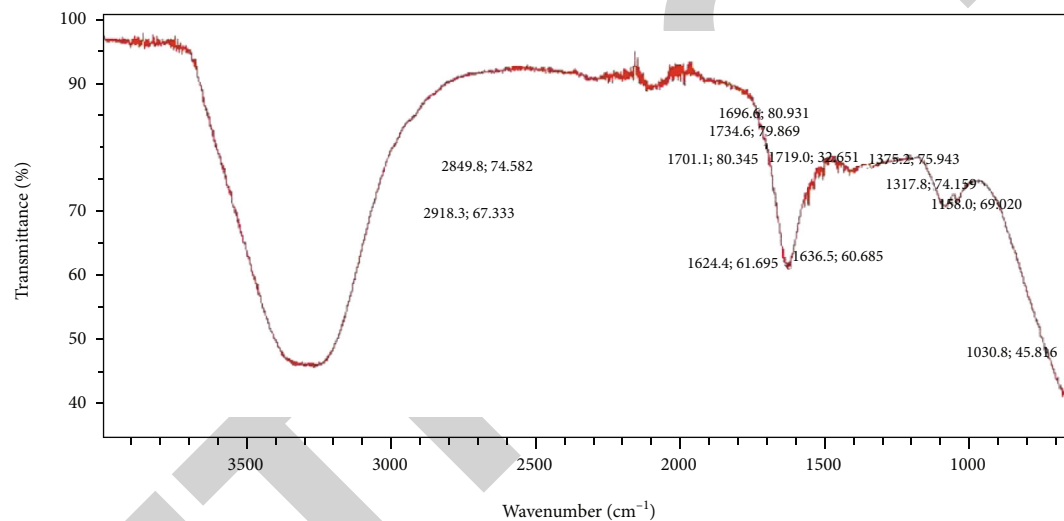
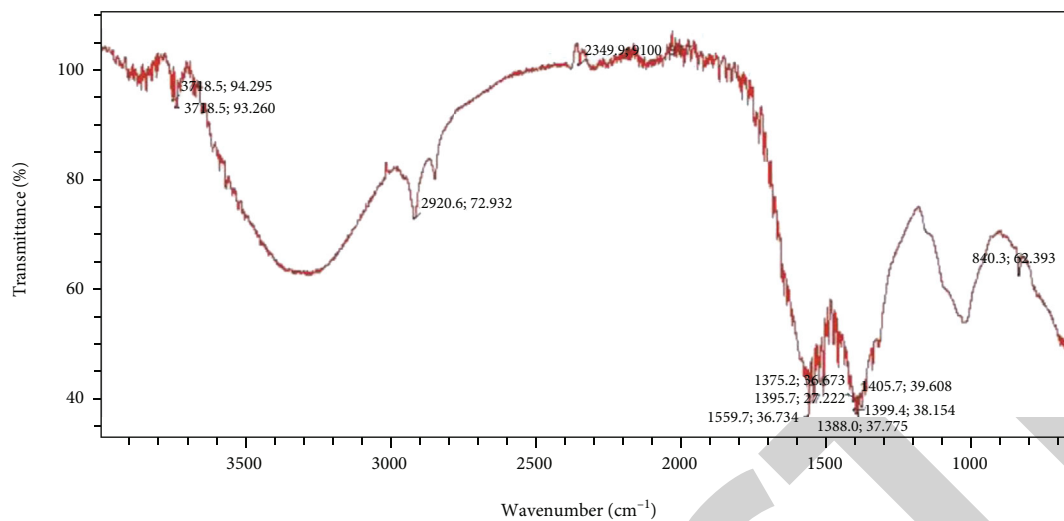
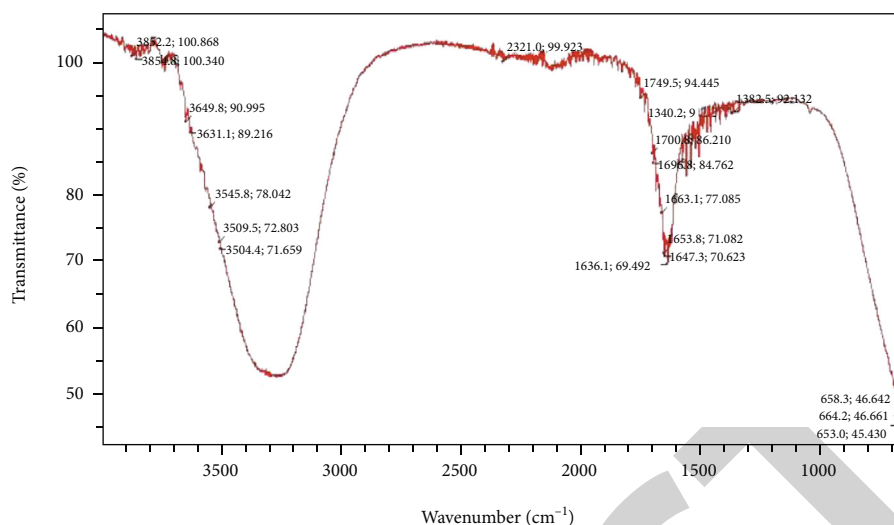
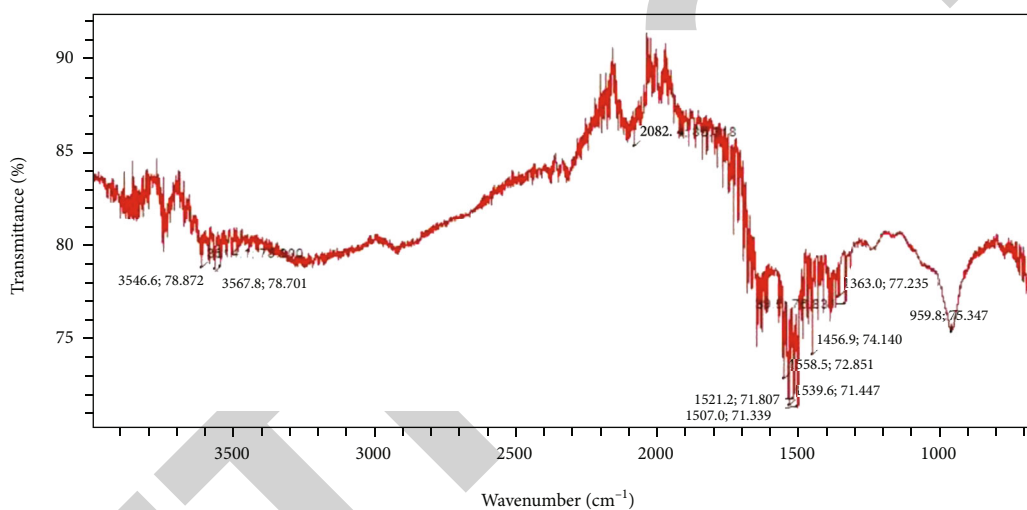


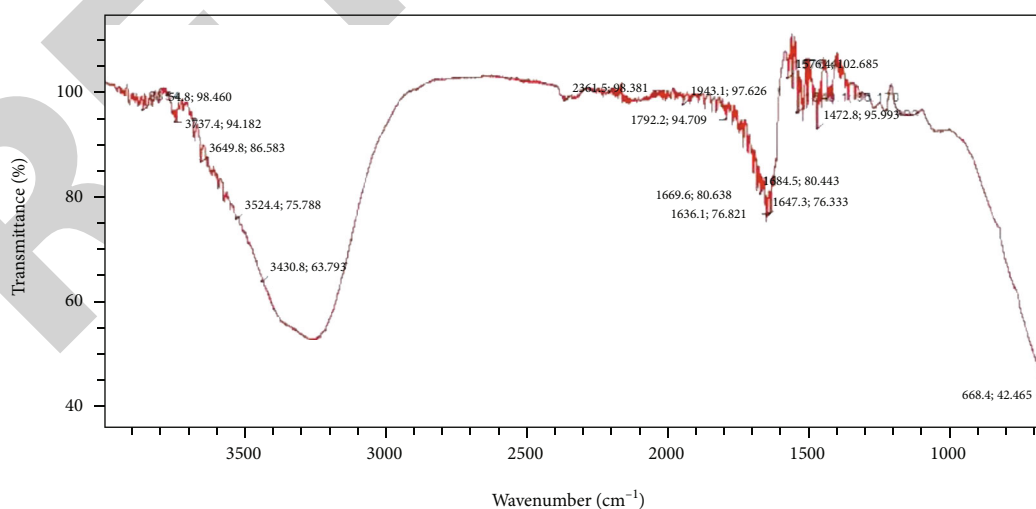
FIGURE 3: Continued.



(d)



(e)



(f)

FIGURE 3: (a) FTIR spectrum of ZnO-NCs of *Elaeagnus umbellata* (autumn olive). (b) FTIR spectrum of *Elaeagnus umbellata* (autumn olive) fruit extract. (c) FTIR spectrum of ZnO-NCs of *Rubus idaeus* (raspberry). (d) FTIR spectrum of *Rubus idaeus* (raspberry) fruit extract. (e) FTIR spectrum of ZnO-NCs of *Rubus fruticosus* (blackberry). (f) FTIR spectrum of *Rubus fruticosus* fruit extract.



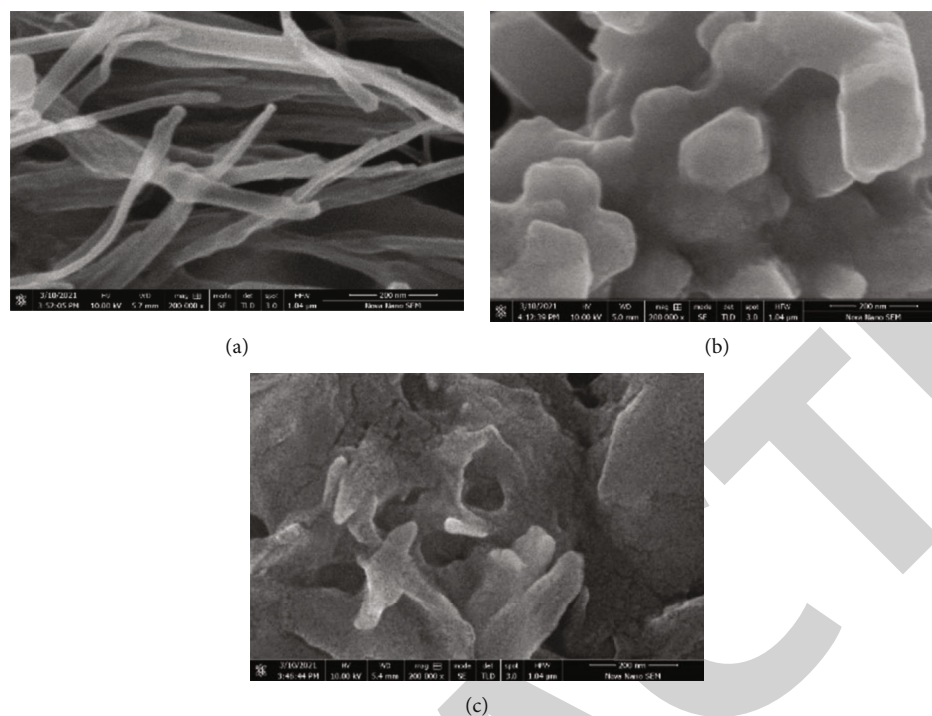


FIGURE 4: SEM image of ZnO-NCs of (a) *Elaeagnus umbellata* (autumn olive), (b) *Rubus idaeus* (raspberry), and (c) *Rubus fruticosus* (blackberry).

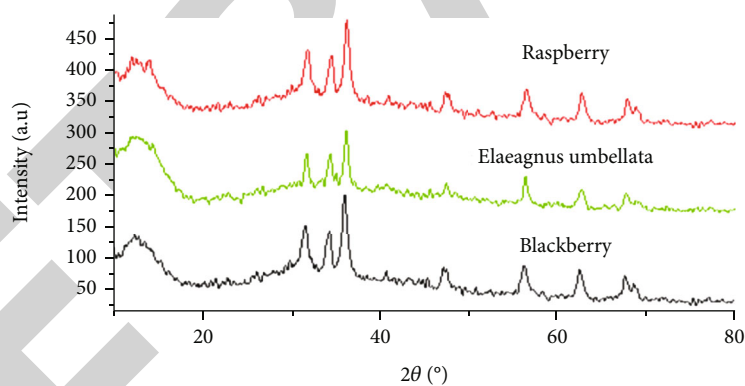


FIGURE 5: XRD pattern of ZnO-NCs of *Elaeagnus umbellata* (autumn olive), *Rubus idaeus* (raspberry), and *Rubus fruticosus* (blackberry).

*fruticosus* were dissolved in 4 mL of DMSO separately for conducting antimicrobial study. All these were then used against the bacterial strains chosen for study. Antimicrobial activity was assessed by the agar disc diffusion method. So, inoculation of testing bacterial strains was done on the agar plates with the help of swab sticks. Filter paper discs that have a diameter of about 6 mm were placed on the surface of agar with the help of sterilized tweezers. 50  $\mu$ L of test solutions were separately introduced on the discs and allowed to diffuse at room temperature. 50  $\mu$ L of DMSO was used as a negative control. Then, bacterial plates were incubated at 37°C for 24 hours. After the incubation period, inhibition zones were formed and then measured.

### 3. Results and Discussion

**3.1. Characterization of ZnO Nanocomposites.** Synthesized zinc oxide nanocomposites were characterized by Fourier transform infrared spectroscopy, X-ray powder diffraction, UV/Visible spectrophotometry, and scanning electron microscopy.

**3.2. UV-Visible Spectroscopy.** The reddish-brown precipitate obtained was dried overnight at room temperature to yield zinc oxide nanocomposites. The powder was resuspended in a 5 mL methanol solution. In Figure 2, the blue band indicates UV/VIS spectra showed an absorption maxima at 340 nm for ZnO-NCs of *Elaeagnus umbellata*, the red band

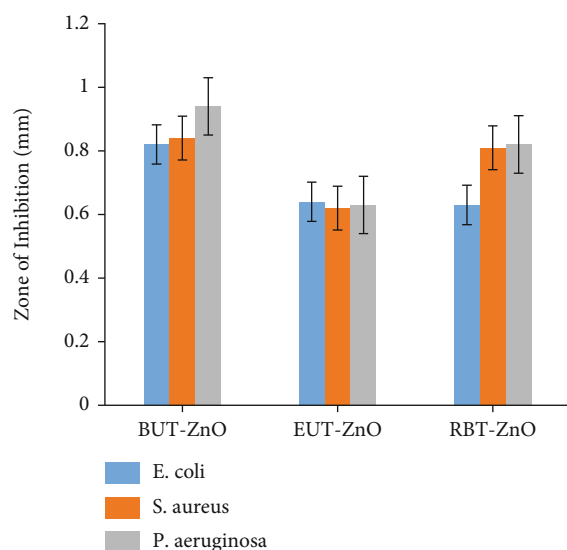


FIGURE 6: Comparison of antimicrobial activity of zinc oxide nanocomposites of *Elaeagnus umbellata* (autumn olive), *Rubus idaeus* (raspberry), and *Rubus fruticosus* (blackberry).

indicates UV/VIS spectra showed absorption maxima at 360 nm for ZnO-NCs of *Rubus idaeus*, and the green band indicates UV/VIS spectra showed an absorption maxima at 360 nm for ZnO-NCs of *Rubus fruticosus*. Researchers have reported comparable results in previous studies [24, 25].

**3.3. Fourier Transform Infrared (FTIR) Spectroscopy.** The FTIR spectrum (Figure 3(a)) of ZnO-NCs *Elaeagnus umbellata* showed band at  $3738\text{ cm}^{-1}$  corresponds to OH stretching vibration. The band at  $2920\text{ cm}^{-1}$  corresponds to  $\text{CH}_2$  stretching vibration. The band at  $2349\text{ cm}^{-1}$  indicates  $\text{CO}_2$  asymmetric stretch. The band at  $1559\text{ cm}^{-1}$  corresponds to aromatic C=C stretching vibrations. The band appears at  $1395\text{ cm}^{-1}$  corresponds to OH bend. The band at  $840\text{ cm}^{-1}$  indicates C-N vibration [24].

The FTIR spectrum (Figure 3(b)) of *Elaeagnus umbellata* fruit extract shows different bands. The band at  $1734\text{ cm}^{-1}$  corresponds to C=O stretching vibration. The band at  $1317\text{ cm}^{-1}$  indicates C-O stretching vibration. The band at  $1696\text{ cm}^{-1}$  corresponds to C=N vibration. The band at  $1030\text{ cm}^{-1}$  indicates S=O vibration.

The FTIR spectrum (Figure 3(c)) of ZnO-NCs *Rubus idaeus* shows different bands. The band at  $3614\text{ cm}^{-1}$  is attributed to OH stretching vibration. The band at  $2082\text{ cm}^{-1}$  corresponds to the strongest C-C stretching vibration. The band at  $1558\text{ cm}^{-1}$  corresponds to aromatic C=C stretching vibrations. The band appears at  $1507\text{ cm}^{-1}$  corresponds to the asymmetric bending of C-H. The band at  $1456\text{ cm}^{-1}$  indicates  $\text{CH}_2$  bending. The band at  $1363\text{ cm}^{-1}$  corresponds to ZnO. The band at  $959\text{ cm}^{-1}$  corresponds to the  $\text{PO}_4$  group of calcium hydroxyapatite [24].

The FTIR spectrum (Figure 3(d)) of *Rubus idaeus* fruit extract showed band at  $3509\text{ cm}^{-1}$  indicating OH stretching vibration. The band at  $1749\text{ cm}^{-1}$  is attributed to C=O stretching vibration. The band at  $1636\text{ cm}^{-1}$  indicates C=C stretching vibration. The band at  $1340\text{ cm}^{-1}$  indicates C-O vibration. The band at  $653\text{ cm}^{-1}$  shows Cl stretching [25].

The FTIR spectrum (Figure 3(e)) of ZnO-NCs *Rubus fruticosus* shows band at  $3750\text{ cm}^{-1}$  that corresponds to OH stretching vibration. The band at  $1684\text{ cm}^{-1}$  corresponds to C-N stretching vibrations. The band at  $1506\text{ cm}^{-1}$  corresponds to  $\text{CO}_2$  vibration. The band at  $1339\text{ cm}^{-1}$  is attributed to aromatic C-H bend. The band at  $1014\text{ cm}^{-1}$  corresponds to  $\text{PO}_4$ . The band at  $697\text{ cm}^{-1}$  confirms the formation of ZnO nanocomposites [24].

The FTIR spectrum (Figure 3(f)) of *Rubus fruticosus* fruit extract shows band at  $3854\text{ cm}^{-1}$ , which specifies OH stretching vibration. The band at  $1792\text{ cm}^{-1}$  is attributed to C=O stretching vibration. The band at  $1636\text{ cm}^{-1}$  indicates C=C stretching vibration. The band at  $668\text{ cm}^{-1}$  shows Cl stretch [25].

**3.4. Scanning Electron Microscopy.** The surface morphology of ZnO-NCs of *Elaeagnus umbellata*, *Rubus idaeus*, and *Rubus fruticosus* were characterized by SEM analysis as shown in Figures 4(a)–4(c). The shape of the ZnO-NCs of *Elaeagnus umbellata* was fiber-like while for ZnO-NCs of *Rubus idaeus* was cubic-like and for ZnO-NCs of *Rubus fruticosus* was leaf-like. The particle size of the nanocomposites was calculated from ImageJ software. The average particle size of synthesized ZnO-NCs of *Elaeagnus umbellata* was 69 nm while the average particle size of synthesized ZnO-NCs of *Rubus idaeus* was 67 nm and the average particle size of synthesized ZnO-NCs of *Rubus fruticosus* was 65 nm.

**3.5. X-Ray Diffraction (XRD).** Bragg's diffraction peaks of ZnO-NCs of *Elaeagnus umbellata*, *Rubus idaeus*, and *Rubus fruticosus*  $2\theta = 31.7^\circ, 34.3^\circ, 36.15^\circ, 47.25^\circ, 56.45^\circ, 62.75^\circ$ , and  $67.7^\circ$  were observed by XRD spectrum. The diffraction intensities were studied from  $20^\circ$  to  $80^\circ$  at  $2\theta$  angles. The existence of ZnO-NCs was verified by a high-intensity broad peak at  $2\theta = 36.15^\circ$  and low-intensity peak at  $2\theta = 67.7^\circ$ . The mean crystallite size of obtained ZnO-NCs was verified by the Debye-Scherrer equation. Figure 5 shows the average particle size of ZnO-NCs of *Elaeagnus umbellata* was 102.97 nm while the average particle size of ZnO-NCs of *Rubus idaeus* was 151.99 nm and the average particle size of ZnO-NCs of *Rubus fruticosus* was 102.47 nm. A similar trend is observed with ZnO/PVA nanocomposite using aqueous Moringa oleifera leaf extract [26].

**3.6. Antimicrobial Activity.** ZnO nanocomposites synthesized by three different berries *Elaeagnus umbellata* (autumn olive), *Rubus idaeus* (raspberry), and *Rubus fruticosus* (blackberry) was assessed for their antimicrobial activity against Gram-positive *Staphylococcus aureus* (345B) bacteria, Gram-negative *Pseudomonas aeruginosa* (5994 NLF), and *Escherichia coli* (341) bacteria. The antimicrobial activity of ZnO nanocomposites was analyzed by the agar disc diffusion method. The presence of a zone of inhibition demonstrated the antimicrobial potential of ZnO nanocomposites.

The antimicrobial potential of ZnO-NCs of *Elaeagnus umbellata* (autumn olive), *Rubus idaeus* (raspberry), and *Rubus fruticosus* (blackberry) shows a wide spectrum of

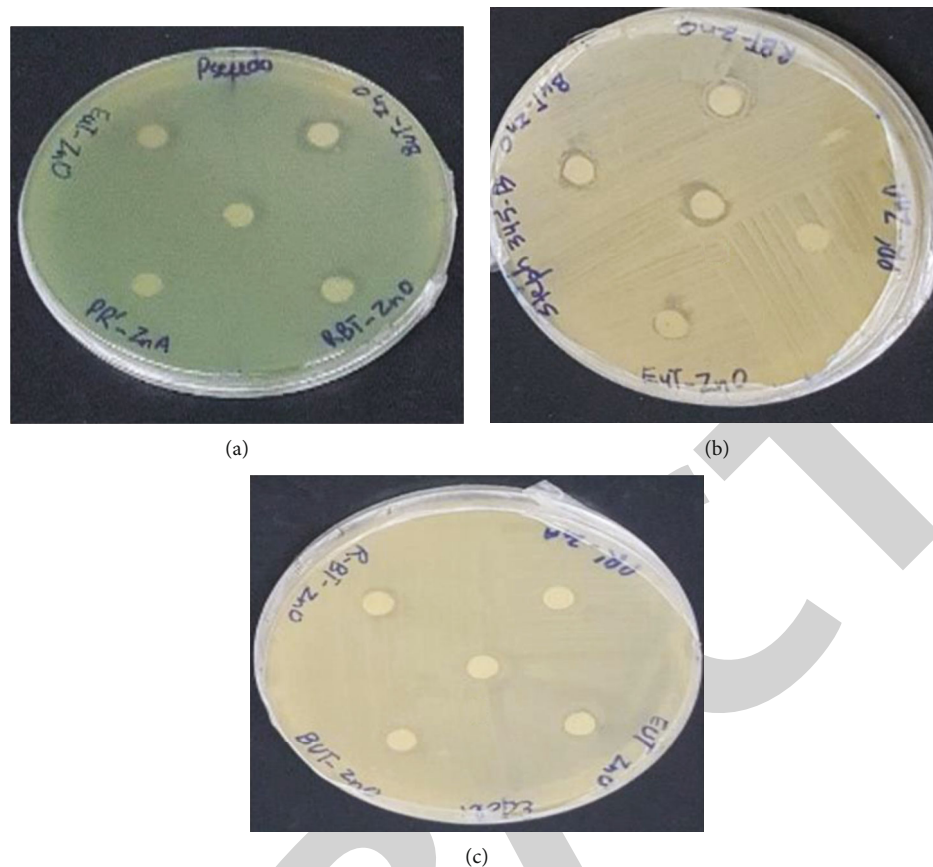


FIGURE 7: Zone of inhibition of ZnO-NCs of *Elaeagnus umbellata* (autumn olive), *Rubus idaeus* (raspberry), and *Rubus fruticosus* (blackberry) against (a) *Pseudomonas aeruginosa*, (b) *Escherichia coli*, and (c) *Staphylococcus aureus*.

antibacterial action. Figure 6 shows the highest zone of inhibition was identified in ZnO-NCs of *Rubus fruticosus* against *Pseudomonas aeruginosa* (5994 NLF) bacteria. The lowest zone of inhibition was observed in ZnO-NCs of *Elaeagnus umbellata* and *Rubus idaeus* against *Escherichia coli* (341) and *Staphylococcus aureus* (345B) bacteria, as given in Figures 7(a)–7(c). Same trend is observed with neem [27] and *Mentha longifolia* extract [28].

#### 4. Conclusion

In this work, zinc oxide nanocomposites were synthesized by using the green approach. A simple method was utilized for the preparation of ZnO nanocomposite using extract of *Rubus fruticosus*, *Elaeagnus umbellata*, and *Rubus idaeus*, thereby, restricting the use of harmful chemicals for the fabrication of nanocomposites. The fruit extract was used instead of toxic reducing and stabilizing chemicals. The fabricated ZnO nanocomposites' average particle size was calculated as 102.47, 102.97, and 151.99 nm by using Debye-Scherrer's equation. Synthesized nanocomposites showed good antimicrobial potential against *Escherichia coli* (341), *Staphylococcus aureus* (345B), and *Pseudomonas aeruginosa* (5994 NLF) strains of bacteria.

#### Abbreviations

SEM:	Scanning electron microscopy
UV/VIS:	Ultraviolet/visible spectroscopy
FTIR:	Fourier transform infrared spectroscopy
XRD:	X-ray diffraction
ZnO-EU:	ZnO- <i>Elaeagnus umbellata</i> nanocomposite
ZnO-Ri:	ZnO- <i>Rubus idaeus</i> nanocomposite
ZnO-Rf:	ZnO- <i>Rubus fruticosus</i> nanocomposite
ZnO-NCs:	Zinc oxide nanocomposites
EU:	<i>Elaeagnus umbellata</i>
Ri:	<i>Rubus idaeus</i>
Rf:	<i>Rubus fruticosus</i> .

#### Data Availability

All data related to this work are presented in Results and Discussion along with references.

#### Conflicts of Interest

The authors declare that they have no conflicts of interest regarding the publications of this paper.

## *Retraction*

# **Retracted: Factors Influencing Cerebrospinal Fluid Leaking following Pituitary Adenoma Transsphenoidal Surgery: A Meta-Analysis and Comprehensive Review**

### **BioMed Research International**

Received 12 November 2022; Accepted 12 November 2022; Published 22 November 2022

Copyright © 2022 BioMed Research International. This is an open access article distributed under the Creative Commons Attribution License, which permits unrestricted use, distribution, and reproduction in any medium, provided the original work is properly cited.

*BioMed Research International* has retracted the article titled “Factors Influencing Cerebrospinal Fluid Leaking following Pituitary Adenoma Transsphenoidal Surgery: A Meta-Analysis and Comprehensive Review” [1] due to concerns that the peer review process has been compromised.

Following an investigation conducted by the Hindawi Research Integrity team [2], significant concerns were identified with the peer reviewers assigned to this article; the investigation has concluded that the peer review process was compromised. We therefore can no longer trust the peer review process and the article is being retracted with the agreement of the editorial board.

### **References**

- [1] J. Zhang, J. Liu, and L. Huang, “Factors Influencing Cerebrospinal Fluid Leaking following Pituitary Adenoma Transsphenoidal Surgery: A Meta-Analysis and Comprehensive Review,” *BioMed Research International*, vol. 2022, Article ID 5213744, 9 pages, 2022.
- [2] L. Ferguson, “Advancing Research Integrity Collaboratively and with Vigour,” 2022, <https://www.hindawi.com/post/advancing-research-integrity-collaboratively-and-vigour/>.



## Review Article

# Factors Influencing Cerebrospinal Fluid Leaking following Pituitary Adenoma Transsphenoidal Surgery: A Meta-Analysis and Comprehensive Review

Jiao Zhang, Jingyun Liu, and Liyan Huang 

Operating Room, The First Hospital of China Medical University, Shenyang, Liaoning 110001, China

Correspondence should be addressed to Liyan Huang; 49298247@qq.com

Received 28 June 2022; Revised 18 July 2022; Accepted 25 July 2022; Published 16 August 2022

Academic Editor: Dinesh Rokaya

Copyright © 2022 Jiao Zhang et al. This is an open access article distributed under the Creative Commons Attribution License, which permits unrestricted use, distribution, and reproduction in any medium, provided the original work is properly cited.

**Background.** Surgical resection is the main method to treat pituitary adenoma. Cerebrospinal fluid leakage (CSF Leak) is the main complication after transsphenoidal surgery. The impact of postoperative CSF Leak can be predicted in advance, and preventive measures can be taken in time. Clinically, a variety of factors may affect the occurrence of postoperative CSF Leak. In this study, meta-analysis was used to investigate the risk factors of postoperative CSF Leak as a clinical reference. **Methods.** The databases PubMed, Medline, Embase, Cochrane library, CNKI, and CBM were searched for all studies on the risk factors of postoperative CSF Leak. Studies were screened and finally included. The quality of the included studies was assessed by the Newcastle-Ottawa scale. We used Revman 5.4 software to conduct the pooled effect size of every potential statistically significant factor. **Results.** 13 articles with a total of 5967 patients with pituitary adenoma and 405 cases of postoperative CSF Leak were finally included, accounting for 6.79%. All of the 13 articles had a quality score > 5, indicating good quality. Meta-analysis showed that patient age (OR = 0.71, 95% CI (0.41, 1.20),  $P = 0.20$ ) was not a factor influencing postoperative CSF Leak, while BMI (MD = 2.26, 95% CI (1.31, 3.20),  $P < 0.00001$ ), tumor size (MD = 1.35, 95% CI (0.22, 2.49),  $P = 0.02$ ), whether a second operation was performed (OR = 2.20, 95% CI (1.45, 3.33),  $P = 0.0002$ ), and intraoperative CSF Leak (OR = 8.88, 95% CI (3.64, 21.69),  $P < 0.00001$ ) were risk factors for postoperative CSF Leak in patients. **Discussion.** BMI, tumor size, reoperation, and intraoperative CSF Leak are the risk factors of postoperative CSF Leak. However, not all the factors were covered in this study, it is still worth continuing to deeply investigate in this topic.

## 1. Introduction

Pituitary adenomas are benign tumors arising from the adenohypophyseal cells of the anterior pituitary gland, located in the saddle region in the middle of the base of the brain, and are characterized by slow growth, small local lesions, and nonmetastasis [1]. According to the size of the tumor, pituitary adenomas can be divided into microadenomas (diameter < 10 mm), macroadenomas (diameter  $\geq$  10 mm), and giant adenomas (diameter  $\geq$  40 mm). According to the function of the tumor and the characteristics of hormone secretion, pituitary adenomas can be divided into functional pituitary adenomas and nonfunctional pituitary adenomas [2]. The vast majority of pituitary adenomas are nonfunctional pituitary microade-

nomas. Patients have no symptoms and signs for their whole life and do not need treatment. Only about 0.1%-0.2% of pituitary adenomas will metastasize into pituitary cancer, which is very rare [2]. Among all intracranial tumors, pituitary adenomas account for about 10%-15% and tend to happen to people aged 30-50, and the incidence is independent of gender [3].

Although most microadenomas are asymptomatic, when pituitary tumors cause pituitary hyperfunction or hypofunction, tumor space occupying effect, and pituitary tumor stroke, they will have a negative impact on the human body [4]. The pituitary gland plays a very important role in maintaining endocrine balance in the human body, functional pituitary adenomas may cause excessive secretion of hormones and cause hyperpituitarism, and the local mass effect of tumors may cause

headache, decreased visual acuity, and hydrocephalus symptoms, while giant adenomas may compress intracranial tissues and lead to hypopituitarism [5]. Therefore, when patients have headache, decreased vision, or visual impairment, combined with sexual dysfunction caused by endocrine abnormalities (male), menopause or lactation stop (female), and abnormal obesity, they should seek medical examination in time to diagnose the existence of pituitary adenoma.

Surgical resection is the mainstay of treatment for pituitary adenomas, and endoscopic transsphenoidal surgery (ETS) has been widely used because of its less trauma and good safety, but this procedure also has complications such as bleeding, infection, cerebrospinal fluid leakage (CSF Leak), and decreased visual acuity [6]. Transsphenoidal surgery has been plagued by cerebrospinal fluid leak and intracranial infection since its inception in the 20th century. It was once abandoned because of the high risk of infection, but with the help of antibiotics, the risk of infection has been greatly reduced. With the application of endoscopic technology in surgery, the visual angle and field of vision during surgery are clearer, which makes transsphenoidal surgery popular again and widely used in neurosurgery today [7].

However, the application of new technology cannot completely avoid the occurrence of surgical complications. The common complications of transsphenoidal surgery include cerebrospinal fluid leak, epistaxis, dysosmia, and sinusitis. CSF Leak is the main complication of transsphenoidal surgery, with an incidence rate between 0.5% and 14%, which may cause meningitis or tension pneumocephalus, increasing the risk of reoperation if no intervention is involved in time [8].

Studying the effect of preoperative and intraoperative factors on the occurrence of postoperative CSF Leak can help to foresee the occurrence and development of CSF Leak after transsphenoidal surgery in advance and carry out prevention or treatment in time. In the meta-analysis by Zhou et al. [9], 34 observational studies and 9144 patients were included; gender, age and body mass index, tumor size and scope, tumor texture, and experience level of surgeons were summarized as the main factors of postoperative CSF Leak. However, most of the included studies were Chinese articles, with great implementation bias. In our study, 13 literatures with study sites in different regions around the world were included to quantitatively analyze the possible influencing factors and provide the basis for taking targeted preventive measures.

## 2. Materials and Methods

**2.1. Search Strategy.** The databases Embase, Medline, PubMed, and Cochrane library were selected as English literature sources for this study, and CNKI and CBM were used as Chinese literature sources. The search was completed in December 2021. Search method: quick search of keywords; combination of keywords: [Predictors/factors] AND [cerebrospinal fluid leak/CSF/Cerebrospinal fluid rhinorrhea] AND [pituitary adenoma] AND [endoscopic transnasal pituitary surgery/transsphenoidal surgery].

**2.2. Inclusion Criteria.** (1) All literatures were retrospective observational study papers, which were limited to cohort study or case-control study. There is no limit to the number of research centers. The randomized controlled study, case analysis, noncontinuous time series study, cross-sectional study, and case report study were excluded. (2) The patient was diagnosed with pituitary adenoma by transsphenoidal surgery. After the opening of nasal sphenoid sinus, the incision was made to expose the tumor and scrape off the tumor tissue. (3) CSF Leak: postoperative CSF Leak is defined as the outflow of clear fluid from the saddle or parasellar region within 1-7 days after surgery. Literatures in which the study purpose is intraoperative (non-postoperative) CSF Leak are excluded. (4) Literature review: the patients were divided into 2 groups for factor analysis: the group with postoperative CSF Leak and the group without postoperative CSF Leak, and complete data could be obtained.

**2.3. Selection of Literatures.** Two researchers independently completed the screening of literatures. After the literatures were searched by keywords, the title and abstract of the literatures were read to exclude the literatures that did not meet the requirements, and then, the full text of the literatures was obtained and read to further determine whether they were included. After this, 2 researchers performed a cross-check, and if there is a disagreement between two researchers, a third researcher is invited to step in to resolve it.

**2.4. Data Extraction.** After the included literatures were determined, two institutes further read the literatures; independently extracted the basic information, study characteristics, and outcome indicators of the literatures; and recorded them using excel table. If the data cannot be determined due to incomplete data, the original author should be contacted to obtain all the data; if the data can still not be obtained, the literature will be excluded. In order to facilitate the final statistical analysis, the data expressed as “%” will be converted to the actual number of cases. After completing this work, two researchers cross-checked the extracted data to resolve disagreements and determine the content of the data.

**2.5. Outcome Indicators.** The factors that may cause postoperative CSF Leak in the literatures were collected (in some literatures, it has become *Predictors*), such as gender, age, BMI, tumor size, total resection or hemisection, intraoperative CSF Leak, operation time, cerebral edema, second operation, and preoperative chemotherapy. The information (number of cases and continuous value) of patients with this factor in different groups was obtained.

**2.6. Literature Quality Evaluation.** The Newcastle-Ottawa scale (NOS scale) [7] was used to analyze the quality of the included articles, and the scale was used to evaluate the object selection, comparability, and outcome indicators of the articles. The maximum score was 9 points, and the score of more than 5 points was considered as good quality. The higher the score, the better the literature quality and the less the bias. The Newcastle-Ottawa scale (NOS) is suitable for evaluating case-control studies and cohort studies. It evaluates cohort and case-control studies by means of three large



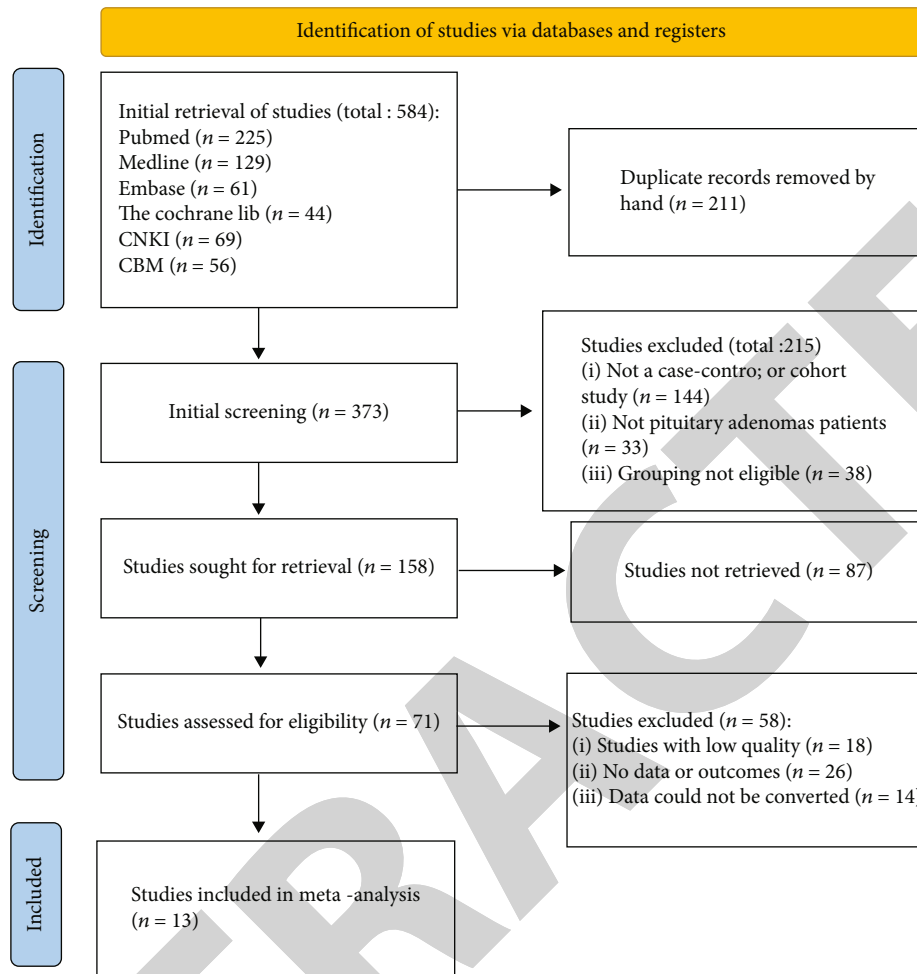


FIGURE 1: Search and selection chart.

blocks of eight entries, specifically including study population selection, comparability, exposure, or outcome assessment. The NOS evaluation of the quality of the literature employs the semiquantitative principle of star system with a total of 9 stars. NOS has its own dedicated website ([http://www.ohri.ca/programs/clinical\\_epidemiology/oxford.asp](http://www.ohri.ca/programs/clinical_epidemiology/oxford.asp)). You can see the site if you are interested.

**2.7. Statistical Analysis.** (1) The analysis tool used is the Revman 5.4 software. (2) Use mean difference (MD) to report continuous variables (BMI and tumor size) and odd rate (OR) value and 95% CI to report binary variables (age, whether there is a second operation, whether there is intraoperative CSF Leak), and use forest plot to present the results. (3) Q test was used to verify literature heterogeneity.  $P > 0.05$  indicated no heterogeneity and good consistency. Fixed effects model analysis could be used to calculate OR the with Mantel-Haenszel method. If heterogeneity existed, random effects model analysis was used to calculate OR with the DerSimonian and Laird method. If fixed effects analysis was consistent with random effects analysis, sensitivity analysis result was stable. (4) Heterogeneity was investigated by subgroup analysis. (5) Funnel plot was used to show the results of publication bias analysis.

### 3. Results

**3.1. Literature Search.** In this study, 584 relevant literatures were initially detected, 211 literatures were filtered out through repeated detection, and the remaining 373 literatures were included in the primary screening, and 13 literatures were finally included. The screening process is shown in Figure 1.

**3.2. Basic Information of the Included Literatures.** 13 literatures were included in this study. The basic data, factors, and quality score of the literatures are shown in Table 1.

**3.3. Excluded Literatures and Reasons for Exclusion.** We present 6 excluded articles (not all) after reading the full text, which were excluded mainly because of the following: (a) the study was for intraoperative CSF leakage, (b) no factor analysis, (c) no data available, and (d) patients with nonpituitary tumors, as shown in Table 2.

#### 3.4. Meta-Analysis Results

**3.4.1. Age.** Four literatures [10–13] reported the effect of age on whether patients had postoperative CSF Leak, including 653 patients aged <40 years and 1165 patients aged >40

TABLE 1: Summary of the basic information and risk factors of the included literatures.

Serial number	Author	Study location	Date of publication	Total cases	Number of cases of postoperative CSF Leak (%)	Factors	Quality score (points)
1	Ivan et al. [10]	California, USA	2015	98	11 (11.2)	(a)	6
2	Fraser et al. [14]	Pennsylvania, USA	2018	615	103 (16.7)	(b) and (c)	6
3	Patel et al. [15]	Vanderbilt, USA	2018	806	38 (4.7)	(b), (c), and (d)	5
4	Zhang et al. [11]	Shanghai, China	2017	474	13 (2.7)	(a) and (e)	5
5	Karnezis et al. [16]	Multicenters of Australia, Canada, and USA	2016	1161	68 (5.9)	(b), (d), and (h)	7
6	Q. Liu et al. [12]	Xuzhou, China	2020	194	25 (12.9)	(a), (d), and (f)	5
7	Tian et al. [13]	Yantai, China	2018	1063	29 (2.7)	(a), (d), (e), (f), and (h)	5
8	Sun et al. [17]	Singapore	2018	123	10 (8.1)	(b)	6
9	Liu et al. [22]	Guangdong, China	2012	397	31 (7.8)	(e) and (f)	5
10	Hannan et al. [18]	Austria	2020	270	24 (9)	(b) and (f)	5
11	Dlouhy et al. [19]	Iowa, USA	2012	96	13 (13.5)	(b), (d), (e), and (f)	6
12	Lee et al. [20]	Los Angeles, USA	2020	78	14 (17.9)	(b), (d), (g), and (h)	6
13	Han et al. [21]	Guangzhou, China	2008	592	26 (4.4)	(b), (e), and (f)	6

Notes: (a) age; (b) BMI; (c) hydrocephalus; (d) tumor size; (e) secondary surgery; (f) intraoperative CSF leaks; (g) operation time; (h) radiation therapy before surgery.

TABLE 2: Excluded literatures and reasons for exclusion (not all).

Serial number	Author	Date of publication	Reason for exclusion
1	Zhou et al. [34]	2017	Not postoperative CFL (intraoperative)
2	Lee et al. [35]	2019	No risk factors of CFL
3	Campero et al. [36]	2019	Not postoperative CFL (intraoperative)
4	Xue et al. [37]	2020	No data available
5	Nishioka et al. [38]	2005	Not pituitary adenomas patients
6	Cheng et al. [23]	2018	Not postoperative CFL (intraoperative)

years. There was no heterogeneity between the literatures ( $I^2 = 46\%$ ,  $P = 0.14$ ). Fixed effects model analysis showed that there was no significant difference in the proportion of patients with CSF Leak in different age groups (OR = 0.71, 95% CI (0.41, 1.20),  $P = 0.20$ ), as shown in Figure 2.

**3.4.2. BMI.** Seven literatures [14–20] reported the comparison of BMI between patients with postoperative CSF leakage and patients without CSF leakage. There was no statistical heterogeneity between the literatures ( $I^2 = 0\%$ ,  $P = 0.88$ ). Fixed effects model analysis showed that the BMI of patients with postoperative CSF leakage was significantly higher than that of patients without CSF leakage (MD = 2.26, 95% CI (1.31, 3.20),  $P < 0.00001$ ), as shown in Figure 3.

**3.4.3. Tumor Size.** Four literatures [15, 19–21] reported the comparison of tumor size between patients with postoperative CSF Leak and patients without CSF Leak, with statistical heterogeneity between the literatures ( $I^2 = 84\%$ ,  $P = 0.0003$ ). Random effects model analysis showed that there was significant difference in tumor size between patients with postoperative CSF Leak and patients without CSF Leak (MD = 1.35, 95% CI (0.22, 2.49),  $P = 0.02$ ), as shown in Figure 4.

**3.4.4. Whether There Is Second Operation.** Four literatures [13, 19, 21, 22] reported whether the type of surgery was secondary surgery affecting the occurrence of postoperative CSF Leak, without statistical heterogeneity between the literatures ( $I^2 = 37\%$ ,  $P = 0.19$ ). Fixed effects model analysis showed that the possibility of CSF Leak in the secondary surgery was higher (OR = 2.20, 95% CI (1.45, 3.33),  $P = 0.0002$ ), as shown in Figure 5.

**3.4.5. Intraoperative CSF Leak.** Six literatures [12, 13, 18, 19, 21, 22] reported whether intraoperative CSF Leak affected the occurrence of postoperative CSF Leak, with statistical heterogeneity between literatures ( $I^2 = 81\%$ ,  $P < 0.0001$ ). Random effects model analysis showed that the patients with intraoperative CSF Leak were more likely to have postoperative CSF Leak (OR = 8.88, 95% CI (3.64, 21.69),  $P < 0.00001$ ), as shown in Figure 6.

**3.4.6. Heterogeneity Investigation and Sensitivity Analysis.** In the analysis of tumor size, after the literatures were divided into 2 subgroups according to the calculation method of tumor size, there was no internal heterogeneity, which indicated that the calculation method of tumor size was the

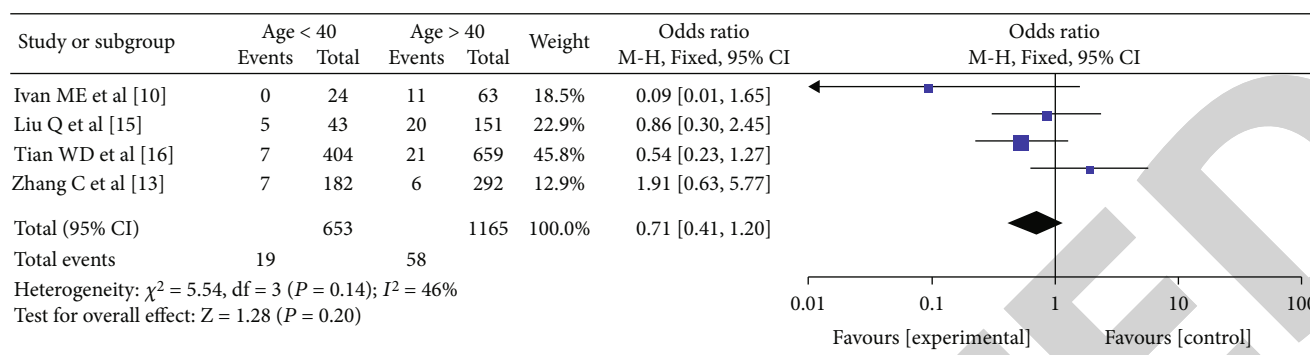


FIGURE 2: Effect of age on CSF Leak after transsphenoidal surgery for pituitary adenoma.

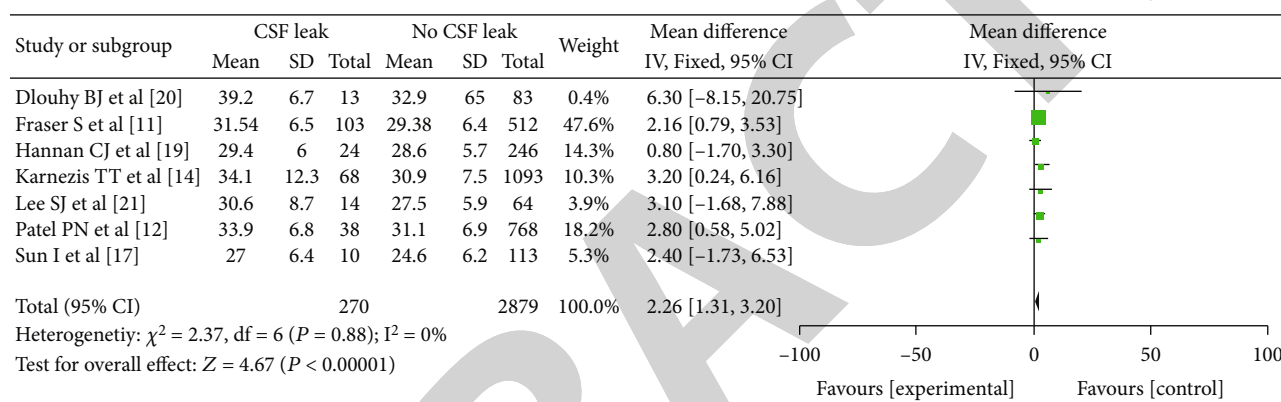


FIGURE 3: Effect of BMI on CSF Leak after transsphenoidal surgery for pituitary adenoma.

source of heterogeneity in the analysis of this factor. The results from the fixed effects model were the same as those from the random effects model in the remaining analyses, indicating that the results were stable.

3.4.7. *Analysis of Publication Bias.* Publication bias analysis was not performed because few articles were included in the study (Figure 7).

#### 4. Discussion

Endoscopic transsellar approach and craniotomy are the two main surgical resection methods for pituitary adenoma. The former is significantly less invasive than the latter, which is a reliable and minimally invasive surgery, but it may still produce complications including cerebrospinal fluid rhinorrhea, epistaxis, olfactory dysfunction, and sinusitis; cerebrospinal fluid leakage is one of the serious complications, which can increase the risk of postoperative intracranial infection (commonly used anti-infective drugs include amoxicillin and metronidazole [23, 24]). The possible cause of CSF Leak is rupture of the top saddle diaphragm or arachnoid membrane caused by resection of the tumor, causing cerebrospinal fluid outflow from the nasal cavity [25]. At present, according to known reports, the incidence of postoperative CSF Leak after endoscopic treatment of pituitary adenoma is between 0.5% and 14% [25, 26]. In this study, the inci-

dence of postoperative CSF Leak was 6.79%, close to 5.6% reported in the literature [9, 26].

The occurrence of CSF Leak may be related to patient's own characteristic factors, tumor characteristic factors, and surgical factors. The reports in various studies are not exactly the same. Therefore, in this meta-analysis, the CSF Leak caused by different factors was summarized and analyzed.

4.1. *Patient's Own Characteristic Factors.* The common factors affecting postoperative CSF leakage include age factor and body mass index (BMI) factor. In the 13 included literatures, gender was not the relevant factor of postoperative CSF Leak. Therefore, no summary analysis is conducted in this study. In this meta-analysis, there was no significant difference in the incidence of postoperative CSF Leak at different age levels, suggesting that age is not a relevant factor for the occurrence of postoperative CSF Leak. However, patients with a postoperative CSF Leak had a significantly higher BMI than those without, suggesting that patients with a higher body mass index (obesity) are more likely to have a postoperative CSF leak, consistent with the observations of some scholars [27, 28]. The pathophysiology of obesity leading to an increased incidence of CSF Leak is uncertain, but the possibility of intracranial hypertension in obese patients was higher; during surgery, persistent elevated intracranial pressure eventually leads to postoperative saddle reconstruction dehiscence, resulting in the occurrence of CSF

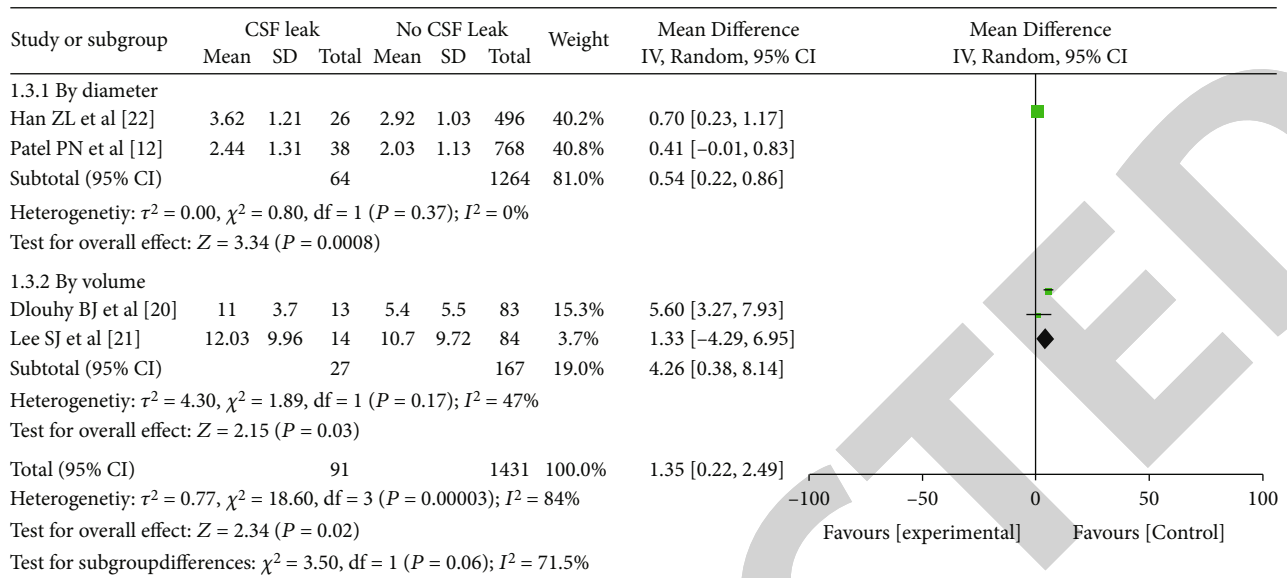


FIGURE 4: Effect of tumor size on CSF Leak after transsphenoidal surgery for pituitary adenoma.

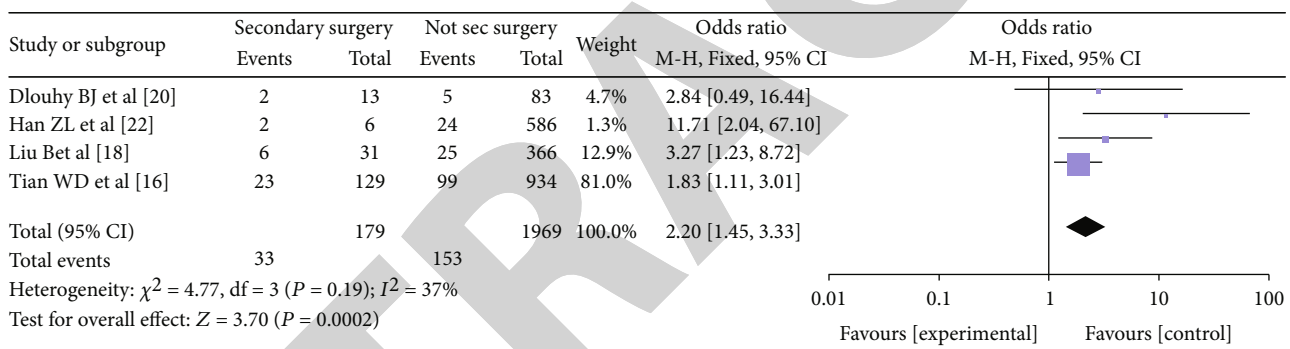


FIGURE 5: Effect of secondary operation on CSF Leak after transsphenoidal surgery for pituitary adenoma.

Leak [27, 29]. Therefore, when time permits, for young and obese patients, preoperative weight loss should be performed, while the operation should more carefully examine whether the intracranial pressure is increased and whether there is intraoperative CSF Leak. Once intraoperative CSF Leak and severe collapse of sellar septum occur, saddle floor reconstruction should be actively performed, and lumbar drainage should be performed when necessary to reduce the intracranial pressure.

**4.2. Tumor Factors.** Many studies [15, 20] have shown that patients with giant adenoma are more prone to have postoperative CSF Leak than microadenoma. This summary shows that patients with CSF Leak have larger tumors (in diameter or volume) than patients without CSF Leak; that means tumor size is one of the factors for the occurrence of CSF Leak. The reason for this is that larger tumors grow parasellar or suprasellar and are more likely to cause injury when surgically removing tumor tissue protruding into the saddle and parasellar region, and the voids left after resection of giant adenomas make the arachnoid membrane on the saddle more likely to collapse and cause damage [30–32]. At the

same time, larger tumors as well as tumors with wider invasion to the surrounding can often only be partially resected, while many surgeons pursue near total resection and have a higher risk of CSF Leak and bleeding. Therefore, for larger adenomas, particular attention should be paid to the occurrence of CSF Leak and timely drainage.

**4.3. Surgical Factors.** Our study also found that the incidence of postoperative CSF Leak in patients undergoing reoperation was higher than that in patients undergoing the first operation (OR = 2.20, 95% CI (1.45, 3.33)), which may be due to the formation of scar and tissue adhesion during the first operation, postoperative vascular proliferation, and tissue fibrosis, making it difficult to find the residual part of the tumor during reoperation, increasing the risk of CSF Leak by more invasive anatomical procedures during resection [31–33]. Our study also found that patients with intraoperative CSF Leak had an increased risk of secondary postoperative CSF Leak, which was a risk factor for postoperative CSF Leak, which may be related to insufficient repair of intraoperative cerebral spinal fluid leakage or postoperative buttress changes that caused the leakage to not close

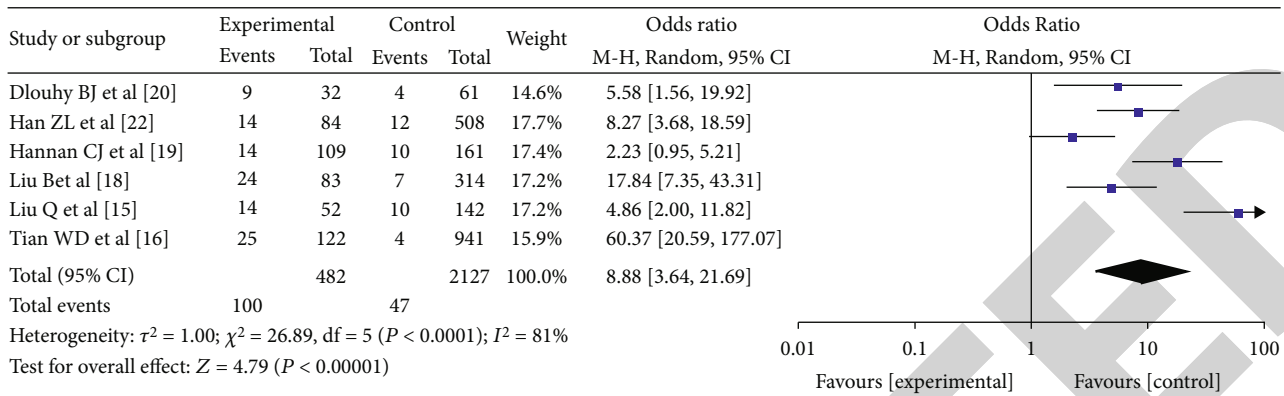


FIGURE 6: Effect of CSF Leak during surgery on CSF Leak after transsphenoidal surgery for pituitary adenoma.

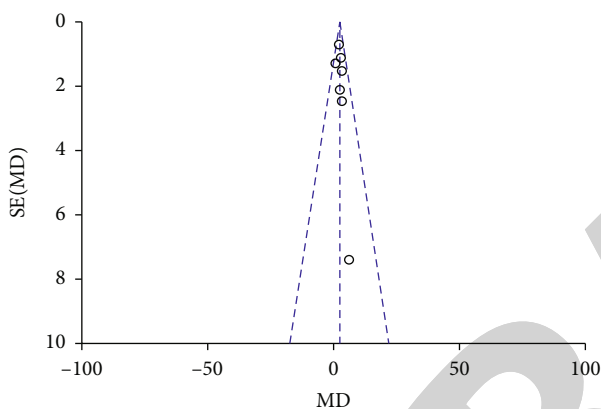


FIGURE 7: Publication bias analysis of the effect of patient BMI on CSF Leak after transsphenoidal surgery for pituitary adenoma.

due to detachment and displacement of the repair material, or pulsatile cerebrospinal fluid impact on the weak sellar septum, or the subsided sellar septum was punctured by the saddle floor bone margin [23]. Therefore, we believe that skull base reconstruction should be actively performed when cerebrospinal fluid leakage occurs during surgery, and prophylactic lumbar drainage of cerebrospinal fluid should be performed if necessary.

Some literatures reported that the type of tumor, texture of tumor, operation time, and preoperative cerebral edema were also risk factors of postoperative CSF Leak. However, there were few reported literatures, so we could not conduct a summary analysis. Although we found in this meta-analysis that age was not a risk factor for CSF Leak, it remains to be further determined because too few articles were included. In our study results, it was determined that BMI, tumor size, reoperation, and occurrence of intraoperative CSF Leak were related factors of postoperative CSF Leak, which were different from 4 related factors of tumor size, adenoma consistency, reoperation, and intraoperative CSF Leak obtained in the meta-analysis [9], which may be related to different literatures included in the two meta-analyses.

In the analysis of tumor size, we observed significant heterogeneity among the literatures ( $I^2 = 84\%$ ,  $P = 0.0003$ ), but when we divided the 4 literatures into two subgroups accord-

ing to different methods of tumor size assessment, the internal heterogeneity disappeared ( $P < 50\%$ ), indicating that the method of assessment was the source of heterogeneity. We also did not find serious publication bias in the publication bias analysis, but there were still few included literatures based on each risk factor, the coverage of risk factors was not comprehensive enough, and the risk factors for the occurrence of CSF Leak after transsphenoidal surgery for pituitary adenoma are still worthy of continued in-depth discussion.

### 5. Summary

This study included 13 studies on the factors that influence CSF Leak after pituitary adenoma transsphenoidal surgery. According to the findings, BMI, tumor size, reoperation, and the presence of intraoperative CSF Leak were the risk factors for postoperative CSF leak. However, there are still few included literatures based on each risk factor, and the coverage of the risk factors is insufficient, and it is still worthwhile to continue to deeply investigate the risk factors for the occurrence of CSF Leak after pituitary adenoma transsphenoidal surgery.

### Data Availability

The simulation experiment data used to support the findings of this study are available from the corresponding author upon request.

### Conflicts of Interest

The authors declare that they have no conflicts of interest.

### References

- [1] N. Inoshita and H. Nishioka, "The 2017 WHO classification of pituitary adenoma: overview and comments," *Brain Tumor Pathology*, vol. 35, no. 2, pp. 51-56, 2018.
- [2] M. G. Lake, L. S. Krook, and S. V. Cruz, "Pituitary adenomas: an overview," *American Family Physician*, vol. 88, no. 5, pp. 319-327, 2013.
- [3] M. Elsarrag, P. D. Patel, A. Chatrath, D. Taylor, and J. A. Jane, "Genomic and molecular characterization of pituitary



- adenoma pathogenesis: review and translational opportunities," *Neurosurgical Focus*, vol. 48, no. 6, p. E11, 2020.
- [4] A. Li, W. Liu, P. Cao, Y. Zheng, Z. Bu, and T. Zhou, "Endoscopic versus microscopic transsphenoidal surgery in the treatment of pituitary adenoma: a systematic review and meta-analysis," *World Neurosurgery*, vol. 101, pp. 236–246, 2017.
  - [5] C. Taweesomboonyat and T. Oearsakul, "Prognostic factors of acromegalic patients with growth hormone-secreting pituitary adenoma after transsphenoidal surgery," *World Neurosurgery*, vol. 146, pp. e1360–e1366, 2021.
  - [6] B. L. Hendricks, T. A. Shikary, and L. A. Zimmer, "Causes for 30-day readmission following transsphenoidal surgery," *Otolaryngology and Head and Neck Surgery*, vol. 154, no. 2, pp. 359–365, 2016.
  - [7] A. Parikh, A. Adapa, S. E. Sullivan, and E. L. McKean, "Predictive factors, 30-day clinical outcomes, and costs associated with cerebrospinal fluid leak in pituitary adenoma resection," *Journal of Neurological Surgery Part B: Skull Base*, vol. 81, no. 1, pp. 43–55, 2020.
  - [8] C. van Lieshout, E. M. H. Slot, A. Kinaci et al., "Cerebrospinal fluid leakage costs after craniotomy and health economic assessment of incidence reduction from a hospital perspective in the Netherlands," *BMJ Open*, vol. 11, no. 12, article e052553, 2021.
  - [9] Z. Zhou, F. Zuo, X. Chen et al., "Risk factors for postoperative cerebrospinal fluid leakage after transsphenoidal surgery for pituitary adenoma: a meta-analysis and systematic review," *BMC Neurology*, vol. 21, no. 1, p. 417, 2021.
  - [10] G. E. Bryce, J. M. Nedzelski, D. W. Rowed, and J. M. Rappaport, "Cerebrospinal fluid leaks and meningitis in acoustic neuroma surgery," *Otolaryngology–Head and Neck Surgery*, vol. 104, no. 1, pp. 81–87, 1991.
  - [11] C. Zhang, X. Ding, Y. Lu, L. Hu, and G. Hu, "Cerebrospinal fluid rhinorrhoea following transsphenoidal surgery for pituitary adenoma: experience in a Chinese centre," *Acta Otorhinolaryngologica Italica*, vol. 37, no. 4, pp. 303–307, 2017.
  - [12] Q. Liu, Y. S. Liu, J. Li et al., "Risk factors of cerebrospinal fluid leakage after endoscopic transsphenoidal pituitary adenoma resection," *Journal of Clinical Neurosurgery*, vol. 17, no. 5, pp. 516–521, 2020.
  - [13] W. D. Tian, X. H. Meng, T. Zhou et al., "Analysis of related factors of cerebrospinal fluid leakage during and after endoscopic transnasal pituitary adenoma resection," *Chinese Journal of Neuromedicine*, vol. 17, no. 6, pp. 563–569, 2018.
  - [14] S. Fraser, P. A. Gardner, M. Koutourousiou et al., "Risk factors associated with postoperative cerebrospinal fluid leak after endoscopic endonasal skull base surgery," *Journal of Neurosurgery*, vol. 128, no. 4, pp. 1066–1071, 2018.
  - [15] P. N. Patel, A. M. Stafford, J. R. Patrinely et al., "Risk factors for intraoperative and postoperative cerebrospinal fluid leaks in endoscopic transsphenoidal sellar surgery," *Otolaryngology and Head and Neck Surgery*, vol. 158, no. 5, pp. 952–960, 2018.
  - [16] T. T. Karnezis, A. B. Baker, Z. M. Soler et al., "Factors impacting cerebrospinal fluid leak rates in endoscopic sellar surgery," *International Forum of Allergy & Rhinology*, vol. 6, no. 11, pp. 1117–1125, 2016.
  - [17] I. Sun, J. X. Lim, C. P. Goh et al., "Body mass index and the risk of postoperative cerebrospinal fluid leak following transsphenoidal surgery in an Asian population," *Singapore Medical Journal*, vol. 59, no. 5, pp. 257–263, 2018.
  - [18] C. J. Hannan, H. Almhanedi, R. Al-Mahfoudh, M. Bhojak, S. Looby, and M. Javadpour, "Predicting post-operative cerebrospinal fluid (CSF) leak following endoscopic transnasal pituitary and anterior skull base surgery: a multivariate analysis," *Acta Neurochirurgica*, vol. 162, no. 6, pp. 1309–1315, 2020.
  - [19] B. J. Dlouhy, K. Madhavan, J. D. Clinger et al., "Elevated body mass index and risk of postoperative CSF leak following transsphenoidal surgery," *Journal of Neurosurgery*, vol. 116, no. 6, pp. 1311–1317, 2012.
  - [20] S. J. Lee, J. Cohen, J. Chan, E. Walgama, A. Wu, and A. N. Mamelak, "Infectious complications of expanded endoscopic transsphenoidal surgery: a retrospective cohort analysis of 100 cases," *Journal of Neurological Surgery Part B: Skull Base*, vol. 81, no. 5, pp. 497–504, 2020.
  - [21] Z. L. Han, D. S. He, Z. G. Mao, and H. J. Wang, "Cerebrospinal fluid rhinorrhea following trans-sphenoidal pituitary macroadenoma surgery: experience from 592 patients," *Clinical Neurology and Neurosurgery*, vol. 110, no. 6, pp. 570–579, 2008.
  - [22] A. J. Psaltis, R. J. Schlosser, C. A. Banks, J. Yawn, and Z. M. Soler, "A systematic review of the endoscopic repair of cerebrospinal fluid leaks," *Otolaryngology–Head and Neck Surgery*, vol. 147, no. 2, pp. 196–203, 2012.
  - [23] X. Cheng, F. Huang, K. Zhang, X. Yuan, and C. Song, "Effects of none-steroidal anti-inflammatory and antibiotic drugs on the oral immune system and oral microbial composition in rats," *Biochemical and Biophysical Research Communications*, vol. 507, no. 1-4, pp. 420–425, 2018.
  - [24] X. Cheng, F. He, M. Si, P. Sun, and Q. Chen, "Effects of antibiotic use on saliva antibody content and oral microbiota in Sprague Dawley rats," *Frontiers in Cellular and Infection Microbiology*, vol. 12, 2022.
  - [25] L. E. Rotman, E. N. Alford, M. C. Davis, T. B. Vaughan, B. A. Woodworth, and K. O. Riley, "Preoperative radiographic and clinical factors associated with the visualization of intraoperative cerebrospinal fluid during endoscopic transsphenoidal resection of pituitary adenomas," *Surgical Neurology International*, vol. 11, p. 59, 2020.
  - [26] S. Cohen, S. H. Jones, S. Dhandapani, H. M. Negm, V. K. Anand, and T. H. Schwartz, "Lumbar drains decrease the risk of postoperative cerebrospinal fluid leak following endonasal endoscopic surgery for suprasellar meningiomas in patients with high body mass index," *Operative Neurosurgery*, vol. 14, no. 1, pp. 66–71, 2018.
  - [27] G. Lam, V. Mehta, and G. Zada, "Spontaneous and medically induced cerebrospinal fluid leakage in the setting of pituitary adenomas: review of the literature," *Neurosurgical Focus*, vol. 32, no. 6, p. E2, 2012.
  - [28] D. J. Lobatto, F. de Vries, A. H. Zamanipoor Najafabadi et al., "Preoperative risk factors for postoperative complications in endoscopic pituitary surgery: a systematic review," *Pituitary*, vol. 21, no. 1, pp. 84–97, 2018.
  - [29] V. Sciarretta, D. Mazzatenta, R. Ciarpaglini, E. Pasquini, G. Farneti, and G. Frank, "Surgical repair of persisting CSF leaks following standard or extended endoscopic transsphenoidal surgery for pituitary tumor," *min-Minimally Invasive Neurosurgery*, vol. 53, no. 2, pp. 55–59, 2010.
  - [30] M. E. Ivan, J. B. Iorgulescu, I. El-Sayed et al., "Risk factors for postoperative cerebrospinal fluid leak and meningitis after expanded endoscopic endonasal surgery," *Journal of Clinical Neuroscience*, vol. 22, no. 1, pp. 48–54, 2015.



## *Retraction*

# **Retracted: Effect of Supplementation of Vitamin D in Patients with Periodontitis Evaluated before and after Nonsurgical Therapy**

### **BioMed Research International**

Received 18 July 2023; Accepted 18 July 2023; Published 27 September 2023

Copyright © 2023 BioMed Research International. This is an open access article distributed under the Creative Commons Attribution License, which permits unrestricted use, distribution, and reproduction in any medium, provided the original work is properly cited.

This article has been retracted by Hindawi following an investigation undertaken by the publisher. This investigation has uncovered evidence that the peer review process was compromised. We cannot, therefore, vouch for its reliability. Please note that this notice is intended solely to alert readers that the peer review of this article is compromised.

We have subsequently provided the authors with the opportunity to re-submit their article and undergo a new and independent peer-review process.

Wiley and Hindawi regret that the usual quality checks did not identify these issues before publication and have since put additional measures in place to safeguard research integrity.

We wish to credit our Research Integrity and Research Publishing teams and anonymous and named external researchers and research integrity experts for contributing to this investigation.



The corresponding author, as the representative of all authors, has been given the opportunity to register their agreement or disagreement to this retraction. We have kept a record of any response received.

## **References**

- [1] S. M. Mishra, P. L. Ravishankar, V. Pramod et al., “Effect of Supplementation of Vitamin D in Patients with Periodontitis Evaluated before and after Nonsurgical Therapy,” *BioMed Research International*, vol. 2022, Article ID 5869676, 5 pages, 2022.

## Research Article

# Effect of Supplementation of Vitamin D in Patients with Periodontitis Evaluated before and after Nonsurgical Therapy

Shree Mohan Mishra,<sup>1</sup> P. L. Ravishankar,<sup>2</sup> V. Pramod,<sup>1</sup> Prem Blaisie Rajula,<sup>2</sup> K. Gayathri,<sup>2</sup> Mohammad Khursheed Alam,<sup>3,4,5</sup> A. Thirumal Raj,<sup>6</sup> Shilpa Bhandi <sup>7,8</sup> and Shankargouda Patil <sup>9,10</sup>

<sup>1</sup>Department of Periodontology, New Horizon Dental College, Bilaspur, 495001 Chattisgarh, India

<sup>2</sup>Department of Periodontology, SRM Kattankulathur Dental College & Hospital, SRM Institute of Science and Technology, SRM Nagar, Kattankulathur, 603203 Kancheepuram, Chennai, Tamil Nadu, India

<sup>3</sup>Orthodontics, Preventive Dentistry Department, College of Dentistry, Jouf University, Sakaka 72345, Saudi Arabia

<sup>4</sup>Center for Transdisciplinary Research (CFTR), Saveetha Dental College, Saveetha Institute of Medical and Technical Sciences, Saveetha University, Chennai, India

<sup>5</sup>Department of Public Health, Faculty of Allied Health Sciences, Daffodil International University, Dhaka, Bangladesh

<sup>6</sup>Department of Oral Pathology and Microbiology, Sri Venkateswara Dental College and Hospital, Chennai 600130, India

<sup>7</sup>Department of Restorative Dental Sciences, Division of Operative Dentistry, College of Dentistry, Jazan University, Jazan 45142, Saudi Arabia

<sup>8</sup>Department of Cariology, Saveetha Dental College & Hospitals, Saveetha Institute of Medical and Technical Sciences, Saveetha University, Chennai- 600 077, India

<sup>9</sup>Department of Maxillofacial Surgery and Diagnostic Science, Division of Oral Pathology, College of Dentistry, Jazan University, Jazan 45142, Jazan 45412, Saudi Arabia

<sup>10</sup>Centre of Molecular Medicine and Diagnostics (COMManD), Saveetha Dental College & Hospitals, Saveetha Institute of Medical and Technical Sciences, Saveetha University, Chennai- 600 077, India

Correspondence should be addressed to Shankargouda Patil; [dr.ravipatil@gmail.com](mailto:dr.ravipatil@gmail.com)

Received 20 April 2022; Accepted 25 July 2022; Published 8 August 2022

Academic Editor: Dinesh Rokaya

Copyright © 2022 Shree Mohan Mishra et al. This is an open access article distributed under the Creative Commons Attribution License, which permits unrestricted use, distribution, and reproduction in any medium, provided the original work is properly cited.

**Background.** Vitamin D has anti-inflammatory properties and the potential to increase the generation of antimicrobial peptides like cathelicidin and defensins that may have a good impact on oral health. Higher vitamin D consumption has also been linked to a reduced risk of periodontal disease progression. Hence, the primary objective of this study was to evaluate and compare the clinical and laboratory parameters of oral supplementation of vitamin D as an adjuvant to scaling and root planing and to assess the bone mineral density via qualitative ultrasound bone density scanner in chronic periodontitis patients. **Methodology.** This study included 40 patients with periodontitis categorized into 2 groups with twenty patients each, Group I comprising scaling and root planing (SRP) alone and Group II comprising SRP along with vitamin D supplementation. Plaque index, gingival index, probing pocket depth, and clinical attachment loss was measured as clinical parameters. Serum vitamin D levels were assessed before and after SRP at both baseline and 6 weeks. **Results.** The intergroup comparison of clinical parameters (PI, GI, PPD, and CAL) at 6 weeks for both the groups showed statistical significance. Intragroup comparison of clinical parameters from baseline to 6 weeks showed a statistically significant reduction in both groups. The mean bone mineral density level in both the control and test groups demonstrated a mean *T* score of -1.3 and -1.21, respectively. The mean vitamin D levels were 27.8460 and 28.1020 for the test and control groups, respectively, which was statistically insignificant ( $p = 0.705$ ) and those at six-week intervals improved to 31.3650 and 28.0240 which were statistically significant ( $p \leq 0.001$ ). **Conclusion.** It could be stated that a positive relationship exists between periodontitis and osteopenia which could aggravate periodontal destruction. All periodontitis cases should thus be evaluated for BMD and supplemented with vitamin D<sub>3</sub> in an appropriate dosage and time frame to treat both these diseases.

## 1. Introduction

The most common type of periodontitis is periodontitis, which is characterized by a slow progression of inflammatory disease. Systemic and environmental variables (e.g., diabetes, smoking) may change the host's immunological response to the tooth biofilm, causing periodontal damage to occur more quickly [1]. Inflammatory and immune reactions that extend deep into the connective tissue beyond the cemento-enamel junction (CEJ) may include loss of connective tissue attachment to the tooth involved as well as loss of the alveolar bone.

Alveolar bone loss is more common in people with osteoporosis or low bone mass, according to research, though this connection is not fully accepted. A negative calcium balance is likely to come from a chronically low intake of vitamin D and calcium, leading to an increase in calcium removal from bone, including the alveolar bone. The tooth attachment system may be weakened as a result of this bone loss.

Vitamin D, namely, 1,25-dihydroxy vitamin D, has anti-inflammatory and antimicrobial properties via modifying immune cell cytokine production and increasing monocyte-macrophage cell secretion of antibacterial peptides. Vitamin D's various functions could help people with periodontal disease.

The inflammatory response, which is triggered by endotoxins or by the stimulation of the host immune system and the production of inflammatory mediators, causes tissue destruction. By initiating osteoclast-mediated bone resorption, these locally generated compounds cause connective tissue degradation and bone loss [2].

The general population's vitamin D and calcium intake should be within current limitations of 400 to 600 IU and 1,000 to 1,200 mg daily, respectively. Despite a growing agreement that such routine limits are insufficient, and professional organizations now prescribe increased vitamin D dosages (800 to 1,000 IU daily), 1 billion people are believed to be vitamin D deficient or insufficient globally. Although many people are aware of the benefits of calcium and vitamin D supplementation for bone health, their role in periodontal disease remains unknown. Taking vitamin D and/or calcium has been shown to prevent alveolar bone breakdown, gingivitis, and attachment loss in several trials [3].

Vitamin D is a potent anti-inflammatory and antimicrobial agent. Vitamin D is also required for bone strength and calcification, which appears to include alveolar bone. It was also recently reported that a higher vitamin D intake may protect against periodontal disease progression in older men. On the other side, no correlation exists between vitamin D levels and radiographic assessments of alveolar crest height (ACH), which are assumed to characterize the chronic stage of damaging periodontitis. Few studies have looked at the relationship between periodontal disease markers and vitamin D levels throughout time [4]. The goal of this study will be whether using vitamin D oral supplementation as an addition to periodontal treatment improves clinical measures of periodontal health.

## 2. Methodology

The present study was approved by the institutional ethics committee of New Horizon Dental College and Research Institute (ref. no NHDC&RI/2014/8340). Informed consent was obtained from all the patients.

The present randomized case-control clinical study comprising 40 patients with periodontitis was designed and implemented in the Department of Periodontology, New Horizon Dental College and Research Institute, Sakri, Bilaspur, Chhattisgarh. Systemically healthy patients within the age group of 19-50 years with generalized moderate to severe periodontitis (stage III) having a minimum of 20 teeth exhibiting probing depth  $\geq 5$  mm and CAL  $\geq 5$  mm were included in the study. Participants who underwent periodontal therapy, in the last 6 months, medically compromised patients (diabetes, hypertension, and CVS), osteoporosis, and patients with a history of disease, disorders, or drugs that might affect mineral metabolism and periodontal health are excluded. A detailed case history was recorded in a designed pro forma for all the patients, and written consent was obtained.

*2.1. Assessment of Parameters.* Plaque index, gingival index, probing pocket depth, and clinical attachment loss was recorded as clinical parameters to assess periodontal condition before and after the intervention. After the clinical examination and biochemical evaluation (blood test), detailed case sheet documentation including medical history was carried out by a single calibrated examiner. Patients who had generalized CP were provisionally recruited into the study and categorized into two groups as follows:

- (i) Group I (control): 20 subjects with periodontitis were subjected to SRP alone. Clinical parameters, bone mineral density, and serum vitamin D levels, were measured at baseline and six weeks after SRP
- (ii) Group II (test): consisting of 20 subjects with periodontitis were administered vitamin D supplements (Medisys® D<sub>3</sub>) (400 IU)/day for 6 weeks as an adjunct to SRP. Clinical parameters, bone mineral density and serum levels of vitamin D, were assessed at baseline and 6 weeks after SRP

Patients of both the groups were put on SRP, patient education, and motivation, and oral hygiene instructions were given.

*2.2. Measurement of Vitamin D Levels and Bone Mineral Density.* Serum vitamin D levels were assessed using the Chemiluminescent immune assay (ADVIA CENTAUR) (Thyrocare) technique at baseline and six weeks after therapy in both groups. Luminescent immunoassays are variations of the standard ELISA, just like fluorescent immunoassays. An enzyme converts a substrate to a reaction product that emits photons of light instead of developing a visible color.

Bone mineral density was measured by quantitative ultrasonography (QUS) using a bone mineral density

TABLE 1: Intragroup comparison of parameters at baseline and six weeks in the test and control groups.

Time interval	Control		Test	
	Mean	<i>p</i> value	Mean	<i>p</i> value
Plaque index	0.152	0.018*	0.246	$p \leq 0.001^{**}$
Gingival index	0.697	$p \leq 0.001^{**}$	0.212	0.037*
Probing pocket depth	2.787	$p \leq 0.001^{**}$	2.377	$p \leq 0.001^{**}$
Clinical attachment level	2.216	$p \leq 0.001^{**}$	0.959	$p \leq 0.001^{**}$
Serum vitamin D	-3.519	$p \leq 0.001^{**}$	0.078	0.236*
Bone mineral density	0.17000	0.495	0.24500	0.349

\*Statistically significant. \*\*Statistically highly significant.

TABLE 2: Inter-group Comparison of Mean values at Baseline and at 6 weeks.

Parameters (mean)	Baseline		<i>p</i> value	6 weeks		<i>p</i> value
	Control	Test		Control	Test	
Plaque index	1.550	1.652	0.128	1.304	1.012	$p \leq 0.001^{**}$
Gingival index	1.560	1.517	0.482	1.348	0.820	$p \leq 0.001^{**}$
Probing pocket depth	5.848	5.557	0.301	3.470	2.770	$p \leq 0.001^{**}$
Clinical attachment level	6.245	6.290	0.869	3.820	2.950	0.035*
Serum vitamin D	28.102	27.846	0.705	28.024	31.365	$p \leq 0.001^{**}$
Bone mineral density	-1.300	-1.210	0.862	-1.545	-1.380	0.456

\*Statistically significant. \*\*Statistically highly significant.

scanner (Sunlight Ultrasound Bone Density Scanner). QUS is a noninvasive approach to determining bone mineral conditions in the periphery bone that is relatively new. QUS methods offer biomechanical information in addition to bone density, which may be useful in assessing fracture risk. The BMD using QUS was assessed in the radial bone and patients were categorized with a *T* score of normal: 0 to -1, osteopenia: -1 to -2.5, and osteoporotic: -2.5 and above. In patients, the density of the maxillary alveolar process bone is linked to the density of the mandibular alveolar ridge, vertebral column, hips, and radius [5].

2.3. *Periodontal Intervention.* Scaling and root planing (SRP) were performed by hand instruments (Gracey's Area Specific cures from #1 to #14).

### 3. Statistical Analysis

The collected data were statistically analyzed. The standard deviation, standard error, and mean were determined. The Student *T*-test was used to determine the level of significance and the correlation of each treatment group's efficacy. All of the data was processed using the statistical program SPSS 15.0, and the findings were obtained using the student *T*-test. *p* value less than 0.05 was regarded as statistically significant (\*), and *p* value less than 0.001 was considered statistically highly significant (\*\*).

### 4. Results

The present study included 40 generalized CP patients who were allocated under the two study groups. The intragroup comparison (Table 1) and intergroup comparison (Table 2) were done between the test and control groups at baseline and six weeks.

The mean plaque index values at baseline between the control and test groups were 1.55 and 1.652 which was statistically insignificant ( $p = 0.128$ ) at the six-week interval reduced to 1.304 and 1.012 which were statistically highly significant ( $p \leq 0.001$ ), respectively. The mean gingival index values at baseline between the control and test groups were 1.560 and 1.517 which was statistically insignificant ( $p = 0.482$ ) and those at six-week intervals reduced to 1.348 and 0.820 which were statistically highly significant ( $p \leq 0.001$ ), respectively. The mean probing pocket depth values at baseline between the control and test groups were 5.848 and 5.557 which was statistically insignificant ( $p = 0.301$ ) and those at the six-week interval were reduced to 3.4702 and 2.7700 which were statistically significant ( $p = 0.037$ ), respectively. The mean clinical attachment values at baseline between the control and test groups were 6.245 and 6.29 which was statistically insignificant ( $p = 0.869$ ) and those at six-week intervals were reduced to 3.8200 and 2.9500 which were statistically significant ( $p = 0.035$ ), respectively. The mean vitamin D levels were 27.8460 and 28.1020 for the test and control groups, respectively, which was statistically insignificant



( $p = 0.705$ ) and those at six-week intervals improved to 31.3650 and 28.0240 which were statistically significant ( $p \leq 0.001$ ), respectively. The mean bone mineral density level values at baseline between the control and test groups were -1.3000 and -1.2100 which was statistically insignificant ( $p = 0.862$ ) and those at six-week interval were -1.5450 and -1.3800 which was not significant ( $p = 0.456$ ), respectively. The intragroup comparison of the clinical parameters from baseline to 6 weeks showed a statistically significant reduction in both the groups. The intergroup comparisons of the clinical parameters at baseline for both the groups were not statistically significant.

## 5. Discussion

Periodontitis is an inflammatory process of the teeth's surrounding tissues induced by a variety of microorganisms that causes progressive degradation of the periodontal ligament and alveolar bone loss, as well as increasing pocket depth, recession, or both [6].

Persons with low bone mass or osteoporosis are more prone to alveolar bone loss. This type of bone loss can hasten the onset of periodontal disease [7]. Vitamin D deficiency affects almost every group of society, including children and young people. The Indian Council of Medical Research (ICMR) suggests consuming 400 IU of vitamin D each day [8]. 1,25-Dihydroxy vitamin (the active form of vitamin D) (vitamin D<sub>3</sub>) is a strong immunological modulator by inhibiting cytokine synthesis by immune cells and stimulating monocytes-macrophages to release antibiotic-active peptides [3].

Southard et al. did a study and concluded that vitamin D is used as a supplement in periodontal maintenance therapy, but very little research has been instituted on its use as an adjuvant to SRP [5]. Hence, this case-control study with 40 patients diagnosed with periodontitis was performed to see if there was a link between periodontitis and skeletal bone mineral density, as well as the effect of vitamin D supplementation combined with nonsurgical periodontal therapy.

The intragroup comparison of the clinical parameters from baseline to 6 weeks showed a statistical significant reduction in both the groups. The intergroup comparisons of the clinical parameters at baseline for both the groups were not statistically significant showing that cases with similar disease severity were recruited for the study.

The intergroup comparison of the clinical parameters (PI, GI, PPD, and CAL) at 6 weeks for both the groups showed statistically significant. This could be attributed to the decrease in gingival inflammation after the removal of local irritants following nonsurgical therapy. The significant decrease in the gingival index values in the test group at six-week intervals may attribute to the anti-inflammatory effects of vitamin D supplements (400 IU). This was in accordance with the study done by Hiremath et al. who found a dose-dependent anti-inflammatory effect of vitamin D supplementation on gingivitis patients [9].

A greater reduction of PPD from baseline to six weeks in both the groups could be attributed firstly to the beneficial effects of scaling and root planing on the soft tissues within

the periodontal pocket leading to shrinkage and decrease in pocket depth. The superior result seen in the test group could be attributed to the positive effect of vitamin D on wound healing. The result of this study was in accordance with the previous study done by Tonguc et al. in which vitamin D administration improved healing potential [10].

QUS is a simple, safe, and feasible technology. These are a compact instrument that takes just a few minutes to complete the measurements and emits minimal or zero radiation [11]. The mean bone mineral density level values at baseline between the control and test groups were -1.3000 and -1.2100 which was statistically insignificant ( $p = 0.862$ ) and those at six-week interval were -1.5450 and -1.3800 which was nonsignificant ( $p = 0.456$ ), respectively. The distinctive feature of this study was that the patients selected in both the control and test groups diagnosed with periodontitis demonstrated a mean *T* score of -1.3 and -1.21, respectively, which could be grouped as osteopenia patients. This exhibits a correlation between osteopenia and periodontitis and is in accordance with a study (Hattatoglu-Sonmez et al.) done previously [12]. Considering this dual relationship, it may be stated that all patients with periodontitis may be screened for their skeletal bone mineral density and treated appropriately as the bone of lesser density may be more prone to rapid destruction caused by periodontal infection [13].

Vitamin D supplementation elevated the bone mineral density in the test group at six weeks (-1.38) as compared to the control (-1.54) though the patients still remained in the osteopenia range. This could be because vitamin D suppresses OPG expression, and the combination of high RANKL expression and low OPG expression mediated by vitamin D would promote osteoclast differentiation and stimulation, as well as enhanced bone resorption [13]. Low vitamin D levels may also raise parathyroid hormone levels in the blood, which can promote bone resorption and elevate blood calcium levels indirectly.

In this study, vitamin D was administered only for six weeks which may have been an insufficient time interval to produce changes in bone mineral density. Thus, it could be stated that a positive relationship exists between periodontitis and osteopenia which could aggravate periodontal destruction. All periodontitis cases should thus be evaluated for BMD and be supplemented with vitamin D<sub>3</sub> in an appropriate dosage and for an adequate time frame to treat both these chronic diseases appropriately [14].

## 6. Conclusion

In conclusion, the current study's findings revealed that there is a link between periodontitis and osteopenia. As a result, these individuals might be tested for bone mineral density and serum vitamin D levels. Vitamin D supplements can be utilized in conjunction with SRP to enhance periodontal disease status and bone mineral density.

## Data Availability

No data were used to support this study.

## Retraction

# Retracted: The Predictive Value of Neutrophil-Lymphocyte Ratio in Patients with Polycythemia Vera at the Time of Initial Diagnosis for Thrombotic Events

### BioMed Research International

Received 20 June 2023; Accepted 20 June 2023; Published 21 June 2023

Copyright © 2023 BioMed Research International. This is an open access article distributed under the Creative Commons Attribution License, which permits unrestricted use, distribution, and reproduction in any medium, provided the original work is properly cited.

This article has been retracted by Hindawi following an investigation undertaken by the publisher [1]. This investigation has uncovered evidence of one or more of the following indicators of systematic manipulation of the publication process:

- (1) Discrepancies in scope
- (2) Discrepancies in the description of the research reported
- (3) Discrepancies between the availability of data and the research described
- (4) Inappropriate citations
- (5) Incoherent, meaningless and/or irrelevant content included in the article
- (6) Peer-review manipulation

The presence of these indicators undermines our confidence in the integrity of the article's content and we cannot, therefore, vouch for its reliability. Please note that this notice is intended solely to alert readers that the content of this article is unreliable. We have not investigated whether authors were aware of or involved in the systematic manipulation of the publication process.

In addition, our investigation has also shown that one or more of the following human-subject reporting requirements has not been met in this article: ethical approval by an Institutional Review Board (IRB) committee or equivalent, patient/participant consent to participate, and/or agreement to publish patient/participant details (where relevant).

Wiley and Hindawi regrets that the usual quality checks did not identify these issues before publication and have since put additional measures in place to safeguard research integrity.

We wish to credit our own Research Integrity and Research Publishing teams and anonymous and named external researchers and research integrity experts for contributing to this investigation.

The corresponding author, as the representative of all authors, has been given the opportunity to register their agreement or disagreement to this retraction. We have kept a record of any response received.

### References

- [1] X. Wang, Y. Tu, M. Cao et al., "The Predictive Value of Neutrophil-Lymphocyte Ratio in Patients with Polycythemia Vera at the Time of Initial Diagnosis for Thrombotic Events," *BioMed Research International*, vol. 2022, Article ID 9343951, 8 pages, 2022.



## Research Article

# The Predictive Value of Neutrophil-Lymphocyte Ratio in Patients with Polycythemia Vera at the Time of Initial Diagnosis for Thrombotic Events

Xuekun Wang <sup>1,2</sup>, Yansong Tu,<sup>3</sup> Mei Cao,<sup>1,2</sup> Xiaoyan Jiang,<sup>1</sup> Yazhi Yang,<sup>1</sup> Xiaoyan Zhang <sup>1,4</sup>, Hurong Lai <sup>1,2</sup>, Huaijun Tu <sup>2,5</sup>, and Jian Li <sup>1,5</sup>

<sup>1</sup>The Key Laboratory of Hematology of Jiangxi Province, The Department of Hematology, The Second Affiliated Hospital of Nanchang University, 1 Minde Road, Nanchang, 330006 Jiangxi, China

<sup>2</sup>Graduate School of Medicine, Nanchang University, 465 Bayi Road, Nanchang, 330006 Jiangxi, China

<sup>3</sup>Faculty of Environment, University of Waterloo, 200 University Avenue, Waterloo, Ontario, Canada N2L 3G1

<sup>4</sup>Laboratory of Infection & Immunology, School of Basic Medical Sciences, Nanchang University, 465 Bayi Road, Nanchang 330006, China

<sup>5</sup>The Department of Neurology, The Second Affiliated Hospital of Nanchang University, 1 Minde Road, Nanchang, 330006 Jiangxi, China

Correspondence should be addressed to Huaijun Tu; [thj127900@163.com](mailto:thj127900@163.com) and Jian Li; [ndefy03048@ncu.edu.cn](mailto:ndefy03048@ncu.edu.cn)

Received 13 May 2022; Revised 18 June 2022; Accepted 24 June 2022; Published 8 August 2022

Academic Editor: Dinesh Rokaya

Copyright © 2022 Xuekun Wang et al. This is an open access article distributed under the Creative Commons Attribution License, which permits unrestricted use, distribution, and reproduction in any medium, provided the original work is properly cited.

**Objective.** To investigate and discuss the predictive value of the neutrophil-to-lymphocyte ratio (NLR) in patients with polycythemia vera (PV) at the time of initial diagnosis, as well as its clinical significance in predicting the occurrence of thrombotic events and the progression of future thrombotic events during follow-ups, with the goal of providing a reference for the early identification of high-risk PV patients and the early intervention necessary to improve the prognosis of PV patients. **Method.** A total of 170 patients diagnosed with PV for the first time were enrolled in this study. The risk factors affecting the occurrence and development of thrombotic events in these patients were statistically analyzed. **Results.** NLR ( $P=0.030$ ), WBC count ( $P=0.045$ ), and history of previous thrombosis ( $P<0.001$ ) were independent risk factors for thrombotic events at the time of initial diagnosis. Age  $\geq 60$  years ( $P=0.004$ ), NLR ( $P=0.025$ ), history of previous thrombosis ( $P<0.001$ ), and fibrinogen ( $P=0.042$ ) were independent risk factors for the progression of future thrombotic events during follow-ups. The receiver operating characteristic curve (ROC curves) showed that NLR was more effective in predicting the progression of future thrombotic events than age  $\geq 60$  years, history of previous thrombosis, and fibrinogen. Kaplan-Meier survival analysis showed progression-free survival time of thrombotic events in the high NLR value group (NLR  $\geq 4.713$ ) (median survival time 22.033 months, 95% CI: 4.226-35.840), which was significantly lower compared to the low NLR value group (NLR  $< 4.713$ ) (median overall survival time 66.000 months, 95% CI: 50.670-81.330); the observed difference was statistically significant ( $P<0.001$ ). The 60-month progression-free survival in the low NLR value group was 58.8%, while it was 32.8% in the high NLR value group. **Conclusion.** Peripheral blood NLR levels in patients with PV resulted as an independent risk factor for the occurrence of thrombotic events at the time of initial diagnosis and for the progression of future thrombotic events during follow-ups. Peripheral blood NLR levels at the time of initial diagnosis and treatment had better diagnostic and predictive value for the progression of future thrombotic events in patients with PV than age  $\geq 60$  years, history of previous thrombosis, and fibrinogen.

## 1. Introduction

Polycythemia vera (PV) is a form of myeloproliferative neoplasm (MPN) originating from hematopoietic stem cells. Thrombotic events are a major complication in patients with PV, as well as the most common cause of death [1, 2]. Therefore, early assessment of the risk of occurrence and progression of thrombotic events and early intervention may be effective in improving the prognosis of patients with PV.

By damaging vascular endothelial cells, promoting platelet adhesion and aggregation, and triggering coagulation reactions, inflammation can induce thrombosis, which is more likely to occur with intense inflammation and poor prognosis. White blood cell (WBC) count is an indicator of the systemic inflammatory response that has an important role in thrombosis [3]. One of the risk factors for MPN thrombotic events is the increase and activation of WBC [4].

NLR is the ratio of neutrophils to lymphocytes [5, 6] that has a more significant role in the diagnosis of inflammation and prognosis than the leukocyte subtype alone [7]. In addition to its predictive efficacy in the prognosis of ischemic diseases [8], it has been shown to be strongly associated with thrombotic events in cardiovascular disease [9–11]. Furthermore, a previous study found that the NLR value at the time of initial diagnosis and treatment is a simple-to-calculate marker for systemic inflammation that has better diagnostic and predictive efficacy for future thrombotic event progression in essential thrombocytosis (ET) than other clinical indices [12]. However, there are no relevant studies on the relationship between NLR in PV and thrombotic events in China and abroad. The study of the relationship between NLR and thrombotic events in patients with PV can provide new experimental basis for clinical workers to evaluate the disease and early intervention in the future. In this study, we retrospectively analyzed clinical and laboratory-related parameters in 170 patients with PV, investigated the risk factors for the occurrence and progression of thrombotic events, and analyzed and discussed the correlation between NLR levels and the occurrence and progression of thrombotic events in patients with PV at the time of initial diagnosis and treatment, as well as their clinical significance.

## 2. Materials and Methods

**2.1. Case Information.** A total of 170 patients admitted diagnosed with PV for the first time at our hospital between July 2013 and July 2019 were enrolled in this study. Inclusion criteria were as follows: (1) a clear diagnosis of PV, meeting the diagnostic criteria established by WHO in 2008 [13]; (2) patients who were undiagnosed before hospital admission and were not treated with antiplatelet, anticoagulant, or blood cell-lowering related medications. Exclusion criteria were as follows: (1) PV was diagnosed before the patient's admission or patients were treated with antiplatelet, anticoagulant, or hematocrit-lowering related therapy; (2) secondary erythrocytosis; (3) the disease had transformed during follow-ups and the diagnosis met other MPN diagnostic criteria such as ET; (4) the disease had progressed to other types of disease such as primary myelofibrosis, myelodysplastic syndrome, or acute leukemia; (5) the patient had coinfection, tuberculosis, surgery,

trauma, malignancy, or the use of immunomodulators or other medications that may affect the blood test.

This study was approved by the Medical Ethics Committee of the Second University Hospital of Nanchang University. Hematocrit is the ratio of red blood cells to the fluid component of your blood or plasma.

Platelets are blood clotting cells that aid in the coagulation of blood. A complete blood count that shows abnormal increases or declines in cell counts may suggest that you have an underlying medical problem that needs to be evaluated further.

**2.2. Relevant Definitions.** Cardiovascular risk factors (CVF) [14]: smoking, hyperlipidemia, diabetes, hypertension, and congestive heart failure. Thrombotic events [15]: arterial thromboembolism refers to acute myocardial infarction, acute ischemic stroke, peripheral arterial disease, and similar. Venous thromboembolism refers to pulmonary embolism, peripheral or visceral venous thrombosis, and similar. Progression of future thrombotic events: a new thrombotic event during follow-up of a patient with no previous history of thrombosis or exacerbation of thrombotic progression at the same site on top of a previous thrombotic event or a new thrombotic event at a different site.

**2.3. Data Collection.** Patient's data in the study were reviewed and collected through the electronic medical record system. All patients were followed up by telephone, outpatient, or inpatient modalities with the future thrombotic event progression as the endpoint of the follow-ups. The last follow-up visit was on September 10, 2019, which included demographic data such as sex, age, cardiovascular risk factors, history of previous thrombosis, future thrombotic event progression, and clinical laboratory findings, such as blood count, biochemistry, coagulation function, JAK2V617F mutation, and bone marrow examination.

**2.4. Breakdown by Group.** Patients with PV were divided into a group with and without thrombotic events based on the presence or absence of thrombotic events at the time of the initial consultation. They were separated into two groups: one group had progression of future thrombotic events throughout the follow-up, while the other group did not have progression of future thrombotic events. These groups were determined based on the progression of future thrombotic events. In order to determine the optimal NLR cutoff value, patients were separated into two groups: those with low NLR values and those with high NLR values. These groups were determined using the receiver operating characteristic curve (ROC curve).

**2.5. Statistical Methods.** Data were statistically processed using SPSS 24.0. One-sample Kolmogorov-Smirnov test was used to assess the distribution of the data, and *t*-tests were used for normally distributed measurements. The multifactor analysis was performed using logistic regression for binary outcomes. ROC curves were applied to analyze the predictive value of peripheral blood NLR levels at the time of initial diagnosis and treatment for the occurrence of thrombotic events in patients with PV and to determine the optimal cutoff values with high sensitivity and specificity. Kaplan-Meier analysis

was used to assess progression-free survival time to thrombotic events.  $P$  value of  $<0.05$  was considered to be statistically significant.

### 3. Results

**3.1. Clinical and Laboratory Test Characteristics.** The median age of onset among 170 patients with PV was 56 years (20-83), while 58 patients (34.1%) were aged  $\geq 60$  years and 112 (65.9%)  $<60$  years. There were 134 male (78.8%) and 36 female (21.2%) patients, a total of 133 CVF (78.2%) and 37 without CVF (21.8%). In addition, 54 (31.8%) patients had a history of previous thrombosis, and 116 (68.2%) had no previous history of thrombosis; 49 (28.8%) had comorbid diseases with thrombotic events at the time of visit and 121 had no comorbid disease (71.2%) at the time of visit. All 170 patients were tested for the JAK2V617F mutation, among which 107 were positive (62.9%) and 63 were negative (37.1%). The first routine blood test at the time of admission in 170 patients with PV showed a white blood cell count (WBC) of  $9.35 \pm 5.07 \times 10^9/L$ , red blood cell count (RBC)  $6.61 \pm 1.03 \times 10^{12}/L$ , hemoglobin count (Hb)  $195.28 \pm 15.97$  g/L, and platelet count (PLT)  $281.31 \pm 190.13 \times 10^9/L$  (Table 1).

**3.2. Thrombosis at Initial Diagnosis.** At the time of consultation, 49 (28.8%) patients with PV had comorbid diseases with the thrombotic event. The results of the single-factor analysis showed that comorbid disease in thrombosis at the time of initial consultation was closely correlated with NLR ( $P < 0.001$ ), history of previous thrombosis ( $P < 0.001$ ), CVF ( $P = 0.020$ ), and WBC ( $P = 0.006$ ) (Table 2). The multifactorial analysis showed that NLR ( $P = 0.030$ ), WBC ( $P = 0.045$ ), and history of previous thrombosis ( $P < 0.001$ ) were an independent risk factor for the occurrence of thrombotic events at the time of initial diagnosis (Table 3).

**3.3. Progress of Future Thrombotic Events during Follow-Up.** All follow-ups for 170 patients were completed within a median follow-up time of 20.33 (1 to 69) months, and 51 (30.0%) patients progressed to thrombotic events. The single-factor analysis showed that future thrombotic event progression during follow-ups was closely associated with age  $\geq 60$  years ( $P < 0.001$ ), NLR ( $P < 0.001$ ), WBC ( $P < 0.001$ ), JAK2V617F mutation ( $P = 0.006$ ), history of previous thrombosis ( $P < 0.001$ ), and fibrinogen (FIB) ( $P = 0.011$ ) (Table 4). The multifactorial analysis showed that age  $\geq 60$  years ( $P = 0.004$ ), NLR ( $P = 0.025$ ), previous thrombosis history ( $P < 0.001$ ), and fibrinogen ( $P = 0.042$ ) were independent risk factors in the progression of future thrombotic events during follow-ups (Table 5). ROC curve analysis showed that the diagnostic efficacy of NLR for the progression of future thrombotic events was more effective than age, history of previous thrombosis, JAK2V617F mutation, and fibrinogen level (AUC<sub>NLR</sub> > AUC<sub>history of previous thrombosis</sub> > AUC<sub>WBC</sub> > AUC<sub>age  $\geq 60$  years</sub> > AUC<sub>JAK2V617F gene mutation</sub> > AUC<sub>fibrinogen</sub>) (Table 6). The sensitivity of the NLR for predicting the progression of thrombotic events was 74.5%, with a specificity of 79.8% when NLR equaled 4.713 (Figure 1).

TABLE 1: Clinical characteristics of 170 patients with PV at the first consultation.

Categories	Values
Age $\geq 60$ years	58
Male	134
History of previous thrombosis	54
JAK2V61F mutation	107
CVF	133
WBC ( $10^9/L$ )	$9.35 \pm 5.07$
RBC ( $10^{12}/L$ )	$6.61 \pm 1.03$
HB (g/L)	$195.28 \pm 15.97$
PLT ( $10^9/L$ )	$281.31 \pm 190.13$

The 170 followed-up patients were divided into a high NLR group (NLR  $\geq 4.713$ ) and a low NLR group (NLR  $< 4.713$ ). Kaplan-Meier survival analysis showed that the progression-free survival time to thrombotic events in the high NLR group (median overall survival time 22.033 months, 95% CI: 4.226 to 35.840) was significantly lower compared to that in the low NLR group (median overall survival time 66.000 months, 95% CI: 50.670-81.330), and the difference was statistically significant ( $P < 0.001$ ) (see Figure 2). Sixty-month progression-free survival after thrombotic events was 58.8% in the low NLR group. However, the 60-month progression-free survival after thrombotic events in the high NLR group was 32.8%.

### 4. Discussion

Recent studies have identified NLR as an essential indicator of immune inflammation [16] that has a wide range of applications. Furthermore, NLR is crucial for the diagnosis and prognosis of infectious diseases. Also, thrombotic events are closely related to noninfectious diseases, such as cardiovascular disease and tumors. However, there are only a few studies on the relationship between NLR and thrombotic events in MPN.

Zhou et al. [12] indicated that a high NLR at the initial diagnosis and treatment is an independent risk factor for future thrombotic events in patients with ET, which suggests that NLR may be related to MPN thrombotic events. Nonetheless, there is no current study on the relationship between NLR and PV thrombotic events. The results of this study indicated that peripheral blood NLR levels at the time of initial diagnosis were not only associated with thrombotic events in patients with PV at the time of initial diagnosis ( $P = 0.030$ ). The high level of NLR at the time of initial diagnosis and treatment indicated a higher risk of combined thrombotic events. Moreover, it had predictive value for the progression of future thrombotic events ( $P = 0.025$ ). In addition, the predictive efficacy in NLR was more significant compared to other indicators. For example, high NLR value indicated shorter survival time in progression-free thrombosis with a higher risk for further development of the original thrombus or new thrombotic events, as well as poor prognosis.

The mechanisms behind NLR and PV thrombotic events are unknown. The process might be analogous to thrombotic events in cardiovascular and tumor disorders [17–22], with

TABLE 2: Single-factor analysis of risk factors for thrombotic events at initial diagnosis.

Item	Thrombosis group (n = 49)	Nonthrombotic group (n = 121)	P value
Gender, male n(%)	37 (75.51)	97 (80.17)	0.501
Age ≥ 60 years n(%)	20 (40.82)	38 (31.40)	0.241
JAK2V617F mutation (%)	36 (73.47)	71 (58.68)	0.070
CVF n(%)	44 (89.80)	89 (73.55)	0.020
History of thrombosis n(%)	41 (83.67)	13 (10.74)	<0.001
NLR	6.602 ± 6.312	4.061 ± 4.131	<0.001
WBC (10 <sup>9</sup> /L)	10.527 ± 5.167	8.870 ± 4.977	0.006
RBC (10 <sup>12</sup> /L)	6.563 ± 0.965	6.632 ± 1.060	0.832
Hb (g/L)	195.510 ± 16.802	195.190 ± 15.691	0.782
HCT	59.653 ± 5.486	59.148 ± 7.307	0.202
PLT (10 <sup>9</sup> /L)	272.220 ± 178.780	285.020 ± 195.179	0.439
Creatinine (μmol/L)	83.535 ± 38.224	77.307 ± 18.908	0.926
Uric acid (μmol/L)	451.397 ± 133.154	439.447 ± 115.753	0.812
eGFR (mL/min)	95.397 ± 38.522	97.528 ± 25.534	0.201
Sodium (mmol/L)	139.016 ± 3.355	138.481 ± 2.703	0.589
Potassium (mmol/L)	4.057 ± 0.608	4.185 ± 0.599	0.220
FIB (g/L)	2.659 ± 0.839	2.573 ± 0.835	0.221
D-dimers (mg/L)	1.558 ± 1.443	1.693 ± 3.248	0.774
APTT (s)	36.045 ± 9.880	36.780 ± 10.143	0.403
PT (s)	13.492 ± 3.585	13.502 ± 3.604	0.561
INR	1.159 ± 0.301	1.151 ± 0.283	0.388
PTA (%)	81.860 ± 26.540	85.493 ± 26.795	0.499
TT (s)	19.420 ± 5.724	19.192 ± 2.161	0.108

TABLE 3: Multifactorial analysis of risk factors for thrombotic events at the time of initial diagnosis.

Variant	P value	OR	95% CI
NLR	0.030	1.192	1.017-1.398
WBC	0.045	0.869	0.758-0.997
History of thrombosis	<0.001	48.912	16.797-142.429
CVF	0.435	1.701	0.449-6.449

NLR acting as an inflammatory-immune signal. There is an increase in neutrophil stress after thrombotic events, indicating an inflammatory response, whereas injured arteries stimulate platelet adhesion and aggregation, triggering a coagulation reaction. On the other hand, lymphocyte stress, which indicates immunological activity, is lowered, lowering immunoprotection and increasing the risk of thrombosis. However, further study is required to fully understand the mechanism.

Age ≥ 60 years has been identified as an independent risk factor for thrombotic events in the conventional thrombotic risk stratification [19]. Patients in this study were divided into two groups based on their age, including ≥60 years and <60 years. The results indicated that even though there was no significant association between age ≥ 60 and PV at the time of

initial diagnosis ( $P > 0.05$ ), it was the independent risk factor for future thrombotic event progression in patients with PV ( $P = 0.004$ ). Therefore, it has an important predictive value in patients with PV for future thrombotic event progression, which is consistent with the conventional risk assessment of thrombotic events. Yet, the International Working Group on Myeloproliferative Neoplasms Research and Treatment (IWG-MRT) developed by Tefferi [11] is one of the overall prognostic stratification schemes used in clinical practice for PV based on age (5 points for ≥67 years and 2 points for 57-66 years) that clearly shows the importance of age on the overall prognosis of PV, as well as subdivides the age groups in more detail. The principle is the same, i.e., advanced age is important for the prediction of thrombotic events and overall prognosis in patients with PV.

History of thrombosis is not only an independent risk factor in the conventional thrombotic risk stratification in PV patients [23] but a history of venous thrombosis also accumulates points in the IWG-MRT developed by Tefferi [13] in patients with PV. This emphasizes the importance of the history of thrombosis in predicting PV thrombotic events. The results of this study also indicated that a history of thrombosis was not only an independent risk factor for thrombotic events at the time of initial diagnosis ( $P < 0.001$ ) but also an independent risk factor for the progression of future thrombotic events



TABLE 4: Single-factor analysis of risk factors for progression to future thrombotic events.

Item	Thrombosis group (n = 51)	Nonthrombotic group (n = 119)	P value
Gender, male n(%)	36 (70.59)	98 (82.35)	0.085
Age ≥ 60 years n(%)	33 (64.71)	25 (21.01)	<0.001
JAK2V617F mutation n(%)	40 (78.43)	67 (56.30)	0.006
CVF n(%)	39 (76.47)	94 (78.99)	0.715
History of thrombosis n(%)	36 (70.59)	18 (15.13)	<0.001
NLR	8.174 ± 7.346	3.344 ± 2.353	<0.001
WBC (10 <sup>9</sup> /L)	12.259 ± 5.926	8.099 ± 4.092	<0.001
RBC (10 <sup>12</sup> /L)	6.589 ± 1.071	6.622 ± 1.019	0.904
Hb (g/L)	196.120 ± 18.938	194.920 ± 14.589	0.723
HCT	59.775 ± 6.070	59.087 ± 7.131	0.115
PLT (10 <sup>9</sup> /L)	306.250 ± 176.270	270.530 ± 195.553	0.120
Creatinine (μmol/L)	82.041 ± 37.003	77.843 ± 19.592	0.735
Uric acid (μmol/L)	445.692 ± 135.430	441.691 ± 114.472	0.938
eGFR (mL/min)	94.897 ± 37.700	97.778 ± 25.753	0.230
Sodium (mmol/L)	138.502 ± 3.515	138.692 ± 2.617	0.199
Potassium (mmol/L)	4.143 ± 0.609	4.151 ± 0.602	0.909
FIB (g/L)	2.895 ± 1.164	2.471 ± 0.606	0.011
D-dimers (mg/L)	2.479 ± 4.897	1.301 ± 0.999	0.059
APTT (s)	37.666 ± 12.108	36.098 ± 9.035	0.661
PT (s)	13.727 ± 3.847	13.401 ± 3.483	0.833
INR	1.187 ± 0.318	1.151 ± 0.283	0.975
PTA (%)	80.302 ± 27.010	86.222 ± 26.473	0.293
TT (s)	19.917 ± 5.588	18.975 ± 2.144	0.243

TABLE 5: Multifactorial analysis of risk factors for the progression of future thrombotic events.

Variant	P value	OR	95% CI
Age ≥ 60 years	0.004	4.378	1.614-11.873
NLR	0.025	1.279	1.032-1.587
History of thrombosis	<0.001	11.604	4.463-30.173
Fibrinogen	0.042	1.820	1.023-3.238
WBC	0.675	0.970	0.841-1.118
JAK2V617F mutation	0.767	1.179	0.396-3.508

( $P < 0.001$ ). Although it has been shown that CVF also increases the risk of MPN thrombotic events [24], CVF is not considered as an independent risk factor in the conventional thrombosis risk stratification [23] nor the PV IWG-MRT [15]. Our results revealed no significant correlation between CVF and PV thrombotic events ( $P > 0.05$ ).

The majority of patients with PV have the JAK2V617F mutation [25, 26]. Still, neither the conventional PV thrombosis risk stratification [23] nor the IWG-MRT [13] for PV patients currently includes the JAK2V617F mutation as an independent risk factor. Our results did not reveal the JAK2V617F mutation

as an independent risk factor for progression of thrombotic events ( $P > 0.05$ ) in PV patients at the time of initial diagnosis and during the follow-ups; however, there was a significant correlation between JAK2V617F mutations and the thrombotic events during follow-ups ( $P = 0.006$ ) from the single-factor analysis. De Grandis et al. [25] and Lu et al. [27] also found that the JAK2V617F mutation is strongly associated with PV thrombotic events, which suggests that the JAK2V617F mutation might be important for the occurrence of PV thrombotic events at the time of initial diagnosis and in the progression of future thrombotic events.

Conventional risk factors for PV thrombosis did not include blood count as an independent risk factor [23], but WBC count  $> 15 \times 10^9/L$  accumulates 1 point in the IWG-MRT in PV patients [13]. Our results revealed that WBC was an independent risk factor for the development of PV thrombotic events at the time of initial diagnosis ( $P = 0.045$ ). Even though it was not an independent risk factor for future thrombotic event progression ( $P > 0.05$ ), there was a significant correlation between WBC and future thrombosis progression when analyzed with single-factor analysis ( $P < 0.001$ ). We also found a small number of cases with WBC count  $> 15 \times 10^9/L$  (19 cases), while 51 patients had elevated WBC above  $10 \times 10^9/L$ . Therefore, it is hypothesized that the risk of future

TABLE 6: ROC curve analysis of aged  $\geq 60$  years, NLR, WBC, JAK2V61F gene mutation, history of previous thrombosis, and fibrinogen in predicting thrombotic events during follow-up of PV patients.

Variant	Area under the curve	<i>P</i> value	95% CI
NLR	0.813	<0.001	0.743-0.883
History of thrombosis	0.777	<0.001	0.695-0.860
WBC	0.757	<0.001	0.677-0.837
Age $\geq 60$ years	0.718	<0.001	0.630-0.806
JAK2V61F mutation	0.611	0.022	0.521-0.700
Fibrinogen	0.584	0.083	0.482-0.687

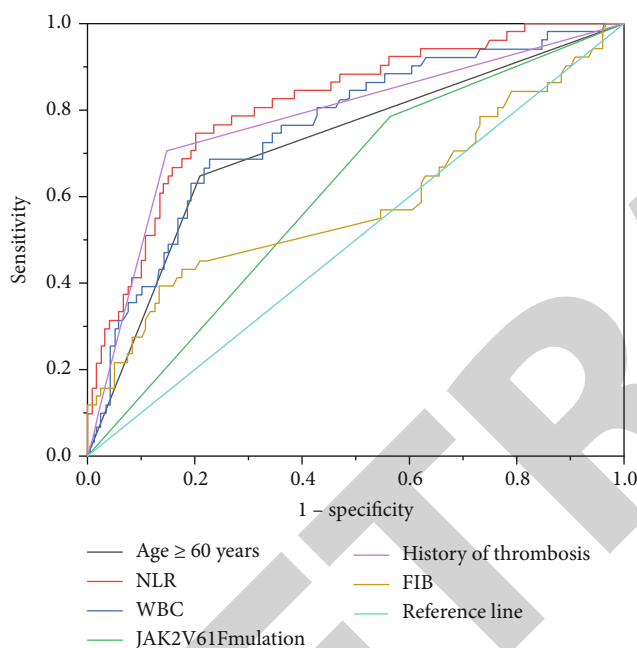


FIGURE 1: ROC curve analysis of age  $\geq 60$  years, NLR, WBC, JAK2V61F mutation, history of previous thrombosis, and fibrinogen in predicting thrombotic events during follow-up of PV patients.

thrombotic events is increased in PV patients with elevated WBC at the time of initial treatment. Moreover, our results also indicated that RBC and platelet counts were not significantly correlated with the initial thrombotic event or the progression of future thrombotic events ( $P > 0.05$ ).

While neither the conventional risk factors for thrombosis in PV [23] nor the IWG-MRT [13] has included coagulation dysfunction as an independent risk factor for PV, Barraco et al. [28] and Krol [29] have indicated that coagulation dysfunction is an important factor in the development of thrombotic events in PV. Our results did not show a significant correlation ( $P > 0.05$ ) between coagulation function and thrombotic events at the time of initial diagnosis. Still, fibrinogen in coagulation function resulted as an independent risk factor for the progression of thrombotic events during the follow-ups of PV patients ( $P = 0.011$ ).

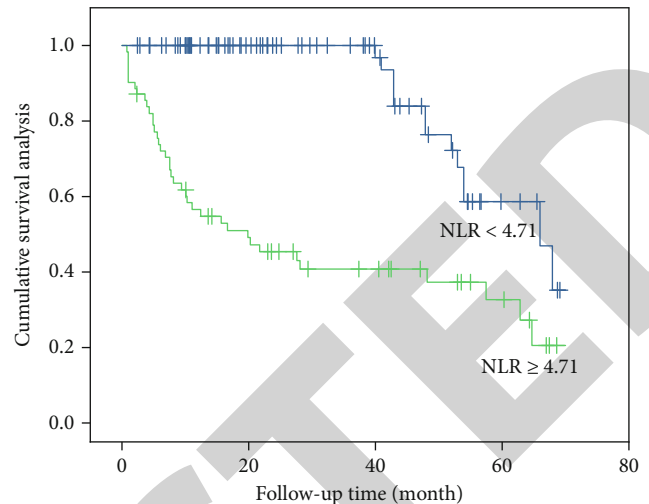


FIGURE 2: Progression-free survival after thrombotic events' survival rate comparison in the high NLR group and the low NLR group.

In the present study, we retrospectively examined the relationship between peripheral blood NLR levels and thrombotic events in patients with PV at the time of initial diagnosis and treatment, finding that NLR is not only an independent risk factor for thrombotic events at initial diagnosis ( $P = 0.030$ ) but also for future thrombotic event progression during follow-ups ( $P = 0.025$ ). The ROC curve also showed that NLR is a stronger predictor of future thrombotic episodes than other factors such as age, past thrombosis history, WBC, and JAK2V617F mutation.

## 5. Conclusion

Peripheral blood NLR levels in patients with PV resulted as an independent risk factor for the occurrence of thrombotic events at the time of initial diagnosis and for the progression of future thrombotic events during follow-ups. Peripheral blood NLR levels at the time of initial diagnosis and treatment had better diagnostic and predictive value for the progression of future thrombotic events in patients with PV than age  $\geq 60$  years, history of previous thrombosis, and fibrinogen.

Therefore, in addition to focusing on factors such as age, previous thrombosis history, blood count, and JAK2V61F mutation in PV patients when assessing the risk of thrombotic events in PV patients, NLR level at the time of initial diagnosis and treatment has more clinical significance in predicting the risk of thrombotic events in PV patients. Moreover, these factors may be useful for early assessment and prediction of thrombotic events in patients with PV, early selection of appropriate therapeutic options and prevention, and improved prognosis of patients with PV. The study's border is that it only looked at NLR levels at the time of the first diagnosis and therapy; nevertheless, NLR levels alter over time as illness progresses. Furthermore, because the inflammatory process is complicated, NLR alone is insufficient to determine the amount of inflammatory response. As a result, future research should



include baseline levels and dynamics of NLR, as well as other inflammatory markers, to better understand its association to the incidence of PB thrombotic events.

## Data Availability

The datasets used and analyzed during the current study are available from the corresponding author on reasonable request.

## Conflicts of Interest

The authors declare that the research was conducted in the absence of any commercial or financial relationships that could be construed as a potential conflict of interest.

## Authors' Contributions

X.K. Wang and Y.S. Tu contribute equally to this study and share first authorship.

## Acknowledgments

This study was supported by the National Natural Science Foundation of China (81760033 and 82160030).

## References

- [1] A. Tefferi and T. Barbui, "Polycythemia vera and essential thrombocythemia: 2019 update on diagnosis, risk-stratification and management," *American Journal of Hematology*, vol. 94, no. 1, pp. 133–143, 2019.
- [2] M. F. Matos, "The role of IL-6, IL-8 and MCP-1 and their promoter polymorphisms IL-6 -174GC, IL-8 -251AT and MCP-1 -2518AG in the risk of venous thromboembolism: A case-control study," *Thrombosis Research*, vol. 128, no. 3, 2011.
- [3] E. Reganon, V. Vila, V. Martínez-Sales et al., "Sialic acid is an inflammation marker associated with a history of deep vein thrombosis," *Thrombosis Research*, vol. 119, no. 1, pp. 73–78, 2007.
- [4] T. Sun and L. Zhang, "Thrombosis in myeloproliferative neoplasms with JAK2V617F mutation," *Clinical & Applied Thrombosis/hemostasis*, vol. 19, no. 4, pp. 374–381, 2013.
- [5] Y. Arbel, A. Finkelstein, A. Halkin et al., "Neutrophil/lymphocyte ratio is related to the severity of coronary artery disease and clinical outcome in patients undergoing angiography," *Atherosclerosis*, vol. 225, no. 2, pp. 456–460, 2012.
- [6] M. B. Alazzam, A. T. Al-Radaideh, N. Binsarif, A. S. AlGhamdi, and M. A. Rahman, "Advanced deep learning human herpes virus 6 (HHV-6) molecular detection in understanding human infertility," *Computational Intelligence and Neuroscience*, vol. 2022, Article ID 1422963, 5 pages, 2022.
- [7] G. Sabri, "Platelet/lymphocyte ratio and risk of in-hospital mortality in patients with ST-elevated myocardial infarction," *Medical Science Monitor: International Medical Journal of Experimental and Clinical Research*, vol. 20, pp. 660–665, 2014.
- [8] A. Celikbilek, S. Ismailogullari, and G. Zararsiz, "Neutrophil to lymphocyte ratio predicts poor prognosis in ischemic cerebrovascular disease," *Journal of Clinical Laboratory Analysis*, vol. 28, no. 1, pp. 27–31, 2014.
- [9] N. Xu, X. F. Tang, Y. Yao et al., "Predictive value of neutrophil to lymphocyte ratio in long-term outcomes of left main and/or three-vessel disease in patients with acute myocardial infarction," *Catheterization and Cardiovascular Interventions*, vol. 91, no. S1, pp. 551–557, 2018.
- [10] M. B. Alazzam, H. Mansour, F. Alassery, and A. Almulihi, "Machine learning implementation of a diabetic patient monitoring system using interactive E-App," *Computational Intelligence and Neuroscience*, vol. 2021, Article ID 5759184, 7 pages, 2021.
- [11] M. Zhai, J. Wang, L. Yu, X. Fu, and L. Li, "Predictive value of neutral granulocyte to lymphocyte ratio on the prognosis of patients with acute cerebral infarction," *Chinese Journal of Cerebrovascular Disease*, vol. 2, pp. 82–86, 2017.
- [12] D. Zhou, H. Cheng, W. Chen, Z. Li, and K. Xu, "Relationship between peripheral thromboplastin ratio and thrombotic events in primary thrombocytopenic patients at the time of initial diagnosis and treatment," *Chinese Journal of Experimental Hematology*, vol. 2, pp. 534–538, 2019.
- [13] Z. Shi and Z. Xiao, "Interpretation of the Chinese expert consensus on the diagnosis and treatment of true erythrocytosis (2016 edition)," *Chinese Journal of Hematology*, vol. 10, pp. 852–857, 2016.
- [14] R. Marchioli, G. Finazzi, R. Landolfi et al., "Vascular and neoplastic risk in a large cohort of patients with polycythemia vera," *Journal of Clinical Oncology*, vol. 23, no. 10, pp. 2224–2232, 2005.
- [15] T. Barbui, G. Finazzi, A. Carobbio et al., "Development and validation of an international prognostic score of thrombosis in World Health Organization-essential thrombocythemia (IPSET-thrombosis)," *Blood*, vol. 120, no. 26, pp. 5128–5133, 2012.
- [16] J. Zhu, L. Zhu, Y. Yin, and Z. Ruan, "Peripheral blood NLR changes in patients with early ventricular arrhythmias in acute myocardial infarction and their significance," *Shandong Medical*, vol. 38, pp. 59–60, 2014.
- [17] M. B. Alazzam, N. Tayyib, S. Z. Alshawwa, and M. K. Ahmed, "Nursing care systematization with case-based reasoning and artificial intelligence," *Journal of Healthcare Engineering*, vol. 2022, Article ID 1959371, 9 pages, 2022.
- [18] P. Ferroni, S. Riondino, V. Formica et al., "Venous thromboembolism risk prediction in ambulatory cancer patients: clinical significance of neutrophil/lymphocyte ratio and platelet/lymphocyte ratio," *International Journal of Cancer*, vol. 136, no. 5, pp. 1234–1240, 2015.
- [19] J. He, J. Li, Y. Wang, P. Hao, and Q. Hua, "Neutrophil-to-lymphocyte ratio (NLR) predicts mortality and adverse-outcomes after ST-segment elevation myocardial infarction in Chinese people," *International Journal of Clinical and Experimental Pathology*, vol. 7, no. 7, pp. 4045–4056, 2014.
- [20] L. Xu and B. Tao, "Correlation of neutrophil lymphocyte ratio and acute myocardial infarction," *China Cardiovascular Research*, vol. 8, pp. 692–695, 2017.
- [21] A. Carobbio, A. M. Vannucchi, V. De Stefano et al., "Neutrophil-to-lymphocyte ratio is a novel predictor of venous thrombosis in polycythemia vera," *Blood Cancer Journal*, vol. 12, no. 2, p. 28, 2022.
- [22] B. Huang, "Regulation of immunity and inflammation in the tumor microenvironment," *Chinese Journal of Cancer Biotherapy*, vol. 2, pp. 111–115, 2012.
- [23] T. Barbui, G. Barosi, G. Birgegard et al., "Philadelphia-negative classical myeloproliferative neoplasms: critical concepts and

## Retraction

# Retracted: Hysterectomy by Transvaginal Natural Orifice Transluminal Endoscopic Surgery versus Transumbilical Laparoscopic Single-Site Surgery: A Single-Center Experience from East China

### BioMed Research International

Received 20 June 2023; Accepted 20 June 2023; Published 21 June 2023

Copyright © 2023 BioMed Research International. This is an open access article distributed under the Creative Commons Attribution License, which permits unrestricted use, distribution, and reproduction in any medium, provided the original work is properly cited.

This article has been retracted by Hindawi following an investigation undertaken by the publisher [1]. This investigation has uncovered evidence of one or more of the following indicators of systematic manipulation of the publication process:

- (1) Discrepancies in scope
- (2) Discrepancies in the description of the research reported
- (3) Discrepancies between the availability of data and the research described
- (4) Inappropriate citations
- (5) Incoherent, meaningless and/or irrelevant content included in the article
- (6) Peer-review manipulation

The presence of these indicators undermines our confidence in the integrity of the article's content and we cannot, therefore, vouch for its reliability. Please note that this notice is intended solely to alert readers that the content of this article is unreliable. We have not investigated whether authors were aware of or involved in the systematic manipulation of the publication process.

In addition, our investigation has also shown that one or more of the following human-subject reporting requirements has not been met in this article: ethical approval by

an Institutional Review Board (IRB) committee or equivalent, patient/participant consent to participate, and/or agreement to publish patient/participant details (where relevant).

Wiley and Hindawi regrets that the usual quality checks did not identify these issues before publication and have since put additional measures in place to safeguard research integrity.

We wish to credit our own Research Integrity and Research Publishing teams and anonymous and named external researchers and research integrity experts for contributing to this investigation.



The corresponding author, as the representative of all authors, has been given the opportunity to register their agreement or disagreement to this retraction. We have kept a record of any response received.

### References

- [1] B. Yan, H. Miao, Y. Wang et al., "Hysterectomy by Transvaginal Natural Orifice Transluminal Endoscopic Surgery versus Transumbilical Laparoscopic Single-Site Surgery: A Single-Center Experience from East China," *BioMed Research International*, vol. 2022, Article ID 8246761, 7 pages, 2022.

## Research Article

# Hysterectomy by Transvaginal Natural Orifice Transluminal Endoscopic Surgery versus Transumbilical Laparoscopic Single-Site Surgery: A Single-Center Experience from East China

Bin Yan,<sup>1,2,3</sup> Hui-Xian Miao,<sup>4</sup> You Wang,<sup>1,2,3</sup> Jia-Mu Xu,<sup>1,2,3</sup> Xiu-Qing Lu,<sup>1</sup> Wan-Hong He,<sup>1</sup> Wen Di <sup>1,2,3</sup> and Wei-Hua Lou <sup>1,2,3</sup>

<sup>1</sup>Department of Obstetrics and Gynaecology, Renji Hospital, School of Medicine, Shanghai Jiao Tong University, Shanghai, China

<sup>2</sup>Shanghai Key Laboratory of Gynaecologic Oncology, Shanghai, China

<sup>3</sup>State Key Laboratory of Oncogenes and Related Genes, Shanghai Cancer Institute, Renji Hospital, School of Medicine, Shanghai Jiao Tong University, China

<sup>4</sup>Jiangsu Province Hospital, The First Affiliated Hospital with Nanjing Medical University, China

Correspondence should be addressed to Wen Di; diwen163@163.com and Wei-Hua Lou; jason19921851540@163.com

Bin Yan and Hui-Xian Miao contributed equally to this work.

Received 10 May 2022; Revised 31 May 2022; Accepted 30 June 2022; Published 8 August 2022

Academic Editor: Dinesh Rokaya

Copyright © 2022 Bin Yan et al. This is an open access article distributed under the Creative Commons Attribution License, which permits unrestricted use, distribution, and reproduction in any medium, provided the original work is properly cited.

**Objective.** To compare hysterectomy by transvaginal natural orifice transluminal endoscopic surgery (VNOTES) versus transumbilical laparoscopic single-site surgery (LESS) as a minimal invasive technique. **Materials and Method.** The women undergoing hysterectomy for benign diseases by VNOTES and LESS from January 2020 to June 2021 in a tertiary hospital in Shanghai were retrospectively analyzed. **Results.** 361 women were included in our study, with 228 in the VNOTES groups, 129 in the LESS groups, and 4 conversions from VNOTES to LESS technique. The length of a VNOTES hysterectomy was shorter than that of LESS (80.76 min versus 112.09 min; MD -31.34 min; 95% CI -40.24 to -22.43 min;  $P < 0.001$ ). VNOTES hysterectomy has a quicker gas passage by the anus (18.80 versus 36.49 hours, MD -17.68 hours, 95% CI -20.23 to -15.14 hours,  $P < 0.001$ ) and associated with a shorter length of hospital stay (2.31 versus 3.77 days, MD -1.46 days, 95% CI -1.75 to -1.17 days,  $P < 0.001$ ), while with no increase in blood loss during the operation (median 50 versus 50 ml,  $P = 0.25$ ). Besides, the VAS pain score in the 24<sup>th</sup> hour after the operation was lower (median 0 versus 0.5,  $P < 0.001$ ) in the VNOTES group. Four unique phases of the learning curve were identified using cumulative analysis: the mean operation time of phase I was  $82.81 \pm 31.45$  min (the initial learning curve of 43 cases), phase II was  $72.48 \pm 23.66$  min (the acquisition of command of 91 cases), phase III was  $103.77 \pm 45.69$  min (the further learning of 26 cases), and phase IV was  $73.18 \pm 26.89$  min (postlearning in 68 cases). **Conclusions.** VNOTES is noninferior to LESS as a new minimal invasive procedure for hysterectomy, which also allows patients a faster recovery from surgery and to suffer less pain, and its efficiency and feasibility in large uterine need further exploring.

## 1. Introduction

Hysterectomy is one of the most common gynecological procedures for benign gynecological diseases and some early-stage tumors, such as abnormal uterine bleeding, adenomyosis, atypical endometrial hyperplasia, and cervical hyperplasia. The procedure has been performed in different ways: abdominal hysterectomy (AH), conventional vaginal

hysterectomy (VH), laparoscopic hysterectomy (LH), and robotically assisted hysterectomy (RH). According to the number of laparoscope, LH can be classified into several types: conventional multiport laparoscopic hysterectomy (CMLH), laparoscopy-assisted vaginal hysterectomy (LAVH), or transumbilical laparoscopic single-site surgery (LESS). As a Cochrane review involving 5012 women reports, VH is superior to LH and AH because of its faster return to normal

activities. When VH is not feasible, LH is preferred but related to more urinary tract injuries [1]. Although patients appear to benefit more from VH, it is not easy to have a good command of VH because of its poor visualization and limited space for manipulation.

Recently, natural orifice transluminal endoscopic surgery (NOTES), which utilizes the natural orifices such as the rectum, mouth, urethra, and vagina to get into the peritoneal cavity, has been developed since its minimal invasions during procedures. After various animal experiments, NOTES started to be used in human and the first transvaginal NOTES (VNOTES) hysterectomy was performed in 2012 [2]. VNOTES is a combination of conventional vaginal surgery and laparoscopic single-site surgery, which overcomes the limitations of conventional VH with the help of endoscopic view and instruments. Several studies have reported VNOTES as a safe procedure, associated with shorter surgical time, faster postoperative recovery, reduced postoperative pain, decreased postoperative wound infections, and cosmetic results [3, 4].

LESS is reported as a feasible, safe, and equally effective alternative to CMPL for hysterectomy [5]. A randomised controlled trial of VNOTES has suggested that VNOTES is noninferior to CMPL for hysterectomy and reduces postoperative pain [6, 7]. Our study was aimed at comparing VNOTES with LESS as a minimally invasive technique for hysterectomy. We explored that VNOTES, as a combination of VH and LESS, not only removes the uterus as safely and effectively as LESS but has a faster recovery from the procedure and better cosmesis. What is more, we evaluated the learning curve of the new technique, evaluating its efficiency and feasibility in uterine with normal weight. Learning curve means the learning time or times required for new technologies or methods.

## 2. Materials and Method

This was a retrospective study of women who underwent hysterectomy by transvaginal NOTES and by LESS with the same indications from January 2020 to June 2021 in Shanghai Jiao Tong University affiliated Renji Hospital, a teaching hospital in China. The surgical indications include atypical endometrial hyperplasia, adenomyosis, uterine myoma, high-grade cervical dysplasia, treatment-refractory dysfunctional uterine bleeding, benign adnexal masses, and uterine prolapse. The following information was collected in all the patients: age, body mass index (BMI), prior vaginal birth, previous abdominal surgery, diabetes, cardiovascular diseases, indication for operation, uterine weight, total operation time, intraoperative and postoperative complications, and the length of hospital stay.

The duration of the operation was defined as the time from the start of circumcising the vaginal mucosa to the removal of the uterus. The VAS pain score was accomplished in the first 24 hours after the operation. The complications were accepted as wound infection, blood transfusion requirement, and readmission into the hospital in 6 weeks.

The learning curve of the VNOTES technique was measured as the operation time over the time course of the study. Cumulative sum (CUSUM<sub>OT</sub>) analysis was used as

reported by previous studies [8, 9]. The CUSUM calculated the total difference between the individual values and mean of all values. Arranging the patients in sequence, graphical information of the trend in the operation time of consecutive procedures could be plotted. The CUSUM<sub>OT</sub> for the 1st case was the difference between the OT for the 1st case and the mean OT for all patients. The CUSUM<sub>OT</sub> of the 2nd case was the CUSUM<sub>OT</sub> of the 1st value added to the difference between the OT of the 2nd case and the mean OT for all patients. The calculation was repeated until the last CUSUM<sub>OT</sub> reached zero. Linear regression with log transformations was performed to determine the sign of the slope of regression.

**2.1. Surgical Procedure.** All participants in our study were admitted into hospital several days earlier (depending on the severity of the complications) to receive the laboratory and imaging assessment to rule out the contraindications of the surgery, especially those who could not tolerate the surgery. The operations were performed by the same expert gynecologist (Lou), who was the first gynecologist to conduct the VNOTES procedures in our department. All women in our study received hysterectomy and either bilateral salpingectomy or salpingo-oophorectomy depending on the indications. The first step of the hysterectomy was to circumcise the vaginal mucosa around the cervix by using a scalpel, then expose the vesical peritoneal reflection after pushing up the anterior vaginal mucosa along the uterine cervical fascia, and dissect the peritoneal reflection to get access to the abdominal cavity anteriorly. Similarly, the posterior vaginal wall was exposed and dissected, and the pouch of Douglas was opened. The uterosacral ligament complexes were then cut as done in the conventional vaginal surgeries, followed by circumcising the cervix to get into the peritoneal cavity. To achieve a pneumoperitoneum, a VNOTES port (Beijing Hang Tian KaDi Technology R&D Institute) was inserted through the vagina into the peritoneal cavity, which had two 5 mm and two 10 mm channels. The two endoscopic instruments were used through the two 5 mm channels and a standard 10 mm rigid mm 30° laparoscope (Stryker) through one 10 mm channel. As done in the conventional vaginal surgery, the hysterectomy was performed caudally to cranially. The bilateral ureters would routinely be identified during the operation but not be dissected unless it was necessary. The uterine vessels and bilateral ligaments, including parametrial tissues, round ligament, ovarian proper ligament, and mesosalpinx, were cut and sealed by the ultrasonic scalpel and the endoscopic instrument with bipolar coagulation (Hangzhou Kangji Medical Instrument). When the salpingo-oophorectomy was indicated, the bilateral infundibulopelvic ligaments would also be cut to enable the ovaries to be disconnected. The free uterine was removed through the vagina. After confirming there was no active bleeding, the VNOTES port was removed and the vaginal cuff was closed using one 1-0 suture (Ethicon Endo-Surgery, Norderstedt, Germany) through the vagina.

In those who received hysterectomy by LESS, the gynecologist performed hysterectomy by transumbilical laparoscopic single-site surgery technique. A LESS port was inserted through the umbilicus to create access to the



abdominal cavity, which also had two 5 mm and two 10 mm channels. A standard 10 mm rigid 30° laparoscope (Stryker) and endoscopic instruments were used. Similarly, the ureters were identified but not dissected to prevent injuries. With the help of a uterine manipulator and endoscopic instruments with bipolar coagulation, the gynecologist performed hysterectomy cranially to caudally. The uterine was removed through the vagina, which in some extent would save surgical time. The vaginal cuff was also closed using the 1-0 suture (Ethicon Endo-Surgery, Norderstedt, Germany). The umbilicus was closed using absorbable suture after ensuring there was no bleeding inside the abdominal cavity. Finally, a wound dressing was used on the umbilicus.

**2.2. Statistical Analysis.** The Fisher exact test or chi-square test was applied for dichotomous secondary outcome measures, while an independent *t*-test or Mann–Whitney *U* test was applied for the continuous secondary outcomes. *P* values of <0.05 were considered to indicate statistical significance. Data analysis was performed by using SPSS software (version 26).

### 3. Results

Between January 2020 and June 2021, a total number of 232 patients received hysterectomy by VNOTES and 129 by LESS. Four cases in the VNOTES group failed to remove the uterus and converted to LESS technique, which resulted in a conversion rate of 1.72% ( $P = 0.30$ ). The 4 conversions were all diagnosed as multiple uterine myoma, 3 of whom failed due to the large size of myoma (up to 12 centimeters) and 1 of whom due to the adhesion between the uterus and the pelvis.

Baseline characteristics were comparable between the two groups except for some certain surgical indications, which are summarized in Table 1. The percentage of uterine myoma and benign adnexal tumor in the VNOTES group was lower than that in the LESS group (36.84% versus 48.44%,  $P = 0.04$ , and 4.82% versus 20.16%,  $P < 0.001$ ), while the percentage of cervical dysplasia and uterine prolapse was higher than that in the controlled group (29.82% versus 14.07%,  $P < 0.001$ , and 4.82% versus 0.78%,  $P < 0.02$ ).

As shown in Table 2, we leave out the 4 conversions and compared the main outcomes between the two groups. In our study, not only the median uterine weight was comparable between the VNOTES group and the LESS group (median 164.00 gram versus 176.90 gram,  $P = 0.58$ ) but also the percentage of uterine weight more than 400 g ( $P = 0.48$ ) was comparable. The total length of a VNOTES hysterectomy was shorter than a LESS one (78.21 minutes versus 112.09 minutes; mean difference (MD) -33.89 minutes; 95% confidence index (CI) -42.55 to -25.22 minutes;  $P < 0.001$ ). Compared with LESS hysterectomy, VNOTES hysterectomy has a quicker gas passage by the anus (18.80 versus 36.49 hours, MD -17.68 hours, 95% CI -20.23 to -15.14 hours,  $P < 0.001$ ) and thus associated with a shorter length of hospital stay (2.31 versus 3.77 days, MD -1.46 days, 95% CI -1.75 to -1.17 days,  $P < 0.001$ ). Surprisingly, the VNOTES and LESS groups shared a similar blood loss dur-

ing the operation (median 50 versus 50 ml,  $U = 2662.5$ ,  $z = -1.152$ ,  $P = 0.25$ , there was no statistical difference; a Mann–Whitney *U* test).

The VAS pain score in the 24th hour after the operation in the VNOTES group was lower than that in the LESS group (median 0 versus 0.5,  $U = 2133.0$ ,  $Z = -3.517$ ,  $P < 0.001$ , there was statistical difference; a Mann–Whitney *U* test). The less analgesic use in the VNOTES group also indicated patients suffered less pain from VNOTES technology (odds ratio 4.00, 95% CI 1.81 to 8.84,  $P < 0.001$ ). There was exudation in the umbilicus wound in 2 women in the LESS group; however, it showed no statistical difference ( $P = 0.13$ ). Besides, no complications and readmission in 6 weeks were reported in both groups.

Then, after getting the raw operation time in each consecutive patient in chronological order (Figure 1), we calculated the  $CUSUM_{OT}$  values and a learning curve was achieved, which was plotted in a graph as shown in Figure 2(a). The learning curve was able to be divided into four distinct phases: cases 1-43 into the initial learning phase (phase I), cases 44-134 into the commanding phase (phase II), cases 135-150 into the further learning phase (phase III), and cases 150-228 into postlearning phase (phase IV). The best fit curves of the learning curve in each phase are shown in Figure 2(b).

There were significant differences among the four phases in operation time and uterine weight (Table 3). Patients in phase III had the longest operation time ( $103.77 \pm 45.69$  min) and the largest uteri ( $423.27 \pm 338.14$  grams, Figures 3(a) and 3(b)) but shared similar BMI and postoperative stay with the other three phases.

### 4. Discussion

Since the VNOTES was introduced into our department in 2019, more and more patients preferred this advanced technique to receive hysterectomy. In our study, we retrospectively analyzed the cases of hysterectomy by VNOTES and LESS, involving as much as 228 patients in the VNOTES group. We found that VNOTES was noninferior to LESS hysterectomy and could be an alternative for hysterectomy in women with benign diseases due to its minimal invasiveness, as previously reported [10–12]. In our study, with no increased risk of blood loss during the procedure, VNOTES had a shorter surgical length compared with the LESS group, which saved almost half an hour, though part of which might resulted from the leave out of suturing the umbilical wound. There were no increase in the intra- and postoperative complications in the VNOTES group, which also proved VNOTES was a safe technique for hysterectomy. Besides, women in the VNOTES group had a faster recovery with less pain from the surgery. Women after the VNOTES surgery had a faster recovery of gastrointestinal function and thus had a reduced length of hospital stay, which no doubt decreased the hospitalization expenses. We investigated the VAS pain score in the 24th hour after the surgery and postoperative analgesic use, which suggested women in the VNOTES group suffered less postoperative pain. No postoperative and wound infection was reported

TABLE 1: Baseline characteristics of the population.

	VNOTES* ( <i>n</i> = 228)	LESS ( <i>n</i> = 129)	<i>P</i> value
Age (years)	53.04 ± 9.44	54.26 ± 10.33	0.27
BMI (kg/m <sup>2</sup> ) (range)	23.96 ± 3.08	24.26 ± 3.84	0.48
Prior vaginal birth, <i>n</i> (%)	155 (67.98)	80 (62.02)	0.25
Previous abdominal surgery, <i>n</i> (%)	84 (36.84)	59 (45.74)	0.10
Cardiovascular disease, <i>n</i> (%)	41 (17.98)	32 (24.81)	0.13
Diabetes, <i>n</i> (%)	13 (5.70)	5 (3.88)	0.45
Indication for surgery, <i>n</i> (%)			
Atypical endometrial hyperplasia	16 (7.02)	5 (3.91)	0.23
Adenomyosis	36 (15.79)	13 (10.16)	0.13
Uterine myoma	84 (36.84)	62 (48.44)	0.04
Cervical dysplasia	68 (29.82)	18 (14.07)	<0.001
Treatment-resistant DUB	2 (0.88)	4 (3.13)	0.20
Benign adnexal tumor	11 (4.82)	26 (20.16)	<0.001
Uterine prolapse	11 (4.82)	1 (0.78)	0.02

DUB: dysfunctional uterine bleeding; SD: standard deviation. \*The 4 conversions were not included.

TABLE 2: Main outcomes in the population.

	VNOTES ( <i>n</i> = 228)	LESS ( <i>n</i> = 129)	<i>P</i> value
Uterine weight (g), median (±IQR)	164.00 (±224.00)	176.90 (±254.00)	0.58
Uterine weight > 400 g, <i>n</i> (%)	31 (13.6)	21 (16.3)	0.48
Total operating time (min), mean (±SD)	78.21 ± 30.79	112.09 ± 44.05	<0.001
Blood loss (ml), median (±IQR)	50 (±10)	50 (±50)	0.25
Duration of anal exhaust (hours) (±SD)	18.80 ± 6.60	36.49 ± 13.71	<0.001
VAS pain score, mean (±IQR)	0 (0-0)	0.5 (0-5)	<0.001
Hospital stay (d), median (±IQR)	2.31 ± 0.69	3.77 ± 1.57	<0.001
Postoperative analgesics use, <i>n</i> (%)	10 (4.39)	20 (15.50)	<0.001
Complications, <i>n</i> (%)	0 (0)	0 (0)	—
Wound infection, <i>n</i> (%)	0 (0)	2 (1.55)	0.13
Readmission after 6 weeks, <i>n</i> (%)	0 (0)	0 (0)	—

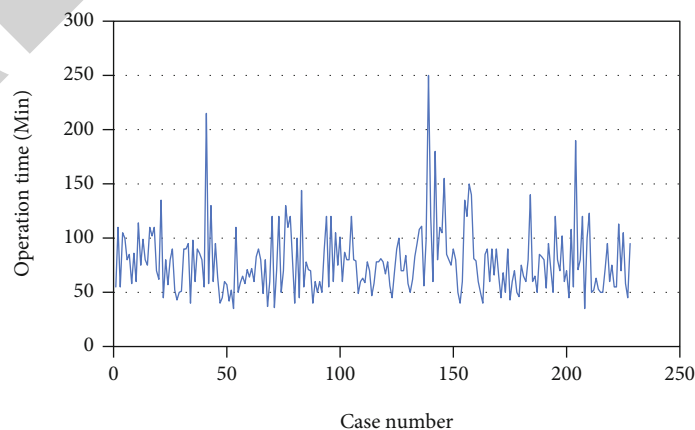


FIGURE 1: Raw operation time (OT) of 228 patients in a chronological order.



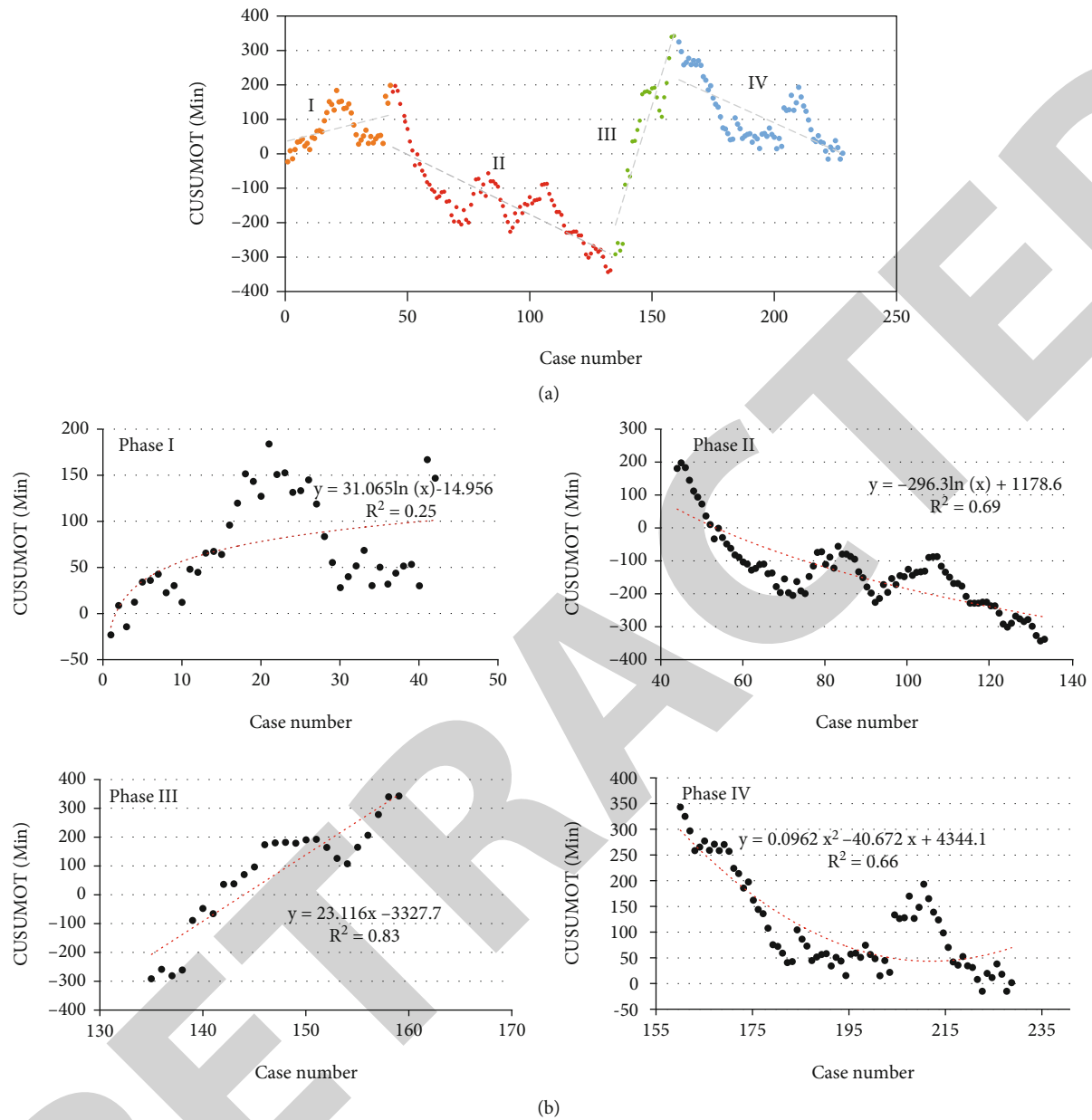


FIGURE 2: (a) The CUSUM<sub>OT</sub> values of operation time in four phases. (b) The best fit curve for each phase.

TABLE 3: Interphase comparison of patient characteristics and postoperative outcomes.

	Phase I (n = 43, cases 1-43)	Phase II (n = 91, cases 44-134)	Phase III (n = 26, cases 135-160)	Phase IV (n = 68, cases 161-228)	P
BMI (kg/m <sup>2</sup> )	24.01 ± 2.74	24.32 ± 3.46	22.57 ± 2.27	24.06 ± 2.93	0.09
Uterine weight (g)	158.92 ± 134.60	195.96 ± 154.25	423.27 ± 338.14	214.30 ± 171.89	<0.001
Operation time (min)	82.81 ± 31.45	72.48 ± 23.66	103.77 ± 45.69	73.18 ± 26.89	<0.001
Blood loss (ml)	50.00 ± 30	50.00 ± 20	50.00 ± 113	50.00 ± 18	0.01*
Postoperative stay (days)	2.23 ± 0.43	2.52 ± 0.94	2.20 ± 0.41	2.14 ± 0.43	0.12

\*There was significant difference between phases I, II, III, and phase IV.

after the procedure. Further, VNOTES had an outstanding cosmetic result since it created no apparent wound. Most patients in the VNOTES group expressed their satisfaction

of this technique when they were followed up in the outpatient clinic. In summary, VNOTES provided a more minimal invasive procedure for women to undergo hysterectomy.

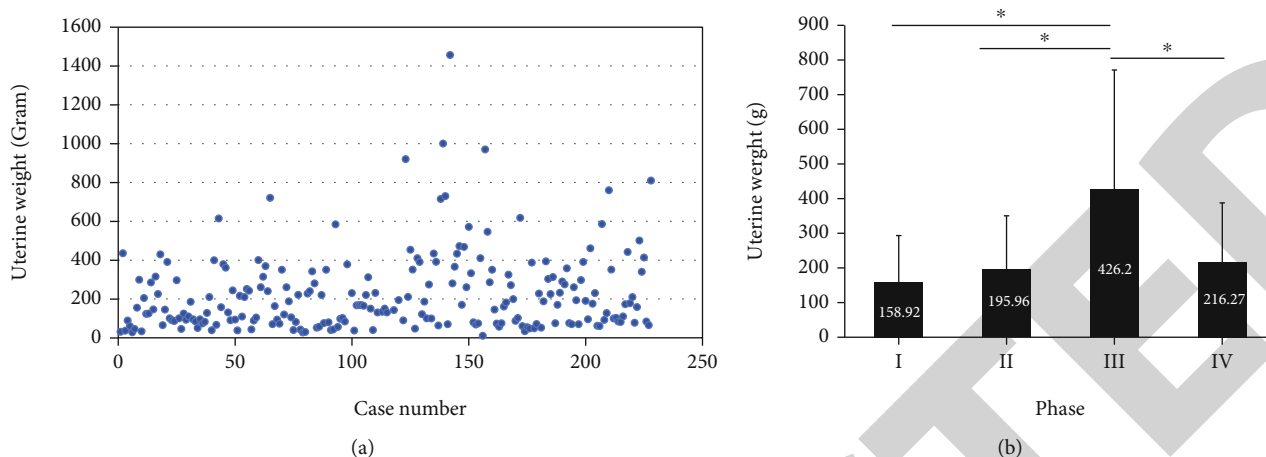


FIGURE 3: (a) Graph of raw uterine weight plotted against a chronological case number (228 consecutive patients). (b) The average uterine weight in four phases.

Four cases in the VNOTES groups were converted to the LESS technique. Large uterine size is reported to have a significant effect on operative time and blood loss [13, 14], and the prior intra-abdominal procedures might contribute to adhesions, which would be challenging to successfully perform the hysterectomy especially for VNOTES and thus increased blood loss and operative time [15, 16], which was corresponding to our findings. We assumed our 4 failures may be contributed to the position of the fibroid and the pelvic adhesion. In one case, a 12-centimeter fibroid grew into right broad ligament and grew caudally to the cervix, which resulted in obstruction in the route to the abdominal cavity. In another case, who had a prior abdominal surgery, it was not easy to separate the vesical peritoneal reflection because of the firm adhesion and therefore caused a failure of entrance into the abdominal cavity.

Due to its feasibility and applicability, we evaluated the learning curve of the VNOTES technique. In phase I, which was the initial stage, it took 43 cases to acquire the basic skill in completing VNOTES with or without adnexectomy. In phase II, the phase of commanding the technique, 91 cases were needed to solidate the technique. In our study, the surgeon practiced 134 cases to fully master the new technique. Therefore, in phase III, the surgeon built up the confidence and tried to perform the surgery in more challenging cases, in which uterine weight was much heavier than the other three phases and two failures happened during this phase. An increasing operation time and blood loss were seen in this phase. This indicated that VNOTES for large uterine might not be so efficient for uterine weight of around 430 g or less. In phase IV, the postlearning phase, the surgeon had achieved proficiency in uterine with normal weight and showed a good command of the technique. In our study, we suggested that increasing operation time might be associated with heavier uterine weight, which implied it of great importance to evaluate the uterine volume before the surgery.

Inevitably, our study had several limitations. Our study was a single-center trial in one teaching hospital and all the operations were performed by one expert gynecologist, which

might result in limitations in the generality of some findings. A multicenter trial involving more gynecologists needs to be conducted to reconfirm the findings. LESS was proved to achieve a lower pain score faster than CMPL [17]. In 1989, laparoscopic technique was introduced into this operation, which changed the surgical approach and concept of hysterectomy [18]. A lot of changes have taken place in laparoscopic technique. In our study, we evaluated the postoperative pain score. Further study could be conducted to find out if the VNOTES group could achieve a lower pain score faster than LESS and whether it could be equally efficient in large uterine.

## 5. Conclusion

VNOTES, a combination of VH and LESS, could be a new minimal invasive procedure for hysterectomy. VNOTES allows patients to have a faster recovery from surgery and to suffer less pain. In the future, a randomised comparison between VNOTES and VH could be done to assess the effectiveness of both techniques.

## Data Availability

The datasets used and analyzed during the current study are available from the corresponding author on reasonable request.

## Conflicts of Interest

The authors declare that the research was conducted in the absence of any commercial or financial relationships that could be construed as a potential conflict of interest.

## Authors' Contributions

Wei-Hua Lou and Wen Di designed and directed the study; Bin Yan and Hui-Xian Miao conducted the data and wrote the paper. You Wang, Jia-Mu Xu, Xiu-Oing Lu, and Wan-Hong He analyzed the data; all authors read and approved the final manuscript. Bin Yan and Hui-Xian Miao contributed equally to this work.

## Retraction

# Retracted: Study on the Mechanism of Xiaotan Sanjie Recipe in the Treatment of Colon Cancer Based on Network Pharmacology

### BioMed Research International

Received 3 October 2023; Accepted 3 October 2023; Published 4 October 2023

Copyright © 2023 BioMed Research International. This is an open access article distributed under the Creative Commons Attribution License, which permits unrestricted use, distribution, and reproduction in any medium, provided the original work is properly cited.

This article has been retracted by Hindawi following an investigation undertaken by the publisher [1]. This investigation has uncovered evidence of one or more of the following indicators of systematic manipulation of the publication process:

- (1) Discrepancies in scope
- (2) Discrepancies in the description of the research reported
- (3) Discrepancies between the availability of data and the research described
- (4) Inappropriate citations
- (5) Incoherent, meaningless and/or irrelevant content included in the article
- (6) Peer-review manipulation

The presence of these indicators undermines our confidence in the integrity of the article's content and we cannot, therefore, vouch for its reliability. Please note that this notice is intended solely to alert readers that the content of this article is unreliable. We have not investigated whether authors were aware of or involved in the systematic manipulation of the publication process.

Wiley and Hindawi regrets that the usual quality checks did not identify these issues before publication and have since put additional measures in place to safeguard research integrity.

We wish to credit our own Research Integrity and Research Publishing teams and anonymous and named external researchers and research integrity experts for contributing to this investigation.

The corresponding author, as the representative of all authors, has been given the opportunity to register their agreement or disagreement to this retraction. We have kept a record of any response received.

### References

- [1] X. Wang, C. Zhang, and M. Ye, "Study on the Mechanism of Xiaotan Sanjie Recipe in the Treatment of Colon Cancer Based on Network Pharmacology," *BioMed Research International*, vol. 2022, Article ID 9498109, 9 pages, 2022.

## Research Article

# Study on the Mechanism of Xiaotan Sanjie Recipe in the Treatment of Colon Cancer Based on Network Pharmacology

Xiao-wei Wang , Ci-an Zhang, and Min Ye 

Department of Traditional Chinese Medicine, Changzheng Hospital, Second Military Medical University, Shanghai 200003, China

Correspondence should be addressed to Min Ye; 13564643706@163.com

Received 28 June 2022; Revised 13 July 2022; Accepted 19 July 2022; Published 5 August 2022

Academic Editor: Dinesh Rokaya

Copyright © 2022 Xiao-wei Wang et al. This is an open access article distributed under the Creative Commons Attribution License, which permits unrestricted use, distribution, and reproduction in any medium, provided the original work is properly cited.

The aim of the study is to investigate the mechanism of action of Disulfiram against colon cancer through a network pharmacology approach. The targets were then imported into the Cytoscape 3.7.2 software to construct a network of active ingredient targets and were imported into the STRING database to construct a protein-protein interaction (PPI) network, and the Bisogenet plug-in in Cytoscape 3.7.2 was used for network topology analysis. Gene ontology (GO) enrichment analysis and Kyoto Encyclopedia of Genes and Genomes (KEGG) enrichment analysis were performed on the potential targets of Yiqi and Baiyu Tang for colon cancer using the R-language Bioconductor platform, and the results were imported into Cytoscape 3.7.2 to obtain KEGG network relationship maps. Molecular docking software Autodock Vina was used to map the core targets to the active ingredients. A total of 119 chemical components and 694 disease targets were obtained, including 113 intersecting targets. The key targets included AKT1 and TP53, and GO functional analysis mainly related to ubiquitination and apoptosis, etc. KEGG analysis showed that the treatment of colon cancer with Ganchenzan mainly acted through cancer-related signaling pathways such as AGE-RAGE and P13K-Akt, and the molecular docking results showed the best binding performance with TP53.

## 1. Introduction

Colon cancer is the fourth leading cause of cancer-related deaths in the world. In symptomatic patients, 60%–70% of confirmed cases are found in the late stage of the disease [1]. At present, the treatment of colon cancer is a comprehensive treatment method led by surgery and supplemented by chemotherapy and radiotherapy [2].

However, the antitumor drugs in chemotherapy inhibit and kill not only tumor cells but also normal cells [3]. Therefore, efficient and low toxicity antitumor drugs are urgently needed. Medicine Food Homology Species demonstrate critical, low toxicity antitumor properties with prospective applications in tumor treatment. The study is aimed at providing theoretical support for the development and utilization of these low toxicity, plant-based drugs.

Network pharmacology is one of the achievements of big data research. Different from traditional single component

and single target thinking, its multicomponent, multitarget, and multichannel network building thinking is more suitable for the complex characteristics of traditional Chinese medicine compound. Networked pharmacology, as a new method, provides a lot of information about compounds, targets, diseases, etc., for pharmacological research of unique Chinese drugs and compounds. It can analyze the mechanism of action of traditional Chinese drugs from the perspective of modern pharmacology and also provide help for the research and development of new Chinese drugs and new dosage forms. At the same time, the network pharmacological method can be used to demonstrate the general concept, differentiation and treatment of the syndrome, different treatments for the same disease, and the same treatment for different diseases in the theory of traditional Chinese medicine, so as to provide data support for accurate medical treatment of traditional Chinese medicine. It can also demonstrate the compatibility theory of monarch,

minister, assistant, drug pair, mutual requirement, mutual assistance, mutual assistance, etc., and clarify the role and changes of drug toxicity in prescription due to compatibility.

Xiaotan Sanjie Recipe (*Pinellia ternata*, Nan-xing, Tianlong, *Scorpio*, tangerine peel, *Galleria Gigerris Endothelium Corneum*, and Zhi Gan Cao) has been Professor Wei Pinkang's empirical prescription for treating gastrointestinal (GI) tumors for more than 40 years. Preliminary clinical studies show that Xiaotan Sanjie Recipe can effectively improve the card score in patients with advanced GI tumors and prolong the survival time [4]. Some studies have found that Xiaotan Sanjie Recipe can inhibit the proliferation of human colorectal cancer HCT116 cells by promoting cell apoptosis in the tumor cells [5]. Xiaotan Sanjie Recipe was found to inhibit the proliferation of colon cancer stem cells, block the cell cycle and induce apoptosis *in vitro*, and inhibit the growth of colon cancer stem cells that are transplanted as tumors *in vivo*. Tumor-bearing mice subjected to high doses of the recipe showed prolonged survival time and improved survival rate. *In vivo* and *in vitro* settings show that the recipe can significantly inhibit the Wnt/ $\beta$ -catenin pathway and downregulate the transcription of target genes and, thereby, the expression of some colon cancer stem cell markers. The upstream regulation mechanism leading to inhibition of pathway activity may follow either of the two mechanisms: The first is caused by inhibition of AKT activity, activation of GSK-3 $\beta$  function, and degradation of  $\beta$ -catenin; the second mechanism likely involves widely downregulating the expression of receptors and ligands that upregulate the Wnt/ $\beta$ -catenin pathway, thereby reducing pathway receptor-ligand response [6, 7]. Although the active components of Xiaotan Sanjie Recipe have been extensively studied, there are few studies on the traditional Chinese medicine (TCM) compound Danshen Decoction.

## 2. Materials and Methods

**2.1. Screening of Target Components of Xiaotan Sanjie Recipe.** TCMSP and TCMID, the pharmacological platforms of the TCM system, enabled finding the active chemical components of the Xiaotan Sanjie Recipe (*Pinellia ternata*, Nan-xing, Tianlong, *Scorpio*, tangerine peel, *Galleria Gigerris Endothelium Corneum*, and Zhi Gan Cao). TCMSP is set with oral bioavailability (OB)  $\geq 30\%$  and druglikeness (DL)  $\geq 0.18$  for screening [5]; TCMID is screened in Swiss adme. Per the screening conditions, GI absorption during pharmacological treatment was high, and more than two parameters in druglikeness were rated as "yes." The ineffective components were removed, and the active components of TCM in the Xiaotan Sanjie Recipe are obtained. Potential protein targets are obtained through the Swiss target prediction database, and the screening condition was set at probability  $\geq 0.1$ . The screened protein targets, like the protein game, were converted into standardized gene names in the UniProt database.

**2.2. Screening of Colon Cancer-Related Targets.** OMIM and GeneCards databases were searched to identify the target genes related to colon cancer using the keyword "colon

cancer." Multiple target genes were retrieved from the GeneCards database. Targets were filtered per the score value: the higher the score, the stronger the correlation between the target and the disease.

**2.3. Acquisition of Effective Targets and Drawing of the Venn Diagram.** A Venn diagram was drawn to determine the intersection of the Xiaotan Sanjie Recipe targets and colon cancer targets. The targets in the intersection were identified as effective targets of Xiaotan Sanjie Recipe in colon cancer treatment.

**2.4. Construction and Analysis of Active Component-Effective Target Network.** The active ingredients from the Xiaotan Sanjie Recipe and the identified effective target genes were introduced into the Cytoscape 3.7.2 [6] software and the drug active component-effective target network diagram was obtained.

**2.5. Construction of Protein Network.** The effective targets of the Xiaotan Sanjie Recipe and colon cancer were imported into the STRING database to construct a protein interaction network. Data with reliability  $\geq 0.900$  were imported into the Cytoscape 3.7.2 software in tsv format for visual analysis, and protein-protein interaction (PPI) data were extracted using R programming. Connection points of core genes were identified, and a histogram of the first 30 core genes was drawn.

**2.6. Enrichment Analysis of Target Function and Pathway.** The R software (<https://www.r-project.org/>) and its background object database <https://org.hs.eg/db> were assessed to obtain the gene ID (entrezID) of potential action targets, and then, the program packages of DOSE, clusterProfiler, and path view accessed using the Bioconductor open-source software were used to conduct gene ontology (GO) function enrichment analysis on the identified potential active targets, which included the following three functions: biological process (BP), cellular component (CC), and molecular function (MF). *P* value and *q* value cutoffs were set at 0.05. Each category was sorted according to its significance, and the top 10 enrichment items were displayed in the form of a histogram and bubble chart.

**2.7. Docking of the Main Active Ingredients and Target Molecules of Xiaotan Sanjie Recipe.** The targets of Xiaotan Sanjie Recipe on colon cancer were searched the PDB database saved in the pdb format. The ligands were stored in mol2 format with the top 2 compounds after topological analysis (degree value). The potential targets Xiaotan Sanjie Recipe colon cancer were connected with the main compounds in Xiaotan Sanjie Recipe by AutoDockTools-1.5.6.

## 3. Results

**3.1. Acquisition of Active Components and Related Targets of Xiaotan Sanjie Recipe.** Taking screening conditions as OB  $\geq 30\%$  and DL  $\geq 0.18$ , GI absorption  $\geq$  two yes in DL, and 119 active components in the phlegm powder were



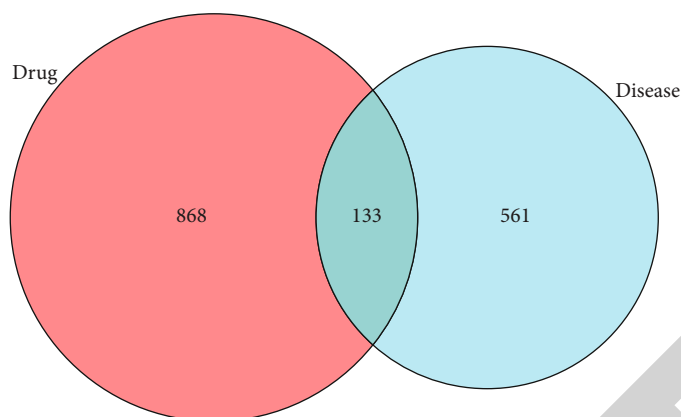


FIGURE 1: Venn diagram of intersection target of Xiaotan Sanjie Recipe and colon cancer.

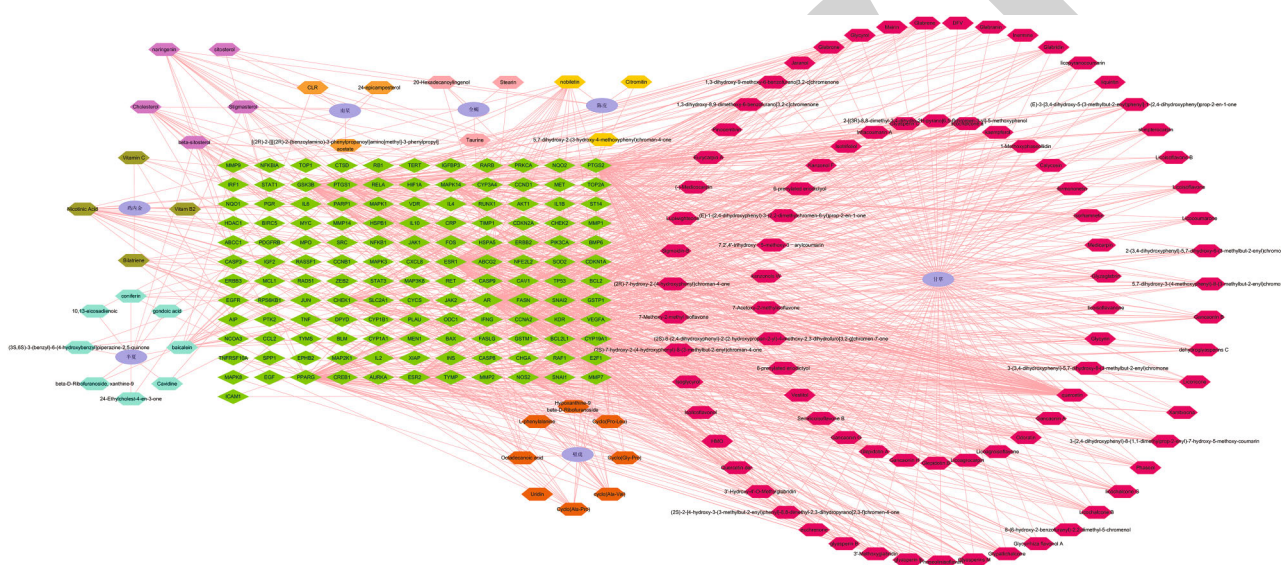


FIGURE 2: Active component-effective target network diagram of Xiaotan Sanjie Recipe.

eliminated. 1001 TCM targets were retrieved by TCMSP and TCMID (see Table S1 for active components).

**3.2. Acquisition of Colon Cancer-Related Targets.** The disease-related genes were obtained from GeneCards and OMIM databases. Targets with a score greater than the median were considered potential targets for disease treatment. Combined with the relevant targets retrieved from the OMIM database, the duplicate values were deleted after merging, and finally, 694 colon cancer-related targets were obtained.

**3.3. Venn Drawing.** Using the Venn tool in TBtools, the intersection of Xiaotan Sanjie Recipe target and colon cancer target was obtained, and 133 intersection targets were obtained. The results are shown in Figure 1.

**3.4. Construction of an Active Component-Effective Target Network Diagram of Xiaotan Sanjie Recipe.** Cytoscape 3.7.2 was used to construct the active component and effective target network of Xiaotan Sanjie Recipe, as shown in Figure 2. The network topology parameters of Xiaotan Sanjie

Recipe in the treatment of colon cancer were calculated by the software to evaluate the importance of the active components and effective targets. The results showed that quercetin, gingerol, nicotinic acid, and other active components of the recipe can act on multiple targets. These components may be the main active components of Xiaotan Sanjie Recipe in the treatment of colon cancer.

**3.5. Construction of Protein Network.** Use Venn tool in TBtools to intersect the target between Xiaotan Sanjie Recipe targets and colon cancer, as shown in Figure 1. Upload the intersection target to STRING database, set the confidence level  $\geq 0.9$ , and obtain the PPI network diagram of the target. Import the data into Cytoscape 3.7.2 to draw the protein network diagram. The bigger the node, the greater the corresponding degree value. According to the degree value, judge the location in the network. According to Figure 3, the targets in the center of the network are TP53, AKT1, Myc, etc.

**3.6. Enrichment Analysis Results of Target Function and Pathway.** Using the R software, GO annotation of effective targets was analyzed to select the top 20 results among BP,



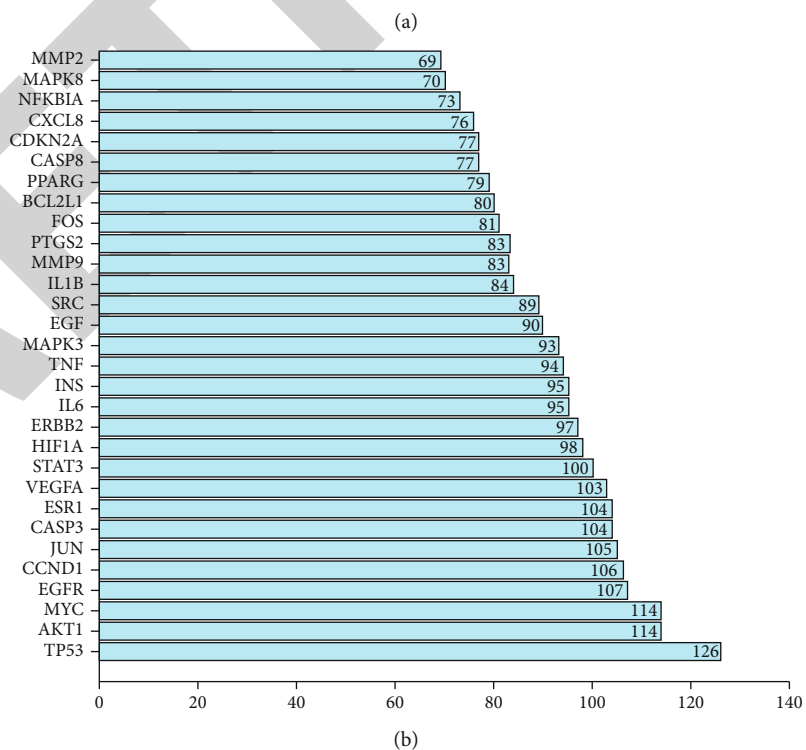
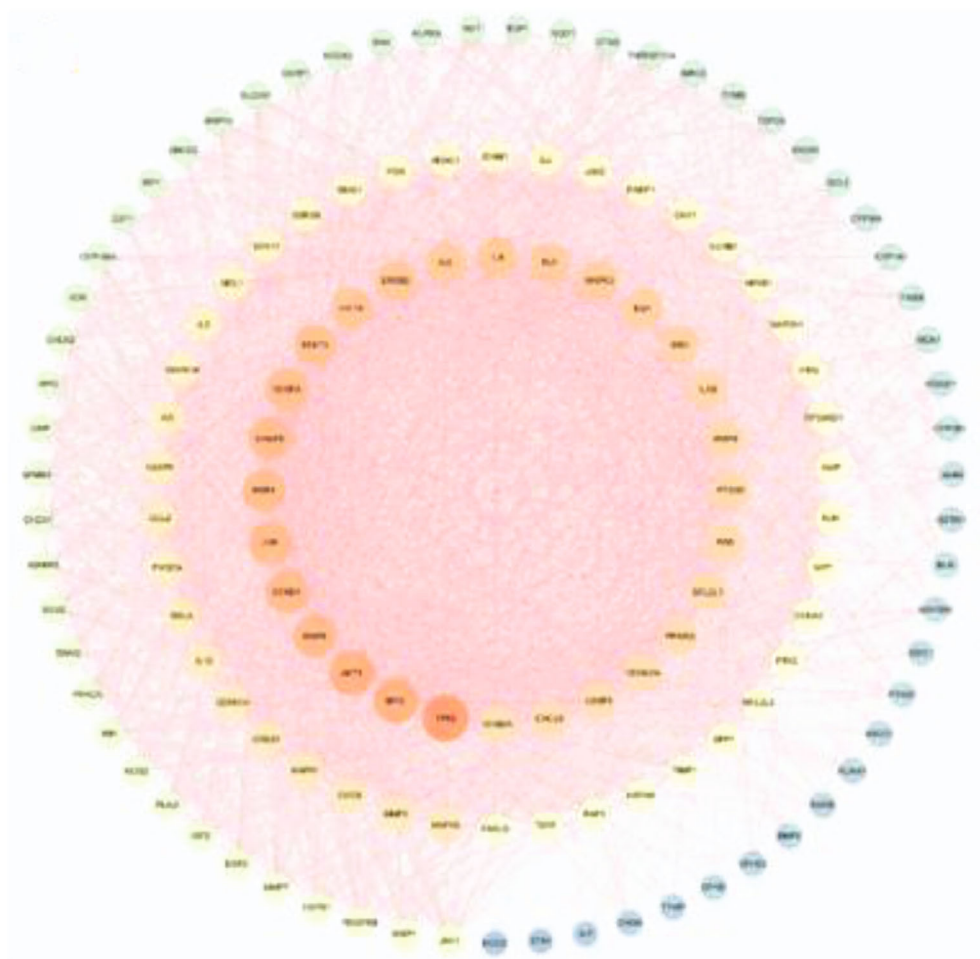
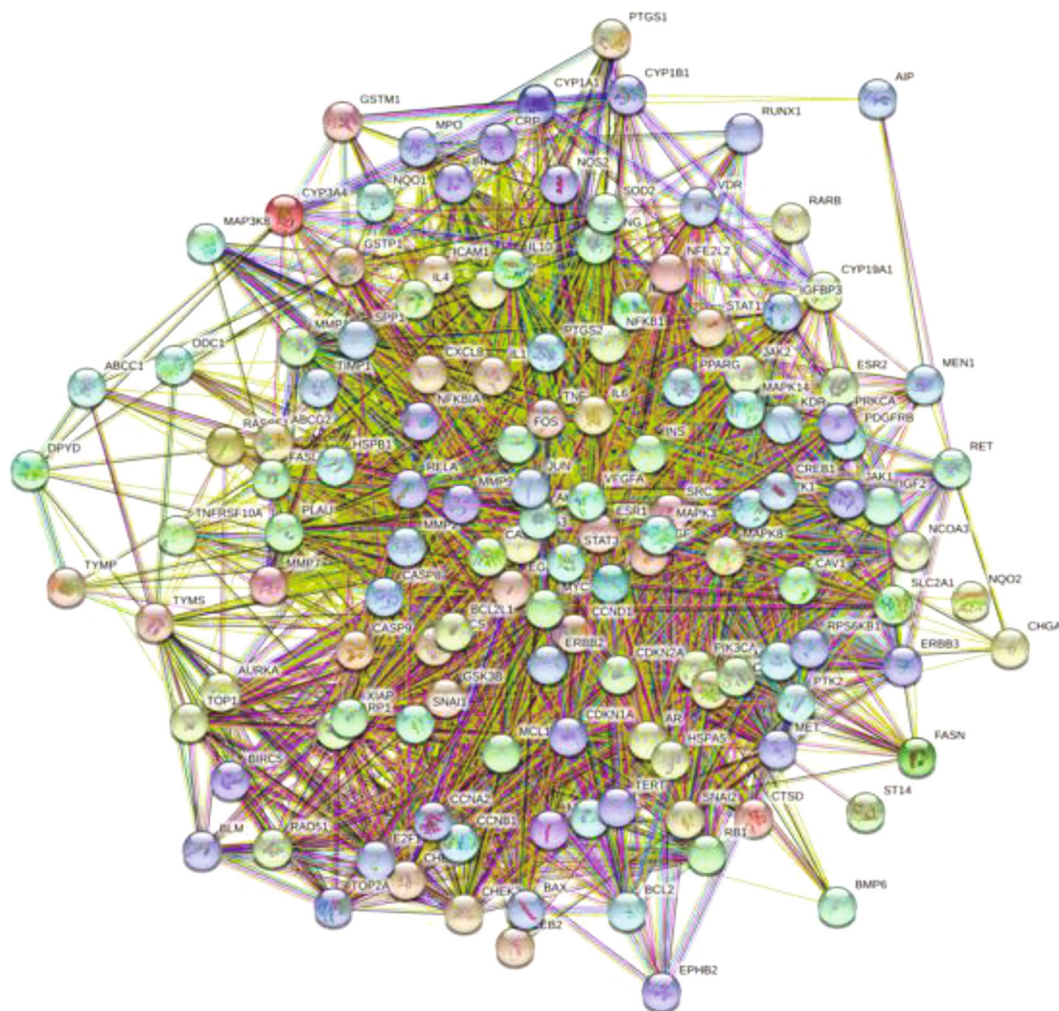


FIGURE 3: Continued.



(c)

FIGURE 3: Target intersection and PPI network diagram: (a) PPI network diagram; (b) core gene map; (c) protein interaction diagram.

CC, and MF, respectively. BP enriched by these targets was mainly related to cellular oxidative stress, apoptosis signal, reproductive structure development, steroid hormones, and so on. MF mainly involved ubiquitinated protein ligase binding, cytokine corresponding binding, transcription factor complex, etc. CC mainly involved nuclear chromatin, membrane raft, and micromembrane area. These results are shown in Figure 4(a). KEGG database enabled to enrichment and analysis of 174 signal pathways, including the AGE-RAGE signaling pathway, TNF signaling pathway, P13K-AKT, and IL-17. The first 20 pathways were selected for visualization. These results are shown in Figure 4(b).

**3.7. Molecular Docking Results of Active Components of Xiaotan Sanjie Recipe.** After topological analysis and calculation, the main compounds of the Xiaotan Sanjie Recipe were obtained. The potential targets and main compounds of Xiaotan Sanjie Recipe acting on colon cancer were docked using AutoDockTools-1.5.6. Greater stability in the conformation of the ligand and receptor binding was predicted to have a greater probability of drug action. Per the degree

value, the top two key targets were found to be serine/threonine kinase (AKT1) and TP53 tumor protein (TP53). Using AutoDock Vina for molecular docking of the components, the following results were observed between ligand small molecules and receptor proteins: binding energy < -4.25 kcal/mol suggested a certain binding activity; binding energy < -5.0 kcal/mol shows good binding activity; binding energy < -7.0 kcal/mol indicates strong binding activity [8]. The binding energies of quercetin and gingerol to the core target were found to be -7.7 and -4.6 kcal/mol, respectively, indicating that the drug recipe has a strong binding activity to the target. The specific docking results are shown in Figure 5.

**4. Discussion**

The number of colon cancer has seen a sharp increase, especially in younger patients, possibly owing to eating habits and lifestyle [9]. About 1 million new cases of colon cancer are annually reported worldwide, and the mortality rate is as high as 40% [10]. Currently, colon cancer treatment involves comprehensive care and is based on surgery.

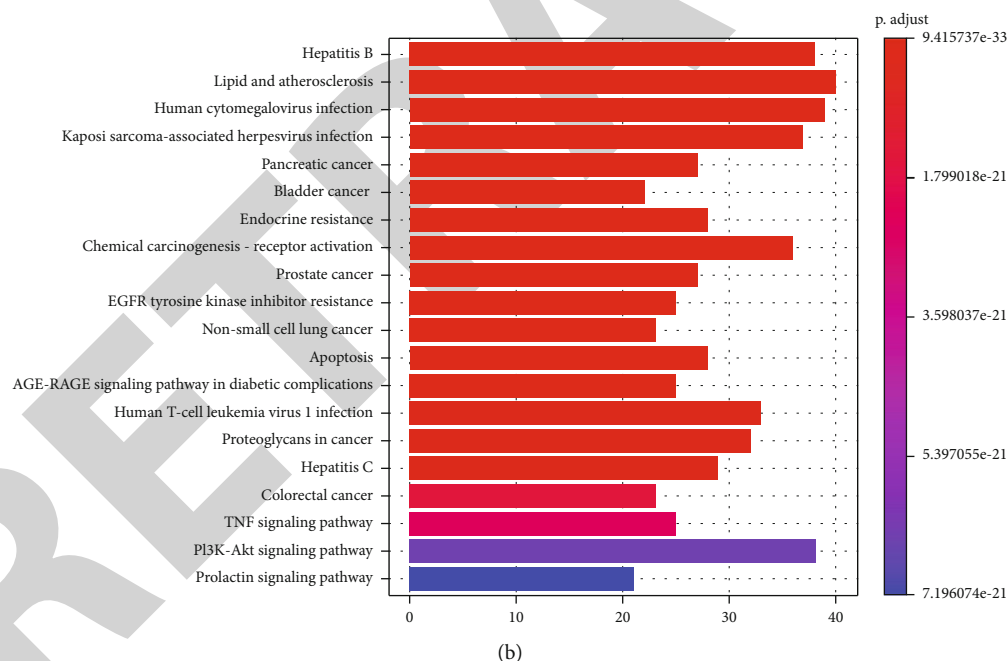
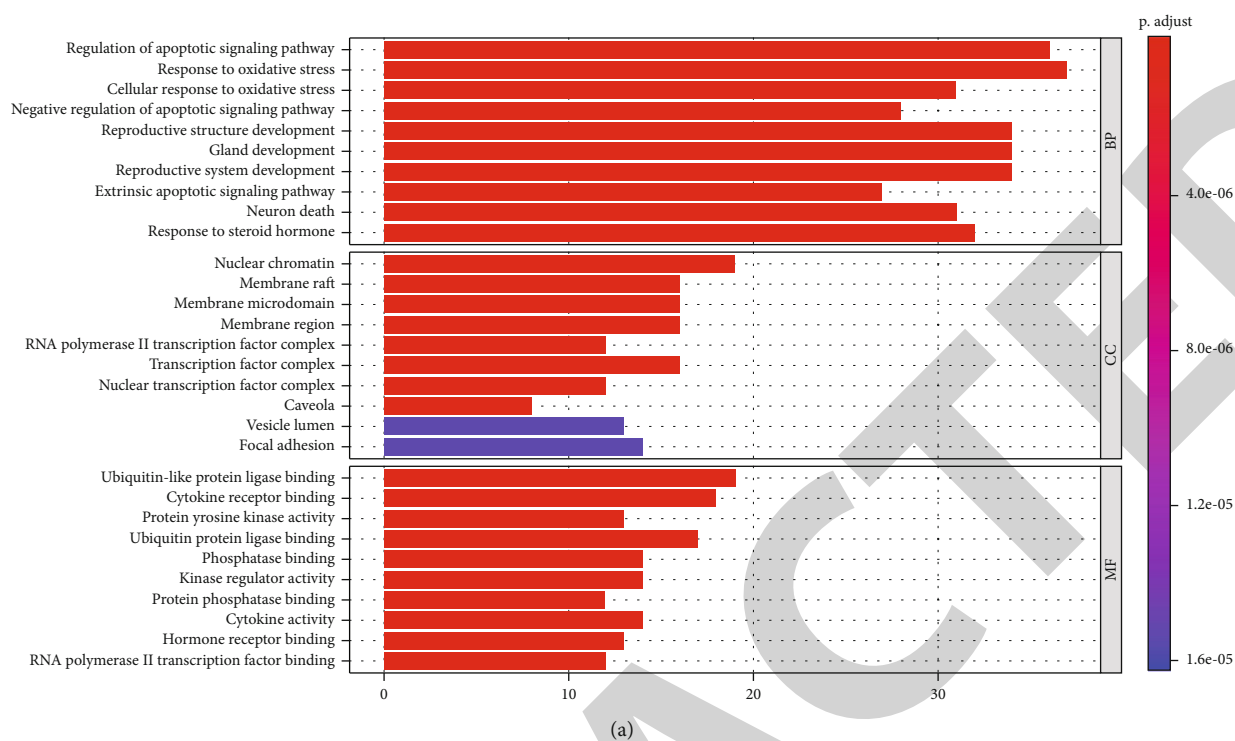


FIGURE 4: Enrichment analysis of Xiaotan Sanjie Recipe in the treatment of colon cancer: (a) GO enrichment analysis; (b) KEGG enrichment analysis.

Developing new, targeted drugs for colon cancer treatment is, therefore, warranted.

Herbal TCMs have shown good tumor curative properties. Active components from Herbal TCMs have been screened for preventing and treating colon cancer and have shown encouraging scientific significance and application prospects [11]. The pathogenesis of colon cancer is not caused by a single target, but rather by multiple targets working cohesively and these targets keep changing based

on the different stages of disease development; this mechanism is aligned with the characteristics and connotation of TCM, i.e., multitarget, multicomponent, and multiregulative [12, 13]. Currently, data mining, network pharmacology, and computer-aided drug design are playing an important role in the modernization of TCM remedies.

In this study, the main active components of Xiaotan Sanjie Recipe in colon cancer treatment were found to be quercetin, kaempferol, and luteolin. Quercetin is a natural

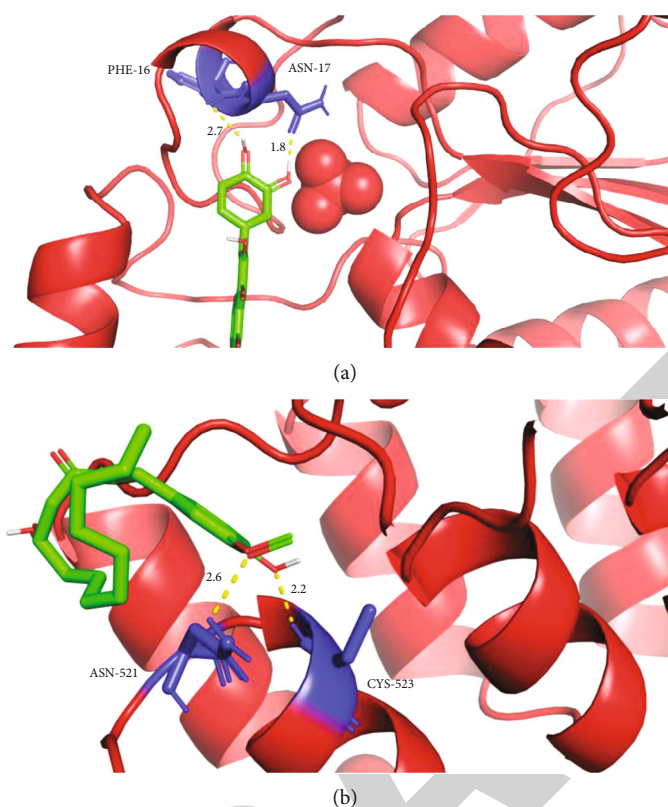


FIGURE 5: Molecular docking mode diagram: (a) docking diagram of quercetin and TP53; (b) docking diagram of gingerol and AKT1.

small molecule flavonoid. Relevant pharmacological studies have shown that quercetin plays an anticolon cancer role by inducing apoptosis in HCT116 colon cancer cells by regulating the Sestrin 2-AMPK-mTOR signal pathway [14]. Kaempferol inhibits the proliferation of human colon cancer SW480 cells by inducing cell cycle arrest and p53-mediated mitochondrial apoptosis pathway [15]. Luteolin has been shown to inhibit colon cancer metastases by inhibiting the proliferation, migration, and epithelial-mesenchymal transformation of colon cancer cell HT-29 [16].

The core proteins determined by PPI were TP53, AKT1, Myc, EGFR, CCND1, JUN, CASP3, STAT3, etc. Among these, AKT1 and AKT2 gene knockout have been shown to reduce metastasis and growth of colon cancer [17].

The KEGG pathway enrichment analysis results showed that the main signal pathways in the treatment of colon cancer using Xiaotan Sanjie Recipe included the cancer pathway, the PI3K-AKT signal pathway, and the apoptotic pathway. PI3K-AKT signaling pathway plays an important role in tumor growth and progression [18, 19]. The overactivation of the PI3K/AKT signaling pathway leads to the decreased expression of tumor suppressor protein p53, leading to increased protein synthesis and tumor cell proliferation and therefore inhibition of cell apoptosis [20]. Tang Jian et al. [21] found that the proliferation of human colon cancer HT-29 cells can be inhibited by inhibiting the PI3K/AKT signaling pathway; this is achieved by inhibiting the downstream expression of the P-glycoprotein transduction pathway and blocking the cell cycle in the G1 phase. Currently, there is limited literature reporting the mechanism

of Xiaotan Sanjie Recipe in the treatment of colon cancer. Some studies have revealed that its mechanism may be related to cell apoptosis. Xiaotan Sanjie decoction inhibits interleukin-8-induced metastatic potency in gastric cancer, blocks the cell cycle, and induces apoptosis *in vitro* [22]. However, other pathways and possible mechanisms of anti-tumor activity need further analysis and experimental verification.

Of course, network pharmacology has many limitations [23]. This is not a simple supplement to the chemical components of traditional Chinese medicine [24]. The content and concentration of traditional Chinese medicine affect the therapeutic effect. The establishment of any theoretical model does not depend on experimental verification, nor does it depend on the laboratory verification of pharmacological research of traditional Chinese medicine network. Ye et al.'s research discusses progress and perspectives in network pharmacology, focusing on the discovery of out-of-target drugs, the identification of disease-associated proteins, and the analysis of the pathway to clarify the relationships between drug targets and disease-associated proteins [25]. Vogt and Mestres's research introduces two approaches to measure the loss of information associated with bipartite network projection. The application to two structurally distinct cases in network pharmacology, namely, bipartite networks target drug and disease gene, confirms that the main determinant of information loss is the degree of vertices omitted during single-party projection [26]. Li et al.'s research highlighted the necessity and proposed the strategies for improving the methodology of conventional network pharmacology [27].



The accuracy and reliability of prediction can only be verified by combining network-based prediction with experimental verification and biological experiment with network pharmacological prediction. Of course, this does not depend on the cooperation and communication between online pharmacology groups.

## 5. Conclusion

In conclusion, using the network pharmacology method, this study preliminarily attempts to predict the possible mechanism of Xiaotan Sanjie Recipe in treating colon cancer. The study also reveals that Xiaotan Sanjie Recipe treats colon cancer from multicomponent, multitarget, and multi-channel mechanisms and provides a basis for further experimental verification and clinical research. There are still some limitations in this study, such as different databases with different targets, which may be missing.

## Data Availability

The datasets used and analyzed during the current study are available from the corresponding author on reasonable request.

## Conflicts of Interest

The authors declared no conflict of interest.

## Acknowledgments

This study was funded by the National Natural Science Foundation of China (81703967).

## Supplementary Materials

In TCMSP and TCMID databases, 119 active components in the phlegm powder were eliminated and were obtained using  $OB \geq 30\%$  and  $DL \geq 0.18$ ; the active components are shown in the Supporting File (Table S1, supporting information). A total of 1001 TCM targets were listed as Table S1 for active components. (*Supplementary Materials*)

## References

- [1] F. Bürtin, C. S. Mullins, M. Linnebacher, C. S. Mullins, and M. Linnebacher, "Mouse models of colorectal cancer: past, present and future perspectives," *World Journal of Gastroenterology*, vol. 26, no. 13, pp. 1394–1426, 2020.
- [2] N. J. McCleary, J. A. Meyerhardt, E. Green et al., "Impact of age on the efficacy of newer adjuvant therapies in patients with stage II/III colon cancer: findings from the ACCENT database," *Journal of Clinical Oncology*, vol. 31, no. 20, pp. 2600–2606, 2013.
- [3] D. Ahmed, N. Graff-Baker Amanda, V. Brooke et al., "Goldfarb Melanie. Neoadjuvant chemotherapy improves survival in patients with clinical T4b colon cancer," *Journal of Gastrointestinal Surgery: Official Journal of the Society for Surgery of the Alimentary Tract*, vol. 22, no. 2, pp. 242–249, 2018.
- [4] G. Qunhao, H. Bo, Z. Xiaodong, J. Jianpeng, L. Long, and W. Pinkang, "Clinical observation on Xiaotan Sanjie formula combined with chemotherapy for 32 cases of advanced gastric cancer," *Journal of Traditional Chinese Medicine*, vol. 54, no. 23, 2013.
- [5] Z. Yu-Qi, M. Ye, C. Lv, and P. Wei, "Effect of Xiaotan Sanjie Recipe on proliferation and apoptosis of HCT116 cell and expression of Caspase3 protein," *Chinese Journal of Information on TCM*, vol. 22, no. 3, 2015.
- [6] Z. Yuqi, Z. Yingcheng, W. Pinkang, and Y. Min, "Study on the effect of Xiaotan Sanjie Recipe on apoptosis of colon cancer stem-like cells and its related mechanism," *China Medical Herald*, vol. 14, no. 24, 2017.
- [7] Z. Yu-Qi, *The role and mechanism of XiaoTanSanJieDecoction in inhibiting the proliferation of colorectal cancer stem cells*, [Ph.D. thesis], 2015.
- [8] K. Y. Hsin, S. Ghosh, and H. Kitano, "Combining machine learning systems and multiple docking simulation packages to improve docking prediction reliability for network pharmacology," *PLoS One*, vol. 8, no. 12, p. e83922, 2013.
- [9] T. Yamada and S. Ohwada, "Scirrhus colon cancer presenting as a pseudokidney sign," *Clinical Case Reports*, vol. 8, no. 12, 2020.
- [10] Q. Wu, W. Jue, Z. Chen, X. Shihao, S. Min, and W. Yugang, "Targeting LncRNA EPIC1 to inhibit human colon cancer cell progression," *Aging*, vol. 12, 2020.
- [11] X. Qingmin and W. Mao, "Anti-tumor effects of traditional Chinese medicine give a promising perspective," *Journal Of Cancer Research and Therapeutics*, vol. 10, no. 5, 2014Supplement 1, 2014.
- [12] Z. Yajie, L. Min, D. Yijiang et al., "Serum microRNA profile in patients with colon adenomas or cancer," *BMC Medical Genomics*, vol. 10, no. 1, pp. 1–9, 2017.
- [13] W. Henri, T. Issa Naiem, W. Byers Stephen, and D. Sivanesan, "Harnessing polypharmacology with computer-aided drug design and systems biology," *Current Pharmaceutical Design*, vol. 22, no. 21, pp. 3097–3108, 2016.
- [14] K. G. Tae, L. S. Hee, and K. Y. Min, "Quercetin regulates Sestrin 2-AMPK-mTOR signaling pathway and induces apoptosis via increased intracellular ROS in HCT116 colon cancer cells," *Journal Of Cancer Prevention*, vol. 18, no. 3, p. 264, 2013.
- [15] J. Zhiliang, Y. Wei, J. Hui, G. Changzheng, and X. Yanhua, "Differential effect of psoralidin in enhancing apoptosis of colon cancer cells via nuclear factor- $\kappa$ B and B-cell lymphoma-2/B-cell lymphoma-2-associated X protein signaling pathways," *Oncology Letters*, vol. 11, no. 1, pp. 267–272, 2016.
- [16] M. Millot, S. Delebassée, B. Liagre, L. Vignaud, V. Sol, and L. Mambu, "Screening of lichen extracts on HT-29 human colon-cancer cells," *Planta Medica*, vol. 80, no. 16, 2014.
- [17] H. S. Sara, C. Mortensen Anja, H. Jakob et al., "Nestor Marika. Different functions of AKT1 and AKT2 in molecular pathways, cell migration and metabolism in colon cancer cells," *International Journal of Oncology*, vol. 50, no. 1, pp. 5–14, 2017.
- [18] L. Yu, W. Jessica, and L. Pengda, "Attacking the PI3K/Akt/mTOR signaling pathway for targeted therapeutic treatment in human cancer," in *Seminars In Cancer Biology*, Academic Press, 2021.
- [19] M. Slomovitz Brian and L. Coleman Robert, "The PI3K/AKT/mTOR pathway as a therapeutic target in endometrial cancer," *Clinical Cancer Research: An official Journal of the American Association for Cancer Research*, vol. 18, no. 21, pp. 5856–5864, 2012.

## *Retraction*

# **Retracted: Hot Air Treatment Elicits Disease Resistance against *Colletotrichum gloeosporioides* and Improves the Quality of Papaya by Metabolomic Profiling**

### **BioMed Research International**

Received 12 November 2022; Accepted 12 November 2022; Published 19 January 2023

Copyright © 2023 BioMed Research International. This is an open access article distributed under the Creative Commons Attribution License, which permits unrestricted use, distribution, and reproduction in any medium, provided the original work is properly cited.

*BioMed Research International* has retracted the article titled “Hot Air Treatment Elicits Disease Resistance against *Colletotrichum gloeosporioides* and Improves the Quality of Papaya by Metabolomic Profiling” [1] due to concerns that the peer review process has been compromised.

Following an investigation conducted by the Hindawi Research Integrity team [2], significant concerns were identified with the peer reviewers assigned to this article; the investigation has concluded that the peer review process was compromised. We therefore can no longer trust the peer review process and the article is being retracted with the agreement of the editorial board.

### **References**

- [1] B. Liu, M. Xue, J. Zhou, H. Zhang, L. Ren, and J. Fan, “Hot Air Treatment Elicits Disease Resistance against *Colletotrichum gloeosporioides* and Improves the Quality of Papaya by Metabolomic Profiling,” *BioMed Research International*, vol. 2022, Article ID 5162845, 13 pages, 2022.
- [2] L. Ferguson, “Advancing Research Integrity Collaboratively and with Vigour,” 2022, <https://www.hindawi.com/post/advancing-research-integrity-collaboratively-and-vigour/>.



## Research Article

# Hot Air Treatment Elicits Disease Resistance against *Colletotrichum gloeosporioides* and Improves the Quality of Papaya by Metabolomic Profiling

Bo Liu,<sup>1,2</sup> Meiling Xue,<sup>1</sup> Jiao Zhou,<sup>3</sup> Hongxia Zhang,<sup>3</sup> Lili Ren <sup>1,4</sup> and Jianting Fan <sup>5</sup>

<sup>1</sup>Institute of Equipment Technology, Chinese Academy of Inspection and Quarantine, Beijing 10029, China

<sup>2</sup>School of Medical Artificial Intelligence, Binzhou Medical University, Yantai, 264003 Shandong, China

<sup>3</sup>Institute of Zoology, Chinese Academy of China, Beijing 100101, China

<sup>4</sup>Science and Technology Research Center of China Customs, Beijing 100026, China

<sup>5</sup>School of Forestry and Biotechnology, Zhejiang A & F University, National Joint Local Engineering Laboratory for High-Efficient Preparation of Biopesticide, Hangzhou, 311300 Zhejiang, China

Correspondence should be addressed to Lili Ren; [renlili@caiq.net.cn](mailto:renlili@caiq.net.cn) and Jianting Fan; [fanjt@zafu.edu.cn](mailto:fanjt@zafu.edu.cn)

Received 2 April 2022; Revised 6 May 2022; Accepted 11 May 2022; Published 3 August 2022

Academic Editor: Dinesh Rokaya

Copyright © 2022 Bo Liu et al. This is an open access article distributed under the Creative Commons Attribution License, which permits unrestricted use, distribution, and reproduction in any medium, provided the original work is properly cited.

Forced air heat treatment could induce defenses to protect fruit from pathogen attacks and has been applied as an alternative to methyl bromide for phytosanitary treatment before exportation. However, few studies were reported on the regulation mechanism of antifungal effect and delayed physiological disorders of papaya by heat treatment. Therefore, we aim to explore the fruit's resistance to pathogens and the inhibition of physiological disorders by metabolomic profiling. In our study, papaya fruits were treated with 47.2°C for 30, 60, and 90 min by forced hot air treatment. The disease resistance against *Colletotrichum gloeosporioides*, quality parameters, and metabolites of papaya fruits were measured during 10 days of storage after heat treatment by metabolomic profiling. Papaya fruits after 30 and 60 min heat treatment had higher firmness, a delayed degreening and yellowing (lower a value) process, and a higher lightness (L) and hue angle (h) during storage. Heat treatment also delayed ripening, inhibiting the growth of *C. gloeosporioides* and softening of papaya. Metabolites and enzymes inhibited ROS scavenging, depressed ABA-regulated respiratory, and activated phenylpropanoid metabolism. Our study provides a broad picture of fruit resistance to pathogens and the inhibition of physiological disorders by metabolomic profiling, which is induced by heat treatment.

## 1. Introduction

Papaya, *Carica papaya* L., is one of the most popular tropical fruits and ranks third with 11.2 million tons in the world and accounts for 15.36% of the total tropical fruit production [1]. It has become an important agricultural export and import product from 60 producing countries, which export nearly 11.2 million tons of papaya fruit from Mexico, Brazil, Belize, and other exporting countries in 2010 [2]. Postharvest diseases especially *Colletotrichum* spp. and quarantine pests, such as mealybugs and fruit flies infesting papaya fruit reduce the commercial value of fruit during storage and impede further exportation to foreign market [3]. Anthrac-

nose disease of papaya caused by *Colletotrichum gloeosporioides* has posed serious problems to commercializing high-quality fruit and causes approximately 40-100% losses during transit, storage, and market in Mexican and many developing countries [2, 4, 5].

Concerned about the risk of chemical residues on fruits, heat treatment (HT) has been used as an alternative and safer technology to replace chemical treatments such as methyl bromide. Heat treatment has been known for a long time as a high level of efficacy and environment-friendly method for fruit decreasing pathogen levels and disease progression [6], inducing the defensive response of the fruit [7], disinfecting quarantine pests [8-10], alleviating chilling

injury and physiological storage disorders [11, 12], and inhibiting fruit ripening [13], thus maintaining fruit quality and prolonging storage [14]. Heat treatments at a temperature ranging from 40 to 60°C also have shown to control diseases [15, 16]. Hot water dip treatment in a 52°C water bath for 2 min could effectively inhibit the germination of blue mold *Penicillium italicum* on pericarp citrus [17]. Heat treatment could improve the antibacterial ability of fruits; however, few studies have revealed the effect of inhibiting physiological disorders and its antibacterial mechanism after HT.

Physical and physiological traits of fruit could be significantly altered after heat treatment that has implications for the changes of consumer acceptance, nutritional quality, and disease resistance. Klein and Lurie reported that prestorage heat treatment at 38°C for 4 d reduced titratable acidity (TA) and respiration and retained firmness in the apple study [18]. 'Waimanalo Solo' papaya showing skin scalding was associated with a reduction of ethylene and TA after heating at 48.5°C over 60 min [19]. HT could suppress post-harvest disease of fruits such as *C. gloeosporioides* on mango and papaya [6, 20], and *Penicillium digitatum* on lemon [21], because of key plant defense-related enzymes, such as phenylalanine ammonia lyase (PAL), peroxidase (POD) and cell wall degradation, and softening-related enzymes such as polygalacturonase (PG) and pectin methylesterase (PME) and the synthesis of metabolites [16, 20]. PG was inhibited, and PME of strawberry was increased by heat treatment at 45°C for 3 h [22]. Phenylpropanoid metabolism in cherry tomato fruit including phenolics and flavonoids, PAL, and cinnamate-4-hydroxylase p-coumaric acid were enhanced related to the reduction of *Alternaria alternata* (black mold) or *Botrytis cinerea* (gray mold) incidence after hot air treatment [7]. Hot water dip treatment at 53°C for 3 min delayed the reduction of SOD in 'Lisbon' lemons and reduced chilling injury compared to the control [23]. Hot air treatment at 48°C for 3 h improved the resistance of Chinese bayberry fruit against green mold rot caused by *L. abietinum*, and the activities of POD were significantly enhanced [24]. In addition, through the ascorbate-gluthathione (AsA-GSH) cycle, ascorbic acid could also impair plant cells from ROS-induced damage by blocking the oxidative chain reaction triggered by ROS [25].

Metabolomics also could help to reveal quality changes and antibacterial mechanism of fruit after heat treatment, which underlies quality phenotypic characteristics in combination with metabolite alterations in response to post-harvest processes [17, 26]. Yun et al. reported that primary metabolic profiling identified 45 detected metabolites. Mostly organic acids and amino acids were regulated in heat-treated pericarp of citrus [17]. In our study, we tested the fungicidal effect of *C. gloeosporioides* in response to HT and investigated heat treatment effect on quality parameters and disease resistance against *C. gloeosporioides* related enzymes of papaya fruit. We determined to adopt the metabolite profiling analysis using HPLC-MS to exhibit heat responses during storage. Our results provide further insights into fruit disease resistance in papaya and shed light on the quality diversity by metabolomics after heat treatment.

## 2. Materials and Methods

**2.1. Materials.** 'Baizhong' papaya fruits were harvested from a commercial orchard of Ledong, Hainan province (N 18°45'; E 109°10'). Fruits were removed from the orchard, held at 20°C overnight after harvest, and transported to our laboratory in Beijing by a refrigerated trailer within 2 days (10°C R.H. 90%). Papaya fruits were selected according to a uniform size and color (90% to 100% yellow), weight (from 700 to 900 g), and absence of external damages [19, 27]. On the third day after harvest, all the papaya fruits were used in our tests.

Strains of *C. gloeosporioides* were purchased from the Query Network for Microbial Species of China and cultured on potato dextrose agar (PDA) at 25°C for 7 d. Spore suspensions were prepared and adjusted to  $1 \times 10^5$  conidia/ml by a hemocytometer.

**2.2. Experiment Design and Heat Treatment.** All tests were designed as two-way factorial arrangements to investigate the quality changes of papaya fruit after heat treatment during storage time. The two factors were heat treatment and storage duration. The fruits were randomly distributed into four treatments: nonheated treatment (CK) and 30, 60, and 90 min heat treatment (HT), respectively. The storage duration treatments were 0, 4, 7, and 10 d in the quality test. After treatment, 38 papaya fruits were randomly picked up in each treatment for quality parameter measurement. A total of 272 papaya fruits were used in our experiments. Heat treatments were heated by forced hot air (HT) at 47.2°C fruit core temperature following periods of 30, 60, and 90 min at 47.2°C hot air treatment chamber (Chongqing well testing instrument Co. Ltd., Chongqing, China). This temperature and time combination can effectively disinfest most invasive fruit flies and is commercially used by USDA. All fruits were placed in plastic bins (48 × 36 × 20 cm) with open lattice bottom and walls. Temperature recorders (JLFX100, Beijing Aerospace Oriental High-tech Development Co. Ltd., Beijing, China) and platinum resistance thermocouples (FK 30-SL, Beijing Aerospace Oriental High-tech Development Co. Ltd., Beijing, China) were used to monitor four fruit center temperatures and the temperature of dry and wet bulb in the chamber. During forced air heat treatment, the airflow rate was set to 1 m/s and a programmable stepped heating process was performed to avoid possible damage of moisture condensation to fruit peel [28–30]. In the first step, the ambient temperature was rising from 30 to 45°C, and relative humidity was rising from 40 to 50%, respectively, within 30 min in the chamber; in the second step, the temperature was rising from 45 to 48°C, and the relative humidity was rising from 50 to 80% within 90 min; in the third step, the temperature was rising to 49°C, and the relative humidity was rising from 80 to 90% within 210 min until all the fruit core temperatures reached to 47.2°C [31]. After the fruit's core temperature reached 47.2°C, the treatment time began to record and the treatment duration continued to 30, 60, and 90 min, respectively. The whole heating process lasted less than four hours. After the heat treatment phase, papayas including control fruits were transferred from the chamber

into a 1 l water tank and hydrocooled with 20°C water for 30 min until fruit temperatures fall to less than 30°C [19]. The process of hydro cool was aimed at avoiding the excessive damage to the peel of papaya. All fruits were then air-dried, kept in cartons, and stored in a chamber with a temperature at 20°C and R.H. at 80% chamber (Binder KMF, Germany) until the start of the following quality evaluation experiments.

### 2.3. Methods

**2.3.1. Antifungal Assay of HT.** *C. gloeosporioides* was chosen to evaluate the disease resistance of papaya to fungal infection after heat treatment. Fruit treated by HT before wounding and inoculation. Fruits were randomly assigned to the HT and control groups. The HT group was incubated at core temperature at 47.2°C for 30, 60, and 90 min, while the control group was incubated at 20°C for 12 h. After the incubation period, a uniform lesion (3 mm deep, 4 mm wide) was wounded at the equator of the papaya [17]. Each wound was inoculated with 10  $\mu$ l of the conidial suspension of *C. gloeosporioides*. All fruits were incubated at 20°C and 85–90% relative humidity for 9 d. Disease incidence and lesion diameters were recorded from 4 to 9 d after inoculation according to Yun et al.'s methods [17]. Disease incidence was the percentage of a number of diseases and total number of fruit in this treatment, and lesion diameter was measured for infected wounds only. Eighty fruits were used for fungal inoculation test.

**2.3.2. Quality Parameter Measurement.** Quality changes of papaya after forced hot air treatment were measured and expressed with sensory, physical, and chemical parameters. Physical parameters include the color, firmness, and weight loss, and chemical parameters consisted of the respiration rate, soluble solids content (SSC), titratable acidity (TA), ascorbic acid (AA), enzymes related to cell wall hydrolytic (PG, PME), and plant disease resistance (AOC, SOD, POD, and PAL). Each treatment had five replicates at each measurement. Each treatment of respiration rate test had three replicates. Each treatment of weight loss test was carried out in nine replicates. Colorimeter (CR-10, Konica Minolta, Inc., Tokyo, Japan) was used to measure the fruit color at four equidistant points from the middle of fruit peel on the equator. *L*, *a*, *b*, *c*, and *h* represent lightness, the spectral changes from green to red, the spectral changes from blue to yellow, saturation, and hue of the surface color, respectively. Weight loss was recorded as the percentage of fruit weight at different storage times divided by the initial weight before treatment. Papaya fruits were weighted with an analytical scale (CP224S, Sartorius, Goettingen, Germany).

Respiration rate was measured as CO<sub>2</sub> emission at 20°C in 2 h. Three fruits were weighted before sealing in a 6 l glass jar. Headspace gas in the jar was collected by a syringe (5  $\mu$ l bevel tip, Agilent Technologies, Waldbronn, Germany) through the rubber septum on the glass jar, and then, 2  $\mu$ l sample gas was quickly injected into Agilent 6890 N gas chromatograph (Agilent Technologies, Waldbronn, Germany) with a thermal conductivity detector (TCD) for carbon

dioxide concentration analysis. The column oven was held at 40°C for 3 min and then programmed to raise from 70 to 200°C, with nitrogen as the carrier gas. A Porapak Q column (Agilent Technologies, Waldbronn, Germany) was used. Quantization data was based on the GC peak area and converted into micrograms of component trapped after calculating micrograms per area count. We also added five different doses of pure CO<sub>2</sub> into syringe with pure N<sub>2</sub>. The standard curve was calculated by the five concentrations of CO<sub>2</sub>, and the levels of CO<sub>2</sub> emission were determined against standards. The respiration rates were calculated by the CO<sub>2</sub> emission and expressed in ml/kg/h [32]. Each sample was tested two times, and each treatment had three replicates.

Fruit pulp was homogenized in a blender and centrifuged at 10,000  $\times$  g for 25 min. The juice was used to test SSC and TA by digital refractometer (GMK-708, G-won HITECH CO LTD, Seoul, South Korea) and saccharometer (GMK-701R, G-won HITECH CO LTD, Seoul, South Korea). Each sample was tested three times, and each treatment had five replicates. After peeling in the middle of a papaya fruit, a manometer probe (TLC 250 N, Food Technology Corporation, USA) was used to put pressure on the test site and test the firmness. The force was recorded at 2.5 mm deformation, and the results were reported in Newtons. Four equidistant points of fruit were recorded, and the average of four points was recorded as a replicate. The process of fruit softening, cell wall solubilization, and membrane breakdown during ripening are highly related to PG and PME [33, 34]. All the chemicals in PG and PME enzyme tests were obtained from Sigma Chemical Co. St. Louis, MO, USA. PG activities were measured by the spectrophotometrically method according to Gross [35] and Chávez-Sánchez et al. [27]. Samples (20 g) were homogenized with 20 ml of 12% polyethylene glycol and 0.2% sodium bisulfite solution (pH 5.0) and centrifuged at 24,000  $\times$  g for 30 min at 4°C. The pellet was washed with distilled water at 4°C, and centrifuged at 5,000  $\times$  g for 30 min. The pellet was held in 20 ml 0.5 mol/l NaCl solution for 30 min and centrifuged at 5,000  $\times$  g for 10 min. The supernatants were used for the enzymatic activity test.

For PG analysis, the supernatants (1 ml) were mixed with 0.8% polygalacturonic acid and 0.4 ml of 0.2 mol/l pH 4.6 sodium acetate buffer and held in a water bath (FK30-SL, Julabo, Germany) at 37°C for 2 h. After 2 h incubated reaction, the solutions were mixed with 0.1 M pH 9 borate buffer and 0.1% 2-cyanoacetamide and immersed in a boiling water bath for 15 min. When the temperature of the sample was reduced to 25°C, the absorbance of the samples was measured at 276 nm. A standard curve of five reducing concentrations from galacturonic acid was also tested as the same methods. The PG activities were expressed as  $\mu$ mol/g at 37°C pH 4.6. Frozen fruit tissue was ground and stored at -80°C to be used.

PME analysis of papaya fruit followed Fayyaz et al.'s [36] and Chávez-Sánchez et al.'s [27] methods. Samples (20 g) were cut by a hole puncher from four parts of papaya and weighted and mixed with 30 ml 2 mol/l NaCl at 4°C by using a tissue homogenizer. The pH of homogenate was adjusted to 7.5 with 0.1 mol/l NaOH or HCl at 4°C. The samples were



centrifuged at 4°C, 24,000×g for 30 min (Eppendorf centrifuge 5417R, Hamburg, Germany). The supernatants were used to analyze the PME following the Hagerman and Austin [37] method using a spectrophotometer (HitachiU-3310, Tokyo, Japan).

Papaya fruits were washed and divided into four parts. Samples (40 g) were cut and weighted by a hole puncher from four parts of papaya and mixed with 20 g of purified water by using a tissue homogenizer (MX-GX1561, Panasonic, Japan). Samples were centrifuged at 15000 rpm for 10 min (Sigma 1-14, Sartorius Sigma, Germany). Ascorbic acid content was determined by 2,6-dichloroindophenol titration method [38].

Samples (0.1 g) were homogenized with 0.1 mol/l potassium phosphate buffer (pH 7-7.4) and carried out at 4°C for AOC, SOD, POD, and PAL activity analyses. These analysis kits of AOC, SOD, POD, and PAL enzymes were purchased from Nanjing Jiancheng Bioengineering Institute.

A standard curve of five reducing concentrations (0.1 to 10 mg/ml) from galacturonic acid was prepared. Both galacturonic acid standards and samples (100 µl) were added to 2 ml of 0.5% citric pectin, 0.5 ml of 0.01% bromothymol blue solution of 3 mmol/l potassium phosphate buffers, and 0.4 ml of distilled water, incubated at room temperature for 5 min, and then, the absorbance was measured at 620 nm. The pH of the mixed solution was adjusted to 7.5 before adding PME enzymatic extract. The PME activities were expressed as µmol/g. AOC activity was determined as described by Vicente et al. and assayed the absorbance at 520 nm [39]. SOD activity was determined by the xanthine-oxidase reaction system producing superoxide anion radicals which can oxidize hydroxylamine to form nitrite. The SOD activity can be quantified by the decrease in absorbance development at 550 nm. POD activity was analyzed by catalyzing hydrogen peroxide reaction and measuring the absorbance at 420 nm [17]. PAL catalyzes the cleavage of phenylalanine into *trans*-cinnamic acid and ammonia. PAL activity was calculated by measuring the absorbance of *trans*-cinnamic acid at 290 nm over a period of 30 min at 30°C.

The freeze-dried samples were crushed with a mixer mill for 60 s at 50 Hz. 20 mg aliquot of individual samples were precisely weighed and were transferred to an Eppendorf tube, after the addition of 500 µl of extract solution (methanol/water = 3 : 1, precooled at -40°C, containing internal standard). After 30 s vortex, the samples were homogenized at 35 Hz for 4 min and sonicated for 5 min in an ice-water bath. Repeat homogenize and sonicate for 3 times. Then, the samples were extracted over night at 4°C on a shaker. Then, centrifuged at 12000 rpm (RCF = 13,800 (× g), R = 8.6 cm) for 15 min at 4°C. The supernatant was carefully filtered through a 0.22 µm microporous membrane, then take 30 µl from each sample and pooling as QC samples, and store at -80°C until the UHPLC-MS analysis.

The UHPLC separation was carried out using an EXIONLC System (SCIEX). The mobile phase A was 0.1% formic acid in water, and the mobile phase B was acetonitrile. The column temperature was set at 40°C. The autosampler temperature was set at 4°C, and the injection volume was 2 µl. A SCIEX QTrap 6500+ (SCIEX Technologies)

was applied for assay development. Typical ion source parameters were as follows: IonSpray voltage: +5500/-4500 V, curtain gas: 35 psi, temperature: 400°C, ion source gas 1: 60 psi, ion source gas 2: 60 psi, and DP: ±100 V.

**2.4. Statistical Analysis.** Significant differences of antifungal activity of HT treatment and quality parameter measurement after heat treatment during storage were separately analyzed using analysis of variance (ANOVA). ANOVA was followed by Tukey's test at the 5% level. Data analyses were performed by Statistical Product and Service Solutions software (SPSS 17.0, IBM Corp, New York). SCIEX Analyst Work Station Software (version 1.6.3) was employed for MRM data acquisition and processing. MS raw data (wiff) files were converted to the TXT format using MSconverter. The in-house R program and database were applied to peak detection and annotation. The metabolomics data was imported to the SIMCA16.0.2 software package (Sartorius Stedim Data Analytics AB, Umea, Sweden) for multivariate analysis. Data were scaled and logarithmically transformed to minimize the impact of both noise and high variance of the variables. After these transformations, PCA (principle component analysis), an unsupervised analysis that reduces the dimension of the data, was carried out to visualize the distribution and the grouping of the samples. 95% confidence interval in the PCA score plot was used as the threshold to identify potential outliers in the dataset. The metabolites with VIP > 1 and  $P < 0.05$  (Student's *t*-test) were considered as significantly changed metabolites. In addition, commercial databases including KEGG (<http://www.genome.jp/kegg/>) and MetaboAnalyst (<http://www.metaboanalyst.ca/>) were used for pathway enrichment analysis.

### 3. Results

**3.1. HT Suppression of *C. gloeosporioides* on Papaya.** Heat treatment effectively inhibited the germination of *C. gloeosporioides* on papaya at 4 d after inoculation (see Figure 1). The disease incidence of HT papaya is significantly reduced by 35%-60% compared with the control treatment ( $F = 21.576$ ,  $df = 3, 16$ ,  $P < 0.05$ ). Lesion diameters were significantly larger in control than the treated treatment (60 min and 90 min from 4 to 9 d) after inoculation ( $P < 0.05$ , see Figure 1(c)). The lesion diameter of papaya that was heat treated (60 min at 8 d) was 16.82 mm, while the lesion diameter of control was 21.49 mm ( $F = 13.986$ ,  $df = 3, 16$ ,  $P < 0.05$ ).

**3.2. Color.** Papaya fruit peel from nonheat treatment turns from green to yellow (increased *a* value and decreased *b* value) during storage. With the increase of the storage period, *L*, *b*, *c*, and *h* values were significantly decreased and only *a* value significantly increased (see Table 1;  $P < 0.01$ ). The highest *b* value showed on the initial day during storage period, and its average was from 43.34 to 53.68. After 10 days of holding at 20°C, nonheated papaya is red peel with a yellow background.

Heated treatment papaya significantly showed delayed darkening (*L*), degreening and yellowing (*a*), and chroma

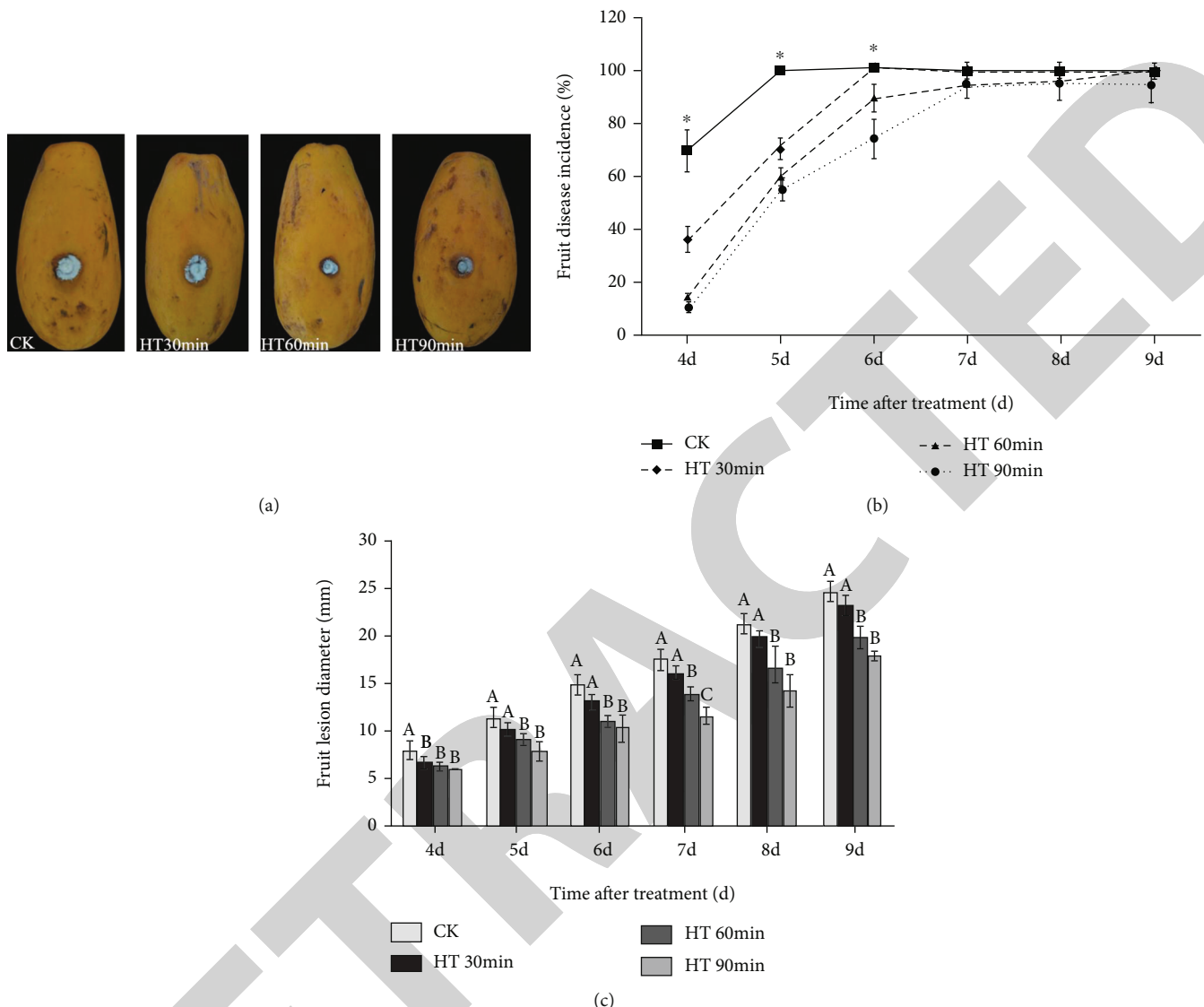


FIGURE 1: Effect of heat treatment on disease development of papayas during storage. (a) Disease incidence of papaya infected by *C. gloeosporioides* on 8<sup>th</sup> day. (b) Fruit disease incidence. (c) Fruit lesion diameter.

and hue change (*h*) processes compared to nonheated papaya. Heated papaya fruits exhibit delayed degreening and yellowing during storage. On the 4th day, *L*, *a*, and *h* values had a significant difference between heated and nonheated papaya ( $P = 0.01$ ). On the 7th day, *h* value in nonheated treatment was notable lower than heated papaya ( $F = 3.87$ ,  $P = 0.03$ ). Similarly, forced hot air (43°C for 220 min) applied to mango fruits significantly affected tristimulus color of the skin and mesocarp including *a*, *b*, and *L* values and slowed down the ripening process. In fresh-cut mangos after hot water treatment, the *L* value could be an indicator of peel browning and the hue angle indicates fruit from yellow to orange-red [40].

3.3. *Weight Loss, Respiration Rate, TA, and SSC.* With the increasing of storage, weight loss was increased ( $P < 0.01$ ). There was no significant difference between the nonheated and heated papaya fruits (see Table 2,  $P > 0.05$ ). Respiration

rate showed at first a slight increase during the first four days of storage and then decreased (see Table 2;  $P < 0.01$ ). Only on the initial day and the 7<sup>th</sup> day, the differences between the heated and nonheated fruits were significant (0 day,  $F = 29.00$ ,  $P < 0.01$ ; 7<sup>th</sup> day,  $F = 5.07$ ,  $P = 0.03$ ). On the initial day, the respiration rate of heated fruits had about 34% reduction compared to nonheated papaya. After removal from heat treatment, respiration of heated papaya was inhibited and then elevated from the 0 to the 4<sup>th</sup> day of storage. Neither heat treatments nor storage time influenced TA and SSC levels (see Table 2;  $P > 0.05$ ), although SSC on the initial day was slightly higher than the SSC level of the other storage time ( $P > 0.05$ ).

3.4. *Firmness, PME, and PG.* The firmness of papaya fruits after 30, 60, and 90 min heat treatment was significantly higher than the nonheated from 4<sup>th</sup> to 10<sup>th</sup> day of storage (see Table 2;  $P < 0.01$ ). PG activity levels were significantly



TABLE 1: Color changes, including *L*, *a*, *b*, *c*, and *h* values of papaya fruits after nonheated and heated treatment during 10 days storage at 20°C.

Parameters	Treatments	Storage period (days)			
		0	4	7	10
L	CK	62.42 ± 0.72 <sup>a</sup>	54.61 ± 0.74 <sup>b</sup>	57.5 ± 0.93 <sup>a</sup>	54.65 ± 1.70 <sup>a</sup>
	HT30min	63.37 ± 0.44 <sup>a</sup>	58.74 ± 1.05 <sup>a</sup>	59.69 ± 0.37 <sup>a</sup>	56.6 ± 0.33 <sup>a</sup>
	HT60min	63.77 ± 0.56 <sup>a</sup>	60.27 ± 0.66 <sup>a</sup>	59.53 ± 1.14 <sup>a</sup>	57.27 ± 1.14 <sup>a</sup>
	HT90min	62.43 ± 0.38 <sup>a</sup>	59.29 ± 1.42 <sup>a</sup>	58.98 ± 1.18 <sup>a</sup>	53.96 ± 1.81 <sup>a</sup>
a	CK	19.37 ± 2.60 <sup>a</sup>	29.44 ± 1.05 <sup>a</sup>	26.76 ± 1.58 <sup>a</sup>	27.33 ± 1.33 <sup>a</sup>
	HT30min	18.81 ± 1.05 <sup>a</sup>	25.33 ± 1.50 <sup>ab</sup>	24.85 ± 1.16 <sup>a</sup>	26.48 ± 1.45 <sup>a</sup>
	HT60min	12.4 ± 3.19 <sup>a</sup>	22.73 ± 1.76 <sup>b</sup>	20.57 ± 2.43 <sup>a</sup>	22.60 ± 2.31 <sup>a</sup>
	HT90min	13.48 ± 2.83 <sup>a</sup>	20.46 ± 1.97 <sup>b</sup>	22.44 ± 2.20 <sup>a</sup>	23.84 ± 2.01 <sup>a</sup>
b	CK	53.68 ± 0.59 <sup>a</sup>	46.1 ± 1.39 <sup>a</sup>	47.96 ± 0.46 <sup>b</sup>	43.34 ± 1.47 <sup>b</sup>
	HT30min	54.75 ± 1.06 <sup>a</sup>	52.60 ± 0.93 <sup>a</sup>	53.43 ± 0.59 <sup>a</sup>	51.41 ± 2.15 <sup>a</sup>
	HT60min	52.82 ± 1.04 <sup>a</sup>	52.02 ± 0.78 <sup>a</sup>	51.36 ± 1.50 <sup>ab</sup>	47.7 ± 1.43 <sup>ab</sup>
	HT90min	51.23 ± 1.17 <sup>a</sup>	51.71 ± 3.11 <sup>a</sup>	51 ± 2.11 <sup>ab</sup>	45.45 ± 2.52 <sup>ab</sup>
c	CK	57.26 ± 1.17 <sup>a</sup>	54.93 ± 1.28 <sup>a</sup>	55.08 ± 0.59 <sup>a</sup>	51.18 ± 1.15 <sup>a</sup>
	HT30min	58.0 ± 1.27 <sup>a</sup>	58.08 ± 1.19 <sup>a</sup>	58.69 ± 0.85 <sup>a</sup>	56.40 ± 1.72 <sup>a</sup>
	HT60min	55.18 ± 1.85 <sup>a</sup>	57.25 ± 1.23 <sup>a</sup>	55.38 ± 1.94 <sup>a</sup>	52.64 ± 2.09 <sup>a</sup>
	HT90min	53.3 ± 1.54 <sup>a</sup>	55.94 ± 2.99 <sup>a</sup>	54.98 ± 1.75 <sup>a</sup>	50.70 ± 2.49 <sup>a</sup>
h	CK	70.35 ± 2.46 <sup>a</sup>	57.40 ± 1.24 <sup>b</sup>	60.49 ± 1.71 <sup>b</sup>	58.08 ± 1.82 <sup>a</sup>
	HT30min	71.05 ± 0.84 <sup>a</sup>	64.37 ± 1.32 <sup>a</sup>	65.09 ± 0.93 <sup>ab</sup>	62.51 ± 0.92 <sup>a</sup>
	HT60min	77.12 ± 3.11 <sup>a</sup>	66.17 ± 1.08 <sup>a</sup>	68.15 ± 2.12 <sup>a</sup>	64.54 ± 2.02 <sup>a</sup>
	HT90min	75.22 ± 2.72 <sup>a</sup>	68.56 ± 2.17 <sup>a</sup>	66.60 ± 1.74 <sup>ab</sup>	62.06 ± 2.09 <sup>a</sup>

Lower case letters (a and b) indicate significantly different means within a row (Tukey test,  $P < 0.05$ ).

decreased on 4<sup>th</sup> and 7<sup>th</sup> day of storage after heat treatment (see Figure 2, 4 days,  $F = 7.23$ ,  $P < 0.05$ ; 7 days,  $F = 14.51$ ,  $P < 0.01$ ). PME from heated treatment fruits had a similar trend during 10 days of storage and significant differences were detected ( $P < 0.01$ ). During the storage, PME from nonheated treatment showed a decreased activity of about 9.90% loss during the first four days of storage and increased to 0.32  $\mu\text{mol/h/g}$  on the 7<sup>th</sup> day of storage ( $F = 11.36$ ,  $P < 0.01$ ). PG of nonheated papaya showed an increased activity of about 1.43-fold in the first 4 days of storage and then decreased to 2.23  $\mu\text{mol/h/g}$  on the 10<sup>th</sup> day ( $F = 6.77$ ,  $P < 0.05$ ).

**3.5. Ascorbic Acid.** With the increasing storage time, it exhibited a decreasing trend of ascorbic acid after heat treatment (nonheated,  $F = 2.17$ ,  $P > 0.05$ ; heated 30 min,  $F = 3.50$ ,  $P = 0.04$ ; heated 60 min and 90 min,  $P < 0.01$ ). In 30 min heat treatment, citric acid on the initial day was 4.27 mg/kg, whereas it dropped to 2.39 mg/kg on the 10<sup>th</sup> day of storage. The significant difference of citric acid between the nonheat and 90 min heat treatments began to appear in the 7<sup>th</sup> day of storage ( $F = 5.57$ ,  $P < 0.01$ ). On the 10<sup>th</sup> day of storage, all citric acid levels of heat treatment papaya were lower than nonheated treatment papaya ( $F = 7.07$ ,  $P < 0.01$ ).

**3.6. Activities of Disease Resistance Enzymes.** The activities of SOD, POD, and PAL enzymes were measured in the control and heat-treated papaya (see Figure 3). SOD activity of control and heat-treated fruits was no significant differences in

first few days after heat treatment, while heat-treated fruit showed significant higher SOD activity than those activities in control between them at 4<sup>th</sup> and 10<sup>th</sup> day (4<sup>th</sup> day  $F = 6.18$ ,  $df = 1, 8$ ,  $P < 0.05$ ; 10<sup>th</sup> day  $F = 14.84$ ,  $df = 1, 8$ ,  $P < 0.05$ ). Increased SOD activity was also found in the heat-treated fruit during storage. POD activity of the heat-treated fruit was significantly higher than controls on the 4<sup>th</sup> and 10<sup>th</sup> days of storage at 20°C (4<sup>th</sup> day  $F = 6.35$ ,  $df = 1, 8$ ,  $P < 0.05$ ; 10<sup>th</sup> day  $F = 17.55$ ,  $df = 1, 8$ ,  $P \leq 0.05$ ). Similarly, PAL activity of the heat-treated fruit was also significantly higher than controls on the 4<sup>th</sup> and 10<sup>th</sup> days of storage (4<sup>th</sup> day  $F = 6.777$ ,  $df = 1, 8$ ,  $P < 0.05$ ; 10<sup>th</sup> day  $F = 20.132$ ,  $df = 1, 8$ ,  $P < 0.05$ ).

**3.7. Overview of the Fruit Metabolomics Profiling in Papaya.** GC-MS was used to analyze the metabolites of papaya after heat treatment. Principal component analysis (PCA) was used to reveal that heat treatment had significant differences in the metabolites of papaya on day 0 and day 10, and the treatment groups could be distinguished ( $R^2 = 0.52$ , see Figure 4). Differential metabolites were selected based on the criteria of VIP (variable importance for the projection) value  $> 1$  and  $P < 0.05$ .

Four groups can be distinguished (different colors). The first component (12.8%) separates each variety and the second component (9.1%) separates the groups with different behavior after treatments.

After heat treatment, a total of 84 metabolic compounds were selected, mainly including carbohydrates, amino acids,

TABLE 2: Firmness, weight loss, respiration rate, TA, SSC, and SSC/TA changes of papaya fruit after nonheated and heated treatment during 10 days storage at 20°C.

Parameters	Treatments	Storage period (days)			
		0	4	7	10
Firmness (N)	CK	4.49 ± 0.46 <sup>a,A</sup>	2.79 ± 0.81 <sup>b,B</sup>	3.06 ± 1.02 <sup>b,B</sup>	2.53 ± 1.34 <sup>b,B</sup>
	HT30min	6.53 ± 1.33 <sup>a,A</sup>	8.71 ± 0.32 <sup>a,A</sup>	8.99 ± 0.70 <sup>a,A</sup>	9.45 ± 0.50 <sup>a,A</sup>
	HT60min	6.44 ± 0.84 <sup>a,A</sup>	8.18 ± 0.79 <sup>a,A</sup>	6.86 ± 0.37 <sup>a,A</sup>	8.28 ± 1.40 <sup>a,A</sup>
	HT90min	7.29 ± 0.55 <sup>a,A</sup>	8.60 ± 0.14 <sup>a,A</sup>	8.79 ± 0.38 <sup>a,A</sup>	9.09 ± 0.14 <sup>a,A</sup>
Weight loss (%)	CK	0.11 ± 0.01 <sup>b,A</sup>	1.73 ± 0.10 <sup>a,A</sup>	1.61 ± 0.14 <sup>a,A</sup>	1.48 ± 0.18 <sup>a,A</sup>
	HT30min	0.11 ± 0.10 <sup>b,A</sup>	2.09 ± 0.10 <sup>a,A</sup>	1.73 ± 0.14 <sup>a,A</sup>	1.66 ± 0.42 <sup>a,A</sup>
	HT60min	0.13 ± 0.01 <sup>a,A</sup>	2.08 ± 0.12 <sup>a,A</sup>	1.68 ± 0.10 <sup>b,A</sup>	1.40 ± 0.13 <sup>b,A</sup>
	HT90min	0.11 ± 0.03 <sup>c,A</sup>	1.97 ± 0.12 <sup>a,A</sup>	1.47 ± 0.10 <sup>b,A</sup>	1.17 ± 0.14 <sup>b,A</sup>
Respiration rate (ml/kg/h)	CK	24.06 ± 0.90 <sup>c,A</sup>	35.23 ± 0.99 <sup>a,B</sup>	21.19 ± 0.59 <sup>b,B</sup>	19.13 ± 1.03 <sup>bc,B</sup>
	HT30min	15.82 ± 0.20 <sup>a,A</sup>	30.07 ± 1.49 <sup>a,A</sup>	18.81 ± 0.84 <sup>a,A</sup>	18.89 ± 0.91 <sup>a,A</sup>
	HT60min	15.74 ± 0.71 <sup>b,AB</sup>	36.17 ± 3.11 <sup>a,B</sup>	21.10 ± 0.61 <sup>b,AB</sup>	18.04 ± 0.30 <sup>b,A</sup>
	HT90min	16.39 ± 0.95 <sup>c,A</sup>	30.94 ± 1.85 <sup>a,A</sup>	22.50 ± 0.65 <sup>b,A</sup>	19.03 ± 0.91 <sup>bc,A</sup>
TA (%)	CK	2.41 ± 0.15 <sup>a,A</sup>	2.60 ± 0.22 <sup>a,A</sup>	2.11 ± 0.23 <sup>a,A</sup>	2.54 ± 0.20 <sup>a,A</sup>
	HT30min	2.38 ± 0.19 <sup>a,A</sup>	2.40 ± 0.08 <sup>a,A</sup>	2.53 ± 0.23 <sup>a,A</sup>	2.67 ± 0.17 <sup>a,A</sup>
	HT60min	2.33 ± 0.12 <sup>a,A</sup>	2.54 ± 0.16 <sup>a,A</sup>	2.66 ± 0.30 <sup>a,A</sup>	2.69 ± 0.14 <sup>a,A</sup>
	HT90min	2.66 ± 0.08 <sup>a,A</sup>	2.74 ± 0.10 <sup>a,A</sup>	2.39 ± 0.19 <sup>a,A</sup>	2.53 ± 0.14 <sup>a,A</sup>
SSC (%)	CK	10.10 ± 0.38 <sup>a,A</sup>	8.48 ± 0.40 <sup>a,A</sup>	8.68 ± 0.28 <sup>a,A</sup>	8.18 ± 0.12 <sup>a,A</sup>
	HT30min	9.30 ± 0.69 <sup>a,A</sup>	8.56 ± 0.19 <sup>a,A</sup>	9.24 ± 0.28 <sup>a,A</sup>	8.78 ± 0.31 <sup>a,A</sup>
	HT60min	9.82 ± 0.73 <sup>a,A</sup>	8.58 ± 0.34 <sup>a,A</sup>	8.10 ± 0.48 <sup>a,A</sup>	7.90 ± 0.40 <sup>a,A</sup>
	HT90min	9.78 ± 0.31 <sup>a,A</sup>	8.20 ± 0.38 <sup>a,A</sup>	8.94 ± 0.54 <sup>a,A</sup>	8.54 ± 0.32 <sup>a,A</sup>
SSC/TA	CK	4.23 ± 0.17 <sup>a,A</sup>	3.92 ± 0.17 <sup>a,A</sup>	4.21 ± 0.24 <sup>a,A</sup>	3.69 ± 0.19 <sup>a,A</sup>
	HT30min	3.39 ± 0.41 <sup>a,A</sup>	3.58 ± 0.15 <sup>a,A</sup>	3.45 ± 0.34 <sup>a,A</sup>	3.03 ± 0.25 <sup>a,A</sup>
	HT60min	4.27 ± 0.40 <sup>a,A</sup>	3.77 ± 0.36 <sup>a,A</sup>	3.31 ± 0.62 <sup>a,A</sup>	3.78 ± 0.28 <sup>a,A</sup>
	HT90min	3.29 ± 0.21 <sup>a,A</sup>	3.32 ± 0.17 <sup>a,A</sup>	2.96 ± 0.17 <sup>a,A</sup>	3.41 ± 0.18 <sup>a,A</sup>

Upper case letters (A and B) indicate significantly different means within a column (Tukey test,  $P < 0.05$ ). Lower case letters (a and b) indicate significantly different means within a row (Tukey test,  $P < 0.05$ ).

and secondary metabolites (see Figure 5). In carbohydrates, the content of D-xylulose and D-maltose increased significantly. Among amino acids, L-alanine, L-phenylalanine, and L-homoglutamic acid was upregulated, while L-arginine was decreased. Nicotinic acid and a vitamin were significantly reduced. Glycerophosphocholine and phosphorylcholine in choline decreased. Among the secondary metabolites, various phenols (benzaldehyde, phloretic acid, and taxiphyllin), 7,8-dihydroxyflavone in flavonoids, and phenethylamine in alkaloids were increased.

On the 10<sup>th</sup> day after heat treatment, 78 metabolites were screened out, mainly including carbohydrates, amino acids and derivatives, lipids, vitamins, and secondary metabolites (see Figure 5). Among carbohydrates, maltotetraose and stachyose were increased significantly. In amino acids and derivatives, the levels of L-phenylalanine and L-glutamic acid were increased, while L-lysine D-glutamine, pyrrolidonecarboxylic acid and L-alanine were decreased. Linolenic acid in lipids was upregulated. Ascorbic acid in vitamins increased significantly. Among the secondary metabolites, abscisic acid, phenols (alpha-tocopherol, eriobofuran, myzodendrone, and p-octopamine), flavonoids (cynaroside, flavone, gallocatechin, karanjin, and puerarin),

coumarins (pteryxin), and alkaloids(indole) were increased significantly.

Normalized values of data are shown on a color scale, which is proportional to the content of each metabolite. SCIEX Analyst Work Station Software (version 1.6.3) was employed for MRM data acquisition and processing.

### 3.8. Pathway Changes Associated with Heat Treatment.

Metabolites VIP (variable importance for the projection) value  $> 1$  and  $P < 0.05$  were selected. According to the pathway analysis of MetaboAnalyst 3.0, 35 metabolic pathways were affected on 0 days after heat treatment and 41 metabolic pathways were affected on 10 days after heat treatment. The pathway impact  $> 0.3$  was analyzed. After heat treatment (0 day), upregulated metabolic pathways included phenylalanine metabolism, phenylalanine, tyrosine and tryptophan biosynthesis metabolism, beta-alanine metabolism, lysine degradation metabolism, glycerophospholipid metabolism, and histidine metabolism. Nicotinate and nicotinamide metabolism pathway was reduced. 10 days after heat treatment, D-glutamine and D-glutamate metabolism; phenylalanine, tyrosine, and tryptophan biosynthesis; phenylalanine metabolism; alpha-linolenic acid metabolism;

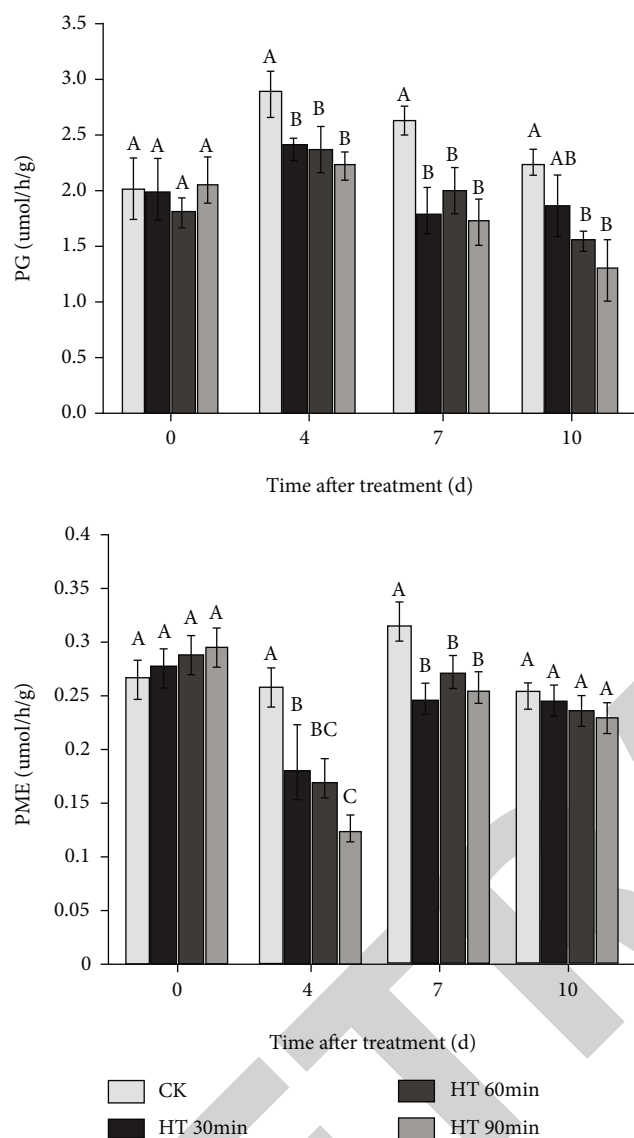


FIGURE 2: PG and PME activity changes of papaya fruit after nonheated and heated treatments during 10 days storage at 20°C. Different lower case letters indicate significantly different between different treatments at  $P < 0.05$ .

alanine, aspartate, and glutamate metabolism; and starch and sucrose metabolism were enhanced. Sphingolipid metabolism was downregulated (see Figure 6).

#### 4. Discussion

HT has an antifungal effect on papaya fruit against *C. gloeosporioides*. Previous studies reported applications of hot water and vapor heat were applied to mango [41, 42]. Disease incidence on mango fruits inoculated with heat treatment at 55°C for 5 min and hot water at 38°C for 5 min combined with vapor heat was reduced by 93% or kept lesion development of *C. gloeosporioides* below 5%. Hot air treatment for phytosanitary treatment of Caribbean fruit flies in mango at 48°C for 2.5 h was reported to control anthracnose [43]. However, these observations were contrary to findings with

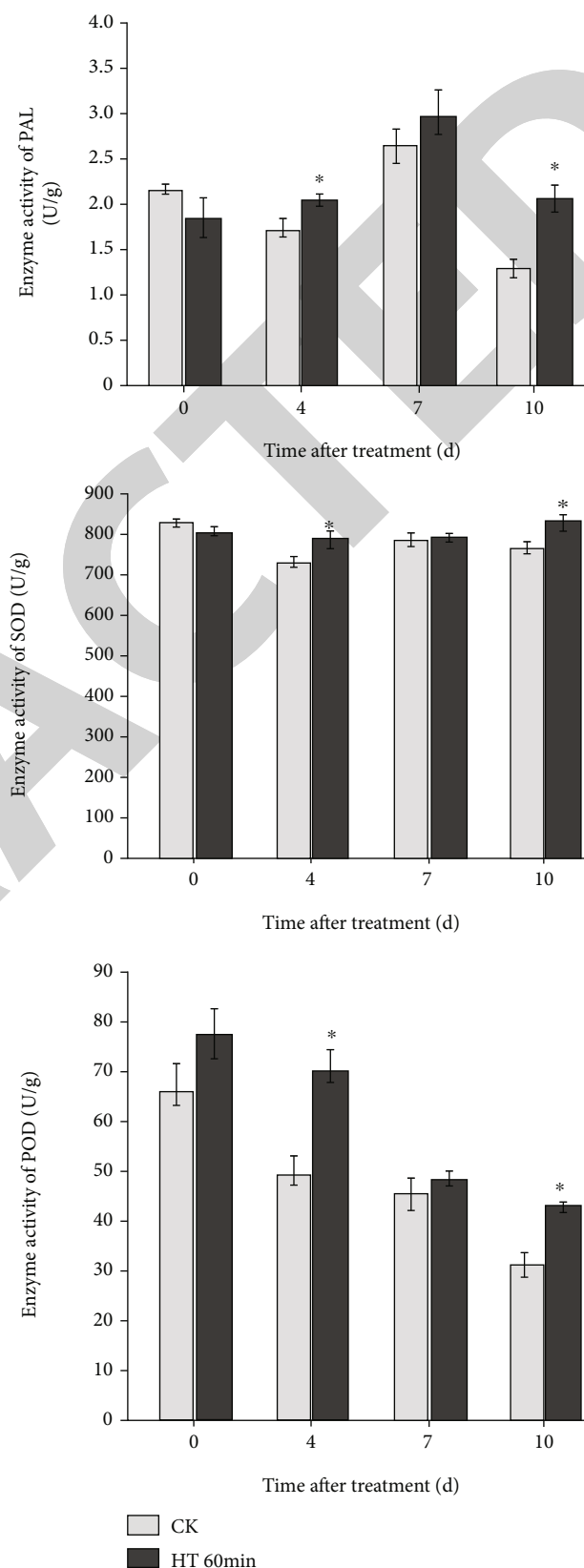


FIGURE 3: SOD, POD, and PAL activity changes of papaya fruit after nonheated and heated treatments during 10 days storage at 20°C. \*Significantly different between nonheated and heated for 60 min at 47.2°C at  $P < 0.05$ .

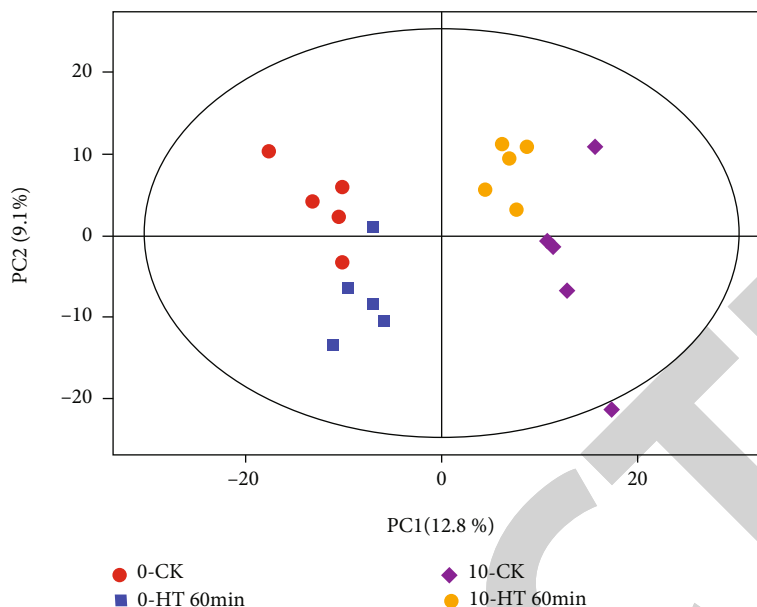


FIGURE 4: Principal component analysis (PCA) of the analyzed metabolites, collected by LC–MS after heat treatment and storage period.

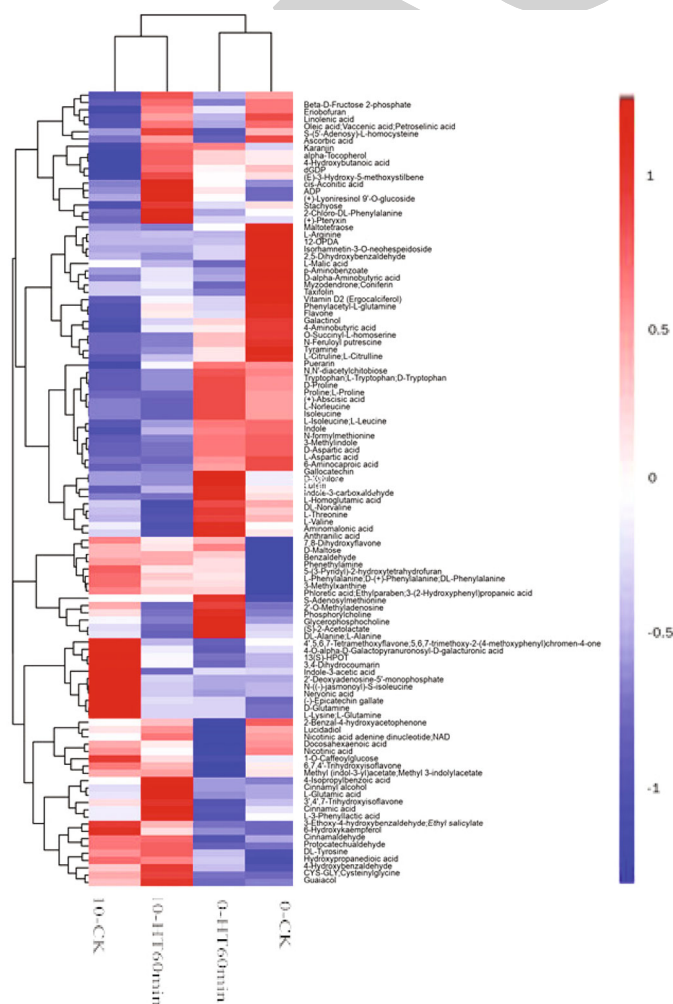


FIGURE 5: Heat map performed with data obtained by GC-MS of the heated and nonheated papaya at storage time.

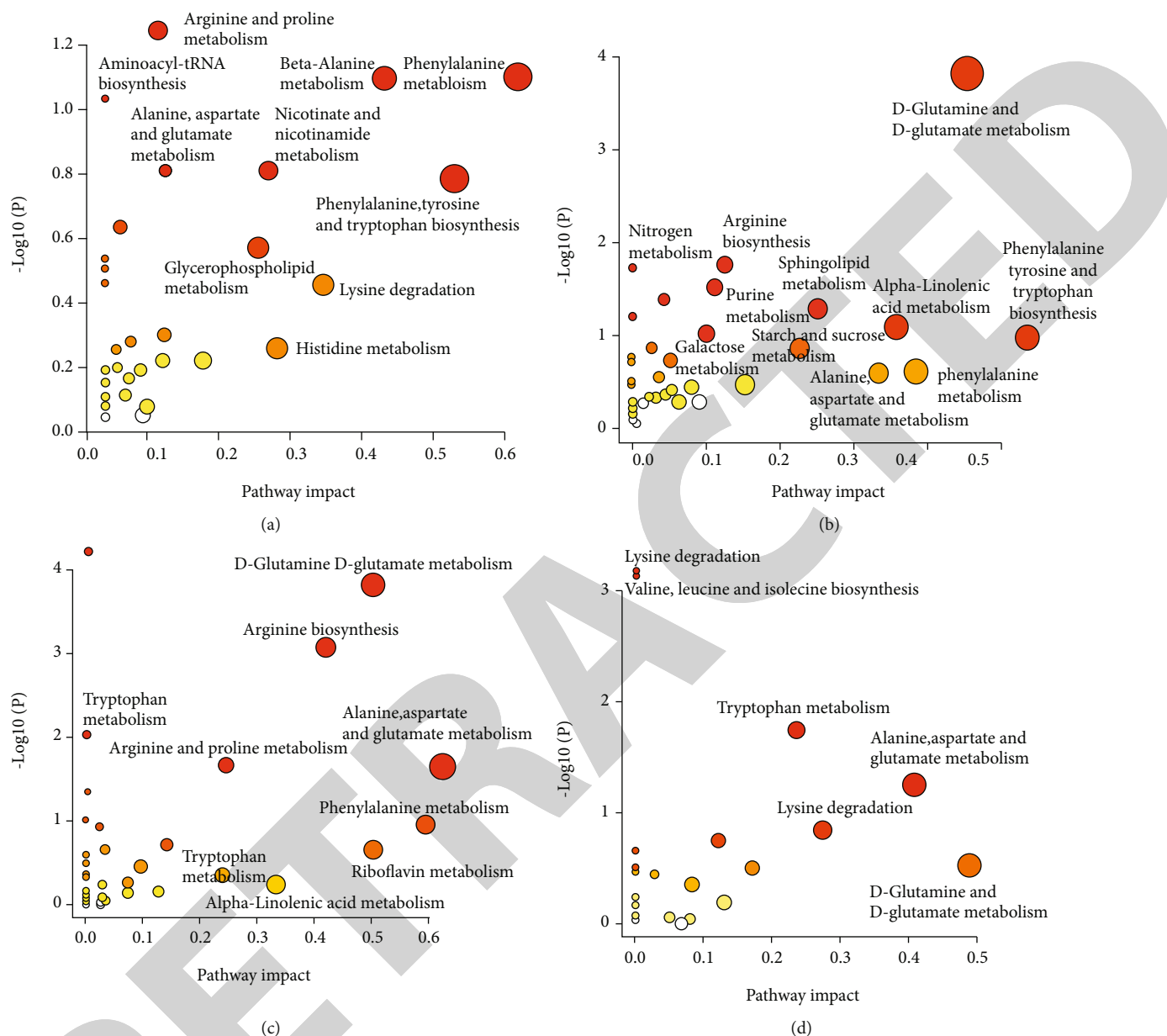


FIGURE 6: Pathway analysis of differentially expressed metabolites ((a) 0-HT60min vs. 0-CK, (b) 10-HT60min vs. 10-CK, (c) 10-CK vs. 0-CK, and (d) 10-HT60min vs. 0-HT60min.).

papaya by Nishijima et al. [44]; forced hot air at 48.5°C for 3-4 hours until center temperatures were 47.2°C did not significantly reduce incidences of *C. gloeosporioides* and was associated with a high rate of internal lumpiness. The differences of results might be related to the heating program, relative humidity of treatment, and fruit ripeness.

The delayed ripening of fruit after heat treatment may contribute to decreasing pathogen susceptibility and the deterioration of fruit tissue [33, 45]. Heat treatment highly depressed color change and firmness loss of papaya, which were related to fruit ripe in our study. Papaya fruit peel from nonheat treatment turns from green to yellow, while heated papaya fruits exhibit delayed degreening and yellowing during storage. These changes were attributed to peel lightness (*L*) decreasing, a loss of green color (*a*), a lowered hue angle (*h*),

and a rise in browning and yellow-orange (*b*). Similarly, forced hot air (43°C for 220 min), vapor heat (47°C for 15 min), and hot water (53°C for 5 min) applied in mango fruits significantly affected tristimulus color of the skin and mesocarp including *a*, *b*, and *L* values and slowed down the ripening process [46, 47]. In fresh-cut mangos after hot water-treated, the *L* value could be an indicator of peel browning and hue angle indicates fruit from yellow to orange-red [40]. Color changes of papaya fruit could due to chlorophyll degradation, carotenoid formation, and other phenolic compounds' accumulation during postharvest ripening process [48].

The host antifungal mechanism induced by heat treatment of papaya could be related to the activity of soften related and ROS-scavenging antioxidant enzymes (SOD and POD) and the enhancement of ascorbic acid. Heat treatment



by dipping in 50 or 55°C water for 5 min reduced PME and PG activities in both peel and pulp tissues of mango [49]. These enzymes catalyze the cleavage of pectin backbones and deesterify methoxylated pectin in cell wall, which contribute to delaying softening process after heat treatment [50, 51]. Plants could scavenge excess reactive oxygen species through SOD and POD to resist the oxidative burst, which originated generated by pathogen infection and reduce oxidative damage [52]. Hot water treatment at 48°C for 10 min reduced internal browning and maintained firmness of peach fruit and enhanced AsA-GSH metabolism and upregulated expressions of PpaSOD5, PpaCAT1, and PpaAPX2 [13].

After heat treatment, the increase of ABA could depress respiration rate and inhibit the growth of *C. gloeosporioides* during papaya storage in our study, since it could induce spiracular closure and helps block the entry of pathogens [53]. The respiration of the apple that was heated at 38°C for 4 days was much lower compared to the nonheated fruit. Li et al. [6] and Zhao et al. [54] reported that hot water treatment (54°C for 4 min) significantly reduced the respiration rate of papaya fruit. The ABA levels and PAL enzyme activity of grape seedlings was significantly increased after hot water treatment at 38°C for 1 h, which was related to improved plant heat tolerance [55].

Phenylpropanoid metabolism is an important metabolic pathway for plants to enhance plant resistance after infecting by pathogenic microorganisms [56, 57]. Phenylalanine is sequentially catalyzed by PAL, cinnamic acid 4-hydroxylase, and 4-coumarate-CoA ligase to generate cinnamic acid, p-hydroxycinnamic acid, and p-coumaroyl coenzyme. These compounds will serve as substrates for the next metabolic reaction, eventually transformed into phenols, flavonoids, and coumarins [58, 59]. After heat treatment, phenylalanine and PAL enzyme activities of papaya were significantly increased, while phenylpropanoid metabolism-related secondary metabolite levels including phenols, flavonoids, and coumarins were also increased. PAL enzyme activity and ROS scavenging genes of peach fruit were found to be induced by hot water at 60°C for 20 s, which was associated with decreased incidence after inoculation with conidia of *Monilinia laxa* [60]. Phenolics, flavonoids, and coumarins play a vital role in the disease resistance of fruits [59], which contribute to the antioxidant properties of plants due to their ability of chelate formation and radical dismutation [61]. Hot water at 52°C for 2 min induced PAL and accumulated flavonoids of citrus fruit, which play a vital role in improving the resistance of fruits to *Penicillium italicum* [17]. Hot air treatment at 38°C for 12 h enhanced phenylpropanoid metabolism of cherry tomatoes, as evidenced by elevated levels of phenolics and flavonoids and higher activities of phenylalanine ammonia lyase [7]. Flavonoids and coumarins accumulated of the citrus fruits may act as phytoantipins and phytoalexins in the resistance mechanism against *Penicillium digitatum* attack to improve the disease resistance of tangor varieties [62].

Heat treatment delayed ripening, inhibiting softening, and induced defenses to protect papaya from pathogen attacks, which rely on efficient resistance mechanisms that involve the inhibition of ROS scavenging systems, ABA-

regulated respiratory depression, and inactivated phenylpropanoid metabolism. Phytosanitary heat treatment (especially 60 min treatment) not only prolonged their shelf life and improved the quality of papaya fruits in our study but also was adequate to satisfy quarantine security conditions. Heating papaya fruit to core temperature at 47.2°C could be a generic heat treatment to provide quarantine security for a broad group of pests, such as Tephritid fruit flies (*C. capitata*, *B. cucurbitae*, and *B. dorsalis* for 20 min) and mealybug *Macronellicoccus hirsutus* (for 5 min) [63, 64]. This study would improve our understanding of the fundamental biological processes after heat treatment. This integrated metabolomic approach will allow gain us to insight into the antifungal mechanisms after heat treatment at quality and molecular perspectives of fruits.

## 5. Conclusion

In conclusion, we tested the fungicidal effect of *C. gloeosporioides* in response to HT and also investigated heat treatment effect on quality parameters and disease resistance against *C. gloeosporioides*-related enzymes of the papaya fruit. Our findings would improve our understanding of the fundamental biological processes after heat treatment. This integrated metabolomic approach will allow us to gain insight into the antifungal mechanisms after heat treatment at the quality and molecular perspectives of fruits.

## Data Availability

The datasets used and/or analyzed during the current study are available from the corresponding author on reasonable request.

## Conflicts of Interest

The authors declare no potential conflicts of interest with the respect to the research, authorship, and/or publication of this article.

## Acknowledgments

This research was funded by the Scientific Research Program of the Chinese Academy of Inspection and Quarantine 2019JK028 and 2020JK030.

## References

- [1] E. A. Evans and F. H. Ballen, "An overview of global papaya production, trade, and consumption," *Food and Resource Economics*, 2015.
- [2] O. S. Bautista-Ba, M. Hernández-López, E. Bosquez-Molina, and C. L. Wilson, "Effects of chitosan and plant extracts on growth of *Colletotrichum gloeosporioides*, anthracnose levels and quality of papaya fruit," *Crop Protection*, vol. 22, no. 9, pp. 1087–1092, 2003.
- [3] R. B. Waghmare and U. S. Annapure, "Combined effect of chemical treatment and/or modified atmosphere packaging (MAP) on quality of fresh-cut papaya," *Postharvest Biology and Technology*, vol. 85, no. 11, pp. 147–153, 2013.

- [4] A. Ademe, "Evaluation of antifungal activity of plant extracts against papaya anthracnose (*Colletotrichum gloeosporioides*)," *Journal of Plant Pathology and Microbiology*, vol. 4, no. 10, pp. 1–4, 2013.
- [5] E. Bosquez-Molina, E. R. Jesús, O. S. Bautista-Ba, J. R. Verde-Calvo, and J. Morales-López, "Inhibitory effect of essential oils against *Colletotrichum gloeosporioides* and *Rhizopus stolonifer* in stored papaya fruit and their possible application in coatings," *Postharvest Biology and Technology*, vol. 57, no. 2, pp. 132–137, 2010.
- [6] X. Li, X. Zhu, N. Zhao et al., "Effects of hot water treatment on anthracnose disease in papaya fruit and its possible mechanism," *Postharvest Biology and Technology*, vol. 86, pp. 437–446, 2013.
- [7] Y. Wei, D. Zhou, J. Peng, L. Pan, and K. Tu, "Hot air treatment induces disease resistance through activating the phenylpropanoid metabolism in cherry tomato fruit," *Journal of Agricultural and Food Chemistry*, vol. 65, pp. 8003–8010, 2017.
- [8] Ippc, "ISPM No. 42, Requirements for the use of temperature treatments as phytosanitary measures," *Food and Agricultural Organization Rome*, 2018.
- [9] J. Tang, J. N. Ikediala, S. Wang, J. D. Hansen, and R. P. Cavalieri, "High-temperature-short-time thermal quarantine methods," *Postharvest Biology and Technology*, vol. 21, no. 1, pp. 129–145, 2000.
- [10] N. W. Heather and G. J. Hallman, "Disinfestation with cold," in *Pest Management and Phytosanitary Trade Barriers*, CABI, 2008.
- [11] M. Schirra, S. D. Aquino, P. Cabras, and A. Angioni, "Control of postharvest diseases of fruit by heat and fungicides: efficacy, residue levels, and residue persistence. A review," *Journal of Agricultural and Food Chemistry*, vol. 59, no. 16, pp. 8531–8542, 2011.
- [12] X. Shao, Y. Zhu, S. Cao, H. Wang, and Y. Song, "Soluble sugar content and metabolism as related to the heat-induced chilling tolerance of loquat fruit during cold storage," *Food & Bioprocess Technology*, vol. 6, no. 12, pp. 3490–3498, 2013.
- [13] H. Chen, H. Shuai, J. Li et al., "Postharvest hot air and hot water treatments affect the antioxidant system in peach fruit during refrigerated storage," *Postharvest Biology and Technology*, vol. 126, pp. 1–14, 2017.
- [14] N. Shadmani, S. H. Ahmad, N. Saari, P. Ding, and N. E. Tajidin, "Chilling injury incidence and antioxidant enzyme activities of *Carica papaya* L. 'Frangi' as influenced by postharvest hot water treatment and storage temperature," *Postharvest Biology and Technology*, vol. 99, pp. 114–119, 2015.
- [15] Y. Sui, M. Wisniewski, S. Droby, J. Norelli, and J. Liu, "Recent advances and current status of the use of heat treatments in postharvest disease management systems: is it time to turn up the heat?," *Trends in Food Science and Technology*, vol. 51, pp. 34–40, 2016.
- [16] J. Usall, A. Ippolito, M. Sisquella, and F. Neri, "Physical treatments to control postharvest diseases of fresh fruits and vegetables," *Postharvest Biology and Technology*, vol. 122, pp. 30–40, 2016.
- [17] Z. Yun, H. Gao, P. Liu et al., "Comparative proteomic and metabolomic profiling of citrus fruit with enhancement of disease resistance by postharvest heat treatment," *Plant Biology*, vol. 13, no. 1, p. 44, 2013.
- [18] J. D. Klein and S. Lurie, "Prestorage heat treatment as a means of improving poststorage quality of apples," *Horticultural Science*, vol. 115, no. 2, pp. 265–269, 1990.
- [19] M. Lay-Yee, G. K. Clare, R. J. Petry, R. A. Fullerton, and A. Gunson, "Quality and disease incidence of 'Waimanalo Solo' Papaya following forced-air heat treatments," *Hort Science: a publication of the American Society for Horticultural Science*, vol. 33, no. 5, pp. 878–880, 1998.
- [20] S. Kanlaya, J. Pongphen, T. Shinji et al., "Combined treatment with hot water and UV-C elicits disease resistance against anthracnose and improves the quality of harvested mangoes," *Crop Protection*, vol. 77, pp. 1–8, 2015.
- [21] B. Nafussi, S. Ben-Yehoshua, V. Rodov, J. Peretz, B. K. Ozer, and G. D'hallewin, "Mode of action of hot-water dip in reducing decay of lemon fruit," *Chemistry*, vol. 49, no. 1, pp. 107–113, 2001.
- [22] A. R. Vicente, M. L. Costa, G. A. Martínez, A. R. Chaves, and P. M. Civello, "Effect of heat treatments on cell wall degradation and softening in strawberry fruit," *Postharvest Biology and Technology*, vol. 38, no. 3, pp. 213–222, 2005.
- [23] M. R. Safizadeh, M. Rahemi, and M. Aminlari, "Effect of post-harvest calcium and hot-water dip treatments on catalase, peroxidase and superoxide dismutase in chilled Lisbon lemon fruit," *International Journal of Agricultural Research*, vol. 2, no. 5, pp. 440–449, 2007.
- [24] K. Wang, S. Cao, J. Peng, H. Rui, and Y. Zheng, "Effect of hot air treatment on postharvest mould decay in Chinese bayberry fruit and the possible mechanisms," *Food Microbiology*, vol. 141, no. 1–2, pp. 11–16, 2010.
- [25] L. D. Gara, M. C. D. Pinto, and F. Tommasi, "The antioxidant systems vis-a-vis reactive oxygen species during plant-pathogen interaction," *Plant Physiology and Biochemistry*, vol. 41, no. 10, pp. 863–870, 2003.
- [26] C. J. Clarke and J. N. Haselden, "Metabolic profiling as a tool for understanding mechanisms of toxicity," *Toxicologic Pathology*, vol. 36, no. 1, pp. 140–147, 2008.
- [27] I. Chávez-Sánchez, A. Carrillo-López, M. Vega-García, and E. M. Yahia, "The effect of antifungal hot-water treatments on papaya postharvest quality and activity of pectinmethylesterase and polygalacturonase," *Journal of Food Science and Technology*, vol. 50, no. 1, pp. 101–107, 2013.
- [28] Aphis, "Treatment Manual," 2018.
- [29] M. Lay-Yee and K. J. Rose, "Quality of 'Fantasia' nectarines following forced-air heat treatments for insect disinfestation," *Hort Science*, vol. 29, no. 6, pp. 663–666, 1994.
- [30] R. Lahoz-Beltra, S. R. Hameroff, J. E. Dayhoff, Krista C. Shellie, and Robert L. Mangan, "Tolerance of red-fleshed grapefruit to a constant or stepped temperature, forced-air quarantine heat treatment," *Postharvest Biology and Technology*, vol. 7, no. 1–2, pp. 151–159, 1996.
- [31] L. M. Coates, G. I. Johnson, and A. W. Cooke, "Postharvest disease control in mangoes using high humidity hot air and fungicide treatments," *Annals of Applied Biology*, vol. 123, no. 2, pp. 441–448, 2008.
- [32] P. Varoquaux, B. Gouble, M. N. Ducamp, and G. Self, "Procedure to optimize modified atmosphere packaging for fruit," *Fruits*, vol. 57, no. 5–6, pp. 313–322, 2002.
- [33] A. Carrillo-Lopez, F. Ramirez-Bustamante, J. B. Valdez-Torres, R. Rojas-Villegas, and E. M. Yahia, "Ripening and quality changes in mango fruit as affected by coating with an edible film," *Journal of Food Quality*, vol. 23, 486 pages, 2000.
- [34] D. J. Huber, "The role of cell wall hydrolases in fruit softening," *Horticultural Reviews*, vol. 5, 1983.

## Retraction

# Retracted: The Expression of the Long Noncoding RNA AFAP1-AS1 in Laryngeal Carcinoma Affects the Proliferation, Invasion, Migration, and Apoptosis of TU212 Cell Line

### BioMed Research International

Received 20 June 2023; Accepted 20 June 2023; Published 21 June 2023

Copyright © 2023 BioMed Research International. This is an open access article distributed under the Creative Commons Attribution License, which permits unrestricted use, distribution, and reproduction in any medium, provided the original work is properly cited.

This article has been retracted by Hindawi following an investigation undertaken by the publisher [1]. This investigation has uncovered evidence of one or more of the following indicators of systematic manipulation of the publication process:

- (1) Discrepancies in scope
- (2) Discrepancies in the description of the research reported
- (3) Discrepancies between the availability of data and the research described
- (4) Inappropriate citations
- (5) Incoherent, meaningless and/or irrelevant content included in the article
- (6) Peer-review manipulation

The presence of these indicators undermines our confidence in the integrity of the article's content and we cannot, therefore, vouch for its reliability. Please note that this notice is intended solely to alert readers that the content of this article is unreliable. We have not investigated whether authors were aware of or involved in the systematic manipulation of the publication process.

In addition, our investigation has also shown that one or more of the following human-subject reporting requirements has not been met in this article: ethical approval by an Institutional Review Board (IRB) committee or equivalent, patient/participant consent to participate, and/or agreement to publish patient/participant details (where relevant).

Wiley and Hindawi regrets that the usual quality checks did not identify these issues before publication and have since put additional measures in place to safeguard research integrity.

We wish to credit our own Research Integrity and Research Publishing teams and anonymous and named external researchers and research integrity experts for contributing to this investigation.

The corresponding author, as the representative of all authors, has been given the opportunity to register their agreement or disagreement to this retraction. We have kept a record of any response received.

### References

- [1] X. Chen, Z. Hu, L. Bing et al., "The Expression of the Long Non-coding RNA AFAP1-AS1 in Laryngeal Carcinoma Affects the Proliferation, Invasion, Migration, and Apoptosis of TU212 Cell Line," *BioMed Research International*, vol. 2022, Article ID 2337447, 8 pages, 2022.

## Research Article

# The Expression of the Long Noncoding RNA AFAP1-AS1 in Laryngeal Carcinoma Affects the Proliferation, Invasion, Migration, and Apoptosis of TU212 Cell Line

Xin Chen,<sup>1</sup> Ziwei Hu,<sup>2</sup> Liao Bing,<sup>3</sup> Xinhua Zhu,<sup>3</sup> Ke Liu,<sup>3</sup> Yuehui Liu,<sup>3</sup> and Jianguo Liu<sup>3</sup> 

<sup>1</sup>Otolaryngology Department of Youxian People's Hospital of Hunan Province, China

<sup>2</sup>Department of Otolaryngology and Head and Neck Surgery, Guangzhou Red Cross Hospital Affiliated to Jinan University, China

<sup>3</sup>Otolaryngology Head and Neck Surgery, Second Affiliated Hospital of Nanchang University, China

Correspondence should be addressed to Jianguo Liu; [ljq0813@163.com](mailto:ljq0813@163.com)

Received 28 June 2022; Revised 18 July 2022; Accepted 22 July 2022; Published 4 August 2022

Academic Editor: Dinesh Rokaya

Copyright © 2022 Xin Chen et al. This is an open access article distributed under the Creative Commons Attribution License, which permits unrestricted use, distribution, and reproduction in any medium, provided the original work is properly cited.

**Background.** lncRNA AFAP1-AS1 has been linked to the pathogenesis of a wide range of tumors. Nevertheless, whether it plays a role in laryngeal carcinoma (LC) remains unclear. **Methods.** Twenty-nine pairs of LC and related normal tissues were collected for the detection of lncRNA AFAP1-AS1 using qRT-PCR. Correlation of lncRNA AFAP1-AS1 level and clinicopathological characters was assessed by the chi-square test. Impacts of lncRNA AFAP1-AS1 silencing on LC phenotypes were tested *in vitro* via CCK-8, clone formation, EdU staining, wound healing, flow cytometry, and Transwell assay. **Results.** Herein, a remarkable elevation of lncRNA AFAP1-AS1 was observed in LC patients. And higher lncRNA AFAP1-AS1 level was correlated to worse clinical pathological characteristics. Moreover, lncRNA AFAP1-AS1 silencing was revealed to repress TU212 malignant phenotypes. **Conclusion.** Our data suggested that lncRNA AFAP1-AS1 acts as an oncogene of LC *in vitro*.

## 1. Background

Laryngeal cancer (LC) is a malignant tumor in otolaryngology, among which 96%-98% consists of squamous cell carcinoma [1]. In comparison, others such as adenocarcinoma, basal cell carcinoma, poorly differentiated carcinoma, lymphosarcoma, and malignant lymphoma are rare [1]. Global cancer analysis data show that in 2002, there were 159,000 new cases and 90,000 deaths [2]. Cancer accounts for 2.4% of all male diseases and is 7-9 times more common in men than in women [1, 2]. In recent decades, the incidence of LC has increased significantly, and the onset age is mainly between 40 and 60 years. Although great progress has been made in the clinical treatment of LC in the past decades, including surgical intervention, radiotherapy, and chemotherapy, the prognosis of advanced LC patients remains unsatisfactory [3]. Therefore, exploring the molecular mechanisms underlying the carcinogenesis or progression of LC is crucial for the development of more effective therapeutic targets.

Long noncoding RNAs (lncRNAs) are known as a group of transcripts with over two hundred nucleotides, which lack of or possess a limited capacity to encode proteins [4]. Numerous researches have argued that lncRNAs participate in various biological events, including transcriptional regulation and tumor occurrence [4, 5]. Recent studies also indicated that dysregulated lncRNAs are linked to human tumor development [5]. lncRNA AFAP1-AS1 is a newly discovered tumor-associated lncRNA originated from the anti-sense strand of the AFAP1 gene [6]. It was reported to be related with multiple malignant tumors, including esophageal cancer, nasopharyngeal cancer (NPC), and tongue squamous cell carcinoma (TSCC) [7-9]. lncRNA AFAP1-AS1 may elevate the protein level of VEGF-C and artemin to enhance esophageal cancer cell invasion and migration. In NPC and TSCC, elevated lncRNA AFAP1-AS1 was found to be related to metastasis and poor prognosis; moreover, lncRNA AFAP1-AS1 silencing could repress NPC and TSCC cell migration and invasion [9, 10]. Nevertheless, the role of lncRNA AFAP1-AS1 in LC remains undetermined.



TABLE 1: Relationship between lncRNA AFAP1-AS1 expression and clinicopathological features in patients with LC.

Parameter	Total (n = 29)	lncRNA AFAP1-AS1		$\chi^2$	P
		Low (n = 8)	High (n = 21)		
		Age (years)			
<60	5	3 (60.0%)	2 (40.0%)	3.178	0.075
≥60	24	5 (20.8%)	19 (79.2%)		
		Gender			
Female	29	8 (27.6%)	21 (72.4%)	—	0.999
Male	0	0	0		
		T-classification			
T1-T2	10	6 (60.0%)	4 (40.0%)	8.028	0.004**
T3-T4	19				
(TNM)		2 (10.5%)	17 (89.5%)		
I-II	8			6.741	0.009**
III-IV	21	5 (62.5%)	3 (37.5%)		
Tumor differentiation		3 (14.3%)	18 (85.7%)		
Well/moderate	23	4 (17.4%)	19 (82.6%)	5.784	0.016*
Poor	6	4 (66.7%)	2 (33.3%)		

\*P < 0.05 and \*\*P < 0.05.

Herein, we aimed to study whether lncRNA AFAP1-AS1 plays a role in the regulation of LC cell proliferation, apoptosis, migration, and invasion. Our results indicated that lncRNA AFAP1-AS1 was elevated in LC. Moreover, loss-of-function assays suggested that lncRNA AFAP1-AS1 acts as an oncogene of LC. Our findings suggested that lncRNA AFAP1-AS1 might act as a potential diagnostic biomarker and therapeutic target for LC.

## 2. Methods

**2.1. Human Tissues.** Twenty-nine LC patients who received therapy between June 2020 and December 2020 at the Otorhinolaryngology Department of the Second Affiliated Hospital of Nanchang University, Jiangxi, China, were included in the study. This population is consisted of 29 males, aged 42-81 (median age = 64.5). Patients did not undergo chemo- or radiotherapy, did not have other tumors, immune system diseases, and blood system diseases, and did not have advanced cardiac, liver, kidney, and other organ dysfunction. The adjacent normal tissues were collected from the 29 LC patients, approximately 1-2 cm away from the tumors as the control group. Informed consents were obtained from all 29 LC patients. Tissues were kept under -80°C until use. The clinicopathologic characteristics of the 29 LC patients are presented in Table 1.

**2.2. Cell Culture.** TU-212 cell line purchased from Beina Bio (BNCC340714) was maintained in DMEM medium plus penicillin/streptomycin and fetal bovine serum (10%). Cells were placed in a humidified condition with 5% CO<sub>2</sub> at 37°C.

**2.3. Vector Establishment and Cell Transfection.** Add 1 mL of 0.25% trypsin for digestion for 2-3 min, then add 2 mL of complete medium to terminate the digestion, centrifuge at

1,000 r/min for 5 min, remove supernatant and collect the pelleted cells, and resuspend in complete culture medium. After the cell suspension is passaged or inoculated according to the required ratio, take logarithmic growth of cells and placed in 6-well plates and cultured for 24 h, and then, Lipofectamine™ 3000 Kit (Invitrogen, L3000015) was employed to conduct cell transfection. Incubate cells at 37°C for 2-4 days.

**2.4. Quantitative Real-Time PCR Analysis.** Total RNAs of LC tissues and cells were extracted using TRIzol reagent (Invitrogen, USA) following the manufacturer's guidance. Then, RNA was reverse transcribed into cDNA using the iScript™ cDNA Synthesis Kit (Bio-Rad, USA). Real-time PCR reaction was conducted on an ABI 7500 system using SYBR Premix Dimer Eraser (Takara, Dalian, China). Sequences of primers are shown in Table 2.

**2.5. CCK-8 Assay.** Briefly, 0.8 × 10<sup>5</sup> cells/mL were seeded into 96-well plates and CCK-8 reagent was added into each well and allowed for another 2 h of incubation. Absorbance of each well was determined at 450 nm by a Quant Reader (BioTek Instruments, USA). Each sample had three replicates.

**2.6. Clone Formation Assay.** Around 400 cells were placed into 6-well plates and allowed for 14 days of incubation, and culture medium was replaced every two days. Afterwards, colonies were washed by PBS for three times and subjected for crystal violet staining. Colonies with more than fifty cells were counted manually.

**2.7. EdU Cell Staining.** Treated cells were seeded in a 6-well culture plate with three replicates. EdU cell proliferation staining was performed using an EdU kit. For the EdU staining assay, the Cell-Light™ EdU Cell Proliferation Detection



TABLE 2: Sequences of primers.

Gene symbols	Sequences
GAPDH	F: ATGGGGAAGGTGAAGGTCG R: TCGGGGTCATTGATGGCAACAATA
Primer of AFAP1-AS1	F: ATAAGAATGGCTTGCTGTGGAC R: GGTTGGTGCGGTTGGAATAG
AFAP1-AS1-siRNA1	F: GATCCGCACGGAGTGTGGACAATAAAGCTCGAGTTATTGTGCCACACTCCGTGCTTTTTGC R: GGCCGCAAAAAGCACGGAGTGTGGACAATAAAGCTCGAGTTATTGTGCCACACTCCGTGCG
AFAP1-AS1-siRNA2	F: GATCCGCACGGAGTGTGGACAATAAAGCTCGAGTTATTGTGCCACACTCCGTGCTTTTTGC R: GGCCGCAAAAAGCACGGAGTGTGGACAATAAAGCTCGAGTTATTGTGCCACACTCCGTGCG
AFAP1-AS1-siRNA3	F: GATCCGCACGGAGTGTGGACAATAAAGCTCGAGTTATTGTGCCACACTCCGTGCTTTTTGC R: GGCCGCAAAAAGCACGGAGTGTGGACAATAAAGCTCGAGTTATTGTGCCACACTCCGTGCG
si-NC	F: TAGTTATTAATAGTAATCAATTACGGGGTCATTAGTTCATAGCCCATATATGGAGT R: GTTCTTTCCTGCGTTATCCCTGATTCTGTGGATAACCGTATTACCGCCATGCAT

Kit (RiboBio) was used. Finally, use Click-iT Additive Solution EdU detected.

**2.8. Transwell Assay.** TU212 cells ( $2.5 \times 10^5$  cell/mL) were included into the top Transwell chamber, and bottom Transwell chamber was filled by FBS-included culture medium. After 24 h of incubation, cells which invade to the lower surface were fixed in methanol and subjected for crystal violet (0.5%) staining.

**2.9. Wound Healing Assay.** Cells seeded in 6-well plate were allowed culturing until full confluence. Then, a scratch was made on the surface of cell layer by a pipette tip followed by PBS washing to discard debris. The scratch was photographed at 0 and 24 h of scratching, and the width was measured.

**2.10. Flow Cytometry.** An apoptosis analysis kit (KeyGEN, KGA1015-1018) was used in flow cytometry analysis. After overnight of fixation with 70% ethanol, cells were subjected for propidium iodide ( $25 \mu\text{g/mL}$ ) staining for 1 h. Afterwards, a FACSCalibur flow cytometer (Becton Dickinson, USA) was adopted to perform apoptosis analysis.

**2.11. Statistical Analysis.** Data analyzed in IBM SPSS21.0 and GraphPad Prism were presented as the mean  $\pm$  SD. Student's *t*-test or one-way ANOVA was employed to compare difference between groups. A *P* value less than 0.05 was considered statistically significant.

### 3. Results

**3.1. lncRNA AFAP1-AS1 Was Elevated in LC.** We firstly tested lncRNA AFAP1-AS1 expression in normal control (NC,  $n = 29$ ) and LC ( $n = 29$ ) tissues using qRT-PCR. Result indicated a remarkable elevation of lncRNA AFAP1-AS1 in LC (Figure 1). Association between lncRNA AFAP1-AS1 level and LC patients' clinicopathologic characteristics was also investigated. LC patients were divided into the low ( $n = 8$ ) and high ( $n = 21$ ) lncRNA AFAP1-AS1 groups. As expected, elevated lncRNA AFAP1-AS1 expression was linked to T-classification, TNM stage, and tumor differenti-

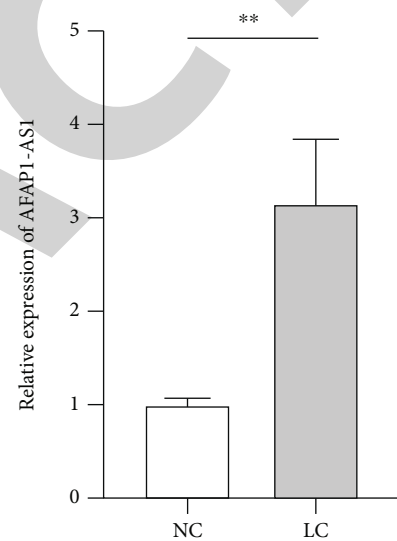


FIGURE 1: Relative lncRNA AFAP1-AS1 level in NC and LC tissue samples. lncRNA AFAP1-AS1 was sharply elevated in the LC group. \* $P < 0.05$ .

ation, but irrelevant to other factors, including age and gender (Table 1).

**3.2. lncRNA AFAP1-AS1 Was Successfully Silenced in TU212 Cells.** To study lncRNA AFAP1-AS1 function in TC, three specific shRNAs target lncRNA AFAP1-AS1 (sh#1, sh#2, and sh#3) were designed and transfected into TU212 cells. Green fluorescence was observed in the sh-NC and shRNAs transfected groups, suggesting that sh-AFAP1-AS1s and sh-NC were successfully transfected into TU212 cells (Figure 2). As shown by qRT-PCR results, relative lncRNA AFAP1-AS1 expression in TU212 cells was dramatically decreased by three shRNAs compared to the mock group (Figure 3).

**3.3. lncRNA AFAP1-AS1 Silencing Repressed TU212 Cell Proliferation.** Afterwards, the influences of lncRNA AFAP1-AS1 silencing on TU212 cell proliferation viability

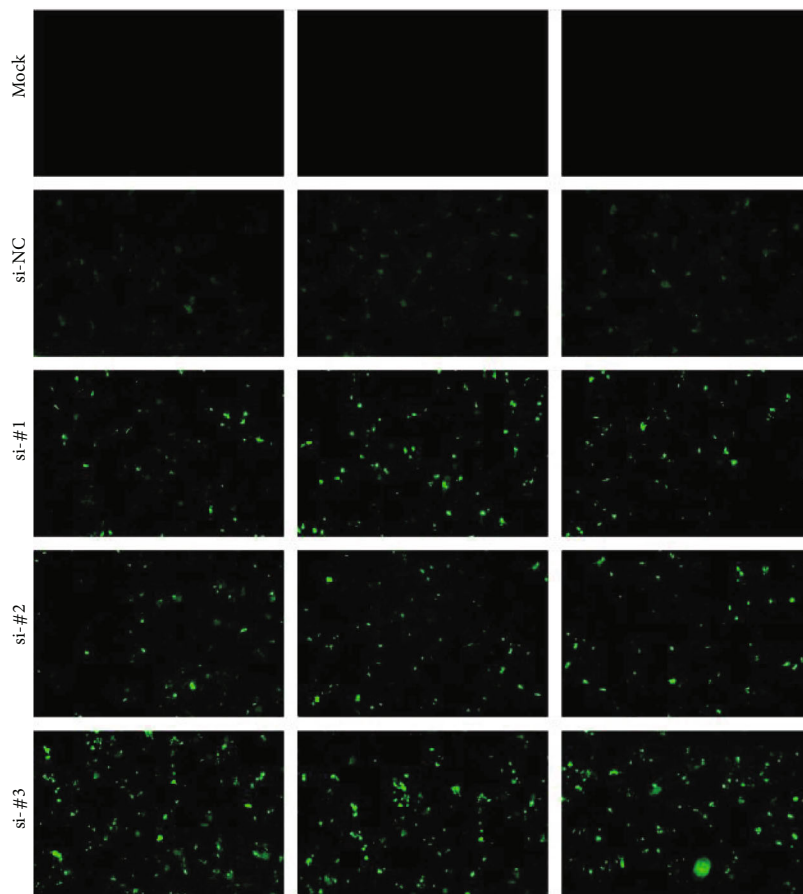


FIGURE 2: Confocal images showing that sh-AFAP1-AS1 and sh-NC were successfully transfected into TU212 cells. Green fluorescence was observed in the sh-NC and sh-RNAs transfected groups.

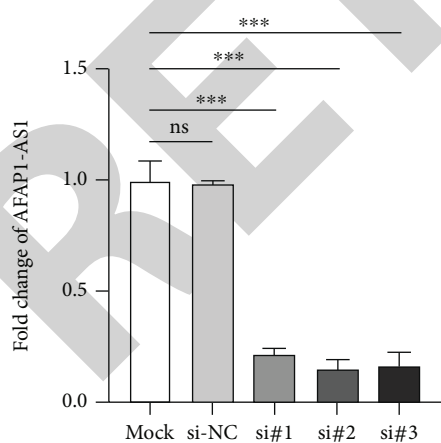


FIGURE 3: Knockdown efficiency of three shRNAs target AFAP1-AS1 (sh#1, sh#2, and sh#3) were tested by qRT-PCR in TU212 cells. All three shRNAs dramatically decreased lncRNA AFAP1-AS1 level.  $***P < 0.01$ .

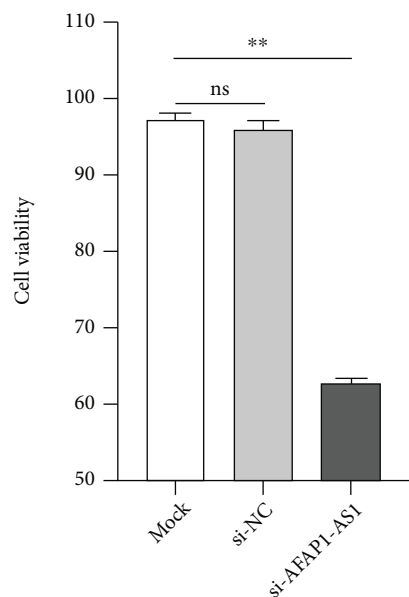


FIGURE 4: Impacts of lncRNA AFAP1-AS1 silencing on TU212 cell viability were estimated via CCK-8 kit. lncRNA AFAP1-AS1 silencing repressed TU212 cell viability.  $***P < 0.001$ .

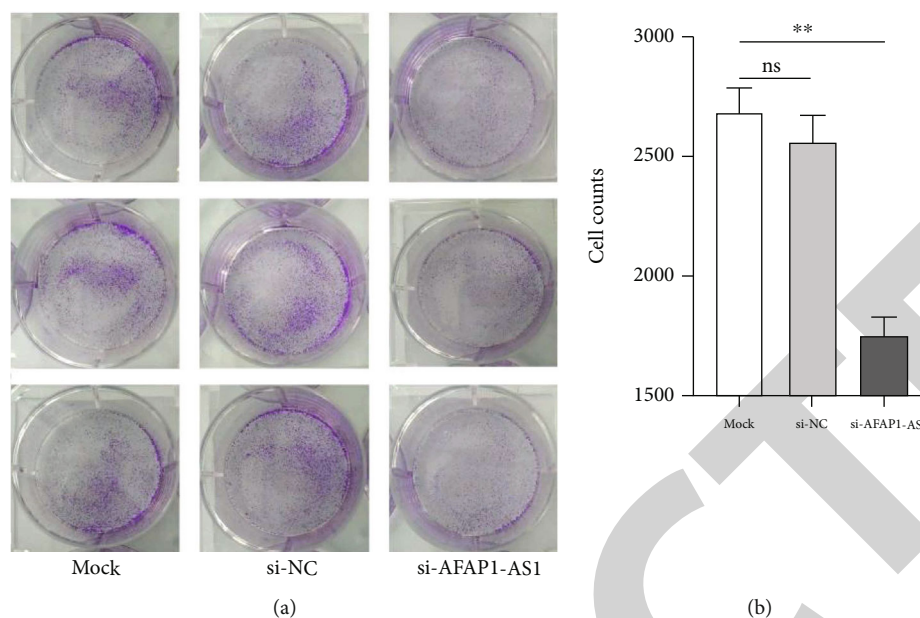


FIGURE 5: Impacts of AFAP1-AS1 silencing on TU212 cell clonogenicity were tested by colony formation assay. (a) Representative images showing the colonies formed by treated TU212 cells. (b) Statistical analysis of clone number in each group.

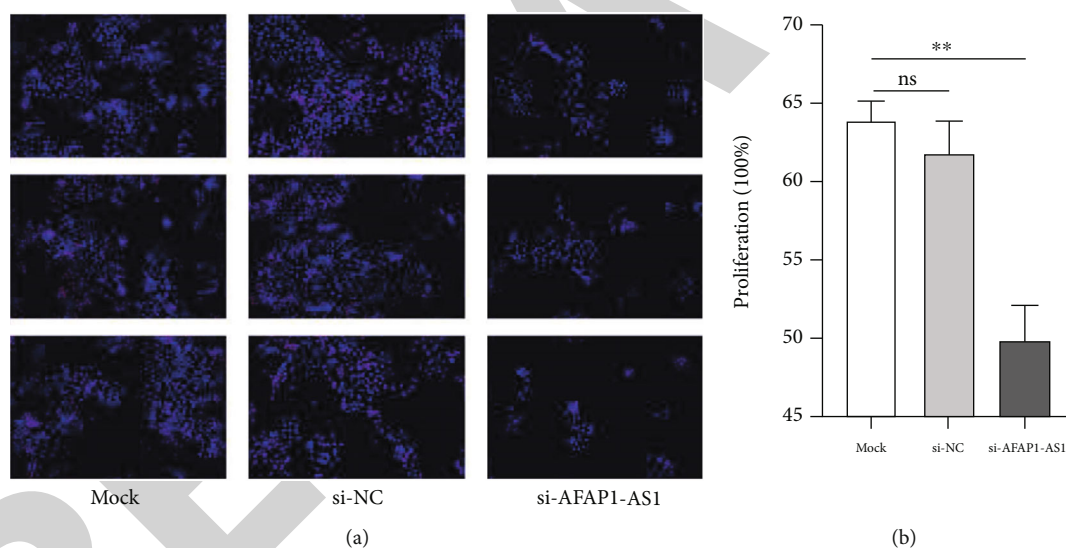


FIGURE 6: EdU staining results showing the influences of AFAP1-AS1 silencing on TU212 cell proliferation. (a) Representative images showing the EdU-stained TU212 cells. (b) Statistical analysis of EdU staining.

were tested. A remarkable viability repression was observed in CCK-8 assay in the lncRNA AFAP1-AS1 silenced group (Figure 4). And, we showed that the number of colonies formed by lncRNA AFAP1-AS1 silenced cells was dramatically reduced (Figure 5). The repressive effects of lncRNA AFAP1-AS1 silencing on TU212 cell proliferation viability were further supported by the results from EdU staining (Figure 6).

**3.4. lncRNA AFAP1-AS1 Silencing Repressed TU212 Cell Migration and Invasion.** Impacts of lncRNA AFAP1-AS1 silencing on LC migration and invasion were also tested *in vitro*. By using Transwell chambers coated with Matrigel,

we demonstrated that lncRNA AFAP1-AS1 silencing led to a remarkable repressive effect on TU212 cell invasion (Figure 7). Additionally, in wound healing assay, a significant repression of migratory capacity was observed in lncRNA AFAP1-AS1 silenced TU212 cells (Figure 8).

**3.5. lncRNA AFAP1-AS1 Silencing Facilitated TU212 Cell Apoptosis.** Finally, the impacts of lncRNA AFAP1-AS1 silencing on LC cell apoptosis were estimated via flow cytometry, as results indicated that the apoptosis rate was significantly higher in the lncRNA AFAP1-AS1 silenced group compared to the mock and sh-NC groups (Figure 9).

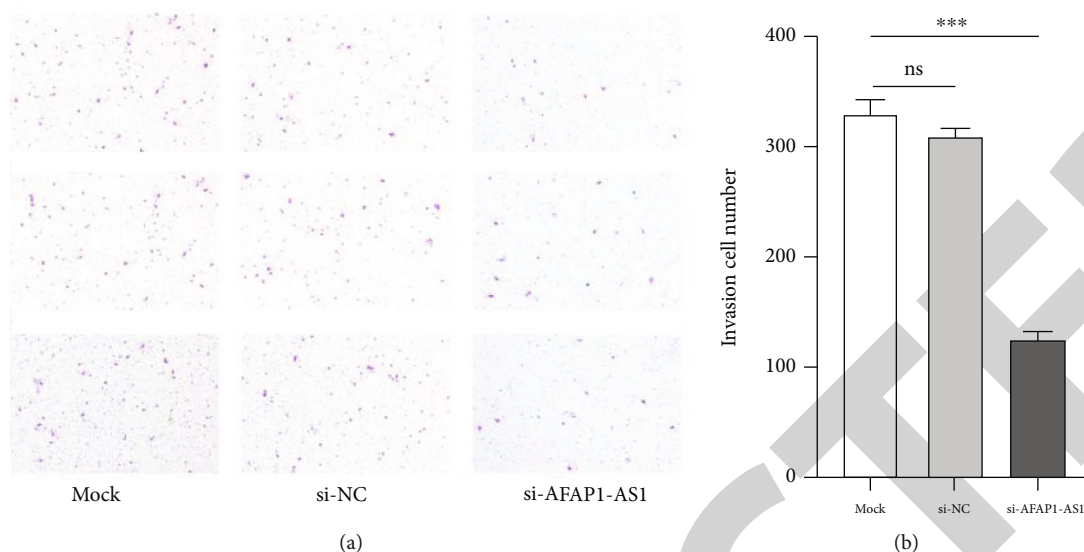


FIGURE 7: Invasive capacity of TU212 cell was assessed through Transwell chamber with Matrigel after transfection with si-AFAP1-AS1 or si-NC. (a) Representative images showing the invasive cells in each group. (b) Statistical analysis of the number of invasive cells.

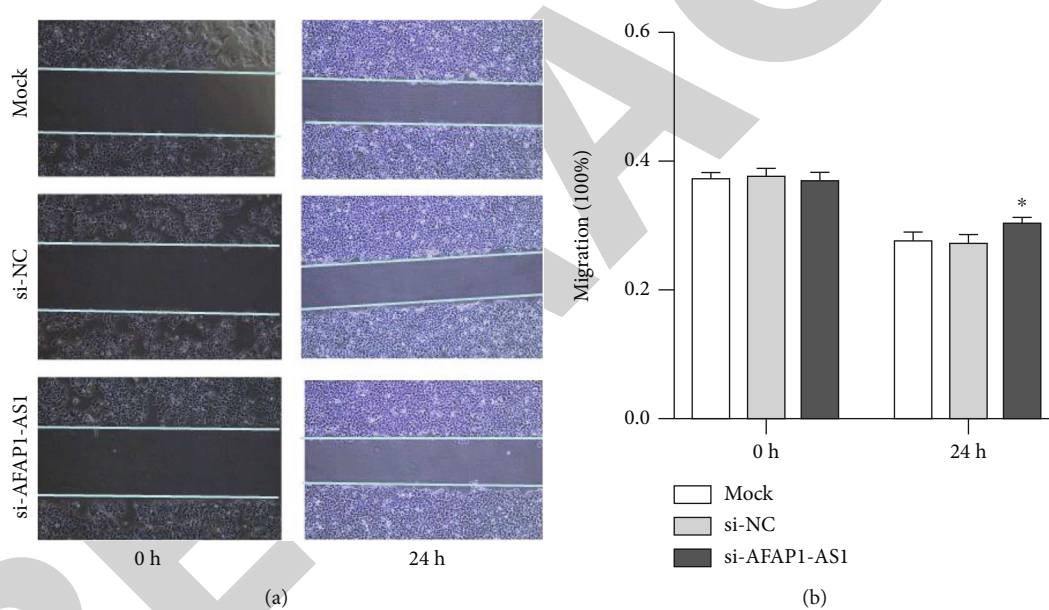


FIGURE 8: Migratory capacity of TU212 cell was assessed via wound healing assay after transfection with si-AFAP1-AS1 or si-NC. (a) Representative images showing the wound width. (b) Statistical analysis of the width of wound from each group.

#### 4. Discussion

The etiology of LC is poorly identified so far [11]. Epidemiological data confirms that it is related to factors including smoking and drinking, viral infection, environmental and occupational factors, radiation, lack of trace elements, and sexual hormone metabolism disorders [12]. At present, the clinical treatment of laryngeal cancer mainly adopts multidisciplinary comprehensive treatment with surgery as the mainstay [12, 13]. Currently, it has been well recognized that the ideal goals of the management of laryngeal cancer are to completely eradicate tumor lesions while preserving and reconstructing the function of the larynx as much as possible

and to improve the patient's quality of life [13]. Therefore, it is particularly important to explore the mechanism of LC tumorigenesis from the molecular level.

Recently, dysregulated expression or functions of lncRNAs have been reported in almost all kinds of tumors, and evidence also suggested an involvement of lncRNAs in all steps of tumor occurrence and progression [4, 14]. lncRNAs are widely believed to exert critical impacts on diagnosis, management, and prognosis of tumors [4, 15]. The discovery of lncRNA provides a novel direction for studying gene regulation. It can act as a carcinogenic or tumor repressive factor to participate in tumor proliferation, invasion, migration, and apoptosis [4, 16]. Numerous



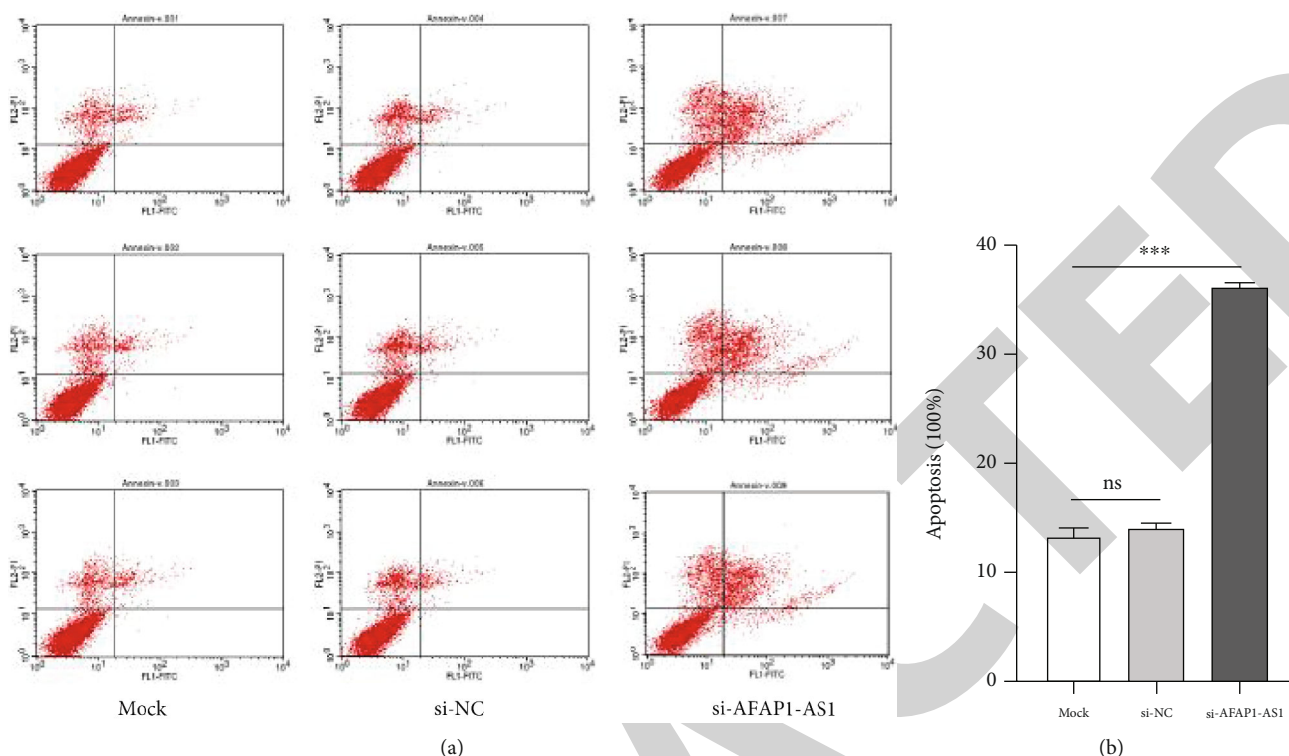


FIGURE 9: Flow cytometry analysis results showing the impacts of transfection with si-AFAP1-AS1 or si-NC on TU212 cell apoptosis. (a) Representative images showing the flow cytometry analysis of cells. (b) Statistical analysis of apoptosis rate.

lncRNAs have been found to be elevated or downregulated in LC, and evidence also demonstrated that lncRNAs play an important role in regulating LC cell growth, apoptosis, invasion, and migration through various of mechanisms [17–19]. lncRNA AFAP1-AS1 has been revealed to play a role in numerous cancers by a large of studies. For instance, it was reported to be an oncogene in gastric cancer by regulating FGF7 expression via miR-155-5p [20]. lncRNA AFAP1-AS1 also promotes the occurrence and development of osteosarcoma by competitively binding miR-497 [21]. lncRNA AFAP1-AS1 is also elevated in lung cancer and mediates lung cancer cell inhibition by modulating the expression of miR-545-3p [22]. However, there are few studies focusing on the role of lncRNA AFAP1-AS1 in LC. Only Yuan et al. have shown that lncRNA AFAP1-AS1 increases RBPJ expression through negative regulation of miR-320a, and the overexpression of RBPJ rescues the repressive effects of lncRNA AFAP1-AS1 on LC [23]. Thus, it is reasonable to believe that AFAP1-AS1 holds a carcinogen potential to participate in the process of tumors. Yet, the specific mechanism of occurrence and development needs to be further studied.

Herein, we tested the expression of lncRNA AFAP1-AS1 in LC tissues and cells, and we also studied its role in LC *in vitro* using TU212 cells. lncRNA AFAP1-AS1 was reported to be an oncogene of a variety of cancers. Similarly, our results also suggested that lncRNA AFAP1-AS1 promotes LC progression *in vitro*.

Although the data from our study revealed that AFAP1-AS1 is an oncogene of LC, there are still a few limitations.

First, sample size of the study is not large enough, but we believe that it has sufficient statistical power. Second, we did not explore the mechanism of lncRNA AFAP1-AS1 in LC.

## 5. Conclusions

lncRNA AFAP1-AS1 is highly presented in LC and is related to the clinicopathological characteristics of LC patients. Moreover, *in vitro* loss-of-function assays suggested that lncRNA AFAP1-AS1 acts as an oncogene of LC.

## Data Availability

The datasets used and analysed during this study are available from the corresponding author on reasonable request.

## Conflicts of Interest

The authors declare that they have no competing interests.

## Funding

This research was supported by a grant (GJJ18075) from the Jiangxi Provincial Education Department and a grant (202110052) from the project of Jiangxi Provincial Health Department.



## Retraction

# Retracted: A Novel Method for Parkinson's Disease Diagnosis Utilizing Treatment Protocols

### BioMed Research International

Received 20 June 2023; Accepted 20 June 2023; Published 21 June 2023

Copyright © 2023 BioMed Research International. This is an open access article distributed under the Creative Commons Attribution License, which permits unrestricted use, distribution, and reproduction in any medium, provided the original work is properly cited.

This article has been retracted by Hindawi following an investigation undertaken by the publisher [1]. This investigation has uncovered evidence of one or more of the following indicators of systematic manipulation of the publication process:

- (1) Discrepancies in scope
- (2) Discrepancies in the description of the research reported
- (3) Discrepancies between the availability of data and the research described
- (4) Inappropriate citations
- (5) Incoherent, meaningless and/or irrelevant content included in the article
- (6) Peer-review manipulation

The presence of these indicators undermines our confidence in the integrity of the article's content and we cannot, therefore, vouch for its reliability. Please note that this notice is intended solely to alert readers that the content of this article is unreliable. We have not investigated whether authors were aware of or involved in the systematic manipulation of the publication process.

In addition, our investigation has also shown that one or more of the following human-subject reporting requirements has not been met in this article: ethical approval by an Institutional Review Board (IRB) committee or equivalent, patient/participant consent to participate, and/or agreement to publish patient/participant details (where relevant).

Wiley and Hindawi regrets that the usual quality checks did not identify these issues before publication and have since put additional measures in place to safeguard research integrity.

We wish to credit our own Research Integrity and Research Publishing teams and anonymous and named external researchers and research integrity experts for contributing to this investigation.

The corresponding author, as the representative of all authors, has been given the opportunity to register their agreement or disagreement to this retraction. We have kept a record of any response received.

### References

- [1] S. Al-Otaibi, S. Ayouni, M. M. H. Khan, and M. Badr, "A Novel Method for Parkinson's Disease Diagnosis Utilizing Treatment Protocols," *BioMed Research International*, vol. 2022, Article ID 6871623, 6 pages, 2022.

## Research Article

# A Novel Method for Parkinson's Disease Diagnosis Utilizing Treatment Protocols

**Shaha Al-Otaibi** <sup>1</sup>, **Sarra Ayouni** <sup>1</sup>, **Md Maruf Haque Khan** <sup>2</sup>, and **Malek Badr** <sup>3,4</sup>

<sup>1</sup>Department of Information Systems, College of Computer and Information Sciences, Princess Nourah bint Abdulrahman University, P.O. Box 84428, Riyadh 11671, Saudi Arabia

<sup>2</sup>Department of Public Health and Informatics, Bangabandhu Sheikh Mujib Medical University, Dhaka, Bangladesh

<sup>3</sup>The University of Mashreq, Research Center, Baghdad, Iraq

<sup>4</sup>Department of Medical Instruments Engineering Techniques, Al-Farahidi University, Baghdad 10021, Iraq

Correspondence should be addressed to Md Maruf Haque Khan; [drmaruf38@bsmmu.edu.bd](mailto:drmaruf38@bsmmu.edu.bd)

Received 19 June 2022; Revised 2 July 2022; Accepted 13 July 2022; Published 2 August 2022

Academic Editor: Dinesh Rokaya

Copyright © 2022 Shaha Al-Otaibi et al. This is an open access article distributed under the Creative Commons Attribution License, which permits unrestricted use, distribution, and reproduction in any medium, provided the original work is properly cited.

It makes no difference whether a person is male or female when it comes to neurodegenerative disorders; both sexes are equally susceptible to their devastating effects. Sometimes, it is unclear why a person in their life got a condition that is well-known in the world, such as Parkinson's disease. Other times, it is evident why the individual obtained the ailment (PD). In modern times, a variety of cutting-edge algorithms that are based on treatment protocols have been developed for the purpose of diagnosing Parkinson's disease. The approach that is presented in this article is the most current one; it was created using deep learning, and it can predict how severely Parkinson's disease would affect a patient. In order to diagnose this condition, it is necessary to conduct a comprehensive medical history, a history of any past treatments, physical exams, and certain blood tests and brain films. Because they are less time-consuming and costly, diagnoses are becoming an increasingly important part of medical practice. The diagnosis of Parkinson's disease by the physician is supported by the findings of the present research, which analyzed the voices of 253 participants. Preprocessing is done in order to get the most accurate results possible from the data. In order to carry out the technique of balancing, a methodical sampling approach was used to choose the data that would afterwards be evaluated. Using a feature selection approach that was determined by the magnitude of the label's influence, many data groups were created and organized. DT, SVM, and kNN are three methods that are used in classification algorithms and performance assessment criteria. The model was developed as a result of selecting the classification method and data group that had the greatest performance value. This decision led to the creation of the model. During the process of building the model, the SVM technique was used, and data comprising 45% of the original data set were utilized. The information was arranged in descending order of significance, beginning with the most pertinent. In addition to achieving exceptional outcomes in every other aspect of the project, the performance accuracy target was successfully met at 86 percent. As a consequence of this, it has been decided that the physician will be provided with medical decision support with the assistance of the data set obtained from the speech recordings of the individual who may have Parkinson's disease and the model that has been developed. This has led to the conclusion that medical decision support will be offered to the physician.

## 1. Introduction

Parkinson's disease (PD) is a progressive neurodegenerative disorder due to the loss of neurons in the substantia nigra, which decreases dopamine levels, an important neurotransmitter whose primary function is the correct control of movements. It is a chronic and incurable disease that mani-

fest itself through a progressive loss of the ability to coordinate actions, presenting several peculiar characteristics such as tremor at rest, slowness in the initiation of movements, difficulty in speaking, and muscular rigidity. PD is characterized as slowness of movement (bradykinesia), tremors, and convulsions [1]. In addition to these, sleep disturbance, symptoms of depression, and speech disorder are observed

[2]. Speech disorder includes difficulties affecting social life, such as low voice, dull speech, inability to start speaking, pronunciation errors, and inability to adjust the volume while speaking [2, 3].

A simple test cannot determine whether a person has PD or not. A neurologist doctor requests biochemical tests and brain tomography from patients to diagnose the disease and understand whether another disease condition causes the disease. In addition, some physical examinations are required to evaluate functional adequacy of legs and arms, muscle condition, free gait, and balance. As the patients are usually aged greater than 60, the required tests are complex for people. Because of all these difficulties, simpler and more reliable methods are needed to diagnose PD [4].

For a decade, many researchers have shown great interest in offering a solution for diagnosing Parkinson's by voice. Initially, voice recordings made in the laboratory used a series of characteristics extracted to use them as predictors to classify Parkinson's patients and healthy controls. These recordings, in general, used to be sustained vowels since, as demonstrated [5], they offer more information than words or short phrases. Usually, a selection of the extracted features is carried out to improve the effectiveness of the data mining methods (kNN, SVM, or random forests). In this way, the characteristics were analyzed and, to avoid redundancies and simplify the problem, those that were strongly correlated were eliminated. There are various algorithms to follow for the selection, and we found an excellent comparison of four of them in [6]. This selection of characteristics is still present and occupies most of the articles, and there are even specific ones such as [7]. Using these traditional methods, it is possible to discriminate whether a patient suffers from PD or not. It is even possible to predict their Unified Parkinson's Disease Rating Scale level; it is a scale for assessing Parkinson's disease that measures motor and nonmotor symptoms and is very useful for monitoring patients. It should be noted that until now, the vast majority of studies have evaluated their models using cross-validation or similar, without noticing that different recordings of the same individual are found both in training and in the test. This may be a significant reason why they get such optimistic results.

Apart from these, there are also studies on nonsmall data sets [4–8]. A comparison was made with the data set in which the adjustable Q-factor wavelet transform was used and the data set in which this transform was not used. It has been stated that the conversion increases the accuracy rate, which is one of the performance criteria, albeit at a low rate. To get more relevant results, it is necessary to use more than one data set in a larger data set and balance the data set. Mei et al. [9] used the subjects' walking data to diagnose PD. The data set was grouped according to the age factor. The proposed model is constructed using the Dual Density 1-D Wavelet Transform method. Badem and Yücelbaş found high accuracy rates in different studies conducted recently by Schwab et al. [10]. A comprehensive data set was used in the studies, but balancing was not done. The data sets generally used in the literature are fundamental vocal frequency, the amount of variation in frequency, and variation in amplitude as features extracted for use in treatment protocols.

## 2. Materials and Method

The investigation followed the flow chart depicted in Figure 1. Separate groupings of similar attribute values were created to ensure an even distribution of data. The data sets were sorted from most relevant to least relevant using a feature selection technique. These ordered data groups were divided into feature groups at a certain percentage, and the performances of each data group were evaluated with classification algorithms. Necessary operations from the arrangements in the data set to the performance evaluation stage were carried out in the MATLAB program.

*2.1. Parkinson's Disease Data Set.* The University of Baghdad's College of Medicine's Treatment Protocols Repository provided us with the data we needed for our investigation. The study included 188 Parkinson's disease patients (107 males and 81 females) and 64 control subjects (23 males and 41 females). Involved individuals are in the range of 33 to 87 years old. The label in the data set represents only one patient group and zero healthy groups. There were 757 measurements recorded from the 253 participants, who were asked to repeat the /a/ vowel three times each. From the data collected, a tag was one of 753 attributes created.

*2.2. Data Preprocessing.* The researchers developed several processes [11] to prepare the data set for analysis. The following sections outline the data preprocessing steps used in this study.

*2.2.1. Separating the Data Set into Related Attribute Groups.* 753 features in the raw data set can be traced back to certain feature groups. In addition to basic characteristics like intensity parameters and formant frequencies (formal phonetic frequencies), wavelet features and MFCCs (mel-frequency cepstral coefficients) are some of the features that can be discovered (wavelet properties). Because of the similarity in the characteristics of the new time features, it was decided to consolidate the three categories (intensity, formant frequency, and bandwidth parameters). As shown in the schematic in Figure 2, data groupings were constructed that contained five core attribute groups and a group that included all attributes.

*2.2.2. Balancing the Data Set.* According to Mei et al. [12], an "unbalanced data set" refers to a data collection that has values for each label class that differs from one another. It is possible that a nonbalanced data collection can result in false accuracy values utilized in performance evaluation, resulting in wrong conclusions being drawn. It was decided to apply a systematic sampling approach to eliminate this unwanted circumstance. This process balanced the system by employing the undersampling method, and the unbalanced state was then retrieved by reversing the procedure. In the downsampling approach, the outnumbered tag class is regarded as the undersampled tag class and vice versa. The data set for this investigation consisted of 757 measurements, with 192 having healthy labels (0) and 564 having patient labels (Figure 3). Following the completion of the

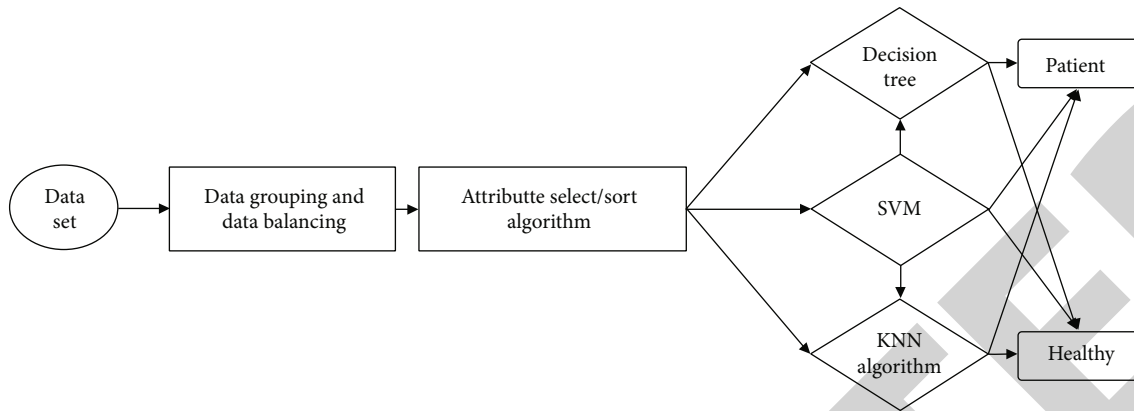


FIGURE 1: Flow chart.

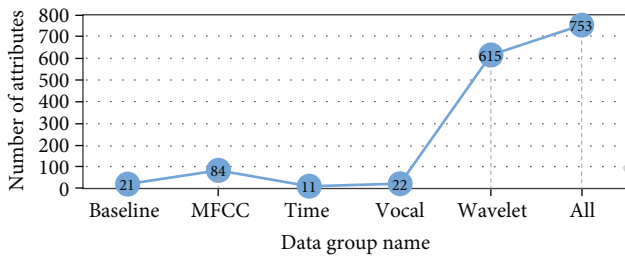


FIGURE 2: Data set attribute groups.

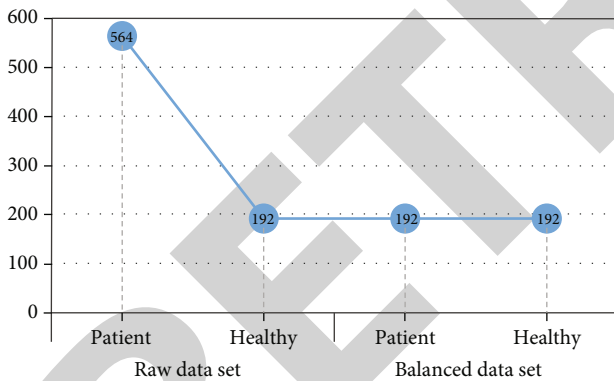


FIGURE 3: Schematic representation of data set balancing.

balancing procedure, 192 nutritional labels and 192 patient labels were obtained as a result of the process.

### 2.3. Feature Selection/Ranking Algorithm

**2.3.1. Fisher Attribute Sorting Algorithm.** The number of features affects positive and negative performance of treatment protocols. The feature selection technique is carried out to reduce the negative effects on the environment. This approach generates a grade from relevant to irrelevant based on the power of any attribute in the tag estimate process. The researcher can include as many features in the data set as he wants, ordered from the most relevant to the most

irrelevant. Thus, it can get more accurate results without unnecessary data and have a faster program cycle. In this study, the feature selection algorithm was used. The model was set up according to the performance values by taking 50% of it as shown in Figure 4.

**2.4. Classification Algorithms.** Classification processes in our study were implemented with a decision tree (DT), support vector machines (SVM), and K-nearest neighbor (kNN) algorithms. The flow chart steps in Figure 5 were applied for the classification process. Half of the data was used in model creation and the other half to test the model to perform classification in the data set. For each data group, the training data set was created with the help of the systematic sampling method. The remaining data set was used in the testing phase. The performance evaluation criteria of the model built on the test data were tested.

**2.4.1. Decision Tree (DT).** The decision tree algorithm's fundamental structure is composed of several components, including roots, branches, nodes, and leaves, to mention a few. When the tree structure is constructed, each attribute is assigned to a particular node in the hierarchy. Between the root and the nodes, there are branches to consider. It is sent from one node to the other via branches from each node. The selection is made in the tree based on the most recently visited leaf [13]. The critical reasoning in forming a decision tree structure can be explained as follows: the relevant questions are asked at each node reached, and the final leaf is reached in the shortest amount of time and space possible based on the responses provided. The responses to the questions serve as the foundation for creating models. It is determined whether or not this trained tree structure performs as expected by using test data, and the model is employed if it gives the desired result.

**2.4.2. Support Vector Machines (SVM).** Support vector machines (SVM) are used to separate data belonging to two classes in the most ideal way. This separation is performed with the appropriate linear and nonlinear lines. The learning data closest to the hyperplane are called support vectors. The maximum distance between the support



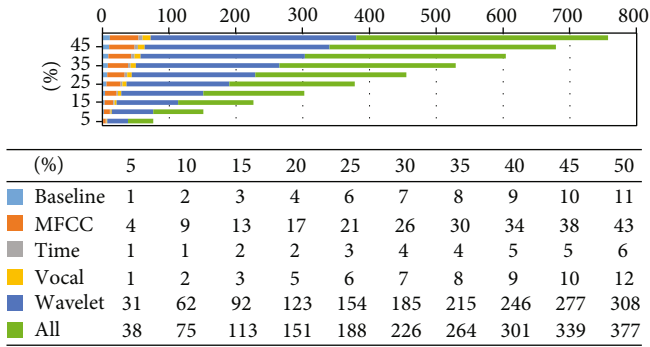


FIGURE 4: Attribute ranking in data groups.

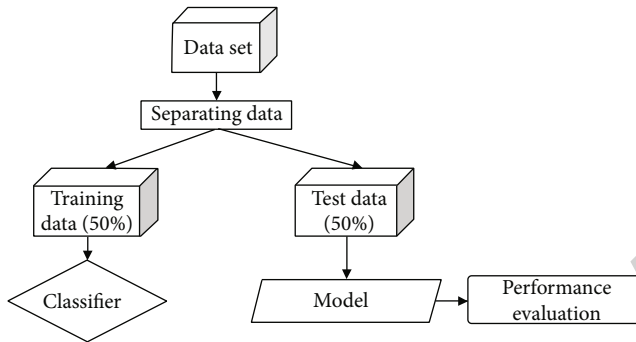


FIGURE 5: Separating the data set into training and test data sets.

vectors is determined and a curve is fitted in between. This curve is accepted as the generalized solution for the classification process [14]. The SVM method is one of the best and simplest algorithms among the supervised learning methods. The SVM algorithm develops a suitable classification method using the training data set. Then, it tries to classify the test data set with the minimum error with the method it has developed. SVM is used effectively in regression analysis as well as classification problems. Most of the objects in the data sets used cannot be separated by linear vectors. If objects cannot be separated with the help of a linear vector, a nonlinear support vector machine algorithm is used for classification. To classify a data set with objects, a size transformation is performed.

**2.4.3. *k*NN (*K*-Nearest Neighbor).** In *k*NN classification, classification is made according to the nearest neighbors. For nearest neighbors, the value of *k* may change to decide how to classify an unknown event; it determines how many values are considered neighbors. In the presence of an unknown sample, a nearest neighbor classifier explores the pattern space in search of the *k* training samples most similar to the unknown sample. The distance measures Euclid, Minkowski, and Manhattan are all employed to calculate the nearest neighbor. In this case, the unknown instance is assigned the most prevalent class among its nearest neighbors. When *k* = 1, the unknown sample is assigned the class of the training sample closest to it in the design area. The time to classify a test sample with the nearest neighbor classifier increases linearly with the number of training samples

TABLE 1: Training and test set distribution.

	Education (50%)	Testing (50%)	Total
Patient	86	86	192
Healthy	86	86	192
Total	192	192	384

retained in the classifier. It has a large storage requirement. It also performs poorly when different properties affect the result for different scopes. The parameter that can affect the performance of the *k*NN classification algorithm is the number of nearest neighbors to be used. A nearest neighbor is used by default. The *K*-nearest neighbor algorithm is created by calculating the neighborhood distances for each object. *K* parameter expresses how many neighbors will be classified in the algorithm [15]. Each object in the data set is checked to which class its *K* neighbors belong. The object is included in the class its neighbors are the most. In order to avoid equality, the value of *K* is generally chosen from odd numbers. In this study, the *K* value was chosen as 3.

**2.5. Performance Evaluation Criteria.** A variety of performance evaluation criteria were employed in this study to assess the overall performance of models developed using decision trees and support vector machines. The details are given in the above sections. While classifying the data set, the training-test ratios were 50-50% (Table 1).

### 3. Results and Discussion

The goal of our research was to use treatment protocols to diagnose Parkinson's disease. For this purpose, classifier algorithms are used. Classifier algorithms are applied to certain data groups and appropriate performance values obtained. Classifier achievements are shown in Table 2. The classifiers give the data groups the highest accuracy rate: 71% for baseline, 75% for MFCC, 72% for time, 64% for vocal, 80% for wavelet, and 85% for all. For each data group, there are classifier achievements with a certain accuracy. However, the highest accuracy is seen in all data groups, including each data group. The highest accuracy rate was seen in support vector machines (SVM) among the classification algorithms. The 85% accuracy (highest value) was obtained when 45% of the data in the group named all was taken and the SVM algorithm was used for classification. It can be said that the better results when 45% of the data set is trained, rather than 50%, maybe due to the ranking of the most relevant to the most irrelevant features in the data set. The support vector machine for sensitivity, F-measure, kappa, and AUC provides the highest success when looking at other performance criteria. Only for the originality criterion, the decision tree algorithm achieved a slightly higher success rate (0.02). Other performance criteria of the group with successful results are as follows: sensitivity: 0.94, specificity: 0.078, F-measure: 0.86, kappa: 0.72, and area under the ROC curve: 0.86.



TABLE 2: Classifier achievement data for each data group.

(a)						
Data set	Baseline data group			MFCC data group		
Performance criteria	Classifier algorithms		Classifier algorithms			
	Decision tree (DT)	kNN	SVM	Decision tree (DT)	kNN	SVM
Accuracy rate (%)	71.35	68.75	66.67	69.79	75	73.44
Sensitivity	0.75	0.7	0.72	0.6	0.72	0.7
Specificity	0.68	0.68	0.61	0.79	0.79	0.78
F-measurement	0.72	0.69	0.66	0.69	0.75	0.73
Kappa	0.43	0.38	0.33	0.4	0.5	0.47
Area under the ROC curve	0.71	0.71	0.68	0.72	0.72	0.72

(b)						
Data set	Time data group			Vocal data group		
Performance criteria	Classifier algorithms		Classifier algorithms			
	Decision tree (DT)	kNN	SVM	Decision tree (DT)	kNN	SVM
Accuracy rate (%)	66.15	67.71	72.4	61.98	64.06	63.02
Sensitivity	0.73	0.82	0.8	0.64	0.58	0.64
Specificity	0.59	0.53	0.65	0.6	0.7	0.63
F-measurement	0.65	0.65	0.72	0.62	0.64	0.63
Kappa	0.32	0.35	0.45	0.24	0.28	0.26
Area under the ROC curve	0.65	0.69	0.70	0.61	0.63	0.64

(c)						
Data set	Wavelet data group			Whole data group		
Performance criteria	Classifier algorithms		Classifier algorithms			
	Decision tree (DT)	kNN	SVM	Decision tree (DT)	kNN	SVM
Accuracy rate (%)	68.23	73.44	79.69	69.79	76.56	85.42
Sensitivity	0.81	0.76	0.97	0.6	0.81	0.94
Specificity	0.55	0.72	0.63	0.79	0.72	0.78
F-measurement	0.66	0.73	0.76	0.69	0.76	0.86
Kappa	0.36	0.47	0.59	0.4	0.53	0.72
Area under the ROC curve	0.69	0.74	0.82	0.70	0.78	0.89

#### 4. Conclusion

In our study, it was aimed to benefit from treatment protocols in diagnosing PD. The data set used in treatment protocols consisted of only the analysis of the voice recordings of the patients. In this way, the diagnostic process will be shorter and less costly. It will also reduce the workload of clinical staff and enable patients to have an easier diagnosis process.

There were many studies in the literature for PD diagnosis [6-20, 26]. Yücelbaş et al. created a data set by conducting the subjects to diagnose PD. The generated data set was grouped according to the age factor and analyzed using the Dual Density 1-D Wavelet Transform method [16-18]. However, it has been studied on a small data set with few features.

In another study, Badem et al. established a model with 87% accuracy using artificial neural networks. Two data sets

were used in the established model. One of the data sets consists of 23 features, while the other consists of 26 features [19-21]. The models with a high accuracy rate will not provide the same accuracy in large data sets. The number of data in the data set we use is quite large. Therefore, the models created in this article can produce more reliable results. Many data sets currently available in the literature have an uneven distribution. In the studies, a model was created without eliminating this imbalance [15]. In 2019, Mei et al., Wroge et al., and Bader Alazzam et al. [12-14] found high accuracy rates in their different studies. A comprehensive data set was used in the studies, but balancing was not done. We think that the data used in this study will work more stable because the model is created by balancing the subsampling method. In models created with unstable data, the system produces results prone to data with excess amount. The models proposed in this study are one step ahead of the literature, built with balanced data sets.

## *Retraction*

# **Retracted: The Current Antimicrobial and Antibiofilm Activities of Synthetic/Herbal/Biomaterials in Dental Application**

### **BioMed Research International**

Received 10 October 2023; Accepted 10 October 2023; Published 11 October 2023

Copyright © 2023 BioMed Research International. This is an open access article distributed under the Creative Commons Attribution License, which permits unrestricted use, distribution, and reproduction in any medium, provided the original work is properly cited.

This article has been retracted by Hindawi following an investigation undertaken by the publisher [1]. This investigation has uncovered evidence of one or more of the following indicators of systematic manipulation of the publication process:

- (1) Discrepancies in scope
- (2) Discrepancies in the description of the research reported
- (3) Discrepancies between the availability of data and the research described
- (4) Inappropriate citations
- (5) Incoherent, meaningless and/or irrelevant content included in the article
- (6) Peer-review manipulation

The presence of these indicators undermines our confidence in the integrity of the article's content and we cannot, therefore, vouch for its reliability. Please note that this notice is intended solely to alert readers that the content of this article is unreliable. We have not investigated whether authors were aware of or involved in the systematic manipulation of the publication process.

In addition, our investigation has also shown that one or more of the following human-subject reporting requirements has not been met in this article: ethical approval by an Institutional Review Board (IRB) committee or equivalent, patient/participant consent to participate, and/or agreement to publish patient/participant details (where relevant).

Wiley and Hindawi regrets that the usual quality checks did not identify these issues before publication and have since put additional measures in place to safeguard research integrity.

We wish to credit our own Research Integrity and Research Publishing teams and anonymous and named external researchers and research integrity experts for contributing to this investigation.

The corresponding author, as the representative of all authors, has been given the opportunity to register their agreement or disagreement to this retraction. We have kept a record of any response received.

### **References**

- [1] A. Moghaddam, R. Ranjbar, M. Yazdani et al., "The Current Antimicrobial and Antibiofilm Activities of Synthetic/Herbal/Biomaterials in Dental Application," *BioMed Research International*, vol. 2022, Article ID 8856025, 26 pages, 2022.

## Review Article

# The Current Antimicrobial and Antibiofilm Activities of Synthetic/Herbal/Biomaterials in Dental Application

Ali Moghaddam,<sup>1</sup> Reza Ranjbar<sup>1,2</sup>,<sup>ORCID</sup> Mohsen Yazdani<sup>1</sup>,<sup>ORCID</sup> Elahe Tahmasebi<sup>1</sup>,<sup>ORCID</sup> Mostafa Alam,<sup>3</sup> Kamyar Abbasi,<sup>4</sup> Zahra Sadat Hosseini,<sup>5</sup> and Hamid Tebyaniyan<sup>6</sup><sup>ORCID</sup>

<sup>1</sup>Research Center for Prevention of Oral and Dental Diseases, Baqiyatallah University of Medical Sciences, Tehran, Iran

<sup>2</sup>School of Dentistry, Baqiyatallah University of Medical Sciences, Tehran, Iran

<sup>3</sup>Department of Oral and Maxillofacial Surgery, School of Dentistry, Shahid Beheshti University of Medical Sciences, Tehran, Iran

<sup>4</sup>Department of Prosthodontics, School of Dentistry, Shahid Beheshti University of Medical Sciences, Tehran, Iran

<sup>5</sup>Department of Genetics and Biotechnology, School of Biological Science, Varamin-Pishva Branch, Islamic Azad University, Tehran, Iran

<sup>6</sup>Science and Research Branch, Islamic Azad University, Tehran, Iran

Correspondence should be addressed to Reza Ranjbar; ranjbarre@yahoo.com and Hamid Tebyaniyan; tebyan.hamid@yahoo.com

Received 26 May 2022; Revised 6 July 2022; Accepted 25 July 2022; Published 2 August 2022

Academic Editor: Zohaib Khurshid

Copyright © 2022 Ali Moghaddam et al. This is an open access article distributed under the Creative Commons Attribution License, which permits unrestricted use, distribution, and reproduction in any medium, provided the original work is properly cited.

Herbal and chemical products are used for oral care and biofilm treatment and also have been reported to be controversial in the massive trials conducted in this regard. The present review is aimed at evaluating the potential of relevant herbal and chemical products and comparing their outcomes to conventional oral care products and summarizing the current state of evidence of the antibiofilm properties of different products by evaluating studies from the past eleven years. Chlorhexidine gluconate (CHX), essential oils (EOs), and acetylpyridinium chloride were, respectively, the most commonly studied agents in the included studies. As confirmed by all systematic reviews, CHX and EO significantly control the plaque formation and gingival indices. Fluoride is another interesting reagent in oral care products that has shown promising results of oral health improvement, but the evidence quality needs to be refined. The synergy between natural plants and chemical products should be targeted in the future to accede to the formation of new, efficient, and healthy anticaries strategies. Moreover, to discover their biofilm-interfering or biofilm-inhibiting activities, effective clinical trials are needed. In this review article, therapeutic applications of herbal/chemical materials in oral biofilm infections are discussed in recent years (2010-2022).

## 1. Introduction

Skin, respiratory and gastrointestinal mucosa, and the oral cavity which covers most of the surface of the human body are colonized by bacteria and provide a specific environment for microorganisms [1]. Oral biofilm or dental plaque in the oral cavity of all mammals is one of the prime examples that is detected to be hosting seven hundred specific bacterial species [2]. As a dynamic microbial biofilm, dental plaque consists extracellular matrices (ECM) and numerous bacterial species containing common and pathogenic microorganisms [1]. In addition to bacteria, the oral cavity of the human contains hundreds of various viral and fungi species. Generally,

there may be over  $10^{11}$  microorganisms per milligram of dental plaque which can cause different dental pathologies including gingivitis, caries, and periodontitis. Biofilm-originated infections can lead to fundamental issues in society in terms of economical and health aspects [3]. Biofilms usually consume natural teeth and dental prosthesis materials including either dentures or implants, as well as organic acids as the substrates. The increased secretion of organic acids is attributed to the consumption of carbohydrate-rich food. With increasing oral bacterial colonization, the extracellular polymeric substance (EPS) such as polysaccharide alginate is also overproduced [2]. Such substance provides a mucoid biofilm that facilitates developing resistance to antibiotics and the host's

immune response [4]. As a result, the risk of chronic infections raises and their treatment becomes more difficult. Untreated infection for any reason causes enamel demineralization and dental caries [2, 4]. Dental caries and periodontal problems are common mouth and tooth diseases all over the world that affect almost every age and geographic communities [2]. In Europe, the incidence of dental caries is about 20-90 % in children at 6 years old and very close to 100% in adults. In the same population, 0.5-3.5 teeth of children at age 12 are conflicted by dental caries on average. Besides, the rate of severe periodontal (gum) disease in adults at middle ages and more advanced ages is 5-20% and 40%, respectively. In addition, people about 30% of the population have no natural teeth [5]. The loss of natural teeth due to dental caries and severe periodontal diseases can substantially affect the patients' tooth function and reduce their quality of life [5]. As a preventive strategy, the biofilms should be controlled appropriately to inhibit their physiological heterogeneity and interactions from developing dental mineralization and systemic inflammation [6]. The relationship between prosthetic loading or bacterial infection and implant failure has been indicated in the literature. The prevalence of mucositis and peri-implantitis has been reported to be around 30% and 9%, respectively [7]. This high prevalence of oral biofilm-related infectious diseases necessitates developing new and more effective treatments; as such in the US, over \$81 billion are spent annually on such research [8]. The accessibility and highly multibacterial environment of the mouth make it a suitable setting for studying new modalities of biofilm inhibition. Results from studies on the oral cavity can be also extended to other biofilm-associated issues pertaining human health or industrial purposes [8]. Despite the difficulties of biofilm eradication, through decades, several conventional strategies have been applied to control dental biofilms. A popular example is brushing as a mechanical method that can effectively remove biofilms. This physical method is a common and important way to remove biofilms from dentures and prevent infection but not enough. Evidence shows that for controlling the oral biofilms, some form of chemical and biological cleanser is also required [9]. Alkaline peroxides, in the form of tablets, are a common popular approach to clean dentures. When these tablets are added to water, an effervescent alkaline solution is produced that generates hydrogen peroxide and active oxygen that penetrate to areas not accessible for brush and clean them [10]. Antiplaque oral rinses play an important role in biofilms. Although rinses containing chlorhexidine gluconate and essential oils can effectively remove plaques, they may have unwanted side effects too. However, such chemicals can be associated with side effects such as tooth discoloration and occasional loss of taste. Therefore, essential oils are increasingly being conveyed and preferred as alternatives with low mammalian toxicities and side effects [11]. Because of the side effects and limited efficiency of classic chemicals in oral planktonic and biofilm eradication, the search for novel nature-inspired antibiofilm methodologies continues. In this regard, the note of Hippocrates saying "nature itself is the best physician" has been updated to the importance of the plant kingdom against biofilm-related dental diseases [12-14]. Then, in addition to using some enzymes for degrading the protein

matrices of biofilm, several naturals, herbal-based materials, or natural plant extracts have been added to some mouth rinse formulations for their anti-inflammatory and antimicrobial properties [11, 15]. Some herbal species with antiplaque properties existing in commercially available products are *Centella asiatica*, *Echinacea purpurea*, and *Sambucus nigra* [15]. Another example is naturally derived polyphenols that are being extensively discussed in scientific studies for their preventive and/or treating effects on many chronic infection/inflammatory-based diseases such as cardiovascular, metabolic, or neurodegenerative disorders and cancers, as well as oral diseases [16]. It is hoped that some of the materials discussed in this article will be able to be employed in dental research and industry, such as the development of dental sealers, lingual cements (are used in clinical dentistry to seal), biocompatible, bacteriostatic, nonshrinking, and nondispersible sealers are ideal for use, so that if a sealer was to extrude from the canal, it could be dissolved without causing damage to the tissue. Regardless of the type of root canal sealer used, all root canal sealers contain a certain level of toxicity. Therefore, even though newer sealers have been introduced that have been deemed highly biocompatible as a result, there is still a concern about their cytotoxicity. There have been numerous studies examining dental materials' cytotoxicity, especially soft tissues [17, 18]. In this review article, therapeutic applications of herbal and chemical materials in oral biofilm therapy in *in vitro*, *in vivo*, and clinical studies are discussed in the recent decade (2010-2022).

## 2. Research Methodology

In this review article, a comprehensive overview of the most important and critical aspects of the topic's knowledge is discussed. Several synthetic/herbal/biomaterials were investigated for their antimicrobial and antibiofilm activities. A search was performed on PubMed (2010-2022) using the keywords: (oral biofilm) OR (dental biofilm) AND (herbal treatment) AND (chemical treatment). A variety of sample types, microorganism species, methods, types of studies (in vitro, in vivo, and clinical), and results were evaluated in the studies.

## 3. Biofilm

**3.1. Biofilm and Diseases.** Similar to growth regulation, heterogeneity, proteolytic systems, and encapsulation in a self-created polymeric matrix, plaque formation is a survival mechanism taken by pathogenic microbes for adapting to stress conditions and host immunological responses. Biofilm formation is affected by the colonization area and matrix. Besides an important physical barrier against drugs, matrix provides a protective ecological niche for single or consortia microorganisms of several species to survive and/or cause diseases. The pathogenic species developing biofilms usually include fungal species (e.g., *Candida albicans*), gram-positive bacteria (e.g., *Staphylococcus epidermidis*, *Mycobacterium tuberculosis*, and *Mycobacterium abscessus*), and gram-negative bacteria (e.g., *Pseudomonas aeruginosa*) as well as *Mycoplasma pneumonia* that can develop resistance against



immune responses and drug leading to serious health concerns [19]. Regarding the endodontic, *Enterococcus faecalis* (*E. faecalis*) is the leading pathogenic agent specifically in secondary and persistent infections [20].

**3.2. Biofilm Formation.** Microbes can form biofilms on almost any surface generally through a sequence of attachment and assembling micro colonies that leads to a differentiated mature structure. Attachment involves bacterial deposition and adhesion by anchoring either of matrix or earlier colonies. Sedimentation, hydrodynamic forces, and Brownian motion account for deposition while intermolecular forces such as acid-base, Lifshitz–Van der Waals, hydrophobic, and electrostatic interactions manage bacterial adhesion to the substratum. OmpA, fibronectin-binding proteins (FnBPs), protein A32, SasG, and biofilm-associated protein (BAP) are other surface-associated proteins that contribute to the microorganismal attachment as the initial stage of biofilm formation [21]. Another main mechanism underlying biofilm formation is quorum sensing (QS) which is a cell-to-cell communication mechanism and has been detected almost in all microorganismal species including gram categories (Figures 1 and 2). Quorum sensing involves small signaling molecules that mediate colonization and control biofilm formation whose disassembly or dispersion only takes place through mechanical and active processes [21]. Resistance to bactericidal or bacteriostatic agents commonly occurs in planktonic cultures at concentrations normally inhibitory [22]. Describe resistance as the mechanisms through which an antimicrobial agent is prevented from interacting with its intended target [23]. Mutations and transfections (interspecies exchange of antibiotic resistance genetic elements) are the main mechanisms recognized as responsible for acquired resistance; however, some species have intrinsic resistance and phenotypes based on their wild-type genes. For example, gram-negative bacteria are intrinsically more resistant to antibiotics because of their less impermeable outer membrane. Accordingly, some biofilm-based resistance mechanisms such as antibiotic efflux pumps, matrix  $\beta$ -lactamases, and antibiotic sequestering molecules (such as eDNA and NdvB-derived periplasmic glucans) are discussed in this review [23].

**3.3. Oral Biofilm.** In the past 100 years, medical literature contained considerable interest toward bacteria at their planktonic phase presenting in host's mouth, while today, we know that oral microbiota is generally organized as biofilms [24]. The humidity, temperature, and nutrient-rich environment of the oral cavity provide an ideal ecosystem for differentiating microorganism communities and microbial biofilms. Biofilm formation respectively includes four main stages (Figure 3): pellicle formation, adhesion, aggregation, and maturation [25]. The structurally and functionally organized biofilm through bacterial succession on any surfaces in the oral cavity—that is not shed—is defined as dental plaque. Including a considerable diversity of microorganism species, the oral microbiota has a key role in protecting the human body by preventing health-affecting extrinsic bacteria from colonization. Losing the balance of this sensitive ecosystem due to immune system failure is proved to be a serious problem fac-

ing the systemic health. This imbalance may lead to oral diseases including caries, periodontitis, and gingivitis. The most common strategy for preventing oral diseases is the mechanical removal of biofilms from oral surfaces by regular tooth brushing; however, restorations and dental prostheses are other golden standard [24]. The summaries of therapeutic application of herbal and chemical materials *in vitro* and *in vivo* are presented in Table 1. In the following, the most applied and promising approaches and materials, including biological, chemical, and herbal agents, for preventing oral diseases due to dentine biofilms are reviewed.

## 4. Probiotics

Probiotics are live microorganisms and seem to be the only biological agents used for antibiofilm properties and benefit the host's health at an optimum amount [26]. Although probiotics are mostly well known for gastrointestinal applications, they can also modify the oral environment by competing with cariogenic and pathogenic oral bacteria and interfere with their colonization [27]. Literature implies the regular consumption of probiotics to be substantially effective in preventing or treating dental caries, halitosis, gingivitis, periodontitis, and even oral diseases due to candida infection [26, 27]. Species that can colonize and establish a healthy environment in the oral cavity mainly include *Lactobacillus*, *Bifidobacterium*, and *Streptococcus* species [27]. One mechanism suggested for the antibiofilm function of some commensals in the oral microbiota is producing alkaline compounds that contrast acidogenic bacteria such as *S. mutans* that causes acid stress [28]. The formed biofilms by probiotic bacteria are seen as beneficial because they are considered capable of promoting colonization and long-term stability in the mucosa of the host, preventing contamination by pathogenic bacteria. However, further research in this field is necessary to obtain more reliable evidence.

## 5. Chemical Antibiofilm Materials

**5.1. Nanoparticles and Nanomaterials.** The application of nanoparticles (NPs) as therapeutic agents was a revolution in medicine [29]. Nanomaterials were discovered in the 1980s and, since then, have been used for different purposes in the field of medicine with an extensive perspective of future development [30]. Nanomaterials are used as either antimicrobials for their inherent antimicrobial properties or drug delivery systems specifically designed to have affinity to dental surfaces [31]. Silver (Ag), copper oxide (CuO, Cu<sub>2</sub>O, Cu<sub>2</sub>O<sub>3</sub>, and CuO<sub>2</sub>), zinc oxide (ZnO), titanium oxide (TiO, TiO<sub>2</sub>, and Ti<sub>2</sub>O<sub>3</sub>), graphene (an allotrope of carbon), quaternary ammonium polyethyleneimine (QA-PEI), chitosan (CH), and silica (SiO<sub>2</sub>) nanoparticles are examples of numerous nanomaterials that can control biofilm formation [29, 32–36]. Among all, silver nitrate (AgNO<sub>3</sub>) and silver nanoparticles (AgNPs) are indicated as specific metal nanomaterials with one of the highest capacities to control the oral biofilm [37]. Despite the disadvantage of dentine discoloration by silver nitrate, it is considered a promising



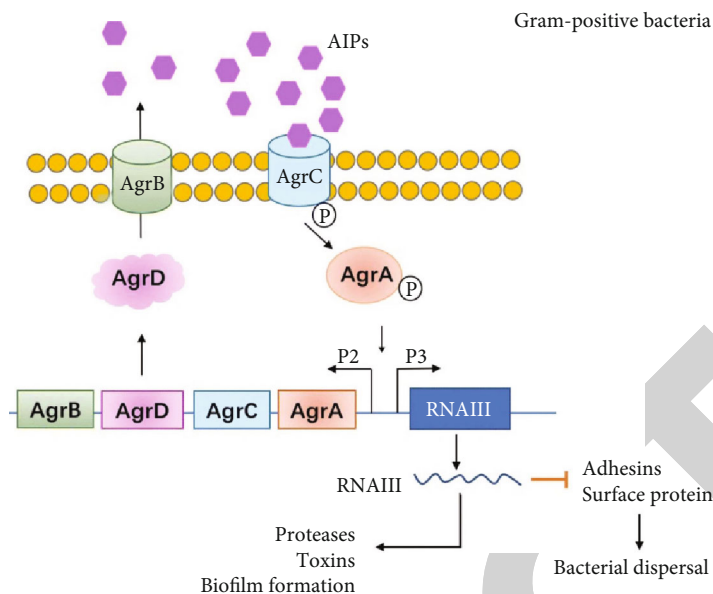


FIGURE 1: QS mechanism in gram-categorized species. The canonical QS signaling and the Agr system are the most typical processes involved in the biofilm formation in gram+ bacteria *S. aureus*. This system includes four genes (AgrA-D) under the control of one operon. The products of this operon include virulence factors such as toxins and proteases. AgrD is converted to autoinducer peptides (AIPs) during secretion through AgrB to out of the cell where it activates the transmembrane AgrC by phosphorylation. The activated AgrC further activates AgrA that promotes the expression of targeted genes by influencing two promoters (P2 and P3). P2 regulates the Agr operon system, and P3 activates the expression of RNAIII which is the key regulator of different factors relating QS and biofilm formation. RNAIII upregulates virulence factors and inhibits factors contributing to bacterial dispersal. The balancing QS function Agr proteins on bacterial swarming and infection makes them promising targets for developing therapeutic antibiofilm agents [69].

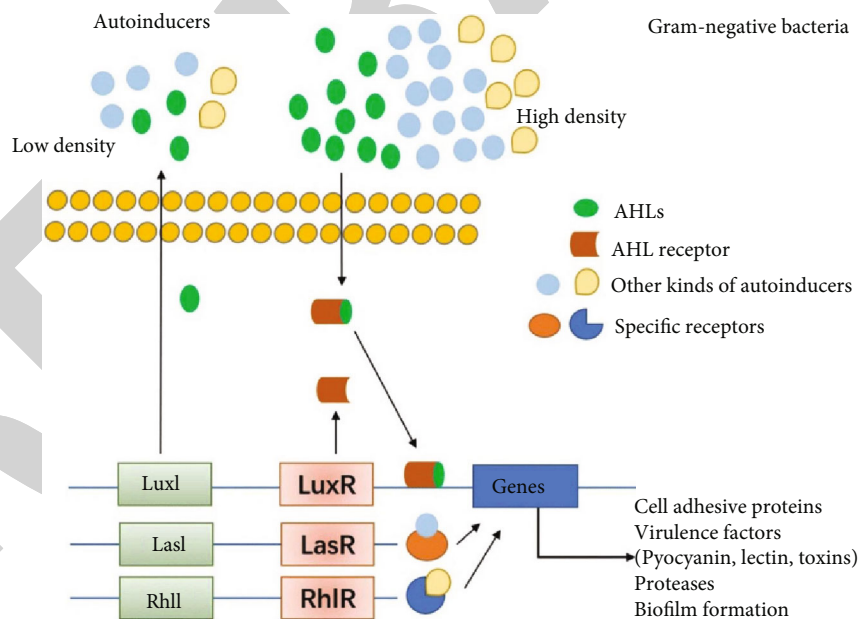


FIGURE 2: QS mechanism in gram-categorized species. In gram- bacteria biofilm formation, QS signaling involve autoinducer acyl-homoserine lactones (AHLs) that help communication among bacteria and modulate targeted genes expression by activating corresponding cytoplasmic receptors. The LuxI/luxR transcriptional factors are other essential regulating factors activated by AHLs and control the expression of various virulence factors in different gram- bacteria such as pigments, carbohydrate-binding proteins, various proteases such as elastase, toxin, different autoinducers such as *Pseudomonas* quinolone signal (PQS), CAI-1, and AI-2, as well as QS receptors such as LasI/LasR, RhII/RhIR, CqsS, and LuxPQ. Specific autoinducers can also further promote other adhesives and virulence factors [69].

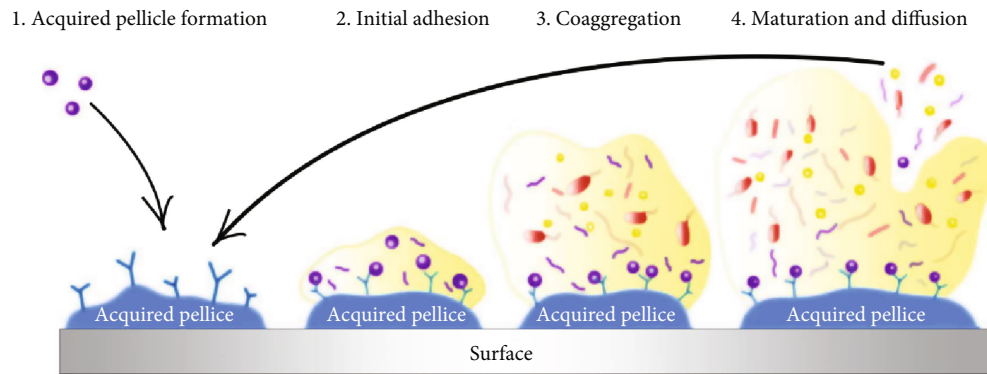


FIGURE 3: The four main stages of biofilm formation process in the oral cavity [25].

approach to coat dentin and prevent biofilm formation on dentin surfaces. AgNP gel can prevent the growth of bacteria and protect teeth from dental plaque formation and secondary caries by disrupting the structural integrity of biofilm created by most oral pathogens such as *E. faecalis* [20, 38]. Silver nanoparticles and silver nitrate can be administered as gel, irritant, and medicament with other materials such as chitosan and calcium hydroxide [28, 38]. Ag-CH-conjugated NPs can reduce biofilm formation contained *Streptococcus* species and *E. faecalis* on implants [24]. On the other hand, mesoporous silica nanoparticles in conjugation with chlorhexidine have a broad spectrum of action [39]. Such NPs have been used with restorative materials for inhibiting biofilm development with no adverse effect on their mechanical properties [40]. An inoculation of fresh *Bacillus subtilis* was used to prepare TiO<sub>2</sub> nanoparticles. Treatment with 5% TiO<sub>2</sub>-GIC (glass ionomer cement) was most effective in treating dental caries without producing any cytotoxic effects [41]. NaOCl is another antibiofilm material commonly used in endodontic treatment against *E. faecalis* with more irritating capacity compared to the AgNP solution. It is also a good vector for calcium hydroxide (Ca(OH)<sub>2</sub>) to be used in short-term as intracanal medication for removing *E. faecalis* dental biofilms [42]. Biological enzymes are also suggested for their potential of antibacterial function. They perform catalytic functions under strict physiological conditions. However, their broad applications are limited because of some drawbacks. Therefore, synthesis of molecules, complexes, and nanoparticles mimicking natural enzymes has recently been developed as an alternative to natural enzymes. The development of artificial biocatalysts has been accelerated by nanozymes exhibiting the properties of enzymes. Nanozymes offer several advantages over natural enzymes [43]. Synthetic polymers such as polyethylenimine or PEI (also known as polyaziridine) in two linear or branched structural architectures are other biomaterials used for their biocidal effects on oral pathogens. The chemical structure of the linear PEI (LPEI) (containing secondary amino groups) and branched PEI (BPEI) (containing primary, secondary, and tertiary amino groups) accounts for their antibacterial activity (Figure 4) [44]. The eradication of biofilms and resident bacteria using nanoparticles holds great promise. The clinical

translation of nanoparticles targeting specific microbial and biofilm features is best done with materials that are nontoxic. The effects of topically applied therapeutic agents on chronic biofilms, such as dental caries, require additional research to characterize.

**5.2. Modified Dental Materials.** Biomaterials have a widespread application in our everyday practice, and they are extensively passed through the next phase of the experiments which is modifications. Research advances indicate that biomaterials precoated with silanes, chlorhexidine, histatins, and antifungal drugs can inhibit biofilm formation at either initiation or development especially on difficult-to-access devices such as dentistry prosthesis [45]. For example, polymeric chlorhexidine-coated implant (the internal chamber) prevents bacterial colonization on the pre-implant locations and improve the microbiota quality by reducing species with a higher risk of future restoration failure [7]. Another surface modification is performed by photocatalytic irradiation of TiO<sub>2</sub>-coated biomaterials to kill bacteria on orthodontic wires and implants. Titanium-modified aminopropyl silane is also used for immobilizing active antibiotics such as vancomycin on surfaces [46]. It is vital that new materials are developed to discourage the formation of biofilms. In this study, dental materials that inhibit biofilm formation, inhibit biofilm growth, inhibit microbial metabolism in biofilms, kill biofilm bacteria, and detach biofilms are sought [47].

**5.3. Arginine.** Dietary carbohydrates such as arginine are considered a good supplement with antibacterial effects by limiting their virulence, growth, aggregation, and biofilm formation [48]. Arginine produced by oral commensals is another antibiofilm material used for preventing tooth enamels to be demineralized by oral acidogenic bacteria [28]. Arginine also reduces the biomass of dental polymicrobiota by inhibiting and limiting their colonization [48, 49]. L-arginine specifically prevents *S. mutans* from adherence to the tooth surface by suppressing glucan production and composition resulting in reduced EPS [48, 49]. The arginine function mechanism is creating periods of alkalization that can lead to remineralization and restoring the integrity of the enamel [28]. Oral pathogens such as *Actinomyces naeslundii*, *Actinomyces odontolyticus*, *Aggregatibacter*

TABLE 1: *In vivo* and *in vitro* studies in oral biofilm treatments.

Type	Method	Outcomes	Year/Ref
Herbal materials			
Apple-boysenberry beverage	Quantitation of <i>Lactobacillus</i> spp., <i>A. naeslundii</i> , and <i>S. mutans</i> in saliva samples using qPCR	The bioactive beverage reduced the proliferation of <i>Actinomyces</i> and <i>Streptococci</i> down to almost half.	2017/ [115]
Cranberry proanthocyanidins	The antibiofilm and anticaries effects of proanthocyanidin's against <i>S. mutans</i> was assessed <i>in vitro</i> and <i>in vivo</i> , respectively.	Proanthocyanidin treatment inhibited smooth-surface caries in rats.	2010/ [80]
Toothpaste and mouth rinse containing natural/herbal agents	Six commercially available products were compared to PBS as control on artificial plaque in animal model.	Four mouth rinses (Tom's Propolis & Myrrh®, Colgate Total 12® toothpaste, Malvatricin® Plus, and PerioGard®) significantly reduced the biofilm viability.	2019/ [116]
<i>Zingiber officinale</i>	The crude and methanolic extracts of ginger were evaluated at sub-MIC levels on <i>S. mutans</i> caries <i>in vitro</i> and <i>in vivo</i> .	Both extracts showed strong anticariogenic effect.	2015/ [117]
<i>Roselle calyx</i>	The antibacterial activity of the herbal extract was studied on eight oral bacterial strains <i>in vitro</i> .	The extract showed antibacterial activity especially against <i>F. nucleatum</i> , <i>P. intermedia</i> , and <i>P. gingivalis</i> .	2016/ [118]
<i>Terebinthifolius</i> and <i>Croton urucurana</i>	The antiadherent and antibiofilm potentials of plants were studied <i>in vitro</i> by evaluating their minimal concentration of adherence (MICA).	Both herbal extracts inhibited <i>S. mutans</i> and <i>C. albicans</i> from forming biofilm.	2014/ [119]
Garlic	The MIC of garlic extract against <i>S. mutans</i> was studied <i>in vitro</i> .	Garlic extract increased the biofilm formation of <i>S. mutans</i> on the orthodontic wires.	2011/ [120]
Limonoids	The antibiofilm activity of limonoids against <i>Vibrio harveyi</i> was evaluated <i>in vitro</i> .	Limonoids showed significant modulatory functions interfering with biofilm formation.	2011/ [73]
Hordenine	The inhibitory activity of hordenine against quorum sensing was studied using high-resolution microscopy and RT-PCR.	Hordenine inhibited quorum sensing of foodborne pathogens by competing with their signaling molecules.	2018/ [74]
Quercetin	The effect of quercetin on <i>P. aeruginosa</i> biofilm and virulence factors was studied <i>in vitro</i> .	Quercetin effectively inhibited the biofilm formation and reduced <i>P. aeruginosa</i> virulence.	2016/ [75]
Red wine Dealcoholized red wine Red wine extract (with or without grape seed)	The effect of seed extract on an oral supragingival plaque model was studied <i>in vitro</i> and using high-resolution microscopy.	Solutions spiked with seed extract showed antimicrobial effect on 3 of 5 studied strains ( <i>F. nucleatum</i> , <i>S. oralis</i> , and <i>A. oris</i> ). Red wine and dealcoholized	2014/ [121]

TABLE 1: Continued.

Type	Method	Outcomes	Year/Ref
<i>Myristica fragrans</i>	MIC and MBC tests were performed using the ethanol and ethyl acetate extracts of seed and mace of plant in vitro.	wine showed antimicrobial effects on 2 strains ( <i>F. nucleatum</i> and <i>S. oralis</i> ). The ethanol extract of the plant displayed better antimicrobial potential compared to the ethyl acetate extracts.	2012/ [122]
<i>Olea europaea</i> , <i>Inula viscosa</i> , and mastic gum	MIC and the MBC assays were performed against oral microbiota (10 bacteria and 1 yeast) in vitro.	The most considerable antimicrobial effect belonged to the ethyl acetate extract of <i>I. viscosa</i> and the total extract of mastic gum.	2014/ [123]
The essential oils of <i>Citrus limonum</i> and <i>Citrus aurantium</i>	The antibiofilm effect was studied in vitro against <i>C. albicans</i> , <i>E. faecalis</i> , and <i>E. coli</i> .	Both essential oils displayed antibiofilm effects against all species.	2014/ [124]
The commercially available essential oils of 15 plants	MIC and MBC test against a panel of oral bacteria was performed in vitro.	The essential oil of <i>Cinnamomum zeylanicum</i> displayed a moderate antimicrobial effect on <i>Fusobacterium nucleatum</i> , <i>Actinomyces naestlundii</i> , <i>Prevotella nigrescens</i> , and <i>Streptococcus mutans</i> .	2016/ [125]
Aqua extract of <i>Hypericum perforatum</i>	Colorimetry, microtitration, and resazurin assays were performed using <i>S. mutans</i> , <i>S. sobrinus</i> , <i>L. plantarum</i> , and <i>E. faecalis</i> .	The extract showed high antibacterial potential against <i>S. sobrinus</i> and <i>L. plantarum</i> but moderate antibacterial potential against <i>S. mutans</i> and <i>E. faecalis</i> .	2016/ [126]
Essential oils extracted from 8 Guatemalan medicinal plants	MIC assay was exerted in vitro on <i>S. aureus</i> , <i>E. coli</i> , <i>S. mutans</i> , <i>L. acidophilus</i> , and <i>C. albicans</i> .	<i>S. mutans</i> showed high sensitivity to all used essential oils. <i>C. albicans</i> was sensitive to 4 species.	2015/ [127]
<i>Ligustrum robustum</i>	In vitro microbial tests and high-resolution microscopy were used to assess the effect of herbal extract against <i>S. mutans</i> biofilm and exopolysaccharide formation.	The extract downregulated the expression of quorum sensing factors and genes encoding glucosyltransferase in <i>S. mutans</i> .	2021/ [96]
Quercetin Kaempferol	MIC and MBC assays were evaluated in vitro using <i>S. mutans</i> .	These materials reduced biofilm formation, protein expression, cell proliferation, and glucan production.	2019/ [128]
<i>Houttuynia cordata</i> ethanol extract (wHCP)	The antimicrobial and antibiofilm potentials of a water solution of extract were evaluated on a number of oral pathogens in vitro.	wHCP showed limited antimicrobial potential but high antibiofilm effects against <i>F. nucleatum</i> , <i>S. mutans</i> , and <i>C. albicans</i> .	2016/ [93]
<i>LongZhang</i> gargle	The antibiofilm and antiacid effects of <i>LongZhang gargle</i> on <i>S. mutans</i> were evaluated in vitro.	<i>LongZhang Gargle</i> displayed a significant antimicrobial activity.	2016/ [129]
<i>Equisetum giganteum</i> <i>Punica granatum</i>	In vitro microbial tests and microscopy were used to test herb extracts' potential against <i>Candida albicans</i> .	Herb extracts synergized the antibiofilm effect of adhesive materials.	2018/ [130]

TABLE 1: Continued.

Type	Method	Outcomes	Year/Ref
<i>Azadirachta indica</i> <i>Mimusops elengi</i> <i>Chlorhexidine gluconate</i> <i>Mangifera indica</i> <i>Ocimum sanctum</i>	The remaining microbial load on the extracted tooth sections after the antimicrobial treatment was evaluated in vitro. <i>E. faecalis</i> planktonic growth was tested in vitro. The molecular effect of sub-MIC volume of the essential oil loaded on a chitosan nanogel was evaluated on biofilm formation-associated gene expression of <i>S. mutans</i> .	Herb extracts displayed significant antimicrobial effects. Herb extracts significantly reduced the growth amount.	2015/ [131] 2013/ [132]
<i>Mentha piperita</i> essential oils	The antibiofilm effects of MIC and MBC levels of herb extracts were evaluated on <i>Enterococcus faecalis</i> .	The expression levels of <i>gtfB</i> , <i>gtfC</i> , <i>gfpD</i> , <i>gpbB</i> , <i>spaP</i> , <i>brpA</i> , <i>relA</i> , and <i>vicR</i> genes showed alterations.	2019/ [82]
Methanolic extracts of <i>Myrtus communis</i> L. and <i>Eucalyptus galbie</i>	Molecular tests were used to assess the antibacterial effect of herbal and chemical medicaments against <i>E. faecalis</i> .	The herb extracts had significant antimicrobial potential.	2019/ [133]
<i>Piper nigrum</i> <i>Piper longum</i> <i>Zingiber officinale</i>	The extract was applied to the polymicrobial plaque model in vitro. The effect of herb oil was studied on <i>Fusobacterium nucleatum</i> and <i>Actinomyces naeslundii</i> biofilm formation in vitro and using high-resolution microscopy.	The herb extracts showed antibacterial activity lower than calcium hydroxide and higher than saline. GCE inhibited excess acid production by the biofilms.	2019/ [134] 2012/ [88]
<i>Galla chinensis</i> extract (GCE)	Three concentrations of herb extract were examined on <i>E. faecalis</i> biofilm formation.	Thymol and thymoquinone (the active constituents of herbal oil) have an inhibitory effect on biofilm formation.	2020/ [87]
<i>Garlic</i> extract	The antibiofilm effect of herb extract against <i>S. mutans</i> was studied ex vivo on tooth substrate.	The biofilm production significantly decreased in a concentration-dependent manner.	2015/ [135]
<i>Triphala</i>	Clinical-isolated coagulase-negative <i>staphylococci</i> and <i>S. epidermidis</i> were used for assessing the antibacterial activity of EEPP in vitro.	<i>Triphala</i> significantly reduced the biofilm formation by <i>S. mutans</i> .	2014/ [136]
Chemical materials	Digital photography was used in orthodontic patients.	EEPP reduced bacterial growth and biofilm formation.	2013/ [137]
Ethanollic extract of Polish propolis (EEPP)	Periodontal therapy was performed for six months, and microbial/clinical outcomes were assessed in the clinic.	Chlorhexidine varnish decreased bacterial growth. Compared to GPAP, EPAP was less abrasive and produced smaller particles.	2015/ [138] 2015/ [139]
Chlorhexidine varnish			2016/ [140]
Erythritol powder			
Dentifrice containing <i>Eugenia uniflora</i>			



TABLE 1: Continued.

Type	Method	Outcomes	Year/Ref
Methylene blue-loaded poly(lactic-co-glycolic) nanoparticles (MB-NP)	The antibacterial effect of the dentifrice on 3 oral bacteria ( <i>S. mutans</i> , <i>S. oralis</i> , and <i>L. casei</i> ) was examined in vitro. MB-NP was applied to multistrain dental biofilm in vitro and followed by photodynamic therapy (PDT).	The tested dentifrice had significant antibacterial effect. The combination of MB-NP and PDT resulted in improving clinical parameters.	2016/ [141]
MB-NP	Dental plaques underwent PDT in a clinical pilot study. Planktonic and biofilm phases were assessed in vitro.	PDT was confirmed as a safe treatment that improved clinical parameters.	2016/ [141]
Stannous fluoride and zinc citrate dentifrice	Mineralized biofilms were used to examine the antibiofilm potential of mouthwash in vitro and in vivo.	The used dentifrice decreased calcium accumulation in the biofilm.	2017/ [142]
Stannous fluoride or triclosan dentifrices	The effects of two dentifrices on oral biofilm models (acid production/glycolysis inhibition) and plaque growth were assessed in vitro and in vivo, respectively.	Stannous fluoride dentifrice significantly reduced glycolysis and plaque growth.	2017/ [143]
3 commercially available kinds of toothpaste Chlorhexidine	The bactericidal effect of materials on a baseline biofilm flora was examined in vitro.	All kinds of toothpaste showed significant bactericidal effects but were lower than the chlorhexidine mouth rinse.	2018/ [144]
Doxycycline hyclate-containing resin	<i>S. mutans</i> microbial load was evaluated after a 3-month clinical trial.	The composite resin could eliminate all bacteria.	2018/ [145]
Toothpaste containing zinc oxide, zinc citrate, and L-arginine	All silica-based kinds of toothpaste were used on the oral bacteria on the teeth, tongue, cheeks, and gums.	The designed product could significantly reduce bacterial load in all samples.	2018/ [146]
Polysiloxane- and chlorhexidine-containing alcoholic solution	The bacterial load on bilateral fixed prostheses or crown restorations with a medicament-coated internal chamber was tested in a clinical study by molecular assays.	Polymeric chlorhexidine-coated implants displayed a limiting effect on the bacterial load of the peri-implant tissue.	2019/ [7]
Propolis solution Alkaline peroxide	Digital photography and microbiological quantifications were performed on <i>Candida spp.</i> and <i>S. mutans</i> biofilms.	Both materials displayed significant bactericidal and antifungal effects.	2019/ [147]

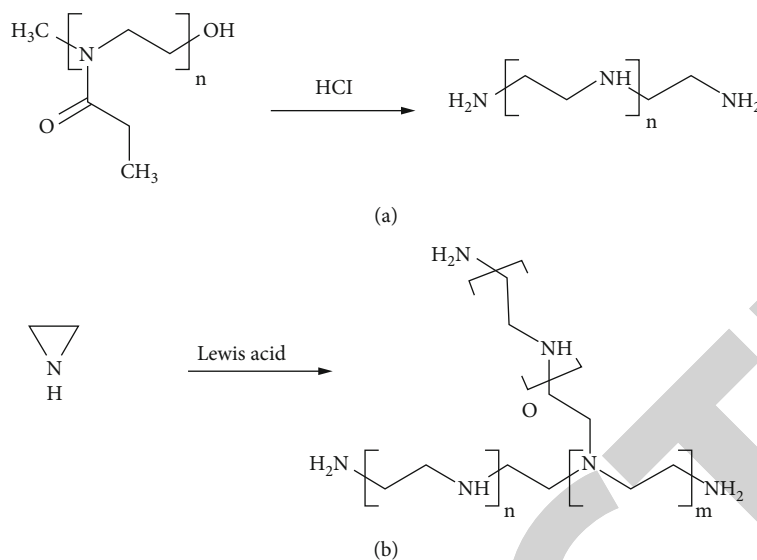


FIGURE 4: The synthesis of (a) linear polyethyleneimine and (b) branched polyethyleneimine [44].

*actinomycetemcomitans*, *Enterococcus faecalis*, *Fusobacterium nucleatum*, *Lactobacillus acidophilus*, *Porphyromonas gingivalis*, and *Candida albicans* are shown to be inhibited by protamine which is a polycationic protein rich in arginine residues [48]. The arginine deiminase system (ADS) is a dominant pathway of arginine metabolism that involves oral streptococci species (e.g., *S. australis*, *S. cristatus*, *S. gordonii*, *S. intermedius*, *S. sanguinis*, and *S. parasanguinis*), some *Lactobacillus* species, and a few numbers of *Spirochete* species [49]. Recently, an in vitro study indicated that L-arginine (1.5%) could enrich *S. gordonii*, suppress *S. mutans*, and inhibit *P. gingivalis/Prevotella oris* coaggregation [48].

Exogenous arginine has been recognized as a promising method for inhibiting biofilm formation, and several arginine-containing products are developed in this regard. An example is arginine-containing toothpaste that has been shown to increase ADS activity in dental caries leading to an oral bacteria composition resembling to that of healthy individuals [49]. 7% arginine added to dental adhesives has been shown to be a safe way to improve the dental biofilm composition without affecting its mechanical properties. Arginine and NaF have offered an ecological control approach on multispecies biofilms since they have shown synergistic preventive effect on *S. mutans*, enriching effect on *S. sanguinis*, and suppressing effect on *P. gingivalis* overgrowth [48]. In a study by Nascimento et al., a HOMIM online analysis tool was used to generate microbial community profiles from the scanned HOMIM arrays (<http://bioinformatics.forsyth.org/homim/>). A specific taxon in a multispecies sample was detected by a fluorescent spot for that particular probe. The hybridization spots were used to calculate the mean intensity for each taxon. There is a limit of detection of about 104 cells for organisms represented by 0.1% of the total sample. Using this method, Nascimento et al. concluded that toothpaste containing 1.5% arginine can induce dental plaque by increasing arginine availability in the oral environment [50].

**5.4. Quaternary Ammonium Salts (QAS).** Various composite resin and adhesive systems are common and favorable restorations recognized for their esthetic properties. However, they show about 50% failure rate within ten years mainly due to secondary caries caused by plaque formation. This is while despite the significant improvement mechanical properties and wear resistance of dental composites, their antibacterial properties have remained limited [51]. Then, some efforts such as antibacterial additives (antibiotics, Ag ions, etc.) in the resin and adhesive systems have been made to inhibit secondary caries. QAS are polycations with beneficial traits such as high molecular weight, nonvolatility, chemical stability, low toxicity, and antimicrobial activity against a wide range of microorganisms [52, 53]. Therefore, QAS are firstly used in mouthwash to control oral biofilm in the 1970s; then, they were examined as additives into the resin and adhesive systems and in the 1990s were added into dental composite materials [52, 53]. QAS antibacterial mechanism includes binding to the negatively charged bacterial cell membrane through their positive charge leading to bacterial cell membrane lysis [54].

Recently, the combination of QAS with other compounds has been considered for the development of new composites. Quaternary ammonium dimethacrylate (QADM) is a type of combined QAS with reactive groups on both dimethacrylate ends and can be incorporated into resin without reducing their mechanical features [55]. Also, Imazato et al. have developed a complex QAS (12-methacryloyloxydodecyl-pyridinium bromide or MDPB) with strong antibacterial and antibiofilm effects against *E. faecalis*, *F. nucleatum*, *Prevotella nigrescens*, and *S. mutans* [56]. MDPB has been also used in combination with methacryloxylethyl cetyl dimethyl ammonium chloride (DMAE-CB) and could have limited oral pathogens' growth and adherence [57]. Another copolymer using QAS has been constructed by copolymerizing ionic dimethacrylate (IDMA) and methacrylates such as bisphenol A glycerolate dimethacrylate. The obtained polymers have displayed antibacterial

effect on dental composites leading to a reduction of *S. mutans* colonization [58]. Furthermore, IDMA-1 in corporation with silver nanoparticles and calcium phosphate (CaP) particles has been used for developing composite resins and showed augmented bactericidal activity without compromising their mechanical properties [59].

**5.5. Small Molecules.** Interfering the formation of oral biofilm using small molecules with adequate biostability, low effective concentration, and low cytotoxicity is a novel strategy to control dental plaques biofilm formation [59]. The imbalanced homeostasis between the oral microflora diversity and the host's immune system is called dysbiosis. Several products have been studied for treating such microbial imbalance. DMTU (1,3-di-m-tolyl-urea) is a small molecule that can inhibit QS communication system in single or multibacterial species. It has proved inhibitory effects against *S. mutans* biofilm formation as well as multispecies biofilm models. For example, Kalimuthu et al. have used *Streptococcus gordonii* as an early colonizer, *Fusobacterium nucleatum* as a bridge colonizer, and *Porphyromonas gingivalis* and *Aggregatibacter actinomycetemcomitans* as late colonizers to develop a multispecies oral biofilm model and demonstrates the anti-microflora effect of DMTU against the planktonic cells in the multispecies biofilm model [60]. ZY354 is another synthetic small molecule with low toxicity against human oral cell lines and acceptable bactericidal function against common oral streptococci (i.e., *S. mutans*, *S. gordonii*, and *S. sanguinis*). A relevant study showed that treating multispecies biofilms with ZY354 reduced demineralizing activity at the interface of biofilm and enamel showing promising potentials for anticaries clinical purposes [61].

## 6. Herbal and Natural Materials in Oral Biofilm Treatments

There are biologically active natural products with uncertain structures that show favorable antibiofilm effects when used as alternative or adjunctive therapies. Polyphenols are examples originated from nature that has at least one aromatic ring with single or several hydroxyl groups and is a group of active compounds found in tea, propolis, cranberry, *Galla chinensis*, grapes, coffee, and cacao [59]. Chemical, herbal, and natural antibiofilm material mechanisms are described in Figure 5.

**6.1. Green Tea.** Firstly, being popular for its effectiveness in reducing body weight, green tea has medical properties such as anticancer, antioxidant, antiprophyllaxis, and antimicrobial as well as anticaries activities. Then, its extract has been used in mouthwash for reducing the bacterial load of saliva (*S. mutans* and *Lactobacilli*) via inhibiting their proliferation, attachment, and some metabolic functions such as acid production of acidogenic species [62]. A main effective component in green tea with antimicrobial properties is catechin whose different types are categorized into four main types: epicatechin (EC), epicatechin-3-gallate (ECG), epigallocatechin (EGC), and epigallocatechin-3-gallate (EGCG). EGC and EGCG constitute the biggest proportions and center most studies showing a variety of antimicrobial properties

[63]. Tea catechins also reduce the cariogenic properties of starch-containing nutrients by suppressing the salivary amylase activity [57, 63]. Even in a study by Xue et al., the anticaries and anticariogenicity effects of EGCG have been shown to be associated [57]. Also, the powerful antimicrobial properties of EGCG against *E. faecalis* and *S. mutans* as well as its suppressive effects on their virulence genes have been verified by multiple studies [63].

**6.2. Propolis.** A powerful antifungal and antibacterial agent, propolis also promotes healing of inflammation and has antioxidant properties. A widely studied active component of propolis is caffeine phenethyl ester (CAPE). Antiviral and antibacterial activities are among the many biological activities of CAPE. A previous CAPE study demonstrated effective antifungal action against *C. albicans*. Biofilm formation and hyphal growth of *C. albicans* are inhibited by it as well [64]. Propolis in the form of ethanol extract (EEPs) is an herb-originated nontoxic product that is usually used as a dietary supplement and antibacterial agent [65]. The flavonoids, cinnamic acid-derived material, and bioactive fatty acid contents are considered the main bioactive constituents that inhibit bacterial growth and adherence and exert anticaries effect in propolis [65]. EEP displays an inhibitory effect comparable to chlorhexidine (CHX) against *A. israelii*, *C. albicans*, *Lactobacilli*, *P. gingivalis*, and *P. intermedia* [65, 66].

**6.3. Garlic.** Garlic or *A. sativum* is known as a plant with various antimicrobial compounds. Its extract exhibits inhibitory effects on QS, QS signaling, and virulence factors such as biofilm formation in several microorganisms [67, 68]. N-(Heptylsulfanylacetyl)-L-homoserine lactone is one of the most potent components in garlic that is responsible for interrupting QS signaling and inhibiting QS and some transcriptional regulators (e.g., LuxR and LasR) [69]. The rapid clearing effect of garlic extract in respiratory burst due to tobramycin-sensitive *P. aeruginosa* through phagocytosis by polymorphonuclear leukocytes (PMNs) was found by Bjarnsholt et al. [70]. There are different components of garlic which are presented in Figure 6. Some other phytochemical compounds in the solvent extract of garlic bulb are carbohydrates, proteins, alkaloids, saponins, flavonoids, tannins, and steroids that exert a wide range of antidental caries (Figure 7) [71]. Many studies have approved that the garlic extract has antibacterial, antiviral, and antifungal activities (Figure 8).

**6.4. Phloretin.** Phloretin is a component found in apple with antioxidant, antibiofilm, and antivirulence properties against strains such as *E. coli* O157:H7 and *S. aureus* RN4220 and SA1199B. Phloretin suppresses fimbria production, adhesion to host cells, and the inflammatory response induced by the tumor necrosis factor-alpha, but does not affect bacterial growth in their planktonic phase. Phloretins repress hlyE and stx (toxin genes), lsrACDBFs (autoinducer-2 importer genes), csgA and csgB (curli genes), and prophage genes and also target efflux proteins [72]. According to mentioned study, phloretin may also act as an anti-inflammatory agent in inflammatory diseases and as an inhibitor of biofilm formation.

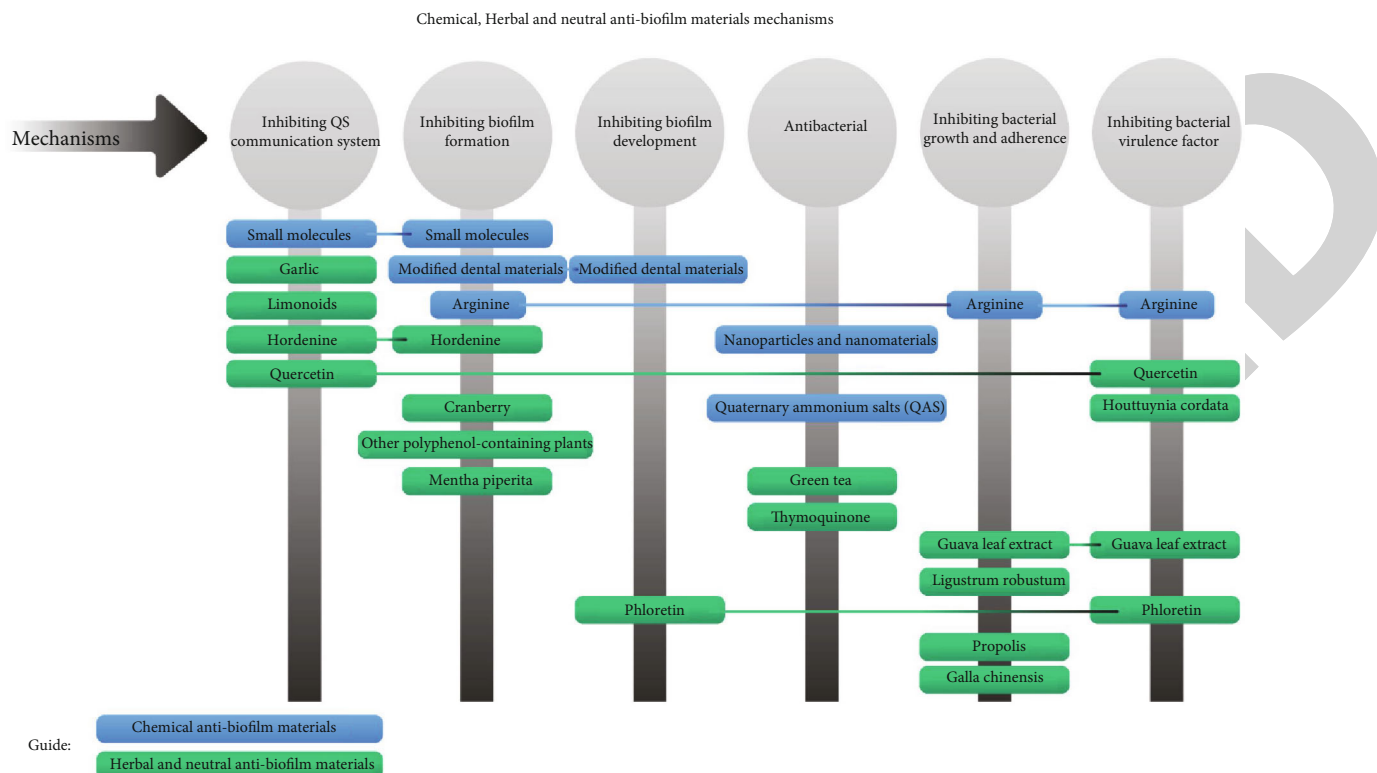


FIGURE 5: Antibiofilm activities and mechanisms of herbal and neutral materials.

6.5. *Limonoids*. Limonoids or triterpenoid are secondary metabolites in citrus that interfere with cell to cell signaling, plaque formation, and the type III secretion system in *Vibrio harveyi*, probably via modulating the luxO expression by isolimonic acid and/or ichangin. Isolimonic acid interferes with QseBC/QseA-dependent cell to cell signaling by inhibiting AI-3/epinephrine activation [73]. Biofilm formation can be inhibited by preventing quorum sensing signaling, as can be seen in other compounds later in this article.

6.6. *Hordenine*. Zhou et al. also showed the concentration-dependent decreasing effect of hordenine on signaling molecule production in foodborne pathogen *P. aeruginosa* and block its QS-controlled phenotypes including biofilm formation [73, 74]. The anti-QS function of hordenine is a competitive inhibition toward signaling molecules [74]. Hordenine in combination with nanoparticles (NPs) such as AuNPs has displayed an enhanced antibiofilm effect on *P. aeruginosa* PAO1 [74].

6.7. *Quercetin*. As a plant-originated polyphenol, quercetin shows effective biofilm-limiting, antivirulence, and anticaries properties, namely, against *P. aeruginosa*, *Streptococcus pneumoniae*, *S. mutans*, and *E. faecalis* [75]. The quercetin found in fruits, grains, and vegetables suppresses the activity of virulence factors such as pyocyanin and proteases at a much lower effective concentration than that of other herbal extracts and substances [74, 75]. From a mechanistic view, quercetin significantly reduces the expression of QS-associated genes including LasI, LasR, RhlI, and RhlR as well

as suppressing sialic acid expression by inhibiting SrtA [75, 76]. These studies explain the potential of quercetin for antimicrobial applications and therapies. Quercetin also shows synergistically increased antibiofilm activities in conjugation with nanoparticles that has opened up a novel therapeutic approach for preventing microbial infections [69, 75].

6.8. *Cranberry*. Cranberry is most popular for antibacterial properties owing to its various antioxidant bioactive contents such as anthocyanins, flavonols, flavan-3-ols, phenolic acid derivatives, and tannins [77]. This potential enables cranberry to fight not only cardiovascular diseases and cancer but also a variety of bacterial infections against pathogens including *E. coli*, *Helicobacter pylori*, *Salmonella species*, *S. aureus*, and *S. mutans* [78]. Accordingly, mouthwash products containing the extract of this fruit have reduced the bacteria counts in dental caries and periodontal diseases after daily use [79]. The most active components in cranberry are proanthocyanins (PACs) and flavonols that show a powerful disruptive effect on biofilm formation. The high concentration of purified A-type PAC leads to reducing *S. mutans* biofilm formation and diminishes its acidogenicity [80]. Kim et al. have indicated that PAC oligomers associated with myricetin break down the microarchitecture of cariogenic biofilms, decrease the insoluble EPS amount, and neutralize the acidic microenvironment at the biofilm-apatite interface. These functions cause alternating cell surface molecules, reducing the bacterial hydrophobicity, and prevention of bacterial coaggregation [81]. Polymerization-degree (DP) investigations on PAC oligomer have shown the highest biofilm disruption effect on the



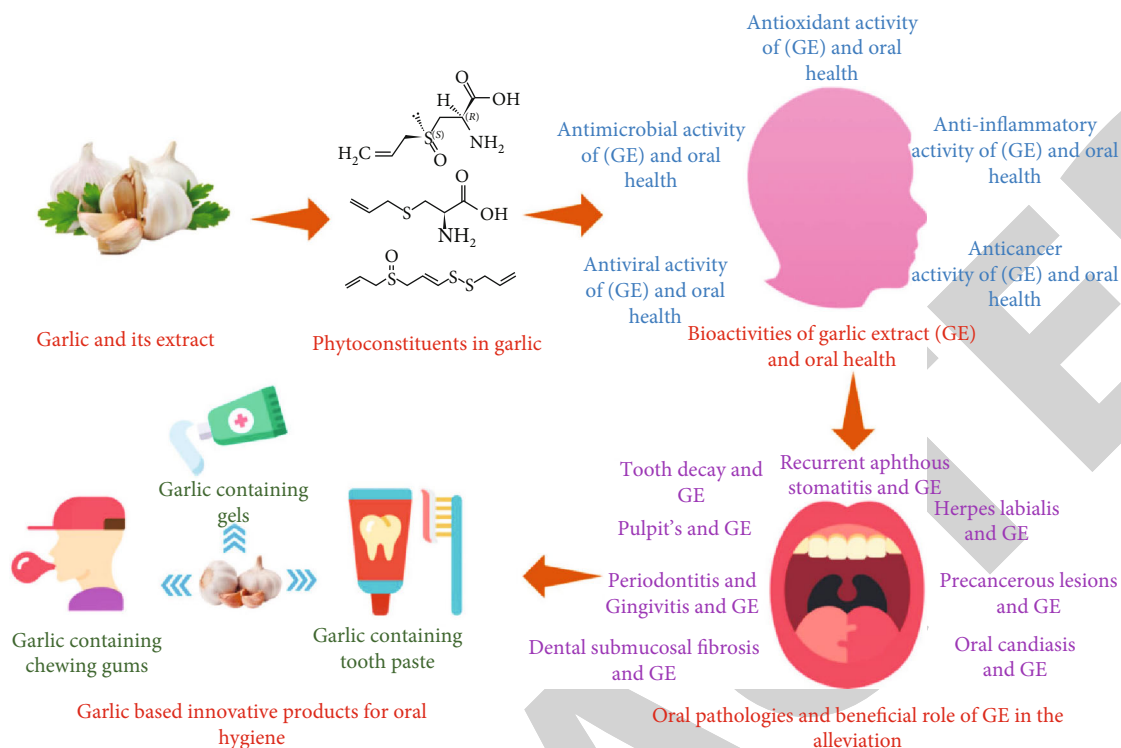


FIGURE 6: Different components of garlic [71].

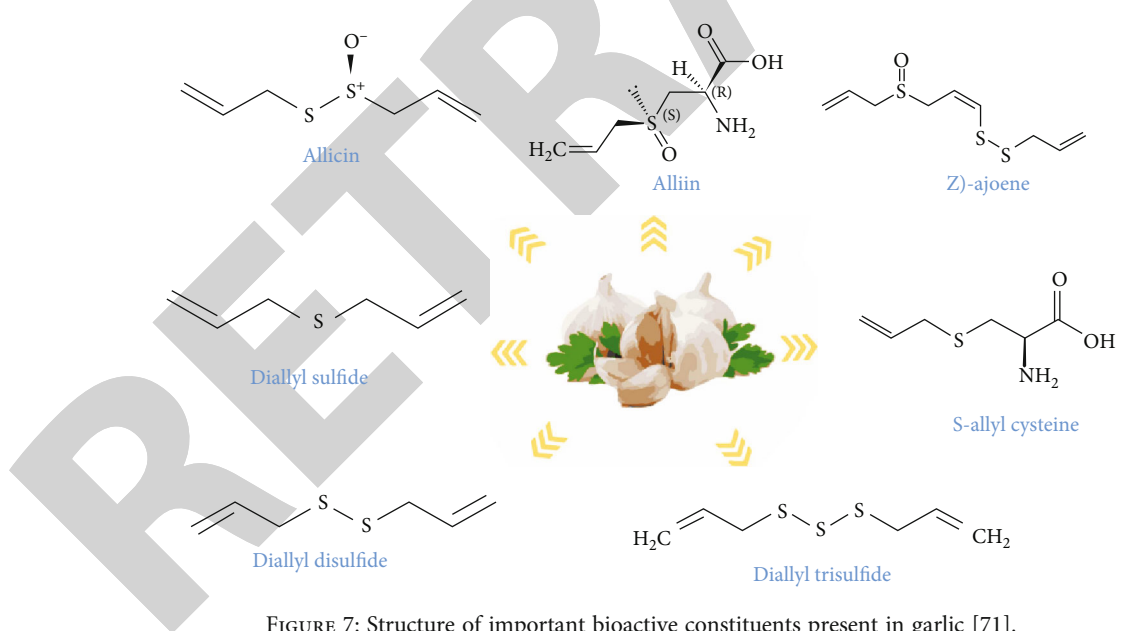


FIGURE 7: Structure of important bioactive constituents present in garlic [71].

bacterial adhesion in DP 4 and DP 8 to 13, especially on smooth surfaces [82–84]. Overall, PACs are suggested as ideal alternatives to or adjunctive for anticaries chemotherapy [85].

6.9. *Thymoquinone*. Black cumin or *Nigella sativa* is an important medicinal plant with treating potentials for a variety of disorders including diabetes, cancer, and reproductive disorders as well as several infectious diseases. Its seeds show anti-inflammatory, antioxidant, immunomodulatory, anal-

gesic, bronchodilatory, hepatoprotective, and spasmolytic properties such as antidiabetic, anticancer, and antimicrobial. Its essential oil components such as thymoquinone (TQ) are responsible for most of its biological activities [86]. In an animal study, Ozdemir et al. fed periodontitis models with thymoquinone and showed a significant reduction in gingival inflammation and alveolar bone loss [86]. These findings warrant further studies on the antibacterial and anti-inflammatory properties of TQ and its potential



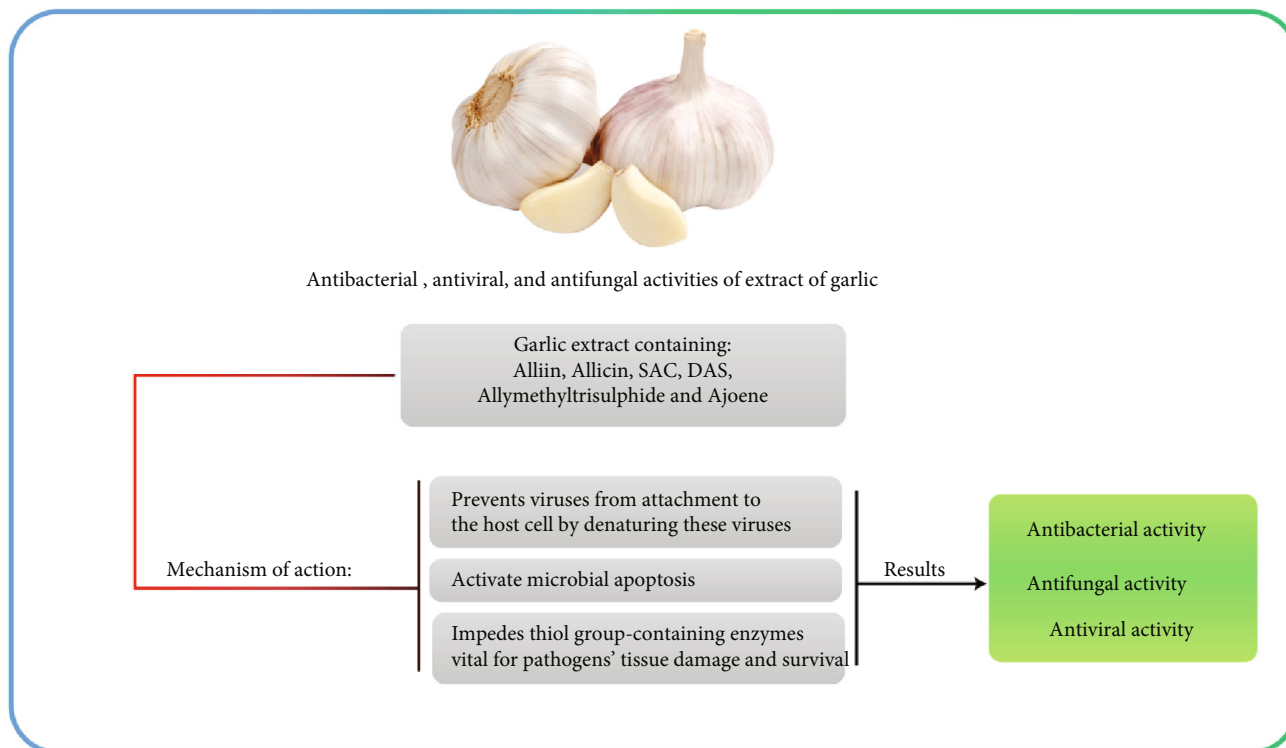


FIGURE 8: Antibacterial, antiviral, and antifungal activities of extract of garlic.

for preventing periodontal diseases [87]. To explore TQ's use as bioactive substances with antibiofilm potential, further research is needed to examine how it prevents biofilm formation.

**6.10. *Galla chinensis*.** *Galla chinensis* has high content of hydrolyzable tannins and broad bioactive materials including polyphenols (e.g., gallotannin and gallic acid). Both laboratory and animal studies on its extract showed enhanced remineralization of enamel, inhibited growth of caries, and reduced metabolism in pathogens by decreasing the enamel demineralization [88]. Clarification of *G. chinensis*'s exact mechanism and evaluation of its effectiveness have proven difficult. These aspects have been examined in numerous studies: inhibitory effect on oral bacteria, inhibition of demineralization, and enhancement of remineralization, stability, and toxicity [89]. Inhibition of cariogenicity by *Galla chinensis* is possible. The *Galla chinensis* plant could be used as a source of new caries-preventive agents.

**6.11. Other Polyphenol-Containing Plants.** There is a wide range of biological activities associated with polyphenols, which are derived from plants. Based on the effects of tea or red wine on glass or cup surfaces, a versatile surface chemistry with polyphenols originated from biomimetic inspiration [90]. Polyphenols are also found in other herbs, namely, cocoa, coffee, hop bract, oat hull, and tea tree or *Melaleuca alternifolia* (MEL). MEL, for example, shows anti-inflammatory and antimicrobial properties against a wide range of microorganisms including bacterial, fungal, and viral species. It has also displayed anticaries and antibio-

film effects against monospecies plaques of periodontopathogens by inhibiting their growth and adhesion. However, its clinical application is limited because of its inadequate clinical stability, water miscibility, and penetrating capacity. Nanotechnology can help remove these limitations and improve its release and selectivity by reducing the size of MEL particles as well as lowering its toxicity [91].

**6.12. *Mentha piperita*.** In Iran and many parts of the world, *Mentha piperita* is a species of the Lamiaceae family that is used for its aroma and therapeutic properties in foods and cosmetic industrial products. Medicinal properties are also found in the leaves and flowers of *M. piperita* [92]. The antibiofilm potential of *Mentha piperita* essential oil (MPEO) has been studied on *S. mutans*; however, it has shown some other biocidal functions against other bacterial, fungal, viral, and larval species. Interestingly, even high doses (2000 mg/kg) of MPEO have shown no toxicity for humans [82].

**6.13. *Houttuynia cordata*.** *Houttuynia cordata* or Thunberg is a common medicinal herb in Japan. Its poultice has been traditionally used for treating purulent skin diseases, and its ethanol extract has proved antimicrobial and antibiofilm effects on a variety of bacterial species including methicillin-resistant *S. aureus* (MRSA). Regarding the mechanism, stimulation of human keratinocytes occurs by the anti-inflammatory effect of HC that inhibits IL-8 and CCL20 productions. Regarding the potential of HCP in fighting various infections, it is suggested as a therapeutically useful antibiotic and anti-inflammatory modulator for infections or inflammation in the skin with high and long-term effectiveness. *Houttuynia*

cordata poultice ethanol extract was reported to prevent oral infectious diseases, such as periodontal disease, when used as mouthwash for oral care by Sekita et al. [93].

**6.14. Guava Leaf Extract.** *Psidium guajava* or guava tree has extensive medicinal properties. The bioactive components existing in its leaf and bark have valuable therapeutic effects with almost no side effects. The phytochemicals in *P. guajava* leaf include alkaloids, carotenoids, essential and fixed oils, flavonoids, glycosides, lectins, reducing-sugars, saponins, tannins, triterpenes, and vitamins (C&A). Flavonoids and quercetin are the constituents accounting for the antibacterial properties, antioxidant effect and strengthening of the immune system [94]. One mechanism for their anti-inflammatory effect is intervening the production of nitric oxide and prostaglandin E2 induced by lipopolysaccharide [95]. Moreover, the guava leaf extract is suggested to be useful for aphthous ulcers displaying marked pain relief and ulcer resolution effects [94].

**6.15. Ligustrum robustum.** *Ligustrum robustum* (Roxb.) Blume is called Ku-Ding-Cha and recognized as a medicinal plant in China where its leaves are used as herbal tea to treat obesity, detoxification, and improving digestion. The Blume's extract has also proved potentials against oxidative stress, inflammation, cancer, infection, and dental caries as well as neuroprotective and hepatoprotective activities with low cytotoxicity. *Ligustrum robustum* extracts were treated for 24 hours with different concentrations of *Ligustrum robustum* extracts to test the inhibitory effects on *S. mutans* UA159 planktonic cells and biofilms by Zhang et al. It was observed in the bacterial growth curve that *Ligustrum robustum* extracts inhibited bacterial proliferation in a dose-dependent manner, with 0.40% (w/v) of *Ligustrum robustum* extracts almost completely inhibiting bacterial growth [96].

## 7. Animal Studies of Chemical Materials in Oral Biofilm Treatments

Dental caries and biofilm formation occur in both animals and humans [97]. Biofilm formation may have several consequences for live organisms that necessitates acquiring more knowledge about their treatments [22]. Accordingly, several studies try to address the anticaries effect of different chemicals on biofilm formation. A turning point in this regard was a dual strategy using microarc oxidation + poly (amidoamine)-loading dimethylaminododecyl methacrylate (PD) to combat biofilm formation that achieved promising results against peri-implantitis [87, 98]. Prates et al. stated that using protoporphyrin derivative as an antimicrobial photodynamic therapy agent exhibits 30% dental bone recovery [99]. Moreover, poly (ethylene) glycol-poly ( $\beta$ -amino esters) micelles have been conjugated with other antimicrobials and could fairly eradicate *S. aureus* infection [100]. The impact of antibiotics and NO-releasing biomimetic nanomatrix gel on different bacterial biofilms has been assessed by Choi et al. and indicated a concentration-dependent antibacterial effect [101]. Despite variations in

chemical structures and collection from different geographical regions, Kharshid et al. clearly established that propolis exhibits remarkable antibacterial properties. This natural resin shows limited activity against gram-negative bacteria, although it seems to be effective against gram-positive rods and *M. tuberculosis*. It was shown that propolis extract is cariostatic in at least three different aspects of caries development, *S. mutans* vulnerabilities, and the activity of glycosyltransferase in rats, in three different studies [66]. Finally, the results of the evaluation of dental hygiene chew and 0.2% W/V chlorhexidine on dental plaque formation in dogs have been successful [102]. Although there are few exceptions where the intervention has not achieved its primary endpoint, the results are generally promising.

## 8. Clinical Studies of Chemical Materials in Oral Biofilm Treatments

As the archetypical biofilms, dental plaques are composed of a heterogeneous community of microbes that underlies many dental and periodontal diseases including dental caries. The balance between the periodontal pathogens and the host immune system determines the clinical representation of dental diseases. If the delicate balance and harmonious relationship of plaque and adjacent tissues are disturbed, the healthy state between them will be ruined and the disease will appear [103]. Patients' oral hygiene home care performance can be measured and motivated using disclosing agents. "Colorimetric technique" describes this method. It is important to apply the disclosing agent correctly and with the right technique. The clinician can motivate patients to prevent periodontal disease by using disclosing agents to reveal the areas around the teeth, including bacterial biofilm [104]. Evaluation of the clinical facet of dental biofilm formation is mentioned in several studies. For example, sucrose exposure to the biochemical and microbiological composition of dental biofilm showed its positive effect on enamel demineralization especially in the presence of fluoride [105]. Moreover, controlling the dental biofilm can be improved by adding a vegetable or mineral oil to dentifrice that confirms the associated benefits of treatments containing essential oils [106]. Similarly, a combination of chlorhexidine, fluoride, and erythrosine has decreased the dental biofilm and gingival bleeding in patients with Down syndrome [107]. Triclosan toothpaste has been evaluated for modulation of the clinical and subgingival condition in children from aggressive periodontitis parents and could effectively control the periodontal parameters and enhance the immune factors in subjects [108]. In another study, a temporal relationship was shown between biofilm composition and enamel demineralization following exposure to sucrose. The findings indicated that sucrose affects the insoluble extracellular polysaccharides differentially higher than monosaccharide components, and changes in the biofilm composition occur earlier than enamel demineralization [109]. Finally, these results verified the clinical implications of chemical treatments for dental biofilms (Table 2).

TABLE 2: Clinical studies in oral biofilm treatments.

Type	Method	Outcomes	Year/Ref
Herbal materials			
Allium tuberosum Coriandrum sativum Cymbopogon martini Cymbopogon winterianus Santolina chamaecyparissus	MIC of extracts and essential oils and their antibiofilm effect against <i>C. albicans</i> were evaluated in vitro. Chromatography, spectrometry, and scanning electron microscopy (SEM) were used for biochemical evaluations.	The <i>C. sativum</i> essential oil and crude oil inhibited biofilm formation and growth.	2011/ [148]
<i>Aloe vera</i> gel	The antimicrobial effect of <i>Aloe vera</i> gel against some oral pathogenic bacteria was evaluated in vitro.	An optimum concentration of <i>Aloe vera</i> gel displayed significant antiseptic function against dental and periodontal pathogens.	2012/ [149]
<i>Equisetum arvense</i> L. <i>Glycyrrhiza glabra</i> L. <i>Punica granatum</i> L. <i>Stryphnodendron barbatimam</i>	The antibacterial effect and cytotoxicity of plant extracts were tested in vitro.	All plant extracts displayed antibacterial effect. <i>E. arvense</i> L. extract and <i>G. glabra</i> L. extract showed the highest and lowest cytotoxic effect, respectively.	2013/ [150]
Mouth rinse containing <i>Acacia nilotica</i>	The antibacterial effect of <i>Acacia nilotica</i> was evaluated against <i>S. mutans</i> in a clinical trial recruiting volunteer.	<i>A. nilotica</i> significantly decreased the bacterial load.	2015/ [151]
Green tea <i>Salvadora persica</i> L. aqueous	Antibacterial effect of the combined mouthwash was evaluated against plaque accumulation.	The combined mouthwash significantly decreased plaque formation.	2016/ [152]
Phloretin	The effect of flavonoids on the growth and biofilm formation of <i>S. aureus</i> strains was evaluated in vitro.	Even sub-MIC values of flavonoids could inhibit the biofilm formation.	2017/ [72]
<i>Ricinus communis</i> and sodium hypochlorite	The antimicrobial effect was evaluated using molecular methods.	The denture cleanser effectively inhibited biofilm formation by <i>C. albicans</i> .	2017/ [153]
Propolis Chlorhexidine	Antioxidative and antibacterial effects of both materials were compared by evaluating clinical parameters.	Propolis-based formula showed similar clinical chlorhexidine.	2018/ [154]
<i>Carica papaya</i> leaf extract	Clinical outcomes were evaluated during a 4-week treatment period.	The herb-containing dentifrice showed similar effect to other used mouthwashes on the gingival bleeding.	2018/ [111]
<i>Juglans regia</i> L.	Antibacterial effect of herb extract against <i>P. aeruginosa</i> isolated from burn, tracheal, and urine infections was evaluated in vitro.	The herb extract displayed antibiofilm effect on a concentration-dependent manner.	2018/ [155]
<i>Melaleuca alternifolia</i> nanoparticles mouthwash with chlorhexidine gluconate	Plaque and gingival clinical parameters as well as participants' perceptions were assessed in recruited subjects.	Chlorhexidine resulted in a better taste, higher antibiofilm effect, and more taste change.	2019/ [91]
Mouth rinse containing <i>guava</i> leaf extract	<i>Guava</i> was compared to chlorhexidine in terms of antimicrobial and antioxidant effects by clinical and microbial assessments.	<i>Guava</i> leaf extract showed similar antibiofilm effects compared to chlorhexidine.	2019/ [94]
<i>Melaleuca alternifolia</i>	The effect of herb was compared to chlorhexidine in terms of clinical parameters.	The anti-inflammatory potential of two materials displayed to be similar.	2019/ [91]
Probiotic yogurt containing <i>Bifidobacterium lactis</i> Bb12	Antibacterial effect of probiotic yogurt on salivary bacteria was evaluated.	The probiotic yogurt significantly reduced the salivary bacteria.	2020/ [156]
<i>Ricinus communis</i> Chloramine-T Sodium hypochlorite	The antimicrobial effect against <i>Candida spp.</i> was compared among the three material counts by clinical assessments and photography.	All materials improved denture stomatitis and reduce biofilm formation while sodium hypochlorite had the highest efficacy.	2020/ [157]
Leaf extracts of <i>Citrus hystrix</i> DC, <i>Moringa oleifera</i> Lam., and <i>Azadirachta indica</i> A. Juss.	The effect of herb extracts was studied on gingivitis and compared to chlorhexidine gluconate in terms of clinical and oral microbial parameters.	<i>Moringa oleifera</i> Lam. significantly reduced gingivitis and plague. <i>Azadirachta indica</i> A. Juss. showed high antimicrobial effect against <i>Staphylococcus</i> and <i>Candida</i> strains.	2021/ [158]
Chemical materials			
Mouthwash containing essential oils	Biofilms were stained and analyzed by microscopy.	Bacterial vitality was reduced significantly.  Taurolidine enhanced antibiofilm effect.	2015/ [159]

TABLE 2: Continued.

Type	Method	Outcomes	Year/ Ref
Taurolidine Chlorhexidine	The efficacy of treatments on biofilm removal was evaluated using clinical outcome parameters.		2015/ [160]
Glycine powder Sodium bicarbonate	Both materials were used as air polishing. Gingival and clinical parameters were evaluated.	Glycine powder air polishing significantly improved the measured parameters.	2015/ [161]
Polymethyl-methacrylate and Ag nanoparticles	Antibacterial potential of two formulations against cariogenic bacteria was assessed.	Both formulations inhibited biofilm formation of all tested bacteria.	2015/ [162]
Toothpaste containing fluoride and fluoride plus sodium trimetaphosphate	The antibiofilm effect of toothpaste was assessed.	The formulations containing sodium trimetaphosphate showed higher antibiofilm potentials.	2015/ [163]
Triclosan formula	The antiplaque effects were assessed in vitro.	Including triclosan in formulation significantly inhibited plaque formation.	2015/ [164]
Floss impregnated with chlorhexidine gluconate	Antibiofilm effect was assessed on 4 different surfaces (mesiobuccal, distobuccal, mesiolingual, and distolingual).	Chlorhexidine-impregnated floss displayed synergic reducing effect on supragingival biofilm.	2015/ [165]
Chlorhexidine gluconate Essential oils Cetylpyridinium chloride Triclosan <i>Hamamelis virginiana</i>	The inhibitory effect of all materials against bacterial plaque was evaluated.	All mouthwashes containing the five ingredients significantly reduced the biofilm formation.	2015/ [166]
Mouthwash containing <i>Matricaria chamomilla L.</i> and chlorhexidine	Clinical parameters were evaluated in a clinical trial.	The mouthwash significantly reduced the visible plaque formation and gingival bleeding.	2016/ [167]
Triclosan	Clinical parameters were evaluated in a clinical trial.	No considerable change occurred in the plaque and gingival indexes of triclosan-treated subjects.	2016/ [168]
Sodium perborate Chlorhexidine	The antibiofilm effect of disinfection agents was assessed in vitro.	Brushing combined with agents successfully inhibited biofilm formation on dentures.	2016/ [169]
Stannous fluoride (SnF <sub>2</sub> )	Dental plaque was sampled and evaluated in terms of gingival inflammation and bleeding.	SnF <sub>2</sub> -containing dentifrice improved clinical outcomes of gingivitis and plaque.	2017/ [170]
—	Scaling and root planing with or without laser diode was assessed in terms of clinical, microbiological, and inflammatory effects.	Diode laser synergically improved parameters.	2017/ [171]
Chlorhexidine solutions	The antiplaque effect on clinical samples was examined in vitro.	The treatment significantly prevented plaque and subgingival biofilm formation.	2017/ [172]
Acidulated phosphate fluoride	The antibiofilm effect against salivary <i>S. mutans</i> was studied in vitro after topical application.	The treatment displayed no inhibitory effect on salivary or biofilm bacterial load.	2017/ [173]
Toothpaste containing arginine	Some biochemical and microbial parameters were evaluated.	The treatment reduced lactic acid production.	2017/ [174]
Fluoride-impregnated toothbrush Fluoride-containing toothpaste	The remained fluoride in saliva and antiplaque effects were evaluated on buccal and lingual surfaces.	Both treatments displayed similar plaque-removing outcomes.	2017/ [175]
Saline Sodium hypochlorite <i>Ricinus communis</i>	The antibiofilm effect against <i>Candida spp.</i> on the intaglio surface of maxillary dentures was evaluated using photography and quantifying software.	Only different concentrations of sodium hypochlorite displayed antimicrobial effect.	2017/ [176]
Hyaluronic acid mouthwash Chlorhexidine	Plaque and clinical parameters were evaluated in clinics.	The mouthwash showed a marginally less inhibitory effect on plaque formation compared to chlorhexidine.	2017/ [176]
Silver/fluoride nanoparticles	The bactericidal and antibiofilm effects were evaluated on <i>S. mutans</i> .	Nanoparticles were reported to be effective and suggested for clinical application in order to limit dental biofilm formation.	2017/ [177]
Mouth rinse containing chlorhexidine gluconate	Antimicrobial effect against <i>S. mutans</i> was analyzed using microscopy.	The intense contamination showed no significant difference in the microbial load.	2017/ [178]



TABLE 2: Continued.

Type	Method	Outcomes	Year/Ref
Probiotic ( <i>B. lactis</i> )-containing lozenges	Lozenges were used with scaling and root planning. Clinical, immunological, and microbial parameters were monitored.	The treated subjects displayed higher antibacterial and lower inflammatory effects.	2018/[179]
Propolis/herbs in antioxidant-based formula Chlorhexidine-based formulae	A couple clinical parameters were monitored in a 3-month trial study.	The two formulas displayed similar clinical outcomes.	2018/[154]
Sodium bicarbonate	A couple clinical parameters were monitored in a clinical trial.	Sodium bicarbonate displayed increasing antibacterial effect.	2018/[180]
Modified antimicrobial peptide	A couple clinical parameters were evaluated in a clinical trial.	The modified peptide displayed antibacterial effect against periodontal bacteria.	2018/[180]
Fluoridated dentifrice containing arginine	A couple clinical and microbial parameters were examined.	Arginine did not display any additional antibiofilm effect.	2018/[181]
Edathamil-containing gel	Antiplaque effect was evaluated by photography.	Edathamil increased the plaque removal.	2018/[182]
Toothpastes containing different concentrations of sodium bicarbonate	Antiplaque effect was measured before and after a single-timed brushing.	No statistically significant difference was observed.	2018/[183]
Dentifrices containing different ratios of sodium fluoride and tara gum	The fluoride concentration was determined using a physicochemical technique.	The antibiofilm effect displayed no statistically significant differences.	2018/[184]
Chlorhexidine digluconate-impregnated dental floss	The plaque index was assessed in clinics.	The impregnated floss significantly reduced the plaque formation.	2018/[185]
Metronidazole Amoxicillin	Subjects were treated with systemic antibiotic as an adjuvant therapy, and antibiofilm outcome was evaluated.	No significant differences were observed in clinical parameters.	2019/[186]
Arginine- or fluoride-containing toothpastes	Caries diagnosis and plaque sampling were performed on tooth surfaces, and antiplaque effects were evaluated in vitro.	The arginine deiminase system was significantly activated, and the acidity was reduced in the plaque. Fluoride reduced plaque lactate production.	2019/[187]
Sodium hypochlorite Chlorhexidine gluconate Sodium bicarbonate	Antimicrobial activity was quantified in healthy complete denture wearers through chemical analysis.	Sodium hypochlorite and chlorhexidine significantly decreased microbial viability.	2019/[188]
Lozenges containing probiotic <i>Streptococcus salivarius</i> M18	Plaque and gingival outcomes were measured in orthodontic brace wearers using molecular analyses.	Treatment had no effect on microbial parameters.	2019/[189]
Mouth rinses containing chlorhexidine and guava	Plaque and gingival indexes were measured.	Plaque and gingival indexes as well as microbial counts showed gradual reduction.	2019/[94]
Triclosan toothpaste	Plaque and gingival indexes were measured.	Triclosan toothpaste displayed antiplaque effect.	2020/[108]
Triclosan toothpaste	Plaque index and gingival bleeding were measured.	Treatment with triclosan toothpaste reduced gingival bleeding and plaque formation.	2020/[190]
Sodium hypochlorite gel	Pocket probing depth was evaluated before and after treatment.	No statistically significant difference was observed.	2020/[191]
Sodium hypochlorite Dettol and Lifebuoy liquid soap Phosphate-buffered saline	The antimicrobial effect against <i>Candida spp.</i> was evaluated in vitro.	All three treatments significantly reduced the microbial load.	2020/[192]
Ozonated water	The antiplaque and antibiofilm effects were assessed in vitro.	No statistical difference was observed.	2021/[193]
Mouth rinses containing chlorhexidine with or without hydrogen peroxide	The antiplaque effect was studied in vitro.	Both mouth rinses significantly controlled the plaque formation. Hydrogen peroxide had a slightly synergistic effect.	2021/[194]



## 9. Clinical Studies of Herbal Materials in Oral Biofilm Treatments

Considering the important role of dental biofilm in oral health and the approved positive effect of herbal materials, several studies have evaluated the effect of medicinal herbs on dental biofilm. Clinically, a mouth rinse containing guava leaf extract was shown to be a useful adjunct to professional oral prophylaxis for chronic generalized gingivitis [94]. In another study, the inhibitory effects of chlorhexidine and MEL nanoparticles against biofilm and inflammation showed similar results on tooth surfaces free of or covered by biofilm [91]. Another randomized clinical trial study used an experimental solution of *Ricinus communis* through a cleansing regimen on a silicone-based denture liner to assess the integrity of liners and showed antibiofilm and antimicrobial effects of solution [110]. Saliasi et al. compared the potential of two dentifrice in reducing the interdental gingival bleeding. One of their used mouthwash contained *Carica papaya* leaf extract (CPLE) and the other one was a classical sodium lauryl sulfate- (SLS-) free dentifrice containing enzyme. This study indicated that CPLE more efficiently reduced the gingival bleeding and inflammation compared to the classical SLS-free dentifrice [111]. In another study, four antimicrobial mouth rinses in different formulations were tested for their effects on the clinical parameters of adjacent tissues and subgingival microbiota composition. The alteration in the composition of subgingival microbiota made by the studied mouth rinses improved the clinical parameters [112]. Collectively, the above-mentioned findings confirm that herbal medicines can be considered important effective agents in treating dental biofilms (Table 2).

## 10. Clinical Studies of the Mixed Materials (Herbal and Chemical) in Oral Biofilm Treatment

Nearly 1000 species of bacteria live in the mouth. In treating caries, hard tissues are usually restored in regard to functional and aesthetic concerns. Nonetheless, this treats only the outcomes of the illness. Typically, in clinical settings, contaminated tissues are removed to prevent the spread of dental caries [113]. Dental materials are designed to kill microbes in contact by strategically incorporating a wide range of antimicrobial agents (such as polycations, quaternary ammonium compounds, and antimicrobial peptides). Covalent compound structures can be formed by combining the compounds with dental materials. Both gram-negative and gram-positive bacteria are strongly affected by these broad-spectrum antimicrobial agents [4]. Recently, antimicrobial dental materials have been prepared using QAMs and AgNPs. In addition to killing bacteria on the surface, the modified materials also kill bacteria away from the surface [3]. An evaluation of barley hordenine, a polyphenolic compound, as well as a combination with netilmicin, an aminoglycoside antibiotic, was carried out by Zou et al. (2018). In a study using hordenine and netilmicin together,

up to 88% of *P. aeruginosa* PAO1 biofilms were reduced, compared to none of the treatments individually [74]. In order to target biofilms more effectively, studies should combine natural antibiofilm compounds from different sources. Moreover, natural compounds are not effective against all bacterial strains, so selecting an effective compound is also necessary [114].

## 11. Conclusion

Supported with strong clinical efficacy proof, antibiofilm materials are being increasingly considered and applied as efficient agents for controlling the dental biofilm and ameliorating gingivitis. However, generally, herbal-based materials produce a lower score in comparison to mouthwashes containing chemical materials such as CHX, fluoride, and EO. In addition, the importance of mechanical removal is still on the top priority among all dental biofilms controlling methods and chemical treatment provides an alternative or adjunctive method by preventing biofilm accumulation rather than oral microflora eradication. The present study reviewed that factors beneficial in preventing dental caries include probiotics, herbs, and spices. Also, it indicated that combining multiple plants or plants with probiotics can exert more efficient results than individual therapies using single herbal products or probiotics. Surveying the literature showed that probiotics act not only as possible antimicrobial agents but also sustain the oral ecosystem's balance. Finally, the combination of functional products containing probiotics and polyphenol extracts is an important research trend in the food industry.

## 12. Future Direction

This review highlighted the recent successful studies on using antibiofilm chemical and herbal materials. Nevertheless, several problems and limitations remained to be addressed. The majority of evidence results from laboratory or preclinical trial studies in short-time projects, whereas longer-time studies are required to provide more reliable quantitative proof that confirms techniques have benefits in vivo and verify that their antibacterial effect is durable. On the other hand, the safety profile of the above-mentioned antimicrobial agents and the emergence of antimicrobial tolerance as a major concern require further investigation. In addition, well-planned and appropriately structured clinical trials conducted across multiple centers are required for accurate comparisons. Such extensive trials are also essential to find the most efficient antimicrobial or antibiofilm approach and suitable criteria for opting them in. Furthermore, the potential synergic functions of nature-originated materials and chemical agents should be targeted in future studies. Such studies and information are necessary to develop novel, efficient, and healthy anticaries strategies. In the end, the biofilm-interfering or biofilm-inhibiting activities of these products should be investigated in cohort clinical trials. Several herbal materials as well as their active ingredients need further study and clarification with regard to their antimicrobial and antioxidant properties.

## Data Availability

This article is a review and does not contain any studies with humans or animals performed by any of the authors.

## Conflicts of Interest

The authors declare that they have no competing interests.

## Acknowledgments

The authors would like to acknowledge the useful comments given by colleagues.

## References

- [1] W. S. Song, J. K. Lee, S. H. Park, H. S. Um, S. Y. Lee, and B. S. Chang, "Comparison of periodontitis-associated oral biofilm formation under dynamic and static conditions," *Journal of Periodontal & Implant Science*, vol. 47, no. 4, pp. 219–230, 2017.
- [2] S. A. Mosaddad, E. Tahmasebi, A. Yazdanian et al., "Oral microbial biofilms: an update," *European Journal of Clinical Microbiology & Infectious Diseases*, vol. 38, no. 11, pp. 2005–2019, 2019.
- [3] Y. Jiao, F. R. Tay, L. N. Niu, and J. H. Chen, "Advancing antimicrobial strategies for managing oral biofilm infections," *International Journal of Oral Science*, vol. 11, no. 3, p. 28, 2019.
- [4] S. Rath, S. C. B. Bal, and D. Dubey, "Oral biofilm: development mechanism, multidrug resistance, and their effective management with novel techniques," *Rambam Maimonides Medical Journal*, vol. 12, no. 1, p. e0004, 2021.
- [5] M. A. Peres, L. M. D. Macpherson, R. J. Weyant et al., "Oral diseases: a global public health challenge," *The Lancet*, vol. 394, no. 10194, pp. 249–260, 2019.
- [6] P. D. Marsh, A. Moter, and D. A. Devine, "Dental plaque biofilms: communities, conflict and control," *Periodontology*, vol. 55, no. 1, pp. 16–35, 2011.
- [7] F. Carinci, D. Lauritano, C. A. Bignozzi et al., "A new strategy against peri-implantitis: antibacterial internal coating," *International Journal of Molecular Sciences*, vol. 20, no. 16, p. 3897, 2019.
- [8] D. S. W. Benoit, K. R. Sims Jr., and D. Fraser, "Nanoparticles for oral biofilm treatments," *ACS Nano*, vol. 13, no. 5, pp. 4869–4875, 2019.
- [9] D. Berger, A. Rakhimova, A. Pollack, and Z. Loewy, "Oral biofilms: development, control, and analysis," *High-Throughput*, vol. 7, no. 3, 2018.
- [10] S. C. Lucena-Ferreira, A. P. Ricomini-Filho, W. J. Silva, J. A. Cury, and A. A. Cury, "Influence of daily immersion in denture cleanser on multispecies biofilm," *Clinical Oral Investigations*, vol. 18, no. 9, pp. 2179–2185, 2014.
- [11] S. C. Cortelli, F. O. Costa, M. Rode Sde et al., "Mouthrinse recommendation for prosthodontic patients," *Brazilian Oral Research*, vol. 28, 2014.
- [12] L. Karygianni, A. Al-Ahmad, A. Argyropoulou, E. Hellwig, A. C. Anderson, and A. L. Skaltsounis, "Natural antimicrobials and oral microorganisms: a systematic review on herbal interventions for the eradication of multispecies oral biofilms," *Frontiers in Microbiology*, vol. 6, p. 1529, 2015.
- [13] M. Yazdanian, P. Rostamzadeh, M. Rahbar et al., "The potential application of green-synthesized metal nanoparticles in dentistry: a comprehensive review," *Bioinorganic Chemistry and Applications*, vol. 2022, Article ID 2311910, 27 pages, 2022.
- [14] M. Yazdanian, P. Rostamzadeh, M. Alam et al., "Evaluation of antimicrobial and cytotoxic effects of Echinacea and Arctium extracts and Zataria essential oil," *AMB Express*, vol. 12, no. 1, p. 75, 2022.
- [15] W. Z. Levine, N. Samuels, M. E. Bar Sheshet, and J. T. Grbic, "A novel treatment of gingival recession using a botanical topical gingival patch and mouthrinse," *The Journal of Contemporary Dental Practice*, vol. 14, no. 5, pp. 948–953, 2013.
- [16] K. Sahni, F. Khashai, A. Forghany, T. Krasieva, and P. Wilder-Smith, "Exploring mechanisms of biofilm removal," *Dentistry*, vol. 6, no. 4, 2016.
- [17] M. T. Khan, F. Moeen, S. Z. Safi, F. Said, A. Mansoor, and A. Khan, "The structural, physical, and in vitro biological performance of freshly mixed and set endodontic sealers," *European Endodontic Journal*, vol. 6, no. 1, pp. 98–109, 2021.
- [18] F. Said, F. Moeen, M. T. Khan et al., "Cytotoxicity, morphology and chemical composition of two luting cements: an in vitro study," *Pesquisa Brasileira em Odontopediatria e Clínica Integrada*, vol. 20, 2020.
- [19] A. Kumar, A. Alam, M. Rani, N. Z. Ehtesham, and S. E. Hasnain, "Biofilms: survival and defense strategy for pathogens," *International Journal of Medical Microbiology*, vol. 307, no. 8, pp. 481–489, 2017.
- [20] W. Song and S. Ge, "Application of antimicrobial nanoparticles in dentistry," *Molecules*, vol. 24, no. 6, p. 1033, 2019.
- [21] R. Roy, M. Tiwari, G. Donelli, and V. Tiwari, "Strategies for combating bacterial biofilms: a focus on anti-biofilm agents and their mechanisms of action," *Virulence*, vol. 9, no. 1, pp. 522–554, 2018.
- [22] D. W. Williams, M. A. Lewis, S. L. Percival, T. Kuriyama, S. da Silva, and M. P. Riggio, "Role of biofilms in the oral health of animals," in *Biofilms and Veterinary Medicine*, pp. 129–142, Springer, 2011.
- [23] C. W. Hall and T. F. Mah, "Molecular mechanisms of biofilm-based antibiotic resistance and tolerance in pathogenic bacteria," *FEMS Microbiology Reviews*, vol. 41, no. 3, pp. 276–301, 2017.
- [24] N. B. Arweiler and L. Netuschil, "The oral microbiota," *Advances in Experimental Medicine and Biology*, vol. 902, pp. 45–60, 2016.
- [25] Y. Hao, X. Huang, X. Zhou et al., "Influence of dental prosthesis and restorative materials interface on oral biofilms," *International Journal of Molecular Sciences*, vol. 19, no. 10, p. 3157, 2018.
- [26] E. Zaura and S. Twetman, "Critical appraisal of oral pre- and probiotics for caries prevention and care," *Caries Research*, vol. 53, no. 5, pp. 514–526, 2019.
- [27] G. Gazzani, M. Daglia, and A. Papetti, "Food components with anticaries activity," *Current Opinion in Biotechnology*, vol. 23, no. 2, pp. 153–159, 2012.
- [28] W. H. Bowen, R. A. Burne, H. Wu, and H. Koo, "Oral biofilms: pathogens, matrix, and polymicrobial interactions in microenvironments," *Trends in Microbiology*, vol. 26, no. 3, pp. 229–242, 2018.
- [29] R. P. Allaker and K. Memarzadeh, "Nanoparticles and the control of oral infections," *International Journal of Antimicrobial Agents*, vol. 43, no. 2, pp. 95–104, 2014.

- [30] J. E. Hulla, S. C. Sahu, and A. W. Hayes, "Nanotechnology," *Human & Experimental Toxicology*, vol. 34, no. 12, pp. 1318–1321, 2015.
- [31] M. Truffi, L. Fiandra, L. Sorrentino, M. Monieri, F. Corsi, and S. Mazzucchelli, "Ferritin nanocages: a biological platform for drug delivery, imaging and theranostics in cancer," *Pharmacological Research*, vol. 107, pp. 57–65, 2016.
- [32] A. Besinis, T. De Peralta, C. J. Tredwin, and R. D. Handy, "Review of nanomaterials in dentistry: interactions with the oral microenvironment, clinical applications, hazards, and benefits," *ACS Nano*, vol. 9, no. 3, pp. 2255–2289, 2015.
- [33] A. Shrestha, Z. Shi, K. G. Neoh, and A. Kishen, "Nanoparticulates for antibiofilm treatment and effect of aging on its antibacterial activity," *Journal of Endodontics*, vol. 36, no. 6, pp. 1030–1035, 2010.
- [34] M. Yazdani, M. N. Motallaei, E. Tahmasebi et al., "Chemical characterization and cytotoxic/antibacterial effects of nine Iranian propolis extracts on human fibroblast cells and oral bacteria," *BioMed Research International*, vol. 2022, Article ID 6574997, 14 pages, 2022.
- [35] M. Yazdani, A. Rahmani, E. Tahmasebi, H. Tebyanian, A. Yazdani, and S. A. Mosaddad, "Current and advanced nanomaterials in dentistry as regeneration agents: an update," *Mini-Reviews in Medicinal Chemistry*, vol. 21, no. 7, pp. 899–918, 2021.
- [36] E. Tafazoli Moghadam, M. Yazdani, M. Alam et al., "Current natural bioactive materials in bone and tooth regeneration in dentistry: a comprehensive overview," *Journal of Materials Research and Technology*, vol. 13, pp. 2078–2114, 2021.
- [37] A. Besinis, T. De Peralta, and R. D. Handy, "The antibacterial effects of silver, titanium dioxide and silica dioxide nanoparticles compared to the dental disinfectant chlorhexidine on *Streptococcus mutans* using a suite of bioassays," *Nanotoxicology*, vol. 8, no. 1, pp. 1–16, 2014.
- [38] C. T. Rodrigues, F. B. de Andrade, L. de Vasconcelos et al., "Antibacterial properties of silver nanoparticles as a root canal irrigant against *Enterococcus faecalis* biofilm and infected dentinal tubules," *International Endodontic Journal*, vol. 51, no. 8, pp. 901–911, 2018.
- [39] D. D. Divakar, N. T. Jastaniyah, H. G. Altamimi et al., "Enhanced antimicrobial activity of naturally derived bioactive molecule chitosan conjugated silver nanoparticle against dental implant pathogens," *International Journal of Biological Macromolecules*, vol. 108, pp. 790–797, 2018.
- [40] H. Yan, H. Yang, K. Li, J. Yu, and C. Huang, "Effects of chlorhexidine-encapsulated mesoporous silica nanoparticles on the anti-biofilm and mechanical properties of glass ionomer cement," *Molecules*, vol. 22, no. 7, p. 1225, 2017.
- [41] A. Mansoor, M. T. Khan, M. Mehmood, Z. Khurshid, M. I. Ali, and A. Jamal, "Synthesis and characterization of titanium oxide nanoparticles with a novel biogenic process for dental application," *Nanomaterials*, vol. 12, no. 7, p. 1078, 2022.
- [42] J. Wong, T. Zou, A. H. C. Lee, and C. Zhang, "The potential translational applications of nanoparticles in endodontics," *International Journal of Nanomedicine*, vol. 16, pp. 2087–2106, 2021.
- [43] S. Singh, "Nanomaterials exhibiting enzyme-like properties (nanozymes): current advances and future perspectives," *Frontiers in Chemistry*, vol. 7, p. 46, 2019.
- [44] M. Chrószcz and I. Barszczewska-Rybarek, "Nanoparticles of quaternary ammonium polyethylenimine derivatives for application in dental materials," *Polymers*, vol. 12, no. 11, p. 2551, 2020.
- [45] S. Patil, G. S. Vidya, H. Baeshen et al., "Current trends and future prospects of chemical management of oral biofilms," *Journal of Oral Biology and Craniofacial Research*, vol. 10, no. 4, pp. 660–664, 2020.
- [46] H. Chouirfa, H. Bouloussa, V. Migonney, and C. Falentin-Daudré, "Review of titanium surface modification techniques and coatings for antibacterial applications," *Acta Biomaterialia*, vol. 83, pp. 37–54, 2019.
- [47] Z. Wang, Y. Shen, and M. Haapasalo, "Dental materials with antibiofilm properties," *Dental Materials*, vol. 30, no. 2, pp. e1–16, 2014.
- [48] X. Zheng, X. Cheng, L. Wang et al., "Combinatorial effects of arginine and fluoride on oral bacteria," *Journal of Dental Research*, vol. 94, no. 2, pp. 344–353, 2015.
- [49] X. Huang, R. M. Schulte, R. A. Burne, and M. M. Nascimento, "Characterization of the arginolytic microflora provides insights into pH homeostasis in human oral biofilms," *Caries Research*, vol. 49, no. 2, pp. 165–176, 2015.
- [50] M. M. Nascimento, C. Browngardt, X. Xiaohui, V. Klepac-Ceraj, B. J. Paster, and R. A. Burne, "The effect of arginine on oral biofilm communities," *Molecular Oral Microbiology*, vol. 29, no. 1, pp. 45–54, 2014.
- [51] N. Beyth, A. J. Domb, and E. I. Weiss, "An in vitro quantitative antibacterial analysis of amalgam and composite resins," *Journal of Dentistry*, vol. 35, no. 3, pp. 201–206, 2007.
- [52] R. J. Worthington, J. J. Richards, and C. Melander, "Small molecule control of bacterial biofilms," *Organic & Biomolecular Chemistry*, vol. 10, no. 37, pp. 7457–7474, 2012.
- [53] P. P. Mahamuni-Badiger, P. M. Patil, M. V. Badiger et al., "Biofilm formation to inhibition: role of zinc oxide-based nanoparticles," *Materials Science & Engineering C, Materials for Biological Applications*, vol. 108, p. 110319, 2020.
- [54] P. Zarparvar, M. A. Amoozegar, H. Babavalian, F. M. Reza, H. Tebyanian, and F. Shakeri, "Isolation and identification of culturable halophilic bacteria with producing hydrolytic enzyme from Incheh Broun hypersaline wetland in Iran," *Cellular and Molecular Biology*, vol. 62, no. 12, pp. 31–36, 2016.
- [55] L. Cheng, M. D. Weir, H. H. Xu et al., "Antibacterial amorphous calcium phosphate nanocomposites with a quaternary ammonium dimethacrylate and silver nanoparticles," *Dental Materials*, vol. 28, no. 5, pp. 561–572, 2012.
- [56] N. Izutani, S. Imazato, Y. Noiri, and S. Ebisu, "Antibacterial effects of MDPB against anaerobes associated with endodontic infections," *International Endodontic Journal*, vol. 43, no. 8, pp. 637–645, 2010.
- [57] J. Xue, J. Wang, D. Feng, H. Huang, and M. Wang, "Application of antimicrobial polymers in the development of dental resin composite," *Molecules*, vol. 25, no. 20, p. 4738, 2020.
- [58] J. M. Antonucci, D. N. Zeiger, K. Tang, S. Lin-Gibson, B. O. Fowler, and N. J. Lin, "Synthesis and characterization of dimethacrylates containing quaternary ammonium functionalities for dental applications," *Dental Materials*, vol. 28, no. 2, pp. 219–228, 2012.
- [59] X. Kuang, V. Chen, and X. Xu, "Novel approaches to the control of oral microbial biofilms," *BioMed Research International*, vol. 2018, Article ID 6498932, 13 pages, 2018.



- [60] S. Kalimuthu, B. P. K. Cheung, J. Y. Y. Yau, K. Shanmugam, A. P. Solomon, and P. Neelakantan, "A novel small molecule, 1,3-di-m-tolyl-urea, inhibits and disrupts multispecies oral biofilms," *Microorganisms*, vol. 8, no. 9, p. 1261, 2020.
- [61] C. Zhang, X. Kuang, Y. Zhou et al., "A novel small molecule, ZY354, inhibits dental caries-associated oral biofilms," *Antimicrobial Agents and Chemotherapy*, vol. 63, no. 5, 2019.
- [62] M. M. Aboulwafa, F. S. Youssef, H. A. Gad, A. E. Altyar, M. M. Al-Azizi, and M. L. Ashour, "A comprehensive insight on the health benefits and phytoconstituents of *Camellia sinensis* and recent approaches for its quality control," *Antioxidants*, vol. 8, no. 10, p. 455, 2019.
- [63] W. C. Reygaert, "Green tea catechins: their use in treating and preventing infectious diseases," *BioMed Research International*, vol. 2018, Article ID 9105261, 9 pages, 2018.
- [64] K. S. Al-Khalifa, M. M. Gad, F. A. Alshahrani et al., "Influence of propolis extract (caffeic acid phenethyl ester) addition on the *Candida albicans* adhesion and surface properties of autopolymerized acrylic resin," *International Journal of Dentistry*, vol. 2022, Article ID 6118660, 7 pages, 2022.
- [65] V. D. Wagh, "Propolis: a wonder bees product and its pharmacological potentials," *Advances in Pharmacological Sciences*, vol. 2013, Article ID 308249, 11 pages, 2013.
- [66] Z. Khurshid, M. Naseem, M. S. Zafar, S. Najeeb, and S. Zohaib, "Propolis: a natural biomaterial for dental and oral healthcare," *Journal of Dental Research, Dental Clinics, Dental Prospects*, vol. 11, no. 4, pp. 265–274, 2017.
- [67] C. Bin, N. A. Al-Dhabi, G. A. Esmail, S. Arokiyaraj, and M. V. Arasu, "Potential effect of *Allium sativum* bulb for the treatment of biofilm forming clinical pathogens recovered from periodontal and dental caries," *Saudi Journal of Biological Sciences*, vol. 27, no. 6, pp. 1428–1434, 2020.
- [68] T. Persson, T. H. Hansen, T. B. Rasmussen, M. E. Skindersø, M. Givskov, and J. Nielsen, "Rational design and synthesis of new quorum-sensing inhibitors derived from acylated homoserine lactones and natural products from garlic," *Organic & Biomolecular Chemistry*, vol. 3, no. 2, pp. 253–262, 2005.
- [69] L. Lu, W. Hu, Z. Tian et al., "Developing natural products as potential anti-biofilm agents," *Chinese Medicine*, vol. 14, no. 1, p. 11, 2019.
- [70] T. Bjarnsholt, P. Ø. Jensen, T. B. Rasmussen et al., "Garlic blocks quorum sensing and promotes rapid clearing of pulmonary *Pseudomonas aeruginosa* infections," *Microbiology*, vol. 151, no. 12, pp. 3873–3880, 2005.
- [71] M. Sasi, S. Kumar, M. Kumar et al., "Garlic (*Allium sativum* L.) bioactives and its role in alleviating oral pathologies," *Antioxidants*, vol. 10, no. 11, p. 1847, 2021.
- [72] L. A. A. Lopes, J. B. Dos Santos Rodrigues, M. Magnani, E. L. de Souza, and J. P. de Siqueira-Júnior, "Inhibitory effects of flavonoids on biofilm formation by *Staphylococcus aureus* that overexpresses efflux protein genes," *Microbial Pathogenesis*, vol. 107, pp. 193–197, 2017.
- [73] A. Vikram, P. R. Jesudhasan, G. K. Jayaprakasha, S. D. Pillai, and B. S. Patil, "Citrus limonoids interfere with *Vibrio harveyi* cell-cell signalling and biofilm formation by modulating the response regulator LuxO," *Microbiology*, vol. 157, no. 1, pp. 99–110, 2011.
- [74] J. W. Zhou, H. Z. Luo, H. Jiang, T. K. Jian, Z. Q. Chen, and A. Q. Jia, "Hordenine: a novel quorum sensing inhibitor and antibiofilm agent against *Pseudomonas aeruginosa*," *Journal of Agricultural and Food Chemistry*, vol. 66, no. 7, pp. 1620–1628, 2018.
- [75] J. Ouyang, F. Sun, W. Feng et al., "Quercetin is an effective inhibitor of quorum sensing, biofilm formation and virulence factors in *Pseudomonas aeruginosa*," *Journal of Applied Microbiology*, vol. 120, no. 4, pp. 966–974, 2016.
- [76] J. Wang, M. Song, J. Pan et al., "Quercetin impairs *Streptococcus pneumoniae* biofilm formation by inhibiting sortase A activity," *Journal of Cellular and Molecular Medicine*, vol. 22, no. 12, pp. 6228–6237, 2018.
- [77] J. B. Blumberg, T. A. Camesano, A. Cassidy et al., "Cranberries and their bioactive constituents in human health," *Advances in Nutrition*, vol. 4, no. 6, pp. 618–632, 2013.
- [78] M. R. Khairnar, G. N. Karibasappa, A. S. Dodamani, P. Vishwakarma, R. G. Naik, and M. A. Deshmukh, "Comparative assessment of cranberry and chlorhexidine mouthwash on streptococcal colonization among dental students: a randomized parallel clinical trial," *Contemporary Clinical Dentistry*, vol. 6, no. 1, pp. 35–39, 2015.
- [79] F. Sadat Sajadi, M. Moradi, A. Pardakhty, R. Yazdizadeh, and F. Madani, "Effect of fluoride, chlorhexidine and fluoride-chlorhexidine mouthwashes on salivary *Streptococcus mutans* count and the prevalence of oral side effects," *Journal of Dental Research, Dental Clinics, Dental Prospects*, vol. 9, no. 1, pp. 49–52, 2015.
- [80] H. Koo, S. Duarte, R. M. Murata et al., "Influence of cranberry proanthocyanidins on formation of biofilms by *Streptococcus mutans* on saliva-coated apatitic surface and on dental caries development in vivo," *Caries Research*, vol. 44, no. 2, pp. 116–126, 2010.
- [81] D. Kim, G. Hwang, Y. Liu et al., "Cranberry flavonoids modulate cariogenic properties of mixed-species biofilm through exopolysaccharides-matrix disruption," *PLoS One*, vol. 10, no. 12, p. e0145844, 2015.
- [82] B. Ashrafi, M. Rashidipour, A. Marzban et al., "Mentha piperita essential oils loaded in a chitosan nanogel with inhibitory effect on biofilm formation against *S. mutans* on the dental surface," *Carbohydrate Polymers*, vol. 212, pp. 142–149, 2019.
- [83] G. Feng, M. I. Klein, S. Gregoire, A. P. Singh, N. Vorsa, and H. Koo, "The specific degree-of-polymerization of A-type proanthocyanidin oligomers impacts *Streptococcus mutans* glucan-mediated adhesion and transcriptome responses within biofilms," *Biofouling*, vol. 29, no. 6, pp. 629–640, 2013.
- [84] K. Feghali, M. Feldman, V. D. La, J. Santos, and D. Grenier, "Cranberry proanthocyanidins: natural weapons against periodontal diseases," *Journal of Agricultural and Food Chemistry*, vol. 60, no. 23, pp. 5728–5735, 2012.
- [85] L. Bonifait and D. Grenier, "Cranberry polyphenols: potential benefits for dental caries and periodontal disease," *Journal of Canadian Dental Association*, vol. 76, p. a130, 2010.
- [86] H. Ozdemir, M. I. Kara, K. Erciyas, H. Ozer, and S. Ay, "Preventive effects of thymoquinone in a rat periodontitis model: a morphometric and histopathological study," *Journal of Periodontal Research*, vol. 47, no. 1, pp. 74–80, 2012.
- [87] A. Tada, H. Nakayama-Imahoji, H. Yamasaki et al., "Effect of thymoquinone on *Fusobacterium nucleatum*-associated biofilm and inflammation," *Molecular Medicine Reports*, vol. 22, no. 2, pp. 643–650, 2020.
- [88] X. Huang, L. Cheng, R. A. Exterkate et al., "Effect of pH on *Galla chinensis* extract's stability and anti-caries properties in vitro," *Archives of Oral Biology*, vol. 57, no. 8, pp. 1093–1099, 2012.

- [89] T. Zhang, J. Chu, and X. Zhou, "Anti-cariogenic effects of *Galla chinensis*: a systematic review," *Phytotherapy Research*, vol. 29, no. 12, pp. 1837–1842, 2015.
- [90] N. Kharouf, Y. Haikel, and V. Ball, "Polyphenols in dental applications," *Bioengineering*, vol. 7, no. 3, p. 72, 2020.
- [91] M. Casarin, J. Pazinato, L. M. Oliveira, M. E. Souza, R. C. V. Santos, and F. B. Zanatta, "Anti-biofilm and anti-inflammatory effect of a herbal nanoparticle mouthwash: a randomized crossover trial," *Brazilian Oral Research*, vol. 33, p. e062, 2019.
- [92] M. J. Saharkhiz, M. Motamedi, K. Zomorodian, K. Pakshir, R. Miri, and K. Hemyari, "Chemical Composition, Antifungal and Antibiofilm Activities of the Essential Oil of *Mentha piperita* L.," *ISRN Pharmaceutics*, vol. 2012, Article ID 718645, 6 pages, 2012.
- [93] Y. Sekita, K. Murakami, H. Yumoto et al., "Preventive effects of *Houttuynia cordata* extract for oral infectious diseases," *BioMed Research International*, vol. 2016, Article ID 2581876, 8 pages, 2016.
- [94] N. Nayak, J. Varghese, S. Shetty et al., "Evaluation of a mouthrinse containing guava leaf extract as part of comprehensive oral care regimen- a randomized placebo-controlled clinical trial," *BMC Complementary and Alternative Medicine*, vol. 19, no. 1, p. 327, 2019.
- [95] M. Jang, S.-W. Jeong, S. K. Cho et al., "Anti-inflammatory effects of an ethanolic extract of guava (*Psidium guajava* L.) leaves in vitro and in vivo," *Journal of Medicinal Food*, vol. 17, no. 6, pp. 678–685, 2014.
- [96] Z. Zhang, J. Zeng, X. Zhou et al., "Activity of *Ligustrum robustum* (Roxb.) Blume extract against the biofilm formation and exopolysaccharide synthesis of *Streptococcus mutans*," *Molecular Oral Microbiology*, vol. 36, no. 1, pp. 67–79, 2021.
- [97] F. A. Hale, "Dental caries in the dog," *Canadian Veterinary Journal*, vol. 50, no. 12, pp. 1301–1304, 2009.
- [98] X. Huang, Y. Ge, B. Yang et al., "Novel dental implant modifications with two-staged double benefits for preventing infection and promoting osseointegration in vivo and in vitro," *Bioactive Materials*, vol. 6, no. 12, pp. 4568–4579, 2021.
- [99] E. L. Belinello-Souza, L. H. Alvarenga, C. Lima-Leal et al., "Antimicrobial photodynamic therapy combined to periodontal treatment: experimental model," *Photodiagnosis and Photodynamic Therapy*, vol. 18, pp. 275–278, 2017.
- [100] Y. Liu, Y. Ren, Y. Li et al., "Nanocarriers with conjugated antimicrobials to eradicate pathogenic biofilms evaluated in murine in vivo and human ex vivo infection models," *Acta Biomaterialia*, vol. 79, pp. 331–343, 2018.
- [101] C. Y. Moon, O. H. Nam, M. Kim et al., "Effects of the nitric oxide releasing biomimetic nanomatrix gel on pulp-dentin regeneration: pilot study," *PloS One*, vol. 13, no. 10, p. e0205534, 2018.
- [102] N. Garanayak, M. Das, R. C. Patra, S. Biswal, and S. K. Panda, "Effect of age on dental plaque deposition and its control by ultrasonic scaling, dental hygiene chew, and chlorhexidine (0.2%w/v) in dogs," *Veterinary World*, vol. 12, no. 11, pp. 1872–1876, 2019.
- [103] C. J. Seneviratne, C. F. Zhang, and L. P. Samaranyake, "Dental plaque biofilm in oral health and disease," *Chinese Journal of Dental Research*, vol. 14, no. 2, pp. 87–94, 2011.
- [104] D. Shrivastava, V. Natoli, K. C. Srivastava et al., "Novel approach to dental biofilm management through guided biofilm therapy (GBT): a review," *Microorganisms*, vol. 9, no. 9, 2021.
- [105] R. A. Ccahuana-Vásquez, C. P. Tabchoury, L. M. Tenuta, A. A. Del Bel Cury, G. C. Vale, and J. A. Cury, "Effect of frequency of sucrose exposure on dental biofilm composition and enamel demineralization in the presence of fluoride," *Caries Research*, vol. 41, no. 1, pp. 9–15, 2007.
- [106] F. Filogônio Cde, R. V. Soares, M. C. Horta, C. V. Penido, and R. A. Cruz, "Effect of vegetable oil (Brazil nut oil) and mineral oil (liquid petrolatum) on dental biofilm control," *Brazilian Oral Research*, vol. 25, no. 6, pp. 556–561, 2011.
- [107] A. P. Teitelbaum, M. T. Pochapski, J. L. Jansen, A. Sabbagh-Haddad, F. A. Santos, and G. D. Czlusniak, "Evaluation of the mechanical and chemical control of dental biofilm in patients with Down syndrome," *Community Dentistry and Oral Epidemiology*, vol. 37, no. 5, pp. 463–467, 2009.
- [108] M. F. Monteiro, H. Tonelli, A. A. Reis et al., "Triclosan toothpaste as an adjunct therapy to plaque control in children from periodontitis families: a crossover clinical trial," *Clinical oral investigations*, vol. 24, no. 4, pp. 1421–1430, 2020.
- [109] G. C. Vale, C. P. Tabchoury, R. A. Arthur, A. A. Del Bel Cury, A. F. Paes Leme, and J. A. Cury, "Temporal relationship between sucrose-associated changes in dental biofilm composition and enamel demineralization," *Caries research*, vol. 41, no. 5, pp. 406–412, 2007.
- [110] L. Segundo Ade, M. X. Pisani, C. Nascimento, R. F. Souza, F. Paranhos Hde, and C. H. Silva-Lovato, "Clinical trial of an experimental cleaning solution: antibiofilm effect and integrity of a silicone-based denture liner," *The Journal of Contemporary Dental Practice*, vol. 15, no. 5, pp. 534–542, 2014.
- [111] I. Saliassi, J. C. Llodra, M. Bravo et al., "Effect of a toothpaste/mouthwash containing *Carica papaya* leaf extract on interdental gingival bleeding: a randomized controlled trial," *International Journal of Environmental Research and Public Health*, vol. 15, no. 12, p. 2660, 2018.
- [112] A. D. Haffajee, C. Roberts, L. Murray et al., "Effect of herbal, essential oil, and chlorhexidine mouthrinses on the composition of the subgingival microbiota and clinical periodontal parameters," *Journal of Clinical Dentistry*, vol. 20, no. 7, pp. 211–217, 2009.
- [113] M. N. Motallaei, M. Yazdani, H. Tebyanian et al., "The current strategies in controlling oral diseases by herbal and chemical materials," *Evidence-Based Complementary and Alternative Medicine*, vol. 2021, Article ID 3423001, 22 pages, 2021.
- [114] R. Mishra, A. K. Panda, S. De Mandal, M. Shakeel, S. S. Bisht, and J. Khan, "Natural anti-biofilm agents: strategies to control biofilm-forming pathogens," *Frontiers in Microbiology*, vol. 11, p. 566325, 2020.
- [115] S. G. Parkar, S. Eady, M. Cabecinha, and M. A. Skinner, "Consumption of apple-boysenberry beverage decreases salivary *Actinomyces naeslundii* and their adhesion in a multi-species biofilm model," *Beneficial Microbes*, vol. 8, no. 2, pp. 299–307, 2017.
- [116] A. S. Braga, L. D. Girotti, L. L. de Melo Simas et al., "Effect of commercial herbal toothpastes and mouth rinses on the prevention of enamel demineralization using a microcosm biofilm model," *Biofouling*, vol. 35, no. 7, pp. 796–804, 2019.
- [117] S. Hasan, M. Danishuddin, and A. U. Khan, "Inhibitory effect of zingiber officinale towards *Streptococcus mutans* virulence and caries development: in vitro and in vivo studies," *BMC Microbiology*, vol. 15, no. 1, p. 1, 2015.



- [118] H. Sulistyani, M. Fujita, H. Miyakawa, and F. Nakazawa, "Effect of roselle calyx extract on in vitro viability and biofilm formation ability of oral pathogenic bacteria," *Asian Pacific Journal of Tropical Medicine*, vol. 9, no. 2, pp. 119–124, 2016.
- [119] D. S. Barbieri, F. Tonial, P. V. Lopez et al., "Antiadherent activity of *Schinus terebinthifolius* and *Croton urucurana* extracts on in vitro biofilm formation of *Candida albicans* and *Streptococcus mutans*," *Archives of Oral Biology*, vol. 59, no. 9, pp. 887–896, 2014.
- [120] H. J. Lee, H. S. Park, K. H. Kim, T. Y. Kwon, and S. H. Hong, "Effect of garlic on bacterial biofilm formation on orthodontic wire," *The Angle Orthodontist*, vol. 81, no. 5, pp. 895–900, 2011.
- [121] I. Muñoz-González, T. Thurnheer, B. Bartolomé, and M. V. Moreno-Arribas, "Red wine and oenological extracts display antimicrobial effects in an oral bacteria biofilm model," *Journal of agricultural and food chemistry*, vol. 62, no. 20, pp. 4731–4737, 2014.
- [122] Z. Shafiei, N. N. Shuhairi, N. Fazly Shah Yap, C. A. Harry Sibungkil, and J. Latip, "Antibacterial activity of *Myristica fragrans* against oral pathogens," *Evidence-Based Complementary and Alternative Medicine*, vol. 2012, Article ID 825362, 7 pages, 2012.
- [123] L. Karygianni, M. Cecere, A. L. Skaltsounis et al., "High-level antimicrobial efficacy of representative Mediterranean natural plant extracts against oral microorganisms," *BioMed Research International*, vol. 2014, Article ID 839019, 8 pages, 2014.
- [124] S. A. Oliveira, J. R. Zambrana, F. B. Iorio, C. A. Pereira, and A. O. Jorge, "The antimicrobial effects of *Citrus limonum* and *Citrus aurantium* essential oils on multi-species biofilms," *Brazilian Oral Research*, vol. 28, no. 1, pp. 22–27, 2014.
- [125] D. K. Bardaji, E. B. Reis, T. C. Medeiros, R. Lucarini, A. E. Crotti, and C. H. Martins, "Antibacterial activity of commercially available plant-derived essential oils against oral pathogenic bacteria," *Natural Product Research*, vol. 30, no. 10, pp. 1178–1181, 2016.
- [126] I. Süntar, O. Oyardi, E. K. Akkol, and B. Özçelik, "Antimicrobial effect of the extracts from *Hypericum perforatum* against oral bacteria and biofilm formation," *Pharmaceutical Biology*, vol. 54, no. 6, pp. 1065–1070, 2016.
- [127] A. B. Miller, R. G. Cates, M. Lawrence et al., "The antibacterial and antifungal activity of essential oils extracted from Guatemalan medicinal plants," *Pharmaceutical Biology*, vol. 53, no. 4, pp. 548–554, 2015.
- [128] Y. Zeng, A. Nikitkova, H. Abdelsalam, J. Li, and J. Xiao, "Activity of quercetin and kaempferol against *Streptococcus mutans* biofilm," *Archives Oral Biology*, vol. 98, pp. 9–16, 2019.
- [129] Y. Yang, S. Liu, Y. He, Z. Chen, and M. Li, "Effect of Long Zhang gargle on biofilm formation and acidogenicity of *Streptococcus mutans* in vitro," *BioMed Research International*, vol. 2016, Article ID 5829823, 8 pages, 2016.
- [130] N. L. M. Almeida, L. L. Saldanha, R. A. da Silva et al., "Antimicrobial activity of denture adhesive associated with *Equisetum giganteum*- and *Punica granatum*-enriched fractions against *Candida albicans* biofilms on acrylic resin surfaces," *Biofouling*, vol. 34, no. 1, pp. 62–73, 2018.
- [131] K. S. Mistry, Z. Sanghvi, G. Parmar, S. Shah, and K. Pushpalatha, "Antibacterial efficacy of *Azadirachta indica*, *Mimusops elengi* and 2% CHX on multispecies dental biofilm," *Journal of Conservative Dentistry: JCD*, vol. 18, no. 6, pp. 461–466, 2015.
- [132] A. Subbiya, K. Mahalakshmi, S. Pushpangadan, K. Padmavathy, P. Vivekanandan, and V. G. Sukumaran, "Antibacterial efficacy of *Mangifera indica* L. kernel and *Ocimum sanctum* L. leaves against *Enterococcus faecalis* dental biofilm," *Journal of Conservative Dentistry: JCD*, vol. 16, no. 5, p. 454–7, 2013.
- [133] M. Raof, M. Khaleghi, N. Siasar, S. Mohannadalizadeh, J. Haghani, and S. Amanpour, "Antimicrobial activity of methanolic extracts of *Myrtus communis* L. and *Eucalyptus Galbie* and their combination with calcium hydroxide powder against *Enterococcus Faecalis*," *Journal of Dentistry*, vol. 20, no. 3, pp. 195–202, 2019.
- [134] R. Kalaiselvam, K. Soundararajan, R. M. Rajan, K. Deivanayagam, C. Arumugam, and A. Ganesh, "Comparative evaluation of the anti-bacterial efficacy of herbal medicaments and synthetic medicaments against *Enterococcus faecalis* using real-time polymerase chain reaction," *Cureus*, vol. 11, no. 7, p. e5228, 2019.
- [135] O. J. Birring, I. L. Vilorio, and P. Nunez, "Anti-microbial efficacy of *Allium sativum* extract against *Enterococcus faecalis* biofilm and its penetration into the root dentin: an in vitro study," *Indian Journal of Dental Research*, vol. 26, no. 5, pp. 477–482, 2015.
- [136] J. Prabhakar, S. Balagopal, M. S. Priya, S. Selvi, and M. Senthilkumar, "Evaluation of antimicrobial efficacy of Triphala (an Indian Ayurvedic herbal formulation) and 0.2% chlorhexidine against *Streptococcus mutans* biofilm formed on tooth substrate: an in vitro study," *Indian Journal of Dental Research*, vol. 25, no. 4, pp. 475–479, 2014.
- [137] R. D. Wojtyczka, M. Kępa, D. Idzik et al., "In vitro antimicrobial activity of ethanolic extract of Polish propolis against biofilm forming *Staphylococcus epidermidis* strains," *Evidence-based complementary and alternative medicine*, vol. 2013, Article ID 590703, 11 pages, 2013.
- [138] H. Pretti, G. L. Barbosa, E. M. Lages, A. Gala-García, C. S. Magalhães, and A. N. Moreira, "Effect of chlorhexidine varnish on gingival growth in orthodontic patients: a randomized prospective split-mouth study," *Dental press journal of orthodontics*, vol. 20, no. 5, pp. 66–71, 2015.
- [139] T. T. Hägi, P. Hofmänner, S. Eick et al., "The effects of erythritol air-polishing powder on microbiologic and clinical outcomes during supportive periodontal therapy: six-month results of a randomized controlled clinical trial," *Quintessence International (Berlin, Germany: 1985)*, vol. 46, no. 1, pp. 31–41, 2015.
- [140] C. Jovito Vde, I. A. Freires, D. A. Ferreira, Q. Paulo Mde, and R. D. Castro, "Eugenia uniflora dentifrice for treating gingivitis in children: antibacterial assay and randomized clinical trial," *Brazilian Dental Journal*, vol. 27, no. 4, pp. 387–392, 2016.
- [141] L. M. De Freitas, G. M. F. Calixto, M. Chorilli et al., "Polymeric nanoparticle-based photodynamic therapy for chronic periodontitis in vivo," *International Journal of Molecular Sciences*, vol. 17, no. 5, p. 769, 2016.
- [142] T. He, M. K. Anastasia, M. Zsiska, T. Farmer, E. Schneiderman, and J. L. Millemann, "In vitro and in vivo evaluations of the anticalculus effect of a novel stabilized stannous fluoride dentifrice," *The Journal of Clinical Dentistry*, vol. 28, no. 4, pp. B21–B26, 2017.
- [143] L. R. Friesen, C. R. Goyal, J. G. Qaqish et al., "Comparative antiplaque effect of two antimicrobial dentifrices: laboratory and clinical evaluations," *The Journal of Clinical Dentistry*, vol. 28, no. 4, pp. B6–11, 2017.

- [144] N. B. Arweiler, F. Grelle, A. Sculean, C. Heumann, and T. M. Auschill, "Antibacterial effect and substantivity of toothpaste slurries in vivo," *Oral Health & Preventive Dentistry*, vol. 16, no. 2, pp. 175–181, 2018.
- [145] A. R. F. D. Castilho, C. Duque, P. F. Kreling et al., "Doxycycline-containing glass ionomer cement for arresting residual caries: an in vitro study and a pilot trial," *Journal of Applied Oral Science*, vol. 26, p. e20170116, 2018.
- [146] K. V. Prasad, S. G. Therathil, A. Agnihotri, P. K. Sreenivasan, L. R. Mateo, and D. Cummins, "The effects of two new dual zinc plus arginine dentifrices in reducing oral bacteria in multiple locations in the mouth: 12-hour whole mouth antibacterial protection for whole mouth health," *Journal of Clinical Dentistry*, vol. 29, pp. A25–A32, 2018.
- [147] R. F. de Souza, C. H. Silva-Lovato, C. N. de Arruda et al., "Efficacy of a propolis solution for cleaning complete dentures," *American Journal of Dentistry*, vol. 32, no. 6, pp. 306–310, 2019.
- [148] V. F. Furletti, I. P. Teixeira, G. Obando-Pereda et al., "Action of *Coriandrum sativum* L. essential oil upon oral *Candida albicans* biofilm formation," *Evidence-Based Complementary and Alternative Medicine*, vol. 2011, Article ID 985832, 9 pages, 2011.
- [149] M. Fani and J. Kohanteb, "Inhibitory activity of Aloe vera gel on some clinically isolated cariogenic and periodontopathic bacteria," *Journal of Oral Science*, vol. 54, no. 1, pp. 15–21, 2012.
- [150] J. R. de Oliveira, V. C. de Castro, P. D. G. F. Vilela et al., "Cytotoxicity of Brazilian plant extracts against oral microorganisms of interest to dentistry," *BMC Complementary Alternative Medicine*, vol. 13, no. 1, pp. 1–7, 2013.
- [151] D. Gupta and R. K. Gupta, "Investigation of antibacterial efficacy of *Acacia nilotica* against salivary mutans streptococci: a randomized control trial," *General Dentistry*, vol. 63, no. 1, pp. 23–27, 2015.
- [152] H. R. Abdulbaqi, W. H. Himratul-Aznita, and N. A. Baharuddin, "Evaluation of *Salvadora persica* L. and green tea anti-plaque effect: a randomized controlled crossover clinical trial," *BMC Complementary Alternative Medicine*, vol. 16, no. 1, p. 493, 2016.
- [153] M. M. Badaro, M. M. Salles, V. M. F. Leite et al., "Clinical trial for evaluation of *Ricinus communis* and sodium hypochlorite as denture cleanser," *Journal of Applied Oral Science*, vol. 25, no. 3, pp. 324–334, 2017.
- [154] E. Giammarinaro, S. Marconcini, A. Genovesi, G. Poli, C. Lorenzi, and U. Covani, "Propolis as an adjuvant to non-surgical periodontal treatment: a clinical study with salivary anti-oxidant capacity assessment," *Minerva stomatologica*, vol. 67, no. 5, pp. 183–188, 2018.
- [155] S. Dolatabadi, H. N. Moghadam, and M. Mahdavi-Ourtakand, "Evaluating the anti-biofilm and antibacterial effects of *Juglans regia* L. extracts against clinical isolates of *Pseudomonas aeruginosa*," *Microbial Pathogenesis*, vol. 118, pp. 285–289, 2018.
- [156] A. Zare Javid, E. Amerian, L. Basir, A. Ekrami, M. H. Haghhighzadeh, and L. Maghsoumi-Norouzabad, "Effects of the consumption of probiotic yogurt containing *Bifidobacterium lactis* Bb12 on the levels of *Streptococcus mutans* and *Lactobacilli* in saliva of students with initial stages of dental caries: a double-blind randomized controlled trial," *Caries Research*, vol. 54, no. 1, pp. 68–74, 2020.
- [157] M. M. Badaró, F. L. Bueno, R. M. Arnez et al., "The effects of three disinfection protocols on *Candida* spp., denture stomatitis, and biofilm: a parallel group randomized controlled trial," *The Journal of Prosthetic Dentistry*, vol. 124, no. 6, pp. 690–698, 2020.
- [158] W. Buakaew, R. P. Sranujit, C. Noysang et al., "Evaluation of mouthwash containing *Citrus hystrix* DC., *Moringa oleifera* Lam. and *Azadirachta indica* A. Juss. leaf extracts on dental plaque and gingivitis," *Plants (Basel)*, vol. 10, no. 6, p. 1153, 2021.
- [159] V. Quintas, I. Prada-López, J. C. Prados-Frutos, and I. Tomás, "In situ antimicrobial activity on oral biofilm: essential oils vs. 0.2 % chlorhexidine," *Clinical Oral Investigations*, vol. 19, no. 1, pp. 97–107, 2015.
- [160] G. John, F. Schwarz, and J. Becker, "Taurolidine as an effective and biocompatible additive for plaque-removing techniques on implant surfaces," *Clinical Oral Investigations*, vol. 19, no. 5, pp. 1069–1077, 2015.
- [161] C. J. Simon, P. Munivenkatappa Lakshmaiah Venkatesh, and R. Chickanna, "Efficacy of glycine powder air polishing in comparison with sodium bicarbonate air polishing and ultrasonic scaling - a double-blind clinico-histopathologic study," *International Journal of Dental Hygiene*, vol. 13, no. 3, pp. 177–183, 2015.
- [162] R. Ghorbanzadeh, B. Pourakbari, and A. Bahador, "Effects of baseplates of orthodontic appliances with in situ generated silver nanoparticles on cariogenic bacteria: a randomized, double-blind cross-over clinical trial," *The Journal of Contemporary Dental Practice*, vol. 16, no. 4, pp. 291–298, 2015.
- [163] E. M. Takeshita, M. Danelon, L. P. Castro, K. T. Sasaki, and A. C. Delbem, "Effectiveness of a toothpaste with low fluoride content combined with trimetaphosphate on dental biofilm and enamel demineralization in situ," *Caries Research*, vol. 49, no. 4, pp. 394–400, 2015.
- [164] E. Andrade, P. Weidlich, P. D. Angst, S. C. Gomes, and R. V. Oppermann, "Efficacy of a triclosan formula in controlling early subgingival biofilm formation: a randomized trial," *Brazilian Oral Research*, vol. 29, no. 1, pp. 1–8, 2015.
- [165] F. W. Muniz, K. S. Sena, C. C. de Oliveira, D. M. Verissimo, R. S. Carvalho, and R. S. Martins, "Efficacy of dental floss impregnated with chlorhexidine on reduction of supragingival biofilm: a randomized controlled trial," *International Journal of Dental Hygiene*, vol. 13, no. 2, pp. 117–124, 2015.
- [166] J. C. E. M. Junior, L. H. Nunes, C. S. Arruda et al., "Effectiveness of oral antiseptics on tooth biofilm: a study in vivo," *The Journal of Contemporary Dental Practice*, vol. 16, no. 8, pp. 674–678, 2015.
- [167] P. Goes, C. S. Dutra, M. R. Lisboa et al., "Clinical efficacy of a 1% *Matricaria chamomile* L. mouthwash and 0.12% chlorhexidine for gingivitis control in patients undergoing orthodontic treatment with fixed appliances," *Journal of oral science*, vol. 58, no. 4, pp. 569–574, 2016.
- [168] B. A. Pancer, D. Kott, J. V. Sugai et al., "Effects of triclosan on host response and microbial biomarkers during experimental gingivitis," *Journal of Clinical Periodontology*, vol. 43, no. 5, pp. 435–444, 2016.
- [169] E. B. Moffa, F. E. Izumida, J. H. Jorge, M. C. Mussi, W. L. Siqueira, and E. T. Giampaolo, "Effectiveness of chemical disinfection on biofilms of relined dentures: a randomized clinical trial," *American Journal of Dentistry*, vol. 29, no. 1, pp. 15–19, 2016.

## *Retraction*

# **Retracted: Big Data Analysis of Manufacturing and Preclinical Studies of Nanodrug-Targeted Delivery Systems: A Literature Review**

### **BioMed Research International**

Received 20 June 2023; Accepted 20 June 2023; Published 21 June 2023

Copyright © 2023 BioMed Research International. This is an open access article distributed under the Creative Commons Attribution License, which permits unrestricted use, distribution, and reproduction in any medium, provided the original work is properly cited.

This article has been retracted by Hindawi following an investigation undertaken by the publisher [1].

This investigation has uncovered evidence of one or more of the following indicators of systematic manipulation of the publication process:

- (1) Discrepancies in scope
- (2) Discrepancies in the description of the research reported
- (3) Discrepancies between the availability of data and the research described
- (4) Inappropriate citations
- (5) Incoherent, meaningless and/or irrelevant content included in the article
- (6) Peer-review manipulation

The presence of these indicators undermines our confidence in the integrity of the article's content and we cannot, therefore, vouch for its reliability. Please note that this notice is intended solely to alert readers that the content of this article is unreliable. We have not investigated whether authors were aware of or involved in the systematic manipulation of the publication process.

Wiley and Hindawi regrets that the usual quality checks did not identify these issues before publication and have since put additional measures in place to safeguard research integrity.

We wish to credit our own Research Integrity and Research Publishing teams and anonymous and named

external researchers and research integrity experts for contributing to this investigation.










The corresponding author, as the representative of all authors, has been given the opportunity to register their agreement or disagreement to this retraction. We have kept a record of any response received.

### **References**

- [1] Q. Cao, X. Li, Q. Zhang et al., "Big Data Analysis of Manufacturing and Preclinical Studies of Nanodrug-Targeted Delivery Systems: A Literature Review," *BioMed Research International*, vol. 2022, Article ID 1231446, 10 pages, 2022.

## Review Article

# Big Data Analysis of Manufacturing and Preclinical Studies of Nanodrug-Targeted Delivery Systems: A Literature Review

Qiang Cao <sup>1</sup>, Xiaochen Li <sup>2</sup>, Qi Zhang <sup>3</sup>, Kexuan Zhou <sup>4</sup>, Ying Yu <sup>3</sup>, Zixu He <sup>5</sup>,  
Zhibiao Xiang <sup>6</sup>, Yi Qiang <sup>7</sup>, and Wei Qi <sup>1</sup>

<sup>1</sup>School of Pharmacy, Macau University of Science and Technology, China

<sup>2</sup>The Third Affiliated Hospital of Shandong First Medical University, China

<sup>3</sup>Taishan University, China

<sup>4</sup>Hainan University, China

<sup>5</sup>University of New South Wales, University of New South Wales, Australia

<sup>6</sup>Second Xiangya Hospital, The Second Xiangya Hospital, China

<sup>7</sup>Kunming University of Science and Technology, China

Correspondence should be addressed to Yi Qiang; 462766753@qq.com and Wei Qi; 2166764636@qq.com

Received 24 June 2022; Revised 8 July 2022; Accepted 21 July 2022; Published 30 July 2022

Academic Editor: Dinesh Rokaya

Copyright © 2022 Qiang Cao et al. This is an open access article distributed under the Creative Commons Attribution License, which permits unrestricted use, distribution, and reproduction in any medium, provided the original work is properly cited.

**Objective.** Nanodelivery is a modern technology involving improved delivery methods and drug formulations. The current development and initial applications of nanocarriers are pointing to new directions in the current development of nanomedicine. Researchers are increasingly applying nanodelivery to the delivery of therapeutic or diagnostic agents. This article discusses the preparation and application of nanocomplexes and nanoparticles, as well as their potential future value in clinical research. Through a review and analysis, it is hoped that this will serve as a guide for the future development of various nanodelivery technologies and help researchers learn more about these technologies. **Materials and Methods.** A literature search was conducted using the keywords “Nano drug delivery” or “Nanomaterials” or “Nano”. A literature search was conducted in three major databases, PubMed, Web of Science, and Google Scholar, using the keywords such as “Nano drug delivery”, “Nanomaterials”, or “Nanobubble drug delivery”. The initial search was screened by title and abstract. In the full-text review, the titles or abstracts were reviewed according to the selection criteria based on the inclusion criteria. The risk of bias and study quality was assessed according to the Cochrane guidelines, and possible biases such as selection bias and good selection bias were included in the review. **Results.** A total of 297 studies were included in this study, of which 219 were excluded based on the screening criteria, resulting in the inclusion of 78 studies, the majority of which were original studies and clinical trials, and a small number of which provided design and route of administration analysis of nanomaterial particles and effect fluorograms and were studied in more depth. This paper summarises and reviews the views and directions of the included articles. The main directions include cyclodextrin-based or grafted cyclodextrin nanomaterials, nanobubbles, and stimuli-sensitive and temperature-sensitive nanodelivery systems. **Conclusion.** The use of innovative, targeted drug delivery systems is effective in cancer drug delivery by summarising the previous studies. However, nanodelivery systems’ risks and therapeutic effects need to be evaluated before clinical application. Future research in the field of targeted drug delivery nanosystems should focus on the development of nanocarriers with high in vivo delivery capacity, good synergy with therapeutic agents, and milder short-term and long-term toxicological effects and conduct comprehensive preclinical trials on nanodrug delivery systems with high potential for clinical application as soon as possible, to find nanodrug delivery systems suitable for clinical use and put them into the clinical application as soon as possible.



## 1. Introduction

The materials chosen for nanodelivery can come from almost any substance, lipophilic colloidal nanoparticles (NPs) from solid lipids and phospholipids and nanomaterials based on carbon, natural, or synthetic polymers, and metal oxides can also be used. In bio-nanotechnology, nanomaterials are used in biomedical applications, including targeted drug delivery, contrast agents, and biosensors. Many nanomaterials' properties allow them to be used in drug delivery processes but can also make them toxic to living cells. Due to their large surface area, nanomaterials are more active and can easily cross environmental barriers, pass through cell membranes, and enter the body. In order to maximize the potential of nanotechnology, a sound scientific approach to nanotoxicology and safety issues is required. There are many different approaches in preparing NF, using both conventional and unconventional techniques in both the solid and liquid phases [1]. The main objective is to obtain NFs of uniform size and shape. Several techniques have addressed this issue; mechanochemistry is used in solvent-free solid-phase synthesis, while microwave radiation and ultrasonication are used for synthesis in aqueous solutions.

As a heat source with a high heating rate, microwave irradiation can produce large quantities of high-quality NS in a short period. The application of microwave irradiation allows for a high degree of homogeneous mixing of raw materials and reduced crystal production during the preparation of nanomaterials. It increases the reaction rate when preparing nanomaterials [2, 3]. Sonochemical and microwave-assisted synthesis development can be effectively applied to the derivatization of carbon-based nanomaterials and the production of nanostructured cyclodextrin oligomers and grafted nanomaterials for biomedical applications. Studies have shown that CD derivatives can retain drug and contrast agent molecules and be used as versatile and efficient carriers and contrast agents for MRI. Grafting CD onto NF can increase its water solubility and surface accessibility. Since the nanobubbles are spherical in structure, multifunctional nanocarriers can be developed on nanobubbles (core/shell) for targeted imaging and therapy. It has become increasingly important to improve the efficacy of antitumor drug nanosystems and to use nanodelivery strategies for successful treatment, as they enable "on-demand" drug release and tailored delivery regimens. In an ideal, it would be able to deliver the appropriate medication at the appropriate time to the appropriate patient.

## 2. Methods

The current literature search was conducted using PubMed, Web of Science, and Google Scholar until 9 May 2022 with the following search terms: "Nano drug delivery" or "Nanomaterials" or "Nanobubble drug delivery", including original research, randomized trials, clinical trials, reports, and guidelines.

The articles were initially screened by title and abstract. The review of titles or abstracts against inclusion criteria was carried out in a full-text review based on selection cri-

teria and assessed for risk of bias and study quality against Cochrane guidelines, with potential bias such as selection bias and good selection bias included in the review, with two members of this group dedicated to bias assessment and ultimately consensus within the group. After the bias assessment, exclusion of some literature that would pose a risk of bias to this study, the contents of the literature were put together, and the references in the literature were used to make a data network from which the data and discussion that would support this study were eventually gathered. This study is a review article conducted following the PRISMA-P statement and did not require approval by the ethics committee before proceeding with the study.

## 3. Results

After a search exercise in three databases, a total of 297 studies were included in this study, of which 219 were excluded based on the selection criteria, resulting in the inclusion of 78 studies, most of which were original studies and clinical trials, and a small number of which provided the design of nanomaterial particles with the route of administration analysis and effect fluorograms of and conducted more in-depth studies. Different members wrote two articles on the same unit or subject group, and their conclusions were similar. Some of the included articles have not been peer-reviewed. This poses a slight challenge to the research work in this paper. The relevance of the included literature is shown in Figure 1. This paper summarises and synthesizes the views and directions of the included articles. It focuses on the current status and prospects of intelligent nanosystems for drug delivery controlled by specific internal or external factors.

### 3.1. Cyclodextrin-Based or Grafted Cyclodextrin Nanomaterials.

The use of nanotechnology for drug delivery offers new opportunities for the delivery of therapeutic drugs to intracellular targets and monitoring target delivery sites, which could influence the future development of the pharmaceutical and biotechnology industries. In the future, nanodrug delivery systems may be able to achieve targets with good biocompatibility and improve the physicochemical properties of drugs (stability, solubility, and bioavailability) [4]. As with other synthetic methods, unconventional techniques using ultrasound and microwaves have been widely used to prepare new versus known structures based on CD, and in experiments, this approach has shown good efficiency and short reaction times. The production of a water-soluble phosphate oligonucleotide isomer by ultrasound as a dendritic multicarrier with high receptivity and its suitability as an MRI contrast agent has been successfully demonstrated in relaxation titration experiments of Gd complexes placed on a dendritic polymer platform and in successful experiments regarding cell viability and binding capacity [5–7]. Microwave radiation has currently been demonstrated to enable the derivatization of carbon nanotubes (SWCNTs) with CD and contrast agents [8, 9]. The effectiveness of microwave exposure has also been demonstrated for producing graphene oxide grafted to porphyrins [10]. With the help of these antecedent studies, it is currently possible to investigate the ability of CD to attach or release drugs concerning magnetic





nanobubbles and improve drug binding capabilities. The presence of polysaccharide shells allows for interaction with specific ligands.

Table 1 shows a list of biomolecules that enter the perfluorocarbon polysaccharide nanobubbles differently. The hybrid system contains a monolayer of phospholipids that can interact with polyelectrolytes. The structure of this hybrid lipid-polymer system is based on the fact that the phospholipid monolayer can adsorb charged polymers, such as polysaccharides, through various types of interactions, including electrostatic hydrophobic. Attempts have been made to create smaller nanobubbles. Most of these involve technical manipulation of the microbubbles during preparation, such as gravity gradient separation, physical filtration, or flotation. An alternative approach to achieving this goal is the initial formation of nanoscale systems. Nanobubbles are obtained mainly by ultrasonic treatment, high shear emulsification, thin layer evaporation, and mechanical stirring; these procedures are also used to obtain microbubbles [13]. Nanobubbles are a versatile tool for developing externally controlled nanocarriers with the controlled release of active drugs and imaging capabilities. Nanobubbles show high drug binding (encapsulation) efficiency and prolonged drug release.

**3.3. Stimulation-Sensitive Nanosystems.** The effectiveness of drug therapy depends mainly on how the active ingredient reaches the target organs and tissues. On the way to the target, drug molecules can be affected by enzymes and have problems accessing the target area and cell selectivity. In this regard, the development of targeted drug delivery systems utilizing LF holds great promise for applications, with both passive and active targeting showing promising results. In addition, the novel properties of such nanosystems have the potential to enhance the bioavailability of drugs at the desired site. Targeted drug delivery systems for PM ensure that the drug leaves the bloodstream only at the target site or “target organ,” where passive or active PM accumulation occurs. The use of low-density drug delivery ensures better access to specific organs and prevents the elimination of drugs due to first-pass effects in the liver. Passive accumulation occurs due to the EPR effect observed in pathological tissues. For example, in tumor cells, NF accumulation is much faster than in other tissues and is characterized by uneven distribution and particle size dependence. Accumulation of activity is achieved due to specific interactions of the nanosystem with the target cells—due to the presence of monoclonal antibodies or bioconjugates on the NS surface [17]. However, NF’s targeted drug delivery systems are often accompanied by systemic side effects associated with nonspecific biodistribution and uncontrolled drug release patterns. Several nanoformulations for cancer treatment have been proposed in the pharmaceutical market, and they have shown a better safety profile than conventional drugs. However, researchers have noted low bioavailability of drugs within the tumor and insufficient therapeutic efficacy [18]. Researchers in related fields are currently seeking modern nanodelivery systems that enable controlled drug release in space and time to overcome these problems. Joint developments in nanomaterials and pharmaceutical research are paving the way for the development of

innovative nanodelivery systems, particularly in the treatment of cancer, where nanomaterials can play a therapeutic role together with drugs. Intelligent nanosystems that are sensitive to external or internal factors can improve drug efficacy and reduce side effects, resulting in intelligent stimulus-sensitive nanosystems [19].

There are two types of stimulus-sensitive nanosystems available, i.e., nanodelivery systems that can respond to changes in the biological environment and thus regulate the rate of drug release based on a feedback system and delivery systems that can activate and release a drug in response to some external trigger. In both systems, sensitivity to internal or external stimuli can be achieved by using nanomaterials carrying functional groups that can change their properties depending on the strength of the signal. This leads to changes in the properties of the nanosystem, such as the ability to release the drug. These changes may have different properties, but a nanodelivery system can only be considered intelligent if these structural changes are reversible and proportional to the intensity of the stimulus [18].

#### 3.4. Nanosystems Sensitive to Internal Stimuli

**3.4.1. Nanoparticles with Redox-Dependent Reactions.** The design and development of NFs with a redox response are another direction for targeted drug delivery to specific sites within tumor cells. Glutathione oxidation systems that have entered clinical trials are being used initially in cancer cell therapy and have been selected as a reference model for developing redox-dependent nanocarriers. It has been shown that the concentration of glutathione localized in tumor cells is 100-500 times higher than in normal cells [19–23]. GSH levels in the intercellular space may cause bond exchange in the thiol-disulfide system. Polymers with disulfide bonds in their structure can successfully exploit this property to release drugs rapidly in response to glutathione stimulation. There are two ways to exploit the properties of disulfide bonds in polymer systems, i.e., modifying disulfide bonds directly on the polymer framework versus creating disulfide bonds in the polymer network as a cross-linking agent.

A 2019 study suggested improvements to active ingredient delivery systems, suggesting that glutathione-sensitive nanofibers that are unstable inside cells could be used [24]. The disulfide bonds of polymers can maintain their stability in the extracellular space for long periods but lose their stability once inside the cell. As a result, the bioavailability and efficiency of redox-dependent nanosystems are improved. The depletion of endogenous antioxidants makes cancer cells more susceptible to chemotherapeutic agents. This research has driven the generation of a new class of glutathione-sensitive CD nanodelivery systems designed to deliver doxorubicin in a targeted manner to cells with high GSH content. Glutathione-specific carriers loaded with doxorubicin inhibited clonal growth, cell viability, and enzyme activity and induced more structural DNA damage than other delivery methods when observed in different cell lines. Notably, the use of this system inhibited prostate tumor development more effectively than the administration of unconjugated drugs, without additional toxicity.

TABLE 1: The case of nanobubble delivery of bioactive substances.

Treatment effects	Medicinal product	Method of administration
Diagnostic systems	Gd complexes	Intravenous
Antibacterial	Vancomycin, erythromycin	Topical delivery
Anti-inflammatory	Prednisolone	Intravenous
Antifungal	Itraconazole	Topical delivery
Antivirus	Acyclovir, valacyclovir	Topical delivery
Gene therapy	DNA, siRNA	Intravenous
Antitumor	Doxorubicin, paclitaxel, doxorubicin, and cisplatin	Intravenous
Other	Curcumin, melatonin	Topical delivery/intravenous

Due to the nanosystem's precise delivery, doxorubicin can act more specifically on cancer cells and less on healthy cells near the cancer cells. This means that doxorubicin delivered by the nanosystem has less of an effect on healthy cells than free doxorubicin, ensuring therapeutic efficacy and minimizing side effects.

**3.4.2. Reaction of Nanoparticles with pH Dependence.** A typical example of a stimulus-dependent nanosystem that responds to internal signals is the operation of pH-sensitive nanocarriers for targeted transport to dense tumors. Low pH in the extracellular matrix caused by glycolytic activity in tumor tissue can be a specific stimulus for the nanosystem. Given that surface potential is directly related to cellular uptake, charge-induced polymeric nanosystems have been proposed for targeted delivery to tumor tissue. Positively charged NF exhibits good permeability due to positive interaction with the cell membrane. Furthermore, this NS can act like a "proton sponge," causing disruption of lysosomes, facilitating intracytoplasmic delivery, and inducing cancer cell death [20]. The new tetrasaccharide-based polymer obtained by Caldera et al. is a chain of cyclic nigrosugar-1-6-nigrosugar (CNN). Cross-linking the four glucose and caramel dihydrates produced the entire NF described as "nanoporous" (NG). The polymer was characterized by its biocompatibility and ability to be selectively assimilated by cells according to pH changes. Doxorubicin is well encapsulated in the nanostructure and shows a slow and stable release pattern. The combination of the pH specificity of doxorubicin and the prolonged release capacity in the CNN nanostructures, which enhanced the antitumor effect, suggests the success of this nanostructure as a nanomedical tool while showing a milder toxicological profile and common side effects of the therapy [21].

The pH-dependent blocking of SiO<sub>2</sub> mesopores using fluorescently labeled CD derivatives has also demonstrated favorable release kinetics of doxorubicin. The ability to monitor the movement of fluorescently stained NPs during treatment provides an advantage for applying this substance [22].

### 3.5. Nanosystems Sensitive to External Stimuli

**3.5.1. Nanoparticles Sensitive to Temperature and Ultrasound.** Controlling the rate of drug release from the nanocarrier by temperature changes is the most common way of delivering drugs. Under pathological conditions, for

example, the temperature of cancerous tissue is higher than the temperature of healthy tissue. This difference can act as a trigger for releasing the drug at the tumor site. Thermosensitive nanocarriers are designed to not release the drug formulation at physiological temperatures (37°C) and to release the drug when the temperature rises to 40-45°C. For safety reasons, the temperature range of most nanocarriers is calculated so that the threshold of sensitivity to temperature signals exceeds the background temperature fluctuations. By combining the effects of thermotherapy in the presence of temperature-sensitive liposomes, a specific release of the drug substance in the tumor can be achieved.

**3.5.2. Nanoparticles and Nanobubbles Sensitive to Ultrasound.** Ultrasound is widely used in clinical diagnosis and treatment, mainly due to its high penetrating power and safety for the body. Low-frequency ultrasound can penetrate body organs and act on body tissues and organs in various ways including local temperature elevation. The effect depends on the frequency of the waveband used, the intensity of the radiation, and the duration of the exposure. Local heating of tissues with ultrasound is widely used in clinical practice (focused high-intensity ultrasound), while the therapeutic effects of nonthermal ultrasound irradiation have been less studied. In addition to thermal effects, ultrasound is also used to convert the permeability of biological barriers and regulate drug delivery; it is used in ultrasound therapy.

Sonodynamic therapy (SRT) is a technique in which low toxicity molecules are activated by physical exposure to ultrasound, leading to oxidation, damage, and death of cancer cells. The effects of SRT are achieved by applying an external stimulus in the presence of the molecules or colloidal systems activated by it. The combination of these two factors, in turn, provides a biological effect. Acoustic cavitation is the formation or operation of a cavity filled with gas or vapor (bubbles) in a medium subjected to ultrasonic action. Two states of acoustic cavitation are distinguished.

A steady state in which oscillations cause the liquid to evaporate and mix with the surrounding microenvironment

Inertial state in which the growing cavity will grow to the maximum volume attainable at the ultrasonic wavelength in which it is located, producing an explosion upon reaching its maximum value. In the second case, the temperature of the microenvironment surrounding the explosion may rise sharply to 10 000°C, and the pressure may reach up to



81 MPa, turning the system into a kind of “acoustic-chemical reactor” [25]. In anticancer therapy, LF can be used as a stimulus-dependent acoustic sensitizer with improved spatial and velocity properties and as an acoustic sensitizer in its own right if cleverly designed [26].

The significant anticancer activity of polymethylmethacrylate containing 4-sulfophenyl porphyrins was demonstrated in an *in vitro* neuroblastoma model when the target site was exposed to ultrasound [27, 28]. These NFs can act as acoustically sensitive systems for *in vivo* applications, as radiolabelling and magnetic resonance imaging agents, and their suitability for targeted therapy and imaging of dense tumors. The nanosystems were loaded with 4-sulfophenyl porphyrin for anticancer or  $^{64}\text{Cu}$ -TPPS for diffusion topography studies in positron emission tomography. Based on a comparison of MR data taken before and after treatment in a synthetic breast cancer model, the TPPS-RMANCH nanosystem showed sensitivity to ultrasound. The 4-sulfophenyl porphyrin and polymethyl methacrylate carried by the TPPS-RMANCH nanosystem can work as an anticancer agent in ultrasound therapy by combining their effects, suggesting that this multimodal system could be successfully used as a selective external control tool for cancer control [29].

In order to better understand the unique properties of inorganic NPs and, in this case, gold, the properties of gold have also been investigated to understand its LPR phenomenon better. NF made from gold coupled to folic acid polyethylene glycol has been shown to act as an adjuvant sensitizer for cancer treatment. Sensitivity to ultrasound exposure was studied on human cancer cell lines with varying numbers of folate receptors. Gold-made NF was selectively sensitive to folate receptors in highly expressed cancer cells, leading to decreased cell growth, increased production of reactive oxygen species, and increased necrotic cells through ultrasound exposure [30]. Exploiting the synergy between the precise targeting of gold NF and the sensitizing effect obtained through local external stimulation could make the nanosystem a promising platform for site-specific cancer treatment. This *in vitro* study can be considered as evidence that gold nanofibres have the potential to be used in the treatment of cancer.

One study investigated the feasibility of combining nanobubbles with ultrasound irradiation for the topical treatment of dermatological conditions. A vehicle was developed to treat localized skin lesions associated with hypoxia while accelerating wound healing [31, 32]. That study also developed decalfluoropentane- or dodecafluoropentane-loaded nanobubbles with dextran and chitosan shells for oxygen delivery, capable of dissolving and storing oxygen in their cores and releasing it slowly and stably due to their perfluorocarbon properties [32–35]. Under both *in vitro* and *in vivo* conditions, the decalfluoropentane system showed significant efficacy in delivering oxygen to hypoxic regions, as evidenced by comparative analysis using oximetry and photoacoustic imaging. By exploiting the antimicrobial properties of chitosan, oxygen-loaded nanodroplets in chitosan shells have been proposed as an innovative tool to aid in treating infections in patients with chronic skin diseases [32, 36]. Oxygen-loaded nanodroplets exhibited high cytostatic activity against methicillin-resistant *Staphylo-*

*coccus aureus* (MRSA) and *Candida albicans*, with no toxic effect on human keratinocytes (HaCaT). In addition, additional ultrasound exposure promoted transdermal delivery of oxygen from nanodroplets to tissues exposed to hypoxia. Research in recent years has focused on an in-depth study of the morphology of nanobubbles that facilitate oxygen transport, as exogenous oxygen delivery to tumors is difficult if removed from the bloodstream. The excellent solubility of oxygen in the bubbles gives them an advantage in delivering oxygen to hypoxic tissues.

Nanobubbles made of dextran sulfate were designed for targeted drug delivery in skin infections [37]. The combined use of targeted drug delivery and ultrasound irradiation facilitated the penetration of antibiotics into the skin through the action of ultrasound electrophoresis, and targeted drug release occurred at the site of disease.

Diethylaminoethyl dextran (DEAE) nanobubbles have been applied to protect proteases and the transport of DNA molecules loaded therein for plasmid DNA transfection across cell membranes. No cytotoxic effects were observed in this case [38]. Another chitosan-based nanobubble formulation has been proposed for the transport of DNA. The nanobubbles containing DNA have dimensions of up to 300 nm while accommodating a considerable amount of DNA [39]. *In vitro* transfection experiments were also performed. Adherent cells of the COS7 line were exposed to ultrasound at a frequency of 2.5 MHz in the presence of different concentrations of nanobubbles filled with plasmid DNA. None of the transfections were successful without ultrasound stimulation in all concentrations tested. Thirty seconds of ultrasound exposure showed a moderate success rate of transfection. Cell viability studies showed that neither ultrasound nor nanobubbles adversely affected the system under the experimental conditions performed.

In recent years, the ongoing efforts of cancer immunotherapy researchers have led to several vaccination concepts based on tumor-associated antigens, such as the oncogene HER2. Anticancer vaccination offers several distinct advantages over standard therapies. These include higher specificity, lower toxicity, and gentler long-term effects caused by immune memory. In this sense, nanotechnology has great potential to improve the quality of immunotherapy significantly. After all, to qualitatively improve the immune response to tumor development, the vaccine must first reach the relevant dendritic cells, which play a crucial role in inducing the correct immune response. In recent years, a novel immunotherapeutic tool, namely, chitosan nanobubbles carrying a DNA vaccine and equipped with anti-CD11C surface antibodies for targeting dendritic cell recognition, has been developed for the treatment of HER2-positive breast cancer [40]. Subcutaneous injection of pHER2-loaded CD11c nanobubbles exhibited migration of skin dendritic cells to excretory lymph nodes and inhibited the growth of HER2-positive tumors. Therefore, researchers are investigating various modifications of nanobubbles as a diagnostic-therapeutic platform to exploit their echogenic properties. Polymeric nanobubbles are a versatile tool for targeting cancer cells, ultrasound imaging, and performing ultrasound-guided cancer therapy.

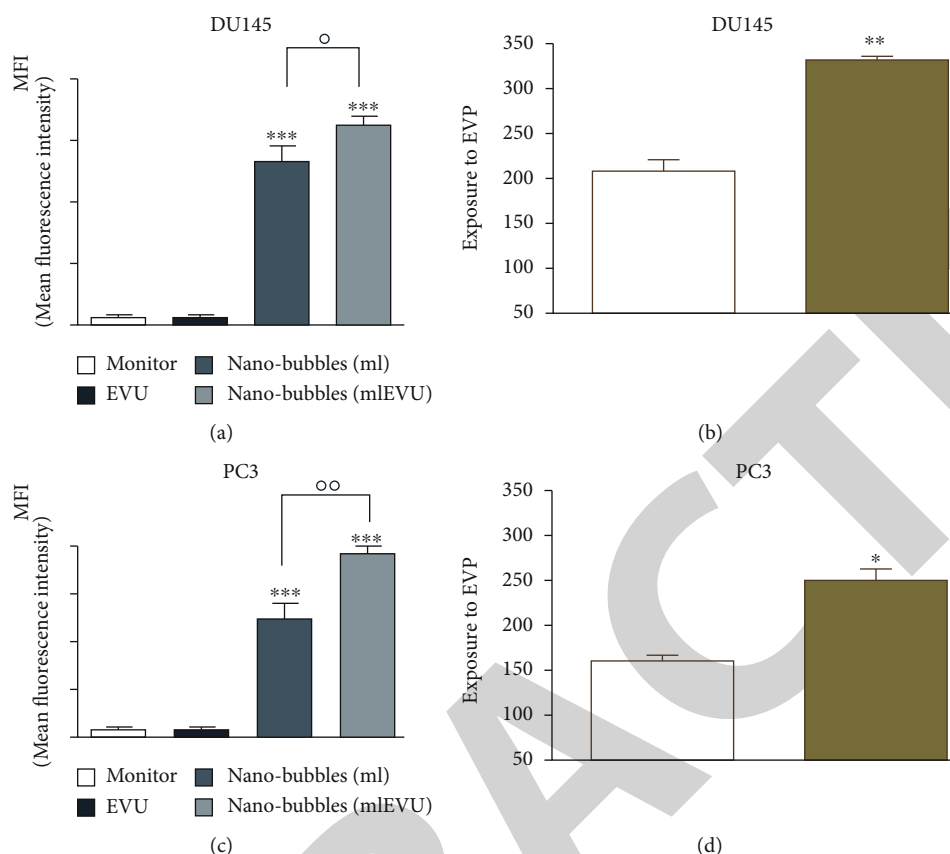


FIGURE 2: Fluorescence intensity of DU145 (a) with PC3 (b) treated with 6-coumarin-labelled glycol chitosan NBs (15-104 NBs/ml) for 24 hours. Quantitative analysis of 6-coumarin-labeled glycol chitosan NBs in DU145 (c) and PC3 (d) cells and significance of DU145 (c) compared to 6-coumarin-labeled glycol chitosan NBs and no ESWs in PC3 (d) cells.

UK researchers have developed a variant of chitosan nanobubbles as a diagnostic-therapeutic system capable of dual visual detection of nanobubbles [41]. A variant of this nanosystem simultaneously delivers prednisolone phosphate, placed at the leading edge of a perfluorobutane core, and electrostatically binds the negatively charged GD-DOTP complex to a cationic chitosan body. The nanobubbles exhibited echogenic properties, which allowed them to be used in real-time imaging systems while showing positive contrast in magnetic resonance studies. The effects of extracorporeal shock waves (ESWs) were investigated as another external stimulus to which the response (in addition to ultrasound) may lead to the release of the active components of the nanosystem. EUV is a brief (less than 10 ms) focused acoustic oscillation widely used in urology for lithotripsy and the treatment of various motor dysfunctions. The efficacy of nanotransport bubbles under EUV stimulation has been extensively studied. Notably, the efficacy of the combined action of nanobubbles and UV light has been studied in at least two aggressive cancers, asexual thyroid cancer and prostate cancer [42–45]. Cotreatment with nanobubbles loaded with paclitaxel or docetaxel and EBV has been reported to increase the cytotoxicity of both drugs in two prostate cancer cell lines (PC3 and DU145). This study reduced the GI50 dose of paclitaxel to 55% and docetaxel to 45% (Figure 2).

**3.5.3. Nanoparticles with Light-Dependent Reactions.** Drug release from light-dependent nanosystems is triggered by exposing the particles to a specific wavelength of light from an external source. However, the low light penetration makes such systems extremely limited in their application. In light-dependent nanodelivery systems, the drug can be bound to a carrier through photodegradation bonds or by a carrier that can change its structure under specific light exposure. The infrared light-dependent resetting effect of doxorubicin, for example, was demonstrated by a matrix made of a lactic acid polymer with a coating [46, 47]. Gold-containing drug delivery nanosystems have attracted more attention in academia due to their ease of fabrication and good biocompatibility. Such NFs can be used as targets for local plasmon resonance, a technique used in multimodal cancer therapy, particularly in photothermal therapy [48]. Under near-infrared irradiation, gold-containing low-frequency resonances lead to local heating (several degrees above body temperature values). After intravenous injection, these NFs are exposed to a laser brought in by a fiber optic, which initiates local heating at the tumor nodes, thus providing photothermal therapy [49]. In addition, the surface of gold-containing NFs is suitable for attaching drugs, oligonucleotides, and peptides [50, 51]. Such nanoparticles can be successfully applied for targeted substance delivery and release tasks under the influence of external signals [52].



#### 4. Discussion

In recent years, research trends in nanoparticle drug delivery systems have fully reflected the interdisciplinary cross-fertilization, synergy, and innovation between biologists, chemists, and clinical researchers. Targeted drug delivery systems based on nanoparticles provide better technical support for clinical disease treatment research. As a new and popular drug delivery system, nanocarriers have excelled in targeted therapy and tumor diagnosis and delivery. However, issues related to potential toxicity, accurate targeting of deep lesions, and true efficacy still need to be addressed. Only a few nanodelivery systems are currently in clinical trials. Most studies are still in the experimental stage. The large-scale clinical application of nanodelivery systems is limited by many factors, including drug release performance, optimization of the preparation process, production costs, surface properties of nanosystems, and in-depth studies of in vivo mechanisms of action. As the design of research nanosystems is optimized and research continues, however, nanodelivery systems are gradually overcoming their inherent limitations and providing more options for the development of new, safe, and effective nanoparticle drug delivery systems.

Compared to drug or gene therapy alone, nanodelivery systems combine nanotechnology and targeted drug delivery technologies. By combining the two different mechanisms of action, the synergistic effect can be improved, and drug tolerance, for example, in tumor cells, can be reduced. The exact intracellular delivery mechanism for drug delivery by nanoparticles is still unclear from the current research. To investigate how to ensure optimal synergy between the drug and the nanodelivery system when the drug is loaded onto the nanoparticles remains. In addition, although nanoparticles can carry and deliver drugs in vivo with relatively mild short-term toxicological effects, their potential long-term toxicity in the body needs to be further investigated and their metabolic pathways and clearance mechanisms. The ideal vehicle should be able to deliver the drug with a good delivery capacity. However, it should also be able to precisely regulate the site, time, and dose of release to achieve the maximum effect of the combination therapy. Further research should focus on the synergy between the therapeutic agent and the carrier.

With the rapid development of nanotechnology and related research, targeted drug delivery systems based on combined therapy have more advantages than single function and composition drug delivery systems in ultrasound therapy and tumor delivery. Nanodelivery systems have shown promising applications, and research on ultrasound therapy and precision killing of cancer cells will hopefully make further progress in the continuous development of nanodelivery systems.

#### 5. Conclusion

A review of previous studies demonstrates that intelligent, targeted drug delivery systems are highly effective for the delivery of anticancer drugs. Prior to their use in clinical

applications, however, a comprehensive assessment of their therapeutic efficacy and potential risks is required. Future research in targeted drug delivery nanosystems should focus on the development of nanocarriers with high in vivo delivery capacity, good synergy with therapeutic agents, and milder short-term and long-term toxicological effects to enhance the clinical benefits of nanodrug delivery systems. Researchers should continue to refine nanodelivery systems and conduct thorough preclinical trials on those with a high potential for clinical application to find suitable nanodelivery systems for clinical use and put them into clinical use as soon as possible.

#### Data Availability

The data used to support the findings of this study are included within the article.

#### Conflicts of Interest

The authors declare that there is no conflict of interest regarding the publication of this paper.

#### Authors' Contributions

Qiang Cao, Xiaochen Li, Qi Zhang, Xuanke Zhou, and Ying Yu are the first authors. Zixu He and Zhibiao Xiang are the second authors. Wei Qi is the third author.

#### References

- [1] S. Adepun and S. Ramakrishna, "Controlled drug delivery systems: current status and future directions," *Molecules*, vol. 26, no. 19, p. 5905, 2021.
- [2] C. Burger, Y. Shahzad, A. Brummer, M. Gerber, and J. du Plessis, "Traversing the skin barrier with nano-emulsions," *Current Drug Delivery*, vol. 14, no. 4, pp. 458–472, 2017.
- [3] V. P. Chavda, "Nanobased nano drug delivery: a comprehensive review," *Applications of targeted nano drugs and delivery systems*, pp. 69–92, 2019.
- [4] J. Chen, C. Gao, Y. Zhang et al., "Inorganic nano-targeted drugs delivery system and its application of platinum-based anticancer drugs," *Journal of Nanoscience and Nanotechnology*, vol. 17, no. 1, pp. 1–17, 2017.
- [5] S. Chen, Z. Song, and R. Feng, "Recent development of copolymeric nano-drug delivery system for Paclitaxel," *Anti-Cancer Agents in Medicinal Chemistry (Formerly Current Medicinal Chemistry-Anti-Cancer Agents)*, vol. 20, no. 18, pp. 2169–2189, 2020.
- [6] S. M. Dieng, N. Anton, P. Bouriat et al., "Correction: pickering nano-emulsions stabilized by solid lipid nanoparticles as a temperature sensitive drug delivery system," *Soft Matter*, vol. 15, no. 42, pp. 8638–8638, 2019.
- [7] X. Fang, J. Cao, and A. Shen, "Advances in anti-breast cancer drugs and the application of nano-drug delivery systems in breast cancer therapy," *Journal of Drug Delivery Science and Technology*, vol. 57, p. 101662, 2020.
- [8] A. Firooz, R. Namdar, S. Nafisi, and H. I. Maibach, "Nano-sized technologies for miconazole skin delivery," *Current Pharmaceutical Biotechnology*, vol. 17, no. 6, pp. 524–531, 2016.

- [9] A. K. Goyal, G. Rath, C. Faujdar, and B. Malik, "Application and perspective of pH-responsive nano drug delivery systems," in *In Applications of Targeted Nano Drugs and Delivery Systems*, pp. 15–33, Elsevier, 2019.
- [10] Q. He and J. Shi, "Mesoporous silica nanoparticle based nano drug delivery systems: synthesis, controlled drug release and delivery, pharmacokinetics and biocompatibility," *Journal of Materials Chemistry*, vol. 21, no. 16, pp. 5845–5855, 2011.
- [11] S. Hua, E. Marks, J. J. Schneider, and S. Keely, "Advances in oral nano-delivery systems for colon targeted drug delivery in inflammatory bowel disease: selective targeting to diseased versus healthy tissue," *Nanomedicine-Nanotechnology Biology and Medicine*, vol. 11, no. 5, pp. 1117–1132, 2015.
- [12] T. Ishii and Y. Sakurai, "Challenges and new directions for next-generation drug delivery system (DDS) research based on nano-technology," *Yakugaku Zasshi-Journal of the Pharmaceutical Society of Japan*, vol. 132, no. 12, pp. 1345–1346, 2012.
- [13] N. R. Jabir, S. Tabrez, C. K. Firoz et al., "A synopsis of nano-technological approaches toward anti-epilepsy therapy: present and future research implications," *Current Drug Metabolism*, vol. 16, no. 5, pp. 336–345, 2015.
- [14] J. Jeevanandam, "Nano-formulations of drugs: recent developments, impact and challenges," *Biochimie*, vol. 128, pp. 99–112, 2016.
- [15] S. G. Klochkov, "Nano-formulations of drugs: recent developments, impact and challenges," *Seminars in Cancer Biology*, vol. 128, pp. 190–199, 2021.
- [16] N. Kumar, "Optimized Targeting of Magnetic Nano Particles for Drug Delivery System," in *IEEE/ASME International Conference on Advanced Intelligent Mechatronics (AIM) - Mechatronics for Human Wellbeing*, Wollongong, AUSTRALIA, 2013.
- [17] L. Kumawat and A. Jain, "Review on gold nano particle for novel drug delivery system," *YInternational Journal of Pharmaceutical Sciences and Research*, vol. 3, no. 1, pp. 53–59, 2012.
- [18] H. Li, "Nano/microscale technologies for drug delivery," *Mechanics in Medicine and Biology*, vol. 11, no. 2, pp. 337–367, 2011.
- [19] J. Liu, Y. Huang, A. Kumar et al., "pH-sensitive nano-systems for drug delivery in cancer therapy," *Biotechnology Advances*, vol. 32, no. 4, pp. 693–710, 2014.
- [20] W. Liu, Z. Dong, K. Liu et al., "Targeting strategies of oral nano-delivery systems for treating inflammatory bowel disease," *International Journal of Pharmaceutics*, vol. 600, p. 120461, 2021.
- [21] Y. Liu and W. Lu, "Recent advances in brain tumor-targeted nano-drug delivery systems," *Expert Opinion on Drug Delivery*, vol. 9, no. 6, pp. 671–686, 2012.
- [22] J. Lopes-Nunes, P. Oliveira, and C. Cruz, "G-Quadruplex-based drug delivery systems for cancer therapy," *Pharmaceutics*, vol. 14, no. 7, p. 671, 2021.
- [23] J. Ma, "Drug-loaded nano-microcapsules delivery system mediated by ultrasound-targeted microbubble destruction: a promising therapy method," *Biomedical Reports*, vol. 1, no. 4, pp. 506–510, 2013.
- [24] M. Mahmoudian, H. Valizadeh, R. Löbenberg, and P. Zakeri-Milani, "Bortezomib-loaded lipidic-nano drug delivery systems; formulation, therapeutic efficacy, and pharmacokinetics," *Journal of Microencapsulation*, vol. 38, no. 3, pp. 192–202, 2021.
- [25] P. Purkayastha, S. S. Jaffer, and P. Ghosh, "Formation and applications of cyclodextrin nano and micro structuresIn ABSTRACTS OF PAPERS OF THE AMERICAN CHEMICAL SOCIETY," in , 1155 16TH ST, NW, WASHINGTON, DC 20036 USA: AMER CHEMICAL SOC, 2011, August.
- [26] S.-S. Qi, J. H. Sun, H. H. Yu, and S. Q. Yu, "Co-delivery nanoparticles of anti-cancer drugs for improving chemotherapy efficacy," *Drug Delivery*, vol. 24, no. 1, pp. 1909–1926, 2017.
- [27] W.-W. Ren, S. H. Xu, L. P. Sun, and K. Zhang, "Ultrasound-based drug delivery system," *Current Medicinal Chemistry*, vol. 29, no. 8, pp. 1342–1351, 2022.
- [28] M. Sharma, *Transdermal and Intravenous Nano Drug Delivery Systems: Present and Future*, 2019.
- [29] S. Sharma, S. S. Pukale, A. Mittal, and D. Chitkara, "Docetaxel and its nanoformulations: how delivery strategies could impact the therapeutic outcome?," *Therapeutic Delivery*, vol. 11, no. 12, pp. 755–759, 2020.
- [30] H. Su, Y. Wang, S. Liu et al., "Emerging transporter-targeted nanoparticulate drug delivery systems," *Pharmaceutica Sinica B*, vol. 9, no. 1, pp. 49–58, 2019.
- [31] M. Su, Q. Dai, C. Chen, Y. Zeng, C. Chu, and G. Liu, "Nanomedicine for thrombosis: a precise diagnosis and treatment strategy," *Nano-Micro Letters*, vol. 12, no. 1, p. 96, 2020.
- [32] S. E. K. Tekkeli and M. V. Kiziltas, "Current HPLC methods for assay of nano drug delivery systems," *Current Topics in Medicinal Chemistry*, vol. 17, no. 13, pp. 1588–1594, 2017.
- [33] V. Uyen Vy, "Synthesize and survey the drug loading efficiency of the porous nano silica modified by gelatin," *Advances in Natural Sciences-Nanoscience and Nanotechnology*, vol. 10, no. 3, 2019.
- [34] Y. Wang, P. Li, T. Truong-Dinh Tran, J. Zhang, and L. Kong, "Manufacturing techniques and surface engineering of polymer based nanoparticles for targeted drug delivery to cancer," *Nanomaterials*, vol. 6, no. 2, p. 26, 2016.
- [35] T. M. Wilbanks and J. A. Schuster, "Aerosol Drug Delivery to the Lung Periphery Using Nano-Scale Technologies," in *International Conference on MEMS, NANO and Smart Systems*, Banff, CANADA, 2005.
- [36] C. Witharana and J. Wanigasekara, "Drug delivery systems: a new frontier in nano-technology," *International Journal of Medical Research & Health Sciences*, vol. 6, no. 9, pp. 11–14, 2017.
- [37] M. Wu, D. Zhang, C. Sun et al., "Drug delivery properties of nano-bundles formed in vitro by Janus-type TA nucleosides," *Journal of Nanoscience and Nanotechnology*, vol. 16, no. 7, pp. 7096–7102, 2016.
- [38] K. Yang, L. Feng, and Z. Liu, "Stimuli responsive drug delivery systems based on nano-graphene for cancer therapy," *Advanced Drug Delivery Reviews*, vol. 105, pp. 228–241, 2016.
- [39] S. Yang, C. Chen, Y. Qiu, C. Xu, and J. Yao, "Paying attention to tumor blood vessels: cancer phototherapy assisted with nano delivery strategies," *Biomaterials*, vol. 268, p. 120562, 2021.
- [40] Y. Yang, "Peptide-mediated nano drug delivery system for tumor targeting," *Progress in Chemistry*, vol. 25, no. 6, pp. 1052–1060, 2013.
- [41] H. Zhang, T. Fan, W. Chen, Y. Li, and B. Wang, "Recent advances of two-dimensional materials in smart drug delivery nano- systems," *Bioactive Materials*, vol. 5, no. 4, pp. 1071–1086, 2020.

## *Retraction*

# **Retracted: Strategies of Bioceramics, Bioactive Glasses in Endodontics: Future Perspectives of Restorative Dentistry**

### **BioMed Research International**

Received 5 December 2023; Accepted 5 December 2023; Published 6 December 2023

Copyright © 2023 BioMed Research International. This is an open access article distributed under the Creative Commons Attribution License, which permits unrestricted use, distribution, and reproduction in any medium, provided the original work is properly cited.

This article has been retracted by Hindawi, as publisher, following an investigation undertaken by the publisher [1]. This investigation has uncovered evidence of systematic manipulation of the publication and peer-review process. We cannot, therefore, vouch for the reliability or integrity of this article.

Please note that this notice is intended solely to alert readers that the peer-review process of this article has been compromised.

Wiley and Hindawi regret that the usual quality checks did not identify these issues before publication and have since put additional measures in place to safeguard research integrity.

We wish to credit our Research Integrity and Research Publishing teams and anonymous and named external researchers and research integrity experts for contributing to this investigation.

The corresponding author, as the representative of all authors, has been given the opportunity to register their agreement or disagreement to this retraction. We have kept a record of any response received.

### **References**

- [1] S. Chitra, N. K. Mathew, S. Jayalakshmi, S. Balakumar, S. Rajeshkumar, and R. Ramya, "Strategies of Bioceramics, Bioactive Glasses in Endodontics: Future Perspectives of Restorative Dentistry," *BioMed Research International*, vol. 2022, Article ID 2530156, 12 pages, 2022.

## Review Article

# Strategies of Bioceramics, Bioactive Glasses in Endodontics: Future Perspectives of Restorative Dentistry

S. Chitra <sup>1</sup>, Nibin K. Mathew,<sup>2</sup> S. Jayalakshmi,<sup>3</sup> S. Balakumar,<sup>2</sup> S. Rajeshkumar <sup>4</sup>,  
and R. Ramya<sup>5</sup>

<sup>1</sup>Department of Prosthodontics, Saveetha Dental College & Hospitals, Saveetha Institute of Medical and Technical Sciences (SIMATS), Chennai 600 077, India

<sup>2</sup>National Centre for Nanoscience and Nanotechnology, University of Madras, Guindy campus, Chennai 600 025, India

<sup>3</sup>White Lab, Materials Research Centre, Saveetha Dental College & Hospitals, Saveetha Institute of Medical and Technical Sciences (SIMATS), Chennai 600 077, India

<sup>4</sup>Department of Pharmacology, Saveetha Dental College & Hospitals, Saveetha Institute of Medical and Technical Sciences (SIMATS), Chennai 600 077, India

<sup>5</sup>Department of Oral Biology, Saveetha Dental College & Hospitals, Saveetha Institute of Medical and Technical Sciences (SIMATS), Chennai 600 077, India

Correspondence should be addressed to S. Chitra; [chitru\\_ashok@yahoo.com](mailto:chitru_ashok@yahoo.com)  
and S. Rajeshkumar; [rajeshkumars.sdc@saveetha.com](mailto:rajeshkumars.sdc@saveetha.com)

Received 30 April 2022; Revised 15 June 2022; Accepted 1 July 2022; Published 30 July 2022

Academic Editor: Dinesh Rokaya

Copyright © 2022 S. Chitra et al. This is an open access article distributed under the Creative Commons Attribution License, which permits unrestricted use, distribution, and reproduction in any medium, provided the original work is properly cited.

Prevalently, there is a primary strategy to cure caries using restorative materials notably bioceramics. Existing synthetic materials stimulate natural tooth structure with acceptable interfacial bonding and esthetic and biomechanical qualities with better durability. Several bioceramics have been introduced and investigated for their potentialities as restorative materials. Biomineralization of tooth initiates repair and regeneration of natural dental tissue and reinstating the integrity of periodontium. In the evolution of bioceramics in the aspects of different essential composition for dental application, recent technology and modern strategies revolutionize the restorative dentistry. Bioglass is one among the important bioceramics as a restorative material, and by regulating the properties of the material, it is possible to construct improved formulation towards restoration. This article reviews the current revolution of endodontics, existing restorative materials, and technologies to be achieve for engineering materials with the better design.

## 1. Introduction

Recently bioceramics-based restorative materials possess a great interest due to their sealing behavior with mineralization potentiality. Lot many materials are emerging day by day to fulfil the required criterion; in that direction, biodentin and Novamin are emerging materials owing to their mineralization potentialities [1]. Many researchers pointed out that a relative restorative material should accommodate the bioactive molecules along with inherent antimicrobial characteristic features, which efficiently deter microbial biofilm formation that indiscriminates the colonization [2]. Dentist

expectation is on materials that are easy to use and inexpensive and give long-lasting cure; hence, research is underway to develop and analyze such kind of materials [3].

Modern sealing materials have evolved with great challenges (toxicity, mechanical strength, and integration). Tracing their historical background, over 170 years ago, silver amalgam- (silver and mercury) based materials have been used to seal the cavities [4]. Later on, tin has been included into the silver amalgam compound [5], but the drawback of this material was, tin-mercury intermetallic phase easily corroded, leading to breakdown of the fillings. Copper (Cu), introduced into amalgam to eliminate the intermetallic



tin-mercury phases, became modern amalgam materials with silver-copper-tin alloy powders along with mercury [6]. These materials survived with both chemical onslaughts and mechanical stability in the oral environment for longer duration. Later, researchers found that release of mercury from the fillings, contaminated and owing to its toxic behavior, increases risk (carcinogenicity, damage to the tooth socket and alveolar bone) to the oral environment. Therefore, alternatives to silver amalgam were fused with gallium-indium-tin alloy at room temperature; with this, silver-copper-tin mixture was combined and formulated as paste [7]. These filling alloys were also prone to corrosion, and toxicological reactions of gallium became a challenge. After this era, resin-based composites progressed as endodontic filling around 1960s [8]. Modernized dental composites consist of paste with the mixture of dimethacrylate monomers along with cross-linking including silane-coatings and ceramic particulates, and this composite paste was used to seal cavities. These resin-based composites have strength similar to amalgam; however, polymerization shrinkage in the resin tooth interface proved to be a dramatic disadvantage of these materials [9]. To overcome such adversities, calcium phosphate-rich apatite with phosphoric acid components and porous organic/inorganic compounds were tried [10]. Consecutively, resin/silica-based porcelain bioactive materials are being attuned to improve the standard of restorative materials [11].

## 2. Milestones in Dentistry

Dentistry evolved and has grown systematically; initially three centuries before started the journey towards the development in dental medicine; many excellent inventions have been introduced and still climbing to progress. In the field of restorative dentistry, American Dental Association recognized endodontics specialty in the year 1963; this field takes credit for their contribution in dental emergencies as defined in "The Surgeon Dentist" [12]. Followed by this, Chinese had clear ideology in dental caries; they introduced arsenical compound (alloy materials) to treat pulp. In this connection, Pierre Fauchard is known as the father of modern dentistry; he introduced concepts of endodontics [13]. Qureshi et al. explained that in the next level Phillip Pfaff took it further into another dimension; he initiated pulp capping using gold/lead in the year 1756 [14]. Then in 1809, for the first time, root canal filling with gold foil was experimented by Edward Hudson; furthermore, the authors also explained in 1834 phenols for canal irrigation [15]. It was reported that the first endodontic instrument was developed by Edwin Maynard (1838), then the most expected gutta-percha recommended by Watt in the year 1857, followed by obturation demonstrated by Bowman (1867) [15]. In this direction, in modern dentistry, electric current was applied and tested for pulp capping by Black in the year 1867, who also suggested zinc oxychloride as a pulp capping material [15]. Then, radiographs were evolved and became essential part of endodontics; dental X-ray instruments were used for diagnostic purposes after 1919 [16]. On the other hand, in restorative research, the first ceramic (calcium hydroxide)

was introduced in the year 1920 to treat infected root canals. After 1993, revolutionary bioceramics materials were evolved for apical sealing, repair, and restorative purposes [15]. Fully reclining dental chairs were publicized in the year 1958; similarly, in the 1990s, aesthetic techniques have been introduced for tooth whitening [17]. On the other hand, in the aspects of diagnostics, laser light, dual wavelength spectrophotometry, thermistor, thermocouple, infrared thermography, fibre optic transillumination, and digital imaging fibre optic transillumination have been sequentially evolved for the better identification of the problems [18]. In this modern era, laser in dentistry, computer aided designing and computer aided milling, and Dental Operating Microscope (DOM) are the supporting tools for better activation of therapies [18].

## 3. Root Canal and Associated Problems

Enamel is the strongest mineralized part of the human body; beneath that layer, a hard portion is dentin existing above the gingiva. Inside the root there is a soft tissue known as pulp, which contains nerves, blood vessels, and connective tissues. This pulp mainly supports the growth of the root canal of the tooth during the development of infants and contains a mass of connective tissue recognized as endodontium [19]. Root is embedded with the jawbone, the pulp provides the moisture and nourish the tooth, and the damage of this pulp is known as the root canal problem, which arise most of the times due to the infections/microbial exposures. The pulp and root canal possess an importance in tooth development; however, a fully developed tooth can possible to survive without pulp and relative cells, since surrounding cells provide the nourishment to the teeth. Root canal therapy mainly includes three steps cleaning the root canal, filling the root canal, and adding a crown/filling [20].

The primary cause of root canal problems such as severe decay, serious infection, cavities, and gum disease also leads to the damage of pulp and soft tissue inside the canal (Figure 1).

Bioceramics are the potential candidates for endodontic sealing, and this class of materials consists of mineral trioxide aggregate (MTA), ERRM (EndoSequence root repair material) Putty, ERRM Paste, Biodentine, and iRoot FS (preloaded paste in a syringe with material delivery tips for intracanal deliverance), iRoot SP, MTA Fillapex, and BC Sealer MTA Plus, gutta-percha, and Bioactive glass. As of now, MTA is the gold standard material for restoration; however, this can be replaced by bioactive glasses by improvising the properties towards mechanical stability and early setting time.

## 4. Restorative Materials and Relative Problems

Gutta percha (GP) is generally used as an obturation material for filling, along with this GP bioceramics composites, glass ionomer cement, or amalgam-based materials were utilized to induce the mechanical bonding between the tooth structure and the materials. Hence, bioceramics composites are the most expected material for restoration; besides, they



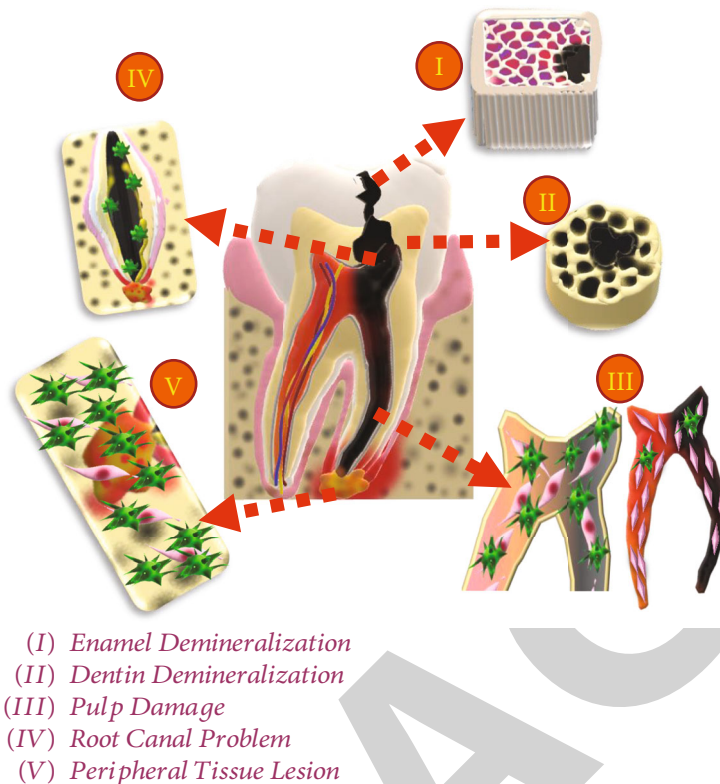


FIGURE 1: The most common stages of tooth problems.

exhibit adorable bonding between teeth and restorative components. The most common complications in the root canal treatments are microbial infections that may be percolated due to the following reasons which leads to root canal failure. (i) Multiple root canals at a time in the same tooth may lead to failure due improper cleaning. (ii) unpredicted or undetected crack in the root, improper sealing, and problem with the restorative materials may provide a way to pave microbes inside the canals [21]. (iii) Dietary habituates, accident wounds, acids by fermentation, and pathological infections may lead to damage in enamel, dentin followed by the (iv) root canal and pulp. To overcome these circumstances, some tooth pastes were used to cure the enamel/dentin remineralization (sensitivity) in the early stage; some of the restorative materials were in the function for root canal sealing and pulp treatment. Deep cavity due to sensitivity, traumatic injury, and microbial exposure may lead to necrosis in the pulp dentin. Hence, pulp capping is one of the important and essential techniques used in dental restorations to secure pulp from necrosis. In this case, initially, calcium hydroxide is used as a pulp capping material followed by many bioceramics.

Endodontic problem is biofilm-mediated disease; it is mostly associated with growth of microorganisms on the surface of canals. Potential pathogenic sealant component/new approaches are required for disinfection. Zaneva-Hristova and Borisova-Papancheva and Vishwanath and Rao [22, 23] stated that gutta-percha is one of the best

restorative materials that was discovered by John Tradescant in the year 1656; then it was introduced to medical society by William Montgomerie in the year 1925 [22, 23]. Traditional gutta-percha is a famous root filling material; it can only act as a filler material but does not possess the capability to completely seal the canal. Owing to the improper sealing, microbes will travel inside the canal; therefore, it is essential to fix this problem with sealer material. Regular sealers have their own setting time and shrinkage behavior; those kinds of materials may or may not bond with the core gutta-percha, and that gap also encourages the microbial invade. Hence, bioceramics-based materials entered into an endodontic restorative industry to revolutionize the restoration society. Bioceramics such as hydroxyapatite, bioactive glasses, calcium phosphates, and their derivatives, alumina, and zirconia are being used as tissue and joint replacement materials in both orthopaedics and dentistry [24, 25]; owing to their biocompatible and osteoconductive properties as well as chemical and dimensional stability. Generally, commercially available bioceramics sealers are composed of calcium silicates such as dicalcium silicate, tricalcium silicate, colloidal silica, calcium hydroxide, and calcium phosphate monobasic. Zirconium, bismuth oxide, and boron can used as a radiopacifier to analyze filling proficiency. Bioceramics are ideal restorative materials; since they are not affected by blood contaminations, sensitivity or shrinkage is not a problem like other sealant materials [26, 27]. They are hydrophilic in nature and induce long-term sealing due to hydration

TABLE 1: The most common restorative materials with their compositions.

Name	Composition	References
Activa BioActive restorative	Powder: silicate bioactive glass, sodium fluoride silicate bioactive glasses, and sodium fluoride Liquid: diurethane modified hydrogenated polybutadiene, methacrylate monomers, altered polyacrylic acid, and distilled water	[32]
Cention N	Powder: barium aluminosilicate glass, isofiller, ytterbium trifluoride, calcium fluorosilicate glass, and calcium barium aluminum fluorosilicate Liquid: urethane dimethacrylate, tetramethyl xylene diurethane dimethacrylate, tricyclodecane dimethanol dimethacrylate, polyethylene glycol 400 dimethacrylate, Ivocerin, and hydroxyperoxide	[33]
Mineral trioxide aggregate (MTA)	Mineral trioxide aggregate is a mixture of tricalcium silicate, dicalcium silicate, tetracalcium aluminoferrite, tricalcium aluminate, gypsum, and bismuth oxide. It is currently marketed mainly in two forms: GMTA (gray) and WMTA (white)	[34]
ERRM Putty, ERRM Paste (ERRM-EndoSequence root repair material)	Both ERRM putty and paste materials are composed of calcium silicates, calcium phosphate monobasic, tantalum oxide, and zirconium oxide	[35]
Biodentine	Biodentine comprises tricalcium silicate, zirconium oxide, calcium carbonate, and liquid-containing calcium chloride as a setting accelerator.	[34]
BC sealer and iRoot SP	Zirconium oxide, dicalcium silicate, tricalcium silicate, calcium silicates, colloidal silica, calcium hydroxide, and calcium phosphate monobasic	[34]
Endo CPM sealer Egeo	Calcium carbonate, silicon dioxide, bismuth trioxide, barium sulfate, sodium citrate, calcium chloride, and propylene glycol alginate	[36]
ProRoot Endo Sealer	Calcium sulphate, dicalcium silicate, tricalcium silicate, bismuth oxide, and traces of tricalcium aluminate along with water-soluble polymer viscous solution	[37]
AH Plus	Calcium tungstate, zirconium oxide, bismuth nitrate, epoxy resin, and silica	[38]
Sealapex	Calcium hydroxide, zinc oxide, barium sulfate, titanium dioxide, and zinc stearate	[38]
Zinc oxide-eugenol-based sealers	Zinc oxide, zinc acetate, rosin, and eugenol	[39]
Glass ionomer	Calcium aluminosilicate and polyacrylic acid	[39]
Amalgam	Silver, copper, zinc, tin, and mercury	[39]

reaction that influences the formation of calcium hydroxide followed by dissolution into calcium and hydroxyl ions.

## 5. Bioceramics in Dentistry

Bioceramics materials are the best choice as an alternative for pulp capping, perforation repair, pulpotomy, root canal filling, and obturation of immature teeth [28, 29], while, setting of bioceramics, pH of the surrounding environment is enhancing up to 12, owing to the hydration reaction (dissolution of ions from the material matrix), which rapidly inhibits the microbial growth. Almost 90% of endodontic treatments are succeeded based on the reports. Failures in endodontics are mostly related to persistence of various pathological infections; root filling materials with the conflicting tissue reactions were very minimal extent. However, sealing materials and relative technique exhibited divergent qualities in terms of sealing with varying clinical performances. Most of the reports enumerate the essentiality of superior biocompatible endodontic sealer, whereas the exact demand in sealant materials is early setting time and it possibly should exhibit improved antimicrobial properties against pathogens, since the major cause of problem was generated due to pathogens and sealing efficiency that is essential than the biocompatibility. Calcium hydroxide is

one of the important bioceramics in endodontics, and it has been used in different forms. This material is less effective to inhibit some microbial species as well as bioactivity; alternatively, it exhibits potential biocompatibility owing to their solubility [30]. It was reported that it does not fulfil the required criteria to become an ideal sealer and concluded that detailed evaluation is required to elaborately analyze the materials' properties in endodontic sealing [31]. Similarly, released ions interreacted and precipitated as a mineral apatite that induces the osteoconductive potential of the material. Thus, there is need of mineralization as well as antimicrobial properties in the sealing materials. Hence, bioactive glass modification towards a sealing material can potentially sort out this existing problem (Table 1).

Amalgam-based resin composite entered into the dental society in the year 1833 [3], after the entry of amalgam, Pierce introduced zinc phosphate cement (1879) and it is a majorly used material in dentistry; these materials are ruled in the 18<sup>th</sup> century [40]; at the same time, clove oils and zinc oxide-clove cements are popularized in this period [41, 42]. Calcium phosphate is the gold standard material for medical applications [43].

In the 19<sup>th</sup> century, also progressive materials were grown; in this connection, polycarboxylate was introduced by Smith (1968) [40]; similarly, Wilson initiated glass ionomer cement (GIC [1972]) [44] and then MTA introduced in

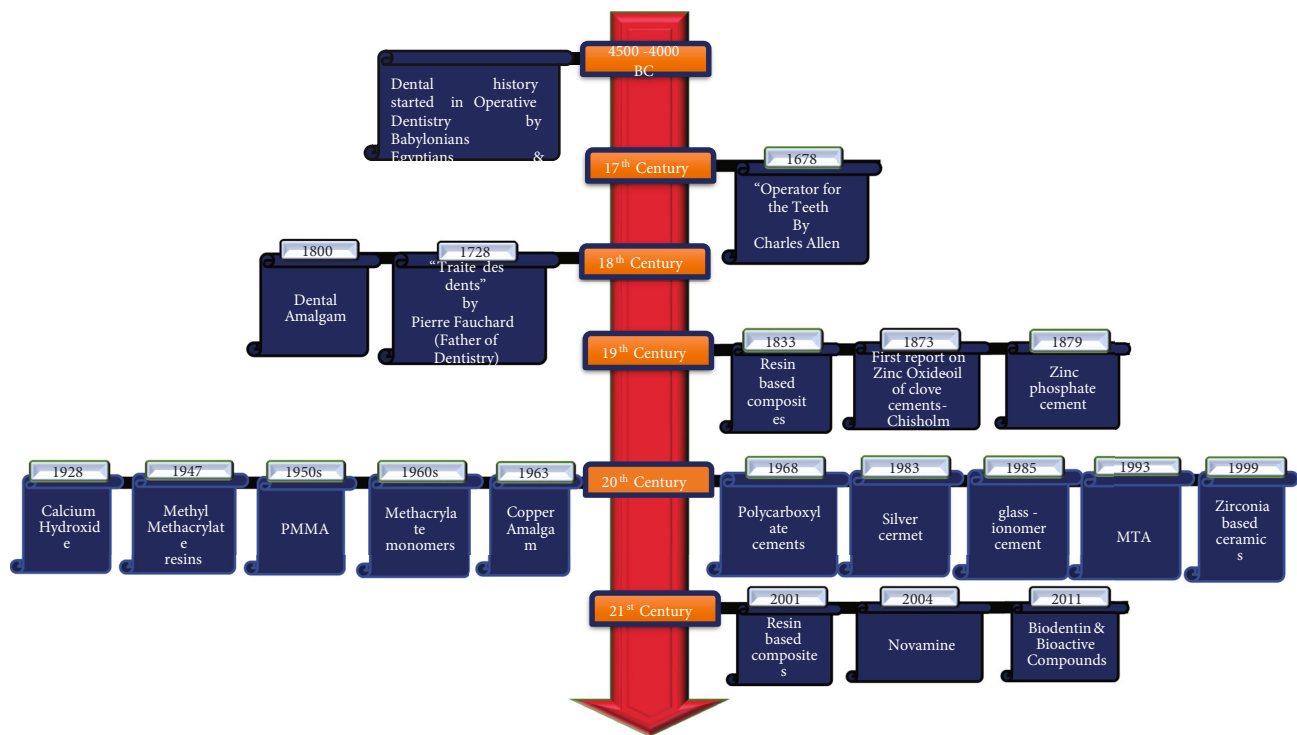


FIGURE 2: Timeline for the evolution of restorative dentistry.

the year 1993 and got FDA approval in a short span [45]. Biodentine is a bioactive and biocompatible material, which potentially overcomes the limitations of calcium hydroxide and MTA [43]. Followed by several bioceramics, bioglass entered into the era of dentistry in the year 2004; demanding bioglass was integrated in toothpaste (Sensodyne®) in the name of Novamin®, and the remineralization efficacy of this material was sequentially reported, and then forth bioglass was potentiality investigated in periodontics, endodontics, and remineralization applications (Figure 2) [46].

## 6. Merits of Bioceramics

Incredible biocompatibility of bioceramics in a physiological environment owing to their similarity with natural mineral apatite encourages these materials for biomedical applications (Figure 3). Osteoinductive, osteoconductive, and bioresorbable properties enrich the bone tissue regeneration [47, 48]. Chemical bonding with the microstructure of tooth and antimicrobial properties induces the improved hermetic seal with tooth structure that leads to relevant dental applications. MTA is one of the best sealants and majorly being used among bioceramics; it has good solubility, improved bioactivity, acceptable antimicrobial properties, and sealing ability. MTA revealed superior biocompatibility with mesenchymal stem cell proliferation without genotoxicity and cytotoxicity according to earlier reports [49, 50]. Elevated solubility of MTA may jeopardise in long-lasting sealability in restorations, and it is critical to withstand like a bioactive material [51, 52]. Further, in this time period, biodentine was evolved; this is also formulated in a manner similar to MTA-based

compositions with some improved properties. In the case of biodentine and MTA, calcium carbonate ( $\text{CaCO}_3$ ) acts a nucleation point to form the calcium silicate hydrate gel (C-S-H). Along with this material, water-soluble polymers balance the viscosity and induce the setting time. The setting time of biodentine starts at 6 minutes, and final setting occurs in about 45 minutes. This is one of the attractive behaviors of biodentine over other calcium silicate-based materials. Biodentine explicates improved mechanical stability and faster setting that lowers the risk of microbial/bacterial contamination than MTA [53]. EndoSequence Root Repair Material exhibited leakage in sealing compared to MTA groups. However, this material revealed similar antimicrobial and biocompatible properties related to MTA [54–56].

## 7. Uses of Bioceramics

The following are the uses of bioceramics:

- (1) Endodontics: obturation, sealers, retrograde filling, perforation repair, apexification, pulpotomy, and regenerative endodontics [27]
- (2) Restoration: dentin hypersensitivity, dentin substitute, dentin remineralization, and pulp capping [57]
- (3) Prosthetics: prosthesis, prosthetic device implants, implant coatings to improve osteointegration, and biocompatibility [58]
- (4) Surgery: fillings in surgical bone defects, joint replacements, alveolar bone augmentation, orbital floor fracture, and sinus obliteration [59, 60]

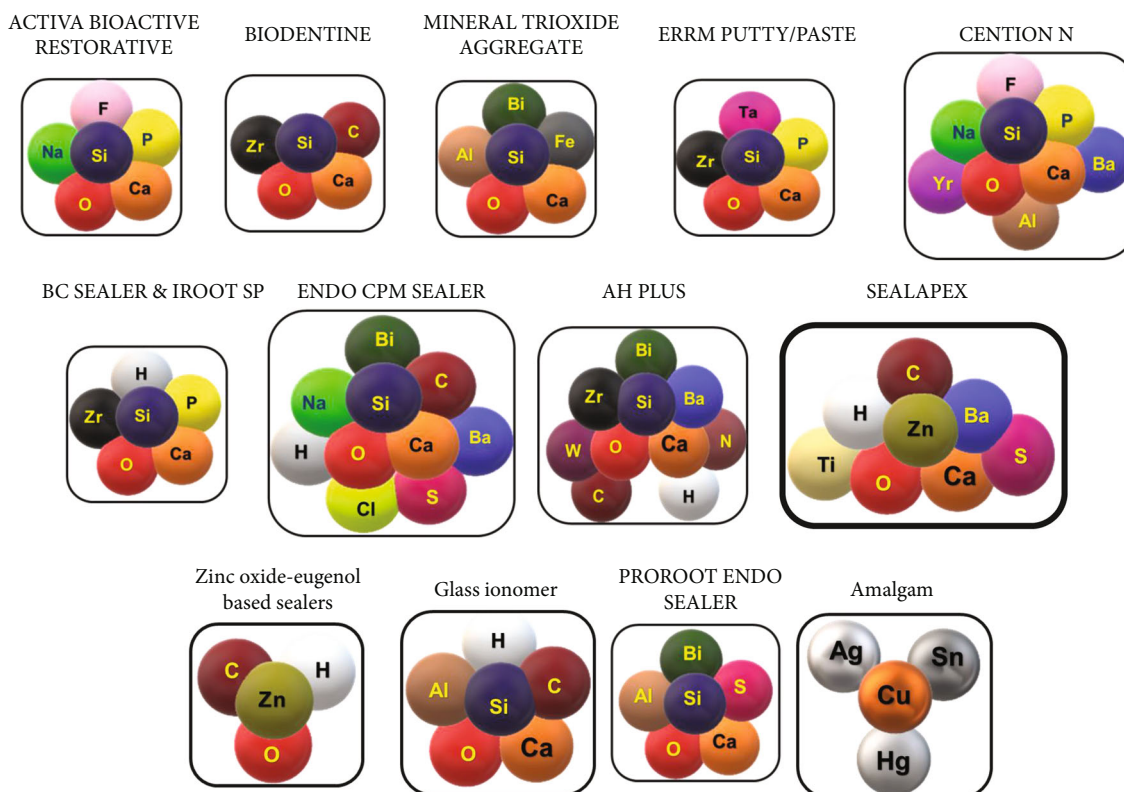


FIGURE 3: Schema explains the formulations of commercial restorative materials.

Bioceramics are prevalently used by the dental community; in this connection, MTA is a benchmark material in endodontics as well as restorative dentistry among bioceramics. However, some limitations are reported by several authors [27, 61]. Hence, based on the understanding from literary reports, it can be expected that up-to-date informative knowledge of new bioactive materials is essential to confirm the suitable materials based on the relevant clinical needs. [27] Modifying the glass network may produce new crystal lattices with required properties in bioactive materials that may enlighten the dentistry with the fulfilment of relevant desires. Biomaterials were drastically designed and developed towards dental research innovations in the last 9 years. Zirconia and relative bioactive scaffolds analyzed for bone regeneration and bioactive molecule demands were also identified in the last decade. Similarly, the importance of silver amalgam, alloys, and nonresinous cements was significantly decreased. Extensive focus is on restorative materials with enhanced regenerative potentiality, aesthetic restorative materials, and dental implants [62].

Bioactive components (Si, C, P, and Na) in restoration compositions induce the formation of mineral apatite crystals that leads to bonding integration in demineralized dentin, which is directly proportional to the incubation time in oral environment. Saliva itself has some essential ions along with that those relevant bioactive ions penetrate deep into dentin to regenerate dentinal tubules and also generate an entanglement that enhances the adhesive strength. Mineral apatite precipitation on the restorative materials produces

beneficial interfaces on the adhesive restorations that encourages the remineralization and induce enzymatic reaction of collagen mesh followed by fossilization of metallo-proteins [63]. It was reported that compared to current restorative materials, inclusion of bioactive glasses, tricalcium phosphate, and hydroxyapatite with the restorative composition positively triggers the chemical as well as biological properties [64, 65]. These bioceramics explicated tremendous biological, bioactive, and exceptional biocompatible properties. However, poor mechanical properties hinder their growth in dental application [66]. Hence, changes in the materials engineering possibly help to overcome this drawback in terms of incorporating mechanically stable ions in the lattices of host materials to reconstruct the crystallinity, material stability, and solubility that may provide a way for these materials into clinical dentistry [66, 67]. Implant failure can be overcome by coating bioactive materials on the implant surfaces in terms of inducing osteointegration, corrosion resistance, antimicrobial properties, and bone bonding ability, and coatings also enhance the biological fixation between metallic implant and bone [68, 69]. Implant biocompatibility and longevity also have positive stimulation on the regeneration of bone in the oral circumstances. It was also reported that direct coatings of therapeutic agents such as proteins, ligands, and growth factors provide beneficial osteoconductive properties, combat infection, stimulate bone growth, and also enhance the lifespan of implants [70, 71]. On the other hand, bioactive ceramics is being used as a coating material, since several



TABLE 2: Importance of bioglass in the journey of dentistry.

Reports	Applications	Summarization	References
Deng et al. investigated the effect of 45S5 bioglass on bleaching efficacy of bovine enamel	Bleaching and whitening	Combination of bioglass and hydrogen peroxide could be a promising adjunct for bleaching therapy	[74]
Resin-modified glass ionomer cement bonded with dentin pretreated by bioglass using a variety of air abrasion techniques to evaluate the material and dentin bonding interfaces	Bonding durability and healing	Bioglass treated dentin samples explored better bonding with resin-ionomer cement and summarized that bioglass-treated surface exhibited improved remineralization and healing ability	[75]
Hydrated calcium silicate filler effect on resin-based pit and fissure sealant to prevent secondary caries, this was reported by Yang et al.	Caries prevention	Incorporation of calcium silicate in the pit resulted in changing the environment from a cariogenic state to a remineralization state	[76]
Gihan et al. explored the epoxy resin bioactivity and bond strength, after the incorporation of bioglass nanoparticles	Endodontic sealer	Incorporation of 10% bioglass into epoxy resin is an effective method to encourage bioactivity without affecting bond strength	[77]
Evaluation of ionic dissolution and apatite forming potential of bioactive glass containing polydimethylsiloxane-(PDMS-) based sealant by Niko-Pekka et al.	Endodontic sealer	Bioglass containing PDMS caused higher absorption and ionic solubility than control; bioglass-PDMS revealed rapid mineralization and feasible antimicrobial properties	[78]
Mohn et al. analyzed the bismuth oxide and barium sulphate including bioactive glass particulates with high alkaline capacity and radioopaque properties for potential root canal dressing material	Root canal filling or dressing material	Bismuth oxide modified bioglass increases radiopacity, and alkaline behaviour promotes the sealing ability	[79]
Another study by Mohn et al. explained that polycaprolactone (PCL) or polyisoprene (PI) mixed 45S5 bioglass could create apatite interface, which ultimately acts as an endodontic sealer	Endodontic sealer	Bioglass filled PI and PCL composite materials resulting in improved bioactivity and immediate sealing	[80]
A study by Stalcin et al. experimented that chemophysical properties of resin infiltrant (ERI) doped bioglass reduce water absorption and solubility	Treatment of white spot lesions	Resin infiltrant-bioglass enhances chemomechanical properties, such that innovative materials might prevent demineralization and induce remineralization on enamel surfaces	[81]
Wang et al. investigated the effect of Ca <sub>3</sub> SiO <sub>5</sub> /CaCl <sub>2</sub> composite paste on setting time, compressive strength, bioactivity, and biocompatibility to explore the use in root canal filling	Root canal filling	Ca <sub>3</sub> SiO <sub>5</sub> /CaCl <sub>2</sub> composite cement revealed biocompatibility and good bioactivity, a potential candidate as a root canal sealing material	[82]



metal implants and screws that are been used for dental treatments damage the tissue and interrupt the blood supply; therefore, cells die, inflammation occurs, and the interfacial atmosphere may be destroyed. Mostly, metals are used as dental materials; thus, there may be a chance of corrosion on the implant surface and corroded ions may percolate inside the tissues and cells that initiate the variety of clinical problems. These problems can be controlled by coating bioactive components on the porous metal surfaces [72].

## 8. Bioglass Journey in Dentistry

Dental resin bonding with tooth is a challenging criterion to overcome, due to the interaction between the hydrophobic resin and the hydrophilic surface of the tooth; despite this, it can be resolved by making resin composites with hydrophilic bioactive glasses (Table 2, Figure 4). Recently, researchers analyzed commercial polymer-based materials (AH plus and poly-c) to formulate a paste of bioglass, from which one of the major issues of bioactive glass with poly-c is the formation of crack, due to shrinkage at the time of drying and evaporation of liquid. Subsequent evaporation probably moves through the interrelated pores of the bioglass network towards inside of the surface, which might generate capillary stresses causing crack propagation. Comparatively, these stresses are smaller in powders than monoliths due to the evaporation path, which are capable of inducing fracture. Narrow porosity distribution with increased grain size can render this problem [73]. Shrinkage of sealant paste (bioglass and poly-C) creates a gap, which leads to poor mechanical properties and instigate failure of dental restorations. Some of the earlier reports towards the development of sealant are tabulated in Table 2.

Amandeep et al. [83] reported the detailed survey of some restorative materials such as zinc oxide eugenol, calcium hydroxide sealers, and resin-based sealers. Zinc oxide eugenol has long successive history over 100 years; however, prolonged setting time, solubility, and shrinkage are the major complications. Antimicrobial activities of calcium hydroxide sealers are appreciable, but solubility is the major disadvantage. Resin-based sealers have been successful over the past few decades due to its improved flowability; however, reduced adhesive property is yet to be overcome. Similarly, Patel et al. [84] reviewed the bioactive dental biomaterials for endodontic therapy and mentioned some limitations of biomaterials including polymers, metals, bioceramics, composites, and natural minerals. Structural stability, cytocompatibility, and mechanical resistance of polymers are not up to the requirement. A metal exhibits complexity in corrosion and challenges due to interaction with the physiological environment. In case of bioceramics, fabrication and processing are difficult; lower impact resistance and brittleness are the major issues. Composites exhibit foreign body reaction at physiological environment; correspondingly, rapid immunological problems were noted in natural materials. It has been reported that bioglass was able to maintain its stability more than two months while soaked in brain heart infusion media and also enumerated similar mechanical behavior rather than decreased fracture resistance compared to commercial

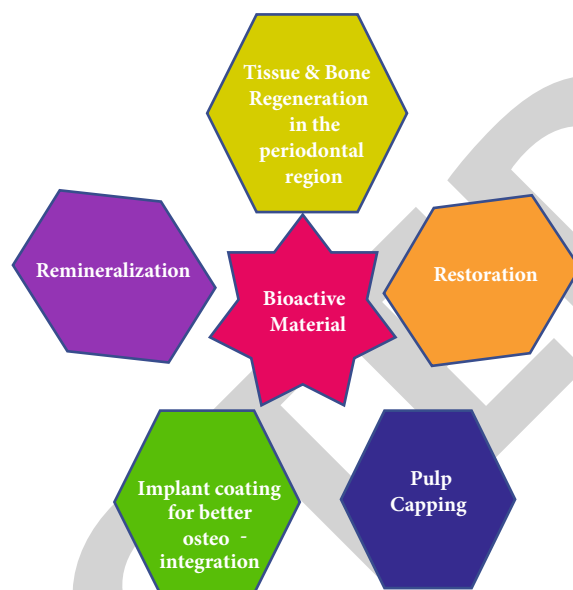


FIGURE 4: Bioactive material's impactful role in dentistry.

materials. Hence, it is easy to construct the structure of bioactive glasses with the relevant properties than some commercially available endodontic sealants.

Generally, bioglass particulates are mixed with phosphoric acid to form a paste, which positively interacts with enamel surfaces and protects orthodontic brackets from erosive solution, as reported by Abbassy et al. [85]. Similarly, Ahmed et al. [86] elaborated that bioglass paste with diluted phosphoric acid has significant effect on remineralization of enamel lesion. Bioglass with 30% phosphoric acid is used to treat dentin hypersensitivity, and sealing was observed in depth of dentinal tubules by Lee et al. [87]. Bioglass formulation was available in commercial toothpaste, which remineralizes the eruption of tubules at the dentin/enamel. Continuous brushing by the respective toothpaste initiates tubule occlusion, by the development of apatite on their surfaces and fixed restorations on the margins to fill gaps, and can also eliminate secondary caries over a period of time [88]. In another report, Adanir et al. [89] studied the sealing ability of resin-based commercial root canal sealers such as Diaket, EndoREZ, and AH26 along with those of zinc oxide-eugenol-based U/P sealer and concluded that none of these sealers completely prevent the leakage of fluids, among which zinc-oxide eugenol exhibited more significant leakage. However, cytotoxicity is one of the major problems in most of the commercially available endodontic sealant materials [90, 91]. Milly et al. [92] evaluated that bioglass/polyacrylic acid treatment enhanced remineralization of enamel white spot lesion. Bioglass with polyacrylic paste was able to increase the surface area, mechanical properties, and mineral content, resulting in augmented mineralization [91].

Generally, bioceramics are the materials that exhibit mineralization, which simulate the natural mineral component on the canal voids of the tooth. Bioactive ions are released from the ceramics material in the exposure of oral fluid in that environment; mineral apatite tends to form over the restorative materials, which enhances the durability of

the restoration. On the other hand, in the absence of bioactive ions, leached ions may not be having the potentiality to regenerate therefore it drops its stability. Bioceramics has the tendency to easily bond with polymer, and it became hardened; hence, it is accessible to use owing to its early setting time and stronger bonding nature. These positive features of bioceramics revolutionize the restorative society [20, 24]. Bioceramics are the most expected materials for restorative purposes; linear development in the aspects of composition was evolved with respect to duration. Initially, bioceramics journey started with calcium and phosphate compositions based on the silica, sodium, fluoride, zinc, carbon, iron, aluminium, bismuth, tantalum, ytterbium, barium, chlorine, sulfur, nickel, tungsten, titanium, silver, copper, tin, and mercury which have been included in different formulations depending on the need while growing ceramic materials. Currently, bioglass is the active material with different formulation and network chemistry. Hence, engineering glass network chemistry initiates the tunable characteristics such as porosity, morphology, structural aspects, degradability, bioactivity, and biocompatibility properties of the material. Besides, deep investigation and understanding the properties of bioglass lead to generate better restorative materials with acceptable stability as well as mineralization potentiality.

## 9. Summary and Future Direction

Starting from calcium silicate, so far, plenty of materials as well as many investigations have been reported in the aspects of various biocompatible and structural properties of existing ceramics. As of now, MTA (calcium silicate based bioceramics) is considered a potential candidate for endodontic restorative material owing to their biological characteristic feature and physicochemical properties. Followed by MTA, recently, biodentine is also gaining impactful attention due to their physico-bio-chemical properties; however, even more *in vitro* and *in vivo* studies are required to exactly assess the properties of this material. Addition of protein (CPNE7) into bioceramics may induce reparative dentin formations while using in pulp capping. Biodentine is similar in composition to that of bioglass, and not many reports are available to elaborate bioactive glass role in dentistry and also with the extended understanding in the characteristic features of the material at oral environment. However, based on the basic properties of bioglass, it can be assumed that it is one of the best materials for bioactivity among all bioceramics; however, this material has limitations in mechanical stability. By engineering stable bioglass with substituting strong metal ion in the glass network in terms of stronger metal ion in the lattice of bioglass or fabricating bioglass with hard polymer composite, it is possible to achieve better material for restoration. It is essential to analyze in detail, such kind of materials in the direction of structural, mechanical properties, and *in vitro/in vivo* compatibility.

## Data Availability

The data used to support the findings of this study are included within the article.

## Conflicts of Interest

The authors declare that they have no conflicts of interest.

## Acknowledgments

This study is self-funding.

## References

- [1] M. S. Zafar, F. Amin, M. A. Fareed et al., "Biomimetic aspects of restorative dentistry biomaterials," *Biomimetics (Basel)*, vol. 5, no. 3, p. 34, 2020.
- [2] A. S. Khan and M. R. Syed, "A review of bioceramics-based dental restorative materials," *Dental Materials Journal*, vol. 38, no. 2, pp. 163–176, 2019.
- [3] L. L. Dai, M. L. Mei, C. H. Chu, and E. C. M. Lo, "Mechanisms of bioactive glass on caries management: a review," *Materials*, vol. 12, no. 24, p. 4183, 2019.
- [4] A. L. Ware, "The control of dental amalgam," *Australian Dental Journal*, vol. 5, no. 5, pp. 298–305, 1960.
- [5] M. Fathi and V. A. S. Mortazavi, "A review on dental amalgam corrosion and its consequences," *Journal of Research in Medical Sciences (Jrms)*, vol. 9, p. 42, 2004.
- [6] C. M. A. Brett, E. Jorge, C. Gouveia-Caridade, and H. Dias, "Influence of protein adsorption on the passivation of dental amalgams," in *Passivation of Metals and Semiconductors, and Properties of Thin Oxide Layers*, Elsevier, 2006.
- [7] D. L. Smith and H. J. Caul, "Alloys of gallium with powdered metals as possible replacement for dental amalgam," *The Journal of the American Dental Association*, vol. 53, no. 3, pp. 315–324, 1956.
- [8] H. Y. Marghalani, "Resin-based dental composite materials," in *Handbook of bioceramics and biocomposites*, pp. 357–405, Springer, Berlin, Germany, 2016.
- [9] M. M. Karabela and I. D. Sideridou, "Synthesis and study of properties of dental resin composites with different nanosilica particles size," *Dental Materials*, vol. 27, no. 8, pp. 825–835, 2011.
- [10] N. Eliaz and N. Metoki, "Calcium phosphate bioceramics: a review of their history, structure, properties, coating technologies and biomedical applications," *Materials (Basel)*, vol. 10, no. 4, p. 334, 2017.
- [11] G. Spagnuolo, "Bioactive dental materials: the current status," *Materials (Basel)*, vol. 15, no. 6, p. 2016, 2022.
- [12] J. L. Gutmann, "The interactive role of tooth trauma, pulpal status, and orthodontic tooth movement: a focused review," *Endo (Lond Engl)*, vol. 8, pp. 267–291, 2014.
- [13] C. D. Lynch, V. R. O'Sullivan, and C. T. McGillicuddy, "Pierre Fauchard: the 'Father of Modern Dentistry'," *British Dental Journal*, vol. 201, no. 12, pp. 779–781, 2006.
- [14] A. Qureshi, E. Soujanya, and P. Nandakumar, "Recent advances in pulp capping materials: an overview," *Journal of Clinical and Diagnostic Research: JCDR*, vol. 8, p. 316, 2014.
- [15] S. K. Aliuddin, P. Prakash, S. Mohiuddin et al., "Historical milestones in endodontics: review of literature," *International Journal of Preventive and Clinical Dental Research*, vol. 4, no. 1, pp. 56–58, 2017.
- [16] N. Shah, N. Bansal, and A. Logani, "Recent advances in imaging technologies in dentistry," *World Journal of Radiology*, vol. 6, no. 10, pp. 794–807, 2014.

- [17] G. Cervino, "Milestones of dentistry: advent of anesthetics in oral surgery," *Dentistry Journal*, vol. 7, no. 4, p. 112, 2019.
- [18] A. Jayaraj, S. S. V. Jayakrishnan, K. N. Shetty, and R. Rai, "Recent advances in endodontics exploring the trends in diagnosis," *International Journal of Innovative Science and Research Technology*, vol. 5, no. 1, 2020.
- [19] R. S. Lacruz, S. Habelitz, J. T. Wright, and M. L. Paine, "Dental enamel formation and implications for oral health and disease," *Physiological Reviews*, vol. 97, no. 3, pp. 939–993, 2017.
- [20] C. Estrela, D. D. A. Decurcio, G. Rossi-Fedele, J. A. Silva, O. A. Guedes, and Á. H. Borges, "Root perforations: a review of diagnosis, prognosis and materials," *Brazilian Oral Research*, vol. 32, 2018.
- [21] S. Tabassum and F. R. Khan, "Failure of endodontic treatment: the usual suspects," *European journal of dentistry*, vol. 10, no. 1, pp. 144–147, 2016.
- [22] D. Zaneva-Hristova and T. Borisova-Papancheva, "Bioceramics in endodontics-advantages and disadvantages," *Journal of the Union of Scientists-Varna. Medicine and Ecology Series*, vol. 23, no. 1, pp. 141–146, 2019.
- [23] V. Vishwanath and H. M. Rao, "Gutta-percha in endodontics-a comprehensive review of material science," *Journal of conservative dentistry: JCD*, vol. 22, no. 3, pp. 216–222, 2019.
- [24] S. Chitra, P. Bargavi, M. Balasubramaniam, R. R. Chandran, and S. Balakumar, "Impact of copper on in-vitro biomineralization, drug release efficacy and antimicrobial properties of bioactive glasses," *Materials Science and Engineering: C*, vol. 109, p. 110598, 2020.
- [25] G. Radha, S. Balakumar, B. Venkatesan, and E. Vellaichamy, "Evaluation of hemocompatibility and *in vitro* immersion on microwave-assisted hydroxyapatite -alumina nanocomposites," *Materials Science and Engineering: C*, vol. 50, pp. 143–150, 2015.
- [26] L. Miyoung, J. Chanyong, S. Dong-Hoon, and C. Yong-bum, "Calcium silicate-based root canal sealers: a literature review," *Restorative Dentistry and Endodontics*, vol. 45, pp. 1–17, 2020.
- [27] S. S. Raghavendra, G. R. Jadhav, K. M. Gathani, and P. Kotadia, "Bioceramics in ENDODONTICS – A review," *Journal of Istanbul University Faculty of Dentistry*, vol. 51, p. S128, 2017.
- [28] S. Chitra, R. Chandran, R. Ramya, D. Durgalakshmi, and S. Balakumar, "Unravelling the effects of ibuprofen-acetaminophen infused copper-bioglass towards the creation of root canal sealant," *Biomedical Materials*, vol. 17, no. 3, p. 035001, 2022.
- [29] D. Durgalakshmi, R. A. Rakkesh, M. Kesavan et al., "Highly reactive crystalline-phase-embedded strontium-bioactive nanorods for multimodal bioactive applications," *Biomaterials Science*, vol. 6, no. 7, pp. 1764–1776, 2018.
- [30] R. Ba-Hattab, M. Al-Jamie, H. Aldreib, L. Alessa, and M. Alonazi, "Calcium hydroxide in endodontics: an overview," *Open Journal of Stomatology*, vol. 6, no. 12, pp. 274–289, 2016.
- [31] A. S. Polinsky, "Evaluation and comparison of periapical healing using periapical films and cone beam computed tomography," *Post-Treatment Follow Up*, 2019.
- [32] J. L. Sanz, F. J. Rodr Águez-Lozano, C. Llana, S. Sauro, and L. Forner, "Bioactivity of bioceramic materials used in the dentin-pulp complex therapy: a systematic review," *Materials*, vol. 12, no. 7, p. 1015, 2019.
- [33] P. Panpisut and A. Toneluck, "Monomer conversion, dimensional stability, biaxial flexural strength, and fluoride release of resin-based restorative material containing alkaline fillers," *Dental Materials Journal*, vol. 39, no. 4, pp. 608–615, 2020.
- [34] W. Song, W. Sun, L. Chen, and Z. Yuan, "In vivo biocompatibility and bioactivity of calcium silicate-based bioceramics in endodontics," *Frontiers in Bioengineering and Biotechnology*, vol. 8, p. 580954, 2020.
- [35] S. M. Abusrewil, W. McLean, and J. A. Scott, "The use of bioceramics as root-end filling materials in periradicular surgery: a literature review," *The Saudi dental journal*, vol. 30, no. 4, pp. 273–282, 2018.
- [36] M. Tanomaru-Filho, R. Bosso, R. Viapiana, and J. M. Guerreiro-Tanomaru, "Radiopacity and flow of different endodontic sealers," *Acta Odontol Á<sup>3</sup>gica Latinoamericana*, vol. 26, pp. 121–125, 2013.
- [37] K. Olcay, P. N. Taşli, E. P. Güven et al., "Effect of a novel bioceramic root canal sealer on the angiogenesis-enhancing potential of assorted human odontogenic stem cells compared with principal tricalcium silicate-based cements," *Journal of Applied Oral Science*, vol. 28, 2020.
- [38] G. A. Marín-Bauza, Y. T. C. Silva-Sousa, S. A. D. Cunha et al., "Physicochemical properties of endodontic sealers of different bases," *Journal of Applied Oral Science*, vol. 20, no. 4, pp. 455–461, 2012.
- [39] T. I. Vieira, A. K. Alexandria, T. K. da Silva Fidalgo, A. de Almeida Neves, A. M. G. Valença, and L. C. Maia, "Chemical and physical modification of carbonated energy beverages to reduce the damage over teeth and restorative materials," in *Sports and Energy Drinks*, pp. 205–227, Woodhead Publishing, 2019.
- [40] J. S. Sivakumar, B. N. S. Kumar, and P. V. Shyamala, "Role of provisional restorations in endodontic therapy," *Journal of Pharmacy & Bioallied Sciences*, vol. 5, no. 5, p. 120, 2013.
- [41] G. M. Brauer, "A review of zinc oxide-eugenol type filling materials and cements," *Revue Belge de Médecine Dentaire*, vol. 20, no. 3, pp. 323–364, 1965.
- [42] E. C. Chisholm, "Proceedings of the Tennessee Dental Association, 7th annual meeting-Nashville," *Dental Register*, vol. 27, p. 517, 1873.
- [43] S. Priyalakshmi and M. Ranjan, "Review on Biodentine-A Bioactive Dentin Substitute," *Journal of Dental and Medical Sciences*, vol. 13, no. 1, pp. 13–17, 2014.
- [44] N. Iftikhar, B. S. Devashish, N. Gupta, and R.-S. Natasha Ghambir, "A comparative evaluation of mechanical properties of four different restorative materials: an in vitro study," *Journal of Clinical Pediatric Dentistry*, vol. 12, no. 1, pp. 47–49, 2019.
- [45] P. Z. Tawil, D. J. Duggan, and J. C. Galicia, "MTA: a clinical review," *Compendium of Continuing Education in Dentistry (Jamesburg, NJ: 1995)*, vol. 36, pp. 247–252, 2015.
- [46] H. E. Skallevoid, D. Rokaya, Z. Khurshid, and M. S. Zafar, "Bioactive glass applications in dentistry," *International Journal of Molecular Sciences*, vol. 20, no. 23, p. 5960, 2019.
- [47] S. Chitra and S. Balakumar, "Insight into the impingement of different sodium precursors on structural, biocompatible, and hemostatic properties of bioactive materials," *Materials Science and Engineering: C*, vol. 123, p. 111959, 2021.
- [48] P. Bargavi, R. Ramya, S. Chitra et al., "Bioactive, degradable and multi-functional three-dimensional membranous scaffolds of bioglass and alginate composites for tissue regenerative applications," *Biomaterials Science*, vol. 8, no. 14, pp. 4003–4025, 2020.



- [49] S. Fayazi, S. N. Ostad, and H. Razmi, "Effect of ProRoot MTA, Portland cement, and amalgam on the expression of fibronectin, collagen I, and TGF $\beta$  by human periodontal ligament fibroblasts in vitro," *Indian Journal of Dental Research*, vol. 22, no. 2, pp. 190–194, 2011.
- [50] V. D'Antò, M. P. Di Caprio, G. Ametrano, M. Simeone, S. Rengo, and G. Spagnuolo, "Effect of mineral trioxide aggregate on mesenchymal stem cells," *Journal of Endodontics*, vol. 36, no. 11, pp. 1839–1843, 2010.
- [51] Á. H. Borges, F. L. Pedro, C. E. Miranda, A. Semenoff-Segundo, J. D. Pécora, and A. M. Cruz Filho, "Comparative study of physico-chemical properties of MTA-based and Portland cements," *Acta Odontológica Latinoamericana*, vol. 23, no. 3, pp. 175–181, 2010.
- [52] L. A. S. Dreger, W. T. Felipe, J. F. Reyes-Carmona, G. S. Felipe, E. A. Bortoluzzi, and M. C. S. Felipe, "Mineral trioxide aggregate and Portland cement promote biomineralization in vivo," *Journal of Endodontics*, vol. 38, no. 3, pp. 324–329, 2012.
- [53] H. Singh, M. Kaur, S. Markan, and P. Kapoor, "Biodentine: a promising dentin substitute," *Journal of Interdisciplinary Medicine and Dental Science*, vol. 2, p. 2, 2014.
- [54] C. S. Hirschberg, N. S. Patel, L. M. Patel, D. E. Kadouri, and G. R. Hartwell, "Comparison of sealing ability of MTA and EndoSequence bioceramic root repair material: a bacterial leakage study," *Quintessence International*, vol. 44, no. 5, pp. e157–e162, 2013.
- [55] K. F. Lovato and C. M. Sedgley, "Antibacterial activity of EndoSequence root repair material and ProRoot MTA against clinical isolates of *Enterococcus faecalis*," *Journal of Endodontics*, vol. 37, no. 11, pp. 1542–1546, 2011.
- [56] M. Martínez-Cortés, C. Tinajero-Morales, C. Rosales, and E. Uribe-Quero, "Evaluación de la citotoxicidad de tres cementos selladores endodóncicos utilizados en cirugía periapical: estudio In vitro," *Revista Odontológica Mexicana*, vol. 21, no. 1, pp. 40–48, 2017.
- [57] A. D. Sonu Gupta, "Endodontic treatment of immature tooth – a challenge," *Journal of Pre-Clinical and Clinical Research*, vol. 14, no. 3, pp. 73–79, 2020.
- [58] F. Leal, G. De-Deus, C. Brandão, A. S. Luna, S. R. Fidel, and E. M. Souza, "Comparison of the root-end seal provided by bioceramic repair cements and white MTA," *International Endodontic Journal*, vol. 44, no. 7, pp. 662–668, 2011.
- [59] C. Prati and M. G. Gandolfi, "Calcium silicate bioactive cements: biological perspectives and clinical applications," *Dental Materials*, vol. 31, no. 4, pp. 351–370, 2015.
- [60] P. Jain and M. Ranjan, "The rise of bioceramics in endodontics: a review," *International Journal of Pharma and Bio Sciences*, vol. 6, pp. 416–422, 2015.
- [61] M. Kaur, H. Singh, J. S. Dhillon, M. Batra, and M. Saini, "MTA versus biodentine: review of literature with a comparative analysis," *Journal of Clinical and Diagnostic Research: JCDR*, vol. 11, p. ZG01, 2017.
- [62] S. Lftikhar, N. Jahanzeb, M. Saleem, S. Ur Rehman, J. P. Matinlinna, and A. S. Khan, "The trends of dental biomaterials research and future directions: a mapping review," *The Saudi Dental Journal*, vol. 33, no. 5, pp. 229–238, 2021.
- [63] L. G. Ladino, A. Bernal, D. Calderón, and D. Cortés, "Bioactive Materials in Restorative Dentistry: A Literature Review," *ScienceVols*, vol. 2, no. 2, pp. 74–81, 2021.
- [64] H. O. Simila and A. R. Boccaccini, "Sol-gel bioactive glass containing biomaterials for restorative dentistry: a review," *Dental Materials*, vol. 38, no. 5, pp. 725–747, 2022.
- [65] R. R. Chandran, S. Chitra, S. Vijayakumari, P. Bargavi, and S. Balakumar, "Cognizing the crystallization aspects of NaCa-PO $_4$  concomitant 5S5 bioactive-structures and their imprints in vitro bio-mineralization," *New Journal of Chemistry*, vol. 45, no. 34, pp. 15350–15362, 2021.
- [66] M. G. Raucchi, D. Giugliano, and L. Ambrosio, *Fundamental properties of bioceramics and biocomposites*, Springer, Cham, 2016.
- [67] M. K. Arifa, R. Ephraim, and T. Rajamani, "Recent advances in dental hard tissue remineralization: a review of literature," *International journal of clinical pediatric dentistry*, vol. 12, no. 2, pp. 139–144, 2019.
- [68] I. V. Antoniac, *Handbook of bioceramics and biocomposites*, Springer, Berlin, Germany, 2016.
- [69] D. Durgalakshmi, S. Balakumar, C. A. Raja, R. P. George, and U. K. Mudali, "Structural, morphological and antibacterial investigation of Ag-impregnated Sol-Gel-Derived 45S5 nanobioglass systems," *Journal of Nanoscience and Nanotechnology*, vol. 15, no. 6, pp. 4285–4295, 2015.
- [70] G. P. Jayaswal, S. P. Dange, and A. N. Khalikar, "Bioceramic in dental implants: a review," *The Journal of Indian Prosthodontic Society*, vol. 10, no. 1, pp. 8–12, 2010.
- [71] A. A. Campbell, "Bioceramics for implant coatings," *Materials Today*, vol. 6, no. 11, pp. 26–30, 2003.
- [72] L. L. Hench, "Bioceramics: from concept to clinic," *Journal of the American Ceramic Society*, vol. 74, no. 7, pp. 1487–1510, 1991.
- [73] J. R. Jones, "Review of bioactive glass: from Hench to hybrids," *Acta Biomaterialia*, vol. 9, no. 1, pp. 4457–4486, 2013.
- [74] M. Deng, H.-L. Wen, X.-L. Dong et al., "Effects of 45S5 bioglass on surface properties of dental enamel subjected to 35% hydrogen peroxide," *International Journal of Oral Science*, vol. 5, no. 2, pp. 103–110, 2013.
- [75] S. Sauro, T. F. Watson, I. Thompson, M. Toledano, C. Nucci, and A. Banerjee, "Influence of air-abrasion executed with polyacrylic acid-Bioglass 45S5 on the bonding performance of a resin-modified glass ionomer cement," *European Journal of Oral Sciences*, vol. 120, no. 2, pp. 168–177, 2012.
- [76] S.-Y. Yang, J.-W. Choi, K.-M. Kim, and J.-S. Kwon, "Prevention of secondary caries using resin-based pit and fissure sealants containing hydrated calcium silicate," *Polymers*, vol. 12, no. 5, p. 1200, 2020.
- [77] G. H. Waly and R. A. Salama, "Addition of bioactive glass to endodontic epoxy resin sealer: effect on bioactivity, flow and push-out bond strength," *Egyptian Dental Journal*, vol. 64, no. 3, pp. 2645–2655, 2018.
- [78] N. P. J. Hoikkala, X. Wang, L. Hupa, J. H. Smått, J. Peltonen, and P. K. Vallittu, "Dissolution and mineralization characterization of bioactive glass ceramic containing endodontic sealer Gutttaflow Bioseal," *Dental Materials Journal*, vol. 37, no. 6, pp. 988–994, 2018.
- [79] D. Mohn, M. Zehnder, T. Imfeld, and W. J. Stark, "Radio-opaque nanosized bioactive glass for potential root canal application: evaluation of radiopacity, bioactivity and alkaline capacity," *International Endodontic Journal*, vol. 43, no. 3, pp. 210–217, 2010.
- [80] D. Mohn, C. Bruhin, N. A. Luechinger, W. J. Stark, T. Imfeld, and M. Zehnder, "Composites made of flame-sprayed bioactive glass 45S5 and polymers: bioactivity and immediate

## *Retraction*

# **Retracted: Ferroptosis-Related lncRNA for the Establishment of Novel Prognostic Signature and Therapeutic Response Prediction to Endometrial Carcinoma**

### **BioMed Research International**

Received 24 November 2022; Accepted 24 November 2022; Published 27 December 2022

Copyright © 2022 BioMed Research International. This is an open access article distributed under the Creative Commons Attribution License, which permits unrestricted use, distribution, and reproduction in any medium, provided the original work is properly cited.

*BioMed Research International* has retracted the article titled “Ferroptosis-Related lncRNA for the Establishment of Novel Prognostic Signature and Therapeutic Response Prediction to Endometrial Carcinoma” [1] due to concerns that the peer review process has been compromised.

Following an investigation conducted by the Hindawi Research Integrity team [2], significant concerns were identified with the peer reviewers assigned to this article; the investigation has concluded that the peer review process was compromised. We therefore can no longer trust the peer review process and the article is being retracted with the agreement of the editorial board.

The authors agree to the retraction.

### **References**

- [1] X.-Y. Zhou, H.-Y. Dai, H. Zhang, J.-L. Zhu, and H. Hu, “Ferroptosis-Related lncRNA for the Establishment of Novel Prognostic Signature and Therapeutic Response Prediction to Endometrial Carcinoma,” *BioMed Research International*, vol. 2022, Article ID 2056913, 16 pages, 2022.
- [2] L. Ferguson, “Advancing Research Integrity Collaboratively and with Vigour,” 2022, <https://www.hindawi.com/post/advancing-research-integrity-collaboratively-and-vigour/>.



## Research Article

# Ferroptosis-Related lncRNA for the Establishment of Novel Prognostic Signature and Therapeutic Response Prediction to Endometrial Carcinoma

Xin-Ying Zhou , Hai-Yan Dai , Hu Zhang , Jian-Long Zhu, and Hua Hu 

Department of Obstetrics and Gynecology, Shanghai Pudong Hospital, Fudan University Pudong Medical Center, 2800 Gongwei Road, Pudong, Shanghai 201399, China

Correspondence should be addressed to Hai-Yan Dai; [daihaiyan0218@sina.cn](mailto:daihaiyan0218@sina.cn) and Hu Zhang; [doczhray@163.com](mailto:doczhray@163.com)

Received 31 May 2022; Revised 16 June 2022; Accepted 8 July 2022; Published 28 July 2022

Academic Editor: Dinesh Rokaya

Copyright © 2022 Xin-Ying Zhou et al. This is an open access article distributed under the Creative Commons Attribution License, which permits unrestricted use, distribution, and reproduction in any medium, provided the original work is properly cited.

**Background.** Ferroptosis is a recently described form of intentional cellular damage that is iron-dependent and separate from apoptosis, cellular necrosis, and autophagy. It has been demonstrated to be adequately regulated by long noncoding RNAs (lncRNAs) in various cancers. However, the predictive profile of ferroptosis-related lncRNAs (FRLs) in endometrial carcinoma (EC) is unknown. Herein, FRLs associated with uterine corpus endometrial carcinoma (UCEC) prognosis were screened to predict treatment response in EC. **Methods.** Samples of EC and adjacent normal tissues were obtained from The Cancer Genome Atlas (TCGA) dataset repository. Limma and survival packages in R software were used to screen FRLs associated with the prognosis of EC. Gene Ontology (GO) and Kyoto Encyclopedia of Genes and Genomes (KEGG) chord and circle plots of FRLs were also plotted. Next, FRLs screened by the least absolute shrinkage and selection operator (LASSO) method were applied to construct and validate a multivariate Cox proportional risk regression model. Nomogram plots were created to forecast the outcome of UCEC patients, and gene set enrichment analysis (GSEA), principal component analysis (PCA), and immunoassays were performed on the prognostic models. Finally, limma, ggpubr, pRRophetic, and ggplot2 programs were used for drug sensitivity analysis of the prognostic models. **Results.** A signature based on nine FRLs (CFAP58-DT, LINC00443, EMSLR, HYI-AS1, ADIRF-AS1, LINC02474, CDKN2B-AS1, LINC01629, and LINC00942) was constructed. The developed FRL prognostic model effectively discriminated UCEC patients into low-risk and high-risk groups. Immunological checkpoints CD80 and CD40 were strongly expressed in the high-risk group. In addition, the nine FRLs were all more expressed in the high-risk group compared to the low-risk group. **Conclusion.** These findings significantly contribute to the understanding of the function of FRLs in UCEC and provide promising therapeutic strategies for UCEC.

## 1. Introduction

Endometrial carcinoma (EC) is the most common malignancy in women worldwide, with approximately 320,000 cases and over 76,000 death annually, and the increasing incidence rate makes it an essential factor for female health [1]. According to the International Federation of Gynecology and Obstetrics (FIGO) staging system, the five-year survival for EC is over 90% for phase I, 70% for phase II, and

60% for phase III [2]. For early-stage cancer, the primary treatment combines surgery with radiotherapy or, more commonly, chemotherapy, which is the backbone of therapy for most patients with advanced cancer. Newer therapies include antiangiogenic and poly(ADP-ribose) polymerase (PARP) inhibitors [3]. Adjuvant treatment for EC remains complex and controversial. Advanced EC has a high risk of recurrence and death, and relatively few treatment options are available for metastatic uterine corpus endometrial carci-

noma (UCEC). Studies have suggested that biomarkers and predictive models could be used to improve targeted therapy and immunotherapy in cancer patients [4]. No reliable biomarkers have been identified to reflect the prognosis and response to drug therapy in UCEC.

Ferroptosis, a form of regulated cell death characterized by the iron-dependent accumulation of lipid hydroperoxides, is associated with tumor growth and therapeutic responsiveness [5]. Unlike unplanned cell death, mediated cellular death is affected by pharmacological or genetic intervention and regulated by specific signal transduction [6]. Apoptosis, cell scorch, necroptosis, and ferroptosis are the most well-studied forms of regulated cell death, each of which has its molecular mechanism [7]. Extrinsic and intrinsic mechanisms can both cause ferroptosis [8]. The former is through inhibiting cell membrane transporters or activating iron transporters serum transferrin and lactotransferrin, while the latter operates by blocking intracellular antioxidant enzymes [5]. Ferroptosis induction requires increased iron storage, oxidative stress, fatty acid supply, and lipid peroxidation. Small molecule-induced ferroptosis has a considerable inhibitory effect on tumor development and improves chemotherapeutic treatment sensitivity, particularly in drug-resistant. This research emphasizes the significance of ferroptosis in anticancer therapy. Ferroptosis impacts chemotherapeutics, radiation, and immunotherapeutic outcomes, and its interaction with drugs targeting ferroptosis pathways can significantly improve treatment outcomes [5].

Recent studies have shown that ferroptosis is associated with various clinical disorders, including malignancies, neurological diseases, ischemia-reperfusion impairment, renal damage, and hematological disorders. Ferroptosis is a biological phenomenon controlled by a cluster of genes [9]. Triple-negative breast carcinoma is a highly aggressive malignancy with limited therapeutic strategies. However, it is susceptible to ferroptosis stimulants, and ferroptosis therapy is predicted to be a novel method for “refractory breast carcinoma” [10]. Noncoding RNA has also been postulated to be a regulator of cancer networks and an indicator of cancer outcomes in the recent decade [11–14]. Several long noncoding RNAs (lncRNAs) have been found to impact tumor outcomes [15]. A nuclear lncRNA LINC00336 is elevated in lung disease and functions as a carcinogen by interacting with indigenous RNAs [16]. Although numerous studies have investigated whether ferroptosis-associated lncRNAs (FRLs) influence UCEC outcomes, little is known about this relationship. The present study sought to develop a predictive model for FRL risk in UCEC and investigate its interaction with tumor immunology and treatment response. As shown in the flow chart (Figure 1), a prognostic model was constructed based on nine FRLs (CFAP58-DT, LINC00443, EMSLR, HYI-AS1, ADIRF-AS1, LINC02474, CDKN2B-AS1, LINC01629, and LINC00942) that predict the overall survival, tumor immune characteristics, and drug treatment response in UCEC. To the best of our knowledge, this is the first study to explore FRLs with UCEC prognosis and drug sensitivity. These findings may help in the identification of markers associated with prognosis and pharmacological therapy in EC patients, which may enhance prognosis.

## 2. Methods and Materials

**2.1. Data Acquisition.** RNA-seq data of 552 EC tissue samples and 23 normal tissue samples were downloaded from The Cancer Genome Atlas (TCGA) database [17]. The Perl software was used to differentiate the extracted RNA data into lncRNAs and mRNA. The transcription of ferroptosis-associated genes obtained from the FerrDb website (<http://www.zhounan.org/ferrdb/>) was calculated using the R tool [18].

**2.2. Functional Enrichment Analysis of FRLs Associated with the Prognosis of EC.** FRLs were firstly screened and correlation analysis was performed on the obtained lncRNAs and ferroptosis genes. The limma program [19], with absolute levels of statistical parameters greater than 0.4 and significant levels just below 0.001, was used to assess the transcription of FRLs. Univariate analysis was used to screen FRLs associated with EC prognosis ( $p < 0.05$ ). Gene Ontology (GO) and Kyoto Encyclopedia of Genes and Genome (KEGG) analyses were performed on the screened FRLs. clusterProfiler, <http://org.Hs.eg.db>, GOplot, and ggplot2 programs were used to plot line, and circle plots of GO and KEGG chord and circle plots of the expression levels of FRLs in UCEC were plotted using clusterProfiler, <http://org.Hs.eg.db>, GOplot, and ggplot2 packages.

**2.3. Construction and Validation of an FRL Prognostic Model.** The screened prognosis-related FRLs were used to establish a prognostic model. FRLs were selected using the least absolute shrinkage and selection operator (LASSO) approach for the multivariable Cox proportionate risk regression analysis. After, the candidate prognostic signatures were filtered using univariate Cox regression, LASSO regression, and multivariate Cox regression analyses. A risk assessment model was developed using the following formula: gene transcription  $\times$  corresponding regression score. Subjects were divided into high- and low-risk groups based on the median risk score value. Patients were classified as high risk if their risk score was above the median and as low risk if their risk score was below the median using glmnet, survivor, and survminer packages in R.

The constructed prognostic model was validated. First, survival curves of the FRLs prognostic model were plotted using survivor and survminer packages in the R software were utilized. Risk graphs, survival condition images, and hazard heat maps for the prognostic models were also plotted using the pheatmap package in R. The receiver operating characteristic (ROC) curves, including time-dependent and clinically relevant ROC curves, were used to assess the accuracy of the predictive model using survival, survminer, and timeROC packages in R [20]. Clinically relevant heat maps were drawn limma and pheatmap packages in R, and the transcription of prognosis-related lncRNAs in low- and high-risk groups was analyzed to determine the relevance of clinical variables to the predictive model. Finally, the Cytoscape software was used to map the coexpression of lncRNAs and ferroptosis-related genes in the prognostic model [21].

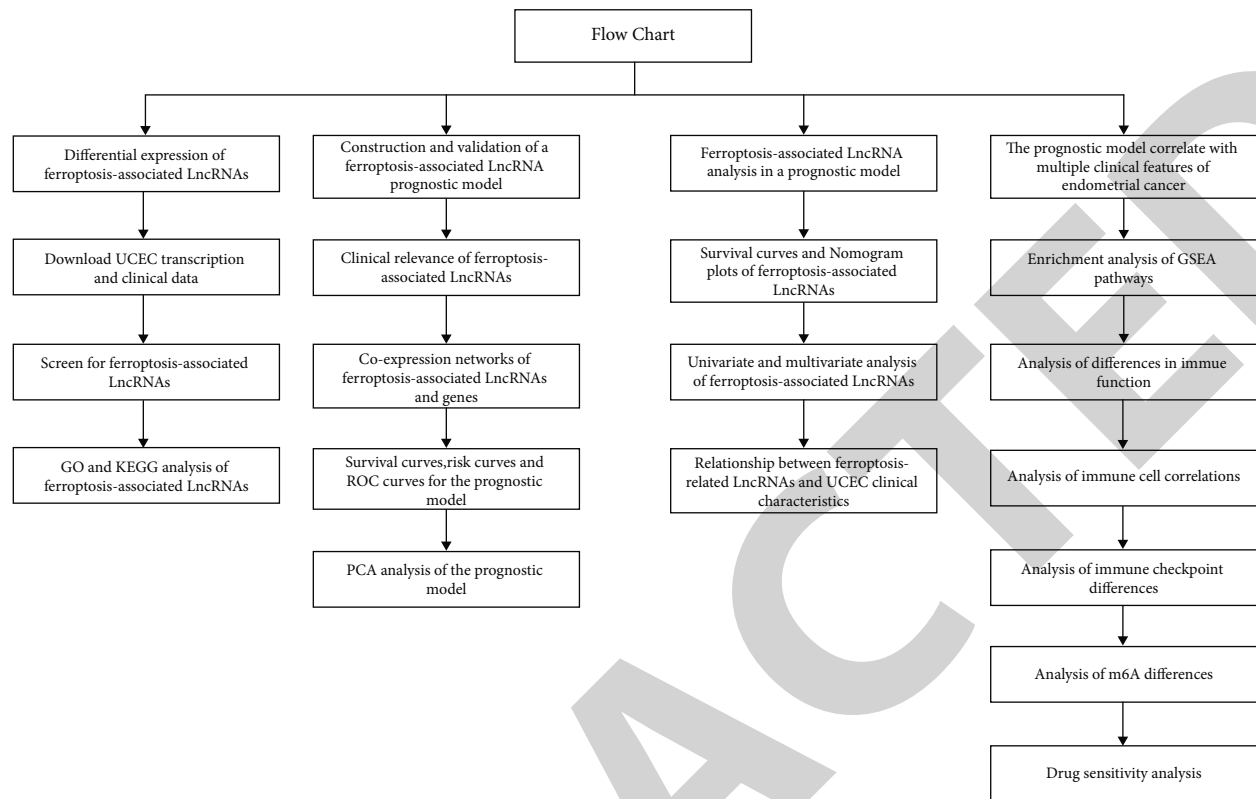


FIGURE 1: Flow chart of the ferroptosis-related lncRNA prognostic model.

**2.4. Correlation between the Prognostic Model and Clinical Features.** The survminer package in R was used to plot the survival curves of FRLs in the prognostic model. Nomogram plots were then constructed using rms and survminer packages in the R software. Column line plots were created to assess how well the risk levels collected predicted prognosis at 1, 3, and 5 years. Univariate and multivariate analyses of FRLs in the predictive model were performed using the survival package in R to evaluate their effects on the outcome of UCEC patients. Clinical features of EC with substantial FRLs were examined using the R program.

**2.5. GSEA and PCA of the Predictive Model.** The GSEA software [22] was used to perform a KEGG analysis of differential pathways of the prognostic model ( $p < 0.05$ ). Subsequently, PCA was employed to verify the ability of the FRL model's UCEC grouping. Differences in gene expression profiles, ferroptosis genes, FRLs, and risk models constructed from FRLs by PCA were examined [23]. Three-dimensional (3D) scatter plots were used to display the spatial distribution of samples. PCA was performed using limma and scatterplot3d packages in the R software.

**2.6. Immune Characteristic and m6A Differential Analysis.** The prognostic model was further subjected to immune cell differential analysis, immunological function differential analysis, and immune checkpoint differential analysis. The association between the predictive model and tumor immunity was investigated. Limma and pheatmap packages in R were employed to conduct correlation studies between

immune cells and low-risk and high-risk groups. Limma, GSVA, GSEABase, ggpubr, and reshape2 packages in R were used to evaluate immune function in the forecast model. R packages limma, ggplot2, and ggpubr were utilized to evaluate immunological checkpoints in the diagnostic model.

In addition, m6A differential analysis was performed on prognostic models. Seven m6A-associated lncRNAs closely associated with UCEC prognosis were selected, including RAB11B-AS1, LINC01812, HM13-IT1, TPM1-AS, SLC16A1-AS1, LINC01936, and CDKN2B-AS1. R packages limma, ggplot2, and ggpubr were used for m6A differential analysis of prognostic models.

**2.7. Drug Sensitivity Analysis of the Prognostic Model.** Drug susceptibility analysis was performed on the developed predictive model to forecast prospective drugs to manage UCEC. The 50% inhibitory concentration (IC50) value was used to assess the drug sensitivity of the predictive model. The IC50 value was used to assess the predictive model's sensitivity to the medication. The 50% inhibitory dosage is the concentration of drug that causes 50% apoptosis in tumor cells. The ability of the drug to trigger apoptosis can be measured using the IC50 value. The lower the level and the better the therapeutic effect, the greater the induction. Limma, ggpubr, pRRophetic, and ggplot2 packages in the R software were used for drug sensitivity analysis of the prognostic model.

**2.8. Statistical Analysis.** All analyses were performed using the R software (version 4.1.2) and Perl tools. The Kaplan–

Meier method and univariate and multivariable Cox proportional hazard regression models were employed to investigate prognosis-related FRLs. A  $p$  value less than 0.05 was considered statistically significant.

### 3. Results

**3.1. Identification of Prognosis-Related FRLs in EC Using GO and KEGG Analyses.** Twenty-one FRLs associated with UCEC outcome were identified from 552 EC tissue samples and 23 normal tissue samples. Figure 2(a) shows that LRRBCB-DT (relative risk (RR) = 3.618, 95% confidence interval (CI) = 1.449 – 9.030;  $P = 0.006$ ), FAM66C (RR = 2.915, 95%CI = 1.366 – 6.219;  $P = 0.006$ ), and CFAP58-DT (RR = 2.291, 95%CI = 1.403 – 3.742) were risk factors for EC, whereas HYI-AS1 (hazard ratio = 0.532, 95 %CI = 0.326 – 0.869;  $P = 0.012$ ) was a protective indicator for patients with EC. GO and KEGG chord and circle plots of FRLs are shown in Figures 2(b) and 2(c), respectively. The KEGG pathway revealed that differentially expressed FRLs mainly enriched in glutathione metabolism (hsa00480). Results of GO and KEGG pathway analysis of FRLs are summarized in Table 1.

**3.2. Establishment and Verification of a Prognostic Model Based on Ferroptosis-Related lncRNAs.** Twenty-one ferroptosis-related lncRNAs with prognostic value in UCEC were identified. The LASSO tool was used to construct multivariate proportional risk regression models. Nine ferroptosis-associated lncRNAs were used for prognostic modelling. Risk values were calculated using the multivariable Cox regression formula: risk score = CFAP58 – DT (0.8267) + LINC00443 (0.2150) + EMSLR (0.0695) + HYI – AS1 (–0.6638) + ADIRF – AS1 (0.1993) + LINC02474 (0.0737) + CDKN2B – AS1 (0.9564) + LINC01629 (0.1711) + LINC00942 (0.0247). As shown in Figure 3(a), the predictive model indicated that the survival score was significantly lower in the high-risk group than in the low-risk group ( $P < 0.001$ ), demonstrating that HYI-AS1 may be a protective factor for UCEC. The other ferroptosis-related lncRNAs used in the model were overexpressed in the high-risk group and influenced the outcomes of UCEC patients. The age and tumor grade of patients with endometrial cancer were different between the low- and high-risk groups as illustrated in Figure 3(b). In addition, Figure 3(c) shows that the area under ROC curves for the 1-year, 3-year, and 5-year overall survival (OS) was 0.714, 0.689, and 0.745, respectively. The AUC of the built prognostic model was higher compared with that of other clinicopathological parameters as shown in Figure 3(c). To test the model's predictive power, a risk score was calculated for each patient. The distribution of ferroptosis-related lncRNAs and their expression levels are shown in Figure 3(d). We, therefore, conclude that high-risk UCEC patients have a shorter life expectancy than those with relatively low risk. Finally, coexpression of lncRNAs and ferroptosis-related genes used to construct the prognostic model is shown in Figure 3(e). LINC00942 was correlated with G6PD, SQSTM1, HMOX1, and AKR1C1, whereas CDKN2B-AS1 and LINC02474 were correlated with ATM.

**3.3. Correlation between Prognostic Model and Clinical Features.** Survival curves were plotted using the R software to analyze the association of the prognostic model with clinical features of UCEC (Figure 4(a)). Several genes such as CFAP58-DT (HR = 1.62, 95 percent CI = 1.07 – 2.44,  $P = 0.023$ ), EMSLR (HR = 1.70, 95 percent CI = 1.12 – 2.58,  $P = 0.012$ ), ADIRF-AS1 (HR = 1.67, 95 percent CI = 1.10 – 2.53,  $P = 0.016$ ), and CDKN2B-AS1 (HR = 1.63, 95 percent CI = 1.08 – 2.46,  $P = 0.021$ ) were found to be unfavorable predictive factors in UCEC. In contrast, HYI-AS1 (HR = 0.65, 95 percent CI = 0.43–0.99,  $P = 0.044$ ) was associated with favorable outcomes in UCEC patients. Survival curves for the remaining ferroptosis lncRNAs were not statistically significant. The predicted OS at 1, 3, and 5 years, column line plots for the risk classes, and clinical risk characteristics were established (Figure 4(b)). Finally, the R software was used to perform univariate and multivariate analysis for the ferroptosis-associated lncRNA (Table 2). In the univariate analysis, CFAP58-DT, EMSLR, ADIRF-AS1, CDKN2B-AS1, and HYI-AS1 were significantly differentially expressed in UCEC patients ( $P < 0.05$ ). High expression of CFAP58-DT, EMSLR, ADIRF-AS1, and CDKN2B-AS1 was correlated with clinical stage, age, histologic grade, OS event, and histological type of endometrial carcinoma (Table 3).

**3.4. GSEA Pathway Enrichment and PCA Analyses.** KEGG analysis of the prognostic model was performed using the GSEA software to explore pathways associated with low- and high-risk groups (Figure 5). The low-risk group showed low KEGG enrichment whereas the alpha linolenic acid metabolism, fatty acid metabolism, and glycan degradation were enriched in the KEGG analysis ( $P < 0.05$ ). The ferroptosis-associated lncRNA prediction model showed good ability to distinguish between high- and low-risk groups as determined by PCA (Figure 6).

**3.5. Differential Analysis of Lymphocytes, Immunological Function, and Immune Checkpoints, as well as Variable Assessment of m6A.** To investigate the association between prognostic models and tumor immunology, immune cells, immune function, and immunotherapy differential analysis related to the prognostic models were analyzed using the R software. The profile of immune cell infiltration in low- and high-risk groups was mapped using several datasets (Figure 7(a)). Enrichment of parainflammation and Type I IFN responses was higher in the high-risk group than in the low-risk group. In the low-risk group, the immunological function was more effective in T cell costimulation and Type II IFN Response (Figure 7(b)). Immune checkpoints found in immune cells regulate the activity of immune system. The high-risk group had relatively higher expression levels of CD80, ICOSLG, IDO2, and CD40. In comparison, TNFSF14, CD276, CD44, CTLA4, and TNFRSF4 were overexpressed in the low-risk group (Figure 7(c)). Furthermore, differential correlation analysis for m6A was performed for the prediction model. Seven m6A-related lncRNAs were found to be closely related to the UCEC outcomes. The expression of remaining m6A-associated lncRNAs was higher in the high-risk group whereas RAB11B-AS1



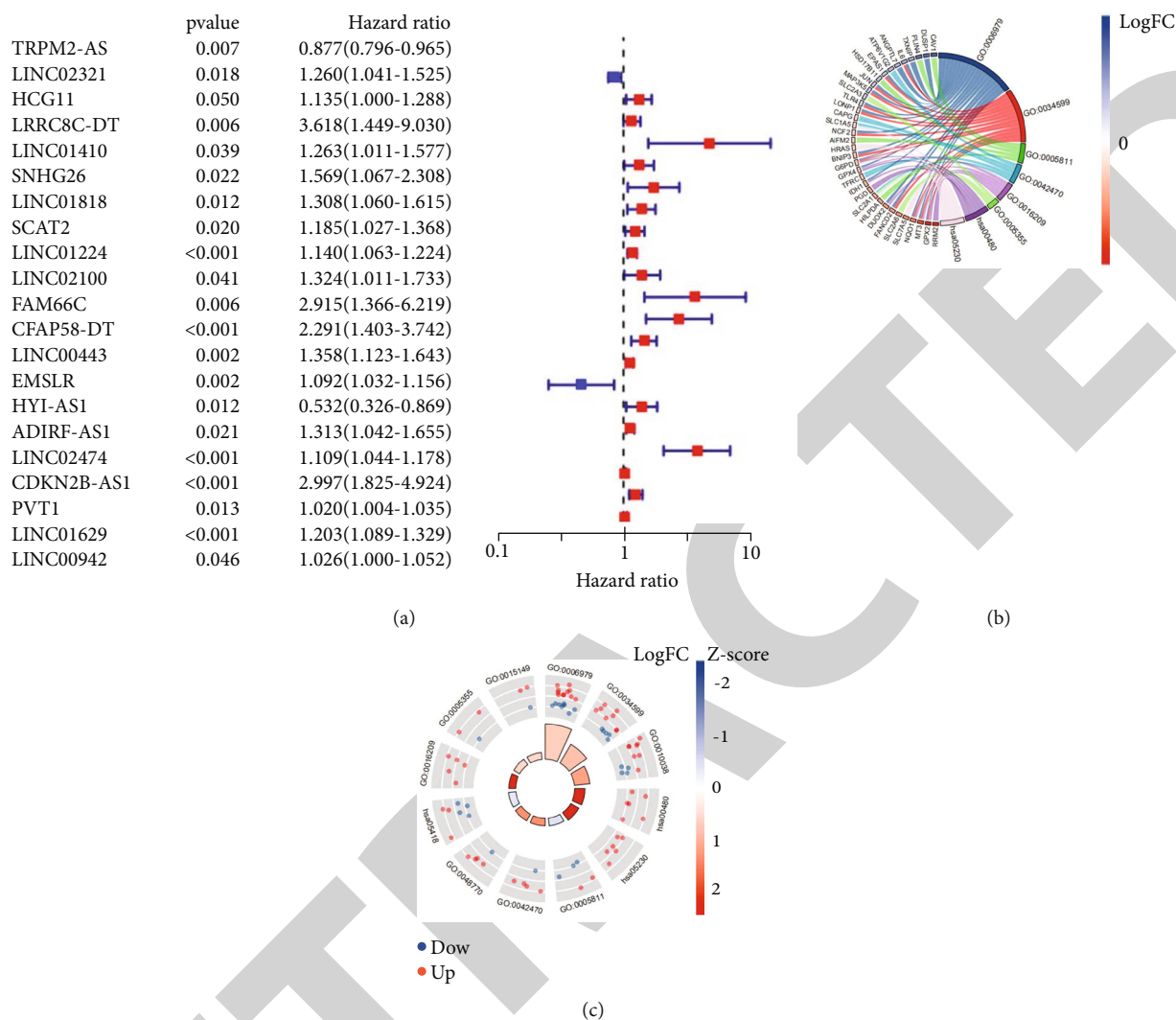


FIGURE 2: Identification of ferroptosis-related lncRNAs with prognostic significance of UCEC based on GO and KEGG assessment. (a) Forest plot of ferroptosis-related prognostic lncRNAs. (b) Chordal and (c) circle plots of GO and KEGG of ferroptosis-related lncRNAs in UCEC.

expression was overexpressed in the low-risk group (Figure 7(d)). RAB11B-AS1 is thought to be a protective factor on the survival of UCEC patients.

### 3.6. Drug Susceptibility Assessment for the Prediction Model.

Drug sensitivity assessment was performed on the developed prediction model to determine drugs with the potential to treat UCEC. The IC50 value, which is used to assess a drug's ability to induce apoptosis, was utilized to evaluate the model's sensitivity to potential medicines. The greater the induction, the lower the level and the more significant the therapeutic impact. The susceptibility of the high and low categories to 11 compounds differed significantly in predicting prospective treatment agents. For high-risk groups, nine compounds were found to have higher sensitivity compared with those in the low-risk group (Figure 8). Two compounds were more sensitive to the low-risk group than to the high-

risk group (Figure 8). These findings are expected to improve the clinician management of UCEC.

## 4. Discussion

EC, one of the three most prevalent malignancies in females, is characterized by angiogenesis, chronic inflammation, and immunogenicity and exhibits variable sensitivity to antiangiogenic drugs and immunotherapy. Studies have suggested that biomarkers and predictive models can improve targeted therapy and immunotherapy in cancer patients [4]. However, the development of a risk prediction model for UCEC remains challenging. According to recent findings, ferroptosis has been linked to several pathological conditions, including tumors, neurological conditions, ischemia-reperfusion impairment, renal damage, and hematological illnesses. Meanwhile, the expression of lncRNAs



TABLE 1: GO and KEGG pathway analyses of ferroptosis-related lncRNAs.

Ontology	ID	Description	P.adjust	Count
BP	GO:0006979	Response to oxidative stress	3.62E - 11	19
BP	GO:0034599	Cellular response to oxidative stress	3.18E - 07	13
BP	GO:0010038	Response to metal ion	2.19E - 05	12
BP	GO:0042594	Response to starvation	5.17E - 05	9
BP	GO:0031667	Response to nutrient levels	5.17E - 05	13
CC	GO:0005811	Lipid droplet	3.11E - 03	5
CC	GO:0042470	Melanosome	3.80E - 03	5
CC	GO:0048770	Pigment granule	3.80E - 03	5
CC	GO:0016323	Basolateral plasma membrane	9.85E - 03	6
CC	GO:0016324	Apical plasma membrane	4.19E - 02	6
MF	GO:0016209	Antioxidant activity	5.82E - 03	5
MF	GO:0005355	Glucose transmembrane transporter activity	5.82E - 03	3
MF	GO:0015149	Hexose transmembrane transporter activity	5.82E - 03	3
MF	GO:0008483	Transaminase activity	5.82E - 03	3
MF	GO:0015145	Monosaccharide transmembrane transporter activity	5.82E - 03	3
KEGG	hsa00480	Glutathione metabolism	6.41E - 04	6
KEGG	hsa05230	Central carbon metabolism in cancer	1.08E - 03	6
KEGG	hsa05418	Fluid shear stress and atherosclerosis	4.17E - 03	7
KEGG	hsa04115	p53 signaling pathway	6.11E - 03	5
KEGG	hsa01230	Biosynthesis of amino acids	6.11E - 03	5

affects the prognosis of various cancers and might be a promising biomarker for tumors. Considerable studies have constructed ferroptosis-related prognostic tumor models, including liver cancer [24] and head and neck tumors [25] models. However, whether FRLs are associated with UCEC outcomes is unknown. The present study sought to establish a predictive risk model for FRL in UCEC and investigate its interaction with tumor immunology and treatment response.

A total of 21 FRLs associated with UCEC prognosis were identified. LRRCBC-DT, FAM66C, CFAP58-DT, and CDKN2B-AS1 were risk factors for EC, whereas HY1-AS1 was a protective indicator for EC. Even though LRRCBC-DT and FAM66C were not included in the development of the FRL prognostic model, they may be risk factors for EC, which requires further investigation and validation. GO and KEGG analyses were used to evaluate differentially expressed FRLs in EC. GO analysis showed that FRLs were primarily enriched in oxidative stress response, cellular response to oxidative stress, and antioxidants. Ferroptosis, a form of regulated cell death characterized by the iron-dependent accumulation of lipid hydroperoxides, has been associated with tumorigenesis and response to therapy. Numerous oxidative and antioxidant mechanisms are thought to collaborate with autophagy and membrane repair processes to modify the lipid peroxidation process during ferroptosis [5]. Oxidative stress is a typical hallmark of cancer due to metabolic and signaling problems [26]. Excessive production of reactive oxygen species (ROS) can harm bio-

logical components such as DNA, proteins, and lipids. Furthermore, Kuang et al. found that the most common ferroptosis cofactors are antioxidant system blockers, which are critical to understanding the antioxidant properties of molecule networks that protect cells from ferroptosis-induced cellular damage [27]. Meanwhile, KEGG analysis revealed that FRLs were predominantly enriched in glutathione metabolism and p53 signal transduction. In ferroptosis, the glutathione reduction process is important because the concentration of iron-dependent lipid ROS outnumbers glutathione peroxidase 4 (GPX4) to convert lipid peroxide to lipid alcohols. Ferroptosis is characterized by impaired lipid peroxidation and lipid peroxidation recovery [28, 29]. Lycopene has also been demonstrated to stimulate ferroptosis in hepatocellular carcinoma (HCC) cells by altering the glutathione redox system produced by GPX4 [30]. Though p53 controls cell cycle arrest, senescence, and apoptosis as a negative regulator, recent data showed that it also controls ferroptosis as a repressor [31]. P53 decreased cystine absorption and rendered cells more susceptible to ferroptosis by downregulation of SLC7A11, a crucial component of the cystine/glutamate reversal transport mechanism [32].

Nine FRLs (CFAP58-DT, LINC00443, EMSLR, HY1-AS1, ADIRF-AS1, LINC02474, CDKN2B-AS1, LINC01629, and LINC00942) were screened from 21 prognosis-associated lncRNAs in UCEC via the LASSO regression analysis to construct a prognostic model. Subjects were divided into two groups based on their median risk scores. The built predictive model was validated by survival, hazard, and ROC curves. The

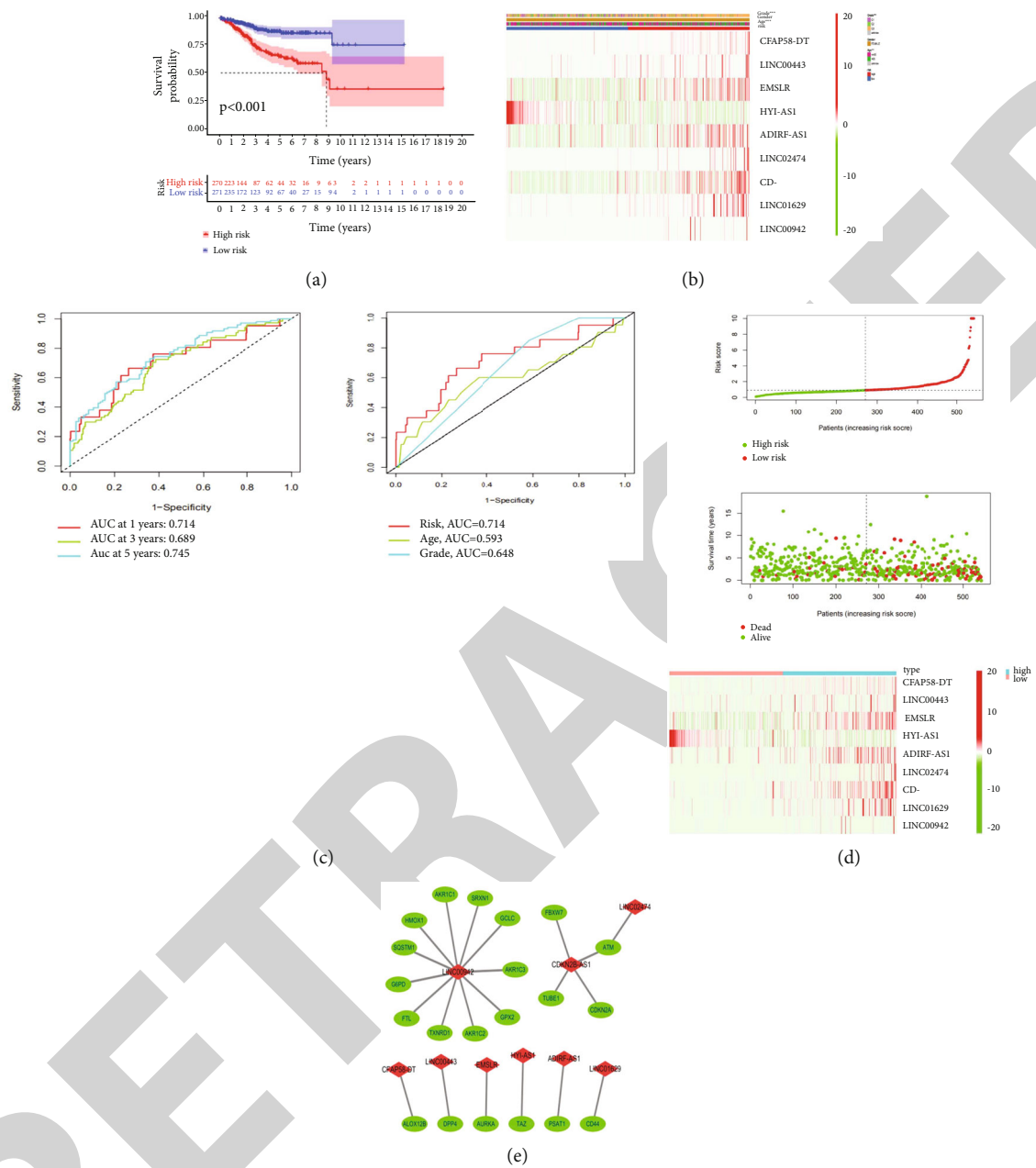


FIGURE 3: Prognosis prediction performance of the lncRNA-associated ferroptosis prognostic model. (a) Survival curves of ferroptosis-associated lncRNA prognostic models. (b) Heat map showing the clinical relevance of prognostic models based on ferroptosis-related lncRNA. (c) ROC diagnostic curves of the prognostic models. (d) Risk curves of the prognostic models. (e) Coexpression plots of lncRNA and ferroptosis-related genes included in the prognostic model.

interaction between FRLs and UCEC was further investigated using univariate and multivariate models. CFAP58-DT, EMSLR, ADIRF-AS1, and CDKN2B-AS1 were possible causes of EC, but HYI-AS1 was found to be a protective gene. The change in transcription was statistically significant ( $P < 0.05$ ). Kaplan–Meier survival curves showed no statistically significant differences in the remaining four lncRNAs, including LINC00443, LINC02474, LINC01629, and LINC00942, suggesting a little impact on EC prognosis. The influence of con-

founding factors, however, cannot be ruled out due to the limited sample size. Increased sample size and external experimental verification are required to assess the influence of these lncRNAs on EC prognosis [33]. CDKN2B-AS1 is a noncoding RNA that is overexpressed in several cancers, including hepatocellular carcinoma, colorectal carcinoma, cervical carcinoma, and ovarian carcinoma. CDKN2B-AS1, a protein involved in tumorigenesis, migration, invasion, and regulation of tumor cell apoptosis, is upregulated in HCC, is significantly associated

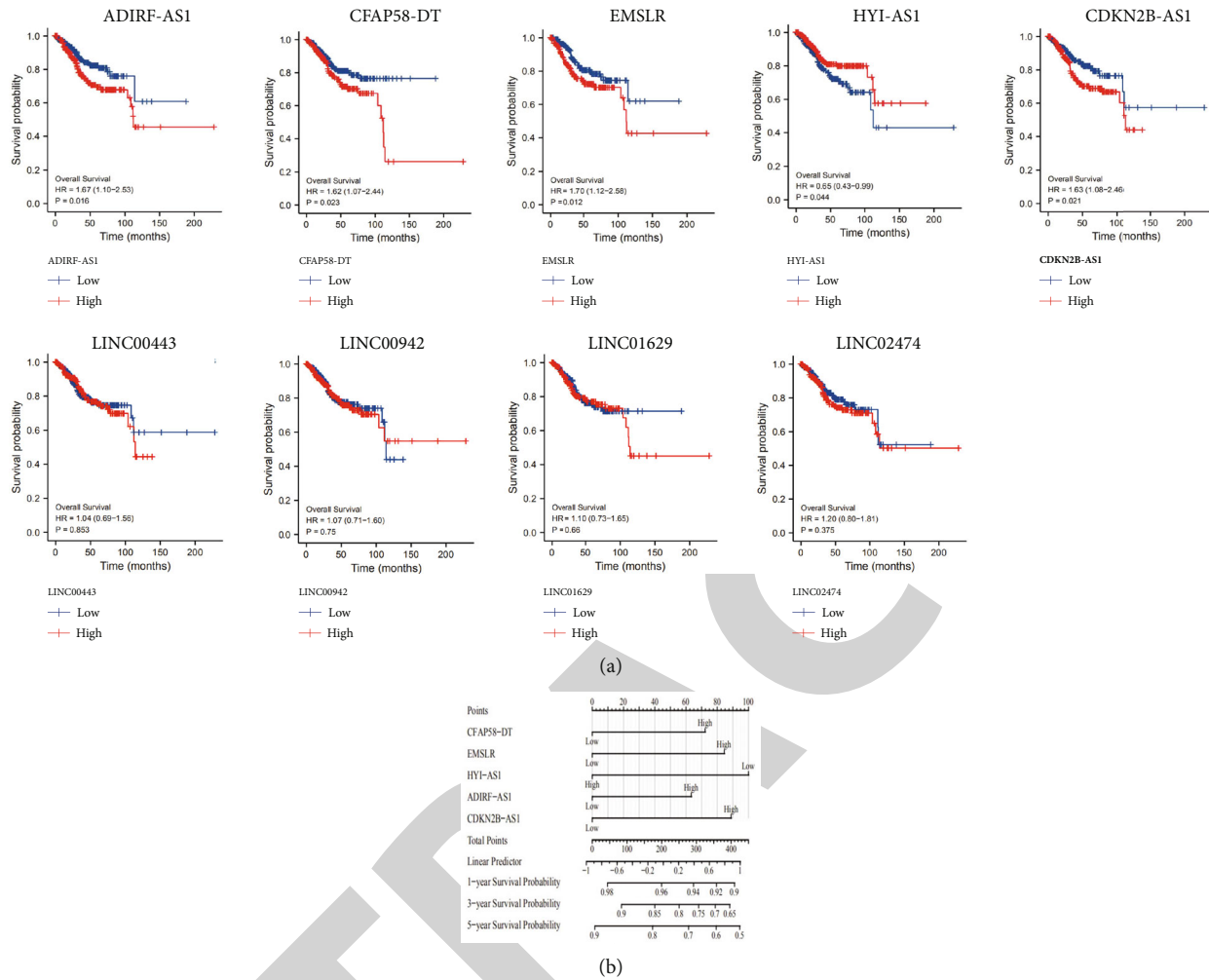


FIGURE 4: Survival curves and nomograms based on ferroptosis-associated lncRNAs. (a) Survival curves of ferroptosis-associated lncRNAs. (b) Nomogram plots of the ferroptosis-associated lncRNAs.

with the growth of the disease, and can be used as a potential treatment or predictive biomarker for the various human diseases. CDKN2B-AS1 knockdown inhibited the proliferation, migration, and invasion of HCC cells in vitro and induced their G1 phase arrest and apoptosis, whereas CDKN2B-AS1 silencing inhibited the growth and metastasis of HCC cells in vivo. CDKN2B-AS1 increased NAP1L1 transcription in HCC cells by adsorbing let-7c-5p, which activates the PI3K/AKT/mTOR activity [34]. Yang et al. observed that CDKN2B-AS1 knockdown inhibited endometrial carcinogenesis both in vivo and in vitro, and the tumor size was smaller in the CDKN2B-AS1 knockdown group than in the nonknockdown group [35]. The current study found that CDKN2B-AS1 is a potential risk for EC. The relationship between the remaining four lncRNAs (LINC00443, LINC02474, LINC01629, and LINC00942) in the predictive model and tumor progression has been established. Wang et al. found that LINC00942 was elevated in lung adenocarcinoma (LUAD) tissues and was associated with LUAD clinical outcomes [XYZ]. The LINC00942/miR-5006-5p/FZD1 pathway may be a therapeutic target for LUAD [36]. Furthermore, Du et al. reported that LINC02474 could affect colorectal cancer migration, invasion, and apoptosis by inhibit-

ing granzyme B transcription, which has been associated with poor outcomes and could be a potential predictor of colorectal cancer lifespan [37].

KEGG analysis was performed on the low-risk and high-risk groups in the predictive model using the GSEA method to investigate changes in the implicated pathways. Artesunate has been shown to inhibit the multiplication of sunitinib-resistant kidney cancerous cells by triggering cell cycle arrest and ferroptosis. The suppression of the proliferation of artesunate was accompanied by cell cycle blockade and modification of cell cycle molecules [38]. Hu et al. found that iron overload-induced ferroptosis disrupted meiosis and lowered the quality of pig oocytes potentially owing to enhanced oxidative stress, mitochondrial malfunction, and autophagy activation [39]. The low-risk group in the predictive model had fewer KEGG enrichment values. KEGG enrichment analysis showed that the low-risk group of the predictive model was enriched in fatty acid metabolism ( $P < 0.05$ ). Acyl-coenzyme with a long-chain A synthase 4 is also involved in fatty acid metabolism and has been recently shown to exert an oncogenic effect in LUAD by lowering tumor survival/invasion and promoting ferroptosis. A high-fat diet reduced ferroptosis in lung

TABLE 2: Univariate and multivariate analysis of lncRNA-related to ferroptosis.

Characteristics	Total (N)	HR (95% CI) univariate analysis	P value univariate analysis	HR (95% CI) multivariate analysis	P value multivariate analysis
CFAP58-DT	551				
Low	275	Reference			
High	276	1.617 (1.070-2.444)	<b>0.023</b>	1.385 (0.907-2.116)	0.131
LINC00443	551				
Low	276	Reference			
High	275	1.039 (0.693-1.557)	0.853		
EMSLR	551				
Low	276	Reference			
High	275	1.703 (1.125-2.577)	<b>0.012</b>	1.464 (0.935-2.293)	0.096
HY1-AS1	551				
Low	275	Reference			
High	276	0.654 (0.433-0.988)	<b>0.044</b>	0.637 (0.421-0.963)	<b>0.033</b>
ADIRF-AS1	551				
Low	275	Reference			
High	276	1.668 (1.099-2.532)	<b>0.016</b>	1.331 (0.844-2.099)	0.219
LINC02474	551				
Low	276	Reference			
High	275	1.202 (0.800-1.806)	0.375		
CDKN2B-AS1	551				
Low	275	Reference			
High	276	1.628 (1.078-2.461)	<b>0.021</b>	1.493 (0.977-2.281)	0.064
LINC01629	551				
Low	276	Reference			
High	275	1.096 (0.729-1.647)	0.660		
LINC00942	551				
Low	275	Reference			
High	276	1.068 (0.712-1.601)	0.750		

carcinoma by downregulating Acyl-CoA synthetase long-chain family member 4 A (CSL4) [40]. PCA 3D scatter plots showed that the developed FRL predictive model in the present study effectively distinguished between high-risk and low-risk groups.

Differential analysis of lymphocytes, immunological function, and immunological checkpoints in the predictive model was conducted using the R tool to investigate the relationship between the model and tumor immunology. EC has a substantial immunological cell invasion in the tumor immunological environment, with cancer-related fibroblasts, CD8<sup>+</sup> T cells, CD4<sup>+</sup> T cells, dendritic cells (DCs), regulatory T cells, tumor-linked macrophages, and monocytes among the lymphocytes. Recent studies have demonstrated that cancer-associated fibroblast-generated exosomes stimulate EC cell invasion more than exosomes derived from normal fibroblasts [41]. Teng et al. also demonstrated that cancer-associated fibroblast from EC cells stimulates EC proliferation in a paracrine or autocrine manner via the SDF-1/CXCR4 pathway [42]. CD8<sup>+</sup> T cells are key for immunological invasion in EC, and their numbers are higher in EC than in noncancerous tissues, but their cytotoxicity is lower. Tumor CD8<sup>+</sup> T cells displayed reduced granzyme A, granzyme B, and PD-1 levels

and lower cytotoxic killing [43]. DCs are a component of the tumor environment that capture tumor antigens and stimulate antigen-specific T lymphocytes. Several studies have reported DC invasion in endometrioid adenocarcinoma. S100- and HLA-DRY-positive DCs may help slow tumor growth and lymph node metastasis [44]. Antitumor immunological activity is suppressed by inhibitor T cells. T-regulatory cells are a type of cells that induces tumor immune tolerance in various cancers. Strauss et al. found that Treg-produced IL-10 and transforming growth factor YA1 may mediate immunosuppression in the tumor environment [45]. Tumor-associated macrophages are abundant in most types of malignant tumors. Tumor-associated macrophages are usually categorized into two subsets M1 and M2. The former produces pro-inflammatory factors and has significant microbicidal and tumor-killing action. However, the latter is immunosuppressive and produces large quantities of anti-inflammatory cytokines, including IL10 and TGF- $\beta$ . Macrophage concentration is predicted to be higher in EC than in benign endometrium due to the prevalence of M1 macrophages in the stroma of type 2 EC [46].

In terms of the immune system function, our study found that parainflammation and type I interferons (IFN) response

TABLE 3: Association of ferroptosis-related lncRNAs with UCEC clinical characteristics.

Characteristic	Low expression of CFAP58-DT	High expression of CFAP58-DT	P	Low expression of EMSLR	High expression of EMSLR	P	Low expression of ADIRF-ASI	High expression of ADIRF-ASI	P	Low expression of CDKN2B-ASI	High expression of CDKN2B-ASI	P
n	276	276		276	276		276	276		276	276	
Clinical stage, n (%)			0.201			<0.001			0.006			0.045
Stage I	182 (33%)	160 (29%)		197 (35.7%)	145 (26.3%)		191 (34.6%)	151 (27.4%)		186 (33.7%)	156 (28.3%)	
Stage II	25 (4.5%)	26 (4.7%)		17 (3.1%)	34 (6.2%)		22 (4%)	29 (5.3%)		25 (4.5%)	26 (4.7%)	
Stage III	58 (10.5%)	72 (13%)		56 (10.1%)	74 (13.4%)		51 (9.2%)	79 (14.3%)		54 (9.8%)	76 (13.8%)	
Stage IV	11 (2%)	18 (3.3%)		6 (1.1%)	23 (4.2%)		12 (2.2%)	17 (3.1%)		11 (2%)	18 (3.3%)	
Age, n (%)			<0.001			0.007			<0.001			<0.001
≤60	123 (22.4%)	83 (15.1%)		119 (21.7%)	87 (15.8%)		123 (22.4%)	83 (15.1%)		132 (24%)	74 (13.5%)	
>60	151 (27.5%)	192 (35%)		156 (28.4%)	187 (34.1%)		151 (27.5%)	192 (35%)		141 (25.7%)	202 (36.8%)	
Histologic grade, n (%)			<0.001			<0.001			<0.001			<0.001
G1	66 (12.2%)	32 (5.9%)		75 (13.9%)	23 (4.3%)		60 (11.1%)	38 (7%)		47 (8.7%)	51 (9.4%)	
G2	73 (13.5%)	47 (8.7%)		80 (14.8%)	40 (7.4%)		78 (14.4%)	42 (7.8%)		81 (15%)	39 (7.2%)	
G3	129 (23.8%)	194 (35.9%)		118 (21.8%)	205 (37.9%)		135 (25%)	188 (34.8%)		145 (26.8%)	178 (32.9%)	
OS event, n (%)			0.054			0.031			0.017			0.054
Alive	238 (43.1%)	220 (39.9%)		239 (43.3%)	219 (39.7%)		240 (43.5%)	218 (39.5%)		238 (43.1%)	220 (39.9%)	
Dead	38 (6.9%)	56 (10.1%)		37 (6.7%)	57 (10.3%)		36 (6.5%)	58 (10.5%)		38 (6.9%)	56 (10.1%)	
Histological type, n (%)			0.024			<0.001			<0.001			<0.001
Endometrioid	219 (39.7%)	191 (34.6%)		234 (42.4%)	176 (31.9%)		246 (44.6%)	164 (29.7%)		249 (45.1%)	161 (29.2%)	
Mixed	10 (1.8%)	14 (2.5%)		10 (1.8%)	14 (2.5%)		7 (1.3%)	17 (3.1%)		5 (0.9%)	19 (3.4%)	
Serous	47 (8.5%)	71 (12.9%)		32 (5.8%)	86 (15.6%)		23 (4.2%)	95 (17.2%)		22 (4%)	96 (17.4%)	
Age, median (IQR)	61 (56, 70.75)	65 (60, 72)	0.003	62 (56, 70)	65 (58, 73)	0.004	63 (55, 71)	64 (60, 72)	0.004	62 (54, 69)	66 (60, 72)	<0.001



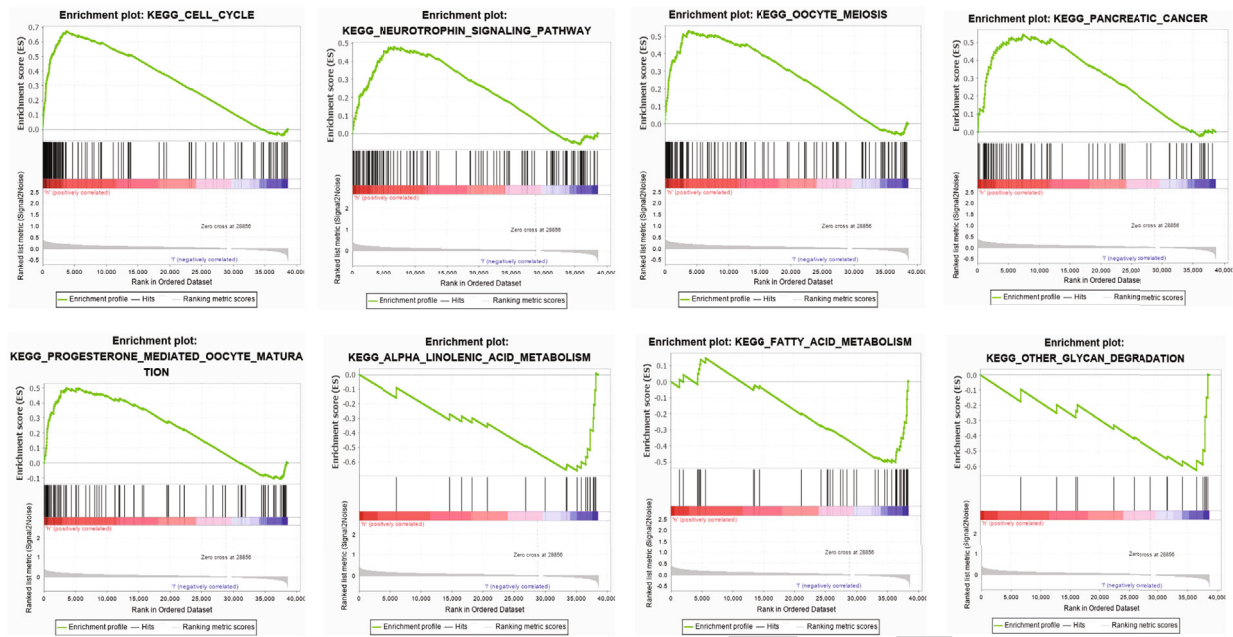


FIGURE 5: GSEA pathway enrichment analysis for the prognostic model.

were more prevalent in the high-risk group than in the low-risk group. T cell costimulation and type II IFN response were considerably more prominent in the low-risk group. Previous studies demonstrated that tumor parainflammation is a low-grade inflammatory process that is common in human cancers, particularly those with p53 mutations, suggesting that tumor parainflammation could be used as a screening marker and clinical indication for nonsteroidal anti-inflammatory drugs (NSAIDs) for cancer therapies [47]. Jacquilot et al. found a connection between type I IFN signaling upregulation and immunotherapy resistance in melanoma patients. IFN receptor- (IFNAR-) induced nitric oxide synthase-2 expression was a PD-1 blockade sustained anticancer, a critical negative regulator of efficacy, which acted at the tumor cell and leucocyte levels [48]. This is consistent with our findings that type I IFN pathway induction was more effective in the high-risk group, presumably matching patient resistance to immunotherapy. Conversely, T cell costimulation was more prevalent in the low-risk group. This could be because cytomegalovirus in the high-risk group inhibits ICOSL transcription on antigen-presenting cells, inhibiting T lymphocyte costimulation, thereby resulting in immunological resistance [49].

TNFSF14 (LIGHT), CD276 (B7-H3), CD44, CTLA4, and TNFRSF4 (OX40) were enormously elevated in the low-risk group, whereas CD80, ICOSLG, IDO2, and CD40 were dramatically improved in the high-risk group. CD80 and CD40 expression on DCs in normal endometrium was higher than on tumor invading DCs in endometrioid adenocarcinoma [50], suggesting a strong variation in CD80 and CD40 transcription in EC compared with normal endometrium. Brunner et al. reported that patients with severe lesions and type II carcinoma expressed substantially more B7-H3 than those with low-grade and endometrioid tumors [51], which is inconsistent with our findings that CD276 was expressed in the low-risk group. B7-H3 transcription may be absent in more aggressive and less

differentiated cancers. Many cancers overexpress CD44, a cellular glycoprotein and adhesion molecule, and its attachment to the cellular surface governs tumor growth [52]. Elbasateeny et al. found that CD44 expression tended to decrease with increasing aggressiveness and progression of EC, and downregulation of CD44 may suggest a more aggressive process and may be associated with carcinosarcomas with poor prognosis [53]. These findings support the theory that CD44 is deleted in more invasive tumors. OX40 is a cancer immunological checkpoint whose presence indicates a favorable prognosis and is a promising target for developing novel immunotherapies. OX40 agonist treatment has been implemented to enhance lifespan in glioblastoma mice and reduce tumorigenesis in ovarian carcinoma [54, 55]. In a subcutaneous mouse model of breast cancer, Dai et al. found that LIGHT caused tumor cell death, enhanced T lymphocyte invasion, and triggered systemic antitumor immune function, making it a promising drug for cancer immunotherapy [56]. Our predictive model was also subjected to an m6A differential analysis. RAB11B-AS1 was discovered to be overexpressed in the low-risk group. However, other m6A-associated lncRNAs were significantly increased in the high-risk group, implying that RAB11B-AS1 may be a protective indicator for outcomes of UCEC patients.

Drug sensitivity analysis was carried out on the constructed prognostic model to predict potential drugs for UCEC treatment. There was significant variation in susceptibility for 11 drugs between the low-risk and high-risk groups. The nine FRLs rendered the high-risk group more vulnerable than the low-risk group. Akt activity is upregulated in most tumors and plays a vital role in creating the malignant phenotype by increasing cell proliferation and lowering apoptosis. Inhibition of Akt could be beneficial for the treatment of cancer. A-443654 and other effective and selective Akt inhibitors reduce Akt-dependent signaling in vitro and in vivo in a dose-dependent manner. Akt inhibitors diminish tumor

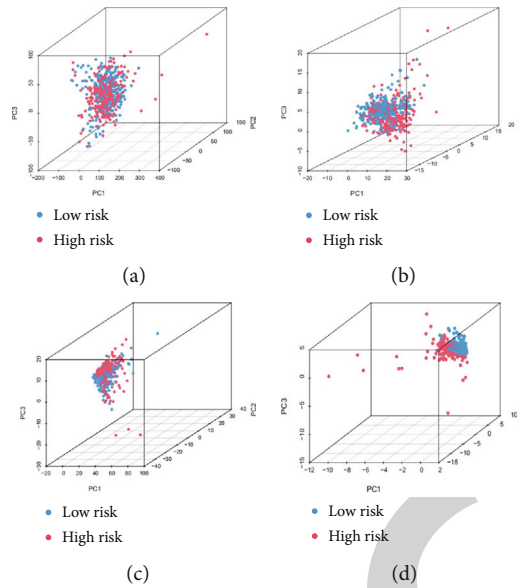


FIGURE 6: PCA for the high- and low-risk groups. (a) PCA for all genes. (b) PCA for ferroptosis genes. (c) PCA for ferroptosis-associated lncRNAs. (d) PCA for ferroptosis-associated lncRNAs included in the prognostic models.

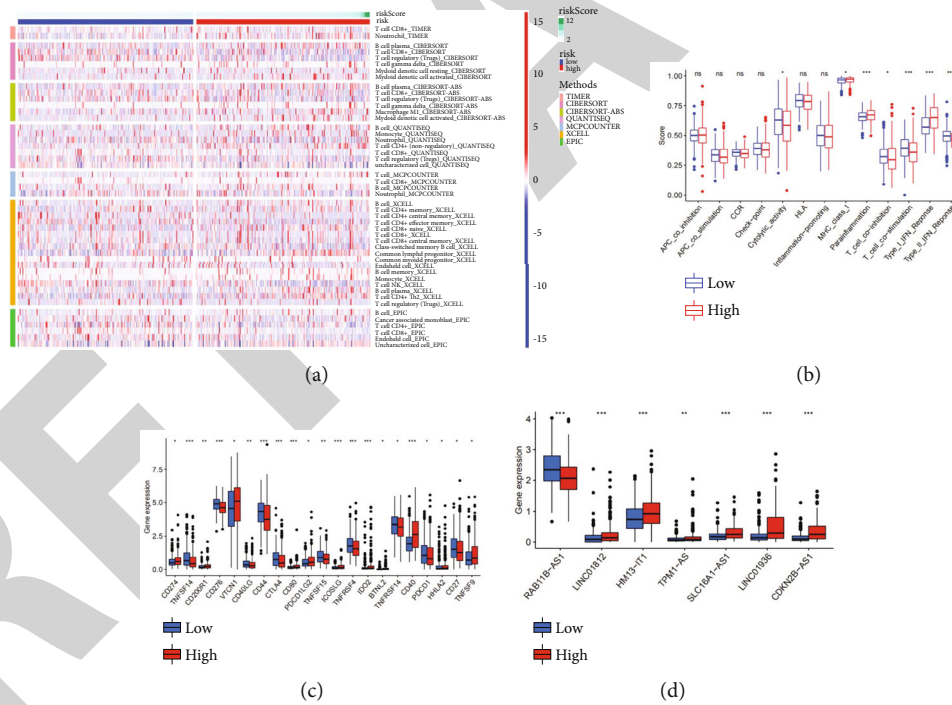


FIGURE 7: Immunological characteristics and differential analysis of m6A. (a) Correlation of immune cells with ferroptosis-associated lncRNA prognostic models. (b) Variable assessment of immunological function in prognostic models. (c) Variable assessment of immunological checkpoints in the prognostic model. (d) Differential analysis of m6A in the prognostic models.

formation when used alone or in conjunction with paclitaxel or rapamycin in vivo [57]. Duan et al. demonstrated that A-770041, a strong blocker of Src family enzymes, could reverse osteosarcoma cell resistance to paclitaxel and adriamycin [58]. ABT-263, a novel oral Bcl-2 blocker that boosts anticancer effects in vitro by reducing the apoptosis threshold, has been shown to have cytotoxic activity against tumor cell lines that

upregulates Bcl-2, such as small cell lung carcinoma and leukemia/lymphoma [59]. The PARP antagonist ABT.888 is quite efficient. EC, glioblastoma, malignant melanoma, prostate carcinoma, and breast carcinoma patients with reduced phosphatase and tensin homolog transcription may benefit from PARP suppression [60]. Zhang et al. found that xenatide prevented the development of Ishikawa xenografts in

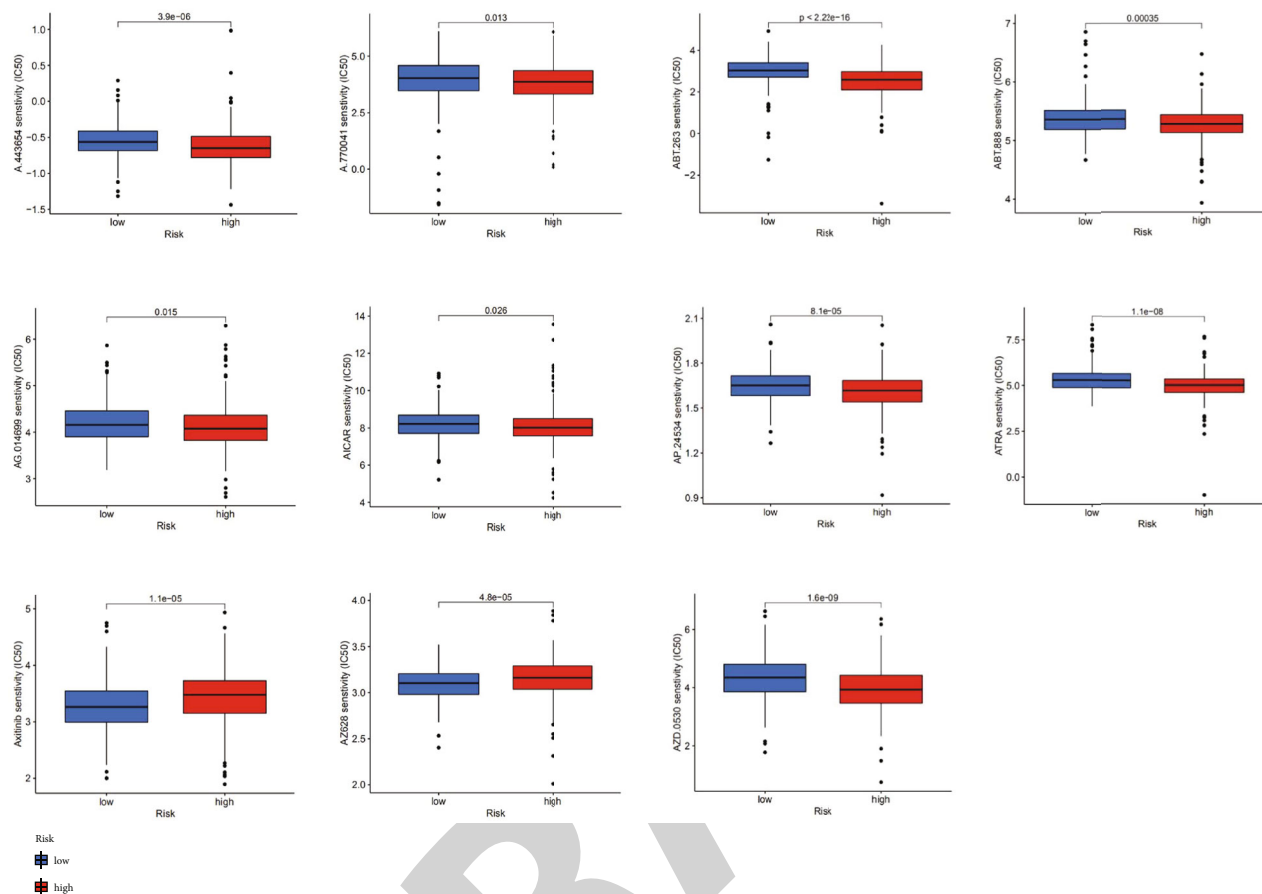


FIGURE 8: Drug susceptibility assessment for the prediction model.

nude mice with EC, and AMPK could be the subject of such a mechanism. According to the results, exenatide plus AICAR (AMPK activator) increased apoptosis and produced more cleaved caspase-3 than exendin-4 alone [61]. ECs are associated with abnormal fibroblast growth factor receptor 2 (FGFR2) mutational stimulation. AP24534 (ponatinib), an oral multitargeted blocker now in clinical trials, suppresses the growth, migration, and infiltration of FGFR2-mutated EC cells. It causes apoptosis by arresting the cell cycle in the G1/S phase [62]. Recent studies showed that retinoic acid (RA) has anti-cancer properties, including the suppression of cell proliferation and invasion in EC cells [63]. Because all-trans-retinoic acid (ATRA) is an analog of RA, it could be used to treat EC.

However, this study has several limitations. First, in vitro and in vivo studies are employed to explain the biological mechanisms and physiological actions of FRLs. Second, a relationship between FRLs and tumor-infiltrating lymphocytes was observed. Thirdly, bias may exist in case inclusion and data processing in retrospective studies. Future studies using clinical samples and external experimental data validation are needed.

### 5. Conclusions

In summary, a predictive model based on nine FRLs (CFAP58-DT, LINC00443, EMSLR, HYI-AS1, ADIRF-AS1, LINC02474, CDKN2B-AS1, LINC01629, and LINC00942)

was developed and validated using bioinformatics analysis. High levels of CFAP58-DT, EMSLR, ADIRF-AS1, and CDKN2B-AS1 were risk factors for EC, whereas HYI-AS1 was a protective factor. These findings suggest that ferroptosis has a mechanistic function in altering the immunological milieu and therapeutic response in EC.

### Abbreviations

- UCEC: Uterine corpus endometrial carcinoma
- EC: Endometrial carcinoma
- TCGA: The Cancer Genome Atlas
- OS: Overall survival
- GO: Gene Ontology
- KEGG: Kyoto Encyclopedia of Genes and Genomes
- GSEA: Gene set enrichment analysis

### Data Availability

The data that support the findings of this study are openly available in TCGA database at <https://portal.gdc.cancer.gov/>.

### Conflicts of Interest

The authors declared no potential conflicts of interest with respect to the research, authorship, and/or publication of this article.

## Authors' Contributions

Writing—original manuscript preparation—was done by ZX; conceptualizing was done by ZX and ZH; material curation and deep analysis were done by ZH and ZX; and writing—review and editing—was done by DH, ZJ, and HH. All contributors have reviewed and approved the completed version of the article.

## Acknowledgments

The Discipline Construction Promoting Project of Shanghai Pudong Hospital (project no.Tszb2020-07 and project no.Zdzk2020-16) and the Scientific Research Foundation provided by Pudong Hospital affiliated to Fudan University (YJ2019-16) supported this research, and we thank TCGA platform for providing useful resources.

## References

- [1] M. E. Urlick and D. W. Bell, "Clinical actionability of molecular targets in endometrial cancer," *Nature Reviews Cancer*, vol. 19, no. 9, pp. 510–521, 2019.
- [2] E. Steiner, O. Eicher, J. Sagemüller et al., "Multivariate independent prognostic factors in endometrial carcinoma: a clinicopathologic study in 181 patients: 10 years experience at the Department of Obstetrics and Gynecology of the Mainz University," *International Journal of Gynecological Cancer*, vol. 13, no. 2, pp. 197–203, 2003.
- [3] R. A. Brooks, G. F. Fleming, R. R. Lastra et al., "Current recommendations and recent progress in endometrial cancer," *CA: a Cancer Journal for Clinicians*, vol. 69, no. 4, pp. 258–279, 2019.
- [4] A. Argentiero, A. G. Solimando, M. Krebs et al., "Anti-angiogenesis and immunotherapy: novel paradigms to envision tailored approaches in renal cell-carcinoma," *Journal of Clinical Medicine*, vol. 9, no. 5, p. 1594, 2020.
- [5] X. Chen, R. Kang, G. Kroemer, and D. Tang, "Broadening horizons: the role of ferroptosis in cancer," *Nature Reviews Clinical Oncology*, vol. 18, no. 5, pp. 280–296, 2021.
- [6] L. Galluzzi, I. Vitale, S. A. Aaronson et al., "Molecular mechanisms of cell death: recommendations of the nomenclature committee on cell death 2018," *Cell Death & Differentiation*, vol. 25, no. 3, pp. 486–541, 2018.
- [7] D. Tang, R. Kang, T. V. Berghe, P. Vandenabeele, and G. Kroemer, "The molecular machinery of regulated cell death," *Cell Research*, vol. 29, no. 5, pp. 347–364, 2019.
- [8] D. Tang and G. Kroemer, "Ferroptosis," *Current Biology*, vol. 30, no. 21, pp. R1292–R1297, 2020.
- [9] J. Li, F. Cao, H. L. Yin et al., "Ferroptosis: past, present and future," *Cell Death & Disease*, vol. 11, no. 2, p. 88, 2020.
- [10] L. L. Sun, D. L. Linghu, and M. C. Hung, "Ferroptosis: a promising target for cancer immunotherapy," *American Journal of Cancer Research*, vol. 11, no. 12, pp. 5856–5863, 2021.
- [11] R. P. Alexander, G. Fang, J. Rozowsky, M. Snyder, and M. B. Gerstein, "Annotating non-coding regions of the genome," *Nature Reviews Genetics*, vol. 11, no. 8, pp. 559–571, 2010.
- [12] M. Esteller, "Non-coding RNAs in human disease," *Nature Reviews Genetics*, vol. 12, no. 12, pp. 861–874, 2011.
- [13] S. Djebali, C. A. Davis, A. Merkel et al., "Landscape of transcription in human cells," *Nature*, vol. 489, no. 7414, pp. 101–108, 2012.
- [14] A. E. Kornienko, P. M. Guenzl, D. P. Barlow, and F. M. Pauler, "Gene regulation by the act of long non-coding RNA transcription," *BMC Biology*, vol. 11, no. 1, p. 59, 2013.
- [15] S. Serghiou, A. Kyriakopoulou, and J. P. Ioannidis, "Long non-coding RNAs as novel predictors of survival in human cancer: a systematic review and meta-analysis," *Molecular Cancer*, vol. 15, no. 1, p. 50, 2016.
- [16] M. Wang, C. Mao, L. Ouyang et al., "Long noncoding RNA LINC00336 inhibits ferroptosis in lung cancer by functioning as a competing endogenous RNA," *Cell Death & Differentiation*, vol. 26, no. 11, pp. 2329–2343, 2019.
- [17] J. Liu, T. Lichtenberg, K. A. Hoadley et al., "An integrated TCGA pan-cancer clinical data resource to drive high-quality survival outcome analytics," *Cell*, vol. 173, no. 2, pp. 400–416.e11, 2018.
- [18] N. Zhou and J. Bao, "FerrDb: a manually curated resource for regulators and markers of ferroptosis and ferroptosis-disease associations," *Database*, vol. 2020, article baaa021, 2020.
- [19] M. E. Ritchie, B. Phipson, D. Wu et al., "limma powers differential expression analyses for RNA-sequencing and microarray studies," *Nucleic Acids Research*, vol. 43, no. 7, article e47, 2015.
- [20] S. P. Walker, "The ROC curve redefined - optimizing sensitivity (and specificity) to the lived reality of cancer," *The New England Journal of Medicine*, vol. 380, no. 17, pp. 1594–1595, 2019.
- [21] R. Saito, M. E. Smoot, K. Ono et al., "A travel guide to Cytoscape plugins," *Nature Methods*, vol. 9, no. 11, pp. 1069–1076, 2012.
- [22] S. Hänzelmann, R. Castelo, and J. Guinney, "GSVA: gene set variation analysis for microarray and RNA-seq data," *BMC Bioinformatics*, vol. 14, no. 1, p. 7, 2013.
- [23] E. Rahmani, N. Zaitlen, Y. Baran et al., "Sparse PCA corrects for cell type heterogeneity in epigenome-wide association studies," *Nature Methods*, vol. 13, no. 5, pp. 443–445, 2016.
- [24] B. Tang, J. Zhu, J. Li et al., "The ferroptosis and iron-metabolism signature robustly predicts clinical diagnosis, prognosis and immune microenvironment for hepatocellular carcinoma," *Cell Communication and Signaling*, vol. 18, no. 1, p. 174, 2020.
- [25] Y. Xu, M. Hong, D. Kong, J. Deng, Z. Zhong, and J. Liang, "Ferroptosis-associated DNA methylation signature predicts overall survival in patients with head and neck squamous cell carcinoma," *BMC Genomics*, vol. 23, no. 1, p. 63, 2022.
- [26] G. Y. Liou and P. Storz, "Reactive oxygen species in cancer," *Free Radical Research*, vol. 44, no. 5, pp. 479–496, 2010.
- [27] F. Kuang, J. Liu, D. Tang, and R. Kang, "Oxidative damage and antioxidant defense in ferroptosis," *Frontiers in Cell and Development Biology*, vol. 8, article 586578, 2020.
- [28] Y. Zou, M. J. Palte, A. A. Deik et al., "A GPX4-dependent cancer cell state underlies the clear-cell morphology and confers sensitivity to ferroptosis," *Nature Communications*, vol. 10, no. 1, p. 1617, 2019.
- [29] H. Zhu, A. Santo, Z. Jia, and Y. Robert Li, "GPx4 in bacterial infection and Polymicrobial sepsis: involvement of ferroptosis



- and pyroptosis," *Reactive Oxygen Species*, vol. 7, no. 21, pp. 154–160, 2019.
- [30] M. Jin, C. Shi, T. Li, Y. Wu, C. Hu, and G. Huang, "Solasonine promotes ferroptosis of hepatoma carcinoma cells via glutathione peroxidase 4-induced destruction of the glutathione redox system," *Biomedicine & Pharmacotherapy*, vol. 129, article 110282, 2020.
- [31] J. Liu, C. Zhang, J. Wang, W. Hu, and Z. Feng, "The regulation of ferroptosis by tumor suppressor p53 and its pathway," *International Journal of Molecular Sciences*, vol. 21, no. 21, p. 8387, 2020.
- [32] L. Jiang, N. Kon, T. Li et al., "Ferroptosis as a p53-mediated activity during tumour suppression," *Nature*, vol. 520, no. 7545, pp. 57–62, 2015.
- [33] C. Song, Y. Qi, J. Zhang, C. Guo, and C. Yuan, "CDKN2B-AS1: an indispensable long non-coding RNA in multiple diseases," *Current Pharmaceutical Design*, vol. 26, no. 41, pp. 5335–5346, 2020.
- [34] Y. Huang, B. Xiang, Y. Liu, Y. Wang, and H. Kan, "lncRNA CDKN2B-AS1 promotes tumor growth and metastasis of human hepatocellular carcinoma by targeting let-7c-5p/NAP1L1 axis," *Cancer Letters*, vol. 437, pp. 56–66, 2018.
- [35] D. Yang, J. Ma, and X. X. Ma, "CDKN2B-AS1 promotes malignancy as a novel prognosis-related molecular marker in the endometrial cancer immune microenvironment," *Frontiers in Cell and Developmental Biology*, vol. 9, article 721676, 2021.
- [36] R. Wang, X. Wang, J. Zhang, and Y. Liu, "LINC00942 promotes tumor proliferation and metastasis in lung adenocarcinoma via FZD1 upregulation," *Technology in Cancer Research & Treatment*, vol. 20, 2021.
- [37] T. Du, Q. Gao, Y. Zhao et al., "Long non-coding RNA LINC02474 affects metastasis and apoptosis of colorectal cancer by inhibiting the expression of GZMB," *Frontiers in Oncology*, vol. 11, article 651796, 2021.
- [38] S. D. Markowitsch, P. Schupp, J. Lauckner et al., "Artesunate inhibits growth of sunitinib-resistant renal cell carcinoma cells through cell cycle arrest and induction of Ferroptosis," *Cancers*, vol. 12, no. 11, p. 3150, 2020.
- [39] W. Hu, Y. Zhang, D. Wang et al., "Iron overload-induced ferroptosis impairs porcine oocyte maturation and subsequent embryonic developmental competence in vitro," *Frontiers in Cell and Developmental Biology*, vol. 9, article 673291, 2021.
- [40] Y. Zhang, S. Li, F. Li, C. Lv, and Q. K. Yang, "High-fat diet impairs ferroptosis and promotes cancer invasiveness via downregulating tumor suppressor ACSL4 in lung adenocarcinoma," *Biology Direct*, vol. 16, no. 1, p. 10, 2021.
- [41] B. L. Li, W. Lu, J. J. Qu, L. Ye, G. Q. du, and X. P. Wan, "Loss of exosomal miR-148b from cancer-associated fibroblasts promotes endometrial cancer cell invasion and cancer metastasis," *Journal of Cellular Physiology*, vol. 234, no. 3, pp. 2943–2953, 2019.
- [42] F. Teng, W.-Y. Tian, Y.-M. Wang et al., "Cancer-associated fibroblasts promote the progression of endometrial cancer via the SDF-1/CXCR4 axis," *Journal of Hematology & Oncology*, vol. 9, no. 1, 2016.
- [43] M. V. Patel, Z. Shen, M. Rodriguez-Garcia, E. J. Usherwood, L. J. Tafe, and C. R. Wira, "Endometrial cancer suppresses CD8+ T cell-mediated cytotoxicity in postmenopausal women," *Frontiers in Immunology*, vol. 12, article 657326, 2021.
- [44] Z. Lijun, Z. Xin, S. Danhua et al., "Tumor-infiltrating dendritic cells may be used as clinicopathologic prognostic factors in endometrial carcinoma," *International Journal of Gynecological Cancer*, vol. 22, no. 5, pp. 836–841, 2012.
- [45] L. Strauss, C. Bergmann, M. Szczepanski, W. Gooding, J. T. Johnson, and T. L. Whiteside, "A unique subset of CD4<sup>+</sup>CD25<sup>high</sup>Foxp3<sup>+</sup> T cells secreting interleukin-10 and transforming growth factor- $\beta$ 1 Mediates Suppression in the tumor microenvironment," *Clinical Cancer Research*, vol. 13, 15, Part 1, pp. 4345–4354, 2007.
- [46] M. G. Kelly, A. M. Francisco, A. Cimic et al., "Type 2 endometrial cancer is associated with a high density of tumor-associated macrophages in the stromal compartment," *Reproductive Sciences*, vol. 22, no. 8, pp. 948–953, 2015.
- [47] D. Aran, A. Lasry, A. Zinger et al., "Widespread parainflammation in human cancer," *Genome Biology*, vol. 17, no. 1, p. 145, 2016.
- [48] N. Jacquelot, T. Yamazaki, M. P. Roberti et al., "Sustained type I interferon signaling as a mechanism of resistance to PD-1 blockade," *Cell Research*, vol. 29, no. 10, pp. 846–861, 2019.
- [49] G. Angulo, J. Zeleznjak, P. Martínez-Vicente et al., "Cytomegalovirus restricts ICOSL expression on antigen-presenting cells disabling T cell co-stimulation and contributing to immune evasion," *eLife*, vol. 10, article e59350, 2021.
- [50] J. Jia, Z. Wang, X. Li, Z. Wang, and X. Wang, "Morphological characteristics and co-stimulatory molecule (CD80, CD86, CD40) expression in tumor infiltrating dendritic cells in human endometrioid adenocarcinoma," *European Journal of Obstetrics, Gynecology, and Reproductive Biology*, vol. 160, no. 2, pp. 223–227, 2012.
- [51] A. Brunner, S. Hinterholzer, P. Riss, G. Heinze, and H. Brustmann, "Immunoexpression of B7-H3 in endometrial cancer: relation to tumor T-cell infiltration and prognosis," *Gynecologic Oncology*, vol. 124, no. 1, pp. 105–111, 2012.
- [52] L. Wang, X. Zuo, K. Xie, and D. Wei, "The role of CD44 and cancer stem cells," in *Methods in Molecular Biology*, pp. 31–42, Humana Press, New York, NY, 2018.
- [53] S. S. Elbasateeny, A. A. Salem, W. A. Abdelsalam, and R. A. Salem, "Immunohistochemical expression of cancer stem cell related markers CD44 and CD133 in endometrial cancer," *Pathology, Research and Practice*, vol. 212, no. 1, pp. 10–16, 2016.
- [54] N. Jahan, H. Talat, and W. T. Curry, "Agonist OX40 immunotherapy improves survival in glioma-bearing mice and is complementary with vaccination with irradiated GM-CSF-expressing tumor cells," *Neuro-Oncology*, vol. 20, no. 1, pp. 44–54, 2018.
- [55] Z. Guo, X. Wang, D. Cheng, Z. Xia, M. Luan, and S. Zhang, "PD-1 blockade and OX40 triggering synergistically protects against tumor growth in a murine model of ovarian cancer," *PLoS One*, vol. 9, no. 2, article e89350, 2014.
- [56] S. Dai, Y. Lv, W. Xu et al., "Oncolytic adenovirus encoding LIGHT (TNFSF14) inhibits tumor growth via activating anti-tumor immune responses in 4T1 mouse mammary tumor model in immune competent syngeneic mice," *Cancer Gene Therapy*, vol. 27, no. 12, pp. 923–933, 2020.
- [57] Y. Luo, A. R. Shoemaker, X. Liu et al., "Potent and selective inhibitors of Akt kinases slow the progress of tumors in vivo," *Molecular Cancer Therapeutics*, vol. 4, no. 6, pp. 977–986, 2005.



## Retraction

# Retracted: Dapagliflozin Improves Diabetic Cardiomyopathy by Modulating the Akt/mTOR Signaling Pathway

### BioMed Research International

Received 20 June 2023; Accepted 20 June 2023; Published 21 June 2023

Copyright © 2023 BioMed Research International. This is an open access article distributed under the Creative Commons Attribution License, which permits unrestricted use, distribution, and reproduction in any medium, provided the original work is properly cited.

This article has been retracted by Hindawi following an investigation undertaken by the publisher [1]. This investigation has uncovered evidence of one or more of the following indicators of systematic manipulation of the publication process:

- (1) Discrepancies in scope
- (2) Discrepancies in the description of the research reported
- (3) Discrepancies between the availability of data and the research described
- (4) Inappropriate citations
- (5) Incoherent, meaningless and/or irrelevant content included in the article
- (6) Peer-review manipulation

The presence of these indicators undermines our confidence in the integrity of the article's content and we cannot, therefore, vouch for its reliability. Please note that this notice is intended solely to alert readers that the content of this article is unreliable. We have not investigated whether authors were aware of or involved in the systematic manipulation of the publication process.

Wiley and Hindawi regrets that the usual quality checks did not identify these issues before publication and have since put additional measures in place to safeguard research integrity.

We wish to credit our own Research Integrity and Research Publishing teams and anonymous and named external researchers and research integrity experts for contributing to this investigation.

The corresponding author, as the representative of all authors, has been given the opportunity to register their agreement or disagreement to this retraction. We have kept a record of any response received.

### References

- [1] M. Ren, D. Pan, D. Zha, and Z. Shan, "Dapagliflozin Improves Diabetic Cardiomyopathy by Modulating the Akt/mTOR Signaling Pathway," *BioMed Research International*, vol. 2022, Article ID 9687345, 10 pages, 2022.

## Research Article

# Dapagliflozin Improves Diabetic Cardiomyopathy by Modulating the Akt/mTOR Signaling Pathway

Mengxiang Ren,<sup>1</sup> Dabin Pan ,<sup>1</sup> Dayong Zha,<sup>2</sup> and Zeyang Shan<sup>3</sup>

<sup>1</sup>Department of Cardiology, Yijishan Hospital, Wannan Medical College, Anhui Province, China 241001

<sup>2</sup>Department of Cardiology, Wuhu Second People's Hospital, Anhui Province, China 241001

<sup>3</sup>Department of Cardiology, Bengbu Second People's Hospital, Anhui Province, China 233000

Correspondence should be addressed to Dabin Pan; [pandabiny12022@hotmail.com](mailto:pandabiny12022@hotmail.com)

Received 20 April 2022; Revised 22 June 2022; Accepted 27 June 2022; Published 26 July 2022

Academic Editor: Dinesh Rokaya

Copyright © 2022 Mengxiang Ren et al. This is an open access article distributed under the Creative Commons Attribution License, which permits unrestricted use, distribution, and reproduction in any medium, provided the original work is properly cited.

**Background.** Dapagliflozin can significantly improve heart failure, and Cx43 is one of the molecular mechanisms of heart failure. This study investigated the effect of dapagliflozin on Cx43 and Akt/mTOR signaling pathway in ventricular myocytes. **Methods.** A rat model of type 2 diabetes mellitus was established by high-fat diet combined with streptozotocin, and the animals were treated randomly with dapagliflozin. The morphological changes of the myocardium were observed by hematoxylin eosin staining, and the expression and distribution of Cx43 in ventricular myocytes were detected by immunohistochemistry. And Western blot determined the expressions of Cx43, Akt, mTOR, p62, and LC3 proteins in rat myocardium. **Results.** Compared with the normal control group, the heart rate of diabetic rats decreased significantly ( $p < 0.05$ ), QRS wave of ECG widened, and QT interval prolonged ( $p < 0.05$ ). Dapagliflozin treatment in diabetic rats resulted in improvements in these ECG indexes ( $p < 0.05$ ) with early administration group obtaining greater efficacy than the late administration group ( $p < 0.05$ ). In the normal control group, the cardiomyocytes were arranged orderly, and the expression of Cx43 was dense, uniform, and regular, which was higher than that in the intercalated disc. In the diabetic control model group, the cardiomyocytes were enlarged and presented disorderly with detection of Cx43 in the cytoplasm. Early use of dapagliflozin better improved these myocardial tissue lesions. Of note, as diabetic rats exhibited decreased expression of Cx43, Akt, and mTOR ( $p < 0.05$ ), increased p62 expression ( $p < 0.05$ ), and decreased LC3-II/I ratio ( $p < 0.05$ ), administration of dapagliflozin partially reversed the expression of the above proteins ( $p < 0.05$ ) with greater improvement in the early administration group compared with the late administration group ( $p < 0.05$ ). **Conclusions.** Dapagliflozin increases the expression of Cx43 in cardiomyocytes of diabetic rats and thereby alleviates heart failure partly through regulating the Akt/mTOR signaling pathway.

## 1. Introduction

Dapagliflozin is a new oral hypoglycemic drug and an inhibitor of sodium-glucose cotransporter 2 (SGLT2) to reduce the reabsorption of glucose by the kidney and promote the excretion of glucose in urine by inhibiting SGLT2 in the kidney [1]. In recent years, studies have depicted its cardioprotective effect, apart from good hypoglycemic effect [2, 3].

For patients with heart failure and a reduced ejection fraction (HFrEF), regardless of the presence or absence of diabetes, administration of dapagliflozin significantly decreases the

risk of worsening heart failure or death from cardiovascular [4–6]. Without obvious side effects on these patients [6], dapagliflozin shortens hospitalization for heart failure in patients with and without HFrEF [7].

Gap junctions have a wide range of physiological functions and play a key role in excitatory and nonexcitatory tissues. Connexin (Cx) is one of the most important proteins of cardiac gap junction. Cx43 is the most important transmembrane aqueous channel connexin expressed in ventricular muscle as it forms an ion channel between cardiomyocytes and maintains the conduction of electrical signals between

cardiomyocytes. Its normal expression and distribution are an important guarantee for normal electrical activity and coordination of cardiac diastolic and systolic functions [8].

Cx43 mRNA and protein are significantly downregulated in left ventricular in patients with end-stage heart failure caused by ischemic cardiomyopathy and idiopathic dilated cardiomyopathy. Congestive heart failure is associated with a significant decrease in the level of Cx43, the main gap junction protein in the left ventricle, which may lead to the enhancement of arrhythmia and systolic dysfunction [9].

Diabetic cardiomyopathy (DCM) is initially described as a human pathophysiological condition of heart failure without coronary heart disease, hypertension, and valvular heart disease. Of note, recent studies in animal models of diabetes have found that declined myocardial cell function is an important mediating mechanism for heart failure [10]. Changes in Cx43 content and distribution possibly contribute to alterations in cardiac function [11], while its expression in cardiomyocytes is closely related to the Akt/mTOR signaling pathway, an important pathway involved in oncogenesis and the cellular processes of metabolism [12]. Studies have found that dapagliflozin can affect autophagy through the Akt/mTOR signaling pathway [13, 14].

Low-after-high glucose promotes cardiomyocyte H9c2 cell autophagy through PI3K/Akt/mTOR and MEK/ERK1/2 signaling pathways, thereby downregulating Cx43. Chloroquine inhibited autophagy and reversed the downregulation of Cx43. U0126 inhibited ERK activation and decreased autophagy protein expression, but increased Cx43 expression, indicating that Cx43 expression is closely related to autophagy, and the mechanism is related to PI3K/Akt/mTOR and MEK/ERK1/2 signaling pathways [15]. As such, when the primary vascular smooth muscle cell (VSMC) is stimulated with ox-LDL, inhibiting Cx43 may activate VSMC autophagy to inhibit foam cell formation by inhibiting the PI3K/AKT/mTOR signaling pathway [16].

Dapagliflozin can significantly improve cardiac function, but whether it has an effect on the expression of Cx43 in cardiomyocytes remains elusive. In this study, we investigated the effects of dapagliflozin on Cx43 expression and Cx43-related Akt/mTOR signaling pathway in cardiomyocytes of type 2 diabetic rats.

## 2. Methods and Materials

**2.1. Materials.** Specific pathogen-free (SPF) grade 4-week-old (70-80 g) male SD rats were purchased from Hunan Changsha Tianqin Biotechnology Co., Ltd. Common feed, high-fat feed, and streptozotocin (STZ) were all obtained from Beijing Boai Port Biotechnology Co., Ltd. Cx43 antibody (#AF0137), mTOR antibody (#AF6308), AKT antibody (#AF6261), GAPDH antibody (#T0004),  $\beta$ -actin antibody (#AF7018), LC3 antibody (#AF5402), p62 antibody (#AF5384), goat anti-rabbit IgG (#S0001), and goat anti-mouse IgG (#S0002) were all purchased from Affinity Biosciences (Affinity Biosciences Milwaukee, WI 53224, America). Dapagliflozin was provided by AstraZeneca Pharmaceutical Co., Ltd.

**2.2. Animal Procedure and Drug Administration.** The experimental procedure was reviewed and approved by the experimental animal welfare and ethics committee of Wannan Medical College (LLSC-2020-144). Rats were housed in the SPF-grade animal room of Wannan Medical College.

The animals were randomly divided into two groups: normal groups and model group. Type 2 diabetes mellitus (T2DM) model was established by feeding with high-fat diet first for 4 weeks and then one-time lower left abdominal intraperitoneal injection of 35 mg/kg STZ. One week later, a random blood glucose measurement  $> 16.7$  mmol/L indicated successful establishment of diabetes models. The control group was fed a normal diet for 4 weeks and then received injection of the same amount of citric acid buffer.

The control group was randomly divided into normal control group (group A,  $n = 10$ ) and normal administration group (group B,  $n = 10$ ). The diabetic model group was randomly split into diabetic control group (group C,  $n = 10$ ), early administration group (group D,  $n = 10$ ), and late administration group (group E,  $n = 10$ ). After modeling, group B and group D began administration with dapagliflozin 1 mg/kg/day via gavage, and the other groups were gavaged with the same amount of normal saline. After 8 weeks, group E began to receive dapagliflozin 1 mg/kg/day via gavage, when the treatment of the other groups remained unchanged until the end of the animal experiment.

**2.3. General Phenotypes and Electrocardiogram (ECG) Observation.** During feeding, an electronic balance (Shanghai Minqiao Scientific Instrument Company, China) and blood glucose meter (ACCU-CHEK, Roche, USA) were used to monitor the weight and blood glucose of the rats in each group every week, and their mental state, diet, and urine output were observed and recorded. After 16 weeks, under anesthesia with sodium pentobarbital (Beyotime, China) at a dose of 40 mg/kg, after supine fixation of the limbs, a needle was inserted into the subcutaneous layer of the rats and connected to an RM6240E multichannel physiological signal acquisition and processing system (Chengdu Instrument Factory, China); the electrocardiogram (ECG) was recorded, and the heart rate, QRS wave width, and QT interval data of the rats in each group were measured three times with the average values taken.

**2.4. Assay of NT-Pro-Brain Natriuretic Peptide (NT-proBNP, BNP).** After establishment of the diabetic model, the BNP content in the blood of all rats was determined in strict accordance with the instructions of the ELISA Kit (Shanghai Enzyme-Linked Biotechnology Co., Ltd). We set 6 standard wells and 2 blank wells, and the rest of the wells were used as sample wells to be tested. 50  $\mu$ L standard of 6 concentration gradients was added to the standard wells, 40  $\mu$ L diluents and 10  $\mu$ L plasma supernatant of rats in normal control group and diabetes model group to each sample well in sequence, and 50  $\mu$ L diluent to the blank wells. After that, the ELISA plate was shaken slowly, and 100  $\mu$ L of enzyme labeled reagent was added into the sample holes and standard holes rather than the blank hole. Then, after the ELISA plate was completely sealed with sealing film, it was

incubated in the incubator at 37°C for 60 min. After incubation, the sealing film was torn off and the liquid in the hole was poured out. We added 300-200  $\mu\text{L}$  of washing solution and then poured it out three times and pat the liquid in the hole as dry as possible on the clean filter paper. Then, 50  $\mu\text{L}$  reagent A ( $\text{H}_2\text{O}_2$ ) and 50  $\mu\text{L}$  reagent B (R&D, DY999) were added into each hole in turn. The ELISA plate was shaken slowly and then sealed with the plate sealing film, covered with tin foil paper, and placed in the incubator for 20 min. Then, 50  $\mu\text{L}$  of termination liquid was added into each hole. When the liquid changes from blue to yellow, this step should be completed quickly. We used the microplate reader to detect the OD value, which were zeroes according to the value of the blank hole, and measured the absorbance at the wavelength of 450 nm of each hole, that is, the OD value of each hole. The data were processed by ELISA Calc software, and the concentration of BNP in each hole was calculated according to the standard curve of the standard.

**2.5. Detection of Serum Lipid Levels.** Blood sample was collected from the rat abdominal aorta and centrifuged at 4000 rpm for 10 minutes. The supernatant was transferred to a 2 mL EP tube and stored at -20°C. Plasma concentrations of total cholesterol (TC), triglycerides (TGs), low-density lipoprotein cholesterol (LDL-C), and high-density lipoprotein cholesterol (HDL-C) were detected by an automatic biochemical analyzer (Nanjing Ono Medical Equipment Co., Ltd., China).

**2.6. Hematoxylin and Eosin (HE) Staining and Immunohistochemistry.** After euthanasia, each rat's heart was removed and washed with normal saline, and the water was removed with filter paper. Partial ventricular muscle tissues were retained and fixed in EP tubes filled with paraformaldehyde for one week. These tissues were dehydrated, embedded in paraffin, sliced at a thickness of 5  $\mu\text{m}$ , dewaxed, dehydrated, and sealed. Morphological changes in the myocardium were observed with HE staining.

Dehydrated and dewaxed glass slides were sealed with 3%  $\text{H}_2\text{O}_2$  at room temperature for 10 minutes and subjected to antigen retrieval. After rewarming, the slides were incubated with the primary antibodies (Cx43) 4°C overnight and then with the corresponding secondary antibodies for 30 minutes at room temperature. After the slides were incubated in streptavidin-biotin complex, the reaction was carried out at 37°C for 20 minutes. The slides were restained with hematoxylin, sealed with glycerol, and observed under a microscope.

**2.7. Western Blot Analysis.** The ventricular tissue (100 mg) was cut, and total protein samples were extracted from the tissues according to the instructions of the total protein extraction kit (Beyotime, China). With protein concentration detection, the proteins were separated by 8%, 10%, and 12% sodium dodecyl sulfate polyacrylamide gel electrophoresis and transferred to PVDF membranes (Beyotime, China). After being blocked for 2 hours with 5% skimmed milk powder, the membranes were washed and incubated in the primary antibody (Akt, mTOR, Cx43, LC3, and p62)

working solution and shaken overnight at 4°C. After being washed, the membranes were probed with the corresponding secondary antibodies (GAPDH,  $\beta$ -Actin) at room temperature for 2 hours. According to the reagent instruction manual, the membranes were treated with a developer (Affinity, USA) and visualized on a Tanon-5500 cold CCD fluorescence image analysis system (Tanon, China). Each detection was repeated at least 3 times for protein quantification. The density of the signal was quantified with ImageJ (version 1.8.0).

**2.8. Statistical Analysis.** SPSS 21.0 (SPSS, Inc., Chicago, IL, USA) was used for statistical analysis. The measurement data are expressed as the mean  $\pm$  standard deviation ( $\bar{x} \pm s$ ). The means between multiple groups were compared by one-way analysis of variance (ANOVA), and the comparison between two groups was performed with the least significant difference (LSD) test. The inspection level was set at  $\alpha = 0.05$ , and  $p < 0.05$  indicated statistical significance.

### 3. Results

**3.1. Serum NT-proBNP (BNP) Levels in Normal Control Rats and Diabetes Rats.** The serum BNP concentration in the diabetic control group was significantly higher than that in the normal control group ( $41.07 \pm 11.18$  vs.  $531.33 \pm 41.68$ ,  $p < 0.01$ ).

**3.2. General Phenotypes of Rats, Changes in Body Weight and Blood Glucose, and Blood Lipid Levels.** The rats in the diabetic model group were generally in poor condition and bad mental state with slow response, polydipsia, polyuria, weight loss, and cataract compared with those in the control group. Before modeling, the weights of rats in each group increased steadily with no significant difference in their weights between groups. After modeling, the weight of the rats in the model group decreased while the weight in the normal control group increased most heavily, and the weight in the normal administration group was lower than that in the normal control group ( $p < 0.05$ ). As diabetic rats exhibited increased blood glucose levels, early or late administration of dapagliflozin noticeably decreased the levels significantly ( $p < 0.05$ ). There was no significant difference in blood glucose between the normal control group and the normal administration group ( $p > 0.05$ ), but the blood glucose in the early administration group was lower than that in the late administration group ( $p < 0.05$ ). Apart from blood glucose, the model group had elevated blood lipid concentration compared with the normal control group ( $p < 0.05$ ), and the concentration in the normal administration group decreased ( $p < 0.05$ ). The elevated lipid levels in the diabetic rats were decreased by early or late treatment with dapagliflozin ( $p < 0.05$ ), but there was no significant difference between the two model administration groups ( $p > 0.05$ ). See Table 1 and Figure 1.

**3.3. Electrocardiogram and Its Related Parameters in Rats.** As shown in Table 2, the heart rate of rats in the diabetic model group decreased significantly ( $p < 0.05$ ), while the rate was restored in the presence of dapagliflozin and early administration of the drug resulted in greater increase in heart rate



TABLE 1: Weight, blood glucose, and blood lipids of rats at the end of the experiment.

	A (n = 10)	B (n = 10)	C (n = 10)	D (n = 10)	E (n = 10)
Body weight (g)	443.02 ± 14.97	375.56 ± 10.54*	260.39 ± 23.98*	317.31 ± 14.25**	347.08 ± 13.18**
Blood glucose (mmol/L)	3.84 ± 0.43	4.07 ± 0.43 <sup>&amp;</sup>	28.71 ± 2.81*	5.69 ± 0.86**	9.24 ± 1.07** <sup>@</sup>
TC (mg/dL)	1.34 ± 0.13	1.07 ± 0.10*	6.28 ± 0.77*	4.08 ± 0.26**	4.23 ± 0.19**
TG (mg/dL)	0.84 ± 0.11	0.68 ± 0.04*	2.40 ± 0.26*	1.08 ± 0.18**	1.62 ± 0.18**
LDL-C (mg/dL)	0.28 ± 0.04	0.23 ± 0.04*	1.09 ± 0.16*	0.46 ± 0.07**	0.52 ± 0.09**
HDL-C (mg/dL)	0.91 ± 0.09	0.87 ± 0.09*	1.38 ± 0.19*	0.64 ± 0.08**	0.57 ± 0.08**

A: normal control group; B: normal administration group; C: diabetes control group; D: early administration group; E: late administration group; TC: total cholesterol; TG: triglyceride; HDL-C: high-density lipoprotein; LDL-C: low-density lipoprotein. \* $p < 0.05$  vs. A; \*\* $p < 0.05$  vs. C; <sup>&</sup> $p > 0.05$  vs. A; <sup>@</sup> $p < 0.05$  vs. D.

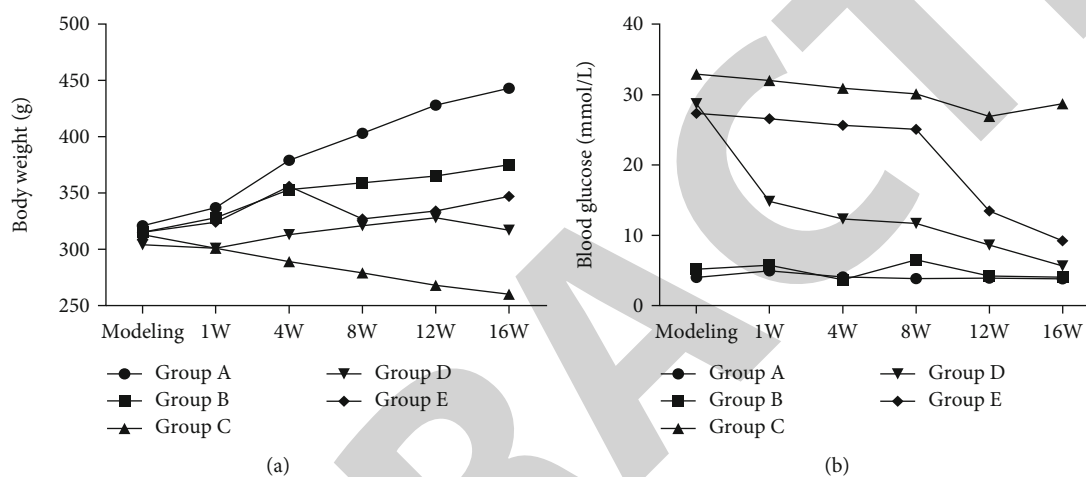


FIGURE 1: Changes in (a) body weight and (b) blood sugar in rats.

TABLE 2: Electrocardiogram indexes of rats in each group.

	A (n = 10)	B (n = 10)	C (n = 10)	D (n = 10)	E (n = 10)
Heart rate (bpm)	381.40 ± 12.14	366.50 ± 6.47	187.88 ± 11.80*	345.75 ± 15.37**	323.11 ± 12.60** <sup>&amp;</sup>
QRS wave (ms)	36.82 ± 0.13	37.39 ± 0.32	73.53 ± 2.56*	37.17 ± 0.87 <sup>#</sup>	40.75 ± 0.33** <sup>&amp;</sup>
QT interval (ms)	57.29 ± 0.13	58.70 ± 1.04	107.27 ± 5.75*	58.78 ± 0.12 <sup>#</sup>	65.45 ± 0.52** <sup>&amp;</sup>

A: normal control group; B: normal administration group; C: diabetes control group; D: early administration group; E: late administration group. \* $p < 0.05$  vs. A; <sup>#</sup> $p < 0.05$  vs. C; <sup>&</sup> $p < 0.05$  vs. D.

( $p < 0.05$ ). The rats in the diabetic control group had ventricular premature beats and ventricular tachycardia, which were not found in other groups. The QRS wave was widened, and QT interval was prolonged in diabetic control rats ( $p < 0.05$ ). These parameters were shortened in the early administration group and the late administration group, especially early administration group where QRS wave and QT interval declined dramatically compared with in the diabetic control group and the late administration group ( $p < 0.05$ ).

**3.4. HE Staining Results of Myocardial Tissue.** The HE results showed that cardiomyocytes in the normal control group were arranged orderly and evenly, myocardial nucleus and cytoplasm were stained clearly, and there was no obvious myocardial fibrosis. There was no significant difference in these characteristics between the normal administration

group and the normal control group. In the diabetic control group, myocardial cells were arranged in disorder with increased myocardial interstitial fibers and myocardial cell fibrosis. These disorders were greatly alleviated by early administration of dapagliflozin rather than later administration. In the late administration group, we still found disordered arrangement of cardiomyocytes and obvious cellular edema and fibrosis. See Figure 2.

**3.5. Cx43 Expression (Immunohistochemical and Western Blot).** Immunohistochemical staining showed that cardiomyocytes were arranged orderly in the normal control group, identifying dense and regular expression of Cx43 mainly in the intercalated disc of myocardium. Dapagliflozin rarely altered these features in the control group with no significant difference between the normal administration group



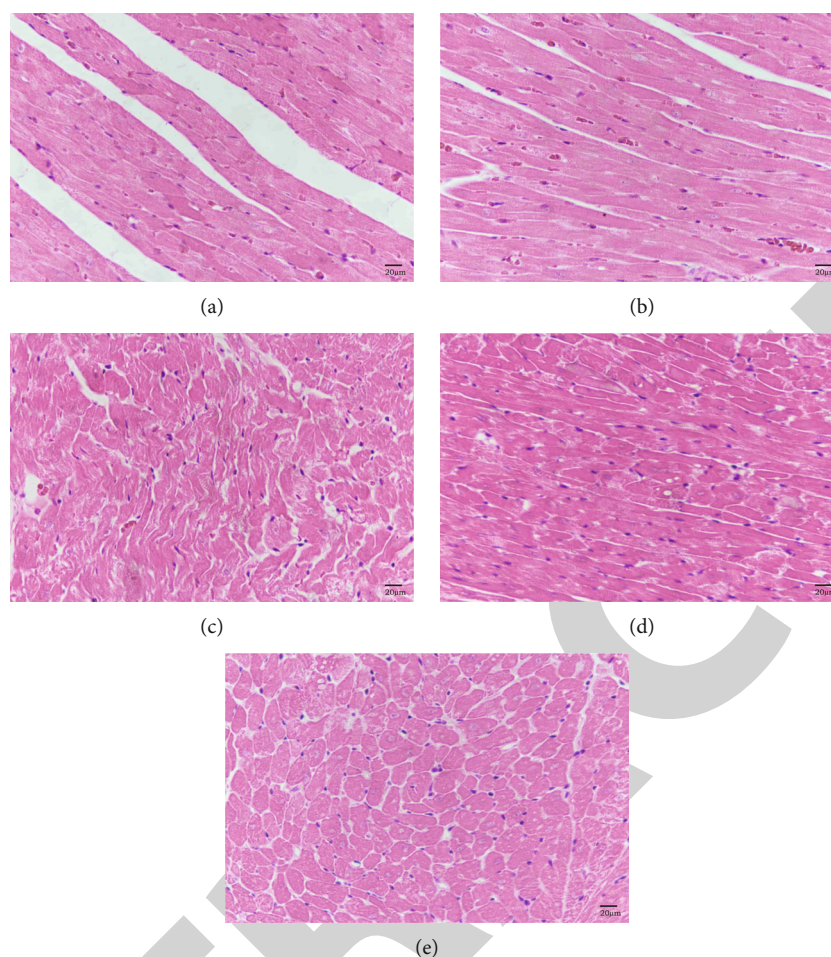


FIGURE 2: HE staining of rat hearts in each group ( $\times 400$ ); (a) normal control group, (b) normal administration group, (c) diabetes control group, (d) early administration group, and (e) late administration group.

and the normal control group. In the diabetic control group, the myocardial cells were enlarged and disordered, and the expression of Cx43 was dispersed in the cytoplasm of the myocardium. Importantly, early dapagliflozin treatment greatly restored the myocardial cell arrangement and gathered the expression of Cx43 to the irrigation area, which was similar to that in the normal control group. The expression level of Cx43 in myocardial cells of the late administration group was higher than that of the model group, but lower than that of the control group.

There was no significant difference in Cx43 protein expression between the normal control group and the normal administration group ( $p > 0.05$ ). The expression level of Cx43 protein in ventricular myocytes decreased significantly in diabetic rats relative to healthy ones ( $p < 0.05$ ), and the expression was improved significantly by the treatment of dapagliflozin ( $p < 0.05$ ), with higher expression of Cx43 in the early administration group ( $p < 0.05$ ). See Figure 3.

**3.6. mTOR Protein Expression.** Injection of dapagliflozin did not cause a significant change in the expression of mTOR in the healthy rats ( $p > 0.05$ ). The mTOR expression was significantly decreased in the diabetic group relative to the normal group ( $p < 0.05$ ). Compared with the diabetic rats, the expres-

sion level of mTOR in the early and late administration groups increased significantly ( $p < 0.05$ ) with the higher level in the early administration group ( $p < 0.05$ ). See Figure 4.

**3.7. p62 Protein Expression.** There was no significant difference in protein expression of p62 between the normal control group and the normal administration group ( $p > 0.05$ ), but compared with these two groups, the level of p62 protein in the diabetic control group increased significantly ( $p < 0.05$ ). Moreover, early or late administration of dapagliflozin dramatically decreased the level of p62 protein ( $p < 0.05$ ), with early treatment exhibiting more significantly inhibitory effect ( $p < 0.05$ ). See Figure 5.

**3.8. Akt Protein Expression.** Compared with the normal control group, there was no significant change in the expression of Akt protein in the normal administration group ( $p > 0.05$ ), but the expression level of Akt protein was significantly inhibited in the diabetic control group ( $p < 0.05$ ). Compared with the diabetic control group, the early administration group and the late administration group had higher protein expression of Akt increased significantly ( $p < 0.05$ ). See Figure 6.

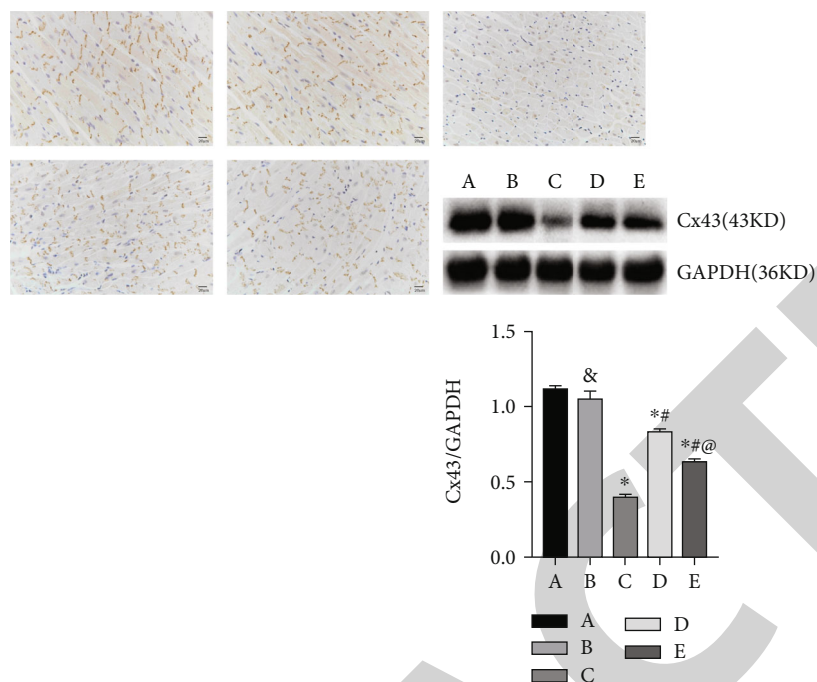


FIGURE 3: Immunohistochemical staining for Cx43 ( $\times 400$ ): A: normal control group, B: normal administration group, C: diabetes control group, D: early administration group, and E: late administration group. \* $p < 0.05$  vs. A; & $p > 0.05$  vs. A; # $p < 0.05$  vs. C; @ $p < 0.05$  vs. D.

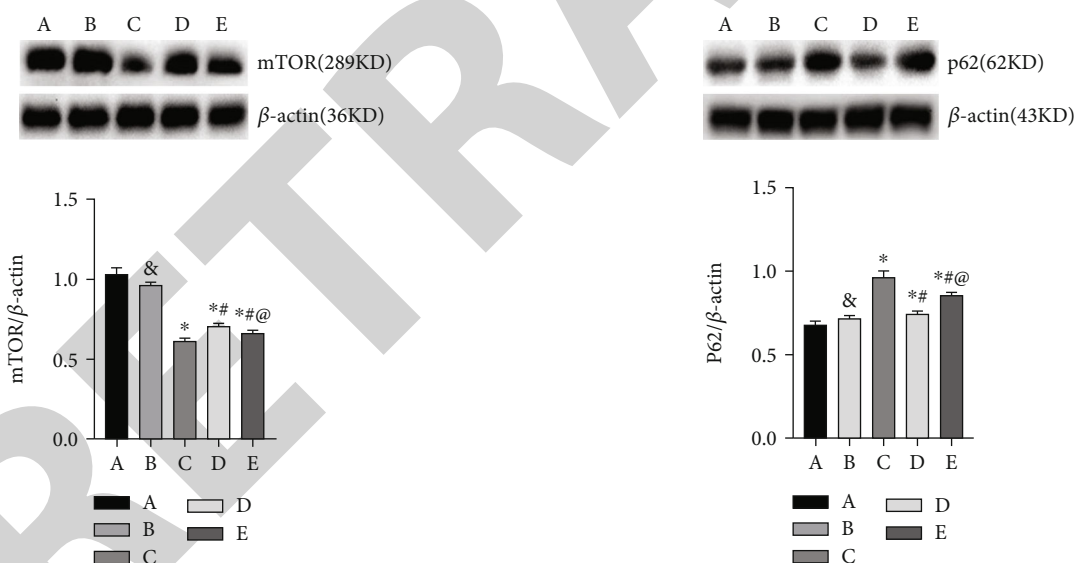


FIGURE 4: Difference in the expression levels of mTOR proteins: A: normal control group, B: normal administration group, C: diabetes control group, D: early administration group, and E: late administration group. \* $p < 0.05$  vs. A; & $p > 0.05$  vs. A; # $p < 0.05$  vs. C; @ $p < 0.05$  vs. D.

3.9. LC3-II Protein Expression. As for LC3-II expression, the difference between the normal control group and the normal administration group as well as the control group did not reach significance ( $p > 0.05$ ), but LC3-II protein expression in the diabetic control group was significantly increased ( $p < 0.05$ ). It was found that dapagliflozin treatment resulted in enhancement of LC3-II expression in the diabetic rats

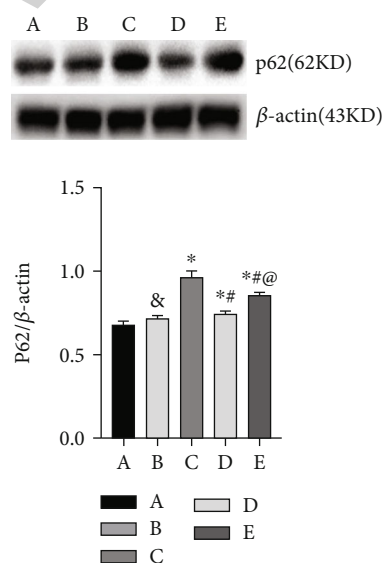


FIGURE 5: Relative expression levels of p62 protein in the ventricles of rats in each group: A: normal control group, B: normal administration group, C: diabetes control group, D: early administration group, and E: late administration group. \* $p < 0.05$  vs. A; & $p > 0.05$  vs. A; # $p < 0.05$  vs. C; @ $p < 0.05$  vs. D.

( $p < 0.05$ ), with greater effect in the early administration group ( $p < 0.05$ ). See Figure 7.

#### 4. Discussion

The onset of diabetes is hidden and usually presents only metabolic dysfunction in the early stage, including

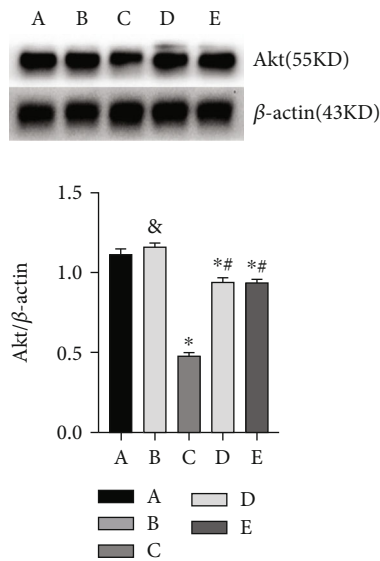


FIGURE 6: Difference in the expression levels of Akt proteins: A: normal control group, B: normal administration group, C: diabetes control group, D: early administration group, and E: late administration group. \* $p < 0.05$  vs. A; & $p > 0.05$  vs. A; # $p < 0.05$  vs. C.

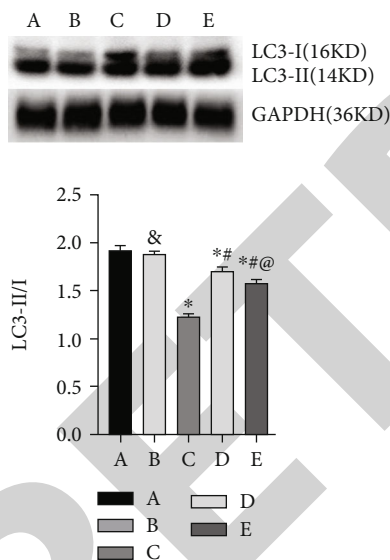


FIGURE 7: Difference in the expression levels of LC3 proteins: A: normal control group, B: normal administration group, C: diabetes control group, D: early administration group, and E: late administration group. \* $p < 0.05$  vs. A; # $p < 0.05$  vs. C; @ $p < 0.05$  vs. D.

hypertension, insulin resistance, oxidative stress, and autophagy. Many patients develop diabetes after the occurrence of complications [17]. Complications of diabetes include renal failure, retinopathy, neuropathy, and cardiovascular and cerebrovascular diseases. These complications seriously affect the quality of life of the patients. DCM is early manifested by myocardial fibrosis, ventricular stiffness, and cardiac enlargement without obvious clinical symptoms.

During diabetes, the patients will undergo structural changes of the heart, cardiac systolic and diastolic dysfunction, and heart failure [18]. The ultrastructure of the diabetic

rats (induced by STZ) changed abnormally at 8-12 weeks, and the heart function changed at 6-14 weeks [19]. Therefore, this experiment was only carried out 16 weeks after the establishment of diabetes rat model, and relevant laboratory tests were carried out to better explore the relevant pathological mechanism and pharmacological effects.

In the present study, we assayed that the blood glucose level, water consumption, and urine volume of diabetes rats increased significantly, but their weight decreased significantly. At the end of this experiment, almost all diabetes rats had the symptoms of lethargy and cataract complications, and the blood lipid increased significantly. HE results depicted orderly arrangement of ventricular myocytes in the normal control group and clear staining of myocardial nucleus and cytoplasm without obvious myocardial fibrosis. In the diabetic group, ventricular myocytes were seriously damaged, myocardial cells were disordered and deformed, cell volume and intercellular space increased, and interstitial fibrosis was serious.

Dapagliflozin functions in the body through inhibition of glucose reabsorption and promotion of the excretion of in urine when hindering the high-glucose transporter SGLT2 in the renal proximal tubule [1]. Dapagliflozin has many mechanisms to protect cardiomyocytes such as blood glucose control effects and protective effect on heart failure, cardiovascular mortality [7, 20], and cardiovascular mortality or hospitalization due to heart failure with safety [21]. Dapagliflozin is indicated to significantly improve health conditions related to heart failure, alleviating symptoms and improving physical function and quality of life which lasts for a long time [22].

Dapagliflozin has a variety of mechanisms to protect cardiomyocytes. By inhibiting the oxidative stress mediated by nicotinamide adenine dinucleotide phosphate (NADPH) oxidase, it obviously ameliorated the cardiac dysfunction, improved myocardial fibrosis, apoptosis, and oxidase stress in vivo, and reduced the enhanced level of reactive oxygen species and cell death of H9c2 cells [23]. Besides, the dapagliflozin can improve the biochemical indexes related to cardiac function, including malondialdehyde (MDA), glutathione (GSH), and catalase (CAT), proinflammatory mediators (NF-κB and tumor necrosis factor-α (TNF-α)), and apoptotic effectors (caspase-3). In addition, it can restore the oxidant/antioxidant balance and attenuates inflammation and downregulates the levels of apoptosis key elements in myocardial tissue [24]. Dapagliflozin obviously improves myocardial hypertrophy caused by T2DM by reducing blood glucose and the expression of calpain-1 in cardiomyocytes [25]. Herein, our experiment was to explore whether dapagliflozin recovered autophagy through the Akt/mTOR signaling pathway and to observe the expression and distribution of Cx43 in ventricular myocytes upon treatment.

We found that blood glucose decreased significantly within one week after treatment with dapagliflozin in the early administration group and the late administration group, and weight was well controlled. The blood glucose level in these two groups at the end of the experiment declined dramatically compared with that in the diabetic



model group as the early administration group exhibited greater effect. Apart from blood glucose, the lipid levels following dapagliflozin treatment were also significantly reduced.

The proportion of complications in the late administration group was similar to that in the diabetic group. Mild complications occurred in rats in the early administration group, and fewer rats had complications of listlessness and cataracts. Such improvement in the complication is largely attributable to the better control of blood glucose in the early stage of the disease.

HE staining showed damaged ventricular myocytes in the early and late administration groups compared with the normal control group, though the pathological changes of cell arrangement, cell edema, and interstitial fibrosis had been improved. The improvement of myocardial lesions in the early administration group was more significant; Shi's study had similar report [26].

The expression of cardiac Cx is influenced by many factors, such as hypertension, diabetes, myocardial remodeling, and heart failure [27]. Cx is essential for coordinating myocardial excitation and contraction to maintain normal cardiac function [28]. In the present study, immunohistochemistry showed a reduction in the expression of Cx43 in ventricular myocytes of the diabetic group relative to the normal control group, and the lateral of Cx43 in cardiomyocytes could be also observed. Compared with the diabetic control group, the fluorescence of Cx43 in ventricular myocytes obviously increased upon treatment with dapagliflozin. The results by Western blot further confirmed downregulation of Cx43 expression in ventricular myocytes of the diabetic control group compared with the normal control group, and dapagliflozin could improve or reverse Cx43 expression. Interestingly, dapagliflozin rarely affected the expression of Cx43 in ventricular myocytes of normal rats. The results of ECG indicated that the heart rate, QRS wave width, and QT interval were significantly abnormal in the diabetic control group, which were improved by administration of dapagliflozin. The effect of dapagliflozin on ECG-related indexes is consistent with that of dapagliflozin on the regulation of Cx43 in ventricular myocytes.

The disorder of Cx43 distribution and abnormal expression are an important pathogenic mechanism to arrhythmia caused by various heart diseases [29]. Cx43 is the main connexin of ventricular myocytes. The lateral Cx43 distribution (remodeling) is a major cause of reduced cardiac conduction reserve and ventricular arrhythmia [30]. Cx43 remodeling is an important pathological mechanism leading to heart failure and arrhythmia [31], and the decrease of Cx43 expression will also increase the incidence of ventricular arrhythmia [32]. Improving the expression and distribution of Cx43 seems to be a new target for the treatment for heart failure and arrhythmia.

The expression and content of Cx43 in cardiomyocytes are closely related to the Akt/mTOR signaling pathway [12]. Autophagy is the main intracellular degradation system and is a process of cell self-degradation and recycling of intracellular components [33]. The amount of LC3-II is

closely correlated with the number of autophagosomes, serving as a good indicator of autophagosome formation [34]. Simple comparison of LC3-I and LC3-II, or summation of LC3-I and LC3-II for ratio determinations, may not be appropriate, and rather, the amount of LC3-II can be compared between samples [35]. Measurement of p62 seems an alternative method for detecting the autophagic flux [36].

Therefore, we measured LC3-II in samples in this experiment. Western blot showed that the increase of LC3-II in the myocardium of the diabetes control group was accompanied by the increase of p62, indicating that autophagy of myocardial cells in the diabetic group was inhibited. After dapagliflozin administration, p62 and LC3-II were inhibited in varying degrees in both early and late stages, suggesting that dapagliflozin administration might recover autophagy and alleviate myocardial damage in diabetes rats. The expression of Akt and mTOR decreased in the diabetic group, but in the early and late administration groups, the expression of Akt and mTOR recovered after dapagliflozin administration, suggesting that the regulatory mechanism of dapagliflozin on autophagy may be related to the Akt/mTOR signaling pathway.

Upregulation of autophagy can reduce cardiac remodeling and dysfunction in DCM, thus hindering the progression of DCM [37]. The Akt/mTOR signaling pathway plays a regulatory role in autophagy and provides a new therapeutic strategy for many diseases, including diabetes, cancer, and neurodegenerative diseases [38].

## 5. Conclusions

Dapagliflozin may be a specific drug for the prevention and administration of DCM. As a new hypoglycemic agent, dapagliflozin can improve blood lipids and body weight in DCM and has a certain cardioprotective effect. This effect may enhance autophagy through the Akt/mTOR signaling pathway and improve the expression and distribution of Cx43 in ventricular myocytes. However, the safety and efficacy of dapagliflozin in the administration for DCM still need more clinical data for verification, and its potential mechanism needs further exploration.

## Data Availability

The data used to support the findings of this study are available from the corresponding author upon request.

## Ethical Approval

The experimental procedure was reviewed and approved by the experimental animal welfare and ethics committee of Wannan Medical College (LLSC-2020-144).

## Conflicts of Interest

The authors have no relevant financial or nonfinancial interests to disclose.

## Authors' Contributions

Dabin Pan and Mengxiang Ren designed the research study, gathered and analyzed the data, and wrote the first draft of the manuscript. All authors contributed to study design, revised, read, and approved the final version of the manuscript. Dabin Pan and Mengxiang Ren contributed equally to this work and should be considered co-first authors.

## Acknowledgments

This work is supported by the Advanced Talents Research Fund Project of Yijishan Hospital of Wannan Medical College (KY20580460).

## References

- [1] S. Dhillon, "Dapagliflozin: a review in type 2 diabetes," *Drugs*, vol. 79, no. 10, pp. 1135–1146, 2019.
- [2] M. Arow, M. Waldman, D. Yadin et al., "Sodium-glucose cotransporter 2 inhibitor dapagliflozin attenuates diabetic cardiomyopathy," *Cardiovascular Diabetology*, vol. 19, no. 1, p. 7, 2020.
- [3] S. Lahnwong, S. Palee, N. Apaijai et al., "Acute dapagliflozin administration exerts cardioprotective effects in rats with cardiac ischemia/reperfusion injury," *Cardiovascular Diabetology*, vol. 19, no. 1, p. 91, 2020.
- [4] J. J. V. McMurray, S. D. Solomon, S. E. Inzucchi et al., "Dapagliflozin in patients with heart failure and reduced ejection fraction," *The New England Journal of Medicine*, vol. 381, no. 21, pp. 1995–2008, 2019.
- [5] M. C. Petrie, S. Verma, K. F. Docherty et al., "Effect of dapagliflozin on worsening heart failure and cardiovascular death in patients with heart failure with and without diabetes," *Journal of the American Medical Association*, vol. 323, no. 14, pp. 1353–1368, 2020.
- [6] J. J. V. McMurray, D. L. DeMets, S. E. Inzucchi et al., "A trial to evaluate the effect of the sodium-glucose co-transporter 2 inhibitor dapagliflozin on morbidity and mortality in patients with heart failure and reduced left ventricular ejection fraction (DAPA-HF)," *European Journal of Heart Failure*, vol. 21, no. 5, pp. 665–675, 2019.
- [7] E. T. Kato, M. G. Silverman, O. Mosenzon et al., "Effect of dapagliflozin on heart failure and mortality in type 2 diabetes mellitus," *Circulation*, vol. 139, no. 22, pp. 2528–2536, 2019.
- [8] M. Rattka, S. Westphal, B. M. Gahr, S. Just, and W. Rottbauer, "Spen deficiency interferes with \_connexin 43\_ expression and leads to heart failure in zebrafish," *Journal of Molecular and Cellular Cardiology*, vol. 155, pp. 25–35, 2021.
- [9] E. Dupont, T. Matsushita, R. A. Kaba et al., "Altered connexin expression in human congestive heart failure," *Journal of Molecular and Cellular Cardiology*, vol. 33, no. 2, pp. 359–371, 2001.
- [10] W. H. Dillmann, "Diabetic cardiomyopathy," *Circulation Research*, vol. 124, no. 8, pp. 1160–1162, 2019.
- [11] M. S. Joshi, M. J. Mihm, A. C. Cook, B. L. Schanbacher, and J. A. Bauer, "Alterations in connexin 43 during diabetic cardiomyopathy: competition of tyrosine nitration versus phosphorylation 在糖尿病心肌病中间隙连接蛋白43的变化:酪氨酸硝化作用与磷酸化作用的竞争," *Journal of Diabetes*, vol. 7, no. 2, pp. 250–259, 2015.
- [12] Y. Chen, X. Qiao, L. Zhang, X. Li, and Q. Liu, "Apelin-13 regulates angiotensin ii-induced Cx43 downregulation and autophagy via the AMPK/mTOR signaling pathway in HL-1 cells," *Physiological Research*, vol. 69, no. 5, pp. 813–822, 2020.
- [13] L. Li, Q. Li, W. Huang et al., "Dapagliflozin alleviates hepatic steatosis by restoring autophagy via the AMPK-mTOR pathway," *Frontiers in Pharmacology*, vol. 12, p. 589273, 2021.
- [14] A. Kogot-Levin, L. Hinden, Y. Riahi et al., "Proximal tubule mTORC1 is a central player in the pathophysiology of diabetic nephropathy and its correction by SGLT2 inhibitors," *Cell Reports*, vol. 32, no. 4, p. 107954, 2020.
- [15] Y. Bi, G. Wang, X. Liu, M. Wei, and Q. Zhang, "Low-after-high glucose down-regulated Cx43 in H9c2 cells by autophagy activation via cross-regulation by the PI3K/Akt/mTOR and MEK/ERK<sub>1/2</sub> signal pathways," *Endocrine*, vol. 56, no. 2, pp. 336–345, 2017.
- [16] X. Qin, W. He, R. Yang et al., "Inhibition of connexin 43 reverses ox-LDL-mediated inhibition of autophagy in VSMC by inhibiting the PI3K/Akt/mTOR signaling pathway," *PeerJ*, vol. 10, article e12969, 2022.
- [17] R. Ambady and S. Chamukuttan, "Early diagnosis and prevention of diabetes in developing countries," *Reviews in Endocrine & Metabolic Disorders*, vol. 9, no. 3, pp. 193–201, 2008.
- [18] G. Jia, A. Whaley-Connell, and J. R. Sowers, "Diabetic cardiomyopathy: a hyperglycaemia- and insulin-resistance-induced heart disease," *Diabetologia*, vol. 61, no. 1, pp. 21–28, 2018.
- [19] W. Xiang, L. Changyun, Z. Qiutang, and C. Linsheng, "Establishment of a rat model of type 2 diabetic cardiomyopathy," *Chinese Journal of pathophysiology.*, vol. 9, pp. 1868–1870, 2006.
- [20] B. Zinman, C. Wanner, J. M. Lachin et al., "Empagliflozin, cardiovascular outcomes, and mortality in type 2 diabetes," *The New England Journal of Medicine*, vol. 373, no. 22, pp. 2117–2128, 2015.
- [21] S. D. Wiviott, I. Raz, M. P. Bonaca et al., "Dapagliflozin and cardiovascular outcomes in type 2 diabetes," *The New England Journal of Medicine*, vol. 380, no. 4, pp. 347–357, 2019.
- [22] M. N. Kosiborod, P. S. Jhund, K. F. Docherty et al., "Effects of dapagliflozin on symptoms, function, and quality of life in patients with heart failure and reduced ejection fraction: results from the DAPA-HF trial," *Circulation*, vol. 141, no. 2, pp. 90–99, 2020.
- [23] Y. J. Xing, B. H. Liu, S. J. Wan et al., "A SGLT2 inhibitor dapagliflozin alleviates diabetic cardiomyopathy by suppressing high glucose-induced oxidative stress *in vivo* and *in vitro*," *Frontiers in Pharmacology*, vol. 12, article 708177, 2021.
- [24] M. El-Shafey, M. S. E. El-Agawy, M. Eldosoky et al., "Role of dapagliflozin and liraglutide on diabetes-induced cardiomyopathy in rats: implication of oxidative stress, inflammation, and apoptosis," *Frontiers in Endocrinology*, vol. 13, article 862394, 2022.
- [25] L. Liu, H. Luo, Y. Liang, J. Tang, and Y. Shu, "Dapagliflozin ameliorates STZ-induced cardiac hypertrophy in type 2 diabetic rats by inhibiting the calpain-1 expression and nuclear transfer of NF- $\kappa$ B," *Computational and Mathematical Methods in Medicine*, vol. 2022, Article ID 3293054, 11 pages, 2022.
- [26] L. Shi, D. Zhu, S. Wang, A. Jiang, and F. Li, "Dapagliflozin attenuates cardiac remodeling in mice model of cardiac pressure overload," *American Journal of Hypertension*, vol. 32, no. 5, pp. 452–459, 2019.



## Retraction

# Retracted: Deep Learning-Based Networks for Detecting Anomalies in Chest X-Rays

### BioMed Research International

Received 20 June 2023; Accepted 20 June 2023; Published 21 June 2023

Copyright © 2023 BioMed Research International. This is an open access article distributed under the Creative Commons Attribution License, which permits unrestricted use, distribution, and reproduction in any medium, provided the original work is properly cited.

This article has been retracted by Hindawi following an investigation undertaken by the publisher [1]. This investigation has uncovered evidence of one or more of the following indicators of systematic manipulation of the publication process:

- (1) Discrepancies in scope
- (2) Discrepancies in the description of the research reported
- (3) Discrepancies between the availability of data and the research described
- (4) Inappropriate citations
- (5) Incoherent, meaningless and/or irrelevant content included in the article
- (6) Peer-review manipulation

The presence of these indicators undermines our confidence in the integrity of the article's content and we cannot, therefore, vouch for its reliability. Please note that this notice is intended solely to alert readers that the content of this article is unreliable. We have not investigated whether authors were aware of or involved in the systematic manipulation of the publication process.

In addition, our investigation has also shown that one or more of the following human-subject reporting requirements has not been met in this article: ethical approval by an Institutional Review Board (IRB) committee or equivalent, patient/participant consent to participate, and/or agreement to publish patient/participant details (where relevant).

Wiley and Hindawi regrets that the usual quality checks did not identify these issues before publication and have since put additional measures in place to safeguard research integrity.

We wish to credit our own Research Integrity and Research Publishing teams and anonymous and named external researchers and research integrity experts for contributing to this investigation.

The corresponding author, as the representative of all authors, has been given the opportunity to register their agreement or disagreement to this retraction. We have kept a record of any response received.

### References

- [1] M. Badr, S. Al-Otaibi, N. Alturki, and T. Abir, "Deep Learning-Based Networks for Detecting Anomalies in Chest X-Rays," *BioMed Research International*, vol. 2022, Article ID 7833516, 10 pages, 2022.

## Research Article

# Deep Learning-Based Networks for Detecting Anomalies in Chest X-Rays

Malek Badr <sup>1,2,3</sup>, Shaha Al-Otaibi <sup>4</sup>, Nazik Alturki,<sup>4</sup> and Tanvir Abir <sup>5</sup>

<sup>1</sup>The University of Mashreq, Research Center, Baghdad, Iraq

<sup>2</sup>Department of Medical Instruments Engineering Techniques, Al-Farahidi University, Baghdad 10021, Iraq

<sup>3</sup>Research Center, The University of Mashreq, Baghdad, Iraq

<sup>4</sup>Department of Information Systems, College of Computer and Information Sciences, Princess Nourah bint Abdulrahman University, P. O. Box 84428, Riyadh 11671, Saudi Arabia

<sup>5</sup>Department of Business Administration, Faculty of Business and Entrepreneurship, Daffodil International University, Dhaka, Bangladesh

Correspondence should be addressed to Tanvir Abir; [tanvir.ba02876.c@diu.edu.bd](mailto:tanvir.ba02876.c@diu.edu.bd)

Received 5 June 2022; Revised 20 June 2022; Accepted 24 June 2022; Published 23 July 2022

Academic Editor: Dinesh Rokaya

Copyright © 2022 Malek Badr et al. This is an open access article distributed under the Creative Commons Attribution License, which permits unrestricted use, distribution, and reproduction in any medium, provided the original work is properly cited.

X-ray images aid medical professionals in the diagnosis and detection of pathologies. They are critical, for example, in the diagnosis of pneumonia, the detection of masses, and, more recently, the detection of COVID-19-related conditions. The chest X-ray is one of the first imaging tests performed when pathology is suspected because it is one of the most accessible radiological examinations. Deep learning-based neural networks, particularly convolutional neural networks, have exploded in popularity in recent years and have become indispensable tools for image classification. Transfer learning approaches, in particular, have enabled the use of previously trained networks' knowledge, eliminating the need for large data sets and lowering the high computational costs associated with this type of network. This research focuses on using deep learning-based neural networks to detect anomalies in chest X-rays. Different convolutional network-based approaches are investigated using the ChestX-ray14 database, which contains over 100,000 X-ray images with labels relating to 14 different pathologies, and different classification objectives are evaluated. Starting with the pretrained networks VGG19, ResNet50, and Inceptionv3, networks based on transfer learning are implemented, with different schemes for the classification stage and data augmentation. Similarly, an ad hoc architecture is proposed and evaluated without transfer learning for the classification objective with more examples. The results show that transfer learning produces acceptable results in most of the tested cases, indicating that it is a viable first step for using deep networks when there are not enough labeled images, which is a common problem when working with medical images. The ad hoc network, on the other hand, demonstrated good generalization with data augmentation and an acceptable accuracy value. The findings suggest that using convolutional neural networks with and without transfer learning to design classifiers for detecting pathologies in chest X-rays is a good idea.

## 1. Introduction

Advances in data acquisition, storage, and processing allow for cheap, large-scale data collection [1]. They have improved the ability to process data into useful information and advance knowledge. This caused a substantial increase in available information in medical imaging, leaving behind the days when health data was scarce. This poses a great

challenge when it comes to developing tools for its analysis and interpretation that aid in decision-making. Many modern hospitals' computer systems store a large volume of chest X-rays and radiological reports [2].

Digital image processing (DIP) allows segmentation and classification of medical images [3]. In this context, segmentation defines a partition so that the obtained regions correspond to anatomical structures, processes, or regions of

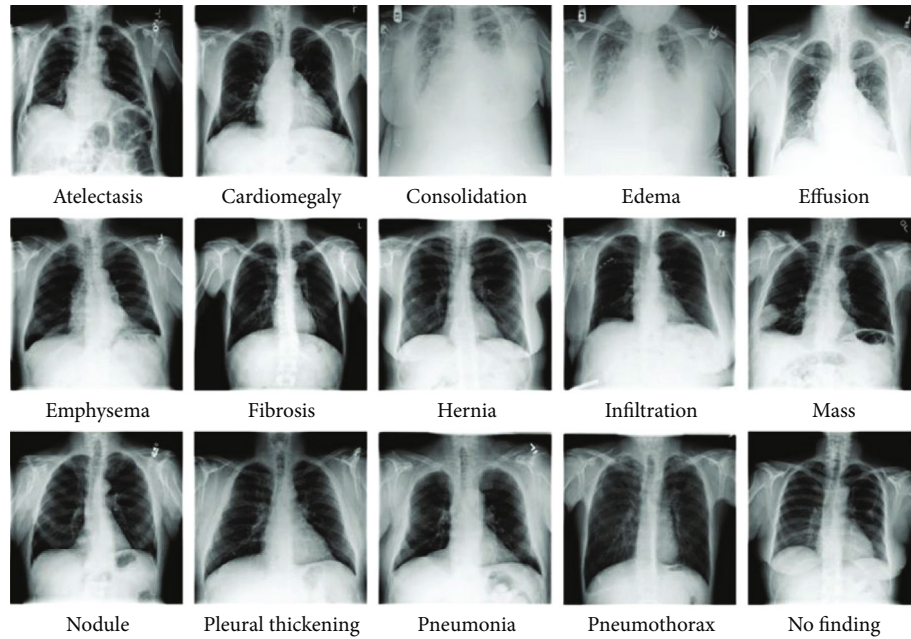


FIGURE 1: Chest X-ray images, with their respective labels, belonging to the ChestX-ray14 data set.

TABLE 1: Pretrained CNN properties used in work.

Architecture	Input image size (pixels)	Depth (layers)	Parameters (millions)
VGG19	224 × 224	19	144
Inception V3	299 × 299	48	23.9
ResNet50	224 × 224	50	25.6

special interest. Its results are used to compare volumes, morphologies, and characteristics with other studies or other regions of the same image; study tissue distribution; detect lesions; understand anatomy; plan surgeries; plan radiation therapies; and detect abnormal tissue, among other tasks. The classification requires global image analysis and helps with diagnosis and treatment.

Neural networks based on deep learning (DNN, from the English Deep Neural Network), specifically convolutional ones (CNN, from the English Convolutional Neural Networks), have seen a huge boom in recent years due to the increased capacity and availability of specific graphics processing units (GPU), the significant reduction in hardware cost, and the recent advances in machine learning [4]. In medical imaging, the number of successful DNN applications is growing [5], including organ and substructure segmentation, tumor detection, sample classification (complete images), and registration.

The automatic detection of anomalies in chest X-rays is an important application of deep learning networks in medical images that has gained momentum in the last year, due to COVID-19 detection [6, 7]. In this work, CNN automatically detects anomalies in chest X-rays from the ChestX-ray14 database [2], which contains more than 100,000 images with 14 possible pathologies. The work includes a deep study of the problem and CNN's and the development

of programs for the design, training, and evaluation of networks using the Keras API on Python and GPU processing. Study, propose, implement, and validate DNN for chest X-ray anomaly detection.

## 2. Material and Methods

**2.1. ChestX-ray14 database.** The ChestX-ray14 database (Figure 1) was compiled by the NIH (National Institute of Health), the main US government agency responsible for biomedical and public health research. It comprises more than 100,000 chest X-ray images with multilabels of common diseases from more than 30,000 anonymous patients, accumulated from the year 2010 to 2020. The data was extracted from the texts of radiology reports using language processing techniques. The data set contains the following 14 varieties of abnormalities: infiltration, effusion, atelectasis, nodule, mass, pneumothorax, consolidation, pleural swelling, cardiomegaly, emphysema, edema, fibrosis, pneumonia, and hernia. Radiographs are tagged with one or more pathology keywords, resulting in single or multitags. On the other hand, the images not associated with any of the 14 classes of pathologies are labeled as "No Finding," which is not equivalent to an image of a healthy person but could contain patterns of disease other than the 14 listed or findings uncertain within the 14 possible categories. The existence of more than one pathology associated with certain radiographs allows to analyze of the correlation between them.

**2.2. CNNs Used in the Work.** Having introduced the basic concepts of the CNNs, this subsection aims to briefly describe the architectures of the pretrained CNNs used during the development of the work; Table 1 shows some of

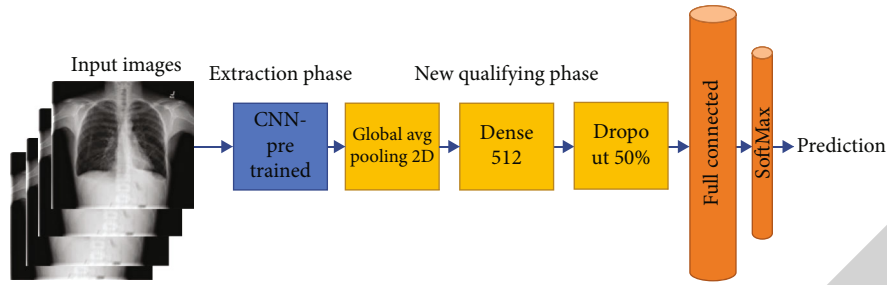


FIGURE 2: General architecture of the model based on transfer learning used.

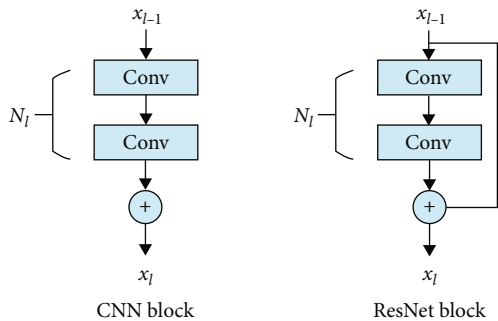


FIGURE 3: Comparison between a typical CNN block and a ResNet residual block.

their properties. Figure 2 shows a general diagram of the implemented models based on transfer learning.

The proposed CNN has five convolution blocks that constitute the feature extraction phase, where  $11 \times 11$ ,  $5 \times 5$ , and  $3 \times 3$  filters are used. For its part, the qualifying phase has 2 fully connected layers, two layers of dropout, and an output layer with the same number of neurons as classes, adjusted according to the problem explored. It was decided to reduce the size of the input images to  $224 \times 224$  pixels. Finally, the built network has 10,721,190 trainable parameters.

**2.2.1. VGGNet.** VGGNet [8, 9] was built and trained by Karen Simonyan and Andrew Zisserman, belonging to the Vision Geometry Group (VGG) of the University of Oxford, being the winner in the location task and obtaining the second place in the classification task of the ILSVRC competition in the year 2014.

This network uses an architecture with very small convolution filters ( $3 \times 3$ ) achieving a significant improvement over previous CNN configurations, where large convolution filters ( $9 \times 9$  or  $11 \times 11$  from AlexNet [10]) were used. The  $3 \times 3$  filter is the smallest filter that can be used without losing track of left/right, top/bottom, and center between neighboring pixels.

There are variants of the VGG depending on the number of hidden layers. In this work the VGG19 is used.

**2.2.2. Inception (GoogLeNet).** GoogLeNet [11], also known as Inception, is a CNN developed by Google researchers. The GoogLeNet architecture presented at the ILSVRC in 2014 won first place in the image classification task, beating VGG. The depth of GoogLeNet is greater than that of

VGGNet. However, the number of parameters is much less, making it a better option to optimize computational costs when available resources are limited. The input data to the network are images of dimension  $224 \times 224$  pixels, pre-processed with an average of zero.

**2.2.3. ResNet.** ResNet introduced the concept of residual learning to address the gradient fading problem, by adding direct connections between neurons, without adding additional parameters or additional computational complexity. In 2015, it was a winner at the ILSVRC in the image classification, detection, and localization categories and the MS COCO in the detection and segmentation categories.

ResNet introduced the residual block concept with the idea of information flowing across connections, allowing it to build much deeper networks. The residual block consists of various network layers and a direct access connection (Figure 3).

**2.3. Regularization.** When developing DNN, it is common to see overfitting, where the model works well with training data but has poor generalization. A neural network learns latent data patterns and adjusts model weights to fit them during training. This becomes complicated when the pattern he finds is just noise. Real-world training data may be affected by noise and differ greatly from real data. If a neural network is overtrained, that is, it overlearns the training data, and these contain noise, then the internal parameters probably move in their adjustment with respect to the values they would obtain in noise-free data, which means the network is less robust to noise and cannot generalize well. The pseudocolor images are segmentation results from the gray PD, T1, and T2 input images. MLP stands for multi-layer perceptron. You cannot train a generalizable model when you have too few samples to learn from. If the data were infinite, the model would be exposed to all data distribution aspects, preventing overfitting. Regularization decreases overfitting. Dropout and data augmentation are two DNN regularization methods.

**2.3.1. Dropout.** The dropout technique is one of the most effective and used techniques. This method, applied to a layer, consists of arbitrarily “deactivating” (zeroing) some neurons of a layer during each training iteration. A number of output features of the layer are randomly discarded. The fraction of the features that are reduced to zero is a parameter of choice known as the dropout rate.

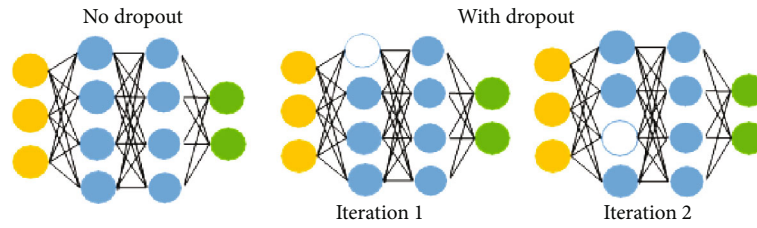


FIGURE 4: Illustrative figure of the dropout technique.

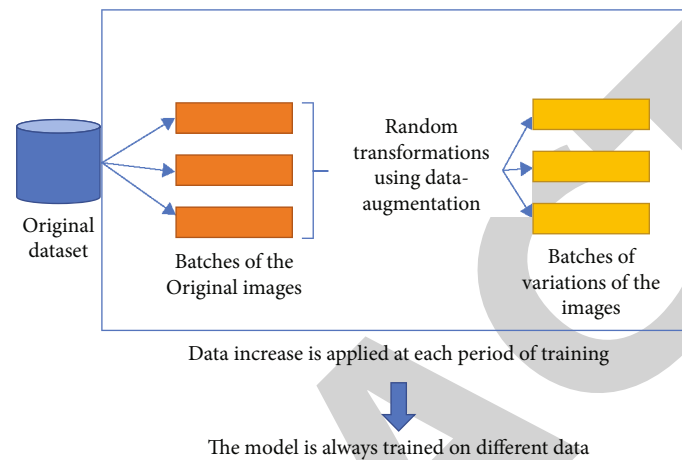


FIGURE 5: Dynamic data augmentation.

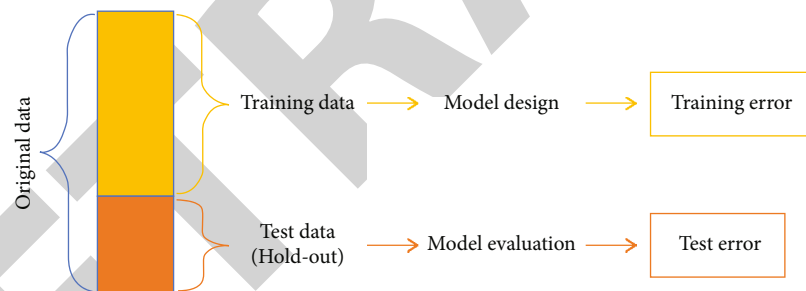


FIGURE 6: Simple hold-out partition of the data set.

It can be seen in Figure 4 how the regular network (left) has all the neurons and connections between two successive layers intact, whereas, with dropout, each iteration induces some defined degree of randomness by arbitrarily deactivating or discarding some neurons and their associated connections.

**2.3.2. Data Augmentation.** Data augmentation consists of generating more training data (in quantity and/or diversity) from the existing training samples, increasing the samples through a series of random transformations that generally consist of rotations, transformations related, translations, and scaling, among others. At the training time, the goal is that the model never sees exactly the same image twice and thus generalizes better [12], known as dynamic data augmentation (Figure 5).

**2.4. Model Validation.** Generalizability is used to evaluate a neural network's quality. To estimate generalization capac-

ity, a suitable metric and mechanism must be defined. This work uses accuracy as the metric and hold-out as the estimation method when working with DNN.

Accuracy is the ratio of correct predictions to total predictions. It measures model generalizability. Correct generalizability estimation requires evaluating the model with untrained data. The hold-out validation method randomly creates two disjoint partitions of the original data set [13]. Figure 6 depicts hold-out.

Given that different subsampling of the data set or random initializations of the internal parameters of the DNNs can usually be used, it is common to carry out more than one entry/test cycle defining a different hold-out for each one. In these cases, the metric is obtained as the average of the values obtained over the different cycles.

**2.5. Development Environment and Implemented Programs.** Python 3.8.5, Keras 2.4.3, and TensorFlow were used to



implement classification models. Python was chosen because it has many data analysis and deep learning libraries, extensive documentation, and a large programming community.

The code was structured in well-defined functions to create clear and readable code. Data loading and preprocessing functions were defined to obtain the necessary data sets for each proposed experimental arrangement, separate training and test data, generate tensor image batches with real-time data augmentation, create classification models and adjust them, graph results, and analyze them. The code was designed to be reused in each experiment with adequate documentation, saving time and reducing redundancy.

Jupyter Notebook, a 2015 client-server application, was used to develop the codes. A Jupyter Notebook is a “computational narrative” that publishes code and data with analyses, hypotheses, and conjectures. “.ipynb” files are simple, documented JSON files. It was chosen because it was accessed through a web browser, allowing the same interface to run locally as a desktop application and on a remote server [14, 15].

Jupyter Notebook was run on a remote server at the ICyTE Image Processing Laboratory using a local web browser and SSH. SSH encrypts client-server connections. Authentication, commands, output, and file transfers are all encrypted.

Conda was a package manager and environment manager. Conda lets you run different versions of Python and its libraries in virtual environments. The work was done in a virtual environment separate from other projects.

Since deep learning training takes a long time, Screen or GNU Screen was used to keep remote sessions active. It is possible to start a screen session, open multiple virtual terminals, and then log out while the processes continue. By establishing a new connection, terminals can be accessed without interrupting processes [12, 13].

*2.5.1. Obtaining New Data Sets from the Original Data Set ChestX-ray14.* Different experimental designs required new data sets from the original database. The open-source libraries NumPy, which manages vectors and matrices in Python, and Pandas were used to obtain these sets.

In this case, the ChestX-ray14 CSV file containing class labels, image paths, radiograph information, and patient information was used. We used the radiograph paths and labels for the proposed analysis, discarding unnecessary data. Only in experiment #1 was radiograph orientation preserved. The main challenge was creating functions for each problem.

The labels had to be pure in #2 and #4; the radiographs had to show a single pathology. In this case, functions were programmed to filter the database by label. Fix #1 used this function to filter images by orientation. To fix #3, all pathological X-ray images (whether pure or not) had to be relabeled as “finding,” generating a new data set with the categories “no finding” and “finding.” A program was developed for this.

Unbalanced data was one of the work’s greatest challenges, so experimental arrangement #2 was proposed. A data balancing function was programmed to obtain the number of pure pathological samples and subsample the majority class until the minority class number was equal.

Reusing the same function for “pure pathology” and “no finding” In array #4, the same logic was used to obtain X-ray images labeled with a single pathology by subsampling the set without substitution.

All cases required a single data set. Multiple sets were obtained in cases where filtering was used, each group belonging to each filtered category (15 categories for array #2 and pure labels with a frequency of 500 or more for fix #4). Therefore, the sets are needed to be concatenated.

The Pandas library’s concatenation function created a new data set with the labels in the same order as the individual sets. Balancing cannot be ensured in partitions performed after a concatenation using this library, which harms the generalization capacity of the models and, consequently, the quality of the experiment and conclusions drawn. Programming a function to partition and concatenate data sets preserved class balance.

*2.5.2. Image Batch Generation.* The preprocessing API in the Keras library has classes and functions for working with images that help convert raw data on disc into an object that can be used to train a model. It was used to both preprocess the input data and apply data augmentation to it.

The ImageDataGenerator class, also known as a generator, allows you to set parameters for preprocessing input data before feeding it to a model. On the one hand, this class was used in the experiments with pretrained CNNs, and the same preprocessing that was used in ResNet, VGG, and Inception was applied to the set of radiographs. The gray levels of the radiographs were normalized to the interval [0.1] for the proposed architecture without transfer learning. Specific functions were programmed in each case.

Most deep-learning classification data sets organize all of the images into separate directories labeled with the names of the classes, making it simple to read the images from the disc. This is not the case with ChestX-ray14, where all images are stored in a single directory and their tags are mapped to a CSV file, as described in the previous subsection.

The method flow from the data frame of the ImageDataGenerator class was used to generate the image batches, which allows the data frames generated with the data set generation functions [16] to be used as input parameters. The method returns an iterator that generates tuples  $(x, y)$ , where  $x$  is an array of batches of tensor images and  $y$  is a vector containing the labels. The batch size refers to the number of images used in each training step before a model’s trainable parameters are updated. Because the GPU’s memory is limited, a batch size of 128 images was chosen, with a validation set of 256 images. Specific functions were created as a result of this stage to define batches to be used in the training and evaluation of the models.

*(1) Augmenting Data with the ImageDataGenerator Class.* The ImageDataGenerator class also allows you to apply data augmentation. Keras augmentation is focused on generating diversity in the data shown to the model from epoch to epoch, maintaining the original amount of data. By instantiating the ImageDataGenerator class, transformations are defined, and then, during training, batches with images

TABLE 2: Proposed architectures from pretrained CNNs.

Proposed architecture base model	Scheme	Multilayer perceptron
#1	ResNet50	#1
#2	ResNet50	#2
#3	VGG19	#1
#4	VGG19	#2
#5	InceptionV3	#1
#6	InceptionV3	#2

TABLE 3: Training hyperparameters used for the experiments.

Hyperparameter	Value
Optimization algorithm	Stochastic gradient descent
Loss algorithm	Cross-entropy
Times	150
Training batch size	128
Validation lot size	256

transformed in real time are assembled. It seeks to make the most of the training examples so that the model never sees exactly the same image twice; this helps to avoid overfitting and the model generalizes better.

To implement data augmentation, a function was defined in such a way that it would return the instance to the ImageDataGenerator class configured to perform transformations on the data. Taking into account previous articles that analyzed chest X-ray images [10, 17–21], the following transformations were defined:

- (i) A random rotation within the range of  $-5/+5$  degrees
- (ii) A random horizontal and vertical shift of 5%
- (iii) A random increase range of 15%
- (iv) A random distortion along an axis of 0.1 degrees creates or rectifies the angles of perception
- (v) A padding to keep the size of the input images constant, mirroring neighboring pixels to fill in the gaps with missing pixels

The programmed function makes use of the `flow_from_dataframe` method to apply the transformations defined by the generator and assemble the image batches. Dynamic data augmentation was applied during model training by calling the function at each epoch.

In order to correctly evaluate the generalization capacity of the model, data augmentation was not applied to the validation data set, so another function had to be programmed with another generator without including the transformation parameters mentioned above. In this case, the implementation uses the `flow_from_dataframe` method prior to classifier training to generate the image batches.

### 2.5.3. Implementation of Classification Models Using Keras.

The classification models were built with the Keras functional API [21–25], allowing for nonlinear topology models and creating more complex networks than the Keras sequential model. This API was chosen because it is extremely useful for implementing transfer learning. It can handle shared layers, which means you can access and reuse a model's middle layer activations, allowing you to use its features to create new feature extraction models that return the activation values. The weights of the convolutional layers were frozen (to avoid their adjustment during training), and the feature extraction phase was extracted for later use in transfer learning-based models.

Specific programs were written to implement both the architecture proposed and the classification phase of the models obtained from pretrained CNNs, in which the model class was used to create the model and the layers class was used to instantiate the necessary layers and define their parameters (number of neurons, activation functions, filters, filter size, type of pooling, dropout, and so on), both of which are part of the Keras library. Layers in Keras are unfrozen by default, allowing them to adjust their weights during network training.

A function was programmed to return the model. The base model and the classification scheme were used as parameters; and the number of classes according to the experimental arrangement, for the creation of the proposed architectures using transfer learning and fine-tuning. A specific function, on the other hand, was created to return the proposed architecture without transfer learning.

## 3. Results and Discussion

This section has the objective of detailing the results obtained for the experiments carried out in the work, using tables and graphs, and also to carry out an analysis of them.

First, the experimentation and analysis carried out for the selection of the base model (CNN pretrained) for the transfer learning tests are explained. Second, the results of experimental arrangements #1 to #4 for transfer learning are shown. Finally, the ad hoc CNN architecture is evaluated on the experimental arrangement that showed the best results.

### 3.1. Selection of the Base Model and Classification Scheme for Transfer Learning.

In the first instance of the development of this work, a study of the classification capacity of CNN chest radiographs defined from transfer learning was carried out. Starting from the ResNet50, VGG19 and InceptionV3 pretrained CNNs, described in the previous sections and considering the two multilayer perceptron structures of the classification phase (schemes #1 and #2). Table 2 shows a summary of the architectures studied in the first stage of the work.

It is important to note that the experimentation was carried out equally for each proposed architecture, seeking that the results obtained are comparable. For this reason, the same hyperparameters were used for training in each of the experiments, which can be seen in Table 3.

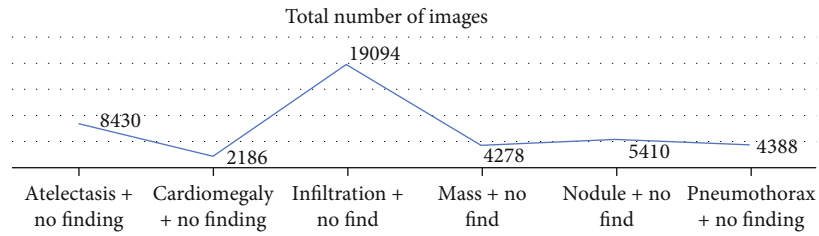


FIGURE 7: Subsets made up of pure pathology and “without finding.”

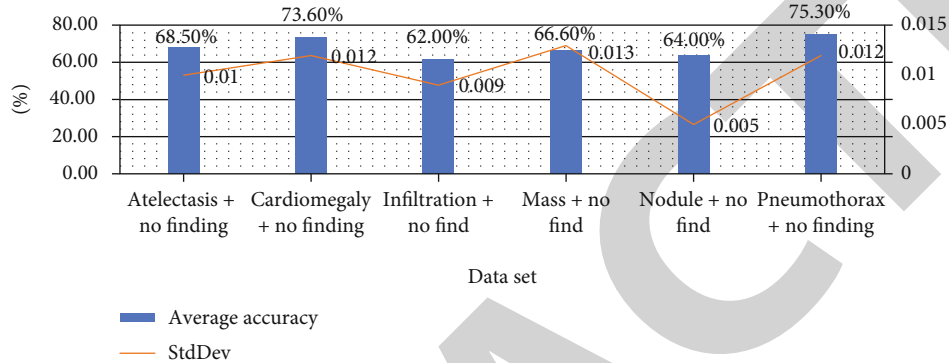


FIGURE 8: Average accuracy results for architecture #1.

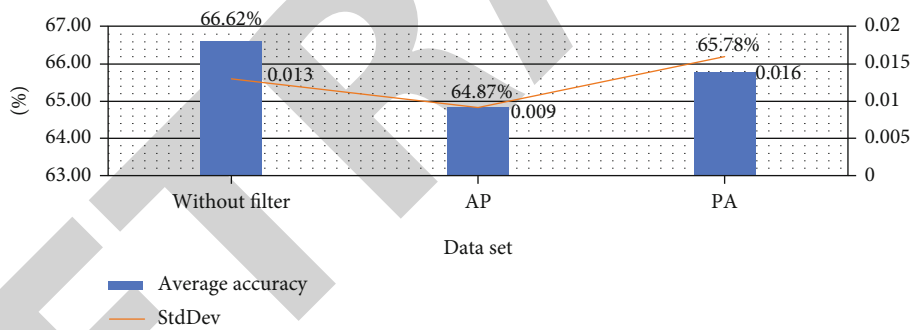


FIGURE 9: Comparison of results obtained by filtering by orientation and without filtering.

In the search to select the best base model and the best classification scheme, the classifiers were trained by adjusting their trainable parameters with the data sets obtained for experimental arrangement #2, the classification between no finding and a specific pathology which are shown in Figure 7.

The best accuracy results were shown for architecture #1, consisting of the ResNet50 pretrained CNN and the first proposed classification scheme, as shown in Figure 8.

The differences in accuracy observed with respect to the rest of the pre-trained architectures and proposed classification schemes were not very significant, but they were minor, so it was decided to continue with the following transfer-learning experiments using architecture #1, that is, combining the ResNet50 qualifying phase and the #1 qualifying phase scheme. It should be noted that all cases presented overfitting, which will be analyzed in more detail later in this section.

### 3.2. Transfer Learning Results

3.2.1. Results of Experimental Setup #1: Evaluation of Robustness in the Classification according to Orientation. After evaluating and comparing the proposed models, it was determined that ResNet50 and the multilayer perceptron #1 produced the best results in identifying pure pathologies in chest X-rays.

The problem defined in experimental arrangement #1, namely the need or not to separate the radiographs according to their orientation for subsequent classification, was investigated using ResNet50 and the classification phase scheme #1. As described in the previous chapter, the database images were filtered according to anteroposterior (AP) and posteroanterior (PA) orientation. The decision was made to perform the analysis only for the classification between “no find” and “mass” due to the lengthy computation times required for CNN training. This filtering

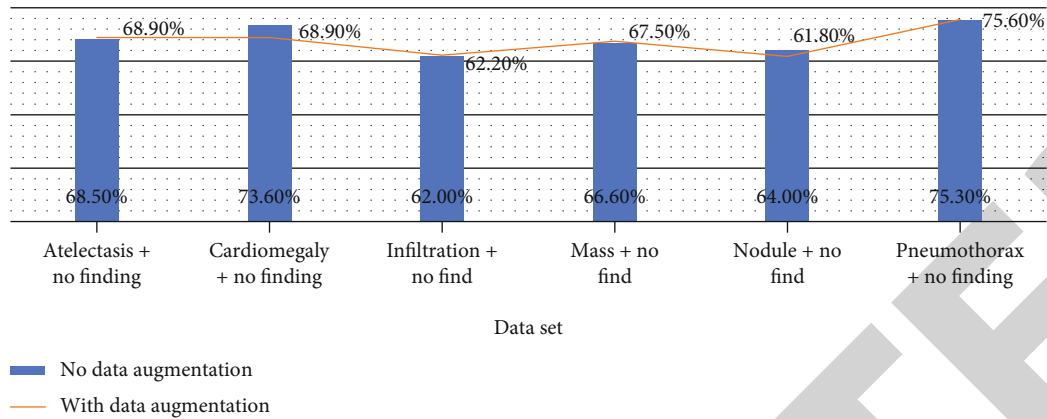


FIGURE 10: Average accuracy without and with data augmentation for the data sets made up of one pathology and “no finding.”

produced two subsets, with 1544 images in the AP data set and 2734 images in the PA data set as a result of the filtering. Five training/test cycles were used to define the validation scheme. Figure 9 summarizes the findings.

As shown in Figure 9, there is no evidence of any improvement in the average accuracy achieved. The behavior varies a lot with respect to the results obtained for the cases evaluated without filtering by orientation; although there is overfitting in both experiments, the model does not seem to improve in generalization. But on the contrary, based on the results obtained, it was decided to continue with the proposed experiments without separating the sets by the orientation of the radiographs.

**3.2.2. Results of Experimental Setup #2: Evaluation of Robustness in the Classification according to Orientation.** Tests were carried out with the different architectures from pretrained CNNs on the data sets shown in Table 2. The results obtained in this stage of the work made evident the need to work with regularization techniques to improve the generalization of the models. Figure 10 shows the average accuracies obtained for each case of pure pathology vs. “no finding” with and without dynamic data augmentation over 5 training/test cycles.

When using dynamic data augmentation, it can be seen that the average validation accuracy improves by more than 5% in relative terms, less for the “nodule” vs. “no finding” classification, which shows a performance degradation. The experimental results show that the use of data augmentation decreases the overfitting that was very marked from the epoch 10.

**3.2.3. Results of Experimental Setup #3: Classification between “Find” and “No Find.”** A new data set called “Find + No Find” was created, which contains all available examples and has a total number of images of 112,120. For this experiment, the “finding” class includes all radiographs that show one or more pathologies, taking into account both simple labels and multilabels. The results obtained with and without dynamic data augmentation are 63.9 percent without data augmentation and 69.5 percent with data augmentation. There was only one training/test cycle because the data set was unique (no subsampling).

When using data augmentation for the classification between “find” and “no find,” there is no improvement in invalidation accuracy for the set. However, the results obtained in both cases are close to 70% accuracy, which is excellent given the problem’s high complexity. However, when comparing the results, there is a significant improvement in overfitting when using dynamic data augmentation.

**3.2.4. Results of Experimental Setup #4: Classification between Different Pure Pathologies.** The validation accuracy results were obtained for the average of the five training cycles of average accuracy without (27.2%) and with (28.1%) data augmentation using a set of 12 pure pathologies. The results of this experimentation were not encouraging, possibly due to the complexity of the problem posed. The use of regularization techniques did not result in any improvement in the model’s lack of generalization. In terms of the validation accuracy obtained from the average of the five training cycles completed, there was a 1% improvement. However, the value obtained is close to 30% in both cases, implying that only about 3 out of every 10 radiographs shown in the model will be correctly classified. As can be seen from the results, increasing the amount of dynamic data improves the model’s generalizability while reducing premature overfitting. The average validation accuracy results obtained, on the other hand, show that the proposed approach is not feasible in this experimental setup.

**3.3. CNN Results without Transfer Learning.** Based on the results obtained with transfer learning for the different experimental arrangements, it was decided to use the data set of experimental arrangement #3, composed of the labels “no finding” and “finding,” which allowed having a large number of images necessary for the training of a complete CNN.

It was decided to train the model for 300 epochs, using dynamic data augmentation and the same training hyperparameters as in the transfer learning experiments. Hold-out was performed with 80% of the data for training and the remaining 20% for testing. The training and test accuracy values for each training epoch are shown in the graph



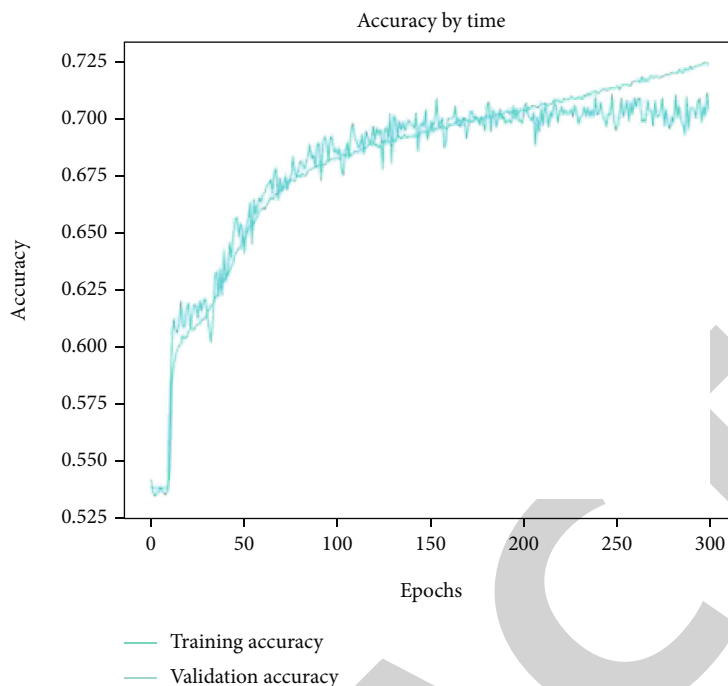


FIGURE 11: Accuracy vs. epoch for the CNN without transfer learning, trained with the data set composed of the labels “no finding” and “finding.”

of Figure 11. As can be seen in Figure 11, the model generalizes very well, beginning to converge between epochs 150 and 200. Compared to the architecture proposed with ResNet50 and the multilayer perceptron, it shows a drastic improvement with overfitting. Likewise, the accuracy value achieved remains close to 70%, as with transfer learning.

#### 4. Conclusions

This work studied deep learning models for identifying chest radiography pathologies. Scarcity of databases of this type of medical image in the public domain limits the state of the art. ChestX-ray14 has the most chest X-rays and the most research, so it was chosen for this work.

The work began with a thorough study of state-of-the-art and the adopted database’s characteristics, from which different experiments were designed to test the models.

ResNet50 showed the best performance for pathology detection using CNN-based transfer learning approaches, followed by VGG19 and Inceptionv3. Transfer learning approaches allow us to affirm that this can be a valid initial strategy for using CNN in cases where there are not enough labeled images, which is common in medicine. Even with chest radiograph classification, considering the complexity of chest radiograph classification, most experiments show acceptable accuracy. Dynamic data augmentation reduced overfitting in all tests without increasing computational cost or classifier stability. The ad hoc architecture proposed to evaluate a CNN without transfer learning showed acceptable accuracy and good generalization using data augmentation, indicating it is a valid strategy to follow when available. Images are enough. DNN models with and without transfer learning proved adequate for classifying chest X-ray pathol-

ogies. The total of the programs developed in this work for the design, training, and validation of CNN, along with its documentation, is an adequate basis for the future development of a library of CNN image functions that will be added to other techniques under development in the laboratory.

#### Data Availability

The data used to support the findings of this study are included within the article.

#### Conflicts of Interest

There is no potential conflict of interest in our paper, and all authors have seen the manuscript and approved to submit to your journal.

#### Authors’ Contributions

All authors have seen the manuscript and approved to submit to your journal.

#### Acknowledgments

The authors acknowledge the support from Princess Nourah bint Abdulrahman University Researchers Supporting Project number (PNURSP2022R136), Princess Nourah bint Abdulrahman University, Riyadh, Saudi Arabia.

#### References

- [1] M. Stead, M. Bower, B. Brinkmann, C. Warren, and G. A. Worrell, “Large-Scale Electrophysiology: Acquisition, Storage and



## Retraction

# Retracted: Hui Medicine Moxibustion Promotes the Absorption of Lumbar Disc Herniation and the Recovery of Motor Function in Rats through Fas/FasL Signaling Pathway

### BioMed Research International

Received 18 July 2023; Accepted 18 July 2023; Published 19 July 2023

Copyright © 2023 BioMed Research International. This is an open access article distributed under the Creative Commons Attribution License, which permits unrestricted use, distribution, and reproduction in any medium, provided the original work is properly cited.

This article has been retracted by Hindawi following an investigation undertaken by the publisher [1]. This investigation has uncovered evidence of one or more of the following indicators of systematic manipulation of the publication process:

- (1) Discrepancies in scope
- (2) Discrepancies in the description of the research reported
- (3) Discrepancies between the availability of data and the research described
- (4) Inappropriate citations
- (5) Incoherent, meaningless and/or irrelevant content included in the article
- (6) Peer-review manipulation

The presence of these indicators undermines our confidence in the integrity of the article's content and we cannot, therefore, vouch for its reliability. Please note that this notice is intended solely to alert readers that the content of this article is unreliable. We have not investigated whether authors were aware of or involved in the systematic manipulation of the publication process.

Wiley and Hindawi regrets that the usual quality checks did not identify these issues before publication and have since put additional measures in place to safeguard research integrity.

We wish to credit our own Research Integrity and Research Publishing teams and anonymous and named external researchers and research integrity experts for contributing to this investigation.






The corresponding author, as the representative of all authors, has been given the opportunity to register their agreement or disagreement to this retraction. We have kept a record of any response received.

### References

- [1] J. Xu, Q. Luo, J. Song et al., "Hui Medicine Moxibustion Promotes the Absorption of Lumbar Disc Herniation and the Recovery of Motor Function in Rats through Fas/FasL Signaling Pathway," *BioMed Research International*, vol. 2022, Article ID 9172405, 9 pages, 2022.

## Research Article

# Hui Medicine Moxibustion Promotes the Absorption of Lumbar Disc Herniation and the Recovery of Motor Function in Rats through Fas/FasL Signaling Pathway

Jianfeng Xu <sup>1,2</sup>, Qiang Luo <sup>1</sup>, Junyao Song <sup>1</sup>, Yanming Zhang <sup>1</sup>, Yingxu Wang <sup>1</sup>,  
Lei Yang <sup>1</sup>, Yinyin Sha,<sup>1</sup> Bowen Sun <sup>3</sup>, Na You,<sup>3</sup> Xinbao Tian <sup>3</sup>, Ruizhu Lin <sup>1</sup>,  
and Yongli Wu <sup>1</sup>

<sup>1</sup>Traditional Chinese Medicine and Traumatology, General Hospital of Ningxia Medical University, Yinchuan, 750004 Ningxia, China

<sup>2</sup>Key Laboratory of Modernization of Traditional Chinese Medicine, Ningxia Medical University, Yinchuan, 750004 Ningxia, China

<sup>3</sup>College of Traditional Chinese Medicine, Ningxia Medical University, Yinchuan, 750004 Ningxia, China

Correspondence should be addressed to Ruizhu Lin; [linrzh22012@163.com](mailto:linrzh22012@163.com) and Yongli Wu; [wuyongli999@163.com](mailto:wuyongli999@163.com)

Received 15 June 2022; Revised 5 July 2022; Accepted 8 July 2022; Published 23 July 2022

Academic Editor: Dinesh Rokaya

Copyright © 2022 Jianfeng Xu et al. This is an open access article distributed under the Creative Commons Attribution License, which permits unrestricted use, distribution, and reproduction in any medium, provided the original work is properly cited.

**Objectives.** To study the resorption of the herniated lumbar disc (RHL) and its mechanism in the SD rats of lumbar intervertebral disc herniation treated with Hui medicine moxibustion (HMM). **Methods.** Forty SD rats were randomly divided into four groups, normal group, lumbar disc herniation (LDH) group, HMM group, and antagonist (HMM+Met12) group, with 10 rats in each group. The rat model of LDH was prepared with the method of lumbar epidural emplacement of the caudal intervertebral disc. In the HMM group and HMM+Met12 groups, 4 weeks after modeling, HMM therapy was performed in the lumbar spine for 3 months with 1 time per day and 20 min each time, the samples were collected 8 weeks after the treatment. The histological degeneration was observed through HE staining, and the neovascularization of intervertebral disc tissues was detected by the expression of CD34 and vascular endothelial growth factor (VEGF). The apoptosis of nucleus pulposus cells was detected by TUNEL assay, and the activity of caspase-3, -8, and -9 and extracellular matrix enzymes was detected by western blotting. **Results.** HMM treatment significantly improved the behavioral ability of rats with LDH surgery. The morphological structure was obviously destroyed in the LDH group, but disc structure was significantly repaired in the HMM group, and mild structure alterations were observed in the HMM+Met12 group. Higher levels of CD34 and VEGF were detected in the HMM group indicating that neovascularization is formed. The expression level of FasL was significantly increased in the HMM group. The protein expression levels of cleaved-caspase-3, cleaved-caspase-8, and cleaved-caspase-9 in nucleus pulposus (NP) tissues were also elevated when treated with HMM, and the TUNEL staining showed the same results. The protein expression levels of matrix metalloproteinases- (MMP-) 1, MMP-2, MMP-3, MMP-13, and ADAMTS-4 were markedly promoted in the HMM group. Met12, a small peptide antagonist of FasL, significantly reduced the effects of HMM. **Conclusion.** HMM can promote the formation of neovascularization of lumbar intervertebral disc, support the apoptosis of NP cells through Fas/FasL signaling, and regulate the degradation of extracellular matrix enzyme, which then accelerates the absorption of lumbar intervertebral disc herniation and the recovery of motor function in rats.

## 1. Introduction

The resorption of the herniated lumbar disc (RHL) refers to the phenomenon of natural absorption or even complete

disappearance after conservative treatment without surgical intervention or chemical drug injection [1]. Since the first report of computed tomography- (CT-) confirmed RHL [2], this phenomenon has been broadly reported in many

pieces of research [3, 4]. RHL theory brings new enlightenment to traditional Chinese medicine and Hui medicine and other conservative therapy in the prevention and treatment of lumbar disc herniation. In the treatment of lumbar disc herniation, Hui medicine moxibustion (HMM) therapy has the effect of promoting blood circulation, detumescence, and strengthening muscle and bone. It can not only prevent the degeneration of the lumbar disc but also promote the resorption of partially ruptured lumbar disc herniation, reduce the recurrence of lumbar disc herniation, and improve the quality of life of patients with lumbar disc herniation [5].

There are many theories about the mechanism of RHL after lumbar disc herniation, such as autoimmunity, inflammatory reaction, neovascularization, imbalance of matrix metabolism, intervertebral disc degeneration, and NP cell apoptosis [6]. More experiments have confirmed that the apoptosis of NP cells mediated by signal pathways may be an important mechanism of reabsorption [7]. Prominent NP cells express a variety of inflammatory factors and matrix-degrading enzymes after contacting with blood supply, which worsens the living environment of NP cells, affects the growth and function of NP cells, and increases the apoptosis of the nucleus pulposus cells. Promoting the apoptosis of NP cells can promote the resorption of NP tissues [8].

Macrophage infiltration after disc herniation can be accompanied by the release of a variety of cytokines, such as IL-1, HIF-1, and monocyte chemoattractant protein-1. These cytokines can participate in the regulation of physiological activities through multiple signaling pathways (such as Fas/FasL, MAPKs, and NF kappa B) [9], among which, the Fas/FasL signaling pathway may be one of the most important pathways regulating the NP cell apoptosis, and moxibustion can regulate this signaling pathway [9].

Fas is a kind of type I transmembrane protein, belonging to the superfamily of tumor necrosis factor (TNF) and nerve growth receptor protein [10]. Fas can induce apoptosis by binding with its ligand FasL. FasL is a type II transmembrane protein belonging to the TNF family [11]. Fas recruits the adaptor protein FADD (Fas-associating protein with death domain) in the cytoplasm through the interaction between DD (death domain) in the intracellular domain and DD in the carboxyl end of FADD. Then, FADD binds with caspase-8 through the death effect domain to form a death-inducing signal complex and activates caspase-8 and downstream caspase-3 family members, which eventually leads to apoptosis. Regulation of the Fas/FasL signaling pathway can lead to a variety of complex biological effects on nucleus pulposus cells: regulating the apoptosis of NP cells and controlling the balance of extracellular matrix anabolism [12]. The Fas/FasL signaling pathway plays an important role in the resorption after lumbar disc herniation, so regulating this signaling pathway becomes an ideal choice to promote the resorption after lumbar disc herniation.

With the deepening of the basic research on the reabsorption of NP, the mechanism of reabsorption is gradually clear. People gradually realize that surgery is not the final

treatment for lumbar disc herniation, and it is not the only treatment. When there is no serious nerve injury, the discovery of reabsorption provides more possibilities for the conservative treatment of lumbar disc herniation with traditional Chinese medicine. It will be the focus of future research to give full play to the advantages of traditional Chinese medicine and develop a more targeted and targeted conservative treatment plan for lumbar disc herniation.

HMM therapy is a treatment method of burning moxa or in the moxibustion tank directly on the body surface of the affected place, making the local skin red and foaming, and promoting the recovery of the body. The treatment needs to achieve the unique moxibustion effect that the skin must be red and foaming. It is the development of the Chinese medical moxibustion with purulent moxibustion therapy to promote the balance of body fluids and to achieve Yin and Yang balance.

HMM therapy has the advantages of fast heat transfer and simple operation, which is deeply loved by patients clinically. However, the mechanism of HMM remains unclear. Herein, we will study the specific mechanism of HMM in traditional Chinese medicine.

## 2. Methods

**2.1. Animals.** Forty healthy male Sprague Dawley rats (2-3 months old and 200-250 g in weight), obtained from Ningxia Medical University Animal Centre, were used in the present study. Rats were cultured in separated cages and fed with distilled water and standard rat chow under a pathogen-free environment of a 12 h light/12 h dark cycle. The rats were fed for 5 days to adapt to the environment before the experiments. Then, the rats were randomly divided into 4 groups: Hui medicine moxibustion (HMM) group, antagonist (Met12) group, LDH model group, and normal group, with 10 rats in each group. Except for 10 rats as a normal group, the remaining 30 rats were made into the model of nucleus pulposus resorption after lumbar disc herniation. Useless laboratory rats were euthanized through carbon dioxide (CO<sub>2</sub>) asphyxiation. Compressed CO<sub>2</sub> gas in cylinders flowed to the rats' chamber at a rate of 10-30% displacing air in the chamber volume per minute. All experiments involving rats in our study were approved by the Ethics Committee of the General Hospital of Ningxia Medical University (approval no.: 2017-052).

**2.2. Establishment of LDH Model.** The method of lumbar epidural emplacement of the caudal intervertebral disc was used to establish the LDH model. Thirty Sprague Dawley rats in the HMM group, Met12 group, and LDH group were anesthetized by intraperitoneal injection of pentobarbital sodium. After successful anesthesia, the back was depilated and the tail was tied with a rubber band. Under the condition of routine disinfection and asepsis, the caudal vertebrae including two complete disc lengths, including the upper and lower cartilage endplates, were cut from each animal. The upper and lower endplates were punctured with needles to expose the NP. The caudal vertebrae were cut with a no. 7 surgical line and put into the normal saline vessel for

standby. The skin of the lumbar vertebrae of rats was depilated and sterilized with 75% alcohol. Under an aseptic condition, the skin and muscle of the back were cut along the posterior midline to expose the spine. The L2-5 spine lamina was removed to expose the dura mater of the lumbar vertebrae. The caudal disc was carefully placed in the lumbar epidural and sutured layer by layer. The rats in the HMM group and Met12 group were intervened for 1 month after the LDH model establishment. According to our previous experimental results, the materials were obtained after 3 months of intervention.

**2.3. Hui Medicine Moxibustion Treatment.** The rats in the HMM group were treated one month after being modeled. LDH rats were fixed on the fixator and shaved along the longitudinal axis of the rat lumbar spine, and then, the special 2 cm × 0.5 cm × 0.5 cm rectangular iron moxibustion device was placed along the longitudinal axis of lumbar vertebrae, covering the surface of L1-L6 vertebrae. The center of the iron moxibustion device was placed in the L3-L4 vertebrae gap of rats, and then, 2 g of moxa was ignited in the moxibustion groove. The hot iron moxibustion device could make the local skin flush, once a day, 10 minutes each time, and the samples were collected 3 months later.

LDH rats in the HMM+Met12 group were intervened one month after modeling, and the method of moxibustion intervention was the same as that of the HMM group. After HMM treatment, the rats were intraperitoneally injected with Met12 (10 μg/kg/week), and the samples were collected 3 months after the intervention.

Rats in the LDH group were fixed on the fixator for 10 min, once a day after 1 month of modeling, without other intervention, and the samples were taken after 3 months of fixation.

Rats in the normal group were LDH rats that were not given modeling and intervention, and the samples were taken after 3 months.

**2.4. Locomotor Activity Test.** The locomotor activity tests were proceeded according to the previous study [13]. Briefly, the gait recovery of rats was observed and recorded every day after the surgery. Rats were placed in the open field to observe their motor function. Rats with a normal gait and no deformity of toes were recorded as having 0 score. Rats with a slight limp in gait were recorded as 1 score. Rats with weakness of hind limbs or moderate claudication were recorded as 2 scores. Rats with paraplegia of hind limbs, obvious claudication, or an abnormal contralateral toe were recorded as 3 scores.

**2.5. Mechanical Allodynia Test.** The pain threshold was measured by a paw tenderness instrument when the rats were waking [14]. Rats were placed in plexiglass boxes with a wire mesh floor. After 15 min, the needle was pointed at the palmar surface of the rat's hind foot through the reflector, and the needle vertically stimulated the middle of the rat's hind foot continuously from the lower part of the metal screen. When the rat's foot retracted or licked, the needle fell, which was regarded as a positive reaction. The stimulation inten-

sity was automatically displayed on the instrument screen, which was the threshold of mechanical claw retraction. Each test was repeated 3 times, with an interval of 5 min. The change percentage of tactile threshold (%) = (immediate pain threshold – basic pain threshold)/basic pain threshold × 100 %.

**2.6. Histopathological Analysis.** Nucleus pulposus tissues were fixed in 4% paraformaldehyde for 24 h and embedded in paraffin and then sliced into 5-6 μm paraffin sections. Sections were stained with hematoxylin and eosin (HE, Beyotime, China) stain. Five fields were randomly selected and observed by light microscopy (Olympus, Tokyo, Japan).

**2.7. Immunohistochemistry (IHC).** IHC experiments were performed as described in a previous report [15]. Briefly, nucleus pulposus tissues were harvested into PBS-buffered formaldehyde, embedded in paraffin, and then cut into 4 μm thick sections. A monoclonal antibody against FasL (Abcam, Cambridge, UK) was used for this analysis. A horseradish peroxidase diaminobenzidine kit was used to detect immunoreactivity, and samples were counterstained with hematoxylin. A microscope (Olympus, Tokyo, Japan) was used to capture a representative area containing FasL-positive tissue (magnification, 200x).

**2.8. Western Blotting.** Based on a previous report, proteins were measured through western blotting [15]. For the isolation of proteins in the tissues, nucleus pulposus tissues were first ground in chilled mortar in the presence of liquid nitrogen. Immediately after grinding, the tissue powder was lysed with radioimmunoprecipitation assay (RIPA) buffer. Total proteins were then separated on polyacrylamide gels and transferred to a polyvinylidene difluoride membrane before being probed overnight at 4°C with antibodies (anticleaved-caspase-3, anticleaved-caspase-8, anti-cleaved-caspase-9, anti-MMP-1, anti-MMP-2, anti-MMP-3, anti-MMP-13, and anti-ADAMTS-4; Abcam, Cambridge, UK), then washed three times with PBST. Then, membranes were treated with the corresponding secondary antibodies. Finally, the membrane was processed using an ECL kit for color reaction. Western blotting results were normalized to those of GAPDH for quantification.

**2.9. TUNEL.** The TUNEL method using an in situ cell death detection kit (Roche, USA) was performed to detect the apoptosis of NP cells. Paraffin sections were deparaffinized and rehydrated with xylene and gradient ethanol. Then, sections were treated with proteinase K at room temperature for 30 min. After washing twice with PBS, specimens were added with 50 μL TUNEL reaction mixture and incubated in the dark for 60 min at room temperature, and then, 50 μL converter POD was added and reacted at 37°C in the dark for 30 min. After rinsing with PBS 3 times, the sections were colored with 50 μL DAB for 10 min at room temperature and counterstained with hematoxylin for a few seconds. A microscope (Olympus, Tokyo, Japan) was used to capture the representative stained pictures.



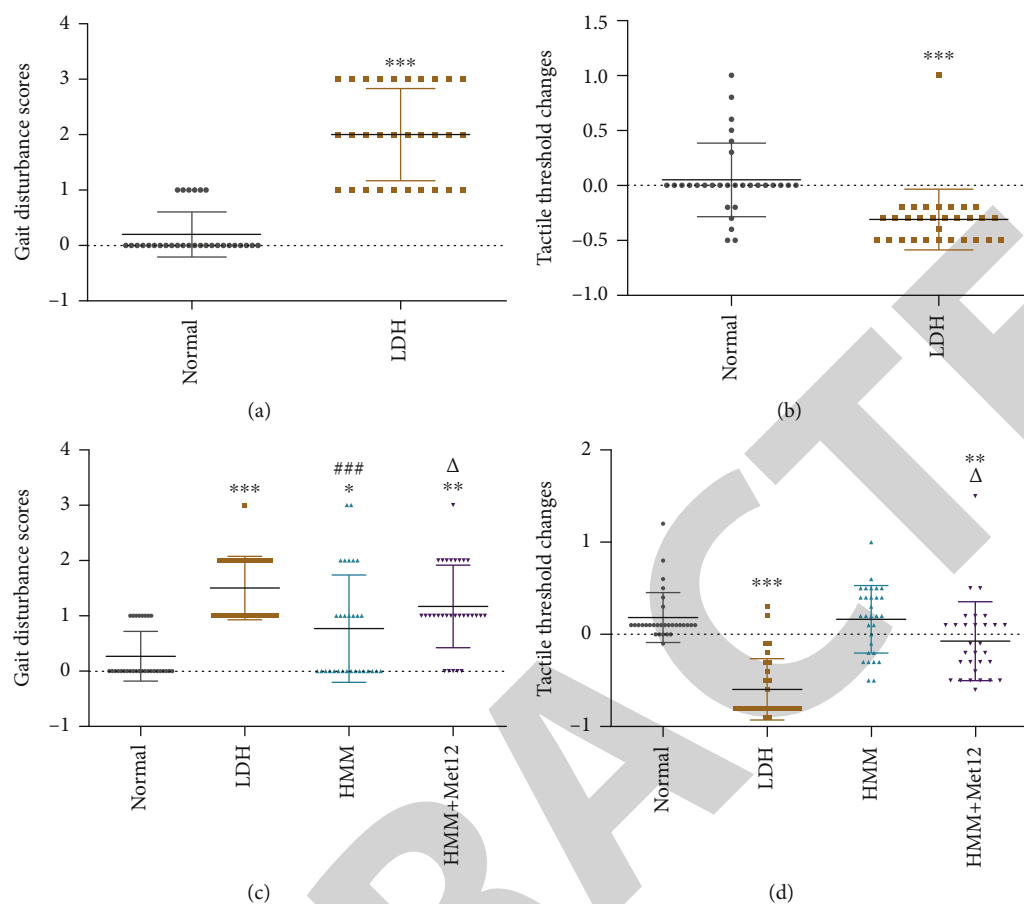


FIGURE 1: Behavioral assessments in lumbar disc herniation (LDH) rats with moxibustion treatment of Hui medicine (HMM). Locomotor activity tests (a) and tactile function tests (b) were performed to assess the success of LDH rat models. Locomotor activity tests (c) and tactile function tests (d) were performed with or without the moxibustion treatment of Hui medicine. A negative value of paw withdrawal latency indicates mechanical hyperalgesia. \* $P < 0.05$ , \*\* $P < 0.01$ , and \*\*\* $P < 0.001$  vs. the normal group; # $P < 0.05$  and ## $P < 0.01$  vs. the LDH group; and  $\Delta P < 0.05$  vs. the HMM group.

**2.10. Statistical Analysis.** The SPSS version 26.0 and GraphPad Prism 8 statistical software packages were used for data analysis. Each result is presented as means  $\pm$  standard deviation. The significance of differences among samples was tested by one-way ANOVA followed by Turkey's post hoc test.  $P < 0.05$  was considered significant. ImageJ software was used to carry out the semiquantitative analysis.

### 3. Results

**3.1. Hui Medicine Moxibustion (HMM) Promotes Recovery of Motor and Tactile Function in Rats with LDH.** We established the LDH rat model by nucleus pulposus transplantation and assessed the behavior of LDH rats. There was no obvious motor dysfunction and no difference in mechanical withdrawal thresholds to stimulations before the LDH surgical procedures in all rats. As shown in Figures 1(a) and 1(b), the locomotor activity of rats with LDH was significantly decreased compared with normal rats, and the mechanical withdrawal thresholds of LDH rats were markedly reduced compared with withdrawal latencies before surgery. HMM treatment significantly improved the behavioral ability of rats with LDH surgery, and the tactile function was also

recovered to a large extent by the end of our experiments. The behavior of LDH rats was improved with HMM treatment but suppressed with the inhibitor of Fas, MET12 (Figures 1(c) and 1(d)).

**3.2. HMM Promotes the Formation of Neovascularization of the Lumbar Intervertebral Disc.** Vascularization plays an important role in the reabsorption process of intervertebral disc herniation. HE staining was used to observe the histological degeneration of the lumbar intervertebral disc. We observed clearly morphological alterations and degenerative nucleus pulposus in the LDH group, which were repaired in the HMM group and mild reparation in the HMM+Met12 group (Figure 2(a)). CD34 immunohistochemical staining further proved the formation of new blood vessels (Figure 2(b)). The expression of VEGF was also detected to further assess the formation of neovascularization of the lumbar intervertebral disc (Figure 2(c)).

**3.3. HMM Induces Apoptosis in Rat NP Tissues through FasL.** To examine whether HMM facilitates the reabsorption of herniated disc tissue by inducing apoptosis, the expression of FasL in NP tissues was assessed by



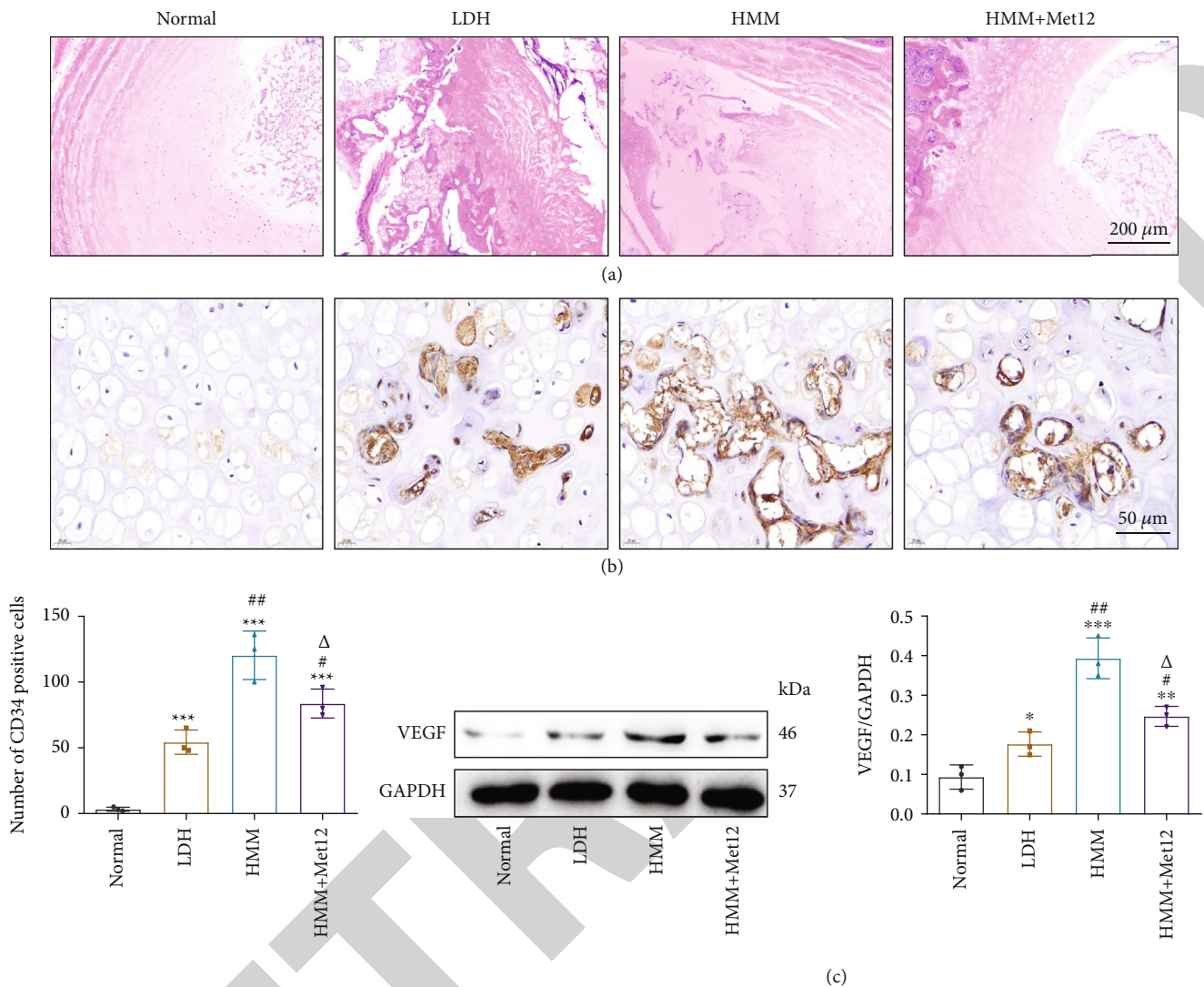


FIGURE 2: HMM promotes the formation of neovascularization of lumbar intervertebral disc tissue. (a) Representative HE staining (10x) of nucleus pulposus tissues, which was used to observe the histological degeneration of the intervertebral disc. Scale bar = 200  $\mu$ m. (b) Representative of CD34 expression, determined by immunohistochemical staining (40x). Scale bar = 50  $\mu$ m. (c) Western blotting was used to detect the protein expression of VEGF. \* $P < 0.05$ , \*\* $P < 0.01$ , and \*\*\* $P < 0.001$  vs. the normal group; # $P < 0.05$  and ## $P < 0.01$  vs. the LDH group; and  $\Delta P < 0.05$  vs. the HMM group.

immunohistochemistry. As shown in Figure 3(a), the number of FasL-positive cells was significantly increased in the LDH group compared with the normal group, with an even higher number in the HMM group, which were then decreased in the HMM+Met12 group. The TUNEL staining in the NP tissues showed a similar trend among the four groups (Figure 3(b)). The protein expression levels of C-caspase-3, C-caspase-8, and C-caspase-9 in NP tissues were also detected to assess the apoptosis of NP cells at the molecular level. The protein expression levels of C-caspase-3, C-caspase-8, and C-caspase-9 were significantly increased in the LDH group compared with the normal group, which were even higher in the HMM group and restored in the HMM+Met12 group (Figure 3(c)).

3.4. HMM Promotes the Reabsorption of Lumbar Disc Herniation through Extracellular Matrix Degradation. The

reabsorption of herniated disc tissue is also related to the imbalance of matrix synthesis and degradation. The protein expression levels of MMP-1, MMP-2, MMP-3, MMP-13, and ADAMTS-4 were detected. The protein expression levels of MMP-1, MMP-2, MMP-3, MMP-13, and ADAMTS-4 were markedly increased in the HMM group and rescued with the FasL inhibitor (Figure 4).

4. Discussion

In recent decades, the incidence rate of LDH has increased worldwide, especially among adolescent and middle-aged people [16]. Not all LDH patients can be treated with surgery. According to statistics, only 10% to 20% of patients are suitable for surgical treatment [17], the incidence of postoperative complications is 15-30%, and the recurrence rate of LDH after the operation can reach 25% [18].

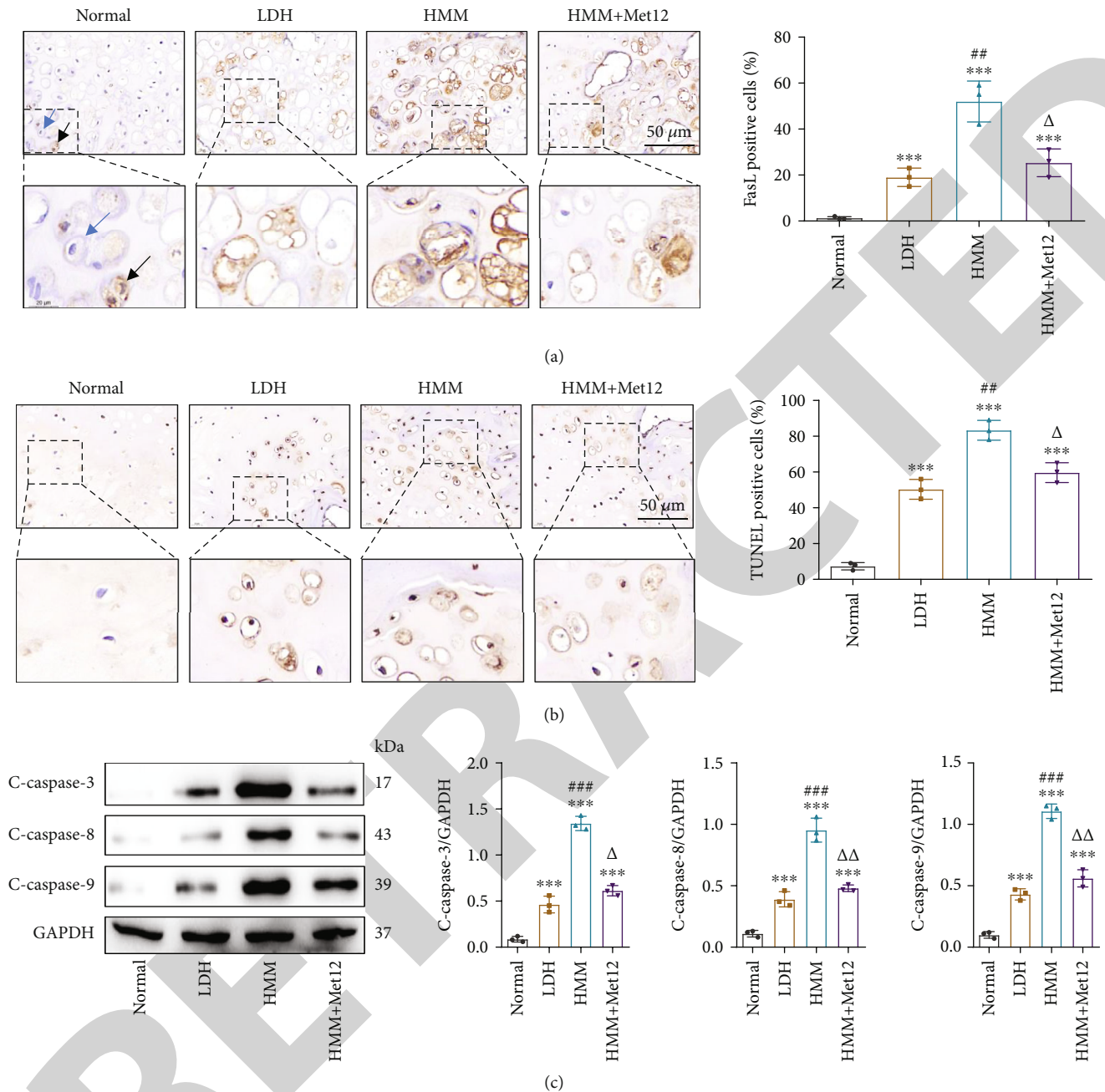


FIGURE 3: HMM promotes the apoptosis of lumbar intervertebral disc tissue through FasL. (a) Representative images of the results of the expression of FasL in nucleus pulposus cells, assessed by immunohistochemistry (40x). Black arrows indicate positive staining, and blue arrows indicate negative staining. Scale bar = 50  $\mu\text{m}$ . (b) Representative images of TUNEL staining (40x) in the nucleus pulposus cells. Scale bar = 50  $\mu\text{m}$ . (c) The expression levels of C-caspase-3, C-caspase-8, and C-caspase-9 in nucleus pulposus cells were detected by western blotting. \* $P < 0.05$ , \*\* $P < 0.01$ , and \*\*\* $P < 0.001$  vs. the normal group; ## $P < 0.01$  and ### $P < 0.001$  vs. the LDH group; and  $\Delta P < 0.05$  and  $\Delta\Delta P < 0.01$  vs. the HMM group.

Therefore, nonsurgical treatment is still the best choice for most LDH patients. HMM is one of the most distinctive treatments of Chinese Hui medicine [19]. This therapy not only has good effects in the treatment of lumbar disc herniation but also can prevent the degeneration of the lumbar disc [20], but the mechanism of HMM remains unclear. In this study, we established the LDH rat model and confirmed that the simulation of self-nucleus pulposus implantation led

to persistent motor dysfunction and mechanical hyperalgesia and revealed that HMM promoted the absorption of the nucleus pulposus through the Fas/FasL pathway and alleviated disc herniation.

Vascularization plays an important role in the resorption of herniated disc tissue, and neovascularization is closely related to the degree of absorption and prognosis of LDH [21]. Previous studies have shown that the higher the degree

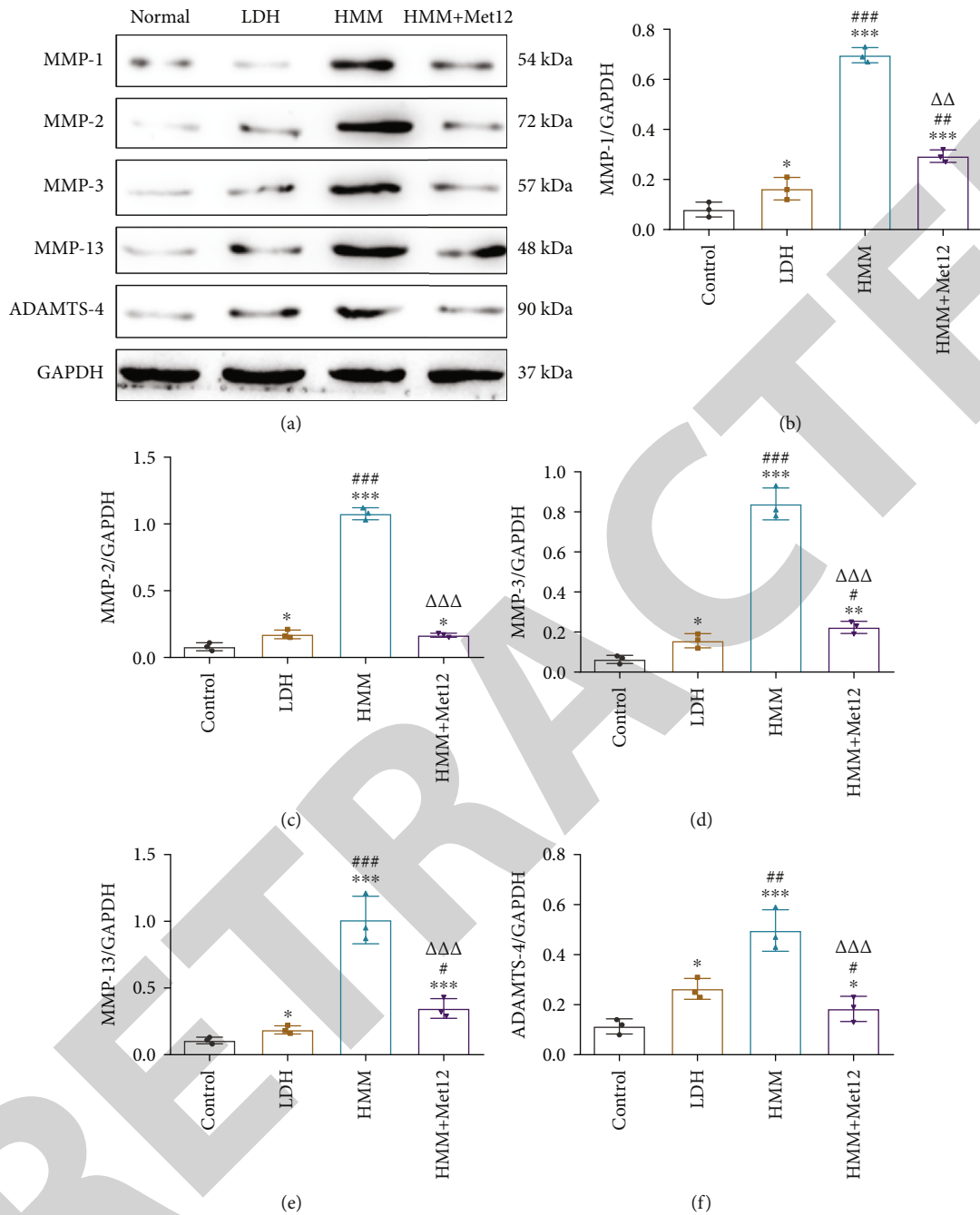


FIGURE 4: HMM promotes the reabsorption of lumbar disc herniation by promoting extracellular matrix degradation. (a) The protein expression levels of MMP-1, MMP-2, MMP-3, MMP-13, and ADAMTS-4 were detected using western blotting. (b–f) Semiquantitative analysis of western blotting. \* $P < 0.05$ , \*\* $P < 0.01$ , and \*\*\* $P < 0.001$  vs. the normal group; ## $P < 0.01$  and ### $P < 0.001$  vs. the LDH group; and ΔΔ $P < 0.01$  and ΔΔΔ $P < 0.001$  vs. the HMM group.

of vascularization of the herniated disc tissue is, the more obvious the spontaneous absorption is. It has been reported that blood vessels have appeared in five types of disc hernia—extruded, bulging, prolapsed, protrusion, and sequestered—and mainly in the extruded type [22]. Therefore, the growth of neovascularization is a potential factor for the resorption of prominent nucleus pulposus. VEGF and CD34 have been proven to be implicated in the neovascularization of herniated disc tissues [23, 24]. In our study, HMM therapy effectively promoted the neovascularization of LDH

rats, with high expression of VEGF and CD34 in the rats treated with HMM.

Apoptosis of the nucleus pulposus plays an important role in the pathological process of RHL. FasL has many effects on maintaining immunity, inducing apoptosis, and mediating inflammation under different conditions. FasL is expressed in the lumbar disc and nucleus pulposus, and the abnormal expression of FasL induces apoptosis of the nucleus pulposus cells, which may play an important role in the pathogenesis of lumbar disc herniation [25].



Apoptosis was observed when the nucleus pulposus cells were cultured with FasL for 24 h, and caspase-3 and caspase-8 expression levels were increased with the increase of the FasL concentration, which indicated that this membrane pathway was involved in the apoptosis of Fas-induced nucleus pulposus cells; caspase-9 was activated when FasL reached a certain concentration, which activated the mitochondrial apoptosis pathway [26]. The effect of the Fas/FasL signaling pathway on nucleus pulposus cells has been widely accepted. Besides, Fas/FasL has also been validated to have a connection with vascularization [27]. Our experiments have also detected that HMM therapy can activate caspase-3, caspase-8, and caspase-9 and observed abnormal expression of FasL.

The resorption of herniated disc tissue is also related to the imbalance of matrix synthesis and degradation. The apoptosis of nucleus pulposus cells will gradually cause the imbalance of extracellular matrix components and metabolic disorder [28]. MMPs are important enzymes in the extracellular matrix. When the activity of MMPs increases, the levels of TIMPs decrease, and matrix synthesis and degradation are unbalanced, which promotes the degradation of protrusions [29]. It is suggested that the reabsorption of the herniated disc is accomplished by the coordination of various protein enzymes. It has been found that the expression of ADAMTS-4 and MMP-3, MMP-8, and MMP-9 in the herniated lumbar disc is highly consistent [30]. Studies have shown that macrophage infiltration and MMP-1 and MMP-3 expression were observed by implanting the disc tissue into the back muscles of rats, and the resorption was promoted by activating the MMPs [31]. As a kind of proteoglycan hydrolase, ADAMTS also participates in the decomposition of the disc matrix and the process of reabsorption [32]. Therefore, it is of great significance to study the effects of the Fas/FasL signaling pathway on the extracellular matrix environment of the nucleus pulposus. We detected the activity of MMP-1, MMP-2, MMP-3, MMP-13, and ADAMTS-4 in the rat nucleus pulposus treated with HMM, which indicated that the treatment of HMM effectively promoted the resorption of the herniated disc.

## 5. Conclusions

Our study found that the Hui medicine moxibustion promoted the apoptosis of the nucleus pulposus cells through the Fas/FasL pathway and then promoted the absorption of the nucleus pulposus. We also clarified the mechanism of the therapeutic effect of the moxibustion on lumbar disc herniation and provided a theoretical and experimental basis for the prevention and treatment of disc herniation by Hui medicine moxibustion.

## Abbreviations

RHLD: Resorption of the herniated lumbar disc  
 HMM: Hui medicine moxibustion  
 LDH: Lumbar disc herniation  
 MMP: Matrix metalloproteinases  
 NP: Nucleus pulposus

VEGF: Vascular endothelial growth factor  
 CT: Computed tomography  
 TNF: Tumor necrosis factor  
 DD: Death domain  
 FADD: Fas-associating protein with death domain.

## Data Availability

The data used to support the findings of this study are available from the corresponding authors upon request.

## Ethical Approval

All experiments involving rats in our study were approved by the Ethics Committee of the General Hospital of Ningxia Medical University (approval no.: 2017-052).

## Conflicts of Interest

The authors declare that they have no competing interests.

## Authors' Contributions

JFX, QL, JYS, and YMZ performed the experiment and analyzed and interpreted the data. JFX was a major contributor in writing the manuscript. YXW, LY, YYS, BWS, NY, and XBT were responsible for literature search, data analysis, and visualization. RZL and WYW were major contributors in critically revising the manuscript; they were listed as corresponding authors. All authors read and approved the final manuscript.

## Acknowledgments

This study was supported by the National Natural Science Foundation of China (Grant Nos.: 81760905 and 82060852), Key Research and Development Project of Ningxia (Grant No.: 2019BEB04027), Scientific Research Project of Ningxia Higher Education Institutions (Grant No.: NGY2020030), Health and Family Planning Appropriate Technology Promotion Project (Grant No.: 2020-007), and Central Government of Ningxia Hui Autonomous Region Guided Local Science and Technology Development Project (Grant No.: 2021YDDF0029).

## References

- [1] C. W. Chang, P. H. Lai, C. M. Yip, and S. S. Hsu, "Spontaneous regression of lumbar herniated disc," *Journal of the Chinese Medical Association*, vol. 72, no. 12, pp. 650–653, 2009.
- [2] J. G. Teplick and M. E. Haskin, "Spontaneous regression of herniated nucleus pulposus," *AJR. American Journal of Roentgenology*, vol. 145, no. 2, pp. 371–375, 1985.
- [3] C. Cunha, A. J. Silva, P. Pereira, R. Vaz, R. M. Gonçalves, and M. A. Barbosa, "The inflammatory response in the regression of lumbar disc herniation," *Arthritis Research & Therapy*, vol. 20, no. 1, p. 251, 2018.
- [4] H. Haro, T. Domoto, S. Maekawa, T. Horiuchi, H. Komori, and Y. Hamada, "Resorption of thoracic disc herniation. Report of 2 cases," *Journal of Neurosurgery. Spine*, vol. 8, no. 3, pp. 300–304, 2008.

## Retraction

# Retracted: The Use of Chest Radiographs and Machine Learning Model for the Rapid Detection of Pneumonitis in Pediatric

### BioMed Research International

Received 20 June 2023; Accepted 20 June 2023; Published 21 June 2023

Copyright © 2023 BioMed Research International. This is an open access article distributed under the Creative Commons Attribution License, which permits unrestricted use, distribution, and reproduction in any medium, provided the original work is properly cited.

This article has been retracted by Hindawi following an investigation undertaken by the publisher [1]. This investigation has uncovered evidence of one or more of the following indicators of systematic manipulation of the publication process:

- (1) Discrepancies in scope
- (2) Discrepancies in the description of the research reported
- (3) Discrepancies between the availability of data and the research described
- (4) Inappropriate citations
- (5) Incoherent, meaningless and/or irrelevant content included in the article
- (6) Peer-review manipulation

The presence of these indicators undermines our confidence in the integrity of the article's content and we cannot, therefore, vouch for its reliability. Please note that this notice is intended solely to alert readers that the content of this article is unreliable. We have not investigated whether authors were aware of or involved in the systematic manipulation of the publication process.

Wiley and Hindawi regrets that the usual quality checks did not identify these issues before publication and have since put additional measures in place to safeguard research integrity.

We wish to credit our own Research Integrity and Research Publishing teams and anonymous and named external researchers and research integrity experts for contributing to this investigation.

The corresponding author, as the representative of all authors, has been given the opportunity to register their agreement or disagreement to this retraction. We have kept a record of any response received.

### References

- [1] K. Alshamrani, H. A. Alshamrani, A. A. Asiri, F. F. Alqahtani, W. T. Mohammad, and A. H. Alshehri, "The Use of Chest Radiographs and Machine Learning Model for the Rapid Detection of Pneumonitis in Pediatric," *BioMed Research International*, vol. 2022, Article ID 5260231, 11 pages, 2022.



## Research Article

# The Use of Chest Radiographs and Machine Learning Model for the Rapid Detection of Pneumonitis in Pediatric

**Khalaf Alshamrani** <sup>1</sup>, **Hassan A. Alshamrani** <sup>1</sup>, **Abdullah A. Asiri**,<sup>1</sup> **F. F. Alqahtani** <sup>1</sup>,  
**Walid Theib Mohammad** <sup>2</sup> and **Ali H. Alshehri**<sup>1</sup>

<sup>1</sup>Radiological Sciences Department, College of Applied Medical Sciences, Najran University, Saudi Arabia

<sup>2</sup>Al-Hussein Bin Talal University, Princess Aisha Bint Al Hussein College for Nursing and Health Sciences, Jordan

Correspondence should be addressed to Hassan A. Alshamrani; hamalshamrani@nu.edu.sa

Received 13 June 2022; Revised 28 June 2022; Accepted 1 July 2022; Published 21 July 2022

Academic Editor: Dinesh Rokaya

Copyright © 2022 Khalaf Alshamrani et al. This is an open access article distributed under the Creative Commons Attribution License, which permits unrestricted use, distribution, and reproduction in any medium, provided the original work is properly cited.

Pneumonia is a common lung disease that is the leading cause of death worldwide. It primarily affects children, accounting for 18% of all deaths in children under the age of five, the elderly, and patients with other diseases. There is a variety of imaging diagnosis techniques available today. While many of them are becoming more accurate, chest radiographs are still the most common method for detecting pulmonary infections due to cost and speed. A convolutional neural network (CNN) model has been developed to classify chest X-rays in JPEG format into normal, bacterial pneumonia, and viral pneumonia. The model was trained using data from an open Kaggle database. The data augmentation technique was used to improve the model's performance. A web application built with NextJS and hosted on AWS has also been designed. The model that was optimized using the data augmentation technique had slightly better precision than the original model. This model was used to create a web application that can process an image and provide a prediction to the user. A classification model was developed that generates a prediction with 78 percent accuracy. The precision of this calculation could be improved by increasing the epoch, among other subjects. With the help of artificial intelligence, this research study was aimed at demonstrating to the general public that deep-learning models can be created to assist health professionals in the early detection of pneumonia.

## 1. Introduction

Pneumonia is a serious infection that affects the lungs and is caused by an acute respiratory infection. Inflammation of the lung sacs is usually caused by one of two pathogens: bacteria or viruses [1]. A common lung disease is the leading cause of death worldwide, affecting primarily children (18% of deaths in children under the age of five), the elderly, and patients with other diseases [2, 3]. Although the initial bacterial and viral pneumonia symptoms are similar, the treatment for each is very different. There are various imaging diagnosis techniques available today. While many of them are becoming more accurate, they are also very expensive and inaccessible to most populations or regions. Furthermore, [3] highlights the “shortage of radiology

experts in low-resource countries or rural areas” or the “endless waiting lists for diagnoses in certain areas,” which leads to an increase in the severity of the disease and, as a result, its mortality rate [2]. And while diagnostic radiography is the cheapest diagnostic technique, it is also the least ionizing and faster to apply than other techniques. However, the opacities that can be visualized can cause the analyst to misinterpret the results [4]. Many of the studies cited in the bibliographic references section develop machine learning techniques based on deep learning models (hereinafter, deep learning) such as convolutional neural networks (CNN), as well as diagnostic techniques for high-resolution images such as computed tomography (CT). It describes the development of a deep learning architecture for diagnosing severe cases of pneumonia via chest X-ray. They used a data set

from the Radiological Society of North America, emphasizing that the data set they provided to the convolutional neural network is specialised in constitutive zones [5].

The goal is to develop a machine learning model that helps minimise diagnostic time and improve diagnostic accuracy with the use of radiographs, taking into account that not all hospitals or health care centres have access to more precise diagnostic techniques, either due to budget or architecture, and that there are differences between different regions of the same country, and with the goal of reaching a larger population faster. This project's data classification (images) will correspond to the data collected [6]. This includes 5,856 JPEG chest X-rays taken on children aged 1 to 5 years old in the Canton region and obtained from the Kaggle and Mendeley database platforms (Guangzhou). This database includes both radiographs with and without pneumonia (normal). This project will be divided into the following phases based on the above information and the study conducted [7].

- (1) Medical detail analysis phase: the most relevant pulmonary radiological characteristics for the detection of pneumonia will be studied, and the differences between viral and bacterial infection will also be analyzed
- (2) Image labeling phase: data classification with which it is going to work already has the validation of 3 expert technicians in diagnostic imaging. So, the information obtained in phase 1 will be validated in this phase
- (3) Processing phase: in this phase, the size of the images and possible treatment of their grayscale will be standardized. There are different studies that have used the CNN learning model. In addition, to pretrain, the model, freely available artificial intelligence (AI) libraries developed with Python can be used, such as TensorFlow. The possibility of learning transfer and open-access AI libraries will be studied [7]
- (4) Training and testing phase: the chosen deep learning model will be trained in this phase. Its performance will be evaluated and validated with the comparisons of the classifications previously made by the experts [7]
- (5) Statistical analysis phase: the results obtained will be analyzed to determine the accuracy of the classification. This will help me decide if a model upgrade is needed
- (6) Information visualization phase: the idea is to bring the classification model closer to the user; for this reason, work will be done to generate a web application that accepts images of chest X-rays in JPEG format and gives a result that is easy to understand for the user

The studies of [3, 7] influenced the method used. They have also influenced the strategies learned in relation to personal problem analysis and resolution. Other methods, such

as those described, have chosen to follow a combined radiograph model that we believe can meet expectations.

*1.1. Deep Learning and Chest Radiographs.* Chest radiography is a diagnostic tool that can be used for the diagnosis of pulmonary pneumonia since it is considered a "fast" tool (the patient has to be exposed to the test for a short time compared to others), less ionizing than others, and the least expensive [3]. Although the final image that an X-ray can offer, in this case of the chest, is full of opacities, the grays usually correspond to known pulmonary structures. Thanks to the studies of opacities, radiologists are able to determine whether or not there is oedema or infection.

With the evolution of medicine and its convergence with artificial intelligence, deep learning comes to our knowledge. Together with the study of chest X-rays, it poses a very powerful diagnostic support tool [8]. As shown in Figure 1(a), with the "naked" eye, it seems almost impossible to differentiate the different lung structures, and the judgment becomes more complicated when the images in Figure 1 are exposed. Grayish tones can be intuited between the viral and bacterial pneumonia images in relation to the normal radiograph. But the difficulty of this diagnosis is clearly appreciated only at first sight.

Thanks to deep learning tools, image classification models can be proposed that help distinguish between the different opacities and grays that usually appear in chest X-rays and can analyze in a minimum time all the peculiarities of the image from a previous training with a database that helps the model to be able to create a classification or prediction relationship, something that has been tested with promising results in the consulted bibliography.

## 2. Methodology

*2.1. Data Set.* The data used in this project was obtained through a platform with a large number of freely accessible databases and images called Kaggle. Mendeley was also used to access the data published in Kaggle. For this project, the data published [7] consisted of chest X-rays performed on children between 1 and 5 years of age in the Canton region. The data has been published in Kaggle by Paul Mooney, its creation is dated March 22, 2018, and its last update (version 2) was on March 24, 2018.

The 1 GB file contains 5856 images in JPEG format classified into different groups:

- (i) Normal chest X-ray images
- (ii) Bacterial pneumonia thoracic X-ray images
- (iii) Viral pneumonia thoracic X-ray images

### 2.2. Environment

*2.2.1. Work Environment.* To carry out this project, Google Collaboratory ("Colab") has been used, which has allowed the code to be executed through the browser and has been able to avoid the problems of lack of memory that occurred in the MacOS (M1) operating system initially used.

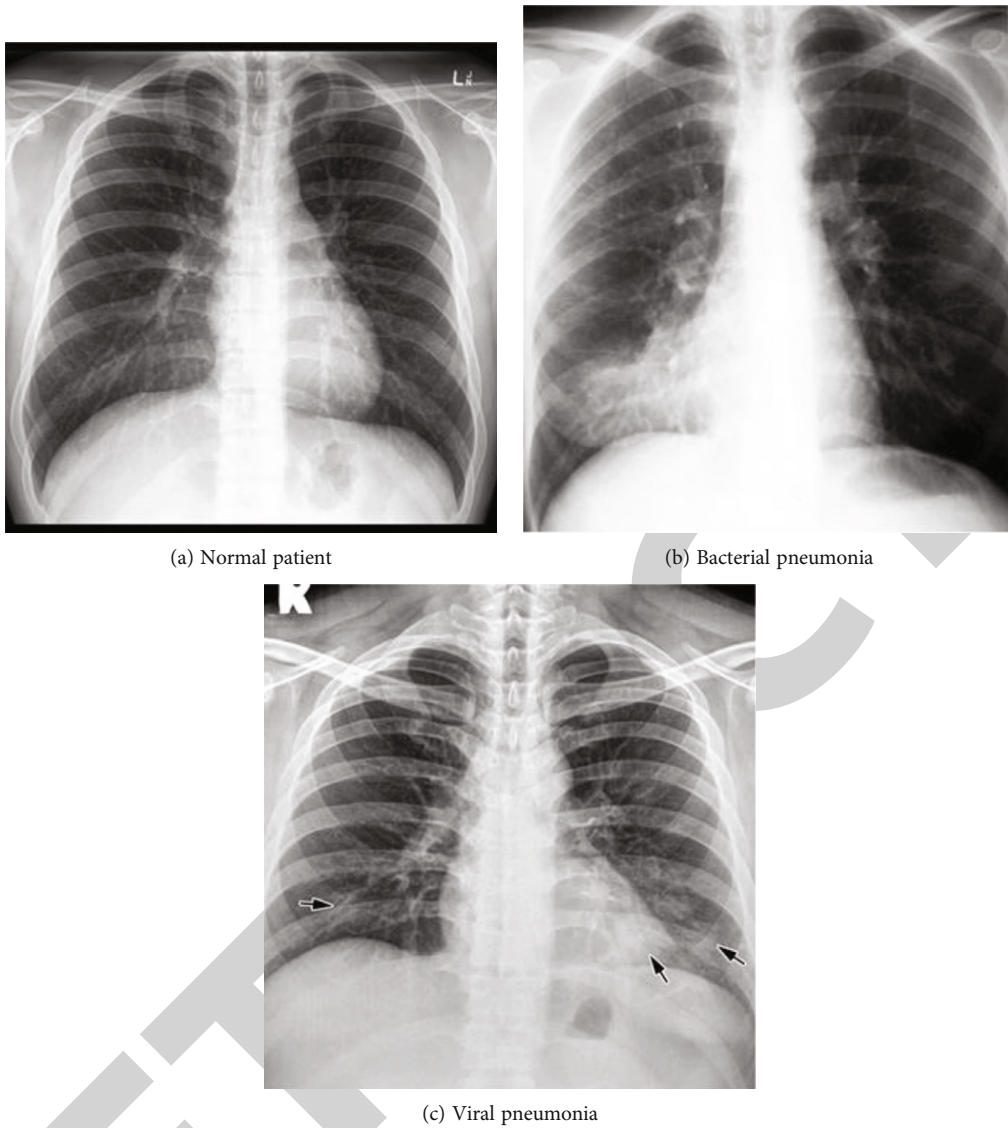


FIGURE 1: Chest radiographs: normal, viral pneumonia, and bacterial pneumonia.

2.2.2. *Programming Language.* Python was chosen as the programming language for the development of this project. It was chosen because it is a simple language when programming and because it has the TensorFlow tool.

2.2.3. *Used Bookstores.* The libraries used (Figure 2) in this project have been presented:

2.3. *Data Environment.* The data was stored in Drive1 of the UOC’s institutional Google account. In the dataset folder, there are the Train (training), Test (Test), and Val (validation) folders that contain the image subgrouped according to diagnosis: normal, pneumonia bacteria (bacterial pneumonia), and pneumonia virus (viral pneumonia). The general working path was drive/MyDrive/TFM\_Raquel\_Sauras/datasets/chest\_xray.

2.3.1. *Data Reconfiguration.* As shown in Figure 3, the images were reconfigured to the same smaller size, 64 × 64,

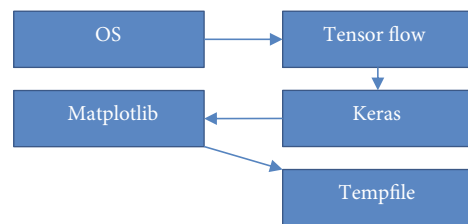


FIGURE 2: Programming libraries.

and transformed to “RGB” so that each of the images had the same number of channels (3).

2.3.2. *Data Classification.* The imported data had already been initially grouped as follows:

- (i) Train (training): images classified as training. These are the images initially used to train the [7]

```

Configuration

[ ] # Resizing
img_height = 64
img_width = 64
channels = 3
batch_size = 32
epochs = 20
color_mode='rgb'

dataset_path = "/content/drive/MyDrive/TFM_Raquel_Sauras/datasets/chest_xray"

```

FIGURE 3: Image size configuration script.

```

Classification datasets

# Classifying train dataset in 3 labels

train_ds = tf.keras.utils.image_dataset_from_directory(
    join(dataset_path, "train"),
    validation_split=0.2,
    subset="training",
    seed=123,
    image_size=(img_height, img_width),
    batch_size=batch_size)

validation_ds = tf.keras.utils.image_dataset_from_directory(
    join(dataset_path, "train"),
    validation_split=0.2,
    subset="validation",
    seed=123,
    image_size=(img_height, img_width),
    batch_size=batch_size)

# Classifying test dataset in 3 labels
test_ds = tf.keras.preprocessing.image_dataset_from_directory(
    join(dataset_path, "test"),
    color_mode=color_mode,
    image_size=(img_height, img_width),
    batch_size=batch_size)

```

FIGURE 4: Script on the classification of images according to groups.

- (a) Test (test): corresponds to the images that are used to test the model in question
- (b) Val (validation) in this folder are the images to evaluate the model

Although initially the data was already regrouped, it was decided not to have the initial validation folder since it only contained images of bacterial pneumonia. A random sample was generated to generate the training (train) and validation

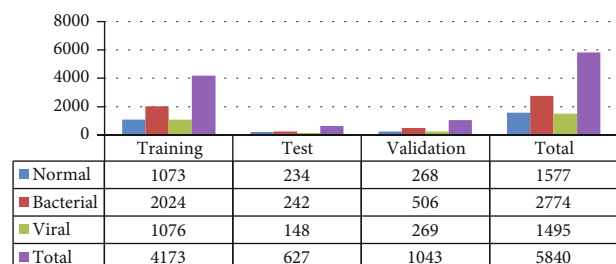


FIGURE 5: Classification of images according to type and group.



```

# Showing found labels
class_names = train_ds.class_names
nClasses = len(class_names)
print("Train classes", class_names)
print('Total number of outputs : ', nClasses)

print("Validation classes", validation_ds.class_names)
print('Total number of validation outputs : ', len(validation_ds.class_names))

print("Test classes", test_ds.class_names)
print('Total number of outputs : ', len(test_ds.class_names))

# Showing 10 images from de training set already resized
show_images(class_names, train_ds)

```

FIGURE 6: Script where the data is displayed according to the random subclassification.

```

Training the model

from tensorflow.keras import datasets, layers, models

num_classes = len(class_names)

model = models.Sequential([
    layers.Rescaling(1./255, input_shape=(img_height, img_width, channels)),
    layers.Conv2D(16, 3, padding='same', activation='relu'),
    layers.MaxPooling2D(),
    layers.Conv2D(32, 3, padding='same', activation='relu'),
    layers.MaxPooling2D(),
    layers.Conv2D(64, 3, padding='same', activation='relu'),
    layers.MaxPooling2D(),
    layers.Flatten(),
    layers.Dense(128, activation='relu'),
    layers.Dense(num_classes)
])

```

FIGURE 7: CNN model script using the Sequential () function.

```

# Compilation of the model
model.compile(optimizer="adam", loss=tf.keras.losses.SparseCategoricalCrossentropy(from_logits=True), metrics=['accuracy'])

# Training the model
training_model = model.fit(train_ds, validation_data=validation_ds, epochs=epochs)

```

FIGURE 8: Compilation and training phase.

(val) subgroups, as can be seen in Figure 4. With this decision, the sample of images that were initially 5,856 remained at 5,840, losing 16 images from the initial validation folder.

The data was classified as follows (Figure 5):

To verify that the images had been subclassified according to the parameters, the number of classes found was also shown (Figures 4 and 6).

**2.4. Creation of the Model.** The different articles consulted used the CNN model as a reference model in deep learning to classify images. So, he used this model for the classification of chest X-ray images.

To train the model, the Sequential () function was used, to which three convolutional layers were added through the Conv2D class (16, 32, and 64), and when the data were normalized, the “ReLU” function was used as an activator.

The MaxPooling2D function is responsible for reducing the sample in width and height (2D) at the end of each added layer. Ultimately, the flatten() layer is added.

Finally, the Dense function of the union of the layers, with 128 units, was used as the output layer [9].

**2.5. Training and Validation of the Model.** As shown in Figure 7, the CNN model was generated and was compiled



```
# Accuracy
acc = training_model.history['accuracy']
val_acc = training_model.history['val_accuracy']

loss = training_model.history['loss']
val_loss = training_model.history['val_loss']
```

FIGURE 9: Study of the accuracy of the CNN model.

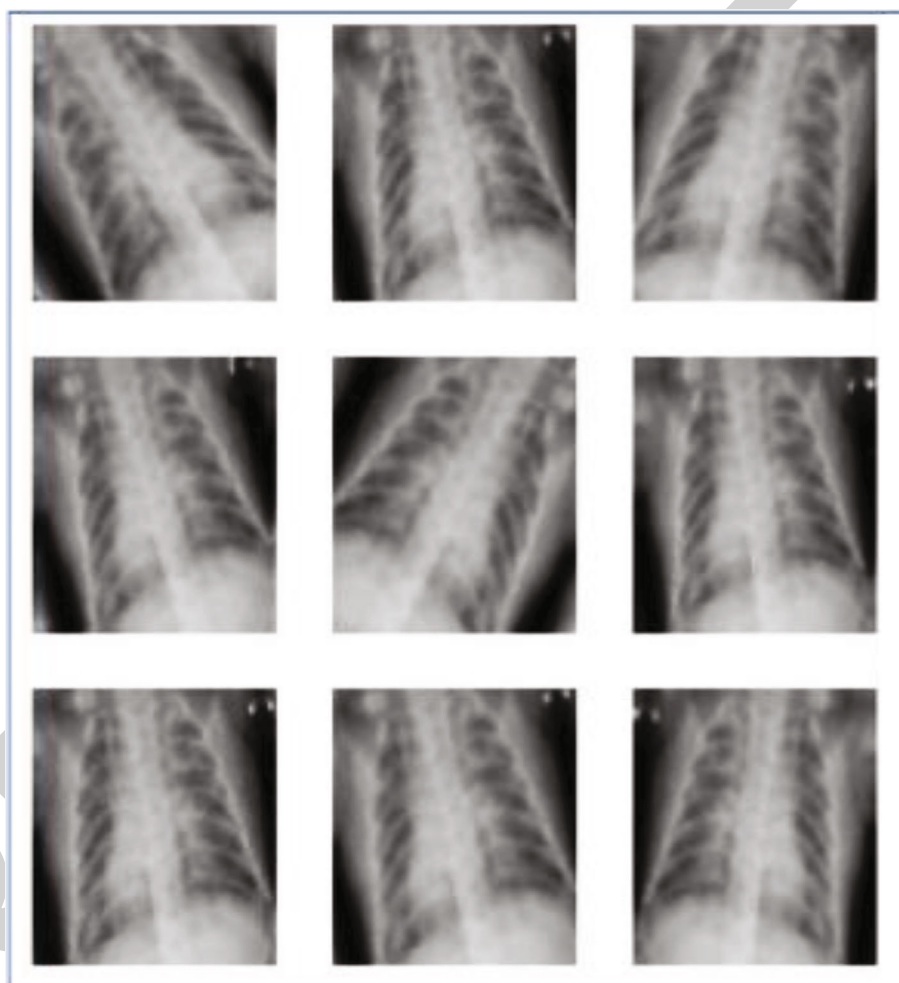


FIGURE 10: Image rotation to increase information.

and trained using the `model.compile` and `model.fit` functions, respectively, shown in Figure 8.

The accuracy parameters of the model were studied and displayed for further evaluation. The `acc` and `loss` functions were used for the precision study, as shown in Figure 9.

**2.6. Model Improvement.** To improve the model, information augmentation function was proposed that consists of rotating the images on the horizontal axis to extract the most information from each layer. With the “prepare” function,

the data of the images destined for training will be increased since what interests us is to improve the model as shown in Figure 10.

In addition, the number of “epoch-” parameters that determine the number of times that the algorithm will work with all the training data (Figures 11 and 12) was increased about the initial model, from 20 to 30.

**2.7. Development of the Web Application.** First, the optimized model was saved, as shown in Figure 13. NextJS, a

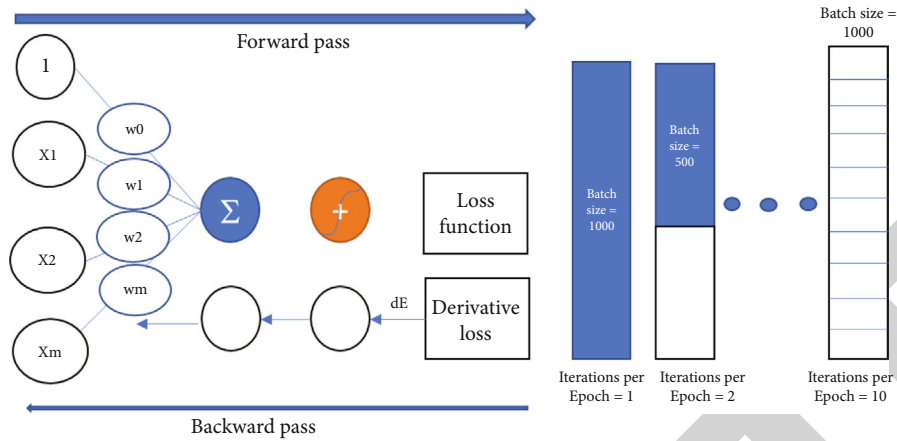


FIGURE 11: Graphic representation of the process in a neural network. Relationship between Batch and iterations to visually understand the concept of an epoch.

```

# Data augmentation
AUTOTUNE = tf.data.AUTOTUNE

data_augmentation = tf.keras.Sequential(
    [
        layers.RandomFlip("horizontal", input_shape=(img_height, img_width, channels)),
        layers.RandomRotation(0.1),
        layers.RandomZoom(0.1),
    ]
)

# Visualizing augmented images
plt.figure(figsize=(10, 10))
for images, _ in train_ds.take(1):
    for i in range(9):
        augmented_images = data_augmentation(images)
        ax = plt.subplot(3, 3, i + 1)
        plt.imshow(augmented_images[0].numpy().astype("uint8"))
        plt.axis("off")

def prepare(ds, shuffle=False, augment=False):
    # Resize and rescale all datasets.

    if shuffle:
        ds = ds.shuffle(1000)

    # Use data augmentation only on the training set.
    if augment:
        ds = ds.map(lambda x, y: (data_augmentation(x, training=True), y), num_parallel_calls=AUTOTUNE)

    return ds
    
```

FIGURE 12: Increased information to improve the model.

JavaScript framework for easily generating web applications, was used to develop the application.

To use the model, it was saved and TensorFlow serving was used, which generates a REST API to be able to interact with the model. A second component uses Flask that is responsible for converting the image that the user uploads to the format that the TensorFlow serving component understands (array of pixels, resizes the image, etc.).

The communication process between the different components can be seen in Figure 14.

2.8. Publishing the Web Application. The web page consists of a form that allows the user to upload a JPEG image and obtain a prediction. For the publication of the web application, an own domain was used, and a server in AWS was used. In addition, Docker was used for its publication, both the web and the

```

Saving model

import tempfile
import os

MODEL_DIR = os.path.join(dataset_path, "model")
version = 2
export_path = os.path.join(MODEL_DIR, str(version))
print(f'export_path = {export_path}')

tf.keras.models.save_model(
    model,
    export_path,
    overwrite=True,
    include_optimizer=True,
    save_format=None,
    signatures=None,
    options=None
)

print('Saved model:')
!ls -l {export_path}

```

FIGURE 13: Script to save the optimized model.

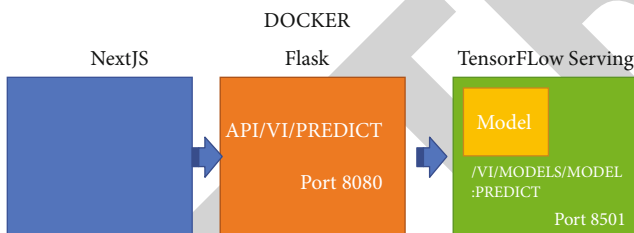


FIGURE 14: Scheme of communication between the different components of the web application development.

two APIs were containerized, and the Docker containers were deployed on the AWS instance using Docker compose.

### 3. Results and Discussion

The results obtained are shown below:

**3.1. Initial Model.** The initial model, model 1, had 4173 images (1073 normal, 2024 bacterial, and 1076 viral, as shown in Figure 5) and generated an accuracy of 70% and a percentage of loss that exceeds 80%.

Figure 15 shows the relationship between precision and loss according to groups (training and validation) according to the evolution of the epoch. If we look at the relationship between training accuracy and validation accuracy, they show the same trend until 4 epoch is reached, at which point the curves diverge; for training accuracy, it tends to increase,

but the same does not happen for validation accuracy, which decreases. In this same figure, the relationship of the loss between training and validation starts with a similar downward trend until epoch 5, when the validation loss increases again until it exceeds the initial levels. On the other hand, the training loss continues with the downward trend.

The accuracy percentage of the model reached 70.19%, and the loss was 2.6756, as can be seen in Figure 16.

**3.2. Optimized Model.** For the optimized model, we observe that (Figure 17) the relationship between training accuracy and validation accuracy tends to increase as the number of epochs increases. Indeed, they do not follow an identical logarithmic increase since the validation precision presents a more “irregular” trend with more increases and decreases depending on the epoch.

In this same figure, the relationship of the loss between training and validation starts with a similar downward trend maintained until the last epoch. A slight rise is observed from epoch 20 on the validation loss graph.

The accuracy percentage of the optimized model reached 78.37%, and the loss was 0.698, as can be seen in Figure 18.

**3.3. Web Application.** The user can now upload the image in JPEG format if they go to “Tria un fixter,” which they want to analyze, and when they have it selected, you can press “Send.” Based on the image chosen by the user, the web page returns the prediction.

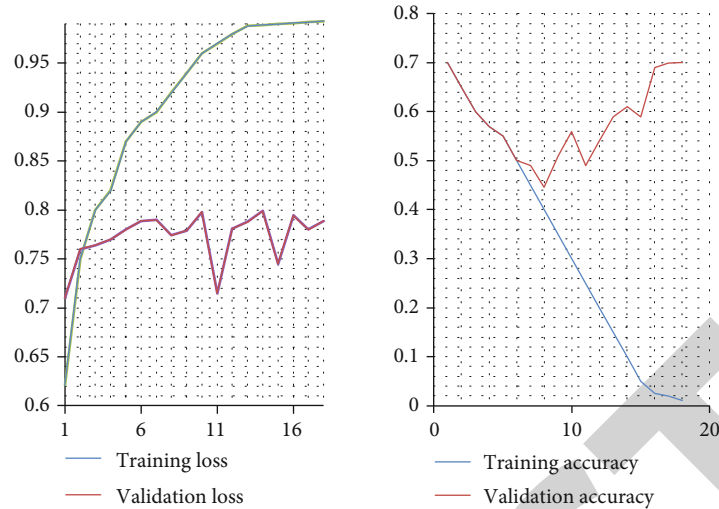


FIGURE 15: Evolution of precision and loss compared to “epoch.”

```
[51] test_loss, test_acc = model.evaluate(test_ds, verbose=2)

print(test_acc)

20/20 - 4s - loss: 2.6756 - accuracy: 0.7019 - 4s/epoch - 201ms/step
0.7019230723381042
```

FIGURE 16: Accuracy value generated in the initial model.



FIGURE 17: Evolution of precision and loss compared to “epoch.”

3.4. Discussion. Due to different socioeconomic factors, there is a shortage of radiology professionals in relation to the volume of patients who come to the clinic with pulmonary symptoms.

Artificial intelligence was aimed at helping professionals establish a faster and more reliable diagnosis that is related or not to the symptoms presented.

Studies such as those reviewed to carry out this work have been able to design applications with very high precision, although always bearing in mind that a radiology professional would have to validate the prediction [10–16]. In this project, data augmentation methods have been used to obtain a classification model with a precision percentage of 78.37%. The generated classification model offers the user a good classification of the images, distinguishing between normal chest X-ray and pneumonia, but the existing opacities can contribute to generating some errors between the differentiation of bacterial and viral pneumonia. For this reason, some studies propose computed tomography as the most effective method for detecting and differentiation of viral and bacterial pneumonia.

One of the limitations that arose during the project was creating the work environment and the lack of memory of the equipment used and the incompatibility of libraries, but thanks to Google Collaboratory, it was possible to solve it. In addition, it allows us to share the code with other researchers [17–22].

Another limitation of the project carried out is that few epochs have been used compared to the studies consulted. In our case, only 20 epochs have been made for the initial model and 30 for the optimized model. This difference in

```

test_loss, test_acc = model.evaluate(test_ds, verbose=2)

print(test_acc)

20/20 - 5s - loss: 0.6988 - accuracy: 0.7837 - 5s/epoch - 232ms/step
0.7836538553237915

```

FIGURE 18: Accuracy value generated in the optimized model.

epochs is due to the lack of adequate equipment to make a model that compiles quickly and efficiently, saving time for the researcher [23–26].

It should also be taken into account that only one type of neural network (CNN) has been worked on, and a single model has been generated, which has been improved. It would have been interesting to make more models and compare them with each other since the time factor has also been a limitation for this work.

#### 4. Conclusions

Pneumonia is a prevalent lung disease and one of the main causes of death worldwide, affecting different groups. Due to its characteristics and mortality rate, we can add that to the current global pandemic by SARS-COV-2, there is currently a lot of literature accessible to the public. In this work, it has been possible to develop a web application that allows the user to classify the image of interest according to whether or not there is pneumonia and what type. In general, all the specific objectives set have been achieved, and the minimum precision established in objective, which was 70%, was exceeded. With the completion of the project, and with the large amount of bibliography currently existing in relation to the chosen topic, machine learning models become more important to help our professionals diagnose diseases faster and with fewer resources than with adequate treatment. In time, it can save lives.

**4.1. Future Recommendations.** The future lines of work that can be proposed as a result of this project could be the following:

- (i) Improve the model until reaching an accuracy percentage of 95%. It is very important to establish a good differentiation between viral and bacterial pneumonia because, as mentioned above, the treatment differs
- (ii) Generate a network of professionals where developed models are shared, and databases are also shared to improve existing models. This would contribute to generating the best possible model and being able to share and implement it in all health centers worldwide
- (iii) Improve the web application. It would be interesting that both the appearance and the functionality of it offer the user more information about the image of

interest and leave a space for the user to share comments such as symptoms or validation (in the case of being a radiologist) of the generated prediction. This would feed and improve the model and open new research lines

- (iv) Implement artificial intelligence in most health centers to support diagnosis, offering training and collaboration with health professionals

#### Data Availability

The data used to support the findings of this study are included within the article.

#### Conflicts of Interest

The authors declare that they have no conflicts of interest.

#### Acknowledgments

Authors would like to acknowledge the support of the Deputy for Research and Innovation-Ministry of Education, Kingdom of Saudi Arabia, for this research through a grant (NU/IFC/ENT/01/008) under the institutional Funding Committee at Najran University, Kingdom of Saudi Arabia.

#### References

- [1] I. Daod, R. Ibrahim, A. Hussein, N. Norsamsi, and N. Mazlan, "Knowledge of pneumonia among nursing staff in Mosul hospitals, Iraq," *International Journal of Medical Toxicology & Legal Medicine*, vol. 23, no. 3and4, pp. 107–116, 2020.
- [2] M. Hassan and I. Al-Sadoon, "Risk factors for severe pneumonia in children in Basrah," *Tropical Doctor*, vol. 31, no. 3, pp. 139–141, 2001.
- [3] N. M. Elshennawy and D. M. Ibrahim, "Deep-pneumonia framework using deep learning models based on chest X-ray images," *Diagnostics*, vol. 10, no. 9, p. 649, 2020.
- [4] S. Güneçli, Z. Atçeken, H. Doğan, E. Altınmakas, and K. Ç. Atasoy, "Radiological approach to COVID-19 pneumonia with an emphasis on chest CT," *Diagnostic and Interventional Radiology*, vol. 26, no. 4, pp. 323–332, 2020.
- [5] A. Jaiswal, P. Tiwari, S. Kumar, D. Gupta, A. Khanna, and J. Rodrigues, "Identifying pneumonia in chest X-rays: a deep learning approach," *Measurement*, vol. 145, pp. 511–518, 2019.
- [6] C. Ortiz, A. García-Pedrero, M. Lillo, and C. Gonzalo-Martin, "Automatic detection of pneumonia in chest X-ray images using textural features," *Computers in Biology and Medicine*, vol. 145, p. 105466, 2022.



## Retraction

# Retracted: Segmentation of Oral Leukoplakia (OL) and Proliferative Verrucous Leukoplakia (PVL) Using Artificial Intelligence Techniques

### BioMed Research International

Received 18 July 2023; Accepted 18 July 2023; Published 19 July 2023

Copyright © 2023 BioMed Research International. This is an open access article distributed under the Creative Commons Attribution License, which permits unrestricted use, distribution, and reproduction in any medium, provided the original work is properly cited.

This article has been retracted by Hindawi following an investigation undertaken by the publisher [1]. This investigation has uncovered evidence of one or more of the following indicators of systematic manipulation of the publication process:

- (1) Discrepancies in scope
- (2) Discrepancies in the description of the research reported
- (3) Discrepancies between the availability of data and the research described
- (4) Inappropriate citations
- (5) Incoherent, meaningless and/or irrelevant content included in the article
- (6) Peer-review manipulation

The presence of these indicators undermines our confidence in the integrity of the article's content and we cannot, therefore, vouch for its reliability. Please note that this notice is intended solely to alert readers that the content of this article is unreliable. We have not investigated whether authors were aware of or involved in the systematic manipulation of the publication process.

In addition, our investigation has also shown that one or more of the following human-subject reporting requirements has not been met in this article: ethical approval by an Institutional Review Board (IRB) committee or equivalent, patient/participant consent to participate, and/or agreement to publish patient/participant details (where relevant).

Wiley and Hindawi regrets that the usual quality checks did not identify these issues before publication and have since put additional measures in place to safeguard research integrity.

We wish to credit our own Research Integrity and Research Publishing teams and anonymous and named external researchers and research integrity experts for contributing to this investigation.




The corresponding author, as the representative of all authors, has been given the opportunity to register their agreement or disagreement to this retraction. We have kept a record of any response received.

### References

- [1] S. Z. Alshawwa, A. Saleh, M. Hasan, and M. A. Shah, "Segmentation of Oral Leukoplakia (OL) and Proliferative Verrucous Leukoplakia (PVL) Using Artificial Intelligence Techniques," *BioMed Research International*, vol. 2022, Article ID 2363410, 11 pages, 2022.

## Research Article

# Segmentation of Oral Leukoplakia (OL) and Proliferative Verrucous Leukoplakia (PVL) Using Artificial Intelligence Techniques

Samar Zuhair Alshawwa <sup>1</sup>, Asmaa Saleh,<sup>1</sup> Malek Hasan <sup>2,3</sup> and Mohd Asif Shah <sup>4</sup>

<sup>1</sup>Department of Pharmaceutical Sciences, College of Pharmacy, Princess Nourah bint Abdulrahman University, P.O. Box 84428, Riyadh 11671, Saudi Arabia

<sup>2</sup>Department of Medical Instruments Engineering Techniques, Al-Farahidi University, Baghdad 10021, Iraq

<sup>3</sup>The University of Mashreq, Research Center, Baghdad, Iraq

<sup>4</sup>Kebri Dehar University, Ethiopia

Correspondence should be addressed to Malek Hasan; [malekb.has@yahoo.com](mailto:malekb.has@yahoo.com)

Received 6 June 2022; Revised 27 June 2022; Accepted 30 June 2022; Published 21 July 2022

Academic Editor: Dinesh Rokaya

Copyright © 2022 Samar Zuhair Alshawwa et al. This is an open access article distributed under the Creative Commons Attribution License, which permits unrestricted use, distribution, and reproduction in any medium, provided the original work is properly cited.

PVL (proliferative verrucous leukoplakia) has distinct clinical characteristics. They have a proclivity for multifocality, a high recurrence rate after treatment, and malignant transformation, and they can progress to verrucous or squamous cell carcinoma. AI can aid in the diagnosis and prognosis of cancers and other diseases. Computational algorithms can spot tissue changes that a pathologist might overlook. This method is only used in a few studies to diagnose LB and PVL. To see if their cellular nuclei differed and if this cellular compartment could classify them, researchers used a computational system and a polynomial classifier to compare OLs and PVLs. 161 OL and 3 PVL specimens in the lab were grown, photographed, and used for training and computation. Exam orders revealed patients' sociodemographics and clinical pathologies. The nucleus was segmented using Mask R-CNN, and LB and PVL were classified using a polynomial classifier based on nucleus area, perimeter, eccentricity, orientation, solidity, entropies, and Moran Index (a measure of disorderliness). The majority of OL patients were male smokers; most PVL patients were female, with a third having malignant transformation. The neural network correctly identified cell nuclei 92.95% of the time. Except for solidity, 11 of the 13 nuclear characteristics compared between the PVL and the LB showed significant differences. The 97.6% under the curve of the polynomial classifier was used to classify the two lesions. These results demonstrate that computational methods can aid in diagnosing these two lesions.

## 1. Introduction

According to the World Health Organization, cancer arises from transforming normal cells into tumor cells in a multistage process [1]. Among the various types of tumors, squamous cell carcinoma (SCC) of the oral cavity is usually preceded by MPDs, which develop from etiological factors such as tobacco, alcohol, autoimmune diseases, and idiopathic or inherited genetic aberrations. We can mention oral leukoplakia (OL), erythroplakia, oral submucosal fibrosis, palatine keratosis associated with inverted smoke, lichen planus, lupus erythematosus, and dyskeratosis congenita [2].

Although each of them has specific histological aspects, some histological characteristics such as hyperkeratosis (increase in keratin), hyperplasia (increase in the number of cells), and even dysplasia (an architectural disorder of epithelial tissue accompanied by cytological atypia) may be shared between them [3].

Premalignant cases are local lesions characterized by a higher risk of malignant change than normal structures or general conditions associated with an increased risk of cancer. Oral mucosa is an area where more than 5% of premalignant cases turn into cancer [4, 5]. Therefore, the diagnosis of premalignant formations gains importance in

the early detection of possible malignant lesions. Problems in evaluating premalignant cases mainly arise from two factors [5]. Although various clinical features are important in determining the risk of malignant change in premalignant cases, histological examinations are the most valid method today to determine these formations' proper structure and malignant potential. Histologically, epithelial dysplasia and cellular atypia are prognostic indicators of premalignancy, which refers to impaired proliferation, maturation, and organization of the epithelium. These changes are seen in three degrees mild, moderate, and severe. Although the relationship between epithelial dysplasia and future carcinoma is not certain, it is generally stated that the degree of dysplasia and the transformation into cancer are directly proportional [6].

Technological advances in the last decade, especially with the advent of high-resolution digitized images and AI, have allowed pathology to adopt computational approaches, such as machine learning, to assess tissue aspects such as minimal or no human interference through algorithms capable of predicting, for example, precancerous lesions' risk of malignant transformation [7]. Thus, several studies have proposed using AI as a tool that adds to existing ones to understand the biology of these lesions better, but with the advantage of eliminating the pathologist's subjectivity regarding the interpretation of histopathological findings [8].

Considering the potential of this tool, this study investigated the nuclear aspects of OL and proliferative verrucous leukoplakia (PVL) cells with the main aim of detecting nuclear alterations and creating a classification algorithm that can be used for differential diagnosis between the two lesions. We hypothesized that the nuclear aspects investigated by AI are different between the two lesions and that this tool can be used for the purpose of differential diagnosis between an OL and PVL, especially in the early stages of both lesions when the clinicopathological aspects overlap, compromising the accuracy of the diagnosis both by the clinician but mainly by the pathologist.

## 2. Material and Methods

Sixty-one cases of OL, three cases of PVL, and five cases of SCC (all these cases were linked to malignant transformation of either OL or PVL) were collected from the Oral Pathology Laboratory of the Faculty of Dentistry of the University of Baghdad, Iraq, in the period from March 2021 to February 2022 to be used in the study in the neural network training, segmentation, and feature extraction phases. Initially, slides stained with hematoxylin and eosin used in the clinical routine were retrieved from their respective cases and reassessed to confirm the diagnosis of each of the lesions. In the case of OLs and PVLs, the degrees of dysplasia were also checked. For this diagnostic confirmation step, the criteria established by the World Health Organization of 2017 were used [9]. The fact of using routine slides stained with hematoxylin and eosin refers to the search in this work of the neural network to learn from the conditions found in oral pathology laboratories, ensuring better applicability of this tool. Clinico-

pathological data (lesion color, location, lesion type, dysplasia, malignant transformation, and size) and sociodemographic (gender, age, and smoking status) of the patients were obtained from the examination requests presented by the pathology laboratory. As a minimum inclusion criterion, only cases of OLs, PVLs, and SCCs had stained and well-preserved slides, and their respective diagnoses were used. Otherwise, the cases were excluded from the study.

**2.1. Computer Analysis.** The slides selected from each case were photographed using a Leica DM500 optical microscope to study the nuclei. On average, ten fields/lesions were obtained at 400× magnification, and all images were saved in JPEG and TIFF format with a resolution of 1600 × 1200. From the capture of these fields, the regions of interest were extracted. Then, the steps were used sequentially: segmentation, postprocessing, feature extraction, and classification, which are detailed below. All steps after extracting the ROIs were performed on a computer with the following configurations: AMD FX-8320 processor, 8GB of RAM, and NVIDIA GTX 1060 GPU with 6GB of VRAM. In the manual segmentation phase for network training, a Wacom Monitor-Cintiq was used to bypass the cores; the GIMP software was used both in this step and to obtain the ROIs obtained through the website <https://www.gimp.org/>. All software used in this work is available free of charge.

**2.2. Segmentation.** The first stage of segmentation is the training phase, in which the segmentation of the nuclei is performed manually from the ROIs extracted from the fields obtained from each lesion, as explained above. For this step, 481 ROIs were used, distributed as follows: 74 ROIs from OL without dysplasia, 77 ROIs from OL with mild dysplasia, 114 ROIs from OL with moderate dysplasia, 43 ROIs from OL with severe dysplasia, 59 PVL ROIs, and 114 SCC ROIs. A total of 15,027 cores were manually segmented and used in network training.

For training, the Mask R-CNN neural network was used together with the ResNet50 convolutional network to detect the cellular nuclei in the images. The ResNet50 convolutional network was first used in the learning stage of the characteristics of cell nuclei. The architecture of this network is shown in Figure 1. The network model is composed of 50 convolutional layers distributed over the input layer (E); four blocks of convolutional layers called Block 1 (B1), Block 2 (B2), Block 3 (B3), and Block 4 (B4); and an output step. Briefly, layer E has 64 convolutional filters with a size of 7 × 7 pixels that process the original image through a sliding window with an offset size of 2 pixels. Then, still in layer E, a max-pooling filter, with a size of 2 × 2 pixels, is used, with a displacement size equal to 2 pixels. This result is then applied to layer C1 of B1, which has 64 convolutional filters of size 1 × 1 pixel, followed by C2, which has 64 filters of size 3 × 3 pixels, and C3, which contains 256 filters of size 1 × 1 pixel. B1 is repeated three times over the image processed in layer E, totaling nine convolutional layers in this block. The result of B1 is applied to B2, passing first through layer C1, with 128 filters of size 1 × 1 pixel, followed by C2, with 128 filters of size 3 × 3 pixels, and C3, with 512 filters of size

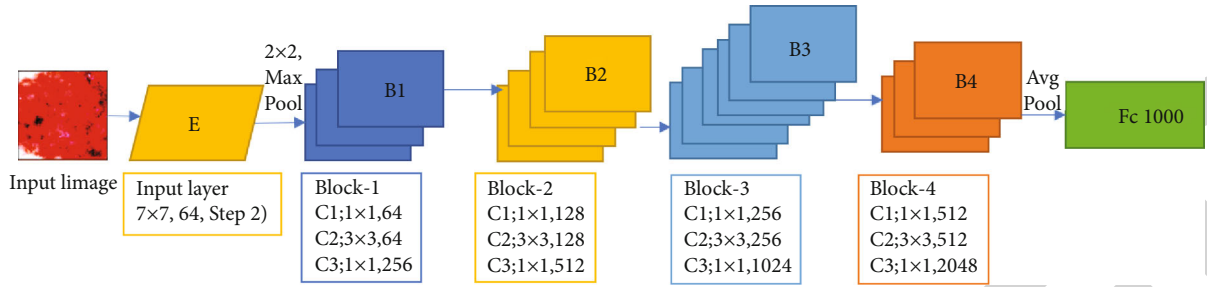


FIGURE 1: Architecture of the ResNet50 neural network used in the segmentation process for the learning of cell nuclei.

$1 \times 1$  pixel. This block has four repetitions, resulting in 12 convolutional layers. The result of B2 is then used in B3, which has 256 filters of size  $1 \times 1$  pixel in C1, 256 filters of size  $3 \times 3$  pixels in C2, and 1024 filters of size  $1 \times 1$  pixel in C3. This block has six repetitions, totaling 18 layers. The result of B3 is used in B4, which also has three layers: C1, which has 512 filters of size  $1 \times 1$  pixel, C2, with 512 filters of size  $3 \times 3$  pixels, and C3, with 2048 filters of size  $1 \times 1$  pixel. Block B4 is repeated three times, presenting nine layers in total. Finally, the generated data is transformed into a vector by an average pooling filter, while the softmax function is used to classify objects between core or background region. For this step, a fully connected layer with 1000 neurons is used. Between each block of convolutional layers (B1, B2, B3, and B4), the feature matrix is reduced in size by a proportionality of 2. For this, a sliding window with a displacement size of 2 pixels is used in the transition convolutions between each block. For the network model used in this work, the activation function adopted was the Rectified Linear Unit (ReLU) [10].

He and others [11] explained that the Mask R-CNN is a convolutional neural network that detects and separates candidate objects into distinct classes from regions. It consists of two stages; the first stage is called Region Proposal Network (RPN) and aims to generate sets of candidate objects in bounding boxes (the smallest square that comprises an object); the second stage aims to classify the objects contained in the bounding boxes and perform the regression of these boxes. In parallel to the second stage, the network also has a branch that provides a binary mask for each ROI.

This network detects and segments nuclei through the core characteristics extracted by ResNet50. For this, Mask R-CNN uses the feature maps generated by ResNet50 and stacks them from the largest (most detailed) to smallest (least detailed) map forming a Feature Pyramid Network (FPN). How ResNet50 has many layers that generate maps, the use of all of them can generate a large pyramid of high execution complexity. To get around this problem, only the last layer of each block is used, that is, C3 of the last B1, C3 of the last B2, C3 of the last B3, and C3 of the last B4. Then, the FPN layers are passed as input to the Region Proposal Network (RPN) to identify the cores in the top-down direction, from the smallest to the largest layer. With this, we classify the regions between core and background regions along with the bounding boxes in the first layer from above (smaller and less detailed). These results are then

combined with the layers below, which are larger and have more detailed core features. As these results are passed through these larger, more detailed layers, the identified regions become more accurate and correct, while the bounding boxes are regressed. Finally, the R-CNN Mask through a convolutional network used in conjunction with feature maps produces a binary mask for each identified nucleus.

A multitasking loss rate is calculated for each region during the network training phase. This rate calculates the training error percentage, that is, how much the training is different from the gold standard (ROIs manually segmented by the expert). Basically, it sums the rate of loss (error) of classification and regression of boxes and masks, and its function is defined by

$$L = L_{cls} + L_{box} + L_{mask}. \quad (1)$$

For the network model applied in this work, 60 ROIs were used for network training, 48 of them for training and 12 for testing, with 40 epochs performed in total.

416 ROIs were used to validate the model. Five of the total ROIs used were discarded during the process because they showed errors that prevented the program from working.

**2.2.1. Postprocessing.** After the network classifies the objects between cores and the background region, some regions may be incompletely filled or even present noise or artifacts that can harm the segmentation process. To prevent this from happening, the postprocessing step is performed through morphological operations to eliminate false-positive regions and refine the segmented nuclei.

**2.2.2. Classification.** The classification was performed using these vectors after the feature extraction process in which the  $\mu$  and  $\sigma$  of the extracted nuclear features were transformed into a single vector for each ROI. The objective was to separate the images in the two different classes of lesions (OL and PVL) through the polynomial classifier (POL) [11]. This classifier employs polynomial expansion over the extracted feature vector to define the coefficients used in the separation of classes. For this to occur, the following discriminant polynomial function is used:

$$g(x) = a^T p_n(x). \quad (2)$$



**2.3. Statistical Analysis.** To assess the method's effectiveness, a comparison was performed by estimating the overlap between the segmented images and the gold standard. With this, measures of true positives, false positives, true negatives, and false negatives are obtained, which were used in segmentation and classification. The ROC curve is obtained from the graph plotted by sensitivity versus false-positive rate (TFP). In order to compare the morphological characteristics of the nuclei between OLs and PVLs, regardless of the degree of dysplasia, the statistical Mann-Whitney tests or the unpaired *t*-test were used, according to the data distribution, as determined by the normality test, Shapiro-Wilk. It was considered statistically significant when  $p < 0.05$ .

### 3. Results

**3.1. Clinicopathological Data.** Most OL patients were male, while all PVL cases were female. The mean age of the patients was 55 years, 54 in the OLs and 72 in the PVLs. Most patients with OL were smokers, while only one patient with PVL had information about smoking. The main locations of both lesions were the buccal mucosa, tongue, alveolar ridge, and lip. For both OL and PVL, the most frequently found dysplastic alteration was mild dysplasia. Two cases of OL and one of PVL underwent a malignant transformation. Regarding the clinical characteristics of both lesions, most were white and had an average size of 1.5 cm.

**3.1.1. Nuclear Segmentation and Neural Network.** For the analysis of nuclear segmentation of the lesions, photomicroscopy of the lesions of OL, PVL, and SCC was obtained, as described in the methodology. Of the total, 568 images of OL, 45 images of PVL, and 58 images of SCC were taken. From these images, the following numbers of ROIs were captured for each image: 1,217 ROIs from OL, 119 ROIs from PVL, and 133 ROIs from SCC. In this step, SCC samples were used to increase the number of nuclei used for neural network training purposes and increase its accuracy in the nuclear segmentation process. After obtaining the ROIs, the manual segmentation of the cellular nuclei belonging to the 481 ROIs selected for learning the algorithm was performed, which represented a supervised training phase. After that, the training of the Mask R-CNN network took place, where the network was fed with information about the cores in the training and the segmentation of cores by the network was performed in the separate ROIs for testing. To evaluate Mask R-CNN's performance in identifying and separating nuclei from background regions, both in testing and validation, the ROIs segmented by it were compared to the gold standard.

After training, Mask R-CNN was used to segment the ROIs extracted from the dataset, and the results of the segmentation process by Mask R-CNN can be seen in Figures 2–4. Figure 2 shows the segmentation of an image with the nuclei being identified by the neural network. After training, it was found that the network successfully separated the nuclei from the background regions of the original image (Figure 2(a)). However, it was observed that the neural network detected perinuclear regions as belonging to the

nuclear regions that were not identified in the gold standard (manual segmentation) and therefore were called false-positive nuclear regions (Figure 2(c), red arrow). This may be due to the similarity of coloration in the regions close to the nuclear limits. Still in Figure 2(c), it can be seen that the neural network did not identify some nuclear regions, as observed in the gold standard, indicating a false-negative result (green arrow). In addition, some segmented images presented noise that was wrongly classified as nuclei, which were considered false positives (Figure 2(e), red arrow). To correct these and other irregularities, a postprocessing step was carried out.

**3.1.2. Postprocessing.** Postprocessing was carried out after segmentation by the neural network to correct some segmentation irregularities. The result can be seen in Figure 3. In this step, dilation (Figure 3(c)), hole filling (Figure 3(d)), and erosion (Figure 3(e)) operations were performed on an image. In Figure 3(b), the region indicated by the green arrow indicates the presence of a hole inside the core, where after the application of the expansion operation, the hole is reduced in size and, subsequently, eliminated by the hole-filling operation. At the end, the erosion operation was applied so that the nuclei returned to their respective original sizes. After the process of identifying the cellular nuclei, the tissues started to be classified based on the extraction of morphological characteristics from the objects classified as nuclei. The morphological characteristics studied were area (A), eccentricity (E), perimeter (PE), orientation (OR), solidity (S), entropy (EN), and Moran Index (IM). These selected characteristics are based on the work of which in turn was based on the studies [11, 12].

The area is calculated by the total value of the number of pixels in an object; eccentricity concerns the difference in the circumference of an object in relation to a circle, that is, the calculation of the elongation of objects; orientation calculates the relationship between the major axis of an object about the *x*-axis; solidity analyzes the deformity of an object, in the case of this work, the level of irregularity of the circular shape by the number of invaginations present.

The entropy measure analyses the intensity levels of a region and calculates the intensity variation present in the texture of a neighborhood of pixels. In this study, 7 neighborhood sizes were used to extract entropy measurements, as follows:  $3 \times 3$ ,  $5 \times 5$ ,  $7 \times 7$ ,  $9 \times 9$ ,  $11 \times 11$ ,  $13 \times 13$ , and  $15 \times 15$  pixels based on in the work of Kleppe et al. (2018). The Moran Index measures spatial autocorrelation by averaging the intensity of neighboring pixels and comparing them with the central pixel.

These 13 features were extracted for each core *n* present in all ROIs. In this way, each ROI has a matrix of size  $13 \times n$  and, from these matrices, the mean ( $\mu$ ) and standard deviation ( $\sigma$ ) were extracted for each characteristic present in the ROI, generating two vectors (one for average and another for standard deviation), each having the descriptors of these characteristics:  $MK = [m_1, m_2 \dots m_{13}]$  and  $DK = [d_1, d_2 \dots d_{13}]$ . In MK, there is a vector with the average of all 13 features extracted from a given image, while in DK, there is a vector with the entire standard deviation of each feature found in the image in question. Finally, these vectors were



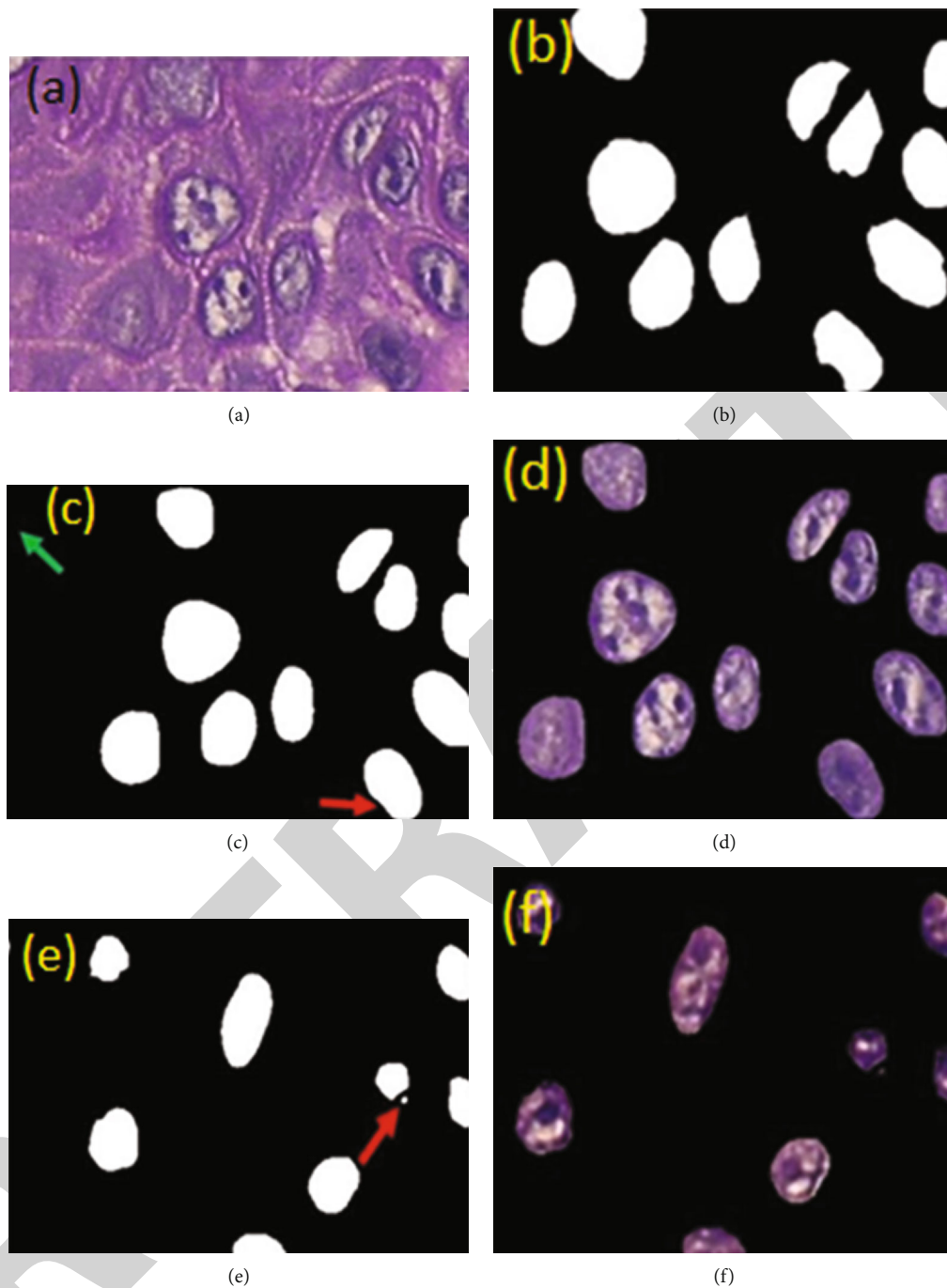


FIGURE 2: Segmentation of an OL image by the gold standard and the neural network. (a) Original image; (b) mask resulting from the gold standard; (c) mask resulting from the Mask R-CNN neural network showing false-positive (red arrow) and false-negative (green arrow) regions; (d) segmentation resulting from (c) and image of SCC showing a small noise that was classified as false positive (red arrow); (e) mask resulting from Mask R-CNN; (f) segmentation resulting from (a).

concatenated (merged), forming a single vector that was used in the classification of each ROI.

The operation to eliminate small artifacts or noise classified as false positives was also performed. Figure 4 shows the result of the operation that aims to eliminate segmented objects smaller than 30 pixels in an image, as identified by the red arrow in Figure 4(a).

The segmentation performed by the neural network obtained a satisfactory performance in identifying the nuclei

and the background regions in the histological images, presenting an average accuracy of 92.95%. Table 1 shows the means and standard deviations of sensitivity (SE), specificity (ES), accuracy (AC), correspondence rate (TC), and dice coefficient (DC) achieved by the Mask R-CNN network in segmenting the different tissue histopathological tests evaluated in this study. As can be seen, the values for each of the indices investigated in the neural network segmentation test were similar between the different lesions. In summary,

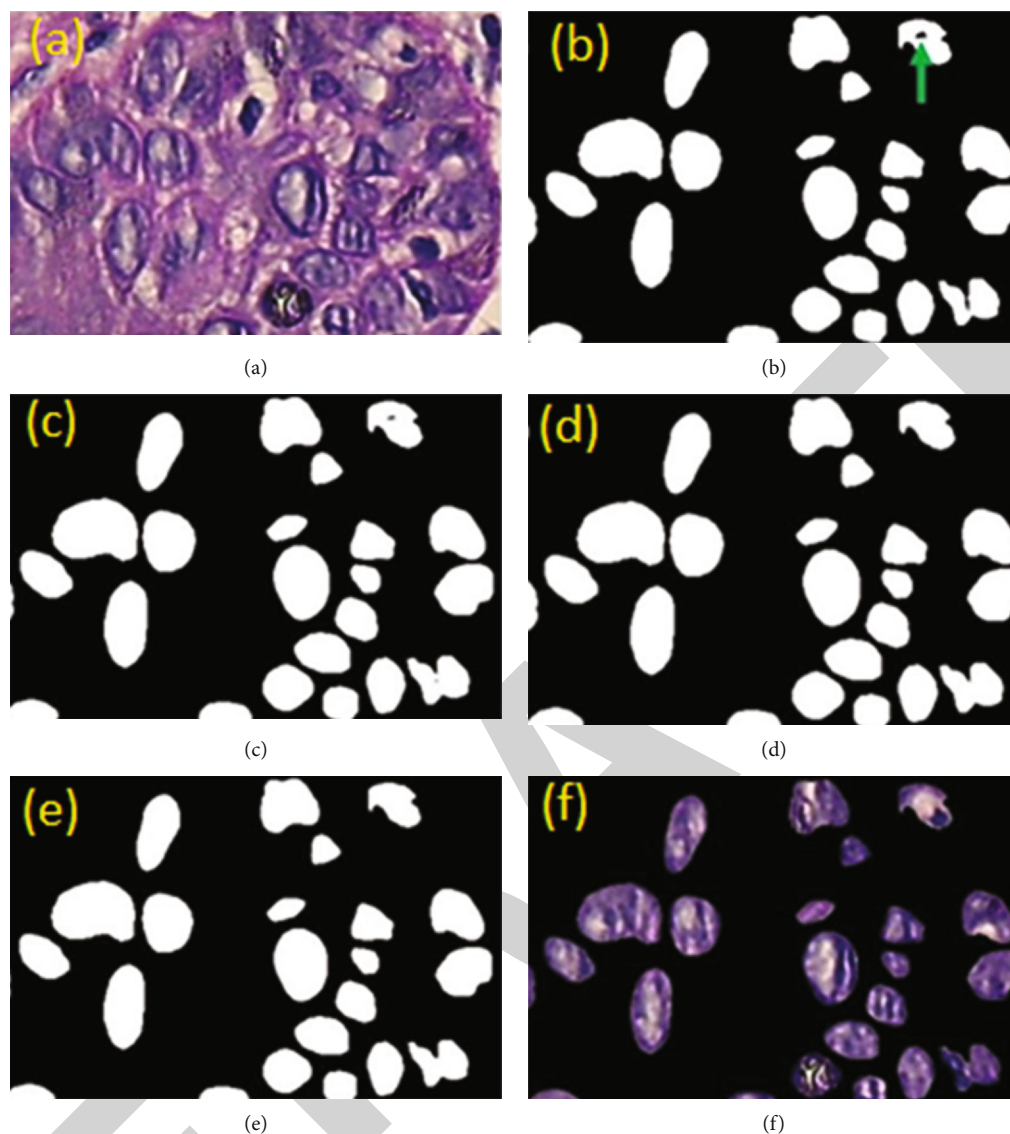


FIGURE 3: Postprocessing step in a SCC image: (a) original image, (b) mask after segmentation, (c) mask after the dilation operation, (d) mask after applying the hole-filling operation, (e) mask after erosion operation, and (f) resulting segmentation.

these data indicate that the neural network presented similar sensitivity, specificity, and accuracy, indicating that the algorithm performed well in identifying cell nuclei in all cases.

**3.2. Morphological Features Extracted by the Neural Network.** The nuclear features extracted by the neural network were compared between OL and PVL. Altogether, the 13 characteristics used in the classification were extracted from the entire PVL ROI dataset and 1,196 of the 1,217 OL ROIs. Regarding entropies, seven entropy measures were used, and the data for each entropy/lesion can be seen in Table 2. The means for all entropies were always higher in the PVLs when compared to the OLs, and the differences were statistically significant ( $p < 0.0001$ ).

The Moran Index revealed a statistically significant difference between OL and PVL, with means of 0.09702 and 0.1022, respectively ( $p = 0.0103$ ). Regarding the area, the averages for OL and PVL were 836.4 and 1,050, respectively,

with  $p < 0.0001$ . Similarly, the mean nuclear perimeters for OL and PVL were 103.3 and 117.9, respectively, with  $p < 0.0001$ . As for solidity, an average of 0.9685 and 0.9621 for OL and PVL was observed, respectively, with  $p < 0.0001$ . Regarding the eccentricity and orientation characteristics, the means for OL and PVL were very similar and with  $p > 0.05$ .

**3.3. OL and PVL.** For the separation between OL and PVL, a polynomial classifier was used. For this, 119 ROIs from PVL and 120 ROIs from OL randomly chosen were used by the classifier to assess the degree of separability between them. The classifier performed the cross-validation by dividing the ROIs into five groups (folds), where four of them were used for training and one for testing, which were alternated until all groups were trained and tested. As a result, the mean AUC of the classifier was 97.06%, the mean sensitivity was 95.83%, the mean specificity was 98.29%, and the mean

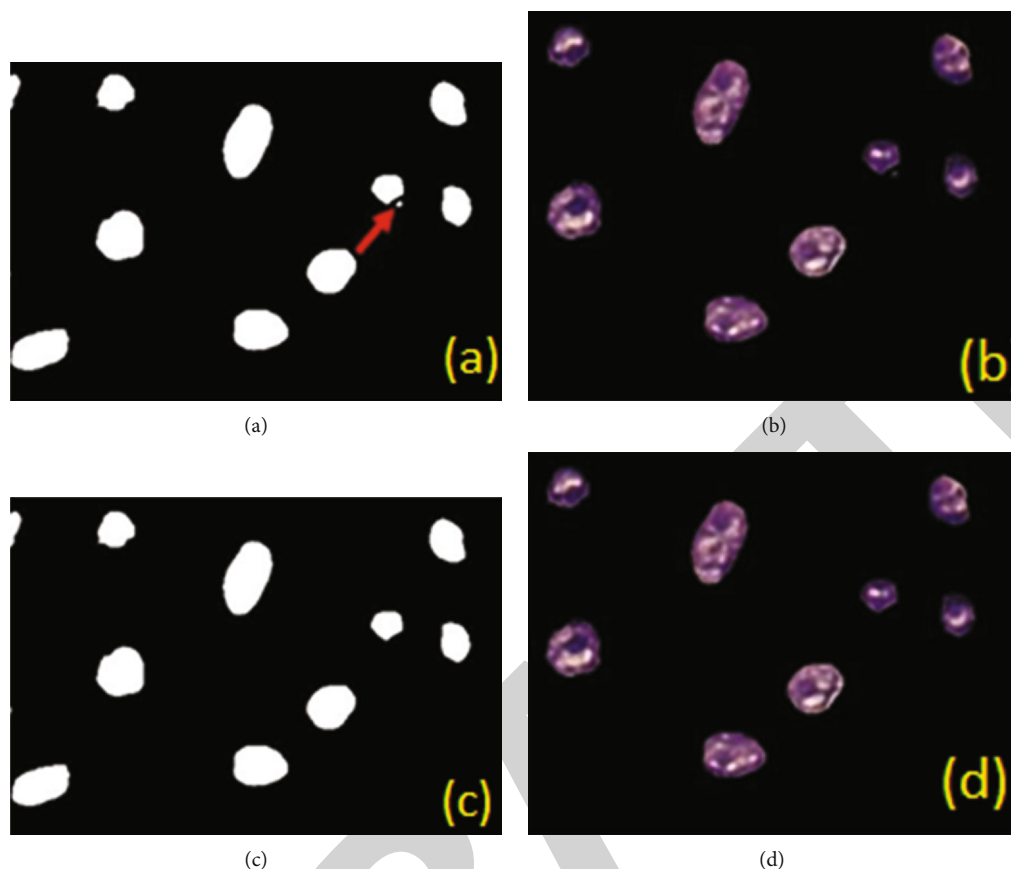


FIGURE 4: Operation to eliminate small artifacts in an SCC image: (a) resulting mask of the neural network; (b) segmentation resulting from (a); (c) mask resulting from the process of eliminating objects smaller than 30 pixels; (d) segmentation resulting from (c).

TABLE 1: Result of the segmentation of the Mask R-CNN in the different histopathological tissues of OL, PVL, and SCC.

Lesion	SE (%)	ES (%)	AC (%)	TC (%)	DC (%)
OL	$81.89 \pm 6.44$	$96.51 \pm 2.28$	$93.15 \pm 2.76$	$74.95 \pm 8.21$	$83.80 \pm 5.60$
PVL	$80.79 \pm 4.58$	$96.64 \pm 1.61$	$92.93 \pm 2.34$	$74.77 \pm 5.71$	$83.82 \pm 3.90$
SCC	$80.24 \pm 9.28$	$97.67 \pm 1.83$	$94.63 \pm 2.85$	$74.42 \pm 8.81$	$83.47 \pm 6.36$

accuracy was 97.05%. These results show that the classifier successfully distinguished the two lesions with a high degree of sensitivity, specificity, and accuracy, indicating that such a tool has great potential for use in the differential diagnosis between them. From the obtained results, it is possible to observe the results obtained in each group and the mean and standard deviation of the metrics used to evaluate the classifier's performance.

#### 4. Discussion

This study aimed to investigate the detection of nuclear alterations in OLs and PVLs using a computer as well as the separation between them through the application of a classifier based on morphological nuclear characteristics. The results of this study shed light on one of the problems of oral pathology, which is to differentially diagnose a OL from a PVL, especially when the latter is at an early stage,

which can generate inconsistencies, difficulties, doubts, and even diagnostic errors, according to pointed out by Al-Rawi (2022) [13]. Since our results showed the presence of detectable nuclear alterations among them, and that these alterations in turn were able to differentiate them with high precision by the polynomial classifier, this study showed the importance of investigating the cell nucleus through machine learning in DBPMs for diagnostic purposes as well as in the elucidation of the characteristic nuclear properties of each one of them. In light of advances in AI, this tool can be another foundation in the search for understanding these lesions together with studies aimed at finding differential molecular biomarkers between them, which do not exist to date.

Analyzing the clinicopathological data collected in this work, it can be seen that they are in line with the specific literature. In general, the incidence of OL was higher in males than in females; on the other hand, all cases of PVL were

TABLE 2: Values of the seven levels of nuclear entropy evaluated between OL and PVL.

Variable	Measures of central tendency and dispersion	LB	LVP	<i>p</i> -value
Entropy 3 × 3	Average	1968	2137	<0.0001*
	Median	1983	2149	
	Minimum	1428	1962	
	Maximum	2314	2284	
Entropy 5 × 5	Average	2769	3049	<0.0001*
	Median	2784	3082	
	Minimum	2017	2759	
	Maximum	3308	3268	
Entropy 7 × 7	Average	3243	3598	< 0.0001*
	Median	3252	3.64	
	Minimum	2363	3232	
	Maximum	3913	3862	
Entropy 9 × 9	Average	3566	3974	< 0.0001*
	Median	3571	4024	
	Minimum	2587	3552	
	Maximum	4.33	4266	
Entropy 11 × 11	Average	3804	4249	< 0.0001*
	Median	3805	4308	
	Minimum	2735	3785	
	Maximum	4636	4574	
Entropy 13 × 13	Average	3986	4459	< 0.0001*
	Median	3987	4518	
	Minimum	2836	3962	
	Maximum	4872	4811	
Entropy 15 × 15	Average	4.13	4624	< 0.0001*
	Median	4.13	4687	
	Minimum	2909	4101	
	Maximum	5059	5	

\*Mann-Whitney test; \*\*unpaired *t*-test.

found in females, which are usually evidenced in studies involving these disorders [14]. Smoking, an important etiological factor of OLs, was also observed in most cases of OL investigated. As for the anatomical site, these lesions can develop anywhere in the oral cavity; however, the oral mucosa and the tongue are the regions constantly affected by them [15]. These aspects were also observed in our patients. Dysplasias, a histopathological finding commonly found in these lesions, were also present in most of our cases, mainly mild dysplasia and, more rarely, severe dysplasia. Although OL incidence is much higher than that of PVL, the rate of transformation of OLs is much lower. In our study, of the 61 cases of OL, only two underwent malignant transformation, while of the three cases of PVL, one patient only progressed to SCC, which in the light of our study can be considered high, even higher than the OLs used [14]. However, it is important to consider that our sample of PVL was small, which somewhat compromises the interpretation of this pathognomonic biological aspect of this lesion. In addition, there is the issue of the follow-up time of these

patients, which seemed short to the point of detecting malignant transformation of their respective lesions, which led us to classify them as tumor-free in the present study. As for the color of the lesions, the vast majority of cases were white, a clinical aspect commonly found in these lesions, but which can alternate between white and red lesions in some cases [14, 15].

The model used in this study for learning and segmenting the cores was the Mask R-CNN network. The choice of this network came from the work of our study group in the area of AI carried out by, who used this network to identify nuclei in dysplastic lesions of the oral cavity developed in mice subjected to oral carcinogenesis by 4NQO. Mask R-CNN couples to ResNet50 or ResNet101 for learning the cores. We chose ResNet50 based on an empirical test carried out in the study by Silva (2019), which showed that ResNet50 performed better in targeting the dysplastic lesions investigated by him.

The different works on core identification have adopted different segmentation methods. In this regard, the Mask



R-CNN proved to be the most effective in detecting nuclei in studies that compared different methods of nuclear identification. The study by Waal, Isaïc (2019) [16, 17], for example, segmented normal and abnormal nuclei of cervical cells using the Mask R-CNN, obtaining an average accuracy of 96%. They also compared this network with other segmentation methods and found that these methods presented lower results than the Mask R-CNN, such as the Multiscale Watershed + Binary Classifier, which achieved an accuracy of 88%, the RGVF of 83%, and Patch-based FCM of 85%. The work by Silva (2019) reached an average accuracy of 89.52% with the segmentation of nuclei of tongue epithelium cells without and with mild, moderate, and severe dysplasias. Also in this study, other methods were tested in comparison to his, and the results were inferior, such as the Otsu method, which presented an average accuracy of 60.78%, K-means of 77.32%, and SegNet of 73.12%. These data reveal that this neural network presents a good performance in terms of nuclear segmentation, which was confirmed by our accuracy results in OLs, PVLs, and SCCs, corresponding to 93.15%, 92.93%, and 94.63%, respectively. Future works may further improve this network so that its use in the area of pathology becomes ubiquitous, as shown by Anantharaman et al. (2018), who developed a network based on the Mask R-CNN exclusively for the detection of nuclei called Nuclei R-CNN, with even better results than the original Mask R-CNN.

As for the core features extracted from the entire OL and PVL dataset after neural network training, including entropy, Moran Index, area, perimeter, eccentricity, orientation, and solidity, they were compared between the two lesions. Significant differences were found between OL and PVL in the seven entropy levels evaluated in our study. Entropy is a measure that assesses the disorder of the nuclear texture, which, in turn, directly reflects the organization of chromatin and, consequently, the genetic and epigenetic changes that occur in the DNA molecule during the tumorigenesis process [18]. Thus, nuclear entropy has been studied in several types of cancers, focusing on determining clinical prognosis and tumor aggressiveness. In the study by, which investigated different types of cancers including the colon, ovary, uterus, prostate, and endometrium, it was observed that patients who exhibited more heterogeneous texture patterns, that is, higher entropy levels, had worse survival for all tumors evaluated. In our study, it is interesting to note that all mean entropy levels analyzed were higher in PVLs than in OLs, suggesting a greater chromatin disorder in those lesions to the detriment of these, which partly may explain the greater potential of PVLs to progress to SCC.

Similarly, [19] found a consecutive increase in entropy in the epithelial cell nuclei of nonsmoking smokers and patients with precancerous conditions. Therefore, these entropy results seem to be useful in distinguishing lesions with lower and higher malignant transformation potential, in the case of LB and PVL, respectively, suggesting the occurrence of distinct genetic and epigenetic alterations between them. Further studies will assess whether higher entropy indices in OLs indicate a greater risk of malignant transformation, as seems to be the case for PVLs.

Another characteristic evaluated in our study and related to the nuclear texture is the Moran Index. There are no works in the literature that use the Moran Index to assess cell nuclei, except for Silva (2019). As in our study, in work by Silva (2019), this feature proved useful in distinguishing the different lesions studied, with significant differences between healthy tissue and tissue with dysplasia; in the present work, a significance was obtained between OL and PVL. In this sense, it can be concluded that both entropy and the Moran Index can be used to detect changes in chromatin in premalignant lesions, a fact reinforced by the study by [20–22], who analyzed some nuclear characteristics and verified that the nuclear texture is an effective variable in differentiating the degrees of dysplasia in Barrett's esophagus, in addition to being efficient in predicting progression to cancer, which, together with our results, further highlights the importance of evaluating the nuclear textures in an attempt to elucidate the pathological conditions of premalignant lesions.

Regarding the area, our results point to a direct relationship with some studies on DBPMs. The work of [23] showed that the area of the cellular nuclei of the oral submucosal fibrosis lesion with dysplasia was greater than that of the normal nuclei, suggesting that this alteration could indicate the occurrence of tumorigenesis, reflecting the increase in the metabolic activity of these cells. Similar to the area, perimeter reflects the size of nuclei and is sometimes used together with area to infer changes in nuclear size. The work by Krishnan et al. (2010) showed an increase in the perimeter of the nuclei between oral submucosal fibrosis with dysplasia and normal oral mucosa. Solidity is a descriptor used in the assessment of nuclear deformity. In our results, a significant difference was found between the two injuries, also proving to be a useful variable in distinguishing between OL and PVL. Here, the mean solidity in the PVLs was slightly lower than in the OLs. Unlike our study, work by Krishnan et al. [23] found no significant differences in the solidity of nuclei in an attempt to discriminate oral submucosal fibrosis from normal oral mucosa. Similarly, the study [19] also did not detect substantial differences in nuclear solidity between nonsmoking smokers and patients with PMBD. One hypothesis is that PVLs have a high power of malignant transformation compared to other MPDs, increasing the chances of nuclear deformity and leaving the nuclei less convex and more irregular, a characteristic found in cancer cells, as described. Solidity is a variable that is still little investigated in studies involving the evaluation of nuclear morphology by computational algorithms. Therefore, it is expected that further research may include it in the evaluation of nuclei in different DBPMs as a possible descriptor that characterizes different lesions, as observed in our study.

We found no significant differences in eccentricity and orientation between OL and PVL. Interestingly, the study by [24–28] also found no differences in eccentricity between oral submucosal fibrosis nuclei and buccal mucosa. Thus, further studies should be conducted in order to determine the value of these variables in DBPMs more clearly. Thus, it is possible to conclude from our investigation that both



lesions carry distinct nuclear alterations. Our findings also support the importance of the nuclear study from computational techniques evaluated by an AI, a promising area in medicine that, without a doubt, will shape the field of pathology soon, finding new ways to interpret the pathological processes that occur. In various diseases. Based on the evidence found in our study and in the works mentioned here, these descriptors may prove to be useful in predicting the progression to SCC of PMBDs, such as OL and PVL. The investigated nuclear features were transformed into vectors so that the classifier could dichotomize the samples between the two lesions. The classifier used all 119 PVL ROIs and 120 OL ROIs to assess the degree of separability. It is worth mentioning that for the classification to perform well, it is important to have a balanced number among the samples to be investigated. Therefore, only 120 OL ROIs were used by the classifier [29–33].

The polynomial classifier proved to be very effective in the studies in which it was adopted, with extremely satisfactory performance [15] in the classification between normal and abnormal tissues of mammograms through texture analysis, reaching an AUC of 98%, a performance superior to the SVM, decision tree, and K-NN classifiers, which were also compared in the study. Similarly, in work by Silva (2019), the polynomial classifier achieved an average AUC of 92% in the classification between healthy tissues and those with different degrees of dysplasia, that is, a superior result than the multilayer perceptron, decision tree, and random classifiers. Forest was compared in their study. Similarly, our result was excellent, with an average UAC of 97.06%, indicating that this classifier can be an additional tool for pathologists in defining a histopathological diagnosis since the diagnosis of PVLs is still a constant challenge in oral pathology, and that can be easily confused with OLs, especially in the initial cases. Thus, our study proposes the use of AI as a tool that raises the criteria currently adopted in the distinction between these two lesions, reducing the margin of doubt and improving the accuracy of the diagnosis with less subjectivity. Further studies are needed to verify whether this method can be used in the early stages of PVLs, when they are usually labeled as OLs without any evidence of evolution to more aggressive forms, which would be of great importance in determining an early diagnosis of PVLs, increasing the chances of successful treatment.

## 5. Conclusion

Based on the investigations carried out in this work, the present study showed that, despite being histologically similar, OLs and PVLs carry distinct nuclear properties that can be used for differential diagnosis between them, thus, helping to resolve one of the major challenges of oral pathology in the search for more effective and accurate ways to establish the differential diagnosis between OL and PVL. The fact that the neural network has achieved an excellent performance in nuclear identification through the supervised training performed reveals that this method can be a great ally in our later works involving histological studies, including the analysis of more cases of OLs and PVLs in the first

time. In addition, the characteristics found in the nuclei of the two lesions can provide important information in the construction of a model to assess the risk of malignant transformation of these disorders, being extremely important in making therapeutic decisions for each case. Added to this, the use of a classifier could also be used in the future as an additional tool for cases of a difficult diagnosis. Finally, our investigations are added to the various works that show machine learning as a new possibility for studies in pathology, being an effective, low-cost method that will possibly be used on a large scale in the near future in clinical routines, adding speed, precision, and prediction in diagnoses.

## Data Availability

The data used to support the findings of this study are included within the article.

## Conflicts of Interest

The authors declare that they have no conflicts of interest.

## Acknowledgments

The authors extend their appreciation to Princess Nourah bint Abdulrahman University Researchers Supporting Project number (PNURSP2022R141), Princess Nourah bint Abdulrahman University, Riyadh, Saudi Arabia.

## References

- [1] World Health Organization, *WHO global report on trends in prevalence of tobacco smoking 2015*, WHO, 2015, <https://apps.who.int/iris/handle/10665/156262>.
- [2] A. G. Zygianni, G. Kyrgias, P. Karakitsos et al., “Oral squamous cell cancer: early detection and the role of alcohol and smoking,” *Head & Neck Oncology*, vol. 3, no. 1, p. 2, 2011.
- [3] A. A. Hamad, M. L. Thivagar, M. B. Alazzam et al., “Dynamic systems enhanced by electronic circuits on 7D,” *Advances in Materials Science and Engineering*, vol. 2021, Article ID 8148772, 2021.
- [4] P. Speight, S. A. Khurram, and O. Kujan, “Oral potentially malignant disorders: risk of progression to malignancy,” *Oral Surgery, Oral Medicine, Oral Pathology, Oral Radiology*, vol. 125, no. 6, pp. 612–627, 2018.
- [5] E. Mustafa, S. Parmar, and P. Praveen, “Premalignant lesions and conditions of the oral cavity,” in *Oral and Maxillofacial Surgery for the Clinician*, K. Bonanthaya, E. Panneerselvam, S. Manuel, V. V. Kumar, and A. Rai, Eds., Springer, Singapore, 2021.
- [6] M. B. Alazzam, W. T. Mohammad, M. B. Younis et al., “Studying the effects of cold plasma phosphorus using physiological and digital image processing techniques,” *Computational and Mathematical Methods in Medicine*, vol. 2022, 5 pages, 2022.
- [7] L. A. Owki, E. Othieno, J. Wandabwa, and A. Okoth, “Prevalence of cancerous and pre-malignant lesions of cervical cancer and their association with risk factors as seen among women in the regions of Uganda,” *Journal of Clinical and Laboratory Medicine*, vol. 2, 2019.

## Retraction

# Retracted: DNMT3A Regulates miR-149 DNA Methylation to Activate NOTCH1/Hedgehog Pathway to Promote the Development of Junctional Osteosarcoma

### BioMed Research International

Received 20 June 2023; Accepted 20 June 2023; Published 21 June 2023

Copyright © 2023 BioMed Research International. This is an open access article distributed under the Creative Commons Attribution License, which permits unrestricted use, distribution, and reproduction in any medium, provided the original work is properly cited.

This article has been retracted by Hindawi following an investigation undertaken by the publisher [1]. This investigation has uncovered evidence of one or more of the following indicators of systematic manipulation of the publication process:

- (1) Discrepancies in scope
- (2) Discrepancies in the description of the research reported
- (3) Discrepancies between the availability of data and the research described
- (4) Inappropriate citations
- (5) Incoherent, meaningless and/or irrelevant content included in the article
- (6) Peer-review manipulation

The presence of these indicators undermines our confidence in the integrity of the article's content and we cannot, therefore, vouch for its reliability. Please note that this notice is intended solely to alert readers that the content of this article is unreliable. We have not investigated whether authors were aware of or involved in the systematic manipulation of the publication process.

In addition, our investigation has also shown that one or more of the following human-subject reporting requirements has not been met in this article: ethical approval by an Institutional Review Board (IRB) committee or equivalent, patient/participant consent to participate, and/or agreement to publish patient/participant details (where relevant).

Wiley and Hindawi regrets that the usual quality checks did not identify these issues before publication and have since put additional measures in place to safeguard research integrity.

We wish to credit our own Research Integrity and Research Publishing teams and anonymous and named external researchers and research integrity experts for contributing to this investigation.

The corresponding author, as the representative of all authors, has been given the opportunity to register their agreement or disagreement to this retraction. We have kept a record of any response received.

### References

- [1] S. Cheng and W. Wang, "DNMT3A Regulates miR-149 DNA Methylation to Activate NOTCH1/Hedgehog Pathway to Promote the Development of Junctional Osteosarcoma," *BioMed Research International*, vol. 2022, Article ID 3261213, 9 pages, 2022.

## Research Article

# DNMT3A Regulates miR-149 DNA Methylation to Activate NOTCH1/Hedgehog Pathway to Promote the Development of Junctional Osteosarcoma

Shigao Cheng<sup>1</sup> and Wanchun Wang<sup>2</sup> 

<sup>1</sup>Department of Orthopedics, Loudi Central Hospital of Hunan Province, Loudi, Hunan, 417000, China

<sup>2</sup>Department of Orthopedics, The Second Xiangya Hospital of Central South University, Changsha, Hunan, 410011, China

Correspondence should be addressed to Wanchun Wang; 161843129@masu.edu.cn

Received 24 April 2022; Revised 24 May 2022; Accepted 27 May 2022; Published 21 July 2022

Academic Editor: Dinesh Rokaya

Copyright © 2022 Shigao Cheng and Wanchun Wang. This is an open access article distributed under the Creative Commons Attribution License, which permits unrestricted use, distribution, and reproduction in any medium, provided the original work is properly cited.

**Purpose.** To investigate the DNMT3A/miR-149/NOTCH1/Hedgehog axis regulating the development of osteosarcoma. **Methods.** First, microRNA and mRNA expression microarrays were downloaded from the GEO database for osteosarcoma and differentially expressed microRNAs were analyzed. Subsequently, we collected cancerous tissues and corresponding paracancerous tissues from 42 osteosarcoma patients and examined the expression levels of miR-149, DNMT3A, and NOTCH1 in the samples. Subsequently, miR-149 was overexpressed in osteosarcoma cells to detect cell proliferation and metastatic ability changes. We then queried the methylation level of the miR-149 promoter on the bioinformatics website and verified it by experiment. We further demonstrated the expression level of miR-149 with NOTCH1 using a dual luciferase assay and confirmed the role of NOTCH1 on osteosarcoma cell growth and metastasis by functional rescue assay. Finally, we detected the activation level of the Hedgehog/catenin signaling pathway by WB and immunofluorescence. **Results.** miR-149 was significantly low expressed in osteosarcoma tissues and cells, while DNMT3A and NOTCH1 were highly expressed in osteosarcoma tissues and cells, and negatively correlated with miR-149 expression levels. Overexpression of miR-149 significantly inhibited the growth and metastasis of osteosarcoma cells in vitro and in vivo, and we found that DNMT3A could promote the methylation modification of the miR-149 promoter, thereby inhibiting the expression of miR-149. Subsequently, the experimental results showed that miR-149 could target negative regulation of NOTCH1, and further overexpression of NOTCH1 in cells with high miR-149 expression could promote the growth and metastasis of osteosarcoma cells in vitro. **Conclusion.** The methyltransferase DNMT3A suppresses miR-149 expression by promoting methylation modification of the miR-149 promoter, resulting in elevated expression levels of NOTCH1 in cells, therefore exacerbating activation of the Hedgehog signaling pathway and therefore exacerbating the development and progression of osteosarcoma.

## 1. Introduction

Osteosarcoma (OS) is the most frequent malignant bone tumor in children and adolescents, and it mostly affects the metaphysis of long bones [1]. The annual incidence of OS varies between 1 and 4 per million, with men having a slightly greater prevalence than women [2]. Despite the low overall prevalence of OS, the prognosis is dismal. The 5-year survival rate for patients without metastases is approximately 65–70 percent when limb salvage surgery and neoadjuvant chemotherapy are combined [3]. Because

osteosarcoma has such a dismal prognosis following metastasis, new therapeutic approaches are desperately needed [4].

Long noncoding RNAs (lncRNAs) with more than 200 nucleotides are thought to regulate protein-coding genes in various ways, including epigenetic regulation, transcription regulation, posttranscriptional regulation, and microRNA (miRNA) regulation [5–7]. MicroRNAs (miRNAs) are single-stranded RNAs with a length of 21–25 nucleotides that do not code for proteins. Its expression alterations are linked to the tumor's occurrence, progression, diagnosis, and prognosis [8]. It is worth noting that miRNAs have a

unique property: they are extremely stable in plasma and serum and are not destroyed by RNase [9]. Finding miRNA biomarkers with unique expression patterns will be critical for the early detection and treatment of OS.

It has been demonstrated that odd DNA methylation regulates carcinogenesis and the course of many cancers. According to growing data, tumorigenesis is linked to strange epigenetic variables such as DNA methylation, histone modification, RNA m6A modification, RNA binding proteins, and transcription factors. [10] Methylation of RNA, notably m6A modifications of RNA, and histone modifications, which are thought to be the essential contributors to cancer development, are among the critical epigenetic alterations in cancer development [11]. DNMT3A (NM 022552.4) belongs to the DNA methyltransferases (DNMTs) family, which catalyzes the addition of a methyl group to the 5-cytosine residue CpG dinucleotides. The DNMT3A gene (2p23.3) encodes a protein that methylates previously unmethylated genomic DNA and is responsible for genome-wide de novo DNA methylation [12]. DNMT3A also acts as a transcriptional corepressor, suppressing gene transcription without the need for its de novo methyltransferase activity [13, 14]. It is frequently mutated in AML and has been linked to a poor prognosis; however, DNMT3A mutations in solid human tumors have not been well studied [15]. Although DNA methylation patterns in OS have attracted attention as an essential biomarker and therapeutic target, the mechanism of regulation of OS by DNMT3A with miR-149 and DNA methylation remains unclear. miR-149 is further overexpressed in cells with NOTCH1, and the growth and metastasis of the resulting tumor cells are also unclear, so tumor recurrence and widespread metastasis also complicates the clinical treatment of osteosarcoma. To date, the molecular mechanisms underlying the malignant biological behavior of osteosarcoma remain unclear, although molecular biology studies associated with osteosarcoma have provided a theoretical basis for its pathogenesis. Exploring the pathogenesis of OS is important for improving diagnosis and finding new therapeutic targets. Therefore, in our study, a functional enrichment study was carried out to investigate the possible mechanisms.

## 2. Materials and Methods

**2.1. Bioinformatics Analysis.** The Gene Expression Omnibus (<https://www.ncbi.nlm.nih.gov/geo/>) was used to download osteosarcoma-related gene expression datasets (DEGs). Three gene expression datasets were obtained: one miRNA (GSE67268) and two gene expression datasets (GSE29001 and GSE20347). Normalized expression data were used to screen DEGs and differentially expressed miRNAs using the limma package (<http://master.bioconductor.org/packages/release/bioc/html/limma.html>) with  $|\log_2 \text{FC}| > 1.5$  and  $\text{adj.}P\text{-Val} = 0.05$ . Also, pheatmap (<https://cran.r-project.org/web/packages/pheatmap/index.html>) was used to create a miRNA heat map. The target genes of differentially expressed miRNAs were predicted using the starBase, TargetScan, and mirRDB databases. jvenn ([\[toulouse.inra.fr/app/example.html\]\(http://toulouse.inra.fr/app/example.html\)\) was also used to screen differentially expressed miRNAs \(GSE29001 and GSE20347\). The HPA website was utilized to retrieve the staining intensity of DNMT3A and NOTCH1 for immunohistochemistry in normal esophageal tissue and osteosarcoma tissue samples.](http://jvenn</a></p>
</div>
<div data-bbox=)

**2.2. EdU Staining.** Osteosarcoma cells in the logarithmic growth phase were seeded in triplicate into 96-well plates at 4 × 10<sup>4</sup> cells/well. After 24 hours, the cells were treated with various chemicals. 2 hours in EdU media at 100l/well, followed by 100l/well cell fixative, 2 mg/ml glycine, and 100l/well permeabilizer (phosphate-buffered saline (PBS) containing 0.5 percent Triton X-100). Incubation with antifluorescence quenching blocking solution (100l/well) followed by staining with Apollo and Ho osteosarcoma hst 33342 reaction solutions. The number of EdU-stained cells was counted using microscope images. Positive cells have red nuclei. In order to obtain the EdU staining rate (%), the number of positive cells was divided by (number of positive cells + number of negative cells) 100 percent.

**2.3. Colony Formation.** Cells were cultured at a density of 1 × 10<sup>3</sup> cells/well in 90 mm cell culture dishes containing 5 ml of complete DMEM complete +10% FBS. All culture dishes were incubated in a sterile incubator at 37°C and 5% CO<sub>2</sub> for 2 weeks. The culture medium was changed every two days. Cells were washed three times with PBS to remove residual cells and then fixed with 4% formaldehyde for 10 min at room temperature. The cells were then stained with crystal violet (0.1%) for 10 minutes at room temperature. The colonies were counted under a light microscope. A population of >50 cells was considered a clone.

**2.4. Caspase-3 Activity Assay.** MG63 or TE-3 cells were transfected in 100l of media in 96-well flat-bottomed microplates. Then, 100l Caspase-Glo 3/7 Reagent (Promega, Madison, WI, USA) was added to each well and shaken for 1-2 minutes, 3h incubation at ambient temperature. A microplate reader measured 485Ex/527Em fluorescence (PerkinElmer, Waltham, MA, USA). The apoptotic index is the ratio of apoptotic nuclei to total cells in each group.

**2.5. Apoptosis Test.** Apoptosis was detected using the Annexin V-FITC/Propidium Iodide Apoptosis Detection Kit (BD Biosciences, San Diego, CA, USA). MG63 and SAOS-2 cells were plated in 6-well plates at 3105 cells per well, collected, washed twice with PBS, resuspended in binding buffer, and stained with Annexin V-FITC and PI. Staining cells for 15 minutes at 4°C in the dark, then analyzing using a B osteosarcoma kman Coulter flow cytometer (B osteosarcoma kman Gallios, Fullerton, CA, USA).

Transwell MG63 and SAOS-2 cells were collected and resuspended in 1 × 10<sup>5</sup> cells/ml serum-free DMEM. 200l of sample was introduced to 8m Transwell chambers pre-coated with Matrigel. The Transwell chambers were then placed in a 24-well plate with 500l DMEM (10% FBS) in each well. Affixed cell membranes from Transwell chambers were collected. Upper surface cells were gently scraped off with a cotton swab, while lower surface cells were gently



washed with PBS. After fixing with 4 percent paraformaldehyde, the cells were stained with 0.1 percent crystal violet for 20 minutes at room temperature. The invading cells were counted under a light microscope (Olympus, 200x).

**2.6. Tumorigenesis In Vivo.** Our Animal Care and Use Committee approved all animal experiments. We injected miR-149 mimic or control transfected MG63 or SAOS-2 cells (7106) into 4-week-old nude mice. Every 5 days, the tumor volume was measured 5 times. Then, the mice were killed and the tumors weighed. Tumor samples were also preserved at  $-80^{\circ}\text{C}$  for histological analysis.

**2.7. Immunohistochemistry.** Xenograft tumors were collected and sectioned. In order to quench endogenous peroxidase, the 4m thick sections were deparaffinized, rehydrated, and then labeled with antibody overnight at  $4^{\circ}\text{C}$ , followed by 30 seconds of hematoxylin counterstaining and slipcovering with secondary streptavidin-horseradish peroxidase-conjugated antibody (Santa Cruz Biot Osteosarcoma h, Santa Cruz, CA).

**2.8. TUNEL Stain.** Tumor sections were stained with 4',6-diamidino-2-phenylindole (DAPI, 1:5000; Beyotime, China) and TUNEL kit to evaluate apoptosis-related alterations (Roche, Basel, Switzerland). We also counted TUNEL-positive cells using a laser scanning confocal microscope (SP8, Leica, Japan).

**2.9. MSP-qPCR.** The DNA Methylation Kit (TIANGEN Biot Osteosarcoma h, Beijing, China) was used to modify human genomic DNA with bisulfite (Zymo Research, Orange, CA, USA). The modified DNA (1 g) was amplified using Winkylbio (Guangzhou, China) MSP methylation and nonmethylation primers. 45 seconds each at  $95^{\circ}\text{C}$ ,  $62^{\circ}\text{C}$ , and  $72^{\circ}\text{C}$  with a final extension of 10 minutes at  $72^{\circ}\text{C}$ . qPCR was used to test PCR products.

**2.10. Assay for Luciferase.** WT NOTCH1-3' untranslated region (UTR) (PGLO-NOTCH1-WT) and MUT NOTCH1 sequence with MUT miR-149 binding site (PGLO-NOTCH1-MUT) were purchased from Guangzhou Land Bio (Guangdong, China). Positive control was renilla luciferase plasmid pRL-TK. They were cotransfected with miR-149mimic and NC mimetic in HEK-293 T cells at 70-80% confluence. Transfection was performed using the following ratios of firefly luciferase reporter vector: mimic: pRL-TK = 0.50 nM: 0.1 g. Lysed cells were tested utilizing the Dual-Luciferase® Reporter Vector Assay System (E1910, Promega, Madison, WI, USA) The relative luciferase activity was calculated as the ratio of firefly luciferase to renilla luciferase activity.

**2.11. Immunofluorescence.** Fixed with prechilled acetone, cells on glass coverslips were rinsed three times with PBS and then reincubated in 10% goat serum with 0.3 percent hydrogen peroxide, followed by overnight incubation with primary antibodies to atenin (both from Abcam). A secondary HRP-conjugated antibody (ZSGB-BIO, Xicheng, Beijing, China) was then incubated for 45 minutes at room temper-

ature. DAPI was used to stain the nuclei (Boster Biot osteosarcoma technology, Wuhan, China).

**2.12. Data Analysis Methods.** SPSS was applied for statistical analysis. The data was noted as "mean  $\pm$  standard deviation." Chi-square test or Student *t*-test was applied for two-sample comparisons. All the tests at *P* value  $< 0.05$  were considered a significant difference.

### 3. Experimental Results

**3.1. miR-149 Is Significantly Underexpressed in Osteosarcoma Tissues and Cells.** The GEO database contained 113 osteosarcoma tumor samples and normal esophagus tissues. We analyzed 63 differently expressed microRNAs (normal vs. cancer) (Figure 1(a)), of which miR-149 expression was most significantly downregulated in osteosarcoma tissues. We then looked at miR-149 expression in 42 osteosarcoma patients' tumors and paraneoplastic organs. Tumor tissues had significantly reduced expression of miR-149 (Figure 1(b)), and we investigated the connection between miR-149 expression and clinical stage, lymph node metastasis, and differentiation levels of osteosarcoma patients. The expression of miR-149 was found to be significantly lower in Stage III and IV patients than in Stage I and II patients (Figure 1(c)), and in lymph node metastasis patients than in nonmetastasis patients (Figures 1(d) and 1(e)). qRT-PCR evaluated miR-149 expression in normal human esophageal epithelial cells HET-1A and osteosarcoma cell lines SAOS-2, 9706, and MG63 (Figure 1(f)). So, we wondered if decreased miR-149 expression was linked to osteosarcoma formation and progression.

**3.2. Exogenous Overexpression of miR-149 Significantly Inhibits the Growth and Metastasis of Osteosarcoma Cells In Vitro.** We transfected miR-149 mimic into MG63 and SAOS-2 cells to confirm the effect of miR-149 on osteosarcoma cell proliferation and development (Figure 2(a)). After transfection with miR-149, the number of cell clones generated by MG63 and SAOS-2 cells was dramatically reduced (Figure 2(b)). Using a caspase-3 kit and flow cytometry, we discovered that miR-149 mimic dramatically increased caspase-3 activity in KYSE-150 and SAOS-2 cells (Figures 2(c) and 2(d)). Using qRT-PCR, we discovered that miR-149 raised E-cadherin and ZO-1 mRNA expression levels while decreasing N-cadherin and vimentin mRNA expression levels (Figure 2(e)), indicating that miR-149 promotes EMT. Using the Transwell experiment, we confirmed our suspicions: miR-149 transfection reduced the migratory and invasion abilities of MG63 and SAOS-2 cells (Figures 2(f) and 2(g)). In vitro, miR-149 appears to slow osteosarcoma cell growth and metastasis.

**3.3. The miR-149 Promoter Has Significant Methylation Modifications.** To clarify the upstream regulatory mechanism of miR-149, we first found that miR-149 belongs to a transcript with HYC gene (Figure 3(a)), and we found that the promoter sequence of miR-149 has a distinct CpG island (Figure 3(b)). Thus, we speculated whether it was because the miR-149 promoter was modified by methylation in



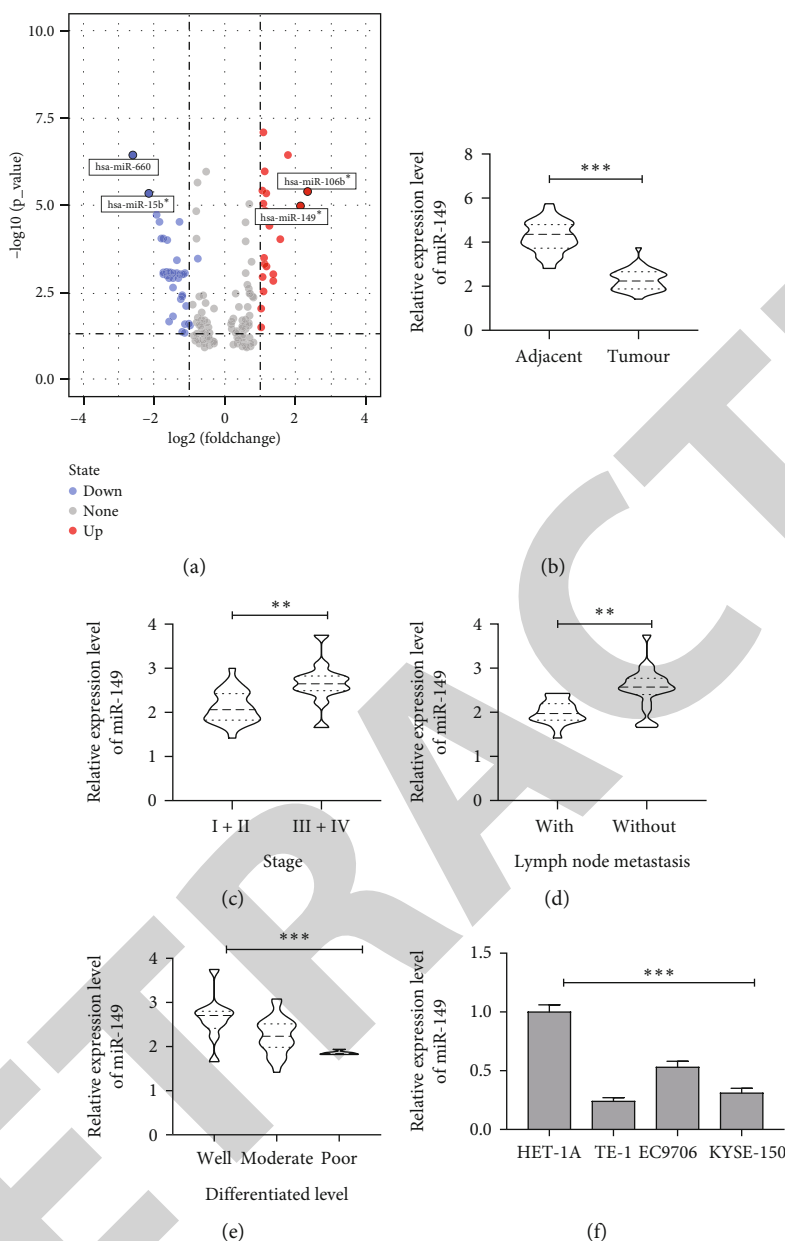


FIGURE 1: miR-149 was significantly low expressed in osteosarcoma tissues and cells. (a) Differentially expressed microRNA in microRNA expression microarray GSE67268 of osteosarcoma tissues. (b) qRT-PCR detection of miR-149 expression levels in cancer tissues and paired paraneoplastic tissues of 42 osteosarcoma patients. (c–e) Analysis of miR-149 451a expression levels in relation to clinical stage, lymph node metastasis, and differentiation level of osteosarcoma patients. (f) miR-149 expression levels in normal human esophageal epithelial cells HET-1A and osteosarcoma cell lines SAOS-2, osteosarcoma 9706, and MG63. In (b–e), each point represents one sample, and data were analyzed for differences using the paired or unpaired test; \*\* $P < 0.01$ , \*\*\* $P < 0.001$ . In (f), data were analyzed for differences using one-way ANOVA and Tukey's multiple comparison test for analysis of variance on data; \*\*\* $P < 0.001$ .

osteosarcoma, thus suppressing its expression. To test our conjecture, we harvested the methylation level of miR-149 promoter in 42 osteosarcoma patients by MSP-qPCR. We found that the methylation level of miR-149 promoter was significantly higher in cancer tissues than in paraneoplastic tissues (Figure 3(c)). Moreover, we further analyzed that the expression level of miR-149 was negatively correlated with its methylation level in 42 osteosarcoma tumor samples (Figure 3(d)). And we also found that the methylation modification level of miR-149 promoter was significantly lower

in normal human esophageal epithelial cells HET-1A than in osteosarcoma cell lines (Figure 3(e)). Moreover, we further found that the expression level of miR-149 in the cells was significantly increased after treatment with 5-aZa-CDR on the osteosarcoma cell line (Figure 3(f)).

**3.4. DNMT3A Promotes Methylation Modification of miR-149 Promoter.** We found in result 4 that the miR-149 promoter has significant methylation modifications, thereby repressing its transcription, which leads to the growth and

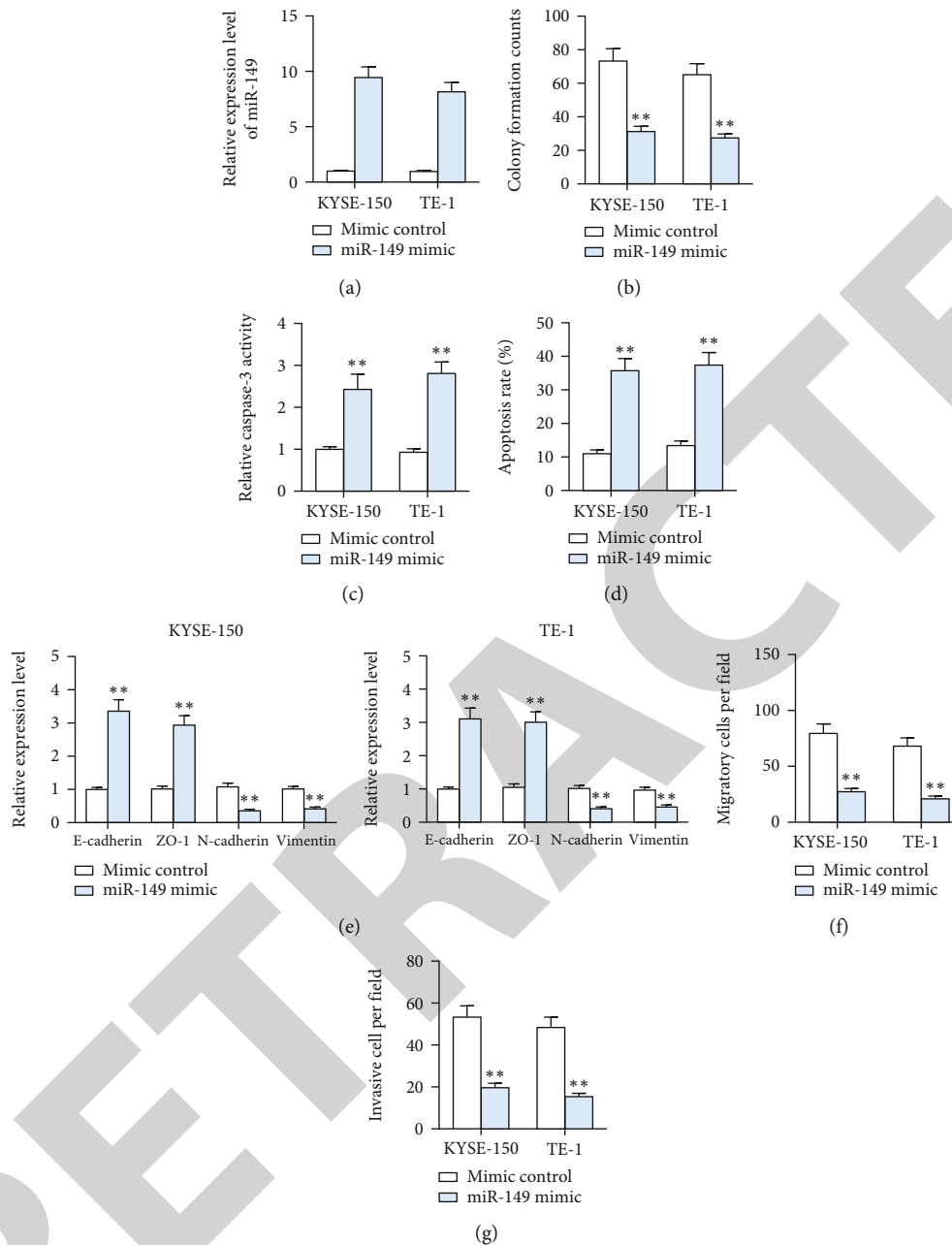


FIGURE 2: Exogenous overexpression of miR-149 significantly inhibits the growth and metastasis of osteosarcoma cells in vitro. (a) qRT-PCR to detect the expression level of miR-149 in MG63 and SAOS-2 cells after transfection with mimic control or miR-149 mimic. (b) Plate cloning assay to detect the number of clones formed in MG63 and SAOS-2 cells. The number of clones formed. (c) Caspase-3 kit to detect changes in caspase-3 activity in MG63 and SAOS-2 cells. (d) Flow cytometry to detect the proportion of apoptosis in MG63 and SAOS-2 cells. (e) qRT-PCR to detect the EMT-related factors E-cadherin, ZO-1, vimentin, and N-cadherin mRNA expression levels. (f, g) Transwell assay to detect the migration and invasion ability of MG63 and SAOS-2 cells. Each experiment was repeated three times, and data were presented as mean plus or minus standard deviation, and in (a–g), 2-way ANOVA and Tukey’s multiple comparison test were used to analyze the data for differences, \*\*\* $P < 0.001$ .

metastasis of osteosarcoma cells. To determine which specific methyltransferase initiates the role, we focused on DNMT1, DNMT3A, DNMT3A, and DNMT3L. We first examined the expression levels of these four genes in 42 paired osteosarcoma tissues and paracancerous tissues and found that they all had significantly high expression in osteosarcoma tissues (Figure 4(a)), and we further found

that the expression levels of DNMT1, DNMT3A, DNMT3B, and DNMT3L were higher in cancer tissues than in normal esophageal tissues, but there was no significant difference, while the expression level of DNMT3A was significantly higher in osteosarcoma tissues than in normal esophageal tissues (Figure 4(b)). Therefore, we further analyzed the correlation between miR-149 and DNMT3A in 42

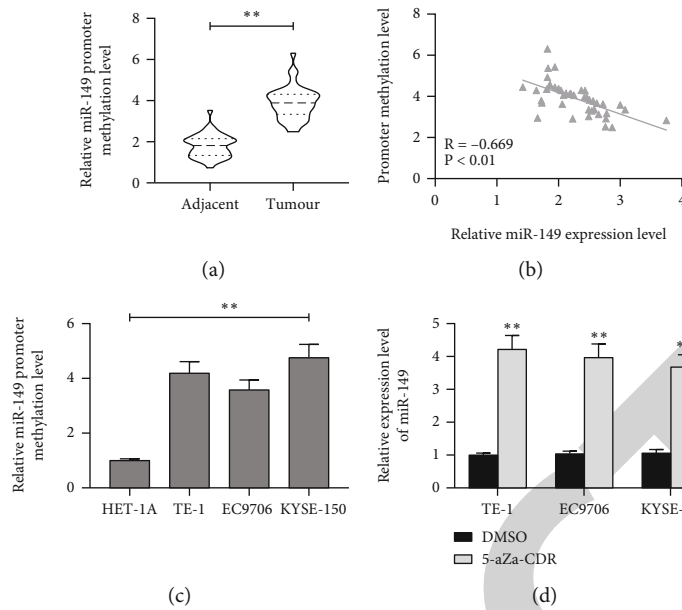


FIGURE 3: miR-149 promoter has significant methylation modification. (a) MSP-qPCR detects the methylation level of miR-149 promoter in cancerous and paraneoplastic tissues of 42 osteosarcoma patients. (b) Correlation between miR-149 and its DNA methylation level in tumor tissues of osteosarcoma patients. (c) MSP-qPCR detects the correlation between miR-149 and its DNA methylation level in normal tissues of osteosarcoma patients. Methylation levels of the promoter of miR-149 in tumor tissues from osteosarcoma patients. (d) Correlation between miR-149 and its DNA methylation levels in tumor tissues from osteosarcoma patients. Each point in CD represents one sample, and the data were tested for significant differences using the paired *t*-test,  $**P < 0.01$ . In (e, f), each experiment was repeated three times, and the data were presented as mean plus or minus standard deviation, using one-way or 2-way ANOVA and Tukey's multiple comparison test for analysis of variance on data,  $**P < 0.01$ ,  $***P < 0.001$ .

osteosarcoma patients, and we found that miR-149 had a significant negative correlation with DNMT3A (Figure 4(c)). We further found in the HPA site that DNMT3A staining intensity was significantly higher in osteosarcoma tissues than in normal esophageal tissues (Figure 4(d)). To further determine that DNMT3A promotes the methylation modification of miR-149, we first examined the binding relationship between DNMT3A and miR-149 promoter in osteosarcoma cell lines by ChIP-qPCR assay, and we found that the enrichment level of miR-149 promoter in the complexes pulled down using anti-DNMT3A antibody was significantly higher than that of IgG (Figure 4(e)). Moreover, we further constructed a luciferase reporter vector pGL3-enhancer containing miR-149 promoter and cotransfected it with different doses of DNMT3A overexpression plasmids into 293T cells, and we found that the luciferase activity in 293T cells decreased significantly with the increase of DNMT3A overexpression plasmid dose (Figure 4(f)). The above results suggest that DNMT3A can bind to miR-149 promoter to promote its methylation modification, thus inhibiting the expression of miR-149.

#### 4. Discussion

OS is the most prevalent malignant bone tumor, and it has a significant impact on patients' quality of life and life expectancy. Early detection and treatment of osteosarcoma patients cannot be overstated [16]. It has an early onset age, a high malignancy, a high rate of metastasis, and a bad prognosis [17]. Its proclivity for metastasizing is the most common cause

of therapy failure and poor prognosis [18]. Despite significant advances in surgery and neoadjuvant treatment, most patients still have a dismal prognosis. Some researchers have attempted to apply gene treatments to OS in recent years, including adenovirus-based gene transfection and siRNA-based gene silencing [19–21], and it is now making progress in certain basic studies. Since the discovery of miRNA, researchers from all around the world have been exploring its involvement in malignancies. Some miRNAs have been discovered to promote or repress malignancy in tumors [22, 23].

lncRNAs are primarily found in the cytoplasm, acting as a miRNA sponge [24]. For patients with osteosarcoma, there are currently few biomarkers with high sensitivity. Bioinformatics research in the past was frequently limited to a single database or single gene prognostic value, which has limits. In recent decades, scientists have uncovered many factors of epigenetic modification influencing gene expression that interfere with tumor formation [25, 26]. DEGs are primarily engaged in DNA replication, mitosis, and cell cycle regulatory signaling pathways, according to the GSEA data. DNA replication is the cellular activity that most easily leads to cancer, and genome instability is a marker of cancer [27].

Abnormal mitosis can promote the unrestricted expansion of faulty cells, making it the most common way for tumors to form [28]. Cell cycle dysregulation is the cause of aberrant cell proliferation, which is a hallmark of cancer, and the loss of cell cycle checkpoint control promotes genetic instability [29].

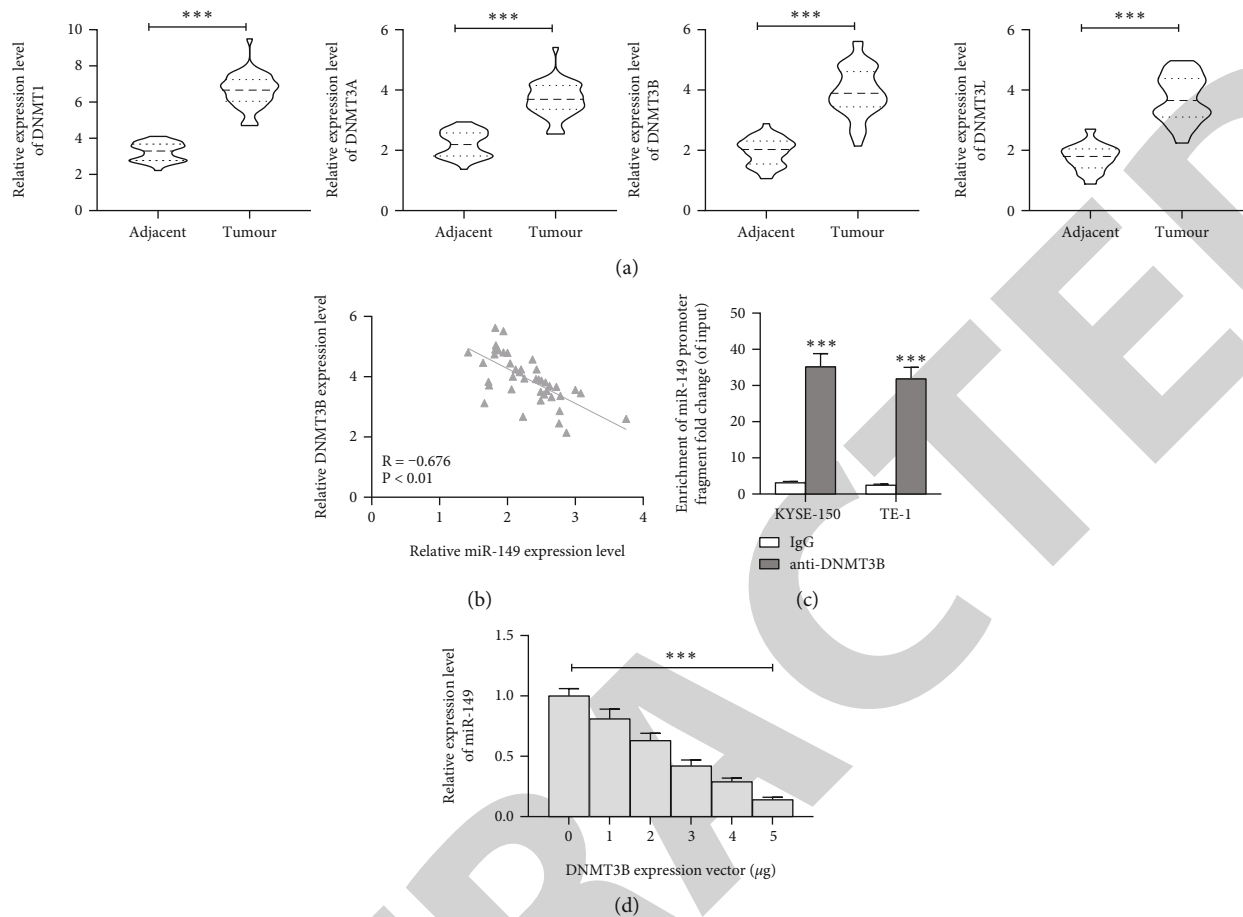


FIGURE 4: DNMT3A promotes miR-149 DNA methylation modification. (a) Pearson correlation test to analyze the correlation analysis between miR-149 and DNMT3A expression levels. (b) HPA website to retrieve the staining intensity of DNMT3A in normal esophageal tissues and osteosarcoma tissue samples by immunohistochemistry. (c) ChIP-qPCR to detect DNMT3A binding relationship with miR-149 promoter. (d) The luciferase reporter vector pGL3-enhancer containing miR-149 promoter was constructed, cotransfected into 293T cells with different doses of DNMT3A overexpression plasmids, and the expression level of miR-149 in the cells was detected. In (a), each point represents one sample, and the data were tested for significant differences using paired *t*-test,  $**P < 0.01$ . In (e, f), each experiment was repeated three times, and the data were presented as mean plus minus standard deviation using one-way or 2-way ANOVA and Tukey's multiple comparison test for analysis of variance on data;  $**P < 0.01$ ,  $***P < 0.001$ .

In our study, firstly, we analyzed the expression levels of miR-149 in the tumor tissues and corresponding paracancerous tissues of 42 patients with osteosarcoma and confirmed that miR-149 was significantly low expressed in osteosarcoma tissues and cells; secondly, to further verify the effect of miR-149 on the growth and development of osteosarcoma cells, the expression levels of EMT-related proteins in the cells were detected by qRT-PCR, and we found that exogenous overexpression of miR-149 significantly inhibited the growth and metastasis of osteosarcoma cells in vitro. Next, our experiments confirmed that miR-149 can significantly inhibit the growth of osteosarcoma cells in vivo and that the upstream of miR-149 has a regulatory mechanism, which suggests that the miR-149 promoter has significant methylation modifications. Then, miR-149 promoter represses its transcription, leading to osteosarcoma cells' growth and metastasis. We focused on DNMT1, DNMT3A, DNMT3A, and DNMT3L, and we found that DNMT3A promotes miR-149 promoter methylation modification. Finally, to clarify the downstream regulatory mechanisms

of miR-149, we confirmed that miR-149 targets the negative regulation of NOTCH1 expression and NOTCH1 promotes osteosarcoma cell progression through activation of the Hedgehog signaling pathway, thus exacerbating the development and progression of osteosarcoma.

Consistently, in OS tissue and cells, the DNA methyltransferase inhibitor 5-AZA-dC decreased DNA methylation in the APCDD1 promoter and restored APCDD1 expression. Furthermore, DNMT3a was the primary DNA methyltransferase that promoted hypermethylation of DNA in the APCDD1 promoter, lowering APCDD1 mRNA levels in OS tissues, but not DNMT1 or DNMT3b [30]. Thus, the present study shows that we provide for the first time that miR-149 is significantly low expressed in osteosarcoma tissues and cells, while DNMT3A and NOTCH1 are highly expressed in osteosarcoma tissues and cells. Thus exacerbating the development and progression of osteosarcoma. DNMT3A is involved in important cancer-related biological processes in OS.

**4.1. Limitation.** This is a study to develop predictive features for osteosarcoma based on epigenetically modified genes. However, our study has some limitations [31]. First, further confirmation of the efficacy of this study in additional independent prospective trials with functional testing of the identified genes is needed in this study. In addition to this, we need more prospective clinical studies and larger sample sizes to evaluate the diagnostic performance of this prognostic model. Therefore, more work remains to be done before the results can be applied to clinical practice.

## 5. Conclusion

Our study created a novel epigenetically relevant gene signature that has demonstrated significant clinical utility in predicting OS in patients with osteosarcoma. The methyltransferase DNMT3A exacerbates osteosarcoma development and progression by promoting methylation modification of the miR-149 promoter, thereby repressing miR-149 expression and leading to elevated levels of NOTCH1 expression in cells, thereby promoting activation of the Hedgehog signaling pathway. This signature may serve as a reliable biomarker for early detection and prognosis of osteosarcoma.

## Data Availability

All data generated or analyzed during this study are included in this published article.

## Conflicts of Interest

The authors declare that they have no competing interests.

## References

- [1] K. Berner, T. B. Johannesen, A. Berner et al., "Time-trends on incidence and survival in a nationwide and unselected cohort of patients with skeletal osteosarcoma," *Acta Oncologica*, vol. 54, no. 1, pp. 25–33, 2015.
- [2] L. Mirabello, R. J. Troisi, and S. A. Savage, "International osteosarcoma incidence patterns in children and adolescents, middle ages and elderly persons," *International Journal of Cancer*, vol. 125, pp. 229–234, 2009.
- [3] R. Siegel, K. Miller, and A. J. C. Jemal, "Cancer statistics, 2018," *CA: a Cancer Journal for Clinicians*, vol. 68, no. 1, pp. 7–30, 2018.
- [4] W. Zhang, L. Wei, J. Weng et al., "Advances in the research of osteosarcoma stem cells and its related genes," *Cell Biology International*, vol. 46, no. 3, pp. 336–343, 2022.
- [5] W. Zhuomin, L. Xiaoxia, L. Li et al., "Regulation of lncRNA expression," *Cellular & Molecular Biology Letters*, vol. 19, no. 4, pp. 561–575, 2014.
- [6] R. He, D. Luo, and Y. J. G. Mo, "Emerging roles of lncRNAs in the post-transcriptional regulation in cancer," *Genes & Diseases*, vol. 6, no. 1, pp. 6–15, 2019.
- [7] C. Wang, L. Wang, Y. Ding et al., "lncRNA structural characteristics in epigenetic regulation," *Regulation*, vol. 18, no. 12, 2017.
- [8] K. Felekis, E. Touvana, C. Stefanou, and C. J. H. Deltas, "MicroRNAs: a newly described class of encoded molecules that play a role in health and disease," *Hippokratia*, vol. 14, no. 4, pp. 236–240, 2010.
- [9] A. Turchinovich, L. Weiz, A. Langheinz, and B. Burwinkel, "Characterization of extracellular circulating microRNA," *Nucleic Acids Research*, vol. 39, no. 16, pp. 7223–7233, 2011.
- [10] S. Liu, B. Wu, X. Li, L. Zhao, W. Wu, and S. Ai, "Construction and validation of a potent epigenetic modification-related prognostic signature for osteosarcoma patients," *Journal of Oncology*, vol. 2021, Article ID 2719172, 2021.
- [11] A. Nebbioso, F. Tambaro, C. Dell'Aversana, and L. J. Altucci, "Cancer epigenetics: moving forward," *PLoS Genetics*, vol. 14, no. 6, article e1007362, 2018.
- [12] M. Okano, D. Bell, D. Haber, and E. J. C. Li, "DNA methyltransferases Dnmt3a and Dnmt3b are essential for de novo methylation and mammalian development," *Cell*, vol. 99, pp. 247–257, 1999.
- [13] F. Fuks, W. A. Burgers, N. Godin, M. Kasai, and T. Kouzarides, "Dnmt3a binds deacetylases and is recruited by a sequence-specific repressor to silence transcription," *The EMBO Journal*, vol. 20, no. 10, pp. 2536–2544, 2001.
- [14] K. E. Bachman, M. R. Rountree, and S. B. Baylin, "Dnmt3a and Dnmt3b Are Transcriptional Repressors That Exhibit Unique Localization Properties to Heterochromatin," *Journal of Biological Chemistry*, vol. 276, no. 34, pp. 32282–32287, 2001.
- [15] T. J. Ley, L. Ding, M. J. Walter et al., "DNMT3A mutations in acute myeloid leukemia," *The New England Journal of Medicine*, vol. 363, no. 25, pp. 2424–2433, 2010.
- [16] T. Wu, B. Wei, H. Lin et al., "Integral analyses of competing endogenous RNA mechanisms and DNA methylation reveal regulatory mechanisms in osteosarcoma," *Frontiers in Cell and Developmental Biology*, vol. 9, article 763347, 2021.
- [17] Y. Lu, G. Cao, H. Lan et al., "Chondrocyte-derived exosomal miR-195 inhibits osteosarcoma cell proliferation and anti-apoptotic by targeting KIF4A in vitro and in vivo," *Translational Oncology*, vol. 16, article 101289, 2022.
- [18] G. Sheng, Y. Gao, Y. Yang, and H. J. Wu, "Osteosarcoma and metastasis," *Frontiers in Oncology*, vol. 11, article 780264, 2021.
- [19] R. Luc, L. Julie, Z. Marianne et al., "Nitric oxide synthase inhibition and oxidative stress in cardiovascular diseases: possible therapeutic targets?," *Pharmacology & Therapeutics*, vol. 140, no. 3, pp. 239–257, 2013.
- [20] Y. Lin, B. E. Jewell, J. Gingold et al., "Osteosarcoma: molecular pathogenesis and iPSC modeling," *Trends in Molecular Medicine*, vol. 23, no. 8, pp. 737–755, 2017.
- [21] A. Czarnecka, K. Synoradzki, W. Firlej et al., "Molecular biology of osteosarcoma," *Cancers*, vol. 12, no. 8, 2020.
- [22] L. Qiang, L. Bowen, L. Qing et al., "Exosomal miR-21-5p derived from gastric cancer promotes peritoneal metastasis via mesothelial-to-mesenchymal transition," *Cell Death & Disease*, vol. 9, no. 9, p. 854, 2018.
- [23] M. Wu, Q. Duan, X. Liu et al., "MiR-155-5p promotes oral cancer progression by targeting chromatin remodeling gene ARID2," *Biomedicine & Pharmacotherapy*, vol. 122, article 109696, 2020.
- [24] H. Dong, J. Hu, K. Zou et al., "Activation of lncRNA TINCR by H3K27 acetylation promotes trastuzumab resistance and epithelial-mesenchymal transition by targeting MicroRNA-125b in breast Cancer," *Molecular Cancer*, vol. 18, 2019.



## Retraction

# Retracted: Use of Composite Acellular Dermal Matrix-Ultrathin Split-Thickness Skin in Hand Hot-Crush Injuries: A One-Step Grafting Procedure

### BioMed Research International

Received 20 June 2023; Accepted 20 June 2023; Published 21 June 2023

Copyright © 2023 BioMed Research International. This is an open access article distributed under the Creative Commons Attribution License, which permits unrestricted use, distribution, and reproduction in any medium, provided the original work is properly cited.

This article has been retracted by Hindawi following an investigation undertaken by the publisher [1]. This investigation has uncovered evidence of one or more of the following indicators of systematic manipulation of the publication process:

- (1) Discrepancies in scope
- (2) Discrepancies in the description of the research reported
- (3) Discrepancies between the availability of data and the research described
- (4) Inappropriate citations
- (5) Incoherent, meaningless and/or irrelevant content included in the article
- (6) Peer-review manipulation

The presence of these indicators undermines our confidence in the integrity of the article's content and we cannot, therefore, vouch for its reliability. Please note that this notice is intended solely to alert readers that the content of this article is unreliable. We have not investigated whether authors were aware of or involved in the systematic manipulation of the publication process.

Wiley and Hindawi regrets that the usual quality checks did not identify these issues before publication and have since put additional measures in place to safeguard research integrity.

We wish to credit our own Research Integrity and Research Publishing teams and anonymous and named external researchers and research integrity experts for contributing to this investigation.

The corresponding author, as the representative of all authors, has been given the opportunity to register their agreement or disagreement to this retraction. We have kept a record of any response received.

### References

- [1] Y. Fan, Y. Pan, C. Chen et al., "Use of Composite Acellular Dermal Matrix-Ultrathin Split-Thickness Skin in Hand Hot-Crush Injuries: A One-Step Grafting Procedure," *BioMed Research International*, vol. 2022, Article ID 1569084, 12 pages, 2022.

## Research Article

# Use of Composite Acellular Dermal Matrix-Ultrathin Split-Thickness Skin in Hand Hot-Crush Injuries: A One-Step Grafting Procedure

**Youfen Fan, Yanyan Pan , Cui Chen, Shengyong Cui, Jiliang Li, Guoying Jin, Neng Huang, and Sida Xu**

*Department of Burns, Hwa Mei Hospital, University of Chinese Academy of Sciences, Ningbo, China*

Correspondence should be addressed to Yanyan Pan; [ningbopanyanyan@126.com](mailto:ningbopanyanyan@126.com)

Received 27 May 2022; Revised 18 June 2022; Accepted 24 June 2022; Published 21 July 2022

Academic Editor: Dinesh Rokaya

Copyright © 2022 Youfen Fan et al. This is an open access article distributed under the Creative Commons Attribution License, which permits unrestricted use, distribution, and reproduction in any medium, provided the original work is properly cited.

**Background.** Hot-crush injuries to the hands can be devastating, and early debridement and coverage with skin autograft remains the golden standard of wound treatment. However, this type of treatment is not feasible or unlikely to succeed due to limited donor sites and wound characteristics of hot-crush injuries on hands. Thus, the composite grafting of acellular dermal matrix (ADM) and split-thickness skin graft (STSG) as a novel alternative method has been attempted. In this series, the results are presented to demonstrate the feasibility and effectiveness of the use of one-stage procedure for early reconstruction in hand hot-crush injuries. **Methods.** All consecutive patients with hand hot-crush injuries, who underwent one-stage procedure of ADM and ultrathin STSG for soft tissue coverage at our institution from December 2018 to November 2019, were retrospectively analyzed. Wound dressings were opened on 7 days after operation to examine graft survival and complications. Patients were followed up for at least 9 months to evaluate their hand profiles. **Results.** Samples of 14 patients with a total of 23 wounds were involved in the study. Thirteen of the 23 third–fourth-degree wounds had varying degrees of tendon exposure. On 7 days postoperation, the composite grafts survived in 12 patients with minimal focal graft losses and liquefaction and necrosis in 2 patients, which achieved successful healing following new coverage of ultrathin STSG. All the wounds healed with hospital stays ranging from 9 days to 32 days (median: 24.5 days). At the final follow-up (from 9 months to 20 months), all patients achieved excellent or good total active motion grade and good scar quality (Vancouver scar scale scored 1–3) with no revision surgery. **Conclusions.** One-stage composite grafting of ADM and ultrathin STSG is a reliable alternative for early reconstruction in hand hot-crush injuries, which delivers good functional outcomes and a good cosmetic appearance.

## 1. Background

As a relatively rare type of burn, hot-crush injuries are more common in industrial settings. The upper extremities are the most common sites of these injuries because they are used for the operation of various machines (e.g., hot roller and hot press machine) that expose them to trauma [1]. Hot-crush injuries combined with the effect of mechanical and thermal components may cause full-thickness skin defect with tendon/bone damage or exposure of the involved segment, resulting in severely limited function and compromised aesthetic appearance. The hand, with complex important structures, such as nerves, blood vessels, tendons, muscles,

and numerous delicate joints all tightly packed in a crowded space, plays a crucial role in our daily life and work. Thus, care of hot-crush injury on hand should be given high priority. At present, the commonly used methods in the treatment of hot-crush injuries are early debridement and coverage with autograft, such as full-thickness skin graft (FTSG), split-thickness skin graft (STSG), and regional flap graft. These methods have a high rate of success with wound closure; however, there are still high risks of graft skin loss with FTSG, scar contracture with STSG, bloated deformity with flap graft, and a burden on the donor site [2–4].

To overcome these limitations, the composite grafting of acellular dermal matrix (ADM) and autograft as a novel

alternative treatment has been attempted. The ADM is a dermal substitute acquired from allogeneic skin after special treatment to remove its cellular components. This type of treatment provides a stable dermal scaffold to facilitate the invasion of normal fibroblasts and capillaries to synthesise new dermis and minimises contracture and scar formation during wound healing [5]. In addition, ADM combined with ultrathin STSG covers the full-thickness skin defect with a minimal aesthetic and functional deficit to the donor site, which is also an advantage of the ADM application. The application of ADMs has been developing in hand surgery over the past 15 years, and it has become the treatment of choice for conditions affecting the hand, wrist, and forearm as a temporary cover after skin tumour excision [6, 7]. However, the use of ADM entails a delay (often approximately 2 weeks) to allow vascular ingrowths and fibroblast infiltration before they can be covered with skin autograft and requires two-stage procedures [7–10]. Animal study in a rat model [10] confirmed that the epithelisation time of one-stage procedure of heterogeneous ADM (Integra) and skin autograft was 13–29 days, which is significantly shorter than the 28–35 days of two-stage grafting. Lee et al. [11] reported that one-stage composite grafting for coverage of the flap donor site contributes to a better scar quality than STSG alone. Nevertheless, a literature search yields only few articles on the simultaneous use of ADM and autograft by one-stage procedure [12, 13] and lets alone for hand hot-crush injuries. We present our experience with composite grafting of ADM and ultrathin STSG in 14 patients to provide supporting evidence for the application of one-stage procedure in early reconstruction for hand hot-crush injuries. Last but not least, the research still needs proofreading.

## 2. Methods

**2.1. Patient Selection.** This work is a retrospective case series of hand hot-crush injury patients treated with one-stage procedure of composite grafting of ADM and ultrathin STSG in our centre from December 2018 to November 2019. The study was approved by our institutional review board (approval no: PJ-KY-NBEY-2020-150-01), and an informed consent was obtained prior to surgery. Patients with a third–fourth-degree wound were included from this report [14]. Patients with over 1.5 cm<sup>2</sup> size or over 1.0 cm maximum width of tendon exposure (1), bone exposure (2), and/or severe infection (3) in the wound were excluded.

**2.2. One-Stage Grafting Procedure.** Surgical procedures were all performed under local anaesthesia. Acute full-thickness wounds without vital dermal and epidermal remnants were excised, and escharotomy was carried out to the deep fascia level within 48 h after admission. Routine treatment of antibiotic anti-infection and analgesia was performed. The involved hand was treated by aggressive debridement and irrigation (if necessary, increasing VSD) [15] to achieve a clean and healthy bed. After haemostasis, the Jieya Matrix of corresponding size was meshed at a ratio of 1:1–1.1 and placed on the open wound surface with a smooth surface (basement membrane surface) facing up and a rough surface

(true skin surface) facing down. The Jieya Matrix (Beijing Jieya Laifu Biotechnology Company, Ltd., Beijing, China) was meshy, 1 mm thick and 5 cm × 6 cm in size and stored at 4°C. The Jieya Matrix was presoaked with 0.1% chlorhexidine solution for 3–5 min before use, trimmed to precisely fit the defect and anchored using 5–0 absorbable sutures at the wound margin. Autologous ultrathin STSG (0.10–0.15 mm) was harvested from the scalp or lateral thigh and fixed over the ADM surface area. Several small stab incisions were made in the autologous skin. In the case of no active bleeding, haematoma, and fluid accumulation, the wound was bandaged with paraffin gauze and 0.05% of chlorhexidine solution presoaked gauze as primary dressing and pressure bandages. Wound dressings were changed at 7 days postoperation to check graft survival and complications (haematomas, liquefaction, necrosis, and infection) and replaced every 3 days on subsequent days until wound closure.

**2.3. Evaluation.** Patients were followed up at least 9 months postoperation, which involved the scar appearance, the hand function, and the presence or absence of second revision surgery. The scar appearance was evaluated by the Vancouver scar scale (VSS) [11]: vascularity (0–3), pigmentation (0–3), pliability (0–5), and height (0–4). The finger range of motion was classified according to the total active motion (TAM) to evaluate the hand function [16].

## 3. Result

From December 2018 to November 2019, a total of 41 patients with hand hot-crush injuries were analysed. Twenty-three isolated wounds of 14 patients (seven males and seven females) met the inclusion criteria and received the ADM combined with an ultrathin STSG. The patients' demographic characteristics are summarised in Table 1. The median age of patients was 40 years (ranging from 16 years old to 59 years old). Most injuries (except case 12) occurred during factory work, caused by automatic machinery (e.g., hot press machine and hot melt mould) in motion. There were seven cases involving the finger, four cases involving the opisthenar, four cases involving the palm, and five cases involving the forearm and/or wrist. All patients were afflicted with third–fourth-degree wound. Phalanx fracture was found in one case and tendon exposure or damage in 10 cases with a range size of 1.0 cm × 0.2 cm–3.0 cm × 0.5 cm. The total area of ADM application ranged from 22 cm<sup>2</sup> to 99 cm<sup>2</sup>.

In Table 1, the patients underwent one to seven times of surgery (median of three times), with a hospital stay from 9 days to 59 days (median of 24.5 days). They underwent the first escharotomy and/or debridement within 48 h after admission, except patient 3. Two patients with third-degree wound underwent escharotomy and one-stage grafting on day 2 postinjury (Figure 1). The remaining 12 patients underwent one-stage grafting at a median time of 12 days postadmission (ranging from 6 days to 48 days) after additional one to three times of debridement and/or one to two times of VSD (continuous drainage for 7–20 days)

TABLE 1: Demographic characteristics and treatment data of patients.

Items	Patients, <i>n</i> = 14 (%)
Age	
Median [min, max], years	40 [16, 59]
Gender	
Male	7 (50.0)
Female	7 (50.0)
Underlying disease	
None	11 (78.6)
Hypertension	2 (14.3)
Diabetes	2 (14.3)
Etiology	
Hot-press	7 (50.0)
Crushed by hot machine	4 (28.6)
Hot melt mould	2 (14.3)
Household electric iron	1 (7.1)
Injury locations	
Hand	12 (85.7)
Forearm/wrist	5 (35.7)
Defect size	
Median [min, max], cm <sup>2</sup>	36.5 [22, 99]
Defect degree	
Third degree	2 (14.3)
Third-fourth degree	5 (35.7)
Fourth degree	2 (14.3)
Escharotomy	
Median [min, max], hours postadmission	31 [2.5, 94.5]
VSD applied	
Yes	12 (85.7)
No	2 (14.3)
Median [min, max], days	13 [7, 20]
Surgery	
ADM and STSG	14 (100)
STSG only	2 (14.3)
Flap	2 (14.3)
Median [min, max], times	3 [1, 7]
Length of stay	
Median [min, max], days	24.5 [9, 59]

(Figures 2 and 3). In addition to composite grafting of ADM and ultrathin STSG, partial deep wounds with a large area of tendon or bone exposure was observed in patients 1 and 2, which were managed by debridement and flap advancement.

Out of the 14 patients who underwent skin graft with ADM, the composite grafts survived in 12 patients with minimal focal graft losses at first dressing open. Two patients (patients 9 and 14, Figure 4) with liquefaction and necrosis of grafts required secondary ultrathin STSG grafting after further debridement. The wounds healed at 14 days (ranging from 9 days to 23 days) after the one-stage grafting procedure on average. At a mean follow-up of 13.9 months (ranging from 9 to 20), all the ADM applied sites were firm and

soft, with a satisfactory hand function. The VSS outcome was observed in 20 skin grafts out of 23 with a score of one to three (Table 2). In most patients, TAM was excellent or good, as shown in Table 3. No scar contractures or flexor tendon adhesions limiting the range of motion severely were found in all patients, except patient 2 with adhesion of third web space that needed revision surgery.

**3.1. Patient 5.** A 59-year-old woman presented at the emergency room with hot-crush injury of her left hand 4 h post-injury, whose hand and forearm were caught between hot press machine heated to 170°C for 20 s. However, she refused to get admission after simple cleaning and bandaging and intramuscular injection of tetanus antitoxin, but was obliged to go to our department again for admission at 18 h postinjury due to the continuous swelling and numbness of the wound. Through examination, she was found to have fourth-degree burns of 78 cm<sup>2</sup> size on the thenar and hypothenar eminence region of the left palm and the ulnar side of left forearm. The X-ray showed fractures of the fourth middle and far phalanx of the left hand. The fractured finger was immediately immobilized with a small splint with the ring finger. On arrival, the left forearm was grossly swollen and paralysed, and the fourth-degree wound of the wrist was crusted and hard. Escharotomy and debridement were urgently performed on the left forearm on the day of admission once partial necrosis was observed in the thenar and hypothenar, and flexor digitorum superficialis aponeurosis was exposed. VSD was given consecutively for the next 6 days. The second surgical debridement of the wounds was performed on day 7 postadmission due to the partial necrotic muscle on the left forearm and the deep wound. VSD treatment was given consecutively for another 4 days. Granulation tissue developed with flexor digitorum superficialis aponeurosis exposure in the burnt area (Figure 5(a)), and one-stage grafting was performed on day 10 postadmission (Figures 5(b) and 5(c)). Two 5 cm × 6 cm ADMs were proportionally trimmed and secured over the wounds on the left palm and forearm. Ultrathin STSGs harvested from the scalp were grafted to the wounds covered with the ADM in the form of large sheet skin. After each operation, the patient received anti-infective therapy (IGTT Mezlocillin/Sulbactam 3.75 g, q 12 h) and given increased analgesia when necessary. During dressing change on day 7 postsurgery, the composite grafts survived without incident. The patient was discharged with wound closure after 20 days of hospitalisation. The patient underwent occupational and physical therapy throughout the entire period and during the following weeks. Approximately 20 months postoperation, no contractures were observed in the hand and forearm. The patient had a good range of motion of the thumb metacarpophalangeal and can flex or extend at will (good TAM). She was contented with the composite grafting.

**3.2. Patient 14.** A 17-year-old man working in a plastic factory was pinned to his right hand by a hot melt mould. Several seconds lapsed before he was able to free his hand. Then, he was transported to our emergency department for burns 2 h postinjury. On examination, he had fourth-





FIGURE 1: View of patient 8. Day of admission (a); debridement and one-step composite grafting on day 2 postadmission (b, c); first dressing change postgrafting (d); and follow-up at 6 months (e) and 17 months (f) postoperation.

degree burns on the ventral aspect of the second and third fingers of the right hand (Figure 4(a)). On the day of admission, he was given escharotomy and debridement, and intra-

operative flexor tendon exposure was observed on involved fingers. Then, the wounds were treated with VSD on the subsequent days (Figure 4(b)). Postoperative patients





FIGURE 2: Continued.



(g)

FIGURE 2: View of patient 6. Before and after escharotomy (a); after debridement and first VSD (b); after debridement and second VSD (c); one-step composite grafting on day 11 postadmission (d); first dressing change postgrafting (e); and follow-up at 1 month (f) and 4 months (g) postoperation.

underwent anti-infection therapy, including intravenous ceftriaxone sodium (1 g, qd) on the same day and oral cefaclor (0.25 g, bid) on the following 5 days. On day 8 postadmission, he was given the second surgical debridement (Figure 4(c)) and one-step operative grafting (Figure 4(d)). One 5 cm × 6 cm ADM was proportionally trimmed and secured over the defect area of 20 cm<sup>2</sup> on the fingers. Then, a large sheet of ultrathin STSG from the right thigh was grafted to close the wound. The patient also underwent anti-infection therapy (OGTT cefaclor 0.25 g, bid) for 4 days and VSD for the next 7 days after surgery. On day 7 postsurgery, the composite grafts completely necrosed and liquefied at the first dressing change (Figure 4(e)). On day 21 postadmission, granulation wounds were formatted (Figure 4(f)) through complete debridement of the necrotic grafts and a third VSD for 7 days. Then, ultrathin STSG grafting was performed. On day 6 postsurgery, the dressings were replaced, and the ultrathin STSG survived. On day 29 postadmission, the patient was discharged with wound closure and returned to the outpatient clinic for further consultation on schedule. After the successful surgery, the patient started to use pressure gloves, and received physical therapy exercises on the subsequent months. An aesthetically acceptable and durable outcome was achieved in the later follow-up period.

#### 4. Discussion

The composite structural anatomy of the hand and paucity of overlying soft tissue often leads to denuded vital structures following hot-crush injuries, such as bones, tendons, and joints [17]. Hence, wound coverage after hot-crush injuries of hand is still challenging. The ideal treatment should focus on providing early, good-quality (thin, pliable) skin cover to promote a quick healing process, prevent contracture, and achieve a functionally and cosmetically acceptable result.

In this series of cases, most wounds were at third–fourth degrees with varying degrees of tendon exposure and surrounding tissue damage. In our previous wound manage-

ment, soft tissue coverage by skin autograft, such as intermediate STSG, FTSG, pedicled abdominal flap, and local rotation flap, was chosen for such hand hot-crush injuries. However, the exposed bone, tendon, or cartilage of patients with full-thickness defects on hand does not have sufficient vascularity to support a granulation bed for re-epithelialisation or neovascularisation for simple skin graft survival [2]. The flap grafts with easier survival and less contracture, especially on the exposed bone and tendon wound, are recommended. However, the appearance and function of the graft area were seriously affected by the bloated skin flap, which required several times of repair, and it is required to conduct follow-up finger splitting operation for patients with hot-crush injuries of fingers. In addition, FTSG and flap graft accompany donor-site morbidity.

In recent years, ADM graft combined with ultrathin STSG is a common technique in complex wounds of hand hot-crush injuries. The efficacy and advantages of ADM have been well documented [6–9, 18, 19]. This technique allows for neovascularised tissue to form overexposed or denuded structures within these wounds, creating a more robust vascularised tissue bed for neovascularisation of subsequently placed skin grafts [20]. The donor site can immediately heal without scarring because ultrathin autologous STSG can be feasible. A prior study [21] by objective measurements verified that the application of ADM with autologous STSG showed superior elasticity and less scar elevation than STSG alone. The complication rate in our one-stage grafting procedure (3/23) was not higher than that in a recent review of dermal regenerative matrix application in full-thickness burn injury [22]. The reported overall complication (infection, graft loss, haematoma formation, and contracture) rate was 13%. In our study, all patients achieved excellent or good TAM grade and good scar quality (VSS scored 1–3) with no revision surgery at a mean of 13.9 month follow-up. Only patient 2 needed revision surgery. The adhesion of the third web space impairing metacarpophalangeal joint motion of the third and fourth fingers (fair

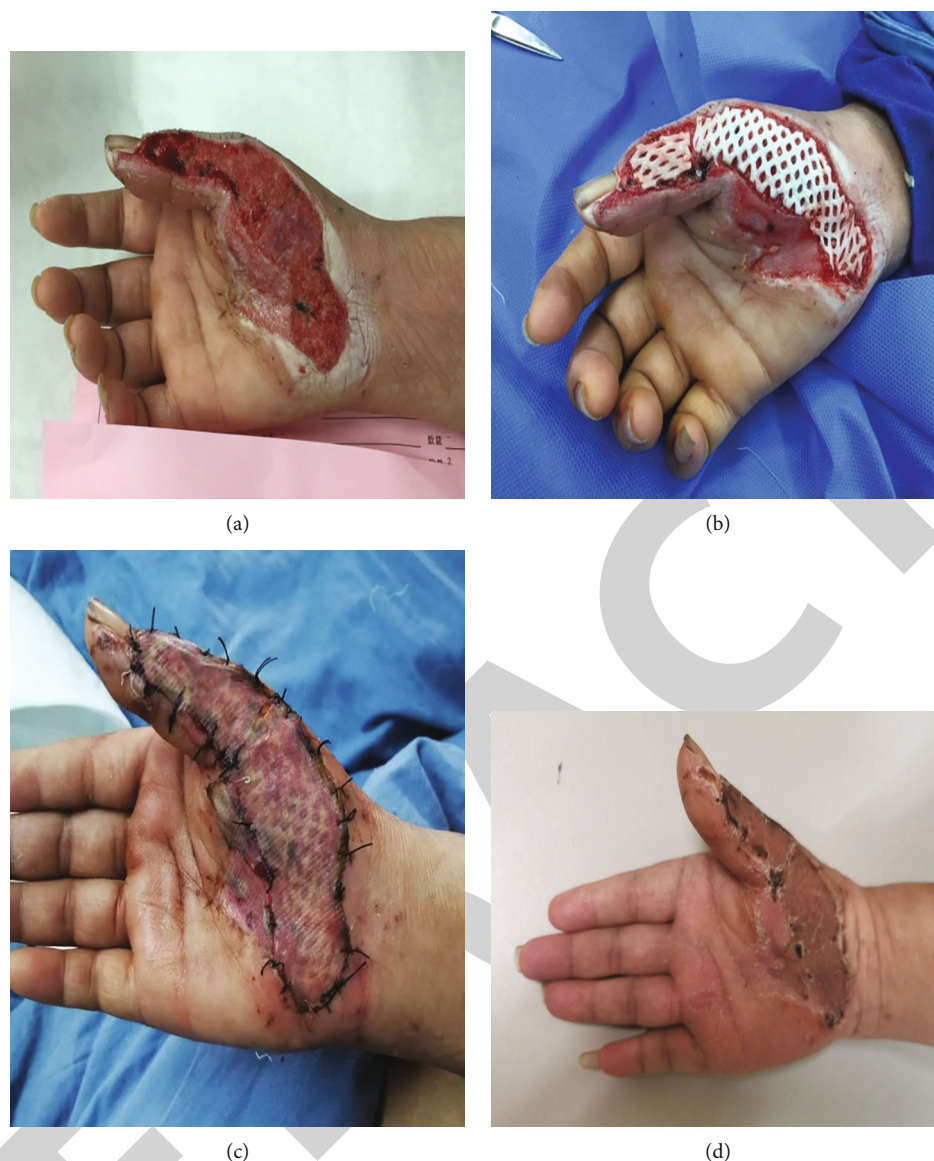


FIGURE 3: View of patient 7. Granulation wounds after debridement and two times of VSD for 14 days (a); one-step composite grafting on day 16 postadmission (b); first dressing change postgrafting (c); and follow-up at 4 months postoperation (d).

TAM grade) was noted in patient 2 after additional local rotation flaps grafting in part wound of opisthenar. This series of cases showed that a one-stage procedure of ADM and ultrathin STSG used in hand hot-crush injury was possible without compromising the functional and aesthetic results. In comparison with two-stage grafting, one-stage composite grafting shortened the wound healing and hospitalisation time (23.5 days in our study vs. 40.2 days in Maruccia et al. [23]), allowing patients to resume physical exercises earlier.

We summarised the successful experience of one-stage grafting as follows:

- (1) Early escharotomy: early escharotomy, sometimes executed within hours, before the damage is irreversible, which not only effectively lowers microbial load under eschar to avoid wound infection deepening but also immediately releases the contracted skin to

relieve the pressure of eschar on blood circulation, resulting in necrosis of muscle and other tissues [13, 24]. In our series of cases, escharotomy was performed within 48 h postadmission. For patients who complained of obvious swelling and numbness on hand, escharotomy would be carried out to the deep fascia within hours to prevent compartment syndrome. It is simple for experienced, skilled hands or burn surgeons, but may be more destructive than curative in unskilled surgeons

- (2) Thorough debridement: one-stage grafting is strict with wound bed, which requires thorough debridement to ensure no necrotic or infected tissue on wound [25]. However, necrotic and viable tissue may not be distinguished in the early stages in patients with hot-crush injury, and one time of debridement may be





FIGURE 4: View of patient 14. Day of admission (a); granulation wounds after debridement and VSD for 7 days (b); second debridement and one-step composite grafting on day 8 postadmission (c, d); necrosis and infection of composite grafts on days 7 postsurgery (e); and granulation wounds after debridement and third VSD for 7 days (f).

inadequate. Therefore, serial debridements and dressing changes may be needed. The application of VSD therapy prevents infection and facilitates granulation growth, which shortens the preparation of wound bed [26]. Our 12 patients were given multiple surgical debridement and VSD for 7–20 days until the wound is clean with no infection and nonviable tissue. However, the parabiologic tissue around the tendon was over-

preserved during early escharotomy and debridement in patients 9 and 14, resulting in liquefaction and necrosis of the composite grafts. After thorough debridement and VSD until the wound was clean, the wounds were repaired by autologous split thickness skin grafting. Incomplete early debridement will lead to prolonged wound healing time and increase in the number of operations

TABLE 2: One-stage grafting procedure related data and VSS score at last follow-up.

Patient	ADM applied area, cm <sup>2</sup>	No. of ADMs used	ADM placement time, days postinjury	ADM placement site	Tendon exposed	Composite grafts survival (at first open)	VSS score (at last follow-up)
1	34	1	48	Forearm	Y	Y	2
				Opisthenar	N	Y	4
2	25	1	23	III	Y	Y	3
				IV	N	Y	3
3	24	1	22	Wrist	Y	Y	3
				III	N	Y	3
4	20	1	11	IV	Y	Y	3
5	72	2	10	Forearm	N	Y	2
				Wrist/palm/I	Y	Y	5
				Thenar	Y	Y	2
6	33	1	12	Hypothenar	Y	Y	2
7	30	1	17	Palm, I	N	Y	2
8	35	1	2	Opisthenar	N	Y	1
9	29	1	11	I/II/first web space	N	Liquefaction/necrosis	3
10	30	1	2	Opisthenar	N	Y	1
11	28	1	15	Forearm	Y	Y	1
				Opisthenar	N	Y	1
				III	Y	Y	1
				Forearm	Y	Y	1
13	91	3	6	Thenar	N	Y	1
				Hypothenar	N	Y	1
				II	Y	Liquefaction/necrosis	4
14	20	1	8	III	Y	Liquefaction/necrosis	2

I: thumb; II: index finger; III: middle finger; IV: ring finger; V: small finger.

TABLE 3: TAM grade at last follow-up.

Patient	Affected fingers	TAM grade (at last follow-up)
1	No finger involved	
2	III/IV	Fair
3	No finger involved	
4	III/IV	Good
5	I	Good
6	I	Excellent
	V	Good
7	I	Excellent
8	I/II	Excellent
9	I/II	Excellent
10	II/III	Excellent
11	No finger involved	
12	II/III/IV	Excellent
13	I/V	Excellent
	II	Good
14	III	Excellent

I: thumb; II: index finger; III: middle finger; IV: ring finger; V: small finger.



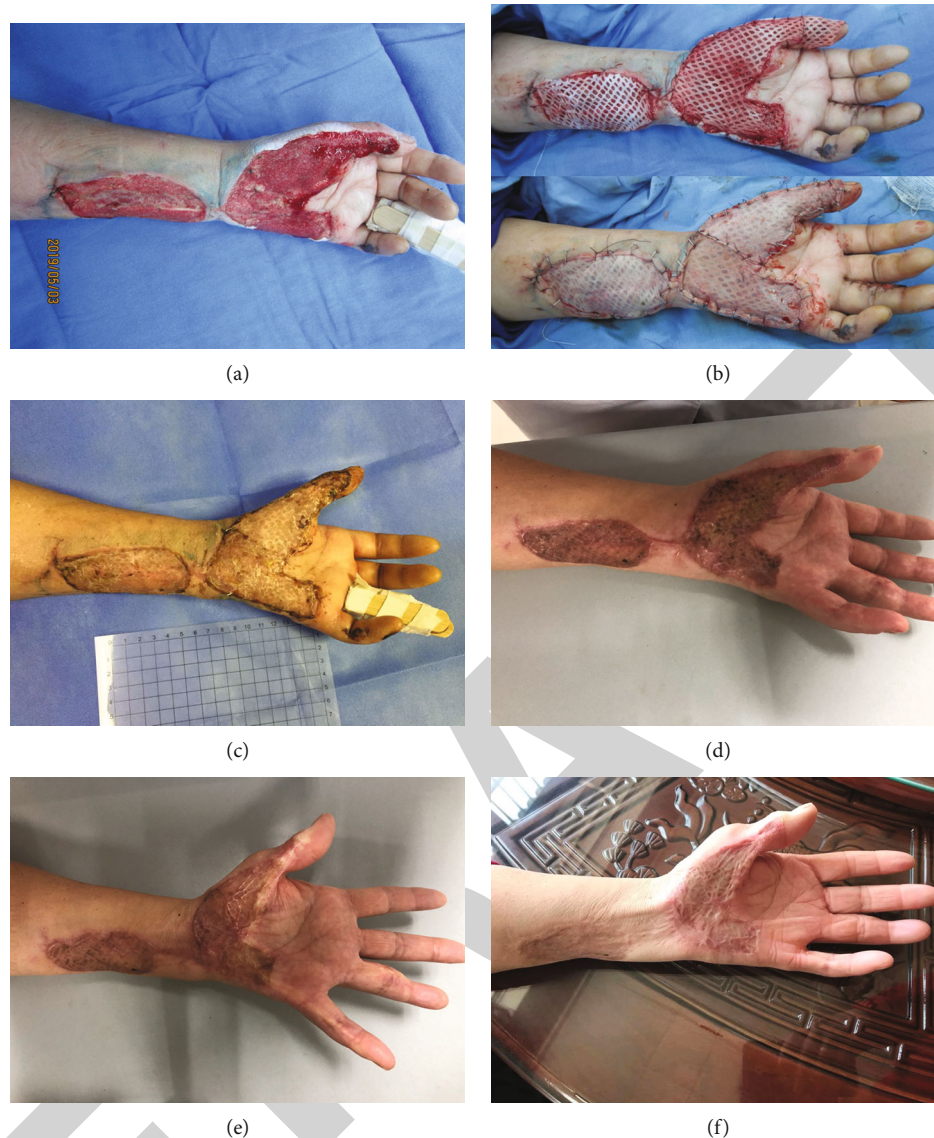


FIGURE 5: View of patient 5. Granulation wounds after debridement and two times of VSD for 10 days (a); one-step composite grafting on day 10 postadmission (b); and follow-up at 1 month (c), 6 months (d, e), and 20 months postoperation (f).

- (3) Complete haemostasis: haematoma must be avoided by careful haemostasis and drainage during application of the one-stage grafting. To address this issue, a combination of multiple haemostatic regimens was carried out, including intraoperative bipolar electrocautery and hot compress. The mesh of Jieya Matrix was properly spread, and several small stab incisions were made in autologous skin during grafting to facilitate drainage. The reticular structure also permitted the autograft from directly contacting with the excised wound bed, which allowed earlier nutrition acquisition and revascularisation of the autograft. In some patients, scattered punctate necrosis and little marginal necrosis on the composite grafts were found at the first dressing change postgrafting. This work speculated that focal haematoma developed under the composite grafts postgrafting, which obstructed the

vascularisation of the dermal scaffold and resulted in necrosis of the covered ultrathin STSG

## 5. Conclusions

The composite grafting of ADM and autograft skin has been proven to be a reliable alternative for wound reconstruction. However, this series represents the rare situation of the method's use of one-stage grafting procedure in hand hot-crush injuries. This series, while small, demonstrates the feasibility and effectiveness of one-stage grafting of ADM and ultrathin STSG in acute closure of hand hot-crush injuries in providing early coverage and preventing contractures. Moreover, our experience highlights the importance of wound bed preparation, including early escharotomy, thorough debridement, and haemostasis. We hope that one-stage grafting of ADM and ultrathin STSG might be applied

in the future in a variety of complex wounds for early reconstruction and release of the moderate or severe postburn contracture to provide patients with less surgery and pain and a better appearance and function improvement of the healing site.

## Abbreviations

ADM: Acellular dermal matrix  
 FTSG: Full-thickness skin graft  
 STSG: Split-thickness skin  
 TAM: Total active motion  
 VSD: Vacuum sealing drainage.

## Data Availability

The datasets used and analysed during this study are available from the corresponding author on reasonable request.

## Ethical Approval

This study was approved by the Institutional Review Board of Hwa Mei Hospital, University of Chinese Academy of Sciences.

## Conflicts of Interest

The authors declare that they have no competing interests.

## Authors' Contributions

CC, SC, JL, NH and SX collected the patient data. YF designed and wrote the article. YP analysed the data and wrote the article. YF and YP were major contributors in editing and revising the manuscript. All authors read and approved the final manuscript.

## Acknowledgments

This study was supported by the Ningbo Medical & Health Leading Academic Discipline Project (project number: 2022-F17), the Zhejiang Provincial Medical and Health Science and Technology Program Project (2021KY290), and the Zhejiang Provincial Medical and Health Science and Technology Program Project (2021KY1004).

## References

- [1] A. Sagi, A. Amir, D. M. Fliss, S. Ozi, G. Ofer, and L. Rosenberg, "Combined thermal and crush injury to the hand and fingers," *Burns*, vol. 23, no. 2, pp. 176–181, 1997.
- [2] J. S. Taras, A. Sapienza, J. B. Roach, and J. P. Taras, "Acellular dermal regeneration template for soft tissue reconstruction of the digits," *The Journal of Hand Surgery*, vol. 35, no. 3, pp. 415–421, 2010.
- [3] M. Reynolds, D. A. Kelly, N. J. Walker, C. Crantford, and A. J. Defranzo, "Use of integra in the management of complex hand wounds from cancer resection and nonburn trauma," *Hand (N Y)*, vol. 13, no. 1, pp. 74–79, 2018.
- [4] S. Dast, R. Vaucher, V. Rotari et al., "Thin flaps in the management of hand and upper limb defects," *Annales de Chirurgie Plastique et Esthétique*, vol. 62, no. 1, pp. 69–78, 2017.
- [5] V. C. van der Veen, M. B. van der Wal, M. C. van Leeuwen, M. M. Ulrich, and E. Middelkoop, "Biological background of dermal substitutes," *Burns*, vol. 36, no. 3, pp. 305–321, 2010.
- [6] C. V. Ellis and D. A. Kulber, "Acellular dermal matrices in hand reconstruction," *Plastic and Reconstructive Surgery*, vol. 130, 5 Suppl 2, pp. 256S–269S, 2012.
- [7] V. Teoh and G. Gui, "Direct to implant breast reconstruction with biological acellular dermal matrices," *British Journal of Hospital Medicine*, vol. 81, no. 3, pp. 1–7, 2020.
- [8] X. Li, X. Meng, X. Wang et al., "Human acellular dermal matrix allograft: a randomized, controlled human trial for the long-term evaluation of patients with extensive burns," *Burns*, vol. 41, no. 4, pp. 689–699, 2015.
- [9] Z. Hu, J. Zhu, X. Cao et al., "Composite skin grafting with human acellular dermal matrix scaffold for treatment of diabetic foot ulcers: a randomized controlled trial," *Journal of the American College of Surgeons*, vol. 222, no. 6, pp. 1171–1179, 2016.
- [10] C. S. Chu, A. T. McManus, N. P. Matylevich, C. W. Goodwin, and B. A. Pruitt Jr., "Integra as a dermal replacement in a meshed composite skin graft in a rat model: a one-step operative procedure," *The Journal of Trauma*, vol. 52, no. 1, pp. 122–129, 2002.
- [11] Y. J. Lee, M. C. Park, D. H. Park, H. M. Hahn, S. M. Kim, and I. J. Lee, "Effectiveness of acellular dermal matrix on autologous split-thickness skin graft in treatment of deep tissue defect: esthetic subjective and objective evaluation," *Aesthetic Plastic Surgery*, vol. 41, no. 5, pp. 1049–1057, 2017.
- [12] Y. Pan, Z. Liang, S. Yuan, J. Xu, J. Wang, and S. Chen, "A long-term follow-up study of acellular dermal matrix with thin autograft in burns patients," *Annals of Plastic Surgery*, vol. 67, no. 4, pp. 346–351, 2011.
- [13] Y. H. Kim, K. T. Hwang, K. H. Kim, I. H. Sung, and S. W. Kim, "Application of acellular human dermis and skin grafts for lower extremity reconstruction," *Journal of Wound Care*, vol. 28, no. Sup4, pp. S12–S17, 2019.
- [14] M. G. Jeschke, M. E. van Baar, M. A. Choudhry, K. K. Chung, N. S. Gibran, and S. Logsetty, "Burn injury," *Nature Reviews Disease Primers*, vol. 6, no. 1, pp. 1–25, 2020.
- [15] Y. Li, P. Y. Li, S. J. Sun et al., "Chinese Trauma Surgeon Association for management guidelines of vacuum sealing drainage application in abdominal surgeries—update and systematic review," *Chinese Journal of Traumatology*, vol. 22, no. 1, pp. 1–11, 2019.
- [16] K. Libberecht, C. Lafaie, and R. Van Hee, "Evaluation and functional assessment of flexor tendon repair in the hand," *Acta Chirurgica Belgica*, vol. 106, no. 5, pp. 560–565, 2006.
- [17] A. Di Castri, L. Quarta, I. Mataro et al., "The entity of thermal crush-avulsion hand injury (hot-press roller burns) treated with fast acting debriding enzymes (nexobrid): literature review and report of first case," *Annals of burns and fire disasters*, vol. 31, no. 1, p. 31, 2018.
- [18] R. E. Lewis, E. A. Towery, S. G. Bhat et al., "Human acellular dermal matrix is a viable alternative to autologous skin graft in patients with cutaneous malignancy," *The American Surgeon*, vol. 85, no. 9, pp. 1056–1060, 2019.

## Retraction

# Retracted: Innovate a Standard for the Future Model of Nursing Care at Medical-Surgical Units in Najran University

### BioMed Research International

Received 3 October 2023; Accepted 3 October 2023; Published 4 October 2023

Copyright © 2023 BioMed Research International. This is an open access article distributed under the Creative Commons Attribution License, which permits unrestricted use, distribution, and reproduction in any medium, provided the original work is properly cited.

This article has been retracted by Hindawi following an investigation undertaken by the publisher [1]. This investigation has uncovered evidence of one or more of the following indicators of systematic manipulation of the publication process:

- (1) Discrepancies in scope
- (2) Discrepancies in the description of the research reported
- (3) Discrepancies between the availability of data and the research described
- (4) Inappropriate citations
- (5) Incoherent, meaningless and/or irrelevant content included in the article
- (6) Peer-review manipulation

The presence of these indicators undermines our confidence in the integrity of the article's content and we cannot, therefore, vouch for its reliability. Please note that this notice is intended solely to alert readers that the content of this article is unreliable. We have not investigated whether authors were aware of or involved in the systematic manipulation of the publication process.

Wiley and Hindawi regrets that the usual quality checks did not identify these issues before publication and have since put additional measures in place to safeguard research integrity.

We wish to credit our own Research Integrity and Research Publishing teams and anonymous and named external researchers and research integrity experts for contributing to this investigation.

The corresponding author, as the representative of all authors, has been given the opportunity to register their agreement or disagreement to this retraction. We have kept a record of any response received.

### References

- [1] A. Y. Mahdy Shalby and D. D. AlThubaity, "Innovate a Standard for the Future Model of Nursing Care at Medical-Surgical Units in Najran University," *BioMed Research International*, vol. 2022, Article ID 2959583, 7 pages, 2022.

## Research Article

# Innovate a Standard for the Future Model of Nursing Care at Medical-Surgical Units in Najran University

Abeer Y. Mahdy Shalby <sup>1</sup> and DaifAllah D. AlThubaity <sup>2</sup>

<sup>1</sup>Medical-Surgical Nursing Department, Faculty of Nursing, Najran University, Saudi Arabia

<sup>2</sup>Pediatric Nursing Department, Faculty of Nursing, Najran University, Saudi Arabia

Correspondence should be addressed to Abeer Y. Mahdy Shalby; [aymahdy@nu.edu.sa](mailto:aymahdy@nu.edu.sa) and DaifAllah D. AlThubaity; [ddalthubaity@nu.edu.sa](mailto:ddalthubaity@nu.edu.sa)

Received 16 June 2022; Revised 30 June 2022; Accepted 7 July 2022; Published 20 July 2022

Academic Editor: Dinesh Rokaya

Copyright © 2022 Abeer Y. Mahdy Shalby and DaifAllah D. AlThubaity. This is an open access article distributed under the Creative Commons Attribution License, which permits unrestricted use, distribution, and reproduction in any medium, provided the original work is properly cited.

**Aim.** Innovate a standard for the future model of nursing care at medical-surgical units in Najran University through a training program for the standard of the future model evaluation on studied nurses' knowledge, attitude about innovation standards, and innovative behavior among nurses. **Methods.** A quasi-experimental research was used to achieve the study's goal; the research was carried out at Najran University Hospital at Najran, in the medical and surgical units, as well as outpatient clinics. The sample is a convenience type; 100 nurses were used. **Tool.** A structured questionnaire sheet was used for data collection that includes nurses' knowledge, attitude, and individual innovative scale. **Results.** This reveals the studied nurses related to their individual innovative scale pre- and postintervention. Concerning resistance to change, the mean of them preintervention is  $x - SD 9.08 \pm 2.60$ . Concerning opinion leadership, the mean of them postintervention is  $x - SD 14.32 \pm 3.16$ . There is a highly significant difference ( $p < 0.01^{**}$ ) preintervention as regards all domains listed. **Conclusion.** The educational program significantly enhances nurses' knowledge and attitude, according to our present study. Nurses' innovative skills are also improved by enhancing their knowledge and attitude. Before and after the educational program was implemented, there was a highly positive linear association between the nurses' knowledge, attitude, and innovative skills at  $p < 0.01$ .

## 1. Introduction

Nurses are critical to high-quality care, so healthcare would come to a stand without them. There is not a single intervention or healthcare program in which they do not play an important role [1, 2].

The innovation idea is nothing new to the profession of nursing. Nurses all over the world engage in new actions on a daily basis with the goal of improving healthy patient care results while minimizing costs. Numerous of these initiatives have resulted in considerable improvements in patients, nations, and all systems of healthcare. On the other hand, nursing support for healthcare innovation is rarely familiar, publicized, or shared through nurses and the broader public [3].

Innovation is often characterized as a new method device. "Practice" is described as a rule or custom of practicing; it is also described as follows: reduplicate action for get-

ting expertise, the resulting state of being skillful, information put into action, and vocation performance. You can be innovative in a variety of ways, including being creative or solving issues to develop a new strategy, product, or service that others enjoy. Innovation is a novel way of doing something that is more effective or less expensive [4]. Doing things differently in order to achieve significant performance improvements is what innovation entails. Unlike popular belief, most discoveries do not come from laboratories, policymakers, or senior executives. Employees within those organizations develop the majority of inventions, whether in the public or private sector [5].

Nursing and nurses will not and cannot be free to innovate and improve practice in isolation as a result of transformation and change. There are successful and long-lasting innovations and changes in practice, despite the fact that nursing is a compound and difficult profession that requires



well-informed, competent, and critical thinkers and doers, as well as a lot of enthusiasm, devotion, and hard work [6].

Nursing application innovation is critical for primary, secondary, and tertiary care, identifying and avoiding hazard factors, promoting good lifestyle attitudes, and assessing care and other techniques. This is because the institutions that employ them can generate and discover new information, methods, and services [7].

Nurses are devising innovative strategies to assist patients who are not receiving the care they require, such as making minute clinics more accessible, improving maternal and infant care, and altering treatment at the bedside. To deal with the problems of new technology as well as an out-of-control nursing shortage, a deeper understanding of how innovation works, what it looks like when people come up with new ideas, and how organizations can encourage or discourage it is required [8, 9].

## 2. Methods

**2.1. Hypothesis.** The hypotheses of the study are as follows:

$H^1$ : nurses' knowledge and attitude about innovation were improved postimplantation.

$H^2$ : nurses' knowledge and attitude about innovation standards had a positive effect postprogram implementation.

$H^3$ : nurses' knowledge and attitude had a positive effect on improving innovative behavior.

**2.2. Research Design.** To achieve the study's goal, a one-group pretest/posttest quasi-experimental research methodology was used. It is an empirical study that uses nonrandom assignment to estimate the effect of an intervention on its target population.

**2.3. Setting.** The study was carried out at Najran University Hospital at Najran, in the following departments: medical units, surgical units, and outpatient clinics.

**2.4. Participant.** Participants were recruited using a convenience sampling technique at Najran University Hospital at Najran, in the following departments: medical units, surgical units, and outpatient clinics. A total of 100 nurses, from the previously mentioned setting, who agreed to share in the study were recruited in the study. The study duration extended over a period of five months, from the 1<sup>st</sup> of September 2021 to the end of January 2022.

**2.5. Sample Size.** The sample size was determined using a statistical power of 90%, a degree of confidence (1 – alpha error) of 95%, an alpha of 0.05, and a beta of 0.1. The sample size was set at 90 nurses. With a 15% sample attrition rate, the ultimate sample size is 100 nurses.

**2.6. Tools of Data Collection.** The current study's data were gathered using a structured electronic questionnaire sheet that the researcher created in English after researching literature reviews [10]. It is divided into four sections as follows:

*Part I:* concerned with the demographic profile of the studied nurses, it included sociodemographic characteristics

of the studied nurses such as age, experience, qualification, nationality, and training courses.

*Part II:* concerned with nurses' knowledge, it included 14 MCQ questions such as the concept of innovation standard "2 items," the benefits of innovation standard at nursing "3 items," the factors affecting innovation standard at nursing "3 items," the principal achievement of innovation standard strategy "3 items," and the ways of achievement of innovation standards "3 items." Each answer was scored with 1 if correct and zero if incorrect. The total knowledge score was divided into two categories such as unsatisfactory (<70.0%) and satisfactory (≥70.0%).

*Part III:* concerned with nurses' attitude, it included 6 questions such as "I think that innovation causes wasting time and effort and that innovation at nursing causes a huge load on nurses without benefits." Each answer was scored on the Likert scale as follows: agree "3," sometimes "2," and disagree "1" for positive items and vice versa for negative points. The total attitude score was categorized as follows: negative attitude (<70.0%) and positive attitude (≥70.0%).

*Part IV:* concerned with the individual innovative scale, it will be adopted from [11]. To assess innovative behavior, it included 20 items divided into five domains such as opinion leadership, openness to experience, resistance to change, cautiousness, and risk-taking. Each answer was scored on the Likert scale as follows: agree "3," sometimes "2," and disagree "1" for positive items and vice versa for negative points. The total innovative score was categorized as follows: high (>70.0%), moderate (50 to 70%), and low (<50.0%).

### 2.7. Operational Design

**2.7.1. Preparatory Phase.** A literature review, tool development, and testing of the validity and reliability of the study's generated tools were all part of this phase, including a review of previous and recent literature and studies relevant, as well as a familiarization with the many components of the study research problems using available books, periodicals, magazines, and articles. A statistician used Cronbach's alpha coefficient test in the SPSS program version 21 to split all questions on the instrument and compute all correlation values for them, ensuring that the constructed tool was reliable. It was carried out on 10% of the nurses tested ( $n = 10$ ), with strong reliability for knowledge Cronbach's = 0.849, attitude = 0.817, and innovative scale = 0.887.

**2.7.2. Pilot Study.** A pilot research with a group of ten breast-feeding women was conducted. It is done prior to gathering data to assess the feasibility, time, cost, and adverse events of a full-scale research plan. The appropriate changes were made as a result. The sample included participants from the pilot research.

**2.7.3. Fieldwork.** This phase started from August 2021 to March 2022; it included taking permission from the hospital director and explaining the aim to the director and head nurses; after that, take consent from them to collect data; after that, distribute the Google form in the hospital WhatsApp group to collect data; the session was divided into an orientation to the innovation standard. Feedback was given



at each session, starting about the last one and finishing each session by summary; after that, the evaluation method was selected to suit the nurses' needs and achieve goals.

**2.7.4. Frame of the Study.** The frame of the study was done through the following phases:

*Assessment phase:* assess nurses' knowledge, attitude, and innovative scale.

*Planning phase:* objectives, priorities, and expected outcomes will be established based on the findings to meet nurses' knowledge and innovative skills and needs.

*Implementation phase:* prepare appropriate media, such as brochures, for the new standard in nursing care throughout the implementation phase. The educational program was implemented in the previously specified environments. The instructional program consisted of four classes held once a week, each lasting 20 to 30 minutes. The first session concentrated on the notion and principles of innovation standards. The second session focused on the characteristics of the nursing innovation standard, as well as the methods and strategies for achieving the goal. The third session focused on the advantages and benefits of innovation in nursing. The fourth session focused on innovation directions for nurses.

*Evaluation phase:* reevaluate nurses' knowledge, attitude, and innovative skills after implementing the educational program, which were compared with pretest levels.

**2.8. Ethical Considerations.** The director of the previously described setting gave his assent to the research. After the researcher briefed each nurse about the study's goal, they signed a consent form. Furthermore, the nurse who volunteered to participate in the study was advised that all information acquired would be kept private. They also have the option to leave the study at any moment.

**2.9. Statistical Analysis.** Organize and categorize the data and display the results in tables. The Statistical Package for the Social Sciences was used to analyze the data on a compatible personal computer (SPSS Inc.; version 21; IBM Corp., Armonk, NY, USA). Means and standard deviations were used to present continuous variables. To compare the pre- and postintervention scores, the chi-square was used. A *t*-test is an inferential statistic that is used to see if there is a significant difference between two groups' means. The results were considered significant when the probability of error is less than 5% ( $p < 0.05$ ) and highly significant when the probability of error is less than 0.1% ( $p < 0.001$ ).

### 3. Results

As shown in Table 1, this study is conducted on 100 nurses. Regarding their characteristics, more than two-thirds of them (68%) range in age from 20 to less than 25 years old, with mean age  $\bar{x} \pm SD$  25.26  $\pm$  4.78 years. As regards their experience, more than half of them (54%) have less than one year, while 8% of them have more than five years. In addition, as regards their qualification, most of them (84%) have a bachelor's degree, while 6% of them have a diploma. The majority of them (92%) are Saudi Arabians. Also, nearly

TABLE 1: Distribution of studied nurses related to their characteristics ( $n = 100$ ).

Items	N	%
Age:		
20-<25	68	68
25-30	17	17
>30	15	15
Mean (SD)	25.26 (4.78)	
Experience:		
<1 year	54	54
1-5 years	38	38
>5 years	8	8
Qualification:		
Diploma	6	6
Bachelor	84	84
Postgraduate	10	10
Nationality:		
Saudi	92	92
Non-Saudi	8	8
Training courses about innovation:		
Yes	38	38
No	62	62

two-thirds of them (62%) have no training courses about innovation, but 38% of them have.

Table 2 illustrates the knowledge of the studied nurses about innovation standards pre- and postintervention. Most of them (86%) have a correct answer as regards the principle achievement of innovation standard strategy "3 items" post-intervention, but 83% of them have an incorrect answer regarding the ways of achievement of innovation standards "4 items" preintervention. There is a highly statistically significant difference ( $p < 0.01^{**}$ ) between pre- and postintervention as regards all features registered.

Figure 1 represents the studied nurses' total knowledge about innovation standards pre- and postintervention. Most of them (88%) have satisfactory knowledge postintervention, while more than three-quarters of them (76%) have unsatisfactory knowledge preintervention.

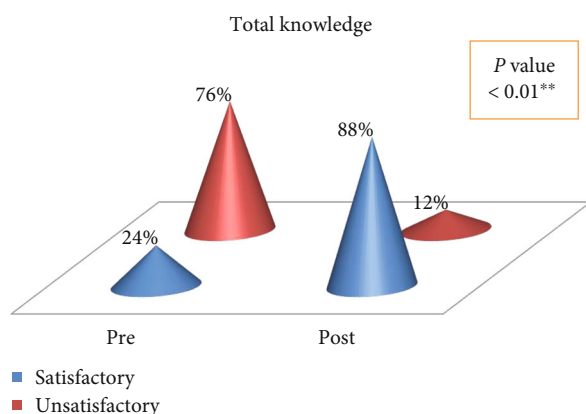
Table 3 reveals the studied nurses related to their individual innovative scale pre- and postintervention. Concerning resistance to change, the mean of them preintervention is  $\bar{x} \pm SD$  9.08  $\pm$  2.60. Concerning opinion leadership, the mean of them postintervention is  $\bar{x} \pm SD$  14.32  $\pm$  3.16. There is a highly statistically significant difference ( $p < 0.01^{**}$ ) between pre- and postintervention as regards all domains listed.

Figure 2 shows the sample of nurses' individual innovative scale pre- and postintervention. More than half of them (52%) have high postintervention, while almost half of them (48%) have low preintervention.

Figure 3 clarifies that most of the studied nurses (84%) have a positive attitude about innovation postintervention,

TABLE 2: Distribution of studied nurses related to their knowledge about innovation pre- and postintervention ( $n = 100$ ).

Domains	Pre		Post		Chi-square	$p$ value
	Correct	Incorrect	Correct	Incorrect		
Concept of innovation standard "4 items"	22	78	69	31	9.868	<0.01**
Benefits of innovation standard at nursing "3 items"	19	81	83	17	11.231	<0.01**
Factors affecting innovation standard at nursing "3 items"	23	77	78	22	12.571	<0.01**
Principle achievement of innovation standard strategy "3 items"	20	80	86	14	14.671	<0.01**
Ways of achievement of innovation standards "4 items"	17	83	72	28	13.901	<0.01**

FIGURE 1: Distribution of nurses related to their knowledge about innovation standards pre- and postintervention ( $n = 100$ ).

while more than two-thirds of them (68%) have a negative attitude preintervention.

Table 4 shows highly statistically significant positive correlations preintervention ( $p < 0.01^{**}$ ) between the total knowledge and the individual innovative scale of the studied nurses ( $r = 0.601$ ), between their total knowledge and their total attitude ( $r = 0.564$ ), and also between their individual innovative scale and their total attitude ( $r = 0.537$ ).

Table 5 shows highly statistically significant positive correlations postintervention ( $p < 0.01^{**}$ ) between the total knowledge and the individual innovative scale of the studied nurses ( $r = 0.577$ ), also between their total knowledge and their total attitude ( $r = 0.498$ ), and between their individual innovative scale and their total attitude ( $r = 0.601$ ).

#### 4. Discussion

The current study revealed that there was a highly statistically significant differentiation ( $p < 0.01^{**}$ ) before and after regarding all domains of knowledge- and attitude-related innovation standards. Moreover, most of them had satisfactory knowledge postintervention, while more than three-quarters of them had unsatisfactory knowledge preintervention. Furthermore, most of the studied nurses had a positive attitude about innovation postintervention, while more than two-thirds of them had a negative attitude preintervention. These results were attributed to the effective training program, which was prepared by the researcher dependent on nurses' needs detected by a pretest and which also used dif-

ferent illustrative teaching methods such as PowerPoint, videos, and attractive animations.

These results were supported by [12] which stated that the theoretical knowledge (88.4 vs. 81.7,  $p = 0.001$ ), operation skills (94.8 vs. 90.3,  $p = 0.001$ ), and total core competency score (156.2 vs. 148.8,  $p = 0.05$ ) were statistically substantially higher in the research group than in the control group. [13] stated that the nurses were enthusiastic about using modern technology, but there were obstacles such as a shortage of nurses, insufficient in-service training for staff on how to use the new technology, and a lack of electricity. [14] detected that there was an improvement in nurse managers' innovative managerial knowledge and skills, which then diminished at follow-up after three months of implementing the training program. Also, [15, 16] detected that nurses' knowledge, attitude, and performance in relation to ethical codes can all be improved through group reflection.

In addition, the current study demonstrated the studied nurses' individual innovative scale pre- and postintervention. More than half of them had high innovative skills postintervention, while almost half of them had low skills preintervention. Also, it was mentioned that it improved in the domains of the innovative scale.

These results were supported by [17, 18] which detected that after the training, nurses' self-rated innovation capacity ( $p = 0.001$ , 95% confidence interval 12.79 to 15.05) and research ability ( $p = 0.001$ , 95% confidence interval 14.39 to 19.09) both improved significantly. Also, [19, 20] revealed that empowering education can help nurses perform their jobs more effectively and master their professional abilities. [21] reported that to equip future generations of medical professionals with the ability to innovate efficiently and effectively, targeted education is required. Besides, [22] revealed that changing and improving nursing management staff's creativity affects their performance at Benha University Hospital. [23] stated that throughout the program, there was a statistically significant increase in the level of creativity and productivity among staff nurses.

Furthermore, the current study discovered highly statistically significant positive correlations between the total knowledge, the attitude, and the individual innovative scale of the studied nurses after intervention ( $p = 0.01^{**}$ ) at  $p$  value 0.01\*\*. These results agree with [24, 25] which showed that at the postintervention and follow-up program phases, there was a highly statistically significant positive link between the head nurses' managerial innovation knowledge, skills, and degree of professional competency.

TABLE 3: Distribution of studied nurses related to their individual innovative scale pre- and postintervention ( $n = 100$ ).

Domains	Pre		Post		<i>t</i> -test	<i>p</i> value
	Mean	SD	Mean	SD		
Opinion leadership	8.96	2.01	14.32	3.16	6.987	<0.01**
Openness to experience	5.03	1.78	10.08	2.31	7.664	<0.01**
Resistance to change	9.08	2.60	13.99	2.87	6.302	<0.01**
Cautiousness	2.33	0.98	4.50	1.01	7.099	<0.01**
Risk-taking	2.51	0.86	4.87	0.76	8.312	<0.01**

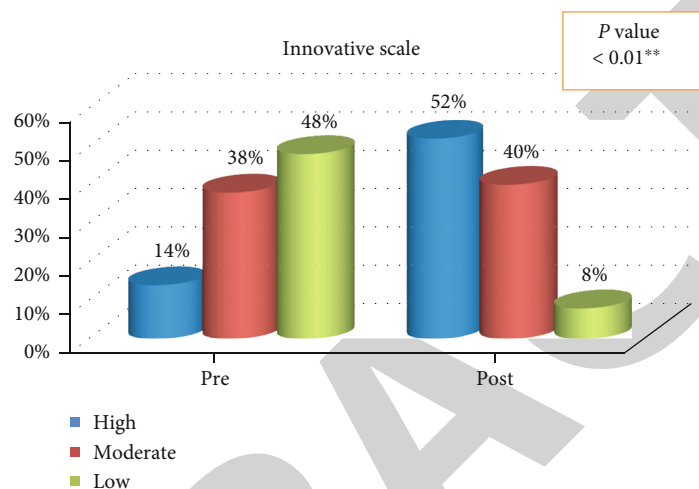


FIGURE 2: Distribution of nurses related to their individual innovative scale pre- and postintervention ( $n = 100$ ).

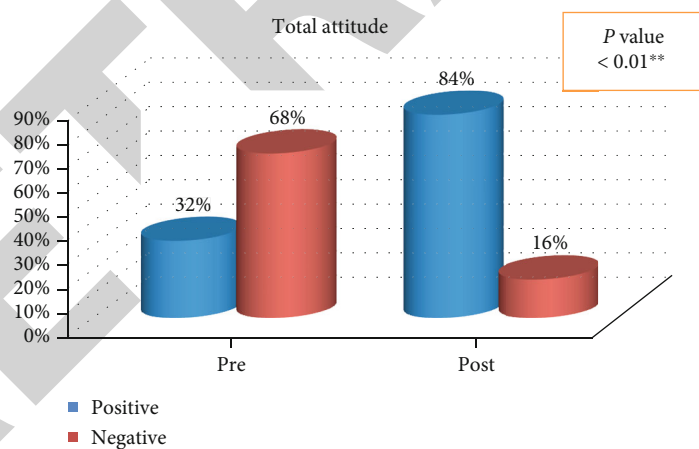


FIGURE 3: Distribution of studied nurses related to their attitude level about innovation pre- and postintervention ( $n = 100$ ).

TABLE 4: Correlation between studied variables preintervention.

		Total knowledge	Individual innovative scale	Total attitude
Total knowledge	<i>r</i>		0.601	0.564
	<i>p</i>		<0.01**	<0.01**
Individual innovative scale	<i>r</i>			0.537
	<i>p</i>			<0.01**
Total attitude	<i>r</i>			
	<i>p</i>			

TABLE 5: Correlation between studied variables postintervention.

		Total knowledge	Individual innovative scale	Total attitude
Total knowledge	<i>r</i>		0.577	0.498
	<i>p</i>		<0.01**	<0.01**
Individual innovative scale	<i>r</i>			0.601
	<i>p</i>			<0.01**
Total attitude	<i>r</i>			
	<i>p</i>			

## 5. Conclusion

The educational program significantly enhances nurses' knowledge and attitude, according to our present study. Nurses' innovative skills are also improved by enhancing their knowledge and attitude. Before and after the educational program was implemented, there was a highly statistically significant positive association between the nurses' knowledge, attitude, and innovative skills at  $p < 0.01$ .

## Data Availability

The data used to support the findings of this study are included within the article.

## Additional Points

*Recommendation.* (1) On-the-job training program for nurses about innovative skills. (2) Further study to assess the barriers of applying innovative skills. (3) Further education with all healthcare workers who are involved in the care of patients in order to reinforce innovative behavior.

## Conflicts of Interest

Concerning the research, writing, and/or publication of this paper, the authors disclosed no potential conflicts of interest.

## Acknowledgments

The authors are thankful to the Deanship of Scientific Research at Najran University for funding this work under the General Research Funding program grant code (NU/-/MRC/10/301). Thank you to all of the nurses who took part in this research.

## References

- [1] A. Purwanto, P. B. Santoso, E. Siswanto et al., "Effect of hard skills, soft skills, organizational learning and innovation capability on Islamic University lecturers' performance," *International Journal of Social and Management Studies*, vol. 2, no. 1, pp. 14–40, 2021.
- [2] M. B. Alazzam, A. T. Al-Radaideh, R. A. Alhamarnah, F. Alassery, F. Hajje, and A. Halasa, "A survey research on the willingness of gynecologists to employ mobile health applications," *Computational Intelligence and Neuroscience*, vol. 2021, Article ID 1220374, 7 pages, 2021.
- [3] M. K. Bhatti, B. A. Soomro, and N. Shah, "Training characteristics and employees' performance among the nurses in Pakistan," *Journal of Economic and Administrative Sciences*, 2021.
- [4] K. Weaver and A. R. Jones, "An innovative educational trio for physical assessment in an undergraduate nursing course," *Nursing Education Perspectives*, vol. 42, no. 4, pp. 257–258, 2021.
- [5] Y. Shen, W. Xie, X. Wang et al., "Impact of innovative education on the professionalism of undergraduate nursing students in China," *Nurse Education Today*, vol. 98, p. 104647, 2021.
- [6] T. C. Cook and L. J. Camp-Spivey, "Innovative teaching strategies using simulation for pediatric nursing clinical education during the pandemic: a case study," *Academic Medicine*, vol. 97, no. 3S, pp. S23–S27, 2022.
- [7] L. Gao, Q. Lu, X. Hou, J. Ou, and M. Wang, "Effectiveness of a nursing innovation workshop at enhancing nurses' innovation abilities: a quasi-experimental study," *Nursing Open*, vol. 9, no. 1, pp. 418–427, 2021.
- [8] N. Kaya, N. Turan, and G. Ö. Aydın, "A concept analysis of innovation in nursing," *Procedia-Social and Behavioral Sciences*, vol. 195, pp. 1674–1678, 2015.
- [9] S. Mamdouh and M. Samir, "Human resource management practices in relation to nurses' innovative work behavior: moderating role of eudaimonic well-being," *International Egyptian Journal of Nursing Sciences and Research*, vol. 2, no. 2, pp. 1–12, 2022.
- [10] T. A. Asurakkody and S. H. Kim, "Effects of knowledge sharing behavior on innovative work behavior among nursing students: mediating role of self-leadership," *International Journal of Africa Nursing Sciences*, vol. 12, p. 100190, 2020.
- [11] S. Yigit and K. Aksay, "A comparison between generation X and generation Y in terms of individual innovativeness behavior: the case of Turkish health professionals," *International Journal of Business Administration*, vol. 6, no. 2, p. 106, 2015.
- [12] F. Xu, L. Ma, Y. Wang et al., "Effects of an innovative training program for new graduate registered nurses: a comparison study," *SAGE Open*, vol. 11, no. 1, p. 215824402098854, 2021.
- [13] O. Olorunfemi, N. R. Osunde, O. M. Olorunfemi, and S. Adams, "Assessing nurses' attitudes toward the use of modern technology to care for patients at selected public and private hospitals, Benin-City, Nigeria, 2020," *International Archives of Health Sciences*, vol. 7, no. 3, p. 143, 2020.
- [14] F. F. Abo Baraka, M. M. Ibrahim, and S. M. Safan, "Developing and implementing an innovative managerial skills training program for nurse managers at Menoufia University Hospitals," *Menoufia Nursing Journal*, vol. 7, no. 1, pp. 157–187, 2022.
- [15] M. Momennasab, M. Ghanbari, and M. Rivaz, "Improving nurses' knowledge, attitude, and performance in relation to ethical codes through group reflection strategy," *BMC Nursing*, vol. 20, no. 1, p. 222, 2021.
- [16] M. B. Alazzam, H. Mansour, F. Alassery, and A. Almulihi, "Machine learning implementation of a diabetic patient monitoring system using interactive E-app," *Computational Intelligence and Neuroscience*, vol. 2021, Article ID 5759184, 7 pages, 2021.
- [17] L. Gao, Q. Lu, X. Hou, J. Ou, and M. Wang, "Effectiveness of a nursing innovation workshop at enhancing nurses' innovation abilities: a quasi-experimental study," *Nursing Open*, vol. 9, no. 1, pp. 418–427, 2022.
- [18] M. B. Alazzam, A. T. Al-Radaideh, N. Binsaif, A. S. AlGhamdi, and M. A. Rahman, "Advanced deep learning human herpes virus 6 (HHV-6) molecular detection in understanding human infertility," *Computational Intelligence and Neuroscience*, vol. 2022, Article ID 422963, 5 pages, 2022.
- [19] M. B. Alazzam, N. Tayyib, S. Z. Alshawwa, and M. Ahmed, "Nursing care systematization with case-based reasoning and artificial intelligence," vol. 2022, Article ID 1959371, 9 pages, 2022.
- [20] M. Chaghari, M. Saffari, A. Ebadi, and A. Ameryoun, "Empowering education: a new model for in-service training of nursing staff," *Journal of Advances in Medical Education & Professionalism*, vol. 5, no. 1, pp. 26–32, 2017.

## Retraction

# Retracted: Knowledge and Behavior toward Venous Thromboembolism Event Prophylaxis and Treatment Protocols among Medical Interns in Riyadh

### BioMed Research International

Received 20 June 2023; Accepted 20 June 2023; Published 21 June 2023

Copyright © 2023 BioMed Research International. This is an open access article distributed under the Creative Commons Attribution License, which permits unrestricted use, distribution, and reproduction in any medium, provided the original work is properly cited.

This article has been retracted by Hindawi following an investigation undertaken by the publisher [1]. This investigation has uncovered evidence of one or more of the following indicators of systematic manipulation of the publication process:

- (1) Discrepancies in scope
- (2) Discrepancies in the description of the research reported
- (3) Discrepancies between the availability of data and the research described
- (4) Inappropriate citations
- (5) Incoherent, meaningless and/or irrelevant content included in the article
- (6) Peer-review manipulation

The presence of these indicators undermines our confidence in the integrity of the article's content and we cannot, therefore, vouch for its reliability. Please note that this notice is intended solely to alert readers that the content of this article is unreliable. We have not investigated whether authors were aware of or involved in the systematic manipulation of the publication process.

Wiley and Hindawi regrets that the usual quality checks did not identify these issues before publication and have since put additional measures in place to safeguard research integrity.

We wish to credit our own Research Integrity and Research Publishing teams and anonymous and named external researchers and research integrity experts for contributing to this investigation.

The corresponding author, as the representative of all authors, has been given the opportunity to register their agreement or disagreement to this retraction. We have kept a record of any response received.

### References

- [1] Z. Al Aseri, J. M. Muammar, N. F. Aldakkan et al., "Knowledge and Behavior toward Venous Thromboembolism Event Prophylaxis and Treatment Protocols among Medical Interns in Riyadh," *BioMed Research International*, vol. 2022, Article ID 7191178, 7 pages, 2022.



## Research Article

# Knowledge and Behavior toward Venous Thromboembolism Event Prophylaxis and Treatment Protocols among Medical Interns in Riyadh

Zohair Al Aseri <sup>1,2</sup>, Jumanah Meshari Muammar <sup>1</sup>, Najd Fahad Aldakkan,<sup>1</sup>  
Afnan A. Alhazmi,<sup>1</sup> Hadeel Hamad Albraik,<sup>1</sup> Aeshah Abdullah Alasmari,<sup>1</sup>  
Lyla Mohammed Ashry,<sup>1</sup> Shaik S. Ahmed,<sup>3</sup> and Aamer Aleem<sup>4</sup>

<sup>1</sup>Department of Clinical Sciences, College of Medicine, Dar Al Uloom University, Riyadh, Saudi Arabia

<sup>2</sup>Departments of Emergency Medicine and Critical Care, College of Medicine, King Saud University, Riyadh, Saudi Arabia

<sup>3</sup>Department of Family and Community Medicine, College of Medicine, King Saud University, Riyadh, Saudi Arabia

<sup>4</sup>Department of Medicine, Hematology/Oncology Division (Oncology Center), College of Medicine, King Khalid University Hospital, King Saud University, Riyadh, Saudi Arabia

Correspondence should be addressed to Zohair Al Aseri; [zalaseri@ksu.edu.sa](mailto:zalaseri@ksu.edu.sa)

Received 13 June 2022; Revised 28 June 2022; Accepted 1 July 2022; Published 20 July 2022

Academic Editor: Dinesh Rokaya

Copyright © 2022 Zohair Al Aseri et al. This is an open access article distributed under the Creative Commons Attribution License, which permits unrestricted use, distribution, and reproduction in any medium, provided the original work is properly cited.

**Objective.** This study was aimed at evaluating the knowledge and behavior toward venous thromboembolism (VTE) prophylaxis among medical interns. **Methods.** This is a questionnaire-based cross-sectional observational cohort study of medical interns that used a validated questionnaire. The questionnaire comprised of items that assessed behavior, knowledge, and self-assessment of VTE risk factors, diagnosis, and prophylaxis. The study was conducted in Riyadh, Saudi Arabia, from October 2020 till September 2021. **Results.** The respondents were 246 medical interns. The overall rate of correct responses to behavior items was 41.82%. The overall rate of correct responses to knowledge items was 47.35%. A total of 61.8% responded negatively to the use of VTE risk assessment guidelines ( $p < 0.0001$ ). For the self-assessment of knowledge of VTE, more than 70% believed they did not have appropriate knowledge, were not prepared to establish the risk of VTE, and were not prepared to provide adequate prophylaxis for VTE ( $p < 0.0001$ ). A high proportion of medical interns (83.3%,  $p < 0.0001$ ) believed they needed further training on this topic. **Conclusion.** Participants in this study showed poor knowledge and negative behavior regarding the assessment of risk factors, diagnosis, and prophylaxis of VTE. The majority of participants reported they needed training on this topic. These findings underscore the need for educational programs during undergraduate training and orientation of medical interns for VTE risk assessment, diagnosis, and prophylaxis at the beginning of their internship.

## 1. Introduction

Venous thromboembolism (VTE) is a common clinical condition and comprises of deep vein thrombosis (DVT) and pulmonary embolism (PE). The incidence rates of VTE range from 0.06 to 0.87 per 1000 person-years and are substantially higher in high-income countries [1]. VTE is associated with significant morbidity and mortality and is considered the third leading cause of vascular-associated deaths worldwide, with mortality rates between 19.4 per

100 000 and 32.3 per 100 000 of population [2]. In a recent retrospective epidemiological study, the World Health Organization (WHO) mortality database (USA and Canada, 2000–17) was accessed to examine the prevalence of conditions contributing to PE-related mortality reported on death certificates and found an increase in PE-related mortality rates [3]. The US Center for Disease Control and Prevention considers VTE, especially PE, the most common cause of preventable death in hospitalized patients (US Centre for disease control and prevention, 2021) [4]. In an autopsy

study, PE was identified as the cause of death in 108 of 982 autopsy cases (11%) in a hospital with an average autopsy rate of  $30\% \pm 0.07\%$  [5].

VTE can be prevented with appropriate thromboprophylaxis, and the need for thromboprophylaxis is determined by VTE risk assessment looking for the presence of risk factors like recent surgery, trauma, immobilization, heart failure, cancer, pregnancy, hormonal therapy, and history of VTE, using various risk assessment tools [6–8]. Evidence from randomized control studies demonstrates significant mortality reduction, safety, and cost-effectiveness of using VTE prophylaxis in appropriate medical and surgical patients [9–12]. Despite wide dissemination of international guidelines on VTE prophylaxis, data show that thromboprophylaxis is under prescribed or misapplied [13–15]. Lack of awareness among physicians is one of the important reasons behind suboptimal thromboprophylaxis utilization [16]. A cross-sectional study performed to assess the awareness of VTE among internal medicine practitioners demonstrated that many practitioners were uncertain of the risk factors for VTE, and the authors concluded that there is a need for ongoing educational program to increase the practitioners' familiarity with the VTE risk factors [16]. Another study showed that internal medicine physicians had different beliefs about VTE prophylaxis than general surgery physicians.

A higher percentage of internal medicine physicians believed that VTE prophylaxis was not required for independent ambulatory patients [17]. Poor knowledge of VTE prophylaxis was also found in a Chinese study which showed clinicians had a low positive response rate regarding their behavior to VTE prophylaxis. The clinicians who responded to the survey suggested the need for more training opportunities on VTE prophylaxis [18].

As poor compliance with VTE prophylaxis is common leading to increased incidence of VTE, the American Heart Association called for action to prevent VTE. Their policy includes VTE knowledge and risk assessment, better implementation of prophylaxis, and reporting, national tracking, and prevention of VTE events [19].

Lack of knowledge of the risk factors for VTE and relevant guidelines can lead to failure among physicians to implement VTE prophylaxis. No study has evaluated the knowledge and behavior of medical interns regarding VTE prophylaxis in Saudi Arabia. This study was aimed at evaluating the knowledge and behavior toward VTE and thromboprophylaxis among medical interns.

## 2. Methods

This was a questionnaire-based cross-sectional observational cohort study of medical interns in Riyadh, Saudi Arabia, using a questionnaire. The study assessed their knowledge and behavior toward VTE risk assessment, diagnosis, and thromboprophylaxis. Ethical approval was obtained from the institutional review boards (IRBs) of the participating institutions. Our target population was medical interns rotating in different specialties at different hospitals in the city of Riyadh who studied at the colleges of medicine in

Riyadh. Interns from other colleges of medicine and health care workers other than interns were excluded. The study was conducted from October 2020 till September 2021, in Riyadh, Saudi Arabia.

The data were collected using a data collection form for the demographic characteristics of the medical interns, with a validated questionnaire to assess the awareness of medical interns about VTE risk assessment, diagnosis, and prophylaxis [20]. The questionnaire comprised 8 items that assessed behavior toward VTE prophylaxis and risk factor assessment using multiple-choice questions with the following possible responses: "always," "often," "not often," and "never"; 16 items that assessed knowledge of VTE risk factors and prophylaxis; 4 items for self-assessment of VTE risk stratification, diagnosis, and thromboprophylaxis using multiple-choice questions with the following possible responses: "totally agree," "somewhat agree," "neither," "somewhat disagree," and "totally disagree"; 3 items for the use of guidelines for VTE risk assessment with "yes" and "no" responses; and 4 items for the self-assessment of VTE risk stratification, diagnosis, and thromboprophylaxis.

Other areas of assessment included general information about VTE. Three items were used for the assessment of knowledge of different methods of thromboprophylaxis and 3 items for the assessment of the diagnostic tools of VTE.

The questionnaire was uploaded to an online survey collection tool, and the link was sent to the colleges of medicine and medical interns across the city of Riyadh by email and WhatsApp. Participation in the survey was anonymous and voluntary.

*2.1. Statistical Analysis.* All data collected were coded in an Excel spreadsheet. SPSS package version 26.0 (IBM Inc., Chicago, USA) was used for data analysis. Descriptive statistics, frequencies, and percentages were used to describe the categorical variables. A nonparametric Pearson's chi-square fitness of test was used to observe the statistical significance of observed categorical binary responses of different items related to VTE prophylaxis. A  $p$  value of  $\leq 0.05$  was used to report the statistical significance of the results.

## 3. Results

Knowledge and behavior toward VTE prophylaxis were assessed among the 246 medical interns. Out of 8 items that assessed behavior, for only 1 item ("How often do you screen for risk factors for venous thromboembolic disease in your hospitalized patients?"), 59.8% of medical intern's responses were positive (always or often) and 40.2% of responses were "never or not always," which indicated a significant difference ( $p = 0.002$ ). In addition, for 2 items that assessed behavior, the responses were not significantly different ( $p = 0.444$  and  $0.524$ ), as the responses ("always or often" and "never or not always") were almost evenly distributed (47.6% and 52.4%; 52% and 48%). For the remaining 5 items that assessed behavior, the binary responses were highly statistically significant ( $p < 0.0001$ ), as a higher proportion (61.8%, 69.5%, 74.8%, 54.1%, and 64.6%) of medical interns

TABLE 1: Distribution of knowledge and behavior responses toward VTE prophylaxis and risk factor assessment ( $n = 246$ ).

Items regarding behaviour toward VTE prophylaxis and risk factor assessment	No. (%)		<i>p</i> value
	Always	Often, not always, never	
How often do you screen for risk factors for VTE in your hospitalized patients?	147 (59.8)	99 (40.2)	0.002
When you are in charge of a hospitalized patient, how often do you consider the possibility of them developing VTE?	117 (47.6)	129 (52.4)	0.444
How often do you ask for a history of deep vein thrombosis in your clinical practice?	94 (38.2)	152 (61.8)	<0.0001
How often do you ask for a history of pulmonary embolism in your practice?	75 (30.5)	171 (69.5)	<0.0001
How often do you suspect a diagnosis of VTE in your clinical practice?	62 (25.2)	184 (74.8)	<0.0001
How often do your hospitalized patients with chronic cardiac or respiratory failure receive pharmacological thromboprophylaxis?	128 (52)	118 (48)	0.524
How often do you suggest the use of a thromboprophylactic measure in patients who require a fixed or mobile splint?	113 (45.9)	133 (54.1)	<0.0001
How often is VTE prophylaxis indicated for a cancer patient?	87 (35.4)	159 (64.6)	<0.0001
Items regarding knowledge about VTE prophylaxis and risk factor assessment	Totally agree	Somewhat agree, disagree, neutral, and totally disagree	<i>p</i> value
1. In all hospitalized patients, should the risk for VTE be stratified?	174 (70.7)	72 (29.3)	<0.0001
2. The risk for VTE is similar for all types of scheduled surgery.	35 (14.2)	211 (85.8)	<0.0001
3. The risk of VTE is greater in surgical patients than in nonsurgical patients.	109 (44.3)	137 (55.7)	0.074
4. The risk of VTE is similar in both oncological and nononcological surgery.	28 (11.4)	218 (88.6)	<0.0001
5. Thromboprophylaxis measures are more useful if they are initiated before the surgery starts as compared to postoperative initiation.	111 (45.1)	135 (54.9)	0.126
6. The presence of varicose veins is a risk factor for VTE.	78 (31.7)	168 (68.3)	<0.0001
7. Patients on mechanical ventilation have a higher risk of VTE.	102 (41.5)	144 (58.5)	0.007
8. Patients with stroke are at an increased risk of VTE.	139 (56.5)	107 (43.5)	0.041
9. Patients with multiple fractures are at an increased risk of VTE.	177 (72.0)	69 (28.0)	<0.0001
10. There is a risk of VTE in patients who require immobilization with fixed or mobile splints.	168 (68.3)	78 (31.7)	<0.0001
11. The use of hormonal medication raises the risk of VTE in women.	182 (74.0)	64 (26.0)	<0.0001
12. The use of hormonal medications raises the risk of VTE in men.	53 (21.5)	193 (78.5)	<0.0001
13. There is strong evidence demonstrating that flights longer than 4 hours are a risk factor for VTE.	142 (57.7)	104 (42.3)	0.015
14. The risk of VTE is significantly increased in cancer patients.	117 (47.6)	129 (52.4)	0.444
15. Gender is a risk factor for VTE.	114 (46.3)	132 (53.7)	0.251
16. Do you consider obesity as a risk factor for VTE?	135 (54.9)	111 (54.1)	0.126

VTE = venous thromboembolism.

TABLE 2: Distribution of responses toward the use of guidelines for VTE risk assessment.

Items regarding the use of guidelines for VTE risk assessment	No. (%)		<i>p</i> value
	Yes	No	
1. Do you know at least one of the published guidelines to assess the risk of VTE?	94 (38.2)	152 (61.8)	<0.0001
2. Do you use any of the published guidelines to stratify the risk of VTE in your patients?	92 (37.4)	154 (62.6)	<0.0001
3. Is there a VTE risk assessment program (model or tool) for the patients in the hospital you work at?	145 (58.9)	101 (41.1)	0.005

VTE = venous thromboembolism.

TABLE 3: Distribution of responses of self-assessment toward VTE risk stratification, diagnosis and thromboprophylaxis.

Items regarding self-assessment toward VTE risk stratification, diagnosis and thromboprophylaxis	No. (%)		<i>p</i> value
	Agree	Disagree	
1. Do you have the appropriate knowledge about VTE?	64 (26.0)	182 (74.0)	<0.0001
2. Are you prepared, in theory, to establish (STRATIFY) the risk for VTE in patients?	41 (16.7)	205 (83.3)	<0.0001
3. Are you prepared, in theory, to diagnose VTE?	51 (20.7)	195 (79.3)	<0.0001
4. Are you prepared, in theory, to provide adequate prophylaxis for VTE in patients?	45 (18.3)	201 (81.7)	<0.0001
5. Do you believe that you need training on the prevention and management of VTE?	205 (83.3)	22 (8.9)	<0.0001

VTE = venous thromboembolism.

TABLE 4: Assessment of responses to general information about VTE, knowledge of different methods of thromboprophylaxis, and diagnostic tools of VTE.

	No. (%)		<i>p</i> value
	Agree	Disagree	
1. VTE disease is a clinical entity that includes deep vein thrombosis and pulmonary embolism?	82.1%	17.9%	<0.0001
2. Pulmonary embolism is a cause of mortality in your clinical practice?	63.8%	36.2%	<0.0001
1. Intermittent pneumatic compression of the lower limbs is a useful nonpharmacological measure to prevent deep vein thrombosis?	43.5%	56.5%	<0.001
2. All anticoagulants have the same risk of causing bleeding?	29.7%	70.3%	<0.0001
3. What test do you request for the control of anticoagulant therapy with vitamin K antagonists?	47.6%	52.4%	<0.0001
1. What is the most appropriate tool for identifying a low probability of deep vein thrombosis?	61.8%	38.2%	<0.0001
2. What is the most appropriate tool for the diagnosis of pulmonary embolism?	86.6%	17.4%	<0.0001
3. The use of D-dimer plus Doppler ultrasound is reliable for the accurate diagnosis of deep vein thrombosis?	72.4%	27.6%	<0.0001

responded with “never” or “not always.” The overall rate of correct responses to behavior items was 41.82%, indicating that medical interns’ behavior toward VTE prophylaxis was not at the optimum level (Table 1).

For the 16 items that assessed the knowledge of VTE prophylaxis and risk factor assessment, the medical interns’ responses for 6 items were positive for items 1 (70.7%), 2 (56.5%), 4 (72%), 6 (68.3%), 9 (74%), and 13 (57.7%), respectively, as they responded with “totally agree,” which was highly statistically significant ( $p < 0.0001$ , Table 1). For a total of 5 items, the medical interns’ distribution of binary responses of “totally agree” and “somewhat agree or did not agree” was not statistically significant, whereas for the remaining 5 items (2, 4, 6, 7, 12, and), a higher proportion of medical interns (85.8%, 88.6%, 68.3%, 58.5%, and 78.5%) responded with “somewhat agree or did not agree” (Table 1), which was highly statistically significant ( $p < 0.0001$ ). The overall rate of correct responses to the items that assessed knowledge was 47.35% (Table 1).

More than 50% of the medical interns (61.8% and 62.6%) responded negatively (with “no”) to the 2 items

related to the use of the guidelines for VTE risk assessment, which was highly statistically significant ( $p < 0.0001$ ). In addition, 58.9% of the interns responded positively (with “yes”) for the item “is there a venous thromboembolic disease risk assessment program (model or tool) for the patients in the hospital you work at?”, which was also statistically significant ( $p = 0.005$ ) (Table 2).

Self-assessment of VTE risk stratification, diagnosis, and thromboprophylaxis was carried out using 5 items, where more than 70% of the interns responded with “disagree and totally disagree” (Table 3), which was highly statistically significant ( $p < 0.0001$ ). A significantly higher proportion of interns (83.3%,  $p < 0.0001$ ) responded with “totally agree” regarding the need for training in the management of VTE (Table 3).

For the two items regarding general information about VTE, approximately 82.1% and 63.8% of medical interns, respectively, responded with “agree,” which was statistically significant ( $p < 0.0001$ ) (Table 4).

For the 3 items for assessment of the diagnostic methods of VTE, 43.5% of medical interns agreed for the use of D-



dimer, 29.7% of them mentioned the use of a chest computed tomogram, and 47.6% of them agreed for the use of D-dimer plus Doppler ultrasound as reliable methods for the accurate diagnosis of deep vein thrombosis (Table 4).

For the 3 items used for the assessment of the interns' knowledge of different methods of thromboprophylaxis (Table 4), approximately 61.8% and 86.6% of medical interns responded with "agree" and "disagree," respectively, whereas for the third item, 72.4% of interns responded positively with international normalized ratio (INR) as the correct response, which was statistically significant ( $p < 0.0001$ ).

#### 4. Discussion

VTE risk assessment and risk stratification is the initial step to evaluate the need for thromboprophylaxis and should be performed in all hospitalized patients [6–8, 19]. Numerous studies of VTE prophylaxis in hospitalized patients have shown that VTE prophylaxis is under prescribed or not properly applied [13–15]. Although VTE risk assessment is needed in all hospitalized patients [19–21], many physicians believe that VTE prophylaxis is not required for independent ambulatory patients and, therefore, may not assess for VTE risk in these patients. Although this attitude varies among different specialties, it is more common among internal medicine physicians as compared to surgeons [17–18]. Poor knowledge and behavior of VTE prophylaxis was shown in a Chinese study, and participants showed a low positive response rate regarding their behaviors to VTE prophylaxis. The clinicians who responded to the survey suggested the need for more training opportunities on VTE prophylaxis [19–23].

To our knowledge, no recent study has evaluated the knowledge and behavior of medical interns toward VTE prophylaxis. In many institutions, medical interns are usually involved in the initial patient assessment. Their awareness and attitude may play an important part in VTE risk assessment and prophylaxis, and hence, poor knowledge and awareness of VTE prophylaxis may result in failure to provide appropriate risk assessment and thromboprophylaxis. Our study showed that overall knowledge of medical interns regarding VTE prophylaxis and risk factor assessment was poor. Respondents of the current study also showed a negative attitude toward VTE risk stratification and prophylaxis. Moreover, there was poor knowledge and adherence to the guidelines for VTE risk assessment; few participants knew about the published guidelines or had used one of them. More than half of the participants reported that they were involved in the VTE risk assessment of their patients in their respective departments. This raises the concern that poor knowledge and attitude of medical interns towards VTE prophylaxis may lead to under prescription and increased risk of VTE among hospitalized patients.

Our study findings highlight that majority of the medical interns did not have appropriate knowledge about VTE and were not prepared to establish the risk for VTE or provide adequate VTE prophylaxis to the patients. Nevertheless, most of the respondents reported and agreed that they

needed further training on this subject. This deficiency underscores the need for more teaching and training regarding VTE prophylaxis prior to starting the internship.

Bearing in mind the widespread poor knowledge and awareness of physicians regarding VTE prophylaxis as shown in other studies [13–18], our study results are not surprising, especially considering the fact that medical interns are at the beginning of their career in clinical practice. This reflects the deficiency of educational programs at the undergraduate level. The importance of educational programs and lectures has been reported in a previous local study that found that education via didactic lectures improved the knowledge of the participants regarding the thromboprophylaxis guidelines [24–27]. The current study showed that there is area for improvement and enhancement of overall knowledge of medical interns toward VTE risk assessment and prophylaxis. Knowledge of medical students needs to be enhanced by incorporating educational courses about VTE risk assessment, diagnosis, and prophylaxis in the undergraduate curricula. Moreover, medical interns should receive orientation on this subject in the beginning of their internships.

Our study has certain limitations. First, all respondents were only from one city, which may not make our findings generalizable to medical interns elsewhere because of the differences in undergraduate curricula and training. Second, the study did not segregate respondents according to their specialty rotations completed before the survey. Third, the timing of the survey was not at a specific period in the internship year, and respondents were in various stages of their internships, which may have influenced the results as interns in the beginning of the internship are expected to have less knowledge of the topic as compared to those at the end.

#### 5. Conclusion

Participants in this study showed poor knowledge and negative behaviors regarding the assessment of risk factors, diagnosis, and prophylaxis of VTE. Majority of the participants agreed that they needed training programs for VTE prophylaxis. Apart from additional educational programs during undergraduate training, medical interns should receive orientation for VTE risk assessment, diagnosis, and prophylaxis in the beginning of their internship.

#### Data Availability

The data used to support the results of this study are available on request from the corresponding author.

#### Ethical Approval

Ethical approval was obtained from the institutional review boards (IRBs) of King Saud University and Dar Al Uloom University.

#### Conflicts of Interest

The authors declare that they have no conflicts of interest.



## Authors' Contributions

ZA was responsible for the concept and design of the study or acquisition, analysis, and interpretation of the data and drafting the article and final approval. AA was responsible for the concept and design of the study or acquisition, analysis, and interpretation of the data and drafting the article and final approval. SA analyzed and interpreted the data and drafted the article and provided final approval. JM, LA, AA, HA, and NA designed the study or acquired the data and drafted the article and provided final approval.

## Acknowledgments

The authors extend their appreciation to the Deanship of Post Graduate and Scientific Research at Dar Al Uloom University for funding this work.

## References

- [1] D. M. Siegal, J. W. Eikelboom, S. F. Lee et al., "Variations in incidence of venous thromboembolism in low-, middle-, and high-income countries," *Cardiovascular Research*, vol. 117, no. 2, pp. 576–584, 2021.
- [2] A. M. Wendelboe and G. E. Raskob, "Global burden of thrombosis," *Circulation Research*, vol. 118, no. 9, pp. 1340–1347, 2016.
- [3] S. Barco, L. Valerio, W. Ageno et al., "Age-sex specific pulmonary embolism-related mortality in the USA and Canada, 2000-18: an analysis of the WHO mortality database and of the CDC multiple cause of death database," *The Lancet Respiratory Medicine*, vol. 9, no. 1, pp. 33–42, 2021.
- [4] M. B. Alazzam, N. Tayyib, S. Z. Alshawwa, and M. Ahmed, "Nursing care systematization with case-based reasoning and artificial intelligence," *Journal of Healthcare Engineering*, vol. 2022, 9 pages, 2022.
- [5] US Centre for Disease Control and Prevention, *Healthcare-associated VTE, data and statistics on HA-VTE*, 2021, January 2022, <https://www.cdc.gov/ncbddd/dvt/ha-vte-data.html>.
- [6] P. H. Sweet, T. Armstrong, J. Chen, E. Maslah, and P. Witucki, "Fatal pulmonary embolism update: 10 years of autopsy experience at an academic medical center," *JRSM Short Reports*, vol. 4, article 2042533313489824, 2013.
- [7] L. N. Godat, L. Kobayashi, D. C. Chang, and R. Coimbra, "Can we ever stop worrying about venous thromboembolism after trauma?," *Journal of Trauma and Acute Care Surgery*, vol. 78, no. 3, pp. 475–481, 2015.
- [8] J. A. Heit, F. A. Spencer, and R. H. White, "The epidemiology of venous thromboembolism," *Journal of Thrombosis and Thrombolysis*, vol. 41, no. 1, pp. 3–14, 2016.
- [9] C. Oedingen, S. Scholz, and O. Razum, "Systematic review and meta-analysis of the association of combined oral contraceptives on the risk of venous thromboembolism: the role of the progestogen type and estrogen dose," *Thrombosis Research*, vol. 165, pp. 68–78, 2018.
- [10] V. Hansrani, M. Khanbhai, and C. McCollum, "The prevention of venous thromboembolism in surgical patients," *Advances in Experimental Medicine and Biology*, vol. 906, pp. 1–8, 2017.
- [11] M. B. Alazzam, A. T. Al-Radaideh, N. Binsaf, A. S. AlGhamdi, and M. A. Rahman, "Advanced deep learning human herpes virus 6 (HHV-6) molecular detection in understanding human infertility," *Computational Intelligence and Neuroscience*, vol. 2022, 5 pages, 2022.
- [12] C. M. Lilly, X. Liu, O. Badawi, C. S. Franey, and I. H. Zuckerman, "Thrombosis prophylaxis and mortality risk among critically ill adults," *Chest*, vol. 146, no. 1, pp. 51–57, 2014.
- [13] M. Nicholson, N. Chan, V. Bhagirath, and J. Ginsberg, "Prevention of venous thromboembolism in 2020 and beyond," *Journal of Clinical Medicine*, vol. 9, no. 8, p. 2467, 2020.
- [14] M. B. Streiff and B. D. Lau, "Thromboprophylaxis in nonsurgical patients," *Hematology*, vol. 2012, no. 1, pp. 631–637, 2012.
- [15] P. D. Hibbert, N. A. Hannaford, T. D. Hooper et al., "Assessing the appropriateness of prevention and management of venous thromboembolism in Australia: a cross-sectional study," *BMJ Open*, vol. 6, no. 3, article e008618, 2016.
- [16] F. Randelli, C. Cimminiello, M. Capozzi, M. Bosco, G. Cerulli, and GIOTTO Investigators, "Real life thromboprophylaxis in orthopedic surgery in Italy. Results of the GIOTTO study," *Thrombosis Research*, vol. 137, pp. 103–107, 2016.
- [17] A. Mamra, A. S. Sibghatullah, G. P. Ananta, M. B. Alazzam, Y. H. Ahmed, and M. Doheir, "Theories and factors applied in investigating the user acceptance towards personal health records: review study," *International Journal of Healthcare Management*, vol. 10, no. 2, pp. 89–96, 2017.
- [18] W. D. Rocher, T. Page, M. Rocher, and D. Nel, "Venous thromboembolism risk and prophylaxis prescription in surgical patients at a tertiary hospital in Eastern Cape Province, South Africa," *South African Medical Journal*, vol. 109, no. 3, pp. 178–181, 2019.
- [19] M. B. Alazzam, H. Al Khatib, W. T. Mohammad, and F. Alassery, "E-health system characteristics, medical performance, and healthcare quality at Jordan's health centers," *Journal of Healthcare Engineering*, vol. 2021, 7 pages, 2021.
- [20] A. Majluf-Cruz, G. Castro Martinez, M. A. Herrera Cornejo, G. Liceaga-Cravioto, F. Espinosa-Larrañaga, and J. Garcia-Chavez, "Awareness regarding venous thromboembolism among internal medicine practitioners in Mexico: a national cross-sectional study," *Internal Medicine Journal*, vol. 42, no. 12, pp. 1335–1341, 2012.
- [21] K. L. Piechowski, S. Elder, L. E. Efirid et al., "Prescriber knowledge and attitudes regarding non-administration of prescribed pharmacologic venous thromboembolism prophylaxis," *Journal of Thrombosis and Thrombolysis*, vol. 42, no. 4, pp. 463–470, 2016.
- [22] X. Gao, H. Qin, C. Hang et al., "Knowledge, behaviors, and attitudes regarding venous thromboembolism prophylaxis: a survey of clinicians at a tertiary hospital of China," *Annals of Vascular Surgery*, vol. 72, pp. 365–372, 2021.
- [23] P. K. Henke, S. R. Kahn, C. J. Pannucci et al., "Call to action to prevent venous thromboembolism in hospitalized patients: a policy statement from the American Heart Association," *Circulation*, vol. 141, no. 24, pp. e914–e931, 2020.
- [24] M. Rasmi, M. B. Alazzam, M. K. Alsmadi, I. A. Almarshdeh, R. A. Alkhasawneh, and S. Alsmadi, "Healthcare professionals' acceptance electronic health records system: critical literature review (Jordan case study)," *International Journal of Healthcare Management*, vol. 13, no. sup1, pp. 48–60, 2020.
- [25] A. Amin, F. Girard, and M. Samama, "Does ambulation modify venous thromboembolism risk in acutely ill medical

## Retraction

# Retracted: Prevalence and Correlation of Metabolic Syndrome in Patients with Bipolar Disorder in NGHA, Riyadh

### BioMed Research International

Received 18 July 2023; Accepted 18 July 2023; Published 19 July 2023

Copyright © 2023 BioMed Research International. This is an open access article distributed under the Creative Commons Attribution License, which permits unrestricted use, distribution, and reproduction in any medium, provided the original work is properly cited.

This article has been retracted by Hindawi following an investigation undertaken by the publisher [1]. This investigation has uncovered evidence of one or more of the following indicators of systematic manipulation of the publication process:

- (1) Discrepancies in scope
- (2) Discrepancies in the description of the research reported
- (3) Discrepancies between the availability of data and the research described
- (4) Inappropriate citations
- (5) Incoherent, meaningless and/or irrelevant content included in the article
- (6) Peer-review manipulation

The presence of these indicators undermines our confidence in the integrity of the article's content and we cannot, therefore, vouch for its reliability. Please note that this notice is intended solely to alert readers that the content of this article is unreliable. We have not investigated whether authors were aware of or involved in the systematic manipulation of the publication process.

In addition, our investigation has also shown that one or more of the following human-subject reporting requirements has not been met in this article: ethical approval by an Institutional Review Board (IRB) committee or equivalent, patient/participant consent to participate, and/or agreement to publish patient/participant details (where relevant).

Wiley and Hindawi regrets that the usual quality checks did not identify these issues before publication and have since put additional measures in place to safeguard research integrity.

We wish to credit our own Research Integrity and Research Publishing teams and anonymous and named external researchers and research integrity experts for contributing to this investigation.

The corresponding author, as the representative of all authors, has been given the opportunity to register their agreement or disagreement to this retraction. We have kept a record of any response received.

### References

- [1] A. Alanazi, S. Alsadhan, S. Aldosari et al., "Prevalence and Correlation of Metabolic Syndrome in Patients with Bipolar Disorder in NGHA, Riyadh," *BioMed Research International*, vol. 2022, Article ID 5847175, 5 pages, 2022.

## Research Article

# Prevalence and Correlation of Metabolic Syndrome in Patients with Bipolar Disorder in NGH, Riyadh

Asma Alanazi <sup>1,2</sup>, Saud Alsadhan,<sup>1</sup> Sultan Aldosari,<sup>1</sup> Abdullah Alharbi,<sup>1</sup> Mohammed Albawardi,<sup>1</sup> Saud Alrabah,<sup>1</sup> Haifa Alhawas,<sup>1,2</sup> and Maram Albalawi<sup>3</sup>

<sup>1</sup>Department of Basic Medical Sciences, College of Medicine, King Saud Bin Abdulaziz University for Health Sciences (KSAU-HS), Riyadh, Saudi Arabia

<sup>2</sup>King Abdullah International Medical Research Centre (KAIMRC), Riyadh, Saudi Arabia

<sup>3</sup>Department of Biostatistics and Bioinformatics, King Abdullah International Medical Research Centre, Riyadh, Saudi Arabia

Correspondence should be addressed to Asma Alanazi; [anazia@ksau-hs.edu.sa](mailto:anazia@ksau-hs.edu.sa)

Received 5 June 2022; Revised 19 June 2022; Accepted 4 July 2022; Published 18 July 2022

Academic Editor: Dinesh Rokaya

Copyright © 2022 Asma Alanazi et al. This is an open access article distributed under the Creative Commons Attribution License, which permits unrestricted use, distribution, and reproduction in any medium, provided the original work is properly cited.

**Background.** Metabolic syndrome is considered dangerous, especially to patients that are diagnosed with a mental condition such as bipolar disorder, since these types of patients can be difficult to deal with. Metabolic syndrome can lead to multiple cardiovascular diseases, strokes, and diabetes. A careful approach is important when it comes to facing a complex condition such as this. This research will contribute to giving more information about the prevalence and statistics of metabolic syndrome in bipolar disorder patients at NGH, Riyadh. No published study in literature has investigated the prevalence of metabolic syndrome in patients with bipolar disorder in NGH, Riyadh. **Methods.** The study was conducted among 191 adult male (66) and female (125) patients at NGH, Riyadh. The medical records were used for the assessment of metabolic syndrome and referrals by using a chart review for individuals. The main variables are metabolic syndrome and bipolar disorder. It was conducted on both males and females. Data was collected on data collection form and further analysis on relations was made by using SAS (Version 9.4). Chi-squared test and the Wilcoxon Two-sample test for two-level continuous variables.  $P \leq 0.05$  was determined to be the significance level. **Results.** Out of 191 patients, 130 were obese, 85 had diabetes, and 89 were hypertensive. Additionally, 50 (40%) females and 29 (43.9%) males had metabolic syndrome, a total of 79 (41.4%) out of 191. **Conclusion.** The findings of this study indicate that there is an elevated prevalence of metabolic syndrome in bipolar disorder patients in NGH, Riyadh. Highlighting the potential danger that people may not be aware of.

## 1. Introduction

Bipolar disorder, which was known as manic depression, is a mental abnormality where a person has a major and a sudden change of mood, and it consists of emotional highs, mania, or hypomania, where a patient may feel energetic and may get over thrilled, and lows, depression, where a patient gets sad and helpless. This abrupt mood fluctuation alters the patient's cognitive capacity, appraisal, and sleep [1, 2]. Bipolar disorder is one of the chronic complicated psychological problems that have an early onset of presentation. Bipolar disorders are considered a range of disorders that include both bipolar I disorder and bipolar II disorder. Bipolar I disorder contains multiple phases of extreme mood

episodes switching from depression to mania. However, bipolar II disorder is considered to be a milder form of mood raising that has a milder occurrence of hypomania which switches, with shifts, to extreme depression.

Cyclothymic disorder explains short sessions of hypomanic symptoms which alternate with short sessions of depressive symptoms which are not as prolonged as seen in entire hypomanic sessions or entire depressive sessions [3]. A cross-sectional scanning of 11 countries indicated that bipolar disorders had a total lifetime prevalence of 2.4%, with 0.6% for bipolar type I and 0.4% for bipolar type II. The mean starting age of bipolar disorder is 25 years [4, 5]. Bipolar disorder is a disabling disorder that has a chronic course. 49 million people were suffering from bipolar

disorder in 2013, which accounts for 9.9 million disability-adjusted life years (DALY) globally [6]. Additionally, patients that are diagnosed with any serious mental conditions, such as bipolar disorder and other mental illnesses, when compared to the general population, have higher rates of untreated medical conditions [7]. Unfortunately, they tend to die 10 to 30 years younger than other people, mainly due to cardiovascular diseases, stroke, and physical illnesses, which account for almost 60% of mortality [8].

A very common group of conditions that arise simultaneously, known as metabolic syndrome, can elevate the chances of type 2 diabetes, heart disease, and stroke. Conditions of metabolic syndrome include excess fat around the waist, increased blood sugar levels, elevated blood pressure, increased triglyceride levels, and decreased levels of HDL [9]. There are three main definitions for metabolic syndrome; we decided to work with the criteria of the International Diabetes Federation (IDF). Additionally, a reliable reporting of the aspects of metabolic syndrome can guide and provide the strategies for prevention and treatment [10]. Both bipolar disorder and metabolic syndrome are suggested to share similar predisposing factors, such as dysregulation of the sympathetic nervous system, endocrine disorders, and detrimental behaviors like smoking, overeating, use of alcohol, and lack of physical activity [4]. Moreover, psychotropic drugs that are used to treat bipolar disorder may result in weight gain and metabolic disruptions, including mutations in glucose and lipid metabolism. Additionally, metabolic syndrome increases the risk of developing cardiovascular diseases, consequently reducing a bipolar patient's life expectancy by 25 to 30 years. The precise mechanism of metabolic syndrome evolution in bipolar patients, however, is unclear. Other biological methods have been proposed, such as anomalies of the immune system, and disruption of the hypothalamic-pituitary-adrenocortical (HPA) axis. In the Middle East and North African region (MENA), a high prevalence of metabolic syndrome is noticed. In Tunisia, for example, it has been proclaimed to be 45.5% using the IDF criteria [11]. However, the prevalence of metabolic syndrome in bipolar disorder patients is rarely studied in Gulf Cooperation Countries (GCC). This research will contribute to giving more information about the prevalence and statistics of metabolic syndrome in patients with bipolar disorder in NGH, Riyadh. No published study in literature has investigated the prevalence of metabolic syndrome in bipolar disorder patients in NGH, Riyadh.

## 2. Methods

**2.1. Study Design, Area, and Setting.** A retrospective cross-sectional study was conducted. The information was collected at one point in time; thus, a cross-sectional study is the best study design. The medical records were checked for the relationship between bipolar disorder and metabolic syndrome in adults. The study was conducted on bipolar disorder patients at King Abdulaziz Medical City in Riyadh, and the data was collected from the Ministry of National Guard Health Affairs NGH. Established in May 1983, King

Abdulaziz Medical City in Riyadh has a bedding capacity of 1501 beds. It provides all types of care to all National Guard soldiers and their families, beginning from primary health care, to complex tertiary specialized care.

**2.2. Study Subjects.** This study constitutes adult male and female bipolar patients older than 18 years. Bipolar patients are patients with a mental disorder that causes unexpected switches in energy, activity levels, mood, concentration, and the ability to carry out ordinary day-to-day tasks. Based on the availability of variables, the sample size was determined to be 191, 125 females and 66 males. A non-probability convenient sample was used. Patient records that met the inclusion criteria between March 2015 and December 2020 were included in the study.

**2.3. Data Collection Process.** All the information and data needed for this study were obtained by reviewing the medical records in the BESTCare system. This study was approved by the institutional Review Board (IRB) from King Abdullah International Medical Research Centre (KAIMRC) IRB #SP21R/247/05. The records were reviewed by the co-investigators. Metabolic syndrome was diagnosed based on the definition of the International Diabetes Federation (IDF).

**2.4. Data Analysis.** The data was coded for entry and analysis using SAS (Version 9.4). For categorical variables, data are presented as frequency and percentage. We used the Chi-squared test and the Wilcoxon Two-sample test for two-level continuous variables.  $P \leq 0.05$  was determined to be the significance level.

## 3. Results

A total of 191 patients (125 females and 66 males) were included in the analysis. A retrospective chart review showed that the mean value for body mass index (BMI) for female patients was 33.76. Similarly, for male patients, it was 33.39, and when including all patients, it was 33.63. According to the IDF, both male patients' and female patients' mean values are considered obese. Furthermore, female patients had a higher prevalence of obesity. 89 (71.2%) female patients, and 41 (62.1%) male patients were obese, which is 130 (68.1%) out of 191 patients. The minimum value for BMI was 17.67, and the maximum value was 63.54.

The mean value for systolic blood pressure (SBP) for female patients was 128.42 compared to 131.44 for male patients. As for all patients, it was 129.47. According to the IDF, the mean SBP value for female patients is considered normal, whereas the mean value for male patients is elevated. Moreover, elevated SBP was observed to be found more in male patients than in females. 54 (43.2%) female patients and 35 (53%) male patients had elevated SBP, which is 89 (46.6%) out of 191 patients. The minimum value for SBP was 81, and the maximum value was 198.

The mean value for fasting blood sugar (FBS) for female patients was 6.68, and for male patients, it was 7.74. As for all patients, it was 7.04. Both male and female mean values are considered high according to the IDF.



Additionally, 56 (51.9%) female patients and 29 (52.7%) male patients had elevated FBS, which is 85 (52.2%) out of 163 patients. The minimum value for FBS was 2.60, and the maximum was 40.30.

The mean value for high-density lipoprotein (HDL) levels for female patients was 1.22 and 0.97 for male patients. As for all patients, it was 1.14. It is important to mention that HDL is the only variable that leads to metabolic syndrome when reduced, rather than elevated as seen in all other variables. Although the IDF's benchmark is different for males and females, both mean values are considered to be reduced. Also, 68 (60.2%) female patients and 41 (67.2%) male patients had reduced HDL levels, which is 109 (62.6%) out of 174 patients. The minimum value for HDL was 0.54, and the maximum value was 2.16.

The mean value for triglyceride levels was 1.38 for female patients and 1.86 for male patients. As for all patients, it was 1.55. In relevance to the IDF's definition, the mean value for females is considered normal, whereas the mean value for males is elevated. In addition to mean values, 25 (23.8%) female patients and 26 (44.1%) male patients had elevated triglyceride levels, which is 51 (31.1%) out of 164 patients. The minimum value for triglyceride was 0.25, and the maximum value was 5.25.

Even though these five variables are the diagnostic variables for metabolic syndrome according to the IDF, other non-diagnostic variables such as LDL and cholesterol levels are also considered important since they accompany HDL and triglyceride levels in the lipid profile test and, thus, they should be mentioned briefly. For cholesterol levels, the mean value for female patients was 4.55 and 4.64 in male patients. For LDL levels, the mean value for females was 2.82 and 2.98 in male patients. As for all patients, it was 4.58 for cholesterol and 2.88 for LDL. The minimum values for cholesterol and LDL were 2.15 and 0.84, whereas the maximum values were 9.02 and 6.92, respectively. For the mean value and prevalence of all variables, see Tables 1, 2, and 3.

When it comes to the prevalence of metabolic syndrome, 50 (40%) females and 29 (43.9%) males had metabolic syndrome, a total of 79 (41.4%) out of 191. When observing the mean values and percentages for all diagnostic variables, male patients were dominant in all except for BMI. Thus, male patients were expected to have a higher prevalence of metabolic syndrome even though obesity is the predominant variable in diagnosing metabolic syndrome according to the criteria of the IDF.

#### 4. Discussion

In Saudi Arabia, this is the first study to assess metabolic syndrome in association with patients suffering from bipolar disorder. Only one research from Saudi Arabia assesses the prevalence of metabolic syndrome in patients with psychiatric disorders not bipolar disorder, however [12, 13]. Throughout the time of economic prosperity, Saudi Arabia's population's dietary patterns went through several alterations. According to some studies, obesity prevalence in adults spans from two-thirds to three-quarters of the population [4]. Women in this region have a higher prevalence of

TABLE 1: Mean, minimum, and maximum values for all patients ( $n = 191$ ).

Variables	Mean $\pm$ SD	Minimum	Maximum
BMI	33.63 $\pm$ 7.64	17.67	63.54
Systolic BP	129.47 $\pm$ 23.93	81	198
FBS	7.04 $\pm$ 4.22	2.60	40.30
HDL	1.14 $\pm$ 0.29	0.54	2.16
Triglyceride	1.55 $\pm$ 0.93	0.25	5.25
Cholesterol	4.58 $\pm$ 1.11	2.15	9.02
LDL	2.88 $\pm$ 1.00	0.84	6.92

obesity than men; other studies have found. Additionally, metabolic syndrome is also more prevalent in women than in men in this region [14].

The prevalence of metabolic syndrome varies from 29.6% to 36.2% in males and 36.1% to 45.9% in females. The rates are comparable to those found in other Arab countries. Also, both diabetes mellitus and hypertension are prevalent [3, 15].

Various aspects, such as a sedentary lifestyle, poor eating habits, and physical inactivity, contribute to the region's high prevalence of metabolic syndrome [16]. Furthermore, high economic status, insufficient education, and advanced aging are other factors that contribute to the region's high prevalence of metabolic syndrome [17–19]. Metabolic syndrome was found to be prevalent in 35.7% of bipolar patients in a Brazilian study [20]. This ratio, however, is comparable to that of the Brazilian general population. Metabolic syndrome is more prevalent in bipolar patients who take antipsychotic medications than in those who do not [21]. Metabolic syndrome is less common in patients who take a mood stabilizer only than in those who take an atypical antipsychotic or a polytherapy of an antipsychotic and a mood stabilizer. Patients with bipolar disorder who have metabolic syndrome have a poor prognosis, function, and insight, as well as recurrent hospitalizations, and a higher chance of developing tardive dyskinesia [22]. The region's high prevalence of metabolic syndrome in the general population can be partly responsible for the development of bipolar disorder.

Women in the region have a higher prevalence of metabolic syndrome and cardiovascular disorders, which could be a result of the region's torrid temperatures preventing people from performing outdoor activities in addition to the social norms. Nowadays, a large number of women work away from home do not have time to cook a proper healthy meal; as a result, an increasing number of families primarily rely on unhealthy junk food. Moreover, studies illustrated a genetic predisposition to diabetes in the Arabian population [23, 24].

A large number of bipolar patients live the majority of their lives depressed, denoted by anhedonia and poor energy, which may lead to a proclivity for an inactive lifestyle and metabolic syndrome. Treatment for bipolar disorder patients is not limited to psychological and pharmacological treatments, but also consists of lifestyle alterations, including, among other things, exercise, and healthy eating habits.



TABLE 2: Mean, minimum, and maximum values with a comparison between male and female patients (n Males=66) (n Females=125).

Variables	Mean $\pm$ SD (males)	Mean $\pm$ SD (females)	Minimum (males)	Maximum (males)	Minimum (females)	Maximum (females)
BMI	33.39 $\pm$ 8.15	33.76 $\pm$ 7.39	19.72	63.54	17.67	51.08
Systolic BP	131.44 $\pm$ 21.07	128.42 $\pm$ 25.34	84	193	81	198
FBS	7.74 $\pm$ 5.73	6.68 $\pm$ 3.17	2.60	40.30	4.10	21.10
HDL	0.97 $\pm$ 0.24	1.22 $\pm$ 0.28	0.54	1.69	0.67	2.16
Triglyceride	1.86 $\pm$ 1.02	1.38 $\pm$ 0.83	0.72	5.25	0.25	5.15
Cholesterol	4.64 $\pm$ 1.31	4.55 $\pm$ 0.99	2.53	9.02	2.15	7.00
LDL	2.98 $\pm$ 1.18	2.82 $\pm$ 0.89	0.84	6.92	0.90	4.88

TABLE 3: Prevalence of metabolic syndrome and its associated signs and symptoms with a comparison between male and female patients.

Variables	<i>n</i> (Males)	%	<i>n</i> (Females)	%	<i>n</i> (Total)	%
Elevated BMI	41	62.1% (Males) 21.47% (Total)	89	71.2% (Females) 46.60% (Total)	130	68.06%
Elevated SBP	35	53.03% (Males) 18.32% (Total)	54	43.2% (Females) 28.27% (Total)	89	46.59%
Elevated FBS	29	52.73% (Males) 17.79% (Total)	56	51.85% (Females) 34.36% (Total)	85	52.15%
Reduced HDL	41	67.21% (Males) 23.56% (Total)	68	60.18% (Females) 39.08% (Total)	109	62.64%
Elevated triglycerides	26	44.07% (Males) 15.83% (Total)	25	23.81% (Females) 15.24% (Total)	51	31.07%
Metabolic syndrome	29	43.9% (Males) 15.18% (Total)	50	40% (Females) 26.18% (Total)	79	41.36%

## 5. Limitations

This study had multiple limitations. To begin with, this study only included bipolar patients that were admitted to NGH, Riyadh. Additionally, the cross-sectional design limited access to the patients' data, since all the information and data needed for this study were obtained by reviewing the medical records from the electronic health record database BESTCare. Furthermore, some patients were missing some variables. Out of 191 patients, 28 patients (17 female and 11 male) were missing FBS, 17 patients (12 female and 5 male) were missing HDL, 27 patients (20 female and 7 male) were missing triglyceride, 16 patients (12 female and 4 male) were missing chole-

sterol, and 17 patients (12 female and 5 male) were missing LDL. As for blood pressure to assess hypertension, we only worked with SBP since all patients had its readings, whereas 108 patients (58 female and 40 male) were missing DBP (diastolic blood pressure) readings (56.5%).

## 6. Conclusion

Metabolic syndrome is a serious hazard to patients with bipolar disorder since it leads to a poor prognosis and poor quality of life (QOL). A thorough and careful approach is required to confront this rising issue with high urgency, in order to achieve greater control of the disorder.

## Retraction

# Retracted: Detection of WBC, RBC, and Platelets in Blood Samples Using Deep Learning

### BioMed Research International

Received 18 July 2023; Accepted 18 July 2023; Published 19 July 2023

Copyright © 2023 BioMed Research International. This is an open access article distributed under the Creative Commons Attribution License, which permits unrestricted use, distribution, and reproduction in any medium, provided the original work is properly cited.

This article has been retracted by Hindawi following an investigation undertaken by the publisher [1]. This investigation has uncovered evidence of one or more of the following indicators of systematic manipulation of the publication process:

- (1) Discrepancies in scope
- (2) Discrepancies in the description of the research reported
- (3) Discrepancies between the availability of data and the research described
- (4) Inappropriate citations
- (5) Incoherent, meaningless and/or irrelevant content included in the article
- (6) Peer-review manipulation

The presence of these indicators undermines our confidence in the integrity of the article's content and we cannot, therefore, vouch for its reliability. Please note that this notice is intended solely to alert readers that the content of this article is unreliable. We have not investigated whether authors were aware of or involved in the systematic manipulation of the publication process.

Wiley and Hindawi regrets that the usual quality checks did not identify these issues before publication and have since put additional measures in place to safeguard research integrity.

We wish to credit our own Research Integrity and Research Publishing teams and anonymous and named external researchers and research integrity experts for contributing to this investigation.

The corresponding author, as the representative of all authors, has been given the opportunity to register their agreement or disagreement to this retraction. We have kept a record of any response received.

### References

- [1] L. Alhazmi, "Detection of WBC, RBC, and Platelets in Blood Samples Using Deep Learning," *BioMed Research International*, vol. 2022, Article ID 1499546, 10 pages, 2022.

## Research Article

# Detection of WBC, RBC, and Platelets in Blood Samples Using Deep Learning

Lamia Alhazmi 

*Department of Management Information System, College of Business Administration, Taif University, P.O Box 11099, Taif 21944, Saudi Arabia*

Correspondence should be addressed to Lamia Alhazmi; lamia.s@tu.edu.sa

Received 13 June 2022; Revised 27 June 2022; Accepted 30 June 2022; Published 14 July 2022

Academic Editor: Dinesh Rokaya

Copyright © 2022 Lamia Alhazmi. This is an open access article distributed under the Creative Commons Attribution License, which permits unrestricted use, distribution, and reproduction in any medium, provided the original work is properly cited.

A blood count is one of the most important diagnostic tools in medicine and one of the most common procedures. It can reveal important changes in the body and is commonly used as the first stage in the process of evaluating patients' health. Even though this is a common practice, delivering examinations in laboratories can be difficult due to the availability of expensive technology that requires frequent maintenance. This study is developing an alternative deep learning computational model capable of automatically detecting cells in images of blood samples. Using object detection libraries, it was possible to train a model that was focused on this task and capable of detecting cells in images with adequate accuracy. When the identification of cells in images of blood samples was taken into account in the best results obtained, it was possible to count white cells with an accuracy of one hundred percent, red cells with an accuracy of 89%, and platelets with an accuracy of 96%, which generated subsidies to develop the primary components of a blood count. The components that were supposed to classify the various types of white cells were not carried out due to the limits of the dataset provided. On the other hand, the study can be broadened to include further works that deal with this issue because it produced satisfactory results.

## 1. Introduction

Health is an important pillar of society, and assisting others is becoming increasingly important. Given the challenges and conditions of the COVID-19 outbreak, it is vital to automate procedures to speed up health professionals' work and focus on emergency care. Automation has grown increasingly important in numerous industries as technology and communication have advanced. Because of the epidemic, laboratory testing has increased, necessitating more health experts' attendance, analysis, and reporting [1, 2]. There is an overflow of functions because not every location has adequate workers to manage this. This research tries to detect blood images to aid in the creation of blood counts, creating a tool for health-care providers. Blood counts are performed using pricey, specialized equipment. To automate this procedure, deep learning algorithms can replace specialized equipment.

Deep learning (DL) algorithms are employed in various fields, including medical, economics, education,

e-commerce, and virtual games. DL is emerging as a viable alternative to traditional job execution and automation methods [3, 4]. Deep learning is being used in some health-related projects to improve decision-making. Deep learning makes use of enormous amounts of data. This data must be collected and preprocessed for deep learning to be effective. The deep learning model is trained and tested with other data to produce results, then postprocessed for better visualization, and delivered to the health professional.

This article analyzes blood test photos to detect and count cells automatically. Because the method is manual, these samples are checked and analyzed using glass slides and a microscope to establish blood counts. Larger labs also employ costly counting machines. This research utilizes a huge collection of images of blood samples to recognize and to count the many types of cells in the sample, assisting clinicians in preparing blood counts. Given the variety of deep learning algorithms and their uses, how could a

computational model for detecting and counting cells in blood sample photos assist laboratory and health-care professionals?

## 2. Theoretical Approach

*2.1. Artificial Intelligence: Machine Learning and Deep Learning.* The deep learning technique, which is the focus of this study, is one of the subfields of machine learning, which is itself a subfield of AI. As a result, the concept of artificial intelligence must be taught before digging into each of these concepts, their differences, and applications. Artificial intelligence is a means of solving issues of many types in an automated manner, that is, without the assistance of a human or a specific user. People are seeking novel ways to automate routine tasks; therefore, this sector is garnering a lot of attention these days [5, 6]. This method is used in a variety of businesses and is now being applied in homes for a variety of reasons. This research aims to figure out how to teach machines and computers to have intelligence that is becoming more human-like. This is usually performed using pattern recognition, which allows computers to be trained to analyze and understand data in a way that is comparable to how people learn. On the other hand, machines usually need a lot of data to understand something simple.

*2.1.1. Machine Learning.* Problem resolution using computational tools and methods designed for specific goals is common, but not in all circumstances because a single line of steps is not always known. To be resolved, a machine learning model can forecast when the data input and the desired result are known, but not the means to get there. We know the parameters and method for obtaining the result in traditional programming methods, but with machine learning, the machine learns and presents the approach (ETHEM, 2016) [7]. Every machine learning model goes through data preparation, training, and testing. Preprocessing is the examination and modification of data in order to improve model comprehension by removing extraneous information and changing the format (RASCHKA, 2015). Before forecasting any value or outcome, the machine learning model must be trained using the specified approach. The person in charge of training must provide a substantial amount of data and the expected results in each, as well as the training parameters and settings. As a result, the model learns to understand and interpret data, and it can predict future data outcomes (RASCHKA, 2015).

The testing follows the model training. The accuracy, precision, and recall of the model are measured in this step. The accuracy of the model reveals how many classes it correctly classified. Precision indicates how many correct positive classifications there are. The recall metric indicates how many positive expected value classifications are correct. The F1-score is a summing of precision and recall (NICK, 2018).

A confusion matrix describes the number of hits and errors associated with true or false positives and true or false negatives for easy display and calculation.

*(1) Traditional Algorithms.* There are two types of machine learning techniques: supervised and unsupervised. In supervised learning, the correct result or where the model should originate from the data is known; however, in unsupervised learning, the model must deal with unstructured input and no obvious outcome (RASCHKA, 2015) [8].

Both regression and classification are supervised learning techniques. Regression methods forecast actual values, whereas classification models categorize data (RASCHKA, 2015).

Methodologies for data regression may be listed (NICK, 2018).

- (i) Linear regression is a simple and traditional method for predicting regression involving drawing a line through the data. Multiple linear regression employs additional variables, whereas polynomial linear regression employs variables with exponentiation to produce a more aggressive outcome
- (ii) Decision tree: This strategy uses model-learned criteria to forecast values. To find patterns in the known data, divide it into related groups

Random forest combines the processing capacity of numerous decision trees to get a more thorough and accurate result.

A list of data classification algorithms is available (RASCHKA, 2015).

- (i) K-nearest neighbors (KNN): This algorithm classifies data by comparing it to similar data. It is lazy since it does not present an intelligent model; it just saves and compares facts
- (ii) Decision tree classifier: Decision trees, like regression, predict classes for specific data based on learned criteria. These criteria will be taught by grouping known data into similar groups in order to find patterns, which in this case, are the necessary classes for interpretation
- (iii) Random forest classifier: Random forest, like regression, combines the processing capabilities of many categorizations decision trees to produce more accurate output

A nontraditional approach, neural networks, can be used for regression and classification. This project will investigate an alternative to standard algorithms.

*(2) Neural Networks.* Neural networks use perceptrons, a computerized representation of a neuron, to mimic the human brain. The perceptron can receive inputs (data) and output. Using numerous perceptrons in a network improves their performance by combining their processing power and achieving a faster, more accurate output. An artificial neural network (ANN) is this structure. Figure 1 shows the structure of a perceptron, where  $x$  is the input,  $w$  is the weights,  $\Sigma$  is the sum,  $f$  is the activation function, and  $y$  is the output [9]. An artificial neural network (ANN) is a structure built using perceptrons to mimic human brain processing. Its

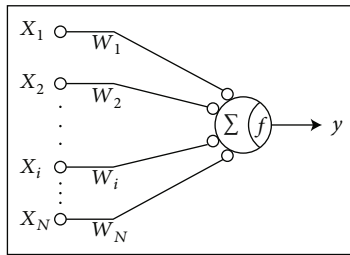


FIGURE 1: Perceptron.

structure is defined at several levels, with an input layer, an output layer, and hidden intermediary layers responsible for overall processing, each with a programmable number of perceptrons. Figure 2 depicts this structure, which includes input, hidden, and output layers. The selected weights are as important as the information transmitted from perceptron to perceptron. Weights are defined values for each piece of information received by the perceptron and are changed to produce the desired output. An ANN can learn to do a variety of tasks, such as classification, by employing a backpropagation strategy that adjusts the model's learning rate in phases.

First, the algorithm uses random weights to train the artificial neural network. During training, the algorithm predicts outcomes that are then compared to the correct numbers to determine success. The backpropagation algorithm calculates the difference between the result and the true result and feeds this error information to all preceding layers in order to alter weights and reduce error [10]. This process is done several times during training until the changes induce an increase in inaccuracy, indicating that the weights have reached their maximum. This stage of modifying the weights of the network is critical because it helps the model learn from its failures.

**2.2. Deep Learning.** In some cases, machine learning is insufficient for data learning because learning occurs through pattern recognition based on data that cannot be used in any case, must be prepared and adapted for each model, or the machine cannot learn on its own because it always requires human intervention to process the data. Deep learning is required to emulate human reasoning. Deep learning uses deep neural networks to enhance neural networks (DNNs). Deep neural networks (DNNs) are deep learning neural network architecture with more neurons, hidden layers in more intricate topologies, and specific neuron connections [11]. Deep neural networks created intriguing versions that focused on a certain specialism, emulating human nature in order to accomplish tasks and produce intelligence. Some of these types are related to natural language processing, such as RNNs, or image recognition and interpretation, such as CNNs.

**2.2.1. Recurrent Neural Networks (RNNs).** Recurrent neural networks are a type of neural network designed to evaluate temporal input sequentially. They can forecast variables in

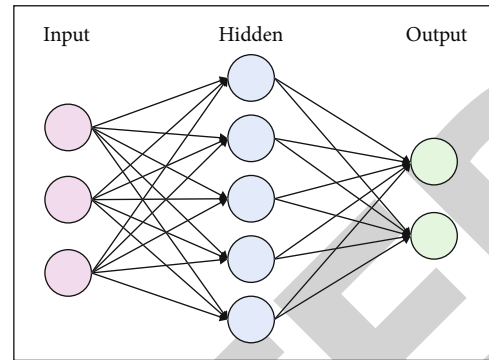


FIGURE 2: Artificial neural network.

relation to time. Its topology facilitates feedback connections of passed-on information; loops allow the information to remain as if the network were repeated. RNNs make use of information in a predefined sequence, such as updated data.

**2.2.2. Convolutional Neural Networks (CNNs).** Convolutional neural networks are a type of neural network architecture created for image recognition that can break down images and analyze them. This network represents height, width, and color as three-dimensional matrices.

Traditional DNNs work well for small images, but with a large amount of data, each pixel in the image, the model would struggle to learn; hence, CNNs were developed. CNNs were constructed with partially connected layers and significant weight reuse to address this issue, resulting in fewer parameters to understand and pass on faster training and less training data required [12–14]. This efficiency is also due to the fact that, unlike DNNs, when a CNN learns to interpret an image feature, it can identify that feature wherever in the image. DNNs are more specialized than CNNs. Figure 3 depicts the convolutional layer at the start of the procedure.

**2.2.3. Libraries and Resources.** Some market-available free libraries assist with deep learning's essential architectures and resources. Tensorflow and Keras are Python and C++ libraries that can communicate with one another and are widely used in the deep learning field (GIANCARLO; REZAUL, 2018).

Tensorflow is a machine learning platform that is open source and focuses on neural networks and deep learning. Keras is the foundation for Tensorflow's neural network APIs. In 2018, Google's Keras library was included in Tensorflow (2021, TENSORFLOW).

Keras focuses on deep neural networks for rapid prototyping and testing. It is straightforward, modular, and extendable. It has layers, loss functions, activation functions, and other features. It also has convolutional and recurrent neural network modules (KERAS, 2021).

The combination of two machine learning and deep learning libraries creates an extremely beneficial tool for this objective, allowing users to work with numbers, text, audio, and image data [15, 16].



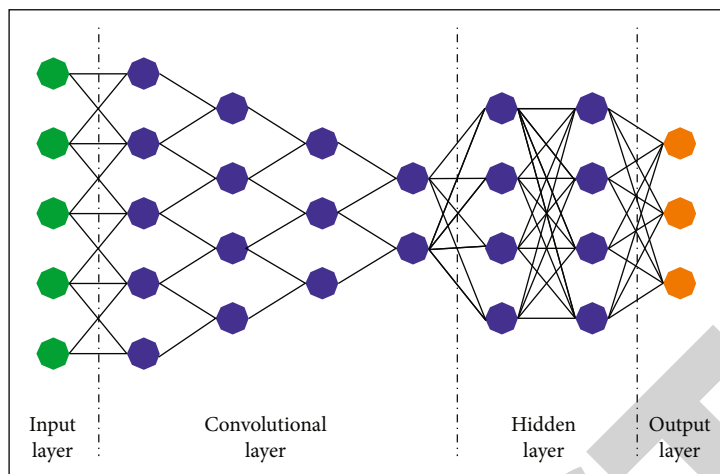


FIGURE 3: Convolutional neural network.

Tensorflow documentation can help you learn how to build a convolutional neural network, providing theory and a practical example. The documentation for this package enables image classification based on a dataset (TENSORFLOW, 2021).

You can also work with different library modules in Tensorflow; object detection was utilized here. This module is responsible for detecting picture objects. Instead of detecting everyday objects, the model is trained to recognize and to differentiate between cells in a picture.

Object detection facilitates image processing and computational model processing while also providing useful training tools. Tensorflow's object detection module was used throughout the model training phase.

### 3. Material and Methods

**3.1. Dataset.** Choosing the dataset for AI work is critical because it influences all subsequent methods. During the search, the best contender for the dataset was the BCCD Dataset (SHENGGAN, 2019).

This dataset was chosen since it is cited in numerous papers. This is the most comprehensive and in-depth dataset for this research area according to the literature. Another important factor was the availability of high-quality pictures for visual interpretation and training deep learning models. WBC (white blood cell), RBC (red blood cell), and platelets are included in the dataset. All of the photos are in one folder, and the XML coordinates for each cell are in another. The investigation into its resources and limits began with the dataset in hand. One of the dataset's limitations is that not all picture cells have mapped coordinates. The dataset contains cells with no coordinates, which can make model training difficult [14].

White cell classification is missing from this dataset. In photos, the dataset distinguishes white, red, and platelet cells. This is insufficient for a complete blood count. In order to provide a more accurate patient diagnosis, white blood cells must be classified (neutrophils, basophils, eosinophils, lymphocytes, and monocytes). White cell classification could be future research.

After getting the dataset, images were modified for model detection. The repository includes images as well as Python data processing programs to demonstrate the dataset's utility. A program outlines cells for a data preview. Because this effort contains deep learning, the data processing will adhere to its specifications. All Python files in the dataset were eliminated, leaving only the images directory and the XML files directory with image coordinates.

**3.2. Object Detection.** The computational model's resources were trained and configured using Tensorflow. Tensorflow contains a large number of functions and utilities for machine learning and deep learning, so selecting the proper ones is critical. Object detection is one of the most exciting components for this job (TENSORFLOW, 2021).

Tensorflow's object detection module locates previously learned picture portions. It recognizes people and things in photographs. It can also be used to recognize people, vehicles, animals, and other common components in security cameras in films, frame by frame. This project develops a computer vision system that can detect cells in a photograph, count them, and generate a histogram [17]. This is where the object detection module comes in. This module is typically used to detect people and things, but it can be customized to learn about blood contents. When the model is trained on a large number of blood images, it may learn from the data and make predictions.

Understanding the library's resources and limitations required extensive documentation. The object identification module had less documentation, but it was useful for a variety of project issues, particularly base codes. The first codes were written using the test cases from the documentation, which provided a solid introduction of the computational model's numerous setups and general behavior.

An environment must be established in order to optimize code execution. The algorithm must be configured to run on the GPU rather than the CPU, which is the default. GPUs provide superior image processing results in less time, especially in large quantities.

The environment was prepared by installing CUDA. The NVIDIA CUDA platform uses parallel computing to optimize graphics card processing and speeds up applications. Use cuDNN in addition to CUDA. cuDNN is a deep neural network library that enables the use of neural network design with machine learning methods, making it appropriate for this job. CUDA improves the efficiency and quality of cuDNN (CUDA, 2021; CUDNN, 2021).

The algorithm can be executed once the environment is ready. At this stage, the documentation's basic examples were run to see how the algorithm behaved on the system, the sample processing outputs, and how long they would take. This step was critical for the project's continuation because it allowed for better planning of the next stages.

**3.3. Computational Model.** The dataset was placed into the model's training and image recognition templates after the resources, libraries, and environment were in place. The photographs were large enough for the algorithm and had the same size and magnification scale. Import and translate XML files into model-readable variables before recognizing image coordinates. The data in the files and the data accepted by the model were of varying scales and proportions. The algorithm was unable to locate the picture cells during import. A function to translate XML coordinates into model scale numbers was required to adopt this method, allowing coordinates and images to be loaded [18].

Thus, a key test for one cell type initially produced satisfactory results with low success rates without modifying the model features. To maximize model notions, the following qualities had to be changed:

- (i) Batch size: The size of the training batch. Larger batches enhance learning but necessitate more machine processing
- (ii) Learning rate: The learning rate of the model. Larger groups learn more quickly. If it becomes too large, the model begins to recognize bogus cells. The model cannot find cells if it is too small
- (iii) Batches: The number of algorithms passes (also known as epochs). The training interval of the algorithm is defined here
- (iv) Hit percentage: A hit occurs when the algorithm is more than 50% certain about a cell

To configure these parameters, each code execution was tested and tweaked. This was repeated until the best values were discovered.

This job necessitates the selection of a pretrained neural network in addition to establishing these settings. Training new models is sped up by leveraging a pretrained network. If it were properly trained with simple information like outlines and common features, the results with more intricate aspects would be better.

This experiment uses the "resnet50" network, but the object identification module accepts a variety of others. This decision was influenced by image size and network speed tests (HE et al., 2015).

"resnet50" aids in the training phase of the model because just the last layers must be learned. Because the model's early layers were already trained with generalities, only the last levels require specific data. After teaching one type of cell, train the others with blood sample photos. First, all cells were trained simultaneously, which took too long and yielded poor results.

This necessitated a different approach. Instead of training all cells at once, a model for white cells, red cells, and platelets was created. This made training more efficient and specific to each type.

Because three models are used, inputting an image for verification in predicting results will result in three separate responses, one for each cell type. This technique allowed for different parameter values for each class, enhancing results. Because this project aims to count individual cells, splitting the models for each cell has no effect on the final result.

**3.4. Evaluation.** Metrics were used to assess the computational model's performance and the output of each trained model. To compare choices, each model option used various metrics and parameters. As a result, it was feasible to determine the best algorithm for the prototype and the best settings to maximize its performance. The first evaluation metric was test accuracy. They were also measured using MSE and rMSE (mean squared error). rMSE (root mean squared error) is an MSE variant that employs the square root. First, the standard accuracy was determined by comparing the number of real cells expected to be discovered by the model to the number discovered. Based on these values, the ultimate accuracy percentage was computed. The MSE formula is shown below. Finally, the mean square error is calculated by averaging all the data.

$$\text{MSE} = \frac{1}{n} \sum_{i=1}^n \left( \underbrace{y_i}_{\text{Predicted Value}} - \underbrace{\hat{y}_i}_{\text{Actual Value}} \right)^2 \quad (1)$$

The ideal value of this number is close to 0, as the higher the number, the greater the model error. As a result is always squared, predictions far from the real are easily noticeable, making this metric interesting for problems where large errors are not tolerated. The rMSE was calculated based on the formula presented below. As the MSE was already calculated, it was possible to calculate the resulting square root to find the final rMSE.

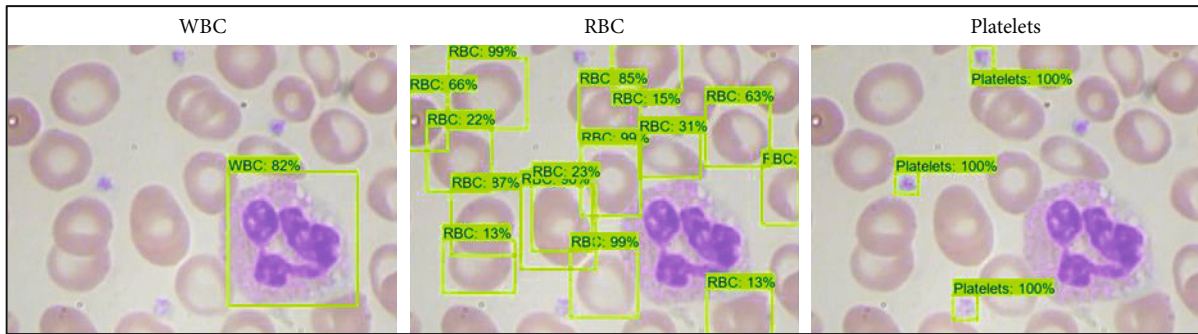


FIGURE 4: Interface of the prototype developed.

$$rMSE = \sqrt{\frac{1}{n} \sum_{i=1}^n \left( \underbrace{y_i}_{\text{Predicted Value}} - \underbrace{\hat{y}_i}_{\text{Actual Value}} \right)^2} \quad (2)$$

This metric is a complement to the normal MSE, because, through this metric, it is possible to measure the final result without changing the scale of the error, facilitating some comparisons. For a while the MSE is squared, the rMSE does not have this problem, as the square root is extracted in the final process.

**3.5. Prototype.** Following the definition of the best viable instance of the computational model, it was exported and used to create a working prototype. The Tensorflow library documentation was examined to understand checkpoints before exporting the model. Checkpoints in Tensorflow save the state of a trained model for later use. As a result, a ready-made model can be employed without retraining for picture predictions only. To use the model elsewhere, simply import a file. The AI algorithm prototype was created using Streamlit. The Streamlit framework in Python makes prototyping simple and quick. A web app with few commands allows you to concentrate on development. As a result, the graphical user interface is unimportant. It is simple to customize, displaying all of the algorithm's capabilities on the screen and allowing the user to give input data and see the algorithm's output (output). This enables user engagement in real time. Figure 4 depicts the interface of the prototype.

The user can send a link to an Internet image in the format of the dataset where the model was trained, as seen in the prototype. The recognition of white, red, and platelet cells in a blood sample using the trained model is illustrated in Figure 4. Additionally, aggression percentages for each cell detection can be calculated.

## 4. Results and Discussion

**4.1. Model Performance Analysis.** The dataset used as a basis for this work has 364 different images of blood samples. Each image can contain up to 30 cells of different classes

located in different image portions. The classes used in this research are red cells (RBC), white cells (WBC), and also platelets (platelets), which are identified through coordinates that indicate the location of each cell in the image and are stored in XML files that accompany the dataset in question.

This dataset was separated into two main groups. The first group refers to the set of images aimed only at training, with 80% of the total images; this group contains 291 randomly selected images, while the second group aimed only at testing, with 20% of the total images, which contains 73 separate images for this purpose. As the training group needs to be larger to have good training of the model and finally to test the remaining images, the selection of 80/20 of the separation of the files was adopted. The model was configured following a few key principles and configurations. First, the pretrained neural network with the best result and performance for this image group was selected, "resnet50", recognized in the code base by "ssd\_resnet50\_v1\_fpn\_640x640\_coco17\_tpu-8." In addition to this choice, four fundamental parameters were carefully selected, seeking the best performance in the shortest time. The definition of batch size, learning rate, number of batches, and the percentage of base hit can be seen in Figure 5.

After model training, predictions were measured using 3 different metrics. The first was standard accuracy, which allows for an overview of the progress of the process. Carrying out the standard accuracy measurement, considering the number of real cells and the number of cells that should be found by the model, the following relationship was arrived at, using the best possible result as a parameter:

- (i) WBC: 74 cells found from 74 real cells (100.00% hit and 0.00% fail)
- (ii) RBC: 1,007 cells found from 908 real cells (89.10% hit and 10.90% fail)
- (iii) Platelets: 57 cells found from 59 real cells (96.61% hit and 3.39% fail)

The MSE and the rMSE are complementary metrics that are easy to use and refer to the performance of the computational model. While the MSE works by calculating the mean square error, the rMSE is the root of this value found. Such metrics are interesting because they allow you to visualize considerably, even small errors. This scale does not have a

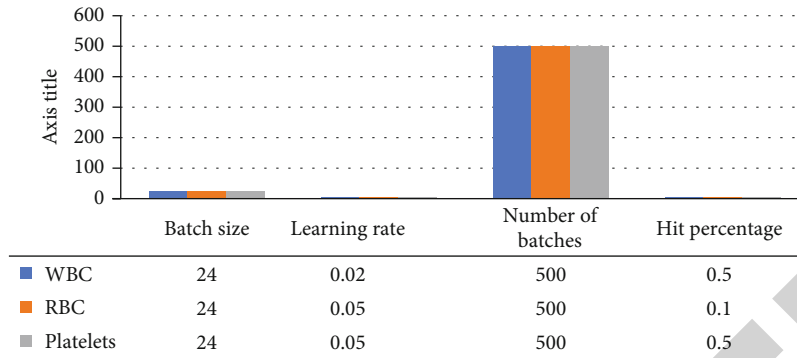


FIGURE 5: Defined parameters.

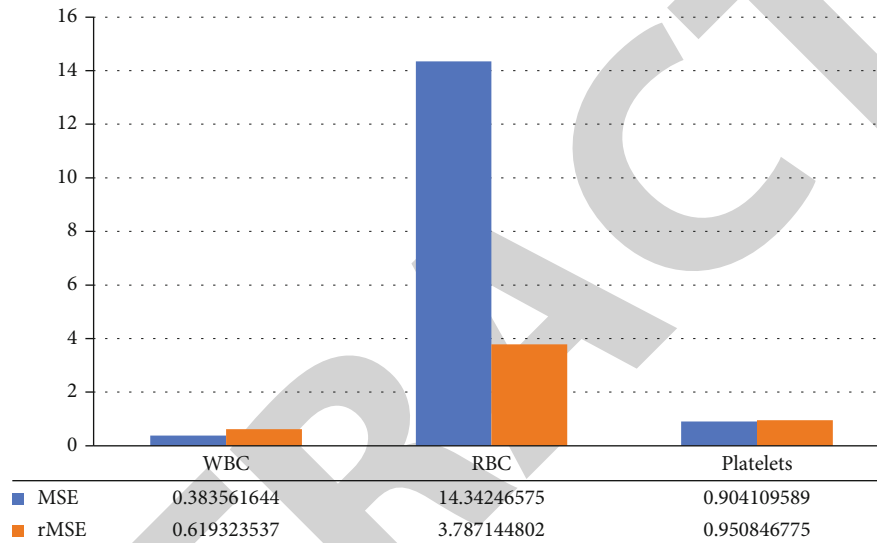


FIGURE 6: MSE and rMSE

maximum or ideal number, but the result should approach zero; the closer, the better. Thus, using the formulas from the previous sections, it was possible to arrive at the relationship in Figure 6. Through the relationship in Figure 6, it was possible to perceive that the best performance is in the detection of white cells, which is in line with the definitions found by the accuracy seen above. This may have happened because, in the dataset, in most of the images, there is at least one white cell that is easily detected about the others. Following this, platelets also show good results, similar to the model’s accuracy relationship. Finally, the red cells present inferior results about the others. This may have happened because of their abundance in all images, while the other classes have one or two cells per image, the red cells may appear in a number greater than 20, which makes it difficult to learn the model and hinders the prediction in this case.

**4.2. Identification of White Cells (WBC).** The first class of cells worked from the first test using the dataset were white cells. This was due to its easy identification about the others, being a great candidate to start the tests and later the first versions of the prototype.

These cells are present in the images in low quantity, as the dataset sought to focus on a white cell in each image. Although it is possible to find even two or three in some cases, in addition to the quantity, they can be distinguished from the others through their coloring.

In Figure 7(a), the model’s detection of the white cell can be observed where it was possible to differentiate and delimit the cell satisfactorily. In Figure 7(b), the same process can also be observed, but in a different situation.

It could be seen that the model had a good hit rate, taking into account both performance metrics and visual analysis of the images. In this way, it is possible to perform cell counts with a good assertiveness index.

**4.3. Identification of Red Cells (RBC).** After the detection of white cells, the next step was the interpretation of red cells. These differ in their detection in relation to the others due to their quantity. Red cells appear in a greater proportion, with more than 20 cells per image.

A large amount of these types of cells is a challenge for the model, mainly due to the delimitation of their areas. As they do not have a defined shape and often overlap, this hinders their identification.



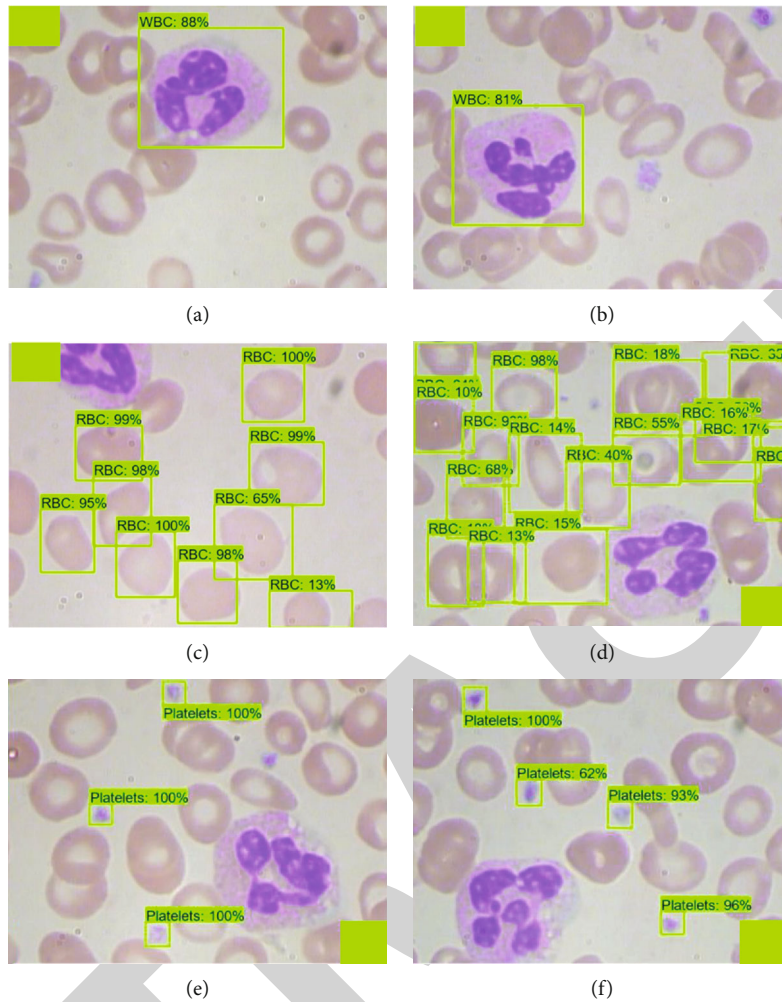


FIGURE 7: Cell detection: WBC (a and b), RBC (c and d), and platelets (e and f).

In Figure 7(c), we can visualize the detection process of red cells. It is possible to count the cells as necessary, with a small margin of error.

However, in Figure 7(d), it is also possible to visualize the identification by the model. However, even with the overlapping of cells at a higher density, the model still managed to identify most of the cells correctly.

It is possible to conclude that although it does not have as positive performance as the other classes, the results are also good as they allow a red cell count with a small margin of error.

**4.4. Identification of Platelets (Platelets).** Finally, platelet detection was performed in a similar way to white cells. Despite being more present in the dataset than the white cells, they are not as high in number as the red cells, presenting small sets by images. Another characteristic factor about the others is its size, which is much smaller and easy to identify with the naked eye.

Although they are easily identified, overlapping cells can also happen in this case, hindering the performance of identification by the model. But this happens in a significantly smaller number compared to red blood cells.

It is possible to visualize in Figure 7(e) the process of identification of platelets, where the model presents a performance considered great.

Figure 7(f) shows a slightly different situation. In this analysis, the model was able to identify the 4 platelets that appear in the image correctly, but with a slightly reduced assertiveness margin of the algorithm.

With this, we can conclude that platelets have adequate performance in their identification, allowing a satisfactory count. Although not as positive as in the detection of white cells, it still outperforms red cells in terms of performance and assertiveness criteria.

**4.5. Elaboration of Hemogram Elements.** It is feasible to generate elements of the hemogram based on the identification and counting of cells, as seen above. A blood count is essentially a count of cells followed by comparing the results to precalculated indices of optimal values for each patient type.

After identifying the cells, the initial values of the blood count can be calculated by counting each kind. The units of measurement are critical in this process since they differ for each type of cell. The cubic millimeter (mm<sup>3</sup>), a unit of volume, serves as the foundation for the calculation. The



count is performed in proportion to one cubic millimeter to compute the leukocytes, which are white cells, and the platelets. However, because erythrocytes, or red blood cells, are in higher abundance than other cells, the computation of millions of cells in a cubic millimeter is conducted.

The erythrogram can be created by multiplying the erythrocytes by millions/mmS. The number of leukocytes found in unit/mmS can be used to create the leukogram. Finally, a platelet count based on the number of platelets recognized in units/mmS can be calculated.

This data is required to diagnose various disorders and abnormalities in the patient's body. For example, the leukogram is the primary test used to assess a person's immunity by measuring the number of leukocytes present in the body. Platelet count also reveals a lot about the body, measuring the individual's blood clotting and bleeding proclivities. In addition to the low amount of red blood cells, it could suggest anemia or another condition, among many other possibilities.

We may conclude that with this data, we can create significant aspects of the hemogram that, when applied to a sample with volume values, will be useful and fascinating to use. When the values provide different outcomes, an in-depth study with particular testing for each circumstance is required.

The restrictions for generating a total blood count are connected to the dataset's limitations. To begin, to perform a complete blood count, it would be necessary to have the ability to count and classify white cells. Its classification into monocytes, leukocytes, neutrophils, eosinophils, basophils, and lymphocytes, among others, is required for the exam to be complete. The dataset, however, does not give these classifications, instead of focusing on the contrasts between the three primary groups. Other volume-related numbers, such as MCV (mean corpuscular volume) and HCM (mean corpuscular hemoglobin), cannot be calculated due to a lack of data. This information can be derived from the data collection when using another dataset in future tasks.

## 5. Conclusions

This project attempted to use deep learning to assist health professionals by automating tasks so that they may focus on others. The blood count is one of the most important routine tests for detecting most illnesses. The best techniques to automate this activity were investigated in subsequent investigations. Deep learning algorithms were used to understand the blood count production process. All cells can be precisely enumerated by developing an intelligent computer model to recognize blood cells. This developed method enables decisions about a patient's health to be made. We can discover any imbalance in their levels by counting white, red, and platelets. More tests can be performed to validate these challenges if there is an aberrant component. Because of limitations in the dataset used and the general classification of white cells are not a comprehensive blood count, you can use these principles in future studies to collect new, more complex data or achieve another purpose. Another possibility is to use evaluation measures

based on this technique, such as forecasts and true values. Based on this finding, the method utilized in this study can estimate the count in proportion to the volume and reproduce all of the information in a blood count.

## Data Availability

The data used to support the findings of this study are included within the article.

## Conflicts of Interest

The authors declare that they have no conflicts of interest.

## References

- [1] K. Talukdar, K. Bora, L. B. Mahanta, and A. K. Das, "A comparative assessment of deep object detection models for blood smear analysis," *Tissue and Cell*, vol. 76, article 101761, 2022.
- [2] J. Pfeil, A. Nechyporenko, M. Frohme, F. T. Hufert, and K. Schulze, "Examination of blood samples using deep learning and mobile microscopy," *BMC Bioinformatics*, vol. 23, no. 1, article 65, 2022.
- [3] M. B. Alazzam, H. Al Khatib, W. T. Mohammad, and F. Alassery, "E-health system characteristics, medical performance, and healthcare quality at Jordan's health centers," *Journal of Healthcare Engineering*, vol. 2021, 7 pages, 2021.
- [4] R. C. Joshi, S. Yadav, M. K. Dutta, and C. M. Travieso-Gonzalez, "An efficient convolutional neural network to detect and count blood cells," *Uniciencia*, vol. 36, no. 1, pp. 1–11, 2022.
- [5] M. B. Alazzam, N. Tayyib, S. Z. Alshawwa, and M. Ahmed, "Nursing care systematization with case-based reasoning and artificial intelligence," vol. 2022, 9 pages, 2022.
- [6] Y. Qin, Y. Wang, F. Meng et al., "Identification of biomarkers by machine learning classifiers to assist diagnose rheumatoid arthritis-associated interstitial lung disease," *Arthritis Research & Therapy*, vol. 24, no. 1, article 115, 2022.
- [7] N. Jain, S. Shah, R. S. Mangrulkar, and P. Sonawane, "Application of deep learning in counting WBCs, RBCs, and blood platelets using faster region-based convolutional neural network," in *Design of Intelligent Applications Using Machine Learning and Deep Learning Techniques*, pp. 77–98, Chapman and Hall/CRC, 2021.
- [8] K. T. Navya, K. Prasad, and B. M. K. Singh, "Classification of blood cells into white blood cells and red blood cells from blood smear images using machine learning techniques," in *2021 2nd Global Conference for Advancement in Technology (GCAT)*, pp. 1–4, Bangalore, India, 2021.
- [9] M. B. Alazzam, W. T. Mohammad, M. B. Younis et al., "Studying the effects of cold plasma phosphorus using physiological and digital image processing techniques," *Computational and Mathematical Methods in Medicine*, vol. 2022, 5 pages, 2022.
- [10] G. Drafus, D. Mazur, and A. Czmil, "Automatic detection and counting of blood cells in smear images using RetinaNet," *Entropy*, vol. 23, no. 11, p. 1522, 2021.
- [11] L. Rayappan and R. J. Karthik, "Deep learning approach to the normal and abnormal blood cells in human blood smear," *Annals of the Romanian Society for Cell Biology*, vol. 12, pp. 3187–3196, 2021.
- [12] N. Indrani and C. S. Rao, "White blood cell image classification using deep learning," vol. 7, no. 9, pp. 7–12, 2021.

## Retraction

# Retracted: A Comparison of Decision Tree Algorithms in the Assessment of Biomedical Data

### BioMed Research International

Received 20 June 2023; Accepted 20 June 2023; Published 21 June 2023

Copyright © 2023 BioMed Research International. This is an open access article distributed under the Creative Commons Attribution License, which permits unrestricted use, distribution, and reproduction in any medium, provided the original work is properly cited.

This article has been retracted by Hindawi following an investigation undertaken by the publisher [1]. This investigation has uncovered evidence of one or more of the following indicators of systematic manipulation of the publication process:

- (1) Discrepancies in scope
- (2) Discrepancies in the description of the research reported
- (3) Discrepancies between the availability of data and the research described
- (4) Inappropriate citations
- (5) Incoherent, meaningless and/or irrelevant content included in the article
- (6) Peer-review manipulation

The presence of these indicators undermines our confidence in the integrity of the article's content and we cannot, therefore, vouch for its reliability. Please note that this notice is intended solely to alert readers that the content of this article is unreliable. We have not investigated whether authors were aware of or involved in the systematic manipulation of the publication process.

Wiley and Hindawi regrets that the usual quality checks did not identify these issues before publication and have since put additional measures in place to safeguard research integrity.

We wish to credit our own Research Integrity and Research Publishing teams and anonymous and named external researchers and research integrity experts for contributing to this investigation.





The corresponding author, as the representative of all authors, has been given the opportunity to register their agreement or disagreement to this retraction. We have kept a record of any response received.

### References

- [1] F. Hajje, M. A. Alohal, M. Badr, and M. A. Rahman, "A Comparison of Decision Tree Algorithms in the Assessment of Biomedical Data," *BioMed Research International*, vol. 2022, Article ID 9449497, 9 pages, 2022.

## Research Article

# A Comparison of Decision Tree Algorithms in the Assessment of Biomedical Data

Fahima Hajje <sup>1</sup>, Manal Abdullah Alohal <sup>1</sup>, Malek Badr <sup>2,3</sup> and Md Adnan Rahman <sup>4</sup>

<sup>1</sup>Department of Information Systems, College of Computer and Information Sciences, Princess Nourah bint Abdulrahman University, P.O. Box 84428, Riyadh 11671, Saudi Arabia

<sup>2</sup>Department of Medical Instruments Engineering Techniques, Al-Farahidi University, Baghdad 10021, Iraq

<sup>3</sup>Research Center, The University of Mashreq, Baghdad, Iraq

<sup>4</sup>Green Business School, Green University of Bangladesh, Bangladesh

Correspondence should be addressed to Md Adnan Rahman; [adnanrahman007@yahoo.com](mailto:adnanrahman007@yahoo.com)

Received 25 May 2022; Revised 7 June 2022; Accepted 14 June 2022; Published 7 July 2022

Academic Editor: Dinesh Rokaya

Copyright © 2022 Fahima Hajje et al. This is an open access article distributed under the Creative Commons Attribution License, which permits unrestricted use, distribution, and reproduction in any medium, provided the original work is properly cited.

By comparing the performance of various tree algorithms, we can determine which one is most useful for analyzing biomedical data. In artificial intelligence, decision trees are a classification model known for their visual aid in making decisions. WEKA software will evaluate biological data from real patients to see how well the decision tree classification algorithm performs. Another goal of this comparison is to assess whether or not decision trees can serve as an effective tool for medical diagnosis in general. In doing so, we will be able to see which algorithms are the most efficient and appropriate to use when delving into this data and arrive at an informed decision.

## 1. Introduction

Over time, many methods for data analysis have been developed, which are mainly based on statistical techniques. However, as the information stored grows considerably, traditional statistical methods have begun to face efficiency and scalability problems. Because most of this information is historical and comes from various sources, it seems clear that there is an imminent need to seek alternative methods for the analysis of this type of data and, from them, to obtain relevant and nonexplicit information. The analysis and interpretation of the data in most cases are made manually; that is, the specialists analyze and prepare a report or a hypothesis about the said data to later reach a conclusion and from this make important decisions and significant. These processes are often very slow and expensive. When the volume of data is excessively large, it exceeds human capacity; then, it becomes very difficult to analyze it without the help of the appropriate tools. Also, with the help of these tools, we can reach an accurate diagnosis [1].

In the case of medicine, it is possible to apply alternative methods due to the large number of conditions involved, the

symptoms, and the patients. Ideally, doctors could count on the support of a tool that allows them to analyze the symptomatological data of each of their patients to determine, based on previous cases, the most accurate diagnosis, as well as the optimal treatment to follow, which would represent support and help for the doctor. An alternative tool for the prediction and classification of large amounts of data widely used in artificial intelligence is decision trees.

## 2. Theoretical Framework Decision Trees

Various fields employ decision trees as a prediction model. Its primary goal is inductive learning based on observation and logical reasoning. Prediction systems that use rules to express and categorize a sequence of events that occur sequentially are very much like this [1].

A tree is used to symbolize the inductive learning process's information. Trees can be depicted by nodes, leaves, and branches in a visual representation. Classification begins with a root node representing the attribute from which all other attributes are subtracted. There are questions regarding the property or problem in the internal nodes or their

children [1]. One of the problem's class variables is represented by the nodes at the end of the graph, known as leaf nodes. There are two stages in the creation process of a decision tree: induction of the tree and categorization. Initial nodes are constructed from training sets, and each node has a test attribute and a part of training data divided according to the possible values of that test attribute.

Decision trees are in the class of supervised machine learning. Decision trees are frequently used because they are easy to implement, can be interpreted easily, are applied to qualitative, quantitative, continuous, and discrete variables, and give reliable results [2]. Decision trees start from a single root. It is a classification tree that progresses towards decision nodes and terminates in labeled leaves. The structure of a simple decision tree is shown in Figure 1. As shown in Figure 1, decision trees consist of roots, branches, and leaves.

After deciding on a test attribute, the training set is divided into two or more subsets; for each subset, a new node is formed and so on. Objects of more than one class in a node generate an internal node; if the node includes only one class, the class label is assigned to a sheet.

When a new object is created and classed, the tree is traversed from its root node to its leaf node, and from there, the object's membership in a certain class is determined. According to the test attribute present in it, the judgments taken at each internal node determine the tree's path. There are many algorithms to generate decision trees, and some that can be found in the WEKA software are the following:

The CART tree is a regression method used to predict values of continuous variables, but when the assumptions to apply this model are not met, its conclusions can be wrong. CART regression trees are a very easy method of interpreting results. The CARTs use historical data, which are used to build regression trees that allow the classification and prediction of new data; these have the advantage that they can easily manipulate numerical variables; their main characteristics are their robustness to outliers or atypical values. [1, 3]. The REETTree decision tree learning method is very easy and very fast to use. This tree is built using the variance information and is pruned using the error reduction criteria. This decision tree classifies only numerical attributes once; the remaining values are obtained from future instances, dividing these instances into information segments [3].

The RandomTree is a randomly drawn tree from a series of possible trees. In this context and other sources of information, we will take "random" to mean that each tree study tree has an equal chance of being tested. Another way of saying this would be that the distribution of trees is uniform. The RandomTree process is a process that produces a random tree of arbitrary permutations [4].

Singh [1] invented C4.5, an algorithm for creating a decision tree. A new version of Quinlan's ID3 algorithm, known as C4.5, has been developed. We will utilize an open-source Java implementation of the C4.5 algorithm, which is the J48 in the WEKA tool, to produce decision trees that may be used for classification.

The J48 algorithm, widely used in data mining, is a decision tree classifier. The J48 classifier is also known as the

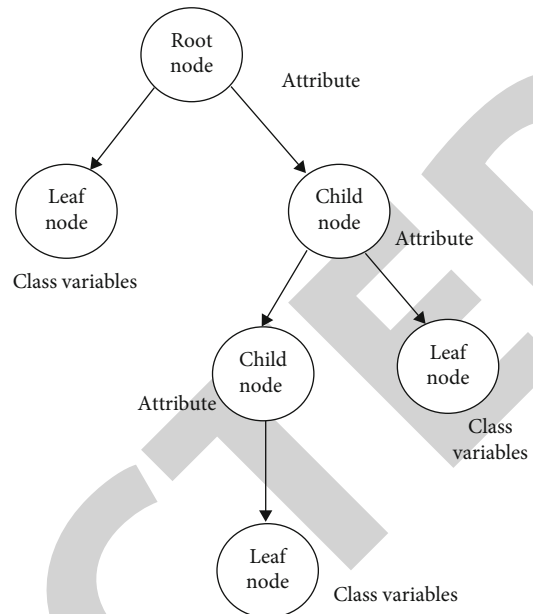


FIGURE 1: Decision tree structure.

C4.5 decision tree. This algorithm classifies the data with a top-down distribution. The final decision tree is reached by dividing the data from the attribute with the highest information gain [3]. The decision tree structure starts with a dataset (training set) partitioned at each node resulting in smaller partitions. In this way, a recursive division strategy is followed. In addition to a dataset, a set of attributes is also transmitted. Objects can be an event, an activity, or attributes which are information about that object. Each tuple in the dataset is associated with a class label, determining whether an object belongs to a particular class. It is tried to reach the highest information gain by using the entropy values at each node. It concludes by starting from the branches created by dividing the data with the highest information gain [4]. The first step in the J48 algorithm is to calculate the information gain [5].

The LMT (logistic model tree) provides a very good description of the data. It consists of a decision tree structure with logistic regression functions on the leaves. As in ordinary decision trees, a test on one of the attributes is associated with each internal node [5–7].

Continuing with the trees that we have the M5P (regression tree) in this decision tree, a standard criterion called M5 is used, which is based on a model tree-type numerical decision tree. It is characterized as follows: build trees using an inductive decision tree algorithm, making routing decisions in nodes taken from the attribute values, and each leaf has an associated class that allows calculating the estimated value of the instance through linear regression [6].

### 3. Review of Literature

Kaur and Wasan's [2] research is an example of a similar research project that we will use to understand our project better. We will conduct a series of comparisons with other works similar to ours to better understand our project.



Decision trees are classification models used in artificial intelligence (AI) that have a visual component to their decision-making process, she argues in advance. The decision tree classification approach was tested using two datasets that contained real patient medical data. It is safe to say that these findings align with the symptoms that a breast cancer specialist would look for to make the diagnosis. One database comprised 692 cases observed by a single physician, whereas the other contained 322 cases from 19 specialists. To put it simply, the study is aimed at discovering whether decision trees, as a medical diagnostic tool, are relevant. Another article of Patel and Prajapati [8] describes the decision trees and the ID3 algorithm (induction decision tree) to determine whether or not to apply drugs to patients with cardiovascular diseases. This research empirically demonstrates that it is possible to diagnose the need to administer drugs in patients with symptoms of cardiovascular disease, using the variable blood pressure, cholesterol, blood sugar, allergies to antibiotics, and other allergies, through the use of trees of decision with the algorithm ID3 (induction decision tree) implemented in the Java language [9].

Another article that is very similar to the previous one but uses another type of decision tree is that by Moghimi-pour and Ebrahimpour [10]. They mention that medical science handles large amounts of information. Advanced machine learning (ML) techniques such as decision trees, support vector machines, and logistic regression can uncover hidden patterns in data. Models developed from these techniques will be very useful for medical science, allowing effective decisions. This article allows us to observe the results obtained about the precision capacity of machine learning techniques, after testing them through a set of data related to cardiovascular diseases provided by the UCI repository. After validating the techniques mentioned with the UCI repository, it is obtained that logistic regression offers the highest levels of precision. It should be noted that support vector machine (SVM) and decision tree (ad) techniques offer acceptable results; however, they are not at the level of the results obtained by logistic regression.

Among other investigations, we have one carried out by Jijo and Abdulazeez [10]; this investigation called “data mining techniques applied to the diagnosis of clinical entities” consists of reducing medical error and improving health processes, which is a priority for all health personnel. In this context, the “clinical decision support systems” (CDSS) arise, a fundamental component in the computerization of the clinical layer. With the evolution of technologies, a large amount of data has been studied and classified through data mining. One of the main advantages of using this in the CDSS has been its ability to generate new knowledge. To this end, through the combination of two mathematical models, it is proposed how it can contribute to the diagnosis of diseases using data mining techniques. To show the models used, arterial hypertension was taken as a case study. The development of the research is governed by the methodology most currently used in the knowledge discovery processes in databases: CRISP-DM 1.0, and is supported by the free distribution tool WEKA 3.6.2, of great prestige among those used for data mining modeling. As a result, data mining

techniques obtained various behavior patterns about the risk factors for hypertension.

Citing another work, we have the one by Hassani and Emami [9] dedicated to the theme of “intelligent system for prognosis of survival of kidney transplant patient” based on obtaining a system based on the hybrid knowledge for the prediction of time of survival renal graft survival of patients. This is developed from the edition of a case base obtained as a result of knowledge engineering; using WEKA the learning methods that generate the best results in the forecast of the objective trait that is continuous and represents graft survival time are determined.

Regression tree is a classification model formed by combining logistic regression and decision tree. Logistic regression tree is a decision tree with a regression analysis structure. In this tree structure, logistic regression analysis is performed for each tree branch; then, branches are separated using the C4.5 decision tree. The final stage is the pruning stage of the tree [8]. Hospital mortality from acute myocardial infarction, in short, was based on carrying out an approximation to the methodology of CART-type decision trees (classification and regression trees) developing a model to calculate the probability of hospital death in acute myocardial infarction (AMI). The method is as follows: the minimum basic dataset at hospital discharge (CMBD) of Andalusia, Catalonia, Madrid, and the Basque country for the years 2001 and 2002 is used, which includes cases with AMI as the main diagnosis.

Another project that we considered was one called “determination of the efficiency of the output bracket. Through this training, the model adjusts the weights of the hidden neurons to optimize the output. The advantage of mining over nomograms is that it has cancer treatment therapy based on data mining” [11]. The said project consisted of using data mining instead of nomograms since there is a wide variety of algorithms, which can learn from experience. They are made up of input nodes, hidden nodes, and nodes with the ability to resolve complex nonlinear relationships between variables without making any prior assumptions about those relationships.

This next project was more striking since it is based on a slightly better-known theme: dengue. We have an investigation carried out [12] whose research is on the “classification of dengue hemorrhagic fever using decision trees in the early phase of the disease.” This work focuses on applying the classification technique of regression and classification trees (ARC), to find decision rules that allow classifying a patient with dengue in the various forms of the disease based on clinical and laboratory characteristics. Performance was evaluated based on the method’s ability to reduce the overall error rate and correctly classify patients [13].

To classify the data, Navada et al. [14] used her article, “decision trees and Bayesian networks for the investigation of genes linked in Alzheimer’s disease,” in which she describes the nested judgments that decision trees reflect. It is possible to classify data using a decision tree employed on the data. The nodes, leaves, and branches of a tree are called its anatomical components. Internal nodes are the queries that are asked regarding a specific attribute of the



problem, referred to as “root” or “primary” nodes. There is a node for each answer to the questions. Each node has a branch that leads to a list of possible values for the attribute. One of the problem’s class variables is represented by the nodes at the end of the graph, known as leaf nodes.

#### 4. Materials and Methods

WEKA’s main interface (Figure 2) [15], the Explorer, provides menu selection and form filling options for all procedures. There are six tabs to choose from when you click on the window on the WEKA main screen. WEKA permits several uses of its capabilities on a same screen using its Knowledge Flow feature. A feature called Knowledge Flow allows jobs to be done repeatedly through separate processes even if only one action may be performed at a time on the Explorer screen itself. Operation beneath the Explorer window takes place with complete automation and readiness. It is necessary for the user to initiate these transactions when using Knowledge Flow.

If you have some data and want to make a decision tree out of it, consider the following scenario. There are a few steps that you must do before you can begin working with your data. Then, select a decision tree creation method, build a tree, and analyze the results. Using a different decision tree algorithm and assessment approach, this process can be easily repeated. If you want to switch between your results, evaluate models created on multiple datasets and graphically examine both models and datasets, including the classification errors generated by the models under an explorer menu. The data and information that were used to carry out our research consisted of a database created from audiology tests; to this database, the different methods that the classification trees have were applied to verify the effectiveness of each one of them. These data indicate a diagnosis for each patient and the person’s characteristics, such as their age and type of eardrum, if they have presented dizziness. Here, the objective is to determine which attributes serve more to predict the diagnosis obtained [15].

Since the CART decision tree has a recursive bipartite structure, it continues until a new split no longer occurs, and in the next stage, pruning starts from the tip to the root. After each pruning, the most successful decision tree is tried to be determined by using the test data. It is tried to reach the highest information gain by generalizing the binomial distribution at each node using the Gini index values obtained. It is said that it does not perform well if there are interrelated variables.

Other data that was also used was a database containing studies on prostate cancer. Still, algorithms that we can find in the regression trees were applied to that database, which present some difference compared to the classification trees. In this study, the objective is to predict the value of PSA (prostate-specific antigen) based on the values of the other characteristics of the patient [16].

One of the main differences that we can find between these two types of trees is that when the “response variable” or to be clearer when our variable of interest is numerical, we



FIGURE 2: WEKA main screen.

speak of regression trees. In contrast, categorical variables are analyzed using regression tree classification, but in any case, the functioning of these two types of trees is relatively similar.

For this reason, if we want to explain and predict characteristics of observations belonging to the objects of a class whose bases can be explanatory or qualitative variables, we will use classification trees, and on the other hand, for an explanatory and predictive model for a dependent quantitative variable whose bases are quantitative variables similarly, we will use regression trees.

Application.

#### 5. Results and Discussion

The observations are as follows:

As shown in Figure 3, the J-48 decision tree algorithm manages to be a practically optimal analysis of the entered data, whose characteristics were modified to present us with a less extensive and understandable tree, reaching a 69.5% classification of the variables.

**5.1. RandomTree.** The random tree starts by choosing a predetermined number of random features at each node. In this algorithm, the branches of the tree are not pruned. Indecision trees, while choosing the most informative feature at each node, are not random in the random tree method. A random tree is a tree in which each tree has an equal chance of being sampled or has a “uniform” distribution. However, each node is considered a randomly generated tree from a set of possible trees of random significance. It also allows the estimation of probabilities for categorical variables [17].

The RandomTree decision tree algorithm, no matter how much work was done on its properties looking for an optimal result and a more simplified tree, only managed to analyze 45% of the data entered. Figure 4 shows the analysis statistics for the best case.

**5.2. REPTree.** The REPTree decision tree algorithm is not a good algorithm to analyze the data that we are working on. No matter how much we tried to increase the percentage of variables evaluated, the algorithm did not present better results. Figure 5 shows the analysis statistics for the best case.

**5.3. DecisionStump.** The DecisionStump decision tree algorithm with the data entered and the configuration of the

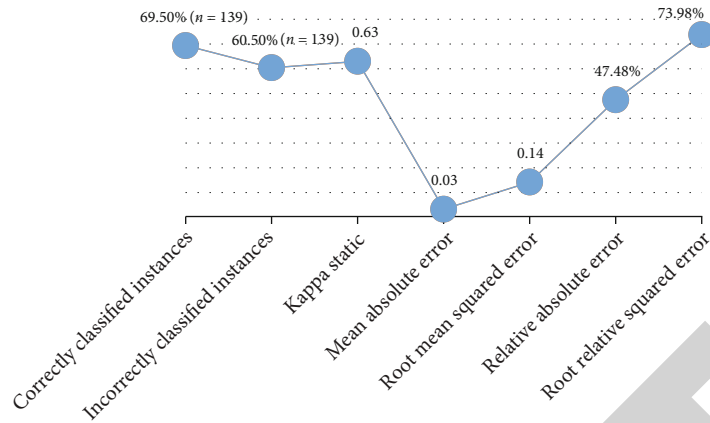


FIGURE 3: Classification trees (audiology exam): J48.

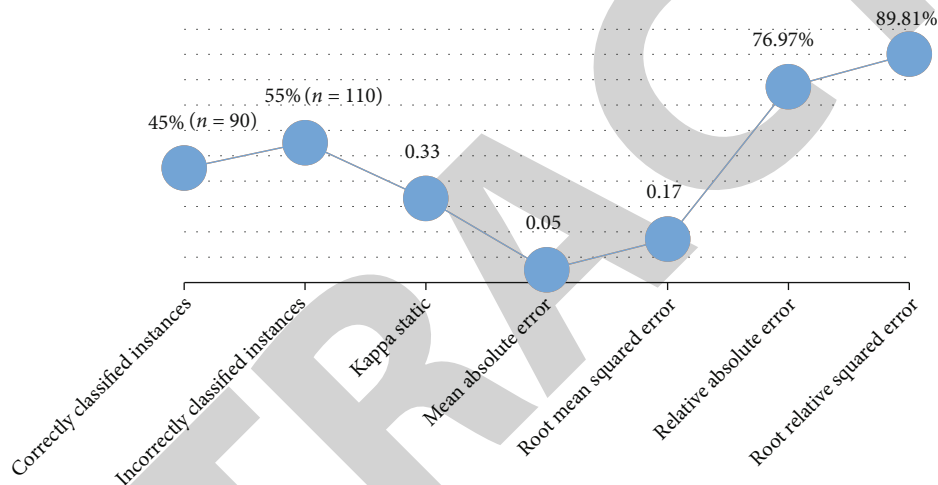


FIGURE 4: Analysis statistics for the best case.

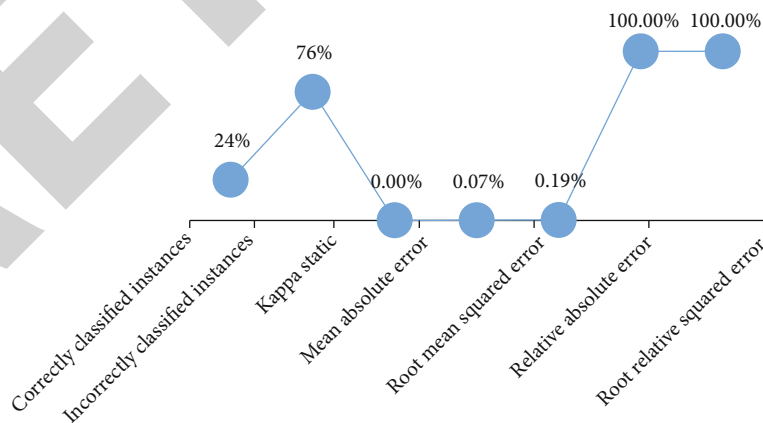


FIGURE 5: Analysis statistics for the best case.

analysis properties only evaluated 47% of the variables. Another disadvantage was that it did not present either a schema of the tree or the tree itself. Figure 6 shows the analysis statistics for the best case.

5.4. *SimpleCART*. The SimpleCART decision tree algorithm presented almost the same disadvantages as the REPTree algorithm with a low percentage when analyzing the variables and with a single level tree, all this with configurations

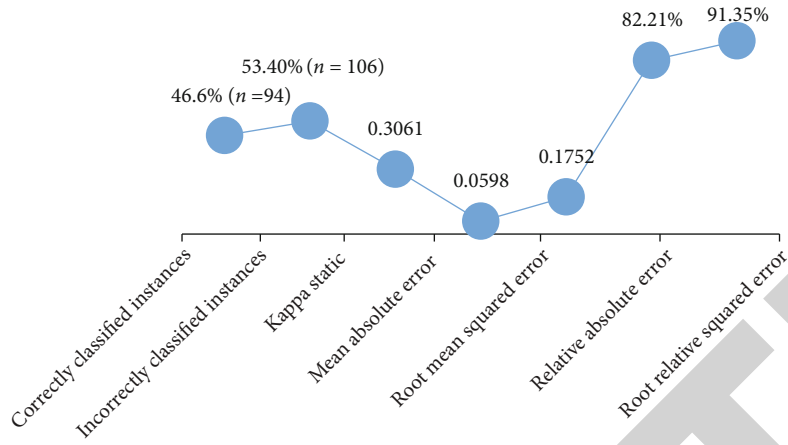


FIGURE 6: Analysis statistics for the best case.

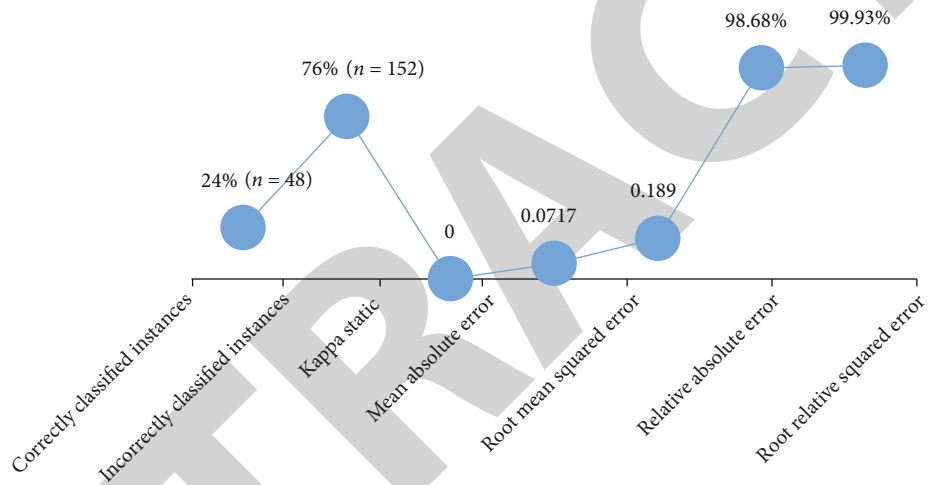


FIGURE 7: Analysis statistics for the best case.

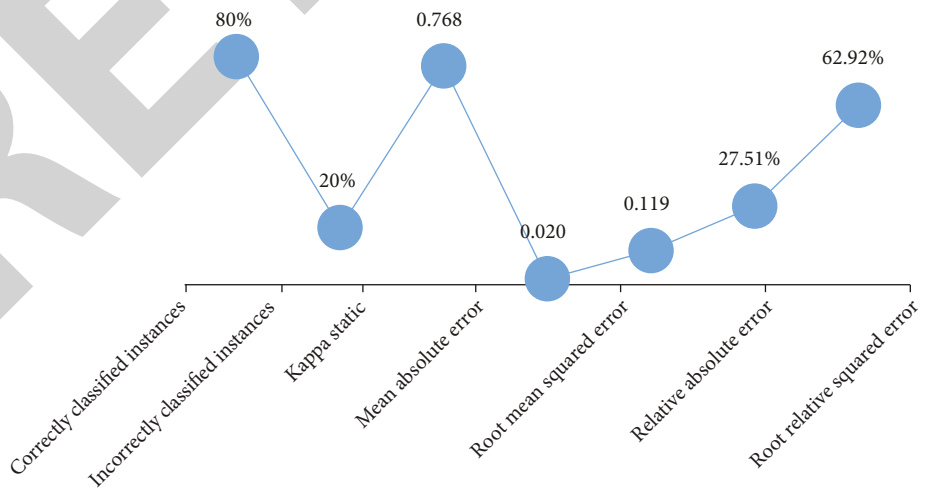


FIGURE 8: Analysis statistics for the best case.

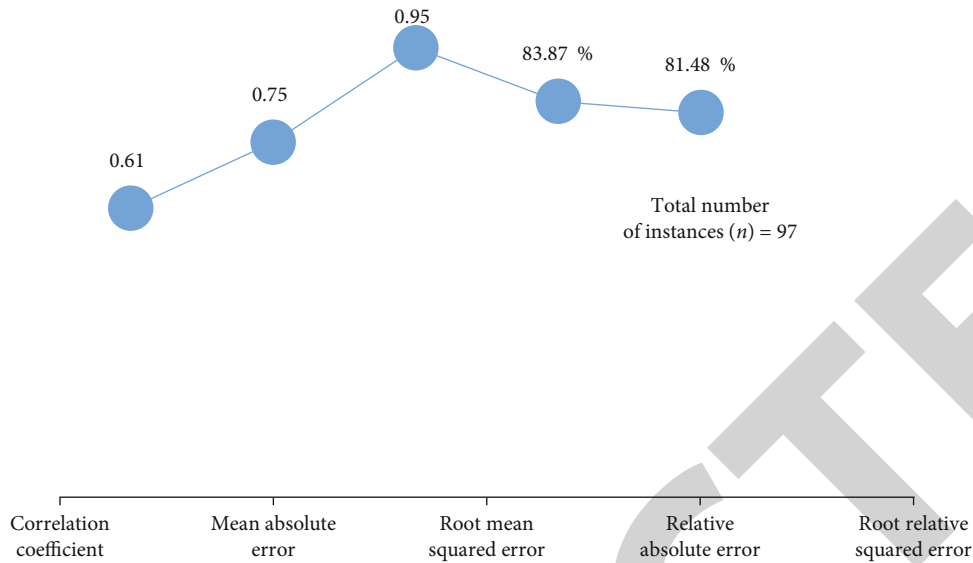


FIGURE 9: Analysis statistics for the best case.

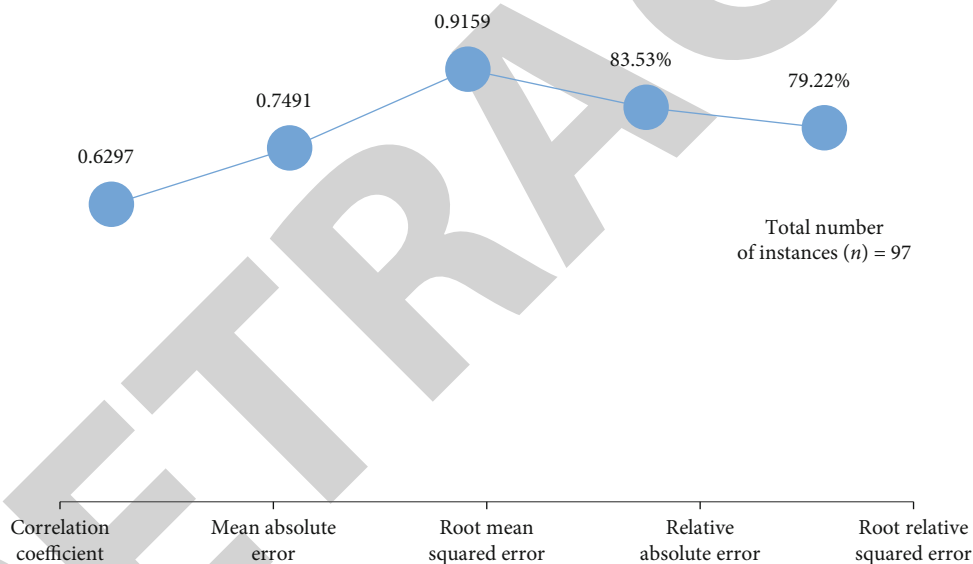


FIGURE 10: Analysis statistics for the best case.

for a better data sampling. Figure 7 shows the analysis statistics for the best case.

5.5. *LMT*. The LMT decision tree algorithm turned out to be the most efficient algorithm when interpreting the type of data presented by the study data, presenting a well-summarized tree and with 80% of the variables analyzed. Figure 8 shows the analysis statistics for the best case.

5.6. *Regression Trees (Prostate Exam): M5P*. The M5P regression tree algorithm turned out to be very efficient when interpreting the attributes and variables that the study database presented, presenting a very well-detailed 7 tree with an approximate frequency of 0.61 of the analyzed variables. Figure 9 shows the analysis statistics for the best case.

5.7. *REPTree*. The REPTree regression tree algorithm is a good algorithm to analyze the data of this class of databases in which we are working since it presented an optimal performance when analyzing the variables evaluated. It presented an approximate frequency of 0.62 (Figure 10).

## 6. Conclusions

The impact that is desired to obtain with the project in applying decision and regression trees as a tool for the prognosis of medical conditions is to take optimal management of the WEKA software [18].

The classification trees are the most competent for these data, more precisely the logistic model tree or LMT [19] classification tree, which statistically turned out to be the type of tree that presented the most efficient results in its

result statistics with an average of 80% correct classifications at the time of executing on the data, whose response or interest variables were the Tymp() variable and the speech() variable, which correspond to the type of eardrum and if the person has problems of speaking [7, 20, 21].

After working on another study which was on the prostate specific antigen which handled quantitative variables, we realize that the regression trees are indicated to analyze this type of data, whose most effective tree was the M5 model tree or the M5P [22–25], whose statistics reached an approximate frequency of 0.62 when analyzing the data, and whose variable of interest was the variables of volume and weight of the prostate (level() and weight()).

## Data Availability

The data used to support the findings of this study are included within the article.

## Conflicts of Interest

The authors declare that they have no conflicts of interest.

## Acknowledgments

This project was supported by Princess Nourah bint Abdulrahman University Researchers Supporting Project number (PNURSP2022R236), Princess Nourah bint Abdulrahman University, Riyadh, Saudi Arabia.

## References

- [1] K. Singh, "The comparison of various decision tree algorithms for data analysis," *International Journal Of Engineering And Computer Science*, vol. 6, no. 6, pp. 21557–21562, 2017.
- [2] H. Kaur and S. Wasan, "Empirical study on applications of data mining techniques in healthcare," *Journal of Computer Science*, vol. 2, no. 2, pp. 194–200, 2006.
- [3] H. Sug, "Performance comparison of decision tree algorithms for medical data sets," *International Journal of Mathematics and Computers in Simulation.*, vol. 8, pp. 107–115, 2014.
- [4] S. N. Chary and B. Rama, "A survey on comparative analysis of decision tree algorithms in data mining," *International Journal of Mathematical, Engineering and Management Sciences.*, vol. 3, pp. 91–95, 2017.
- [5] A. S. Abdullah, S. Selvakumar, P. Karthikeyan, and M. Venkatesh, "Comparing the efficacy of decision tree and its variants using medical data," *Indian Journal of Science and Technology*, vol. 10, pp. 1–8, 2017.
- [6] M. B. Alazzam, N. Tayyib, S. Z. Alshawwa, and M. Ahmed, "Nursing care systematization with case-based reasoning and artificial intelligence," vol. 2022, Article ID 1959371, 9 pages, 2022.
- [7] Y. Zhang, Y. Xin, Q. Li et al., "Empirical study of seven data mining algorithms on different characteristics of datasets for biomedical classification applications," *BioMedical Engineering OnLine.*, vol. 16, no. 1, pp. 1–15, 2017.
- [8] S. Pathak, I. Mishra, and A. Swetapadma, "An Assessment of Decision Tree Based Classification and Regression Algorithms," in *2018 3rd International Conference on Inventive Computation Technologies (ICICT)*, pp. 92–95, Coimbatore, India, November 2018.
- [9] H. Patel and P. Prajapati, "Study and analysis of decision tree based classification algorithms," *International Journal of Computer Sciences and Engineering.*, vol. 6, no. 10, pp. 74–78, 2018.
- [10] Z. Hassani and N. Emami, "Prediction of the Survival of Kidney Transplantation with imbalanced Data Using Intelligent Algorithms," *Computer Science Journal of Moldova*, vol. 77, pp. 163–181, 2018.
- [11] I. Moghimipour and M. Ebrahimpour, "Comparing decision tree method over three data mining software," *International Journal of Statistics and Probability.*, vol. 3, no. 3, 2014.
- [12] B. Charbuty and A. Abdulazeez, "Classification based on decision tree algorithm for machine learning," *Journal of Applied Science and Technology Trends.*, vol. 2, pp. 20–28, 2021.
- [13] M. B. Alazzam, W. T. Mohammad, M. B. Younis et al., "Studying the effects of cold plasma phosphorus using physiological and digital image processing techniques," *Computational and Mathematical Methods in Medicine*, vol. 2022, Article ID 8332737, 5 pages, 2022.
- [14] A. Navada, A. Ansari, S. Patil, and B. Sonkamble, "Overview of use of decision tree algorithms in machine learning," in *2011 IEEE control and system graduate research colloquium*, pp. 37–42, Malaysia, June 2011.
- [15] A. A. Hamad, M. L. Thivagar, J. Alshudukhi et al., "Secure complex systems: a dynamic model in the synchronization," *Computational Intelligence and Neuroscience*, vol. 2021, Article ID 9719413, 6 pages, 2021.
- [16] S. L. Gutiérrez, M. Herrera-Rivero, N. Cruz-Ramírez, M. Hernandez, and G. Aranda-Abreu, "Decision trees for the analysis of genes involved in Alzheimer's disease pathology," *Journal of Theoretical Biology*, vol. 357, pp. 21–25, 2014.
- [17] B. Gupta, A. Rawat, A. Jain, A. Arora, and N. Dhama, "Analysis of various decision tree algorithms for classification in data mining," *International Journal of Computer Applications.*, vol. 163, no. 8, pp. 15–19, 2017.
- [18] I. Witten, M. Hall, E. Frank, G. Holmes, B. Pfahringer, and P. Reutemann, "The WEKA data mining software: an update," *SIGKDD Explorations.*, vol. 11, pp. 10–18, 2009.
- [19] A. Abdullah Hamad, M. L. Thivagar, M. Bader Alazzam, F. Alassery, F. Hajje, and A. A. Shihab, "Applying dynamic systems to social media by using controlling stability," *Computational Intelligence and Neuroscience*, vol. 2022, Article ID 4569879, 7 pages, 2022.
- [20] G. Wang, L. Wang, B. S. Mohammed, and A. A. Hamad, "An investigation on the risk awareness model and the economic development of the financial sector," *Annals of Operations Research*, vol. 12, pp. 1–23, 2022.
- [21] T. Lakshmi, M. Aruldoss, R. M. Begum, and V. Venkatesan, "An analysis on performance of decision tree algorithms using student's qualitative data," *International Journal of Modern Education and Computer Science.*, vol. 5, no. 5, pp. 18–27, 2013.
- [22] S. Panigrahi, B. S. Nanda, and T. Swarnkar, "Comparative analysis of machine learning algorithms for histopathological images of oral cancer," in *Advances in Distributed Computing and Machine Learning*, Springer, Singapore, 2022.



## *Retraction*

# **Retracted: Silencing lncRNA 93358 Inhibits the Apoptosis of Myocardial Cells in Myocardial Infarction Rats by Inducing the Expression of SLC8A1**

### **BioMed Research International**

Received 5 December 2023; Accepted 5 December 2023; Published 6 December 2023

Copyright © 2023 BioMed Research International. This is an open access article distributed under the Creative Commons Attribution License, which permits unrestricted use, distribution, and reproduction in any medium, provided the original work is properly cited.

This article has been retracted by Hindawi, as publisher, following an investigation undertaken by the publisher [1]. This investigation has uncovered evidence of systematic manipulation of the publication and peer-review process. We cannot, therefore, vouch for the reliability or integrity of this article.

Please note that this notice is intended solely to alert readers that the peer-review process of this article has been compromised.

Wiley and Hindawi regret that the usual quality checks did not identify these issues before publication and have since put additional measures in place to safeguard research integrity.

We wish to credit our Research Integrity and Research Publishing teams and anonymous and named external researchers and research integrity experts for contributing to this investigation.

The corresponding author, as the representative of all authors, has been given the opportunity to register their agreement or disagreement to this retraction. We have kept a record of any response received.

## **References**

- [1] J. Cai, X. Wang, W. Liao, Y. Zhong, L. Chen, and Z. Zhang, "Silencing lncRNA 93358 Inhibits the Apoptosis of Myocardial Cells in Myocardial Infarction Rats by Inducing the Expression of SLC8A1," *BioMed Research International*, vol. 2022, Article ID 1138709, 11 pages, 2022.

## Research Article

# Silencing lncRNA 93358 Inhibits the Apoptosis of Myocardial Cells in Myocardial Infarction Rats by Inducing the Expression of SLC8A1

Jiumei Cai,<sup>1,2,3</sup> Xiaoping Wang,<sup>2</sup> Wei Liao,<sup>2</sup> Yiming Zhong,<sup>2</sup> Lingling Chen,<sup>2</sup> and Zhiwei Zhang<sup>1,3</sup> 

<sup>1</sup>The Second School of Clinical Medicine, Southern Medical University, Guangzhou, Guangdong 510515, China

<sup>2</sup>Department of Cardiology, First Affiliated Hospital of Gannan Medical University, Ganzhou, Jiangxi 341000, China

<sup>3</sup>Department of Pediatric Cardiology, Guangdong Cardiovascular Institute, Guangdong Provincial People's Hospital, Guangzhou, Guangdong 510080, China

Correspondence should be addressed to Zhiwei Zhang; [drzhangzw@sohu.com](mailto:drzhangzw@sohu.com)

Received 12 April 2022; Revised 10 June 2022; Accepted 14 June 2022; Published 7 July 2022

Academic Editor: Dinesh Rokaya

Copyright © 2022 Jiumei Cai et al. This is an open access article distributed under the Creative Commons Attribution License, which permits unrestricted use, distribution, and reproduction in any medium, provided the original work is properly cited.

**Objective.** To explore the inhibitor effects and mechanism of lncRNA 93358 against the apoptosis of myocardial cells in rats with myocardial infarction. **Methods.** The myocardial infarction model was established in rats, which were identified by cardiac ultrasound. TTC staining was used to evaluate the degree of heart infarction, and HE staining was utilized to determine the pathological state in myocardial tissues. The apoptotic state in myocardial tissues was confirmed by TUNEL assay. lncRNA 93358 was screened out using a high-throughput sequencing which was confirmed by RT-qPCR. The interaction between miR-466c-3p and SLC8A1 was identified using the dual-luciferase reporter assay. The expression level of Bax, Bcl-2, and SLC8A1 was determined in lncRNA 93358 knockdown cells using RT-qPCR and Western blotting. **Results.** Massive myocardial necrosis was observed in model rats according to the results of TTC staining, HE staining, and TUNEL assay. lncRNA 93358 and Bax were found significantly upregulated, and Bcl-2 and SLC8A1 were greatly downregulated in model rats, which were dramatically reversed by the knockdown of lncRNA 93358, accompanied by the decline area of myocardial necrosis and decreased apoptotic myocardial cells. **Conclusion.** Silencing lncRNA 93358 inhibits the apoptosis of myocardial cells in rats with myocardial infarction by inducing the expression of SLC8A1.

## 1. Introduction

Myocardial infarction (MI) is a fatal cardiovascular disease with millions of deaths annually all over the world, the morbidity and mortality of which remains high in recent years [1, 2]. It is reported that physiological and pathological processes, such as inflammatory reactions, cell apoptosis, and fibrosis, play important roles in impacting the prognosis and survival rate of MI patients [3, 4]. Long noncoding RNAs (lncRNAs) are a group of functional molecules at a greater length than 200 nt and play a critical role in multiple cellular progressions, such as proliferation, apoptosis, and differentiation. lncRNA is reported to be involved in the processes of development, differentiation, myocardial hypertrophy, heart

failure, and MI by regulating transcription, posttranscriptional gene regulation, competitive endogenous RNA, and protein translation [5, 6]. In addition, lncRNA metastasis-associated lung adenocarcinoma transcript 1 (MALAT1) is regarded as a key gene involved in the development of cardiovascular diseases such as MI [7]. The progression of MI is reported to be abnormally aggravated by lncRNA taurine upregulated gene 1 (TUG1) [8]. lncRNA cardiac conduction regulatory RNA (CCRR) shows significant impacts on cardiac conduction. However, not sufficient importance has been attached to the function of lncRNA in the regulation of myocardial apoptosis post MI. The present study will investigate the differentially expressed lncRNAs in MI through the high-throughput sequencing assay and explore the potential genes related to

the function of differentially expressed lncRNAs utilizing the methods of bioinformatics, coexpression network analysis, and fluorescence quantitative PCR.

## 2. Materials and Methods

**2.1. Animals and MI Modeling.** 25 SD rats weighing from 220 g to 250 g were raised at the condition of 18°C-26°C temperature and 40%-70% humidity. After being anesthetized by intraperitoneally injected with 2% pentobarbital sodium, the skin on the back of rats was cut off and the trachea was separated out, followed by making a small hole in the trachea with a needle to insert an endotracheal tube. The tidal volume was modulated to 10, and the electrocardiograph was connected, followed by opening the chest to expose the heart. Ligation was performed with a 6-0 circular wire through the upper 1/3 of the left coronary artery until the myocardial tissues turned pale. The successful establishment of the MI model was confirmed by the electrocardiogram. In the sham group, the ligation was absolved. The animal experiments described in this study were authorized by the Committee of the First Affiliated Hospital of Gannan Medical University (No. LLSC-20201022011).

**2.2. lncRNA High-Throughput Sequencing and Expression Profiling.** The samples were myocardial tissue of MI rats and control groups. The TRIzol reagent (Invitrogen, USA) was used to extract RNA and reverse transcription to synthesize cDNA. High-throughput sequencing was performed by Shanghai Jingneng Biotechnology Co., Ltd. Qualified double-stranded cDNA samples were interrupted by the Covaris ultrasonic system and subjected to end repair. A tail and sequencing adapter addition and the sequence of about 200 bp were recovered and enriched by PCR, and then, a cDNA library was established, and the quality of the library was evaluated. After statistics, samples with a mapping ratio lower than 50% were excluded. The DESeq2 software was used to screen the differentially expressed (DE) lncRNAs between the two groups [9]. Differences in gene expression with  $|\log_2 \text{FC}| \geq 1$  and  $P$  value  $< 0.05$  were considered to be significantly differentially expressed.

For functional analyses, Gene Ontology (GO, <http://geneontology.org/>) analysis and Kyoto Encyclopedia of Genes and Genomes (KEGG, <https://www.kegg.jp/>) were used for the functional annotation and classification of pathway according to the DAVID database (<https://david.ncicrf.gov/>) [10]. Significantly enriched GO and significant pathways were screened according to  $P < 0.05$ .

**2.3. Silencing of lncRNA 93358 in MI Rats.** siRNA (GenScript, Nanjing, China) was designed according to the sequence of lncRNA 93358. MI rats were divided into three groups: model group (injected with the same amount of normal saline), NC group (injected with 100 nM siRNA NC), and shRNA group (injected with 100 nM siRNA lncRNA 93358). Each group received continuous intervention for 5 days.

**2.4. Primary Cardiomyocyte Culture.** Take the rat's heart and cut the heart into about 1 mm<sup>3</sup> tissue pieces. After adding a mixture of digestive enzymes, digest with slow shaking in a 37°C water bath. The single cell suspension was transferred to

DMEM complete medium containing 15% fetal bovine serum (FBS) to end the digestion. The above process was repeated until the digestion of the tissue block was complete. All digested cells were collected, filtered through a 200-mesh cell screen, and centrifuged at 1000 rpm/min for 10 min, the supernatant was discarded, the pellet was resuspended in DMEM complete medium with 15% FBS, and the pellet was repeatedly pipetted gently to form a single cell suspension. The cell suspension was transferred to a Petri dish, and the myocardial cells in the supernatant were collected by differentially adhering to the wall for 60 min. The cells were seeded in a sterile 6-well plate pre-coated with laminin at  $5 \times 10^4$  cells per well. After 24 hours of culture, the medium changed. After 48 hours, the myocardial cells were flattened into a monolayer, which could be used for subsequent experiments.

**2.5. The Establishment of lncRNA 93358 Knockdown Myocardial Cells.** ShRNA was designed and analyzed by GenScript (Nanjing, China), which was used to transfect myocardial cells to establish the lncRNA 93358 knockdown myocardial cells. The transfection reagent was Lipofectamine 3000 (Invitrogen, California, USA), and the duration of the transfection was 48 hours. The control group was myocardial cells from sham-operated rats, the model group was untreated MI rat myocardial cells, the NC group was myocardial cells from MI rat transfected with shRNA NC, and the shRNA group was myocardial cells from MI rat transfected with shRNA-lncRNA 93358. The efficacy of transfection was confirmed using the RT-qPCR assay.

**2.6. Dual-Luciferase Reporter Assay.** The synthesized SLC8A1 3'-UTR sequence (RiboBio, Guangzhou, China) or a mutant sequence was cloned into pmirGlo vectors (GenePharm) to construct the luciferase reporters SLC8A1-WT and SLC8A1-MUT. 293 T cells were cotransfected with SLC8A1-WT (or SLC8A1-MUT) and miR-466c-3p mimics (or mimics NC) at 70–80% confluency. The luciferase activities were assessed 48 h posttransfection using a Dual-Luciferase Reporter Assay System (Promega Biotech Co., Madison, USA).

**2.7. Western Blot.** The lysis buffer was utilized to isolate total proteins from rat myocardial tissue, and the isolated proteins were quantified with the BCA kit (Takara, Tokyo, Japan), followed by loading 30  $\mu$ g proteins for each sample onto the 12% SDS-PAGE. After being separated for 1 hour, proteins in the gel were further transferred onto the PVDF membrane (Takara, Tokyo, Japan), followed by incubation with 5% skim milk. Then, the membrane was incubated with the primary antibody against SLC8A1 (1 : 1000, 55075-1-AP, Proteintech, Chicago, USA), Bcl-2 (1 : 1000, bs-34012R, Bioss, Beijing, China), Bax (1 : 1000, 50599-2-Ig, Proteintech, Chicago, USA), and Tubulin (1 : 1000, 10094-1-AP, Proteintech, Chicago, USA). Then, the secondary antibody (1 : 2000, ZB-2301, SolelyBio, Shanghai, China) was utilized to incubate with the membrane for 1.5 h at room temperature. Finally, the bands were incubated with the ECL solution, followed by quantification using the ImageJ software.

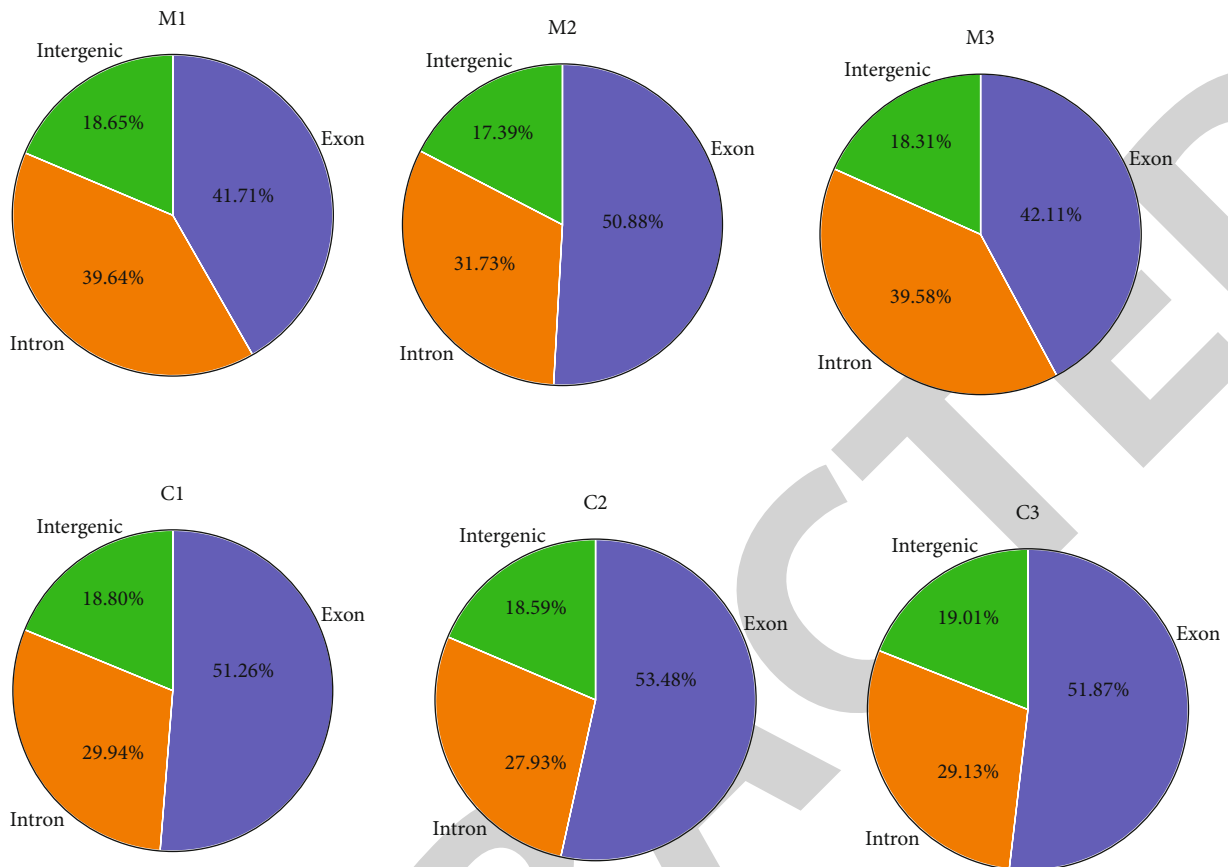


FIGURE 1: The pie chart of gene structure distribution. Percent of reads mapped to genome regions. M1-M3: model group; C1-C3: control group. Blue represents exons, orange represents introns, and green represents intergenic.

TABLE 1: The number and percentage of lncRNAs achieved by 4 different methods of prediction.

Method	Number of transcripts	Percentage (%)
Assessment noncoding in Pfam	7002	52.45
Assessment noncoding in CPC2	4680	35.05
Assessment noncoding in PLEK	4734	35.46
Assessment noncoding in CNCI	4477	33.53
Assessment noncoding in at least one method	8169	61.19
Assessment noncoding in all methods	2997	22.45
Total transcripts	13351	100

**2.8. Quantitative Real-Time PCR (RT-qPCR).** The TRIzol® reagent (Leagene, Beijing, China) was applied for the extraction of total RNAs from myocardial tissues in each group, which were further reverse-transcribed to cDNA using the TaqMan miRNA reverse transcription kit (Invitrogen, California, USA). The RT-PCR was performed with HiScript II Q RT SuperMix (R223-01, Vazyme, Jiangsu, China) using SYBR® Green Real-time PCR Master Mix (Lifeint, Fujian, China). GAPDH was utilized for normalizing gene expression, which was determined using the  $2^{-\Delta\Delta Ct}$  method.

**2.9. Hematoxylin and Eosin (H&E) Staining.** After collecting the myocardial tissues from each rat and washing, the tissues were successively dehydrated with a 70%, 80%, and 90% eth-

anol solution, followed by incubation with equal quality of ethanol and xylene for 15 min. Subsequently, the samples were incubated with equal quality of xylene for another 15 min, followed by repeated incubation until the tissues appeared transparent. Then, the tissues were embedded in paraffin, sectioned, and stained with H&E staining, followed by randomly selecting the images from 5 fields at 100× magnification that were captured, and all phases of follicles and corpora lutea were counted by using an inverted microscope (Olympus, Tokyo, Japan).

**2.10. TUNEL Assay.** The tissue slides were baked in the oven at 65°C for 2 hours, followed by dehydrating with xylene, 100% ethyl alcohol, 95% ethyl alcohol, 80% ethyl alcohol

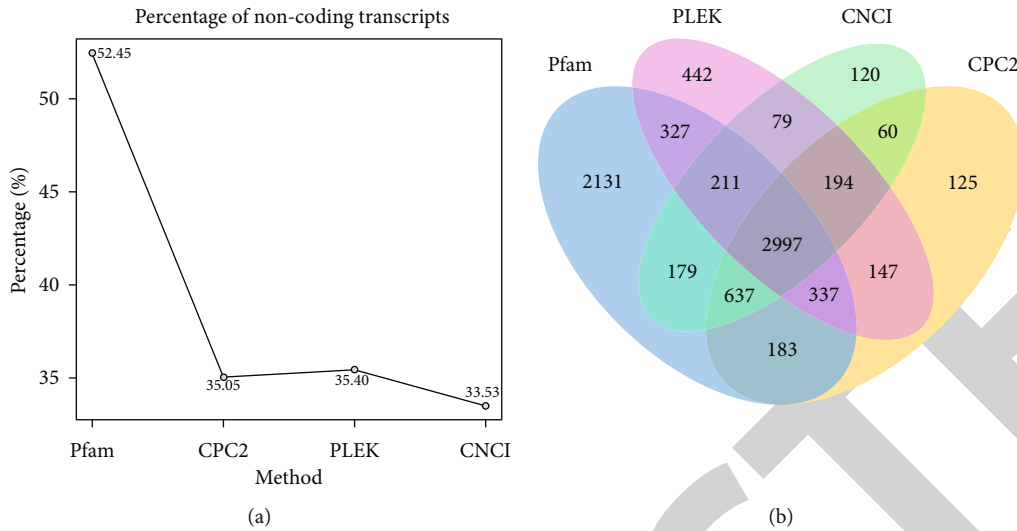


FIGURE 2: The line chart (a) and Venn diagram (b) of lncRNA concentrations.

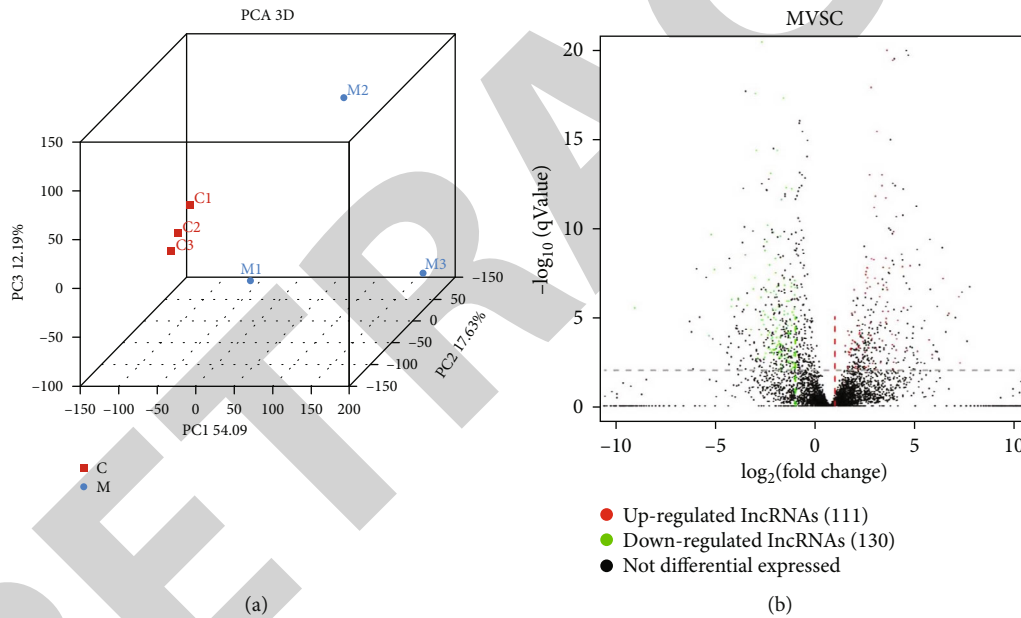


FIGURE 3: Identification of differentially expressed lncRNA. (a) The PCA diagram. (b) Volcano map of differential expression analysis. The horizontal axis represented the expression multiple of the transcript between different groups of samples and the vertical axis represented the statistical significance of changes in transcript expression levels ( $q$  value). Red dots represented an upregulated transcript, green dots represented a downregulated transcript, and black represented a nondifferential transcript.

solution, and pure water, successively. The slides were then added to a 50  $\mu\text{g}/\text{mL}$  proteinase K working solution to incubate at 37°C for 30 min. After 3 washes using PBS buffer, the slides were added with the TUNEL detection buffer to be incubated at 45°C for 2 hours. Lastly, the images were taken under an inverted microscope (Olympus, Tokyo, Japan).

**2.11. Statistical Analysis.** Data achieved was presented as mean  $\pm$  standard deviation (SD) and analyzed using the GraphPad software (Harvey Motulsky). The Student's  $t$ -test was applied to check the difference between the two groups, and the one-way ANOVA method followed by the Tukey post hoc test

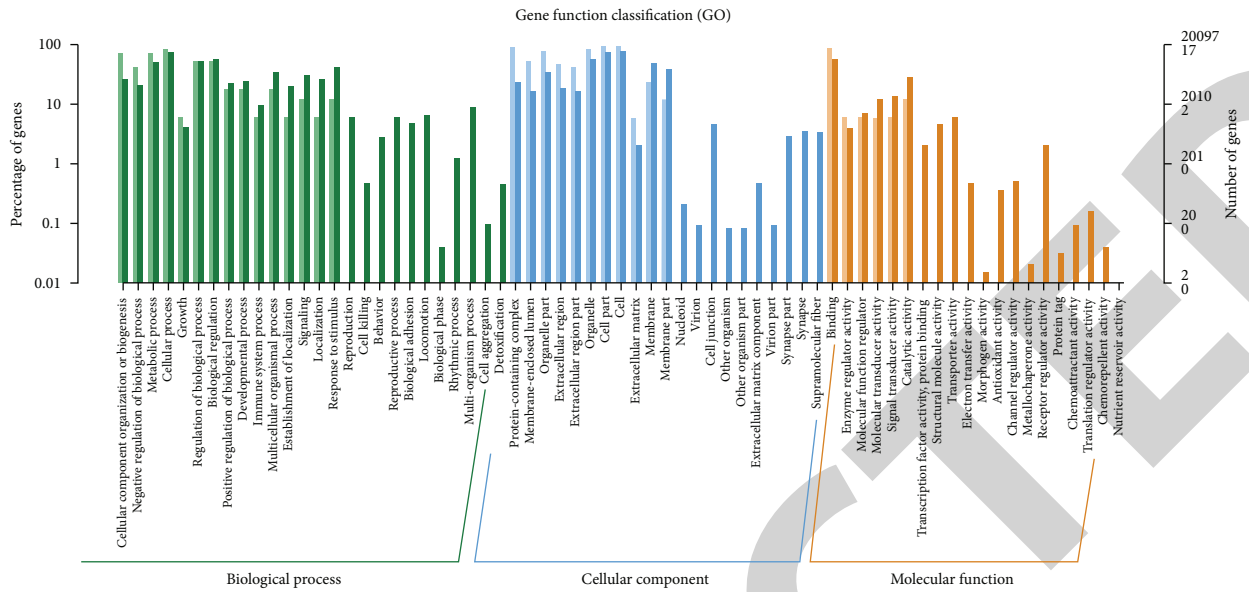
was applied to check the differences among groups.  $P < 0.05$  was regarded as a significant difference.

### 3. Results

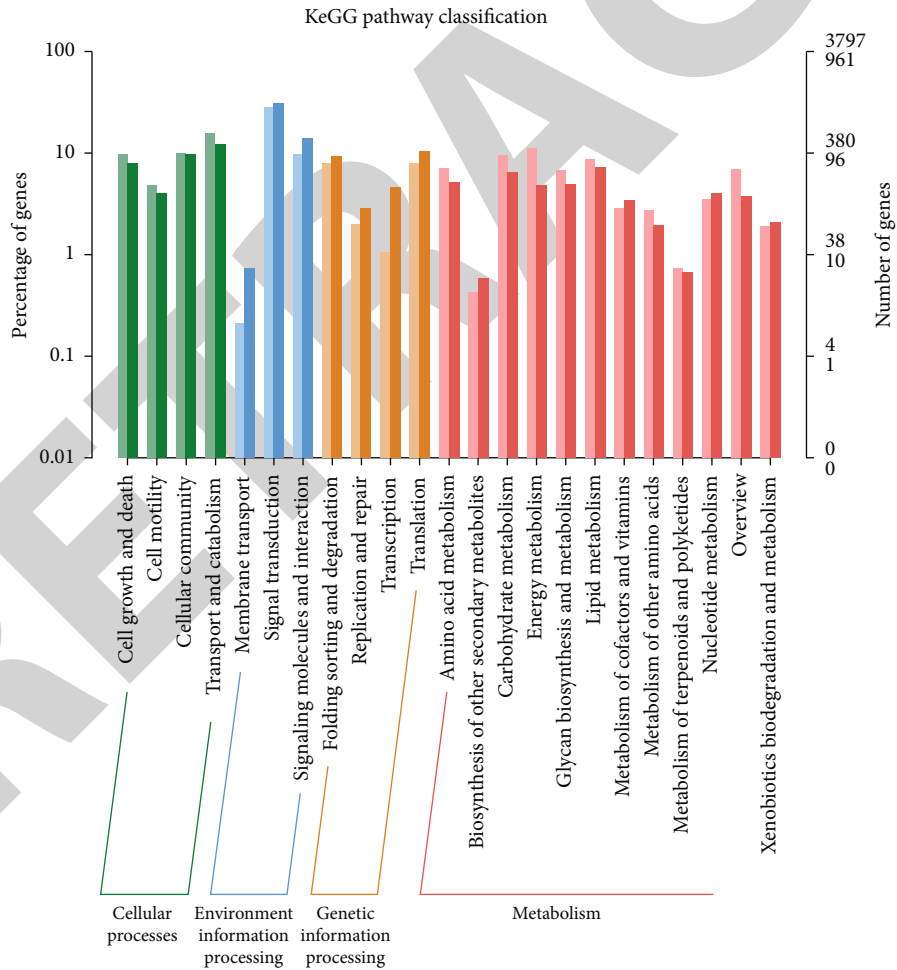
**3.1. lncRNA Screening.** According to the comparison of reads, the proportion of each gene occupied in total reads was shown in Figure 1, including exons, introns, and intergenic.

The conditions for screening were shown as follows: (1) transcripts with more than 2 exons were selected; (2) transcripts with a length longer than 200 bp were selected; (3) transcripts with known annotation were selected; and (4)





(a)



(b)

FIGURE 4: Functional enrichment of differentially expressed lncRNAs. (a) GO analysis on the differentially expressed lncRNAs. The horizontal axis represented a functional classification, and the vertical axis represented the number of genes in the classification (right) and their percentage in the total number of genes annotated (left). (b) KEGG analysis on the differentially expressed lncRNAs. The vertical axis represents the pathway category, and the vertical axis represents the number of genes in the classification (right) and its percentage in the total number of annotated genes (left). Different colors represent different categories.

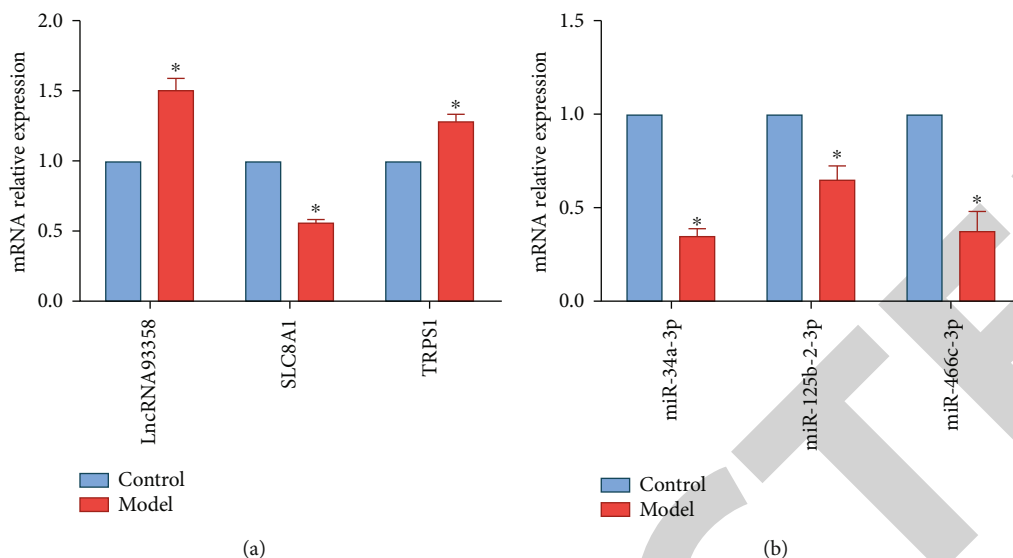


FIGURE 5: Validation of sequencing data. (a and b) The expression levels of lncRNA 93358, SLC8A1, and TRPS1 (a) and miR-34a-3p, miR-125b-2-3p, and miR-466c-3p (b) in the rat myocardial tissues were detected by RT-qPCR. \*\* $P < 0.01$ .

transcripts without coding potential in the intersection of such software as CPC2, CNCI, Pfam, and PLEK were selected. Based on these conditions, the predicted lncRNAs were shown in Table 1 and Figures 2(a) and 2(b).

**3.2. Differentially Expressed lncRNA Identification.** As shown in Figure 3(a), the data from the control group flocked together, and the difference within the group was small. The distance within the model group was relatively significant, indicating that there was a significant difference among individuals in the model group.

A total of 241 DE lncRNAs were then identified, of which 111 were upregulated and 130 were downregulated. Volcano plots were used to assess the DE lncRNAs between the control and model groups (Figure 3(b)).

**3.3. Functional Enrichment of Differentially Expressed lncRNAs.** To further investigate the biological functions of DE lncRNAs, we performed functional enrichment analysis for the DE mRNA regulated by lncRNAs. The GO terms of biological processes, cellular components, and molecular functions were illustrated in Figure 4(a). The results showed that DE mRNAs were enriched in cellular process, protein-containing complex, and binding. Moreover, the KEGG analysis showed that the DE mRNAs significantly enriched in cell growth and death, signal transduction, translation, and energy metabolism (Figure 4(b)).

**3.4. Validation of Sequencing Data.** lncRNA 93358 was proved to be differentially expressed in myocardial tissues in MI rats and by prediction using miRDB (<http://mirdb.org/index.html>); it was predicted that miR-34a-3p, miR-125b-2-3p, and miR-466c-3p interact with lncRNA 93358. Furthermore, we predicted the potential myocardial diseases that interact with these three miRNAs, which were SLC8A1 and TRPS1. Subsequently, the expression level of lncRNA 93358, miR-34a-3p, miR-125b-2-3p, miR-466c-3p, SLC8A1, and TRPS1

was determined by RT-qPCR. We found that lncRNA 93358 and TRPS1 were significantly upregulated in the model group, while the expression of SLC8A1, miR-34a-3p, miR-125b-2-3p, and miR-466c-3p was downregulated (Figures 5(a) and 5(b)).

**3.5. SLC8A1 Was a Target of miR-466c-3p.** To confirm the regulation among lncRNA 93358, miRNAs, and SLC8A1, we collected heart tissues from each group of rats. RT-qPCR results showed that lncRNA 93358 was highly expressed in the model group, which was significantly downregulated by the knock-down of lncRNA 93358. And the expression levels of miR-466c-3p in the model group and NC group were significantly downregulated, which were greatly reversed after the knock-down of lncRNA 93358 ( $P < 0.05$ , Figures 6(a) and 6(b)).

Compared to the WT-SLC8A1 and WT-SLC8A1+mimic NC groups, the fluorescence value in the WT-SLC8A1+miR-466c group declined significantly ( $P < 0.05$ ). After mutation was induced on the binding site, there was no significant difference in the fluorescence value between the mut-SLC8A1+mimic NC and mut-SLC8A1+miR-466c group. This data indicated that miR-466c interacted with SLC8A1 (Figure 6(c)).

**3.6. lncRNA 93358 Knockdown Improves Cardiac Function in MI Rats.** Further, we investigated the effect of lncRNA 93358 expression on cardiac function in MI rats. Echocardiographic results (Figure 7) showed that IVSd, LVIDd, and LVIDs were significantly increased, while LVFE, LVFS, HR, and CO were significantly decreased in the model rats compared with the control group ( $P < 0.05$ ). Interference with lncRNA 93358 expression significantly reduced IVSd, LVIDd, and LVIDs and increased LVFE and LVFS in MI rats. There was no significant difference in LVPWd and LVPWs between the groups ( $P > 0.05$ ).

The infarcted myocardium appeared white after TTC staining, and the percentage of infarct area in each group was calculated. As shown in Figure 8(a), compared to the model and NC groups, the infarct area in the lncRNA 93358-shRNA group

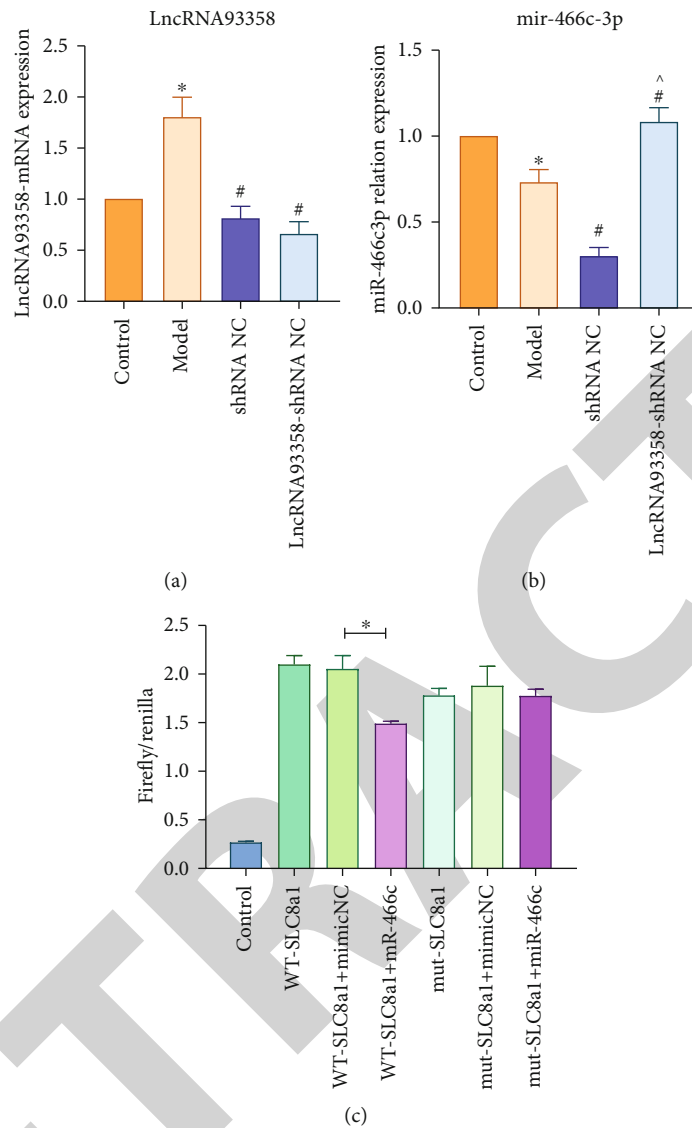


FIGURE 6: The regulation axis of lncRNA 93358/miRNA/SLC8A1. (a and b) The expression of lncRNA 93358 and miR-466c-3p in the four rat myocardial tissues was measured by RT-qPCR. \* $P < 0.05$  vs. control, # $P < 0.05$  vs. model, and ^ $P < 0.05$  vs. NC group. (c) The binding between SLC8A1 and miR-466c-3p was measured by dual-luciferase reporter. \* $P < 0.05$ .

declined significantly, indicating that the infarction could be ameliorated by the knockdown of lncRNA 93358.

In the control group, myocardial cells were neatly arranged, clearly defined, and evenly stained, indicating that the myocardial cells were in good condition. Myocardial cells in the model group and NC group were widely dissociated, necrotic and, severely damaged, and the cells showed incomplete contour. In the shRNA group, myocardial cells underwent necrosis, which was less than that in the model group and NC group. Although myocardial cells were damaged, there were still large areas of live myocardial cells (Figure 8(b)).

**3.7. lncRNA 93358 Knockdown Inhibits Apoptosis in MI Rat Cardiomyocytes.** As shown in Figure 9(a), compared with the control group, a large number of apoptosis cells was observed in the model group and NC group with green fluorescence. However, the green fluorescence was significantly

reduced in the shRNA group, indicating that apoptotic cells were significantly reduced after the knockdown of lncRNA 93358.

In addition, the apoptosis-related protein Bax in myocardial cells in the model group and NC group was significantly increased compared with the control group, while the expression of Bcl2 and SLC8A1 was significantly decreased. However, the expression levels of Bax, Bcl2, and SLC8A1 were significantly reversed by the knockdown of lncRNA 93358 (Figures 9(b) and 9(c)).

**4. Discussion**

In the present study, DE lncRNA in MI rats was screened by high-throughput sequencing, namely, lncRNA 93358. It was predicted that lncRNA 93358 might interact with miR-34a-3p, miR-125b-2-3p, and miR-466c-3p by the miRDB method.

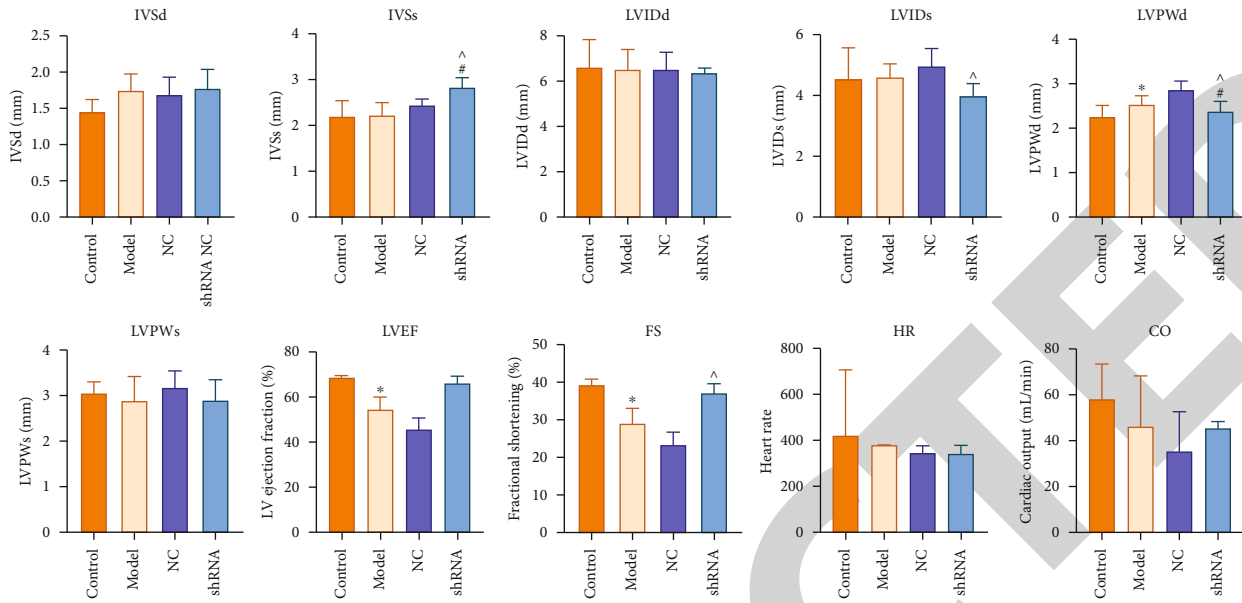


FIGURE 7: The results of cardiac ultrasound in rats. \* $P < 0.05$  vs. control, # $P < 0.05$  vs. model, and ^ $P < 0.05$  vs. NC group. IVSd: interventricular septum size (diastole); IVSs: interventricular septum size (systole); LVIDd: left ventricular internal size (diastolic); LVIDs: internal size of left ventricle (systole); LVPWd: left ventricular posterior wall size (diastolic); LVPWs: posterior wall size of left ventricle (systole); EF: left ventricular ejection fraction (LVEF); FS: percentage of left ventricular fraction shortening; HR: heart rate; CO: cardiac output.

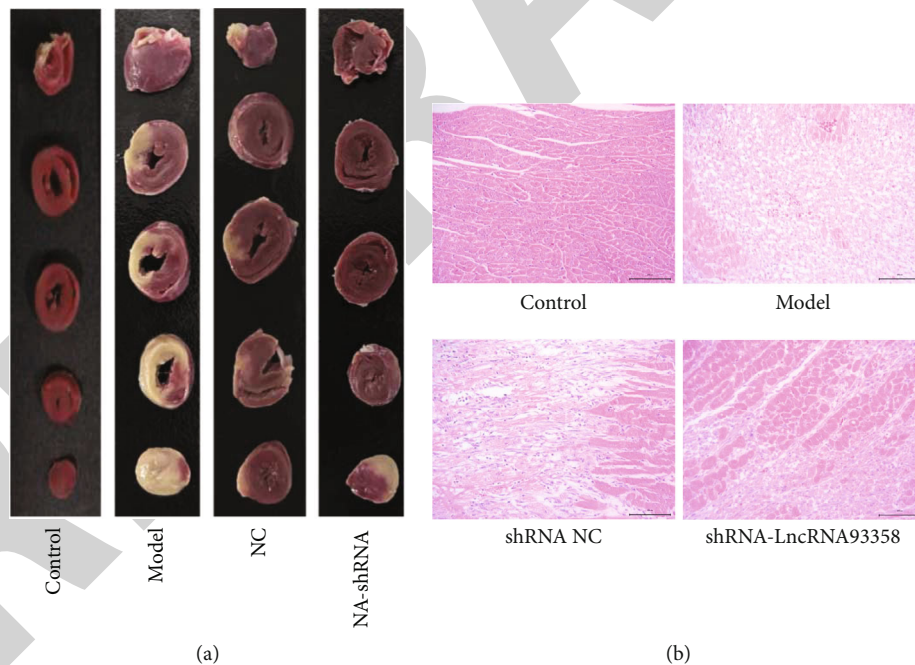


FIGURE 8: Pathological changes in the heart of rats in each group. (a) TTC staining of rat heart. (b) The images of HE staining.

SLC8A1 and TRPS1 were predicted as a target of these miRNAs. lncRNA 93358 regulated the expression of SLC8A1 and participated in the MI process by acting as a competitive endogenous RNA (ceRNA) through absorbing and inhibiting miRNA function.

As further research develops, lncRNAs have proven to play an important role in the occurrence and development of tumors and cardiovascular diseases [11, 12]. lncRNA

aggregates in specific regions near transcription sites and forms lncRNA-protein complexes to organize nuclear structure, modify chromatin state, participate in gene expression regulation, and stabilize subcellular structure and protein complexes [13, 14]. Current sequencing results indicate that a variety of lncRNAs play a critical role in the development of heart diseases. For example, the expression level of lncRNA MIAT is increased and maintains a high level after

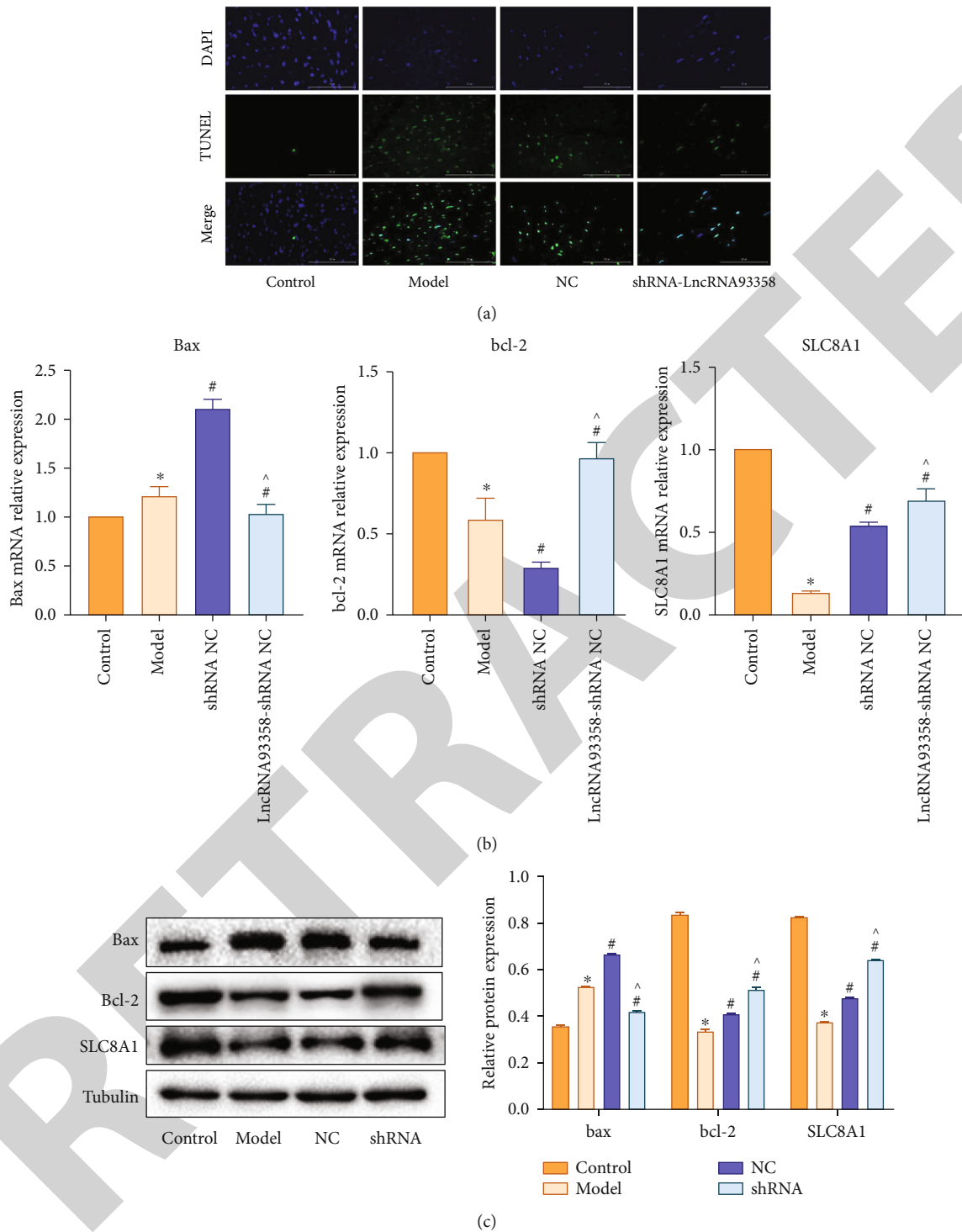


FIGURE 9: Effect of lncRNA 93358 on apoptosis in myocardial infarction rat cardiomyocytes. (a) The apoptosis of myocardial tissues was determined by TUNEL assay. (b and c) The expression level of Bax, Bcl-2, and SLC8A1 in the myocardial cells was determined by RT-qPCR (b) and Western blotting (c). \* $P < 0.05$  vs. control, # $P < 0.05$  vs. model, and ^ $P < 0.05$  vs. NC group.

myocardial death [15]. lncRNA CCRR improves cardiac conduction and inhibits arrhythmias by upregulating Cx43 in the myocardial gap [16]. Downregulating lncRNA MEG3 and lncRNA H19 significantly reduces the size of MI and myocardial cell apoptosis [17, 18]. In the present study, lncRNA93358 was screened out by high-throughput

sequencing, which was highly expressed in MI rats. In addition, current studies indicate that myocardial cell apoptosis plays an important role in ventricular remodeling and heart failure caused by MI in the early stage of MI. Blocking MI is of great significance for inhibiting myocardial injury [19–21]. Therefore, the present study continued to explore



the effects of lncRNA93358 on myocardial apoptosis in MI rats, and cardiac ultrasound results showed that downregulation of lncRNA93358 improved cardiac function in MI rats. The results of HE staining, TTC staining, and TUNEL assay showed that downregulation of lncRNA93358 expression significantly improved the myocardial pathological morphology of MI rats, reduced the myocardial infarction area and myocardial cell apoptosis rate, downregulated Bax, and upregulated Bcl-2. These results suggested that the knockdown of lncRNA93358 significantly ameliorated MI in rats.

The solute carrier (SLC) superfamily is a family of membrane proteins capable of transporting solutes. More than 400 members of the SLC family have been identified, encoding passive transporter, ion complex transporter, and exchanger genes, respectively. The sequence identity of SLC superfamily members is about 20%, with diverse functions. For example, SLC6A3, an amine transporter, plays an important role in signal transmission in the nervous system and provides targets for the design of a variety of drugs [22]. SLC22A20, an organic anion transporter, mainly mediates the transmembrane input and output of organic anions [23]. SLC8A1 is a calcium ion exchanger that is expressed in high abundance in cardiomyocytes. SLC8A1 mainly mediates the exchange between  $\text{Ca}^{2+}$  and  $\text{Na}^+$ , and its memory loss or mutation may lead to arrhythmia and abnormal cardiac contraction, which further induces cardiac diseases such as heart failure and ischemic injury [24, 25]. Studies on SLC8A1 are mainly focused on diseases such as arrhythmia, diabetes, and cancer, which are mainly mediated by the working mode of  $\text{Ca}^{2+}$  entry and  $\text{Na}^+$  excretion [26]. lncRNA-SLC8A1-AS1 alleviates myocardial injury, inhibits the release of pro-inflammatory factors, and reduces infarct size by regulating SLC8A1 and activating the CGMP-PKG signaling pathway, which finally protects the myocardium from injury [27]. In the present study, the expression of SLC8A1 was significantly decreased in MI rats, which was greatly reversed by the knockdown of lncRNA 93358, accompanied by the ameliorated MI in rats. In addition, the dual-luciferase reporter assay results showed that SLC8A1 interacted with miR-466c, indicating that lncRNA93358 was involved in the MI process by inhibiting the function of miR-466c and regulating the expression of SLC8A1.

The injury of cardiomyocytes after MI is an important part of mitochondrial apoptosis. As the antiapoptotic molecule Bcl-2 continues to decrease, the proapoptotic molecule Bax gradually increases, resulting in a large amount of cytochrome C in the mitochondria entering the cytoplasm. The reaction causes procaspase-3 to be cleaved into cleaved-caspase-3 to induce apoptosis. We found that silencing lncRNA 93358 in MI rats can inhibit rat cardiomyocyte apoptosis, which may be a potential target for the treatment of myocardial injury, but more experiments are needed to prove it.

In conclusion, lncRNA 93358 in MI rats was obtained by high-throughput sequencing in this study. Downregulation of lncRNA93358 suppressed the apoptosis of myocardial cells in MI rats, which was achieved by inhibiting the function of miR-466c and regulating the expression of SLC8A1. However, the feedback regulation of miR-466c and SLC8A1 needs to be further studied for our future work.

## Data Availability

The data used to support the findings of this study are available from the corresponding author upon request.

## Ethical Approval

The animal experiments described in this study were authorized by the Committee of the First Affiliated Hospital of Gannan Medical University (No. LLSC-20201022011).

## Conflicts of Interest

The authors declare that they have no conflict of interest.

## Acknowledgments

This study was supported by the doctoral research start-up project of The First Affiliated Hospital of Gannan Medical University (No. QD034).

## References

- [1] D. Jenča, V. Melenovský, J. Stehlik et al., "Heart failure after myocardial infarction: incidence and predictors," *ESC Heart Fail*, vol. 8, no. 1, pp. 222–237, 2021.
- [2] V. Ruddox, I. Sandven, J. Munkhaugen, J. Skattebu, T. Edvardsen, and J. E. Otterstad, "Atrial fibrillation and the risk for myocardial infarction, all-cause mortality and heart failure: a systematic review and meta-analysis," *European Journal of Preventive Cardiology*, vol. 24, no. 14, pp. 1555–1566, 2017.
- [3] N. G. Frangogiannis, "Pathophysiology of myocardial infarction," *Comprehensive Physiology*, vol. 5, no. 4, pp. 1841–1875, 2015.
- [4] M. Smit, A. R. Coetzee, and A. Lochner, "The pathophysiology of myocardial ischemia and perioperative myocardial infarction," *Journal of Cardiothoracic and Vascular Anesthesia*, vol. 34, no. 9, pp. 2501–2512, 2020.
- [5] S. Ghafouri-Fard, T. Azimi, and M. Taheri, "Myocardial infarction associated transcript (MIAT): review of its impact in the tumorigenesis," *Biomedicine & Pharmacotherapy*, vol. 133, p. 111040, 2021.
- [6] M. Kowara, S. Borodzicz-Jazdzzyk, K. Rybak, M. Kubik, and A. Cudnoch-Jedrzejewska, "Therapies targeted at non-coding RNAs in prevention and limitation of myocardial infarction and subsequent cardiac remodeling-current experience and perspectives," *International Journal of Molecular Sciences*, vol. 22, no. 11, p. 5718, 2021.
- [7] S. F. Huang and W. C. Ye, "lncRNA MALAT1 facilitated the progression of myocardial infarction by sponging miR-26b," *International Journal of Cardiology*, vol. 335, p. 24, 2021.
- [8] B. Li and Y. Wu, "lncRNA TUG1 overexpression promotes apoptosis of cardiomyocytes and predicts poor prognosis of myocardial infarction," *Journal of Clinical Pharmacy and Therapeutics*, vol. 45, no. 6, pp. 1452–1456, 2020.
- [9] M. I. Love, W. Huber, and S. Anders, "Moderated estimation of fold change and dispersion for RNA-seq data with DESeq2," *Genome Biology*, vol. 15, no. 12, p. 550, 2014.
- [10] D. W. Huang, B. T. Sherman, Q. Tan et al., "DAVID bioinformatics resources: expanded annotation database and novel

## *Retraction*

# **Retracted: Effect of Early Low-Calorie Enteral Nutrition Support in Critically Ill Patients: A Systematic Review and Meta-analysis**

### **BioMed Research International**

Received 9 February 2023; Accepted 9 February 2023; Published 14 February 2023

Copyright © 2023 BioMed Research International. This is an open access article distributed under the Creative Commons Attribution License, which permits unrestricted use, distribution, and reproduction in any medium, provided the original work is properly cited.

*BioMed Research International* has retracted the article titled “Effect of Early Low-Calorie Enteral Nutrition Support in Critically Ill Patients: A Systematic Review and Meta-analysis” [1] due to concerns that the peer review process has been compromised.

Following an investigation conducted by the Hindawi Research Integrity team [2], significant concerns were identified with the peer reviewers assigned to this article; the investigation has concluded that the peer review process was compromised. We therefore can no longer trust the peer review process and the article is being retracted with the agreement of the editorial board.

### **References**

- [1] Q. Jiang and T. Xu, “Effect of Early Low-Calorie Enteral Nutrition Support in Critically Ill Patients: A Systematic Review and Meta-analysis,” *BioMed Research International*, vol. 2022, Article ID 7478373, 8 pages, 2022.
- [2] L. Ferguson, “Advancing Research Integrity Collaboratively and with Vigour,” 2022, <https://www.hindawi.com/post/advancing-research-integrity-collaboratively-and-vigour/>.

## Review Article

# Effect of Early Low-Calorie Enteral Nutrition Support in Critically Ill Patients: A Systematic Review and Meta-analysis

Qidong Jiang and Tao Xu 

Department of Critical Care Medicine, The Affiliated Hospital of Southwest Medical University, Luzhou, China

Correspondence should be addressed to Tao Xu; 2172396208@qq.com

Received 17 May 2022; Revised 11 June 2022; Accepted 14 June 2022; Published 4 July 2022

Academic Editor: Dinesh Rokaya

Copyright © 2022 Qidong Jiang and Tao Xu. This is an open access article distributed under the Creative Commons Attribution License, which permits unrestricted use, distribution, and reproduction in any medium, provided the original work is properly cited.

**Objective.** The purpose of this research was to rigorously assess the impact of early low-calorie enteral feeding supplementation in critically sick patients. **Methods.** PubMed, Embase, Web of Science, Cochrane Central Register of Controlled Trials, Cumulative Index to Nursing and Allied Health Literature, and Physiotherapy Evidence Database were searched for randomized controlled trials related to enteral nutrition support of critically ill patients (retrieval time was limited to June 30, 2021); data were extracted after screening the literature, and the quality of meta-analysis was evaluated. **Results.** When compared to adequate caloric enteral nutrition support, early low-caloric enteral nutrition support reduces the incidence of intolerance to nutrition support (MD = 0.60, 95 percent CI: -0.18 to 1.39,  $P = 0.13$ ) and the insulin dose during enteral nutrition support (MD = -17.21, 95 percent CI: -19.91 to -14.51,  $P = 0.00001$ ). However, it had no effect on intensive care unit (ICU) treatment duration (MD = 0.60, 95 percent CI: -0.18 to 1.39,  $P = 0.13$ ), in-hospital mortality (MD = 0.60, 95 percent CI: -0.18 to 1.39,  $P = 0.13$ ), or infection incidence (OR = 1.00, 95 percent CI: 0.85, 1.19,  $P = 0.98$ ). **Conclusion.** When compared to sufficient caloric enteral nutrition support, early low-calorie enteral nutrition support lowers the risk of severe illness. The rate of intolerance to nutritional assistance and the decrease in insulin dosage supplied had no effect on the length of ICU therapy, patient death, or infection incidence.

## 1. Introduction

Critical sickness is a disease that has an abrupt start, is severe, is quickly changing, and is unintentional, resulting in lasting repercussions [1]. The clinical needs for treating and caring for critically sick patients are exceedingly high. Critically ill individuals have an exceedingly poor clinical state; endure life-threatening complications, trauma, and stress; and have a high metabolic rate for extended periods of time; as a result, their physical function and immunity may swiftly diminish [2]. Meanwhile, as a result of the disease's impacts, many patients may develop swallowing difficulties and become unable to eat; the nutritional condition of critically sick patients is generally poor [3]. Early enteral nutrition assistance is essential to enhance patients' nutritional status. The optimum timing of enteral feeding for critically sick patients must also be decided throughout the course of early enteral nutrition [4]. In patients with active

upper gastrointestinal bleeding, for example, enteral nutrition should be postponed; once the bleeding ceases, enteral nutrition therapy may be started [5]. To address the nutritional demands of individuals suffering from diarrhea, enteral nutrition therapy should be administered as soon as possible [6]. Problems such as ileus, malabsorption, and gastrointestinal bleeding should be evaluated before providing enteral nutritional assistance [7].

The transnasogastric and transnasoenteric channels comprise the majority of the early enteral nutrition support pathway [8]. The feeding channel must be chosen depending on the patient's real state during the selection process; for example, patients with more severe reflux aspiration may utilize a nasoenteric tube; in general, nasogastric tube feeding is the major feeding approach [9]. Some research on early enteral feeding in critically sick patients has shown that nasoenteric tube insertion is difficult, and the tube is softer and more prone to clogging; hence, the primary kind of

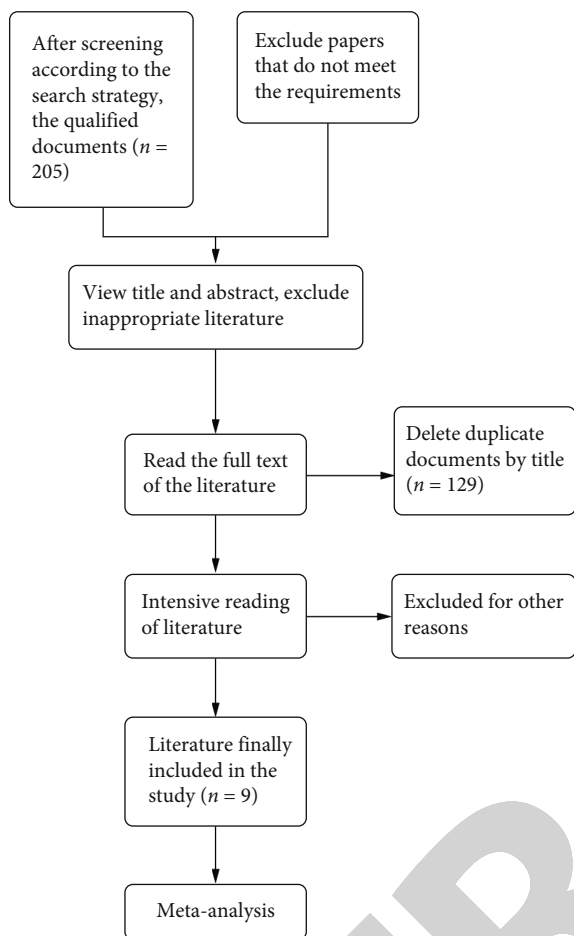


FIGURE 1: Screening procedure for the included literature.

nasogastric tube is used. Whatever feeding route is used, it is critical to ensure the patency of the gastric tube, nutritional fluids, and appropriate food distribution based on the patient's absorption status during feeding; oral care should be performed, and the nasogastric tube should be flushed with warm water after each feeding [10]. Critically ill patients are in critical condition; in order to ensure optimal health and meet their nutritional needs, each critically ill patient should be placed in a single room, and early enteral nutrition should be implemented in accordance with the practice guidelines for nutrition in critically ill patients. For example, while giving enteral nutrition, feeding should be started initially and progressively raised depending on the patient's need and tolerance level; subsequently, the concentration and dosage of the nutrition solution should be gradually increased. The pace of instillation and volume of nutrition should be carefully adjusted at any moment based on the patient's nutritional status, tolerance, and clinical symptoms to ensure that the patient's nutritional demands are satisfied [11].

The guidelines for the provision and evaluation of nutritional support therapy for critically ill adult patients in the United States, as well as the Chinese Medical Association's guidelines for perioperative nutritional support for adults,

both recommend enteral nutritional support for critically ill patients 24-48 hours after admission and emphasize that implementing adequate calorie nutritional support for critically ill patients is beneficial to reduce complications. However, as compared to insufficient caloric intake in recent years, optimal caloric intake in critically ill patients did not improve outcomes; furthermore, increasing the patients' caloric intake increased the risk of ventilator-associated pneumonia [12]. Due to the lack of previous research on the effectiveness of early low-calorie enteral nutrition support in critically ill patients, this systematic review set out to look into the effectiveness of early low-calorie enteral nutrition support in this patient population and determine its feasibility going forward [13].

## 2. Materials and Methods

**2.1. Literature Search Strategy.** The terms "critically ill/critically ill/ICU," "enteral nutrition," "low heat card/hypocaloric/low-energy/restricted heat card/caloric restriction/caloric restriction/energy restriction," and "normal heat card/normocal/normal energy/caloric restriction/caloric restriction/caloric restriction/energy restriction" were used to search for RCTs, random assignments, and randomization group/clinical-controlled trials/clin.

**2.2. Literature Inclusion and Exclusion Criteria.** The literature inclusion and exclusion criteria are the following: (1) randomized controlled trials (RCTs) published in English; (2) studies involving participants aged 18 years and critically ill patients requiring enteral nutrition support; (3) studies involving the early implementation of enteral nutrition support (24-48h from admission to the intensive care unit, within 36h from surgery, and within 36h from admission, enteral nutrition support provided for 14 days); and (4) studies involving the provision of low-heat enteral nutrition. On the other hand, duplicate studies were removed from consideration.

**2.3. Literature Screening and Data Extraction.** After two scientists independently evaluated the aforementioned resources and read the literature, the material was vetted based on inclusion vs. exclusion criteria in order to determine whether or not it should be included. In situations when the two investigators could not come to an agreement, they either talked it out until they did or brought in a third investigator. We obtained a variety of information, including the name of the original author, the publication date of the literature, the demographic characteristics of the research participants, baseline comparability, interventions, sample size, and outcome measures.

**2.4. Quality Assessment of Included Studies.** The following Cochrane Handbook judgment criteria were used to evaluate the quality of the literature: (1) if an RCT was utilized, (2) whether allocation concealment was employed, (3) whether blinding was used, (4) whether withdrawals or losses to follow-up were recorded, (5) whether an intention-to-treat analysis was performed, and (6) whether baseline comparability compliance was reached. The degree of quality of the



TABLE 1: Baseline characteristics of all included studies.

Study Author (year)	Object	Sample		Index
		Intervene	Control	
Arabi (2011)	Patients expected to stay in ICU for >2 D	120	120	Mortality, ICU treatment time, and infection rate during hospitalization
Rice (2011)	Patients with acute respiratory failure with mechanical ventilation time $\geq$ 72 h	98	102	Mortality, ICU treatment time, and infection rate during hospitalization
Rice (2012)	Patients requiring mechanical ventilation within 48 hours of acute lung injury	508	492	ICU treatment time, patient mortality during hospitalization, incidence of infection, and days without mechanical ventilation
Rugeles (2013)	ICU adult critically ill patients	40	40	ICU treatment time, insulin treatment amount, 48 h $\Delta$ SOFA, mechanical ventilation time, and incidence of hyperglycemia
Charles (2014)	Patients expected to stay in surgical ICU for >2 D	41	42	ICU treatment time, patient mortality during hospitalization, incidence of infection, and amount of insulin treatment
Arabi (2015)	Patients expected to stay in ICU > 3 D	448	446	During hospitalization, the mortality of patients, the incidence of intolerance to enteral nutrition support, the incidence of infection, the number of days without mechanical ventilation, and the amount of insulin treatment
Petros (2016)	Patients expected to stay in ICU > 3 D	46	54	The incidence of enteral nutrition intolerance, infection, and mortality during hospitalization
Rugeles (2016)	Patients admitted to ICU and expected enteral nutrition time $\geq$ 96 h	60	60	ICU treatment time, patient mortality during hospitalization, 48 h $\Delta$ SOFA, 96 h $\Delta$ SOFA, mechanical ventilation time, and incidence of hyperglycemia
Zhang (2017)	Severe adult patients in internal medicine	92	91	Mortality, incidence of enteral nutrition intolerance, duration of mechanical ventilation, length of hospital stay, incidence of hypoglycemia, and amount of insulin treatment during hospitalization

literature was divided into three categories: Grade A indicates a low degree of bias and that all six quality criteria were met, Grade B indicates a moderate degree of bias and that some of the quality requirements were met, and Grade C indicates that all six quality criteria were not met. Two investigators who have participated in evidence-based nursing training independently evaluated the quality of the literature.

**2.5. Statistical Methods.** The RevMan 5.3 software was utilized to carry out the meta-analysis; the odds ratio (OR) was utilized to express dichotomous data, while the mean difference (MD) or standard mean difference (SMD) was utilized to express continuous data obtained from an efficacy analysis; each effect size was expressed along with the 95 percent confidence interval (CI). If there was no heterogeneity in the findings of the study ( $I^2 = 50$  percent,  $P > 0.1$ ), then the fixed-effects model was used. If there was heterogeneity in the findings of the research ( $I^2 > 50$  percent,  $P > 0.1$ ), then the root cause of the heterogeneity was investigated, and the random-effects model was used.

### 3. Results

**3.1. Inclusion of the Literature.** Figure 1 depicts the literature screening method and findings. Figure 1 depicts the detection of 205 articles published in English. After removing

duplicates, titles, and abstracts, 59 articles were found. After reviewing the complete text of 59 publications, 9 RCT articles were included. Figure 1 depicts the screening procedure for the included literature.

**3.2. Baseline Characteristics and Evaluation of the Quality of All Included Literatures.** Table 1 shows the baseline characteristics of all included studies. Nine publications with 1,212 research participants (614 in the test group and 598 in the control group) were published in English; the intervention procedures and outcome measures in these studies were fully explained. Figure 2 shows the quality assessment findings for all included studies.

### 3.3. Meta-analysis

**3.3.1. Duration of Patient's Hospital Stay.** Six randomized controlled trials (RCTs) with a total of 1,723 study participants reported on ICU duration of stay. Because the pooled findings revealed acceptable between-study heterogeneity ( $P = 0.26$ ,  $I^2 = 55$  percent), the fixed-effects model was chosen. The duration of ICU stay did not vary significantly between the two patient groups (MD = 0.60, 95 percent CI : -0.18 to 1.39,  $P = 0.13$ ) (Figure 3).



	Random sequence generation (selection bias)	Allocation concealment (selection bias)	Blinding of participants and personnel (performance bias)	Blinding of outcome assessment (detection bias)	Incomplete outcome data (attrition bias)	Selective reporting (reporting bias)	Other bias
Arabi 2011	+	+		+	+	+	+
Arabi 2015	-		+	+	+	+	+
Charles 2014	+	+	+	+	+	+	+
Petros 2016	+	+	+		+	+	+
Rice 2011	+	+	-	+	+	+	-
Rice 2012	+	+	-	+	+	+	
Rugeles 2013	+	+	+		+	+	
Rugeles 2016	+	+	+		-	+	
Zhang 2015	+	+	+	+	+	+	+

FIGURE 2: Literature quality assessment.

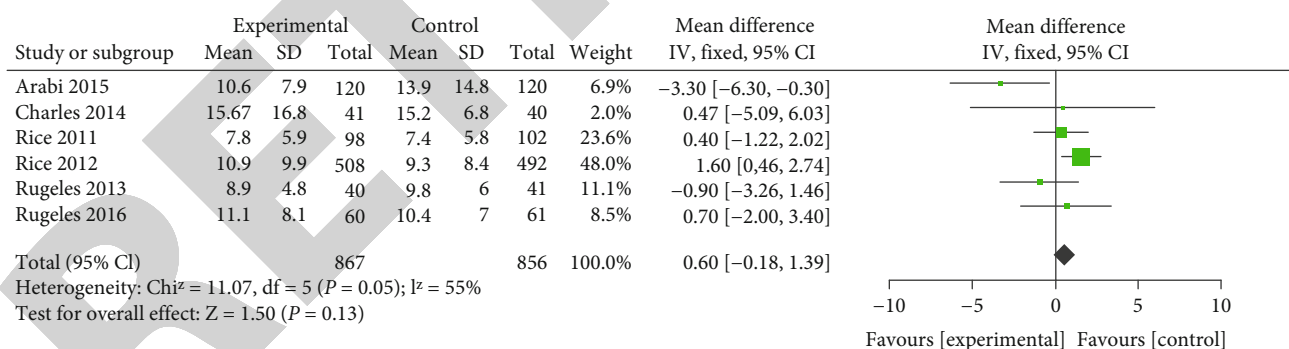


FIGURE 3: Duration of patient’s hospital stay.

3.3.2. *Patient Mortality.* An in-hospital death rate of 2,801 individuals was observed in eight RCTs. Because the pooled findings revealed acceptable between-study heterogeneity ( $P = 0.74, I^2 = 0\%$ ), the fixed-effects model was chosen. There was no significant difference in in-hospital mortality between the two groups (OR = 0.94, 95 percent CI : 0.79 to 1.11,  $P = 0.46$ ) (Figure 4).

3.3.3. *Incidence of Infection.* Infection was reported in seven RCTs with a total of 2,693 participants. Because the pooled findings revealed acceptable between-study heterogeneity

( $P = 0.21, I^2 = 3$  percent), the fixed-effects model was chosen. The incidence of infection did not change significantly between the two patient groups (OR = 1.00, 95 percent CI: 0.85, 1.19,  $P = 0.98$ ) (Figure 5).

3.3.4. *Incidence of Intolerance to Enteral Nutrition.* In three randomized controlled trials with 1,177 subjects, the incidence of enteral nutritional intolerance was documented. The random-effects model was utilized to pool the findings, which revealed study heterogeneity ( $P = 0.0007, I^2 = 86$  percent). The incidence of intolerance to nutritional

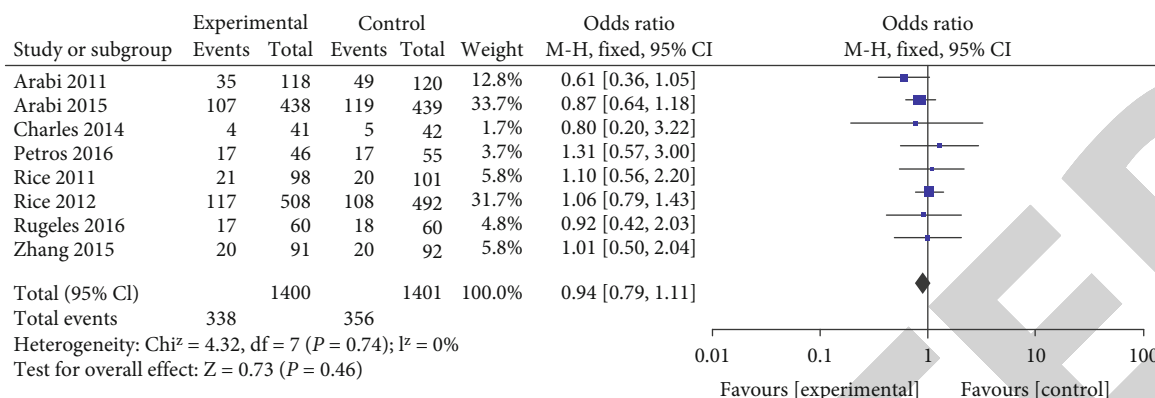


FIGURE 4: Patient in-hospital mortality.

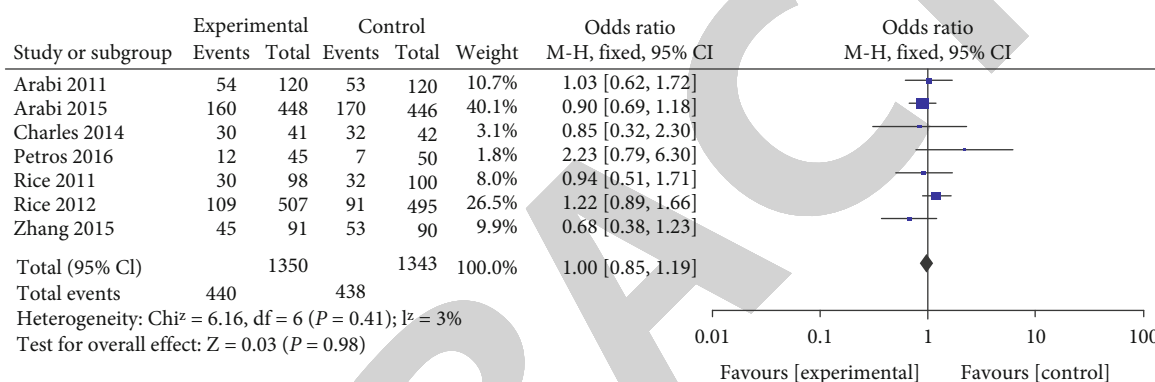


FIGURE 5: Patient incidence of infection.

supplementation differed significantly between the two patient groups (OR = 0.61, 95 percent CI: 0.48, 0.77,  $P < 0.0001$ ) (Figure 6).

3.3.5. *Insulin Dose during the Course of Nutritional Therapy.*

The dosage of insulin delivered over the duration of nutritional treatment was reported in four RCTs with 1,241 participants, and the research comprised 1,241 patients. Because the pooled findings revealed acceptable between-study heterogeneity ( $P < 0.00001$ ,  $I^2 = 97$  percent), the fixed-effects model was chosen. The dosage of insulin delivered during nutritional treatment differed significantly between the two groups (MD = -17.21, 95 percent CI: -19.91 to -14.51,  $P < 0.00001$ ) (Figure 7).

4. Discussion

Sugars, proteins, essential and nonessential amino acids (or peptides), lipids, vitamins, minerals, and dietary fiber are all necessary nutritional components of enteral feeding. The matrix composition of various formulation types varies [14]. Product formulation based on patient needs, which varied in formulation content ratio and ingredient focus ratio, resulted in the development of a wide range of nutritional products, including basic nutrition formulas, special nutrition formulas (for patients with hyperglycemia, liver disease, kidney disease, tumor, and so on), high-energy for-

mulas, high-mineral formulas, and immunomodulatory or dietary fiber formulas [15]. The nutritional base, the patient’s organ and illness condition, and protein needs all influence the choice of enteral formula. The energy density in enteral formula ranges from 0.5 to 2.0 kcal/ml (1 kcal = 4.184 kJ), which can be tailored to the individualized needs of different patients; the initial volume of enteral formula can range from 0.5 to 1.0 kcal/ml, and it can be increased to 1.5–2.0 kcal/ml to meet the energy needs of most critically ill patients [16]. The features of enteral formulations may have a direct impact on their clinical use and patient acceptability. The following variables must be addressed throughout the selecting process: (1) Osmolality: there were significant variances in the osmolality of the various enteral formulations. The enteral formulation’s constituents all contributed to the production of osmotic pressure [17, 18]. The electrolyte is the most important component and influencer in the creation of osmotic pressure. Large molecular sugars, such as polysaccharides and oligosaccharides, have a lower osmolarity than tiny molecular sugars, such as glucose. Sugar infusion and decomposition had a stronger influence on osmotic pressure. Protein has a big molecular weight and has minimal influence on osmotic pressure, but amino acids have a tiny molecular weight and have a substantial effect on osmotic pressure. Excessive osmolality may have an effect on the patient’s GI tract in principle; nevertheless, clinical hyperosmolar formulations

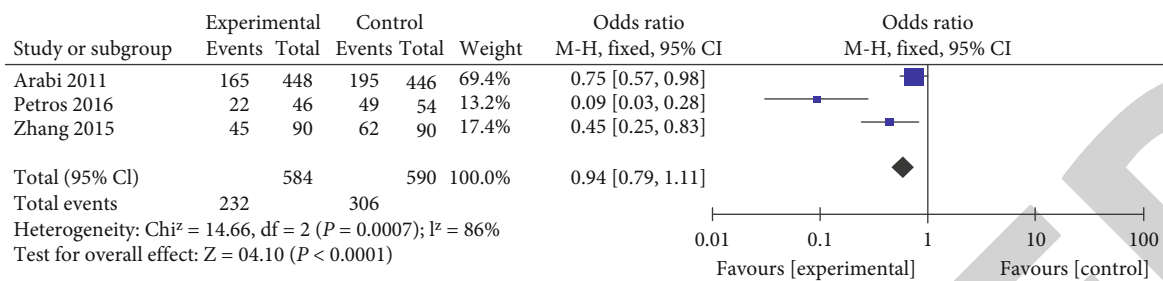


FIGURE 6: Incidence of intolerance to enteral nutrition.

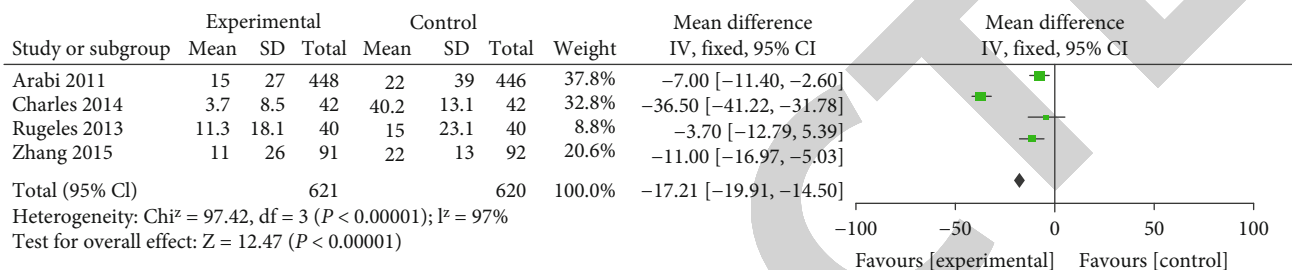


FIGURE 7: Insulin dose during the course of nutritional therapy.

(>300 mOsm/L) do not offer a clinical concern under normal settings since hyperosmolality can be caused by gastrointestinal dilution [19]. However, in individuals with predisposing or synergistic variables that induce diarrhea (e.g., low protein levels, inflammation, or pharmacological side effects), osmolality in a nutritional formula may be associated with diarrhea development. (2) Solubility: the nutritional formula may be made into a powder, solution, or suspension. When all of the components are combined, a range of products are formed that may be employed in various populations and patients with varying calorie needs. The pH varied from 4 to 7, indicating a moderate level. Despite the above results, research on the calorie content of nutritional solutions is scarce [20].

Scholars have presented the “hypocaloric hypothesis” in recent years, which states that energy supply should be lowered during the early stages of the illness (during the first week after admission), although the particular recommended calories vary and range between 10 and 20 kcal/kg/day [21]. The following is the mechanism: a low-heat diet may increase phagocytosis, impact metabolism, hormone levels, and the inflammatory response and play an important role in defense and immunological responses. When compared to appropriate calorie nutrition treatment, early low-calorie enteral nutrition therapy reduced the prevalence of nutritional therapy intolerance in critically sick patients. This could be due to the relatively lower total intake of nutrient solution during the course of enteral nutrition therapy with a low incidence of fever, the short duration of enteral nutrition support, the slow infusion rate, a greater tendency to tolerate the feeding, and the possibility of developing intolerant situations such as diarrhea, constipation, gastric retention, and aspiration [22]. Although several studies have shown that a reduced calorie diet improves patient out-

comes, not all of their findings are consistent [23]. This is due to the fact that the hypermetabolic response in critically sick patients during the first week of hospitalization is characterized by greatly increased protein metabolism and nitrogen loss, resulting in a negative nitrogen balance, as well as low carbohydrate levels and fat loss [24]. As a consequence, whether a suitable amount of protein (>1.5–2.0 g/kg/day) is provided based on ideal body mass determines the effectiveness of a low-calorie diet. When compared to adequate caloric nutrition support, early enteral low-calorie nutrition support did not extend ICU stays or increase in-hospital mortality or infection rates [25, 26]. This might be because appropriate dietary assistance has little effect on metabolic processes or immunological responses in critically sick individuals.

## 5. Limitations

There are obvious limitations to this systematic review. (1) Only published RCTs were included; owing to language restrictions, only Chinese and English literatures were retrieved, and perhaps, incomplete literature was included in the review. (2) Because just nine RCTs were included, the volume of literature was limited, the quality grade was primarily B, and credibility was harmed. (3) Because the majority of the included studies were conducted in the Western population and only one in the Chinese population and the protocol and duration of early enteral nutrition support in each study were not identical, a large-scale study is required to confirm whether early enteral nutrition support is applicable in critically ill patients in China. (4) Because this systematic review comprised just ten papers, a funnel plot analysis was not done; hence, a publication bias may exist.

## 6. Conclusions

Early low caloric enteral nutrition support, when compared to adequate caloric enteral nutrition support, reduces the incidence of intolerance to nutritional support and reduces the dose of insulin required but does not prolong ICU stay, increase patient mortality, or increase the incidence of infection; early enteral nutrition support can be provided in critically ill patients. All nine included publications said that ensuring protein intake (1.2–2.0 g/kg/day) was a necessity for the early introduction of enteral nutrition low-heat nutrition support, which was consistent with the suggestion in national and international nutrition support recommendations. Various researches have shown conflicting findings when it comes to the length of an early enteral low-calorie nutrition assistance program. In two trials, the length of the enteral nutrition low-fever nutrition support program was 14 days, 6 days in another two studies, 4 days in one research, and 7 days in the other four studies. Finally, if enough protein intake is ensured, a low-calorie enteral nutrition assistance regimen for critically sick patients may be commenced between 4 and 14 days after admission. Because the number of included studies is limited, more high-quality, large-sample, and multicenter RCTs should be conducted in the future to standardize the intervention methods, contents, timing, and evaluation indicators of early low-fever enteral nutrition support for critically ill patients and to strengthen and validate the evidence on its outcomes.

## Conflicts of Interest

We define that all authors have not been involved in a set of conditions affecting our professional judgment concerning the validity of research, and we are not influenced by financial gain.

## References

- [1] G. Geller, E. D. Branyon, L. K. Forbes et al., "ICU-RESPECT: an index to assess patient and family experiences of respect in the intensive care unit," *Journal of Critical Care*, vol. 36, pp. 54–59, 2016.
- [2] M. L. Mitchell, F. Coyer, S. Kean, R. Stone, J. Murfield, and T. Dwan, "Patient, family-centred care interventions within the adult ICU setting: an integrative review," *Australian Critical Care*, vol. 29, no. 4, pp. 179–193, 2016.
- [3] D. Lane, M. Ferri, J. Lemaire, K. McLaughlin, and H. T. Stelfox, "A systematic review of evidence-informed practices for patient care rounds in the ICU," *Critical Care Medicine*, vol. 41, no. 8, pp. 2015–2029, 2013.
- [4] M. Mermiri, G. Mavrovounis, D. Chatzis et al., "Critical emergency medicine and the resuscitative care unit," *Acute Crit Care*, vol. 36, no. 1, pp. 22–28, 2021.
- [5] J. R. Smith and F. S. Cole, "Patient safety: effective interdisciplinary teamwork through simulation and debriefing in the neonatal ICU," *Critical Care Nursing Clinics of North America*, vol. 21, no. 2, pp. 163–179, 2009.
- [6] K. Allen and L. Hoffman, "Enteral nutrition in the mechanically ventilated patient," *Nutrition in Clinical Practice*, vol. 34, no. 4, pp. 540–557, 2019.
- [7] D. L. Nguyen, "Guidance for supplemental enteral nutrition across patient populations," *The American Journal of Managed Care*, vol. 23, 12 Suppl, p. S210-210S219, 2017.
- [8] H. Zhang, Y. Wang, S. Sun et al., "Early enteral nutrition versus delayed enteral nutrition in patients with gastrointestinal bleeding: a PRISMA-compliant meta-analysis," *Medicine (Baltimore)*, vol. 98, no. 11, article e14864, 2019.
- [9] P. F. Padilla, G. Martinez, R. W. Vernooij, G. I. Urrutia, M. R. Figuls, and X. B. Cosp, "Early enteral nutrition (within 48 hours) versus delayed enteral nutrition (after 48 hours) with or without supplemental parenteral nutrition in critically ill adults," *Cochrane Database of Systematic Reviews*, vol. 2019, no. 10, 2019.
- [10] F. Tian, P. T. Heighes, M. J. Allingstrup, and G. S. Doig, "Early enteral nutrition provided within 24 hours of ICU admission: a meta-analysis of randomized controlled trials," *Critical Care Medicine*, vol. 46, no. 7, pp. 1049–1056, 2018.
- [11] S. Petros, M. Horbach, F. Seidel, and L. Weidhase, "Hypocaloric vs normocaloric nutrition in critically ill Patients," *JPEN Journal of Parenteral and Enteral Nutrition*, vol. 40, no. 2, pp. 242–249, 2016.
- [12] S. Rugeles, L. G. Villarraga-Angulo, A. Ariza-Gutiérrez, S. Chaverra-Kornerup, P. Lasalvia, and D. Rosselli, "High-protein hypocaloric vs normocaloric enteral nutrition in critically ill patients: a randomized clinical trial," *Journal of Critical Care*, vol. 35, pp. 110–114, 2016.
- [13] Y. M. Arabi, H. M. Tamim, G. S. Dhar et al., "Permissive underfeeding and intensive insulin therapy in critically ill patients: a randomized controlled trial," *The American Journal of Clinical Nutrition*, vol. 93, no. 3, pp. 569–577, 2011.
- [14] T. W. Rice, S. Mogan, M. A. Hays, G. R. Bernard, G. L. Jensen, and A. P. Wheeler, "Randomized trial of initial trophic versus full-energy enteral nutrition in mechanically ventilated patients with acute respiratory failure," *Critical Care Medicine*, vol. 39, no. 5, pp. 967–974, 2011.
- [15] T. W. Rice, A. P. Wheeler, and B. T. Thompson, "Initial trophic vs full enteral feeding in patients with acute lung injury: the EDEN randomized trial," *JAMA*, vol. 307, no. 8, pp. 795–803, 2012.
- [16] S. J. Rugeles, J. D. Rueda, C. E. Diaz, and D. Rosselli, "Hyperproteic hypocaloric enteral nutrition in the critically ill patient: a randomized controlled clinical trial. Indian," *JCritCareMed*, vol. 17, no. 6, pp. 343–349, 2013.
- [17] X. Cheng, F. He, M. Si, P. Sun, and Q. Chen, "Effects of antibiotic use on saliva antibody content and oral microbiota in Sprague Dawley rats," *Frontiers in Cellular and Infection Microbiology*, vol. 12, 2022.
- [18] E. J. Zarling, J. R. Parmar, S. Mobarhan, and M. Clapper, "Effect of enteral formula infusion rate, osmolality, and chemical composition upon clinical tolerance and carbohydrate absorption in normal subjects," *Journal of Parenteral and Enteral Nutrition*, vol. 10, no. 6, pp. 588–590, 1986.
- [19] Y. M. Arabi, A. S. Aldawood, S. H. Haddad et al., "Permissive underfeeding or standard enteral feeding in critically ill adults," *The New England Journal of Medicine*, vol. 372, no. 25, pp. 2398–2408, 2015.
- [20] M. M. Berger, A. Reintam-Blaser, P. C. Calder et al., "Monitoring nutrition in the ICU," *Clinical Nutrition*, vol. 38, no. 2, pp. 584–593, 2019.

## *Retraction*

# **Retracted: Systematic Review and Meta-Analysis of Complications after Laparoscopic Surgery and Open Surgery in the Treatment of Pelvic Abscess**

### **BioMed Research International**

Received 12 November 2022; Accepted 12 November 2022; Published 22 November 2022

Copyright © 2022 BioMed Research International. This is an open access article distributed under the Creative Commons Attribution License, which permits unrestricted use, distribution, and reproduction in any medium, provided the original work is properly cited.

*BioMed Research International* has retracted the article titled “Systematic Review and Meta-Analysis of Complications after Laparoscopic Surgery and Open Surgery in the Treatment of Pelvic Abscess” [1] due to concerns that the peer review process has been compromised.

Following an investigation conducted by the Hindawi Research Integrity team [2], significant concerns were identified with the peer reviewers assigned to this article; the investigation has concluded that the peer review process was compromised. We therefore can no longer trust the peer review process and the article is being retracted with the agreement of the editorial board.

### **References**

- [1] X. Chen, S. Jun, L. Xu, and H. Zhang, “Systematic Review and Meta-Analysis of Complications after Laparoscopic Surgery and Open Surgery in the Treatment of Pelvic Abscess,” *BioMed Research International*, vol. 2022, Article ID 3650213, 8 pages, 2022.
- [2] L. Ferguson, “Advancing Research Integrity Collaboratively and with Vigour,” 2022, <https://www.hindawi.com/post/advancing-research-integrity-collaboratively-and-vigour/>.



## Review Article

# Systematic Review and Meta-Analysis of Complications after Laparoscopic Surgery and Open Surgery in the Treatment of Pelvic Abscess

Xiaolu Chen, Jun Su, Lina Xu, and Huiping Zhang 

Department of Obstetrics and Gynecology, Taizhou First People's Hospital, Taizhou, Zhejiang 318020, China

Correspondence should be addressed to Huiping Zhang; zhanghp1986@163.com

Received 25 May 2022; Revised 16 June 2022; Accepted 20 June 2022; Published 2 July 2022

Academic Editor: Dinesh Rokaya

Copyright © 2022 Xiaolu Chen et al. This is an open access article distributed under the Creative Commons Attribution License, which permits unrestricted use, distribution, and reproduction in any medium, provided the original work is properly cited.

**Background.** Pelvic abscess surgery consists mostly of open laparotomy and laparoscopic surgery. Open surgery is regarded as a classic procedure. With the rise and promotion of laparoscopic indications in recent years, comparative studies of the two's postoperative effectiveness have been limited. **Objective.** To compare the clinical effects of laparoscopic exploratory surgery and open surgery in the treatment of pelvic abscess. **Methods.** Through computer searches of PubMed, EMBASE, Web of Science, China National Knowledge Infrastructure (CNKI), Wanfang, and Weipu databases, we found publicly available case-control research on laparoscopic surgery and open surgery for treating pelvic abscess. The papers that met the evaluation criteria were screened, and meta-analysis was used to look at 8 papers on laparoscopic surgery and open surgery for treating pelvic abscess from 2010 to 2021. **Results.** The results of this study showed that compared with the open laparotomy group, the incidence of laparoscopic group in the incision infection rate (RR = 0.29, 95% CI (0.20, 0.41), and  $P < 0.00001$ ), the incidence of intestinal injury (RR = 0.08, 95% CI (0.04, 0.14), and  $P < 0.00001$ ), incidence of intestinal obstruction (RR = 0.26, 95% CI (0.08, 0.90), and  $P = 0.03 < 0.05$ ), and postoperative pelvic abscess recurrence rate (RR = 0.34, 95% CI (0.13, 0.86), and  $P = 0.02 < 0.05$ ) are lower than open surgery, and the difference of these four items is statistically significant. There was no difference in the risk of urinary tract injury between laparoscopic surgery and open surgery (RR = 0.92, 95% CI (0.27, 3.17), and  $P = 0.89 > 0.05$ ). **Conclusion.** In terms of incision infection, intestinal damage, intestinal obstruction, and recurrence of pelvic abscess, the laparoscopic group clearly outperforms the open group, and it merits clinical promotion and use.

## 1. Introduction

Pelvic inflammatory disease (PID) is a group of common infectious diseases in the lower abdomen. In recent years, with the improvement of people's health awareness and the advancement of diagnostic technology, the detection rate of PID patients is getting higher and higher [1]. Pelvic abscess is a more serious gynecological disease, which includes fallopian tube abscess, ovarian abscess, fallopian tube ovarian abscess, and abscesses caused by acute peritonitis and pelvic connective tissue inflammation [2]. Among the infections of the reproductive tract, pelvic abscess is the most serious infection, usually manifested as acute, subacute, chronic attack, or repeated infection of pelvic organs [3–5]. The clinical manifestations of pelvic abscess are complex

and diverse. Most of them manifest as recurrent pain, fever, loss of appetite, and tender masses in the lower abdomen. Some patients feel anal drop, and there are also patients with hidden disease in clinical practice, so it is a serious threat women's health.

The diagnosis of pelvic abscess is based on the minimum diagnostic criteria, additional diagnostic criteria, and specific diagnostic criteria of PID. Its clinical diagnostic accuracy is not enough [6, 7]. However, delay in diagnosis and treatment may lead to unnecessary sequelae, such as infertility and ectopic pregnancy. Early diagnosis, especially early effective treatment, is the best strategy to ensure that PID will not develop into pelvic abscess. The incidence of pelvic abscess in PID hospitalized patients is as high as 34% [8]. Therefore, the pelvic abscess should be promptly and

effectively intervened. At present, the treatment of pelvic abscess is still based on conservative treatment of drugs, and try to choose antibiotics that have a wide coverage and are directed against the pathogenic bacteria of PID [9]. However, repeated antibiotic treatment can easily lead to drug resistance and flora imbalance in patients [10, 11].

Patients with more complex or critical pelvic abscesses should seek surgical therapy to accomplish the goal of full eradication of the lesions. The following are some indications [12] for pelvic abscess surgery: (1) ineffective medical therapy, chronic, or increasing growth of the abscess mass; (2) the occurrence or suspicion of an abscess rupture; and (3) peritonitis and possibly toxic shock are possibilities. The major surgical procedures include open surgery and laparoscopic surgery, with the purpose of removing the abscess lesion. Since Reich H performed the first laparoscopic hysterectomy in 1989, the discipline of gynecology has seen tremendous advancements in laparoscopic surgery. Laparoscopic surgery is becoming more popular among physicians and patients [13].

Laparoscopic surgery provides the physiological benefits of tiny incisions, less bleeding, and less damage as compared to standard open laparotomy surgery [14]. Can, however, laparoscopic surgery prevent organ damage during pelvic abscess treatment? Can the patient gain more? There are still concerns about the aforementioned difficulties. As a result, this article employs meta-analysis to investigate open or laparoscopic surgery for pelvic abscess, observe the occurrence of surgical complications, investigate the best surgical method for pelvic abscess, and provide patients with reasonable and optimal surgical methods, thereby reducing complications.

## 2. Methods

**2.1. Search Strategy.** Using a computer, search the databases of PubMed, EMBASE, Web of Science, Cochrane Library, CNKI, Wanfang, and Weipu. A collection of publications published between January 2010 and May 2021 are relevant to case-control studies of laparoscopic surgery and conventional laparotomy in the treatment of pelvic abscesses. Laparoscopy, laparotomy, pelvic abscess, fallopian tube abscess, fallopian tube ovarian abscess, ovarian abscess, pelvic inflammatory illness, and case-control study are the search phrases.

**2.2. Inclusion Criteria.** All the included study cases were pathologically diagnosed after surgery and had positive bacterial cultures; they were all patients in the same period; they were all analyzed through case-control on the occurrence of complications after laparoscopic surgery and open surgery for the treatment of pelvic abscess. All included studies are the clinical effects of laparoscopic surgery and open surgery in the treatment of pelvic abscess; the research methods are case-control trials; the clinical data are complete. Research indicators include the following: postoperative wound infection, intestinal injury, postoperative intestinal obstruction, recurrence of pelvic abscess, and urinary tract injury. The language is Chinese or English.

**2.3. Exclusion Criteria.** Preoperative patients with pregnancy; postoperative confirmation of patients with malignant tumors; data provided in the article is incomplete; the type of study is not a case-control study; there is too little information about clinical cases reported in the article; the article is of the type of case reports, reviews, etc.

**2.4. Paper Screening and Data Extraction.** Carry out the preliminary screening of articles according to the following steps: ① preliminary screening. Preliminary screening was performed according to the title and abstract of the literature, and the literature that had nothing to do with the surgical method of pelvic abscess was excluded. ② Research the full text of all selected articles. ③ Read the full text of the selected articles one by one, and exclude the articles that do not meet the requirements of the inclusion criteria. As a result, a total of 5 Chinese literatures and 3 English literatures were included. All literature research types were retrospective case-control studies.

The title of the article, the first author, the date of publication, and the source of the article; the sample size of the laparoscopic surgery group for pelvic abscess treatment and the sample size of patients with pelvic abscess treated by laparotomy; whether the grouping is randomized; and postoperative complications data such as wound infection, intestinal injury, postoperative intestinal obstruction, and recurrence of p. According to the characteristics of these data, only RCT research can be selected.

**2.5. Quality Assessment.** The quality of the included literature is evaluated separately by two researchers. When the assessment reveals a discrepancy, it is resolved via conversation. If the debate fails, the third researcher's view will be requested. The NOS scale (Newcastle-Ottawa Scale) quality evaluation contains a total of 10 points, with 7 split into high-quality research and 7 divided into low-quality research; the assessment material includes the following: patient selection, group comparability, and exposure variables.

**2.6. Statistical Analysis.** The statistical software uses the RevMan 5.3 software provided by the Cochrane Collaboration to perform meta-analysis on the data extracted from the literature. The heterogeneity test is to analyze the heterogeneity of the statistics in the included similar research literature. This study uses statistics  $P$  value and  $I^2$  value to detect heterogeneity. When  $P > 0.10$  and  $I^2 \leq 50\%$ , it means that the statistics included in the literature are less heterogeneous, and the fixed effects model is more reliable; when  $P < 0.10$  and  $I^2 > 50\%$ , it means that the statistic is highly heterogeneous, and it is recommended to choose a random effects model.  $P < 0.05$  indicates that the difference between the two is statistically significant, and vice versa, the difference between the two is deemed not to be statistically significant. For the binary variable data, the risk ratio (RR) is used as the effect indicator, and the combined RR value and 95% confidence interval (CI) are calculated. The publication bias of the article is identified by the funnel plot generated by the RevMan 5.3 software, and this study only performed the

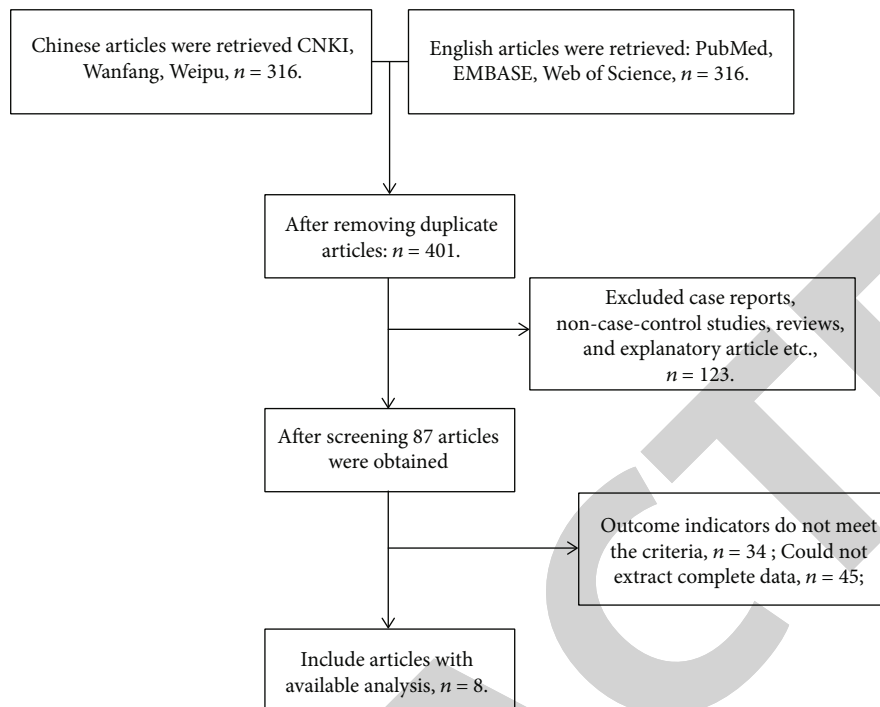


FIGURE 1: Flow diagram of the search, screening, and inclusion process.

funnel plot analysis bias on the research index of the included article amount to 5. For the sensitivity analysis of the included article, the changes in the combined effect were observed by excluding one article at a time during the meta-analysis process to illustrate the stability and accuracy of the results.

### 3. Results

**3.1. Search Results and Study Characteristics.** A total of 439 related articles were retrieved as required, and a total of 316 articles were retrieved through Chinese-related databases, including 127 on CNKI, 113 on Wanfang, and 76 on Weipu; a total of 123 articles were retrieved through English-related databases, including 78 on PubMed, 25 on EMBASE, and 20 on Web of Science; other search methods failed to obtain qualified articles. Then, the retrieved related literature was screened again, and based on the title and abstract content, noncase-control studies, incomplete content information, review, and explanatory literature were excluded, and finally, a total of 8 articles were included in this study, including 5 in Chinese and 3 in English. The literature screening process is shown in Figure 1.

After screening, a total of 8 articles, including Chinese and English articles, were included in 2836 patients, including 1254 cases in the laparoscopic group and 1582 cases in the traditional open laparotomy group. The study types are all case-control studies. Basic information such as authors, countries, and publication dates included in the literature are shown in Table 1.

Eight articles were finally included in quality assessment study, all of which were clinical case-control studies.

According to the NOS evaluation criteria of case-control studies, the included literatures were evaluated objectively. The results showed that all the included literature scores were  $\geq 7$  points, and the literature quality was generally good.

### 3.2. Meta-Analysis Results

**3.2.1. Incision Infection Rate.** Seven of the included studies reported on the incidence of incision infections after laparoscopic surgery and open surgery. A total of 2769 patients participated, including 1217 patients in the laparoscopic group and 1552 patients in the open laparotomy group. The result of the heterogeneity test was calculated by RevMan 5.3 software  $I^2 = 0\% < 50\%$ , so the fixed effects model was adopted,  $RR = 0.29$ , 95% CI (0.20, 0.41),  $P < 0.00001$ , the comparison of the incidence of incision infection between the two groups is statistically significant, it showed that the incidence of incision infection is different between the laparoscopic surgery group and the open surgery group, and the risk of incision infection is lower in laparoscopic surgery than open surgery Figure 2.

**3.2.2. Intestinal Injury Rate.** Five of the included articles reported on the occurrence of intestinal injury in laparoscopic surgery and open surgery. A total of 2073 patients participated, including 1004 patients in the laparoscopic group and 1069 patients in the open group. The result of the heterogeneity test was calculated by RevMan 5.3 software  $I^2 = 0\% < 50\%$ , so the fixed effects model was adopted,  $RR = 0.08$ , 95% CI (0.04, 0.14),  $P < 0.00001$ , the incidence of intestinal injury between the two groups was statistically significant, indicating that for the incidence of intestinal injury,

TABLE 1: Basic characteristics of the study articles.

Author	Country	Year	Journal	Laparoscopic (n)	Open (n)
Carlson et al. [4]	Ohio	2021	J Minim Invasive Gynecol	133	234
Fan [15]	China	2012	Chongqing Medicine	111	101
Huang [16]	China	2010	Chinese Journal of Family Planning	37	30
Li et al. [17]	China	2020	Journal of Fujian Medical university	18	16
Shigemi et al. [18]	Japan	2019	Obstetrics & Gynecology	749	740
Yang et al. [19]	China	2002	J Am Assoc Gynecol Laparosc	19	37
Sun [5]	China	2018	China Medical University	102	382
Yang [20]	China	2019	Qingdao University	85	42

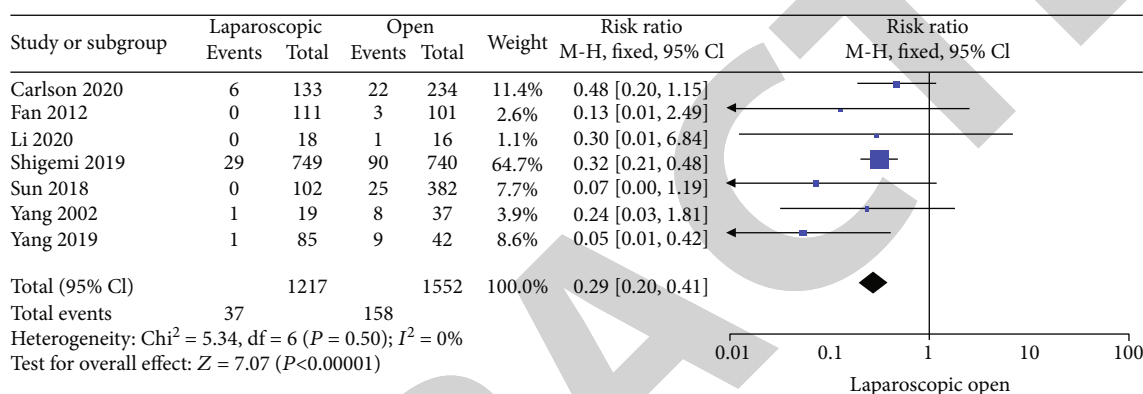


FIGURE 2: Forest plot of incision infection rate. Comparison of incision infection rate between the laparoscopic surgery group and the open laparotomy group. Statistical method: Mantel-Haenszel of fixed effects model (RR: relative risk; 95% CI: 95% confidence interval).

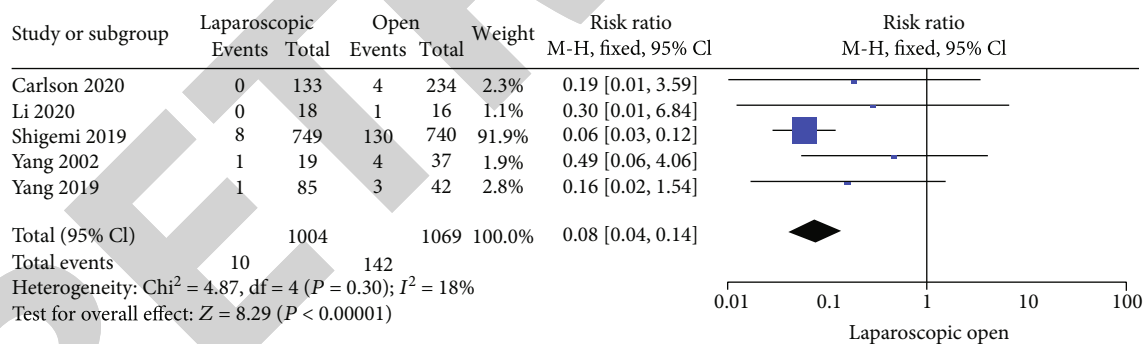


FIGURE 3: Forest plot of intestinal injury rate. Comparison of intestinal injury rate between the laparoscopic surgery group and the open laparotomy group. Statistical method: Mantel-Haenszel of the fixed effects model (RR: relative risk; 95% CI: 95% confidence interval).

laparoscopic surgery is different from open surgery, and laparoscopic surgery has a lower risk of intestinal injury than open surgery Figure 3.

**3.2.3. Intestinal Obstruction Rate.** Three of the included articles reported on the occurrence of intestinal obstruction in laparoscopic surgery and open surgery. A total of 359 patients participated, including 205 patients in the laparoscopic group and 154 patients in the open group. The result of the heterogeneity test is calculated by RevMan5.3 software  $I^2 = 0\% < 50\%$ , so the fixed effects model is adopted,  $\text{RR} = 0.26$ ,  $95\% \text{ CI} (0.08, 0.90)$ ,  $P = 0.03 < 0.05$ , and the compari-

son of the occurrence of intestinal obstruction between the two groups is statistically significant, indicating that the occurrence of intestinal obstruction is different between laparoscopic surgery and open surgery. Laparoscopic surgery has a lower risk of intestinal obstruction than open surgery Figure 4.

**3.2.4. Pelvic Abscess.** Three of the included articles reported on the occurrence of pelvic abscess recurrence in both laparoscopic surgery and open surgery. A total of 678 patients participated, including 224 patients in the laparoscopic group and 454 patients in the open group. The result of

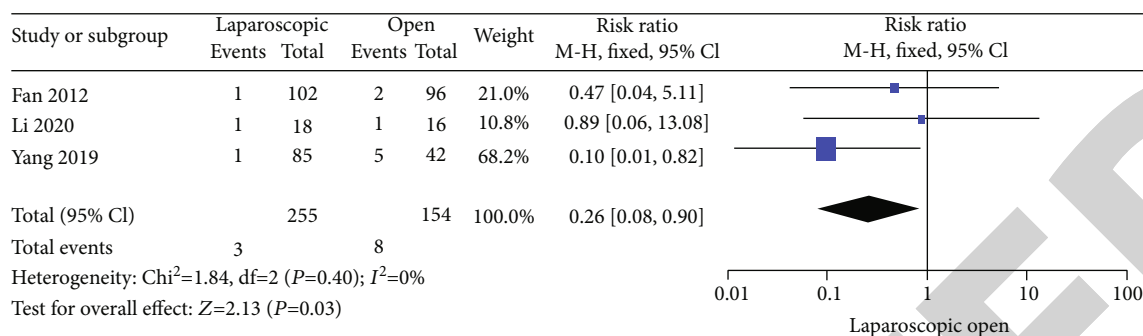


FIGURE 4: Forest plot of intestinal obstruction rate. Comparison of intestinal obstruction rate between the laparoscopic surgery group and the open laparotomy group. Statistical method: Mantel-Haenszel of the fixed effects model (RR: relative risk; 95% CI: 95% confidence interval).

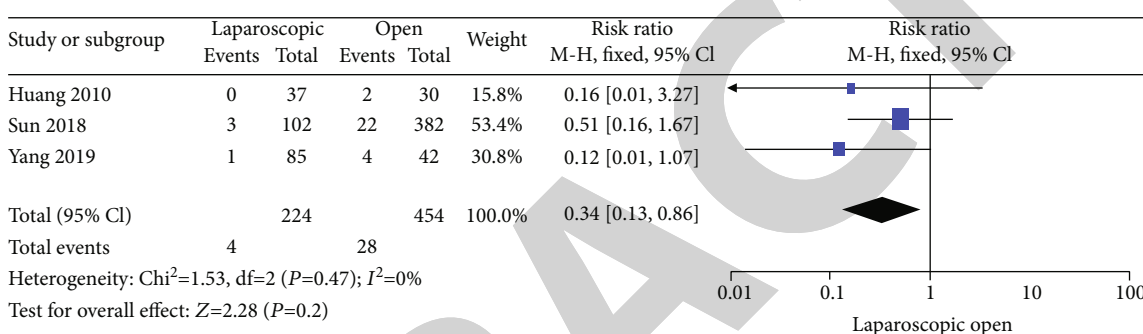


FIGURE 5: Forest plot of pelvic abscess rate. Comparison of pelvic abscess rate between the laparoscopic surgery group and the open laparotomy group. Statistical method: Mantel-Haenszel of the fixed effects model (RR: relative risk and 95% CI: 95% confidence interval).

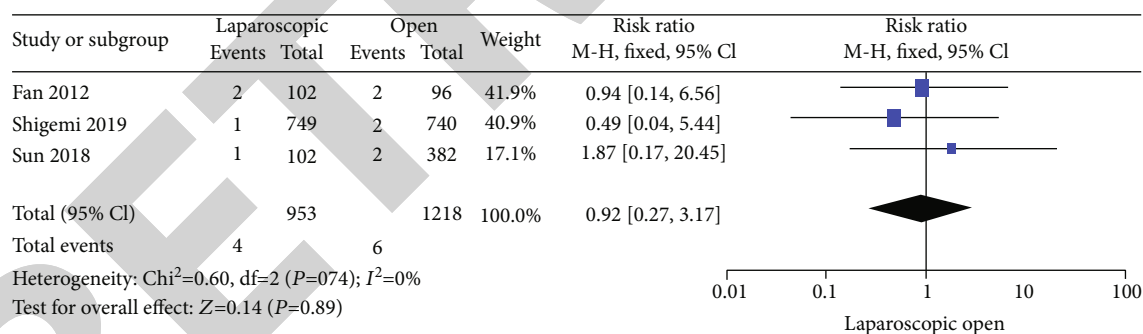


FIGURE 6: Forest plot of urinary system damage rate. Comparison of urinary system damage rate between the laparoscopic surgery group and the open laparotomy group. Statistical method: Mantel-Haenszel of the fixed effects model (RR: relative risk; 95% CI: 95% confidence interval).

the heterogeneity test is calculated by RevMan 5.3 software  $I^2 = 0\% < 50\%$ , so the fixed effects model is adopted,  $RR = 0.12$ , 95% CI (0.13, 0.86),  $P = 0.02 < 0.05$ , and the incidence of pelvic abscess recurrence between the two groups was statistically significant, indicating that for the incidence of pelvic abscess recurrence, laparoscopic surgery is different from open surgery. Laparoscopic surgery has a lower risk of pelvic abscess recurrence than open surgery Figure 5.

3.2.5. *Urinary System Damage.* The study indicators involved a total of 3 included articles and a total of 2171 patients participated, including 953 patients in the laparo-

scopic group and 1218 patients in the open laparotomy group. The result of the heterogeneity test was calculated by RevMan 5.3 software  $I^2 = 0\% < 50\%$ , so the fixed effects model was adopted,  $RR = 0.92$ , 95% CI (0.27, 3.17), and  $P = 0.89 > 0.05$ . The comparison of the occurrence of urinary tract injury between the two groups was not statistically significant, indicating that there was no significant difference in the risk of urinary tract injury between laparoscopic surgery and open surgery Figure 6.

3.2.6. *Publication Bias.* As the number of articles used to analyze the rate of incision infection and intestinal injury



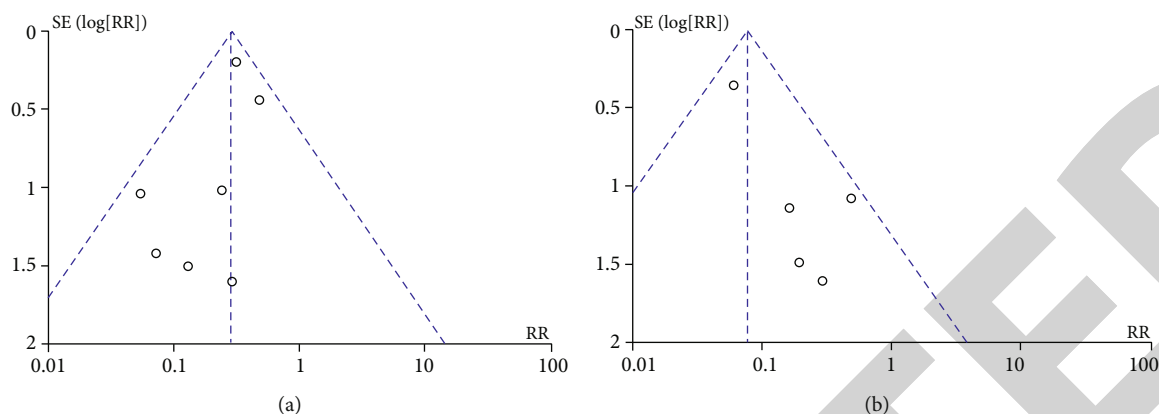


FIGURE 7: Publication bias is analyzed by funnel plot. Comparison of (a) incision infection rate and (b) intestinal injury rate. RR: relative risk; SE: standard error of the mean.

after laparoscopic surgery and open surgery for the treatment of pelvic abscess has reached 5, the funnel chart of these two indicators is used to analyze the publication bias, and both funnel charts are asymmetry, so there is publication bias. The articles with other indicators included in the study were all below the publication bias requirement ( $<5$ ), so no publication bias analysis was performed Figure 7.

**3.2.7. Risk of Bias.** According to the evaluation tool of risk of bias in the Cochrane Collaboration, the low risk of random sequence generation was described in 7 articles [4, 5, 15–19], and the remaining 1 study did not specify the risk of bias [20]. The 8 articles all describe the implicit bias of allocation (low risk = 5 [4, 17–20] and risk = 3 [5, 15, 16]), and the risk of bias for blinding subjects and researchers (low risk = 6 [4, 5, 16–19] and high risk = 2 [15, 20]). Six articles describe the risk of bias in blinded result evaluation (low risk = 4 [4, 15–17] and high risk = 2 [19, 20]). All articles are low risk for incomplete result data, selective reporting domains, and other risks of bias.

#### 4. Discussion

Common pathogens of pelvic inflammatory diseases include *Streptococcus*, *Staphylococcus aureus*, *Neisseria gonorrhoeae*, *Chlamydia trachomatis*, *Mycoplasma*, and viruses [4, 7, 10, 14]. If acute pelvic inflammatory disease is not treated in time, it can evolve into pelvic abscess as the disease progresses. Adhesion of tissues in the pelvic cavity has a serious impact on fertility [3]. In addition, diffuse peritonitis caused by the rupture of a pelvic abscess can cause toxic shock to the patient, and the life of the patient is seriously threatened. Therefore, early diagnosis and treatment can not only reduce complications but also preserve the patient's fertility and save the patient's life.

Because there is an abscess wall in a pelvic abscess, antibiotics cannot enter the abscess and cannot play a therapeutic role. The posterior fornix incision and drainage can achieve a certain therapeutic effect, but the effect is not ideal for patients with pelvic abscess and intestinal tube adhesion and tubal empyema and may cause injury [19, 21]. The

puncture effect under ultrasound is better, but the puncture site has limitations. Traditional open laparotomy can drain the abscess, but the surgical trauma is large, the incision is easy to split or heal poorly, and there are many adverse reactions after the operation [22, 23]. In the past, the surgical treatment of pelvic abscess was mainly traditional open surgery, while laparoscopic surgery has always been regarded as a relatively taboo. With the popularity of laparoscopic surgery and the advancement of the technical level of the surgeon, laparoscopic surgery has gradually become the first choice for the diagnosis and treatment of pelvic abscess. Studies have shown that laparoscopic surgery has the advantages of less trauma and faster recovery, and there are fewer adverse reactions after surgery [24, 25].

This study compared the efficacy of laparoscopic exploratory surgery and laparotomy in the treatment of conservatively treated pelvic abscesses. The results showed that the laparoscopic group's incision infection rate, intraoperative intestinal injury rate, intestinal obstruction rate, and postoperative pelvic abscess recurrence rates were better than those in the open surgery group, but there was no significant difference in the urinary system injury rate between the laparoscopic group and the open surgery group. Laparoscopic surgery can reduce complications such as organ damage during the treatment of pelvic abscess, and patients can benefit more.

There may be several reasons why laparoscopic surgery has a better therapeutic effect. Laparoscopy is a minimally invasive surgery, with a small incision and less damage to the operation area. Patients can get out of bed earlier after surgery. Therefore, intestinal function recovers better and faster, and the risk of intestinal obstruction is lower. Laparoscopy has a magnifying effect, can clearly display the operation field, can observe the lesion from multiple angles, and find the hidden lesion, which can remove the lesion and surrounding necrotic tissue more thoroughly and can completely separate the adhesions, reducing the probability of readhesion and recurrence after surgery [9, 21, 26]. During the operation, the normal saline is repeatedly flushed, and the drainage tube after the operation can reduce the inflammatory exudation, which is safer and more effective.

This study only retrieved Chinese and English articles, which would have a certain degree of influence on the results of the study. The total number of articles included in this study is 8 with 2836 subjects. Because the sample size of the included study is not large enough, and the articles included in this study are heterogeneous in samples and methods, a multicenter and large sample size study is needed to further confirm the difference between laparoscopic and open surgery. In addition, due to publication bias, it affects the veracity and validity of the conclusions to a certain extent.

## 5. Conclusion

Laparoscopic surgery for patients with pelvic abscess has a lower risk of incision infection, intestinal injury, intestinal obstruction, and recurrence of pelvic abscess than open surgery, but there is no significant difference in the risk of urinary tract injury. In summary, laparoscopic surgery has more advantages than open surgery in the treatment of pelvic abscess.

## Conflicts of Interest

The authors declare that there is no conflict of interest.

## References

- [1] J. L. Brun, O. Graesslin, A. Fauconnier et al., "Updated French guidelines for diagnosis and management of pelvic inflammatory disease," *International Journal of Gynaecology and Obstetrics*, vol. 134, no. 2, pp. 121–125, 2016.
- [2] J. Ross, S. Guaschino, M. Cusini, and J. Jensen, "2017 European guideline for the management of pelvic inflammatory disease," *International Journal of STD & AIDS*, vol. 29, no. 2, pp. 108–114, 2018.
- [3] Y. Taira and Y. Aoki, "Tube-ovarian abscess caused by *Rothia aeria*," *BML Case Reports*, vol. 12, no. 8, 2019.
- [4] S. Carlson, S. Batra, M. Billow, S. A. El-Nashar, and G. Chapman, "Perioperative complications of laparoscopic versus open surgery for pelvic inflammatory disease," *Journal of Minimally Invasive Gynecology*, vol. 28, no. 5, pp. 1060–1065, 2021.
- [5] R. Halperin, R. Svirsky, Z. Vaknin, I. Ben-Ami, D. Schneider, and M. Pansky, "Predictors of tuboovarian abscess in acute pelvic inflammatory disease," *The Journal of Reproductive Medicine*, vol. 53, no. 1, pp. 40–44, 2008.
- [6] H. W. Cho, Y. J. Koo, K. J. Min, J. H. Hong, and J. K. Lee, "Pelvic inflammatory disease in virgin women with tubo-ovarian abscess: a single-center experience and literature review," *Journal of Pediatric and Adolescent Gynecology*, vol. 30, no. 2, pp. 203–208, 2017.
- [7] M. V. Revzin, M. Mathur, H. B. Dave, M. L. Macer, and M. Spektor, "Pelvic inflammatory disease: multimodality imaging approach with clinical-pathologic correlation," *RadioGraphics*, vol. 36, no. 5, pp. 1579–1596, 2016.
- [8] L. H. Sordia-Hernandez, L. G. Serrano Castro, M. O. Sordia-Pineyro, A. Morales Martinez, M. C. Sepulveda Orozco, and G. Guerrero-Gonzalez, "Comparative study of the clinical features of patients with a tubo-ovarian abscess and patients with severe pelvic inflammatory disease," *International Journal of Gynaecology and Obstetrics*, vol. 132, no. 1, pp. 17–19, 2016.
- [9] Y. X-l and W. S-b, "Application status analysis on therapeutic appraisable methods of sequelae of pelvic inflammatory disease," *CJT CMP*, vol. 31, no. 10, pp. 4132–4134, 2016.
- [10] Q.-Q. Wang, H.-O. Xu, W.-W. Xu, L. Huang, L.-F. Chen, and X.-F. Zhao, "Cluture of pathogens from cervical secretions of patients with pelvic abscess and non-infectious benign adnexa mass: a comparative study," *Chinese Journal of Nosocomiology*, vol. 27, no. 10, pp. 2359–2362, 2017.
- [11] X. Wang, Y. Lu, H. Pan, M. Lin, X. Luo, and M. Li, "Changes of peritoneal fluid microbial flora ditribution and inflammatory factors levels of patients with anti-infection treatment of acute pelvic abscess surgery," *Chinese Journal of Nosocomiology*, vol. 26, no. 23, pp. 5456–5458, 2016.
- [12] R. Zhang, S. Chen, and Z. Liu, "Analysis of pelvic abscess with 25 cases," *Chinese Journal of Clinical Obstetrics and Gynecology*, vol. 19, no. 3, pp. 226–228, 2018.
- [13] T. Straub, M. Reynaud, and M. Yaron, "Intrauterine device and pelvic inflammatory disease: myth or reality?," *Gynecologie, Obstetrique, Fertilité & Senologie*, vol. 46, no. 4, pp. 414–418, 2018.
- [14] X. Jiang, M. Shi, M. Sui et al., "Clinical value of early laparoscopic therapy in the management of tubo-ovarian or pelvic abscess," *Experimental and Therapeutic Medicine*, vol. 18, no. 2, pp. 1115–1122, 2019.
- [15] Y. Fan and W. Kong, "Clinical analysis of surgical treatment of pelvic abscess Chongqing Medicine," *Chongqing Medicine*, vol. 41, no. 23, pp. 2410–2412, 2012.
- [16] Z. Huang, "Analysis of the clinical effect of laparoscopy in the treatment of pelvic abscess Chinese Journal of," *Family Planning*, vol. 12, no. 183, pp. 742–744, 2010.
- [17] Q. Li, F. Wang, and P. Chen, "The clinical analysis of cases of pelvic abscess," *Journal of Fujian Medical University*, vol. 54, no. 5, pp. 352–354, 2020.
- [18] D. Shigemi, H. Matsui, K. Fushimi, and H. Yasunaga, "Laparoscopic compared with open surgery for severe pelvic inflammatory disease and tubo-ovarian abscess," *Obstetrics and Gynecology*, vol. 133, no. 6, pp. 1224–1230, 2019.
- [19] C.-C. Yang, P. Chen, J.-Y. Tseng, and P.-H. Wang, "Advantages of open laparoscopic surgery over exploratory laparotomy in patients with tubo-ovarian abscess," *The Journal of the American Association of Gynecologic Laparoscopists*, vol. 9, no. 3, pp. 327–332, 2002.
- [20] C. A. Chappell and H. C. Wiesenfeld, "Pathogenesis, diagnosis, and management of severe pelvic inflammatory disease and tuboovarian abscess," *Clinical Obstetrics and Gynecology*, vol. 55, no. 4, pp. 893–903, 2012.
- [21] X. Yin, G. Bian, D. Wang, H. Sun, and X. Qiu, "Progress in diagnosis and treatment of pelvic abscess," *Journal of Chinese Physician*, vol. 21, no. 2, pp. 309–311, 2019.
- [22] L. Chu, H. Ma, J. Liang et al., "Effectiveness and adverse events of early laparoscopic therapy versus conservative treatment for tubo-ovarian or pelvic abscess: a single-center retrospective cohort study," *Gynecologic and Obstetric Investigation*, vol. 84, no. 4, pp. 334–342, 2019.
- [23] C. Villette, A. Bourret, P. Santulli, V. Gayet, C. Chapron, and D. de Ziegler, "Risks of tubo-ovarian abscess in cases of endometrioma and assisted reproductive technologies are both under- and overreported," *Fertility and Sterility*, vol. 106, no. 2, pp. 410–415, 2016.

## *Retraction*

# **Retracted: Red Raspberry Extract Decreases Depression-Like Behavior in Rats by Modulating Neuroinflammation and Oxidative Stress**

### **BioMed Research International**

Received 20 June 2023; Accepted 20 June 2023; Published 21 June 2023

Copyright © 2023 BioMed Research International. This is an open access article distributed under the Creative Commons Attribution License, which permits unrestricted use, distribution, and reproduction in any medium, provided the original work is properly cited.

This article has been retracted by Hindawi following an investigation undertaken by the publisher [1]. This investigation has uncovered evidence of one or more of the following indicators of systematic manipulation of the publication process:

- (1) Discrepancies in scope
- (2) Discrepancies in the description of the research reported
- (3) Discrepancies between the availability of data and the research described
- (4) Inappropriate citations
- (5) Incoherent, meaningless and/or irrelevant content included in the article
- (6) Peer-review manipulation

The presence of these indicators undermines our confidence in the integrity of the article's content and we cannot, therefore, vouch for its reliability. Please note that this notice is intended solely to alert readers that the content of this article is unreliable. We have not investigated whether authors were aware of or involved in the systematic manipulation of the publication process.

Wiley and Hindawi regrets that the usual quality checks did not identify these issues before publication and have since put additional measures in place to safeguard research integrity.

We wish to credit our own Research Integrity and Research Publishing teams and anonymous and named external researchers and research integrity experts for contributing to this investigation.

The corresponding author, as the representative of all authors, has been given the opportunity to register their agreement or disagreement to this retraction. We have kept a record of any response received.

### **References**

- [1] Y. Chen, X. Yang, H. Li, and J. Fang, "Red Raspberry Extract Decreases Depression-Like Behavior in Rats by Modulating Neuroinflammation and Oxidative Stress," *BioMed Research International*, vol. 2022, Article ID 9943598, 11 pages, 2022.

## Research Article

# Red Raspberry Extract Decreases Depression-Like Behavior in Rats by Modulating Neuroinflammation and Oxidative Stress

Yanhua Chen,<sup>1</sup> Xia Yang,<sup>2</sup> Hui Li,<sup>3</sup> and Jianqun Fang<sup>1</sup> 

<sup>1</sup>Mental Health Center, General Hospital of Ningxia Medical University, Yinchuan, Ningxia 750001, China

<sup>2</sup>Information Center, Health Commission of Ningxia Hui Autonomous Region, Yinchuan, Ningxia 750002, China

<sup>3</sup>Minkang Hospital Department of Civil Affairs of Ningxia, Yinchuan, Ningxia 750011, China

Correspondence should be addressed to Jianqun Fang; [fjq-7887@163.com](mailto:fjq-7887@163.com)

Received 20 April 2022; Revised 23 May 2022; Accepted 27 May 2022; Published 2 July 2022

Academic Editor: Dinesh Rokaya

Copyright © 2022 Yanhua Chen et al. This is an open access article distributed under the Creative Commons Attribution License, which permits unrestricted use, distribution, and reproduction in any medium, provided the original work is properly cited.

**Objective.** Red raspberry serves as a proven natural product to produce anti-inflammatory, antioxidant, and anticancer functions, but limited findings are available on its effects on depression. This study, by using a chronic unpredictable mild stress- (CUMS-) induced depression model, thus investigated the effects and underlying mechanism of red raspberry extract (RRE) on depressive behavior, inflammation, and oxidative stress. **Methods.** Different treatments were given after random grouping of Sprague-Dawley rats, including no intervention (control), CUMS induction, and CUMS+different concentrations of RRE, and subsequently, depression-like behavior tests were performed. HE staining was designed to observe the pathological damage of the hippocampal tissue in rats. The levels of oxidative stress, endocrine hormones, and inflammatory factors were determined by biochemical assay and ELISA, and gene expression (mRNA and protein) in the hippocampal tissue by qRT-PCR and Western blot. **Results.** On completion of CUMS treatment, the rats showed severe depression-like behavior, with obvious hippocampal tissue damage, oxidative inflammatory response, and endocrine imbalance. Importantly, RRE treatment significantly improved such depression-like behavior and attenuated histopathological damage in CUMS rats when reducing inflammation and oxidative stress and endocrine imbalance with upregulation of glutathione (GSH), superoxide dismutase (SOD), and interleukin- (IL-) 10 and downregulation of adrenocorticotrophic hormone (ACTH), corticosterone (CORT), malondialdehyde (MDA), IL-1 $\beta$ , cyclooxygenase- (COX-) 2, and human macrophage chemoattractant protein- (MCP-) 1. In addition, for CUMS rats, RRE was a contributor to increasingly expressed brain-derived neurotrophic factor (BDNF), neurotrophic tyrosine receptor kinase 2 (TrkB), and p-mTOR but inhibited p-GSK-3 $\beta$  expression in the hippocampal tissue. All the above antidepressant effects of RRE were concentration-dependent. **Conclusion.** By regulating neuroinflammation, oxidative stress response, endocrine level, and BDNF/TrkB level, RRE showed potential efficacy in alleviating depression-like behavior and histopathological damage of hippocampal tissue in CUMS rats by regulating the GSK3 $\beta$  and mTOR signaling pathways.

## 1. Introduction

Depression, the second most disabling condition worldwide, is a mental disorder that causes serious harm to human health. It is characterized by persistent low mood, slow thinking, anhedonia, disturbed sleep, and appetite loss. In severe cases, the patients may self-mutilate and commit suicide [1, 2]. Epidemiological surveys have found an increase in the year by year incidence, disability, and mortality of depression in recent years [3]. Moreover, depression has severe impacts on a person's physical and mental health

and social economy, accounting for 10.3% of the total disease burden [4, 5]. Depression is a multifactorial disease attributed to heredity, environment, epigenetics, and others, whose underlying mechanism is complex and has not yet been elucidated [6], thereby making its clinical diagnosis and treatment difficult. Meanwhile, most antidepressant drugs are associated with severe adverse events and unsatisfactory responses. Therefore, finding new and effective drugs with fewer side effects for treating depression is important.

Red raspberry (*Rubus idaeus* L. (RB)) is a berry of the Rosaceae family. It contains various essential nutrients and



active compounds, such as anthocyanins, tannin, brass, organic acids (including phenolic acids), fatty acids, xylan, and superoxide dismutase (SOD) [7, 8], which have been shown to have antioxidant, anti-inflammatory, and anticancer functions and other pharmacological effects [9, 10]. RB can inhibit the production of superoxide anion in the heart and aorta of obese mice and promote the activities of hepatic glutathione peroxidase and superoxide dismutase [11]. Also in obese mice (liver tissue), NLRP3 inflammasome activation and production of interleukin- (IL-) 1 $\beta$  and IL-18 are shown to be inhibited as a consequence of RB treatment [12]. It has been reported that red raspberry extract (RRE) has a central role in several diseases, such as arthritis, whereby RRE can significantly inhibit inflammation and the onset of clinical symptoms [13, 14]. RRE, based on in vitro experiments by Zhang et al., suppresses hepatoma cell growth (HepG2 and Huh7 cells) through the PTEN/AKT signaling pathway [15]. However, the role of RRE in depression, however, is still unknown to the medical community.

In this study, for determining the effect and mechanism of RRE on depression, we traced the changes in depressive behavior, serum neuroendocrine hormone, inflammatory factors, and brain-derived neurotrophic factors in chronic unpredictable mild stress- (CUMS-) treated rats. The theoretical basis for the clinical treatment of depression can be derived from the research.

## 2. Materials and Methods

**2.1. Model Establishment and Grouping.** A CUMS-induced depression rat model was established as previously described [11]. Rats from the control group remained untreated, while the others were subjected to CUMS and randomly given two or three kinds of stimulation every day. The stimuli comprised of (a) moist bedding, (b) no water overnight, (c) overnight fasting, (d) tilting their cage to 45° for 24 h, (e) overnight light flashing, (f) reversal of day/night light cycle, (g) odor, (h) white noise at 80 dB for 3 h, (i) overnight staying in a crowded cage, (j) cold swimming at 8°C lasting 5 min, and (k) restraint behavior for 4 h. The same stimulation was given discontinuously for 4 weeks.

Fifty male Sprague-Dawley rats were acquired from the Shanghai Southern Model Organisms Center (Shanghai, China). These 6–8-week-old rats weighing 180–220 g were subjected to random grouping ( $n = 10$ , each group) which consisted of the control group, CUMS group, and three RRE groups (30 mg/kg, 60 mg/kg, and 120 mg/kg). Rats as controls were fed normally and given normal saline by gavage in the 3rd to 4th week. The remaining animals were also given gavage with normal saline or 30 mg/kg, 60 mg/kg, or 120 mg/kg RRE in the 3rd to 4th week, respectively, based on CUMS induction for 4 consecutive weeks (Figure 1). After completing the behavioral test, the rats in each group were sacrificed, followed by collection of their blood and brain hippocampal tissue for the next steps. This study was approved by the Ethics Committee of the General Hospital of Ningxia Medical University (Ningxia, China) (KYLL-2021-1080) and performed in accordance with the approval guidelines.

## 2.2. Behavioral Testing

**2.2.1. Weight Determination.** The rats in each group were weighed every week, and the following formula was applied to the calculation of the change in body weight:

$$\text{Body weight change (\%)} = \frac{W_n - W_0}{W_0} \times 100\%. \quad (1)$$

Here,  $W_n$  refers to the body weight on the last day of the  $n$ th week and  $W_0$  refers to the body weight on the last day of adaptive feeding.

**2.2.2. Sucrose Preference Test.** The sucrose preference test (SPT) was performed as a measurement to evaluate the responsiveness of the rats to positive stimuli, including habituation training and formal testing. Sucrose AR grade reagent was purchased from Shanghai Sinopharm Co., Ltd. During the adaptation training, a bottle of 1% ( $w/v$ ) sucrose solution (200 mL) and a bottle of pure water (200 mL) were placed in the rats' cage in sequence, and the order of the left and right liquids was switched after 12 h to prevent the rats from habitually drinking only one side of the liquid. Baseline measurements were recorded. During the formal test, the rats were fasted for 12 h and kept in separate cages with free access to sucrose solution (200 mL) and pure water (200 mL). After 12 h, the drinking consumption was recorded, and the water intake was measured once before and once after treatments. The following formula was applied to the quantization of sucrose preference [16]:

$$\text{Sucrose preference (\%)} = \frac{\text{sucrose solution intake}}{\text{water intake} + \text{sucrose solution intake}} \times 100\%. \quad (2)$$

**2.2.3. Open Field Test.** The open field test (OFT), a test to assess exploratory activity and anxiety-like behavior in open boxes, was performed using a square box (150 cm  $\times$  150 cm  $\times$  50 cm) as an open field. After being carefully placed in the center of the field without restriction of movement for 5 min, with traces of their movement by a video camera above them, SMART software served to analyze the total moving distance moved and time spent in the central area. The apparatus was wiped utilizing a damp cloth and then dried with a hot air blower after each test [17].

**2.2.4. Elevated Plus Maze.** The elevated plus maze (EPM) is a common measure apparatus (100 cm above the floor) with two open arms and two closed arms, both measuring 50 cm  $\times$  10 cm  $\times$  40 cm. All the rats were transferred to the behavior testing room 15 min prior to the first trial for them to adapt to the environment, with the room volume maintained at 30 decibels as far as possible. After being gently placed in the center of the apparatus facing the open arms, the rats had no restriction of movement for a period of 5 min. Then, with records of their movement by a video camera above them, the calculation of open arm entries and time spent in open arms was achieved [18].



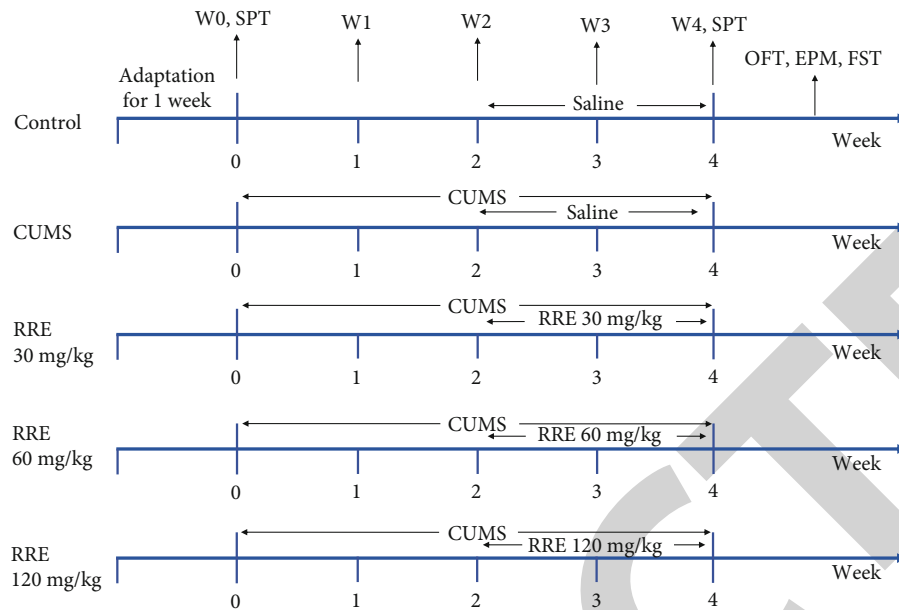


FIGURE 1: Grouping treatment of Sprague-Dawley rats and the behavioral experimental process. W0-W4 represent the rat's body weight on the 0th to 4th week, respectively. OFT: open field test; FST: forced swim test; EPM: elevated maze test; SPT: sucrose preference test.

**2.3. Forced Swim Test.** The forced swim test (FST), an examination of depression-like behaviors, can be divided into a training and a testing phase [19]. The experiments were performed following the protocol of Rogoz et al. [20]. During the training phase, the rats were gently placed in a transparent cylindrical glass container with a water depth of 30 cm (50 cm in height and 23 cm in diameter) to swim alone for 15 min (water temperature  $24^{\circ}\text{C} \pm 1^{\circ}\text{C}$ ). After 24 h, they were put into the water for the swimming test for 6 min. All test procedures were recorded from the other side of the cylinder by a camera. Their immobility time and swimming time were recorded.

**2.4. Hematoxylin and Eosin (HE) Staining.** On completion of drying at ambient temperature, the rats' hippocampal tissue sections were processed as follows: 30 s fixation (ambient temperature, 30 s), 2 s rinsing in 1x PBS, 60 s staining in hematoxylin ( $60^{\circ}\text{C}$ ), 10 s rinsing in 1x PBS, 3 s differentiation with 1% hydrochloric acid alcohol, 2 s rinsing in 1x PBS, 3 min staining in eosin, and 2 s rinsing in 1x PBS again. The treated sections were dehydrated using 70%, 80%, 95%, and absolute ethanol for a period of 5 min and washed using xylene ( $3 \times 5$  min). Finally, they were mounted by transparent neutral gum, followed by use of a microscope (BX63, Olympus, Japan) for observation and photograph.

**2.5. Biochemical Tests.** Saline was added to the rats' hippocampal tissues, which were then grounded into tissue homogenates using a tissue grinder. On completion of centrifugation, the supernatant was collected to dilute separately into different concentration gradients of stock solutions. Measuring the levels of malondialdehyde (MDA), superoxide dismutase (SOD), and glutathione (GSH) was achieved using an automatic biochemical analyzer following the instructions of the biochemical detection kit (Elabscience, China).

**2.6. Enzyme-Linked Immunosorbent Assay (ELISA).** Adrenocorticotropic hormone (ACTH) and corticosterone (CORT) in serum and IL- $1\beta$ , IL-10, cyclooxygenase- (COX-) 2, and human macrophage chemoattractant protein- (MCP-) 1 in the hippocampal tissues were measured on the basis of the instructions of the ELISA kit (Nanjing Jiancheng Bioengineering Institute, China). Homogenates of the hippocampal tissues were taken from the rats, and the supernatant was diluted, to which the sample/standard and reagents were sequentially added to the ELISA plate for the reaction. The absorbance (OD value) at 450 nm wavelength was detected using an ELISA plate reader. The levels of CORT, ACTH, IL- $1\beta$ , IL-10, COX-2, and MCP-1 in the samples were calculated using the standard curve.

**2.7. Real-Time Quantitative Reverse Transcription PCR (qRT-PCR).** Determination of the concentration of total RNA was carried out with the Nanodrop machine and total RNA extraction gained from hippocampal tissues using the Trizol reagent (Sigma, USA). Then, reverse transcription of RNA into cDNA was completed according to the reverse transcription kit instructions (Takara, Japan). The mRNA expression level was detected following the instructions of the fluorescence quantitative kit (Takara, Japan). The  $2^{-\Delta\Delta\text{Ct}}$  method was used for data analysis [21], and GAPDH served to provide an internal reference. The primer sequences used are displayed in Table 1.

**2.8. Western Blot.** Determination of the concentration of total protein was carried out with a BCA kit and with total protein extraction gained from hippocampal tissues using the Trizol reagent (Beyotime, China). Then, after separation using SDS-PAGE, the protein was blotted onto the polyvinylidene fluoride (PVDF) membrane by wet transfer. Next, total protein was then blocked using 5% nonfat dry milk

TABLE 1: qRT-PCR primer sequences.

Gene names	Primer sequences (5' to 3')
BDNF	F AAAACCATAAGGACGCGGACTT
	R AAAGAGCAGAGGAGGCTCCAA
TrkB	F CACACACAGGGCTCCTTA
	R AGTGGTGGTCTGAGGTTGG
GAPDH	F AGTGCCAGCCTCGTCTCATA
	R GGTAACCAGGCGTCCGATAC

for 2 h and subsequently incubated overnight at 4°C with the primary antibodies (BDNF, TrkB, mTOR, p-mTOR, GSK-3 $\beta$ , p-GSK-3 $\beta$ , and  $\beta$ -actin). On the following day, the rinsing step using phosphate buffer was carried out first, and subsequently, the membrane was subjected to 1 h of incubation with secondary antibodies at ambient temperature. Then, ECL was added after thorough washing, and the Flourescence HD2 imaging system was used for scanning and analysis [22]. Quantification of immunoreactive bands was conducted using ImageJ software, with  $\beta$ -actin as the internal reference.

**2.9. Statistics.** The data were analyzed using SPSS 21.0 employed for analyzing data, with statistics in the form of the mean  $\pm$  standard deviation (SD). Comparison between two groups and multiple groups was made using a *t*-test and one-way analysis of variance, respectively.  $P < 0.05$  served as the criterion to determine the significance of difference.

### 3. Results

**3.1. RRE Significantly Inhibits Depression-Like Behavior in CUMS Rats and Ameliorates Histopathological Damage in the Hippocampal Tissue.** We first used the CUMS method to establish a rat model for depression. Before the experiments, the initial body weight of the rats in each group had no marked difference. To determine the effects of CUMS and RRE on depression-like or anxiety behaviors in rats, we evaluated the behaviors of the rats in each group via SPT, OFT, and FST. Comparison between the control and CUMS groups and between the CUMS and RRE groups revealed that CUMS cause significant weight change in the rats over four weeks, but the change could be restored after RRE treatment (Figures 2(a) and 2(b)). Further, CUMS treatment was associated with a reduction in sucrose preference and worse performance in OFT (decreases in time spent in the central area and total movement distance), EPM (decreases in time spent in open arm and open arm entries), and FST (decreased swimming time and prolonged immobility time). The above depression-like behaviors were significantly improved by gavage of RRE in a concentration-dependent manner (Figures 2(c)–2(i)).

The pathological changes of hippocampal tissues were further assessed by HE staining. We found obvious pathological damage to hippocampal tissue in the CUMS group, which could be alleviated to different degrees by RRE treatment (Figure 2(j)). The above results showed that we had successfully established a CUMS-induced depression model

and that RRE treatment could significantly inhibit depression-like behavior and improve the histopathological damage of the hippocampal tissue in CUMS rats.

**3.2. RRE Decreases the Levels of ACTH and CORT in the Serum of CUMS Rats.** ACTH and CORT, as previously reported, have higher levels in patients with depression [23]. We also confirmed CUMS induced increased serum levels of ACTH, and CORT in the serum of rats in the CUMS was markedly increased but could be reduced by RRE in a concentration-dependent manner (Figures 3(a) and 3(b)).

**3.3. RRE Reduces Inflammatory Responses in Hippocampal Tissue of CUMS Rats.** Depression development has an association with inflammatory cytokines secreted by the activated immune system [24]. We measured the levels of proinflammatory factors (IL-1 $\beta$ , COX-2, and MCP-1) and anti-inflammatory factor IL-10 in the hippocampal tissue in each group using ELISA to look into what effect RRE had on neuroinflammation in CUMS-treated rats. In comparison with the control group, the CUMS group presented with a significant elevation of IL-1 $\beta$ , COX-2, and MCP-1 expression in the hippocampal tissue (Figures 4(a)–4(d)), while IL-10 expression had a marked reduction. Further, a dose-dependent decline in the levels of IL-1 $\beta$ , COX-2, and MCP-1 and an increase in IL-10 occurred as a consequence of RRE treatment.

**3.4. RRE Inhibits Oxidative Stress Response in Hippocampal Tissue of CUMS Rats.** To explore the effect of RRE on the oxidative stress response of CUMS rats in each group, we examined the content of oxidative stress-related molecules in the hippocampal tissue of rats using biochemical tests. The CUMS rats had relatively high levels of GSH and SOD and low levels of MDA, but administration of RRE increased the GSH and SOD levels and decreased the MDA level in a dose-dependent manner (Figures 5(a)–5(c)).

**3.5. RRE Promotes the Expression of BDNF and TrkB in the Hippocampal Tissue of CUMS Rats.** In this study, qRT-PCR and Western blot were conducted to detect the expression of BDNF and TrkB in the hippocampal tissues of rats in each group. The results in the hippocampal tissue showed decreased protein and mRNA expression levels of TrkB and BDNF after CUMS treatment (Figures 6(a)–6(c)). However, after administration of RRE treatment in different concentrations, the two were increased significantly, except for the mRNA expression levels of TrkB in CUMS rats in the RRE 30 mg/kg group which remained almost unchanged.

**3.6. RRE Regulates mTOR and GSK-3 $\beta$  Signaling in the Hippocampal Tissue of CUMS Rats.** As reported, the mTOR pathway was involved in depression and antidepressant [25], and the GSK-3 $\beta$  pathway was shown to regulate learning and memory impairment in depressed rats [26]. Here, we attempted to give an account of the possible mechanism of RRE in CUMS rats by detecting relevant protein levels of the mTOR and GSK-3 $\beta$  signaling pathways. As shown in Figures 7(a) and 7(b), the phosphorylation level of mTOR

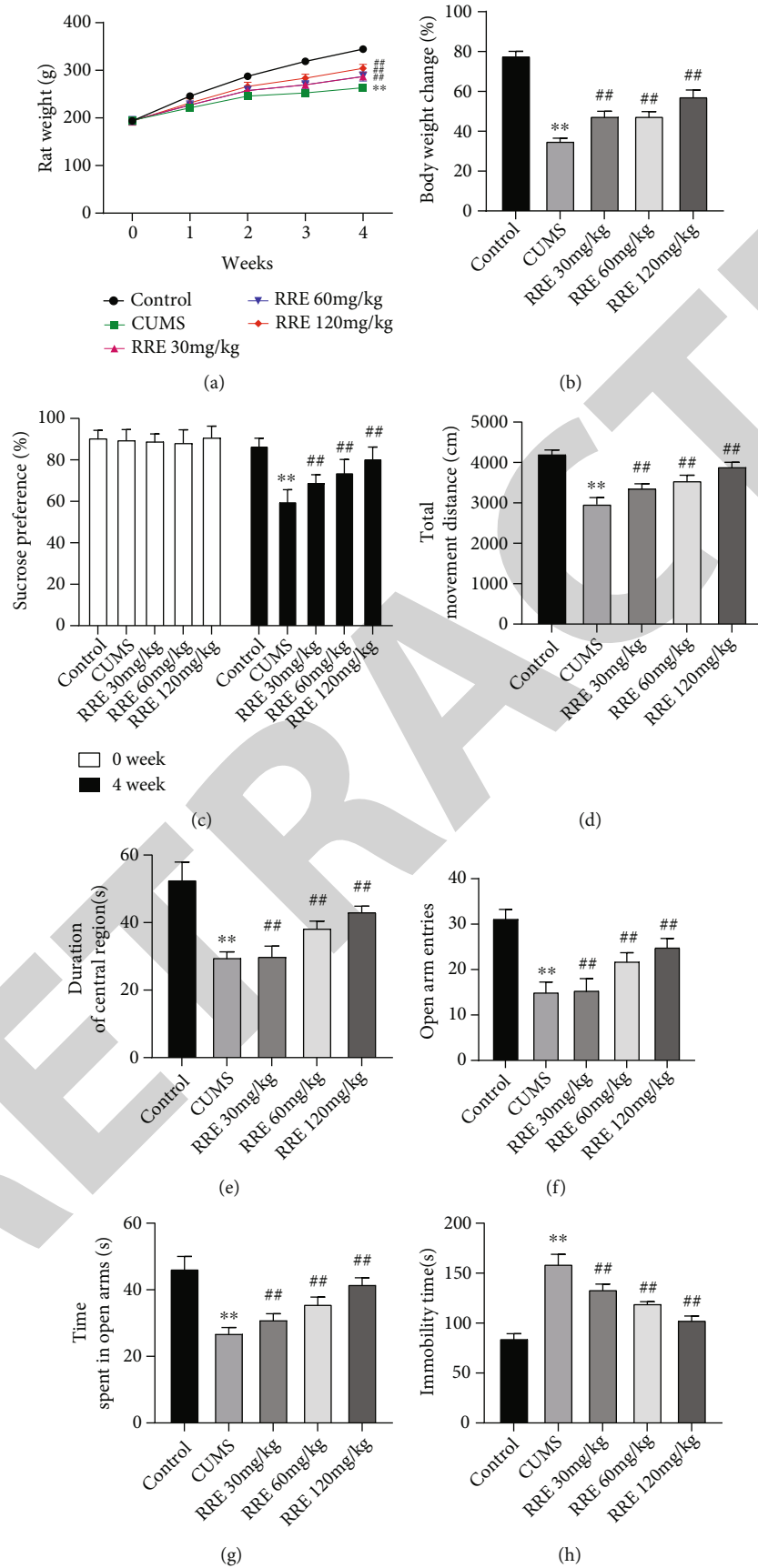


FIGURE 2: Continued.

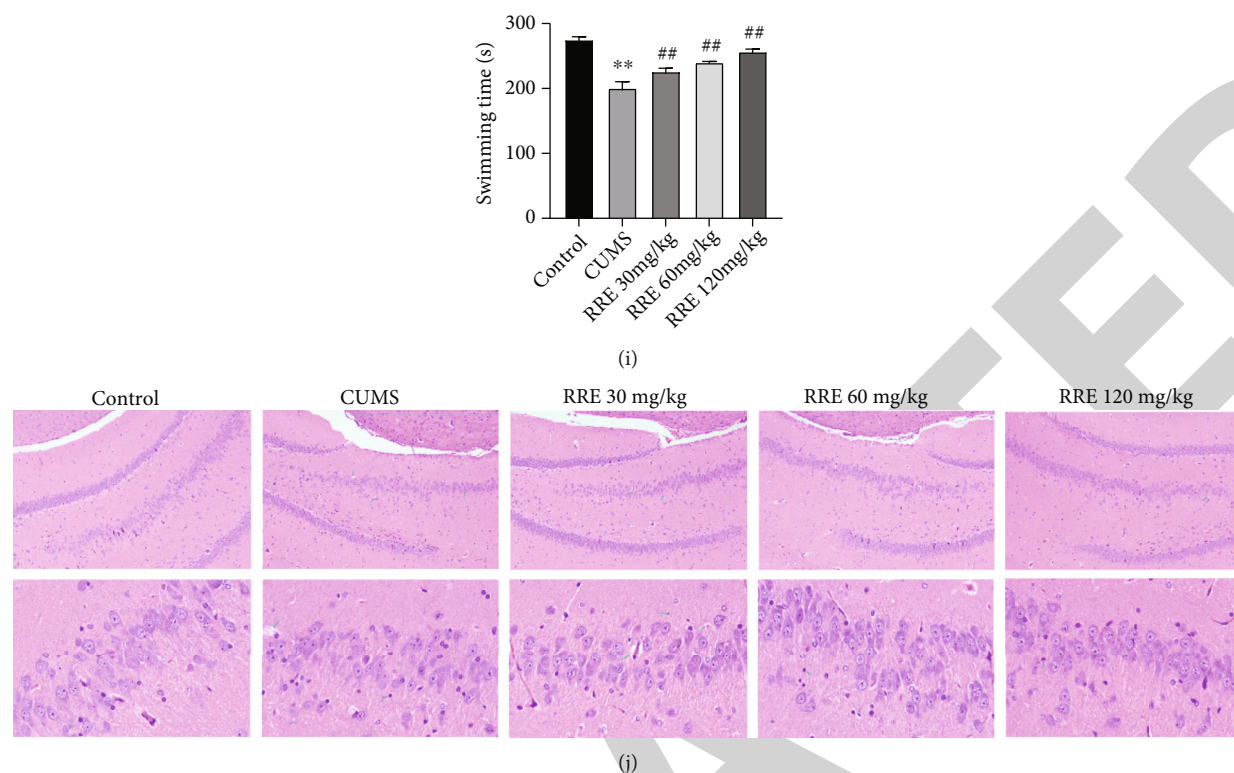


FIGURE 2: Effect of RRE on depression-like behavior and histopathological damage in the hippocampal tissues of rats in each group: (a, b) body weight of rats during weeks 0-4; (c) sucrose preference test before and after CUMS; (d, e) total distance moved; (d) time spent in the central area of rats (e) in open field test; (f, g) open arm entries (f) and time spent in open arms (g) in elevated plus maze test; (h, i) immobility (h) and swimming (i) time in force swim test; (j) HE staining showing the pathological damage of the hippocampal tissue. \*\* $P < 0.01$  vs. control group, ## $P < 0.01$  vs. CUMS group.

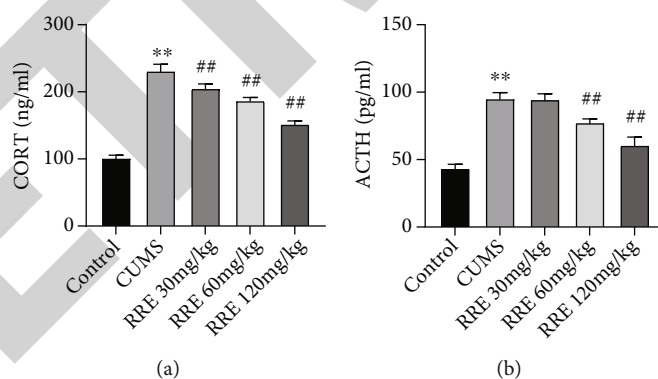


FIGURE 3: Effects of RRE on ACTH and CORT levels in the serum of CUMS rats. (a, b) ELISA detecting the levels of CORT (a) and ACTH (b) in the serum: \*\* $P < 0.01$  vs. control group, ## $P < 0.01$  vs. CUMS group.

and the ratio of p-mTOR/mTOR in the hippocampal tissue presented with reduction in CUMS rats compared with those receiving no interventions, while the phosphorylation level of GSK-3 $\beta$  was significantly increased and the ratio of p-GSK-3 $\beta$ /GSK-3 $\beta$  significantly increased. RRE treatment could reverse the changes in the expression of the above proteins.

#### 4. Discussion

Globally, the CUMS model is one of the classic depression models widely recognized by researchers [27] for searching

for depression, a psychiatric disorder with high prevalence [6]. According to our experiments, a decline was identified in CUMS rats in body weight, preference for sucrose, time spent in the central area and total distance traveled in OFT, time spent in open arms and open arm entries in EPM, and swimming time in FST. Moreover, as confirmed by HE staining, the hippocampal tissue of CUMS rats displayed obvious pathological damage, which indicated the successful establishment of the depression model. In addition, administration of different concentrations of RRE significantly improved the body weight change, sucrose

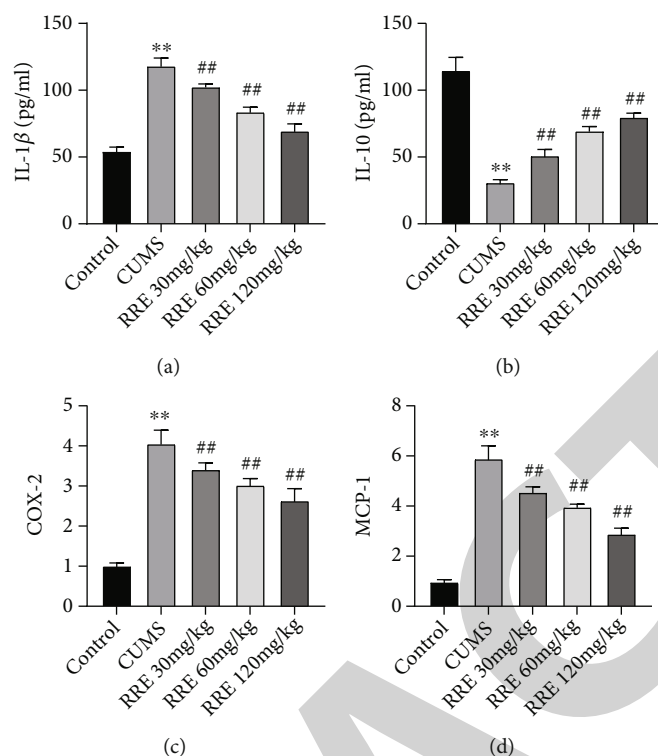


FIGURE 4: Effects of RRE on neuroinflammation in CUMS rats. (a–d) The secretion levels of IL-1 $\beta$  (a), IL-10 (b), COX-2 (c), and MCP-1 (d) in hippocampal tissue measured by ELISA, \*\* $P < 0.01$  vs. control group, ## $P < 0.01$  vs. CUMS group.

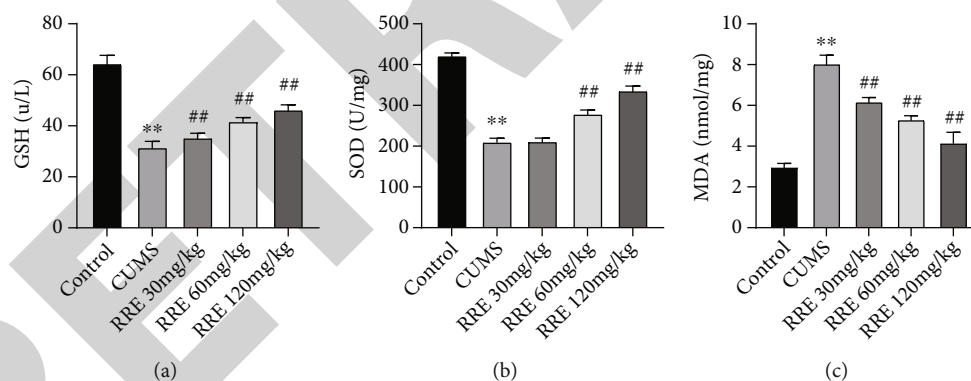


FIGURE 5: Effects of RRE on oxidative stress response in CUMS rats: (a–c) the contents of GSH (a), SOD (b), and MDA (c) in the hippocampal tissue determined by biochemical tests, \*\* $P < 0.01$  vs. control group, ## $P < 0.01$  vs. CUMS group.

preference, free movement ability, memory, and pathological damage of rats to varying degrees. This evidence indicates that RRE is a contributor to alleviating depression-like behaviors like anhedonia, bradykinesia, and histopathological damage in the hippocampal tissue of CUMS rats by having an antidepressant effect that was directly proportional to its concentration.

Studies have found that the abnormal excitation of the hypothalamic-pituitary-adrenal axis is closely related to depression. Stress may promote the release of serum CORT, corticotropin-releasing hormone, and ACTH in rats by inducing the activation of the HPA axis to deregulate its negative feedback regulation, damaging tissues such as the

hippocampus and prefrontal cortex, and further leading to depression and cognitive impairment [28]. In this study, observation of CORT and ACTH in serum produced an increased result in CUMS rats, and RRE treatment could significantly inhibit the increase in ACTH and CORTs.

Patients with depression are usually associated with increased secretion of cytokine IL-1 $\beta$  and decreased IL-10 and a significant increase in the expressions of proinflammatory genes COX-2 and MCP-1 [29–31]. Consistently, our work demonstrated that CUMS rat hippocampal tissue had greatly increased IL-1 $\beta$ , COX-2, and MCP-1, while IL-10 was significantly decreased. These changes, however, were reversed with the addition of RRE, indicating that regulation



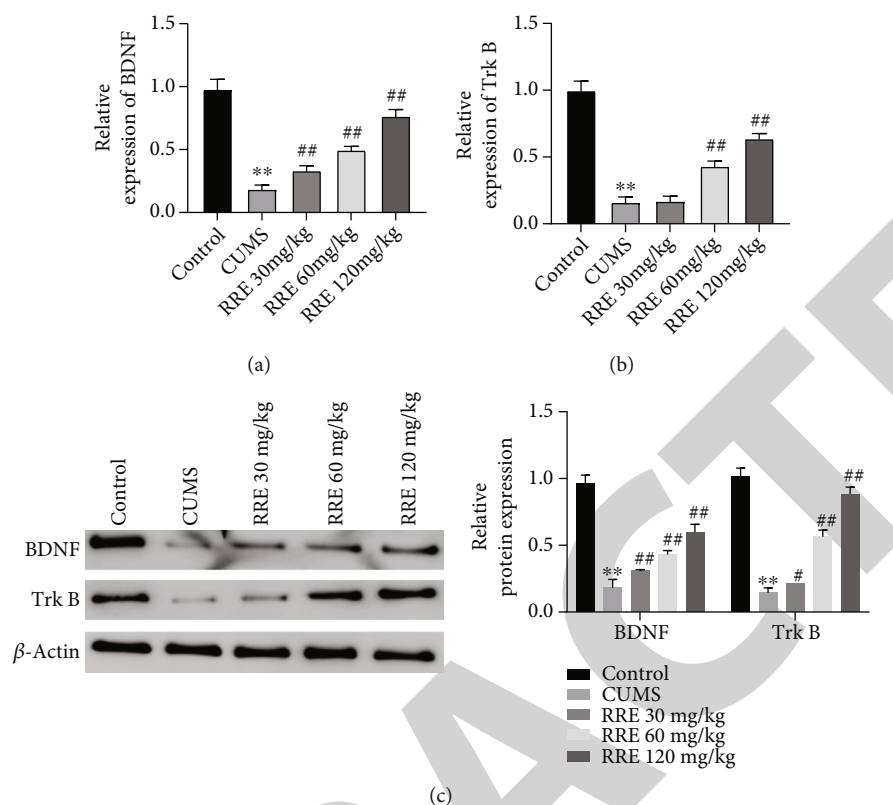


FIGURE 6: Effects of RRE on BDNF and TrkB expression levels in the hippocampal tissue of CUMS rats: (a) qRT-PCR was used to detect BDNF (a) and TrkB (b) expression in the hippocampal tissues; (c) Western blot to measure protein expression of BDNF and TrkB in the rats' hippocampal tissue. \*\* $P < 0.01$  vs. control group, # $P < 0.05$  and ## $P < 0.01$  vs. CUMS group.

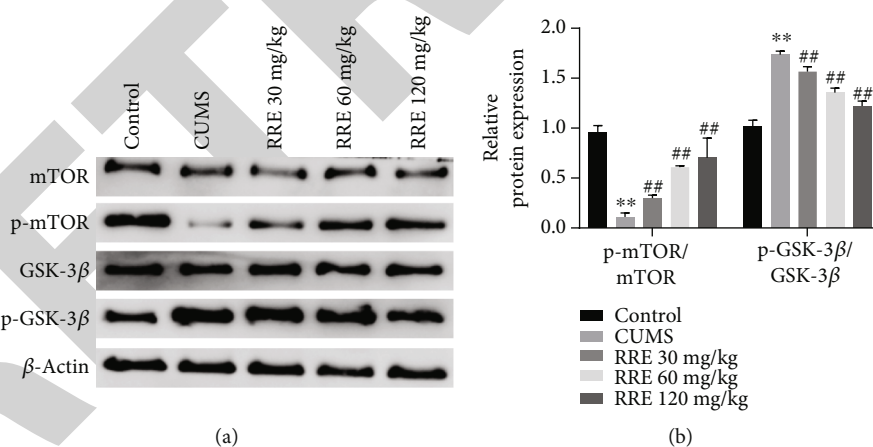


FIGURE 7: Effects of RRE on GSK-3 $\beta$  and mTOR signaling pathways in CUMS rats: (a) mTOR, p-mTOR, GSK-3 $\beta$ , and p-GSK-3 $\beta$  in the hippocampal tissue measured by Western blot; (b) grayscale analysis of p-mTOR/mTOR and p-GSK-3 $\beta$ /GSK-3 $\beta$  ratios. \*\* $P < 0.01$  vs. control group, ## $P < 0.01$  vs. CUMS group.

of the release of inflammatory factors could be the reason for RRE-caused relief of depression.

In recent years, investigators have explored whether an oxidative stress injury has a role as being a trigger for depression and what its mechanism is. In a physiological state, free radicals are normal metabolites in the process of mitochondrial circulation and oxidative phosphorylation, which can be eliminated by the body's SOD, GSH-PX, CAT, and other enzymes or nonenzymatic molecules such as vitamin C, vita-

min E, and other antioxidant stress systems. In a pathological state, oxidative stress is dominant, and insufficiency in antioxidative stress function could lead to oxidative stress damage in the body. MDA, the main product of lipid peroxidation, has been used to reflect the degree of lipid peroxidative damage in the body [32]. The present study also found that the activities of GSH and SOD in CUMS rat hippocampal tissue significantly downregulated while upregulation occurred in the content of MDA, suggesting that the

imbalance of oxidative stress in the brain may lead to peroxidative damage to neurons. The advent of RRE greatly restored the activities of GSH, and SOD were restored with the advent of RRE, accompanied by decreased MDA contents. The antioxidant effect of RRE on CUMS rats was closely related to its concentration.

Besides, our study also found markedly decreased BDNF and TrkB in the hippocampal tissue from CUMS rats, but their expression could be greatly restored after RRE treatment. BDNF, known as brain-derived neurotrophic factor, is ubiquitous in the central nervous system and crucial to nervous system development and neuronal remodeling [33]. A significant decrease in BDNF expression has been noticed in the central nervous system and peripheral blood of patients with depression [34]. BDNF activates the intracellular functional region and triggers the autophosphorylation of TrkB by specifically binding to TrkB elements, thereby activating the downstream Ras-MAPK pathway to mediate synaptic plasticity and the growth and proliferation of hippocampal neurons. These processes may thereby maintain and promote memory and spatial recognition functions [35, 36]. The above studies suggest that the antidepressant effects of RRE on rats could be related to the reversal of the expression of BDNF and TrkB.

GSK-3 is a glycogen synthase kinase with two isoforms,  $\alpha$  and  $\beta$ . GSK-3 $\beta$  is widely expressed in all brain regions [37]. Studies have shown that the phosphorylation level of GSK-3 $\beta$  is increased in depressed animals after stress. Injection of GSK-3 $\beta$ -specific inhibitor increased the content of  $\beta$ -catenin in the hippocampal tissue and rapidly produced an antidepressant effect [38]. The activity of brain tissue GSK-3 $\beta$  significantly increased in depression and suicidal patients [39]. mTOR is a serine/threonine kinase. Activation of mTOR could promote the synthesis of local synaptic proteins and the maturation and formation of new synapses, thereby affecting the pathogenesis of depression and antidepressant treatment. The mTOR signaling pathway has an impact on the efficacy of many classic antidepressants [40]. In this present study, CUMS rats showed decreased p-mTOR and reduced ratio of p-mTOR/mTOR in the hippocampal tissue, while phosphorylation of GSK-3 $\beta$  and the ratio of p-GSK-3 $\beta$ /GSK-3 $\beta$  greatly increased. In addition, RRE treatment activated the activity of mTOR and inhibited the activity of GSK-3 $\beta$ , suggesting that the protective effect of RRE on rat behavior could be related to the regulation of GSK-3 $\beta$  and mTOR signaling pathways, but the specific mechanism needs further experimental exploration.

Moreover, RRE contains a variety of active substances, such as tannin and anthocyanins. In this study, RRE was used to directly study the therapeutic effect, but its main components were not detected, and the separation and purification were not performed. Therefore, the specific active substances in RRE that exert antidepressant effects could not be determined, and the clarification of its active substances requires further isolation and experimental exploration. Nevertheless, there is no doubt that this study has depicted the important role of RRE in antidepressant therapy.

## 5. Conclusion

In summary, this study showed that RRE was associated with an improvement in CUMS-induced depression-like behavior and regulated inflammatory factor secretion, oxidative stress substance secretion, hormone levels, and the expression levels of BDNF and TrkB in CUMS rats. The antidepressant effects of RRE were related to the GSK-3 $\beta$  and mTOR signaling pathway. Although these could suggest a possible association between RRE and alleviation of hippocampal tissue damage, additional investigations are warranted to confirm these findings and shed more light on the possible underlying mechanism.

## Data Availability

The data used to support the findings of this study are available from the corresponding author upon request.

## Ethical Approval

This study was approved by the General Hospital of Ningxia Medical University Ethics Committee (KYL-2021-1080) and performed in accordance with the approval guidelines.

## Conflicts of Interest

The authors declare that they have no competing interests.

## Acknowledgments

This study was supported by the Development of Rehabilitation Training System for Drug Self-Disposal Skills for Recovering Patients with Severe Mental Disorders (No. 2021BEG03057).

## References

- [1] D. M. Howard, M. J. Adams, M. Shirali et al., "Genome-wide association study of depression phenotypes in UK Biobank identifies variants in excitatory synaptic pathways," *Nature Communications*, vol. 9, no. 1, p. 1470, 2018.
- [2] M. Marcus, M. T. Yasamy, M. V. van Ommeren, D. Chisholm, and S. Saxena, *Depression: A Global Public Health Concern*, American Psychological Association, Washington, DC, 2012.
- [3] J. P. Lepine and M. Briley, "The increasing burden of depression," *Neuropsychiatric Disease and Treatment*, vol. 7, Supplement\_1, pp. 3–7, 2011.
- [4] L. F. Faulconbridge, T. A. Wadden, R. I. Berkowitz et al., "Changes in symptoms of depression with weight loss: results of a randomized trial," *Obesity (Silver Spring)*, vol. 17, no. 5, pp. 1009–1016, 2009.
- [5] P. Zagorscak, M. Heinrich, D. Sommer, B. Wagner, and C. Knaevelsrud, "Benefits of individualized feedback in internet-based interventions for depression: a randomized controlled trial," *Psychotherapy and Psychosomatics*, vol. 87, no. 1, pp. 32–45, 2018.
- [6] R. V. Saveanu and C. B. Nemeroff, "Etiology of depression: genetic and environmental factors," *The Psychiatric Clinics of North America*, vol. 35, no. 1, pp. 51–71, 2012.
- [7] H. Kuang, J. Feng, Q. Fan, P. Wang, and J. Wang, "Composition analysis and in vitro anti-lipid peroxidation activity of

- red raspberry polyphenols," *Food Science*, vol. 39, no. 3, pp. 83–89, 2018.
- [8] J. God, P. L. Tate, and L. L. Larcom, "Red raspberries have antioxidant effects that play a minor role in the killing of stomach and colon cancer cells," *Nutrition Research*, vol. 30, no. 11, pp. 777–782, 2010.
- [9] D. Del Rio, A. Rodriguez-Mateos, J. P. Spencer, M. Tognolini, G. Borges, and A. Crozier, "Dietary (poly) phenolics in human health: structures, bioavailability, and evidence of protective effects against chronic diseases," *Antioxidants & Redox Signaling*, vol. 18, no. 14, pp. 1818–1892, 2013.
- [10] H. A. Ross, G. J. McDougall, and D. Stewart, "Antiproliferative activity is predominantly associated with ellagitannins in raspberry extracts," *Phytochemistry*, vol. 68, no. 2, pp. 218–228, 2007.
- [11] J. H. Suh, C. Romain, R. González-Barrío et al., "Raspberry juice consumption, oxidative stress and reduction of atherosclerosis risk factors in hypercholesterolemic golden Syrian hamsters," *Food & Function*, vol. 2, no. 7, pp. 400–405, 2011.
- [12] M. J. Zhu, Y. Kang, Y. Xue et al., "Red raspberries suppress NLRP3 inflammasome and attenuate metabolic abnormalities in diet-induced obese mice," *The Journal of Nutritional Biochemistry*, vol. 53, pp. 96–103, 2018.
- [13] M. E. Figueira, M. B. Câmara, R. Direito et al., "Chemical characterization of a red raspberry fruit extract and evaluation of its pharmacological effects in experimental models of acute inflammation and collagen-induced arthritis," *Food & Function*, vol. 5, no. 12, pp. 3241–3251, 2014.
- [14] D. Jean-Gilles, L. Li, H. Ma, T. Yuan, C. O. Chichester III, and N. P. Seeram, "Anti-inflammatory effects of polyphenolic-enriched red raspberry extract in an antigen-induced arthritis rat model," *Journal of Agricultural and Food Chemistry*, vol. 60, no. 23, pp. 5755–5762, 2012.
- [15] H. Zhang, J. Liu, G. Li et al., "Fresh red raspberry phytochemicals suppress the growth of hepatocellular carcinoma cells by PTEN/AKT pathway," *The International Journal of Biochemistry & Cell Biology*, vol. 104, pp. 55–65, 2018.
- [16] W. Jieqiong, W. Chuanbo, L. Zegeng, T. Jiabing, and Y. Cheng, "Action mechanism research of Qibai Pingfei capsules on COPD rat model of depression," *Clinical Journal of Chinese Medicine*, vol. 5, no. 24, pp. 11–13, 2013.
- [17] T. D. Gould, D. T. Dao, and C. E. Kovacsics, *The Open Field Test*, Humana Press, 2009.
- [18] D. Dan, Z. Shuang, and D. Suzhen, "SKF83959 regulates locomotion activity and anxiety in rats," *Journal of East China Normal University (Natural Science)*, vol. 4, pp. 103–110, 2010.
- [19] R. Yankelevitch-Yahav, M. Franko, A. Huly, and R. Doron, "The forced swim test as a model of depressive-like behavior," *Journal of Visualized Experiments*, vol. 97, no. 97, 2015.
- [20] Z. Rogoz, M. Kabziński, W. Sadaj, P. Rachwalska, and A. Gądek-Michalska, "Effect of co-treatment with fluoxetine or mirtazapine and risperidone on the active behaviors and plasma corticosterone concentration in rats subjected to the forced swim test," *Pharmacological Reports*, vol. 64, no. 6, pp. 1391–1399, 2012.
- [21] Z. He, X. Wang, C. Huang et al., "The FENRRR/miR-214-3P/TET2 axis affects cell malignant activity via RASSF1A methylation in gastric cancer," *American Journal of Translational Research*, vol. 10, no. 10, pp. 3211–3223, 2018.
- [22] Q. Song, Z. He, B. Li et al., "Melatonin inhibits oxalate-induced endoplasmic reticulum stress and apoptosis in HK-2 cells by activating the AMPK pathway," *Cell Cycle*, vol. 19, no. 20, pp. 2600–2610, 2020.
- [23] C. M. Pariante and S. L. Lightman, "The HPA axis in major depression: classical theories and new developments," *Trends in Neurosciences*, vol. 31, no. 9, pp. 464–468, 2008.
- [24] X. Yan, D. Zeng, H. Zhu et al., "miRNA-532-5p regulates CUMS-induced depression-like behaviors and modulates LPS-induced proinflammatory cytokine signaling by targeting STAT3," *Neuropsychiatric Disease and Treatment*, vol. 16, pp. 2753–2764, 2020.
- [25] H. M. Abelaira, G. Z. Réus, M. V. Neotti, and J. Quevedo, "The role of mTOR in depression and antidepressant responses," *Life Sciences*, vol. 101, no. 1–2, pp. 10–14, 2014.
- [26] J. Hui, J. Zhang, M. Pu et al., "Modulation of GSK-3 $\beta$ / $\beta$ -catenin signaling contributes to learning and memory impairment in a rat model of depression," *The International Journal of Neuropsychopharmacology*, vol. 21, no. 9, pp. 858–870, 2018.
- [27] S. Antoniuk, M. Bijata, E. Ponimaskin, and J. Wlodarczyk, "Chronic unpredictable mild stress for modeling depression in rodents: meta-analysis of model reliability," *Neuroscience and Biobehavioral Reviews*, vol. 99, pp. 101–116, 2019.
- [28] P. W. Gold, "The organization of the stress system and its dysregulation in depressive illness," *Molecular Psychiatry*, vol. 20, no. 1, pp. 32–47, 2015.
- [29] R. C. Drexhage, E. M. Knijff, R. C. Padmos et al., "The mononuclear phagocyte system and its cytokine inflammatory networks in schizophrenia and bipolar disorder," *Expert Review of Neurotherapeutics*, vol. 10, no. 1, pp. 59–76, 2010.
- [30] D. Edberg, D. Hoppensteadt, A. Walborn, J. Fareed, J. Sinacore, and A. Halaris, "Plasma MCP-1 levels in bipolar depression during cyclooxygenase-2 inhibitor combination treatment," *Journal of Psychiatric Research*, vol. 129, pp. 189–197, 2020.
- [31] Y. Yingjie, L. Maohang, Y. Fangxin, and Q. Jihong, "Role of preinflammatory cytokines in depression," *Medical Recapitulate*, vol. 23, no. 22, pp. 4393–4396, 2017.
- [32] F. Li Haiyan, C. T. Xiaoyan, J. Qingsong, and Q. Hongmei, "Depressive behaviors of rats induced by unpredictable stress involved in up-regulation of GSK-3 $\beta$  expression and imbalance of oxidative and anti-oxidative system in rat brain," *Journal of Chongqing Medical University*, vol. 41, no. 8, pp. 792–796, 2016.
- [33] L. F. Reichardt, "Neurotrophin-regulated signalling pathways," *Philosophical Transactions of the Royal Society of London. Series B, Biological Sciences*, vol. 361, no. 1473, pp. 1545–1564, 2006.
- [34] W. Dan, "The influence of hippocampus and neurotransmitters on the pathological mechanism of depression," *Journal of Xi'an University of Arts and Sciences (Natural Science Edition)*, vol. 14, no. 2, pp. 9–13, 2011.
- [35] M. Thompson Ray, C. S. Weickert, E. Wyatt, and M. J. Webster, "Decreased BDNF, trkB-TK+ and GAD67 mRNA expression in the hippocampus of individuals with schizophrenia and mood disorders," *Journal of Psychiatry & Neuroscience*, vol. 36, no. 3, pp. 195–203, 2011.
- [36] B. Zhou, Q. Cai, Y. Xie, and Z. H. Sheng, "Snapin recruits dynein to BDNF-TrkB signaling endosomes for retrograde axonal transport and is essential for dendrite growth of cortical neurons," *Cell Reports*, vol. 2, no. 1, pp. 42–51, 2012.
- [37] Y. C. Chen, Q. R. Tan, W. Dang et al., "The effect of citalopram on chronic stress-induced depressive-like behavior in rats

## *Retraction*

# **Retracted: Peroxisome Proliferator-Activated Receptor Gene Knockout Promotes Podocyte Injury in Diabetic Mice**

### **BioMed Research International**

Received 12 November 2022; Accepted 12 November 2022; Published 23 November 2022

Copyright © 2022 BioMed Research International. This is an open access article distributed under the Creative Commons Attribution License, which permits unrestricted use, distribution, and reproduction in any medium, provided the original work is properly cited.

*BioMed Research International* has retracted the article titled “Peroxisome Proliferator-Activated Receptor Gene Knockout Promotes Podocyte Injury in Diabetic Mice” [1] due to concerns that the peer review process has been compromised.

Following an investigation conducted by the Hindawi Research Integrity team [2], significant concerns were identified with the peer reviewers assigned to this article; the investigation has concluded that the peer review process was compromised. We therefore can no longer trust the peer review process and the article is being retracted with the agreement of the editorial board.

### **References**

- [1] R. Yan, Y. Zhang, Y. Yang et al., “Peroxisome Proliferator-Activated Receptor Gene Knockout Promotes Podocyte Injury in Diabetic Mice,” *BioMed Research International*, vol. 2022, Article ID 9018379, 8 pages, 2022.
- [2] L. Ferguson, “Advancing Research Integrity Collaboratively and with Vigour,” 2022, <https://www.hindawi.com/post/advancing-research-integrity-collaboratively-and-vigour/>.



## Research Article

# Peroxisome Proliferator-Activated Receptor Gene Knockout Promotes Podocyte Injury in Diabetic Mice

Rui Yan,<sup>1</sup> Ye Zhang,<sup>1</sup> Yuxing Yang,<sup>2</sup> Lingling Liu,<sup>3</sup> Lirong Liu,<sup>4</sup> Ziwei Guo,<sup>1</sup> Haiyan Yu,<sup>1</sup> Yuanyuan Wang<sup>3</sup> ,<sup>3</sup> and Bing Guo<sup>3</sup> 

<sup>1</sup>Department of Nephrology Affiliated Hospital of Guizhou Medical University, Guiyang, 550004 Guizhou, China

<sup>2</sup>Department of Endocrinology Affiliated Hospital of Guizhou Medical University, Guiyang, 550004 Guizhou, China

<sup>3</sup>Guizhou Provincial Key Laboratory of Pathogenesis and Drug Research on Common Chronic Diseases, Guizhou Medical University, Guiyang, 550025 Guizhou, China

<sup>4</sup>Department of Clinical Hematology, School of Clinical Laboratory Science, Guizhou Medical University, Guiyang, 550004 Guizhou, China

Correspondence should be addressed to Yuanyuan Wang; [guizmedyuanyuan@hospt-edu.cn](mailto:guizmedyuanyuan@hospt-edu.cn) and Bing Guo; [guobingbs@126.com](mailto:guobingbs@126.com)

Rui Yan and Ye Zhang contributed equally to this work.

Received 21 April 2022; Accepted 14 May 2022; Published 30 June 2022

Academic Editor: Dinesh Rokaya

Copyright © 2022 Rui Yan et al. This is an open access article distributed under the Creative Commons Attribution License, which permits unrestricted use, distribution, and reproduction in any medium, provided the original work is properly cited.

**Objective.** To investigate the effects of peroxisome proliferator-activated receptor (PPAR $\gamma$ ) expression on renal podocyte in diabetic mice by conditionally knockout mouse PPAR $\gamma$  gene. **Methods.** Wild-type C57BL mice and PPAR $\gamma$  gene knockout mice were used as research objects to establish the diabetic mouse model, which was divided into normal control group (NC group), normal glucose PPAR $\gamma$  gene knockout group (NK group), diabetic wild-type group (DM group), and diabetic PPAR $\gamma$  gene knockout group (DK group), with 8 mice in each group. After 16 weeks, the mice were sacrificed for renal tissue collection. Morphological changes of renal tissue were observed by HE and Masson staining, and ultrastructure of renal tissue was observed by transmission electron microscope. Protein expressions of PPAR $\gamma$ , podocin, nephrin, collagen IV, and fibronectin (FN) in renal tissues were detected by immunohistochemistry and Western blot, and mRNA changes of PPAR $\gamma$ , podocin, and nephrin in renal tissues were detected by qRT-PCR. **Results.** Compared with the NC group, the protein and mRNA expressions of PPAR $\gamma$ , podocin, and nephrin decreased in the kidney tissue of mice in the DM group, while the protein expressions of collagen IV and FN increased. The expression of various proteins in kidney tissues of the DK group was consistent with that of the DM group, and the difference was more obvious. The expression of PPAR $\gamma$  protein and mRNA decreased in the NK group, while the expression of podocin, nephrin protein and mRNA, collagen IV, and FN protein showed no significant difference. **Conclusion.** In diabetic renal tissue, the loss of PPAR $\gamma$  can aggravate podocellular damage and thus promote the occurrence of diabetic renal fibrosis. Increasing the expression of PPAR $\gamma$  may effectively relieve renal podocyte impairment in diabetic patients, which can be used for the treatment of diabetic nephropathy.

## 1. Introduction

Diabetic nephropathy (DN) is a serious complication of diabetes [1, 2] and one of the main reasons that causes end-stage renal disease. Studies have shown that podocyte injury plays a very important role in the occurrence and development of diabetic nephropathy [3, 4].

Glomerulosclerosis is characterized by progressive proliferation of mesangial cells, deposition of extracellular matrix, and reduction of intrinsic glomerular cell composition. Podocytes, namely, the glomerular visceral epithelial cells, are attached to the lateral side of the glomerular basement membrane (GBM) and together with vascular endothelial cells and glomerular basal membrane constitute the



glomerular filtration barrier [5, 6]. Podocytes have unique structures of foot processes, and abnormal expressions of the interconnecting slit diaphragm (SD) proteins nephrin, podocin, and CD2AP are characteristic markers of early injury of podocytes [7]. In 1998, Tryggvason discovered the podocyte slit diaphragm protein nephrin, which is specifically located in the podocyte slit diaphragm region and participates in maintaining the normal morphology and function of podocyte [8]. Podocin can form complex with nephrin to regulate the filtration permeability of filtered SD [9]. With the progression of DN, podocyte processes disappearance, fusion to sertoli cell apoptosis and abscission, destruction of glomerular basement membrane, and massive proteinuria may occur, and proteinuria itself may further aggravate podocyte injury, forming a vicious cycle, and eventually develop into end-stage renal disease [10–12].

Peroxisome proliferator-activated receptor  $\gamma$  (PPAR $\gamma$ ) is expressed in renal tubular epithelial cells, and its systemic activation has been shown to be protective against renal fibrosis [13]. The injury and shedding of podocyte are closely related to proteinuria, which is the key factor in the formation and development of glomerulosclerosis [14, 15]. Studies have found that pioglitazone, a peroxisome proliferator-activated receptor (PPAR $\gamma$ ) agonist, can reduce glomerular hypertrophy and glomerular hyperfiltration in KK/TA mice [16]. These results suggest that activation of PPAR $\gamma$  is closely related to remission of DN [17, 18]. In addition, activation of PPAR $\gamma$  has been documented to slow down podocyte damage and protect its integrity. Downregulation of PPAR $\gamma$  expression in renal tubular epithelial cells also affects podocyte function [19]. However, the current study only observed the treatment of PPAR $\gamma$  agonists and inhibitors, and the relationship between the expression changes of PPAR $\gamma$  gene or protein itself in renal tissues and podocyte injury is not clear [20]. Therefore, this study intends to use conditional PPAR $\gamma$  gene knockout diabetic mice as the research object and observe the expression changes of podocyte-related molecules in mouse kidney tissue after PPAR $\gamma$  gene knockout.

## 2. Materials and Methods

**2.1. Main Materials and Reagents.** C57BL wild-type mice and C57BL renal tubule conditional PPAR $\gamma$  gene knockout mice (SPF grade), with a body weight of  $30 \pm 5$  g, were self-bred and identified (Professor Guan Youfei of Peking University Health Science Center presented a rat as a gift, SYXK (Beijing) 2011-0012). The following are the main materials and reagents: streptozotocin (STZ; SIGMA company); two-step immunohistochemistry detection reagent, horseradish peroxidase-labeled sheep anti-rabbit IgG, and DAB coloration kit (ZSGB Bio Co., Beijing); bicinchoninic acid protein concentration determination kit and ECL chromogenic agent (Beyotime Biotechnology, Beijing); prestained marker (Thermo Fisher Scientific); mouse anti- $\beta$ -actin antibody (Bioworld, Nanjing); rabbit anti-PPAR $\gamma$  antibody, rabbit anti-NPHS2 antibody, and rabbit anti-collagen-IV antibody (Proteintech); rabbit antinephrin antibody (Abcam); total RNA kit (TIANGEN Biochemical Technology Co., Beijing);

real-time PCR assay kit (TaKaRa); and light microscopy and transmission electron microscopy (Precise, Beijing).

**2.2. Establishment of Mouse DM Model and Experimental Grouping.** Mice were randomly divided into 4 groups (the mice were presented by Professor Guan Youfei of Peking University Health Science Center): wild-type normal control group (NC), normal glucose PPAR $\gamma$  gene knockout group (NK), wild-type diabetes group (DM), and diabetic PPAR $\gamma$  gene knockout group (DK), with 8 mice in each group. For renal tubular epithelial cell conditional PPAR $\gamma$  gene knockout mouse [21], triple loxE gene targeting strategy was adopted. Three loxP loci were introduced into the mouse PPAR $\gamma$  gene to determine the DNA sequence of the PPAR- $\gamma^{\text{lox}}$  allele. Male mice heterozygous with the target allele (PPAR $^{\text{w/lox} + \text{neo}}$ ) were crossbred with wild-type female mice to obtain single-celled embryos. Cre mediated partial or total recombination was achieved by microinjection of 0.1 ng/ $\mu$ L Cre expressing plasmid (pBS185) into embryos. This resulted in the creation of wild-type (PPAR $^{\text{w}}$ ) and knockout (PPAR $^{\text{del}}$ ) PPAR $\gamma$  allele mouse embryos, which were isolated by further reproduction.

The DM and DK groups received intraperitoneal injection of streptozotocin (STZ) (SIGMA company) 55 mg/(kg·day) for 5 days. After 2 weeks, tail venous blood was collected to measure blood glucose, and blood glucose above 16.7 mmol/L was considered as successful modeling. The mice in the four groups were fed to 16 weeks, fasted for 6 h, anaesthesia with ether, collected blood from femoral artery, and separated serum (centrifugation at 4°C). Blood glucose (BG) was measured by oxidase method. The kidneys were taken from both sides after laparotomy. One side was used for prepare paraffin sections (the kidney tissue was fixed in 4% paraformaldehyde) for pathological examination and immunohistochemical staining, and the other side was used for protein and RNA extraction (stored at -80°C) for Western blot and real-time PCR.

**2.3. Immunohistochemical Test.** PPAR $\gamma$ , podocin, nephrin, collagen IV, and fibronectin proteins in renal tissues were determined by streptavidin-peroxidase (SP) two-step immunoassay kit. Paraffin sections of kidney tissues were dewaxed and hydrated and added 3% H<sub>2</sub>O<sub>2</sub> to inhibit endogenous peroxidase. After microwave antigen repair, PPAR $\gamma$  (1:200), podocin (1:250), nephrin (1:200), collagen IV (1:100), and fibronectin (1:50) specific primary antibodies were added and incubated overnight at 4°C. The next day, it was rewarmed to room temperature, rinsed, and incubated with secondary antibody (horseradish peroxidase labeled) for 30 min (37°C). Diaminobenzidine (DAB) was added for color rendering; hematoxylin was redyed, rinsed, dehydrated, and transparent; and the tablet was sealed with neutral gum. Leica microscope was used to randomly observe 5 fields at 200x magnification and collect images. The average number of stained cells was calculated for semiquantitative analysis.

Histopathological examination was performed by light microscopy and transmission electron microscopy at 400 times and 20000 times, respectively. Five visual fields were randomly selected for each group.

TABLE 1: Primer sets used in real time RT-PCR.

Gene	Upstream primer	Reverse primer
PPAR $\gamma$	5'-TTTCAAGGGTGCCAGTTTCG-3'	5'-ATCCTTGCCCTCTGAGATGAG-3'
Podocin	5'-TGAGGATGGCGGCTGAGAT-3'	5'-GGTTTGGAGGAACCTTGGGT-3'
Nephrin	5'-CCCAACACTGGAAGAGGT-3'	5'-CTGGTCGTAGATCCCCCTTG-3'
$\beta$ -Actin	5'-GCTACAGCTTCACCACCACA-3'	5'-AAGGAGGCTGGAAAAGAGC-3'

TABLE 2: Biochemical indexes of mice.

Index	NC	NK	DM	DK
Weight (g)	31.0 $\pm$ 2.3	30.3 $\pm$ 2.5	29.6 $\pm$ 4.3	25.6 $\pm$ 5.2*
Blood glucose (mmol/L)	12.3 $\pm$ 1.4	11.0 $\pm$ 2.9	33.6 $\pm$ 12.1**	32.2 $\pm$ 6.9**
Blood creatinine ( $\mu$ mol/L)	10.2 $\pm$ 2.5	13.5 $\pm$ 3.2	17.3 $\pm$ 2.5*	18.7 $\pm$ 4.0*
Blood urea nitrogen (mmol/L)	6.9 $\pm$ 1.2	8.1 $\pm$ 1.7	13.9 $\pm$ 3.4*	16.7 $\pm$ 3.2*

Note: \* $P < 0.05$ ; \*\* $P < 0.01$ .

**2.4. Western Blot.** The cortical part of the kidney tissue was taken and added with histone lysate for full grinding; then, the supernatant was taken, and the protein concentration was determined with BCA protein detection kit (Beyotime Institute of Biotechnology, Beijing). Then, 50 ng supernatant was added into  $2 \times$  SDS sample buffer to prepare the sample. After fully mixing, the sample was bathed in water at 100°C for 10 min. Cool to room temperature, set aside at 4°C, or store at -20°C. After sample loading, electrophoresis, membrane transfer, and sealing, specific anti-PPAR $\gamma$  (1:1000), anti-podocin (1:5000), anti-collagen-IV (1:500), anti-fibronectin (1:800) (Proteintech company), anti-nephrin (1:300) (Abcam), anti- $\beta$ -actin (1:6000), (Bioworld Technology, Nanjing) were added, sealed, 4°C gently shake overnight. TBST was added to wash the membrane for 5 min  $\times$  3 times. The specific secondary antibody (ZSGB-Bio company) was incubated for 1 h, and the membrane was washed again with TBST for 5 min  $\times$  3 times. Add ECL (Beyotime Institute of Biotechnology, Beijing) development and exposure. Scans were performed using Shanghai Qinxiang gel imaging system. The ImageJ software analyzed the absorbance value of each band and detected the relative expression of each target protein, three times for each group.

**2.5. Real-Time PCR.** According to the kit instructions of TIANGEN Company, total RNA was extracted from renal tissues of mice in each group by TRIzol method. The cDNA was synthesized by reverse transcription-polymerase chain reaction with 20  $\mu$ L reaction system. Primers for PPAR $\gamma$ , podocin, and nephrin mRNA were synthesized by Shanghai Sangon Biotech Co., Ltd. Primer sequences are shown in Table 1. TB Green<sup>TM</sup> Premix Ex Taq<sup>TM</sup> II (Takara) was used for quantitative PCR. The experiment was repeated three times for each group.

**2.6. Statistical Treatment.** The experimental data were processed and analyzed by the GraphPad Prism 5 and SPSS 19.0 softwares. Mean  $\pm$  SD ( $\bar{x} \pm s$ ) was used to represent measurement data. After the data passed the test of variance, one-

way ANOVA was used between multiple groups, and least significant difference (LSD) method was used to analyze and compare the two groups of samples. When  $P < 0.05$ , the difference was statistically significant.

### 3. Results

**3.1. General Situation and Biochemical Indexes of Mice.** After the replication of the DM model induced by STZ, mice in the DM and DK groups showed polydipsia, polyphagia, polyuria, and weight loss. Compared with the NC group or NK group, blood glucose ( $P < 0.01$ ), blood creatinine, and blood urea nitrogen ( $P < 0.05$ ) in the DM and DK groups were increased. Compared with the DM group, the increase of above indexes in the DK group was more significant, but the difference was not statistically significant, as shown in Table 2.

**3.2. Renal Histomorphology.** The renal tissues of mice were examined by pathological examination. HE staining showed complete glomerular morphology, no dilation and necrosis of renal tubules, and complete basement membrane of mice in the NC and NK groups. In the DM group, the lumen of renal tubules was dilated, the epithelial cells were swollen and vacuolated, the basement membrane was irregular thickened, and there were many inflammatory cells infiltrating in the interstitium. The above changes were more obvious in the DK group. Masson staining showed no collagen deposition in the glomerular basement membrane, mesangial area, and interstitial area of renal tubules in the NC and NK groups. The above changes were more serious in the DK group, presenting extensive fibrosis (Figure 1(a)). Transmission electron microscopy showed that the renal ultrastructure was normal in the NC group and NK group. The basement membrane of glomerular capillaries was thickened and mesangial matrix was increased structural changes of podocytes, extensive fusion of foot processes, and increase of hiatus between foot processes were observed in renal tissues of the DM and DK groups (Figure 1(b)).

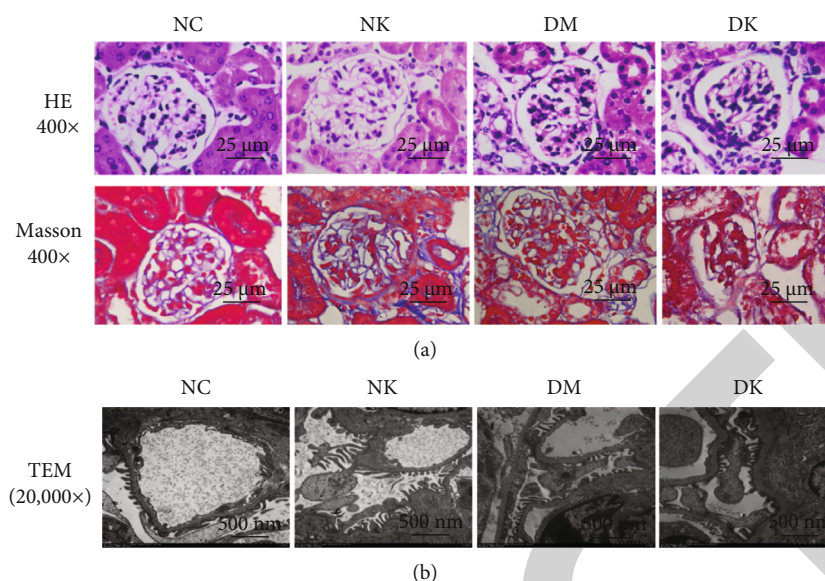


FIGURE 1: (a) Pathological examination of renal tissues of mice in each group by light microscopy (400x). (b) The ultrastructure of renal tissue was observed by transmission electron microscope (20,000x).

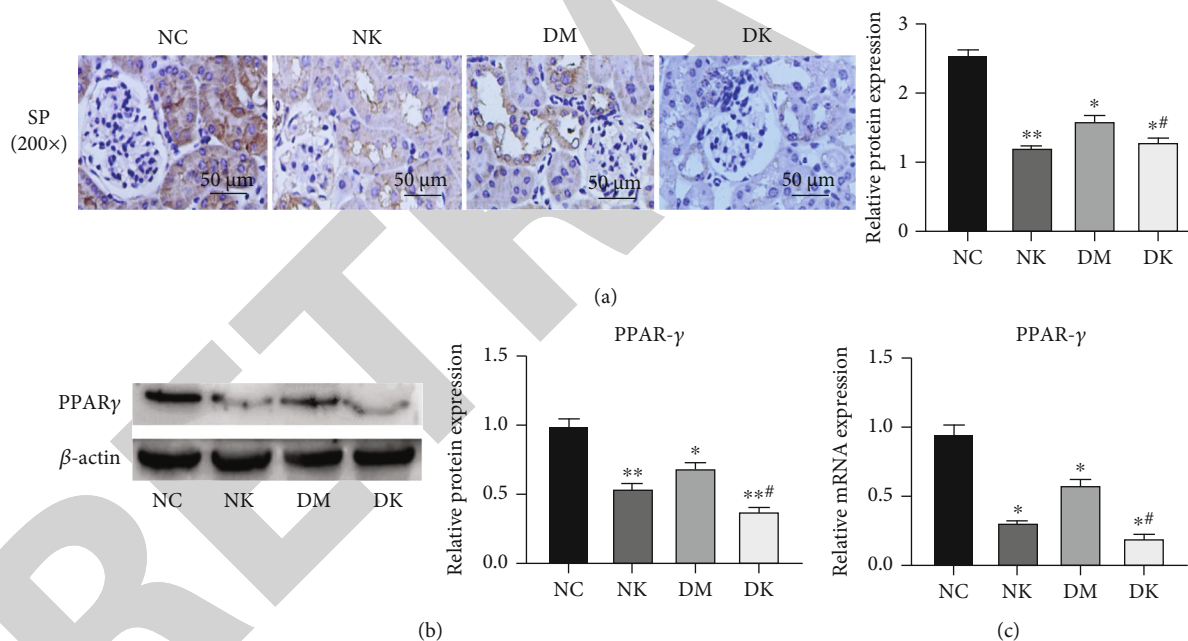


FIGURE 2: (a) The expression of PPAR $\gamma$  in renal tissues of each group was detected by immunohistochemistry (400x). (b) The expression of PPAR $\gamma$  was detected by WB. (c) The expression of PPAR $\gamma$  was detected by RT-qPCR. Compared with the NC group, \* $P < 0.05$  and \*\* $P < 0.01$ . Compared with the DM group, # $P < 0.05$ .

**3.3. Expression of PPAR $\gamma$  Protein in Renal Tissues of Each Group.** The expression levels of PPAR $\gamma$  protein in kidney tissues of mice in four groups were detected by immunohistochemistry and Western blot. Immunohistochemical results showed that PPAR $\gamma$  was highly expressed in renal tissues of mice in the NC group, and the staining result was strongly positive (+++). The expression level of PPAR $\gamma$  protein in the NK group and DM group was lower than that in the normal group, and the staining result was medium positive (++)

The protein expression level was lowest in the DK group, and the staining result was weakly positive (+) (Figure 2(a)). WB results were consistent with immunohistochemical results (Figure 2(b)). qRT-PCR results showed that compared with the NC group, PPAR $\gamma$  mRNA levels in the NK, DM, and DK groups were decreased, and the differences were statistically significant (\* $P < 0.05$ ). Compared with the DM group, PPAR $\gamma$  mRNA level in the DK group was significantly lower (# $P < 0.05$ ) (Figure 2(c)).



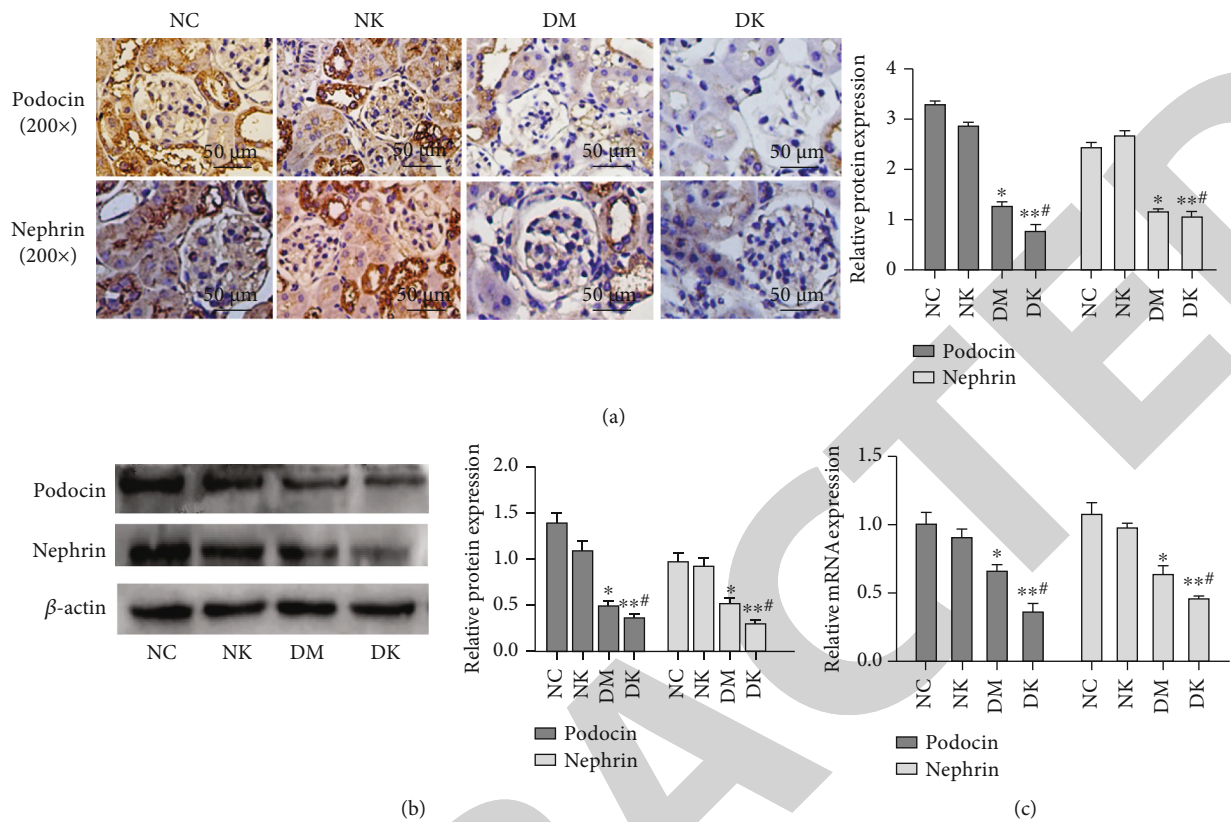


FIGURE 3: (a) The expression of podocin and nephrin in renal tissues of each group was detected by immunohistochemistry (SP assay, 200x). (b) WB detected the expression of podocin and nephrin in tissues. (c) RT-qPCR detected the expression of podocin and nephrin in tissues. Compared with the NC group, \* $P < 0.05$  and \*\* $P < 0.01$ . Compared with the DM group, # $P < 0.05$ .

**3.4. Podocin and Nephrin Protein Expressions in Renal Tissues of Each Group.** Immunohistochemical results showed that podocin staining was strongly positive (+++) and nephrin staining was moderately positive (++) in the NC group. NK group podocin and nephrin staining results were medium positive (++). Podocin and nephrin staining results were weakly positive (+) in the DM group. Podocin and nephrin staining results were negative (-) in the DK group (Figure 3(a)). qRT-PCR results showed that compared with the NC group, the mRNA levels of podocin and nephrin in the DM group were decreased, and the expression level of podocin and nephrin in the DK group was the lowest; the difference was statistically significant (\* $P < 0.05$ , \*\* $P < 0.01$ ). No significant difference was found in the NK group ( $P > 0.05$ ) (Figure 3(b)). The results of Western blotting showed that podocin and nephrin were highly expressed in renal tissues of the NC group and NK group, while the expression levels of podocin and nephrin in the DM and DK groups were lower than those in the NC group. Compared with the DM group, the protein expression level of the DK group was the lowest (Figure 3(c)).

**3.5. Protein Expression of Collagen IV and Fibronectin in Renal Tissues of Each Group.** Immunohistochemical results showed that the staining results of the NC group and NK group were the same: collagen IV and fibronectin staining

were negative. Collagen IV and fibronectin staining were weakly positive (+) in the DM group. In the DK group, collagen IV staining was strongly positive (+++), and fibronectin staining was moderately positive (++) (Figure 4(a)). WB results showed that the expression levels of collagen IV and fibronectin in renal tissues of the NC group and NK group were very low, and the expression levels of collagen IV and fibronectin in the DM group and DK group were higher than those in the normal group (\* $P < 0.05$ , \*\* $P < 0.01$ ), and the protein expression level of the DK group was the highest (Figure 4(b)).

#### 4. Discussion

The pathological changes of diabetic nephropathy mainly include glomerulosclerosis and tubulointerstitial fibrosis [22]. The main pathological processes of renal interstitial fibrosis include changes in tissue microenvironment caused by renal injury, myofibroblast activation and proliferation, production and deposition of a large amount of extracellular matrix (ECM), renal tubular atrophy, and capillary loss [23]. ECM is a noncellular scaffold structure located in the renal interstitium, which provides physical support for renal tubules and capillaries and regulates tissue homeostasis under physiological conditions [24]. ECM is rich in fibrin, matrix proteins, proteoglycans, and other cytokines that

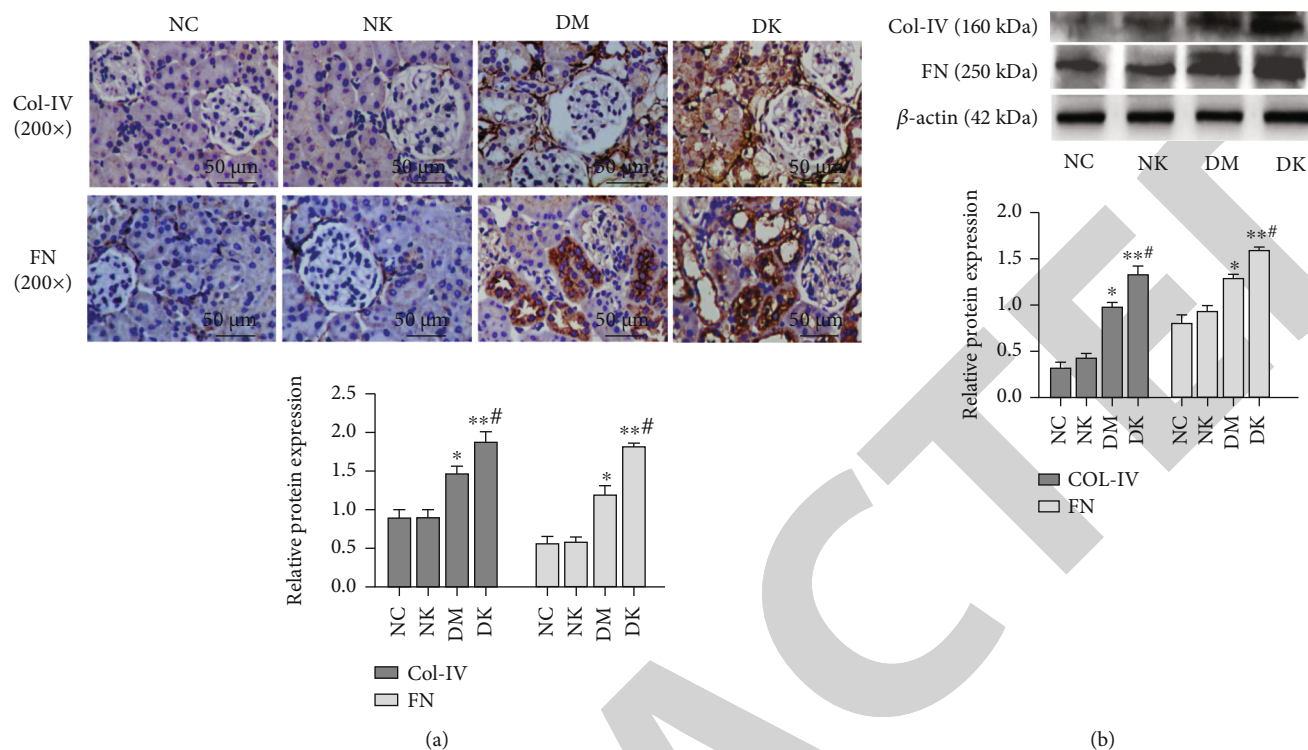


FIGURE 4: (a) The expression of collagen IV and fibronectin in renal tissues of each group was detected by immunohistochemistry (SP assay, 200x). (b) WB detected the expression of collagen IV and fibronectin in tissues. Compared with the NC group, \* $P < 0.05$  and \*\* $P < 0.01$ . Compared with the DM group, # $P < 0.05$ .

promote fibrosis [25]. Fibrin forms the framework of ECM and is the main component of ECM. Fibrin mainly includes collagen, fibronectin, and elastin. Therefore, these protein changes can be a marker of fibrotic lesions.

A large number of studies have confirmed that PPAR $\gamma$  receptor agonists have a significant renal protective effect in the treatment of DN. Choi et al. [26] found that the phosphorylation of PPAR $\gamma$  mediated by cyclin-dependent kinase 5 (Cdk5) may be involved in the pathogenesis of insulin resistance, while rosiglitazone can block the phosphorylation of CK5-PPAR. This inhibition is effective both in vivo and in vitro. Meanwhile, rosiglitazone has significant antidiabetic effects [27] and insulin sensitization [28]. It has been proved that the expression of PPAR $\gamma$  in NRK-52E cells was inhibited and phosphorylated in high glucose environment, but no such changes occurred in mannitol environment [29]. And PPAR $\gamma$  agonist can effectively protect podocyte and regulate podocyte injury [30].

Therefore, in order to investigate the correlation between the expression of PPAR $\gamma$  in mouse renal tissue and podocytes injury, this study used renal tubular epithelial cell conditioned PPAR $\gamma$  gene knockout mice, and intraperitoneal injection of STZ was used to replicate the normal wild mice and the DN model of PPAR $\gamma$  knockout mice. Subsequently, the changes of renal tissue structure were observed by light microscope and electron microscope, and the protein and mRNA expressions of PPAR $\gamma$ , podocin, nephrin, collagen IV, and fibronectin were detected by immunohistochemistry, Western blot, and real-time PCR. Under light micro-

scope, the renal tubule lumen of mice in the DM group and DK group was dilated, epithelial cells were swollen and vacuolated, basement membrane was irregular thickened, and there were many inflammatory cells infiltrating in the interstitium. The above changes were more obvious in the DK group. The glomerular mesangial matrix was increased, and the foot process was fused extensively under electron microscope. In protein level detection, it was found that the expression levels of PPAR $\gamma$ , podocin, and nephrin in renal tissue of mice in the DN group were decreased, accompanied by upregulated expressions of collagen IV and fibronectin; markers of renal interstitium fibrosis and the above protein expression changes were more obvious in renal tissue of mice in the DK group. However, there was no statistical significance in the NK group. In conclusion, PPAR $\gamma$  deletion promoted podocyte injury and aggravated DN fibrosis in DN condition, while in normal glucose condition, PPAR $\gamma$  deletion did not cause obvious podocyte injury and renal fibrosis, which may be related to the absence of PPAR $\gamma$  phosphorylation. Meanwhile, mRNA changes of PPAR $\gamma$ , podocin, and nephrin were consistent with protein level changes. In conclusion, in DN mouse kidney tissue, PPAR $\gamma$  deletion can reduce the expression of podocyte marker protein podocin and nephrin and aggravate the occurrence of renal fibrosis.

In this study, we elucidated the changes of PPAR $\gamma$  and Podocyte marker expression in mouse renal tissue under DN condition and their relationship with renal fibrosis. However, there are still some deficiencies in this study. It is not clear how PPAR $\gamma$  regulates podocyte injury. In the



future, we will further study specific regulatory links and mechanisms from in vitro and clinical trials.

## Data Availability

The datasets used and/or analyzed during the current study are available from the corresponding authors on reasonable request.

## Ethical Approval

Research experiments conducted in this article with animals were approved by the Ethical Committee of Affiliated Hospital of Guizhou Medical University and following all guidelines, regulations, legal, and ethical standards as required for animals.

## Conflicts of Interest

The authors declared no potential conflicts of interest with respect to the research, authorship, and/or publication of this article.

## Acknowledgments

This paper is supported by the National Natural Science Foundation of China (81960140), the Science and Technology Foundation of Guizhou Provincial Health Commission (GZWKJ2020-1-002), and the Innovative and Entrepreneurial Funding Project for High-Level Overseas Talents in Guizhou Province (Scholarship Contract for Overseas Talents (2018) 01).

## References

- [1] C. Qi, X. Mao, Z. Zhang, and H. Wu, "Classification and differential diagnosis of diabetic nephropathy," *Journal Diabetes Research*, vol. 2017, article 8637138, 7 pages, 2017.
- [2] C. E. Meza Letelier, C. A. San Martín Ojeda, J. J. Ruiz Provoste, and C. J. Frugone Zaror, "Pathophysiology of diabetic nephropathy: a literature review," *Medwave*, vol. 17, no. 1, article 6839, 2017.
- [3] H. Kadoya, M. Satoh, Y. Haruna, T. Sasaki, and N. Kashihara, "Klotho attenuates renal hypertrophy and glomerular injury in Ins2Akita diabetic mice," *Clinical and Experimental Nephrology*, vol. 20, no. 5, pp. 671–678, 2016.
- [4] J. S. Lin and K. Susztak, "Podocytes: the weakest link in diabetic kidney disease?," *Current Diabetes Reports*, vol. 16, no. 5, pp. 1–9, 2016.
- [5] M. Nagata, "Podocyte injury and its consequences," *Kidney International*, vol. 89, no. 6, pp. 1221–1230, 2016.
- [6] K. Asanuma, "The role of podocyte injury in chronic kidney disease," *Nihon Rinsho Men'eki Gakkai kaishi= Japanese Journal of Clinical Immunology*, vol. 38, no. 1, pp. 26–36, 2015.
- [7] J. A. Jefferson, S. J. Shankland, and R. H. Pichler, "Proteinuria in diabetic kidney disease: a mechanistic viewpoint," *Kidney International*, vol. 74, no. 1, pp. 22–36, 2008.
- [8] G. I. Welsh and M. A. Saleem, "Nephrin-signature molecule of the glomerular podocyte?," *The Journal of Pathology*, vol. 220, no. 3, pp. 328–337, 2010.
- [9] Y. Hu, S. Ye, Y. Xing, L. Lv, W. Hu, and W. Zhou, "Saxagliptin attenuates glomerular podocyte injury by increasing the expression of renal nephrin and podocin in type 2 diabetic rats," *Acta Diabetologica*, vol. 57, no. 3, pp. 279–286, 2020.
- [10] B. Denhez and P. Geraldes, "Regulation of nephrin phosphorylation in diabetes and chronic kidney injury," *Advances in Experimental Medicine and Biology*, vol. 966, pp. 149–161, 2017.
- [11] S. Fakhruddin, W. Alanazi, and K. E. Jackson, "Diabetes-induced reactive oxygen species: mechanism of their generation and role in renal injury," *Journal Diabetes Research*, vol. 2017, article 8379327, 30 pages, 2017.
- [12] K. Yasuno, S. Ishihara, R. Saito et al., "Early-onset podocyte injury and glomerular sclerosis in Osborne-Mendel rats," *The Journal of Veterinary Medical Science*, vol. 72, no. 10, pp. 1319–1327, 2010.
- [13] M. Zhao, Y. Chen, G. Ding et al., "Renal tubular epithelium-targeted peroxisome proliferator-activated receptor- $\gamma$  maintains the epithelial phenotype and antagonizes renal fibrogenesis," *Oncotarget*, vol. 7, no. 40, pp. 64690–64701, 2016.
- [14] K. Matsui, A. Kamijo-Ikemori, M. Hara et al., "Clinical significance of tubular and podocyte biomarkers in acute kidney injury," *Clinical and Experimental Nephrology*, vol. 15, no. 2, pp. 220–225, 2011.
- [15] S. Merscher and A. Fornoni, "Podocyte pathology and nephropathy - sphingolipids in glomerular diseases," *Frontiers in Endocrinology*, vol. 5, p. 127, 2014.
- [16] M. Tanimoto, Q. Fan, T. Gohda, T. Shike, Y. Makita, and Y. Tomino, "Effect of pioglitazone on the early stage of type 2 diabetic nephropathy in KK/Ta mice," *Metabolism*, vol. 53, no. 11, pp. 1473–1479, 2004.
- [17] Z. Zhou, J. Wan, X. Hou, J. Geng, X. Li, and X. Bai, "Micro-RNA-27a promotes podocyte injury via PPAR $\gamma$ -mediated  $\beta$ -catenin activation in diabetic nephropathy," *Cell Death & Disease*, vol. 8, no. 3, article e2658, 2017.
- [18] Z. W. Dai, K. D. Cai, L. C. Xu, and L. L. Wang, "Perilipin2 inhibits diabetic nephropathy-induced podocyte apoptosis by activating the PPAR $\gamma$  signaling pathway," *Molecular and Cellular Probes*, vol. 53, p. 101584, 2020.
- [19] C. Platt and R. J. Coward, "Peroxisome proliferator activating receptor- $\gamma$  and the podocyte," *Nephrology, Dialysis, Transplantation*, vol. 32, no. 3, pp. 423–433, 2017.
- [20] Y. Zhang and Y. Guan, "PPAR- $\gamma$  agonists and diabetic nephropathy," *Current Diabetes Reports*, vol. 5, no. 6, pp. 470–475, 2005.
- [21] J. R. Jones, K. D. Shelton, Y. Guan, M. D. Breyer, and M. A. Magnuson, "Generation and functional confirmation of a conditional null PPAR $\gamma$  allele in mice," *Genesis*, vol. 32, no. 2, pp. 134–137, 2002.
- [22] T. W. C. Tervaert, A. L. Mooyaart, K. Amann et al. Pathologic classification of diabetic nephropathy," *Journal of the American Society of Nephrology*, vol. 21, no. 4, pp. 556–563, 2010.
- [23] B. D. Humphreys, "Mechanisms of renal fibrosis," *Annual Review of Physiology*, vol. 80, no. 1, pp. 309–326, 2018.
- [24] C. Bonnans, J. Chou, and Z. Werb, "Remodelling the extracellular matrix in development and disease," *Nature Reviews. Molecular Cell Biology*, vol. 15, no. 12, pp. 786–801, 2014.
- [25] M. Walraven and B. Hinz, "Therapeutic approaches to control tissue repair and fibrosis: extracellular matrix as a game changer," *Matrix Biology*, vol. 71, pp. 205–224, 2018.

## *Retraction*

# **Retracted: Processing Decision Tree Data Using Internet of Things (IoT) and Artificial Intelligence Technologies with Special Reference to Medical Application**

### **BioMed Research International**

Received 20 June 2023; Accepted 20 June 2023; Published 21 June 2023

Copyright © 2023 BioMed Research International. This is an open access article distributed under the Creative Commons Attribution License, which permits unrestricted use, distribution, and reproduction in any medium, provided the original work is properly cited.

This article has been retracted by Hindawi following an investigation undertaken by the publisher [1]. This investigation has uncovered evidence of one or more of the following indicators of systematic manipulation of the publication process:

- (1) Discrepancies in scope
- (2) Discrepancies in the description of the research reported
- (3) Discrepancies between the availability of data and the research described
- (4) Inappropriate citations
- (5) Incoherent, meaningless and/or irrelevant content included in the article
- (6) Peer-review manipulation

The presence of these indicators undermines our confidence in the integrity of the article's content and we cannot, therefore, vouch for its reliability. Please note that this notice is intended solely to alert readers that the content of this article is unreliable. We have not investigated whether authors were aware of or involved in the systematic manipulation of the publication process.

Wiley and Hindawi regrets that the usual quality checks did not identify these issues before publication and have since put additional measures in place to safeguard research integrity.

We wish to credit our own Research Integrity and Research Publishing teams and anonymous and named external researchers and research integrity experts for contributing to this investigation.

The corresponding author, as the representative of all authors, has been given the opportunity to register their agreement or disagreement to this retraction. We have kept a record of any response received.

### **References**

- [1] L. H. Al Fryan, M. I. Shomo, M. B. Alazzam, and M. A. Rahman, "Processing Decision Tree Data Using Internet of Things (IoT) and Artificial Intelligence Technologies with Special Reference to Medical Application," *BioMed Research International*, vol. 2022, Article ID 8626234, 9 pages, 2022.

## Research Article

# Processing Decision Tree Data Using Internet of Things (IoT) and Artificial Intelligence Technologies with Special Reference to Medical Application

Latefa Hamad Al Fryan <sup>1</sup>, Mahasin Ibrahim Shomo <sup>2</sup>, Malik Bader Alazzam <sup>3</sup>,  
and Md Adnan Rahman <sup>4</sup>

<sup>1</sup>Educational Technology, Faculty of Education, Princess Nourah University, Saudi Arabia

<sup>2</sup>Applied College Education (Curriculum & Instruction), Princess Nourah University, Saudi Arabia

<sup>3</sup>Information Technology College, Ajloun National University, Jordan

<sup>4</sup>Adjunct Faculty at Green Business School, Green University of Bangladesh, Dhaka, Bangladesh

Correspondence should be addressed to Md Adnan Rahman; [adnanrahman007@yahoo.com](mailto:adnanrahman007@yahoo.com)

Received 18 May 2022; Revised 31 May 2022; Accepted 9 June 2022; Published 28 June 2022

Academic Editor: Dinesh Rokaya

Copyright © 2022 Latefa Hamad Al Fryan et al. This is an open access article distributed under the Creative Commons Attribution License, which permits unrestricted use, distribution, and reproduction in any medium, provided the original work is properly cited.

Alternative methods are available for a wide range of medical conditions. Idealistically, doctors would have a tool that would analyse their patients' symptoms and suggest the most accurate diagnosis and treatment plan. Artificial intelligence uses decision trees to predict and classify large datasets. A decision tree is a versatile prediction model. Its main purpose is to learn from observations and logic. Rule-based prediction systems represent and categorize events. We discuss the basic properties of decision trees and successful medical alternatives to the classic induction strategy. The study reviews some of the most important medical applications of decision trees (classification). We show researchers and managers how to accurately assess hospital and epidemic management behaviour. Additionally, we discuss decision trees and their applications. The results showed the effectiveness of decision trees in processing medical data by using internet of things (IoT) and artificial intelligence technologies in medical applications. Accordingly, the researchers recommend the use of these technologies in other fields of studies.

## 1. Introduction

Industry research was an early adopter of data mining. Inductive processes based on decision trees developed in decision theory were also introduced at the same time. Specialized technologies such as learning (machine learning) and pattern recognition have emerged as a result of the advancement of computing (pattern recognition). Since the development of modern computers, a decision tree (DT) is a representation of a multivariate function that can be used in everyday life. Sonquist-Morgan (1964) seminal work on the AID (Automatic Interaction Detection) [1] software sparked interest in the practical use of DTs, which arose from the needs of the social sciences. As a result, the DTs have progressed from being merely an illustrative represen-

tation in decision-making courses to becoming a practical and easy-to-use tool. "Classification Stone's and regression trees" [2, 3] completed these advancements. It was proposed that a practical method of induction be used to build DTs recursively. CART is the acronym for this. Creating the ID3 (Iterative Dichotomiser 3) algorithm creates trees based on information entropy. The author improved it and dubbed it C4.5 (1993) [4]. These methods are capable of correcting the flaws in the DT used in classical decision theory. Some patient data may be missing in medical practice due to broken or missing equipment, the inability to perform the test, or other factors. On the other hand, by using only one training sample, this results in a single DT. If there is a variable missing from the patient's information, this is the case. The doctor will want to have DT and use it before deciding

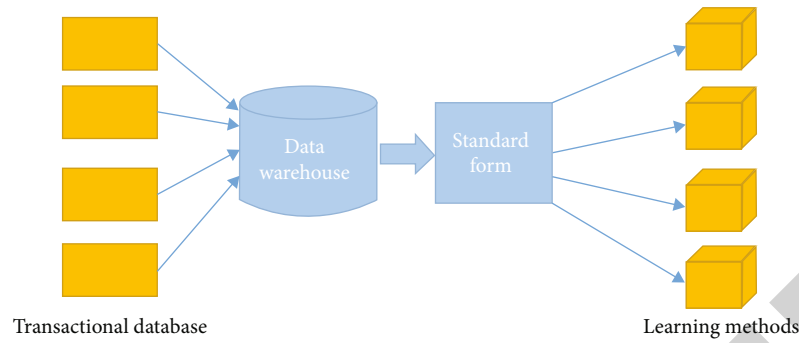


FIGURE 1: Diagram of the selection process, accumulation, and processing of data.

so that he does not miss out on the benefits of using DT as an auxiliary tool. On the other hand, the user would value the ability to analyse multiple DTs and the fact that the DT's predictive efficiency would improve as a result of the new information. These algorithms largely compensate for these flaws. Cremilleux-Robert (1997) [5] created a framework for using DTs in medicine. [6] criticised this, citing the limitations of this technique when used with medical students. With 2637 cases used DT's to consider in the treatment of fractures. Contribution of study identifies and predicts massive datasets, and artificial intelligence used decision trees. Some of the most important medical uses of decision trees are discussed in the research (classification). The goal of this research was to find the best induction method.

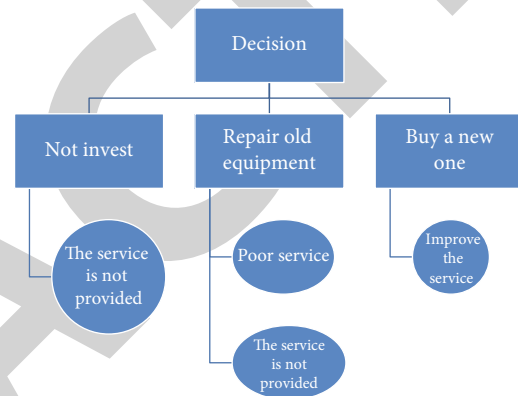


FIGURE 2: A decision tree for investment in new equipment when the old one breaks.

## 2. Data Mining and Classification Trees

**2.1. Data Mining.** Data mining (DM) necessitates operations that must be analysed by a statistician, or someone who understands both the concepts and how to interpret the data when changes occur. One of the issues raised by the dialectic of the exploratory-inferential statistics pair is this. The first performs data analysis, and data mining is used in this process. The second tool allows you to conclude data generated by a phenomenon. As a result, DM necessitates iteration between the fields of computing and statistics and the areas where it is applied by experts, such as doctors in medicine [7].

Because of its features, transparency, and low cost of data storage, the DM became increasingly popular. This is usually only classified when it comes to its role in the study of large databases, and it falls under the heading of "Knowledge Discovery in Databases." It is more accurate to define DM as a process that extracts essential information from large databases without requiring any prior knowledge to make decisions and learn about the phenomenon.

DM should be viewed as a multidisciplinary field that connects procedures, methods, models, and techniques from statistics, pattern recognition, and machine learning, among other fields. The presence of variety in the DM facilitates the selection of tools, which is critical. Inductions lead to inferences, which lead to general models from a concrete example that generates a sample or population. By analysing known

cases, the goal is to learn to classify the items. The importance of such a process in medicine, for example, is obvious in identifying the best therapies for various ailments as shown in Figure 1.

The potential of the DM to work with the size of the databases to be analysed is of great importance. As there are several possible sources of data, the application of the DM requires the so-called "Data Warehouse." This is a relational database management system. It is used to extract archived operational data, resolve inconsistencies between different data formats, and integrate them. Once processed and accumulated in the Data Warehouse, the data is not updated or altered and simply loaded or accessed [8]. Let us think about patient records and the information that can be collected about them from databases in various health centres. The need to use a Data Warehouse that collects data from various databases, classifies them, and cleans up inconsistencies is exemplified.

**2.2. Decision Trees.** Decision trees provide a very powerful classification tool. Its use in data management makes it popular, given the possibilities it offers and the ease with which its results are understood by any user. The tree itself, when obtained, determines a decision rule. This technique allows:

TABLE 1: Equivalence of terms between statistics and artificial intelligence.

Statistics	Artificial intelligence
Model	Network
Observations, individuals, and items	Examples of patterns (features, inputs, and outputs)
Independent, explanatory variables, and regressors	Inputs
Dependent variables, responses, and returning	Outputs (outputs and targets)
Waste	Mistakes
Parameters	Weights and synaptic coefficient (weights and synapsis)
Estimation and prediction	Training and learning (training and learning)
Fit criteria	Error function and cost
Regression. Discrimination	Supervised learning
Classification	Unsupervised learning

TABLE 2: Results in the study of successes in emergency surgery.

Atributo	Characteristics	Decision	Attribute
Nivel de la urgencia ( $A_1$ )	High	Medium	Under
Estado del salón ( $A_2$ )	Okay	Regular	—
Nivel de preparación del personal en la guardia quirúrgica			
Cirujano ( $A_3$ )	Optimum	Acceptable	
Personal auxiliary ( $A_4$ )	Optimum	Acceptable	
Condiciones físicas del enfermo ( $A_5$ )	Okay	Regular	Bad

TABLE 3: Entropy gain of attributes.

Attribute	Gain
Urgency level ( $A_1$ )	0.2728
Hall status ( $A_2$ )	0
Level of preparation of the personnel in the surgical ward	0.015
Surgeon ( $A_3$ )	0.226
Auxiliary staff ( $A_4$ )	0.015

Sample.

- (i) *Segmentation*. Establish which groups are important to classify a certain item. *Classification*. Assign items to one of the groups in which a list is partitioned
- (ii) *Prediction*. Establish rules to make predictions of certain events. *Reduction of the Dimension of the Data*. Identify which data are important to make models of a phenomenon
- (iii) *Identification-Interrelation*. Identify which variables and relationships are important for certain groups identified from analysing the data
- (iv) *Recoding*. Discretize variables or establish qualitative criteria losing the least possible amount of relevant information

The need to make new investments is constant in the health sector, especially in the public sector where decisions involve politicians. In particular, these investments are associated with the acquisition of new instruments, which can be

expensive, expendable material, or extensions-repairs. For them, decisions involve the demand for large sums of money from financial sources. These decisions have repercussions with a delay in the service quality, but it immediately affects the finances and the long-term goals previously set. Investments are strategic decisions and are associated with a high degree of uncertainty [9]. All these investment decisions are supported by expert predictions. In investment analysis, the use of the concept of expected value is popular, and we can use it in the construction of decision trees.

The expected value represents the long-term average to be obtained under the principle of repeated sampling. It is assumed that a probability measure  $P(X)$  allows establishing several scenarios whose result is characterized by a realization  $X$  that can take  $k$  possible values  $x_1, \dots, x_k$ . The expected value  $E(X)$  is as follows

$$E(X) = \sum_{i=1}^k x_i P(X = x_i). \tag{1}$$

The decision tree will allow us to represent and analyse the result of the investment. Before purchasing new equipment, the management of a hospital has a decision tree. Each decision leads to one of the terminal nodes and is associated with a monetary and/or prestige cost. The probability of travelling each path is established by them. It is clear that if the purchase was not made, the service would not be provided with probability one and that if it were, the improvement would be provided with the same probability. In the first case, there is no monetary cost, but socially, the prestige of the health third will be affected.



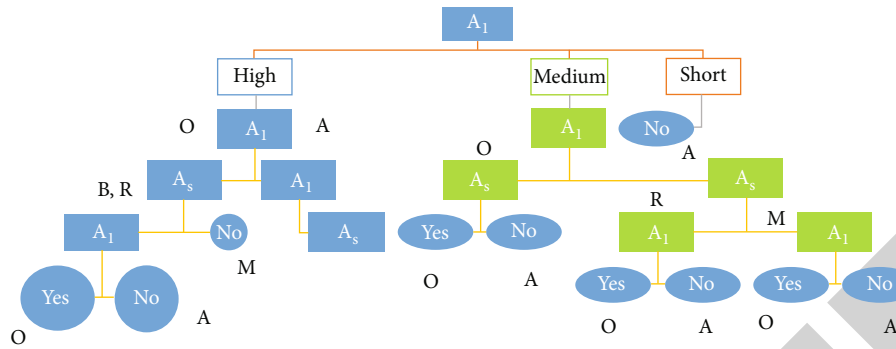


FIGURE 3: Decision tree of the behaviour of the total success of emergency surgery cases.

TABLE 4: Results of treatment with a placebo ointment of psoriasis.

Cell	Considered cured				Total
	Improved	Did not improve	Relapsed	They did not relapse	
Red	53	127	0	0	180
Blue	0	62	54	64	180
Total	53	189	54	64	360

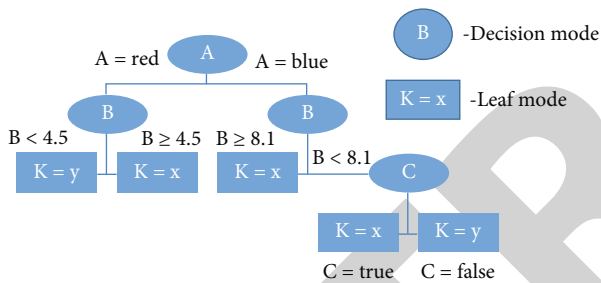


FIGURE 4: Decision tree of psoriasis patients treated with a placebo ointment.

TABLE 5: Results of the audit of 6 surgical hospitals.

Hospital	Category	Primary assistance	Surgery	Hygiene	Staff qualification
Hospital-1	NC	M	B.	R	R
Hospital-2	C	M	B.	M	B
Hospital-3	NC	M	R	B.	R
Hospital-4	NC	B	M	M	R
Hospital-5	C	M	B.	M	R
Hospital-6	C	MM	MM	M	R

In the evaluations, the reasoning present in the dynamic programming of “backward induction” is used: starting at a final node, it returns to the initial node. This decision tree is the one used in classical decision theory. These lead to poor

algorithms for making inductions when the data is incomplete (missing) or with many errors (noisy data).

On the other hand, when evaluating a patient’s symptoms, a doctor detects information through answering questions and rules out possible diseases that may afflict him. In her mind, she has a decision tree and reaches a conclusion, or several possible ones, by considering how plausible the path she follows based on her questions’ answers. When evaluating a questionnaire or analysis, the doctor traces a path in a graph reaching a final node (leaf) [10]. Thus, a doctor’s interest is to use the information collected and establish in which nodes the possible disorders are concentrated. Similarly, a researcher could analyse a health system to detect which care centres concentrate on certain properties, such as the level of efficiency, for example, see Figure 2.

In many medical problems, it is interesting to design the tree described by its users to consider the performance of a health system, which can range from a national system to that of a hospital.

To make such trees, a sample is taken, the path followed by the interviewees is observed, and any campaign or development plan would focus on satisfying the quality interests expressed by the interviews. Some paths will be followed more frequently, allowing a statistical analysis to be made of how the interviewees, who are nothing more than clients, evaluate the system and its components. For example, if we consider the use of a specialized hospital such as a heart centre, several paths traveled before reaching it can be considered [11]. For example, the general medical path-proximity-confidence-speed-poor diagnosis can be more opposite than polyclinic-proximity-confidence-slowness-correct diagnosis to reach treatment in a heart centre. This would lead us to obtain that the largest part of those who attend the emergency room of the cardio centre are patients who go to the polyclinic and live near it. This may lead to the

TABLE 6: Results of the hygiene analysis in the audit of 6 surgical hospitals.

Good hygiene	Primary assistance	Surgery	Hygiene	Staff qualification	Category
Hospital 3 regular hygiene	M	R	B.	R	NC
Hospital 1 poor hygiene	M	B.	R	R	NC
Hospital 2	M	B.	M	B.	C
Hospital 4	B.	M	M	R	NC
Hospital 5	M	B.	M	R	C
Hospital 6	MM	MM	M	R	C

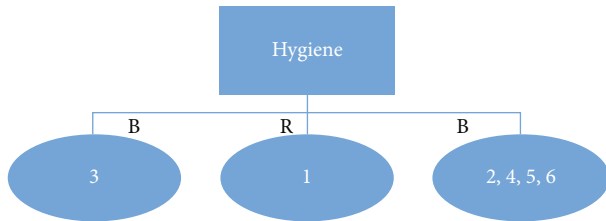


FIGURE 5: Decision tree of the hygiene analysis in the audit of 6 surgical hospitals. The analysis of surgery leads us to Table 7.

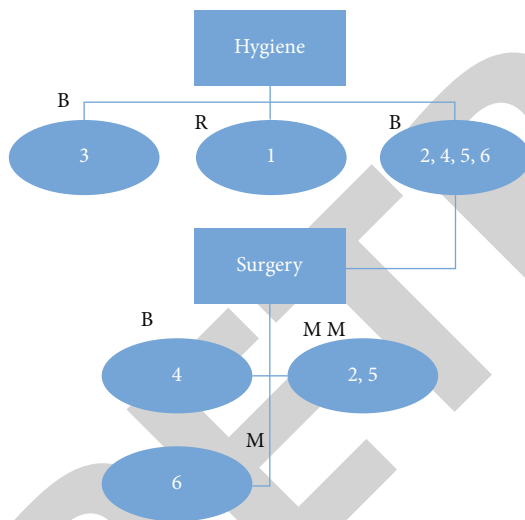


FIGURE 6: Decision tree of the analysis when including surgery together with hygiene in the audit of 6 surgical hospitals.

need to establish closer permanent cardiology services in the municipalities and/or provide specialized training to general practitioners.

In medicine, decision making is very important and systematic. Think of diagnostics, for example. In advanced institutions, there are systems known as “Decision support systems,” decision support systems, which are used to help the doctor to establish alternative decisions, which are efficient and reliable in complex situations. These systems are generally capable of automatically training themselves with new information and learning (Automatic Learning). For such tasks, decision trees are a convenient tool. Given their performance in many applications, the experts in the various

areas taken regularly use them because their behaviour is transparent. The use of a tool that leads us to determine DT is highly recommended when:

- (i) We study concepts of the attribute-value type
- (ii) The objective function is associated with an RV with discrete values
- (iii) Item descriptions are disjunctive
- (iv) The learning set  $T$  has errors and/or has missing values

A DA formalizes a problem mapping by determining connections between tree nodes where the population study process is expressed by determining subtrees and leaves. Each leaf or terminal node determines a class that determines the decision. Some nodes are called test nodes, and output is elaborated based on the analysis of the data that has entered it from the previous nodes with which it connects. In its practical uses, DT begins by analysing known cases. The items are divided into two subsets. One is used to determine the tree (training sample) and the other to evaluate the effectiveness of the DT (test sample). An attribute is set to represent the decision of interest (response variable (RV)). The problem is determined by fixing a set of attributes that can be represented as a vector  $\vec{X} \in \mathcal{R}^k$  for each item. Then, we can say that the training sample is  $T = \{x_1, x_2, \dots, x_m\}$ .

Attributes can take discrete, continuous, or qualitative values. In the discrete case, each value determines a class. If the variable is continuous, intervals will be determined. Qualitative variables are discretized. At each step, the set of items is subdivided according to a certain criterion into two or more classes until reaching the set of final nodes [12]. The usual method of partitioning is done by determining hyperplane orthogonal to the selected attribute. Thus, the DT divides the space  $\mathcal{R}^k$  into hyperrectangles, and each one identifies a decision. There is  $m - 1$  possible partitioning of  $T$ . A pruning criterion is used to determine when to stop the segmentation to make a partition. If the number of VS's is high, the DT will be very large, making it difficult to interpret.

In the case of continuous attributes, intervals can be determined using one of the following criteria

- (i) *Intervals with the Same Amplitude.* The number of classes is fixed, and the intervals are determined

TABLE 7: Results of the analysis when including surgery together with hygiene in the audit of 6 surgical hospitals.

Good surgery	Primary assistance	Surgery	Hygiene	Staff rating	Category
Hospital 2	M	B.	M	b.	C
Bad surgery					
Hospital 5	M	B.	M	R	C
Surgery very bad					
Hospital 4	B.	M	M	R	NC
Hospital 6	MM	MM	M	R	C

- (ii) *Intervals Determined by Percentiles.* The number of classes is finalized, and the intervals are determined, looking for them to contain the same approximate number of items

Following [4], we can fix the search for DT as follows:

- (i) If there are  $k$  classes denoted  $\{C_1, C_2, \dots, C_m\}$ , and a training set,  $T$ , then

If  $T$  contains one or more objects belonging to a single class  $C_j$ ; then, the decision tree is a leaf identifying class  $C_j$ .

- (ii) If  $T$  contains no objects, the decision tree is a leaf determined from information other than  $T$
- (iii) If  $T$  contains objects that belong to a mixture of classes; then, a test is chosen, based on a single attribute, that has one or more mutually exclusive outcomes  $\{O_1, O_2, \dots, O_n\}$
- (iv)  $T$  is partitioned into subsets  $T_1, T_2, \dots, T_n$ , where  $T_i$  contains all the objects in  $T$  that have the outcome  $O_i$  of the chosen test

The same method is applied recursively to each subset of the training object.

Let  $S \subset \Omega$

$$\Omega = \text{study population} = \bigcup_{1 \leq i \leq n} C_i. \quad (2)$$

When selecting a sample, a signal is obtained about the belonging of an item to a class. If

$$f(j_i, S) = \text{number of objects in } C_i, P_i = \frac{f(j_i, S)}{|S|}. \quad (3)$$

Thinking in terms of information theory, this signal in terms of bits is  $-\log_2 f(j_i, S)/|S|$ . Considering  $S$ , the information expected from the signal is

$$\text{inf}(S) = -\frac{\log_2 f(C_j, S)}{|S|}. \quad (4)$$

If we have a training sample

$$\text{inf}(T | \Omega) = \sum_{i=1}^n \left( \frac{|T_i|}{|T|} \right) \text{inf}(T_i | \Omega). \quad (5)$$

We then have a series of measures of interest on the partition.

We then have a series of measures of interest on the partition. We are interested in  $g(\Omega) = \text{info}(T) - \text{info}_\Omega(T) = \text{gain in information by partitioning } T \text{ according to } \Omega$ . If we partition  $T$  into  $n$  subsets, we have

$$\text{part} - \text{info}(\Omega)_i = \text{inf}(T | X) = i = \sum_{i=1}^n \left( \frac{|T_i|}{|T|} \right) \log_2 \left( \frac{|T_i|}{|T|} \right). \quad (6)$$

The partition generates information that is useful for classification, and a measure of the gain is  $gr(\Omega) = g(\Omega) / \text{part} - \text{info}(\Omega)_i = \text{impurity function}$ .

This measures the mixing of a subset and partitions to decrease impurity. It seeks to maximize it. Ultimately, this carries the same meaning as the Gini index, used in economics, [7]. This function considers the probability of misclassifying an additional sample given the result obtained by using the training sample  $T$ .

A classification rule will assign a new item to a node seeking to minimize the misclassification rate.

So a DT is a graph determined from some method that models decision making using easily understood rules. The items grouped from the attributes (explanatory or segmentation variables, VS) are obtained by segmenting  $T$ . When determining a group, a study is made, preferably statistical, of the VR. The homogeneity of this attribute is performed to explain the effect of the VS's on the VR. From the VS's, the members of the groups are identified, and it is easier to predict the value of the VR. This is nothing more than a marketing problem with particular characteristics. Thus, if we interview the system's users, it faces several questions. Your answers establish movement from one node to another in the tree, and at the end, you have traced a path to a conclusion represented by one of the final nodes [13]. Thus, the interviewee is classified. In the diagnostic area, the path leads to evaluating a decision rule. The symptoms that lead to certain diseases and the elements that most frequently identify them can be particularized by analysing the final nodes. The doctor will be able, using them, to have a group of possible diagnoses on which he will develop alternative treatments for the patient's ailment. This is of particular importance in diseases with many symptoms that are common to others, such as dengue.

In both cases presented, the interest is to determine a highly plausible tree. Also, in both, a certain decision-maker, faced with different conditions, has evaluations that determine the decision-making that leads to a terminal node. If the tree design from taking a sample is plausible, it will affect the decisions made using them.

TABLE 8: Results of the analysis when including personnel qualification and surgery and hygiene in the audit of 6 surgical hospitals.

Staff rating	Primary assistance	Surgery	Hygiene	Staff qualification	Category
Good					
Hospital 2	M	B.	M	B.	C
Regular staff qualification					
Hospital 5	M	B.	M	R	C

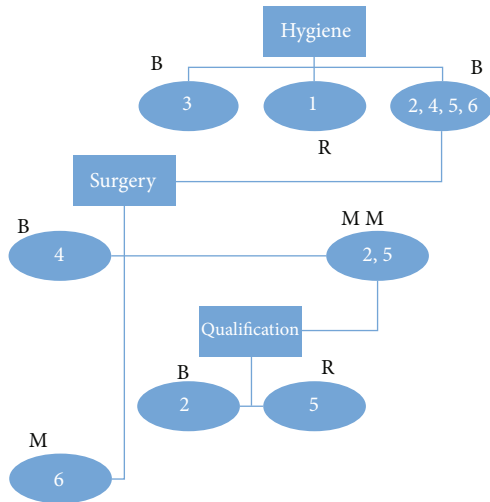


FIGURE 7: Decision tree of the analysis by including personnel qualification and surgery and hygiene in the audit of 6 surgical hospitals.

2.3. *Decision Trees and Neural Networks.* Most of the problems we tackle doing exploratory statistics have clear connections to AI. However, statisticians and AI specialists often do not communicate effectively. The terms used by one and the other are different, although the methods used are similar or the same. In practice, the entire arsenal of statistical methods and tools is wasted by AI. New and generally theoretically inefficient methods are created to solve problems that have been obtained and seem to be found in simple statistics textbooks [14]. AI has focused on making efficient algorithms and not using efficient inferential models.

To illustrate the difference in concepts' denomination, we use the table presented by Lebart (1998), Table 1.

RN is generalizations of classical statistical models that apply sequential learning and successfully address transformations of the original variables to make predictions and overcome the problems posed to statisticians by nonlinear models characterizing complex phenomena. This is a black box where the algorithm uses inputs and provides outputs. The system is expected to learn by improving its predictions. The methods of constructing DT and RN are complementary [15]. Representation through DT is transparent to the doctor and any user, but this is not the case with RN.

On the other hand, the DT technique fails when there are many outliers, which does not happen with the RN. Also, if we use DT to learn, learning is slow, but RNs do it quickly.

Hence, the success of combining both techniques. The proposals use an RN that they train and turn into DT at the end of the learning. If the learning is good, the determined DT is better than the DT used as input data for the RNs.

2.4. *Evolutionary Algorithms.* Another technique used contemporaneously to build DT is the evolutionary algorithms (EVOP). These are commonly used in optimization if there is no efficient heuristic algorithm. [6–15].

The quality of the DT is measured by

$$LFF = \sum_{i=1}^k w_i(1 - acc_i) + \sum_{i=1}^N c(w_i) + w_u + nu1, \quad (7)$$

where  $k$  is the number of decision classes.  $N$  is the number of attribute nodes in the tree.  $acc_i$  is the accuracy of the classification of items of a decision class  $d_i$ .  $w_i$  is the importance given (weight) to classify the items in the decision class  $d_i$ .  $c(w_i)$  is the cost of using the attribute in a node  $t_i$ .  $nu$  is the number of nodes not used.  $w_u$  is the weight of the presence of unused nodes in the tree.

A tree will be better if LFF is smaller. The EVOP searches for the tree with the minimum value of LFF.

### 3. Its Success in Some Applications in Medicine

DT's have been used in medical and community health studies for more than two decades. We will see some applications made using the tools discussed.

Letourneau et al. (1998) took a sample of two groups of nurses and developed a DT to guide the work of one of them. It was concluded that this was of great help when comparing the group's efficiency helped by the DT and the one that did not use it. Tsien et al. (2000) used data obtained in Edinburgh and established how DT could be helpful in rapid decision making when making predictions in Sheffield.

Jones (2001) studied the use of DT's to fix signals suggestive of drug side effects. The DT technique has been proposed in the hospital setting to improve alarm systems in intensive care units, see Tsien et al. (2000). Bonner (2001) conducted a similar study with the mentally ill.

3.1. *Study of the Behaviour of the Total Success of Emergency Surgery Cases.* A study of 285 cases admitted to the emergency room in hospitals of a health system was carried out. All of them had to undergo emergency surgery. The hospital conditions at the time of the intervention, the conditions under which it was carried out, and the total success of the same were analysed. Total success refers to the absence of

postoperative complications. Deaths were not considered in the study, as shown in Table 2, Table 3, and Figure 3.

The study of information entropy (EI) was carried out. The entropy is  $I(S) = 0.8631$ .

So the most important thing for the success of an urgent intervention is the level of urgency. It is followed by the level of the surgeon's auxiliary staff. This must be analysed carefully, meaning that the surgeon's level is important (being good or average according to a previous evaluation). This reflects that surgeons are not especially distinguished in such cases but that the intervention depends a lot on the qualification of the auxiliary personnel (nurses, anesthesiologists, etc.).

**3.2. Evaluation of a Placebo Ointment in Patients with Psoriasis on Less than 10% of Their Body.** Three hundred sixty people who have psoriasis underwent placebo treatment. The medication was an ointment that came in two colours,  $A = \text{blue and red}$ . The results were evaluated, obtaining the results in the following Table 4.

The classification tree appears in Figure 4. It is noted that those who selected the red ointment considered they obtained improvement in less than 4.5 weeks (29.44%) and those of the blue in dismay without improvement after 8.1 (34.44%). Those who used the blue ointment were first considered cured, not improved, and 35.55% were discharged.

**3.3. Study of Hygienic Conditions and Efficiency in Surgical Hospitals.** Six classified hospitals poorly valued by their patients were analysed. The interest was to classify them into unreliable and reliable. The results of the audits led to Table 5 and Table 6.

Calculating the entropy of information (EI), we have that the entropy of primary care is  $I(A1) = 0.66$  since the EI for the values are

$$I_{10} = 0; I_{11} = 1; I_{12} = 0. \quad (8)$$

For surgery, the EI is  $I(A2) = 0.79$  because

$$I_{20} = 1; I_{21} = 0; I_{22} = 0.9183. \quad (9)$$

For hygiene, we have  $I(A3) = 0.54$  since

$$I_{30} = 0; I_{31} = 0.8811; I_{32} = 0.0. \quad (10)$$

Regarding the qualification of the personnel  $I(A_4) = 0.81$  given that

$$I_{40} = 0; I_{41} = 0. \quad (11)$$

Figure 5 is the DT it generates.

The corresponding DT appears in Figure 6.

See Table 8 below for the inclusion in the analysis of staff qualification. The worst hospital is between 6 and 5; the best two are followed by 1.

Then, the complete DT of the problem is obtained, see Figure 7.

**3.4. A Study of Environmental Conditions in Homes: A Campaign against the Transmitting Agent of Dengue.** A

study was carried out in 22.422 dwellings to establish whether they had good conditions (they were not prone to mosquito outbreaks) or bad conditions. Homeownership was considered as the VR, and they used as SVs:

- (i) Highest educational level of one of the family members
- (ii) Location
- (iii) C is house in a city
- (iv) D is apartment in a multifamily building
- (v) M is a room in a condominium
- (vi) S is housing in a semiurban area
- (vii) U is urban housing
- (viii) V is housing in a village

This DT leads us to detect that:

Those classified as middle-level students differentiate between type n S-U-D-V dwellings (which do not differ from each other) and those of type C.

The percentages classified as good in the two groups cannot be accepted as similar.

For those who have completed primary school, the same thing happens with M and F.

Those who have graduated have the same behaviour in all types of locations. Homeowners differ from nonowners regardless of the level of schooling or location of their home.

## 4. Conclusion

The impact that is desired to obtain with the project in the application of decision and regression trees as a tool for the prognosis of medical conditions is to take optimal management, taking it as a reference in our research and allowing us to use it as a support to be able to carry out an exhaustive and highly comparative analysis of the analysed data and how the algorithms internally carry out their functions and different analysis methods. Results obtained in this study allow us to focus the campaign to eliminate outbreaks and make propaganda aimed at nonuniversity students without property.

## Data Availability

The data used to support the findings of this study are included within the article.

## Conflicts of Interest

The authors declare that they have no conflicts of interest.

## Acknowledgments

With great appreciation, the authors would like to express deep gratitude to Princess Nourah University (PNU) for providing such a wonderful opportunity for pursuing this research to attain their career goals as a university instructor.



## *Retraction*

# **Retracted: Clinical Efficacy and Safety Analysis of PD-1/PD-L1 Inhibitor vs. Chemotherapy in the Treatment of Advanced Non-Small-Cell Lung Cancer: A Systematic Review and Meta-Analysis**

### **BioMed Research International**

Received 24 November 2022; Accepted 24 November 2022; Published 25 December 2022

Copyright © 2022 BioMed Research International. This is an open access article distributed under the Creative Commons Attribution License, which permits unrestricted use, distribution, and reproduction in any medium, provided the original work is properly cited.

*BioMed Research International* has retracted the article titled “Clinical Efficacy and Safety Analysis of PD-1/PD-L1 Inhibitor vs. Chemotherapy in the Treatment of Advanced Non-Small-Cell Lung Cancer: A Systematic Review and Meta-Analysis” [1] due to concerns that the peer review process has been compromised.

Following an investigation conducted by the Hindawi Research Integrity team [2], significant concerns were identified with the peer reviewers assigned to this article; the investigation has concluded that the peer review process was compromised. We therefore can no longer trust the peer review process and the article is being retracted with the agreement of the editorial board.

The authors do not agree to the retraction.

### **References**

- [1] W.-w. Guo, T.-w. Zhang, B.-l. Wang, L.-q. Mao, and X.-b. Li, “Clinical Efficacy and Safety Analysis of PD-1/PD-L1 Inhibitor vs. Chemotherapy in the Treatment of Advanced Non-Small-Cell Lung Cancer: A Systematic Review and Meta-Analysis,” *BioMed Research International*, vol. 2022, Article ID 9500319, 9 pages, 2022.
- [2] L. Ferguson, “Advancing Research Integrity Collaboratively and with Vigour,” 2022, <https://www.hindawi.com/post/advancing-research-integrity-collaboratively-and-vigour/>.

## Review Article

# Clinical Efficacy and Safety Analysis of PD-1/PD-L1 Inhibitor vs. Chemotherapy in the Treatment of Advanced Non-Small-Cell Lung Cancer: A Systematic Review and Meta-Analysis

Wei-wei Guo, Tian-wei Zhang, Bin-liang Wang, Li-qun Mao, and Xiao-bo Li 

Department of Respiratory and Critical Care Medicine, Taizhou First People's Hospital, Taizhou City, Zhejiang Province, China 318020

Correspondence should be addressed to Xiao-bo Li; [lixiaobo17591@163.com](mailto:lixiaobo17591@163.com)

Received 25 May 2022; Revised 11 June 2022; Accepted 14 June 2022; Published 25 June 2022

Academic Editor: Dinesh Rokaya

Copyright © 2022 Wei-wei Guo et al. This is an open access article distributed under the Creative Commons Attribution License, which permits unrestricted use, distribution, and reproduction in any medium, provided the original work is properly cited.

**Objective.** To systematically evaluate the efficacy and safety of pembrolizumab (PD-1/PD-L inhibitor) and adjuvant chemotherapy to treat NSCLC and provide evidence-based reference for clinical use. **Methods.** By searching the Cochrane Library, EMBASE, PubMed, and Web of Science, according to the inclusion criteria, literature selection, data extraction, and quality evaluation were carried out for the included literature. The  $I^2$  test was used to evaluate heterogeneity between studies, and the meta-analysis was performed using RevMan 5.3 software provided by Cochrane. **Results.** Finally, 14 relevant documents meeting the standards were included. It is a statistical difference in one-year survival rate [OR = 1.50, 95% CI (1.28, 1.76),  $P < 0.00001$ ,  $I^2 = 0\%$ ,  $Z = 4.99$ ]; overall response rate [OR = 1.57, 95% CI (1.29, 1.90),  $P < 0.00001$ ,  $I^2 = 0\%$ ,  $Z = 4.58$ ]; progression-free survival [OR = 2.99, 95% CI (2.29, 3.91),  $P < 0.00001$ ,  $I^2 = 26\%$ ,  $Z = 8.00$ ]; and overall survival [OR = 1.38, 95% CI (1.07, 1.78),  $P = 0.01$ ,  $I^2 = 46\%$ ,  $Z = 2.50$ ] and reduces the incidence of adverse drug reactions [OR = 2.54, 95% CI (1.99, 3.25),  $P < 0.00001$ ,  $I^2 = 69\%$ ,  $Z = 7.43$ ]. **Conclusion.** Pembrolizumab adjuvant chemotherapy is effective in the treatment of advanced NSCLC, but attention should be paid to the occurrence of adverse reactions in clinical. Due to the limitations of the methodology included in the study, this conclusion required more validation of large-sample RCT.

## 1. Introduction

In recent years, the research achievements of immunotherapy are outstanding, and a number of clinical trials are reported frequently [1]. Lung cancer is one of the most deadly malignancies, with a 5-year survival rate of less than 18%, among which non-small-cell lung cancer (NSCLC) accounts for 85% of the total. The treatment of lung cancer takes a period of 10 years, from the era of chemotherapy, antivasular therapy, and targeted therapy to the current era of immunotherapy [2–4]. With the deepening of the research on the mechanism of tumor immune escape, it is found that negative immune regulation of some immune checkpoints plays an important role in the formation of tumor. Programmed cell death 1 (PD-1) and PD-1 ligand (PD-L1) enhance the resistance of tumor microenvironment to normal immunity through immune escape, inhibition of

immune response, avoidance of killing, and elimination [5]. The efficacy and safety of immunosuppressants targeting the PD-1/PD-L1 pathway have been confirmed in large clinical trials of the local late maintenance therapy, late second-line therapy, and late first-line therapy of NSCLC [6]. In 2020, a multicenter, open Phase III trial test also verified the effect [7]. It is only 20% efficient and has an overall survival period of only 8 to 10 months [8]. EGFR(+) is found in about 80% of NSCLC patients, so the targeted treatment regimens acting on EGFR have become a new direction for NSCLC therapy [9]. Pembrolizumab suppresses epidermal growth factor activation and the conduction of downstream intracellular signaling. In 2009, pembrolizumab was added to the first-line treatment with the NCCN guidelines for relapse and metastatic NSCLC regimen. However, pembrolizumab has not been approved for any first-line and maintenance therapy for NSCLC in China. The US FDA approved

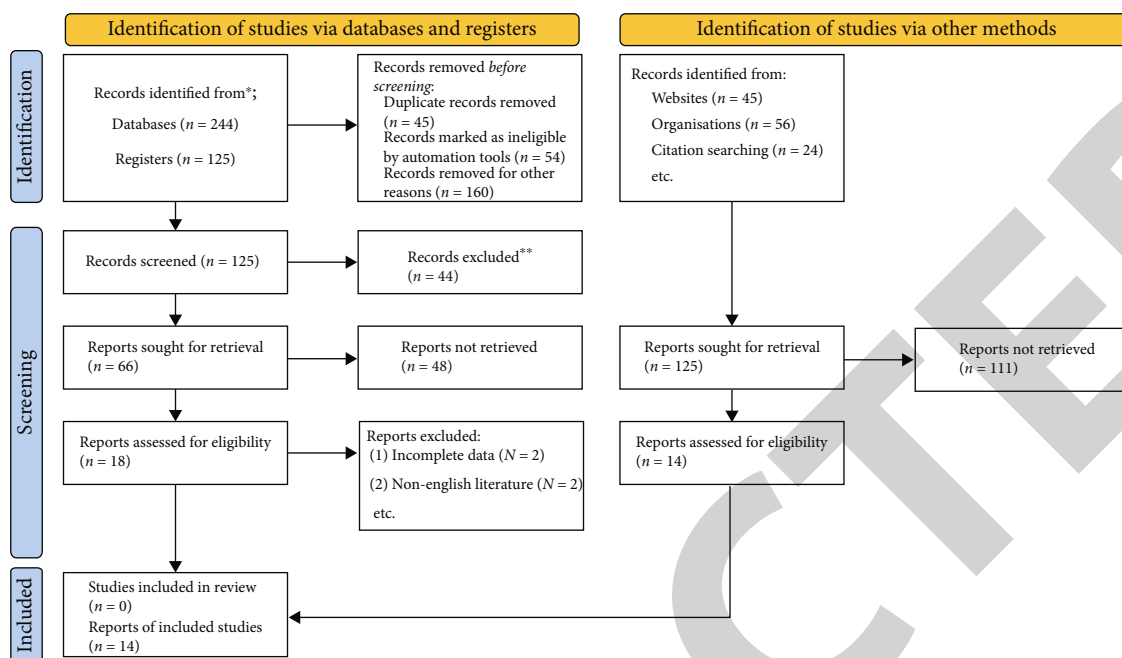


FIGURE 1: Flow chart of the literature screening.

only pembrolizumab for the treatment of metastatic colorectal and head and neck cancers and did not for the treatment of NSCLC. NSCLC has a short survival period and a high mortality rate, and it is difficult for the traditional chemotherapy regimen to achieve a better therapeutic effect. Targeted treatment has gradually become a major trend to treat NSCLC [10]. At present, pembrolizumab has entered phase clinical trials for NSCLC, but pembrolizumab has not been granted for any first-line and maintenance treatment of NSCLC, and pembrolizumab is not sure to benefit NSCLC patients.

Therefore, in this study, the clinical efficacy and safety of pembrolizumab adjuvant chemotherapy were compared according to the Cochrane systematic evaluation method, providing a scientific basis for first-line use of pembrolizumab for advanced NSCLC.

## 2. Materials and Methods

**2.1. Search Strategy.** Using the literature tracing approach, we carefully searched PubMed and EMBASE and gathered relevant literatures published both at home and abroad. The following are the keywords used: pembrolizumab, lung cancer, chemotherapy, PD-1/PD-L1, and others. The retrieval date ranges from the moment the database was created to December 31, 2021. At the same time, included references were tracked, and relevant conference papers were manually retrieved to recover unretrieved material, and the literature gathered was separately appraised by the two reviewers (Figure 1).

**2.2. Research Type.** RCTS have been published at both home and abroad, whether blind or not.

**2.3. Research Objects.** The following are the research objects: (1) age 18 with no gender restriction; (2) pathological diagnosis of NSCLC; (3) stage II/IV NSCLC confirmed by imaging or other clinical examinations; (4) Karnofsky score of 60 or ECOG score of 0-2; and (5) no absolute contraindication to chemotherapy prior to treatment and no obvious abnormality of liver and kidney function, hematology, or electrocardiogram

**2.4. Intervention Methods.** The experimental group was given pembrolizumab+platinum-based chemotherapy, while the control group was given only platinum-based chemotherapy. Dose and course of pembrolizumab and other chemotherapy drugs are not limited.

**2.5. Outcome Indicators.** Therapeutic indexes include 1-year survival rate (1 year after randomization cases/total number of cases of survival); complete remission rate (complete response cases/total number of cases, complete response referring to the lumps disappearing completely, and duration of 1 month or more); partial remission rate (relieving some cases/total number of cases, partial response refers to the mass decrease 50% or higher, and duration  $\geq 1$  month); and total response rate [ORR (total response+partial response)/total response]. Safety indicators included the incidence of anemia, thrombocytopenia, leukopenia, rash, dyspnea, infusion response, vomiting, fever, and mortality.

**2.6. Exclusion Criteria.** The following are the exclusion criteria: (1) patients with a history of small-cell lung cancer or other malignant tumors; (2) patients with severe impairment of heart, liver, or kidney function; (3) a prior history of chemotherapy; and (4) a prior history of EGFR-targeted drugs or monoclonal antibodies with poorly controlled BMS.



FIGURE 2: Literature quality evaluation chart. (a) Risk of bias graph; (b) risk of bias summary.

2.7. Literature Quality Assessment. Two researchers independently extracted data and cross-checked to ensure the accuracy of the data. The quality evaluation method of RCT was based on the standard of Cochrane Handbook 5.0.2 (Figures 2 and 3).

2.8. Statistical Analysis. RevMan 5.2 statistical software was used for meta-analysis, while for continuous variables, Weighted Mean Difference (WMD) and 95% confidence interval (CI) were used to represent the effect size. A  $\chi^2$  test was used for hypothesis testing to determine the heterogeneity among the results of each included study, and  $P < 0.05$  was considered statistically significantly different. The studies without statistical heterogeneity ( $P > 0.1$ ,  $I^2 < 50\%$ ) were analyzed by a fixed-effects model. For studies with statistical heterogeneity ( $P < 0.1$ ,  $I^2 \geq 50\%$ ), a random-effects model was used for pooled analysis.

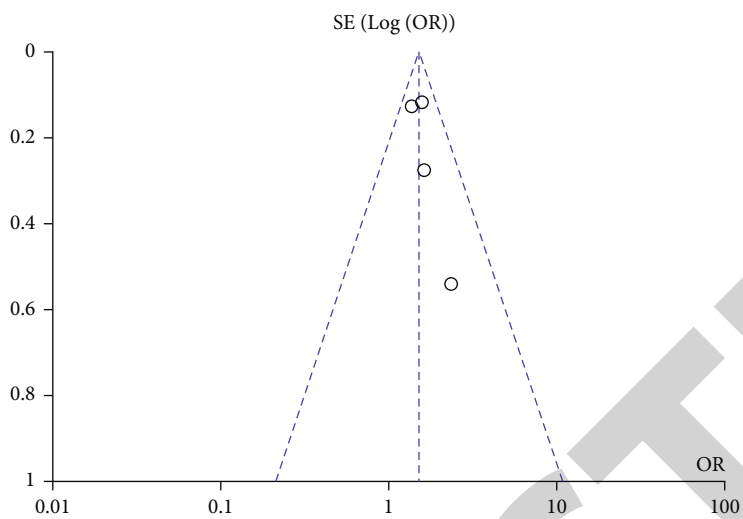
### 3. Result

3.1. Literature Retrieval Results and Included Research Characteristics. A total of 369 literatures were obtained in the preliminary examination, and 259 duplicated literatures

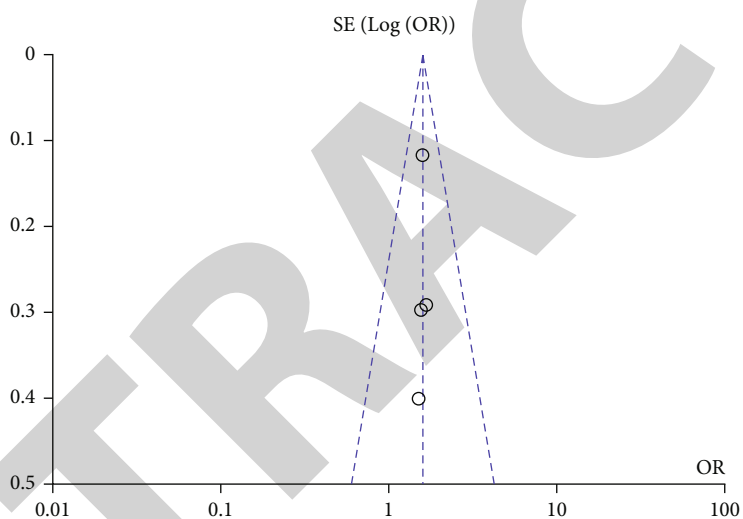
were excluded. 96 literatures were screened out after reading the title and abstract, and 14 literatures were included after reading the full text. Figure 1 is the literature retrieval and screening process (Table 1).

3.2. One-Year Survival Rate. The HR value of one-year survival rate and 95% confidence interval were combined, and there was no statistical heterogeneity among the included studies ( $I^2 = 0\%$ ,  $P < 0.00001$ ), and a fixed-effects model was used for meta-analysis. Therefore, there was a statistical difference in one-year survival rate between two groups [OR = 1.50, 95%CI (1.28, 1.76),  $P < 0.00001$ ,  $I^2 = 0\%$ ,  $Z = 4.99$ ] (Figure 4).

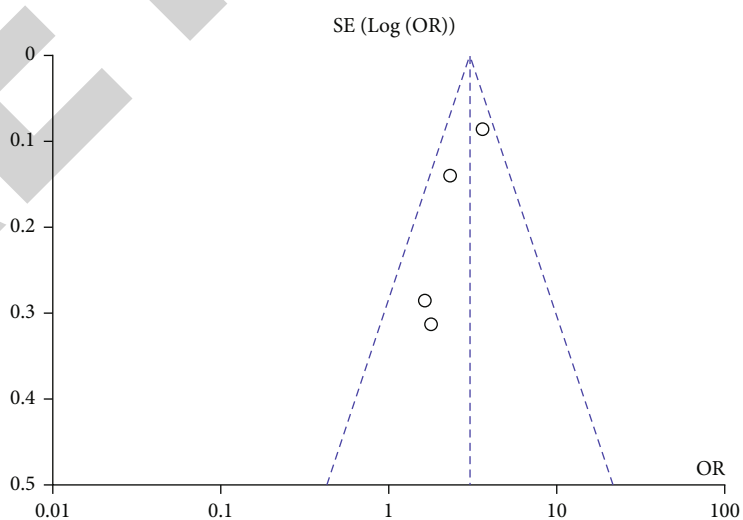
3.3. Overall Response Rate(ORR). The HR value of overall response rate and 95% confidence interval were combined, and there was no statistical heterogeneity among the included studies ( $I^2 = 0\%$ ,  $P < 0.00001$ ), and a fixed-effects model was used for meta-analysis. Therefore, there was a statistical difference in overall response rate between two groups [OR = 1.57, 95%CI (1.29, 1.90),  $P < 0.00001$ ,  $I^2 = 0\%$ ,  $Z = 4.58$ ] (Figure 5).



(a)



(b)



(c)

FIGURE 3: Continued.



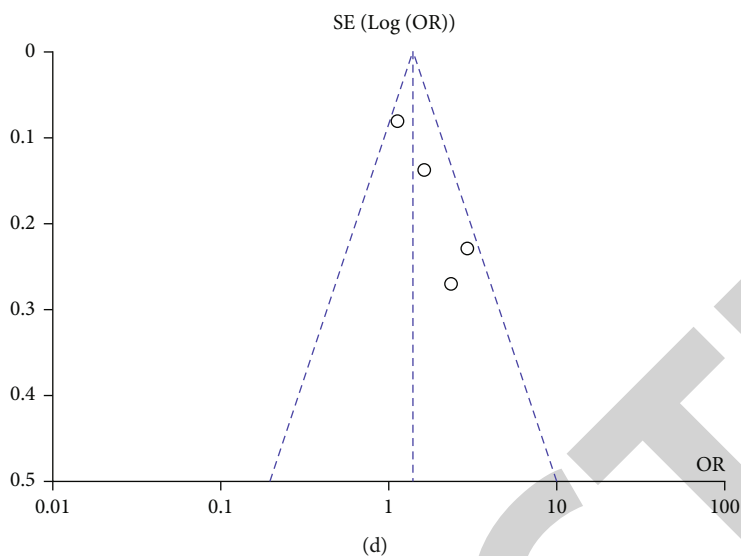


FIGURE 3: (a-d) Funnel plot of literature publication bias.

TABLE 1: Basic clinical features of 14 literatures were included in our study.

Study	Age	Gender (man)	Hospitalization days	Experimental group (N)	Control group (N)	NOS score	Research type
Reck M [11]	63.25 ± 12.2	42.25%	6.8 ± 1.1	200/305	105/305	7	RCT
Garon EB [12]	65.55 ± 13.4	68.12%	6.2 ± 1.3	315/495	278/495	7	RCT
Reck M [13]	63.32 ± 14.5	46.72%	5.4 ± 3.9	167/305	158/305	8	RCT
Goldberg SB [14]	67.15 ± 13.5	45.12%	6.9 ± 4.9	33/52	28/52	7	RCT
Eichhorn F [15]	62.85 ± 8.5	51.89%	9.8 ± 3.4	21/30	15/30	8	RCT
Amrane K [16]	64.26 ± 10.2	63.45%	5.2 ± 5.1	67/108	54/108	7	RCT
Jabbour SK [17]	62.62 ± 12.1	68.10%	6.9 ± 2.1	12/21	9/21	7	RCT
Middleton G [18]	62.61 ± 13.5	49.75%	5.9 ± 1.4	78/112	56/112	7	RCT
Herbst RS [19]	57.15 ± 14.5	59.23%	6.4 ± 4.1	51/92	41/92	7	RCT
Lisberg A [20]	66.22 ± 15.1	57.22%	7.8 ± 1.5	14/25	11/25	8	RCT
Eichhorn F [21]	61.35 ± 8.1	54.16%	6.1 ± 5.9	10/15	5/15	7	RCT
Hellmann MD [22]	67.15 ± 16.0	67.34%	7.5 ± 1.6	322/601	255/601	7	RCT
Weiss GJ [23]	58.11 ± 8.6	49.34%	5.0 ± 5.6	39/49	28/49	9	RCT
Hui R [24]	66.34 ± 6.4	54.12%	6.4 ± 1.7	68/101	56/101	8	RCT

3.4. *Progression-Free Survival*. The HR value of progression-free survival and 95% confidence interval were combined, and there was no statistical heterogeneity among the included studies ( $I^2 = 26\%$ ,  $P < 0.00001$ ), and a fixed-effects model was used for meta-analysis. Therefore, there was a statistical difference in progression-free survival between two groups [OR = 2.99, 95%CI (2.29, 3.91),  $P < 0.00001$ ,  $I^2 = 26\%$ ,  $Z = 8.00$ ] (Figure 6).

3.5. *Overall Survival (OS)*. The HR value of overall survival and 95% confidence interval were combined, and there was no statistical heterogeneity among the included studies ( $I^2 = 46\%$ ,  $P = 0.01$ ), and a fixed-effects model

was used for meta-analysis. Therefore, there was a statistical difference in overall survival between two groups [OR = 1.38, 95%CI (1.07, 1.78),  $P = 0.01$ ,  $I^2 = 46\%$ ,  $Z = 2.50$ ] (Figure 7).

3.6. *Incidence of Coincidences*. The HR value of incidence of coincidences and 95% confidence interval were combined, and there was no statistical heterogeneity among the included studies ( $I^2 = 69\%$ ,  $P < 0.00001$ ), and a fixed-effects model was used for meta-analysis. Therefore, there was a statistical difference in incidence of coincidences between two groups [OR = 2.54, 95%CI (1.99, 3.25),  $P < 0.00001$ ,  $I^2 = 69\%$ ,  $Z = 7.43$ ] (Figure 8).

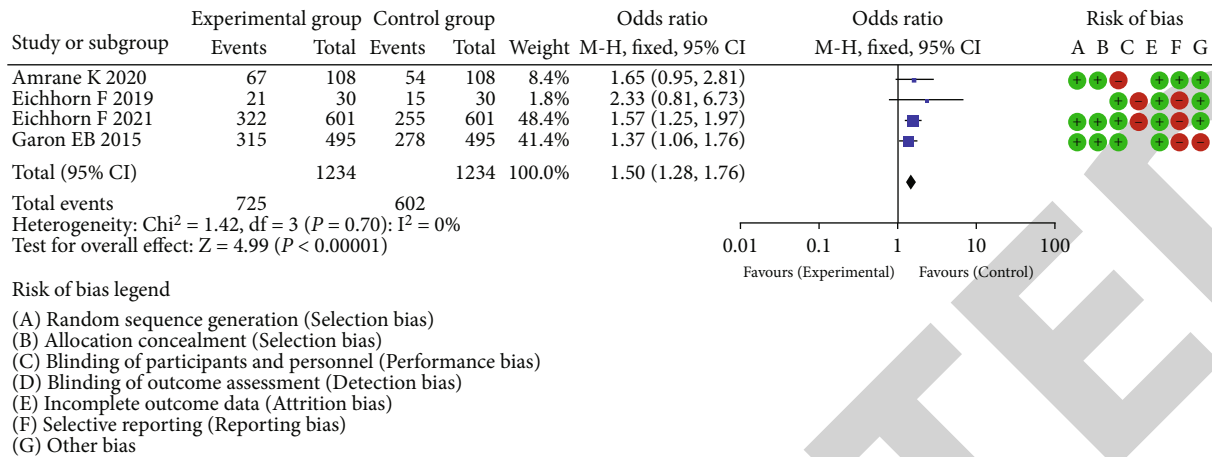


FIGURE 4: Meta-analysis of one-year survival rate between two groups.

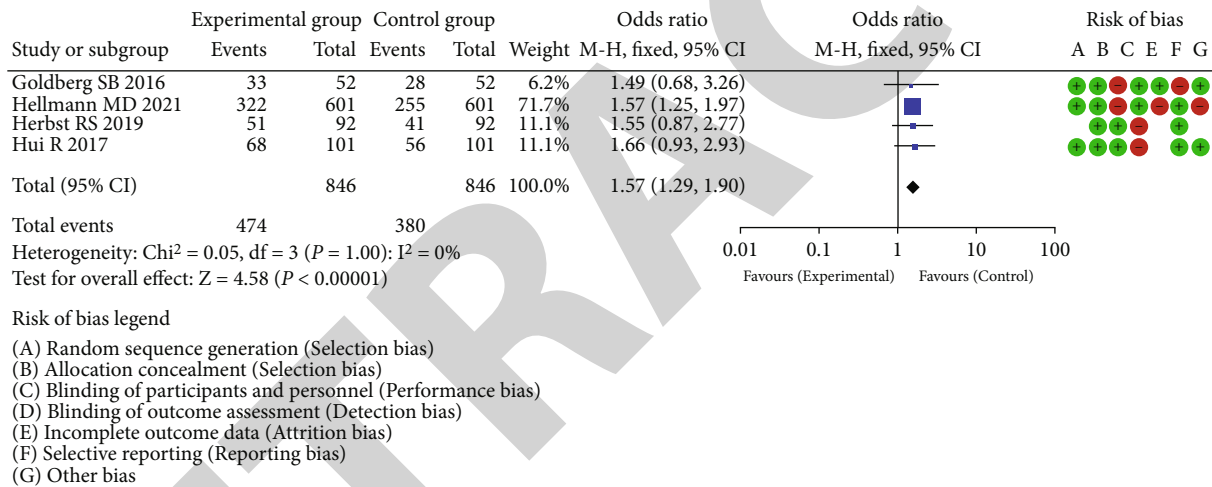


FIGURE 5: Meta-analysis of overall response rate between two groups.

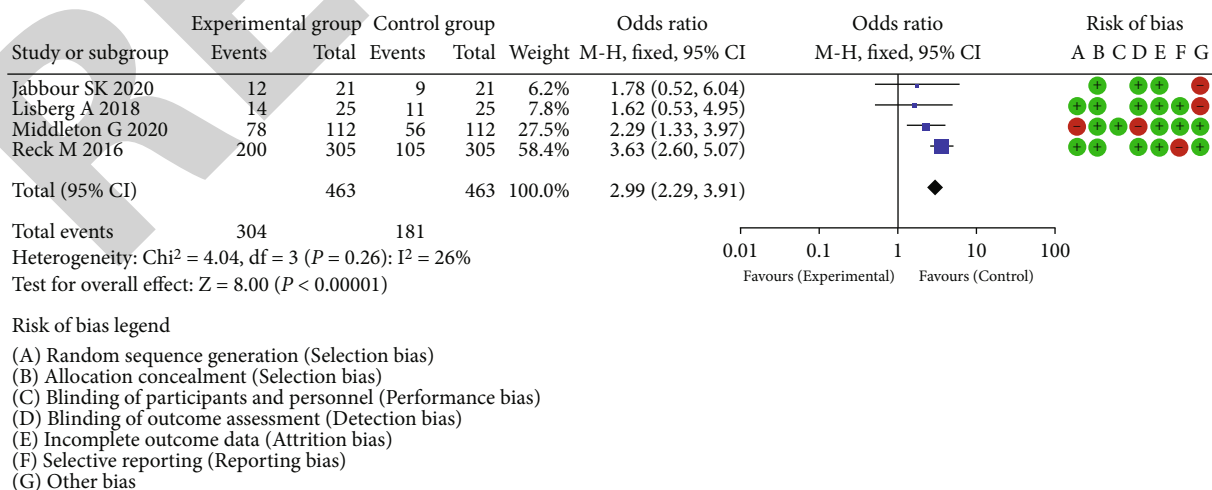


FIGURE 6: Meta-analysis of progression-free survival between two groups.



OS, with statistically significant differences compared with chemotherapy alone, while complete response rate, PFS, and chemotherapy alone showed no statistically significant differences. Relevant studies [36–38] also showed that pembrolizumab combined with chemotherapy had a higher proportion of grade 3 and 4 leukopenia, rash, and infusion reaction than chemotherapy alone, and the difference was statistically significant, but there was no increase in the mortality rate. Therefore, pembrolizumab is effective and safe.

The following are some of the restrictions that apply to this study: (1) The criteria for what constitutes a positive PD-L1 test, known as the cutoff value, may vary [39]. The weakness of this work is that it does not conduct a subgroup analysis of shortened values, which may contribute to an increase in research bias. (2) Responses to immunotherapy might vary depending on the molecular profile of non-small-cell lung cancer [40].

In conclusion, the administration of pembrolizumab in conjunction with chemotherapy for patients with NSCLC may enhance treatment effectiveness. This occurs even if the frequency of certain adverse responses has risen; nevertheless, it does not raise the mortality rate. Therefore, pembrolizumab may be tolerated and should be used in clinical settings on a more extensive scale.

## Conflicts of Interest

We define that all authors have not been involved in a set of conditions affecting our professional judgment concerning the validity of research, and we are not influenced by financial gain.

## References

- [1] D. De Ruyscher, C. Faivre-Finn, K. Nackaerts et al., “Recommendation for supportive care in patients receiving concurrent chemotherapy and radiotherapy for lung cancer,” *Annals of Oncology*, vol. 31, no. 1, pp. 41–49, 2020.
- [2] U. Dafni, Z. Tsourti, K. Vervita, and S. Peters, “Immune checkpoint inhibitors, alone or in combination with chemotherapy, as first-line treatment for advanced non-small cell lung cancer. A systematic review and network meta-analysis,” *Lung Cancer*, vol. 134, pp. 127–140, 2019.
- [3] A. El-Hussein, S. L. Manoto, S. Ombinda-Lemboumba, Z. A. Alrowaili, and P. Mthunzi-Kufa, “A review of chemotherapy and photodynamic therapy for lung cancer treatment,” *Anti-Cancer Agents in Medicinal Chemistry*, vol. 21, no. 2, pp. 149–161, 2021.
- [4] F. Griesinger, E. E. Korol, S. Kayaniyil, N. Varol, T. Ebner, and S. M. Goring, “Efficacy and safety of first-line carboplatin-versus cisplatin-based chemotherapy for non-small cell lung cancer: a meta-analysis,” *Lung Cancer*, vol. 135, pp. 196–204, 2019.
- [5] C. Wang, W. Qiao, Y. Jiang et al., “The landscape of immune checkpoint inhibitor plus chemotherapy versus immunotherapy for advanced non-small-cell lung cancer: a systematic review and meta-analysis,” *Journal of Cellular Physiology*, vol. 235, no. 5, pp. 4913–4927, 2020.
- [6] L. T. Curtis and H. B. Frieboes, “Modeling of combination chemotherapy and immunotherapy for lung cancer,” in *2019 41st Annual International Conference of the IEEE Engineering in Medicine and Biology Society (EMBC)*, pp. 273–276, Berlin, Germany, 2019.
- [7] L. Wen, F. Tong, R. Zhang, L. Chen, Y. Huang, and X. Dong, “The research progress of PD-1/PD-L1 inhibitors enhancing radiotherapy efficacy,” *Frontiers in Oncology*, vol. 11, article 799957, 2021.
- [8] L. Jimbu, O. Mesaros, C. Popescu et al., “Is there a place for PD-1-PD-L blockade in acute myeloid leukemia?,” *Pharmaceuticals (Basel)*, vol. 14, no. 4, p. 288, 2021.
- [9] M. Nie, Y. Liu, X. X. Li et al., “PD-1/PD-L pathway potentially involved in ITP immunopathogenesis,” *Thrombosis and Haemostasis*, vol. 119, no. 5, pp. 758–765, 2019.
- [10] M. Grecea, O. Soritau, D. Dulf, T. E. Ciuleanu, and M. Zdrenghea, “Potential biomarkers for the efficacy of PD-1-PD-L blockade in cancer,” *Oncotargets and Therapy*, vol. Volume 14, no. 14, pp. 5275–5291, 2021.
- [11] M. Reck, D. Rodríguez-Abreu, A. G. Robinson et al., “Pembrolizumab versus chemotherapy for PD-L1-positive non-small-cell lung cancer,” *The New England Journal of Medicine*, vol. 375, no. 19, pp. 1823–1833, 2016.
- [12] E. B. Garon, N. A. Rizvi, R. Hui et al., “Pembrolizumab for the treatment of non-small-cell lung cancer,” *The New England Journal of Medicine*, vol. 372, no. 21, pp. 2018–2028, 2015.
- [13] M. Reck, D. Rodríguez-Abreu, A. G. Robinson et al., “Five-year outcomes with pembrolizumab versus chemotherapy for metastatic non-small-cell lung cancer with PD-L1 tumor proportion score  $\geq 50\%$ ,” *Journal of Clinical Oncology*, vol. 39, no. 21, pp. 2339–2349, 2021.
- [14] S. B. Goldberg, S. N. Gettinger, A. Mahajan et al., “Pembrolizumab for patients with melanoma or non-small-cell lung cancer and untreated brain metastases: early analysis of a non-randomised, open-label, phase 2 trial,” *The Lancet Oncology*, vol. 17, no. 7, pp. 976–983, 2016.
- [15] F. Eichhorn, L. V. Klotz, H. Bischoff et al., “Neoadjuvant anti-programmed death-1 immunotherapy by pembrolizumab in resectable nodal positive stage II/IIIa non-small-cell lung cancer (NSCLC): the NEOMUN trial,” *BMC Cancer*, vol. 19, no. 1, p. 413, 2019.
- [16] K. Amrane, M. Geier, R. Corre et al., “First-line pembrolizumab for non-small cell lung cancer patients with PD-L1  $\geq 50\%$  in a multicenter real-life cohort: The PEMBREIZH study,” *Cancer Medicine*, vol. 9, no. 7, pp. 2309–2316, 2020.
- [17] S. K. Jabbar, A. T. Berman, R. H. Decker et al., “Phase 1 trial of pembrolizumab administered concurrently with chemoradiotherapy for locally advanced non-small cell lung cancer: a nonrandomized controlled trial,” *JAMA Oncology*, vol. 6, no. 6, pp. 848–855, 2020.
- [18] G. Middleton, K. Brock, J. Savage et al., “Pembrolizumab in patients with non-small-cell lung cancer of performance status 2 (PePS2): a single arm, phase 2 trial,” *The Lancet Respiratory Medicine*, vol. 8, no. 9, pp. 895–904, 2020.
- [19] R. S. Herbst, H. T. Arkenau, R. Santana-Davila et al., “Ramucirumab plus pembrolizumab in patients with previously treated advanced non-small-cell lung cancer, gastro-oesophageal cancer, or urothelial carcinomas (JVDF): a multicohort, non-randomised, open-label, phase 1a/b trial,” *The Lancet Oncology*, vol. 20, no. 8, pp. 1109–1123, 2019.
- [20] A. Lisberg, A. Cummings, J. W. Goldman et al., “A phase II study of pembrolizumab in EGFR-mutant, PD-L1+, tyrosine

## Retraction

# Retracted: Gait Improvement in Patients with Knee Osteoarthritis after Proximal Fibular Osteotomy

### BioMed Research International

Received 20 June 2023; Accepted 20 June 2023; Published 21 June 2023

Copyright © 2023 BioMed Research International. This is an open access article distributed under the Creative Commons Attribution License, which permits unrestricted use, distribution, and reproduction in any medium, provided the original work is properly cited.

This article has been retracted by Hindawi following an investigation undertaken by the publisher [1]. This investigation has uncovered evidence of one or more of the following indicators of systematic manipulation of the publication process:

- (1) Discrepancies in scope
- (2) Discrepancies in the description of the research reported
- (3) Discrepancies between the availability of data and the research described
- (4) Inappropriate citations
- (5) Incoherent, meaningless and/or irrelevant content included in the article
- (6) Peer-review manipulation

The presence of these indicators undermines our confidence in the integrity of the article's content and we cannot, therefore, vouch for its reliability. Please note that this notice is intended solely to alert readers that the content of this article is unreliable. We have not investigated whether authors were aware of or involved in the systematic manipulation of the publication process.

Wiley and Hindawi regrets that the usual quality checks did not identify these issues before publication and have since put additional measures in place to safeguard research integrity.

We wish to credit our own Research Integrity and Research Publishing teams and anonymous and named external researchers and research integrity experts for contributing to this investigation.

The corresponding author, as the representative of all authors, has been given the opportunity to register their agreement or disagreement to this retraction. We have kept a record of any response received.

### References

- [1] X. Li, Y. Cao, Z. Cao et al., "Gait Improvement in Patients with Knee Osteoarthritis after Proximal Fibular Osteotomy," *BioMed Research International*, vol. 2022, Article ID 1869922, 8 pages, 2022.



## Research Article

# Gait Improvement in Patients with Knee Osteoarthritis after Proximal Fibular Osteotomy

Xiaotong Li <sup>1</sup>, Yuqing Cao <sup>1</sup>, Zhenguo Cao <sup>2</sup>, Pengfei Zheng <sup>3</sup>,  
Andrew Merryweather <sup>4</sup>, Hui Wang <sup>1</sup>, Ding Chen <sup>5</sup>, and Hang Xu <sup>1</sup>

<sup>1</sup>School of Medical Imaging, Xuzhou Medical University, Xuzhou, China

<sup>2</sup>Department of Orthopedics, The Second Affiliated Hospital of Xuzhou Medical University, Xuzhou, China

<sup>3</sup>Department of Orthopaedic Surgery, Children's Hospital of Nanjing Medical University, Nanjing, China

<sup>4</sup>Department of Mechanical Engineering, University of Utah, Salt Lake City, UT, USA

<sup>5</sup>School of Medical Information and Engineering, Xuzhou Medical University, Xuzhou, China

Correspondence should be addressed to Ding Chen; [chending224@163.com](mailto:chending224@163.com) and Hang Xu; [h\\_xu@xzhmu.edu.cn](mailto:h_xu@xzhmu.edu.cn)

Received 19 May 2022; Revised 6 June 2022; Accepted 13 June 2022; Published 23 June 2022

Academic Editor: Dinesh Rokaya

Copyright © 2022 Xiaotong Li et al. This is an open access article distributed under the Creative Commons Attribution License, which permits unrestricted use, distribution, and reproduction in any medium, provided the original work is properly cited.

Proximal fibula osteotomy (PFO) is a relatively new surgery to treat medial compartment knee osteoarthritis (KOA), which can improve varum deformity and relieve knee joint pain. However, the gait alterations in KOA patients after PFO are still poorly understood. The purpose of this study was to evaluate the gait patterns change in patients of medial compartment KOA after PFO. Gait data were collected for 9 females with unilateral medial compartment KOA before and at 6 months after PFO and also for 9 healthy age-matched females. Paired *t*-test was used to determine the effect of PFO within the KOA group, and independent *t*-test were performed to compare between KOA and control groups for spatiotemporal, kinematic, and kinetic variables. The results showed that patients with KOA had significantly increased knee peak flexion angle, knee sagittal range of motion, and peak external hip adduction moment but decreased knee frontal range of motion in the affected limb after PFO. The gait symmetry was improved postoperatively confirmed by single support and swing phases, knee peak flexion angle and sagittal range of motion, peak external hip and knee adduction moments, and peak anterior and peak posterior ground reaction forces. These findings provided evidence of a biomechanical benefit and gait improvement following PFO to treat medial compartment KOA.

## 1. Introduction

Knee osteoarthritis (KOA) is one of the most common degenerative diseases, which causes pain and disability and seriously deteriorates the quality of life. KOA mostly occurs in adults over 50 years old with an increase incidence with age [1]. Women are more severely impacted by KOA than men, including more advanced stages, more pain and disability, and even higher prevalence [2]. Since the medial compartment of the knee joint bears 60% to 80% of the load during gait, medial compartment KOA is commonly observed by knee varus deformities [3].

There are many surgery options for medial compartment KOA when conservative measures cannot relieve pain or the knee joint has obvious deformities, such as high tibial osteot-

omy and total knee arthroplasty [4]. To date, total knee arthroplasty remains the most common and effective treatment choice for KOA patients, but the cost of surgery is high, and the procedure is invasive [5]. Although high tibial osteotomy can preserve the knee joint and is less invasive, a strict weight-bearing restriction in the early postoperative period is required, and the recovery time after surgery is relatively long [6].

In recent years, proximal fibula osteotomy (PFO) has become a new choice for the management of medial compartment KOA, which has advantages of a smaller surgical incision, local anesthetic operation, shorter hospital stays, and lower treatment cost compared to high tibial osteotomy and total and knee arthroplasty [7]. However, the biomechanical mechanism of how PFO treats medial compartment

KOA is still largely unknown. Previous research concludes that the support of the fibula on the lateral tibial plateau leads to nonuniform settlement of medial and lateral tibial plateaus, which is the medial shift mechanical axis of the knee joint [3, 8]. According to this theory, PFO could disrupt the lateral strut effect of the fibula and redistribute the load and pressure between tibial plateaus, thus relieving knee pain [9].

Most previous studies of PFO to treat KOA focus on the clinical outcomes and radiographic analysis rather than biomechanics [8–10]. PFO was reported to significantly improve patients' knee function as well as pain evidenced by the Western Ontario and McMaster Universities Osteoarthritis Index (WOMAC), American Knee Society Score (KSS), and hospital for special surgery score [10–13]. The radiographic results show that the hip-knee-ankle (HKA) angle and femorotibial angle are corrected, and the medial space of the knee joint increased on average after PFO [3, 10, 12, 14].

There is a paucity of research on the effect of gait alteration after PFO. Biswas et al. collected gait data from 22 KOA patients preoperatively and postoperatively for PFO, respectively. They reported an increased cadence and reduced step width and peak knee inversion angle after PFO, which relieved the knee pain and improved the biomechanical alignment [15]. However, this study distinguished the lower limb by right and left side, not by affected and unaffected limb. Huang et al. analyzed gait parameters from KOA patients with PFO preoperatively, 1 day, 3 months, and 6 months postoperatively, and also healthy adults [12]. They found that gait speed and the range of knee flexion overall increased, but the knee adduction moment (KAM) decreased after PFO at 6 months compared to 1 day postoperatively [12]. However, pain experienced immediately postoperatively might have interfered with the gait result 1 day following surgery [15], and the controls were much younger than the patients, resulting in unclear comparisons between groups.

To our knowledge, the change of gait pattern after PFO to treat medial compartment KOA is still largely unknown. Therefore, the aim of this study was to evaluate the gait alterations in patients of medial compartment KOA after PFO.

## 2. Methods

**2.1. Participants.** Nine females with unilateral medial compartment KOA were recruited from local hospital (Table 1). The sample size was determined using the software G\*Power (version 3.1.9) with the input as follows: paired *t*-test, effect size of 0.8, statistical power of 70%, and significance level of 0.05. Inclusion criteria included (1) medial compartment KOA based on Kellgren-Lawrence (grade 2 or 3); (2) age between 60 and 70 years; (3) the presence of knee deformity with narrowing of the medial compartment; and (4) ambulatory without using an assistive device. Exclusion criteria included (1) any fracture, infection, and surgical history in lower limb joints and (2) other neurologic diseases that affects gait. All the participants with medial compart-

ment KOA underwent PFO by the same orthopedic surgeon, and the surgery was performed as per standard protocol [16]. Nine healthy females were also included as the control group, which met the following criteria: (1) age between 60 and 70 years and (2) free from injuries or disorders which would affect their gait. Institutional review board approval was obtained from Xuzhou Medical University (IRB\_2019651972), and all participants provided written informed consent.

**2.2. Experimental Procedures.** Prior to the gait analysis, the HKA angle was measured for radiographic evaluation, which was defined as the angle between the mechanical axes of the femur and the tibia in the frontal plane. KSS and WOMAC were recorded for all participants before and after PFO. Gait data were collected twice for each participant in Biomechanics and Motion Analysis Laboratory of Xuzhou Medical University, one was before PFO and the other was 6 months after surgery. A 10-camera motion capture system (Vicon Motion Systems Ltd., Oxford, UK) and two force plates (AMTI, Watertown, MA) were used to collect kinematic and ground reaction force (GRF) data. Subjects wore tight fitting clothing, and 28 reflective markers were attached to the body based on an improved plug-in gait lower body marker set [17]. Then, a static trial was collected to build the model and participants barefoot walked along a 10-meter walkway several times to familiarize the laboratory environment. Finally, five successful barefoot gait trials were collected for each subject at a self-selected speed. A successful trial was defined as one which involved a heel strike by a foot as it was isolated on the specific force plate. The marker trajectory and GRF data were recorded at 100 Hz and 1000 Hz and postprocessed with a fourth-order low-pass filter at 6 Hz and 20 Hz, respectively.

**2.3. Data Analysis.** The variables of interest were spatio-temporal, kinematic, and kinetic parameters. The spatio-temporal variables included gait speed, step and stride lengths, step time, step width, step cadence, swing phase, and single-support and double-support phases. Kinematic variables included the peak and range of motion (RoM) of the hip, knee, and ankle joints in three body planes. Kinetic variables included the peak moments of the hip, knee, and ankle joints in the frontal plane and also peak GRFs in vertical, anteroposterior, and mediolateral directions.

The data were processed using Vicon Nexus 2.10 (Vicon Motion Systems Ltd., Oxford, UK). The dynamic plug-in-gait program was run firstly to detect the gait events (heel strike and toe off) which were defined via force plate with a 20 N threshold. Then the joint angles and moments were calculated. Finally, gait data were exported to the Vicon Polygon 4.4 (Vicon Motion Systems Ltd., Oxford, UK) to obtain the spatiotemporal variables. The kinematic and kinetic variables were normalized to 101 points for gait cycle. Additionally, joint moment and GRF were normalized to body mass for each subject. For the patients with medial compartment KOA, all the variables were averaged across five trials for each subject and then averaged across nine participants for both affected and unaffected limbs. For the

TABLE 1: Mean (SD) participants' demographics.

	Age (years)	Height (m)	Weight (kg)	BMI (kg/m <sup>2</sup> )	Affected limb (L/R)	KOA grade (2/3)
KOA group	65.2 (3.4)	1.62 (0.09)	68.4 (9.4)	25.8 (2.1)	4/5	5/4
Control group	65.7 (2.1)	1.62 (0.06)	68.4 (10.1)	26.1 (2.7)	N/A	N/A

TABLE 2: Clinical and radiographic measurement expressed as mean (SD) for KOA group.

	Preoperation	Postoperation
HKA angle (degree)	173.2 (3.5)*	176.5 (2.9)
KSS functional score	57.1 (10.8)*	84.3 (11.3)
WOMAC pain score	20.7 (9.3)*	7.7 (2.6)

\*Significant difference compared with postoperation.

controls, the variables were averaged across two limbs for five within-subject trials and then across subjects to obtain group-averaged data.

**2.4. Statistical Analysis.** Statistics were performed using SPSS 20.0 (IBM Corporation, Armonk, NY, USA). Descriptive statistics were calculated for gait variables, and normality of data was confirmed using the Shapiro-Wilk test. Paired *t*-test was used to assess the gait symmetry between affected and unaffected limbs for patient group and also gait alterations before and after PFO. Independent *t*-test was used to compare between KOA patients and controls. A significance level of 0.05 was used for comparisons.

### 3. Results

The average HKA angle significantly increased for affected limb after PFO ( $p < 0.001$ ), and the KSS functional score and WOMAC pain score also improved ( $p = 0.001$  and  $p = 0.002$ ) (Table 2).

**3.1. Spatiotemporal Variables.** The single support phase and swing phase were significantly different between the affected and unaffected limbs in the KOA group preoperatively ( $p = 0.008$  and  $p = 0.013$ ) (Table 3), but no significant differences were observed for these two variables postoperatively. The KOA patients showed a decreased gait speed, step length, step cadence, stride length, single support phase, and swing phase but increased step time and double support phase compared to controls in both preoperation and postoperation (all  $p < 0.05$ ).

**3.2. Kinematic Variables.** The affected limb showed an increased knee peak flexion and sagittal RoM ( $p = 0.010$  and  $p = 0.011$ ) but decreased frontal RoM for the hip and knee joints after PFO ( $p = 0.039$  and  $p = 0.017$ ) (Figure 1). The significant between-limb differences were observed for knee peak flexion and sagittal RoM preoperatively ( $p = 0.009$  and  $p < 0.001$ ), which were disappeared postoperatively (Table 4). Additionally, the significant difference for knee transverse RoM between the affected limb and control preoperatively ( $p = 0.004$ ) were also disappeared postopera-

tively. Moreover, compared with the controls, KOA patients showed reduced peak angle of knee flexion and ankle plantar flexion, decreased hip frontal RoM, and also sagittal RoM for the hip, knee, and ankle joints for both limbs in preoperation and postoperation (all  $p < 0.05$ ).

**3.3. Kinetic Variables.** The affected limb showed an increased peak external hip adduction moment (HAM) after PFO ( $p = 0.021$ ) (Figure 2). The significant between-limb differences were observed preoperatively for peak external HAM ( $p = 0.042$ ) and KAM ( $p = 0.038$ ), peak propulsion ( $p = 0.015$ ), and braking GRFs ( $p = 0.035$ ) which were disappeared postoperatively (Table 5). Compared with controls, KOA patients showed significantly different peak moments preoperatively, including external HAM ( $p = 0.015$ ) and ankle inversion moment ( $p = 0.028$ ) for the affected limb and external HAM ( $p = 0.028$ ) and KAM ( $p = 0.003$ ) for the unaffected limb. The peak external KAM was larger for the unaffected limb postoperatively than controls ( $p = 0.001$ ). Additionally, KOA patients also showed reduced first and second peak vertical GRFs, decreased peak propulsion, and braking GRFs when comparing with control group in preoperation and postoperation (all  $p < 0.05$ ).

### 4. Discussion

An asymmetrical gait pattern was often observed for KOA patients. In order to reduce the knee pain in the affected limb, KOA patients increased single support phase and decreased swing phase in the unaffected limb preoperatively. However, this phenomenon disappeared after PFO indicating an improvement of gait symmetry postoperatively. Although significant difference still existed between the postoperative KOA patients and controls for most of the spatiotemporal variables, the results after PFO were encouraging, such as increased gait speed, larger step and stride lengths, and decreased double support phase, which agreed with previous findings [7, 12] and also the postoperative reduced WOMAC pain score.

Reduced RoM is usually considered as a response to the pain and dysfunction associated with degenerative joint disease [18, 19]. In our study, decreased sagittal RoM for all lower extremity joints in KOA patients aligned with previous findings, especially for the affected limb [19]. The significant differences between affected and unaffected limbs preoperative observed only in knee sagittal plane suggested that the KOA patients did not use a dynamic hip and ankle compensation strategy for the reduced knee flexion. Although a smaller sagittal RoM was found for both hip and ankle joints in KOA patients preoperatively and postoperatively than controls, further analyses indicated that reduced hip sagittal RoM was related to both peak flexion

TABLE 3: Spatiotemporal variables expressed as mean (SD) for KOA and control groups.

	Preoperation		Postoperation		Control
	Affected	Unaffected	Affected	Unaffected	
Step length (m)	0.44 (0.10)*	0.44 (0.11)*	0.48 (0.08)*	0.49 (0.08)*	0.61(0.04)
Step time (s)	0.61 (0.11)*	0.57 (0.04)*	0.60 (0.14)*	0.57 (0.06)*	0.52 (0.04)
Step cadence (step/s)	1.68 (0.25)*	1.76 (0.13)*	1.74 (0.30)*	1.77 (0.19)*	1.94 (0.12)
Single support phase (%gait cycle)	31.23 (7.28)*	34.89 (5.64)*#	35.30 (3.80)*	36.17 (3.44)*	39.15 (3.80)
Swing phase (%gait cycle)	36.44 (3.94)*	32.78 (5.39)*#	35.92 (3.72)*	34.66 (3.66)*	38.94 (8.18)
Gait speed (m/s)	0.73 (0.23)*		0.85 (0.19)*		1.18 (0.09)
Gait width (m)	0.14 (0.04)		0.12 (0.04)		0.11 (0.01)
Stride length (m)	0.87 (0.20)*		0.97 (0.15)*		1.22 (0.08)
Double support phase (%gait cycle)	32.33 (9.11)*		29.17 (6.50)*		22.11 (8.18)

\*Significant difference compared with control. #Significant difference compared with affected limb preoperatively.

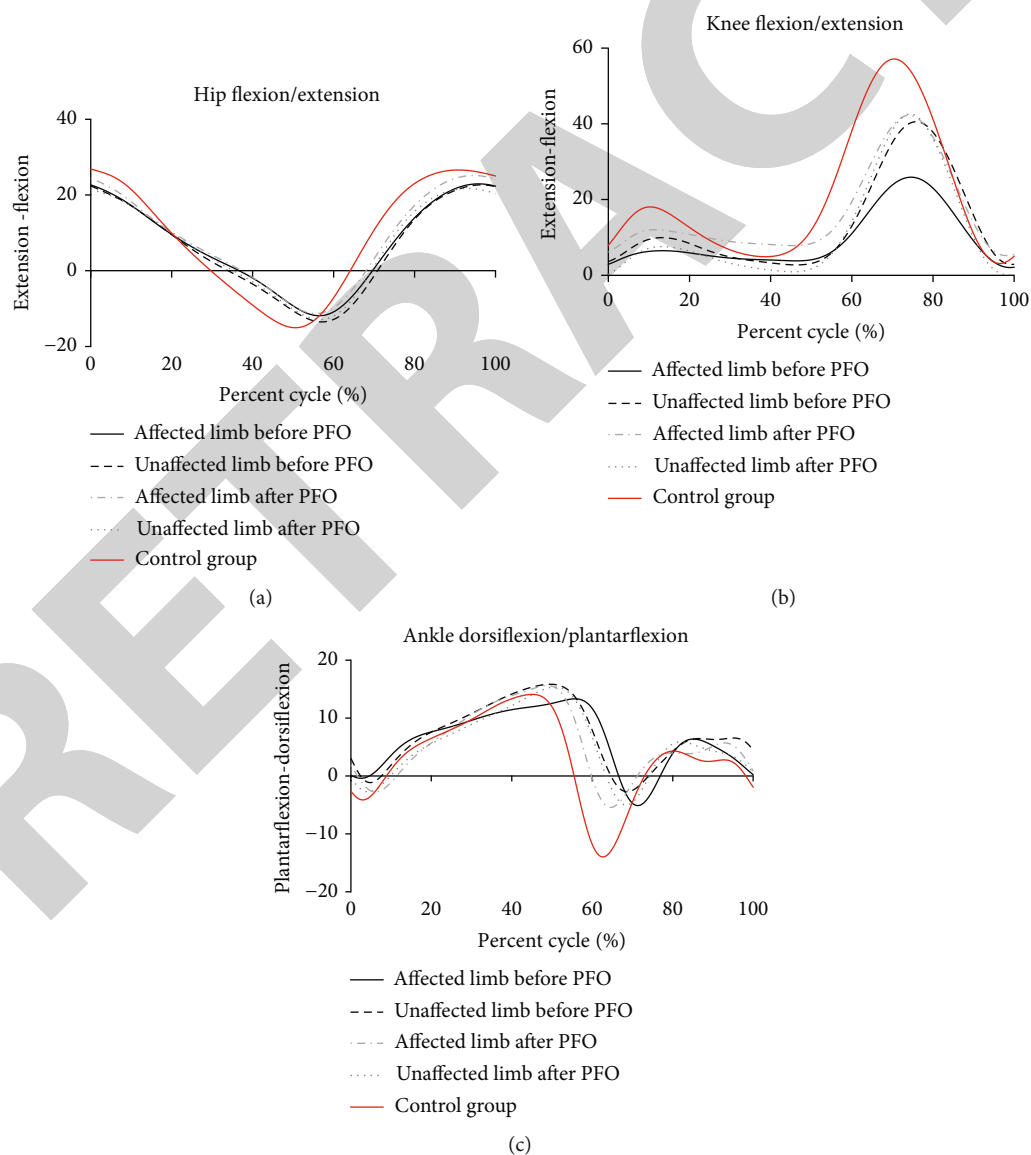


FIGURE 1: Average lower limb joint kinematics in sagittal plane: (a) hip flexion/extension; (b) knee flexion/extension; (c) ankle dorsiflexion/plantar flexion.



TABLE 4: Kinematic variables expressed as mean (SD) for KOA and control groups.

	Preoperation		Postoperation		Control
	Affected	Unaffected	Affected	Unaffected	
<b>Hip joint (degree)</b>					
Peak flexion	23.83 (7.52)	24.02 (5.65)	25.02 (7.77)	22.47 (6.33)	26.92 (5.02)
Peak extension	12.21 (10.38)	13.65 (6.57)	11.20 (11.73)	14.06 (7.10)	16.37 (6.79)
Sagittal RoM	36.03 (7.83)*	37.67 (7.13)*	36.22 (6.80)*	36.54 (6.13)*	43.28 (3.98)
Frontal RoM	8.80 (2.74)*	7.14 (1.66)*	7.29 (2.13)*#	7.11 (0.99)*	10.99 (1.03)
Transverse RoM	20.99 (15.32)	23.71 (12.70)	18.44 (5.27)	24.41 (8.53)	19.71 (6.52)
<b>Knee joint (degree)</b>					
Peak flexion	27.41 (19.03)*	44.03 (10.58)*#	42.75 (17.08)*#	42.72 (14.14)*	57.69 (4.73)
Peak extension	-1.02 (12.87)	-0.42 (7.04)	-3.67 (8.69)	1.69 (4.91)	0.84 (4.23)
Sagittal RoM	26.40 (13.48)*	43.62 (8.39)*#	39.08 (15.47)*#	44.42 (11.84)*	58.53 (4.24)
Frontal RoM	25.33 (14.41)	17.77 (7.67)	13.80(9.62)#	16.09 (7.50)	16.28 (4.24)
Transverse RoM	10.82 (5.01)*	14.41 (4.56)	13.69 (6.45)	15.12 (6.31)	18.06 (3.49)
<b>Ankle joint (degree)</b>					
Ankle peak dorsiflexion	15.33 (6.26)	16.54 (3.24)	16.21 (7.91)	16.24 (5.43)	15.38 (3.87)
Ankle peak plantar flexion	4.97 (5.01)*	7.60 (5.84)*	6.11 (7.51)*	6.83 (5.54)*	14.71 (8.28)
Ankle sagittal RoM	20.30 (5.61)*	24.14 (5.70)*	22.32 (4.09)*	23.07 (5.94)*	30.09 (5.86)
Ankle frontal RoM	4.09 (2.00)	4.83 (2.76)	4.47 (2.96)	5.19 (2.23)	3.66 (1.48)
Ankle transverse RoM	20.10 (5.93)	25.42 (8.64)	21.63 (6.71)	25.06 (7.22)	24.68 (6.01)

\*Significant difference compared with controls; #Significant difference compared with affected limb preoperatively.

and extension, but the ankle sagittal RoM difference was mainly caused by a smaller peak plantar flexion which may result in a decreased push off and short step length.

The previous guidelines for the management of KOA mainly focus on knee pain relief and functional improvement [20]. Beside the relieved pain and improved knee function based on WOMAC and KSS scores after PFO, the knee peak flexion and sagittal RoM also significantly increased postoperatively for the affected limb, and the magnitudes were similar to the unaffected limb, which supported the feasibility and effectiveness of PFO to treat medial compartment KOA. Whether the PFO affected the ankle stability is still controversial. Some research indicated that PFO could damage the conduction path of external condyle and reduce the stabilizing effect of the ankle joint, resulting in ankle joint looseness or valgus [21, 22]. However, similar ankle frontal and transverse RoM between postoperative KOA and control groups suggests that preserving enough distal fibula length could reduce the influence of PFO on the ankle joint movement [23].

Frontal plane knee laxity and instability were commonly reported during gait in KOA patients [24], which contributes to the altered gait pattern including an increased knee adduction angle [25]. Our results found that the preoperative KOA group showed an approximately eight-degree larger knee frontal RoM in the affected limb than unaffected limb and controls. After PFO for 6 months, a comparable knee frontal RoM was observed for the affected limb indicating a likely improvement in knee stability during movement.

The KAM reflected the magnitude of medial joint loading, and medial KOA patients usually showed a large

peak external KAM during stance phase [26], which was also observed in our study, especially for the unaffected limb. In order to relieve knee pain and reduce knee loading, a compensatory strategy of laterally shifting the trunk to the affected side was previously reported to reduce KAM [27, 28], which may increase the loading and risk of osteoarthritis in the contralateral knee joint. Surprisingly, a decreased peak external KAM in postoperative KOA patients was not presently observed. This result could be partially explained by the increased gait speed and corrected HKA angle. On one hand, KAM had a positive correlation with gait speed [29], so increased gait speed postoperatively raised the peak external KAM. On the other hand, the corrected HKA angle could decrease the peak external KAM by shortening the adduction moment arm. Therefore, the phenomenon of knee pain relief in the affected limb postoperatively seemed to not cause a reduction of knee loading in the medial compartment but a redistributed knee pressure due to a more neutral alignment and improved medial knee joint space [1, 8].

KOA not only affects the knee joint, but also the hip and ankle joint, as these three joints operate as a kinetic chain during gait. Decreased peak external HAM were observed for the KOA patients preoperatively compared to the controls, especially for the affected limb, which reduced the demand on hip abductors and lead to muscle weakness [25, 30]. After PFO at 6 months, the peak external HAM for both affected and unaffected limbs increased, and the HAM differences disappeared between patients and controls, which was the results of improved gait speed and HKA angle [12, 14]. Interestingly, the peak external ankle inversion moment was about 47% higher in the affected limb



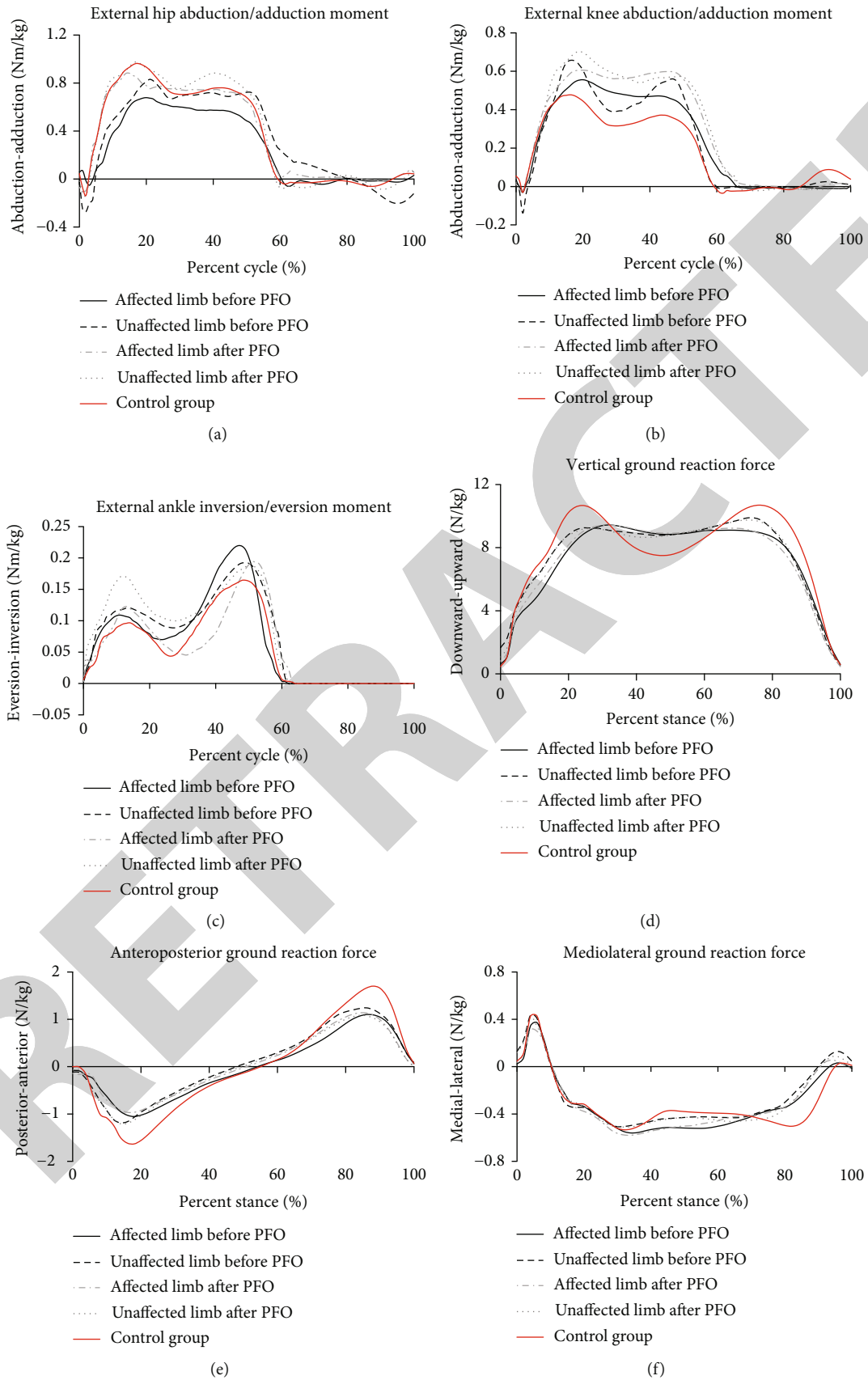


FIGURE 2: Average joint kinetics and GRF during gait: (a) hip abduction/adduction moment; (b) knee abduction/adduction moment; (c) ankle inversion/eversion moment; (d) vertical GRF; (e) anteroposterior GRF; (f) mediolateral GRF.

TABLE 5: Peak kinetic variables expressed as mean (SD) for KOA and control groups.

	Preoperation		Postoperation		Control
	Affected	Unaffected	Affected	Unaffected	
Hip adduction moment (nm/kg)	0.71 (0.22)*	0.83 (0.20)*#	0.88 (0.24)#	0.97 (0.15)	0.97 (0.09)
Knee adduction moment (nm/kg)	0.55 (0.16)	0.67 (0.11)*#	0.59 (0.15)	0.70 (0.13)*	0.49 (0.14)
Ankle inversion moment (nm/kg)	0.22 (0.11)*	0.19 (0.07)	0.19 (0.07)	0.17 (0.06)	0.15 (0.05)
First vertical GRF (N/kg)	9.77 (0.48)*	10.04 (0.53)*	9.89 (0.65)*	10.09 (0.70)*	10.57 (0.51)
Second vertical GRF (N/kg)	9.75 (0.27)*	10.00 (0.51)*	9.78 (0.29)*	9.97 (0.57)*	10.58 (0.51)
Anterior propulsion GRF (N/kg)	1.11 (0.48)*	1.30 (0.37)*#	1.22 (0.44)*	1.19 (0.42)*	1.71 (0.18)
Posterior braking GRF (N/kg)	1.15 (0.34)*	1.28 (0.45)*#	1.12 (0.32)*	1.27 (0.45)*	1.61 (0.18)
Medial GRF (N/kg)	0.61 (0.07)	0.62 (0.07)	0.63 (0.10)	0.62 (0.10)	0.61 (0.10)
Lateral GRF (N/kg)	0.46 (0.18)	0.56 (0.20)	0.42 (0.17)	0.50 (0.16)	0.51 (0.19)

\*Significant difference compared with controls. #Significant difference compared with affected limb preoperatively; GRF: ground reaction force.

for the preoperative KOA patients than controls; such change could be a risk factor for secondary arthritis and the reason of the ankle subluxation commonly seen in KOA patients [31]. The ankle inversion moment was reduced for both limbs postoperatively and was close to the magnitude of the control group, indicating the positive effect of PFO on the ankle joint [11].

KOA patients showed a reduced gait speed that smooths out the vertical acceleration and deceleration to reduce knee stress [15], which explained the observation of smaller peaks in the first and second vertical GRF compared with controls. KOA patients depended on the unaffected limb more to prevent the foot slipping at heel strike and propel the body forward at toe off before PFO [32], which was reflected by the larger propulsion and braking GRFs than the affected limb. This asymmetrical phenomenon disappeared postoperatively due to the knee pain relief and functional improvement. The mediolateral GRF depended mostly on the relationship between the position of body center of mass and the foot. Therefore, the increased gait speed combined with similar medial and lateral GRFs indicated an enhancement in body control in the mediolateral direction after PFO [33].

Two limitations existed in this study. First, the sample size was relatively small, the follow-up period was relatively short, and a larger sample size with longer follow-up period is needed to better understand the potential benefits and limitations of PFO. Second, the magnitude and distribution of knee loads was not directly addressed. Future research focused on gait simulation with musculoskeletal models could help further identify the biomechanical mechanisms of PFO to treat medial KOA.

## 5. Conclusions

This study investigated the gait characteristics in patients with medial compartment KOA after PFO. The improved hip and knee joint functions in the affected limb after PFO were verified by knee peak flexion, peak external HAM, knee sagittal, and frontal RoMs. Moreover, gait symmetry improved postoperatively and was confirmed by sin-

gle support and swing phases, knee peak flexion and sagittal RoM, peak external HAM and KAM, and peak anterior and posterior GRF. The present results provided biomechanical evidence of a benefit from PFO, which may be applied to gait training and rehabilitation interventions for KOA patients after PFO.

## Data Availability

The datasets used and/or analyzed during the current study are available from the corresponding author on reasonable request.

## Conflicts of Interest

The authors declare no conflict of interest.

## Acknowledgments

This work was supported by the China Postdoctoral Science Foundation (2019M651972), Scientific Research Foundation for Excellent Talents of Xuzhou Medical University (D2017018), Key Research and Development Program of Xuzhou (KC21242), Primary Research & Development Plan (Social Development) of Jiangsu Province (BE2019608), Young Medical Talents Project of Science and Education Health Project in Jiangsu Province (QNRC201609).

## References

- [1] M. Vitaloni, A. Botto-van Bemden, R. M. S. Contreras et al., "Global management of patients with knee osteoarthritis begins with quality of life assessment: a systematic review," *BMC Musculoskeletal Disorders*, vol. 20, no. 1, pp. 1–12, 2019.
- [2] S. L. Hame and R. A. Alexander, "Knee osteoarthritis in women," *Current Reviews in Musculoskeletal Medicine*, vol. 6, no. 2, pp. 182–187, 2013.
- [3] Z.-Y. Yang, W. Chen, C.-X. Li et al., "Medial compartment decompression by fibular osteotomy to treat medial compartment knee osteoarthritis: a pilot study," *Orthopedics*, vol. 38, no. 12, pp. e1110–e1114, 2015.

## *Retraction*

# **Retracted: Kukoamine A Improves *Mycoplasma pneumoniae* Pneumonia by Regulating miR-222-3p/Superoxide Dismutase 2**

### **BioMed Research International**

Received 5 December 2023; Accepted 5 December 2023; Published 6 December 2023

Copyright © 2023 BioMed Research International. This is an open access article distributed under the Creative Commons Attribution License, which permits unrestricted use, distribution, and reproduction in any medium, provided the original work is properly cited.

This article has been retracted by Hindawi, as publisher, following an investigation undertaken by the publisher [1]. This investigation has uncovered evidence of systematic manipulation of the publication and peer-review process. We cannot, therefore, vouch for the reliability or integrity of this article.

Please note that this notice is intended solely to alert readers that the peer-review process of this article has been compromised.

Wiley and Hindawi regret that the usual quality checks did not identify these issues before publication and have since put additional measures in place to safeguard research integrity.

We wish to credit our Research Integrity and Research Publishing teams and anonymous and named external researchers and research integrity experts for contributing to this investigation.

The corresponding author, as the representative of all authors, has been given the opportunity to register their agreement or disagreement to this retraction. We have kept a record of any response received.

### **References**

- [1] X.-X. Liu, M.-J. Wang, Q.-N. Kan et al., “Kukoamine A Improves *Mycoplasma pneumoniae* Pneumonia by Regulating miR-222-3p/Superoxide Dismutase 2,” *BioMed Research International*, vol. 2022, Article ID 2064013, 12 pages, 2022.

## Research Article

# Kukoamine A Improves *Mycoplasma pneumoniae* Pneumonia by Regulating miR-222-3p/Superoxide Dismutase 2

Xiu-Xiu Liu,<sup>1</sup> Ming-Jing Wang,<sup>1</sup> Qian-Na Kan,<sup>1</sup> Cui Li,<sup>2</sup> Zhen Xiao,<sup>1</sup> Yong-Hong Jiang,<sup>1</sup> Wen Li,<sup>1</sup> Xiao Li,<sup>1</sup> and Zhi-Yan Jiang<sup>1</sup> 

<sup>1</sup>Department of Pediatrics, Longhua Hospital Affiliated to Shanghai University of Traditional Chinese Medicine, Shanghai 200032, China

<sup>2</sup>Institute of Respiratory Diseases, Longhua Hospital Affiliated to Shanghai University of Traditional Chinese Medicine, Shanghai 200032, China

Correspondence should be addressed to Zhi-Yan Jiang; [jiangzhiyan@shutcm.edu.cn](mailto:jiangzhiyan@shutcm.edu.cn)

Received 13 April 2022; Revised 13 May 2022; Accepted 2 June 2022; Published 21 June 2022

Academic Editor: Abo Omer

Copyright © 2022 Xiu-Xiu Liu et al. This is an open access article distributed under the Creative Commons Attribution License, which permits unrestricted use, distribution, and reproduction in any medium, provided the original work is properly cited.

*Mycoplasma pneumoniae* pneumonia (MPP) represents a common respiratory disease in children patients. Kukoamine A (KuA) is a spermine alkaloid found in the Chinese herb *Cortex Lycii radices*, which has a variety of pharmacological properties. However, no study has been reported on the role of KuA in MPP. Exosomes, a type of lipid bilayer-enclosed extracellular vesicles, can be delivered to the target cells, where they regulate function and physiology. With the use of human alveolar basal epithelial cells (HABECs) as an *in vitro* model, in this study, we sought to characterize the changes in levels of superoxide dismutase 2 (SOD2) and proinflammatory cytokines including IL-6 and TNF- $\alpha$  in HABECs in response to exosomes, which were isolated from peripheral blood serum of MPP patients. We found that, compared to normal, MPP patients exhibited a significant up-regulated miR-222-3p. Further, exosomal miR-222-3p downregulated SOD2 activity but promoted nuclear NF- $\kappa$ B activity and expression of IL-6 and TNF- $\alpha$  in HABECs, ultimately leading to an oxidative stress condition. Interestingly, such stimulating effects were attenuated by the pretreatment of KuA. This study suggests a critical role possessed by KuA in MPP by regulating the miR-222-3p/SOD2 axis, which represents a promising strategy for the treatment of MPP.

## 1. Introduction

*Mycoplasma pneumoniae* pneumonia (MPP) is a common respiratory disease in pediatric patients, which results from an infection of *Mycoplasma pneumoniae* (*M. pneumoniae*). *M. pneumoniae* accounts for approximately 40% of community acquired pneumonia while about 18% of cases usually require hospitalizations [1–3]. *M. pneumoniae* respiratory diseases usually present similar clinical features to those observed with other atypical pathogens, for example, *Chlamydia pneumoniae*, and other various respiratory viruses and bacteria [4–6]. However, the etiology and pathogenesis of MPP remain largely unknown. A number of studies have shown that excessive host immune reactions may have partially contributed to the development of MPP, resulting in activation of lymphocytes including T helper (Th)1 and

Th17 cells [7, 8]. While this activation and differentiation of Th1 and Th17 is tightly regulated by costimulatory molecules expressed on antigen presenting cells [9]. Moreover, the levels of various types of proinflammatory cytokines including IL-6 and TNF- $\alpha$  are also increased in MPP [10]. With regard to treatment, MPP could be self-limiting. However, clinicians routinely treat this disease with antibiotics. Interestingly, Qingfei Tongluo formula (QTF), a traditional Chinese medicine formula, can be an effective therapeutic approach for clinical treatment of MPP [11]. At molecular levels, we found that a treatment of QTF led to effective inhibition of activation of phosphorylation of c-Jun N-terminal kinase (JNK), extracellular signal-regulated kinase (ERK), and nuclear factor- $\kappa$ B (NF- $\kappa$ B) signaling pathways in the MPP mouse model [12]. Notably, Kukoamine A (KuA) constitutes a major active ingredient in the QTF formula. KuA is

TABLE 1: The primer sequences (forward or F/reverse or R).

Name	Sequences
SOD1	Primer F 5' CAGGGCATCATCAATTTC 3' Primer R 5' AGCCTGCTGTATTATCTC 3'
SOD2	Primer F 5' ACAGGTTATGGTGGATTCAAAG 3' Primer R 5' AAACAATAGCCAGGGAAGTTAG 3'
SOD3	Primer F 5' CCTCCATTTGTACCGAAAC 3' Primer R 5' GAAGATCGTCAGGTCAAAG 3'
NF- $\kappa$ B	Primer F 5' GCACAAGGAGACATGAAACAG 3' Primer R 5' CAGCCGGAAGGCATTATTAAG 3'
GAPDH	Primer F 5' AATCCCATCACCATCTTC 3' Primer R 5' AGGCTGTTGTCATACTC 3'
Hsa-miR-222-3p	Primer F 5' GCGCGAGCTACATCTGGCTA 3' Primer R 5' AGTGCAGGGTCCGAGGTATT 3'
U6	Primer F 5' CTCGCTTCGGCAGCACA 3' Primer R 5' AACGCTTCACGAATTTGCGT 3'

a spermine alkaloid present in traditional Chinese medicine *Cortex Lycii radices* and has various pharmacological properties [13]. However, there are no studies on the role of KuA in MPP.

Through their metabolites, exotoxin and exotoxin-like toxic substances of *M. pneumoniae* can cause remarkable toxin-like effects [14]. *M. pneumoniae* can infiltrate bronchial mucous membranes to release hydrogen peroxide, thereby causing swelling and necrosis of bronchial epithelial cells; consequently, leading to a reduced microvilli movement and deformation of structure for dissemination of lymphocytes and other immune cells [15]. Superoxide dismutase 2 (SOD2) and catalases are antioxidant enzymes and play a crucial role in controlling reactive oxygen species production, and the latter is a natural by-product of oxidative phosphorylation. ROS damages multiple components of the cell and thereby disturbs diverse biological processes, such as cell metabolism, aging, and death [16]. The other prevailing virulence factors influencing the pathogenesis of *M. pneumoniae* also include accumulated hydrogen peroxide within the host cells and deleterious effects by superoxides on host cellular ultrastructure [17]. In addition, *M. pneumoniae*-produced ions can effectively impede activities of SOD and catalases in the host cells. As such, host cells become more susceptible to toxic oxygen, thus leading to mitochondrial enlargement and impaired cilia movement in lung epithelium [18].

An increasing body of evidence supports that noncoding RNAs including microRNAs (miRNAs) play important roles in regulation of varied types of physiological processes including cell differentiation and proliferation and apoptosis [19]. Indeed, Chu and colleagues have recently profiled miRNAs in the peripheral blood of pediatric MPP patients and found that 26 miRNAs were differentially regulated between MPP and normal controls [20]. Their further *in vivo* study revealed that miR-222-3p, an upregulated miRNA in MPP

patients, could be a meaningful indicator for diagnosis and prognosis of MPP [18].

Over the past decades, evidence has begun to accumulate that exosomes can be transported to the target cells, where they are capable of regulating function and physiology. Exosomes are lipid bilayer-enclosed extracellular vesicles that encompass constituents including protein, DNA, and RNA of the cells that generate them, with a size range of 40 to 160 nm in diameter with an endosomal origin [21, 22]. Such discoveries suggest that exosomes circulating in patients' blood may also play a role in regulating the physiology and function of lung cells and tissues in MPP. Indeed, through employing miRNA-sequencing (miRNA-seq) on peripheral blood serum exosomes from pneumoniae patients caused by human adenovirus, Huang et al. found that four miRNAs can distinguish pneumoniae patients from healthy controls, suggesting these miRNAs may contribute to the pathogenesis of this virus-induced pneumonia [23].

In the present study, using human alveolar basal epithelial cells (HABECs) as an *in vitro* model, we focused on characterizing the changes in levels of SOD2 and proinflammatory cytokines including IL-6 and TNF- $\alpha$  in HABECs, in response to exosomes, which were isolated from peripheral blood serum of MPP patients.

## 2. Materials and Methods

**2.1. Medicine Information.** Kukoamine A (KuA) was purchased from the company (75288-96-9, MedChemExpress (MCE), New Jersey, USA) and dissolved in DMSO.

**2.2. Cell Culture.** The human type-II alveolar epithelial (A549) cells were obtained from American Type Culture Collection (ATCC) and cultured in DMEM medium (Hyclone, SH30243.01; Logan, UT, USA) added with 10% fetal bovine serum (FBS; GIBCO, 16000-044; Carlsbad, CA,



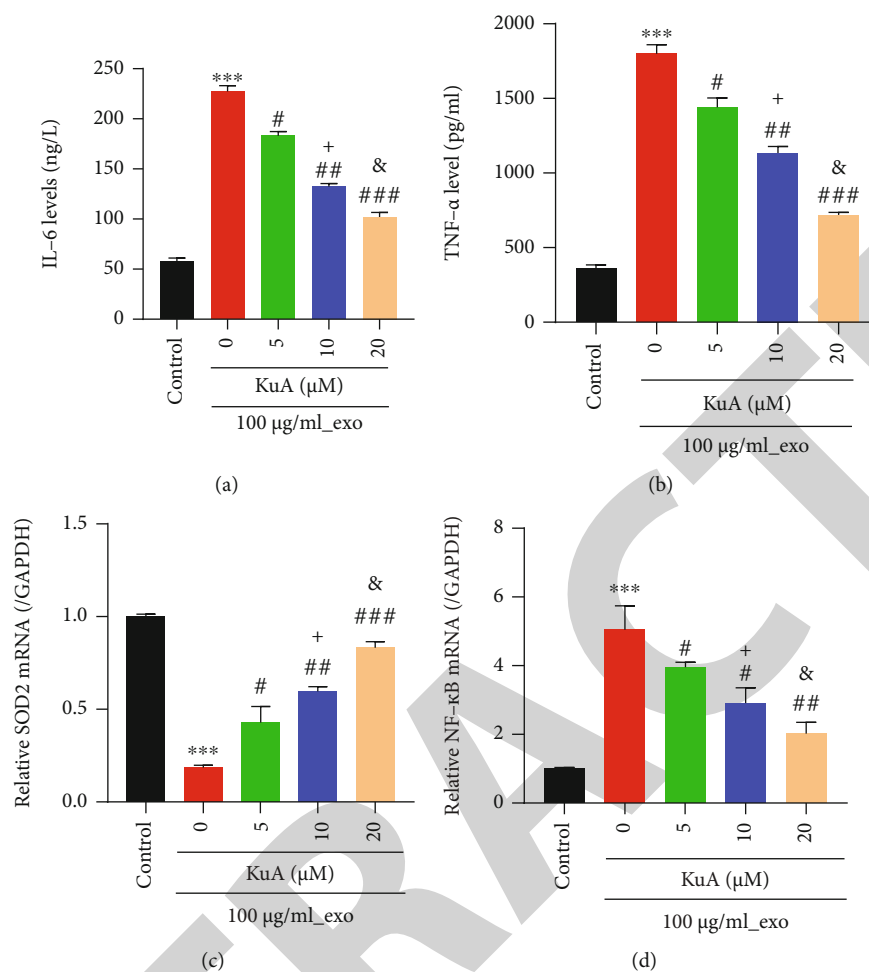


FIGURE 1: Serum exosomes of MPP patients induce inflammation in human alveolar basal epithelial cells A549. MPP serum exosomes (100 μg/mL) were treated with A549 cells, followed by 24 h of treatment with KuA at different concentrations (0, 5, 10, and 20 μM) as indicated. (a, b) ELISA assay for assessment expression of IL-6 (a) and TNF-α (b) in the cell supernatant. (c, d) RT-qPCR was used for assaying the mRNA expression levels of SOD2 (c) and NF-κB (d) (3 repeats in each treatment group). \*\*\*  $P < 0.001$  vs. control (A549 cells without treatment); #  $P < 0.05$ , ##  $P < 0.01$ , ###  $P < 0.001$  vs. 100 μg/ml\_exo + 0 μM\_KuA; +  $P < 0.05$  vs. 100 μg/ml\_exo + 5 μM\_KuA; &  $P < 0.05$  vs. 100 μg/ml\_exo + 10 μM\_KuA.

USA) and 1% penicillin-streptomycin (Solarbio, P1400, Beijing, China) and incubated in an incubator at 37°C with 5% CO<sub>2</sub>.

**2.3. Plasmid Construction and Cell Transfection.** The open reading frame sequences of SOD2 (NM\_000636.4) were amplified with primers harboring Hind III/EcoR I restriction sites and ligated into pCDNA3.1 (+) to overexpress SOD2: SOD2-F: 5'-CCCAAGCTTATGTTGAGCCGGGCAGTG-3' (Hind III) SOD2-R: 5'-CGGAATTCTTACTTTTTC AAGCCATGTATC-3' (EcoR I).

**2.4. Cell Transfection.** When in the logarithmic growth phase, A549 cell transfection was performed as recently described [24]. Briefly, A549 cells were trypsinized and counted to  $1 \times 10^6$  cells/ml suspension, and then, 2 ml of suspension was inoculated into 6-well plates for overnight culture at 37°C in a 5% CO<sub>2</sub> incubator. When grown to 60-70% confluency, the cells were transfected with WT + NC, WT + inhibitor,

WT + mimic, Mut + NC, Mut + inhibitor, Mut + mimic, or control, vector, and oeSOD2 by Lipo2000 (11668-019, Invitrogen). After 24 hours of transfection, serum-free transfer solution was instead of complete medium to culture for 48 hours. The sequences of miR-222-3p mimics and miR-222-3p inhibitor are 5'-AGCUACAUCUGGCUACUGGGU-3' and 5'-ACCCAGUAGCCAGAUGUAGCU-3', respectively. Non-specific sequences are 5'-CAGUACUUUUGUGUAGUAC AA-3'. miR-222-3p mimics and inhibitor were obtained from GenePharma (Shanghai, China).

**2.5. Clinical Specimens.** Patients' blood was prepared to collect exosomes as recently described [25]. All serum specimens (MPP patients:  $n = 10$ ; healthy:  $n = 10$ ) were stored at -80°C and further used for exosomes isolation. The protocol for the present study was approved by the Ethics Committee of Longhua Hospital Affiliated to Shanghai University of Traditional Chinese Medicine (Shanghai, China), and it

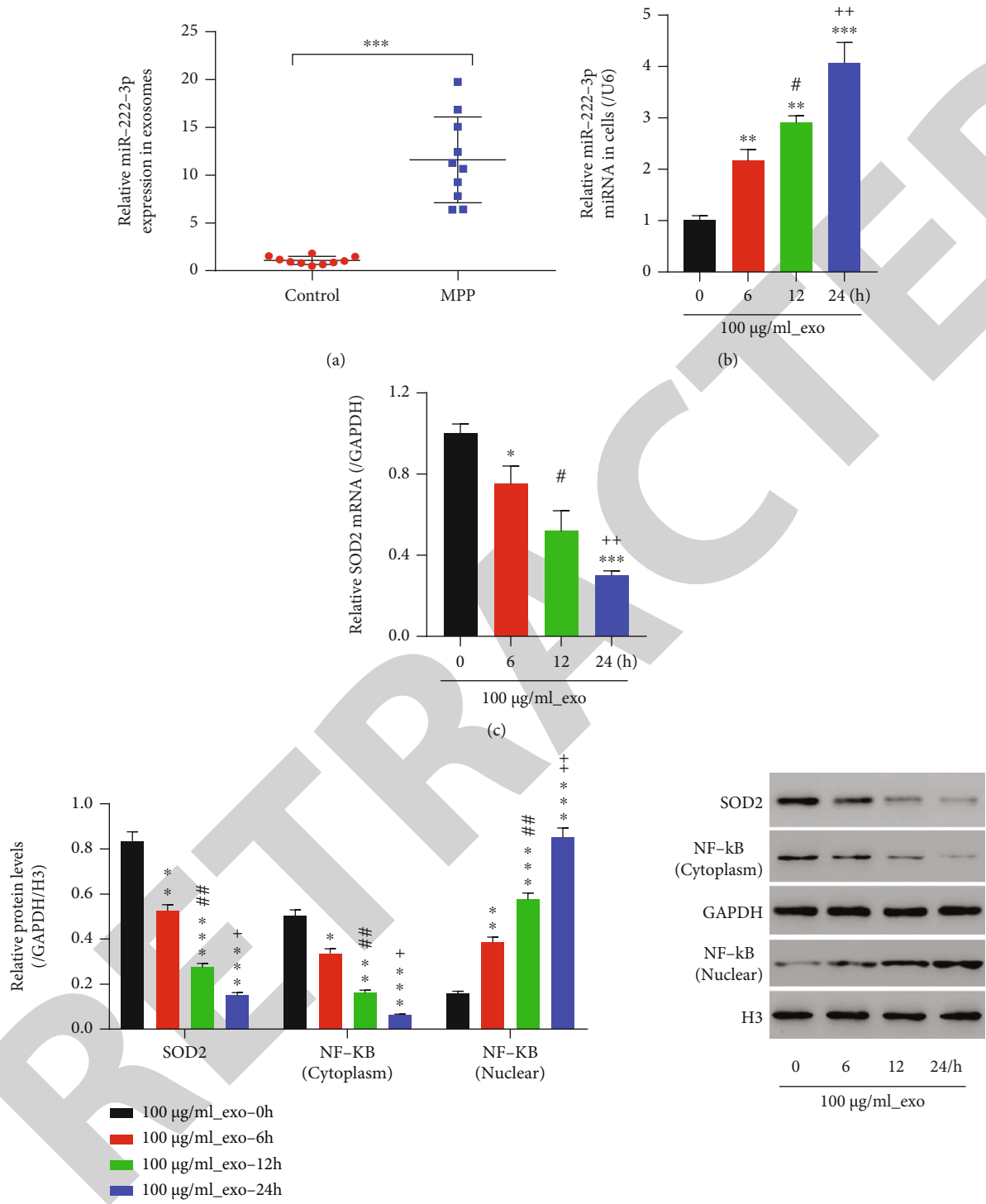


FIGURE 2: Continued.

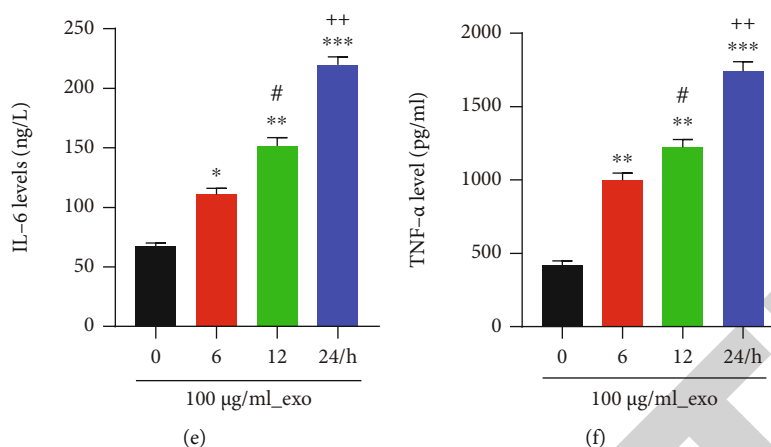


FIGURE 2: miR-222-3p is highly expressed in exosomes and induces inflammation in human alveolar basal epithelial cells. (a) Exosomes extracted from serum samples from MPP patients and normal healthy controls, and then RT-qPCR was used for detecting the expression levels of miR-222-3p ( $n = 10$ ;  $*** P < 0.001$  vs. control). (b)–(f) A549 cells were treated with MPP serum exosomes ( $100 \mu\text{g}/\text{mL}$ ) for 6, 12, and 24 h. (b, c) RT-qPCR was used to detect the mRNA expression levels of miR-222-3p (b) and SOD2 (c). (d) Western blot was used to detect the protein expression levels of SOD2 and NF- $\kappa$ B. (e, f) at 6, 12, and 24 h, the expression of IL-6 (e) and TNF- $\alpha$  (f) in the cell supernatant was detected by ELISA.  $*P < 0.05$ ,  $**P < 0.01$ ,  $***P < 0.001$  vs. 0 h;  $\#P < 0.05$ ,  $\#\#P < 0.01$  vs. 6 h;  $^+P < 0.05$ ,  $^{++}P < 0.01$  vs. 12 h.

conforms to the provisions of the Declaration of Helsinki in 1995. All participants have provided their written informed consent to participate in the study.

**2.6. Isolation and Identification of Serum Exosomes.** This procedure was performed as recently described [25]. Briefly, serum exosomes were individually extracted from the healthy ( $n = 10$ ) and patients ( $n = 10$ ) with MPP with  $10,000 \times g$  for 30 min at  $4^\circ\text{C}$ . Supernatants were then transferred to 5 mL ultrahigh speed centrifugal tubes (supplemented with  $1 \times \text{PBS}$ ) and centrifuged twice at  $17,000 g$  for another 2 h at  $4^\circ\text{C}$ , after which the supernatants were removed. The supernatants were then centrifuged again under the same conditions. The pellets were resuspended in the corresponding  $1 \times \text{PBS}$ , filtered with a  $0.22 \mu\text{m}$  filter, and then the exosomes were quantified using a BCA protein quantification kit, and then aliquoted and stored at  $-80^\circ\text{C}$  for further analysis. Serum exosomes were identified by Western blot with the use of antibodies of anti-CD9 (Ab92726), anti-CD63 (Ab271286), and anti-CD81 (Ab109201) supplied from Abcam (Cambridge, England).

**2.7. Fluorescent Labeling of Exosomes.** Serum exosomes were labeled with PKH-67 Exosomes Green Fluorescent Dye (Umibio, USA) as recently described [24]. In brief, preparation of PKH67 dyeing working solution: at room temperature, the “PKH67 linker” was mixed with “Diluent C” at a ratio of 1:9 in the dark. Exosomes staining: exosomes were stained at room temperature by PKH67 for 4 h in the dark and visualized under a fluorescent microscope (Nikon, Japan).

**2.8. Real Time-Quantitative PCR (RT-qPCR).** RT-qPCR was used to measure mRNA levels as previously described [26]. RNA samples were isolated using TRIZOL reagent and then reverse transcribed to cDNA using the RevertAid First

Strand cDNA Synthesis Kit (Fermentas, Hanover, MD, USA), followed by amplified with the SYBR Green qPCR Master Mixes (#K0223, Thermo Fisher, Rockford, IL, USA) according to the manufacturers’ instructions. The relative mRNA levels were estimated using the  $2^{-\Delta\Delta\text{Ct}}$  method after normalized to GAPDH. The primer sequences (forward or F/reverse or R) were listed in Table 1.

**2.9. Western Blot Analysis.** Western blot assay was performed as recently described [26]. The lysates were separated by electrophoresis. Interest proteins were transferred to polyvinylidene fluoride (PVDF) membrane and blocked with 5% nonfat milk. Then, the bands were incubated with optimally diluted primary antibodies and HRP-labeled (antimouse and antirabbit) second antibodies sequentially. Protein expression was assessed with a chemiluminescent imaging system (Tanon 5200, Shanghai, China). Anti-CD9 (Ab92726, 1:1000), anti-CD63 (Ab271286, 1:2000), anti-CD81 (Ab109201, 1:700), and anti-SOD2 (Ab13534, 1:2000) from Abcam (Cambridge, England), and anti-NF- $\kappa$ B (#8242, 1:1000), anti-H3 (#4499, 1:1000), and anti-GAPDH (#5174, 1:2000) from CST (Boston, USA) served as primary antibodies.

**2.10. ELISA Assay.** The levels of IL-6 and TNF- $\alpha$  in supernatants were determined using an ELISA kit (X-Y Biotechnology, Shanghai, China) according to the manufacturer’s instructions.

**2.11. Luciferase Reporter Assays.** All plasmids were constructed as recently detailed [24]. The sequence of SOD2 (NM\_000636.4) promoter was amplified by PCR and placed into a pGL3-enhancer plasmid containing the firefly luciferase gene. SOD2 3’-UTR was inserted into pGL3-promoter vector to construct pGL3-promoter-wtSOD2. According to hsa-miR-222-3p and SOD2 3’-UTR binding site, the site-directed mutation SOD2 3’-UTR was inserted into pGL3-

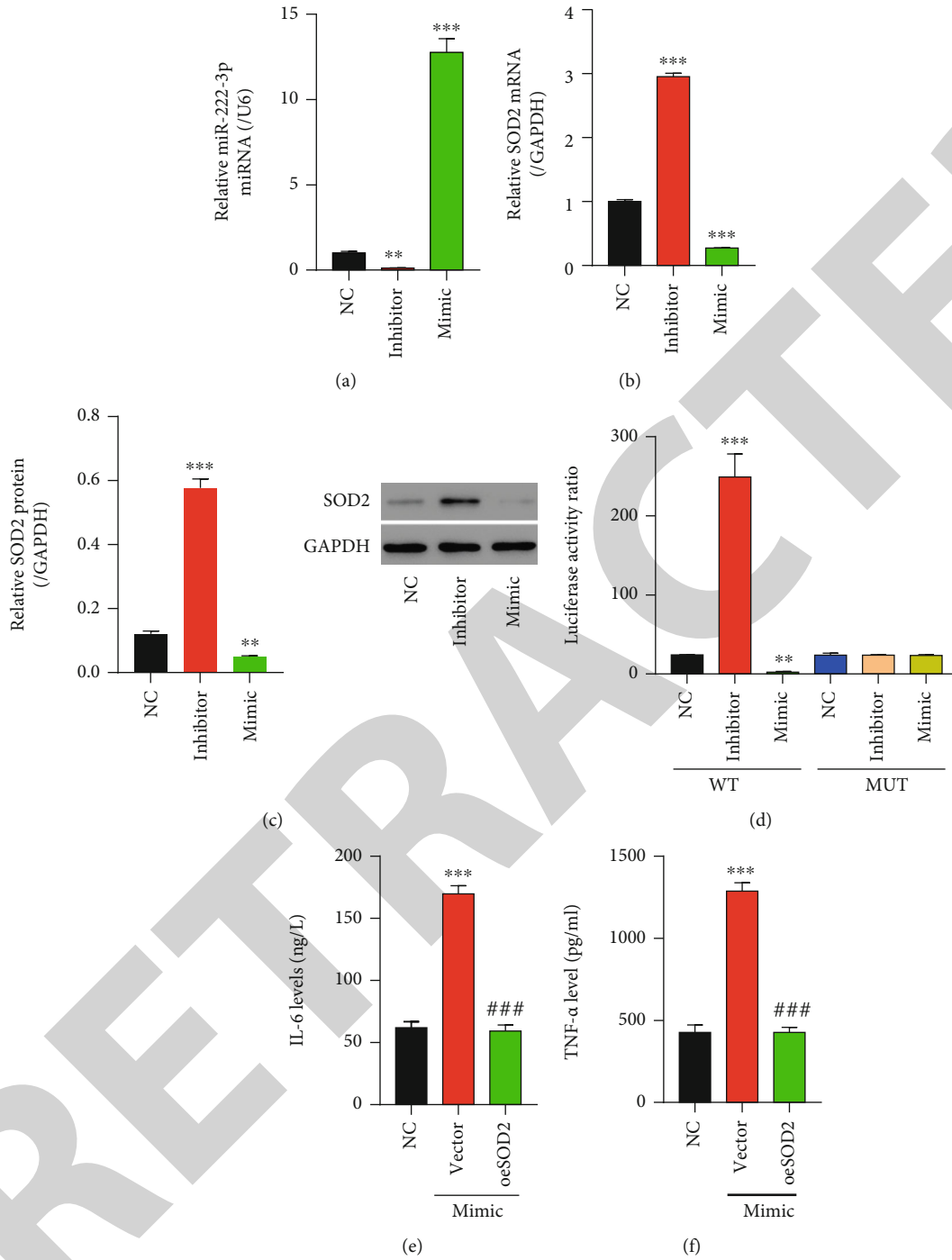


FIGURE 3: Continued.

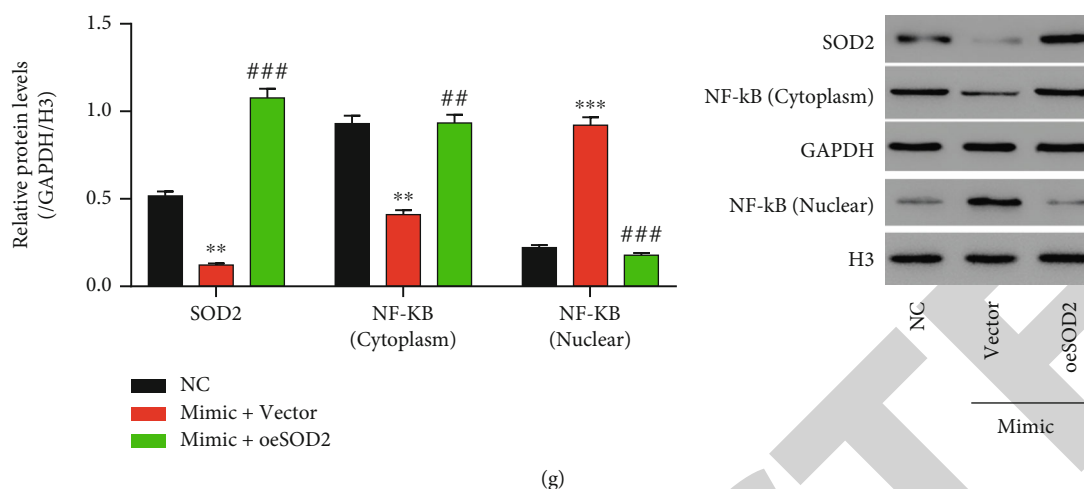


FIGURE 3: Mechanisms of miR-222-3p repression of SOD2 transcription in human alveolar basal epithelial cells. (a)–(c) miR-222-3p inhibitors or mimics were transfected into A549 cells. (a) The miRNA expression of miR-222-3p was detected by RT-qPCR. \*\* $P < 0.01$ , \*\*\*  $P < 0.001$  vs. NC (negative control of mimics or inhibitors). (b, c) The mRNA (b) and protein (c) expression of the endogenous expression of SOD2 in A549 cells was detected by RT-qPCR. \*\* $P < 0.01$ , \*\*\*  $P < 0.001$  vs. NC. (d) Assay of luciferase activities in A549 cells transfected with wild-type (WT) or mutant (Mut) constructs along with miR-222-3p mimics or inhibitors as indicated. \*\* $P < 0.01$ , \*\*\*  $P < 0.001$  vs. WT + NC. (e)–(g) miR-222-3p mimics and SOD2 overexpression vectors were concomitantly or individually transfected into cells A549 cells. (e, f) ELISA for detecting the expression levels of IL-6 (e) and TNF- $\alpha$  (f) in the cell supernatant. (g) The protein expression of SOD2 and NF- $\kappa$ B was detected by western blot. \*\* $P < 0.01$ , \*\*\*  $P < 0.001$  vs. NC; ##  $P < 0.01$ , ###  $P < 0.001$  vs. mimic + vector.

promoter vector to construct pGL3-promoter-mutSOD2. Cultured cells were cotransfected directly with the pGL3-promoter-wtSOD2 and the pRL-TK-Renilla reporter, or pGL3-promoter-mutSOD2 and the pRL-TK-Renilla reporter. After 6 h of transfection, cells were divided to treat with WT + NC, WT + inhibitor, WT + mimic, Mut + NC, Mut + inhibitor, and Mut + mimic. After 24 h, the dual-luciferase assay was conducted with Dual-Promoter Luciferase Assay Kit (Promega, USA).

**2.12. Statistical Analysis.** GraphPad Prism 7.0 software (San Diego, CA, USA) was used for statistical analysis. Each experiment was repeated at a minimum of three times. Data was shown in mean  $\pm$  standard deviation (SD). One-way analysis of variance (ANOVA) was applied to analyze the differences of multiple groups.  $P < 0.05$  was statistically significant.

### 3. Results

**3.1. Serum Exosomes of MPP Patients Induce Inflammation in A549 Human Alveolar Basal Epithelial Cells.** To study the role of serum exosomes from MPP patients, exosomes were isolated from the serum of healthy controls (normal control-exo) and MPP patients (MPP patients-exo) using ultrahigh-speed centrifugation. The purity was validated by transmission electron microscope (Supplementary Figure 1A) and characterized by the measurement of exosomes surface markers CD9, CD63, and CD81 (Supplementary Figure 1B). PKH-67 staining revealed that exosomes were endocytosed by A549 cells (Supplementary Figure 1C). All these results suggested that exosomes were successfully isolated and ready for further analysis.

Next, the effects of isolated serum exosomes on proinflammatory cytokines including IL-6 and TNF- $\alpha$  have been analysed. As shown in Figures 1(a) and 1(b), treatment of A549 cells with MPP patients' serum exosomes led to a significant increase of levels of IL-6 and TNF- $\alpha$  in supernatant, which was remarkably reversed by the addition of KuA in a dose-dependent manner. KuA possesses potent antihypertensive, antioxidant, and anti-inflammatory effects [27]. In our recent study, we also found that KuA constitutes a major active ingredient in QTF formula that has remarkably ameliorative effects on MPP in a mouse model [12].

Furthermore, Figures 1(c) and 1(d) showed that MPP exosomal treatment significantly inhibited SOD2 mRNA levels and resulted in increased expression of NF- $\kappa$ B, while such a trend of decreased expression of SOD2 and increased level of NF- $\kappa$ B can be reversed by KuA in a dose-dependent manner.

Taken together, these results suggest that MPP patients' serum exosomes can potentially induce inflammation in human alveolar basal epithelial cells, and SOD2/NF- $\kappa$ B pathway may be involved in this process.

**3.2. miR-222-3p Is Highly Expressed in Exosomes and Induces Inflammation in Human Alveolar Basal Epithelial Cells.** A previous study has shown that miR-222-3p was increased in MPP patients' serum [20]. Here, we hypothesized that such an increase in serum was attributed to the increased abundance of exosomes in serum, which was actually confirmed by RT-qPCR assay (Figure 2(a)).

In order to investigate the effects of miR-222-3p on levels of proinflammatory cytokines in A549 cells, first, we treated A549 cells with MPP serum exosomes as shown in Figure 2(b). The results suggested that the miR-222-3p level



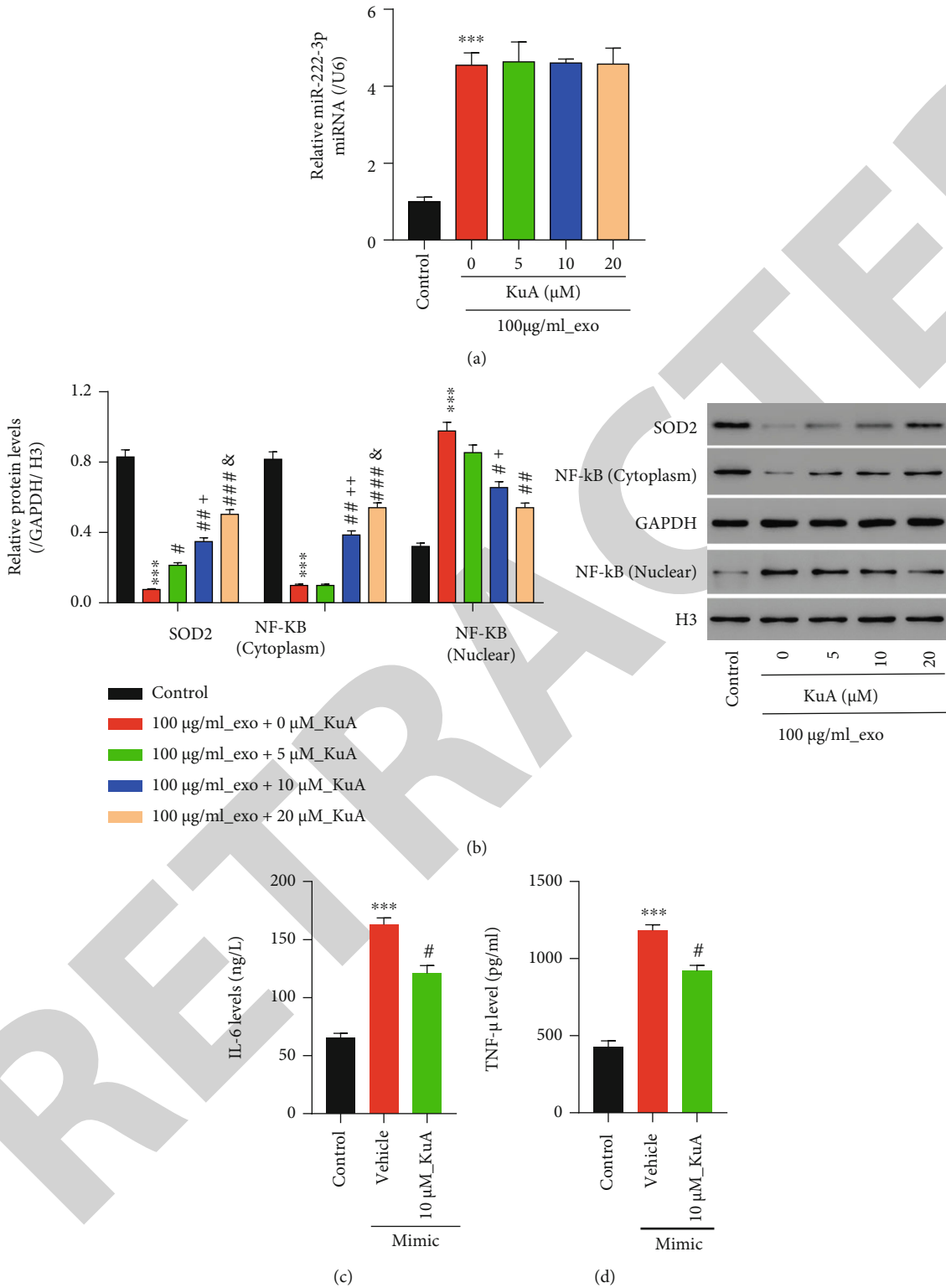


FIGURE 4: Continued.

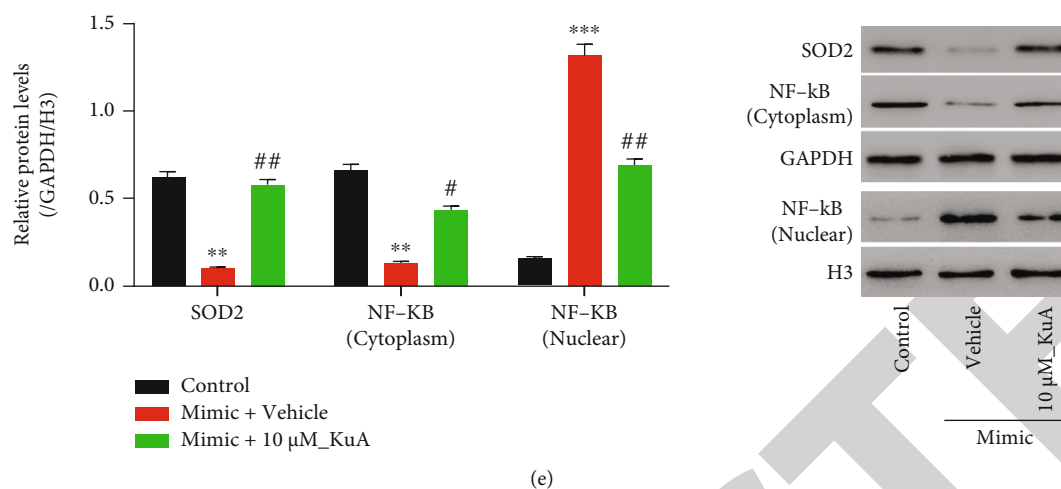


FIGURE 4: KuA attenuates miR-222-3p mimic-induced inflammation by targeting SOD2. (a, b) A549 cells were treated with MPP serum exosomes (100  $\mu$ g/mL), followed by 24 h treatment of KuA at different concentrations (0, 5, 10, and 20  $\mu$ M) of as indicated. (a) The mRNA expression of miR-222-3p was detected by RT-qPCR. (b) The protein expression of SOD2 and NF- $\kappa$ B (cytoplasm and nuclear) was detected by western blot. \*\*\*  $P < 0.001$  vs. control (A549 cells without treatment); #  $P < 0.05$ , ##  $P < 0.01$ , ###  $P < 0.001$  vs. 100 g/mL\_exo + 0  $\mu$ M\_KuA; +  $P < 0.05$ , ++  $P < 0.01$  vs. 100 g/mL\_exo + 5  $\mu$ M\_KuA; &  $P < 0.05$  vs. 100 g/mL\_exo + 10  $\mu$ M\_KuA. (c)–(e) A549 cells were treated with miR-222-3p mimics, followed by treatment of KuA at 10  $\mu$ M for 24 h. (c, d) ELISA to identify the levels of IL-6 (c) and TNF- $\alpha$  (d) in the cell supernatant. (e) The protein levels of SOD2 and NF- $\kappa$ B (cytoplasm and nuclear) were examined by western blot. \*\*  $P < 0.01$ , \*\*\*  $P < 0.001$  vs. control; #  $P < 0.05$ , ##  $P < 0.01$  vs. mimic + vehicle.

in A549 cells was augmented along with an increased incubation time with exosomes, while the parallel extracellular miR-222-3p levels at the corresponding incubation time points were significantly decreased (Supplementary Figure 2A), and there is no significant change in miR-222-3p level by A549 cells during the incubation (Supplementary Figure 2B). These findings suggest that A549 cells were highly capable of taking these serum exosomes. In Figures 2(c) and 2(d), SOD2 levels were reduced at both mRNA and protein levels along with extended exosomal exposure, which was coupled with increased nuclear NF- $\kappa$ B activity in A549 cells (Figure 2(d)). In addition, IL-6 and TNF- $\alpha$  were also increased during exosomal exposure in a time-dependent manner (Figures 2(e) and 2(f)). Statistical test showed that the SOD2 level was negatively correlated with miR-222-3p level, whereas IL-6 and TNF- $\alpha$  levels were positively correlated with miR-222-3p level (Supplementary Figure 2C-2D).

Taken together, these data suggest that miR-222-3p may play an important role in serum exosomes from MPP patients, which can be delivered into A549 cells, triggering inflammation.

**3.3. Mechanisms of miR-222-3p Repression of SOD2 Transcription in Human Alveolar Basal Epithelial Cells.** Here, the molecular mechanisms underlying miR-222-3p-induced inhibition of SOD2 activity in A549 cells were further dissected. MicroRNA usually modulate gene expression through interaction with the 3'-UTR of the mRNA. And then 3'-UTR of wild-type (WT) and mutant SOD2 mRNA into luciferase reporter plasmid were constructed to test the effects of miR-222-3p on SOD2 expression. Figures 3(a)–3(c) revealed that transfection of miR-222-3p

mimics caused a significant increase of miR-222-3p expression but significantly reduced endogenous mRNA and protein levels of SOD2, while miR-222-3p inhibitors had opposite effects. Furthermore, Figure 3(d) showed that miR-222-3p mimics significantly inhibited the activities of the SOD2 3' UTR. Next, a eukaryotic expression vector, allowing an ectopic expression of SOD2, was constructed, and the overexpression efficiency was detected (Supplementary Figure 3A-3B). Consistent with the above mentioned results, miR-222-3p mimics increased IL-6 and TNF- $\alpha$  levels. However, such effects were reversed by overexpressed SOD2 (Figures 3(e) and 3(f)). In addition, miR-222-3p-mediated elevation of nuclear NF- $\kappa$ B activity was also reversed by an ectopic expression of SOD2 (Figure 3(g)). These findings further support that miR-222-3p promotes inflammation in A549 by inhibiting SOD2 activity.

**3.4. KuA Attenuates miR-222-3p Mimic-Induced Inflammation by Targeting SOD2.** We found that treatment of KuA did not alter miR-222-3p levels in A549 cells treated with MPP serum exosomes (Figure 4(a)). However, KuA was able to efficiently reverse MPP serum exosomes-mediated inhibition of SOD2 and increased nuclear NF- $\kappa$ B activity in A549 cells (Figure 4(b)). Furthermore, treatment of KuA partly reversed miR-222-3p mimics increased IL-6 (Figure 4(c)) and TNF- $\alpha$  (Figure 4(d)) levels, as well as decreased SOD2 expression and elevation of nuclear NF- $\kappa$ B activity (Figure 4(e)). Combined with the results showing that KuA had no discernable effects on levels of SOD1 and SOD3 in A549 cells (Supplementary Figure 4A-4B), it can be inferred that KuA partly attenuates miR-222-3p mimic-induced inflammation in A549 cells, which probably by targeting SOD2.

## 4. Discussion

*M. pneumoniae* represents a leading cause of community-acquired pneumonia and causes excessive inflammation that significantly exacerbates the severity of this disease. However, the mechanism and pathophysiology of such excessive inflammation are poorly understood. In this study, we found that MPP patients had a significantly increased expression of miR-222-3p in their peripheral blood serum exosomes as compared to the healthy counterparts.

Our investigation has found that upregulation of miR-222-3p in MMP has potential to decrease the activity of SOD2 and increase the expression of NF- $\kappa$ B followed by upregulation of proinflammatory cytokines such as IL-6 and TNF- $\alpha$  in human alveolar basal epithelial cells and A549 cells and resulted in induction ROS generation. On the other hand, dose-dependent treatment of KuA partly reversed miR-222-3p mimic effects by inducing increased expression of proinflammatory cytokines, as well as elevation of nuclear NF- $\kappa$ B activity. Our findings go hand in hand with a recent study showing that KuA-containing QTF formula alleviated MPP in mice [12, 28]. Studies have found that KuA protects against MDA-induced neurotoxicity by the induction of oxidative stress [29, 30]. Thus, it can be inferred that KuA alleviated MPP probably through regulating oxidative stress. This study provides a novel molecular route linking peripheral blood serum exosomes and induction of inflammation and oxidative stress in lung tissues of MPP patients.

Here, we first reported that miR-222-3p negatively regulates SOD2 but positively regulates proinflammatory cytokines in human alveolar basal epithelial cells A549. A number of studies on the functions of miR-222-3p in regulating gene expression in immune cells, such as macrophages, have mainly focused on its role in cancer [31, 32]. Recent studies by Lodge et al. suggest that miR-222-3p plays a role in the induction of viral infection through targeting CD4, a surface molecule on macrophages that actively participates in a variety of proinflammatory responses [33, 34]. Interestingly, few studies have suggested that MPP patients had a significantly increased abundance of miR-222-3p but a reduced level of CD4 mRNA in their peripheral blood monocytes [20]. Our study presented that MPP patients' serum exosomes can efficiently deliver miR-222-3p into human alveolar basal epithelial cells and thus suppress the SOD2 activity. Our study offers significant insights into the identification of novel targets through miR-222-3p in human alveolar basal epithelial cells and provides a novel mechanism involved in the pathogenesis of MPP.

This study highlights an important role of serum exosomes in the induction of inflammation and pathogenesis of MPP. Effective communication between various types of cells can be exemplified through exosomes. Indeed, the existence and possible role of extracellular vesicles in bacterial and viral infection have been well documented [35]. Exosomes released in response to stress conditions can be obviously distinguished by their contents including RNA and protein in comparison with those liberated from normal cells [36, 37]. The quality and amount of such extracellular

vesicles also change with the physiological conditions of cells that release them. Furthermore, the release of extracellular vesicles can be prominently triggered by various stress factors, including bacterial infections. In consistent with these observations, our study supports that an increased secretion of exosomes and their contents in peripheral blood in response to *M. pneumoniae* infection can remarkably modulate the functions of effectors gene involved in the induction of inflammation, thus further contributing to a complicated pathophysiological condition in human lung tissues. The cellular origin of these miR-222-3p-containing exosomes is unknown in this study, but could be a subject for future research.

In conclusion, this study supports a critical role of serum exosomal miR-222-3p in dysregulation of SOD2 activity and proinflammatory cytokines in human alveolar basal epithelial cells. Thus, blocking exosomes access to these cells could represent a promising strategy for the treatment of MPP.

## Abbreviation

MPP:	Mycoplasma pneumoniae pneumonia
HABECs:	Human alveolar basal epithelial cells
SOD2:	Superoxide dismutase 2
KuA:	Kukoamine A
QTF:	Qingfei Tongluo formula
JNK:	c-Jun N-terminal kinase
ERK:	Extracellular signal-regulated kinase
NF- $\kappa$ B:	Nuclear factor- $\kappa$ B.

## Data Availability

The data that support the findings of this study are available from the corresponding author upon reasonable request.

## Conflicts of Interest

The authors declare that they have no competing interests.

## Authors' Contributions

Zhi-Yan Jiang did the conceptualization, methodology, and software. Xiu-Xiu Liu and Ming-Jing Wang did the data curation and writing—original draft preparation. Qian-Na Kan and Cui Li did the visualization and investigation. Yong-Hong Jiang did the supervision. Wen Li did the software and validation. Xiao Li and Zhen Xiao did the writing—reviewing and editing. All authors read and approved the final manuscript and agree to be accountable for all aspects of the research in ensuring that the accuracy or integrity of any part of the work is appropriately investigated and resolved. Xiu-Xiu Liu and Ming-Jing Wang contributed equally to this work.

## Acknowledgments

This research is funded by National Natural Science Foundation of China (81804144 and 81674024).

## Supplementary Materials

Figure 1: clinical serum samples from children infected with *Mycoplasma pneumoniae* and normal healthy controls were collected. Then, serum exosomes were extracted by ultra-high speed centrifugation. (a) Transmission electron microscope analysis of contents and purity of exosomes. (b) Western blot to assess the abundances of exosomal markers CD81, CD63, and CD9. (c) Exosomes extracted from serum samples of MPP patients and normal healthy controls were incubated with A549 cells ( $2 \times 10^5$  cells) for 4 h in the dark, and then uptake of PKH-67-labeled exosomes by A549 cells was performed. Figure 2: expression level of miR-222-3p in control and MMP patients has been detected. (a) A549 cells were treated with MPP serum exosomes (100  $\mu\text{g}/\text{mL}$ ) for 6, 12, and 24 h, the parallel extracellular miR-222-3p levels were detected by RT-qPCR. (b) A549 cells were treated with MPP serum exosomes (100  $\mu\text{g}/\text{mL}$ ) and RNA scavenger, then, RNA expression levels of miR-222-3p were detected by RT-qPCR. (c)–(e) The correlations between the miR-222-3p expression and expression levels of SOD2 (c), IL-6 (d), and TNF- $\alpha$  (e) in the exosomes extracted from serum samples from MPP patients ( $n = 10$ ). Figure 3: SOD2 overexpression plasmid vectors were transfected into A549 cells. RT-qPCR (a) and Western blot (b) were used to discern SOD2 overexpression efficiency.  $**P < 0.01$ ,  $***P < 0.001$  vs. vector group. Figure 4: expression level MMPP serum exosomes after coinubation with A549 cell line have been detected followed by in control and MMP patients have been detected KuA treatment. (a, b) RT-qPCR was used to detect the abundances of SOD1 and SOD3.  $**P < 0.01$ , control group.  $^{\#}P < 0.05$  vs. 0 group. (Supplementary Materials)

## References

- [1] C. Yan, H. Sun, and H. Zhao, "Latest surveillance data on *Mycoplasma pneumoniae* infections in children, suggesting a new epidemic occurring in Beijing," *Journal of Clinical Microbiology*, vol. 54, no. 5, pp. 1400–1401, 2016.
- [2] A. Ferwerda, H. A. Moll, and R. de Groot, "Respiratory tract infections by *Mycoplasma pneumoniae* in children: a review of diagnostic and therapeutic measures," *European Journal of Pediatrics*, vol. 160, no. 8, pp. 483–491, 2001.
- [3] S. Kashyap and M. Sarkar, "Mycoplasma pneumonia: clinical features and management," *Lung India*, vol. 27, no. 2, pp. 75–85, 2010.
- [4] A. Becker, T. R. Kannan, A. B. Taylor et al., "Structure of CARDS toxin, a unique ADP-ribosylating and vacuolating cytotoxin from *Mycoplasma pneumoniae*," *Proceedings of the National Academy of Sciences of the United States of America*, vol. 112, no. 16, pp. 5165–5170, 2015.
- [5] J. Hu, C. Chen, G. Ou et al., "Nrf2 regulates the inflammatory response, including heme oxygenase-1 induction, by *Mycoplasma pneumoniae* lipid-associated membrane proteins in THP-1 cells," *Pathogens and Disease*, vol. 75, no. 4, 2017.
- [6] S. R. Somarajan, T. R. Kannan, and J. B. Baseman, "Mycoplasma pneumoniae Mpn133 is a cytotoxic nuclease with a glutamic acid-, lysine- and serine-rich region essential for binding and internalization but not enzymatic activity," *Cellular Microbiology*, vol. 12, no. 12, pp. 1821–1831, 2010.
- [7] L. Guo, F. Liu, M. P. Lu, Q. Zheng, and Z. M. Chen, "Increased T cell activation in BALF from children with *Mycoplasma pneumoniae* pneumonia," *Pediatric Pulmonology*, vol. 50, no. 8, pp. 814–819, 2015.
- [8] S. Kurata, T. Osaki, H. Yonezawa, K. Arae, H. Taguchi, and S. Kamiya, "Role of IL-17A and IL-10 in the antigen induced inflammation model by *Mycoplasma pneumoniae*," *BMC Microbiology*, vol. 14, no. 1, p. 156, 2014.
- [9] J. Wen, H. Wang, T. Dong et al., "STAT3-induced upregulation of lncRNA ABHD11-AS1 promotes tumour progression in papillary thyroid carcinoma by regulating miR-1301-3p/STAT3 axis and PI3K/AKT signalling pathway," *Cell Proliferation*, vol. 52, no. 2, article e12569, 2019.
- [10] Z. R. Chen, G. B. Zhang, Y. Q. Wang et al., "Soluble B7-H3 elevations in hospitalized children with *Mycoplasma pneumoniae* pneumonia," *Diagnostic Microbiology and Infectious Disease*, vol. 77, no. 4, pp. 362–366, 2013.
- [11] Z. Y. Jiang, Z. Xiao, Y. H. Jiang, and X. X. Liu, "Effect of Qingfei Tongluo decoction on TCM syndrome score and serum inflammatory factors in children with *Mycoplasma pneumoniae* pneumonia," *World Science and Technology-Modernization of Traditional Chinese Medicine*, vol. 21, no. 4, pp. 623–628, 2019.
- [12] Y. H. Jiang, J. E. Yu, A. H. Guo et al., "Ameliorative effects of Qingfei Tongluo formula on experimental Mycoplasmal pneumonia in mice," *Journal of Natural Medicines*, vol. 70, no. 2, pp. 145–151, 2016.
- [13] G. Li, F. Zhou, Y. Chen, W. Zhang, and N. Wang, "Kukoamine A attenuates insulin resistance and fatty liver through down-regulation of Srebp-1c," *Biomedicine & Pharmacotherapy*, vol. 89, pp. 536–543, 2017.
- [14] A. J. McDermott, B. M. Taylor, and K. M. Bernstein, "Toxic epidermal necrolysis from suspected *Mycoplasma pneumoniae* infection," *Military Medicine*, vol. 178, no. 9, pp. e1048–e1050, 2013.
- [15] S. Grosshennig, S. R. Schmidl, G. Schmeisky, J. Busse, and J. Stulke, "Implication of glycerol and phospholipid transporters in *Mycoplasma pneumoniae* growth and virulence," *Infection and Immunity*, vol. 81, no. 3, pp. 896–904, 2013.
- [16] L. Han, H. Wang, L. Li et al., "Melatonin protects against maternal obesity-associated oxidative stress and meiotic defects in oocytes via the SIRT3-SOD2-dependent pathway," *Journal of Pineal Research*, vol. 63, no. 3, 2017.
- [17] S. Maenpuen, P. Watthaisong, P. Supon et al., "Kinetic mechanism of l- $\alpha$ -glycerophosphate oxidase from *Mycoplasma pneumoniae*," *The FEBS Journal*, vol. 282, no. 16, pp. 3043–3059, 2015.
- [18] C. Kariya, H. W. Chu, J. Huang, H. Leitner, R. J. Martin, and B. J. Day, "Mycoplasma pneumoniae infection and environmental tobacco smoke inhibit lung glutathione adaptive responses and increase oxidative stress," *Infection and Immunity*, vol. 76, no. 10, pp. 4455–4462, 2008.
- [19] V. S. Patil, R. Zhou, and T. M. Rana, "Gene regulation by non-coding RNAs," *Critical Reviews in Biochemistry and Molecular Biology*, vol. 49, no. 1, pp. 16–32, 2014.
- [20] C. Chu, X. Lei, Y. Li et al., "High expression of miR-222-3p in children with *Mycoplasma pneumoniae* pneumonia," *Italian Journal of Pediatrics*, vol. 45, no. 1, p. 163, 2019.
- [21] Y. Zhang, Y. Liu, H. Liu, and W. H. Tang, "Exosomes: biogenesis, biologic function and clinical potential," *Cell & Bioscience*, vol. 9, no. 1, p. 19, 2019.



## Retraction

# Retracted: Automatic Segmentation of Calcification Areas in Digital Breast Images

### BioMed Research International

Received 10 October 2023; Accepted 10 October 2023; Published 11 October 2023

Copyright © 2023 BioMed Research International. This is an open access article distributed under the Creative Commons Attribution License, which permits unrestricted use, distribution, and reproduction in any medium, provided the original work is properly cited.

This article has been retracted by Hindawi following an investigation undertaken by the publisher [1]. This investigation has uncovered evidence of one or more of the following indicators of systematic manipulation of the publication process:

- (1) Discrepancies in scope
- (2) Discrepancies in the description of the research reported
- (3) Discrepancies between the availability of data and the research described
- (4) Inappropriate citations
- (5) Incoherent, meaningless and/or irrelevant content included in the article
- (6) Peer-review manipulation

The presence of these indicators undermines our confidence in the integrity of the article's content and we cannot, therefore, vouch for its reliability. Please note that this notice is intended solely to alert readers that the content of this article is unreliable. We have not investigated whether authors were aware of or involved in the systematic manipulation of the publication process.

In addition, our investigation has also shown that one or more of the following human-subject reporting requirements has not been met in this article: ethical approval by an Institutional Review Board (IRB) committee or equivalent, patient/participant consent to participate, and/or agreement to publish patient/participant details (where relevant).

Wiley and Hindawi regrets that the usual quality checks did not identify these issues before publication and have since put additional measures in place to safeguard research integrity.

We wish to credit our own Research Integrity and Research Publishing teams and anonymous and named external researchers and research integrity experts for contributing to this investigation.

The corresponding author, as the representative of all authors, has been given the opportunity to register their agreement or disagreement to this retraction. We have kept a record of any response received.

### References

- [1] A. A. Abdulrazzaq, Y. Muhammed, A. T. Al-Douri, A. A. H. Mohamad, and A. M. Ibrahim, "Automatic Segmentation of Calcification Areas in Digital Breast Images," *BioMed Research International*, vol. 2022, Article ID 2525433, 7 pages, 2022.



## Research Article

# Automatic Segmentation of Calcification Areas in Digital Breast Images

**Ammar Akram Abdulrazzaq,<sup>1</sup> Yasser Muhammed,<sup>2</sup> Asaad T. Al-Douri,<sup>3</sup>  
A. A. Hamad Mohamad,<sup>4,5</sup> and Abdelrahman Mohamed Ibrahim<sup>6</sup>**

<sup>1</sup>Department of Medical Laboratory Technologies, Al-Maarif University College, Iraq

<sup>2</sup>College of Technical Engineering, Al-Farahidi University, Baghdad, Iraq

<sup>3</sup>Department of Dental Industry, College of Medical Technology, Al-Kitab University, Iraq

<sup>4</sup>Department of Medical Laboratory Techniques, Dijlah University College, Baghdad 10021, Iraq

<sup>5</sup>The University of Mashreq, Research Center, Baghdad, Iraq

<sup>6</sup>Accounting and Financial Management, School of Management Studies, University of Khartoum, Sudan

Correspondence should be addressed to Abdelrahman Mohamed Ibrahim; [amibrahim@uofk.edu](mailto:amibrahim@uofk.edu)

Received 24 April 2022; Revised 3 May 2022; Accepted 18 May 2022; Published 3 June 2022

Academic Editor: Dinesh Rokaya

Copyright © 2022 Ammar Akram Abdulrazzaq et al. This is an open access article distributed under the Creative Commons Attribution License, which permits unrestricted use, distribution, and reproduction in any medium, provided the original work is properly cited.

In this study, the authors hope to demonstrate that when mammography is combined with intelligent segmentation techniques, it can become more effective in diagnosing breast abnormalities and aiding in the early detection of breast cancer. In conjunction with intelligent segmentation techniques, mammography can be made more effective in diagnosing breast abnormalities and aiding in the early diagnosis of breast cancer, hence increasing its overall effectiveness. The methodology, which includes some concepts of digital imaging and machine learning techniques, will be described in the following section after a review of the literature on breast cancer (categories, prevention involving the environment and lifestyle, diagnosis, and tracking of the disease) has been completed (neural networks and random forests). It was possible to achieve these results by working with an image collection that previously had questionable regions (per the given technique). Fiji software extracted problematic candidate regions from mammography images, which were subsequently subjected to further examination. To categorize the results of the picture segmentation, they were sorted into three groups, which were as follows: random forest and neural networks both generated promising results in the segmentation of suspicious parts that were emphasized in the highlight of the image, and this was true for both algorithms. Detection of contours of the regions was carried out, indicating that cuts of these segmented sections may be created. Later on, automatic categorization of the targets can be carried out using a learning algorithm, as illustrated in the experiment.

## 1. Introduction

In Arab countries, the large number of women dying from breast cancer makes the disease a significant public health problem, both because of the commotion of morbidity and mortality, as well as the high personal and social cost related to the disease and its treatment, and even more because of the harmful physical and psychological sequel in patients [1]. It is a tumour that originates from breast cells that grow disorderly. 60% to 70% of this type of cancer appears in the

form of an “irregular or spheroid” nodule, with speculated, indistinct or microlobulated margins, without calcifications. Close to 20% of cases are nodules with calcifications. Calcifications without an associated nodule constitute just under 20% of all cases [2].

Breast cancer is quite frightening because of its high frequency and the physical (either by total mastectomy or segmental resection – the scar left behind is essential) and psychological (low self-esteem, reduced sexuality, and stigma) that generally harm patients. It is one of the diseases

that most cause mortifications and disorders in a wide dimension: it affects the patient, close family members, and caregivers [3].

The most significant risk of this disease is the late diagnosis of the tumour, which can be avoided with digital technologies advancing at an ever-increasing pace to support the early diagnosis of the disease. Mammography, for example, is a test used to diagnose breast abnormalities; it is used in programs for screening women; it reduces the mortality rate due to breast cancer by more than 40% [4], obviously if the diagnosis is still in the preclinical stage, that is, in the early stage of the evolution of malignant tumours.

Because breast cancer is the second with the highest incidence globally and its prevention and mainly treatment are costly for the country's public health, thresholding is a more uncomplicated implementation technique for image processing and computational speed. They are applied very frequently in the image segmentation scenario. It is also called binarization because the technique is based "on partitioning the histogram of the image to convert all pixels [picture element] whose grey tone is greater than or equal to a certain threshold value  $T$  into white and the others in blacks" [5].

That said, the question arises: among the many real possibilities of breast cancer prevention, what would be the relevance of the threshold in this effort? The search for answers to this question makes it possible to achieve the objective of this research, which is to discuss the advantages and limits of the threshold technique applied to mammography in the search for areas suspected of malignant neoplastic, facilitating the interpretation of the findings by the physician and, therefore, way, helping the early diagnosis of breast cancer.

*1.1. Literature Review.* Although there is no defined etiology, breast cancer is studied as multifactorial so that certain interacting risk factors determine the disease. Farhadhosseini-nabadi, et al. (2020) [6] discuss the two categories of risk factors:

- (1) Modifiable: subject to modifications, interventions, and controls, such as "obesity, high-carbohydrate eating habits, exaggerated consumption of red meat and fats, high intake of alcoholic beverages, the performance of combined hormone replacement therapy for more than five years and excessive radiation exposure" [6]. It is read in Vieira that "overweight is considered a risk factor for the development of the disease and this can be explained by the high estrogen levels resulting from peripheral conversion in adipose tissue"
- (2) Nonmodifiable: they do not change. They are inherent to the patient, such as gender (higher incidence in females), age (predominance in those over 50 years of age), race, and ethnicity (more frequent among non-Hispanic whites and blacks). Furthermore, the reproductive and hormonal status of women, with early menarche and late menopause one of the most associated, with family history, association when first-degree relatives (mother, sister,

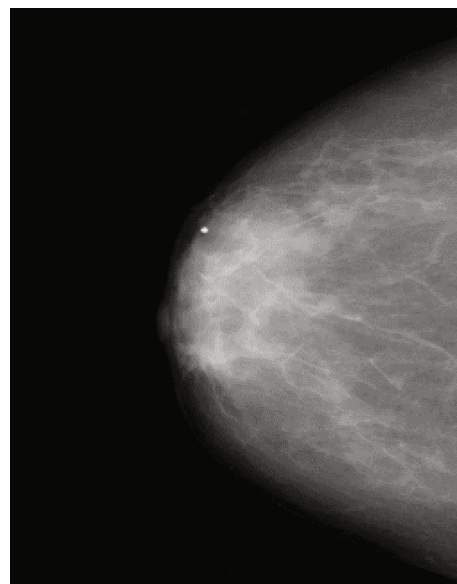


FIGURE 1: Mammography digital image.

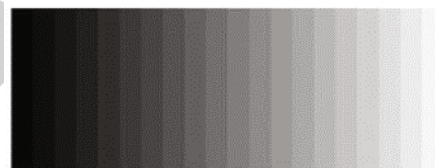


FIGURE 2: Monochrome image grayscale.

daughter, father, brother, and son) developed breast cancer. Mutation in the BRCA1 and BRCA2 genes [7], families carrying these mutations have strong indications for the disease and also the presence of previous breast pathology, women with previous breast cancer have a 1.5x increased risk of developing breast cancer again

How to best prevent breast cancer? This is the question that should be part of the questioning of women, mainly because the answers would allow primary prevention of the disease, that is, before the beginning of the pathological process, even avoiding exposure to many modifiable risk factors, such as the environment and lifestyle, for example, thus preserving health and reducing mortality as a result of this disease.

Some habits should be part of every woman's life, namely, practising physical activities, breastfeeding an infant, regularly eating with fruits, vegetables, fish and nuts, and olive oil, and, on the other hand, avoiding the intake of fat and red meat (which is still not very clear), processed foods, and foods with a high glycemic index, reducing the use of sugar [8].

Therefore, they are simple practices to be cultivated, especially when it is confirmed that, in Arab countries, the risk of having breast cancer is 8% throughout life, which means that one woman in twelve is an expressive risk female.

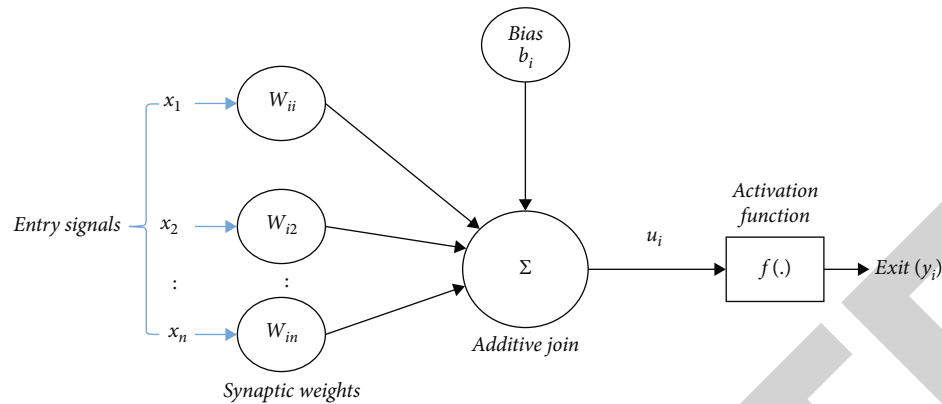


FIGURE 3: Model of an artificial neuron for collection of decision trees.

Because of this, the American Society of Mastology, the American Society of Oncological Surgery, and the American Society of Radiology recommend screening the disease in women from the age of forty undergoing mammography annually [4] to detect any breast abnormalities.

Therefore, the early diagnosis of the preclinical stage, even before the presentation of any symptoms, considerably increases the chances of cure. There is secondary prevention, whose main objective is universal and early screening and the performance of mammography, applied “to large populations, in screening programs, significantly reduces mortality rates from breast cancer (reduction above 40%)” [6].

Secondary prevention was aimed at changing the course of the disease since its biological onset has already occurred through interventions that allow its early detection and timely treatment. For this, there must be clear evidence that the disease in question can be identified at an early stage when it is not yet clinically apparent, allowing a practical therapeutic approach, altering its course or minimizing the risks associated with clinical therapy. Furthermore, the resulting drop in morbidity or mortality must be achieved without the adopted strategy’s significant burden of adverse effects. Early detection of a disease is possible through education for early diagnosis in symptomatic people or screening (screening) in asymptomatic populations [9].

On the other hand, tertiary prevention occurs in a clinical and symptomatic phase of the disease in the face of findings such as a nodule, oedema—a phase in which mammography is no longer a screening to be diagnostic. “It is important to point out that mammography presents false positives and false negatives, an inherent flaw in the method, but it is the best screening method available at the moment” [10].

There are two groups of mammography exams: screening (in asymptomatic patients, primary prevention, which should be performed annually after age forty in the post-menstrual period) and diagnostic (in symptomatic patients suggestive of breast cancer or even those who need to be supplemented with another exam) [9].

Therefore, early diagnosis and treatment of the disease are essential so that the consequences are less harmful, avoiding or reducing mastectomies and the risk of death. Even if diagnosed early, there are great chances of recovery



FIGURE 4: Banalization for binary image.

and even cure. Treatment is usually long, not less than a year. One of the most critical phases is chemotherapy, which, although very effective, its side effects are generally perverse: frequency of nausea, vomiting and mucositis, and somatic changes (alopecia, weight gain, ovarian failure, hormone reduction (testosterone and estrogen causing menopause and vaginal atrophy), various lows, such as libido, vaginal lubrication, anorgasmia, and dyspareunia, affecting sexuality). Inconvenient evaluative judgments emerge for the patient, including the feeling of pity. Even more sinister is the feeling of finitude in the face of the devastating disease [6, 9].

In the face of such nefarious problems, it is never too much to insist on prevention, nor is it too much to insist on good eating and behavioral habits, physical exercise, and a regulated life with sleep patterns, which are basic concepts of public health. We insist that mammography is essential in this prevention, although its sensitivity is approximately 85% and can be reduced to 50% in very dense breasts. In this sense, any alteration identified in the exam must be described according to the Breast Imaging

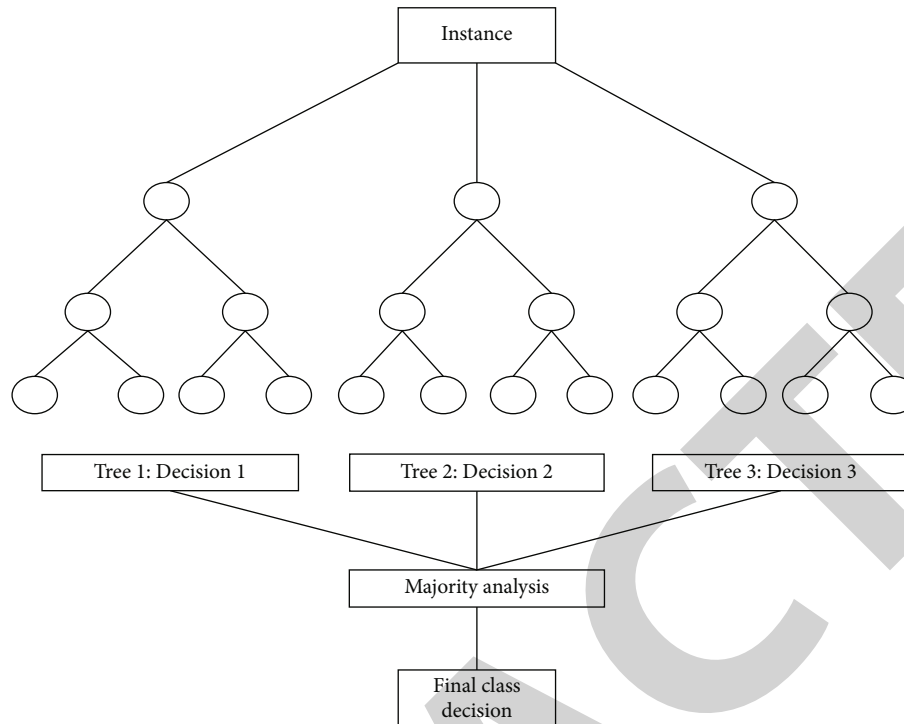


FIGURE 5: Model of a random forest.

Reporting in the Data System (BI-RADS), “a system created to standardize the reports of breast diagnostic exams regarding the terms used, report creation and recommendation of conduct, which facilitates communication between the multidisciplinary team that assists the patient” [9, 10]. Also, images can be improved using the threshold technique.

## 2. Methodology

It was necessary to obtain a previously classified image bank to evaluate the proposed methodology, with suspicious regions already segmented. [11] provided updated and standardized version of the Digital Database for Screening Mammography (DDSM). The CBIS-DDSM (DDSM Cured Breast Images Subset) dataset includes uncompressed images, data selection, and curation by trained mammographers. In this work, the tool used to extract suspicious candidate regions in mammography images was the Fiji software, a free software distribution of the *ImageJ* project. *Fiji* is a software focused on the analysis of biological images. It relies on the combination of powerful software libraries with a wide variety of scripting languages that allow rapid prototyping of image processing algorithms.

**2.1. Digital Image.** Guzman et al., (2013) [12] define an image as a two-dimensional function  $f(x, y)$  of light intensity, where  $x$  and  $y$  denote the spatial coordinates of a point and the value of the function  $f$  (Figure 1) is proportional to the brightness of the image at that point (monochrome image). A digital image is a function  $f(x, y)$  discretized in spatial coordinates and brightness. This function produces luminance and reflectance at each point  $(x, y)$ .

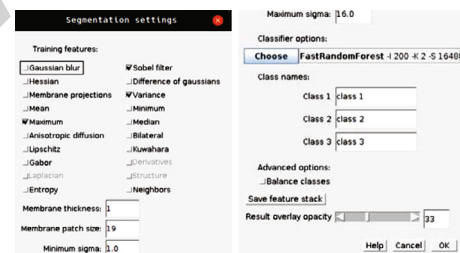


FIGURE 6: Screen of parameters by segmentation with random forest.

**2.2. Monochrome Image.** Figure 2, a monochrome image, contains pixels with only one shade of grey (grayscale). Every scale has a minimum and maximum value. In the case of grayscale (with 8 bits), pixels that approach zero are the darkest pixels, while those that approach the maximum value minus one (L-1) are the lightest pixels [13].

**2.3. Thresholding.** It is a technique that separates the regions of an image when it has two classes (the background and the object). Because thresholding produces a binary image as an output, this process is often called binarization. Like the monochromatic image, a binary image is a two-dimensional matrix with only two values. Sometimes they are called logical images: black corresponds to the value 0 and white corresponds to the value 1 [14].

**2.4. Neural Networks.** Neurophysiologist McCulloch and mathematician Walter Pitts in 1943 modelled simple artificial neural networks using electrical circuits. According to



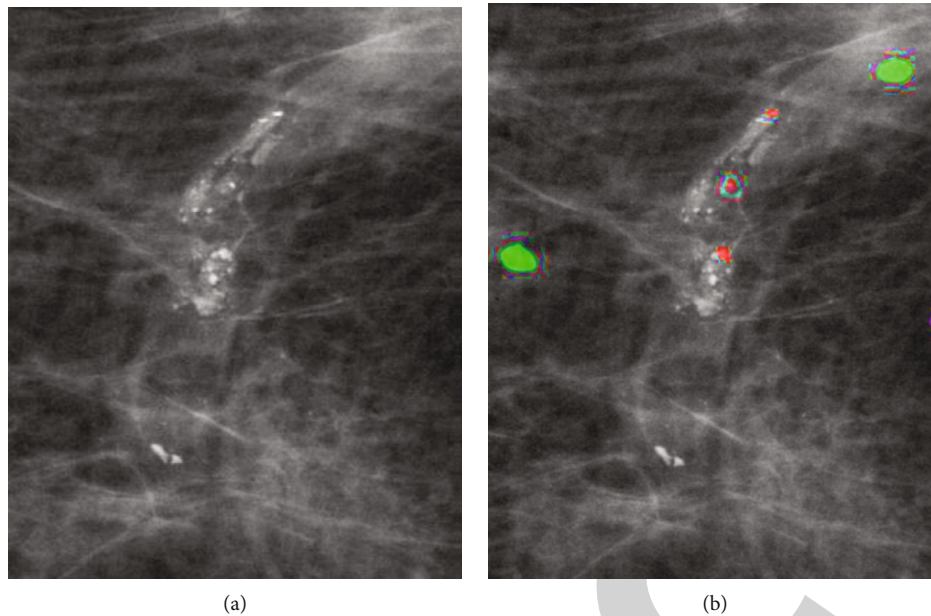


FIGURE 7: (a) Original image. (b) Image with the classes.

McCulloch and Pitts (1943) [15], a neuron can be represented through binary logic (0 or 1). Artificial neural networks emerged from the search to solve problems analogous to the brain (see Figure 3).

**2.5. Random Forest.** Random forest is a classifier that consists of a collection of decision trees. The idea is that if a tree is good, a forest should be even better, as long as there is enough variety within it. The most exciting thing about a random forest is how it creates randomness from a standard dataset.

### 3. Results and Discussion

The segmenting of the candidate suspect regions is based on a feature vector generated for each pixel in the image. In this way, it is possible to obtain a pattern of attributes that can distinguish calcifications. This method uses various image processing filters on the exam image, generating an image of multiple channels. Each image obtained by applying the filters will be used as an attribute for training a machine learning algorithm [16].

As shown in Figures 4 and 5, the machine learning algorithms are provided by the Waikato Environment for Knowledge Analysis (WEKA) data mining and machine learning toolkit [17].

The image filters that best meet the extraction of calcification characteristics in mammographic images were selected through this Fiji plugin. Figure 6 demonstrates the selection of filters and the learning algorithm used in this study.

Three filters were selected, an edge detector, variance, and maximum value. For each applied filter, new images are generated, making changes to the attributes required for each feature extractor filter. Therefore, the plugin applies different settings for each chosen filter.

In addition to the filter definition settings and the learning algorithm, three classes were defined for the image segmentation result.

Figures 7(a) and 7(b) represent the classes in three colors: red is the sample regions of calcification; the green samples represent other regions of the image; and, finally, purple represents the darkest regions to be ignored.

Once the training samples are defined, the feature vectors will be generated; the values of the sample regions will be used as training data for the random forest algorithm. After the training phase, the prediction will occur for each pixel of the image that will be segmented.

The images resulting from the segmentation algorithm can be seen in Figure 8(a): the first represents the three previously defined classes, and the second is the probability map of the candidate suspect regions.

The algorithm applied for image segmentation returns the probability for each image pixel to belong to the first defined class, calcifications; in this way, Figure 8(b) presents lighter tones for a greater possibility of the suspicious region. The probability of each pixel in the image has a value between 0 (zero) and 1 (one), so 1 (one) corresponds to one hundred percent of accuracy.

To evaluate using the same image feature extraction method, segmentation tests were performed using neural networks as a learning algorithm. The image filters to create the vector of features for each image pixel were the same applied to the random forest algorithm, with only the learning technique being different.

The neural network presented an excellent result in this segmentation methodology. Note that the probability map image presents values closer to white, thus less noise from suspicious regions. The segmentation results, shown in Figures 9(a) and 9(b), demonstrate that it can highlight suspicious regions. Through these probability images, it is possible to detect the contours of the regions; in this way, cuts of



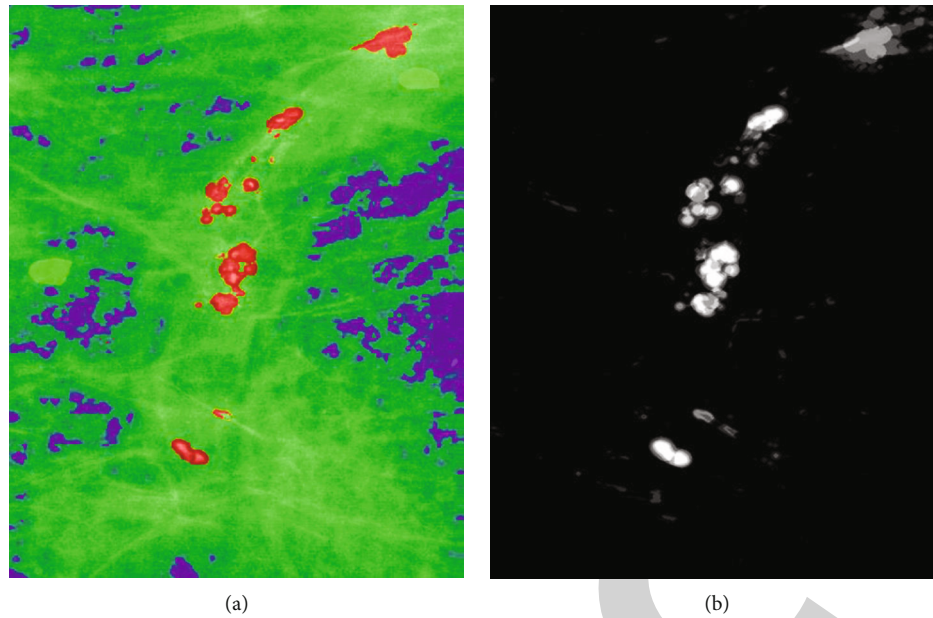


FIGURE 8: (a) Prediction using random forest. (b) Random forest probability map.

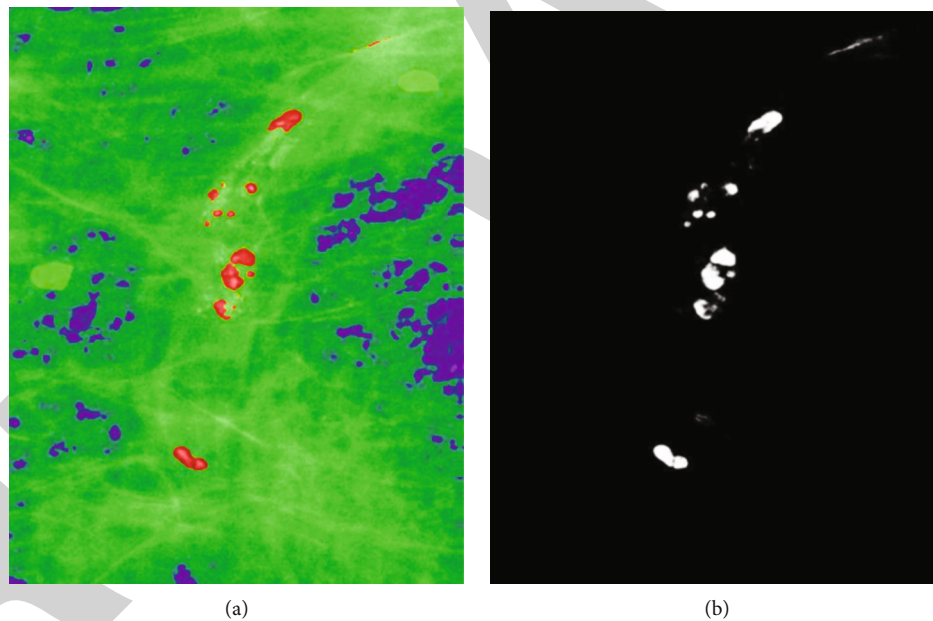


FIGURE 9: (a) Prediction using neural network. (b) Neural network probability map.

these segmented regions can be performed, and, later, an automatic classification of the targets can be performed using a learning algorithm.

#### 4. Conclusions

In this study, the relevance of the intelligent segmentation technique associated with the mammography exam in breast cancer diagnosis was evidenced due to the efficiency of image processing and identification of the suspicious region. In this sense, the research's initial objective was to verify that

this technique facilitates the interpretation of findings by the physician, greatly helping the early diagnosis of breast cancer.

The results were satisfactory in the test of the segmentation methodology, which seeks to solve problems in a similar way to the human brain, which, in the contour of suspicious segmented regions, made possible cuts and, from which, classify the targets, automatically, with support in a learning algorithm.

The random forest algorithm combines several decision criteria to obtain a more accurate prediction, thus allowing

## *Retraction*

# **Retracted: miR-211-5p Alleviates the Myocardial Ischemia Injury Induced by Ischemic Reperfusion Treatment via Targeting FBXW7**

### **BioMed Research International**

Received 12 November 2022; Accepted 12 November 2022; Published 18 January 2023

Copyright © 2023 BioMed Research International. This is an open access article distributed under the Creative Commons Attribution License, which permits unrestricted use, distribution, and reproduction in any medium, provided the original work is properly cited.

*BioMed Research International* has retracted the article titled “miR-211-5p Alleviates the Myocardial Ischemia Injury Induced by Ischemic Reperfusion Treatment via Targeting FBXW7” [1] due to concerns that the peer review process has been compromised.

Following an investigation conducted by the Hindawi Research Integrity team [2], significant concerns were identified with the peer reviewers assigned to this article; the investigation has concluded that the peer review process was compromised. We therefore can no longer trust the peer review process and the article is being retracted with the agreement of the editorial board.

### **References**

- [1] Y. Liu, J. Meng, H. Di, L. Zheng, and Z. Meng, “miR-211-5p Alleviates the Myocardial Ischemia Injury Induced by Ischemic Reperfusion Treatment via Targeting FBXW7,” *BioMed Research International*, vol. 2022, Article ID 5423929, 7 pages, 2022.
- [2] L. Ferguson, “Advancing Research Integrity Collaboratively and with Vigour,” 2022, <https://www.hindawi.com/post/advancing-research-integrity-collaboratively-and-vigour/>.

## Research Article

# miR-211-5p Alleviates the Myocardial Ischemia Injury Induced by Ischemic Reperfusion Treatment via Targeting FBXW7

Yonghui Liu,<sup>1</sup> Jiatian Meng,<sup>2</sup> Hongqin Di,<sup>3</sup> Liheng Zheng,<sup>4</sup> and Zili Meng<sup>1</sup> 

<sup>1</sup>Department of Cardiovascular Surgery, Hebei Chest Hospital, Hebei Lung Cancer Research Center, Shijiazhuang, 050041 Hebei, China

<sup>2</sup>Department of Radiology, Hebei Chest Hospital, Hebei Lung Cancer Research Center, Shijiazhuang, 050041 Hebei, China

<sup>3</sup>Molecular Biology Laboratory, Hebei Chest Hospital, Hebei Lung Cancer Research Center, Shijiazhuang, 050041 Hebei, China

<sup>4</sup>Department of Laboratory, Hebei Chest Hospital, Hebei Lung Cancer Research Center, Shijiazhuang, 050041 Hebei, China

Correspondence should be addressed to Zili Meng; mengzili@hbsxkyy.org.cn

Received 19 April 2022; Revised 6 May 2022; Accepted 14 May 2022; Published 3 June 2022

Academic Editor: Dinesh Rokaya

Copyright © 2022 Yonghui Liu et al. This is an open access article distributed under the Creative Commons Attribution License, which permits unrestricted use, distribution, and reproduction in any medium, provided the original work is properly cited.

Cardiovascular diseases, a class of the most common diseases, seriously threaten human health, which is a direct inducement of death in most countries. The restoration of blood supply is an impactful intervention way for cardiovascular disease treatments while the injury induced by oxygen-glucose deprivation and ischemic reperfusion (I/R) may further impact the tissues of the patients. Myocardial reperfusion is a precondition for saving ischemic myocardial tissues in acute myocardial infarction while the injury induced by immediate reperfusion takes a great challenge for cardiovascular disease treatment. However, the reperfusion of coronary blood could aggravate the injury triggered by ischemia. At present, several studies have focused on the etiopathogenesis and therapeutic strategies of ischemia-reperfusion injury of the myocardium. The report has verified that miR-211-5p was elevated in the pathological specimens, while the influence of miR-211-5p in I/R-mediated injury of myocardial cells remains unclear. This research is aimed at illustrating the role of miR-211-5p in the progression of I/R injury of myocardial cells, and qRT-PCR, western blot, CCK-8, and TUNEL assay were used to investigate the functions of miR-211-5p on I/R-mediated injury of myocardial cells. The result mirrored that miR-211-5p was distinctly reduced in the I/R-induced AC16, and reduced miR-211-5p could evidently improve the viability of I/R-induced AC16. miR-211-5p could directly target FBXW7, and FBXW7 upregulation could reverse the improvement of AC16 in viability and apoptosis level after suffering I/R. Moreover, it was also proved that miR-211-5p can mediate the activation of Wnt/ $\beta$ -catenin via attenuating FBXW7. Consequently, this investigation identified miR-211-5p as a positive role to attenuate the injury of myocardial cells when suffering I/R treatment.

## 1. Introduction

Cardiovascular diseases, a class of the most common diseases, seriously threaten human health, which is a direct inducement of death in most countries [1, 2]. At present, surgery and drug interventions are major strategies for cardiovascular disease, and the restoration of blood supply effectively reduced the damage and the infarct induced by ischemic reperfusion (I/R), thus minimizing the rate of mortality [3, 4]. However, the research has shown that immediate blood supply may cause extra cardiovascular trauma in patients, which can trigger some harmful events such as myocyte apoptosis and even cardiac arrest [5]. Consequently, it remains valuable to delve

the corresponding theory underlying this pathema and to examine the practical values of conceivable strategies that alleviate myocardial I/R injury.

In recent ten years, the roles of noncoding RNA in the progression of diseases have been found, and the regulation of those factors has also been confirmed as effective strategies for treatments of multiple diseases [6]. MicroRNAs (miRNAs) can negatively influence gene abundance by mediating the deterioration of mRNAs, effectively inhibiting protein translation [7, 8]. Several researches have evidenced that miRNA dysfunction is associated with the formation and development of cardiovascular disease, and they are also involved in the progression of the apoptosis and inflammation of myocardial cells

induced by ischemic reperfusion [8, 9]. A previous report has evidenced the reduced miR-211-5p in PC12 cells after I/R treatment [10]. Nevertheless, the role of miR-211-5p in the development of ischemic reperfusion injury remains unclear. Analogously, the investigation also evidenced that miR-211-5p was dramatically reduced in IR-induced human kidney cells. Moreover, miR-211-5p has also been recognized as a protector to keep neonates from heart injury induced by ischemia, suggesting that decreased miR-211-5p may be related to the jury of cardiomyocytes.

This research arranged to investigate the connection of miR-211-5p and the ischemic reperfusion injury of myocardial cells and mirrored the corresponding characteristics of miR-211-5p in the ischemic reperfusion injury of myocardial cells. Moreover, this research determined that miR-211-5p could induce the activation of Wnt pathway while this phenomenon could be abolished by FBXW7 upregulation. It has been found that FBXW7 serves as an inhibitor to suppress the activation of Wnt pathway in lung cancer [11]. Hence, this study sustains that attenuated miR-211-5p can promote the injury and apoptosis of myocardial cells suffering I/R via regulating FBXW7 mediated the inactivation of Wnt pathway [12].

## 2. Material and Methods

**2.1. Cells and Cell Models.** AC16, the human cardiomyocyte cell line (Manassas, VA, USA), was selected for model establishment. DMEM (Gibco, NY, USA) was selected as medium. Besides, 10% fetal bovine serum (FBS) was applied to maintain cell growth. Finally, the cells were cultured in a condition with 5% CO<sub>2</sub> and 37°C. AC16 cells were treated with 94% N<sub>2</sub>, 5% CO<sub>2</sub>, and 1% O<sub>2</sub> for 6, 12, and 24h to establish the ischemic cell models.

**2.2. Cell Transfection.** Six-well plates was applied to cell culture, and the miR-211-5p mimics pcDNA-FBXW7 and the related negative controls (NCs) were transfected added into the related well (cellular confluence: 70%). Briefly, the transfectants and Lipofectamine 2000 were thinned with 250 μl medium, respectively. Subsequently, the thinned transfectants were mixed with Lipofectamine 2000 diluent (1:1). Immediately, the mixtures stood at 25°C for 20 min. Immediately, 500 μl of the incubated transfectants was added in related wells. Finally, the cells were cultured for the subsequent experiments.

**2.3. qRT-PCR.** TRIzol (Sobao Biological Technology Co., Ltd., Shanghai, China) was selected for RNA extraction, and the RNAs were quantified with spectrophotometry. Subsequently, cDNA reverse transcription was executed with the commercial kit (MBL Beijing Biotech Co., Ltd., China). Besides, the primers were provided by RiboBio (Guangzhou, China). After that, the PCR reaction systems were prepared referred to the instruction of the kit (Sigma-Aldrich, Missouri, USA). Besides, the parameters of reactions are as follows: denaturation (95°C, 3 min), amplification (95°C for 12 s and at 53°C for 40 s), and final 70°C for 30 s. Ultimately, the 2<sup>-(ΔΔCt)</sup> method was applied to quantification of miRNAs. The information of the primers is displayed in Table 1.

TABLE 1: The information of the primers.

Genes	Primers
miR-211-5p-F	5'-ATGCCGCAGCAACATCCAGA-3'
miR-211-5p-R	5'-AGGATGCTGCATGCA CTCGAT-3'
FBXW7-F	5'-ATTGGCAATGAGCGGTTC-3'
FBXW7-R	5'-CGTGGG TGCCACAGGACT-3'
U6-F	5'-CTCGCTTCGGCAGCACA-3'
U6-R	5'-AACGCTTCACGAATTTGCGT-3'

**2.4. Western Blot.** RIPA solution was applied to protein extraction at 4°C. The commercial BCA kit (Borif Biotechnology Co., Ltd., Wuhan, China) was applied to the protein quantification. After that, the thermal denaturation of the proteins was executed for 5 min. Protein isolation was performed by SDS-PAGE gels, and then, the wet transfer method was applied to transmembrane. Immediately, the membranes blocking were executed with 5% milk (no fat) for 1 h. After that, the membrane incubation was executed with the first and second antibodies in turn. Finally, a chemiluminescence detection system was applied to quantify the abundances of targets. Antibody information is as follows: anti-FBXW7 (1:1000, ab2533451, ThermoFisher, Massachusetts, USA), anti-Wnt (1:1000, ab11154198, ThermoFisher, Massachusetts, USA), anti-β-catenin (1:1000, ab2533039, ThermoFisher, Massachusetts, USA), and cleaved Caspase-3 (1:1000, ab325431, ThermoFisher, Massachusetts, USA).

**2.5. Dual-Luciferase Reporter Assay.** The mutant 3'-UTR sequences of FBXW7 were designed according to the prediction of the Targetscan database. Subsequently, the mutant types and related wild types were, respectively, linked with the pmirGLO vectors (Yanjiang Bio Co., Ltd., China) and named as FBXW7-mut and FBXW7-wt, respectively. Subsequently, FBXW7-mut or FBXW7-wt were, respectively, cotransfected with miR-211-5p mimics or the related NCs into the cells. Thereafter, the cells were incubated for 48 h. Ultimately, the luciferase activity of the cells was quantified.

**2.6. TUNEL Assay.** The 10% neutral formalin buffer was applied to cell fixation (25°C, 30 min), and then, the mixture of methanol and 0.3% H<sub>2</sub>O<sub>2</sub> was applied to inactivate endogenous peroxidase. The cells were treated with permeabilizing solution (0.1% sodium citrate and 0.1% Triton X-100) at 4°C for 2 min. After that, the cells were treated with the reagent of terminal transferase-mediated biotin dUTP nick end labeling (TUNEL) at 37°C for 1 h. Finally, the Leica fluorescence microscope (Wetzlar, Germany) was applied to investigate cellular apoptosis.

**2.7. CCK-8 Assay.** CCK-8 Kit was provided by Amyjet (Wuhan, China). Firstly, the cells were cultured in 96-well plates (5 × 10<sup>4</sup>/well). Secondly, after transfection and I/R intervention, the cells were treated with CCK-8 reagent (10 μL/well). Immediately, the cells were incubated for 4 h. Ultimately,

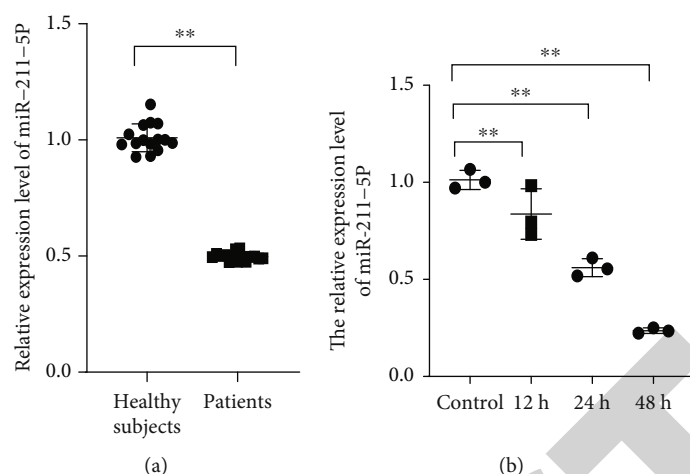


FIGURE 1: miR-211-5p was significantly reduced in I/R-induced AC16. (a) The relative abundance of miR-211-5p in the patients' serums. (b) The relative abundance of miR-211-5p was quantified by qRT-PCR (\*\* $P < 0.01$ ).

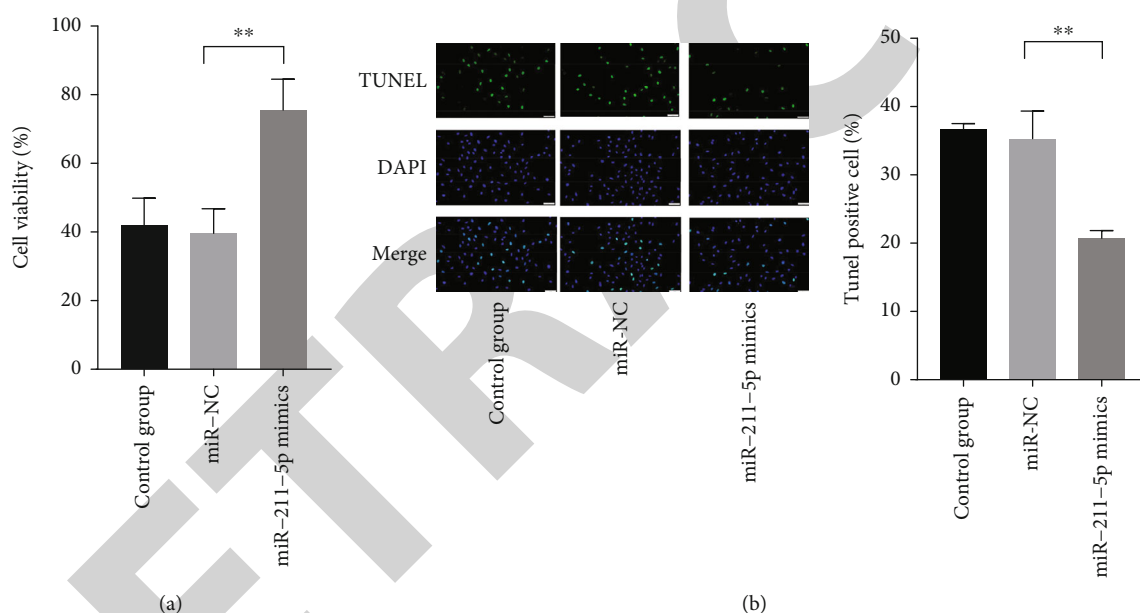


FIGURE 2: miR-211-5p attenuated the apoptosis of I/R-treated AC16. (a) The CCK-8 assay was applied to reveal the influence of miR-211-5p on the viability of I/R-induced AC16. (b) The influence of reduced miR-211-5p on the apoptosis of I/R-induced AC16 was analyzed by TUNEL (\*\* $P < 0.01$ ).

cellular absorbance measurement (450 nm) was executed by a microplate reader (Molecular Devices, Shanghai, China).

**2.8. Statistical Analysis.** All experiments were repeated 3 times. Moreover, SPSS 20.0 and Graphpad Prism 8.0 were applied to data analysis and visualization, respectively. Besides, the difference of the data was tested with Chi-squared test or ANOVA with Tukey's post hoc-test. Moreover,  $P < 0.05$  represented the difference was significant.

### 3. Results

**3.1. Reduced miR-211-5p Was Detected in Patients' Serums.** The abundance of miR-211-5p in patients' serums was quantified to reveal the relationship of miR-211-5p disorder

and ischemic cardiomyopathy. The results mirrored that miR-211-5p was distinctly downregulated in patients' serums (Figure 1(a),  $P < 0.01$ ). Then, AC16 cell models were established with I/R treatment. The results evidenced that the abundance of miR-211-5p was extremely reduced in I/R-treated cells (Figure 1(b),  $P < 0.01$ ).

**3.2. Reduced miR-211-5p Influenced the Phenotype of the Cells when Suffered I/R Treatment.** To delve the miR-211-5p's functions in the development of myocardial inflammation, the miR-211-5p mimics were upregulated in I/R-induced cells, and the phenotype changing of I/R-treated cells was monitored. The CCK-8 reflected that miR-211-5p remarkably improved the viability of the I/R-treated cells. Besides, the



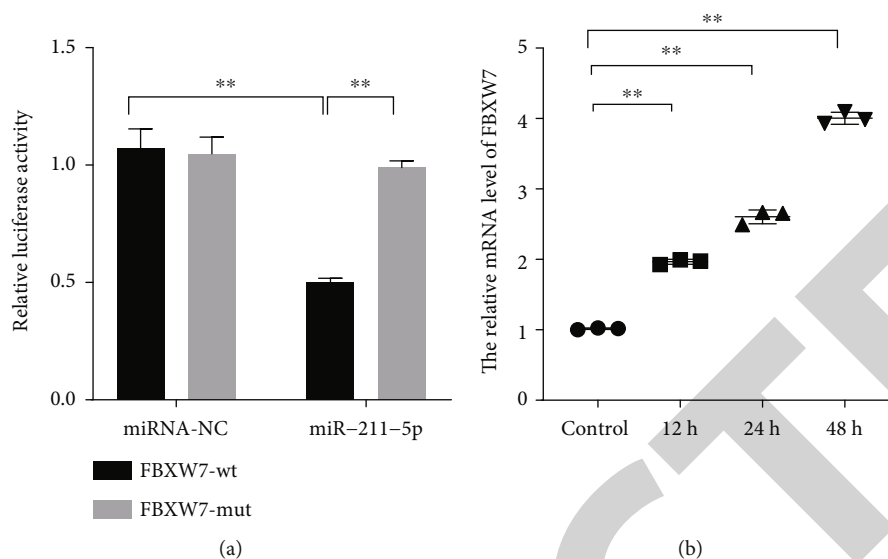


FIGURE 3: miR-211-5p acted as an upregulator of FBXW7, and FBXW7 was extremely elevated in I/R-induced AC16 cells. (a) The interaction of miR-211-5p and FBXW7 was verified by luciferase assay. (b) The quantification of FBXW7 by qRT-PCR (\*\* $P < 0.01$ ).

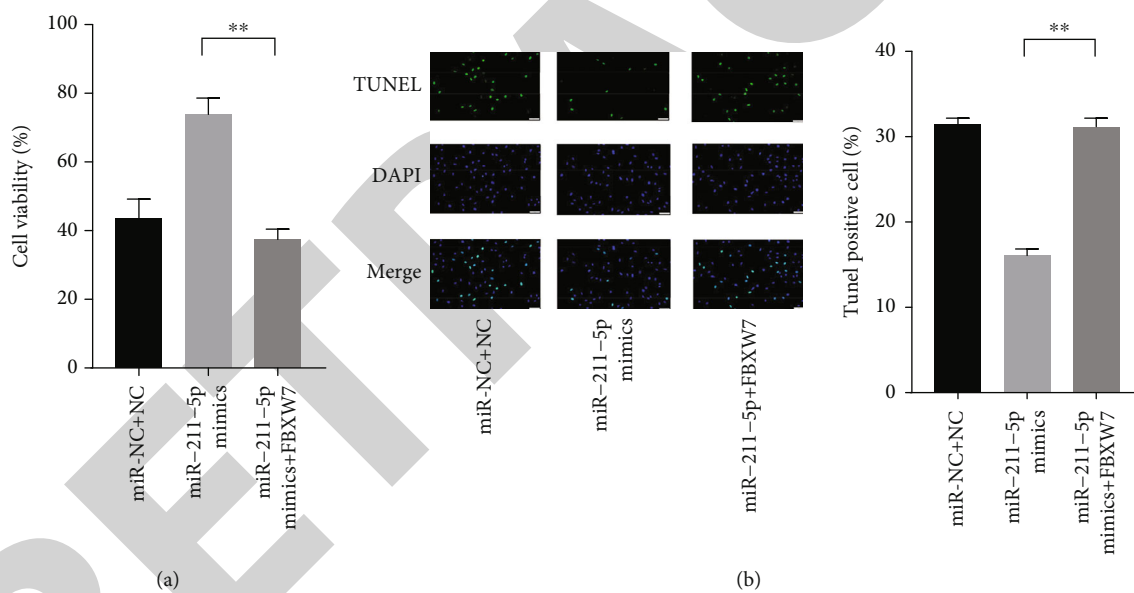


FIGURE 4: FBXW7 upregulation reversed the influence of reduced miR-211-5p in I/R-induced AC16 cells. (a) The viability of I/R-induced AC16 cells. (b) The apoptosis of I/R-induced AC16 (\*\* $P < 0.01$ ).

TUNEL assay proved that miR-211-5p distinctly increased the apoptosis of I/R-treated cells (Figure 2,  $P < 0.01$ ).

**3.3. miR-211-5p Was an Upregulator of FBXW7.** The targets of miR-211-5p were screened through Targetscan. According to Targetscan, FBXW7 was screened as a target of miR-211-5p. Moreover, the luciferase assay was further applied to evidence the connection of miR-193-5p and FBXW7 (Figure 3(a),  $P < 0.01$ ). Besides, the evidence proved that miR-211-5p could effectively affect the 3'-UTR of FBXW7. Besides, the decreased mRNA level of FBXW7 was also detected in I/R-treated cells (Figure 3(b),  $P < 0.01$ ).

**3.4. FBXW7 Abolished the Influences of miR-211-5p in the I/R-Treated Cells.** Although the FBXW7 was proved as a target of miR-211-5p, whether FBXW7 was a pivotal downstream node of miR-211-5p in I/R-induced cells remains unknown. The miR-211-5p and FBXW7 were artificially upregulated in AC16 cells before I/R treatment, and the changes in cellular viability were monitored. Besides, the CCK-8 assay mirrored that reduced FBXW7 extremely inhibited the viability abolished the influence of reduced miR-211-5p on the I/R-treated cells (Figure 4(a),  $P < 0.01$ ). Moreover, the TUNEL assay mirrored that the apoptosis of the cells contra-transfected with FBXW7 and miR-211-5p mimics was remarkably increased (Figure 4(b),  $P < 0.01$ ).

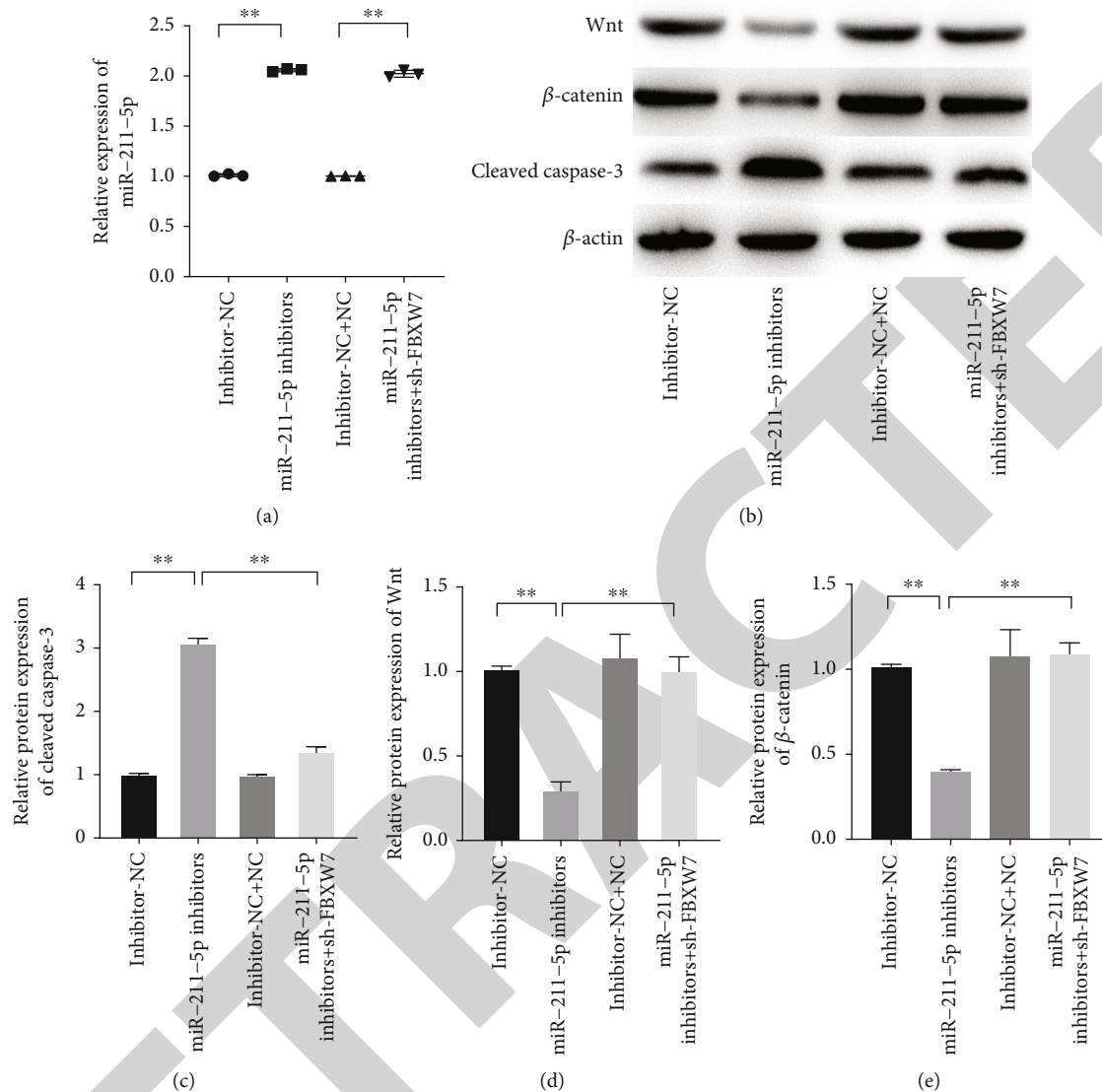


FIGURE 5: Reduced miR-211-5p induced the activation of Wnt pathway through activating the FBXW7. (a) The quantification of miR-211-5p by qRT-PCR. (b–e) The abundances of Wnt,  $\beta$ -catenin, and cleaved Caspase-3 were quantified by western blot (\*\* $P < 0.01$ ).

**3.5. miR-211-5p Was Involved in Wnt Pathway.** For illustrating the related characters of miR-211-5p in the deterioration of myocardial ischemia injury, the abundance of the proteins in Wnt/ $\beta$ -catenin pathway was quantified. The results evidenced that reduced miR-211-5p remarkably attenuated the abundances of Wnt and  $\beta$ -catenin in AC16 cells, which could be abolished by FBXW7 downregulation (Figure 5,  $P < 0.01$ ). Consequently, it suggested that attenuated miR-211-5p influenced the progression of myocardial ischemia injury via targeting FBXW7 mediated the inactivation of Wnt/ $\beta$ -catenin pathway.

#### 4. Discussion

Myocardial reperfusion is a precondition for saving ischemic myocardial tissues in acute myocardial infarction while the injury induced by immediate reperfusion takes a great challenge for cardiovascular disease treatment [4, 13]. Howbeit,

the reperfusion of coronary blood could aggravate the injury triggered by ischemia [14]. At present, several studies have focused on the etiopathogenesis and therapeutic strategies of ischemia-reperfusion injury of myocardium [2]. MicroRNAs (miRNAs) can negatively influence gene abundance via mediating the deterioration of mRNAs, effectively inhibiting protein translation. Several researches have evidenced that miRNA dysfunction is associated with the formation and development of cardiovascular disease, and they are also involved in the progression of the apoptosis and inflammation of myocardial cells induced by ischemic reperfusion. A previous report has evidenced the reduced miR-211-5p in PC12 cells after I/R treatment [10]. Nevertheless, the role of miR-211-5p in the development of ischemic reperfusion injury remains unclear. The study confirmed the connection between miR-211-5p and the injury in myocardial cells induced by ischemic reperfusion, revealed the target of miR-211-5p, and illustrated the related mechanism of miR-

211-5p in the development of the ischemic reperfusion of myocardial cells.

Several reports have indicated that the profiling of the miRNAs in myocardial cells exists visible difference before and after ischemic reperfusion [8]. Shan et al. have proved that the abundance of miR-93 in the myocardial cells induced by I/R treatment was extremely elevated, and miR-93 inhibition could effectively alleviate the injury on myocardial cells induced by oxidative stress and restrain the cellular apoptosis [15]. Analogously, the investigation also evidenced that miR-211-5p was dramatically reduced in IR-induced human kidney cells [16]. Moreover, miR-211-5p has also been recognized as a protector to keep neonates from heart injury induced by ischemia, suggesting that decreased miR-211-5p may be related to the jury of cardiomyocytes [17]. Thus, this report suggests that miR-211-5p can attenuate I/R-induced myocardial injury by targeting the downstream factors. The present evidences in this research reflected that miR-211-5p was an upregulation of FBXW7, and reduced FBXW7 was also observed in the myocardial cell induced by I/R treatment. This study also found that the changes induced by miR-211-5p in the phenotype of I/R-induced HBMECs could be abolished by elevated FBXW7. Besides, Tan et al. have observed that FBXW7 upregulation is related to the aberrant apoptosis of intestinal epithelial cells induced by I/R treatment, and reduced FBXW7 could effectively suppress the abundance of Caspase-3 and Caspase-9 in the IR-induced cells [18]. Therefore, this research sustains that miR-211-5p could attenuate the angiogenesis of HBMECs by reducing FBXW7. In this investigation, it was proved that the abundance of miR-211-5p in myocardial cells was extremely decreased after suffering I/R treatment. Moreover, it was also proved that increased miR-211-5p could significantly attenuate the apoptosis level and improve the viability of I/R-induced AC16 cells, which confirmed that miR-211-5p dysfunction plays a pivotal role in myocardial ischemia injury.

miRNA dysfunction has been proved as key reasons of development of many diseases, and increasing evidences have suggested the regulation of key proteins via impeding the transcription of the mRNAs [19]. Multifactorial regulation has also been proved as an important ability of the miRNA [20]. Besides, the function of miR-211-5p in protecting the brain tissues from I/R injury has been reported by a recent study. Interestingly, the recent report has evidenced the dramatically reduced miR-211-5p in the brains of I/R rat models, and elevated miR-211-5p can availably alleviate the focal cerebral injuries of the rats induced by I/R treatment via targeting COX2 [21].

Several studies have indicated that miRNAs mediated progressions of diseases are related to the changes in activities of multiple pathways [22, 23]. Huang et al. have confirmed that miR-374a-mediated MAPK6 pathway inhibition could effectively protect mouse models away from injury of I/R treatment and reduce the apoptosis of myocardial cells [24]. In this investigation, reduced miR-211-5p was identified to inactivate Wnt pathway. Various researches have confirmed that the inactivation of Wnt pathway plays a key role in the injury and apoptosis process of the myocar-

dial cells. The dysfunction of Wnt pathway has been also evidenced as a key reason of myocardial injury, and the study has found that miR-21/PDCD4 mediated the activation of Wnt pathway could effectively protect myocardial cells away from the damage and apoptosis induced by I/R treatment [25]. Moreover, this research determined that miR-211-5p could induce the activation of Wnt pathway while this phenomenon could be abolished by FBXW7 upregulation. It has been found that FBXW7 serves as an inhibitor to suppress the activation of Wnt pathway in lung cancer [11]. Hence, this study sustains that attenuated miR-211-5p can promote the injury and apoptosis of myocardial cells suffering I/R via regulating FBXW7 mediated the inactivation of Wnt pathway [12].

## 5. Conclusion

This study illustrated the role of miR-211-5p in myocardial ischemia injury triggered by I/R treatment and illustrated the related characters of miR-211-5p in protecting myocardial cells from I/R injury. It is suggested that miR-211-5p can attenuate the myocardial ischemia injury induced by ischemic reperfusion treatment via targeting FBXW7. However, this study still has limitations. The dysfunction of Wnt pathway has been also evidenced as a key reason of myocardial injury, but the mechanism of how it causes cardiomyocyte damage requires further studies to verify.

## Data Availability

The datasets used and/or analyzed during the current study are available from the corresponding author on reasonable request.

## Conflicts of Interest

The authors declare no potential conflicts of interest with the respect to the research, authorship, and/or publication of this article.

## Acknowledgments

This work was supported by grants from the Department of Health of Hebei Province (20150146, 20150148, and 20130129).

## References

- [1] F. B. Tuncer, F. N. Durmus Kocaaslan, A. Yildirim et al., "Ischemic preconditioning and Iloprost reduces ischemia-reperfusion injury in Jejunal flaps: an animal model," *Plastic and Reconstructive Surgery*, vol. 144, no. 1, pp. 124–133, 2019.
- [2] M. Forte, S. Palmerio, F. Bianchi, M. Volpe, and S. Rubattu, "Mitochondrial complex I deficiency and cardiovascular diseases: current evidence and future directions," *Journal of Molecular Medicine*, vol. 97, no. 5, pp. 579–591, 2019.
- [3] S. E. Boag, E. Andreano, and I. Spyridopoulos, "Lymphocyte communication in myocardial ischemia/reperfusion injury," *Antioxidants & Redox Signaling*, vol. 26, no. 12, pp. 660–675, 2017.
- [4] J. Curran, D. Burkhoff, and R. A. Kloner, "Beyond reperfusion: acute ventricular unloading and cardioprotection during

## Retraction

# Retracted: Early Detection of Autism Spectrum Disorders (ASD) with the Help of Data Mining Tools

### BioMed Research International

Received 20 June 2023; Accepted 20 June 2023; Published 21 June 2023

Copyright © 2023 BioMed Research International. This is an open access article distributed under the Creative Commons Attribution License, which permits unrestricted use, distribution, and reproduction in any medium, provided the original work is properly cited.

This article has been retracted by Hindawi following an investigation undertaken by the publisher [1]. This investigation has uncovered evidence of one or more of the following indicators of systematic manipulation of the publication process:

- (1) Discrepancies in scope
- (2) Discrepancies in the description of the research reported
- (3) Discrepancies between the availability of data and the research described
- (4) Inappropriate citations
- (5) Incoherent, meaningless and/or irrelevant content included in the article
- (6) Peer-review manipulation

The presence of these indicators undermines our confidence in the integrity of the article's content and we cannot, therefore, vouch for its reliability. Please note that this notice is intended solely to alert readers that the content of this article is unreliable. We have not investigated whether authors were aware of or involved in the systematic manipulation of the publication process.

Wiley and Hindawi regrets that the usual quality checks did not identify these issues before publication and have since put additional measures in place to safeguard research integrity.

We wish to credit our own Research Integrity and Research Publishing teams and anonymous and named external researchers and research integrity experts for contributing to this investigation.

The corresponding author, as the representative of all authors, has been given the opportunity to register their agreement or disagreement to this retraction. We have kept a record of any response received.

### References

- [1] A. A. Abdulrazzaq, S. S. Hamid, A. T. Al-Douri, A. A. H. Mohamad, and A. M. Ibrahim, "Early Detection of Autism Spectrum Disorders (ASD) with the Help of Data Mining Tools," *BioMed Research International*, vol. 2022, Article ID 1201129, 10 pages, 2022.

## Research Article

# Early Detection of Autism Spectrum Disorders (ASD) with the Help of Data Mining Tools

**Ammar Akram Abdulrazzaq,<sup>1</sup> Sana Sulaiman Hamid,<sup>2</sup> Asaad T. Al-Douri,<sup>3</sup>  
A. A. Hamad Mohamad,<sup>4,5</sup> and Abdelrahman Mohamed Ibrahim<sup>6</sup>**

<sup>1</sup>Department of Medical Laboratory Techniques, Al-Maarif University College, Al-Anbar, Iraq

<sup>2</sup>Al-Farahidi University, Communication Technical Engineering, Baghdad, Iraq

<sup>3</sup>Department of Dental Industry, College of Medical Technology, Al-Kitab University, Iraq

<sup>4</sup>Department of Medical Laboratory Techniques, Dijlah University College, Baghdad 10021, Iraq

<sup>5</sup>The University of Mashreq, Research Center, Baghdad, Iraq

<sup>6</sup>Accounting and Financial Management, School of Management Studies, University of Khartoum, Sudan

Correspondence should be addressed to Abdelrahman Mohamed Ibrahim; [amibrahim@uofk.edu](mailto:amibrahim@uofk.edu)

Received 23 April 2022; Revised 4 May 2022; Accepted 11 May 2022; Published 23 May 2022

Academic Editor: Dinesh Rokaya

Copyright © 2022 Ammar Akram Abdulrazzaq et al. This is an open access article distributed under the Creative Commons Attribution License, which permits unrestricted use, distribution, and reproduction in any medium, provided the original work is properly cited.

Autism is a disorder of neurobiological origin that originates a different course in the development of verbal and nonverbal communication, social interactions, the flexibility of behavior, and interests. The results obtained offer relevant information to reflect on the practices currently used in assessing the development of children and the detection of ASD and suggest the need to strengthen the training of health professionals in aspects such as psychology and developmental disorders. This study, based on genuine and current facts, used data from 292 children with an autism spectrum disorder. The input dataset has 20 characteristics, and the output dataset has one attribute. The output property indicates whether or not a certain person has autism. The research study first and foremost performed data pretreatment activities such as filling in missing data gaps in the data collection, digitizing categorical data, and normalizing. The features were then clustered using *k*-means and *x*-means clustering methods, then artificial neural networks and a linguistic strong neurofuzzy classifier were used to classify them. The outcomes of each strategy were examined, and their respective performances were compared.

## 1. Introduction

Autism spectrum disorders (ASD) are a collection of illnesses characterized by anomalies in the formation and function of neural circuits. Recent epidemiological studies suggest an increase in autism cases [1], for example, 5 cases per 10,000 in 1985, but now 1 case per 100 children and adolescents. It is unknown if this is related to a change in diagnostic criteria or an actual rise in occurrence. It is probable because other illnesses that influence language, learning, and/or mental retardation are now classified better. The sex ratio is 4 to 11. Despite the lack of consensus, it appears that the peak occurrence age is 8 years; mental retardation: 75% (45-60% in other studies) [2]. These percentages are

more akin to typical autism, with PDD being less common and AS being almost nonexistent, with roughly 30% of cases associated with mental retardation. These people are probable carriers of unknown illnesses in which autism is one aspect of a more complex neurological picture. Secondary autisms, on the other hand, occur when another pathology is found in the same person with ASD, usually a rare disease that has been linked to autism—fragile X syndrome, tuberous sclerosis, Angelman syndrome, rubella, etc.—or where it is suspected that all manifestations are part of the same syndromic complex, severe intellectual disability (PID), cognitive disability (CD), ataxia (motor difficulties), blindness and other eye ailments (BAE), deafness (BAE), hyperactivity (hyperactivity), anxiety (anxiety), and insomnia (insomnia)



[3]. There is a lot of discussion in the literature and several research about the early detection of ASD [4]. Most studies in this field agree that early intervention can help these people overcome their shortcomings (IQ, social skills, coping skills, etc.) and help them integrate. The consensus is that these improvements do not suggest a cure but rather a reduction in family and social load and patient well-being. For these reasons, many studies have concentrated on finding instruments that allow early identification, both in high-risk groups like autistic siblings and in general or low-risk populations, the Autism Observation Scale for Infants (AOSI) for studies of autistic siblings and the Childhood Autism Spectrum Test (CAST) for children aged 4 to 6. The Autonomous Scale has been validated in Arabic nations [5].

Data mining is a search for knowledge. Data mining seeks out previously unknown patterns. In other terms, data mining is a set of technologies that allow the creation of meaningful expressions from raw and unintelligible data. When the objective of data mining is considered, it is similar to ore mining [6].

Technology is heavily employed in medicine as in every field. With the advancement of technology, new medical equipment and treatment procedures are being produced. These methods, which are constantly evolving in hardware and software, allow for more professional diagnosis and treatment [7]. Because medicine deals with human health, it is critical to encourage and support R&D. Many treatments rely on early diagnosis. Delaying treatment may cause disease progression and make treatment more difficult. It can potentially result in irreversible losses. For these reasons, data mining strategies to help doctors diagnose and treat patients are common in the literature [8]. Medicine's technological studies are a mix of numerous fields. Because vital information from the patient or examination findings cannot be reviewed without one or more physicians who are experts in the condition and diagnosis, nonexperts in the subject cannot evaluate disease-related findings. To assess if a person has an illness, a specialist must know precise details about the disease. Otherwise, erroneous diagnoses and treatment delays may occur. This may cause more serious issues. As a result, professionals in the subject must be consulted when applying information technologies in diagnosis. Experts agree that collecting the parameters and analyzing them later is best. These analyses require someone who can use information technologies to translate expert data into relevant information.

As a result, the collaboration between disciplines is critical to a successful study. There are classification procedures employing logistic regression, naive Bayes, artificial neural networks, and linguistic strong neurofuzzy classifiers and any classification. No method of clustering was found. This study used data pretreatment approaches such as filling in missing data and standardization, followed by a clustering method that was lacking in the literature and two unproven methods for classification. The study compares the methodologies' success rates using criteria including accuracy, sensitivity, determination, and  $F$ -measure to add to the literature. Artificial neural networks and strong linguistic neurofuzzy

classifier approaches were employed for classification. Regarding estimation accuracy, classification methods outperform clustering methods in data on autism spectrum disorder in children. The linguistic strong neurofuzzy classifier approach has a greater success rate than many other methods in the literature, properly classifying all data.

## 2. Methodology

### 2.1. Classification Method

**2.1.1. Artificial Neural Networks.** Artificial neural networks (ANNs) are an algorithm inspired by how the human brain works. Biological findings of neurophysiologists and psychologists on how neural networks work are used as its basis. These biological findings were systematized structurally and functionally, and a mathematical model was tried to be created. This model is called the neural network model [9].

**2.1.2. Linguistic Strong Neurofuzzy Classifier.** The linguistic strong neurofuzzy classifier (DKSBS) classifies data. Before classifying, determine the relevance of the features. Fuzzy inference is used to rank the features' relevance [10]. Thus, high-importance features are selected while low-importance features are disabled. This is the key distinction between classical and fuzzy logic. Sets can be made up of elements in fuzzy logic. In other words, the state of being an element with one and not being an element with 0 can be represented as 0.3 and 0.5 degrees. Also, since elements do not have to be in the same cluster, an element can be included in one cluster at 0.3 and another at 0.5. This eliminates the clear separation between black and white in classical clusters, allowing for grey spaces. So, by using a fuzzy technique, partial memberships can be established. To classify the features, the fuzzy inference is utilized first. The success rate of training the ANN is high due to the inclusion of fuzzy inference features. Memory is saved by not using attributes that do not split sets. This condition not only speeds up the process but also reduces costs. There is no need to use certain features if the classification success does not diminish when they are removed [8], because in real-life problems, the influence degree of the solutions developed can be different. The goal is to find faster and more accurate solutions. In this sense, the linguistically powerful fuzzy neuroclassifier provides a solution very near to real-life challenges. The data mining process is divided into two steps. First, the preprocessing stage of identifying the importance of the features is carried out. The artificial neural network is then trained using these importance levels and performed classification. The linguistic strong neurofuzzy classifier distinguishes itself from other classification methods by performing feature detection using fuzzy inference. The linguistic strong neurofuzzy classifier employs fuzzy rules to classify features. Fuzzy rules gradually define the features. Blurring frees the system from binary replies like yes or no. In other words, rather than being categorical, whether an attribute affects the outcome is described as "few," "there is," or "a lot." So, fuzzy inferences become more human-like.

## 2.2. Clustering Method

**2.2.1. K-Means.** Clustering is the process of grouping components together. Clustering is a popular strategy for grouping datasets and disclosing crucial and secret information [11]. The distinction between clustering and classification, another data mining process, is that classes in clustering are not predetermined. *K*-means is one of the oldest nonhierarchical clustering algorithms. Clustering uses unsupervised learning. In other words, clustering is not preset. Clusters are constructed by establishing the cluster's center points. The parameter *k* specifies the number of clusters. Because the *K* parameter also contains the number of cluster centers, it must be entered before employing the *K*-means algorithm. When determining clusters, the goal is to have the most in-group and least intergroup similarities. Distances between data points are used while forming similar clusters. Here, the appropriate number of cluster centres is determined (*k* parameter), and the distances of each element to these cluster centers are calculated one by one. Due to noncomputation, each data is included in the nearest cluster center. The new cluster centres are recalculated, as are the distances between each element and the new cluster centres. This cycle repeats until the set with no element changes. To finish the procedure, each element is assigned to the cluster in which it was found last. The elements that share the most similarities are grouped following the algorithm's distance calculations. The main flaw of *k*-means is that it cannot predict how many clusters the data will be divided into. If the number of clusters in the data is known, the *k* parameter can be entered, or the most relevant one can be identified by inputting different *k* parameters.

**2.2.2. X-Means.** *K*-means is a well-known clustering technique. The popularity of *K*-means is due to its simple structure and high model performance rate. However, despite its popularity, it has certain flaws. The user must supply a fixed value for the *k* parameter, representing the number of clusters. Limiting the number of clusters to a set *k*-value means ignoring other options. *X*-means stores the data in a *kd*-tree and stores the statistics for each stage. The statistical data also contains a list of centers to consider for a certain region. So, by comparing all options, the best one can be chosen. Pelleg and Moore developed the *X*-means method in 2000 as an upgraded version of the *K*-means algorithm. It was built to fill in the gaps in the *K*-means algorithm and to use the *K*-means algorithm's working style [12].

The method cannot calculate the number of clusters, which is viewed as a shortcoming of *X*-means and *K*-means. Instead of a predetermined number of clusters, *X*-means specifies an appropriate range. *X*-means may estimate the number of clusters it considers optimal from this range of values. The *X*-means structure runs the *K*-means algorithm progressively. Each time *K*-means creates subsets, it decides which centres to divide them between. Calculate the Bayes information criteria to make division judgments. These are the best results of existing centres (parent) and newly developed offspring (child). The *k* parameter values used to score the model selection criteria are kept adjacent

to the cluster centres. So, the centre positions can be studied attentively. The procedure starts with *k* equal to the range's lower limit and adds new centres until the upper limit is reached. During these operations, the best-scoring centroid set is noted. The new score is added if the following transaction's score is higher than the system's score. So, the list is always updated. A list of probable centroids for locations within a region is kept recursively updated. Its job is to update the region's centre points with the proper values. It starts by recording the randomly generated centre points equal to the *k* parameter list's smallest integer. The new values are updated as better ones are found. Finally, the highest-valued centres are outputs.

**2.3. Preprocessing Techniques.** Data mining methods may collect incomplete data. In such circumstances, missing data analyses are possible. At the same time, it is preferable to repair missing data to increase the dataset's quality. Analysing entire data also helps improve the method's success rate [13]. Missing data correction is part of preprocessing. It is possible to correct missing data by removing records or completing them in various ways. There are numerous approaches for completing missing data in the literature. A value assigned by taking into account the features of other data (such as mean, mode, or median) or values determined as a consequence of guesses might be used to fill in the missing values (regression analysis, hot deck value with Naive Bayes assignment, decision trees, expectation-maximization, and multiple assignment). This study assigned values based on other data's properties to fill in the gaps. The dataset's frequency was evaluated, and the value with the highest frequency was utilized to fill in the gaps.

Data mining is commonly used nowadays to extract meaning from data. Data mining is the process of discovering knowledge through data collecting, preprocessing, transformation, applying data mining tools, and assessing the results. The quality of the data acquired is important in enhancing the method's success rate. Many data preparation techniques exist to increase data quality. Preprocessing approaches include filling in missing data, eliminating noisy data, assessing feature relevance, and normalising particular features. Preprocessing methods and normalisation were employed to fill in missing data. The literature accepts various types of normalisation. Normalization methods include *Z*-score, min-max, median, and Sigmoid. Several normalising approaches can be employed concurrently. This study employed min-max normalisation.

## 3. Application

**3.1. Autism Spectrum Disorder Dataset.** This study used a subset of genuine ASD data for youngsters. The dataset used is called Autism Spectrum Disorder Screening Data for Children [14]. The dataset was developed using the latest parameters acknowledged in the literature for ASD diagnosis. The ASD Tests app gathered the answers. The application has age-specific categories. Each category has ten questions, each illustration to help users choose the correct answer. Participants were told their data would be kept confidential and

TABLE 1: Details of the attributes in the dataset.

Attribute	Datatype	Description
1 Answer to question 1		He usually notices small sounds when others cannot hear it.
2 Answer to question 2		It usually focuses on the whole picture rather than the small details.
3 Answer to question 3		In a social group, he can easily follow the conversation of several different people.
4 Answer to question 4		He finds it easy to commute between different activities.
5 Answer to question 5		He does not know how to continue the conversation with candidates.
6 Answer to question 6	Binary (0,1)	He is good at social chat.
7 Answer to question 7		He has trouble deciphering the character's intentions or feelings when he reads a story.
8 Answer to question 8		While in preschool, she enjoys playing with other children.
9 Answer to question 9		You can easily tell what someone is thinking or feeling by looking at their face.
10 Answer to question 10		He has a hard time making new friends.
11 Age	Number	Information on how old the individual is in years.
12 Gender	String	Knowledge of whether an individual is male or female
13 Ethnicity	String	Information about the ethnic origin of the individual.
14 Being born with jaundice	Boolean (yes-no)	Information on whether an individual is born with jaundice.
15 Family members with PDD	Boolean (yes-no)	Information on whether the individual has any family members with PDD.
16 Country of residence	String	Information of the individual's country of residence.
17 Using the scanning application before	Boolean (yes-no)	Information whether the user has used a scanning application before.
18 Scoring result	Integer	The final score was obtained based on the scoring algorithm of the screening method used.
19 Who completes The test	String	The information of who performed the individual's test (parent, herself, caregiver, health personnel, clinician, etc.).
20 Autistic status (output)	Boolean (yes-no)	Knowledge of the individual's autistic status

used only for research. Participants were briefed on the research's goal, privacy policy, and data use before completing the evaluation. The data collection includes ten items measuring autism spectrum disorder and demographic data. This test included data from three subgroups, totalling 1100 persons. Youth and adults make up the groups. ASD diagnoses are divided into groups based on the questions addressed. The produced dataset for children contains 292 samples, and only this subset was used in this investigation. Data kinds include numerical and categorical. Some data samples in the collection are missing. 20 attributes were used as inputs because they contained information on individuals' general and health state, and 1 attribute was used as output since it included the individual's autistic status. The attribute field "kind of screening method" expresses the individual's age range. In other words, it shows which child, teen, or adult group the autism screening tester belongs to. Only the kid subset was employed in this investigation. Data was unnecessary as it was all about the kids. So, it was eliminated from the dataset. So, there are now only 19 input parameters. Table 1 details the qualities and questions.

The attribute "kind of screening procedure," which indicates which age category the dataset applies to, has been removed from the dataset. The autism status of the Boolean individual was employed as a class label. First, all features were translated into numerical values in the study. Data pre-treatment techniques such as filling in missing data and standardising data between 0 and 1 were performed to eval-

uate the dataset more efficiently. The data were then categorised with DKSBS and grouped with  $k$ -means and  $x$ -means. The number of neurons employed in the planned feedforward ANN on the success rate was investigated. The data were divided into 70% training and 30% testing to examine the model success rate of classification approaches. When the data were categorized by artificial neural networks and DKSBS, the success rate was 100% in the test and training sets. Clustering algorithms lack a pretutorial. Thus, the clustered data were used for both training and testing. 89.73% success rate in  $k$ -means and 88.0% success rate in  $x$ -means.

**3.2. Findings and Evaluation.** Many studies on autism use data mining approaches, according to the literature. Vellanki et al. [15] addressed this issue in his work, stating that the data was outdated, despite the positive results. So, he stressed the need to work with current data. Aloumi et al. [16] supplied the current scale data with a fresh investigation. Aloumi et al. [16] used a subset of data from scientific articles for children in this investigation. The dataset used 292 samples and 21 characteristics. Because the data are relatively new, the findings of this study were compared to other investigations.

The dataset originally had numeric and textual expression variables. The methods employed for normalization and classification cannot be used with string expressions. So, first, the dataset was converted to numerical values. This

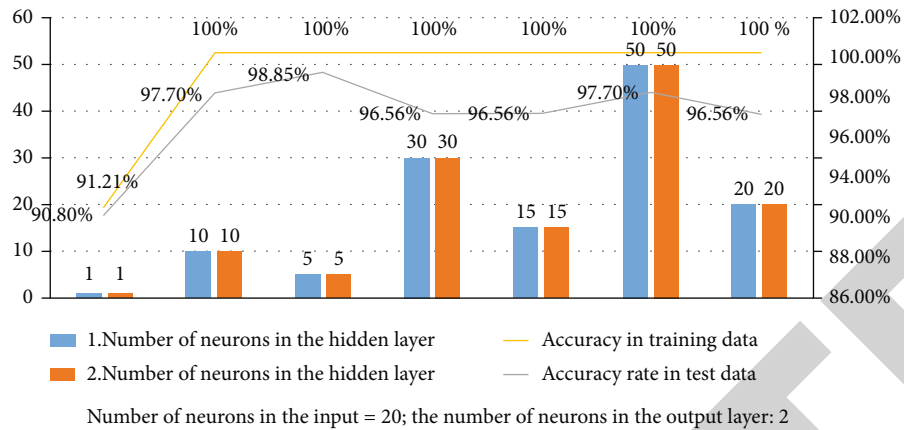


FIGURE 1: Performance of neural network.

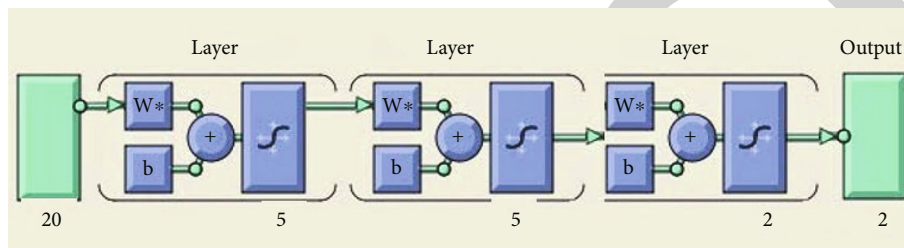


FIGURE 2: ANN model with the highest success rate.

conversion converts category data tagged with string expressions to numeric expressions. For example, gender categorical data has been replaced by 0 and 1. Ethnicity and residency are also designated consecutively starting at 1.

After digitizing the data, the frequency of each characteristic was recovered. The dataset's null values are filled with the most frequent value. Then, the values acquired with the min-max normalization approach, which has the best success rate of all normalizing methods, were constructed. Part of the dataset is allocated for training and a half for testing to compare the methods' success. The literature shows that several ratios are employed, but 70% of training data and 30% of test data are most typical. This study used 205 randomly selected training samples (70%) and 87 randomly selected testing samples (30%) to comply with the general methodology. Data were grouped using *K*-means and *X*-means.

**3.2.1. Results Obtained with Artificial Neural Network.** With the designed feedforward ANN, the effect of the number of neurons used on the success rate was examined, and models with different structures were tested. The performance of ANN is given in Figure 1.

When the success rate of the designed models is examined, it has been seen that a very high rate of success has been achieved. Among the models designed with different neuron numbers, the highest performance was seen in the model designed using 20 neurons in the input layer, 5 neurons in the two hidden layers, and 2 neurons in the output layer. Success was achieved with an accuracy of 100% in the training set and 98.85% in the test set. All samples in

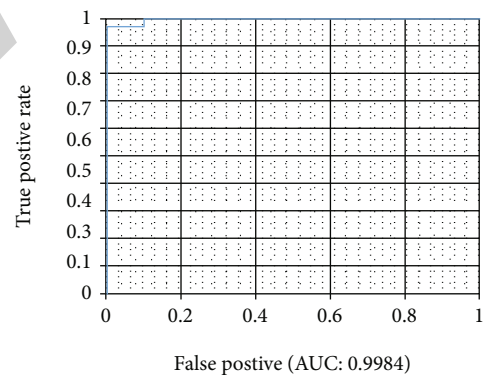


FIGURE 3: ROC curve plotted for the test data of the trained network.

the training set are classified correctly, while only one sample in the test dataset is classified incorrectly. As seen in Figure 1, increasing the number of neurons in the hidden layer is not directly proportional to the increase in the success rate. While increasing the number of neurons increases the model's success rate for some datasets, it decreases the model's success rate for some datasets. Therefore, instead of always adopting a fixed approach related to using too many or too little of the number of neurons, choosing the most successful model by determining several alternatives can increase the success rate. The ANN model with the highest success rate is shown in Figure 2.

The ROC curve (receiver-operating characteristic) drawn for the test data of the trained network is given in Figure 3.



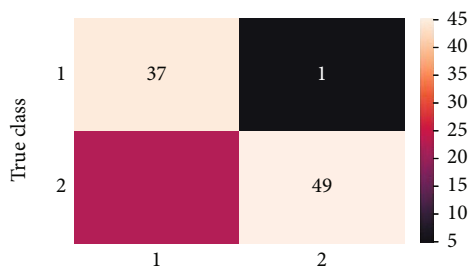


FIGURE 4: Error matrix plotted for the test data of the trained network.

As seen in Figure 3, the area under the ROC curve (AUC) value is very close to 1. This shows that a very high success was achieved in the classification made on the test data. The error matrix drawn for the test data of the trained network is given in Figure 4.

As shown in Figure 4, a very high part of the classification performed by the trained network for the test dataset was predicted correctly, and only one sample was misclassified. This means a very high success for the test data. When the error values produced by the network for the test data are examined in detail, the MSE value is  $4.822e-04$ ; it is seen that the RMSE value is 0.022. As can be seen from the MSE and RMSE values for the training data of the trained network, the error values of the network are quite low. The accuracy, sensitivity, determination, and  $F$ -measure values of the trained network for the test data are 0.989, 0.974, 1, and 0.987, respectively. This shows that the trained network gives very successful results in the test data.

**3.2.2. Results Obtained with the Linguistic Strong Neurofuzzy Classifier.** Firstly, feature selection was performed with DKSBS, and then, classification was performed. The data was divided into 70% training and 30% test data in the classification. When the classification results were examined, it was seen that 100% success was achieved in the training and test data. When the error values calculated for the training data of the method are examined, it is seen that the MSE value is  $3.099e-32$ , and the RMSE value is  $1.760e-16$ . The feature selection performed was determined by looking at the importance level of the features. The importance levels of the features are determined by DKSBS. The order of the numbered features are the same as the order in Table 1 and progressed sequentially from 1 to 19. Considering the importance levels determined by the linguistic strong neurofuzzy classifier on the features for classification, it is seen that groups with five different importance levels are formed. If these groups are to be rated from 5 to 1, with 5 of them being the most important, attributes with 5 significance levels 1, 2, 3, 5, 6, 7, 10, 18, and 4 importance attributes with 4 and 3 significance levels 8, 9, 11, 12, 13, 14, and 15. The numbered ones are the attribute number 16 with a significance level of 2 and the attribute number 17 with a severity level of 1. The significance level of attribute number 19 is set to 0—the contribution degrees of the features expressed by the linguistic strong neurofuzzy classifier. The child is with attributes 1, 2, 3, 5, 6, 7, and 10 in Table 1, whether he usually notices

small sounds when others are not hearing it, whether he usually focuses on the whole picture rather than the small details, whether he can easily follow the conversation of several different people in a social group, whether he knows how to continue the conversation with the candidates, and whether he is good at social conversation, when he reads a story; the character and the features that have the most impact on the classification were determined whether they had difficulty in deciphering their intentions or feelings and whether they found it difficult to make new friends. The final score was obtained based on the screening method's scoring algorithm. Expressed with the number 4 as the second most effective attribute, he found it easy to go back and forth between different activities. The third most effective attributes are expressed with the numbers 8, 9, 11, 12, 13, 14, and 15, whether he likes to play with other children when he is in preschool education and whether he can easily understand what someone is thinking or feeling, just by looking at their face, the age of the individual in years, the information of whether the individual is male or female, the information of the individual's ethnic origin, and the information of the individual's jaundice. It is the information of whether to be born with or not and whether any individual family member has PDD. The fourth most effective attribute is expressed with the number 16, information of the country in which the individual resides. The fifth most effective attribute is expressed with the number 17; it is the information whether the user has used a scanning application before or not. The training performance of the linguistic strong neurofuzzy classifier is shown in Figure 5.

As shown in Figure 5, the error values of the linguistically strong neurofuzzy classifier are quite low. The error matrix drawn for the test data after the linguistic strong neurofuzzy classifier is trained is given in Figure 6.

As shown in Figure 6, the classification performed by the trained linguistic strong neurofuzzy classifier for the test dataset is all correct. The test data's accuracy, sensitivity, determination, and  $F$ -measure values performed by the trained linguistic strong neurofuzzy classifier are 1, 1, 1, and 1, respectively. This shows that all of the training data are classified correctly.

**3.2.3. Results with K-Means.** Clustering algorithms are methods without prior tutorials, and the data classes are not predetermined. For this reason, parents were not separated as training and test data; all of them were used for training. In the  $k$ -means algorithm, the number of clusters expressed by the  $k$  parameter should be determined beforehand and given to the algorithm before running. There are two classes of data in this study to show whether it is OSB or not. Therefore, two clusters were desired when creating the clusters, so the  $k$  parameter was entered as two, and the data were clustered into two. When the classes of the data clustered with the  $K$ -means algorithm are compared with the real cluster classes, 262 of the 292 data in total were correctly classified, and the accuracy of the classification was 89.73%. The real classes and the classes were obtained with  $K$ -means.



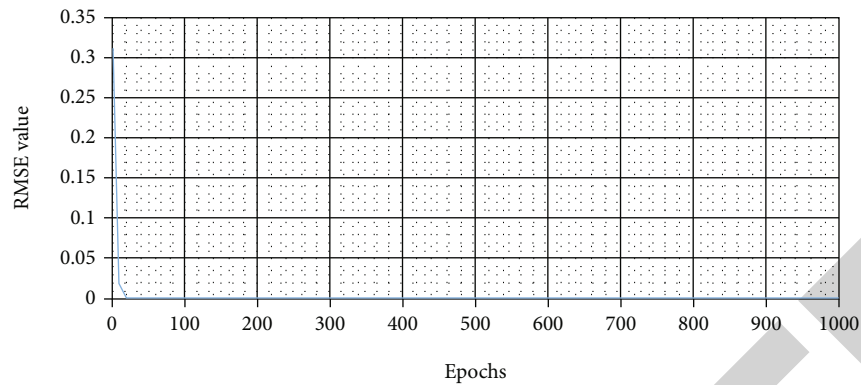


FIGURE 5: Educational performance of the linguistic strong neurofuzzy classifier.

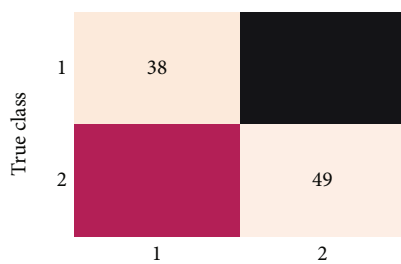


FIGURE 6: Error matrix plotted for test data.

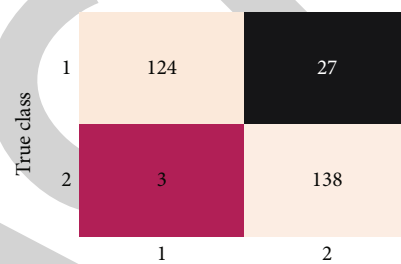


FIGURE 7: Error matrix plotted for the results obtained with the K-means algorithm.

As seen in Figure 7, the classes of the data clustered with the K-means algorithm were mostly predicted correctly, and the total number of incorrectly predicted samples was 30. Accuracy, sensitivity, determination, and *F*-measure values of the data clustered with the K-means algorithm are 0.897, 0.821, 0.979, and 0.892, respectively.

**3.2.4. Results with X-Means.** The X-means algorithm is a more up-to-date clustering method created by the development of the K-means algorithm. X-means is an improved version of K-means besides using the working structure of K-means. It works by specifying a range instead of determining the number of clusters as a fixed value. Thus, the algorithm determines the most suitable number of clusters for the dataset. While determining the number of clusters, the Bayesian information criterion is used to determine the best number of clusters. In this study, the number of clusters in the X-means algorithm, which was run by entering the class range between 2 and 4, was determined as 2 by the algorithm. When the classes of data clustered in two with the X-means algorithm were compared with the real cluster classes, 257 out of 292 data were correctly classified, and the classification accuracy was 88.02%. The real classes and the classes were obtained with X-means. The error matrix drawn for the results obtained with the X-means algorithm is given in Figure 8.

As seen in Figure 8, the data classes clustered with the X-means algorithm were mostly predicted correctly, and the total number of incorrectly predicted samples was 35. Accuracy, sensitivity, determination, and *F*-measure values of the

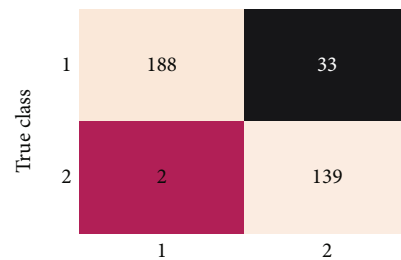


FIGURE 8: Error matrix plotted for the results obtained with the X-means algorithm.

data clustered with the X-means algorithm are 0.880, 0.781, 0.986, and 0.871, respectively.

**3.2.5. Comparison of the Prediction Achievements of Autism Spectrum Disorder Data for Children Analyzed with Different Methods.** In this study, the subset of the ASD dataset for children was classified with ANN and DKSBS and clustered with K-means and X-means methods. The performance values of the methods used are given in Figure 9.

As seen in Table 1, although the classification success rate with ANN is quite high, the highest success rate was obtained with DKSBS. In the classification made with DKSBS, 100% accuracy was achieved for training and test data. This means that the linguistic strong neurofuzzy classifier correctly classifies all samples in the dataset. When the success rates of clustering methods are examined, it is seen

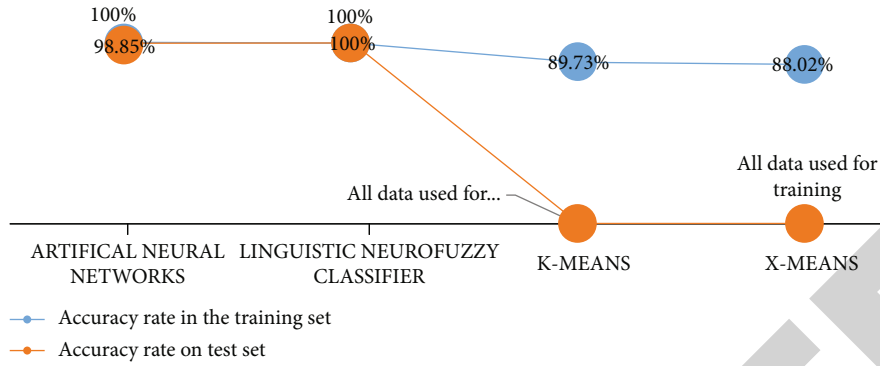


FIGURE 9: Performance values of the methods used.

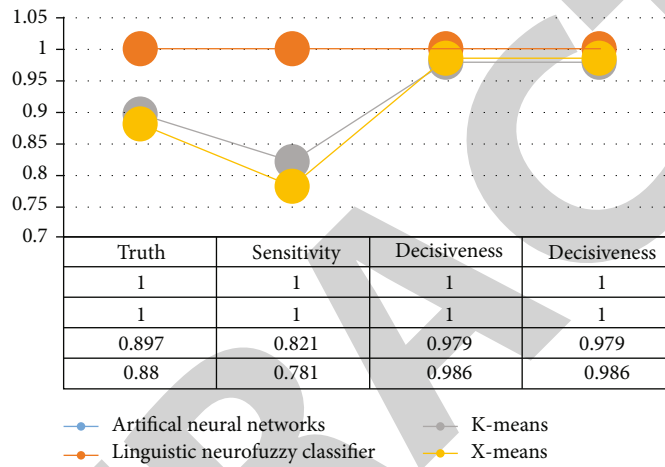


FIGURE 10: Accuracy, sensitivity, determination, and *F*-measure values for the training datasets of the methods used.

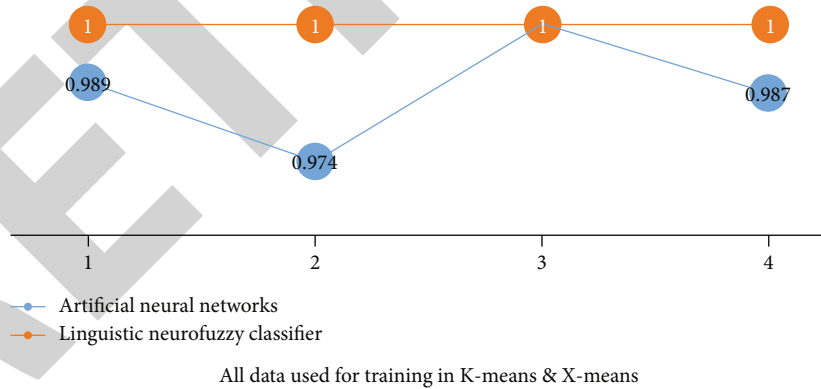


FIGURE 11: Accuracy, sensitivity, specificity, and *F*-measure values for the test datasets of the methods used.

that they are less successful than classification methods in general, and the results obtained with the *K*-means method are more successful than the *X*-means method. The accuracy, sensitivity, determination, and *F*-measure values for the training datasets of the methods used are given in Figure 10.

Figure 10 shows the accuracy, sensitivity, determination, and *F*-measure values calculated for the training data of the classification and clustering methods. As can be seen, all values calculated in the classification methods are 1. In

clustering methods, on average, the calculated values for *K*-means are higher than *X*-means. The accuracy, sensitivity, determination, and *F*-measure values for the test datasets of the methods used are given in Figure 11.

As seen in Figure 11, the accuracy, sensitivity, determination, and *F*-criterion values of the classification made with DK SBS for the test data were calculated as 1. This means that the linguistic strong neurofuzzy classifier classifies all the test data correctly. Accuracy, sensitivity, determination, and *F*-measure values of the classification made with ANN

for test data were also close to 1. This situation reveals that it is a method that can be used for test data, although it is more unsuccessful than the linguistic strong neurofuzzy classifier. All data clustered with *K*-means and *X*-means were used for training, so there are no accuracy, sensitivity, determination, and *F*-measure values calculated for the test data. The performance values of the study and the performance values of other studies were compared and found that different methods in different studies classified the same dataset. Still, no clustering process was found outside of this study. When the results of the studies are examined, it is seen that the success rate is above 90% in general, but there is also a study that is 100%. When the results obtained in this study are compared with the results obtained in other studies, it is seen that the classification success is higher when DKSBS and ANN classify the data than in studies classified with logistic regression, naive Bayes, fuzzy rule logistic regression combination, and j48 decision tree. The success rates of classification with fuzzy neural network architecture and classification with DKSBS within the scope of this study are the same. The accuracy in the data classified by the two methods is at the same rate, and this rate is 100%. This means that both methods correctly classify all samples. When the results of the clustering process carried out within the scope of this study are examined, it is concluded that the *K*-means method, one of the clustering methods, is more successful than the *X*-means method, and the success rate of both clustering methods is lower than the classification methods.

#### 4. Discussion

This study examined studies on OSB using techniques such as data mining and artificial intelligence. It is seen that many studies have achieved very successful results in this regard. In addition to this, the criticism that outdated datasets are used in the studies carried out in recent years with a scientific publications draws the attention [7]. When the details of the publication are examined, it is seen that technological developments are used by using current and successful methods. Still, it is emphasized that the data used in experimental studies are out of date. In the continuation of the study, outdated data, which is seen as a deficiency, were collected based on the last scale developed and shared after some operations were performed. The dataset includes 1100 samples, grouped as children, teenagers, and adults. This study used the subset for children containing 292 samples of the same dataset. Classification and clustering, which is one of the data mining methods [9], was applied to the dataset to estimate the output expressing the autistic status of the individual as a result of the inputs, which consisted of 20 inputs in total but were reduced to 19 after an attribute that was removed because it was the same in all samples. Before applying the classification and clustering processes, the missing data were first completed by looking at the frequency of the features on the dataset, which was completely converted to numeric values, and normalization processes were carried out. The dataset, which was prepared for the methods, was finally separated as 70% training and 30% test

data. The data were classified as test and training data for the classification process, and the results were expressed with many parameters. The methods used for the classification process were ANN and DKSBS. Since the clustering methods are not pretutorial, the dataset is not separated as training and test, but it is clustered as all training data. *K*-means and *X*-means methods were used for clustering. Although the results obtained were expressed with many parameters, accuracy, sensitivity, determination, and *F*-measure were used to compare the common denominator in all methods. When the classification results are examined, it is seen that the success rate for the training dataset is 100% in two methods, namely, ANN and DKSBS [17].

Therefore, the accuracy, sensitivity, determination, and *F*-measure values calculated for the training dataset of the two methods were calculated as 1. This means that both methods correctly classify all of the training data. When the results obtained for the test set are examined, it is seen that the success rates are different from each other. The success rate of the linguistic strong neurofuzzy classifier for the test data was the same as the success rate for the training data. Therefore, the accuracy, sensitivity, determination, and *F*-measure values calculated for the test set were calculated as 1. This means that all of the test data are correctly classified by DKSBS. The success rate of ANN for test data was 98.85%. Accuracy, sensitivity, determination, and *F*-measure values calculated for the test set were 0.989, 0.974, 1, and 0.987, respectively. These results mean that ANN classification misclassified only 1 of 87 samples in the test data and correctly classified the remaining 86 samples. Considering the success of classification methods [9], two methods are used.

#### 5. Conclusion

The contributions of this study to the literature are as follows: when the studies conducted with the same dataset are examined first, it is seen that the classification processes are made by using methods such as logistic regression, Naive Bayes, fuzzy rule logistic regression combination, fuzzy neural network architecture, and j48 decision tree. Still, it is seen that the clustering process is performed with any method in the subset for children. Although no study has been found, a classification made with ANN and DKSBS has not been found. When we look at the results, it is seen that the classification methods are more successful than clustering methods in the data of ASD for children in terms of estimation accuracy. It is concluded that the DKSBS method can be one of the best methods that can be preferred, especially since it has a higher success rate than many methods in the literature by correctly classifying all the data. Therefore, it allows to try different methods for the dataset used in this study and allows classification with a method that has more successful results than many studies in the literature. In addition, the parameters used to evaluate the results obtained are given in more detail than many studies. This allows for a more detailed interpretation of the obtained results.

## Retraction

# Retracted: *In Vivo* Growth Inhibition of Human Caucasian Prostate Adenocarcinoma in Nude Mice Induced by Amygdalin with Metabolic Enzyme Combinations

### BioMed Research International

Received 18 July 2023; Accepted 18 July 2023; Published 19 July 2023

Copyright © 2023 BioMed Research International. This is an open access article distributed under the Creative Commons Attribution License, which permits unrestricted use, distribution, and reproduction in any medium, provided the original work is properly cited.

This article has been retracted by Hindawi following an investigation undertaken by the publisher [1]. This investigation has uncovered evidence of one or more of the following indicators of systematic manipulation of the publication process:

- (1) Discrepancies in scope
- (2) Discrepancies in the description of the research reported
- (3) Discrepancies between the availability of data and the research described
- (4) Inappropriate citations
- (5) Incoherent, meaningless and/or irrelevant content included in the article
- (6) Peer-review manipulation

The presence of these indicators undermines our confidence in the integrity of the article's content and we cannot, therefore, vouch for its reliability. Please note that this notice is intended solely to alert readers that the content of this article is unreliable. We have not investigated whether authors were aware of or involved in the systematic manipulation of the publication process.

In addition, our investigation has also shown that one or more of the following human-subject reporting requirements has not been met in this article: ethical approval by an Institutional Review Board (IRB) committee or equivalent, patient/participant consent to participate, and/or agreement to publish patient/participant details (where relevant).

Wiley and Hindawi regrets that the usual quality checks did not identify these issues before publication and have since put additional measures in place to safeguard research integrity.

We wish to credit our own Research Integrity and Research Publishing teams and anonymous and named external researchers and research integrity experts for contributing to this investigation.

The corresponding author, as the representative of all authors, has been given the opportunity to register their agreement or disagreement to this retraction. We have kept a record of any response received.

### References

- [1] A. M. Alwan and J. T. Afshari, "In Vivo Growth Inhibition of Human Caucasian Prostate Adenocarcinoma in Nude Mice Induced by Amygdalin with Metabolic Enzyme Combinations," *BioMed Research International*, vol. 2022, Article ID 4767621, 7 pages, 2022.

## Research Article

# **In Vivo Growth Inhibition of Human Caucasian Prostate Adenocarcinoma in Nude Mice Induced by Amygdalin with Metabolic Enzyme Combinations**

**Ahmed Mohammed Alwan** <sup>1,2</sup> and **Jalil Tavakol Afshari** <sup>1,2</sup>

<sup>1</sup>Department of Immunology and Allergy, Faculty of Medicine, Mashhad University of Medical Sciences, Mashhad, Iran

<sup>2</sup>Section of Immunogenetic, Cell Culture Unit, Bu-Ali Research Institute, Mashhad University of Medical Sciences, Mashhad, Iran

Correspondence should be addressed to Ahmed Mohammed Alwan; [dr.ahmed.mosawy@gmail.com](mailto:dr.ahmed.mosawy@gmail.com) and Jalil Tavakol Afshari; [tavakolaj@gmail.com](mailto:tavakolaj@gmail.com)

Received 6 April 2022; Revised 20 April 2022; Accepted 30 April 2022; Published 21 May 2022

Academic Editor: Dinesh Rokaya

Copyright © 2022 Ahmed Mohammed Alwan and Jalil Tavakol Afshari. This is an open access article distributed under the Creative Commons Attribution License, which permits unrestricted use, distribution, and reproduction in any medium, provided the original work is properly cited.

Cancer of the prostate is an indicated type that is often recorded as a kind of cancer in men and the second critical cause of mortality through cancer cases. Many pharmacological investigations have shown that numerous herbal substances possess anticancer action. Amygdalin (AMD) has antitumour capabilities and works as an antioxidant, antibacterial, anti-inflammatory, and immune-regulating characteristics. The anticancer effects of amygdalin and its metabolizing enzymes, rhodanese (RHD) and betaglucoisidase (BGD), were examined *in vivo*, as well as their antitumour processes. Novel, effective combination agents are necessary to increase existing cancer treatment rates. This research was aimed at determining the anticarcinogenic impact of amygdalin (AMD) *in vivo*. This research was aimed at determining the RHD and BGD on the anticarcinogenic impact of AMD *in vivo*. Subcutaneously, PC3 prostate cancer cell lines were implanted into nude mice. Mice were treated every day with 0.5 ml of 50 mg/ml (AMD), AMD+ (RHD 0.1 mg/ml), AMD+(BGD 0.1 mg/ml), and doxorubicin (DOX 50 mg/ml). Mice were normalized for negative control with untreated mice. *In vivo*, morphopathological alterations in the tumour tissue were analyzed by histopathological staining methods. After 35 days of therapy, tumour growth and size inhibition were evident, indicating a function for the metabolic enzymes BGD and RHD in regulating AMD's anticancer effect *in vivo*. We concluded the critical role of metabolic enzymes BGD and RHD in elevating the antitumour effect of PC3 cancer cell lines in Balb/c nude mice treated with AMD.

## **1. Introduction**

Prostate cancer (PC) is by far the most widely recognized malignancy in males [1] and the second most common cancer mortality [2], with new cases expected to emerge globally and a high death rate [3]. Due to PC's great clinical and economic significance [4], extensive research has resulted in the fast growth of metastatic therapeutic options [5, 6]. AMD (Figure 1) (formerly known as laetrile) is a nitriloside present in the seed of prunasin group plants such as apricots, almonds, peaches, fruits, and many other rosaceous species [7, 8]. AMD has been commonly used to treat malignancy and pain [9–11]. AMD activation by BGD produces hydro-

cyanic acid, limiting cellular respiration and ultimately resulting in cell death. Cancer cells have a lower level of sulfur hydroxylase than healthy ones [9–13]. As a result, such cells can only detoxify the hydrocyanic acid produced during AMD hydrolysis. AMD's anticancer activity is enhanced when combined with BGD [10, 11, 13, 14]. In cancer cells, anaerobic glycolysis is the primary route [15]. Consequently, acidic circumstances boost betaglucoisidase activity, which results in increased hydrocyanic acid and benzaldehyde formation and a deadly impact on cancer cells [12]. In contrast to other medications with low molecular weight, hydrocyanic acid is a nonspecific agent since it diffuses due to cyanide's toxicity and results in its removal. AMD



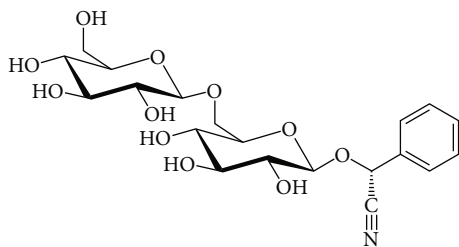


FIGURE 1: AMD structure.

concentrations less than 15 mmol/L were previously shown to be nontoxic to bladder cancer cells. However, activation of BGD reduced cell growth and migration [10, 14, 16]. Additionally, cells were arrested, and apoptosis was enhanced dose-dependently [17]. In recent years, the antitumour effect of AMD has been a gold stone topic [8, 9, 11]. It acts as an anticancer agent by liberating cyanogenic compounds in the body and leads to death of cancer cells, impeding tumour cell growth, and possibly reducing the occurrence of prostate cancer and some other types of cancer [17–19]. RHD is an enzyme of the normal cells that, in the presence of sulfur-containing chemicals, converts free cyanide to thiocyanate, a completely nontoxic molecule [20–22]. Thiocyanate is subsequently eliminated in the urine. RHD role can neutralize the AMD [19, 23–27]. As a result, these cells do not liberate HCN; from AMD, instead, it acts as glucose for healthy cells, supplying energy. In contrast, malignant cells lack RHD, and so the creation of HCN is stored in these cells [18, 28–30]. AMD may have a therapeutic impact on prostate cancer by inhibiting the viability of PC3 cells in vitro [17, 31, 32]. Additionally, no report of the same outcomes in vivo has been recorded. The indication of this research is to investigate the function of enzymatic control of AMD in vivo using BGD and RHD in nude mice tumoured with PC3 cell lines.

## 2. Materials and Methods

**2.1. Animals.** BALB/c (nude) mice (7 weeks of age,  $24 \pm 3.1$  gram weight) were purchased from Iran's Pasteur Institute (NCBI) and housed for one week in the animal house of Mashhad University of Medical Sciences. Environment adaptation was used to normalize new settings for mice, which included in dividing the day into 2 halves, one of them dark and the other half is light, and a temperature of  $22^{\circ}\text{C}$ , with a portion of comprehensive food and water routine. Subcutaneous injection of PC3 cell lines was used to prepare mice for xenograft tumour induction. All conditions and handling with mice were included under class 2 biosafety cabinet. Food and water and all administrative solutions were sterilized carefully. All needs and conditions were met following animal rights and Mashhad University of Medical Sciences' guidelines for laboratory animals, which were approved using the ethical approval code [IR.MUMS.MEDICAL.REC.1397.417].

**2.2. Chemical Reagents.** AMD was obtained by Sigma-Aldrich Company (Germany, catalogue no. A6005), RHD was prepared by Sigma-Aldrich Company (Germany, cata-

logue no. G4511-5MG), BGD was brought from Sigma-Aldrich Company (Germany, catalogue no. R1756-5MG), and DOX was obtained by Merck Company (USA, CAS: 24385-10-2).

**2.3. Cell Culture.** Cell lines PC3 (human Caucasian prostate cancer) were acquired from Iran's Pasteur institution. RPMI culture medium (Gibco, Carlsbad, CA, USA) was used to culturing cells. Culture media were supplemented by FBS 10% and antibiotic 1% pen./strept. (Pan-Biotech, Germany). Cells were trypsinized with trypsin from Sigma-Aldrich Company (Germany) after culture and 75% growth (CAS: 9002-07-7) and cells were counted at a concentration of 106 cells/ $50 \mu\text{l}$  PBS.

**2.4. Tumour Induction.** At a concentration of  $2 \times 10^7$  cells/ $50 \mu\text{l}$  PBS, cells were counted. Suspended cells were administered to each animal using insulin syringes. After seeing the first tumour bud (about ten days after cell injection), chemical compounds were delivered intraperitoneally into the treatment groups using an insulin syringe.

**2.5. Treatment of Animals.** Nude mice were divided into five groups and daily given 0.5 ml AMD alone, AMD 50 mg/ml+0.1 mg/ml RHD, or AMD 50 mg/ml+0.1 mg/ml BGD. Mice were administered with  $1 \mu\text{M}$  DOX doxorubicin as a positive control, whereas control animals were left untreated (002-07-7).

**2.6. Tumour Volume Measurement.** After visually inspecting and measuring the tumour with a calliper throughout the treatment procedure, the tumours were measured using a digital calliper every five days.

**2.7. Animal Weight Measurement.** For data analysis, the weights of all mice were determined every five days and compared to the untreated mice group.

**2.8. Histopathology.** Dissection of the mice resulted in the collection of representative tumours from each of the five groups in 10% neutral buffered formalin. The tumours were fixed in paraffin blocks, and standard Hematoxylin-Eosin staining was used to assess and compare histological features. Numerous characteristics such as tumour growth, mitotic index, and angiogenesis were investigated and compared in each animal group.

**2.9. Data Analysis.** The findings were provided as mean records and standard deviation. The data analyses were informed by using GraphPad Prism version 9.00, with significant differences proposed as  $P < 0.05$ .

## 3. Results

**3.1. Tumour Volume.** The volume of tumours in all mice groups did not record any change from day zero to the day 10. Tumours after day 10 started in the growth rates, and in untreated mice, continued in growth from day 10 to day 35. Tumours in mice treated with AMD+BGD was significantly inhibited, while they did not record significant inhibition in groups DOX and AMD+RHD (Figure 2).

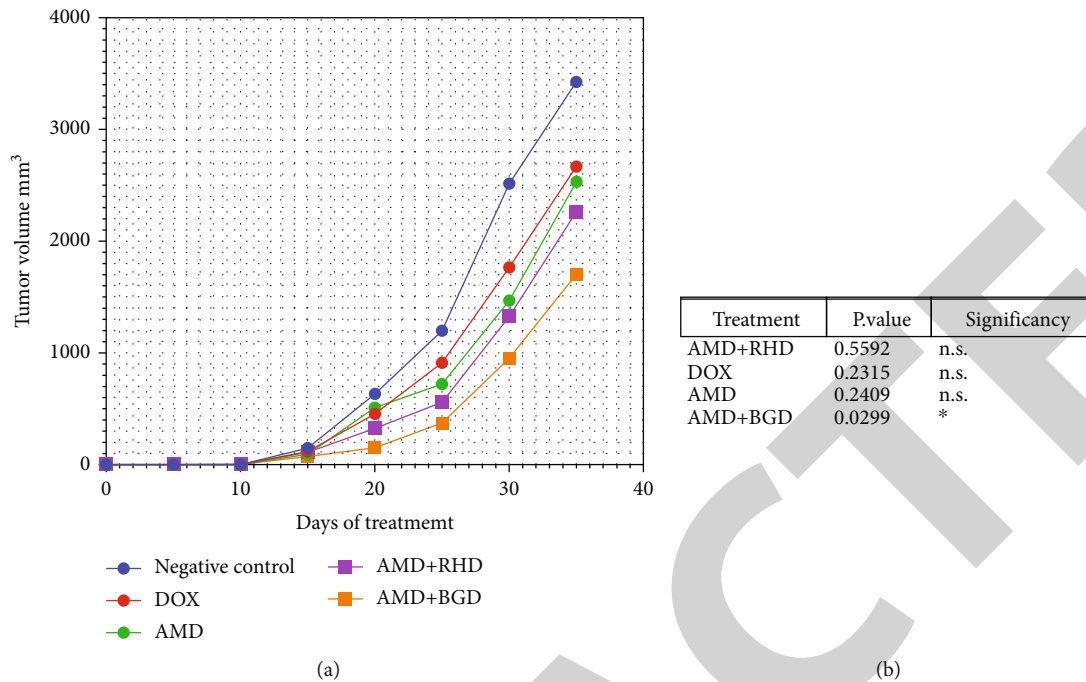


FIGURE 2: Tumour volume analysis. (a) Graph of tumour volume analysis from day zero to day 35. (b) Comparison between groups one-way ANOVA  $P$  value < 0.05.

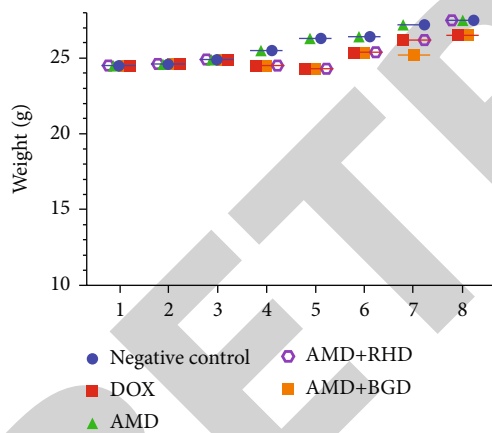


FIGURE 3: Mouse weight every five days during treatment.

3.2. *Mouse Body Weight.* The weight of mice did not show significant alterations in all groups (Figure 3).

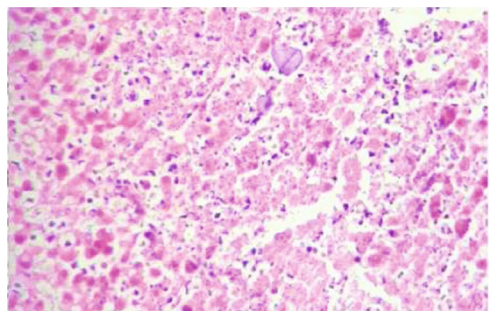
3.3. *Histopathological Analysis.* Tumours from each of the five groups were collected and analyzed according to conventional histopathology procedures. Several microscopic aspects such as angiogenesis, invasiveness, and mitotic index were examined on Hematoxylin-Eosin-stained tumour sections. Angiogenesis was found in tumour sections from the control mice and mice treated with AMD, AMD+RHD, and AMD+BGD. Microscopic analysis of tumour sections demonstrated significantly more tumour growth and invasion in the control group than in the AMD, AMD+RHD, and AMD+BGD treatment groups. Treatment with AMD+

BGD had a substantial effect on tumour growth morbidity compared to the other groups (Figure 4).

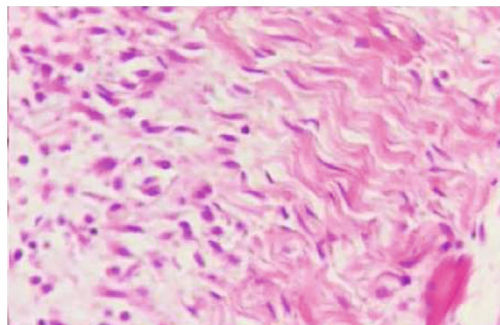
#### 4. Discussion

The first objectives of this research was to verify the concept that amygdalin triggers growth inhibition in human prostate cancer cell line PC3 cells in vivo and to analyze its metabolic enzymes rhodanese and betaglucosidase as a potential adjunct to the existing prostate cancer therapy regimen (Figure 5). In in vivo, amygdalin injection reduced tumour development in PC3 cells through an apoptotic mechanism induced by betaglucosidase activation [32, 33]. According to specific research, cancer cells have a high concentration of betaglucosidase, which may be used to break down amygdalin and produce cyanide, which is harmful to cancer cells. According to several other research, rhodanese, which is capable of detoxifying cyanide, is secreted in normal cells but insufficient in malignant tumours [23, 34, 35]. The combination activity of the both of rhodanese and betaglucosidase may be the reason for producing cyanide in cancer cells treated with amygdalin which can be toxic for cancer cells while leaving normal cells unaffected [36, 37].

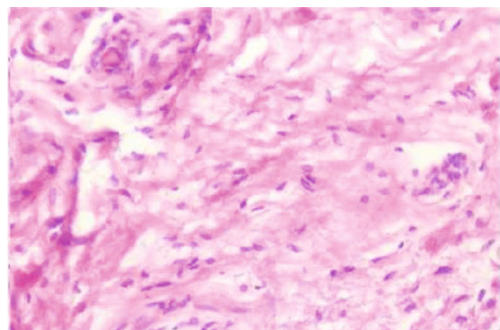
Further research is necessary to discover if betaglucosidase is concentrated in PC3 cells and rhodanese is absent and whether these characteristics are responsible for amygdalin's specificity for PC3 cell growth. Amygdalin was shown in this research to be capable of suppressing the progression of PC3 cell tumours in mice [17, 31, 38, 39]. As a result, we suspect that amygdalin decreases the viability of PC3 cells through a mechanism involving the betaglucosidase enzyme [17, 40]. Amygdalin substantially decreased the development



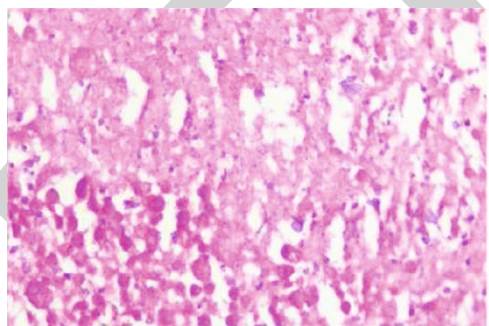
(a)



(b)

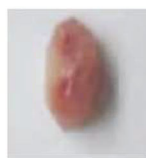
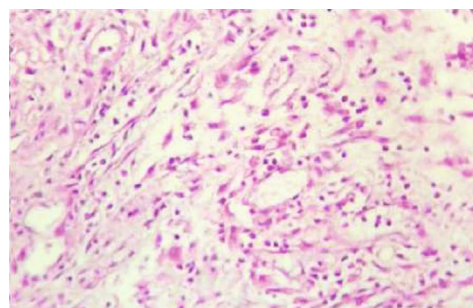


(c)



(d)

FIGURE 4: Continued.



(e)

FIGURE 4: Tumour histopathology. (a) Negative control group (untreated mice). (b) Mice treated with AMD+RHD. (c) Mice treated with AMD only. (d) Mice treated with DOX. (e) Mice treated with AMD+BGD.

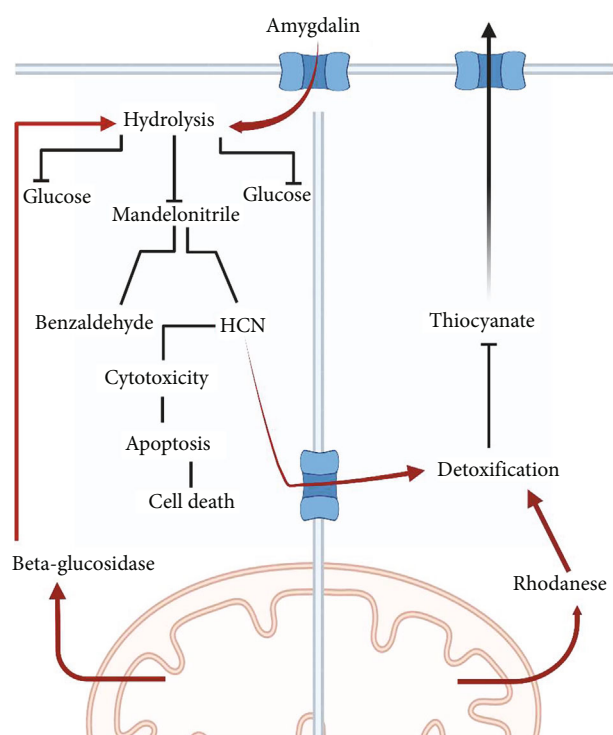


FIGURE 5: RHD and BGD in controlling AMD in cancer and normal cells.

of transplanted PC3 cell athymic mice through induction of the betaglucosidase enzyme, as reported in this work [41, 42]. The findings of our in vivo investigation are reporting nonpublished before. There were no apparent adverse effects seen in naked mice after amygdalin treatment. Amygdalin may be accurate since it naturally occurs as a plant or vitamin [43, 44]. Although it includes a harmful hydrocyanic group to live cells, it is harmless as long as the amygdalin component remains intact and does not release the hydrocyanic group enzymatically [11, 45].

## 5. Conclusion

Our study determined the inhibitory role of amygdalin treatment of PC3 in the mouse in vivo experiment. The mecha-

nism of betaglucosidase and rhodanese played a critical role in controlling the efficacy of amygdalin. We suggested using amygdalin in more in vivo investigations to develop the treatment of cancer by cyanogenic glucoside compound.

## Data Availability

All data are available within the manuscript, and additional data will be provided on request.

## Conflicts of Interest

I hereby declare that I have no pecuniary or other personal interest, direct or indirect, in any matter that raises or may raise a conflict with my duties as a manager of the Incorporated Management Committee of Mashhad University of Medical Sciences.

## References

- [1] M. Haghdoost, N. Serajkhorrani, and B. Makvandi, "The effectiveness of mindfulness based on stress management on death anxiety, disaster of imagination, acceptance and severity of pain in prostat cancer patients," *Journal of Ilam University of Medical Sciences*, vol. 29, no. 6, 2022.
- [2] K. Nishimoto, K. Nakajima, M. Oyama et al., "Predictive factors for effectiveness from novel androgen-receptor-axis-targeted agents in patients with metastatic prostate cancer," *Journal of Clinical Oncology*, vol. 40, Supplement\_6, p. 33, 2022.
- [3] A. Mizokami, K. Nishimoto, H. Matsuyama et al., "Efficacy of new therapies for relapse after docetaxel treatment of bone metastatic castration-resistant prostate cancer in clinical practice," *Anticancer Research*, vol. 42, no. 3, pp. 1465–1475, 2022.
- [4] J. Ellinger, A. Alajati, P. Kubatka et al., "Prostate cancer treatment costs increase more rapidly than for any other cancer—how to reverse the trend?," *The EPMA Journal*, vol. 13, no. 1, pp. 1–7, 2022.
- [5] M. S. Leapman, M. Dinan, S. Pasha et al., "Mediators of racial disparity in the use of prostate magnetic resonance imaging among patients with prostate cancer," *JAMA Oncology*, vol. 25, 2022.
- [6] L. Luo, J. F. Jiang, H. H. Luan et al., "Spatial and temporal patterns of prostate cancer burden and their association with



- socio-demographic index in Asia, 1990–2019,” *Prostate*, vol. 82, no. 2, pp. 193–202, 2022.
- [7] T. Zhang, S. Yang, B. Zhang, D. Yang, Y. Lu, and G. Du, “Insights into the properties of amygdalin solvatomorphs: X-ray structures, intermolecular interactions, and transformations,” *ACS Omega*, vol. 7, no. 10, pp. 8906–8918, 2022.
- [8] C. Zhang, J. Lin, C. Zhen et al., “Amygdalin protects against acetaminophen-induced acute liver failure by reducing inflammatory response and inhibiting hepatocyte death,” *Biochemical and Biophysical Research Communications*, vol. 602, pp. 105–112, 2022.
- [9] A. Abudoukelimu, X. Yang, L. Ge, X. Zeng, Y. Shu, and Z. Zhao, “Effects of amygdalin on TLR4/NF- $\alpha$ B signaling pathway-mediated proliferation and apoptosis of gastric cancer cells,” *Current Topics in Nutraceutical Research*, vol. 20, no. 1, pp. 153–158, 2022.
- [10] C. Zhang, D. Zhang, Y. Wang et al., “Pharmacokinetics and anti-liver fibrosis characteristics of amygdalin: key role of the deglycosylated metabolite prunasin,” *Phytomedicine*, vol. 99, article 154018, 2022.
- [11] S. M. Motawea, S. A.-A. Youssef, G. A. Abdel-Aleem, M. F. Mohamed, and M. S. Mostafa, “Effect of amygdalin (vitamin B17) on induced mammary tumor in virgin female albino rats: histological and morphometric study,” *Egyptian Journal of Histology*, vol. 12, 2022.
- [12] M. Halenár, M. Medveďová, N. Maruniaková, and A. Kolesárová, “Amygdalin and its effects on animal cells,” *Journal of Microbiology, Biotechnology and Food Sciences*, vol. 2021, pp. 2217–2226, 2021.
- [13] V. Jaswal, J. Palanivelu, and C. Ramalingam, “Effects of the gut microbiota on amygdalin and its use as an anti-cancer therapy: substantial review on the key components involved in altering dose efficacy and toxicity,” *Biochemistry and Biophysics Reports*, vol. 14, pp. 125–132, 2018.
- [14] M. M. Abboud, W. Al Awaida, H. H. Alkhateeb, and A. N. Abu-Ayyad, “Antitumor action of amygdalin on human breast cancer cells by selective sensitization to oxidative stress,” *Nutrition and Cancer*, vol. 71, no. 3, pp. 483–490, 2019.
- [15] K. Hönigova, J. Navratil, B. Peltanova, H. H. Polanska, M. Raudenska, and M. Mašarik, “Metabolic tricks of cancer cells,” *Biochimica et Biophysica Acta (BBA)-Reviews on Cancer*, vol. 1877, article 188705, 2022.
- [16] F. Resech, B. Lehmann, W. Weinmann, and K. W. Klingberg, “Akute cyanidintoxikation durch amygdalin,” in *Swiss Medical Forum*, vol. 22, pp. 75–77, EMH Swiss Medical Publishers, 2022.
- [17] J. Makarević, I. Tsaour, E. Juengel et al., “Amygdalin delays cell cycle progression and blocks growth of prostate cancer cells in vitro,” *Life Sciences*, vol. 147, pp. 137–142, 2016.
- [18] B. B. Przemysław Liczbiński, P. Liczbiński, and B. Bukowska, “Molecular mechanism of amygdalin action in vitro: review of the latest research,” *Journal of Microbiology, Biotechnology and Food Sciences*, vol. 40, no. 3, pp. 212–218, 2018.
- [19] M. Aminlari, A. Malekhusseini, F. Akrami, and H. Ebrahimnejad, “Cyanide-metabolizing enzyme rhodanese in human tissues: comparison with domestic animals,” *Comparative Clinical Pathology*, vol. 16, no. 1, pp. 47–51, 2007.
- [20] R. Sabelli, E. Iorio, A. de Martino et al., “Rhodanese–thioredoxin system and allyl sulfur compounds,” *The FEBS Journal*, vol. 275, no. 15, pp. 3884–3899, 2008.
- [21] A. Jamshidzadeh, H.-R. R. Rasekh, L. M. Amin et al., “Rhodanese and arginase activity in normal and cancerous tissues of human breast, esophagus, stomach and lung,” *Archives of Iranian Medicine*, vol. 4, no. 2, pp. 88–92, 2001.
- [22] M. Aminlari and H. Gilanpour, “Comparative studies on the distribution of rhodanese in different tissues of domestic animals,” *Comparative Biochemistry and Physiology. B*, vol. 99, no. 3, pp. 673–677, 1991.
- [23] R. Cipollone, P. Ascenzi, P. Tomao, F. Imperi, and P. Visca, “Enzymatic detoxification of cyanide: clues from *Pseudomonas aeruginosa* Rhodanese,” *Journal of Molecular Microbiology and Biotechnology*, vol. 15, no. 2–3, pp. 199–211, 2008.
- [24] W. F. Gorman, E. Messinger, and M. Herman, “Toxicity of thiocyanates used in treatment of hypertension,” *Annals of Internal Medicine*, vol. 30, no. 5, pp. 1054–1059, 1949.
- [25] Y. Xu, S. Szép, and Z. Lu, “The antioxidant role of thiocyanate in the pathogenesis of cystic fibrosis and other inflammation-related diseases,” *Proceedings of the National Academy of Sciences*, vol. 106, no. 48, pp. 20515–20519, 2009.
- [26] W. Weuffen, C. Franzke, and B. Thürkow, “Fortschrittsbericht Zur alimentären Aufnahme, Analytik und biologischen Bedeutung des Thiocyanats,” *Food/Nahrung*, vol. 28, no. 4, pp. 341–355, 1984.
- [27] E. L. Thomas, “Lactoperoxidase-catalyzed oxidation of thiocyanate: equilibriums between oxidized forms of thiocyanate,” *Biochemistry*, vol. 20, no. 11, pp. 3273–3280, 1981.
- [28] H. Barakat, “Amygdalin as a plant-based bioactive constituent: a mini-review on intervention with gut microbiota, anticancer mechanisms, bioavailability, and microencapsulation,” *Multi-disciplinary Digital Publishing Institute Proceedings*, vol. 61, no. 1, p. 15, 2020.
- [29] J. Mani, J. Rutz, S. Maxeiner et al., “Cyanide and lactate levels in patients during chronic oral amygdalin intake followed by intravenous amygdalin administration,” *Complementary Therapies in Medicine*, vol. 43, pp. 295–299, 2019.
- [30] J. Xu, N. Qin, W. Jiang, and T. Chen, “Amygdalin suppresses the proliferation, migration and EMT of gastric cancer cells by inhibiting TGF- $\beta$ /Smad signal pathway,” *Tropical Journal of Pharmaceutical Research*, vol. 21, pp. 721–726, 2022.
- [31] J. Mani, J. Neuschäfer, C. Resch et al., “Amygdalin modulates prostate cancer cell adhesion and migration in vitro,” *Nutrition and Cancer*, vol. 72, no. 3, pp. 528–537, 2020.
- [32] J. Zhou, J. Hou, J. Rao, C. Zhou, Y. Liu, and W. Gao, “Magnetically directed enzyme/prodrug prostate cancer therapy based on  $\beta$ -Glucosidase/Amygdalin,” *International Journal of Nanomedicine*, vol. 15, pp. 4639–4657, 2020.
- [33] D. Sireesha, B. S. Reddy, B. A. Reginald, M. Samatha, and F. Kamal, “Effect of amygdalin on oral cancer cell line: An in vitro study,” *Journal of Oral and Maxillofacial Pathology: JOMFP*, vol. 23, no. 1, pp. 104–107, 2019.
- [34] B. Mosayyebi, M. Imani, L. Mohammadi et al., “An update on the toxicity of cyanogenic glycosides bioactive compounds: possible clinical application in targeted cancer therapy,” *Materials Chemistry and Physics*, vol. 246, article 122841, 2020.
- [35] S. Milazzo, E. Ernst, S. Lejeune, and K. Boehm, “Laetrile treatment for cancer,” *Cochrane Database of Systematic Reviews*, vol. 5, no. 4, p. 296, 2015.
- [36] J. Newmark, R. O. Brady, P. M. Grimley, A. E. Gal, S. G. Waller, and J. R. Thistlethwaite, “Amygdalin (laetrile) and prunasin beta-glucosidases: distribution in germ-free rat and



## Retraction

# Retracted: Investigation of the Role of *Leuconostoc mesenteroides* subsp. *cremoris* in Periodontitis around Abutments of Fixed Prostheses

### BioMed Research International

Received 10 October 2023; Accepted 10 October 2023; Published 11 October 2023

Copyright © 2023 BioMed Research International. This is an open access article distributed under the Creative Commons Attribution License, which permits unrestricted use, distribution, and reproduction in any medium, provided the original work is properly cited.

This article has been retracted by Hindawi following an investigation undertaken by the publisher [1]. This investigation has uncovered evidence of one or more of the following indicators of systematic manipulation of the publication process:

- (1) Discrepancies in scope
- (2) Discrepancies in the description of the research reported
- (3) Discrepancies between the availability of data and the research described
- (4) Inappropriate citations
- (5) Incoherent, meaningless and/or irrelevant content included in the article
- (6) Peer-review manipulation

The presence of these indicators undermines our confidence in the integrity of the article's content and we cannot, therefore, vouch for its reliability. Please note that this notice is intended solely to alert readers that the content of this article is unreliable. We have not investigated whether authors were aware of or involved in the systematic manipulation of the publication process.

In addition, our investigation has also shown that one or more of the following human-subject reporting requirements has not been met in this article: ethical approval by an Institutional Review Board (IRB) committee or equivalent, patient/participant consent to participate, and/or agreement to publish patient/participant details (where relevant).

Wiley and Hindawi regrets that the usual quality checks did not identify these issues before publication and have since put additional measures in place to safeguard research integrity.

We wish to credit our own Research Integrity and Research Publishing teams and anonymous and named external researchers and research integrity experts for contributing to this investigation.

The corresponding author, as the representative of all authors, has been given the opportunity to register their agreement or disagreement to this retraction. We have kept a record of any response received.

### References

- [1] S. A. M. Hussein, R. A. Kareem, A. M. H. Al-Dahbi, and M. Birhan, "Investigation of the Role of *Leuconostoc mesenteroides* subsp. *cremoris* in Periodontitis around Abutments of Fixed Prostheses," *BioMed Research International*, vol. 2022, Article ID 8790096, 6 pages, 2022.

## Research Article

# Investigation of the Role of *Leuconostoc mesenteroides* subsp. *cremoris* in Periodontitis around Abutments of Fixed Prosthesis

Saif Ali Mohammed Hussein,<sup>1</sup> Rehab Aamer Kareem,<sup>2</sup> Ali Maki Hamed Al-Dahbi,<sup>3</sup> and Mequanint Birhan <sup>4</sup>

<sup>1</sup>Department of Medical Laboratory Technique, Dijlah University College, Iraq

<sup>2</sup>Department of Prosthodontics, College of Dentistry, University of Dijlah, Iraq

<sup>3</sup>Dentistry Department, Dijlah University College, Iraq

<sup>4</sup>Department of Mechanical Engineering, Mizan-Tepi University, Ethiopia

Correspondence should be addressed to Mequanint Birhan; [mequanint@mtu.edu.et](mailto:mequanint@mtu.edu.et)

Received 18 April 2022; Revised 3 May 2022; Accepted 7 May 2022; Published 20 May 2022

Academic Editor: Dinesh Rokaya

Copyright © 2022 Saif Ali Mohammed Hussein et al. This is an open access article distributed under the Creative Commons Attribution License, which permits unrestricted use, distribution, and reproduction in any medium, provided the original work is properly cited.

This study included the role of *Leuconostoc mesenteroides* subsp. *cremoris* in oral diseases such as periodontitis. **Material and Method.** Isolation and identification of *Leuconostoc mesenteroides* subsp. *cremoris* from a saliva sample of twenty patients wearing fixed dental prostheses suffering from periodontitis followed by estimating susceptibility generally to the most common antibiotics and specifically to chlorhexidine (CHX) to determine the MIC of CHX and also screening of the strength of biofilm production under aerobic and anaerobic conditions; here, the study included six groups: Group I: screening of biofilm formation under aerobic condition, Group II: screening the MIC of CHX effect on biofilm formation under aerobic condition, Group III: screening of the MIC of CHX effect on preformed biofilm under aerobic condition, Group IV: screening of biofilm formation under anaerobic condition, Group V: screening of MIC of CHX effect on biofilm formation under anaerobic condition, and Group VI: screening of MIC of CHX effect on preformed biofilm under anaerobic condition. **Results.** The results showed that about 5 (25%) isolates were identified as *L. mesenteroides* subsp. *cremoris*, while 75% are other isolates. Furthermore, susceptibility results to antibiotic showed the sensitivity to penicillin (100%), azithromycin (100%), ciprofloxacin (100%), tetracycline (100%), gentamicin (100%), doxycycline (100%), vancomycin (100%), ofloxacin (60%), chloramphenicol (80%), ampicillin (80%), and ceftiofloxacin (60%). On the other side, the biofilm production assays revealed that all isolates were moderate biofilm former under the aerobic and anaerobic conditions but for the biofilm treated with MIC of CHX, the current study noticed that the strength of the biofilm became weaker in aerobic and anaerobic conditions; regardless, the strength of the biofilm under anaerobic conditions was higher than in that under aerobic conditions, with no significant differences at  $p \leq 0.05$  depending on the statistical analysis (*T*-test) before and after the treatment with MIC of CHX in aerobic and anaerobic conditions. **Conclusions.** The presence of *mesenteroides* subsp. *cremoris* in the oral cavity is due to eating foods and vegetables; based on the strength of the biofilm and sensitivity tests, the isolates have less pathogenicity in the oral cavity due to the weakness of the biofilm production and the lack of resistance to antibiotics.

## 1. Introduction

Probiotics are live nonpathogenic microorganisms that are provided to the host to enhance microbial community balance [1]. The use of microbiome treatment in oral cavity homeostasis is a relatively recent notion, as a viable alternative to antibiotics in the treatment of a variety of oral disor-

ders such as periodontitis and dental caries. The mode of mechanism action can be characterized as direct or indirect. For the effect in direct mode, the probiotic organisms have an effect on pathogenic organism itself [2].

The indirect route of action involves probiotic microbes regulating the host's response to infections [2]. Some researches focused on *Leuconostoc mesenteroides* subsp.

mesenteroides as a viable probiotic. Furthermore, this microorganism has important technological properties, such as the ability to produce acetaldehyde, dextran, acetoin, and diacetyl; also, proteolytic enzymes and lipolytic enzymes at the same time have the ability to grow under extremely stressful conditions [3].

Many *L. mesenteroides* species generate a variety of organic acids, as well as a class of antibacterial chemicals known as bacteriocins (such as carnosin and leuconocin). These chemical substances inhibit both gram-negative and gram-positive bacteria [4]; few studies have found that employing Leuconostoc as a probiotic strain has a high potential. [5] demonstrated that the use of Leuconostoc as a probiotic strain was superior to the probiotic Lactobacillus strain currently in clinical use in generating cytokines [6].

Furthermore, it has been found that *L. mesenteroides* can prevent pathogen growth and can be employed as a safe probiotic for further research [7, 8]. *L. mesenteroides* has shown significant antibacterial activity against gram-positive and gram-negative bacteria [9] like *S. pyogenes* [10] and *G. anatis* [11].

## 2. Material and Method

**2.1. Sample Collection.** A total of 20 specimens (saliva) were collected from fixed dental prosthesis patients complaining from periodontal diseases and suspended in 1 ml phosphate buffer saline (PBS) then transported to the microbiology and immunology laboratory in Dijla University.

**2.2. Isolation and Identification of Bacteria.** Approximately 100  $\mu$ l of samples was inoculated into MRS agar plates for 24 hr in 37°C; the isolates were characterized by cultural and morphological features [12] and Vitek 2 system.

**2.3. Antimicrobial Susceptibility.** Antibiotic susceptibility testing will be carried out using a modified Kirby-Bauer Disk diffusion method and commercially available antibiotic discs. The size of the inhibitory zone was used to classify stains as susceptible, intermediately resistant, or resistant, according to the manufacturer's instructions; this corresponded to the WHO's interpretation criteria: penicillin (P, 10 g), azithromycin (AZM, 15 g), ciprofloxacin (CIP, 5 g), tetracycline (T, 30 g), gentamicin (G, 10 g), doxycycline (DO, 30 g), vancomycin (VA, 30 g), ofloxacin (OF, 5 g), chloramphenicol (C, 30 g), and ampicillin (A, 10 g).

**2.4. CHX Susceptibility Test.** Agar diffusion method was followed as described in [CLSI, 2016]. The isolates were adjusted to  $1.5 \times 10^8$  CFU/ml and cultured on Mueller-Hinton agar-containing wells (6 mm in diameter). 0.1 ml of chlorhexidine gluconate 2% w/v was added into the wells, then incubated under aerobic condition; the same steps were repeated under anaerobic conditions (GasPak Jar) for 24 hr at 37°C.

**2.5. Estimation of Minimum Inhibitory Concentration (MIC) of CHX.** The inoculums were adjusted to roughly  $1.5 \times 10^8$  CFU/ml, and 1 ml was transferred to tubes containing 1 ml of MIC. The tubes were incubated at 37°C for 24 hours,

and the quantity of growth in the tubes containing CHX was matched to the growth-control tubes (no CHX) as the control. The organism's development in the tubes was impeded, as seen with the naked eye [13].

**2.6. Screening the Biofilm Formation.** This assay included six groups as shown in Table 1.

**2.7. Screening of Biofilm Production in Bacterial Isolates under Aerobic and Anaerobic Condition.** In the procedure described by O'Toole [14], 24 hr old isolates were inoculated in tryptic soy broth and incubated for 18 hours at 37°C in, then diluted 1:100 with fresh tryptic soy broth; then, wells of plates (96-well flat-bottom tissue culture plates) were loaded with 0.2 ml of the diluted bacteria and with only broth media (without bacteria) serving as a control (blank) to verify sterility; the following formula was used to determine the biofilm formation strength:

- (1)  $OD \leq ODC$  = nonbiofilm former (NBF)
- (2)  $ODC < OD \leq 2X ODC$  = weak biofilm former (WBF)
- (3)  $2XC < OD \leq 4XC$  = moderate biofilm former (MBF)
- (4)  $OD > 4X ODC$  = strong biofilm former (SBF)

OD stands for optical density and ODC stands for optical density of control.

**2.8. Screening Effect MIC of CHX on Biofilm Production under Aerobic and Anaerobic Condition.** This assay was performed according to Tanner et al. [15] and modified. 200  $\mu$ l of the particular antibiotic (MIC of CHX) dilution in tryptic soy broth was put into the wells (96-well plate); then, the isolates were diluted with 0.2 ml fresh tryptic soy broth; subsequently, 200  $\mu$ l of the suspension was loaded into the wells and the other wells were loaded only with broth (without bacteria) serving as control (blank) to check sterility followed by incubation at 37°C for 24 hr; the following formula was used to determine the biofilm formation strength:

- (1)  $OD \leq ODC$  = nonbiofilm former (NBF)
- (2)  $ODC < OD \leq 2X ODC$  = weak biofilm former (WBF)
- (3)  $2XC < OD \leq 4XC$  = moderate biofilm former (MBF)
- (4)  $OD > 4X ODC$  = strong biofilm former

OD stands for optical density and ODC stands for optical density of control.

**2.9. Screening Effect of MIC of CHX on Performed Biofilm under Aerobic and Anaerobic Condition.** Isolates of 24 hr old were diluted to 0.2 ml of tryptic soy broth followed by 100  $\mu$ l loaded into the wells of plate; after the incubation period at 37°C for 24 hr for biofilm formation, the medium was removed gently, the generated biofilm was then rinsed three times with PBS to eliminate nonadherent cells, and at that time, 200  $\mu$ l of MIC of CHX was added and then, the plate was incubated at 37°C for 24 hr; this test was renewed

TABLE 1

Groups	Biofilm formation methods
Group I	Screening of biofilm formation under aerobic condition
Group II	Screening of MIC of CHX effect on biofilm formation under aerobic condition
Group III	Screening of MIC of CHX effect performed biofilm under aerobic condition
Group IV	Screening of biofilm formation under anaerobic condition
Group V	Screening of MIC of CHX effect biofilm formation under anaerobic condition
Group VI	Screening of MIC of CHX effect performed biofilm under anaerobic condition

in the absence of MIC of CHX as a control [15], and the biofilm production strength was calculated as follows:

- (1)  $OD \leq ODC$  = nonbiofilm former (NBF)
- (2)  $ODC < OD \leq 2X ODC$  = weak biofilm former (WBF)
- (3)  $2 XC < OD \leq 4 XC$  = moderate biofilm former (MBF)
- (4)  $OD > 4X ODC$  = strong biofilm former

OD stands for optical density and ODC stands for optical density of control.

2.10. *Statistical Analysis.* The statistical analysis was achieved by *T*-test probability  $\leq 0.05$ .

### 3. Results and Discussion

A total of 20 samples were collected from patients with gradient collected; approximately 5 (25%) *L. mesenteroides* isolates were identified according to morphological and Vitek system beside 75% of other isolates in Figure 1.

These findings agreed with [16, 17], which identified *S. salivarius*, *S. anginosus*, *L. mesenteroides*, and *L. sakei* (through morphological and genetic analysis from dental caries patients). However, the presence of these bacteria may be ascribed to food residues in the mouth in persons who have been diagnosed with acute severe caries. According to Ananieva et al. [18], both *L. sakei* and *L. mesenteroides* have been proven in some studies to be environmentally sustainable agents against foodborne pathogens in the mouth [19].

The isolates showed sensitivity to penicillin (100%), azithromycin (100%), ciprofloxacin (100%), tetracycline (100%), gentamicin (100%), doxycycline (100%), vancomycin (100%), ofloxacin (60%), chloramphenicol (80%), ampicillin (80%), and ceftioxin (60%) (see Figure 2).

The findings of the current study agreed with [20] during the study of *Leuconostoc* sp. from acute cellulitis and acute apical periodontitis showing. Among the 93 exudate samples, 2 (1.6%) were positive for *Leuconostoc* spp. that have been isolated from one acute facial cellulitis and an acute apical periodontitis. *Leuconostoc* isolates showed 100% sensitivity to lincosamides (lincomycin and clindamycin). The beta-lactam antibiotics to which isolates were 100% sensitive are piperacillin, tobramycin, amoxicillin-clavulanic acid, gentamycin, piperacillin-tazobactam, and penicillin G. By contrast, isolates were 100% resistant to trimethoprim-sulfamethoxazole. Sensitivity was 50% for

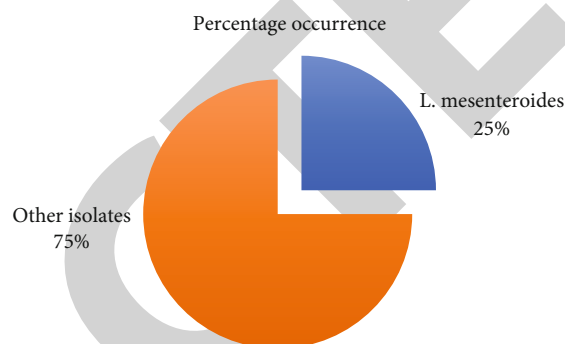


FIGURE 1: Percentage occurrence of *L. mesenteroides* in 20 patients suffering from periodontitis.

macrolides (spiramycin and erythromycin) and for the 3rd-generation cephalosporin antibiotics (cefotaxime, cefuroxime, cefixime, and ceftriaxone).

Anyways, the dental surgeons currently use broad-spectrum antibiotics. In most cases, the prescription of antibiotics in endodontic infections is empirical and an overuse is observed [21]. This contributes to the emergence of antibiotic-resistant bacterial strains [22]. The study reported in this work is about the isolate. Unlike many gram-positive bacteria, *Leuconostoc* species commonly demonstrate high-level resistance to vancomycin, with preserved sensitivity to most other antibacterial agents [23]. Furthermore MIC of CHX for isolates was  $\leq 3.5$  ( $\mu\text{g/ml}$ ) depending on the inhibition zones, under aerobic conditions and under anaerobic conditions in the inhibition zone ( $7.5 \pm 0.06, 7 \pm 0.46$ ), respectively; however, CHX's antibacterial activity caused the bacterial cytoplasmic membrane being damaged. However, resistance to CHX was attributed to the alterations in the cell membrane [24].

Moreover, *L. mesenteroides* isolates were moderate biofilm former (MBF) under aerobic and anaerobic conditions (Table 2). But when the biofilm was treated by MIC of CHX, that noticed the biofilm became weaker under aerobic and anaerobic conditions; however, in the anaerobic conditions, the strength of the biofilm formation was higher than that in aerobic condition; the statistical analysis in the *t*-test has no significant difference between the aerobic and anaerobic conditions after and before the treatment by CHX (Table 3).

Leathers and Bischoff [25] revealed that *L. citreum* and *L. mesenteroides* produce glucans that are comparable to commercial dextran; however, these strains differed significantly

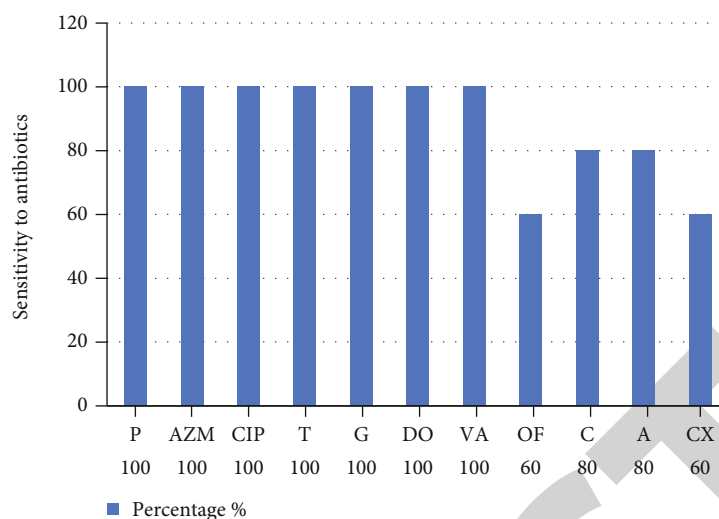


FIGURE 2: Susceptibility of *L. mesenteroides* forward antibiotics.

TABLE 2: Biofilm formation and effect of CHX toward the biofilm formation under aerobic and anaerobic condition.

Biofilm groups	Mean	S.D	S.E
Group I	0.123	0.029	0.021
Group II	0.114	0.007	0.005
Group III	0.103	0.009	0.011
Group IV	0.240	0.130	0.092
Group V	0.170	0.087	0.062
Group VI	0.261	0.230	0.012

TABLE 3: Paired sample test (*T*-test).

Paired groups	Mean	<i>T</i>	Sig.
Group I-Group II	0.008	0.321	0.802
Group IV-Group V	0.0700	2.333	0.258
Group I-Group IV	-0.117-	-1.035-	0.489
Group II-Group V	-0.055-	-0.982-	0.506
Group III-Group VI	-0.035-	-0.882-	0.406

in their ability to build biofilms. Biofilm density was found in these strains. As a result, biofilm-forming capability differed greatly between strains in both species, and the kinds of polysaccharides generated did not appear to have an effect on biofilm formation.

However, CHX has lower effectiveness against the formed biofilm after 24 hr due to the biofilm previously developed by isolates as known by the bacterial biofilm used by bacteria to avoid drugs, ingestion by phagocytosis, and other antimicrobial agents [26, 27], but the activity of antibiotic CHX showed more against preformed biofilm formation attributed to the antimicrobial action against free bacterial isolates and no biofilm formed yet [28].

Regardless, the CHX showed to be less effective under anaerobic condition against biofilm formation and preformed biofilm. *Leuconostoc* is a lactic acid bacterium that produced biofilms [29]. A prior study found that when *L.*

*mesenteroides* was incubated in a high CO<sub>2</sub> environment, the exudate volume and dextran quantity were much larger than when incubated in an aerated environment. The over-expression of the dextransucrase-encoding genes *dsrD* and *dsrT* in *L. mesenteroides* during the first 4 to 8 hours of exposure to high CO<sub>2</sub> levels relative to aerated conditions is linked to dextran synthesis [30, 31].

*L. mesenteroides* subsp. has important technological properties and ability to grow under stress conditions [3], although few research studies have observed the probiotic characteristics of this bacterium [32, 33].

On the other hand, various studies isolated *L. mesenteroides* from the oral cavity [18]; recently, different studies [19, 34] reported that *L. mesenteroides* biofilm has an important role as an antibacterial, including the oral bacteria as *Streptococcus mutans* in which dextran-producing *Leuconostoc* strains are capable to inhibit *S. mutans* biofilm formation [35]. Ahmaed and Awad [34] revealed that the biofilm produced by *L. mesenteroides* showed antimicrobial activity; *Staphylococcus aureus*, *Salmonella* spp., *Escherichia coli*, *Klebsiella* spp., *Pseudomonas aeruginosa*, *Streptococcus mutans* that appear to have *L. mesenteroides* can produce exopolysaccharides especially soluble dextran [36]. Many *Leuconostoc mesenteroides* species produce many organic acids in addition to a group of antimicrobial compounds, especially protein products called bacteriocines and like bacteriocines (such as carnosin and leuconocin). This compound inhibited gram-negative and gram-positive bacteria by damaging the cell or protein synthesis and nucleic acid [4].

#### 4. Conclusion

Based on the results of this study, the existence of *L. mesenteroides* subsp. *cremoris*, in the oral cavity is due to eating foods and vegetables; based on the strength of the biofilm and sensitivity tests, the isolates have less pathogenicity in the oral cavity due to the weakness of the biofilm production



and the lack of resistance to antibiotics; finally, these isolates are more active under anaerobic conditions.

## Data Availability

The data underlying the results presented in the study are available within the manuscript.

## Conflicts of Interest

The authors declare that they have no conflicts of interest regarding the publication of this paper.

## References

- [1] E. Metchnikoff, *Optimistic Studies*, Putman's Sons, New York, 1908.
- [2] G. Nanavati, T. Prasanth, M. Kosala, S. K. Bhandari, and P. Banotra, "Effect of probiotics and prebiotics on oral health," *Studies*, vol. 9, no. 1, pp. 01–06, 2021.
- [3] P. Nieto-Arribas, S. Seseña, J. M. Poveda, L. Palop, and L. Cabezas, "Genotypic and technological characterization of *Leuconostoc* isolates to be used as adjunct starters in Manchego cheese manufacture," *Food Microbiology*, vol. 27, no. 1, pp. 85–93, 2010.
- [4] J. Hitendra, V. C. Suvarna, and S. B. Niveditha, "Antimicrobial attributes of *Leuconostoc* isolates against fruit and vegetable spoilage organisms," *International Journal of Current Microbiology and Applied Sciences*, vol. 4, no. 11, pp. 160–166, 2015.
- [5] R. A. Kekkonen, E. Kajasto, M. Miettinen, V. Veckman, R. Korpela, and I. Julkunen, "Probiotic *Leuconostoc mesenteroides* ssp. *cremoris* and *Streptococcus thermophilus* induce IL-12 and IFN- $\gamma$  production," *World Journal of Gastroenterology*, vol. 14, no. 8, pp. 1192–1203, 2008.
- [6] Z. Benmechernene, H. F. Chentouf, B. Yahia et al., "Technological aptitude and applications of *Leuconostoc mesenteroides* bioactive strains isolated from Algerian raw camel milk," *BioMed Research International*, vol. 2013, Article ID 418132, 2013.
- [7] M. M. C. Casado, N. Benomar, L. L. Lerma, A. Gálvez, and H. Abriouel, "Antibiotic resistance of *Lactobacillus pentosus* and *Leuconostoc pseudomesenteroides* isolated from naturally-fermented Aloreña table olives throughout fermentation process," *International Journal of Food Microbiology*, vol. 172, pp. 110–118, 2014.
- [8] A. Abdullah Hamad, M. Lellis Thivagar, M. Bader Alazzam et al., "Dynamic systems enhanced by electronic circuits on 7D," *Advances in Materials Science and Engineering*, vol. 2021, Article ID 8148772, 2021.
- [9] V. K. Bajpai, I. A. Rather, R. Majumder, F. H. Alshammari, G. J. Nam, and Y. H. Park, "Characterization and antibacterial mode of action of lactic acid bacterium *Leuconostoc mesenteroides* HJ69 from kimchi," *Journal of Food Biochemistry*, vol. 41, no. 1, article e12290, 2017.
- [10] G. Zoumpopoulou, K. Papadimitriou, V. Alexandraki et al., "The microbiota of Kalathaki and Melichloro Greek artisanal cheeses comprises functional lactic acid bacteria," *LWT*, vol. 130, article 109570, 2020.
- [11] H. Zhang, H. HuangFu, X. Wang et al., "Antibacterial activity of lactic acid producing *Leuconostoc mesenteroides* QZ1178 against pathogenic *Gallibacterium anatis*," *Science*, vol. 8, 2021.
- [12] M. J. Leboffe and B. E. Pierce, *A Photographic Atlas for the Microbiology Laboratory*, Morton Publishing Company, 2021.
- [13] I. Wiegand, K. Hilpert, and R. E. Hancock, "Agar and broth dilution methods to determine the minimal inhibitory concentration (MIC) of antimicrobial substances," *Nature Protocols*, vol. 3, no. 2, pp. 163–175, 2008.
- [14] G. A. O'Toole, "Microtiter dish biofilm formation assay," *JoVE Journal of Visualized Experiments*, vol. 47, pp. 24–37, 2011.
- [15] A. C. R. Tanner, J. M. J. Mathney, R. L. Kent et al., "Cultivable anaerobic microbiota of severe early childhood caries," *Journal of Clinical Microbiology*, vol. 49, no. 4, pp. 1464–1474, 2011.
- [16] X. Chen, E. B. M. Daliri, R. Chelliah, and D. H. Oh, "Isolation and identification of potentially pathogenic microorganisms associated with dental caries in human teeth biofilms," *Microorganisms*, vol. 8, no. 10, p. 1596, 2020.
- [17] M. L. Thivagar, A. S. Al-Obeidi, B. Tamilarasan, and A. A. Hamad, "Dynamic analysis and projective synchronization of a new 4D system," in *IoT and Analytics for Sensor Networks*, vol. 244, pp. 323–332, Springer, Singapore, 2022.
- [18] M. Elhai, C. Meune, M. Boubaya et al., "Mapping and predicting mortality from systemic sclerosis," *Annals of the rheumatic diseases*, vol. 76, no. 11, pp. 1897–1905, 2017.
- [19] X. Shao, K. Fang, D. Medina, J. Wan, J. L. Lee, and S. H. Hong, "The probiotic, *Leuconostoc mesenteroides*, inhibits *Listeria monocytogenes* biofilm formation," *Journal of Food Safety*, vol. 40, no. 2, article e12750, 2020.
- [20] W. A. D. Kaboré, S. R. Dembélé, and N. Barro, "Occurrence and antimicrobial susceptibility of *Leuconostoc*: an emergent pathogen associated with acute endodontic infections," *Turkish Endodontic Journal*, vol. 6, no. 1, pp. 1–6, 2021.
- [21] D. F. Bogari, N. A. Alzebiani, R. M. Mansouri et al., "The knowledge and attitude of general dental practitioners toward the proper standards of care while managing endodontic patients in Saudi Arabia," *Saudi Endodontic Journal*, vol. 9, pp. 40–50, 2019.
- [22] J. J. Segura-Egea, K. Gould, B. H. Şen et al., "Antibiotics in endodontics: a review," *International Endodontic Journal*, vol. 50, no. 12, pp. 1169–1184, 2017.
- [23] J. A. Starr, "Leuconostoc-species-associated endocarditis," *Pharmacotherapy*, vol. 27, no. 5, pp. 766–770, 2007.
- [24] F. Cieplik, N. S. Jakubovics, W. Buchalla, T. Maisch, E. Hellwig, and A. Al-Ahmad, "Resistance toward chlorhexidine in oral bacteria—is there cause for concern?," *Frontiers in Microbiology*, vol. 10, p. 587, 2019.
- [25] T. D. Leathers and K. M. Bischoff, "Biofilm formation by strains of *Leuconostoc citreum* and *L. mesenteroides*," *Biotechnology Letters*, vol. 33, no. 3, pp. 517–523, 2011.
- [26] M. Cizek-Lenda, M. Strus, M. Walczewska et al., "Pseudomonas aeruginosa biofilm is a potent inducer of phagocyte hyperinflammation," *Inflammation Research*, vol. 68, no. 5, pp. 397–413, 2019.
- [27] M. Alsaffar, A. A. Hamad, A. Alshammari et al., "Network management system for IoT based on dynamic systems," *Computational and Mathematical Methods in Medicine*, vol. 2021, Article ID 9102095, 2021.
- [28] E. J. Sallum, D. F. Nouer, M. I. Klein et al., "Clinical and microbiologic changes after removal of orthodontic appliances," *American Journal of Orthodontics and Dentofacial Orthopedics*, vol. 126, no. 3, pp. 363–366, 2004.
- [29] E. Díaz-Montes, "Dextran: sources, structures, and properties," *Polysaccharides*, vol. 2, no. 3, pp. 554–565, 2021.

## Retraction

# Retracted: Mutation Detection and Functional Analysis of MSX1, PAX9, AXIN2, and BMP in Nonsyndromic Congenital Missing Teeth Based on Intelligent Image Detection

### BioMed Research International

Received 3 October 2023; Accepted 3 October 2023; Published 4 October 2023

Copyright © 2023 BioMed Research International. This is an open access article distributed under the Creative Commons Attribution License, which permits unrestricted use, distribution, and reproduction in any medium, provided the original work is properly cited.

This article has been retracted by Hindawi following an investigation undertaken by the publisher [1]. This investigation has uncovered evidence of one or more of the following indicators of systematic manipulation of the publication process:

- (1) Discrepancies in scope
- (2) Discrepancies in the description of the research reported
- (3) Discrepancies between the availability of data and the research described
- (4) Inappropriate citations
- (5) Incoherent, meaningless and/or irrelevant content included in the article
- (6) Peer-review manipulation

The presence of these indicators undermines our confidence in the integrity of the article's content and we cannot, therefore, vouch for its reliability. Please note that this notice is intended solely to alert readers that the content of this article is unreliable. We have not investigated whether authors were aware of or involved in the systematic manipulation of the publication process.

Wiley and Hindawi regrets that the usual quality checks did not identify these issues before publication and have since put additional measures in place to safeguard research integrity.

We wish to credit our own Research Integrity and Research Publishing teams and anonymous and named external researchers and research integrity experts for contributing to this investigation.

The corresponding author, as the representative of all authors, has been given the opportunity to register their agreement or disagreement to this retraction. We have kept a record of any response received.

### References

- [1] X. Yao, C. Zhang, P. Gao et al., "Mutation Detection and Functional Analysis of MSX1, PAX9, AXIN2, and BMP in Nonsyndromic Congenital Missing Teeth Based on Intelligent Image Detection," *BioMed Research International*, vol. 2022, Article ID 6217399, 7 pages, 2022.

## Research Article

# Mutation Detection and Functional Analysis of MSX1, PAX9, AXIN2, and BMP in Nonsyndromic Congenital Missing Teeth Based on Intelligent Image Detection

Xueqin Yao , Cheng Zhang, Peipei Gao, Zixuan Meng, Yonghong Hao, Jingjing Yan, and Wenbo Yao

*Pediatric Stomatology of Beijing Tongzhou Xinhua Hospital, China*

Correspondence should be addressed to Xueqin Yao; 41823029@xs.ustb.edu.cn

Received 12 April 2022; Revised 25 April 2022; Accepted 3 May 2022; Published 20 May 2022

Academic Editor: Dinesh Rokaya

Copyright © 2022 Xueqin Yao et al. This is an open access article distributed under the Creative Commons Attribution License, which permits unrestricted use, distribution, and reproduction in any medium, provided the original work is properly cited.

Due to the complexity of clinical manifestations and the lack of standardized diagnostic criteria, it is still difficult to distinguish the etiological types of congenital edentulousness corresponding to genetic defects. This paper studies the application of deep learning image processing and digital image processing in medical images in detail and analyzes the functions of congenital edentulous hotspot genes. The cases in the control group and the study group were collected, and the gene mutations of direct sequence MSX1, PAX9, AXIN2, and BMP were analyzed, and new pathogens were found. The experimental results suggest that PAX9 and MSX1 genes may have a synergistic effect in nonsyndromic congenital edentulous patients. In severely missing teeth, the role of PAX9 may be greater than that of MSX1. The experimental results will help us lay the foundation for further understanding of the disease in the future.

## 1. Introduction

Congenital tooth loss is a disease of dental hypoplasia that only manifests as the loss or abnormality of the number of teeth, which belongs to the number hypoplasia in congenital dental hypoplasia [1, 2]. Congenital lack of teeth affects the normal development of the oral and maxillofacial system of patients, causing developmental deformities of the cranio-maxillofacial region, which further affects the patient's appearance (such as bony crossbite and midface collapse), pronunciation, facial aesthetics, general development, and mental health. These complications are seriously endangering people's physical and mental health. In addition, congenitally missing teeth are often accompanied by allergic diseases [3, 4].

The clinical manifestations of nonsyndromic congenital edentulous generally involve the permanent dentition, rarely involving the deciduous dentition, the third molar is most often missing, and the number of other teeth is variable. There are obvious racial differences in missing teeth. Except

for the third molars, the most common missing teeth in Asian populations are mandibular incisors, and the most common ones in European and American populations are mandibular second premolars and maxillary lateral incisors. After tooth loss, the chewing efficiency is reduced or even lost, which increases the burden on the gastrointestinal system, reduces the quality of life, and affects aesthetics and mental health.

Using computer technology to extract the basic information of teeth in panoramic X-ray films can significantly reduce the workload of doctors [5]. Weon et al. have developed an algorithm for fusing a 3D LIDAR (Light Detection and Ranging) system that receives objects detected in a deep learning-based image sensor and object data in the form of 3D point clouds. Match 3D LIDAR data to 2D image data through fusion of mixed-level multisensors. First, since 3D LIDAR data represents all objects within the sensor's detection range as points, all unnecessary data, including ground data, is filtered out. The 3D Random Sample Consensus (RANSAC) algorithm can extract ground data perpendicular

to the reference estimated 3D plane and data at both ends through ground estimation [6]. Divya and Leena utilize smart devices for fall detection. Vision-based detection with compressed neural networks running on smart devices built using transfer learning. Leverage image augmentation to build datasets to improve model performance. The model is evaluated in terms of accuracy, and the strength of the fog layer is evaluated in terms of latency. Compared with the existing state-of-the-art algorithms available for detection, the accuracy of the proposed model is 98.5% [7]. It is of practical significance to study the mutation detection of congenitally missing teeth by intelligent image detection.

At present, the epidemiological investigation and genetic research on congenitally missing teeth in my country is basically blank. In view of this situation, in order to explore the mutation detection in nonsyndromic congenitally missing teeth, this paper carried out the incidence of such diseases in the population and analyzed them. It was found that the mutation detection of the disease was different in MSX1, PAX9, AXIN2, and BMP, and there were statistically significant differences. In conclusion, the study of the clinical characteristics and pathogenesis of congenital edentulous patients not only has a clinical diagnosis and treatment of the disease. It has important guiding significance and also has important practical significance for the etiology research of the disease.

## 2. Mutation Detection and Functional Study in Nonsyndromic Congenital Edentulous

**2.1. Deep Learning Image Processing.** Deep convolutional neural networks enable complex training models of traditional machine learning algorithms [7]. The structure of the convolutional neural network is shown in Figure 1. It has a fixed-size convolution kernel and an input image that performs integration to capture features such as edges, textures, and contours in the image. The pooling layer is also based on a fixed size. The scale is downsampling, so that the receptive field of the feature image can be enlarged according to the scale [8, 9]. Then, the obtained feature information is mapped to a fixed-length feature vector through the fully connected layer to achieve the effect of classification.

In practical applications, the scale of medical image databases is always small, and in the eyes of complex models, training from scratch can easily lead to overcorrection. To avoid this, preliminary descriptions of models have become a common practice. This feature directly uses some template templates on ImageNet and COCO datasets [10]. In this case, the pre-existing templates act as feature suppliers, and they can restore the data simply by replacing the new layers in the new template [11].

**2.2. Digital Image Processing.** Image augmentation is often employed when faced with small sample image datasets. Since most medical image datasets are small sample datasets, these techniques are often used in the image enhancement process of medical images [12].

Commonly used basic image enhancement methods include cropping, flipping, rotating, adding noise, filtering, and sharpening [13]. Taking horizontal mirroring as an example, if the height and width of an image are known as ( $lHeight$ ,  $lWidth$ ), set the coordinates of a point in the image to be  $(x_0, y_0)$ , and after horizontal mirroring, the coordinates of this point will become  $(lWidth - x_0, y_0)$ , which can be expressed as follows:

$$\begin{bmatrix} x_1 \\ y_1 \\ 1 \end{bmatrix} = \begin{bmatrix} -1 & 0 & lwidth \\ 0 & 1 & 0 \\ 0 & 0 & 1 \end{bmatrix} \begin{bmatrix} x_0 \\ y_0 \\ 1 \end{bmatrix}. \quad (1)$$

The inverse operation matrix expression is as follows:

$$\begin{bmatrix} x_0 \\ y_0 \\ 1 \end{bmatrix} = \begin{bmatrix} -1 & 0 & lwidth \\ 0 & 1 & 0 \\ 0 & 0 & 1 \end{bmatrix} \begin{bmatrix} x_1 \\ y_1 \\ 1 \end{bmatrix}. \quad (2)$$

To realize the mirror image of the whole image, all the points in the image need to be calculated. Similarly, the realization of vertical mirroring is to change the coordinates of all points  $(x_0, y_0)$  to  $(x_0, lHeight - y_0)$  [14].

The noise in the image can be regarded as the interference signal in the image signal. For example, "snowflakes" in a TV image can be seen as image noise that interferes with the original image. In the process of image acquisition, various problems such as equipment and environment often cause interference and introduce image noise, thereby affecting the image quality [15]. Therefore, in the process of image enhancement, filtering is usually used to remove noise. In data enhancement, in order to increase the diversity of the data, noise will be artificially added to the image.

The main purpose of image sharpening is to make blurry images clear. Image sharpening methods are usually divided into two types: one is the differential method, which mainly enhances the pixels with large gradients through image gradient operations to highlight image details, so as to achieve the purpose of sharpening. The other is to use high-pass filtering to accept high-frequency signals and suppress low-frequency signals, thereby highlighting the details of the image and sharpening the image [16]. Both methods are now more popular image sharpening methods.

**2.3. Dental X-Ray Images.** In dentistry, X-ray examinations are divided into two categories: intraoral X-ray examination, which is a technique in which a film is placed in the mouth, that is, the X-ray image is obtained in the patient's mouth, and a technique placed between the radiograph and the X-ray source, where the X-ray image is acquired outside the patient's mouth. This results in the following types of X-ray images: bitewing, apical (intraoral), and panoramic (extraoral) [17].

The bite wing X-ray image is used to display the details of the upper and lower teeth in the oral area, while the periapical X-ray image is used to monitor the entire tooth, which



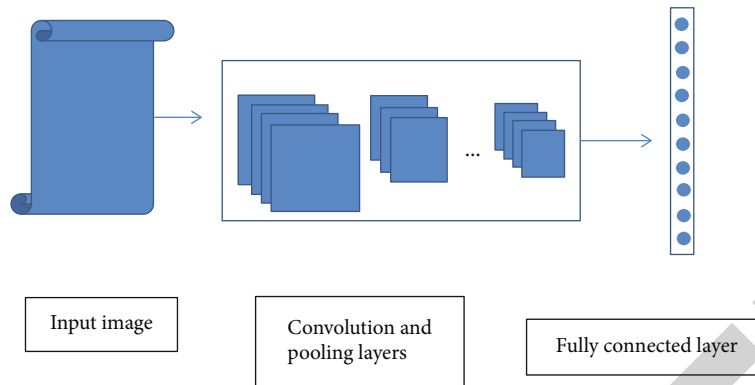


FIGURE 1: Typical convolutional neural network structure.

can display the enamel, dentin, cementum and other dental hard tissues and pulp soft tissues [18]. Panoramic radiography, also known as orthodontic radiography, is a radiological examination that can obtain basic information for the diagnosis of dental abnormalities.

#### 2.4. Congenital Missing Tooth Hotspot Genes

**2.4.1. PAX9.** The PAX transcriptional gene family plays an integral role in vertebrate ontogeny [19]. All members of this family have a paired control domain, an octapeptide domain, and a paired homology domain. These structures play an important role in fetal development and tumor formation. As a transcription factor, it has the ability to bind to DNA. PAX9 is involved in a variety of regulatory mechanisms and plays a crucial role in tumorigenesis. PAX9 is highly expressed in salivary gland tumors, especially malignant tumors, and may play a negative role in the prognosis of patients with esophageal squamous cell carcinoma [20]. Regular screening of patients with PAX9 gene mutations is essential for clinical screening, especially for tumors in tissues with high PAX9 expression such as esophagus, salivary glands, prostate, lung, thyroid, and bladder [21].

**2.4.2. MSX1.** MshHomeobox1 (MSX1) is located on human chromosome 4 q.16.2 with a full length of 5.6k bases, including two exons. As a negative regulator of tooth differentiation, it plays an important role in tooth differentiation and development. Abnormalities of this gene not only show abnormal number of teeth but also affect the morphological development of teeth. Mutations in this gene are highly associated with congenital edentulous and nonsyndromic cleft lip and palate in humans. The MSX1 gene exhibits cleft lip, cleft palate, and dental developmental disorders and affects development. The effect of MSX gene mutation seems to be caused by its influence on downstream genes. The lack of MSX1 gene downregulates the expression of downstream gene BMP4 and transcription factor LEF. Through a series of complex biological regulation, it leads to tooth loss and the formation of cleft lip and palate.

**2.4.3. AXIN2.** AXIN2 is a central axis arrestin 2 gene, located on chromosome 17 q.23, with a full-length gene of 43k bases, including 10 exons. The transcribed mRNA is 4241

bases, the CDS translation transcript is 2532 bases, and the translation forms 843 amino acids. This gene encodes axon arrestin 2, which mainly functions as a structural support protein and plays an important role in the WNT signaling pathway. AXIN protein regulates the expression level of  $\beta$ -catenin in the nucleus by negative feedback and maintains the stability of  $\beta$ -catenin inside and outside the cell. In the absence of WNT pathway ligands,  $\beta$ -catenin can still stimulate the continuous action of the signaling pathway. The deficiency of  $\beta$ -catenin hinders the excitation of WNT signaling pathway and destroys the second important function of  $\beta$ -catenin-adhesion function.

**2.4.4. BMP signaling pathway.** USAG-1 (uterine sensitization associated gene-1, uterine sensitivity-related gene) is a BMP antagonist and can regulate the WNT signaling pathway. Murashima-Suginami et al. found that USAG-1-deficient mice developed multiple teeth with enhanced BMP signaling. Subsequent studies found that blockade of BMP signaling could relieve the formation of supernumerary teeth.

The fine regulation of these signal molecules is very important to maintain the proper number of teeth, such as the inhibition of Shh signal expression in the early stage of tooth germ development and the regulation of WNT signal expression. Epiprofin is expressed in tooth germ epithelium and can interact with BMP, Shh, and WNT signaling pathways and participate in the regulation of the number of teeth. In mice lacking Epiprofin expression, supernumerary incisors and molars can be seen. In addition, inactivation of IL11 signaling can cause craniosynostosis, maxillary dysplasia, delayed tooth eruption, and the occurrence of supernumerary teeth.

### 3. Investigation and Study of Mutation Detection and Function in Nonsyndromic Congenital Absence of Teeth

**3.1. Research Objects.** The cases in the research group came from patients who were treated in the Dental Clinic Center of Xinhua Hospital in Tongzhou District. After excluding the history of tooth extraction, X-ray examination confirmed that there was no permanent tooth germ in the edentulous area. The number of simple missing teeth (except third



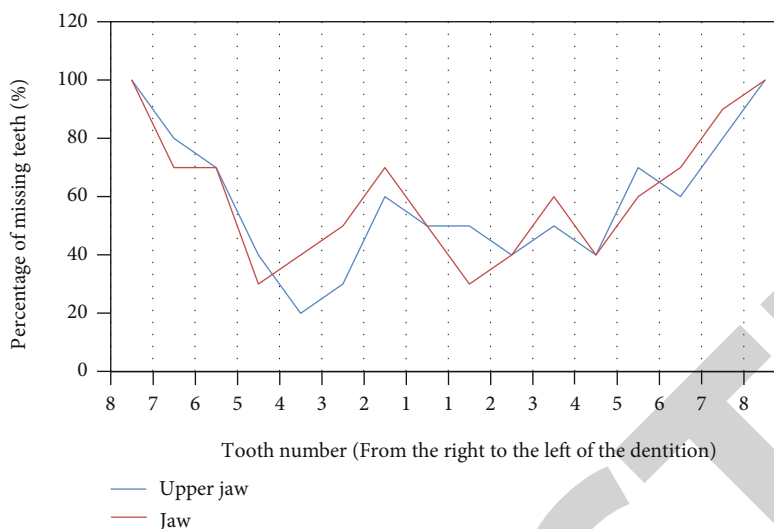


FIGURE 2: Frequency of tooth loss in each tooth position in 10 patients.

molars) with no syndrome and more than 10 teeth was selected. Congenitally edentulous patients or other developmental deformities were included in the study group after informed consent. The frequency of tooth loss in each tooth position of the 10 patients is shown in Figure 2.

**Control group case selection:** 100 noncongenitally edentulous patients were randomly selected as normal controls, 50 males and females, aged between 20 and 60 years old, screened the found mutations of unknown pathogenic nature, and further excluded the mutation as possibility of SNP. If the mutation does not exist in the normal population, it suggests that it is a possible pathogenic mutation; if the mutation exists in the normal population, it suggests that it may be a SNP.

### 3.2. Experimental Reagents

- (1) *Red blood cell lysate*: provided by the Laboratory of Molecular Biology Technology, Medical University
- (2) *Isopropyl alcohol and anhydrous ethanol*: all of analytical grade, products of Bengbu Chemical Reagent Factory
- (3) *Tris-phenol*: product of M company
- (4) *Chloroform*: analytically pure, chemical preparation factory product
- (5) *Proteinase K*: provided by the Laboratory of Molecular Biology Technology, Medical University

### 3.3. Experimental Method

- (1) Backup preservation of genomic DNA and preparation of template DNA

Measure the purity and concentration of the DNA stock solution using a spectrophotometer and divide it into 2-3 tubes. One is kept in a freezer at  $-80^{\circ}\text{C}$  and the rest at  $-20^{\circ}\text{C}$  and  $4^{\circ}\text{C}$  for DNA detection and analysis.

Prepare template DNA at a concentration of  $50\text{ ng}/\mu\text{l}$  depending on the concentration of the DNA stock.

#### (2) Gene primer design

The length of primers was controlled at 16~24 bp. The GC content is controlled between 40% and 60%. The primers themselves cannot have 4 consecutive bases complementary. The energy values of primer dimers and hairpin structures should not be too high.

#### (3) Polyacrylamide gel electrophoresis

After amplification, take  $2\ \mu\text{l}$  of PCR amplification product, use 6% polyacrylamide gel (30% acrylamide 6 ml,  $10\times$  TBE 1.5 ml, TEMED409l, and 10% APS30091, add distilled deionized water 30 ml) electrophoresis detection, 300 V constant pressure. Electrophoresis was performed for 50 minutes, stained with silver nitrate, and the results were observed and recorded.

## 4. Mutation Detection and Functional Analysis and Research in Nonsyndromic Congenitally Missing Teeth

**4.1. Sequencing Results of PAX9 Gene.** In the sequencing results of the PAX9 gene, there is a heterozygous/homozygous mutation of  $c.631+41g>a$  in the intron position of 41 bases downstream of exon 1. After searching the SNP database, it was found that he was an intron SNP site (No. rs5214607), so the site is far away from the exon, and it does not participate in the coding of proteins and does not affect the splicing site at the end of the exon, so it is a nonpathogenic polymorphism.

There is a heterozygous or pure sum mutation of  $c.717-718CG>TC$  in exon 2 of PAX9 gene. There are 5 main sequencing results of these two loci, as shown in Table 1. The heterozygous change at position 717 causes the amino

TABLE 1: Classification of sequencing results at position c.717.718 of the PAX9 gene.

Cdna.717	Cdna.718	Electrophoresis results
Without	G>C pure	Single strip
G>C miscellaneous	Without	Single strip
Without	C>T pure	Single strip
C>T miscellaneous	Without	Single strip
C>T miscellaneous	G>C miscellaneous	Two belts

acid codon CAC to change to CAT, which is still a histidine codon, c. The heterozygous change at position 718 causes the amino acid codon GCG to change to CCG, and the amino acid changes from alanine to histidine. After searching the SNP database, it was found that these two loci are SNP loci, numbered rs6254140 and rs9251432, and the control test of a large sample of normal people proved that they were nonpathogenic mutations. However, by analyzing the results of this study, it can be found that it can be determined that the heterozygous double peak caused the structural change of the DNA template strand, which showed double bands in electrophoresis; The cases with heterozygous mutation, that is, heterozygous double peaks, occupy a certain proportion of 3/10, and the proportion is relatively large. It can be speculated that it has an impact on the pathogenic factors of congenital edentulousness.

**4.2. Sequencing Results of MSX1 Gene.** In the sequencing results of MSX1 gene, the detected SNP loci are as follows: C.119C>G pure and change on exon 1, and after searching the SNP database, it is found that it is an exon SNP locus (number rs62514851). For exon 1 c.348C>T heterozygous/homozygous change, after searching the SNP database, it was found that it was an exon SNP site (number rs825146241). The above two sites have a large sample of normal people controlled studies abroad, indicating that the base changes at these two sites are not the cause of congenital lack of teeth directly, and we can speculate that it is an indirect cause of congenital lack of teeth. There is a t insertion change at the c.470.24 intron upstream of exon 2. After searching the SNP database, it is found that it is an exon SNP site (number rs5618512). Due to the insertion of a single base, a unidirectional repeat appears in the sequencing results. Sequence and electrophoresis result is a single band, indicating that the DNA structure has not changed, and this insertion mutation due to repeated base sequence is a common SNP site, which is a nonpathogenic polymorphic change. The heterozygous change of c>t in the intron position c.912+68 downstream of exon 2 was searched in the SNP database, and it was found that it was an exon SNP site (number rs6914), so the site was far away from the exon, and it was not participating in coding proteins does not affect the splice site at the end of the exon, so it can be determined to be a nonpathogenic polymorphic change.

The relationship between lineage genotype and edentulous interval can be found. In this study, most patients with missing teeth were concentrated in the anterior teeth area.

TABLE 2: Relationship between genotype and edentulous interval.

Genotype	Front teeth	Back teeth
MSX1 mutation	4	2
PAX9 mutation	8	7
Both genes have mutations	11	5
Without	1	1

When the posterior teeth were missing, PAX9 had a greater impact than MSX1. The relationship between genotype and the missing teeth interval is shown in Table 2.

PAX9 has 8 anterior teeth and 7 posterior teeth, as shown in Figure 3. In summary, the two genes PAX9 and MSX1 may have a synergistic effect in patients with simple congenital edentulousness.

**4.3. Analysis of AXIN2 Sequencing Results.** The sequencing results of this study showed that the codon corresponding to the 264th position of exon 2 changed from ACA→GCA, threonine to alanine, and a missense mutation occurred; the 547th position CAA→CGA, glutamine changed from arginine, and a missense mutation also occurred. At position 162 of exon 6, CCG→CTG, a missense mutation occurred, and proline was changed to leucine. At position 922 of exon 11, GAT→GAG, a missense mutation occurred, and the aspartic acid was changed to glutamic acid; the position 1141, ACT→ACA, still encoded threonine, and a synonymous mutation occurred. No mutation sites were found in DNA testing of 100 healthy controls.

**4.4. Analysis of BMP Sequencing Results.** The Ct value of the sample qRT-PCR detection results is shown in Table 3, and the amplification of PAX9 and BMP genes is shown in Figure 4.

In the overall analysis, the genotype distribution of only two BMP polymorphisms, rs2518516 and rs42815, was significantly different between cases and controls among the five loci (rs2518516,  $P=0.028$  and rs42815,  $P=0.032$ ), which is the first time that two loci associated with missing teeth were found in this study. In a stratified analysis by edentulous type, the recessive models of rs3178250 and rs15705 were associated with congenital loss of lower incisors and increased the risk of congenital loss of lower incisors compared with wild type (rs2518516, ORrec = 1.50 and rs42815, ORrec = 1.42). The recessive model and mutant homozygotes of rs235768 have a protective effect on congenital odontogenesis compared with the wild type.

## 5. Conclusions

Nonsyndromic congenital missing teeth are common in clinic. Most of the existing solutions are to restore the missing part through various clinical repair methods, but the effect is not ideal. If the disease can be completely prevented and intervened from the pathogenesis, it would be a major breakthrough. In this paper, the gene mutation detection in the research group and the control group collected through the investigation and combined with clinical analysis, the

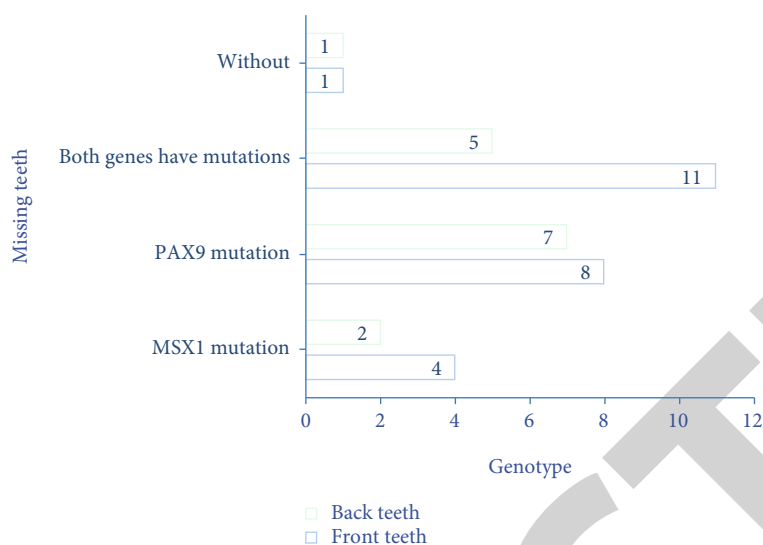


FIGURE 3: Relationship between genotype and edentulous interval.

TABLE 3: PAX9 and BMP gene amplification Ct values.

Sample	Ct duplicate 1	Ct duplicate 1	Ct duplicate 3	Internal reference Ct duplicate well 1	Internal reference Ct duplicate well 2	Internal reference Ct duplicate well 3
mut-PAX9	25.47	25.55	25.63	25.14	25.98	25.46
nor-PAX9	24.61	24.11	24.21	23.11	23.10	23.28
mut-BMP	28.14	28.06	28.30	24.88	24.79	24.92
nor-BMP	22.08	22.39	22.63	23.89	23.99	23.68

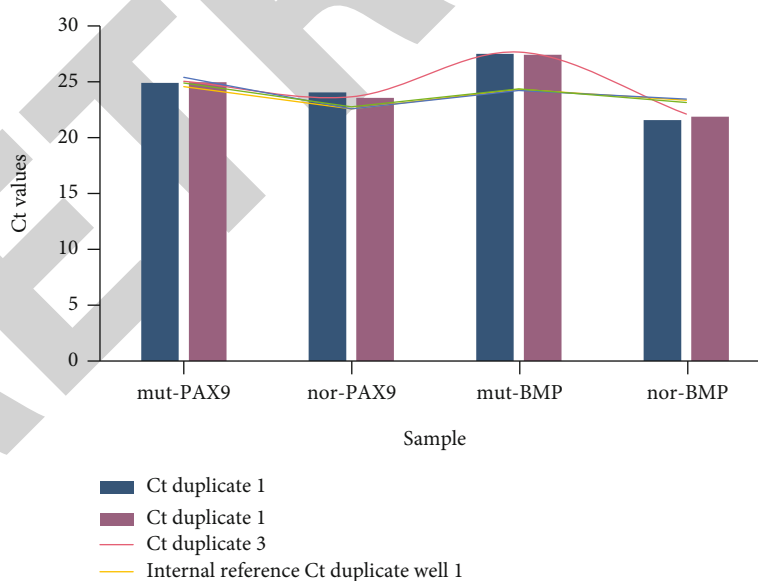


FIGURE 4: PAX9 and BMP gene amplification Ct values.

following conclusions are drawn: several popular genes PAX9, MSX1, EDA, AXIN2, etc. Missing teeth and related diseases (cleft lip and palate, ectodermal hypoplasia, colorectal tumorigenesis, etc.) have research significance. The heterozygosity change of PAX9 gene c.717.718CG>TC may be the cause of the disease in patients with simple congenital

edentulous. MSX1 gene c.469+5G>A heterozygous mutation is a pathogenic mutation in severe nonsyndromic congenital edentulous. In addition, the homozygous change of c.119C>G and the heterozygous change of c.348C>T may also be the cause of the onset of nonsyndromic congenital edentulous patients.